

# **Polymeric Materials in Organic Synthesis and Catalysis**

*Edited by Michael R. Buchmeiser*

***Further Reading from WILEY-VCH***

F. Zaragoza Dörwald

**Organic Synthesis on Solid Phase**

2002, 2nd, Completely Revised and Enlarged Edition

ISBN 3-527-30603-X

K. C. Nicolaou, R. Hanco, W. Hartwig (Eds.)

**Handbook of Combinatorial Chemistry, 2 Vols.**

2002

ISBN 3-527-30509-2

C. Reichardt

**Solvents and Solvent Effects in Organic Chemistry**

2002, 3rd, Updated and Enlarged Edition

ISBN 3-527-30618-8

A. Loupy

**Microwaves in Organic Synthesis**

2002

ISBN 3-527-30514-9

# Polymeric Materials in Organic Synthesis and Catalysis

*Edited by Michael R. Buchmeiser*

*Foreword by Rolf Mülhaupt*



WILEY-  
VCH

WILEY-VCH GmbH & Co. KGaA

**Prof. Dr. Michael R. Buchmeiser**

Institut für Analytische Chemie und Radiochemie  
Universität Innsbruck  
Innrain 52a  
6020 Innsbruck  
Austria

This book was carefully produced. Nevertheless, editor, authors and publisher do not warrant the information contained therein to be free of errors. Readers are advised to keep in mind that statements, data, illustrations, procedural details or other items may inadvertently be inaccurate.

**Library of Congress Card No.: applied for**

**British Library Cataloguing-in-Publication Data**

A catalogue record for this book is available from the British Library.

**Bibliographic information published  
by Die Deutsche Bibliothek**

Die Deutsche Bibliothek lists this publication in the Deutsche Nationalbibliografie; detailed bibliographic data is available in the Internet at <<http://dnb.ddb.de>>

© 2003 WILEY-VCH Verlag GmbH & Co. KGaA, Weinheim

All rights reserved (including those of translation in other languages). No part of this book may be reproduced in any form – by photoprinting, microfilm, or any other means – nor transmitted or translated into machine language without written permission from the publishers. Registered names, trademarks, etc. used in this book, even when not specifically marked as such, are not to be considered unprotected by law.

Printed in the Federal Republic of Germany  
Printed on acid-free paper

**Typesetting** K+V Fotosatz GmbH, Beerfelden

**Printing** betz-druck gmbh, Darmstadt

**Bookbinding** J. Schäffer GmbH & Co. KG, Grünstadt

ISBN 3-527-30630-7

**To Andrea**

## Foreword

At the beginning of the 21st century the remarkable progress achieved in the synthetic chemistry of both small molecules and polymers is stimulating the renaissance of the development of polymer-bound reagents and catalysts. The scope of modern polymer supports is expanding well-beyond that of the traditional Merrifield resins. Advanced polymer supports are offering new opportunities for the development of the modern automated high-throughput screening methods as well as of the advanced manufacturing processes with simplified product recovery. Applications include the production of fine chemicals and new intermediates for the chemical and life sciences industries. An increasing number of academic and industrial labs are employing modern polymer supports to facilitate product purification. Novel reagents are being designed to combine the advantages typical for homogeneous and heterogeneous reactions. This strict borderline between heterogeneous and homogeneous reactions is gradually fading away with continuing progress in the development of polymer-mediated reactions. Precise control of polymerization processes using modern living polymerization methods affords an unprecedented control of three-dimensional polymer architectures and allows selective placement of functional groups and linker molecules. Prominent examples of new polymer carrier generations are highly functional nanometer-sized dendritic and hyperbranched polymers with core/shell topology and the high loading of functional groups on the surface. Polymer self-assembly is being exploited to prepare confined environments which can serve as nanoreactors for a variety of chemical reactions. Design and application of polymer supports is attracting attention in combinatorial chemistry, drug discovery research, catalysis, and biosynthesis. Progress in this field is closely related to interdisciplinary research in the various fields of science and reaction engineering. This book meets very successfully the important challenge to bring together leading experts and pioneers from all these relevant fields in order to highlight the outstanding advances and the future potential of the emerging new strategies for the rational development of modern synthetic reactions based upon innovative polymer supports.

The individual chapters address important contributions relevant to the ongoing progress and future success of polymer-mediated reactions in organic synthesis, catalysis, and biosynthesis. All facets of the modern development are presented in this book. Most authors give their complementary views from different

angles on the novel strategies exploiting new methods introduced in polymer synthesis, polymer characterization, and application of functional polymer supports. This includes synthesis of structured polymer supports using living polymerizations and advanced graft copolymerization, the preparation of novel dendritic and hyperbranched carriers with very high loadings, as well as the formation of structured particles, films, membranes, and monolithic systems. Reaction engineering topics cover monitoring and optimization of reactions on solid supports and liquid-phase systems, the development of polymer membrane reactors, the design of combinatorial libraries, and the use of polymer-bound reagents and scavengers in organic multistep syntheses. Several comprehensive overviews focus on the different aspects and the practical applications of such modern polymeric supports in organic syntheses and the emerging new opportunities of nanoreactor design by means of micellar catalysis and novel molecular nanoparticles. Without any doubt this book represents a very valuable asset to everybody who is interested in getting a close-up view on the current state of the art and the exciting new opportunities relating to the use of novel functional polymer systems being applied in catalysis, modern organic synthesis, combinatorial chemistry, and biosynthesis.

May 2003  
Albert-Ludwigs-Universität Freiburg

ROLF MÜLHAUPT

## Contents

**Foreword** VII

**Preface** XIX

**List of Contributors** XXI

<b>1</b>	<b>Structure, Morphology, Physical Formats and Characterization of Polymer Supports</b>	<b>1</b>
	<i>Yolanda de Miguel, Thomas Rohr and David C. Sherrington</i>	
1.1	Synthesis and Molecular Structure of Polymer Supports	1
1.2	Suspension Polymerized Particulate Resin Supports – Structural and Morphological Variants	2
1.2.1	Suspension Polymerization	2
1.2.2	Resin Morphology	3
1.2.3	Novel Morphologies	7
1.2.3.1	Solvent Expanded Gel-type Resins	7
1.2.3.2	Collapsible Macroporous Resins	8
1.2.3.3	Davankov Hypercross-linked Resins	8
1.2.4	Resins with Branched Molecular Architecture	9
1.3	Polymer Supports in Film and Monolithic Format	11
1.3.1	Thin Film Supports	11
1.3.2	Self-supporting Rods, Discs and Plugs	12
1.3.3	PolyHIPE-based Supports	13
1.3.4	Supported Monolithic Structures	15
1.4	Morphological Characterization of Polymer Supports	15
1.4.1	Solvent Imbibition	16
1.4.2	N <sub>2</sub> Sorption Porosimetry Involving Dry Supports	18
1.4.2.1	Adsorption/Desorption Mechanisms Isotherm Hysteresis Loops	20
1.4.2.2	Models for Calculation of Surface Area and Pore Sizes	20
1.4.2.3	Network and Pore Connectivity Effects	23
1.4.3	Hg Intrusion Porosimetry Involving Dry Supports	24
1.4.3.1	Theory	24
1.4.3.2	Comparison between Nitrogen Sorption and Mercury Intrusion	27

*Polymeric Materials in Organic Synthesis and Catalysis.*

Edited by Michael R. Buchmeiser

Copyright © 2003 WILEY-VCH Verlag GmbH & Co. KGaA, Weinheim

ISBN: 3-527-30630-7



1.4.4	Inverse Size Exclusion Chromatographic (ISEC) Analysis of Solvent Wetted Polymer Supports	29
1.4.5	Other Methods for Characterizing Porous Polymer Morphology	30
1.5	Analytical Techniques for Monitoring Polymer-supported Chemistry	31
1.5.1	Off-bead Analysis	32
1.5.1.1	Cleave-and-Characterize	32
1.5.1.2	Mass Spectrometry	33
1.5.1.3	Analytical Constructs	33
1.5.2	Destructive On-bead Analysis	34
1.5.2.1	Elemental Microanalysis	34
1.5.2.2	Color tests	34
1.5.3	Nondestructive On-bead Analysis	35
1.5.3.1	Mass Balance	35
1.5.3.2	Other Nondestructive Quantitation Methods	35
1.5.3.3	Infrared and Raman Spectroscopy	35
1.5.3.4	Nuclear Magnetic Resonance (NMR) Spectroscopy	41
1.5.4	Spatial Analysis of Resins	44
1.6	Challenges for the Future	46
1.7	References	46
<b>2</b>	<b>Supported Reagents and Scavengers in Multi-Step Organic Synthesis</b>	<b>53</b>
	<i>Ian R. Baxendale, R. Ian Storer and Steven V. Ley</i>	
2.1	Introduction	53
2.1.1	Solid-supported Synthesis and Solution – Solution Manipulation	53
2.1.2	Solid-supported Reagents and Catalysts	54
2.1.2.1	Supporting Materials	55
2.1.2.2	Facilitation of Work-up and Purification	56
2.1.2.3	Immobilization of Toxic and Malodorous Reagents	57
2.1.2.4	Microwaves as a Reliable Heating Method for Polymers	58
2.1.2.5	Effects of Site Isolation	59
2.1.2.6	Mutually Incompatible Reagents in the Same Reaction Compartment	60
2.1.3	Solid-supported Purification Processes	61
2.1.3.1	Supported Scavengers	61
2.1.3.2	Catch and Release	62
2.2	Multi-step Organic Transformations	63
2.2.1	The Early Developments of Polymer-supported Processes in Organic Synthesis	63
2.2.1.1	One Pot Multi-reagent Combinations	63
2.2.1.2	Sequential Multi-step Transformations	69
2.2.2	The Further Development of Scavenging Protocols	72
2.2.3	Immobilized Reagents and Scavenging Techniques in Library Synthesis	76

2.2.3.1	Incorporation of Solid-supported Scavengers into Library Synthesis	76
2.2.3.2	The Application of Immobilized Reagents and Scavengers to Library Synthesis	89
2.2.4	Natural Product Synthesis	116
2.3	Conclusion	131
2.4	References	132
<b>3</b>	<b>Organic Synthesis on Polymeric Supports</b>	<b>137</b>
	<i>Carmen Gil, Kerstin Knepper and Stefan Bräse</i>	
3.1	Introduction	137
3.2	Linkers for Organic Synthesis on Polymeric Supports	138
3.2.1	Linker Families	139
3.2.1.1	Benzyl-Type Linkers including Trityl and Benzhydryl Linkers	139
3.2.1.2	Allyl-Based Linkers	141
3.2.1.3	Ketal/Acetal-Based Linkers	141
3.2.1.4	Ester-, Amide- and Carbamate-Based Linkers	143
3.2.1.5	Silyl Linkers	144
3.2.1.6	Boronate Linkers	144
3.2.1.7	Sulfur-, Stannane- and Selenium-Based Linkers	144
3.2.1.8	Triazene-Based Linkers	149
3.2.1.9	Photocleavable Linkers	151
3.2.2	Linker Strategies	152
3.2.2.1	Safety Catch Linkers	152
3.2.2.2	Cyclative Cleavage (Cyclorelease Strategy)	155
3.2.2.3	Cleavage-Cyclization Cases	156
3.2.2.4	Fragmentation Strategies	156
3.2.2.5	Traceless Linkers	157
3.2.2.6	Multifunctional Cleavage	157
3.2.2.7	Linkers for Asymmetric Synthesis	159
3.2.3	Linkers for Functional Groups	162
3.3	Organic Transformations on Polymeric Supports	164
3.3.1	Oxidation and Reduction Reactions	164
3.3.2	C-C Bond Formation Reactions	165
3.3.2.1	Palladium-Catalyzed Reactions	166
3.3.2.2	Grignard and Similar Reactions	168
3.3.2.3	Michael Reactions and 1,2-Addition Reactions	168
3.3.2.4	Wittig and Horner – Wadsworth – Emmons Reactions	169
3.3.2.5	Alkene Metathesis	169
3.3.3	Cycloaddition Reactions	170
3.3.3.1	Diels-Alder Reactions	170
3.3.3.2	1,3-Dipolar Cycloaddition Reactions	171
3.3.4	Organometallic Chemistry on Polymeric Supports	171
3.3.5	Multicomponent Reactions	172
3.3.5.1	Grieco Reactions	172

3.3.5.2	Ugi Reactions	172
3.3.6	Mannich Reactions	173
3.3.6.1	Hantzsch Reactions	173
3.3.6.2	Biginelli Reactions	173
3.4	Targets for Synthesis on Polymeric Supports	174
3.4.1	Natural Products	174
3.4.1.1	Solid-phase Target-Oriented Total Synthesis of Natural Products	175
3.4.1.2	Combinatorial Derivatization for Immobilized Natural Product Skeletons and Combinatorial Semi-synthesis	176
3.4.1.3	Construction of Natural Product-Like Libraries	176
3.4.2	Adaptation of New Synthetic Methods for the Solid-phase Synthesis of Combinatorial Libraries	178
3.4.2.1	Heterocycles	178
3.5	Conclusion, Summary and Outlook	187
3.6	List of Abbreviations	187
3.7	References	189
<b>4</b>	<b>Solid-Phase Bound Catalysts: Properties and Applications</b>	<b>201</b>
	<i>Thomas Frenzel, Wladimir Solodenko and Andreas Kirschning</i>	
4.1	Introduction	201
4.2	The Solid Support	203
4.2.1	Polymer Supports	203
4.2.2	Inorganic Supports	207
4.2.3	Selected Examples for Attachment of Ligands to Solid Supports	208
4.3	Applications in Catalysis	211
4.3.1	Polymer Supported Oxidations	211
4.3.1.1	Oxidation of Alcohols	212
4.3.1.2	Epoxidation of Alkenes	213
4.3.1.3	Dihydroxylation and Aminohydroxylation of Alkenes	216
4.3.2	Lewis Acid-mediated Reactions	219
4.3.2.1	Addition Reactions to Carbonyl Compounds	219
4.3.2.2	Addition Reactions to Imines	221
4.3.2.3	Addition Reactions to Carbon–Carbon Double Bonds	222
4.3.2.4	Cycloaddition Reactions	223
4.3.2.5	Miscellaneous Applications	225
4.3.3	Transition Metal Catalysts	226
4.3.3.1	Palladium-catalyzed Coupling Reactions	227
4.3.3.2	Olefin Metathesis	229
4.3.3.3	Transition Metal-catalyzed Hydrogenation and Hydroformylation	229
4.3.4	Miscellaneous	232
4.4	Outlook	234
4.5	Acknowledgments	234
4.6	References	234

<b>5</b>	<b>Soluble Polymers as Catalyst and Reagent Platforms:</b>	
	<b>Liquid-Phase Methodologies</b>	241
	<i>Tobin J. Dickerson, Neal N. Reed and Kim D. Janda</i>	
5.1	Introduction	241
5.2	Overview of Soluble Polymers in Organic Synthesis	242
5.2.1	Properties of Soluble Polymeric Supports	242
5.2.2	Methods for Separating Polymers from Reaction Mixtures	243
5.2.3	Analytical Methods in Liquid-phase Synthesis	244
5.2.4	Listing of Polymers	245
5.2.4.1	Polyethylene Glycol (PEG)	245
5.2.4.2	Non-cross-linked Polystyrene	247
5.3	PEG-supported Catalysts	248
5.3.1	Hydrogenation Catalysts	248
5.3.2	Chinchona Alkaloid Ligands for the Sharpless AD Reaction	249
5.3.3	Phase-transfer Catalysts	251
5.3.4	Epoxidation Catalysts	253
5.3.5	Carbon – Carbon Bond-forming Catalysts	253
5.4	Soluble Polymer-supported Reagents	256
5.4.1	Phosphine Reagents	256
5.4.2	Oxidants	261
5.4.3	Reducing Agents	263
5.4.4	Microgel-supported Reagents	265
5.4.5	Miscellaneous Reagents	266
5.5	Conclusions	272
5.6	Acknowledgements	272
5.7	References	273
<b>6</b>	<b>Polymers for Micellar Catalysis</b>	277
	<i>Oskar Nuyken, Ralf Weberskirch, Thomas Kotre, Daniel Schönfelder and Alexander Wörndle</i>	
6.1	Introduction	277
6.2	Amphiphilic Block Copolymers for Micelle Formation	281
6.2.1	Transition Metal Catalysts Solubilized in Micellar Aggregates	281
6.2.2	Metal Colloids Stabilized in Micellar Aggregates	283
6.2.3	Catalysts Covalently Bound to the Amphiphilic Block Copolymer	286
6.2.3.1	Phosphine-Functionalized Amphiphiles for Rhodium-Catalyzed Hydrogenation	286
6.2.3.2	Triphenylphosphine-Functionalized Amphiphiles for Rhodium-Catalyzed Hydroformylation and Palladium-Catalyzed Heck Coupling Reaction	287
6.2.3.3	ATRP of Methyl Methacrylate in the Presence of an Amphiphilic, Polymeric Macroligand	291
6.3	Amphiphilic Polymers Forming Micelle Analogous Structures	294
6.3.1	Amphiphilic Star Polymers with a Hyperbranched Core	295
6.3.2	Polysoaps	298

6.4	Summary and Outlook	301
6.5	References	302
<b>7</b>	<b>Dendritic Polymers as High-Loading Supports for Organic Synthesis and Catalysis</b>	<b>305</b>
	<i>Rainer Haag and Sebastian Roller</i>	
7.1	Introduction	305
7.2	General Aspects of Dendritic Polymers and Solid-phase Hybrid Polymers	305
7.2.1	Special Properties of Soluble Dendritic Polymeric Supports	307
7.2.2	Methods for Separating Dendritic Polymer Supports from Reaction Mixtures	307
7.2.3	Dendritic Hybrid Polymers as High-Loading Solid-phase Supports	310
7.3	Dendritic Polymer-supported Organic Synthesis	312
7.3.1	Perfect Dendrimers as Supports in Organic Synthesis	312
7.3.2	Hyperbranched Polymeric Supports in Organic Synthesis	316
7.3.3	Other Soluble Multivalent Supports in Organic Synthesis	319
7.3.4	Dendronized Solid-phase Supports for Organic Synthesis	322
7.4	Dendritic Polymer-supported Reagents and Scavengers	328
7.5	Dendritic Polymers as High-Loading Supports for Catalysts	331
7.5.1	Dendritic Polymeric Supports in Homogeneous Catalysis	331
7.5.1.1	Selected Examples for Dendritic Polymer-supported Catalysis	332
7.5.2	Dendritic Polymeric Supports in Heterogeneous Catalysis	338
7.6	Conclusions	339
7.7	Acknowledgements	340
7.8	Abbreviations	341
7.9	References	342
<b>8</b>	<b>Metathesis-Based Polymers for Organic Synthesis and Catalysis</b>	<b>345</b>
	<i>Michael R. Buchmeiser</i>	
8.1	Introduction	345
8.2	Polymeric Catalytic Supports Prepared by ROMP	345
8.2.1	Precipitation Polymerization-based Techniques	345
8.2.2	Grafting Techniques	347
8.2.2.1	Grafted Supports for Heck Reactions	347
8.2.2.2	Grafted Supports for ATRP	349
8.2.2.3	Grafted Supports for Ring-closing Metathesis (RCM) and Related Reactions	350
8.2.2.4	Other Grafted Supports	351
8.2.3	Coating Techniques	351
8.2.3.1	Heck Supports Based on Coated Silica	351
8.2.3.2	ATRP Supports Based on Coated Silica	353
8.2.3.3	RCM Supports Based on Coated Silica	353
8.3	ROMPgels and Other Functional Metathesis-based Polymers	354
8.4	Monolithic Catalytic Supports	358

8.4.1	Basics and Concepts	358
8.4.2	Manufacture of Metathesis-based Monolithic Supports	359
8.4.3	Microstructure of Metathesis-based Rigid Rods	360
8.4.4	Functionalization, Metal Removal and Metal Content	361
8.4.5	Applications of Functionalized Metathesis-based Monoliths in Catalysis	364
8.4.5.1	Grafted Supports for Ring-closing Metathesis (RCM) and Related Reactions	364
8.4.5.2	Poly-(N,N-dipyrid-2-yl-7-oxanorborn-2-en-5-ylcarbamido·PdCl <sub>2</sub> )-grafted Monolithic Supports for Heck Reactions	366
8.4.5.3	Poly-(N,N-dipyrid-2-yl-7-oxanorborn-2-en-5-ylcarbamido·PdCl <sub>2</sub> )-coated Monolithic Supports for Heck Reactions	367
8.5	Conclusion, Summary and Outlook	367
8.6	Acknowledgement	368
8.7	References	368
<b>9</b>	<b>New Strategies in the Synthesis of Grafted Supports</b>	<b>371</b>
	<i>R. Jordan</i>	
9.1	Introduction and Scope	371
9.2	Self-assembled Monolayers	372
9.2.1	Two Dimensional Self-assembly	372
9.2.2	Self-assembled Monolayers of Alkanethiols	374
9.2.3	Self-assembled Monolayers of Silanes	376
9.2.4	Self-assembled Monolayers for Surface Engineering	378
9.2.5	Surface Reconstruction: A Dynamic View of Self-assembled Monolayer Systems	381
9.2.6	Self-assembled Monolayers of Rigid Mercaptobiphenyls	382
9.2.6.1	Self-Assembly of Dipoles	386
9.2.7	Patterned Self-assembled Monolayers	388
9.2.8	Self-assembled Monolayers as Tailored Functional Surfaces in Two and Three Dimensions	393
9.3	Polymers on Surfaces	397
9.3.1	Polymer Brushes by Surface-initiated Polymerizations	400
9.3.2	Surface-initiated Polymerization Using Free Radical Polymerization	406
9.3.3	Surface-initiated Polymerization Using Living Ionic Polymerization	413
9.3.3.1	Surface-initiated Polymerization Using Living Anionic Polymerization	414
9.3.3.2	Surface-initiated Polymerization Using Living Carbocationic Polymerization (LCSIP)	417
9.3.4	Surface-initiated Polymerization Using Controlled Radical Polymerization	423
9.3.5	Surface-initiated Polymerization by Miscellaneous Techniques	430
9.4	Summary and Outlook	433
9.5	References	434

<b>10</b>	<b>Biocatalyzed Reactions on Polymeric Supports: Enzyme-Labile Linker Groups</b>	<b>445</b>
	<i>Reinhard Reents, Duraiswamy Jeyaraj and Herbert Waldmann</i>	
10.1	Introduction	445
10.2	Endo-linkers	446
10.3	Exo-linkers	458
10.4	References	465
<b>11</b>	<b>Polymer-Supported Olefin Metathesis Catalysts for Organic and Combinatorial Synthesis</b>	<b>467</b>
	<i>Jason S. Kingsbury and Amir H. Hoveyda</i>	
11.1	Introduction	467
11.2	The First Polymer-supported Ru Catalyst for Olefin Metathesis	468
11.3	Homogeneous Catalysis through Heterogeneous Ru Carbenes	469
11.3.1	Recyclable Monomers Act through a 'Release/Return' Mechanism	469
11.3.2	The First Carbene-tethered Polymeric Catalyst	470
11.3.3	A Poly(ethylene glycol)-based Catalyst with Solvent-dependent Solubility	472
11.4	Dendrimers as Recyclable Metathesis Catalysts	475
11.4.1	Synthesis and Metathesis Activity of Ru-based Carbosilane Dendrimers	475
11.4.2	Evidence for Ru Release and Return During Olefin Metathesis	477
11.4.3	Dendrimer Microfiltration: A New but Underdeveloped Strategy for Catalyst Recovery	479
11.5	A Recent Approach to Permanent Immobilization of a Ru-based Catalyst	480
11.6	A PS-supported Ru Catalyst with Unsaturated N-Heterocyclic Carbene Ligation	482
11.7	A New Recyclable Catalyst Based on the Bidentate Styrene Ether	484
11.8	Alternative Solid Supports Expand the Scope of Existing Catalyst Systems	486
11.8.1	A Comparative Study of Three Poly-DVB-supported Ru Carbenes	486
11.8.2	A Wang-supported Styrene Ether Catalyst for Stereoselective Cross Metathesis	487
11.9	Easily Recyclable Ru Catalysts for Combinatorial Synthesis	489
11.10	The First Supported Chiral Metathesis Catalyst	493
11.11	Conclusions and Future Outlook	499
11.12	References	499

<b>12</b>	<b>Monitoring and Optimizing Organic Reactions Carried Out on Solid Support</b>	<b>503</b>
	<i>Bing Yan</i>	
12.1	Introduction	503
12.1.1	Quality of Combinatorial Libraries	503
12.1.2	Purification and the Chemical Yield of Synthesis	504
12.1.3	Methods for Monitoring the Reaction Completion	505
12.2	Non-chemical Factors Affecting the Completion of Solid-phase Reactions	507
12.2.1	Esterification Reaction Using Resin Beads of Various Sizes	507
12.2.2	Bromination Reaction on Resin Beads of Various Sizes	510
12.3	Monitoring the Reaction Completion	510
12.3.1	Reaction Completion Monitored by Single Bead FTIR	510
12.3.2	Reaction Completion Monitored by Combination of Methods	511
12.3.3	Pitfalls to Avoid in Reaction Monitoring	511
12.4	Monitoring the Cleavage Completion	516
12.4.1	Cleavage from Acid-labile Linker	516
12.4.1.1	TFA Cleavage of Resin-Bound Products	517
12.4.1.2	Comparison of TFA Cleavage Reactions	518
12.4.2	Cleavage from Marshall Linker	520
12.4.2.1	Cleavage of Resin-Bound Thiophenol Esters with <i>n</i> -Butylamine	520
12.4.2.2	Cleavage with 3,4-Dimethoxyphenethylamine	523
12.4.2.3	Cleavage with 1-Piperonylpiperazine	524
12.4.2.4	Effect of Temperature on Cleavage Reaction	524
12.4.2.5	Cleavage Rate after Linker Oxidation	524
12.5	Concluding Remarks	524
12.6	Acknowledgements	525
12.7	References	526
<b>13</b>	<b>Polymeric Membranes for Integrated Reaction and Separation</b>	<b>527</b>
	<i>J.T.F. Keurentjes</i>	
13.1	Introduction	527
13.2	Membrane Systems for Improved Chemical Synthesis	528
13.2.1	Efficient Catalyst Recycle	528
13.2.2	Pervaporation Membranes for Shifting Chemical Equilibrium	530
13.3	Membrane Bioreactors	536
13.3.1	Lactic Acid Production	537
13.3.2	Bioreactors for Environmental Applications	538
13.3.3	Enzyme Reactors	540
13.4	Concluding Remarks	544
13.5	References	545



## Preface

It was in December 2001, when Dr. Peter Göllitz called me and “encouraged” me to edit a book on recent relevant aspects of polymer chemistry in organic synthesis and catalysis. Facing the bitter cup of sorrow I accepted for four reasons.

First, I could not turn down Peter Göllitz’ suggestion. Second, the area of polymer science is a rapidly developing field that certainly deserved another book. Third, hardly any other discipline has had such a strong influence on almost all other areas of chemistry. And finally, though already introduced to both organic synthesis and catalysis in the 1960s, the most substantial improvements in these areas have been made during the last ten years. Therefore, I soon found myself contacting colleagues asking for contributions, tables of contents and manuscripts. Quite surprising, I received hardly any negative replies. This and the professional attitude of all contributors in terms of deadlines and quality of their manuscripts soon sweetened the cup.

As a result, it is now my pleasure to present this book. As can be deduced from its title, it was intended to cover the most relevant achievements of polymer chemistry in the areas of organic synthesis and catalysis. For this purpose, 30 authors have contributed to this venture in 13 chapters. The book commences with some general properties of cross-linked polymers relevant to the above-mentioned applications, then turns to polymer-bound reagents, scavengers, catalysts and reactions (including biocatalyzed reactions) that can be carried out. Special attention has been given to soluble polymers including dendritic polymers and micelles used in organic synthesis and catalysis as well as to the synthetic advancements in the preparation of these materials. Metathesis-based techniques have had an enormous impact, so two chapters covering both heterogeneous metathesis catalysts and metathesis-derived supports have been added. Finally, the on- and off-bead monitoring of reactions as well as technical aspects including those of high-throughput screening and the use of membranes are summarized.

Any edited book strongly depends on the quality of every single contribution. It was both my privilege and honor to win such well-known authors. With their contributions, I am convinced that we have now a book in hand that represents the state of the art and a comprehensive summary on the present status quo. It is designed to attract equally students and advanced readers working in the areas of organic chemistry, organometallic chemistry, catalysis, polymer science, physical

chemistry and technical chemistry by providing both substantial background information and interdisciplinary up-to-date knowledge. Special consideration has been given to the literature sections, which should facilitate further reading. Unfortunately, for economical and practical reasons, every book has to be limited to a certain number of pages. Therefore, few additional, interesting aspects had to be shortened or even neglected. Nevertheless, I am sure Peter Gölitz will find somebody else to write a book on these topics.

Finally, one thing remains to be done, that is to thank all those who have helped me in putting this book together: The contributing authors and Wiley-VCH, in particular Dr. Elke Westermann, for her support, encouraging e-mails and patience.

Innsbruck, Spring 2003

MICHAEL R. BUCHMEISER

## List of Contributors

Dr. IAN R. BAXENDALE  
Department of Chemistry  
University of Cambridge  
Lensfield Rd.  
Cambridge, CB2 1EW, UK

Prof. Dr. STEFAN BRÄSE  
Kekulé-Institut für  
Organische Chemie und Biochemie  
Rheinische Friedrich-Wilhelms-  
Universität Bonn  
Gerhard-Domagk-Str. 1  
D-53121 Bonn

Prof. Dr. MICHAEL R. BUCHMEISER  
Institut für Analytische Chemie  
und Radiochemie  
Universität Innsbruck  
Innrain 52a  
A-6020 Innsbruck

TOBIN J. DICKERSON  
Department of Chemistry and  
The Skaggs Institute for Chemical  
Biology  
The Scripps Research Institute  
10550 North Torrey Pines Rd.  
La Jolla, CA 92037

CARMEN GIL  
Kekulé-Institut für  
Organische Chemie und Biochemie  
Rheinische Friedrich-Wilhelms-  
Universität Bonn  
Gerhard-Domagk-Str. 1  
D-53121 Bonn

Dr. RAINER HAAG  
Freiburger Materialforschungszentrum  
und Institut für Makromolekulare  
Chemie  
Albert-Ludwigs-Universität Freiburg  
Stefan-Meier-Str. 21  
D-79104 Freiburg

Prof. Dr. AMIR H. HOVEYDA  
Department of Chemistry  
Merkert Chemistry Center  
Boston College  
Chestnut Hill MA 02467

Prof. Dr. KIM D. JANDA  
Department of Chemistry and  
The Skaggs Institute for Chemical  
Biology  
The Scripps Research Institute  
10550 North Torrey Pines Rd.  
La Jolla, CA 92037

DR. DURAISWAMY JEYARAJ  
MPI für Molekulare Physiologie  
Abteilung Chemische Biologie  
Otto-Hahn Str. 11  
D-44227 Dortmund

DR. RAINER JORDAN  
Lehrstuhl für Makromolekulare Stoffe  
TU München  
Lichtenbergstr. 4  
D-85747 Garching

Prof. Dr. KEURENTJES  
Chemical Engineering and Chemistry  
Process Development  
Eindhoven University of Technology  
NL-5600 MB Eindhoven

DR. JASON S. KINGSBURY  
Department of Chemistry  
Merkert Chemistry Center  
Boston College  
Chestnut Hill MA 02467

Prof. Dr. ANDREAS KIRSCHNING  
Institut für Organische Chemie  
der Universität Hannover  
Schneiderberg 1B  
D-30167 Hannover

KERSTIN KNEPPER  
Kekulé-Institut für  
Organische Chemie und Biochemie  
Rheinische Friedrich-Wilhelms-  
Universität Bonn  
Gerhard-Domagk-Str. 1  
D-53121 Bonn

Prof. Dr. J. T. F. KEURENTJES  
Process Development Group  
Eindhoven University of Technology  
P.O. Box 513  
NL-5600 MB Eindhoven

THOMAS KOTRE  
Lehrstuhl für Makromolekulare Stoffe  
TU München  
Lichtenbergstr. 4  
D-85747 Garching

Prof. Dr. STEVEN V. LEY  
Department of Chemistry  
University of Cambridge  
Lensfield Rd.  
Cambridge, CB2 1EW, UK

Y. DE MIGUEL  
Department of Chemistry  
King's College  
London, UK

Prof. Dr.-Ing. OSKAR NUYKEN  
Lehrstuhl für Makromolekulare Stoffe  
TU München  
Lichtenbergstr. 4  
D-85747 Garching

NEAL N. REED  
Department of Chemistry and  
The Skaggs Institute for Chemical  
Biology  
The Scripps Research Institute  
10550 North Torrey Pines Rd.  
La Jolla, CA 92037

DR. REINHARD REENTS  
MPI für Molekulare Physiologie  
Abteilung Chemische Biologie  
Otto-Hahn Str. 11  
D-44227 Dortmund

SEBASTIAN ROLLER  
Freiburger Materialforschungszentrum  
und Institut für Makromolekulare  
Chemie  
Albert-Ludwigs-Universität Freiburg  
Stefan-Meier-Str. 21  
D-79104 Freiburg

Prof. Dr. DAVID C. SHERRINGTON  
Department of Pure and Applied  
Chemistry  
University of Strathclyde  
Cathedral Street  
Glasgow UK

Dr. THOMAS ROHR  
Chemical Technology of Organic  
Materials  
Vienna University of Technology  
A-1010 Vienna

DANIEL SCHÖNFELDER  
Lehrstuhl für Makromolekulare Stoffe  
TU München  
Lichtenbergstr. 4  
D-85747 Garching

R. IAN STORER  
Department of Chemistry  
University of Cambridge  
Lensfield Rd.  
Cambridge, CB2 1EW, UK

Dr. RALF WEBERSKIRCH  
Lehrstuhl für Makromolekulare Stoffe  
TU München  
Lichtenbergstr. 4  
D-85747 Garching

Prof. Dr. HERBERT WALDMANN  
MPI für Molekulare Physiologie  
Abteilung Chemische Biologie  
Otto-Hahn Str. 11  
D-44227 Dortmund

ALEXANDER WÖRNDLE  
Lehrstuhl für Makromolekulare Stoffe  
TU München  
Lichtenbergstr. 4  
D-85747 Garching

DR. BING YAN  
ChemRx Division  
Discovery Partners International Inc.  
385 Oyster Point Blvd.  
South San Francisco, CA 94080

## 1

## Structure, Morphology, Physical Formats and Characterization of Polymer Supports

YOLANDA DE MIGUEL, THOMAS ROHR and DAVID C. SHERRINGTON

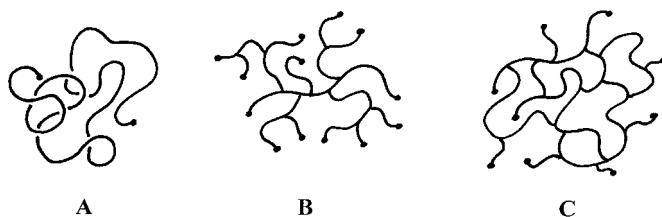
## 1.1

### Synthesis and Molecular Structure of Polymer Supports

The overwhelming majority of synthetic macromolecules used as supports are vinyl addition polymers. Styrene-based species are by far the most important of these, with methacrylate- and acrylamide-based systems finding more limited application. Styrene-based polymer supports have the major advantage of being relatively chemically inert and yet readily functionalized by powerful electrophiles. The ester and amide functions in methacrylate- and acrylamide-based polymer supports make these more susceptible to chemical degradation, and so more care is required in exploiting these species. Though these monomer types can be polymerized via a variety of mechanisms involving free radical [1, 2], cationic, anionic [3] and dipolar [4] reactive intermediates, in practice most polymers destined for use as supports are produced by a free radical polymerization process.

Vinyl polymers can be synthesized as linear macromolecules (Fig. 1.1a) which will dissolve to form isotropic solutions in a suitable solvent. They can also be produced in a highly branched form (Fig. 1.1b) and again these macromolecules are completely soluble in appropriate solvents. Linear polymers and branched or dendritic polymers can be used as supports and these species form the subject of other chapters in this book. If however a vinyl monomer is copolymerized with a divinyl monomer then an infinite cross-linked network (Fig. 1.1c) results, and though these macromolecular species will swell in a thermodynamically compatible solvent, their molecular weight is effectively infinite and this prevents their dissolution to form isotropic solutions. Instead the solvent swollen material appears as a highly flexible gel when low levels of cross-linking comonomer are used or indeed a relatively rigid one when high levels of cross-linker are employed. However, if the individual particles of the cross-linked species are small enough they will disperse in a suitable solvent and may superficially appear to dissolve, while in practice they will be present as microgel.

This chapter will focus exclusively on cross-linked vinyl polymer supports either in a spherical bead or resin form, or in some other macroscopic format. These essentially insoluble materials lead to considerably simplified reaction work-up and product isolation procedures when used e.g. in solid phase synthesis or as catalyst or



**Fig. 1.1** Synthetic macromolecular architectures A) linear B) branched C) cross-linked.

scavenger supports. They are also readily adaptable to continuous flow technologies and robotic instrumentation, and not surprisingly have become the work-horse of many combinatorial and parallel synthetic and screening procedures. Further details are available in extensive reviews [5, 6] and in a number of textbooks [7–12].

## 1.2

### **Suspension Polymerized Particulate Resin Supports – Structural and Morphological Variants**

#### 1.2.1

##### **Suspension Polymerization**

Since cross-linked polymers cannot be re-formed or re-shaped it is necessary to synthesize them in the final physical form appropriate for each particular application. Particles in the size range  $\sim 50\text{--}1000\ \mu\text{m}$  are suitable for laboratory scale chemistry, while larger particles have advantages in large scale continuous processes. Irregularly shaped particles are susceptible to mechanical attrition and breakdown to ‘fines’, whereas the process of suspension polymerization [13] yields uniform spherical cross-linked polymer particles often referred to as beads, pearls or resins. These are much more mechanically robust and are widely exploited on both a small and large scale e.g. as the basis of ion exchange resins [14].

Particles of a suitable size and symmetry (Fig. 1.2) are readily prepared by suspension polymerization in which the organic monomer phase containing dissolved free radical initiator is dispersed as droplets in a continuous aqueous phase. The latter usually contains a water-soluble polymer (e.g. polyvinyl alcohol or a polysaccharide) to aid stabilization of the monomer droplets, and the whole system is efficiently stirred. Polymerization is initiated by raising the temperature typically to  $\sim 70^\circ\text{C}$  and maintaining this for  $\sim 6$  hours. The spherical monomer droplets are converted to solid spherical polymer resin beads. In the laboratory the batch reaction can be performed in a round-bottomed flask, but it is better to use a baffled parallel sided reactor with a flattish base typically 0.5–2 liter in volume. More details are available in Ref. [15]. This technology is also practiced widely on an industrial scale where the reactor size is larger and can yield 100s kg of resin in one batch. The major challenge in suspension polymerization is to

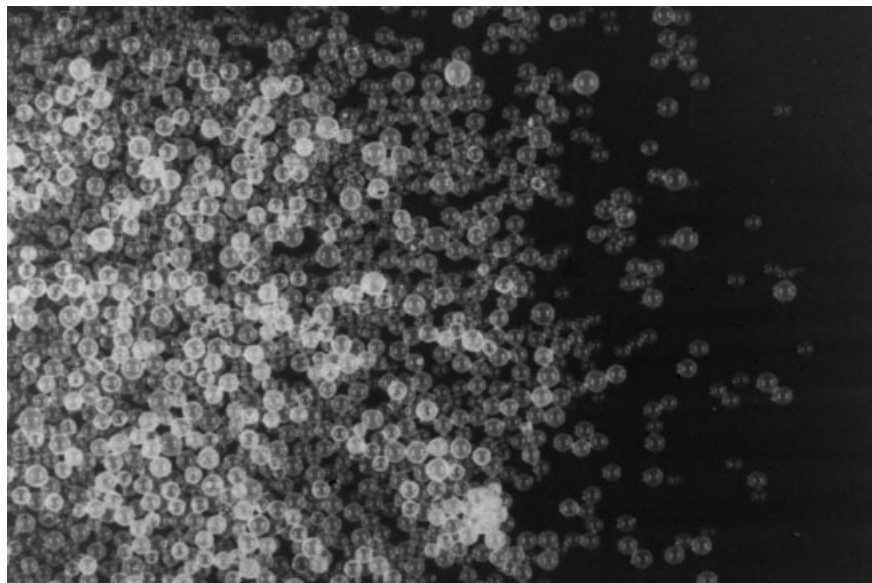


Fig. 1.2 Optical micrograph of suspension polymerized resin beads  $\sim 200\ \mu\text{m}$  diameter.

avoid agglomeration of the polymerizing droplets, and since aggregation arises from surface interactions, perhaps somewhat counter-intuitively, small scale suspension reactions are more problematical than large ones. Recently however the use of a small scale oscillatory baffled reactor (Fig. 1.3) has been described allowing efficient suspension polymerization on a gram scale [16].

### 1.2.2

#### Resin Morphology

So-called **gel-type** resins are prepared from a vinyl monomer typically in the presence of a low level ( $\leq 5\ \text{mol}\%$ ) of a divinyl cross-linking comonomer and no other component other than the free radical initiator. Such materials (shown in Fig. 1.4, left) are hard and glassy in the solid state with a surface area  $\leq 5\ \text{m}^2\text{g}^{-1}$  (measured by e.g.  $\text{N}_2$  sorption and application of the BET equation see Section 1.4.2). However, these species can swell readily in a thermodynamically good solvent to provide access to essentially all the segments of the polymer network e.g. to carry out chemical derivatization. The negative aspect of these resins, however, is that they are relatively impenetrable in the dry state and in contact with thermodynamically poor solvents. Their use is therefore restricted to processes involving swelling solvents. Despite this 1–2% cross-linked poly(styrene-divinylbenzene) (PS-DVB) gel-type resins are the supports most used in solid phase synthesis applications.

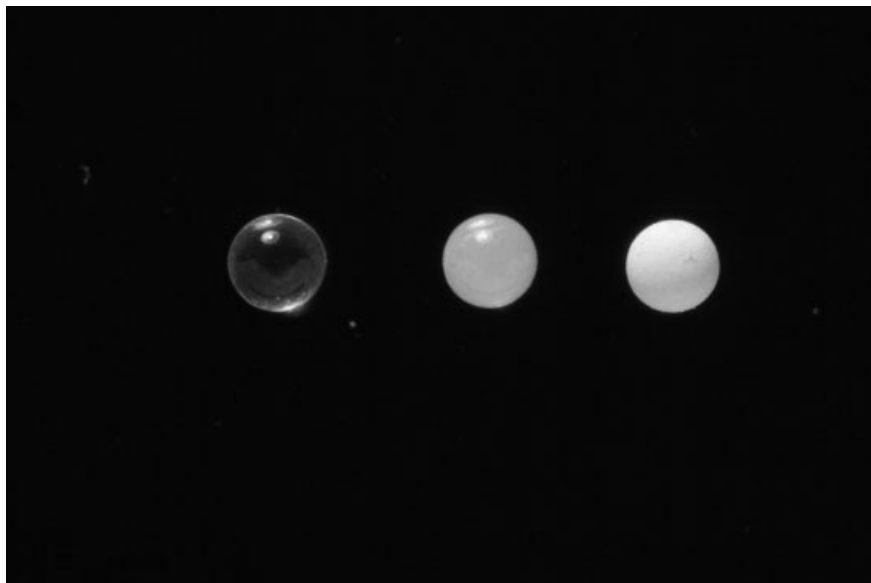
So-called **macroporous resins** (shown in Fig. 1.4, right) are prepared from a vinyl monomer typically in the presence of higher levels of a divinyl cross-linking





**Fig. 1.3** Small scale oscillatory baffled reactor (OBR) for gram scale suspension polymerization.

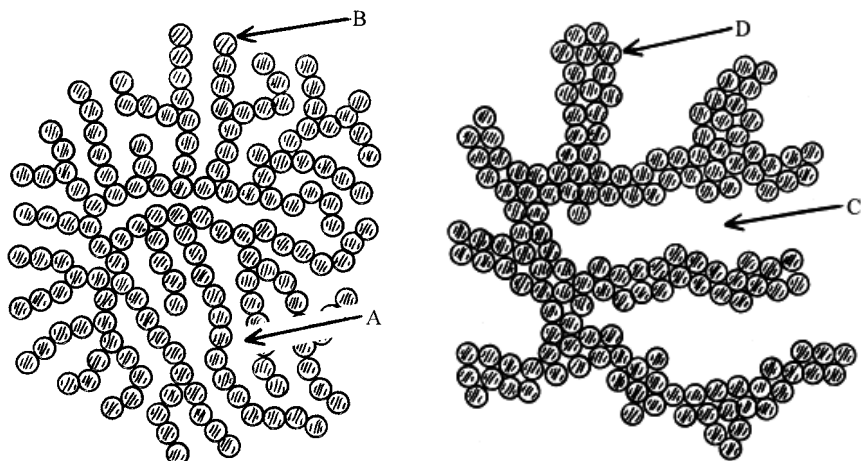
comonomer (from  $\sim 10$ – $80$  mol%). The term ‘macroporous’ is an old one which in the present context means permanently porous; it is *not* an indication of pore size. The permanently porous morphology of these species is generated by inducing the growing polymer network to phase separate or precipitate during the suspension polymerization. This is achieved by using a porogen in the polymerizing mixture, typically present in an equal volume to that of the comonomers. The porogen is more often than not a simple organic solvent, chosen to form an isotropic solution with the comonomers but to cause precipitation of the copolymer at some desired point in the polymerization. When the network does phase separate, microgel particles typically  $\sim 100$  nm in diameter form and these aggregate within each polymerizing droplet to form a discrete polymer phase, separate from



**Fig. 1.4** Optical micrograph of resin bead morphological types: left, gel-type; right, macroporous; center, mixed morphology;  $\sim 200 \mu\text{m}$  diameter.

the liquid porogen phase. At the end of the polymerization when the porogen is removed, e.g. vacuum drying, the pore structure is revealed. In effect the porogen acts a template for formation of the pores. A wide variety of morphological variants can be prepared using this technique and more details are available in Refs [17–20].

In general macroporous resins tend to have a wide pore size distribution stretching from the microporous region ( $\leq 2 \text{ nm}$ ), through the mesoporous region (2–50 nm) and into the macroporous ( $> 50 \text{ nm}$ ) regime (IUPAC nomenclature [21]). It is possible however to design resins with on the one hand a large micropore contribution, yielding a high dry state surface area (say  $\sim 500 \text{ m}^2\text{g}^{-1}$ ), and on the other a large macropore contribution, yielding a rather low dry state surface area (say  $\sim 50 \text{ m}^2\text{g}^{-1}$ ). Sections 1.4.2 and 1.4.3 describe the physical characterization of these materials. A large population of micropores and high surface area can be achieved by delaying the phase separation process in the polymerization until a high conversion of comonomers into polymer has been achieved. This is possible by choosing a porogenic solvent which is relatively thermodynamically compatible with the polymer matrix (e.g. toluene or xylene in the case of PS-DVB) and simultaneously using a relatively high level of cross-linking comonomer (typically  $\geq 50 \text{ mol}\%$ ). The late precipitation of polymer means that the microgel particles that form substantially retain their individuality. The residual monomers in the porogen phase continue to polymerize and weld the microgel particles together, but there is not excessive in-filling of the fine porous texture and no significant loss of micropore



**Fig. 1.5** Connectivity of microgel particles within macroporous resin beads showing formation of small pores, A, from a network of

interconnecting individual microgel particles, B, and large pores, C, from a network of fused or aggregated microgel particles, D.

volume (Fig. 1.5, left). The high level of cross-linker however serves to produce a mechanically strong network of microgel particles. Conversely a large population of macropores and low surface area can be achieved by arranging for the phase separation process in the polymerization to occur at relatively low conversion of the comonomers into polymer. This is possible by choosing a porogenic solvent which is relatively thermodynamically incompatible with the polymer matrix (e.g. alcohols or aliphatic hydrocarbons in the case of PS-DVB), and simultaneously using a relatively low level of cross-linking comonomer (typically 10–20 mol%). The early precipitation of polymer means that the microgel particles that form gradually fuse, and then become extensively welded and in-filled by the formation of large levels of polymer in the period following the point of phase separation. In extreme cases the microgel particles may all but disappear and be replaced by much bigger poorly defined aggregates (Fig. 1.5, right). At the same time much of the micropore structure is lost and is replaced by macroporous voids between the large aggregates.

Between these two extreme morphologies many possibilities exist, and bearing in mind that the solvation quality of a given porogenic solvent will be very sensitive to the chemical nature of any comonomers used in the polymerization, designing the porous morphology of a functional resin can be difficult. Almost inevitably some preliminary synthesis and screening is necessary to provide a composition/morphology relationship upon which to base the design of a particular targeted pore structure.

## 1.2.3

**Novel Morphologies****1.2.3.1 Solvent Expanded Gel-type Resins**

Typically lightly cross-linked gel-type resins are prepared in the absence of any solvent or porogen. However it is possible to include relatively large volumes of thermodynamically compatible solvent in the polymerization without inducing any phase separation at the low levels of cross-linker used in gel-type resin synthesis. As a result the final product is a swollen gel-type resin or 'solvent expanded' gel-type. Interestingly resins of this type are reported from time to time in the literature [22] and it seems that the researchers involved are unaware of the nature of the morphological variants they are producing. The potential advantage of these species is that for a given cross-link ratio they can provide higher levels of swelling than a resin with the same cross-link ratio prepared in the absence of solvent. This is illustrated by the data in Tab. 1.1 for resins prepared from styrene/divinylbenzene/vinylbenzyl chloride [23]. In the case of resins R1–R5 where the DVB content is increased from 0.5 to 5.0 wt% the resins progress from being rather physically fragile to mechanically much more robust. However, the swelling in toluene declines from 13.1 to 2.4 ml g<sup>-1</sup>. With resins R6–R8 (with comparable vinylbenzyl chloride (VBC) content to the earlier group) each has a DVB content of 5 wt% but were prepared with progressively larger levels of toluene present. While 33 vol% toluene has virtually no effect on the resin swelling, at 66 vol% toluene the subsequent resin swelling, 6.4 ml g<sup>-1</sup> also in toluene, lies somewhere between that of conventional 1 and 2 wt% DVB gel-types. Since R8 has a DVB content of 5 wt% it is more mechanically robust. Clearly such materials offer the prospect of optimizing both of these important properties simultaneously and they seem well worthy of further evaluation in specific applications.

**Tab. 1.1** Comparison of chloromethylated styrenic gel-type resins and solvent expanded analogs.

Resin Code	Comonomer mixture (wt%)			Toluene in comonomer phase (vol %)	Resin product	
	St	DVB	VBC		–CH <sub>2</sub> Cl content (mmol g <sup>-1</sup> )	Swelling capacity in toluene
R1	87.5	0.5	12	–	0.80	13.1
R2	87.0	1.0	12	–	0.88	8.7
R3	86.0	2.0	12	–	0.84	5.3
R4	85.0	3.0	12	–	0.73	3.3
R5	83.0	5.0	12	–	0.96	2.4
R6	85.0	5.0	10	33	0.55	2.3
R7	85.0	5.0	10	50	0.64	3.3
R8	85.0	5.0	10	66	0.63	6.4

St = styrene; DVB = divinylbenzene; VBC = vinylbenzylchloride.

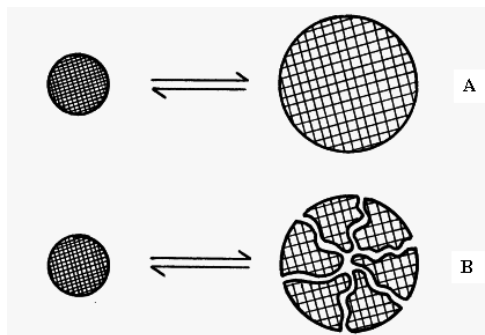
### 1.2.3.2 Collapsible Macroporous Resins

A second group of resins with a novel morphology are the ‘collapsible’ macroporous species. Typically a low surface area PS-DVB resin with rather large pores would be prepared with  $\sim 12$  wt% cross-linker and a thermodynamically poor porogen as described above. However in the case of styrene-divinylbenzene a series of resins with decreasing levels of cross-linker  $10 \rightarrow 1$  wt% each prepared with the poor porogen 2-ethylhexan-1-ol afford products which when dried from toluene or dichloromethane form clear glassy resins with no dry state surface area. Superficially these are therefore very like gel-types. However, when dried from acetone, methanol or  $\text{scCO}_2$  they exhibit dry state surface area typical of a macroporous resin prepared using the same porogen. In fact these species are also macroporous; however, at the lower levels of cross-linker the porous state cannot be maintained when dried from a highly solvating solvent and the porous structure folds or collapses slowly and reversibly.

Addition of good solvent to the dried resin re-establishes the porous structure (Fig. 1.6) [24]. When such resins are dried from a thermodynamically poor solvent the precipitated network is sufficiently rigid to resist folding and at least some of the pore structure and hence surface area is retained in the dry state. The potential advantage of this hybrid morphology is that the macroporous structure allows rapid ingress and egress of molecules to and from the core of the resin particle; however, the level of cross-linking in the polymer phase can be as low as  $\sim 2$  wt% and so the mass transfer limitation (into the polymer phase) often exhibited by conventional macroporous resins is minimized. These novel species therefore also seem well worthy of further evaluation in specific applications.

### 1.2.3.3 Davankov Hypercross-linked Resins

A third group of resins with an unusual morphology are the hypercross-linked species introduced by Davankov and his group some years ago now [25, 26]. For many years these species were not widely appreciated as having unique morphological characteristics, although today technological exploitation of these is under way [27]. In perhaps the most interesting form of these resins a conventional



**Fig. 1.6** Schematic representation of swelling/deswelling of A) a gel-type resin; B) a collapsible macroporous resin.

styrene-divinylbenzene lightly cross-linked gel-type resin is exhaustively cross-linked in a post-polymerization chemical modification involving a bis-alkylating agent generated in situ from e.g. *a,a'*-dichloro-*p*-xylene (*p*-xylylenedichloride) and a Lewis acid such as FeCl<sub>3</sub> or AlCl<sub>3</sub>. This procedure is often termed 'secondary' cross-linking. The reaction is carried out in a swelling solvent such as 1,2-dichloroethane and sufficient secondary bridging (cross-linking) components are employed to ensure on average alkylation of all aromatic groups. In practice careful quantitative solid state single pulse excitation (SPE) magic angle spinning (MAS) <sup>13</sup>C NMR (nuclear magnetic resonance) analysis of solid resins has shown that typically the level of secondary cross-links introduced is so high that a large fraction of aromatic groups must be bridged twice [28]. The whole network must therefore be extremely rigid and this seems to be the source of the unusual properties of these materials. Once the reaction solvent is removed, along with catalyst fragments and other residues, the dry resins display a surface area, calculated from N<sub>2</sub> sorption data, typically up to 1000 m<sup>2</sup>g<sup>-1</sup>. In fact the network is highly microporous. Even more strangely the essentially hydrophobic system readily sorbs water as well as all other solvents and so these resins are quite different to other styrene-divinylbenzene based systems. The explanation for this remains tentative, but it seems that removal of the reaction solvent causes some shrinkage of the matrix and the introduction of considerable strain. The latter is relieved even on wetting with water and this is the driving force for imbibition of the latter. With such very high surface areas and dense micropore network there is interest in these materials as efficient and high capacity sorbents. In addition its use as a catalyst support has recently been reported [29].

#### 1.2.4

##### Resins with Branched Molecular Architecture

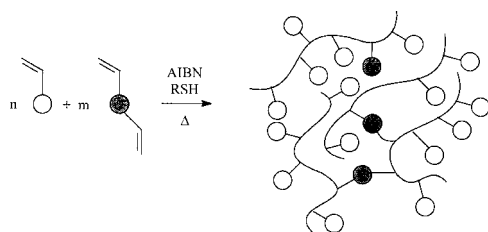
Interestingly, almost certainly the first premeditated synthesis of branched resins was by Professor Bruce Merrifield although he did not publish this in the open literature. The grafting of linear polystyrene chains via living anionic polymerization onto a styrene-divinylbenzene resin is however recorded in his biography [30]. A similar grafting of poly(*N,N*-dimethylacrylamide) chains onto polyethylene and polypropylene particles was reported by Sherrington *et al.* [31]. In both of these works the objective was develop chemical functionality with good accessibility. Perhaps the first important branched architecture in a resin, however, is that reported by Bayer and Rapp [32–34] although their primary motivation was to generate a resin with good swelling characteristics in a broad range of solvents including water. To this end a 1–2% cross-linked styrene resin was grafted with long poly(ethylene glycol) (PEG) sidechains or 'tentacles' in order to improve compatibility with protic solvents and also to provide high flexibility and accessibility to the terminal functional groups. This so-called 'Rapp resin' or TentaGel<sup>®</sup> produced by Rapp Polymere (Tubingen, Germany) has become a benchmark resin for solid phase peptide and other solid phase synthesis despite related materials being made available from time to time. More details are available in Ref. [34]. An im-

provement introduced by Argonaut Technologies Inc. (San Carlos, USA) [35] involves a bifurcated PEG chain which increases the capacity available and effectively increases the level of branching.

Developing a branched architecture on a resin therefore offers the potential for increasing the loading of a functional group, particularly the loading of groups on or near chain ends, and also might improve accessibility to such groups. Dendrimers of course provide highly branched architectures and not surprisingly these species are now being examined as supports in their own right [36], and indeed this subject is dealt with in another chapter in this book. The attachment of a suitable dendrimer wedge to a pre-formed resin is an attractive method of achieving improved loading and a number of groups have reported this approach [37–41]. It is important to realize, however, that building large (additional) structures within a resin can be costly and might actually **reduce** the loading of a functional group in terms of mmole **per gram** if the mass of the structure introduced overcomes the increase in functional group content. An increase in mass transfer limitation may also be observed. The parameter that is unambiguously improved is the functional group content **per bead**, and of course this can be an important parameter in some applications e.g. screening technologies.

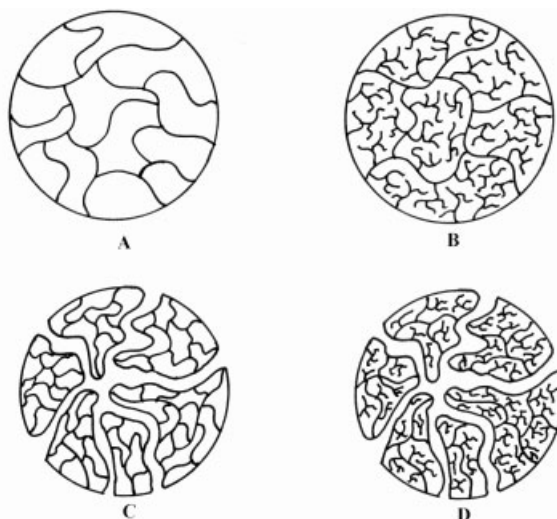
Recently a novel generic method for synthesizing branched vinyl polymers (and potentially other chain growth species) was reported [42, 43]. In this a conventional free radical polymerization of a vinyl monomer with a divinyl comonomer is carried out, but the formation of a cross-linked network and associated gelation is inhibited by use of appropriate levels of a chain transfer agent such as a thiol (Fig. 1.7). This methodology offers the prospect of synthesizing a wide range of branched polymers easily and cheaply from routinely available starting materials in a process that can be readily scaled. The same researchers have now reported that restricting the level of chain transfer agent allows a branched polymer to be synthesized but which overall is cross-linked. Carrying out such polymerizations of styrene and divinylbenzene in aqueous suspension they have produced highly branched gel-type and similarly branched macroporous resins [44] (Fig. 1.8).

Most importantly the procedure is a facile one-pot method. The branching in this instance is an integral part of the resin architecture and a large proportion of chain ends is provided without resort to decorating an existing conventional resin. Functional analogues of these seem likely to form the basis of supported species with improved mass transfer characteristics.



**Fig. 1.7** Synthesis of branched vinyl polymer using a divinyl comonomer and balancing level of thiol-free radical transfer agent – the Cross-linker/Transfer Method (CTM).

**Fig. 1.8** Schematic representation of A) gel-type, B) branched gel-type, C) macroporous and D) branched macroporous resins.



### 1.3

#### Polymer Supports in Film and Monolithic Format

##### 1.3.1

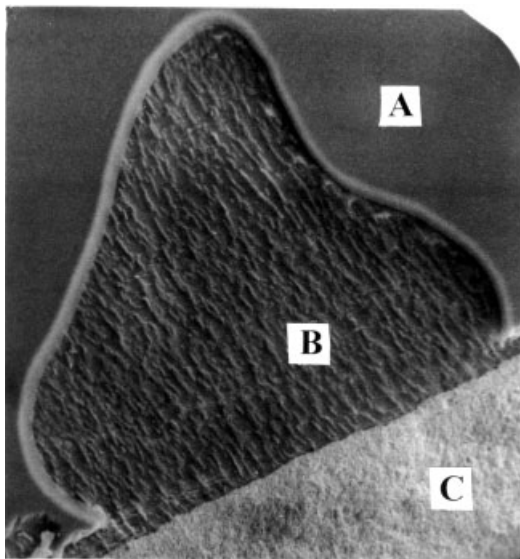
##### Thin Film Supports

Although resin beads have proved to be very useful and successful supports there are disadvantages associated with these. For example manipulating beads robotically is not straightforward and hence various 'tea-bag' [45] or 'kan' technologies [46, 47] have evolved. In addition the particulate nature of beads can exacerbate the problems of spectroscopic analysis by encouraging the scattering of probe light beams. These problems can be reduced by using larger supports that can be more readily manipulated by hand or with a robot although use of these formats is also not routine, not the least because of lack of a convenient source of supply.

The various morphological variants available in bead form can be replicated in thin films ( $\sim 2\text{ cm} \times 8\text{ cm} \times 50\text{--}100\text{ }\mu\text{m}$ ) produced simply by photo-initiated free radical polymerization of comonomer mixtures introduced by capillary action into an appropriate mold formed with microscope slides [48]. With appropriate choice of comonomers, and porogen in the case of macroporous films, reasonably mechanically robust self-supporting films can be removed from the mold for further exploitation (Fig. 1.9).

While such a film format is not intended for routine use in e.g. solid phase synthesis, it has proved useful for spectroscopic mechanistic investigation of polymer-supported metal complex catalysts [49] and we, with our collaborators, are employing such films as a component in nanosecond fluorescence sensing devices [50].





**Fig. 1.9** Scanning electron micrograph ( $\times 750$ ) of a macroporous film showing: A, superficially smooth surface originally in contact with glass slide; B, surface layer cleaved away (serendipitously) to show rough porous interior; C) rough porous interior, edge view (bar =  $10\ \mu\text{m}$ ).

### 1.3.2

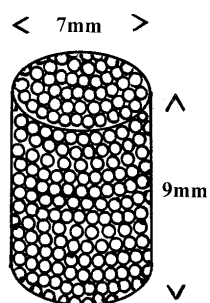
#### Self-supporting Rods, Discs and Plugs

The synthesis of self-supporting monolithic cylindrical rods ( $\sim 1\text{ cm} \times 10\text{ cm}$ ) again with compositions and morphologies similar to resins has been reported [51]. These can also be prepared with a texture that allows each rod to be cleaved into discs. ( $\sim 1\text{ cm} \times 0.2\text{ cm}$ , mass 250–500 mg) (Fig. 1.10). The latter can be handled by a robot arm and solid phase synthesis on one disc allows up to  $\sim 0.5\text{ mmole}$  of a single compound to be produced. Similar disc and alternative shaped macroscopic supports have now been reported [52–54].



**Fig. 1.10** Optical micrograph of cross-linked polymethacrylate-based discs ( $\sim 10\text{ mm} \times 2\text{ mm}$ ); left hand sample swollen in xylene.

Fig. 1.11 Schematic representation of Polymer Laboratories StratoSphere Plugs™ ( $\sim 7\text{ mm} \times 10\text{ mm}$ ).



One of the problems with larger self-supporting monoliths is that often the pore volume is restricted in order to provide sufficient mass for the monolith to be mechanically robust. This is not the case, for example, where the monolith is formed within a supporting structure e.g. a chromatographic or other column. The consequence of the limited pore volume is that mass transfer to the inner parts of the self-supporting monolith can be severely restricted. In the case of a disc upon which a solid phase synthesis was carried out the physical appearance of the support changed significantly during one step in the synthesis. Incomplete reaction in the inner slice of the disc was visually obvious with the disc appearing as a sandwich. The author has referred to this as the 'Big Mac' effect [51].

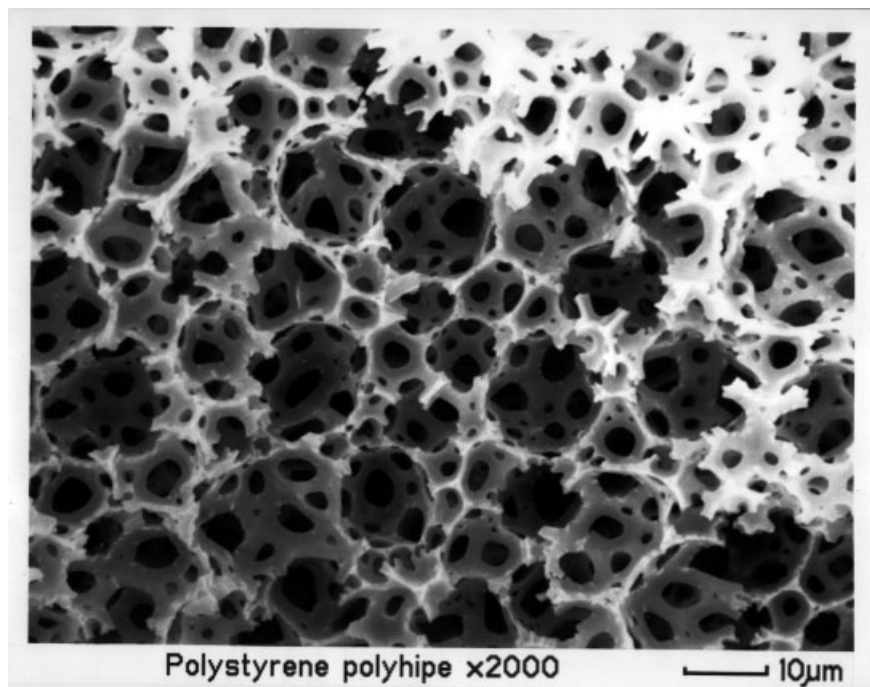
Recently this problem has been circumvented by the synthesis of so-called 'plugs' which are in effect conventional resins that have been sintered and melt fused with a polyalkene (Fig. 1.11) [55]. Each cylindrical 'plug' is  $\sim 7\text{ mm} \times 10\text{ mm}$  and the level of polyalkene employed is low enough for much of the interstitial space between the resin beads to be retained hence providing ready access by solvent and reagents to the core of the plug.

In principle any pre-functionalized resin can be formed into a plug and the monoliths show good solvent resistance except to e.g. hot toluene or xylene. The size of each plug makes them easily manipulated by a robot and use in scavenging situations seems very attractive. Some applications have already been reported [56] and the monoliths will be made available as StratoSphere Plugs™ via Polymer Laboratories (Church Stretton, UK).

### 1.3.3

#### PolyHIPE-based Supports

A high internal phase liquid-liquid emulsion (HIPE) is one where the internal or dispersed phase droplets occupy  $>74\%$  of the total volume of the emulsion. At this point the droplets contact each other and beyond this volume % the droplets are forced into distorted polyhedra. If for example styrene and divinylbenzene are employed as the continuous phase and water droplets dispersed in this oil phase using a suitable surfactant to form a HIPE, the comonomers can be polymerized to form a poly(styrene-divinylbenzene) polyHIPE. Typically the water droplets are



**Fig. 1.12** Scanning electron micrograph of poly(styrene-divinylbenzene) polyHIPE ( $\times 2000$ , bar =  $10\ \mu\text{m}$ ).

$\sim 5\text{--}10\ \mu\text{m}$  in diameter and if the aqueous phase volume is large enough the ‘walls’ of polymer between the aqueous droplets become so thin that holes form between the water droplets. The resulting system is therefore open cell, and all the water can be removed e.g. in a vacuum oven. The final monolith is a material of very low bulk density  $\sim 0.1\ \text{g ml}^{-1}$  as a result of the large volume of water in the original emulsion, and the total pore or cell volume is correspondingly very high (Fig. 1.12). Although closely related materials were reported earlier, Unilever scientists described this particular form in 1982 [57].

The basic poly(styrene-divinylbenzene) polyHIPE can be chemically modified in the same manner as a resin, and other monomer-based species can be prepared. More details are available in references [58, 59]. The granular and monolithic materials have been investigated in many applications including chemical ones, e.g. as a solid phase synthesis support [60], as a catalyst support [61, 62] and as a scavenger [63], where the monolithic form in particular has attracted attention. High surface area analogs have also been synthesized and characterized [64, 65]. While the unique morphology of polyHIPE materials has made them an intense subject of research effort, in practice the specific combination of their physical characteristics coupled with the rather inconvenient method of synthesis, and resulting costs relative to other not too dissimilar materials, has made it difficult to find a

suitable technology niche. Early efforts focused on rather high volume/low unit cost possibilities, but recently greater effort has been made to find more value-added outlets. Overall the high pore (cell) volume and potentially low activity/capacity of any functional derivative per unit volume (as opposed to unit mass) has to be given major consideration, and these two parameters taken together preclude use in many reactive and separative processes. Nevertheless, appropriate examples of the latter in particular seem to offer one of the best opportunities. Since the cell size and pore volume is also compatible with biological cell growth within a polyHIPE it is not surprising that biological and medical applications are now receiving serious evaluation [66]. (**Note:** involvement of cell biologists means that the terms ‘voids’ and ‘void volume’ are now preferred to ‘cells’ and ‘cell volume’ in referring to polyHIPE morphology).

#### 1.3.4

#### **Supported Monolithic Structures**

This chapter has focused on porous polymer supports all of which are self-standing i.e. particles, rods, discs, plugs and larger monoliths. This requirement means that the procedure for synthesizing the support species must not only generate the required porous morphology, but it must also provide the final support with sufficient mechanical stability (to shear, compression, elongation etc) for it to find successful exploitation. Many of the porous materials described here might also be formed within some scaffold or supporting device e.g. a chromatography or capillary electrophoresis column, or could be reinforced using e.g. a heat-shrink wrap-around. Once protected from excess mechanical stress in this way then significant opportunity exists for broadening the morphological range of support materials e.g. increasing pore size, pore volume etc. This area is currently attracting a great deal of intensive research, and the active topics parallel closely those of interest with conventional supports. For further information readers are directed to a research review textbook currently in preparation edited by Svev, Deyl and Tennikova [67].

### 1.4

#### **Morphological Characterization of Polymer Supports**

The enormous practical advantages provided by polymer supports in synthesis and screening methodologies has encouraged their widespread use by scientists who wish to use the support simply as a ‘black-box’ convenience. Many of these practitioners have no expertise, desire nor requirement to understand the detail make-up of the ‘black box’ but are content to exploit its advantages. Others however have a need to optimize problematical systems, and yet others have to design and develop novel systems. For the latter groups an understanding of polymer support morphology and an appreciation of the methods of revealing the morphological characteristics are essential. In the present context morphology refers to

the nano- and microscopic structure of the dry support at dimensions above the molecular structural level. This translates into physical parameters such as surface area, pore volume, average pore size and pore size distribution, and where possible an understanding of how these change, if indeed they do, in the working state of the polymer, i.e. typically when wetted by a solvent. Unfortunately there is no single physical technique which allows evaluation of the above parameters across all the required dimensional ranges, and applicable to all states (dry, wetted, hot, cold, low/high pressure etc.) in which a support might be used. There are however some key techniques which are very widely exploited. These almost inevitably involve some physical measurement, followed by the application of some theoretical model, and finally some mathematical manipulation which is associated with the model. How real are the parameters such as surface area etc., is therefore debatable, but providing consistent models and calculations are employed then at the very least the data have relative significance. Some of the important techniques that are widely employed are described here.

#### 1.4.1

##### **Solvent Imbibition**

A very valuable indication of the porous nature of a polymer support can be deduced from observations of solvent imbibition or uptake. Furthermore such measurements can be reasonably quantitative. It is, however, important to understand the possible processes that can occur when a polymer is contacted with a solvent otherwise the data obtained can be misleading or misinterpreted.

Two major processes must be distinguished. Firstly swelling occurs when a solvent interacts with entangled polymer chains, initially in the solid state, and gradually and progressively solvates the chains. If the solvent is highly compatible with the polymer then significant expansion of the polymer coils will take place, and in due course linear polymer coils will fully dissolve and migrate apart. If the polymer is cross-linked, however, the polymer matrix will expand to thermodynamic equilibrium forming an isotropically solvated polymer gel. This process is true swelling and can be measured as a volume increase of a known mass of dry resin if the volume increase is sufficiently large say  $\geq 10\%$ . Typically this can be carried out using a small measuring cylinder to record the volume increase of a pre-weighed sample of resin [68]. To ensure full expansion the sample should be left in contact with the resin for 24 hours and any trapped air bubbles removed by gentle agitation with a spatula before recording the final volume. The experimental error is potentially high with this method and an alternative is to carry out the same procedure on an optical microscope slide and to measure the diameter of a representative number of resin beads before and after swelling using a calibrated graticule [69]. The average change in this linear dimension can then be converted to a volume expansion. This approach is more accurate but time consuming and tedious. A third method of monitoring swelling employs a small bench-top centrifuge [70, 71]. A known mass of dry resin is introduced into a small pre-weighed glass sinter stick and allowed to swell to equilibrium with sol-

vent. The sinter stick is then gently centrifuged ( $\sim 1000$  rpm for 1 minute) to remove the interstitial volume of solvent and the stick re-weighed. The increase in mass can be converted to a volume by assuming a density for the solvent, and so the volume swelling per gram of dry resin determined. This method is more accurate than the direct volume charge method especially when the swelling is rather low. This method is also useful when evaluating permanently porous resins when the swelling may be extremely low.

The second phenomenon which can occur on contacting a resin with solvent is **pore-filling** when the resin has dry state porosity. This can occur with or without a volume change depending on the degree of interaction between the solvent and the resin and the nature of the resin, in particular its degree of cross-linking. Highly cross-linked porous resins may display virtually no swelling, and yet imbibe significant levels of solvent into the accessible pore volume. Use of the centrifuge method is effective for quantifying the solvent imbibition in these cases. More often than not however a solvent will not only fill the pore volume of a porous resin but also solvate the polymer chains and hence expand the microgel particles comprising the resin. The measured imbibition is therefore a composite of the phenomena of swelling and pore-filling. Millar has suggested a criterion for defining a macroporous resin as being one which imbibes at least  $0.1 \text{ ml g}^{-1}$  dry polymer of a nonsolvating (nonswelling solvent) [72]. In the case of rigid resins with good dry state porosity there is usually a good correlation between the volume uptake of a nonsolvating solvent and the total intrusion volume of Hg (see Section 4.3). In addition there is also often a good correlation between the volume of solvent imbibed by a macroporous resin and the volume of porogen used in templating the pores in the macroporous resin.

The distinction between swelling and pore-filling is illustrated very clearly with data for the uptake of aqueous/acetone mixtures by PS-DVB resins prepared with toluene as a solvent/porogen. With a divinylbenzene content of 5 and 20% the resins display an uptake of  $< 0.5 \text{ ml g}^{-1}$  dry resin for acetone contents of 10–80%. However, a resin prepared with 50% divinylbenzene shows a remarkable rise in the imbibition data to  $> 2 \text{ ml g}^{-1}$  dry resin across the same aqueous/acetone composition range [73]. This result seems strange bearing in mind the high level of cross-linking in the latter resin, but is readily rationalized when it is realized (and was demonstrated) that the latter resin is macroporous, and the imbibition observed is primarily pore-filling. The former two resins are in fact solvent expanded gel-types (see Section 1.2.3.1). Considerable care is therefore needed in interpreting these apparently simple data, and even today papers appear in literature where such data is completely misinterpreted as demonstrating an unusual effect, when in reality a clear distinction between swelling and pore-filling has not been recognized [74].

Increasingly there is a need to evaluate simple physical properties such as solvent imbibition in a more rapid manner for high-throughput materials studies, or for real-time evaluation. Recently this issue has been addressed and a very elegant solution developed [75] based on earlier work [76, 77]. In this a polypropylene disposable syringe containing a known mass of polymer is suspended from a microbalance and the balance reading set to zero. A reservoir of the solvent to be inves-

tigated is raised until the solvent surface is just brought into contact with the syringe. The microbalance simply reads the mass increase on imbibition of the solvent and the data is acquired in real-time. Not only is this a very convenient approach, it provides important kinetic data on solvent uptake as well as equilibrium sorption data.

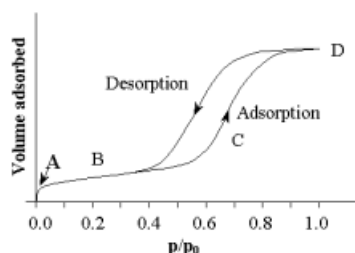
#### 1.4.2

#### **N<sub>2</sub> Sorption Porosimetry Involving Dry Supports**

Among several methods for the characterization of porous solids, e.g. pycnometry, gas adsorption, fluid penetration, calorimetric measurements, radiation scattering, xenon NMR, size exclusion chromatography and ultrasonic techniques [78], gas adsorption is one of the most widely used [21, 79–81]. In this method, the pressure dependence of adsorption of a gas has to be determined. When an adsorbable gas (the adsorptive) is brought into contact with the surface of a solid (the adsorbent) adsorption occurs. If the intermolecular forces involved are weak, i.e. the adsorbate is bound only by van der Waals dispersion forces and dipole–dipole interactions, physisorption occurs. This process is exothermic, with the exothermicity increasing with decreasing temperature and increasing pressure. Many gases can be adsorbed (e.g. CO<sub>2</sub>, N<sub>2</sub>, Ar, etc.), but the most commonly used is N<sub>2</sub> at liquid nitrogen (LN<sub>2</sub>) temperatures around the boiling point (77.35 K) at normal pressure. The quantity of gas adsorbed is usually expressed as its volume under standard conditions. The pressure is reported as the relative pressure, i.e. the actual pressure  $p$  divided by the vapor pressure  $p_0$  of the adsorbing gas at the temperature at which the test is performed.

Typical adsorption and desorption isotherms for a porous solid are indicated in Fig. 1.13. Following the adsorption branch, the steep initial rise (A) is caused by adsorption in the most energetic regions of the solid (single layer adsorption). Thereafter, in the flat region (B), gas molecules adsorb on sites already occupied by other molecules (multilayer adsorption).

The abrupt rise in the middle (C) is caused by starting bulk condensation of the adsorbing gas in small pores. On increasing the pressure, bulk condensation occurs in even larger pores, and if all pores are filled, finally the isotherm becomes horizontal again (D). Adsorption and desorption branches retrace each other only for nonporous materials or special cases with pores of certain conical geometry.



**Fig. 1.13** Adsorption and desorption isotherm for a porous solid.

Usually, a hysteresis loop appears because of different adsorption and desorption mechanisms and network or connectivity effects.

The majority of physisorption isotherms (Fig. 1.14 Type I–VI) and hysteresis loops (Fig. 1.14 H1–H4) are classified by IUPAC [21]. Reversible Type I isotherms are given by microporous (see below) solids having relatively small external surface areas (e.g. activated carbon or zeolites). The sharp and steep initial rise is associated with capillary condensation in micropores which follow a different mechanism compared with mesopores. Reversible Type II isotherms are typical for nonporous or macroporous (see below) materials and represent unrestricted monolayer–multilayer adsorption. Point B indicates the stage at which multilayer adsorption starts and lies at the beginning of the almost linear middle section. Reversible Type III isotherms are not very common. They have an indistinct point B, since the adsorbent–adsorbate interactions are weak. An example for such a system is nitrogen on polyethylene. Type IV isotherms are very common and show characteristic hysteresis loops which arise from different adsorption and desorption mechanisms in mesopores (see below). Type V and Type VI isotherms are uncommon, and their interpretation is difficult. A Type VI isotherm can arise with stepwise multilayer adsorption on a uniform nonporous surface.

With hysteresis loops of Type H1, the two branches are almost vertical and nearly parallel. Such loops are often associated with porous materials which are known to have very narrow pore size distributions or agglomerates of approximately uniform spheres in fairly regular array. More common are loops of Type H2, where the pore size distribution and shape are not well defined. This is attributed to the difference in adsorption and desorption mechanisms occurring in ‘ink-bottle’ pores, and network effects. The Type H3 hysteresis loop does not show any limiting adsorption at high relative pressures and is observed in aggregates and macroporous materials. Loops of Type H4 are often associated with narrow

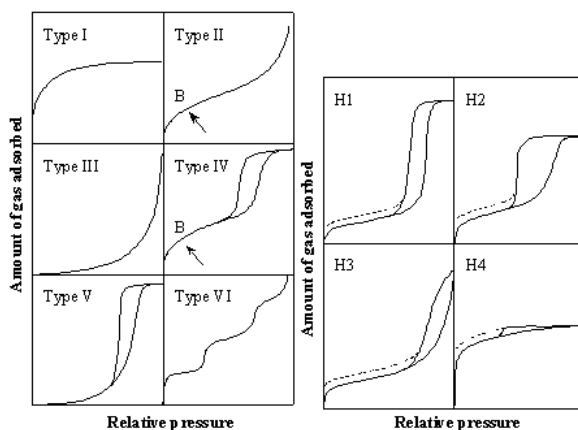


Fig. 1.14 Types of physisorption isotherms (I–VI) and hysteresis loops (H1–H4) according to the IUPAC classifications.



pores size distributions. In many systems, but especially those containing micropores (e.g. permanently porous polymers), a low pressure hysteresis may also be observed, indicated by the dotted lines in Fig. 1.14. This arises when there is residual adsorbed material that cannot be removed at the lowest attainable pressure but by outgassing at higher temperature, or if chemisorption occurs.

#### 1.4.2.1 Adsorption/Desorption Mechanisms Isotherm Hysteresis Loops

The IUPAC classification of pores into micro-, meso- and macropores [21] was introduced because of different pore-filling mechanisms in these ranges. For micropores (pore width < 2 nm), the interaction forces between the adsorbate and the pore walls have to be taken into account. In mesopores (pore width 2–50 nm), the adsorbate can be considered as having the same properties as the bulk liquid. Macropores (pore width > 50 nm) cannot be measured by gas adsorption because already bulk condensation would occur at the pressure required for adsorption to occur. For many applications of polymer supports the mesopore region is very important, but macropores aid access to these. Interest in microporous systems is also growing. Considering nitrogen adsorption in a cylindrical mesopore, capillary condensation occurs dependent on the pore size and the pressure applied. The relationship between pore radius and pressure is described by the Kelvin equation [79], such that with increasing relative pressure, larger pores are filled. The mechanism of adsorption proceeds via the formation of a monolayer of dense gas on the pore walls. This is followed by other layers and the formation of density fluctuations along the pore walls finally leading to collapse into a biconcave lens of liquid, i.e. capillary condensation [79, 82]. Stated another way, condensation occurs from the pore walls inwards towards a central core of decreasing diameter. In contrast, evaporation starts from the pore ends by the menisci receding inwards. The different adsorption and desorption mechanisms are one explanation for the formation of hysteresis loops, but provides an over-simplified picture. It is now well accepted that network effects also have to be taken into account (see Section 1.4.2.3.).

#### 1.4.2.2 Models for Calculation of Surface Area and Pore Sizes

##### BET Theory for the determination of surface area

This acronym is derived from the names of its originators Brunauer, Emmett and Teller [83]. A major advance relative to the monolayer approach of Langmuir [84] is the incorporation of multilayer adsorption. The BET equation can be written as follows [79],

$$\frac{p}{V_a(p_0 - p)} = \frac{1}{V_m C} + \frac{C - 1}{V_m C} \left( \frac{p}{p_0} \right) \quad (1)$$

where  $p$  is the pressure during the experiment,  $p_0$  the saturation pressure of the gas,  $V_a$  the quantity of gas adsorbed at pressure  $p$ ,  $C$  a constant and  $V_m$  the

quantity of gas adsorbed if the entire surface is covered with a monolayer. A plot of  $p/[V_a(p_0-p)]$  versus  $p/p_0$  should yield a straight line having an intercept of  $1/V_m C$  and a slope of  $(C-1)/V_m C$ . The values for  $V_m$  and  $C$  may be obtained from a regression line. The space occupied by a single molecule can be calculated from its van der Waals dimensions (for nitrogen  $0.162 \text{ nm}^2$  at  $\text{LN}_2$  temperature). From this value and  $V_m$ , and assuming hexagonal close packing of adsorbed molecules the surface area of the sample can be derived.

Still, this theory is over-simplified, and holds only for a limited part of the sorption isotherm, which is usually the case for relative pressures between 0.05–0.30, and the presence of point B (Fig. 1.14). Thus, isotherms of Types II (macroporous polymer supports) and IV (mesoporous polymer supports), but not Type I and III, are those amenable to BET analysis [21, 80]. Attention should also be paid to the constant  $C$ , which is exponentially related to the enthalpy of adsorption of the first layer. A negative or high value of  $C$  exceeding  $\sim 200$ – $300$ , is likely to indicate the presence of micropores and the calculated surface area should be questioned since the BET theory would not be applicable [79, 80].

Empirical methods can be applied in order to determine the validity of the BET surface area. The derived standard isotherms can be obtained by normalization of the y-axis (volume adsorbed) of adsorption isotherms. It is strongly recommended that data should always be derived from standard isotherms related to a nonporous sample of the same type of material. Various methods have been established like the  $\alpha_s$ -method where the quantity of gas adsorbed  $V_a$  is related to the value at a relative pressure of 0.4. In the t-plot, the vertical axis is normalized in relation to the average thickness of the adsorbed layer. The shape of the constructed reduced isotherms reveal the presence or absence of micropores and allows the determination of their volume [79, 80].

### BJH Theory for the characterization of mesopores

As discussed in Section 1.4.2.1, the critical condensation pressure in mesopores as a function of pore radius is described by the Kelvin equation. Capillary condensation always follows after multilayer adsorption, and is therefore responsible for the second upwards trend in the S-shaped Type II or IV isotherms (Fig. 1.14). If it can be completed, i.e. all pores are filled below a relative pressure of 1, the isotherm reaches a plateau as in Type IV (mesoporous polymer support). Incomplete filling occurs with macroporous materials containing even larger pores, resulting in a Type II isotherm (macroporous polymer support), usually accompanied by a H3 hysteresis loop. Thus, the upper limit of pore size where capillary condensation can occur is determined by the vapor pressure of the adsorptive. Above this pressure, complete bulk condensation would occur. Pores greater than about 50–100 nm in diameter (macropores) cannot be measured by nitrogen adsorption.

The calculation method for the mesopore size distribution generally follows that described by Barret, Joyner and Halenda [79, 85]. With the so-called BJH method, the pore sizes using a certain pore geometry are calculated along the isotherm. This involves an imaginary emptying of condensed adsorptive in the pores in a

stepwise manner as the relative pressure is decreased. The mathematics is equally applicable whether following the adsorption or desorption branch. In either case, the condition must be set where all pores are considered as being filled. Typically, this is taken at a relative pressure of about 0.995. The amount of adsorptive lost at each step of the desorption process represents the core volume of the pores emptied at this step. The thickness of the remaining adsorbed layer can be calculated from a certain thickness relationship. Depending on which branch of the hysteresis loop is used for the calculation, different pore size distribution curves will be obtained. Recent work has drawn attention to the complexity of capillary condensation in pore networks, and indicated that calculations from the desorption branch are likely to be unreliable for certain isotherm shapes because of pore blocking effects (see Section 1.4.2.3).

Modern  $N_2$  sorption porosimeters are very sophisticated and generally reliable. Typically they come supplied with customized user-friendly software which enables the experimental data to be readily computed using the above models and mathematical expressions. Usually the raw isotherm data is displayed graphically along with various forms of the derived pore size distribution curve and tabulated data for surface area, pore volume and average pore diameter.

### Characterization of micropores

The classical Kelvin equation assumes that the surface tension can be defined and that the gas phase is ideal. This is accurate for mesopores, but fails if applied to pores of narrow width. Stronger solid–fluid attractive forces enhance adsorption in narrow pores. Simulation studies [86] suggest that the lower limit of pore sizes determined from classical thermodynamic analysis methods lies at about 15 nm. Correction of the Kelvin equation does lower this border to about 2 nm, but finally also the ‘texture’ of the fluid becomes so pronounced, that the concept of a smooth liquid–vapor interface cannot accurately be applied. Therefore, analysis based on the Kelvin equation is not applicable for micropores and different theories have to be applied for the different ranges of pore sizes.

No current theory is capable of providing a general mathematical description of micropore filling and caution should be exercised in the interpretation of values derived from simple equations. Apart from the empirical methods described above for the assessment of the micropore volume, semi-empirical methods exist for the determination of the pore size distributions for micropores. Common approaches are the Dubinin–Radushkevich method, the Dubinin–Astakhov analysis and the Horvath–Kawazoe equation [79].

### Statistical-mechanical methods

Instead of the classical approaches, a molecular-based statistical thermodynamic theory can be applied to allow a model of adsorption to be related to the microscopic properties of the system in terms of fluid–fluid and fluid–solid interactions, pore size, pore geometry and temperature. Using such theories the whole range of pore sizes measured can be calculated using a single approach. Two simulation

methods are commonly used to determine the distribution of gas molecules in a system in equilibrium. The molecular dynamics and the Monte Carlo method. Both can yield the same results and are considered in principle to be exact, however they require large computational time. Density functional theory offers a practical alternative to both methods and provides an accurate method requiring fewer calculations. However, the surface structure of the solid must be known and pores have to be of well-defined shape, which limits this approach to very specific materials such as activated carbon or zeolites [79, 80, 87].

#### 1.4.2.3 Network and Pore Connectivity Effects

As discussed above, hysteresis loops can appear in sorption isotherms as result of different adsorption and desorption mechanisms arising in single pores. A porous material is usually built up of interconnected pores of irregular size and geometry. Even if the adsorption mechanism is reversible, hysteresis can still occur because of network effects which are now widely accepted as being a percolation problem [21, 81] associated with specific pore connectivities. Percolation theory for the description of connectivity-related phenomena was first introduced by Broadbent et al. [88]. Following this approach, Seaton [89] has proposed a method for the determination of connectivity parameters from nitrogen sorption measurements.

A typical network effect is illustrated in Fig. 1.15 in the case of three pores of different size. During adsorption the smallest pores are filled first and the largest pores last, resulting in the filling sequence A, B and C. The vapor needed to fill remote pores can be transported either through the liquid or vapor phase. During the desorption process, the order in which the liquid nitrogen would become unstable is C, B and A, i.e. the reverse.

However, desorption follows the meniscus receding mechanism, and vaporization occurs only in pores connected to the vapor phase. As a result, pore C remains filled until pore B is emptied, and the sequence of evaporation is in fact B and C together followed by A. This mechanism can lead to very steep Type H2 hysteresis loops. Indeed, a common diagnostic feature of many hysteresis loops is that the steep region leading to the lower closure point occurs at nearly the same relative pressure. It is almost independent of the porous adsorbent, but mainly dependent on the adsorptive. In case of nitrogen this happens at a relative pressure  $p/p_0 \sim 0.4$  [21].

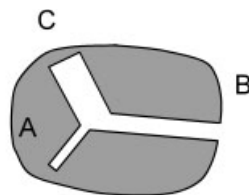


Fig. 1.15 Network with three pores of different sizes A, B and C.

In the past it was very common to derive the mesopore size distribution from the desorption branch of the isotherm. The above considerations make it clear that this practice is questionable especially for Type H2 hysteresis loops, and can lead to misinterpretations [90]. Indeed a significant downward turn in the desorption branch of a  $N_2$  isotherm at  $p/p_0 \sim 0.4$  leads to an apparent sharp maximum in the pore size distribution curve at  $\sim 2$  nm which is totally artefactual. Although no general guidelines exist on whether the adsorption or desorption branch should be used for computation, it should be understood that with Type H2 and H3 hysteresis loops, reliable results are much more likely to be obtained if the adsorption branch is used [21].

#### 1.4.3

#### **Hg Intrusion Porosimetry involving Dry Supports**

Mercury intrusion porosimetry has evolved as a standard technique for the characterization of porous materials [79, 91]. It was developed by Ritter and Drake in 1945 [92] and was originally designed for the characterization of materials having rather large pores, e.g. geological samples and structural materials. Further development finally allowed also the characterization of smaller pores, and now pore diameters in the range between 360–0.003  $\mu\text{m}$ , i.e. a span over 5 orders of magnitude, can be covered [79]. The method is destructive, partly because the very high compression forces may cause mechanical destruction of the sample, but mainly since some mercury remains entrapped in the pores. Despite concerns over the ecological and toxicological effects of mercury, this method remains an indispensable tool for the characterization of porous solids in the macro and mesoporous regimes [78].

##### 1.4.3.1 Theory

As a nonwetting liquid, mercury does not penetrate pores by capillary action. Filling of a pore requires an external force, inversely proportional to the pore size. The relationship below was first described by Washburn [93] considering the pores as cylindrical, nonintersecting capillary tubes.

$$d = \frac{-4\gamma \cos \theta}{p} \quad (2)$$

Since the surface tension  $\gamma$  of mercury is  $0.485 \text{ N m}^{-1}$  at  $20^\circ\text{C}$  with a contact angle of  $\theta = 130^\circ$ , a pore of  $d = 1 \mu\text{m}$  and greater will be filled if a pressure  $p$  of 1.25 MPa is applied. Hence, the amount of mercury forced into pores increases with pressure (intrusion), but releasing the pressure, the pores are emptied again (extrusion). Typical intrusion and extrusion curves are represented schematically in Fig. 1.16A. The intrusion branches in this illustration are typical for samples such as suspension polymerized polymer particles ( $\sim 200 \mu\text{m}$ ).

### Intrusion

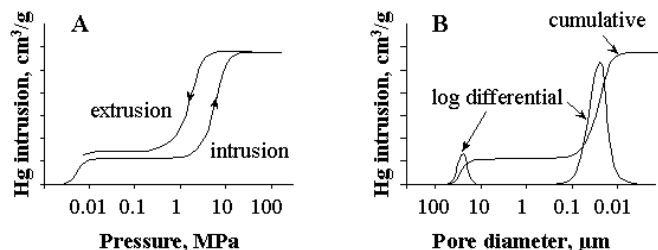
Following the intrusion branch with increasing pressure (Fig. 1.16A), the steep initial rise at low pressures is caused by the filling of interparticle spaces. The breakthrough pressure, i.e. the pressure when the voids between the particles are filled, follows in principle the theory of Mayer and Stowe [94], and is inversely proportional to the particle size [95]. The demarcation between interparticle spaces and actual intraparticle pores may be unclear for microparticles, but in the case of polymer beads from suspension polymerization having particle sizes between 50–500  $\mu\text{m}$ , usually no interference occurs. The second rise of the intrusion branch is caused by pores inside the particles. Shown in Fig. 1.16A is a porous material of rather narrow pore size distribution.

More illustrative than the representation in Fig. 1.16A are plots of incremental or differential pore volume versus pore size as shown schematically in Fig. 1.16B. The pore diameter on the abscissa is calculated by employing a particular pore model, usually to the intrusion branch. As a matter of convenience, a cylindrical pore model is traditionally applied. On the ordinate, steep changes in the cumulative diagram are reflected as peak maxima in the incremental curve. From several possible representations (incremental, differential, log differential), the log differential plot seems to be the most revealing, since the areas under the peaks are proportional to the pore volume [79]. Data that can easily be derived from mercury intrusion are the pore size distribution, median or average pore size, pore volume, pore area, bulk and skeletal density, and porosity.

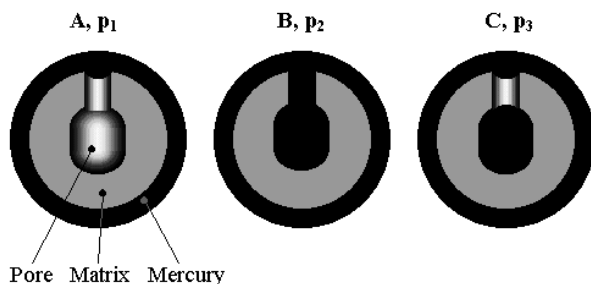
### Extrusion and Hysteresis

The extrusion curve shown in Fig. 1.16A cannot retrace the intrusion curve exactly because mercury is not expelled completely because it is entrapped in so-called ink-bottle pores [79, 96] (Fig. 1.17).

In contrast to nitrogen adsorption, mercury fills the largest pores first, and the smallest pores last. A narrow neck in between a larger cavity and the mercury will cause the volume behind the neck to be registered as a pore having the smaller diameter (A). After filling all pores at high pressure  $p_2$  (B) and releasing the pressure again, extrusion leaves mercury entrapped in the void (C) even when  $p_3 < p_1$ .



**Fig. 1.16** Typical intrusion and extrusion schematic curves for porous beads (A) and the log differential pore volume versus pore radius calculated from the intrusion branch (B).



**Fig. 1.17** Mercury intrusion and extrusion for “ink-well” pores at three different pressures.

The differences of the intrusion and extrusion mechanisms are the main factors, leading to the different pathways (hysteresis) of the branches in Fig. 1.16A. Furthermore, this effect causes the pore size distribution obtained from the intrusion curve to be incorrectly shifted towards smaller pore sizes. Unlike some inorganic materials of very regular pore structure (e.g. zeolites), permanently porous organic polymers consist of a very complex network of pores of different sizes connected to each other. Correction of these falsifications in the results described above is virtually impossible, since it implies a detailed understanding of the network.

### Compression

An important aspect of characterizing a polymer support by Hg intrusion is its elasticity in response to high compression forces. This results in an apparent increase of mercury intruded at high pressures. A nonporous polymer can easily exhibit apparent surface areas around  $50\text{--}100\text{ m}^2\text{ g}^{-1}$  just because of compressibility. The reason is the inherent softness of organic polymers, but also the possible contribution of closed pores which can allow the polymer beads to be compressed like a sponge or even destroyed. Similar studies on the elastic behavior of coals [97] suggest, that the correction for compressibility is more complicated, because of nonlinear response to high applied pressures. Also the distinction between pore-filling and compression, especially compression because of closed pores, is problematic. In principle, intrusion data can be corrected using compressibility moduli [98], but in the case of organic polymers the problems described are complex and not readily corrected. Therefore, pore volumes measured at pressures above 100 MPa, or in terms of pore sizes, values below about  $0.01\text{ }\mu\text{m}$ , start being inaccurate. Hence, mercury porosimetry can be used accurately only for measurements of macro- and large mesopores. Information about smaller pores should be obtained from nitrogen sorption measurements.

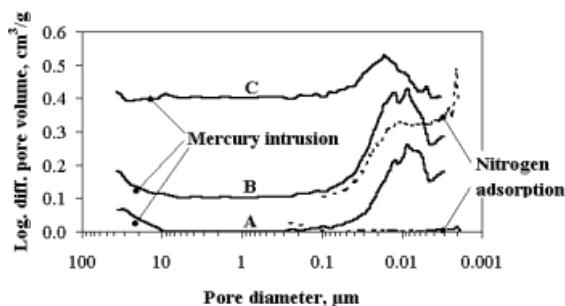
### 1.4.3.2 Comparison between Nitrogen Sorption and Mercury Intrusion

In both nitrogen sorption and mercury intrusion methods a pore volume is measured as a function of pressure, and in principle, one might expect that the results in terms of surface area, pore volume and pore size distribution would be comparable. However, the different physical interactions involved, and artefacts during pore-filling and emptying as pointed out earlier, make direct comparison difficult. In many cases good agreement has been found between the derived data [99], but a general judgment is not possible, and results may or may not agree well [79], depending very much on the material. Nevertheless, a few guidelines should be pointed out with respect to polymer based porous materials.

Fig. 1.18A shows the pore size distribution for nonporous methacrylate based polymer beads with a mean particle size of about  $250\text{ }\mu\text{m}$  [100]. The black line indicates the vast range of mercury intrusion, starting at  $40\text{ }\mu\text{m}$  because interparticle spaces are filled, and down to  $0.003\text{ }\mu\text{m}$  at highest pressure. Apparent porosity is revealed below a pore size of  $0.1\text{ }\mu\text{m}$ , although the dashed line derived from nitrogen adsorption shows no porosity at all. The presence or absence of meso- and micropores is definitely being indicated in the nitrogen sorption experiment.

For mercury porosimetry on the other hand, the compressibility of the sample material has to be considered, and a pore size of  $0.1\text{ }\mu\text{m}$  requires already a pressure of more than 12 MPa to fill the pore. Since polymers are rather soft in contrast to inorganic materials, the peak in Fig. 1.18A is entirely caused by compressibility. Fig. 1.18B shows the pore size distribution of a mesoporous polymer from the same material and particle size as for A. For the sake of clarity, the values on the ordinate are offset by  $0.1\text{ cm}^3\text{ g}^{-1}$ . The dashed line calculated from nitrogen adsorption shows unambiguously the presence of meso- and micropores. The black line from mercury intrusion agrees very well with the curve from the  $\text{N}_2$  adsorption data, however, its shape looks exactly like the one from polymer A indicating compression. Correction of the mercury intrusion data of polymer B with nonporous polymer A (Fig. 1.18C, offset by  $0.4\text{ cm}^3\text{ g}^{-1}$ ) shows that below a pore size of  $0.02\text{ }\mu\text{m}$  intrusion diminishes and data from mercury porosimetry become irrelevant. Thus, e.g. for porous polymer supports based on styrene or methacrylate monomers, the agreement between the two methods appears to be fairly acceptable in the overlapping range between  $0.1\text{--}0.01\text{ }\mu\text{m}$ . Larger pores can

**Fig. 1.18** Pore size distribution from mercury intrusion (—) and nitrogen adsorption (----) data for methacrylate-based polymer beads: Nonporous (A), mesoporous (B) and mesoporous pressure corrected (C).





be covered only by mercury intrusion, for smaller ones nitrogen sorption is much more reliable.

Precise agreement is however exceptional, and even if both methods reveal porosity in the overlapping range, the pore volume may be different and the pore size shifted. Fig. 1.19A gives an example of such with a mesoporous methacrylate based polymer resin. The contribution of interparticle filling has been removed. The pore size distribution from mercury intrusion is shifted towards smaller pore sizes compared with that from the nitrogen adsorption data. This may be caused by ink-bottle pores, but is not generally observed, and other effects can easily reverse the two curves. The shift may also be very significant in the range of an order of magnitude. Such conditions make interpretation of porosity data difficult and it has to be pointed out that none of the values derived with the two methods are true, but rather should be regarded as complementary data for characterization, since they are highly reproducible.

Another example of a macroporous methacrylate-based polymer support is shown in Fig. 1.19 [101]. Again, only the relevant pore range is displayed. The pores around 1  $\mu\text{m}$  are fully revealed by mercury intrusion, whereas with nitrogen sorption, above 0.1  $\mu\text{m}$ , essentially no pores can be detected.

In a summary therefore, for the characterization of porous polymers, mercury intrusion and nitrogen sorption experiments are complementary, and depending on the morphology of the material, data from one or the other method should be questioned. As long as the requirements described in Section 1.4.2.2 are met, the surface area may always be characterized by the BET method from nitrogen adsorption since it does not require pore-filling. Nitrogen sorption data can be used to characterize microporous materials but care is needed in the data acquisition and appropriate models should be applied. The best data for pore sizes and pore volume depend on the individual sample. If only small mesopores are present, nitrogen sorption data are probably more reliable; for macroporous polymers, the

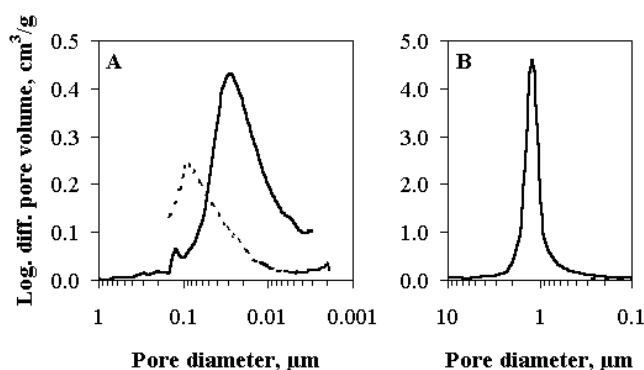


Fig. 1.19 Pore size distribution from mercury intrusion (—) and nitrogen adsorption (-----) data for mesoporous methacrylate-based (A) and macroporous methacrylate-based (B) polymer beads.

method of choice is mercury intrusion. In between no general guidelines are possible, but it may be advantageous if data from both methods are presented.

#### 1.4.4

#### **Inverse Size Exclusion Chromatographic (ISEC) Analysis of Solvent Wetted Polymer Supports**

Although resin morphology data obtained from instrumental techniques such as  $N_2$  sorption and Hg intrusion porosimetry are invaluable, they do have the potentially severe limitation in that they refer to the **dry state** resin. Using such data to interpret resin effects observed e.g. in reactions carried out in solvents does therefore require the assumption that the morphology is not changed significantly when the resin is wetted with solvent. In the case of gel-type resins with a dry state surface area  $<5 \text{ m}^2 \text{ g}^{-1}$  this is clearly not a valid assumption since appropriate compatible solvents swell such resins extensively creating 'solvent porosity' which allows ingress into and egress from the resin. For many macroporous resins the assumption is probably reasonable at least in relative terms for a series of such resins. Almost certainly some swelling of the microgel matrix occurs in these resins along with pore-filling when a compatible solvent is employed, but to a first approximation the effect of swelling might be regarded as similar for a related series of macroporous resins.

Unfortunately there are no routine methodologies for evaluating the morphology of solvent wet resins at least in terms of generating quantitative data on surface area and pore size distribution. It is possible to use the adsorption of a suitable molecule from the solvent, assume monolayer coverage and an molecular area for the molecule, and hence compute a surface area. This technique has been used in assessing the surface area of e.g. silica and alumina but has not proved valuable in the case of resins.

Recently however the technique of inverse size exclusion chromatography (ISEC) has attracted attention as a methodology for probing morphology in the wet state. Size exclusion chromatography (SEC) previously known as gel permeation chromatography (GPC) or gel filtration (GF) is a chromatographic technique for the assessment of analyte molecular size or volume, and with assumptions or appropriate calibration, analyte molecular weight. The technique has become an absolutely essential tool for polymer chemists for determining the molecular weight and molecular weight distribution of soluble synthetic macromolecules. The methodology relies on a porous chromatographic stationary phase which has a distribution of pore sizes. High molecular weight analytes enter relative few pores, while low molecular weight species enter a much larger proportion of the pores. Hence somewhat unusually the larger molecules move down the chromatography column more quickly than the smaller ones and in due course elute first. The column stationary phase is typically a macroporous PS-DVB resin, indeed to achieve optimum resolution of molecular weights it is usual to use 2–4 columns packed with porous resins with different pore size distributions. Polymer chemists typically calibrate their instruments using polymer samples of known molecular weight and with narrow molecular weight dis-

tributions determined using more tedious absolute techniques such as light scattering or membrane osmometry.

ISEC [102] is indeed the inverse of SEC. In this technique the porous structure of e.g. a resin is evaluated quantitatively in the solvent wetted state by packing the resin as the stationary phase in a chromatographic column and then recording the elution volume of a series of solutes of known molecular weights. Typically the latter are C5–C30 alkanes and narrow molecular weight polystyrene standards (580–1 800 000), and tetrahydrofuran is the most used solvent. This generates a molecular weight/elution volume profile characteristic of the morphology of the resin in the solvent swollen state. In order to translate this data into porosity parameters characteristic of the resin, it is necessary to assume some model describing the porous structure of the resin and to relate this mathematically to the elution of solutes of known sizes through the pore structure. For materials with a well developed pore structure a cylindrical pore model is a reasonable one to use and this seems to generate porosity data which relates closely to what might be expected from dry state porosity data [24, 103]. However, both the dry state and wet state derived parameters are both subject to the limitations of their respective models used to compute the porosity parameters, and so care is always needed in the use of such data and particularly in comparing data produced from one technique with that from another. With ISEC a complication arises with very small pores (*i.e.* micropores and smaller) and in particular distinguishing between diffusion of a very small solute through very small but discrete pores, and diffusion of the same solute through a uniform solvent swollen polymer gel network. The latter situation is conveniently treated using the Ogston model [104], but there is no unambiguous way of deciding when such a model should be applied in place of e.g. a cylindrical pore model. Indeed whether or not there is any distinct physical difference between diffusion through very small but discrete pores, and diffusion through a uniform gel network is a debatable point. In recent work involving characterizing branched resins, data for solute molecules below C16, corresponding to a size of  $\sim 2$  nm, was computed in terms of diffusion through a gel rather than very small pores. All other data was handled using a cylindrical pore model [44].

Using the above methodologies we and our collaborators have successfully evaluated the wet state morphology of both collapsible macroporous resins [24] and branched gel-type and macroporous resins [44]. Dry state porosity data alone would have been inadequate in revealing the morphology of these species. The ISEC technique is attracting increased interest from resin designers and exploiters and it seems likely that commercially sourced instrumentation and software will emerge in due course.

#### 1.4.5

#### Other Methods for Characterizing Porous Polymer Morphology

Perhaps one obvious technique for evaluating pore structure is electron microscopy, and indeed numerous papers have been published showing visually attractive scanning electron micrographs (SEM). In fact these studies seldom provide

any quantitative data, indeed taken in isolation such micrographs can be very misleading. Variation of magnification, contrast and exposure can yield quite different images from the same area of a sample. In the extreme the latter can appear smooth or pore ridden by appropriate manipulation of the SEM instrument. The images can however provide rewarding confirmatory evidence for the morphology picture painted by porosity data obtained by the techniques described earlier.

In contrast transmission electron microscopy (TEM) can in skilled hands yield detailed quantitative data on pore structure, and can even provide valuable information on the wet state of resins by plunge freezing such samples and microtoming on a cold stage [105]. To obtain quantitative information it is necessary to use advanced image analysis methodology which is extremely powerful [106]. Unfortunately the approach is time consuming and costly and can rarely be applied routinely in morphology studies.

Thermoporometry [107] has also been used in evaluating resin porosity [108] and in effect gives information on the solvent wetted state of resins. The technique exploits the phenomenon that the freezing point of a liquid is depressed when it is confined in pores of small radius. Calorimetric measurements on solvent imbibed resins at increasingly reduced temperatures allows a distribution curve to be generated. This in turn can be related to a pore size distribution. The technique is not routine nor widely practiced and more information is available in reference [17].

Small angle X-ray scattering monitoring the distribution of electron density has been used to probe resin morphology [109]. More recently contrast matched small angle neutron scattering has also been employed [110, 111]. These techniques can also be applied to wet resins and tend to probe the very low dimensions of the polymer matrix structure. More studies are needed to identify the real value of these approaches.

## 1.5

### Analytical Techniques for Monitoring Polymer-Supported Chemistry

The application of polymer supports in facilitating chemical synthesis was first drawn to the attention of the broader chemical community by Merrifield [112] in 1963 when he described the use of a support in so-called 'solid phase peptide synthesis' (SPPS). In practice though the ion exchange resin community had been using sulfonic acid ion exchangers as solid acid catalysts for many years prior to this, and indeed had developed industrial processes using such polymeric catalysts [113]. Since Merrifield's pioneering work however there has been an accelerating interest in polymer-supported catalysts [5, 6, 12] and in solid phase organic synthesis (SPOS) most recently in the context of high-throughput (parallel and combinatorial) synthesis [9, 11]. Rapid solid phase synthesis (SPS) and screening have been carried out of large numbers of new chemical entities with the aim of accelerating the discovery of new drugs [114–118]. This approach has also been employed successfully in the search for new catalysts and materials [119–123]. All

these activities involve the use of polymer supports which have been specifically chemically derivatized, with supports based on cross-linked PS-DVB beads being overwhelmingly the most commonly used. One of the main challenges in this area remains the adaptation of solution-phase reactions onto polymer supports. This can still be a frustrating and time-consuming process. This is in part caused by the difficulty of monitoring the molecular structural changes taking place during chemical reactions on polymer supports, and of characterizing molecularly the supported species, since conventional techniques such as thin layer chromatography (TLC) and solution phase NMR spectroscopy cannot be employed. Perhaps not surprisingly therefore in recent years there has been a drive towards developing new rapid and sensitive methods for molecular structural analysis of support-bound species [124–128]. This includes different approaches, such as off-bead analysis as well as destructive and nondestructive on-bead analysis. There is also interest in some circumstances in assessing the spatial distribution of functional groups throughout a resin bead. Here we will cover all of these aspects but will focus in particular on the major advances in methods of on-bead analysis such as single bead Fourier transform infrared (FT-IR) spectroscopy, and gel phase high resolution magic angle spinning (HR-MAS) NMR spectroscopy. These techniques are leading to an improved understanding of polymer-supported chemistry.

### 1.5.1

#### Off-bead Analysis

##### 1.5.1.1 Cleave-and-Characterize

In solid-phase synthesis, reactions on polymer supports have been traditionally monitored whenever possible by cleavage of the bound molecule from the resin, followed by conventional analysis of the soluble species, i.e. using the “cleave-and-characterize” strategy. However, this off-bead method has several disadvantages. It is time-consuming, destructive and indirect, hence it is unsuitable for reaction monitoring. In addition, some reactive species may not be stable under the cleavage conditions, and the use of certain cleavage reagents could lead to contamination of the desired product. Furthermore, the cleave-and-characterize approach cannot always be used for accurate quantitative analysis. Since polymer loadings are usually low large amounts of resin need to be cleaved and this is neither cost-effective nor practical in multi-step syntheses. Finally, this strategy cannot be employed in cases where there is no cleavable linker present, such as in the analysis of many polymer-supported catalysts, reagents and scavengers.

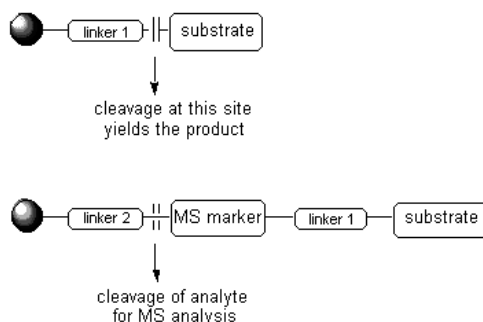
One important methodology falling into the ‘cleave-and-characterize’ category is metal ion analysis, applicable to polymer-supported metal complex catalysts. Here a key and particularly sensitive analytical tool remains the option of chemical digestion of the organic polymer matrix and extraction of the inorganic residue into an aqueous solution suitable for atomic absorption spectrophotometric analysis or inductively coupled plasma emission analysis. The very high sensitivity offered by the latter translates into accurate metal ion content data providing the digestion procedures are carried out quantitatively [129].

### 1.5.1.2 Mass Spectrometry

The rapid analysis of solid-bound compounds may be achieved by cleavage from a small number of beads, followed by mass spectrometry (MS) (mainly electrospray ionization (ESI) or matrix assisted laser desorption ionization (MALDI)) [130–133]. Despite its destructive nature, this technique is extremely fast and sensitive and is therefore widely used for the detection of the desired product in the library synthesis of small molecules. The molecular weight of the cleaved molecule is readily determined as no fragmentation takes place when using these mild ionization methods. A variety of approaches have been described for direct MALDI analysis [134, 135] of resins with photolabile linkers, as well as *in situ* cleavage of supported molecules using trifluoroacetic acid (TFA). The use of ESI Fourier transform ion cyclotron resonance (FT-ICR) MS has also been described [136, 137] for the rapid analysis of compounds from combinatorial libraries. Although significant advances have recently been made in the use of MS in the combinatorial sciences, these have already been reviewed elsewhere [138, 139].

### 1.5.1.3 Analytical Constructs

Resins with two orthogonal linkers, known as *Analytical Constructs* [140–145], have now been designed for applications requiring high-throughput analysis. Cleavage of one linker yields the desired product while the other linker (cleaved under different conditions) is present in order to facilitate the mass spectral analysis of the cleaved molecule. For example, a small amount of a resin with a dual linker (Fig. 1.20) can be employed in conjunction with a traditional resin during solid-phase synthesis. The majority of the resin contains one linker (linker 1) that upon cleavage yields the desired product, whereas a small amount (*ca.* 5%) of a second resin is used in order to facilitate MS analysis upon cleavage (of linker 2), by incorporating a MS marker onto the analyte, the marker acting as a sensitizes and isotopic label. The labeling can be used to ensure that all peaks in the mass spectrum correspond to species cleaved from the resin.



**Fig. 1.20** The design of resins containing analytical constructs for MS analysis.

## 1.5.2

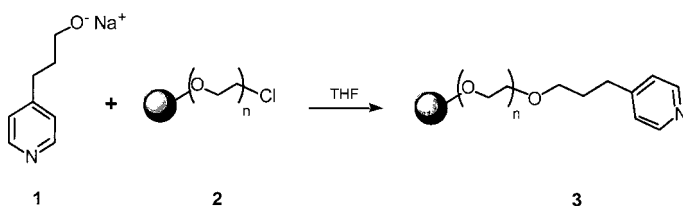
**Destructive On-bead Analysis****1.5.2.1 Elemental Microanalysis**

Another traditional method used for polymer support characterization is elemental analysis. Its use as an accurate quantitative technique for monitoring solid-phase reactions has also been demonstrated [146]. Microanalysis can be extremely valuable if a solid-phase reaction results in the loss or introduction of a heteroatom (usually N, S, P or halogen). In addition, this method can be used for determination of the loading level of a functional group (e.g. usually calculated directly from the observed microanalytical data). For example, in many cases, the displacement of chloride from Merrifield resin has been used as a guide to determine the yield of the solid-phase reaction.

However, one example that demonstrates the limitations of using elemental microanalysis to determine the extent of solid-phase organic reactions is the study reported by de Miguel *et al.* [147] on the reaction between the alkoxide anion (**1**) and ArgoGel chloride (**2**) (a PS-PEG resin see Section 1.2.4) (Scheme 1.1) monitored using chlorine and nitrogen microanalysis. After the reaction, analysis of the washed and dried beads showed complete displacement of chloride (0% Cl) suggesting quantitative yield of the supported pyridine (**3**). However the nitrogen content value (0.39% N) indicated a lower yield (66% by nitrogen analysis), and was therefore in disagreement with the chlorine microanalysis result. The yield was found to be lower than expected because an unexpected enol ether is formed as a side-product (Section 1.5.3.4.).

**1.5.2.2 Color tests**

Other destructive methods that are widely used for qualitative analysis, on account of their simplicity and speed, are color tests specific for particular functional groups. These have been developed mainly for the detection of amines in SPPS. Titrations and derivatizations can also be performed, but are often inaccurate, time-consuming and of limited use. A review of all these methods has been published recently by Kay *et al.* [148] More recently, new color tests for alcohol [149, 150], thiol [151] and aldehyde [152, 153] functionalities have also been reported.



**Scheme 1.1** Attachment of a pyridyl ligand and (**1**) to ArgoGel resin (**2**).

## 1.5.3

**Nondestructive On-Bead Analysis****1.5.3.1 Mass Balance**

Many techniques have been developed for qualitative analysis in solid-phase synthesis, and will be described in this section. However the determination of a solid-phase reaction yield is not trivial. In Section 1.5.2.1, the use of elemental analysis to establish resin loadings has already been discussed. The change in mass during a polymer-supported reaction has also been frequently employed to estimate the yield. However, this is not suitable in most cases, unless the change is significant, and its accuracy is always questionable because of the possibility of trapped solvents, polymer losses during handling or even incomplete removal of reagents during the polymer washing stage.

**1.5.3.2 Other Nondestructive Quantitation Methods**

If a soluble reagent containing an ultraviolet (UV)-active group or dye can be used, then it may be possible to estimate the reaction yield from the amount of unreacted reagent still remaining in the supernatant solution at the end of the reaction. For example, the derivatization of aldehydes and aliphatic ketones with dansylhydrazine has been monitored by fluorescence spectroscopy of the supernatant solution, and has been used to quantify the amount of supported aldehyde or ketone.

An alternative approach is the cleavage of a UV-active protecting group from the resin, such as the widely used Fmoc Test. The quantitation of the 9-fluorenylmethyloxycarbonyl (Fmoc) protecting group for amines is used in SPPS as an indirect method to determine the extent of a peptide coupling reaction. Similar approaches have also been recently reported for the quantitation of supported thiols [151, 154] and have also been the subject of an excellent review [148].

More recently, the synthesis of a novel dihydropyran with a UV-handle has also been reported as a protecting group for supported alcohols [155].

**1.5.3.3 Infrared and Raman Spectroscopy**

Infrared and Raman spectroscopy are nondestructive, quick and convenient techniques for monitoring the course of solid-phase reactions, and have therefore been widely used for the characterization of polymer supports and supported species [156–160]. In fact, the application of infrared spectroscopy in solid-phase synthesis has received much attention and has been the subject of several recent reviews [127, 128, 161–164]. Reactions involving either the appearance or disappearance of an IR-active functional group can be easily monitored using any of the IR techniques described in this section. Some beads are typically removed from the reaction mixture, then they are quickly washed and dried prior to IR analysis. Traditionally, polymer supports are diluted and ground with KBr, then conventional FT-IR analysis of the KBr disk is carried out. Although this is a commonly used



method, the resulting FT-IR spectra are often of poor quality, and the technique is time and sample-consuming [165].

### Single Bead FT-IR or FT-IR Microspectroscopy

FT-IR microspectroscopy is a new nondestructive, fast and reliable technique for solid-phase reaction monitoring. It is the most powerful of the currently available IR methods as it usually requires only a single bead for analysis, thus it is referred to as single bead FT-IR [166]. (See also Chapter 12 for further details). The high sensitivity of the FT-IR microscope is achieved thanks to the use of an expensive liquid nitrogen-cooled mercury cadmium telluride (MCT) detector. Despite the high cost of the instrument, this technique should become more widely used in the future as it represents the most convenient real-time reaction monitoring tool in SPOS [166, 167].

The IR spectrum of a single intact bead (typically containing *ca.* 100–800 pmol of bound substrate) can be obtained using the FT-IR microscope, in transmittance mode, but is marred by broad peaks which blur the resolution of adjacent bands. Improvements in resolution are achieved by simply flattening the bead in a diamond compression cell [168]. This method is particularly useful as there is no sample preparation and only minute amounts of material are needed. One or more beads are placed on one of the diamond windows of the cell and then, after flattening the sample to a uniform thickness, the optical microscope is used to select and focus on the bead of interest. The spectrum of the single bead is then acquired, as well as that of the background. The excellent quality of the resulting IR spectra combined with the high reproducibility and speed of acquisition make this technique a very powerful on-bead analytical tool, which can be used as a solid-phase equivalent of TLC. It has been shown by Yan *et al.* [166] that any one bead taken from a reaction mixture is indeed representative of the entire population of beads in that mixture, and that this technique can be used to follow the course of multi-step reactions, such as in the example shown in Scheme 1.2.

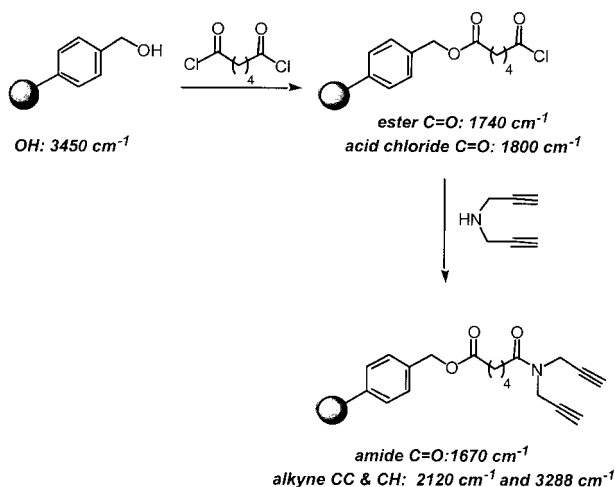
The kinetics of solid-phase reactions have also been investigated by Yan and co-workers [166, 169]. The relative intensities of the IR bands that either disappear or develop during the reaction (compared with an internal reference polymer band) can be plotted against time. This approach can be used to determine when the reaction has reached completion.

*In situ* IR spectral monitoring of solid-phase reactions carried out in dichloromethane, using a flow-through cell [170, 171] has also been described.

Further kinetic studies [172] have focused on the comparison of the rates of reactions on a solid support and in solution-phase, and have served to demonstrate that solid-phase reactions are not always slower than those in solution-phase.

Finally, single bead FT-IR has been further exploited in many applications, such as the study of the tetrapropylammonium perruthenate (TPAP)-catalyzed oxidation of supported alcohols [167], the ring opening of a supported oxazolidinone [173], and the solid-phase synthesis of a benzimidazole [174].

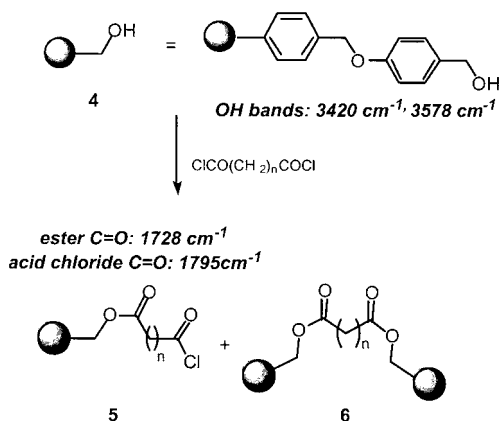
The technique has also been used to gain a better understanding of site–site interactions within a polymer support. Yan *et al.* [175] have investigated the reaction be-



**Scheme 1.2** Monitoring of a multi-step reaction by Single-bead FT-IR spectroscopy.

tween hydroxyl groups on Wang resin (**4**) and different amounts of a diacid chloride (Scheme 1.3). The cross-linked product (**6**) arises from the interaction between neighbouring sites within the resin. It was demonstrated that independent of linker length, large amounts of the reactive acid chloride were required (a 10-fold excess) to avoid formation of the cross-linked diester (**6**) and favor the formation of the supported acid chloride (**5**). Conversely, the diester (**6**) was formed in significant amounts if only a small (2-fold) excess of the acid chloride was employed.

The most important application of this technique has been in the determination of the yield of solid-phase reactions. Several reports have appeared recently focusing on the use of single bead FT-IR as a reliable quantitative technique in SPS [164, 176–178].



**Scheme 1.3** Investigation of site-site interactions using FT-IR microspectroscopy.

Finally, the small sample requirement makes this a suitable method for the analysis of combinatorial libraries. Furthermore, the coupling of a microscope to a motorized stage allows for fully automated analyses [179]. However, the high cost of this instrumentation means that many researchers need to use alternative techniques.

### Beam Condenser Accessory (BCA)

The spectra obtained from an FT-IR instrument fitted with a beam condenser [165] are of the same quality as those obtained using the FT-IR microscope. Again, the sample (usually less than 50–100 beads) is placed in the diamond compression cell but, in this case, the spectrum is recorded for the entire collection of beads present in the cell. The FT-IR spectra of Wang alcohol (**4**) and Wang-supported alanine (**7**) (Fig. 1.21) obtained using a BCA, are shown in Figs. 1.22 and 1.23, respectively. The greater ease of operation and lower cost of this instrument makes this an attractive alternative to the FT-IR microscope for reaction monitoring on polymer beads.

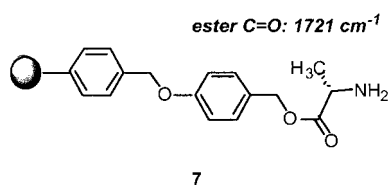


Fig. 1.21 Wang resin-supported alanine (**7**).

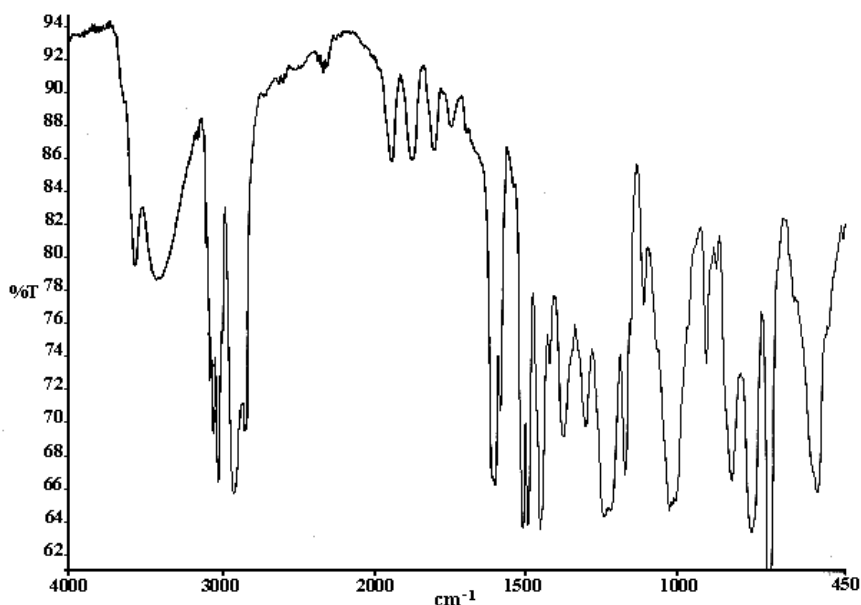


Fig. 1.22 FT-IR spectrum obtained using the BCA for Wang alcohol resin (**4**).

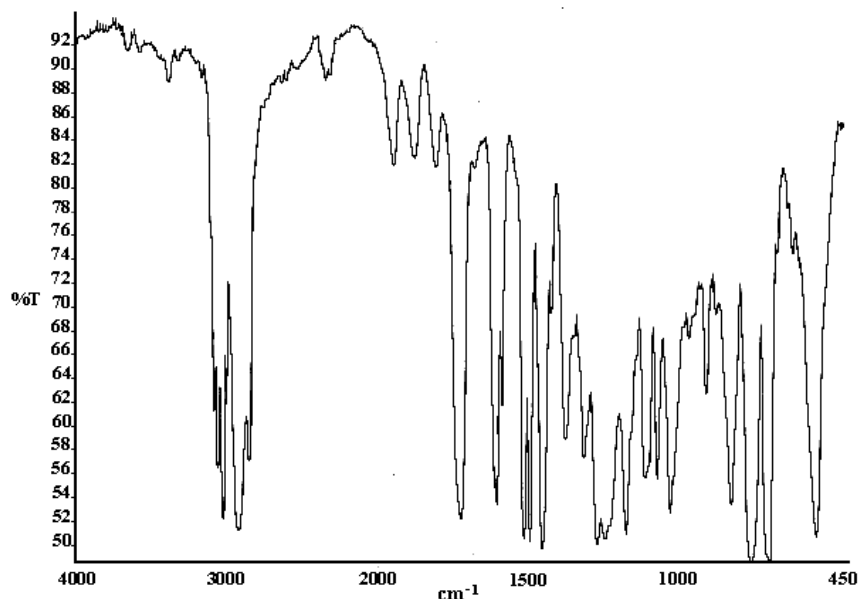
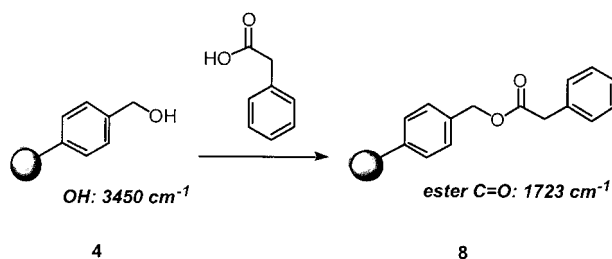


Fig. 1.23 FT-IR spectrum obtained using the BCA for Wang resin-supported **alanine (7)**.

#### Attenuated Total Reflection (ATR) FT-IR

ATR FT-IR spectroscopy allows for analysis of the polymer surface, rather than the bulk of the sample. Whereas the spectra obtained from the FT-IR microscope and BCA are recorded in transmittance mode and are used to analyze the entire bead, an ATR objective can be brought into direct contact with the sample in order to yield information about the chemistry taking place mainly on the periphery of the bead. Some FT-IR microscopes are equipped with an ATR crystal, and ATR analysis can be achieved on a single bead [172], but there have been no reports of automated ATR instruments. This technique has been used in kinetic studies, to prove that the esterification of Wang resin (**4**) (Scheme 1.4) to give the corre-



Scheme 1.4 Esterification of Wang resin (**4**) monitored by ATR FT-IR.

sponding ester (**8**) occurs at the same rate at the surface and in the interior of the bead (where more than 99% of the active sites are located).

ATR FT-IR spectroscopy has also been employed to monitor the solid-phase synthesis of substituted benzopyranoisoxazoles [180]. Finally, Huber *et al.* [181] have also reported that this technique is particularly suitable for the characterization of supported molecules in combinatorial chemistry, as well as for the identification of side products and for Photoacoustic (PA) FT-IR.

#### **Photoacoustic (PA) FT-IR**

PA FT-IR has been successfully used by Gosselin *et al.* [182] for monitoring a solid-phase multi-step synthesis. However the use of PA FT-IR is not yet widespread, even though it is nondestructive and allows surface analysis. This could be caused by the high cost of the instrumentation coupled with larger sample requirements and slightly longer acquisition times.

#### **Diffuse Reflectance FT-IR (DRIFT) spectroscopy**

The IR spectra of supported compounds can be obtained using a DRIFT accessory on a conventional FT-IR instrument. The quality of a DRIFT spectrum is usually higher than that obtained from the traditional KBr disk or pellet (recorded using the transmission mode). It is now possible to avoid the need for KBr dilution of the sample, by use of a specially constructed metal cup. This method is nondestructive and therefore allows recovery of the resin after analysis. Chan and co-workers [183] have successfully demonstrated the advantages of this technique in their study of the conversion of a supported azide to the amine derivative. The complete disappearance of the azide band (at  $2108\text{ cm}^{-1}$ ) could be easily monitored using this instrumentation. In addition, this rapid technique has also been used in conjunction with automation for high-throughput analysis [183]. Finally, Deben *et al.* [184] have reported the development of a DRIFT microcup with a smaller sample volume (0.5–1 mg), which gives similar results to those obtained using the conventional DRIFTS.

#### **Raman spectroscopy**

Raman has also been reported for the analysis of supported compounds, and is complementary to the infrared techniques described above. FT-Raman spectroscopy can be used to detect those functional groups which are IR-inactive or that only give rise to weak signals. A potential disadvantage is that, depending on the wavelength of the exciting light used, significant levels of fluorescence can also arise e.g. from polystyrene resins, and mask the bands being sought. In this respect an instrument employing a near IR laser source is more versatile. Despite this, single bead FT-Raman and FT-IR have been used successfully in conjunction to identify tagged supported molecules present in a combinatorial library [185]. IR or Raman-active functional groups present in each compound had been carefully chosen and used as tags to allow rapid and unambiguous identification of each li-

brary member. More recently, Raman spectroscopy has been used to determine that active sites within polymer beads are uniformly distributed [186]. In addition there have also been several other excellent reports on the application of FT-Raman spectroscopy in the characterization of polymer supports and in the monitoring of solid-phase reactions [165, 187–191].

#### 1.5.3.4 Nuclear Magnetic Resonance (NMR) Spectroscopy

##### Solid state $^{13}\text{C}$ NMR

NMR spectroscopy is perhaps the most important and valuable analytical tool for characterizing the molecular structure of molecules in solution, and it is not surprising that considerable efforts have been made to apply analogous techniques in the evaluation of polymer samples. Unfortunately the cross-linked nature of polymer resins means that isotropic solutions cannot be prepared and hence normal solution phase NMR methodologies cannot be applied. In principle of course solid phase NMR spectroscopy should be useful but again unfortunately the chemical shift anisotropy of  $^{13}\text{C}$  centers in a solid sample arising from the low level of molecular motion means that the resonances are broadened significantly, typically to a degree that fingerprinting of chemical structures becomes very difficult. The situation with  $^1\text{H}$  nuclei is even worse since the high abundance of  $^1\text{H}$  gives rise to excessive dipolar interactions, which adds further to the broadening of signals. In the case of  $^{13}\text{C}$  spectra but not  $^1\text{H}$  spectra the situation is improved considerably by magic angle spinning (MAS) which reduces the broadening, and signal intensity is improved by applying cross-polarization (CP) techniques. Solid state  $^{13}\text{C}$  CP-MAS NMR analysis can therefore be very valuable in analyzing resins [192]. The conventional instrumental methodologies used mean that the data produced is qualitative only i.e. it is not possible to deduce the relative numbers of different  $^{13}\text{C}$  nuclei present. However, by applying the single pulse excitation (SPE) technique quantitative spectra can be obtained and interpreted to give accurate relative abundance of different  $^{13}\text{C}$  nuclei. Using this approach Snape *et al.* have been able to evaluate the structure of anion exchange resins and their precursors [193], similarly they have been able to quantify the structural composition of high surface area highly cross-linked polystyrene resins [194], and indeed made similar evaluation of Davankov hypercross-linked resins [195]. Having said this the SPE technique is not routine and is time consuming. Furthermore the quality, and particularly the resolution, of the spectra obtained are far below that of solution phase spectra and hence the potential scope for application of these methods is limited.

Interestingly however as early as 1971 Sternlicht *et al.* [196] realized that cross-linked resins sufficiently swollen with solvent were sufficiently mobile to yield much improved  $^{13}\text{C}$  NMR spectra, and from this early work gel-phase NMR has emerged.

**Gel-phase  $^{13}\text{C}$  NMR spectroscopy**

The gel-phase  $^{13}\text{C}$  NMR spectrum of solvent-swollen beads can be obtained using a conventional NMR spectrometer. Appropriate gels display a higher degree of motional freedom, giving rise to sharper resonances compared with their solid counterparts. Sternlicht *et al.* [196] reported an NMR study of PS-DVB beads and found that the line width was crucially dependent on the amount of cross-linking of the polymer support, the lower the cross-link ratio the sharper the NMR resonances. Hence gel-phase NMR is mainly used for PS beads with low DVB content (1–2%). It was also found that the signals from the rigid polymer backbone were much broader than those of highly mobile pendant chains. For this reason, resins containing long spacer chains are excellent for such NMR analysis. For example, the commercially available TentaGel (**9**) and ArgoGel (**10**) resins contain a PEG chain grafted onto PS-DVB beads (Fig. 1.24) and indeed the optimal length of the PEG chain in TentaGel was deduced from a  $^{13}\text{C}$  NMR relaxation time study [197].

In several early reports [198–200] the gel-phase  $^{13}\text{C}$  NMR spectra of chloromethylated polystyrenes clearly showed the characteristic signal at  $\delta$  46.3 ppm (for  $\text{CH}_2\text{Cl}$ ). Some reports also indicated that the intensity of this signal could be used to estimate the level of chloromethylation of the resin. Since these early studies, this technique has been exploited by a number of groups in the area of solid-phase peptide synthesis [192, 197, 201–203]. Epton's group for example have published remarkably detailed  $^{13}\text{C}$  NMR spectra from their 'high load' gels [204]. More recently, the technique has also been reported in SPOS studies as a tool for reaction monitoring. For instance, the solid-phase synthesis of a thiazolidinone (**12**) (Scheme 1.5) using isotopically-labeled (**11**) attached to a PS-PEG (TentaGel)

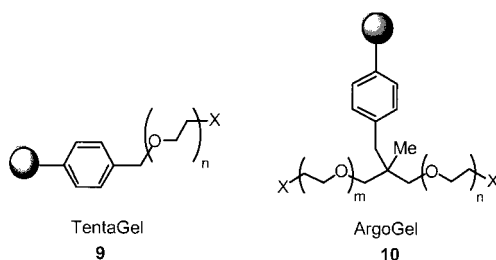
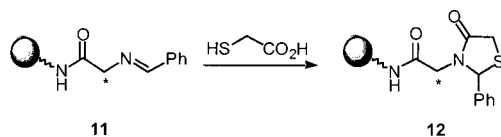


Fig. 1.24 Structures of TentaGel (**9**) and ArgoGel (**10**) resins.



Scheme 1.5 Solid phase synthesis of  $^{13}\text{C}$ -labelled thiazolidinone (**12**) monitored by Gel-phase  $^{13}\text{C}$  NMR spectroscopy.

resin could be easily monitored [205]. The signal for the labeled carbon at  $\delta$  64 ppm for (**11**) gradually disappeared as the peak at  $\delta$  46 ppm for (**12**) increased over the course of the reaction.

Despite the success with gel-phase  $^{13}\text{C}$  NMR spectroscopy the spectra obtained are of limited value because of the broad peaks, and indeed the  $^{13}\text{C}$  NMR spectra of unlabelled samples need relatively long acquisition times (because of the low abundance of  $^{13}\text{C}$ ) especially with lightly loaded resins such as TentaGel and Argo-Gel.  $^{19}\text{F}$  NMR [206, 207] and  $^{31}\text{P}$  NMR [208, 209] spectroscopy of gel beads have also been shown to be a convenient NMR technique for monitoring reactions of fluorine or phosphorous-containing molecules, respectively, attached to solvent-swollen polymer supports.

### Gel-phase (HR-MAS) NMR

As mentioned earlier magic angle spinning (MAS) NMR spectroscopy has been widely used to reduce spectral peak width in the characterization of solids. The method relies on spinning the sample at the angle of  $54.7^\circ$  in order to remove the orientational anisotropy in the solid and hence reduce some of the line broadening found in heterogeneous samples. Frechet *et al.* [210] first reported the use of a MAS NMR probe in conjunction with gel-type resins, which resulted in the reduction of line widths and improvement of signal-to-noise ratios. In the case of Merrifield resins with low degrees of cross-linking, it was shown that the disappearance of the peak at  $\delta$  4.38 ppm (for  $\text{CH}_2\text{Cl}$ ) could be used to monitor the progress of the reaction [211].

The most significant development in this field however has been the design of a high resolution MAS (HR-MAS) NMR probe by Varian [212]. This was shown to be superior to previously used NMR techniques [213] and to give high quality 1-D and 2-D  $^1\text{H}$  NMR spectra using only small quantities of the resin-bound substrates [214]. This convenient and fast technique was also shown to be suitable for monitoring of solid-phase reactions [215]. An elegant example was reported by Sarkar and co-workers [216] where a single-bead HR-MAS NMR spectrum was obtained for a  $^{13}\text{C}$ -labelled substrate.

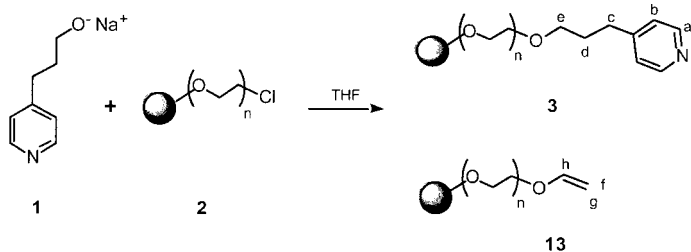
The use of this analytical technique for the characterization of polymer-supported molecules has been the subject of several excellent review articles [217–220].

HR-MAS NMR can also be used to identify reaction side-products, as well as to explore molecular recognition processes [147, 221] taking place between receptors and ligands attached to the support. In a recent example reported by de Miguel *et al.* [147] the attachment of a pyridyl ligand (**1**) onto an ArgoGel resin (**2**) was investigated (Scheme 1.6). The  $^1\text{H}$  HR-MAS NMR spectrum (Fig. 1.25) allowed confirmation of the structure of the bound ligand (**3**) (without the need for cleavage of the product) as well as the detection of the enol ether side-product (**13**).

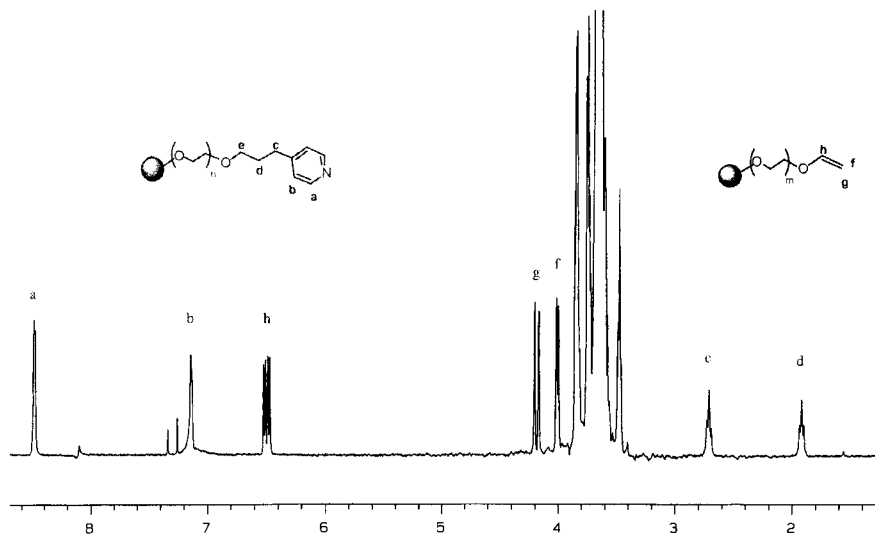
### NMR as a quantitative tool

Resin loadings can be determined using either gel-phase  $^{19}\text{F}$  NMR, [222, 223]  $^{13}\text{C}$  MAS NMR (in a conventional solid-state probe) [187, 224] or using  $^1\text{H}$  HR-MAS





**Scheme 1.6** Immobilization of pyridyl ligand (1) via Williamson ether formation.



**Fig. 1.25** Gel-phase  $^1\text{H}$  HR-MAS NMR spectrum of resin containing pyridyl ligand (3) and the enol ether side-product (13).

NMR spectroscopy [225]. The measurement of enantiomeric excesses of supported substrates has also been achieved by HR-MAS NMR [226].

#### 1.5.4

#### Spatial Analysis of Resins

All of the previously described chemical structural analysis provides an average molecular picture of a resin bead, or more often a collection of resin beads. For most applications this is all that is required. In some circumstances however it is important to have a knowledge of the spatial distribution of functional groups in a resin bead in order to interpret experimental data in an optimal way. This might be true for example in a screening methodology involving beads, or when resin particles are being exploited as catalysts.

As early as 1971 Merrifield [227] was keen to show that oligopeptide synthesis on a resin occurred uniformly throughout the swollen bead and he demonstrated

this very elegantly with an autoradiograph of a single 1% cross-linked polystyrene bead containing a tritium labeled peptide.

With polymer-supported catalysts the behavior of a catalyst, and in particular its mass transfer characteristics, can be influenced significantly with differences in spatial distribution of the catalyst sites. At one extreme the catalytic centers may be uniformly distributed throughout beads and at the other they may be restricted to a pellicular or surface shell on the bead. In the case of macroporous resins they may also be distributed specifically on or near the surface of the pores within the bead. Since the spatial resolution of all current techniques is relatively limited, the latter situation is particularly difficult to detect and in particular to distinguish from a uniform distribution throughout a bead. Nevertheless the cross-sectional area of a single bead can be examined in a SEM fitted with a microprobe. The latter can be tuned to a particular element and then scanned across a diameter of the bead section to give a concentration profile of the particular element. Thus for example depending on the method of preparation a sulfonic acid resin catalyst might display a high sulfur content at the ends of the diameter (i.e. in the bead periphery) or yield a uniform signal across the whole diameter [228]. Much higher resolution information can be obtained using a suitable transmission electron microscope (TEM). Many of these are able to produce an image tuned to a particular element, again when sampling a section of a bead. Typically the latter may have been microtomed to  $\sim 90$  nm thickness. Spratt *et al.* [229] have reported on the distribution of Mo centers in a polymer-supported alkene epoxidation catalyst using this method. In this case the Mo  $K_{\alpha}$  X-ray was used to generate the elemental map. Heavy atoms of this type are relatively easily monitored but to produce elemental maps of light atoms requires an appropriate camera. Nevertheless, providing this is available light atom maps can also be produced in the TEM. Huxham *et al.* [230] have, for example, mapped the sorption of cephalosporin C on a macroporous resin. In this case the element mapped was the nitrogen in the antibiotic molecule.

Useful as the above methods are the techniques are complex, involve costly instrumentation and are time consuming. In terms of making spatially and time-resolved single bead analysis more accessible, and hence more broadly applicable, optical microscopic techniques have much to offer. Whole bead analysis using conventional fluorescence labeling [231, 232] appears to have thrown up conflicting and confusing results in terms of the uniformity of fluorophore distribution presumably arising from the 'lensing' effect of a bead. Scanning confocal Raman spectroscopy on single beads in which 'slices' of the bead are probed successively seems to deliver more realistic and reliable results [233]. However, in a comparison of single bead confocal and nonconfocal fluorescence microscopy data with fluorescence images of microtomed slices of beads, the latter seem to provide the most realistic representations [234]. Clearly therefore these techniques also need to be applied with considerable care in order to avoid the generation of artefactual data.

## 1.6

## Challenges for the Future

Other chapters in this book will describe the developments of new polymer supports which move on and away from conventional resin beads. However, there is no 'magic' polymer support which is optimal for all applications and the novel morphological variants of resin beads reviewed in this chapter offer new opportunities and require extensive evaluation in a range of applications. This work is already ongoing.

The characterization of support morphology in the physical state in which the support is used remains problematical. ISEC offers one solution and the provision of a commercially available instrument and associated software would be a big step forward. Again there are signs that this development is underway. Notwithstanding this there remains considerable scope for alternative user-friendly techniques to be developed and this is a challenge for physical chemists and physicists.

Although the latest developments in molecular structural analysis on-the-bead using FT-IR and HR-MAS NMR have improved our understanding of resin chemistry, these instrumental techniques are costly and not widely accessible. Alternative cheaper instrumentation is required that is capable of providing equally definitive structural information. One major area remains almost totally inaccessible in terms of high resolution molecular structural analysis and that is heavily cross-linked macroporous resins. Where the structure to be probed is a bound inorganic complex e.g. in a polymer-supported metal complex catalyst, then X-ray absorption fine structure (EXAFS) analysis can be useful [229]. However, this technique requires a synchrotron radiation source and anyway is of no value for structural analysis of organic moieties. Some breakthrough in NMR techniques is required.

What is clear however is that polymer-supported chemistry now has a solid base in chemistry and will play an increasing role in the discipline as it expands and interacts with other scientific disciplines.

## 1.7

## References

- 1 G. MOAD, D.H. SOLOMON, *The Chemistry of Free Radical Polymerisation*, Pergamon, Oxford, UK, 1995.
- 2 *Controlled Radical Polymerisation* ed. K. Matyjaszewski, ACS Symposium Series 685, Amer. Chem. Soc., Washington DC, USA, 1998.
- 3 M. SZWARC, M. VAN BEYLEN, *Ionic Polymerisation and Living Polymers* Chapman and Hall, New York, USA, 1993.
- 4 W. KURAN, *Principles of Co-ordination Polymerisation* J. Wiley and Sons, Chichester, UK, 2001.
- 5 A. AKELAH, D.C. SHERRINGTON, *Chem. Rev.*, **1981**, 81, 557–587.
- 6 S.V. LEY, I.R. BAXENDALE, R.N. BREAN, *et al.*, *J. Chem. Soc., Perkin 1.*, **2000**, 3815–4195.
- 7 *Polymer-Supported Reactions in Organic Synthesis*, ed. P. HODGE, D.C. SHERRINGTON, J. Wiley and Sons, Chichester, UK, 1980.

- 8 *Syntheses and Separations using Functional Polymers*, ed. D.C. SHERRINGTON, P. HODGE, J. Wiley and Sons, Chichester, UK, **1988**.
- 9 *Combinatorial Peptide and Non-peptide Libraries*, ed. G. JUNG, VCH, Weinheim, Germany, **1996**.
- 10 *Solid-supported Combinatorial and Parallel Synthesis of Small-Molecular-Weight Compound Libraries*, eds. D. OBRECHT, J.M. VILLALGORDO, Pergamon, Oxford, UK, **1998**.
- 11 P. SENEĆI, *Solid-phase Synthesis and Combinatorial Technologies*, Wiley-Interscience, New York, USA, **2000**.
- 12 *Chiral Catalyst Immobilisation and Recycling*, eds. D.E. DE Vos, I.F.J. VANKELECOM, P.A. JACOBS, Wiley-VCH, Weinheim, Germany, **2000**.
- 13 E.A. GRULKE, *Suspension Polymerisation in Encyclopedia of Polymer Science and Engineering* eds H.F. MARK, N.M. BIKALES, C.G. OVERBERGER, *et al.*, John Wiley and Sons, New York, **1989**, Vol. 16, p. 443.
- 14 *Ion Exchangers*, ed. K. Dorfner, Walter de Gruyter, Berlin, Germany, **1991**.
- 15 See Appendix in ref 7.
- 16 D.C. SHERRINGTON, A. LANVER, H-G. SCHMALZ, *et al.*, *Angew. Chem.*, **2002**, 114, 3808–3811, *Angew. Chem. Int. Ed.*, **2002** 41, 3656–3659.
- 17 A. GUYOT in Ref 8, chapter 1, p 1.
- 18 R.L. ALBRIGHT, *React. Polym.*, **1986**, 4, 155–174.
- 19 D.C. SHERRINGTON, *Chem. Commun.*, **1998**, 2275–2286.
- 20 O. OKAY, *Prog. Polym. Sci.*, **2000**, 25, 711–779.
- 21 K.S.W. SING, D.H. EVERETT, R.A.W. HAUL, *et al.*, *Pure Appl. Chem.*, **1985**, 57, 603–619.
- 22 S. KIATKAMJORNWONG, P. CHIENACHAKUL, P. PRASASSARAKICH *et al.*, *J. Appl. Polym. Sci.*, **2001**, 82 1521–1540.
- 23 M.G.J.T. MORRISON, Ph.D Thesis, University of Strathclyde, Glasgow, UK., **2000**.
- 24 S.M. HOWDLE, K. JERABEK, V. LEOCORBO, *et al.*, *Polymer Comm.*, **2000**, 41, 7273–7277.
- 25 V.A. DAVANKOV, S.V.R. ROGOSHIN, M.P. TSYRUPA, *J. Polym. Sci., Polym. Symp.*, **1974**, 47, 95–101.
- 26 V.A. DAVANKOV, M.P. TSYRUPA, *React. Polym.*, **1990**, 13, 27–42.
- 27 J.A. DALE, N.V. NIKITIN, Technical Notes on Hypersol-Macronet, Purolite Intl, Pontyclun, S. Wales, UK.
- 28 R.V. LAW, D.C. SHERRINGTON, C.E. SNAPE, *et al.*, *Macromols.*, **1996**, 29, 6284–6293.
- 29 S.N. SIDOROV, I.V. VOLKOV, V.A. DAVANKOV, *et al.*, *J. Am. Chem. Soc.*, **2001**, 123, 10502–10510.
- 30 J.E. SEEMAN, *Life During a Gold Age of Peptide Chemistry* Amer. Chem. Soc., Washington, D.C., USA, **1993** p 82.
- 31 J.G. HEFFERNAN, S.B. KINGSTON, D.C. SHERRINGTON *J. App. Polym. Sci.*, **1983**, 28, 3137–3144.
- 32 E. BAYER, *Angew. Chem.*, **1991**, 103, 117, *Angew. Chem. Int. Ed.- Engl.*, **1991**, 30, 113–129.
- 33 E. BAYER, W. RAPP, GP DE-A3714258 (**1988**).
- 34 W. RAPP, see ref 9, p 425.
- 35 Argonaut Technologies Inc., San Carlos, CA 94070, USA – ArgoGel® and Argo Pore-resins.
- 36 R. HAAG, *Chem. Eur. J.*, **2001**, 7, 327–335.
- 37 V. SWALI, N.J. WELLS, G.J. LANGLEY *et al.*, *J. Org. Chem.*, **1997**, 62, 4902–4903.
- 38 P. BHARATHI, J.S. MOORE, *J. Am. Chem. Soc.*, **1997**, 119, 3391–3392.
- 39 A. MAHAJAN, S.R. CHABRA, W.C. CHAN, *Tetrahedron Lett.*, **1999**, 40, 4909–4912.
- 40 P. ARYA, N.V. RAO, J. SINGKHONRAT, *J. Org. Chem.*, **2000**, 65, 1881–1885.
- 41 C. FROMONT, M. BRADLEY, *Chem. Commun.*, **2000**, 283–284.
- 42 N. OBRIEN, A. MCKEE, D.C. SHERRINGTON, *et al.*, *Polymer Comm.*, **2000**, 41, 6027–6031.
- 43 P.A. COSTELLO, A.T. SLARK, D.C. SHERRINGTON *et al.*, *Polymer*, **2002**, 43, 245–254.
- 44 S. DURIE, K. JERABEK, C. MASON *et al.*, *Macromolecules.*, **2002**, in press.
- 45 R.A. HOUGHTON, *Proc. Natl. Acad. Sci.*, **1985**, 82, 5131–5134.
- 46 K.C. NICOLAU, X.-Y. XIAO, Z. PARANDEOSH, *et al.*, *Angew. Chem.*, **1995**, 107, 2476–2479. *Angew. Chem. Intl. Ed.*, **1995**, 34, 2289–2291.
- 47 A.G. BECK-SICKINGER, G. JUNG in ref. 9 p82.

- 48 P. H. FINDLAY, S.-M. LEINONEN, M. G. J. T. MORRISON, *et al.*, *J. Mater. Chem.*, **2000**, 10, 2031–2034.
- 49 A. HAYNES, P. M. MAITLES, R. QUYOUM, *et al.* in *Supported Catalysts and their Applications* ed. D. C. SHERRINGTON, A. P. KYBETT, Royal Soc. Chem., Cambridge, UK, **2001**, p166.
- 50 W. J. OHAGAN, M. MCKENNA, D. C. SHERRINGTON, *et al.*, *Meas. Sci. Technol.*, **2002**, 13, 84–91.
- 51 N. HIRD, I. HUGHES, D. HUNTER, *et al.*, *Tetrahedron*, **1999**, 55, 9575–9584.
- 52 J. A. TRIPP, F. SVEC, J. M. J. FRÉCHET, *J. Combi. Chem.*, **2001**, 3, 216–223.
- 53 A. R. VAINO, K. JANDA, *Proc. Natl. Acad. Sci, USA*, **2000**, 97, 7692–7696.
- 54 U. MEYER, F. SVEC, J. M. J. FRÉCHET, *et al.*, *Macromolecules*, **2000**, 33, 7769–7775.
- 55 R. KOBYLECKI, GB Patent Application GB99/03406 (to Povair Sciences).
- 56 B. ATRASH, M. BRADLEY, R. KOBYLECKI, *et al.*, *Angew Chem.*, **2001**, 113, 967–970, *Angew. Chem. Intl. Ed.*, **2001**, 40, 938–941.
- 57 D. BARBY, Z. HAQ, *Europ. Pat. Appl. EP 60138*, 1982 (to Unilever).
- 58 N. R. CAMERON, D. C. SHERRINGTON, *Adv. Polym. Sci.*, **1996**, 126, 163–214.
- 59 N. R. CAMERON in *Monolithic Materials: Preparation, Properties and Applications*, eds. F. SVEC, Z. DEYL, T. B. TENNIKOVA, Elsevier, Amsterdam, **2002**, in press.
- 60 D. C. SHERRINGTON, P. W. SMALL, *Chem. Commun.*, **1989**, 21, 1589–1591.
- 61 H. F. M. SCHOO, G. CHALLA, B. ROWATT *et al.*, *React. Polym.*, **1991/2**, 16, 125–136.
- 62 M. OTTENS, G. LEENE, A. A. C. M. BEEN-ACKERS, *et al.*, *Ind. Engng. Chem. Res.*, **2000**, 39, 259–266.
- 63 P. KRAJNC, J. F. BROWN, N. R. CAMERON, *Org. Lett.*, **2002**, 4, 2497–2500.
- 64 P. HAINEY, I. M. HUXHAM, B. ROWATT, *et al.*, *Macromolecules*, **1991**, 24, 117–121.
- 65 N. R. CAMERON, A. BARBETTA, *J. Mater. Chem.*, **2000**, 10, 2466–2472.
- 66 W. BUSBY, N. R. CAMERON, C. A. B. JAHODA, *Biomacromols.*, **2001**, 2, 154–164.
- 67 *Monolithic Materials: Preparation, Properties and Applications*, eds. F. SVEC, Z. DEYL, T. B. TENNIKOVA, Elsevier, Amsterdam, ISBN 0-444-50879-1, 2003
- 68 S. ROE, D. C. SHERRINGTON, *Europ. Polym. J.* **1987**, 23, 195–199.
- 69 F. L. BERNARDIS, Ph.D Thesis, University of Strathclyde, Glasgow, **2002**, p. 48.
- 70 K. W. PEPPER, D. REICHENBERG, D. K. HALE, *J. Chem. Soc.*, **1952**, 3129.
- 71 J. A. GREIG, D. C. SHERRINGTON, *Polymer*, **1978**, 19, 163–172.
- 72 I. M. ABRAMS, J. R. MILLAR, *React. Funct. Polym.*, **1997**, 35, 7–22.
- 73 S. P. ROE, D. C. SHERRINGTON, *React. Polym.*, **1989**, 11, 301–308.
- 74 X. H. WANG, J. YAN, C. C. ZHOU, *J. Appl. Polym. Sci.*, **2000**, 78, 250–258.
- 75 M. C. MCCAIRN, S. R. TONGE, A. J. SUTHERLAND, *J. Org. Chem.*, **2002**, 67, 4847–4855.
- 76 M. E. WILSON, K. PAECH, W. JING ZHOU *et al.*, *J. Org. Chem.*, **1998**, 63, 5094–5099.
- 77 J. BUCHARDT, M. MELDAL, *Tetrahedron Lett.*, **1998**, 39, 8695–8698.
- 78 J. ROUQUEROL, D. AVNIR, C. W. FAIRBRIDGE, *et al.*, *Pure Appl. Chem.* **1994**, 66, 1739–1758.
- 79 P. A. WEBB, C. ORR, *Analytical Methods in Fine Particle Technology*, Micromeritics Instrument Corp., Norcross, GA, USA **1997**.
- 80 K. SING, *Colloids Surf., A* **2001**, 187–188, 3–9.
- 81 C. K. LEE, A. S. T. CHIANG, C. S. TSAY, *Key Eng. Mater.* **1996**, 115, 21–43.
- 82 K. MORISHIGE, M. SHIKIMI, *J. Chem. Phys.* **1998**, 108, 7821–7824.
- 83 S. BRUNAUER, P. H. EMMETT, E. TELLER, *J. Am. Chem. Soc.* **1938**, 60, 309–319.
- 84 I. LANGMUIR, *J. Am. Chem. Soc.* **1916**, 38, 2221–2295.
- 85 E. P. BARRETT, L. G. JOYNER, P. P. HALENDA, *J. Am. Chem. Soc.* **1951**, 73, 373–380.
- 86 C. LASTOSKIE, K. E. GUBBINS, N. QUIRKE, *J. Phys. Chem.* **1993**, 97, 4786–4796.
- 87 P. I. RAVIKOVITCH, A. V. NEIMARK, *Colloids Surf., A* **2001**, 187–188, 11–21.
- 88 S. R. BROADBENT, J. M. HAMMERSLEY, *Proc. Cambridge Phil. Soc.* **1957**, 53, 629–641.
- 89 N. A. SEATON, *Chem. Eng. Sci.* **1991**, 46, 1895–1909.
- 90 T. ROHR, S. KNAUS, H. GRUBER, *et al.*, *Macromolecules* **2002**, 35, 97–105.
- 91 C. A. LEÓN Y LEÓN, *Adv. Colloid Interface Sci.* **1998**, 76–77, 341–372.

- 92 H. L. RITTER, L. C. DRAKE, *Ind. Eng. Chem., Anal. Ed.* **1945**, *17*, 782–786.
- 93 E. W. WASHBURN, *Proc. Natl. Acad. Sci. U.S.A.* **1921**, *7*, 115–116.
- 94 R. P. MAYER, R. A. STOWE, *J. Colloid Sci.* **1965**, *20*, 893–911.
- 95 R. POSPECH, P. SCHNEIDER, *Powder Technol.* **1989**, *59*, 163–171.
- 96 J. W. MCBAIN, *J. Am. Chem. Soc.* **1935**, *57*, 699–700.
- 97 E. M. SUUBERG, S. C. DEEVI, Y. YUN, *Fuel* **1995**, *74*, 1522–1530.
- 98 L. ABRAMS, R. MAYNARD, C. FAVORITE, *Microreport* **2002**, *7*, 1–7.
- 82 (Available from Micromeritics Instrument Corp., Norcross, GA, USA)
- 99 B. D. ADKINS, B. H. DAVIS, *Adsorpt. Sci. Technol.* **1988**, *5*, 76–93.
- 100 T. ROHR, Ph.D Thesis, Technical University of Vienna, Vienna, Austria, 1999.
- 101 T. ROHR, C. YÜ, M. H. DAVEY, *et al.*, *Electrophoresis*, **1999**, *50*, 286–292.
- 102 K. JERABEK in *Cross evaluation strategies in size exclusion chromatography* eds. M. POTSCHKA, P. L. DUBIN, Amer. Chem. Soc. Symp. Series No 635, Amer. Chem. Soc., Washington, D.C., USA, p 211.
- 103 K. JERABEK, *Anal. Chem.*, **1985**, *57*, 1598–1602.
- 104 G. OGSTON, *Trans. Faraday Soc.*, **1958**, *54*, 1754–1757.
- 105 I. M. HUXHAM, B. ROWATT, D. C. SHERRINGTON *et al.*, *Polymer*, **1992**, *33*, 2768–2777.
- 106 I. M. HUXHAM, B. ROWATT, D. C. SHERRINGTON *et al.*, *J. Mater. Chem.*, **1994**, *4*, 253–255.
- 107 M. BRUN, A. LALLEMAND, J. F. QUINSON *et al.*, *Thermochim. Acta*, **1977**, *21*, 59–63.
- 108 M. BRUN, J. F. QUINSON, R. BLANC, *et al.*, *Makromol. Chem.*, **1981**, *182*, 873–882.
- 109 J. BALDRIAN, B. N. KOLARZ, H. GALINA *Collect. Czech. Chem. Commun.* **1981**, *46*, 1675–1682.
- 110 P. J. HALL, W. R. MACHADO, D. G. GALAN, *et al.*, *J. Chem. Soc., Farad. Trans.*, **1996**, *92*, 2607–2610.
- 111 P. J. HALL, D. G. GALAN, W. R. MACHADO, *et al.*, *J. Chem. Soc., Farad. Trans.*, **1997**, *93*, 463–466.
- 112 R. B. MERRIFIELD, *J. Am. Chem. Soc.*, **1963**, *85*, 2149–2154.
- 113 D. C. SHERRINGTON in Ref 7, chapter 3, p 157.
- 114 F. BALKENHOHL, C. VONDEMBUSCHE-HUNNEFELD, A. LANSKY *et al.*, *Angew. Chem., Int. Ed. Engl.*, **1996**, *35*, 2289–2337.
- 115 I. C. CHOONG, J. A. ELLMAN, *Annual Reports In Medicinal Chemistry*, **1996**, *31*, 309–318.
- 116 J. S. FRUCHTEL, G. JUNG, *Angew. Chem.* **1996**, *108*, 19–46, *Angew. Chem., Int. Ed. Engl.*, **1996**, *35*, 17–42.
- 117 P. H. H. HERMKENS, H. C. J. OTTENHEIJM, D. REES, *Tetrahedron*, **1996**, *52*, 4527–4554.
- 118 P. H. H. HERMKENS, H. C. J. OTTENHEIJM, D. C. REES, *Tetrahedron*, **1997**, *53*, 5643–5678.
- 119 K. W. KUNTZ, M. L. SNAPPER, A. H. HOVEYDA, *Curr. Opin. Chem. Biol.*, **1999**, *3*, 313–319.
- 120 H. WENNEMERS, *Comb. Chem. High T. Scr.*, **2001**, *4*, 273–285.
- 121 F. GENNARI, P. SENEĆI, S. MIERTUS, *Catal. Rev. Sci. Eng.*, **2000**, *42*, 385–402.
- 122 P. P. PESCARMONA, J. C. VAN DER WAAL, I. E. MAXWELL *et al.*, *Catal. Lett.*, **1999**, *63*, 1–11.
- 123 E. W. MCFARLAND, W. H. WEINBERG, *Trends Biotechnol.*, **1999**, *17*, 107–115.
- 124 B. J. EGNER, M. BRADLEY, *Drug Discov. Today*, **1997**, *2*, 102–109.
- 125 M. A. GALLOP, W. L. FITCH, *Curr. Opin. Chem. Biol.*, **1997**, *1*, 94–100.
- 126 B. YAN, *Analytical methods in combinatorial chemistry*, Technomic, Pennsylvania, USA, **2000**.
- 127 N. K. TERRETT, Chapter 8: Analysis of chemistry and products, in *Combinatorial chemistry*, in *Oxford Chemistry Masters*, eds. S. G. DAVIES, R. G. COMPTON, J. EVANS, Oxford University Press, New York, **1998**.
- 128 P. SENEĆI, Chapter 1.3: Reaction monitoring in Solid-phase synthesis, in *Solid-phase synthesis and combinatorial technologies*, Wiley, New York, **2000**.
- 129 G. OLASON, D. C. SHERRINGTON, *Macromolecular Symposia*, **1998**, *131*, 127–146.
- 130 C. ENJALBAL, J. MARTINEZ, J. L. AUBAGNAC, *Mass Spectrom. Rev.*, **2000**, *19*, 139–161.

- 131 J. W. METZGER, K.-H. WIESMULLER, V. GNAU, *et al.*, *Angew. Chem.*, **1993**, *105*, 901, *Angew. Chem., Int. Ed. Engl.*, **1993**, *32*, 894–896.
- 132 O. VORM, P. ROEPSTORFF, M. MANN, *Anal. Chem.*, **1994**, *66*, 3281–3287.
- 133 F. HILLENKAMP, M. KARAS, R. C. BEAVIS *et al.*, *Anal. Chem.*, **1991**, *63*, 1193–1203a.
- 134 B. J. EGNER, G. J. LANGLEY, M. BRADLEY, *J. Org. Chem.*, **1995**, *60*, 2652–2653.
- 135 B. J. EGNER, M. CARDNO, M. BRADLEY, *Chem. Commun.*, **1995**, 2163–2164.
- 136 T. B. WALK, A. W. TRAUTWEIN, H. RICHTER *et al.*, *Angew. Chem.*, **1999**, *111*, 1877–1880, *Angew. Chem., Int. Ed. Engl.*, **1999**, *38*, 1763–1765.
- 137 D. G. SCHMID, P. GROSCHE, H. BANDEL *et al.*, *Biotechnol. Bioeng.*, **2000**, *71*, 149–161.
- 138 R. D. SUSSMUTH, G. JUNG, *J. Chromatogr. B*, **1999**, *725*, 49–65.
- 139 V. SWALI, G. J. LANGLEY, M. BRADLEY, *Curr. Opin. Chem. Biol.*, **1999**, *3*, 337–341.
- 140 M. S. CONGREVE, S. V. LEY, J. J. SCICINSKI, *Chem. Eur. J.*, **2002**, *8*, 1768–1776.
- 141 O. LORTHIOIR, R. A. E. CARR, M. S. CONGREVE, *et al.*, *Anal. Chem.*, **2001**, *73*, 963–970.
- 142 M. R. CARRASCO, M. C. FITZGERALD, Y. ODA *et al.*, *Tetrahedron Lett.*, **1997**, *38*, 6331–6334.
- 143 M. S. CONGREVE, C. JAMIESON, *Drug Discov. Today*, **2002**, *7*, 139–142.
- 144 P. J. MURRAY, C. KAY, J. J. SCICINSKI, *et al.*, *Tetrahedron Lett.*, **1999**, *40*, 5609–5612.
- 145 M. S. CONGREVE, M. LADLOW, P. MARSHALL, *et al.*, *Org. Lett.*, **2001**, *3*, 507–510.
- 146 B. YAN, C. F. JEWELL, S. W. MYERS, *Tetrahedron*, **1998**, *54*, 11755–11766.
- 147 Y. R. DE MIGUEL, N. BAMPOS, K. M. N. DE SILVA, *et al.*, *Chem. Commun.*, **1998**, 2267–2268.
- 148 C. KAY, O. E. LORTHIOIR, N. J. PARR, *et al.*, *Biotechnol. Bioeng.*, **2000**, *71*, 110–118.
- 149 O. KUISLE, M. LOLO, E. QUINOJA *et al.*, *Tetrahedron*, **1999**, *55*, 14807–14812.
- 150 M. E. ATTARDI, A. FALCHI, M. TADDEI, *Tetrahedron Lett.*, **2000**, *41*, 7395–7399.
- 151 J. P. BADYAL, A. M. CAMERON, N. R. CAMERON, *et al.*, *Tetrahedron Lett.*, **2001**, *42*, 8531–8533.
- 152 J. J. COURNOYER, T. KSHIRSAGAR, P. P. FANTAUZZI, *et al.*, *J. Comb. Chem.*, **2002**, *4*, 120–124.
- 153 J. VAZQUEZ, F. ALBERICIO, *Tetrahedron Lett.*, **2001**, *42*, 6691–6993.
- 154 C. E. FREEMAN, A. G. HOWARD, *Analyst*, **2001**, *126*, 538–541.
- 155 A. G. M. BARRETT, Y. R. DE MIGUEL, *Tetrahedron*, **2002**, *58*, 3785–3792.
- 156 S. L. HSU, Chapter 20: IR Spectroscopy, in *Comprehensive Polymer Science*, Vol. 1, eds. C. Booth, C. Price, Pergamon, Oxford, UK, **1989**.
- 157 J. L. KOENIG, Chapter 3: Experimental IR Spectroscopy of Polymers, in *Spectroscopy of Polymers*, Amer. Chem. Soc., Washington, USA, **1991**, 43.
- 158 J. M. CHALMERS, N. J. EVERALL, *Internat. J. Polym. Anal. Characterisation*, **1999**, *5*, 223–245.
- 159 H. U. GREMLICH, *Biotechnol. Bioeng.*, **1998**, *61*, 179–187.
- 160 H. U. GREMLICH, *Am. Lab.*, **1998**, *30*, 33–37.
- 161 Y. R. DE MIGUEL, A. S. SHEARER, *Biotechnol. Bioeng.*, **2000**, *71*, 119–129.
- 162 B. YAN, H. U. GREMLICH, *J. Chromatogr. B*, **1999**, *725*–102.
- 163 B. YAN, Chapter 3: Solid-Phase Reaction Optimisation Using FTIR Methods, in *Analytical Methods in Combinatorial Chemistry*, Technomic, Pennsylvania, USA, **2000**, 52.
- 164 B. YAN, *Acc. Chem. Res.*, **1998**, *31*, 621–630.
- 165 B. YAN, H. U. GREMLICH, S. MOSS, *et al.*, *J. Comb. Chem.*, **1999**, *1*, 46–54.
- 166 B. YAN, G. KUMARAVEL, H. ANJARIA, *et al.*, *J. Org. Chem.*, **1995**, *60*, 5736–5738.
- 167 B. YAN, Q. SUN, J. R. WAREING *et al.*, *J. Org. Chem.*, **1996**, *61*, 8765–8770.
- 168 B. YAN, G. KUMARAVEL, *Tetrahedron*, **1996**, *52*, 843–848.
- 169 B. YAN, H. GSTACH, *Tetrahedron Lett.*, **1996**, *37*, 8325–8328.
- 170 D. E. PIVONKA, T. R. SIMPSON, *Anal. Chem.*, **1997**, *69*, 3851–3853.
- 171 D. E. PIVONKA, K. RUSSELL, T. GERO, *Appl. Spectrosc.*, **1996**, *50*, 1471–1478.
- 172 B. YAN, J. B. FELL, G. KUMARAVEL, *J. Org. Chem.*, **1996**, *61*, 7467–7472.
- 173 R. E. MARTI, B. YAN, M. A. JAROSINSKI, *J. Org. Chem.*, **1997**, *62*, 5615–5618.

- 174 Q. SUN, B. YAN, *Bioorg. Med. Chem. Lett.*, **1998**, 8, 361–364.
- 175 B. YAN, Q. SUN, *J. Org. Chem.*, **1998**, 63, 55–58.
- 176 B. YAN, W. B. LI, *J. Org. Chem.*, **1997**, 62, 9354–9357.
- 177 K. RUSSELL, D. C. COLE, F. M. McLAREN *et al.*, *J. Am. Chem. Soc.*, **1996**, 118, 7941–7945.
- 178 B. YAN, H. B. YAN, *J. Comb. Chem.*, **2001**, 3, 78–84.
- 179 W. J. HAAP, T. B. WALK, G. JUNG, *Angew. Chem.* **1998**, 110, 3506–3509, *Angew. Chem., Int. Ed. Engl.*, **1998**, 37, 3311–3314.
- 180 E. Y. CHAO, D. J. MINICK, D. D. STERNBACH, *et al.*, *Org. Lett.*, **2002**, 4, 323–326.
- 181 W. HUBER, A. BUBENDORF, A. GRIEDER *et al.*, *Anal. Chim. Acta*, **1999**, 393, 213–221.
- 182 F. GOSSELIN, M. DI RENZO, T. H. ELLIS *et al.*, *J. Org. Chem.*, **1996**, 61, 7980–7981.
- 183 T. Y. CHAN, R. CHEN, M. J. SOFIA, *et al.*, *Tetrahedron Lett.*, **1997**, 38, 2821–2824.
- 184 I. DEBEN, J. GOORDEN, E. VAN DOORNUM, *et al.*, *Eur. J. Org. Chem.*, **1998**, 697–700.
- 185 S. S. RAHMAN, D. J. BUSBY, D. C. LEE, *J. Org. Chem.*, **1998**, 63, 6196–6199.
- 186 J. KRESS, A. ROSE, J. G. FREY, *et al.*, *Chem. Eur. J.*, **2001**, 7, 3880–3883.
- 187 B. OTTENBOURGS, P. ADRIAENSSENS, R. CARLEER, *et al.*, *Polymer*, **1998**, 39, 5293–5300.
- 188 D. E. PIVONKA, R. B. SPARKS, *Appl. Spectrosc.*, **2000**, 54, 1584–1590.
- 189 D. E. PIVONKA, *J. Comb. Chem.*, **2000**, 2, 33–38.
- 190 J. RYTTERSGAARD, B. D. LARSEN, A. HOLM, *et al.*, *Spectrochim. Acta, Part A*, **1997**, 53, 91–98.
- 191 B. ALTAVA, M. I. BURGUETE, E. GARCIA-VERDUGO, *et al.*, *Tetrahedron*, **2001**, 57, 8675–8683.
- 192 R. V. LAW, D. C. SHERRINGTON in *Solid State NMR of Polymers*, eds. I. Ando, T. Asakura, Elsevier, Amsterdam, **1998**, Chap. 25, p. 509.
- 193 R. V. LAW, D. C. SHERRINGTON, C. E. SNAPE, *et al.*, *Ind. Eng. Chem. Res.*, **1995**, 34, 2740–2749.
- 194 R. V. LAW, D. C. SHERRINGTON, C. E. SNAPE, *Macromolecules*, **1997**, 30, 2868–2875.
- 195 R. V. LAW, D. C. SHERRINGTON, C. E. SNAPE, *et al.*, *Macromolecules*, **1996**, 29, 6284–6293.
- 196 H. STERNLICHT, G. L. KENYON, E. L. PACKER *et al.*, *J. Am. Chem. Soc.*, **1971**, 93, 199–208.
- 197 E. BAYER, K. ALBERT, H. WILLISCH, *et al.*, *Macromolecules*, **1990**, 23, 1937–1940.
- 198 S. MOHANRAJ, W. T. FORD, *Macromolecules*, **1985**, 18, 351–356.
- 199 S. L. MANATT, D. HOROWITZ, R. HOROWITZ *et al.*, *Anal. Chem.*, **1980**, 52, 1529–1532.
- 200 W. T. FORD, T. BALAKRISHNAN, in *Polymer Characterisation, Advances in Chemistry Series*, Vol. 203, ed. C. D. CRAVER, Amer. Chem. Soc., Washington, USA, **1983**, 475.
- 201 E. GIRALT, F. ALBERICIO, F. BARDELLA, *et al.*, in *Innovation and Perspectives in Solid Phase Synthesis*, Vol. ed. R. Epton, SPCC, UK, **1990**, 111.
- 202 E. GIRALT, J. RIZO, E. PEDROSO, *Tetrahedron*, **1984**, 40, 4141–4152.
- 203 A. G. LUDWICK, L. W. JELINSKI, D. LIVE, *et al.*, *J. Am. Chem. Soc.*, **1986**, 108, 6493–6496.
- 204 F. G. W. BUTWELL, R. EPTON, E. J. MOLE, N *et al.* in *Innovation and Perspectives in Solid Phase Synthesis*, ed. R. EPTON, SPCC, Birmingham, UK, **1990**, p. 121.
- 205 G. C. LOOK, C. P. HOLMES, J. P. CHINN *et al.*, *J. Org. Chem.*, **1994**, 59, 7588–7590.
- 206 A. SVENSSON, T. FEX, J. KIHLEBERG, *Tetrahedron Lett.*, **1996**, 37, 7649–7652.
- 207 M. J. SHAPIRO, G. KUMARAVEL, R. C. PETER *et al.*, *Tetrahedron Lett.*, **1996**, 37, 4671–4674.
- 208 R. QUARRELL, T. D. W. CLARIDGE, G. W. WEAVER *et al.*, *Molecular Diversity*, **1996**, 1, 223–232.
- 209 C. M. G. JUDKINS, K. A. KNIGHTS, B. F. G. JOHNSON, *et al.*, *Chem. Commun.*, **2001**, 2624–2625.
- 210 H. D. H. STOVER, J. M. J. FRECHET, *Macromolecules*, **1989**, 22, 1574–1576.
- 211 H. D. H. STOVER, J. M. J. FRECHET, *Macromolecules*, **1991**, 24, 883–888.
- 212 W. L. FITCH, G. DETRE, C. P. HOLMES, *et al.*, *J. Org. Chem.*, **1994**, 59, 7955–7956.
- 213 P. A. KEIFER, L. BALTUSIS, D. M. RICE, *et al.*, *J. Magn. Reson., Ser. A*, **1996**, 119, 65–69.



- 214 R. C. ANDERSON, J. P. STOKES, M. J. SHAPIRO, *Tetrahedron Lett.*, **1995**, 36, 5311–5314.
- 215 T. WEHLER, J. WESTMAN, *Tetrahedron Lett.*, **1996**, 37, 4771–4774.
- 216 S. K. SARKAR, R. S. GARIGIPATI, J. L. ADAMS *et al.*, *J. Am. Chem. Soc.*, **1996**, 118, 2305–2306.
- 217 M. J. SHAPIRO, J. R. WAREING, *Curr. Opin. Chem. Biol.*, **1998**, 2, 372–375.
- 218 P. A. KEIFER, *Drug Discov. Today*, **1997**, 2, 468–478.
- 219 M. J. SHAPIRO, J. S. GOUNARIDES, *Biotechnol. Bioeng.*, **2000**, 71, 130–148.
- 220 M. J. SHAPIRO, J. S. GOUNARIDES, *Prog. Nucl. Magn. Reson. Spectrosc.*, **1999**, 35, 153–200.
- 221 Y. F. NG, J. C. MEILLON, T. RYAN, *et al.*, *Angew. Chem.*, **2001**, 113, 1807–1810, *Angew. Chem., Int. Ed. Engl.*, **2001**, 40, 1757–1760.
- 222 M. DREW, E. ORTON, P. KROLIKOWSKI, *et al.*, *J. Comb. Chem.*, **2000**, 2, 8–9.
- 223 D. STONES, D. J. MILLER, M. W. BEATON, *et al.*, *Tetrahedron Lett.*, **1998**, 39, 4875–4878.
- 224 R. HANY, D. RENTSCH, B. DHANAPAL *et al.*, *J. Comb. Chem.*, **2001**, 3, 85–89.
- 225 R. WARRASS, G. LIPPENS, *J. Org. Chem.*, **2000**, 65, 2946–2950.
- 226 R. RIEDL, R. TAPPE, A. BERKESSEL, *J. Am. Chem. Soc.*, **1998**, 120, 8994–9000.
- 227 R. B. MERRIFIELD, *Intra-Sci. Chem. Rept.*, **1971**, 5, 184–198.
- 228 J. KLEIN, H. WIDDECKE, N. BOTHE, *Makromol. Chem. Suppl.*, **1984**, 6, 211–226.
- 229 S. M. LEINONEN, D. C. SHERRINGTON, A. SNEDDON, *et al.*, *J. Catalysis*, **1999**, 183, 251–266.
- 230 I. M. HUXHAM, B. ROWATT, D. C. SHERRINGTON, *Die Makromol. Chem.*, **1991**, 192, 1695–1703.
- 231 S. R. MCALPINE, S. L. SCHREIBER, *Chem. Eur. J.*, **1999**, 5, 3528–3531.
- 232 S. R. MC ALPINE, C. W. LINDSLEY, J. C. HODGES, *et al.*, *J. Comb. Chem.*, **2001**, 3, 1–5.
- 233 J. KRESS, A. ROSE, J. G. FREY, *et al.*, *Chem. Eur. J.*, **2001**, 7, 3880–3883.
- 234 J. RADEMANN, M. BARTH, R. BROCK, *et al.*, *Chem. Eur. J.*, **2001**, 7, 3884–3889.

## 2

# Supported Reagents and Scavengers in Multi-step Organic Synthesis

IAN R. BAXENDALE, R. IAN STORER and STEVEN V. LEY

## 2.1

### Introduction

Developments in genomics and proteomics, coupled with advances in ultra high throughput screening methods, have revolutionized pharmaceutical and agrochemical research. The capacity to design and test thousands of compounds per day has resulted in an unprecedented number of new drug targets arising that possess an increasing level of structural diversity. As a result, there is a requirement for new high throughput synthetic methods and technologies to rapidly assemble these potentially therapeutic molecules in ways which are environmentally clean and lead to structural variation in as short a period of time as possible. New methods have been sought that avoid labor-intensive practices such as aqueous work-up and complex chromatographic purification, to allow efficient multi-parallel synthesis and offer a practical simplicity that is compatible with automated robotic workstations. One of the most promising of these solutions has been the development of solid-supported reagents, catalysts and sequestering agents, especially for multi-step reactions [1]. These ideas require robust thinking and confidence to challenge established concepts, consequently, it is often easier to criticize than to adopt these new methods. This is typical of many new areas of science but a receptive attitude can lead to major advantages.

### 2.1.1

#### Solid-supported Synthesis and Solution – Solution Manipulation

Probably the most thoroughly investigated of the methods reported is that of solid phase organic chemistry, following the pioneering works of Letsinger [2], and Merrifield [3] in 1963. This uses a polymer support as the molecular platform for rapid compound handling and purification. Substrates are temporarily immobilized on a polymeric resin, taken through a synthetic sequence, and then cleaved back into solution. An excess of reactants and reagents are frequently used at each step of the synthesis to drive reactions to completion prior to removal by simple filtration. This solid-phase technique revolutionized polypeptide and polynucleotide synthesis and, almost thirty years later, it set the stage for combinatorial chemis-

try. Although this strategy has many advantages and has been proven to be an essential tool for specific areas of synthesis, it also has several drawbacks which have limited its use in more general syntheses: reactions can be slow and are often difficult to monitor compared with solution-phase chemistry; extra steps are required to attach and release the substrate from the resin, making convergent syntheses less feasible; part of the resin attachment is often found in the final product; resin loading is often poor; resin swelling and solvent compatibilities can also be a problem; optimization of reactions can be very time consuming and long linear sequences are difficult and sometimes unreliable [4].

Recently, other alternative methods to solid-phase synthesis have been investigated which retain more of the advantageous aspects of solution phase chemistry. Several groups have developed elegant methods for separating desired library products from excess reactants, reagents and by-products by liquid phase manipulation. Examples include the use of fluorous reagents and ionic liquids, wherein the desired products are uniquely isolated in one liquid phase and all non-product species are fractionated into other immiscible liquid phases [5]. Soluble polymers have also emerged as viable supports across a broad spectrum of immobilized applications. However, these systems have not been used extensively because of limiting factors, such as their intrinsic solubility and low loadings [6]. Although these methods have shown some promising applications within specialized systems, their general use in multi-step syntheses are problematic.

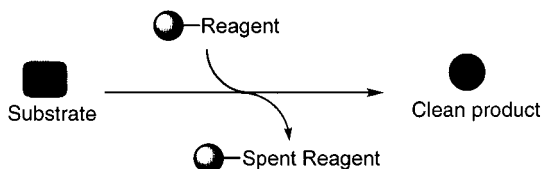
Many of the issues and requirements of high throughput synthesis have been successfully addressed by the application of solid-phase reagents, catalysts and scavenging techniques [1 g]. These strategies assimilate the advantages of product isolation and purification from solid-phase organic synthesis with the flexible choice of chemistry from the vast repertoire of solution-phase organic reactions, whilst at the same time eliminating many of their inherent disadvantages resulting overall in a more efficient methodology. Their combined use has already seen application in both combinatorial and general synthetic chemistry programs. In this chapter we focus on the principles of their use and describe their application in multi-step applications. We begin with a brief introduction to set the scene for the more complex processes. Throughout the following discussion every effort has been made to use appropriate representative examples, and where libraries have been constructed, a selected example rather than a generic scheme has been presented. The chosen examples display what we believe to be the most revealing and interesting aspects of the chemistry applied and the compounds prepared. We therefore urge the reader to regard the yields and purities of the representative compounds as only indicators which may not be illustrative of all other molecules prepared in the library.

### 2.1.2

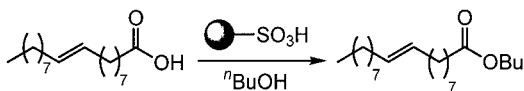
#### **Solid-supported Reagents and Catalysts**

Supported reagents and catalysts are reactive species that are associated with a support material. They transform a substrate into a new chemical product, with the excess or spent reagent being easily removed by filtration (Fig. 2.1). The prod-

**Fig. 1.1** Solid-supported reagents in clean synthesis.



**Scheme 2.1** Ester formation using supported sulfonic acid.



uct build up can be analyzed in real time so information can be used to modify reaction parameters by a feedback approach.

Although solid-phase synthesis was first introduced by Merrifield [3] and Lettinger [2a] in 1963, it is necessary to trace back to as early as the 1930s to discover the origins of polymer-supported reagents and catalysts. In 1935 Adams and Holms [7] described some phenol-formaldehyde based ion exchange particles and the preparation of such keep particles was patented in 1949 [8]. The development of polystyrene-divinylbenzene based ion exchange resins occurred during the late 1940s [9] with an early example of a published organic transformation in 1946 by Sussman [10]. This paper described the synthesis of octadec-9-enoic acid butyl ester using a sulfonic acid resin as the catalyst (Scheme 2.1).

The 1950s saw the further development of acidic and basic ion exchangers and their application as catalysts in water treatment and purification [11]. In light of the fact that the first review of ion exchange resin catalysts was published in 1957 [12], the concept of immobilized reagents had been conceived and established within certain fields prior to the advent of solid phase synthesis and the invention of combinatorial ideals. However, although a steady number of publications appeared over the following decades, it was not until the 1990s, with the demands for high throughput synthesis, that greater interest was shown for the further development and application of these reagent systems [1g].

### 2.1.2.1 Supporting Materials

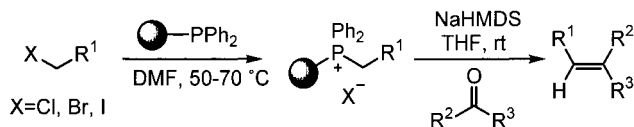
In general, immobilization means tethering a reagent to an insoluble or semi-soluble polymeric resin, usually a functionalized DVB-cross-linked polystyrene, although many other organic polymers and inorganic support materials have also been developed. These include scaffolds such as glass beads, silica, alumina, cellulose, zeolites, graphite and clays. The reagent is then rendered either completely insoluble or selectively soluble in certain solvents. However, in all cases the bound reactive species largely remains freely accessible within the support matrix to both the solvent and to the solution-dissolved reactants. The most common support material is polystyrene cross-linked by an amount of divinylbenzene (DVB). The

physical characteristics, such as solvent swelling, depends on the degree of cross-linking and hence on the proportion of DVB. Microreticular resins, which contain a low degree of cross-linking (1–2% DVB), show a greater swelling capacity, and thus solvent dependency, than the higher cross-linked macroreticular resin (> 5% DVB). Although resin swelling has some effects on reaction kinetics in supported reagent based chemistry, it is less important than with substrate bound chemistry where a higher degree of swelling is necessary to ensure complete reaction.

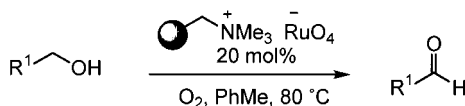
### 2.1.2.2 Facilitation of Work-up and Purification

Often supported reagents are used in stoichiometric excess to rapidly force reactions to completion, resulting in fewer impurities and the requirement of only simple filtration and solvent evaporation to isolate the reaction products. Particularly notable are cases where traditional phase reagents leave by-products which are difficult to remove even by the use of aqueous work-up or conventional purification. Situations where the product and reagent by-products display similar solubilities and polarities or where the products are not stable to exposure to water or silica gel can be successfully improved by taking advantage of the fast and anhydrous work-up that supported reagents permit. Although triphenylphosphine is a versatile reagent in a variety of reactions including Wittig, Staudinger, Mitsunobu and ozonide reductions, the separation of reaction products from any excess reagent and phosphine oxide by-products can be difficult. The use of polymer-supported triphenylphosphine allows straightforward removal of both excess reagents and by-products by filtration, as illustrated by immobilized Wittig reactions (Scheme 2.2) [13].

This ease of isolation of the supported material following a reaction is also beneficial in situations where the reagent functions as a catalyst and/or can be recycled. The example below displays the benefit of using the recyclable heterogeneous polymer-supported perruthenate (PSP) over the conventional homogeneous reagent, which is not easily isolated and re-used (Scheme 2.3) [14].

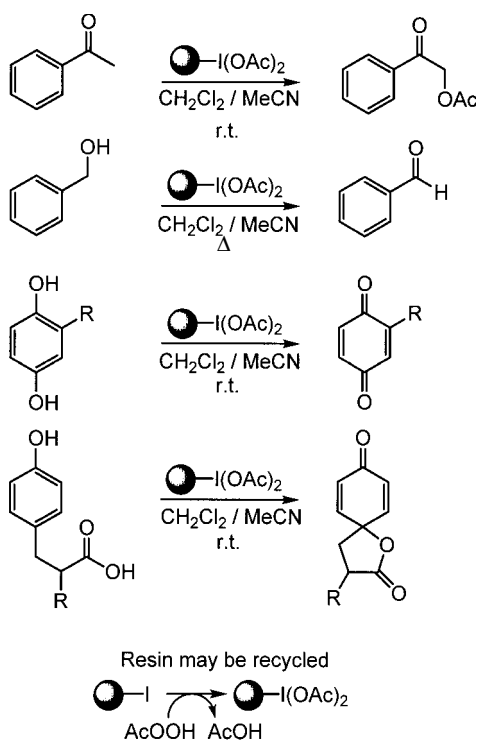


**Scheme 2.2** Polymer-supported triphenylphosphine equivalents for use in Wittig reactions.



**Scheme 2.3** Oxidation of alcohols using the PSP reagent.

**Scheme 2.4** Polymer-supported oxidations using a hypervalent iodine reagent.



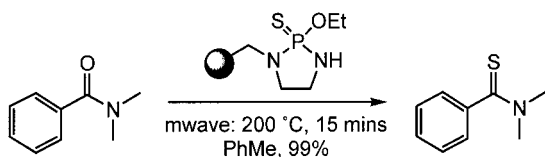
Additionally, many of the stoichiometric reagents which have been developed can be regenerated following reaction. Immobilized hypervalent iodine oxidizing reagents which have been shown to be effective in a range of functional group oxidations and spirocyclizations (Scheme 2.4) can be regenerated simply by oxidative treatment using peracetic acid [15].

### 2.1.2.3 Immobilization of Toxic and Malodorous Reagents

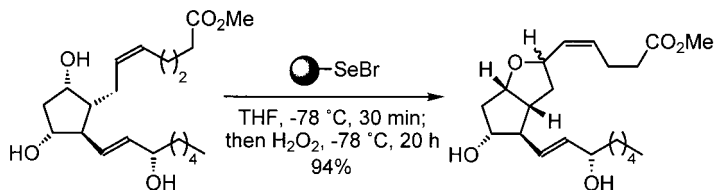
One of the most attractive aspects of reagent immobilization is that analogs of toxic, noxious or hazardous reagents and their by-products are made heterogeneous, thus resulting in reduced odour, easier handling and increased general safety. This situation is aptly exemplified by the elimination of the volatile malodorous sulfur components from thionation reactions by the preparation of a heterogeneous equivalent to Lawesson's reagent [16], which has been used for the conversions of amides to thioamides (Scheme 2.5) [17].

There are also immobilized versions of selenium reagents (Scheme 2.6), which are not only stable to the air, but have no odor, unlike the pungent solution phase equivalents [18].

In both cases, the toxicity and stench that is associated with the sulfur and selenium by-products is eliminated, making the reaction desirable, especially when



**Scheme 2.5** Polymer-supported thionating reagent.



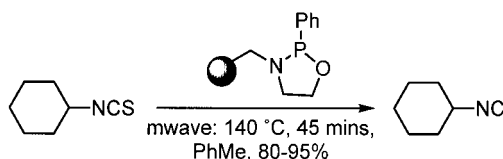
**Scheme 2.6** An immobilized selenium species for cyclo-addition reactions.

considering the possibilities of using the reagents on a larger scale or in multi-parallel arrays.

#### 2.1.2.4 Microwaves as a Reliable Heating Method for Polymers

As with solution-phase chemistry, some reactions require elevated temperatures, although prolonged heating can result in decomposition of substrates or products and additionally, many immobilizing supports and reagents are thermally unstable. A convenient solution to this problem has been proven to be the use of short heating sequences by focused microwave irradiation. Under these conditions, the thermally enhanced reactions proceed without visible or chemical damage to the polymeric supports, but frequently produce enhanced levels of reactivity [19]. The value of this union of technologies has been shown both in the synthesis of small compound libraries and also in key steps within the preparation of natural products [20, 21]. In addition ionic liquids can be used as heat exchangers for non or poorly absorbing solvents to achieve rapid heating without having to resort to a change of solvent [17, 20, 22].

A supported [1.3.2]oxazaphospholidine has been used for the conversion of isothiocyanates to isocyanides and their subsequent incorporation in Ugi multi-component couplings (Scheme 2.7). The reaction was slow to proceed when heated under conventional heat bath conditions and led to low yields, following decompo-



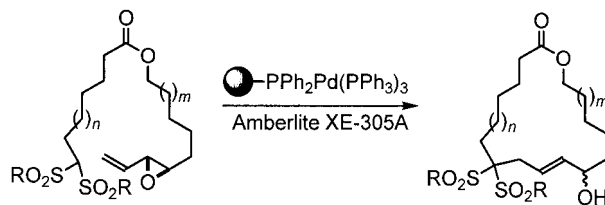
**Scheme 2.7** Supported [1.3.2]oxazaphospholidine for the conversion of isothiocyanates to isocyanides.

sition of the product by rearrangement to the corresponding nitriles. However, under microwave heating the reactions proceeded much quicker and in higher overall yield [23].

### 2.1.2.5 Effects of Site Isolation

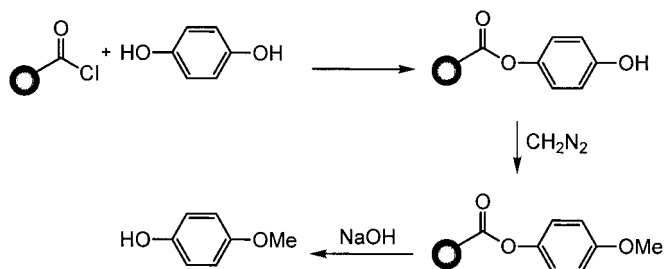
It is important to consider the support material used as it confers certain chemical and physical characteristics to the immobilized reagent. In a similar way to the choice of solvent, the polarity of the support can affect the reactivity of the attached functional groups. The three-dimensional steric environment of the support matrix can also create many pore-like structures and unusual topographies, because phase partitioning means they exist in complete isolation. These characteristics produce reagent systems with *unique reactivities* that can provide several advantages when attempting to overcome solvent-specific reactions or situations in which the solubility of a reactant/product and the solution reagent is problematic [24, 25, 26]. Furthermore, a structural detail commonly referred to as ‘site-specific isolation’ or ‘pseudodilution effect’ can allow many reactions that are only possible in solution at extremely high dilution to be conducted at much higher relative concentrations, as a result of intermolecular reactions being restricted owing to attachment to isolated sites on the supports [25, 26]. A beneficial application of this phenomenon is with macrocyclization reactions to make large rings (Scheme 2.8). In conventional solution-phase reactions, conditions of high dilution are used to reduce the rate of intermolecular coupling. Trost showed that, by using a bound coupling reagent, the concentration problem is circumvented. In these examples the electrophilic and nucleophilic sites are not unmasked until the substrate encounters an active site on the polymer, allowing the reactions to be run at high concentrations without the formation of any dimeric or oligomeric side-products [27].

The same effect has been observed for the monoselective protection/modification of equivalently difunctional molecules [28]. The binding is only temporary for the duration of the reaction but permits the other pendant functional group to react in preference. An example of this was shown by Leznoff for the preparation of monoethers of symmetrical dihydroxy aromatic compounds [29]. Under conventional conditions such reactions are problematic, providing mixtures of mono and

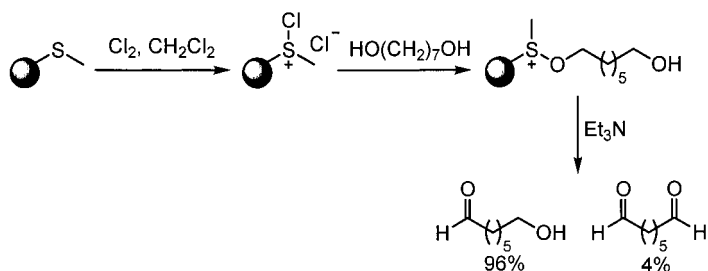


**Scheme 2.8** Palladium-catalyzed allylic substitution an example of pseudodilute conditions.





**Scheme 2.9** Mono-protection of symmetrical diol moieties.



**Scheme 2.10** Mono-oxidation of symmetrical diols.

diether products. However, site isolation allowed attachment and therefore protection of one phenolic group to the polymer, leaving the other alcohol terminus free for alkylation prior to cleavage of the product from the support (Scheme 2.9).

A slightly different variation on this concept was developed by Crosby, who used a polymer for selective activation of one alcohol for a supported sulfur based mono-oxidation of heptanediol (Scheme 2.10) [30]. Here the reactant interacts with the support directly (under pseudo high dilution), becoming chemically transformed in the process.

#### 2.1.2.6 Mutually Incompatible Reagents in the Same Reaction Compartment

As these reagent systems are anchored on a solid, they also allow the simultaneous use of multiple reagents to achieve one-pot transformations where, because of incompatibility of the reagents, no solution-phase equivalent exists or would require intermediate isolation. Many examples of this are illustrated in the following sections where it can be seen that these concepts add a new dimension to how one can think about organic synthesis and will certainly have important ramifications on the design and implementation of new chemical reactions and processes in the future.

## 2.1.3

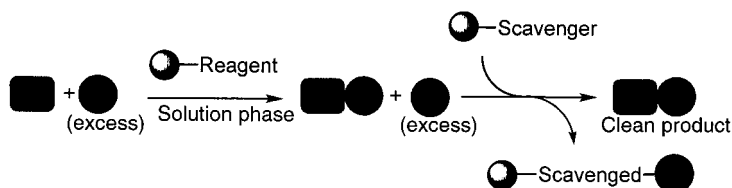
**Solid-supported Purification Processes**

Unfortunately, many reactions do not occur with quantitative conversion and in near absolute purity. The work-up and purification of most chemical processes probably takes up most of a bench chemist's time. Therefore techniques that simplify and accelerate these operations not only free up valuable time, but allow greater creativity and increased levels of output. Here again, supported systems can be used to aid the chemist in the guise of scavengers, quenching agents and catch and release systems.

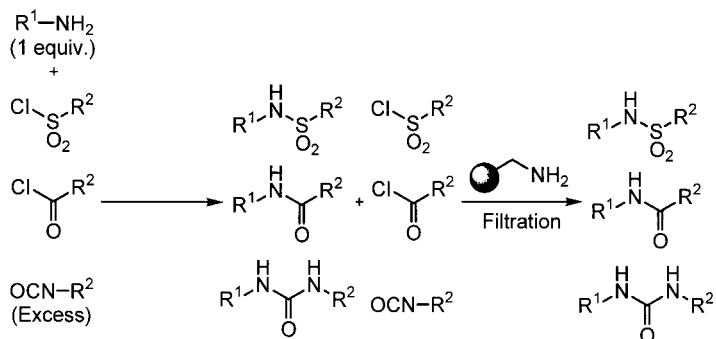
**2.1.3.1 Supported Scavengers**

Supported scavengers are reactive species that selectively quench and/or sequester by-products of the reaction or remove any excess starting materials, and are subsequently removed by filtration (Fig. 2.2). These species, which allow 'liquid-solid phase extraction' are also often referred to as 'sequestering agents' or 'quenching agents'.

The use of insoluble polymers and other solid-supported agents to scavenge by-products and excess starting materials from complex reaction streams is of significant strategic advantage as it effects purification without the need to resort to liquid-liquid extractions or nonspecific column chromatography. Both scavengers



**Fig. 2.2** The concept of combining solid-supported reagents and scavengers in chemical synthesis.



**Scheme 2.11** Polyamine scavenger purification of electrophilic reagents.

which form ionic interactions and those that form covalent bonds are commonly employed to bind organic functionality or to chelate ions and inorganic complexes.

Most conventional scavenging is based on the concept of complementary reactivity. In the simplest cases, electrophilic and nucleophilic species are sequestered via a reciprocally functionalized support (Scheme 2.11; see also Tab. 2.1); likewise, acids and bases can be removed via salt formation with a solid-supported base or acid.

In a similar way, many acidic and basic ion-exchange polymers have been used to quench and work-up reactions as an alternative to aqueous conditions. This is especially valuable if the compound in question is moisture sensitive or hydroscopic, or if a rapid quench and work-up procedure is required.

### 2.1.3.2 Catch and Release

So far, we have considered only the purification methods for the rapid clean up of reaction mixtures that are facilitated by sequestration of either by-products, excess reactants or spent reagents. The idea that one can use a suitably functionalized solid support to selectively capture the required product away from any contaminating impurities, filter and then re-release it in a pure form is also an important purification concept (Fig. 2.3) [31].

The trapping and subsequent liberation of the product can, in essence, be accomplished using any type of reversible physical or chemical mechanism. The variety and generality of these systems are such that it is now conceivable to purify large chemical libraries in a very efficient manner, so they may be directly submitted into biological screens. In the simplest sense a polymer can be used following reaction to bind a product, as illustrated in work by Hodge in which carbonyl compounds were removed by formation of an acetal onto a diol resin. Separation by filtration was followed by hydrolysis to recover clean product (Scheme 2.12) [28a].

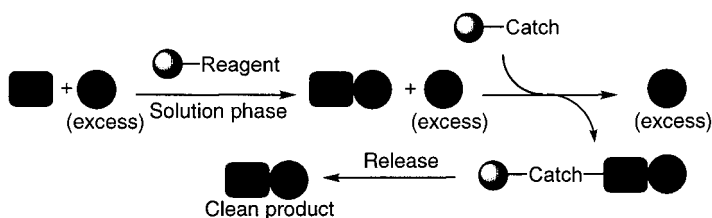
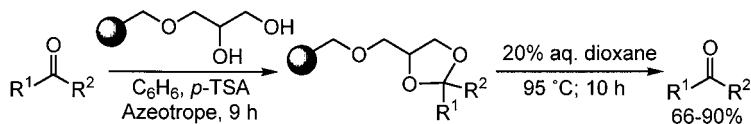
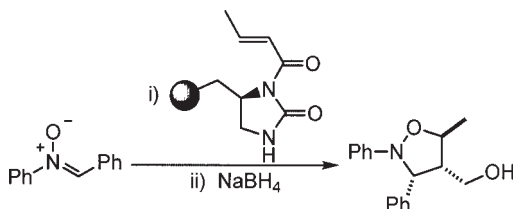


Fig. 2.3 Catch and release purification strategies.



Scheme 2.12 Catch and release purification of carbonyl compounds.

**Scheme 2.13** Systematic reaction/catch and release purification.



Another, slightly different method, is to use the resin to capture a molecule followed by release of a modified product. This is illustrated by the example shown in Scheme 13 where a nitrone undergoes a 1,3-dipolar cyclo-addition with an immobilized chiral auxiliary followed by a reductive cleavage to yield an isoxazolidine (Scheme 2.13) [32]. Here the polymer is acting as both an active reagent and as a purification technique [33].

## 2.2

### Multi-step Organic Transformations

Expedient work-up and purification procedures have increased in importance, so all the aforementioned methods are valuable additions to the repertoire of rapid purification techniques that can be used either independently or in conjunction with other supported reagent systems. So far, however, we have only discussed the ways in which supported reagents or scavenger quench technology can be employed to effect single step modifications. In a variety of cases they have been effectively integrated into synthetic programs to expedite the isolation and purification of a key intermediate or to permit a reaction that, under conventional solution phase methodologies, is extremely problematic. In the following sections these principles, and the inherent advantages offered, are further exemplified through the combined application of supported reagents, scavengers and quenching systems to sequential multi-step organic synthesis. The initial historical groundwork to multi-step application from the 1970s to late 1980s is considered, followed by an in depth examination of the integration into library synthesis and automated combinatorial programs during the 1990s. Finally, recent developments and applications within complex drug and natural product synthesis are reviewed.

#### 2.2.1

#### The Early Developments of Polymer-supported Processes in Organic Synthesis

##### 2.2.1.1 One Pot Multi-reagent Combinations

In 1974 Rebek published the first example of the simultaneous application of two immobilized systems. This pioneering mechanistic study exploited the site isolation properties of polymers for an examination of the existence and movement of short-lived solution species between two insoluble polymeric trapping agents suspended in a common solution (Fig. 2.4). It was demonstrated that a polymer

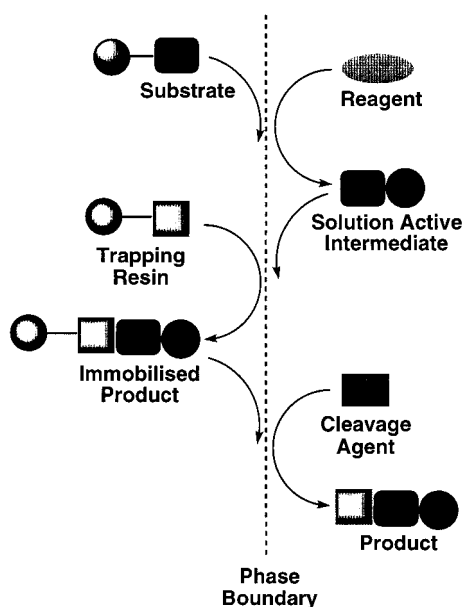
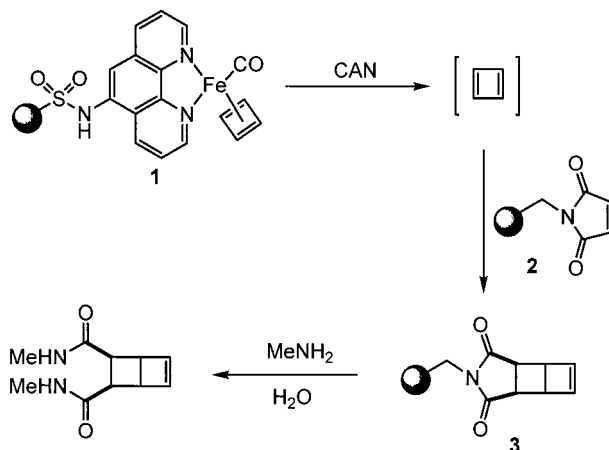


Fig. 2.4 Reactive species transportation between polymeric resins.

bound iron complex (**1**), following treatment with ceric ammonium nitrate, released free cyclobutadiene into solution, which was immediately trapped in a Diels-Alder reaction by a second succinimide substituted polymer (**2**) (Scheme 2.14) [34]. The tricyclic intermediate (**3**) was cleaved back into solution by treatment with excess methylamine. This type of method was later used in a more general sense as a three phase test analysis for the detection of highly reactive solution labile species. The presence of the product trapped on the second resin of

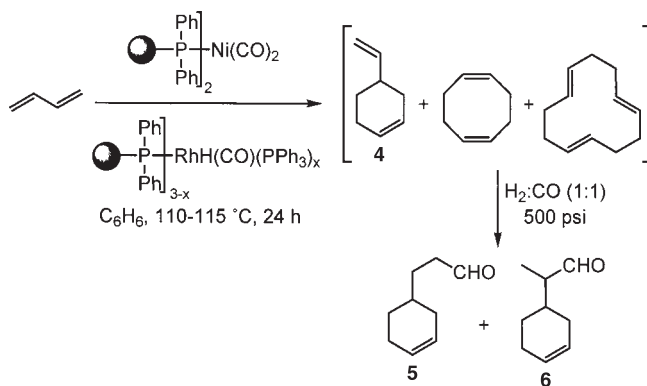


Scheme 2.14 Mutually incompatible reagents in a single reaction vessel.

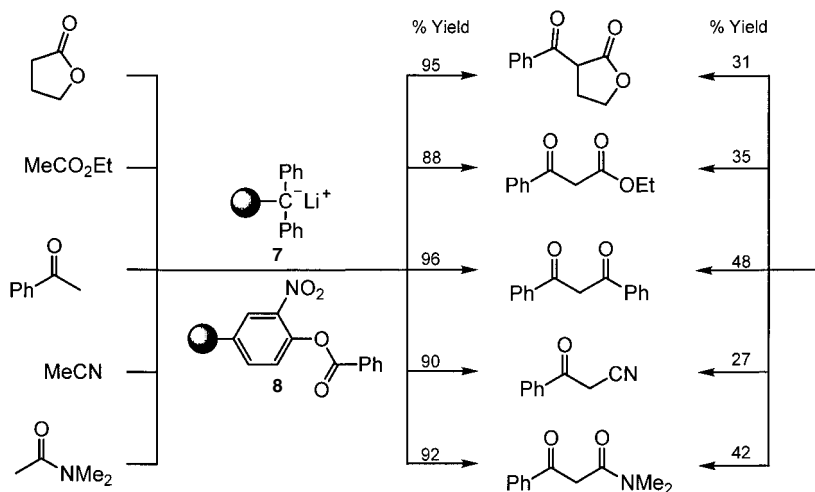
fers support for the existence of a solution active component that has diffused between the polymers (Fig. 2.4). Although the method does not establish irrefutable evidence for the existence of the intermediate, the test does provide a rapid handle to investigate the potential for the involvement of a free transient intermediate. Since its development, the method has been primarily used to prove the involvement of free cyclobutadiene (Scheme 2.14), although an intermediate acylimidazole species in imidazole-catalyzed acylations has also been demonstrated [35] and a similar approach was applied to elucidate the existence of free oxocarbenium ions in the Fries rearrangement [36]. Although these investigations were not directly useful in a synthetic context, they do represent a landmark as the first example of two polymeric systems being used for sequential reactions within the same reaction vessel.

The following year, in 1975 Pittman published an extensive report describing the application of various polymer-supported triphenylphosphine ligated transition metal complexes as catalysts for the functionalization of alkenes through sequential oligomerization and hydrogenation or hydroformylation reactions [37]. A catalytic tandem nickel and rhodium system was applied for the conversion of butadiene to a mixture of cyclo-oligomerized products (Scheme 2.15). Without removal of the reagents, the resulting mixture underwent direct treatment with hydrogen and carbon monoxide to produce aldehydes (**5**) and (**6**) *via* selective hydroformylation of the exocyclic double bond of (**4**). The use of this method remains important to industry because it not only delivers commercially important feedstock, but also has the added advantage that the supported catalysts can be easily recovered and recycled [1].

Two years later in 1977 the Cohen group stimulated the next major development by the introduction of the simultaneous use of two antagonistic supported reagents which they named the “wolf and lamb” approach [38]. This allowed two immobilized systems to be used in conjunction with one another to achieve one-pot reaction sequences that were not possible by employing their homogeneous



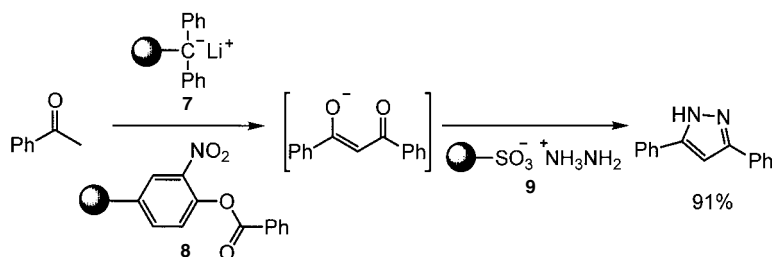
**Scheme 2.15** Supported metal catalysts for hydrogenation and hydroformylation reactions.



**Scheme 2.16** Wolf and Lamb reactions.

counterparts. In a series of experiments, enolizable substrates were deprotonated by a polymer-bound trityllithium base to generate anions that subsequently underwent a rapid C-acylation reaction with a benzoyl-transfer polymer contained in the same reaction vessel (Scheme 2.16). These reaction cascades gave excellent yields and represented the first synthetically useful application of polymer-supported technologies using the site-isolation concept.

This multi-step, one-pot process was taken further by integration of a third supported reagent for the sequential preparation of 3,5-diphenylpyrazole (Scheme 2.17). Following the previously established procedure, acetophenone was deprotonated and acylated to afford the 1,3-dicarbonyl species. This intermediate was easily separated from the spent polymers by filtration and passed without isolation into a suspension of the resin bound hydrazine salt (9), affording the desired pyrazole in 91% yield. In a subsequent publication, the authors reported that the depleted polymeric reagents from the first step of the conversion (i.e. (7) and (8)) were recovered and separated *via* a selective flotation procedure, enabling them to



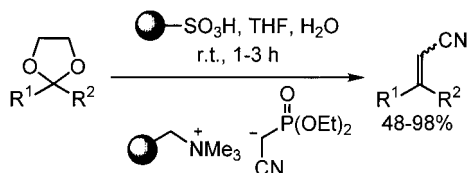
**Scheme 2.17** Preparation of 3,5-diphenylpyrazole in a one-pot procedure.

be regenerated for use in subsequent reactions. This work not only illustrates a new concept as a consequence of site isolation, but also displays the first attempt to use a multi-step application of supported reagents to affect a targeted synthesis.

In 1979 Cainelli described a novel two-step, one-pot procedure for the direct conversion of acetals to the corresponding unsaturated nitriles (Scheme 2.18) [39]. In this process a phosphonate nitrile was treated with an ion exchange resin in its hydroxide form to deprotonate the phosphonate and concurrently immobilize the anion onto the resin. The simultaneous use of an acidic Amberlyst 15 resin and the resin bound phosphonate then permitted the sequential acetal hydrolysis and subsequent Wadsworth-Horner-Emmons alkene formation. Isolation of the products consisted of only a rapid filtration and solvent evaporation to obtain pure material in yields ranging from 40–98%. Although the *E/Z* ratio was not as high as would be expected under normal solution phase conditions, it was however noted that the process was independent of the solvent used, indicating the possibility that the resin provided a microenvironment which made the reaction independent of the external medium. The preparation of this small collection of compounds again demonstrated the potential for progressing a substrate through a planned sequence of chemical transformations, resulting in stepwise activation and immediate chemical modification by a second orthogonal-supported reagent to yield a more advanced product. This is a process that continued to be elaborated on in the subsequent literature.

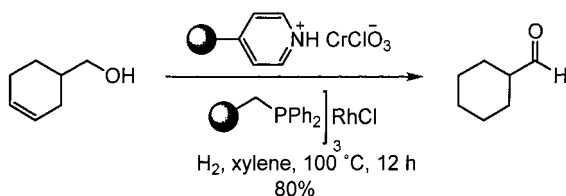
An interesting example was later shown by Bergbreiter [40], who used a two-polymer combination which incorporated the use of both a soluble and an insoluble polymer. A polyethylene diphenylphosphine immobilized Wilkinson's catalyst, which becomes homogeneous under the elevated reaction temperature, was used in conjunction with an insoluble poly(vinylpyridiniumchlorochromate) (PVPCC) system, a reagent previously described by Frechet [41], for the dual oxidation of an alcohol and hydrogenation of an olefin (Scheme 2.19). The physical difference in the behavior of the two polymers facilitated their independent isolation. The PVPCC species was removed by direct filtration at the end of the reaction prior to cooling of the reaction mixture which then caused the hydrogenation catalyst to precipitate from solution. A second filtration then allowed the separate isolation of the majority of the semi-soluble Wilkinson's catalyst equivalent.

In the same year an efficient one-pot oxidation and reduction sequence was also described for the cleavage of 1,2-diols to their corresponding primary alcohols [42]. This process was an excellent demonstration of two immobilized incompati-



**Scheme 2.18** Direct one pot transformation of acetals to nitriles.



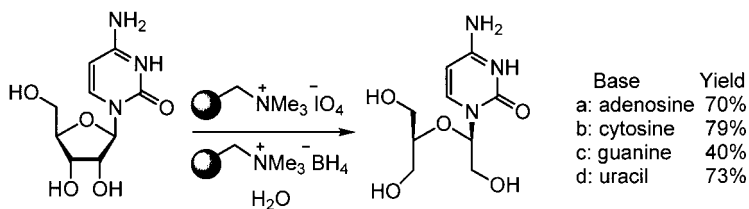


**Scheme 2.19** Multiple reagent combinations for sequential staged reactions.

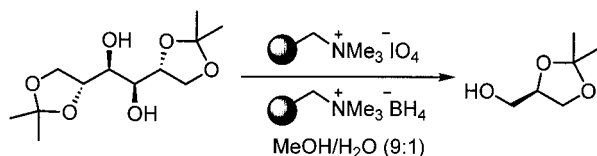
ble reagents being rendered mutually inert by attachment to two different polymeric supports. The transformation was carried out by slowly pumping a solution of the substrates through a column packed with a 1:1 mixture of the periodate and borohydride polymers (Scheme 2.20). In this way the reaction stream could be directly collected from the base of the column and the alcohol products obtained by simple solvent evaporation.

A particular advantage in the synthesis of this series of trihydroxy nucleosides was that the unstable intermediate dialdehyde resulting from diol cleavage was immediately reduced *in situ* by the polymer-supported borohydride, thus minimizing the lifetime of this species and improving the overall yield for the two step process. As would be expected, when the reagents were employed sequentially with isolation, the product was obtained in much lower yield, owing to the increased handling and instability of the intermediate. This process has also been used in the cleavage of 1,2,5,6-diisopropylidene mannitol in a synthesis of Bola-form phosphatidylcholines (Scheme 2.21) [43].

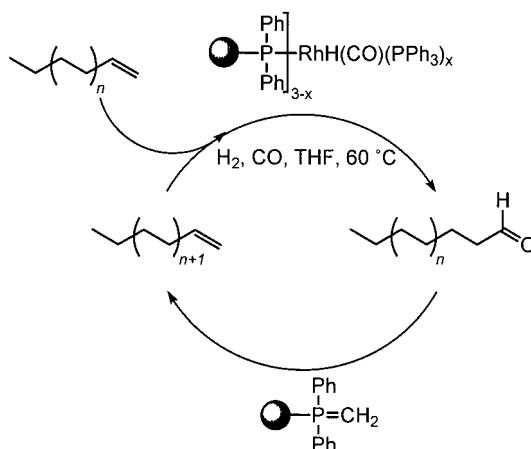
In an interesting example of a continuous one pot, two step iterative chain homologation process, Regen [44] used a polymeric rhodium catalyst to effect the hydroformylation of alkenes which then underwent supported Wittig reactions using a polymer-supported ylide, thereby generating new olefins and creating a sustainable reaction cycle controlled by the quantity of ylide available (Scheme 2.22). The advantages of such a strategy included much milder reaction conditions and the generation of less complex mixtures than were obtained from more traditional alkene homologation methods.



**Scheme 2.20** The simultaneous application of an oxidant and reductant for 1,2-diol cleavage.



**Scheme 2.21** Oxidative cleavage of protected mannitol in the synthesis of Bolaform.

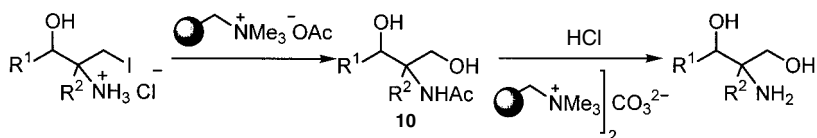


**Scheme 2.22** Living chain homologation using two complementary immobilized catalysts.

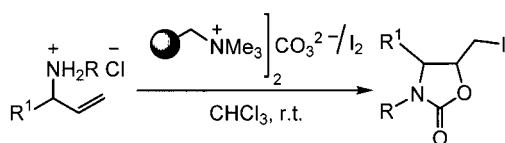
### 2.2.1.2 Sequential Multi-step Transformations

In 1982 Cardillo used a three-step sequence involving two supported reagent systems to convert  $\beta$ -iodoamines into amino alcohols (Scheme 2.23) [45]. Polymer-supported acetate ions were used for the substitution of the iodide which immediately underwent acyl transfer to the amine. The resulting compound (**10**) was directly treated with hydrochloric acid to cleave the amide and the free base was subsequently obtained from the reaction by treatment with a resin-bound carbonate. This was of particularly synthetic value because of the high water solubility of these amino alcohol compounds that would have made aqueous work-up challenging.

Other reagent systems have been created that function as multi-purpose species in order to mimic classical solution phase reactions, an example of this is shown



**Scheme 2.23** A rapid three-step preparation of amino alcohols.



**Scheme 2.24** Rapid assembly of oxazolidin-2-ones using solid-supported reagents.

$R = \text{H}, R^1 = \text{C}_3\text{H}_7$  95%

$R = \text{H}, R^1 = \text{BnO}$  94%

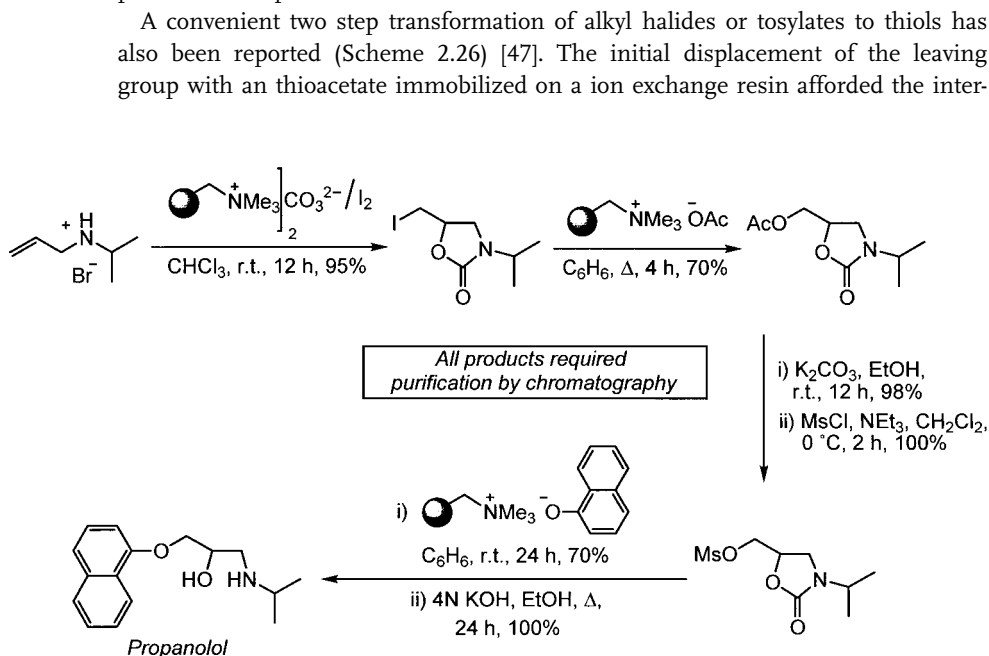
$R = \text{H}, R^1 = \text{OH}$  80%

$R = \text{Bn}, R^1 = \text{C}_3\text{H}_7$  95%

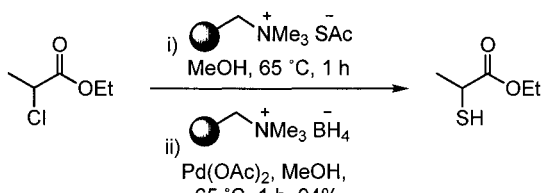
$R = \text{Bn}, R^1 = \text{BnO}$  90%

$R = \text{H}, R^1 = \text{THPO}$  95%

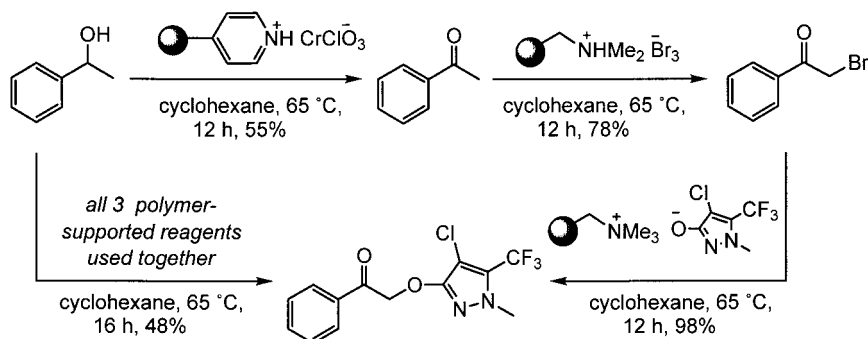
below. The one-pot generic formation of various oxazolidin-2-ones has been elegantly accomplished starting from allylic amine salts using a dual purpose polymeric reagent prepared by adsorbing iodine onto Amberlyst A-26 in its carbonate form. The modified polymeric species acted as both a supported source of iodine for iodolactonization and carbon dioxide for the carbamate formation (Scheme 2.24) [46]. To emphasize the utility of this reagent, it was also used to construct the core of ( $\pm$ )-propanolol, a  $\beta$ -adrenergic receptor agonist, in a six step synthesis which used three different immobilized reagents in individual steps (Scheme 2.25). Nevertheless chromatography was still necessary in order to guarantee high purities of the products.



**Scheme 2.25** Synthesis of the  $\beta$ -adrenergic receptor agonist ( $\pm$ )-propanolol.



**Scheme 2.26** Rapid conversion of alkyl halides or tosylates to thiols.



**Scheme 2.27** Multi-reagent combinations in single pot transformations.

mediate thioester. Subsequent addition of polymer-supported borohydride, doped with a catalytic amount of palladium(II) acetate, gave a smooth reductive cleavage of the thioacetate to the thiol. The only work-up purification required was the filtration of the spent resins and evaporation of the solvent.

After such an encouraging start, the field of supported-reagents lay relatively dormant for a number of years. Although there remained a steady dissemination of papers covering the topic these were almost entirely dedicated to reagent preparations and/or single step transformations. Then, during the mid 1990s, there was a revitalization of the area triggered by the enormous advances in the development and application of high-throughput strategies for the generation of small, discrete and highly pure compounds. One of the first papers on multi-step reactions to appear from this activity was a three step sequence published by Parlow (1995) in which each transformation was mediated by a different polymeric reagent, either in a stepwise sequence or simultaneously as a one-pot process (Scheme 2.27) [48]. Despite being an impressive example of multi-step synthesis using supported reagents, this was the only example reported and no mention was made of how these processes could be used in combinatorial chemistry or parallel synthesis programs.

## 2.2.2

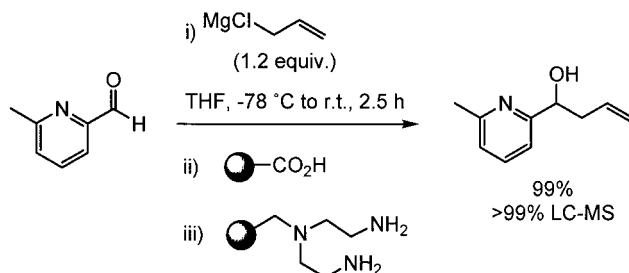
**The Further Development of Scavenging Protocols**

The generation of a solution-phase library using supported reagents is essentially identical to the preparation of a single compound in classical organic synthesis, however the overall throughput is increased by the simultaneous handling of multiple solutions that are reacted, worked-up and purified according to a generic reaction protocol. However, using classical synthesis, the focus of the synthesis becomes directed more at the work-up and purification steps. For this reason substantial work has been carried out which involves solution-phase library synthesis with extensive use of polymeric reagents to scavenge unwanted by-products or excess starting materials from the post-reaction mixture. Although many of these sequestration principles were well established in the early literature, they had not been applied to the rapid isolation of large numbers of new chemical entities as was now needed for discovery programs. It is therefore not very surprising that many of the key developments were made by industrial laboratories including Eli-Lilly, Merck, Glaxo, Warner-Lambert/Parke-Davis, Bristol-Myers Squibb and Searle/Monsanto. Although many of these methods significantly expedited the purification of chemical libraries and in many cases were used in extremely effective automated sequences, they appeared only as single steps within the overall synthetic scheme. (Most examples were based purely on a scavenger clean-up operation.)

A comprehensive list of the most common applications of supported scavenger agents can be found in several reviews [49].

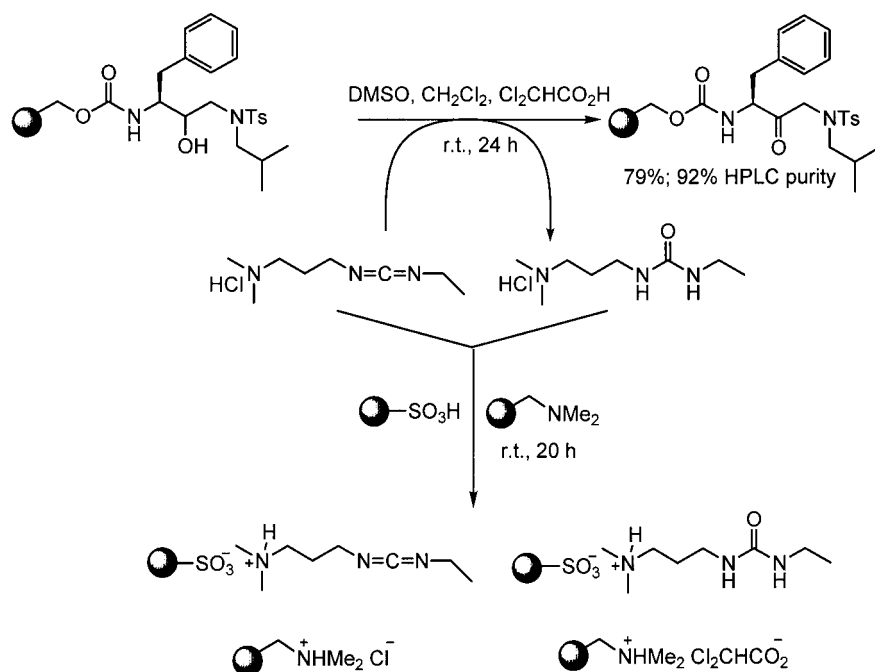
During the late 1990s a team of Monsanto chemists, led by Parlow and Flynn, proposed several general methods for reaction quenching and scavenging aimed at chemical library purification. These procedures were based on the fundamental principles of complementary molecular reactivity and recognition [50] and involved the chemoselective scavenging of product impurities (by-products, reagents or excess substrates) through the interaction of functionalized molecules and solid supports possessing the requisite reactive functionality. In an elegant demonstration of these concepts a series of six different aldehydes were reacted with excess organolithium or Grignard reagents in order to generate the corresponding secondary alcohols (Scheme 2.28). Avoiding traditional work-up procedures, carboxylic acid functionalized Amberlite IRC-50S was used as a quenching agent in order to protonate the metalated alkoxides, decompose excess organometallics and sequester metal ions as resin associated salts (proton-metal transfer). Any residual aldehyde was also removed as a polymer-bound adduct by addition of a polymer-supported trisamine resin, thus allowing isolation of the products in 88–99% yield and purities in excess of 95%, as determined by GC/MS. These techniques illustrated the application of supported scavengers in order to avoid the need to progress reactions through sequences of immiscible liquid-phase extractions. This is of particular importance when the compound in question are either unstable or create solubility/extraction problems.

In addition to describing an alternative to aqueous phase work-up, a novel approach to solution phase chemistry was shown using bifunctional or ‘tagged’ re-



**Scheme 2.28** Complementary molecular reactivity and molecular recognition for library purification.

agents. These artificially modified reagents bear a functional group that does not affect their reactivity, is preserved in the reagent by-products and enables purification by reacting with a complementary functionalized polymeric scavenger at the end of the reaction. In the described procedure, EDCI was exploited as a tagged carbodiimide and was applied to the Pfitzner-Moffat oxidation of secondary alcohols (Scheme 2.29). Upon completion of the reaction, the modified urea and remaining excess carbodiimide were removed by employing two ion-exchange resins to target the pendant amine functionality and effect a simultaneous acid and base

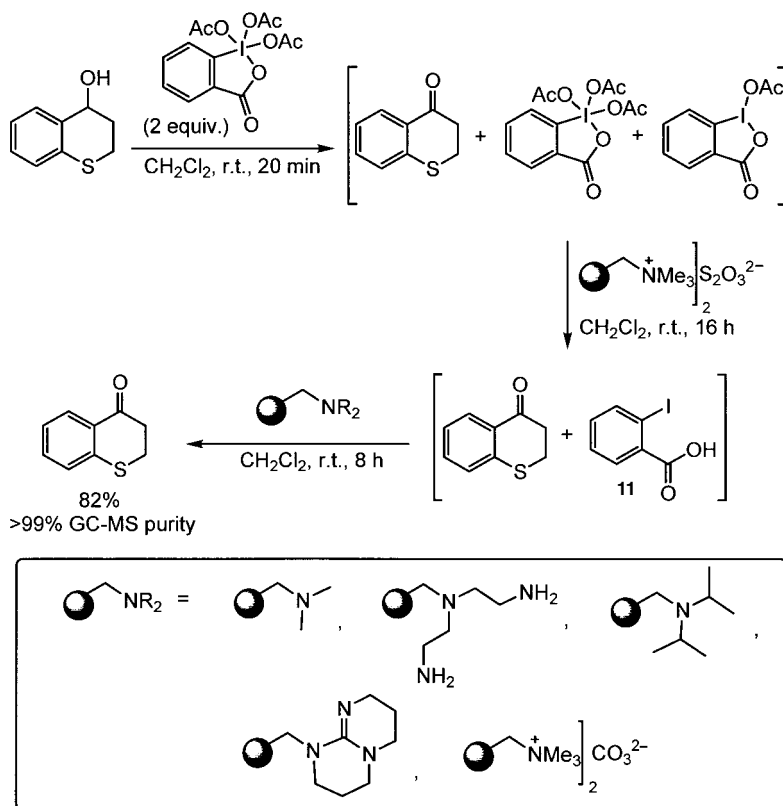


**Scheme 2.29** Rapid purification using tagged reagents for organic synthesis.

extraction. Under these conditions the various keto compounds prepared were isolated in 48–92% yield and purities ranging from 71–93%.

Following a similar strategy, an ingenious mixed resin bed quench and purification strategy was devised for the Dess-Martin periodinane mediated conversion of alcohols to carbonyls. This hypervalent iodine oxidant was viewed as containing an inherent masked carboxylic acid functionality that was revealed at the end of the reaction (Species **(11)**; Scheme 2.30). Therefore purification was easily achieved by treatment of the reaction mixture with a mixed-resin bed containing both a thiosulfate resin and a polymeric base. The thiosulfate polymer was used to reduce excess hypervalent iodine {Iodine(V) and (III) oxidation states} species to 2-iodobenzoic acid (**11**), which was in turn scavenged by the polymeric base [51].

The concept of removing solution phase reagents in post reaction clean-up operations through the use of sequestering agents offers many advantages for synthetic chemists. This is especially true if the reagent in question is commercially available at a low cost and performs a valuable and efficient synthetic transformation. Tetrabutylammonium fluoride (TBAF) is such a species that offers tremen-



**Scheme 2.30** Sequestration of Dess-Martin periodinane.





The introduction of these alternative approaches has permitted the direct transference and smooth integration of many versatile solution phase reagents from mainstream chemistry catalogues straight into practical protocols for use in combinatorial parallel library generation thus broadening the amenable chemistry base. As with all procedures it is the flexibility and synthetic scope provided by these simple operations that has enhanced their utility as alternative reaction conditions and purification strategies.

### 2.2.3

#### **Immobilized Reagents and Scavenging Techniques in Library Synthesis**

##### **2.2.3.1 Incorporation of Solid-supported Scavengers into Library Synthesis**

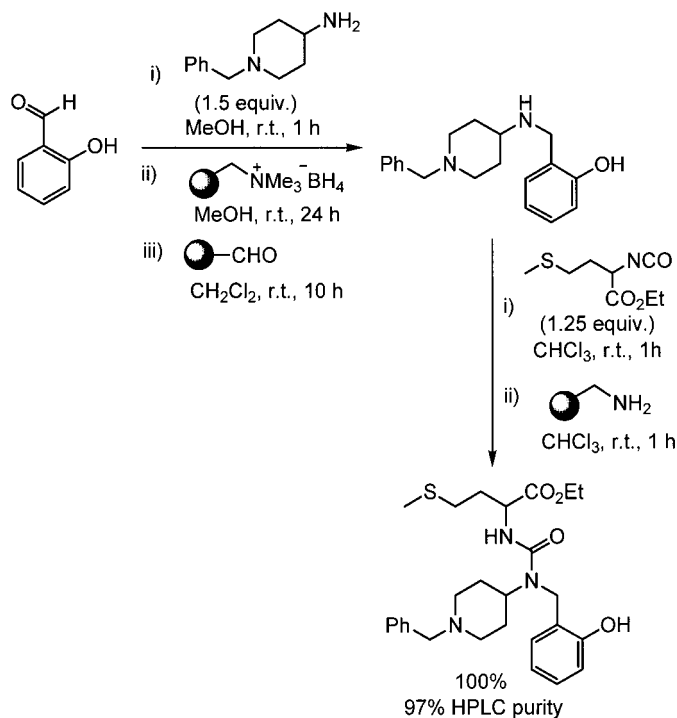
During the early days of combinatorial chemistry, compound library generation was almost solely dominated by the concepts and design characteristics imposed by solid-phase organic synthesis. Although this methodology can and still does offer tremendous faculty for large array synthesis, it does however have a number of drawbacks and limitations (see Section 1.1). One of the principle considerations being the extensive optimization and customization needed to progress immobilized molecules through even a short sequence of chemical modifications. The main difficulty as previously described is that the monitoring of such transformations can be both a time and labor intensive operation. Alternatively, parallel array synthesis in the solution phase, using solid-supported reagents in conjunction with scavengers and quenching resins, is highly attractive because it integrates all aspects of synthesis, work-up and purification into a process that is highly amenable to automated real time reaction monitoring. Consequently, in recent years a great deal of research has been conducted in order to prepare a representative selection of supported reagent systems and validated synthetic protocols that permit multi-reagent and multi-step organic synthesis. In this article we discuss the use of scavengers and various quenching techniques prior to describing the use of immobilized reagent systems. However it should be recognized that only by the combined operation of all these techniques and methods is one able to properly express the full range of synthetic opportunities.

Kaldor [49i, 55] demonstrated the advantages of applying solid-supported scavengers to the preparation of parallel arrays in a multi-step fashion. In these studies he examined the clean-up of multiple amine alkylation and acylation reactions using a variety of immobilized electrophilic and nucleophilic scavenger reagents including an amine, isocyanate, aldehyde and acid chloride (Tab. 2.1).

Following the initial investigation of the scavenging potentials of these systems they were used in the construction of a small library of ureas (Scheme 2.33). The initial reductive amination using polymer-supported borohydride also required the use of excess primary amine to facilitate formation of the imine. The residual primary amine was selectively removed from the reaction mixture following reduction using a supported aldehyde. Then the resulting solution of secondary amine was treated with an excess of isocyanate to provide the urea. In a final purification step, the additional unreacted isocyanate was scavenged through the use of an

Tab. 2.1 Immobilized electrophilic and nucleophilic scavenger reagents

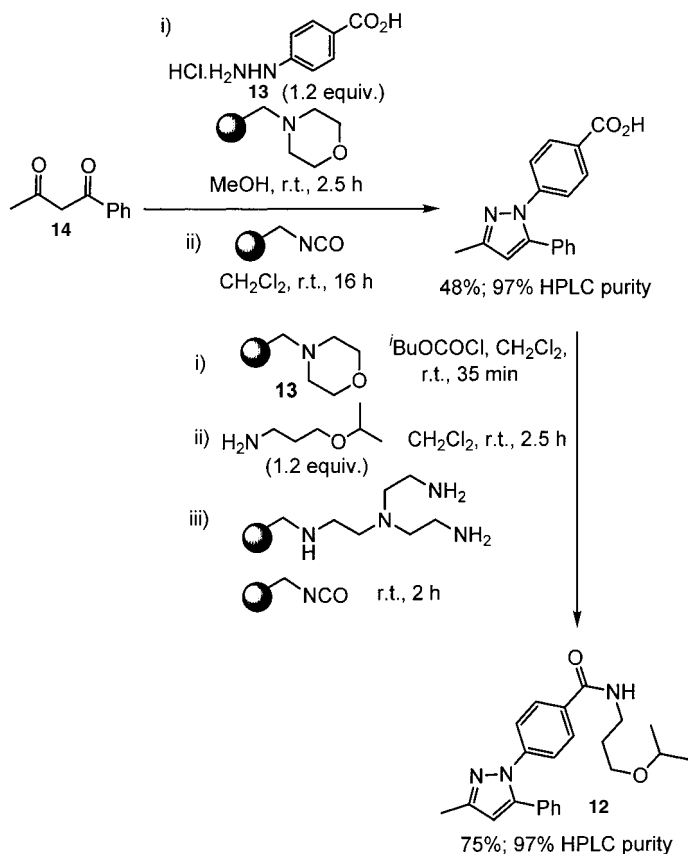
Entry	Electrophile	Nucleophile	Scavenger	Representative Product	Yield	Purity (HPLC)
1	$R^3NCO$ $R^3COCl$ $R^3SO_2Cl$	$\begin{array}{c} R^1 \\ \diagdown \\ NH \\ \diagup \\ R^2 \end{array}$			67%	94%
2		$\begin{array}{c} R^1 \\ \diagdown \\ NH \\ \diagup \\ R^2 \end{array}$			94%	93%
3	$R^3-X$	$\begin{array}{c} R^1 \\ \diagdown \\ NH \\ \diagup \\ R^2 \end{array}$			96%	> 95%
4	$\begin{array}{c} O \\    \\ R^2-C-R^3 \end{array}$	$R^1-NH_2$			73%	90%
5	$\begin{array}{c} O \\    \\ R^2-C-R^3 \end{array}$	$\begin{array}{c} R^1 \\ \diagdown \\ NH \\ \diagup \\ R^2 \end{array}$			62%	> 95%



**Scheme 2.33** Urea library generation and purification using polymer-supported systems.

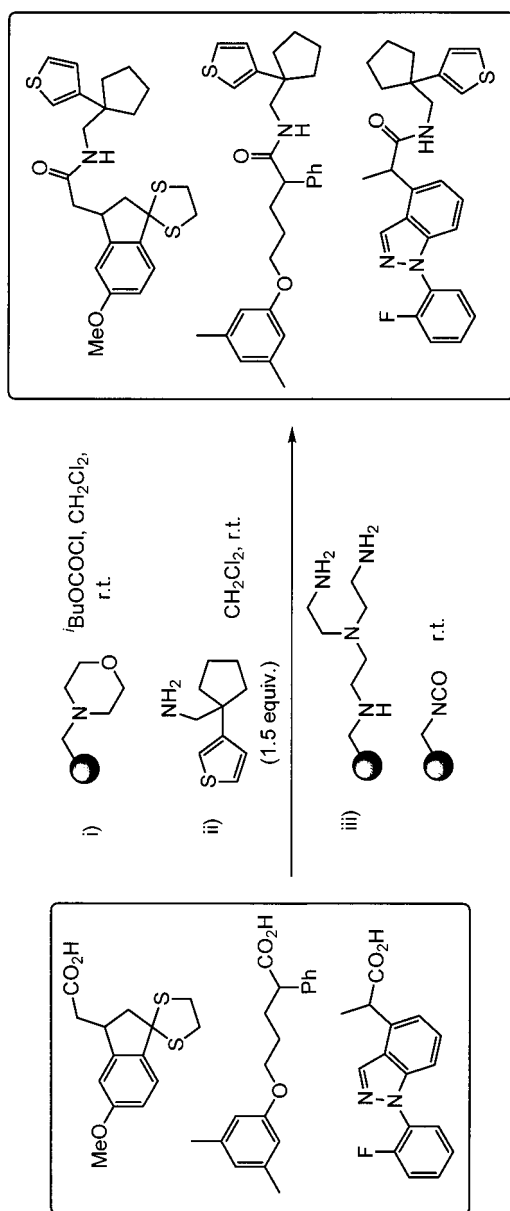
aminomethylated polystyrene resin. The authors report that these general concepts were used to prepare thousands of different amides, sulfonamides, ureas and thioureas compounds for biological evaluation. As exemplification of these procedures the authors reported the discovery of a selection of novel antirhinoviral leads possessing sub-micromolar potency. These were identified by screening a combinatorial library of ureas (4000 member) which was prepared using aminomethylpolystyrene as a covalent scavenger to remove isocyanate impurities [55].

In a seminal paper [56] entitled 'Polymer-Supported Quenching Reagents for Parallel Purification' Hodges and Booth from Parke-Davis described the preparation and application of a high loading polyamine resin for the removal of highly reactive monomers such as acid chlorides, sulfonyl chlorides, isocyanates and isothiocyanates for use in the parallel purification of solution-phase libraries. A number of classical transformations were reported yielding products with high purity following the scavenging process. In the same paper the authors also described the development of a polystyrene-based methylene isocyanate for covalently trapping nucleophilic substrates such as amines. Both of these reagents were used in conjunction with a third weakly basic morpholine resin to assist in the multi-step construction of the pyrazole (**12**) (Scheme 2.34). The condensation reaction be-



**Scheme 2.34** Polymer-supported quenching reagents for parallel purification.

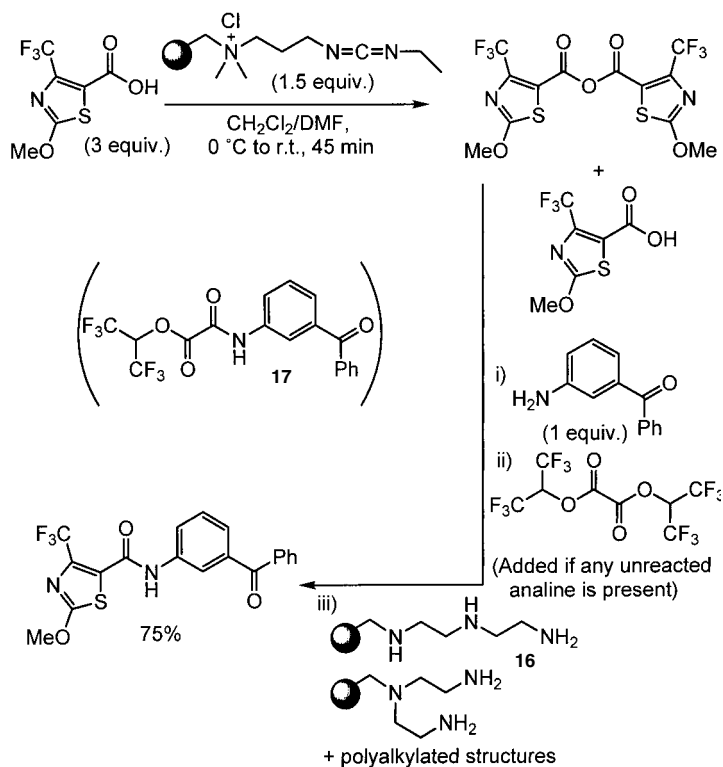
tween the aryl hydrazine (**13**) and the 1,3-diketone (**14**) was performed in the presence of the morpholinomethyl resin acting as both a basic catalyst and acid scavenger. The removal of the excess hydrazine was achieved using the polystyrene-bound isocyanate to give the arylpyrazole in high overall purity. Next, the derivatization of the carboxylic acid moiety to the amide was achieved *in situ* via initial conversion to the mixed anhydride followed by substitution with the primary amine (**15**). The reaction mixture was then purified by treatment with the trisamine resin to remove unreacted isobutyl chloroformate and remnants of the anhydride, while the supported isocyanate was used to extract the excess primary amine. In a similar manner, the same three supported reagents were shown to be effective for the simultaneous synthesis of a mixed solution of compounds (Scheme 2.35). In this example a set of three diverse carboxylic acids were converted to the corresponding mixed anhydrides, then coupled with an excess of a single primary amine to generate a mixture of amides. The crude reaction was treated by the scavenger clean up procedure to remove any trace amounts of start-



Scheme 2.35 Mixed solution phase library synthesis.

ing material then analyzed by HPLC and  $^1\text{H}$  NMR, this confirmed an approximately equimolar mixture containing only the three possible amides. It was proposed that following exactly the same sequence a larger more complex collection of amides could be synthesized with comparable results, thus increasing the scope of solution-phase library generation.

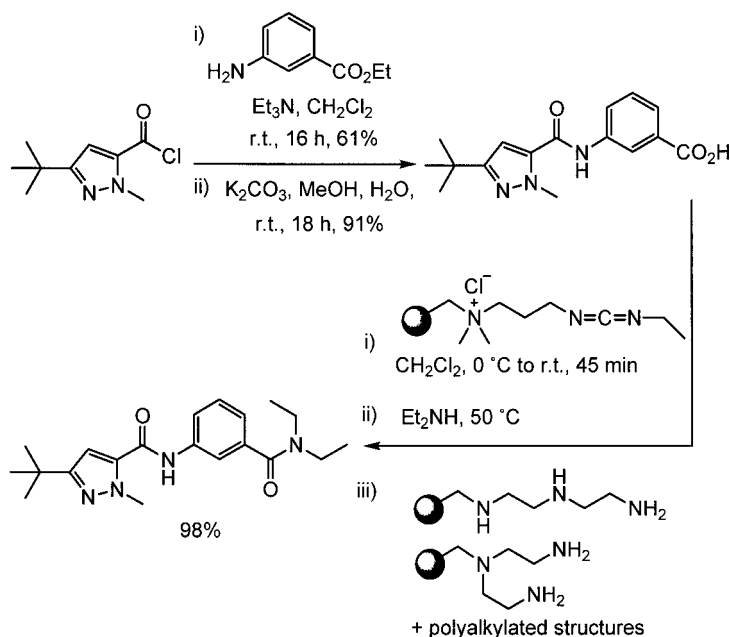
Parlow and co-workers continued to develop the concepts of complementary molecular reactivity and recognition through the preparation of an improved polyamine scavenging reagent [57]. This new immobilized amine had a sequestering capacity in the order of 2–3 times that of the commercially available systems, with the added advantages that it was cheaper and extremely easy to synthesize. Its simple preparation from Merrifield resin and excess diethylene triamine produced a polymer with an irregular architecture (**16**), because the varying composition of mono- and dialkylated units results in significant levels of cross-linking (~40%). This however did not effect its activity and the scavenger was subsequently used in the parallel solution-phase lead optimization of a heterocyclic amide based library (Scheme 2.36).



**Scheme 2.36** Combinatorial library generation using novel polyamine scavengers.

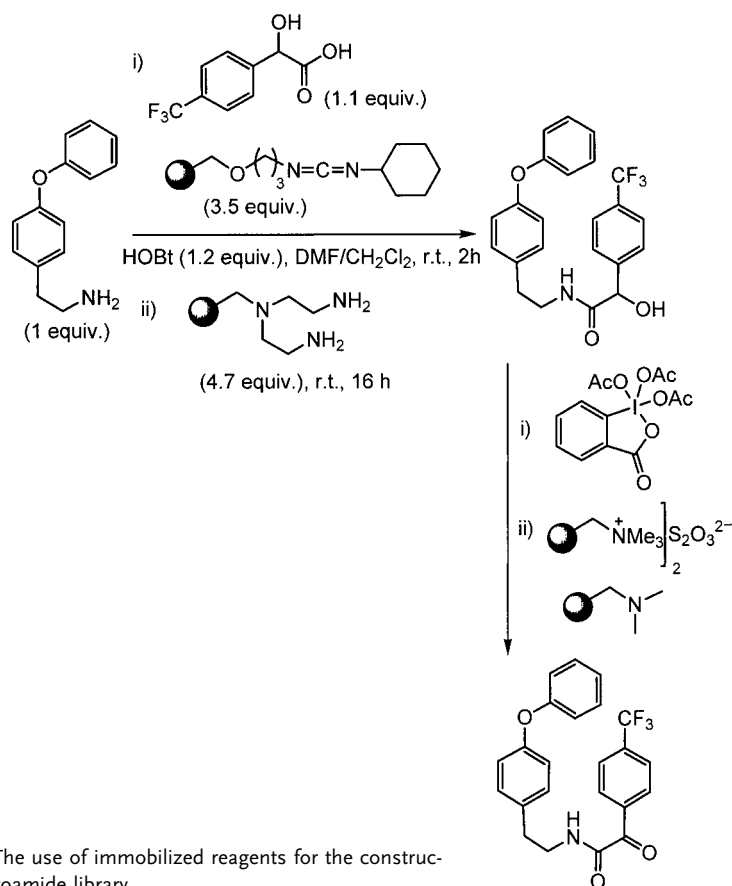
In this sequence a variety of substituted carboxylic acids were accessed and readily converted to their respective anhydrides using a supported carbodiimide reagent. These *in situ* generated anhydrides were immediately reacted with a variety of amines to furnish the desired amides which were contaminated with residues of the original acid component and by-products from the anhydride and aniline. In an interesting extension to the sequestering procedure the aniline component was modified using a 'scavenger enabling reagent' (SER), in this case hexafluoroisopropyl oxalate, resulting in exclusive formation of (**17**). This transformation permitted the simultaneous removal of the now activated aniline component (**17**) in combination with the anhydride and acid by-products following the use of only a single universal scavenge with the mixed polyamine resin (**16**). A similar method was also applied to the combinatorial refinement of the amine fragment (Scheme 2.37). In this synthesis the amine unit was methodically changed to optimize the structural diversity of the right hand fragment thus preparing a second complementary library of amide products. In total, over 400 compounds were produced for biological screening and this resulted in the successful identification of an active herbicide with a four-fold increase in potency over the original lead compound.

A number of polymer assisted procedures have been described that have subsequently become standard practice within the domain of solution-phase library synthesis (complementary molecular reaction and recognition, scavenging, tagged reagent systems and catch and release protocols). A number of these concepts have



**Scheme 2.37** Combinatorial library generation using novel polyamine scavengers.

been effectively homogenized in two multi-step parallel syntheses, the first a  $\alpha$ -ketoamide array (Scheme 2.38) [58] and the second a diaminobenzamide library (Scheme 2.39) [59]. South and co-workers reported both of these examples. The preparation of the  $\alpha$ -ketoamide library was initiated by amide coupling of an  $\beta$ -hydroxy acid with an amine using an immobilized carbodiimide and 1-hydroxybenzotriazole (HOBt) promoter. A basic polyamine resin was then used to remove the various coupling related impurities, leaving the desired hydroxyamides in solution. The oxidation to the corresponding ketoamides was then achieved using excess Dess-Martin periodinane which, as previously described was converted to 2-iodobenzoic acid and sequestered following reaction using a mixed bed of thiosulfate resin and Amberlyst A-21. Likewise the synthesis of the functionalized diaminobenzamide library involved an amide bond forming reaction using the same polymer-bound carbodiimide/HOBt system followed by a scavenging step. In addition, early in the reaction scheme a resin capture and release protocol was employed to remove both organic and inorganic impurities resulting in the isolation



**Scheme 2.38** The use of immobilized reagents for the construction of an  $\alpha$ -ketoamide library.



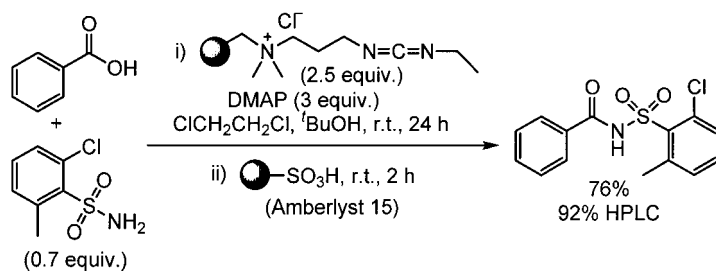


of the majority of compounds in very high overall purity (>95%). These reports are significant in that functionalized polymers are used in a number of situations, not only as reagents and scavengers, but also to effect a catch and release purification.

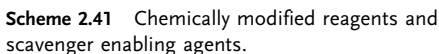
Acylsulfonamides have been readily prepared through the simple condensation of carboxylic acids with sulfonamides in the presence of a dehydrating agent. Accordingly, a convenient preparation has been described using a combination of a polymer-supported carbodiimide and excess dimethylaminopyridine (DMAP) to activate various carboxylic acid components towards coupling with primary sulfonamides (Scheme 2.40) [60]. In addition, an effective and practical method was devised for the removal of the unwanted DMAP by treatment of the reaction mixture with a sulfonic acid resin followed by filtration. Optimization of the reaction stoichiometry established that the use of excess acid coupling component gave improved yields and purity with any unreacted acid remaining attached to the carbodiimide resin. Consequently 25 different acylsulfonamide products were synthesized in respectable yields (56–81%) and excellent purities (85–92% by HPLC).

Previously developed ideas of using chemically modified reagents and scavenger enabling systems for the preparation of solution-phase libraries were soon used together in powerful combinations (Scheme 2.41) [61]. Initial ester formation under Mitsunobu conditions was conducted using specially designed phosphine and azodicarboxylate reagents (step i; Scheme 2.41). Addition of trifluoroacetic acid (TFA) to the post reaction mixture conveniently hydrolyzed the pendant *tert*-butyl ester groups to the corresponding acids which were then scavenged using a polymer-supported carbonate base. This sequence also had the added advantage of removing the Boc protecting group, thus revealing the 2° amine, which was easily acylated. Treatment of the reaction mixture with tetrafluorophthalic anhydride derivatized any hydroxylic starting materials or free unreacted 2° amine and was itself removed, along with any remaining acid chloride, by the addition of a polyamino scavenger resin [62].

A synthesis of a library of benzoxazinones was also accomplished by blending several of the previously described methods (Scheme 2.42) [63]. This creative piece of work used a polymeric DMAP equivalent to mediate a coupling between aniline frag-

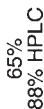


**Scheme 2.40** Facile acylsulfonamide preparation using a sequence of immobilized reagents.

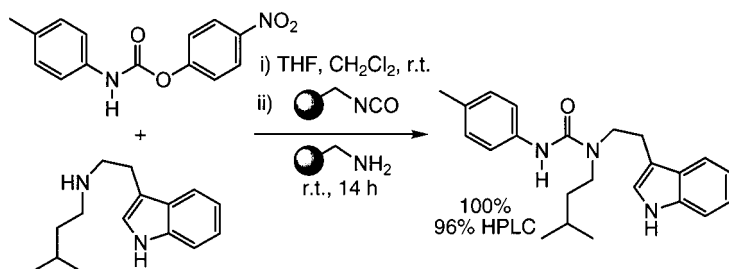


ment (18) and a variety of isocyanates. The reactions were then purified by the application of tetrafluorophthalic anhydride as an enabling reagent, followed by universal scavenging of the electrophilic components using aminomethylpolystyrene. An acid-catalyzed Boc deprotection revealed a second aniline unit which was in turn functionalized with a range of different electrophiles such as acid chlorides. Cleavage of the 2-(trimethylsilyl)ethyl ester group proceeded smoothly using TBAF, which was then quenched and purified using the previously described combination of a calcium sulfonate and sulfonic acid resins. Finally, cyclodehydration with a polymer-supported carbodiimide afforded the benzoxazinone material in good purity. Conducting this route in a parallel fashion permitted the synthesis of an eight by eight array of compounds all isolated in respectable yields.

The combinatorial library synthesis of a diverse set of trisubstituted ureas has been described [64]. The synthetic pathway involves the preliminary preparation of various nitrophenylcarbamates from commercially available nitrophenyl chloroformate and a selection of amines allowing for wide scope in the divergence of the final urea products. In a further reaction of the nitrophenylcarbamates with a second amine, the urea was generated. Simultaneous addition of an electrophilic and basic scavenger resin removed all by-products, again allowing rapid isolation of the products in excellent yield and purity (Scheme 2.43).



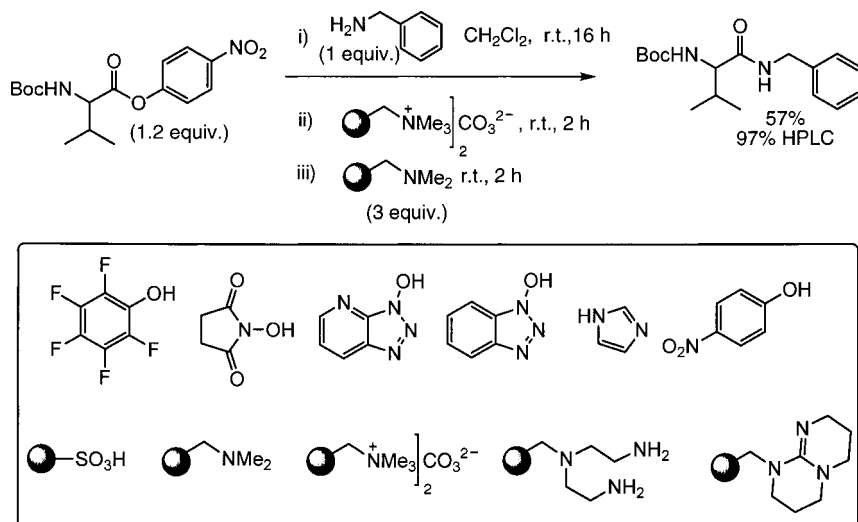
**Scheme 2.42** Parallel synthesis of a benzoxazinone library.



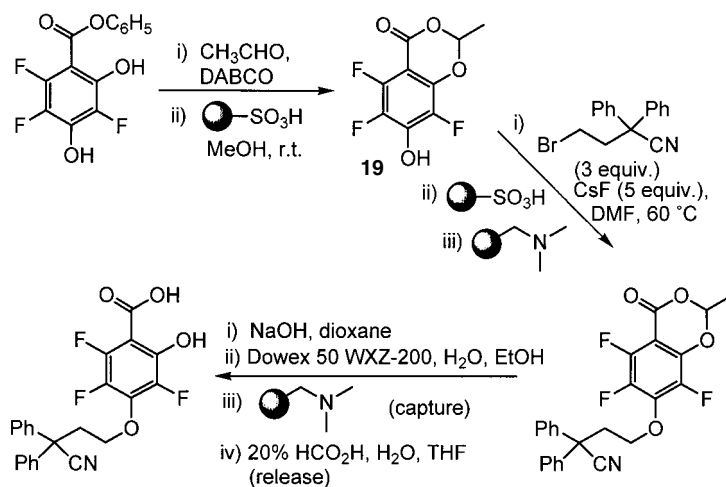
**Scheme 2.43** Combinatorial library synthesis of trisubstituted ureas.

In a very similar strategy, the Monsanto group applied a range of scavenger resins for the extraction of the activated ester components and their leaving group by-products during amide bond formation (Scheme 2.44) [65]. This sequence was designed following an extensive investigation of the scavenging capabilities of several commonly used polymers for removal of acyl transfer agents (Scheme 2.44; boxed area). An interesting discovery was the ability of the immobilized carbonate base to partially sequester the imidazole (70–80%), presumably as the anion.

The selective alkylation of a chemically distinct phenolic site on a perfluorinated aromatic has been achieved following a polymer assisted solution phase protection of an alternative *o*-hydroxybenzoic acid unit as the dioxin-4-one (**19**) (Scheme 2.45) [66]. A diverse set of 22 different alkyl and benzyl bromides were then attached to the free phenol using cesium fluoride as the base, followed by treatment with Amberlyst 15 and Amberlyst A-21 as the work-up. Subsequent hydrolysis of the dioxin-4-one group with NaOH proceeded smoothly and was quenched



**Scheme 2.44** Amide bond formation using activated esters and scavenger resins.



**Scheme 2.45** Synthesis of potential enzyme farnesyl transferase inhibitors.

with an acidic Dowex 50WX2-200 resin. Finally, a solid supported tertiary amine base (A-21) and a 20% solution of formic acid were used to facilitate a catch and release purification. The final compounds were isolated in very variable yields from 2–46% but in purities ranging from 85–100%. These compounds were screened as potential inhibitors of the enzyme farnesyl transferase, an important target in many cancer therapies, but unfortunately showed very disappointing biological activities.

### 2.2.3.2 The Application of Immobilized Reagents and Scavengers to Library Synthesis

#### Small molecule construction

Many of the routes reported for the construction of diverse chemical libraries are often constrained by the commercial availability of the monomer sets used as the primary building blocks. While there are a large number of *simple* starting materials currently available, chemists would prefer to have ready access to more sophisticated and highly functionalized monomer units which would lead rapidly to drug-like molecules.

One of the most versatile functionalities in organic chemistry is the carbonyl group or more specifically aldehydes. These are important starting materials for many synthetic transformations and so a clean scalable preparative method that offers additional sources of aldehydes for integration into combinatorial chemistry programs would represent a valuable supplement. This need has been met through the use of catalytic amounts of polymer-supported perruthenate (PSP) [67] to convert gram quantities of primary alcohols to novel aldehydes. In addition this has provided the opportunity for splitting of these batches and their diversion

into many different synthetic routes to form a diverse library of small drug-like molecules and building blocks (Scheme 2.46).

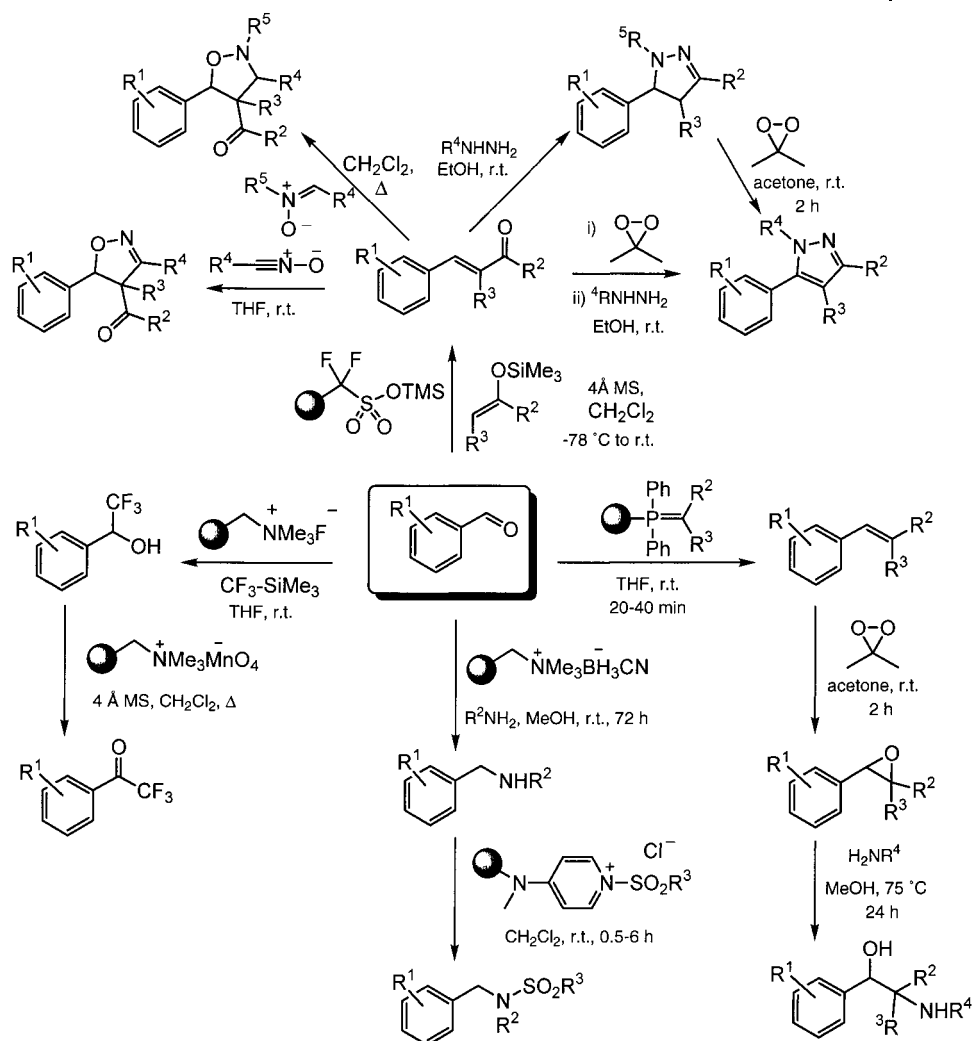
The Mukaiyama aldol reaction of aldehydes with silyl enol ethers catalyzed by Nafion-TMS in the presence of 4 Å molecular sieves has been used to generate  $\alpha,\beta$ -unsaturated carbonyl compounds in high yields and purity. These products have proven to be useful building blocks in many synthetic sequences, for example, treatment with various hydrazines resulted in the formation of a range of dihydro-pyrazole molecules (Scheme 2.46) [68]. These products can in turn be *in situ* oxidized with dimethyldioxirane to their aromatic derivatives. Alternatively, the synthetic sequence can be reversed so that the epoxide is initially formed from the unsaturated carbonyl and the pyrazole subsequently generated directly from addition of the hydrazine. Both the 1*H*-pyrazoles and 4,5-dihydro-1*H*-pyrazoles have found diverse applications in both medicine and agriculture. In particular, they are known as potent antibiotic and antioxidant agents [69]. These methods therefore represent rapid routes to the identification of new therapeutic target molecules.

Again starting from the aldehyde, the reaction with a trifluoromethyl anion, generated from  $\text{Me}_3\text{SiCF}_3$  and polymer-supported fluoride, affords the corresponding alcohols which can be readily oxidized using solid-supported oxidants to generate trifluoroacetyl derivatives (Scheme 2.46) [70]. These compounds again represent very valuable building blocks for medicinal chemistry programs.

The use of an automated synthesis (Advanced ChemTech 496 synthesizer) has expedited the synthesis of a small collection of sulfonamides. This has been accomplished starting with a PSP promoted alcohol to aldehyde oxidation followed by reductive amination mediated by a polymer-bound cyanoborohydride reagent. Finally, the amine functionality was elaborated with a series of polymer-supported aminomethylpyridine sulfonylating agents (Scheme 2.46) [71]. This concept of rapid molecular assembly allows for a wide range of chemical diversity to be incorporated at all stages of the synthesis and so is extremely useful in the generation of arrays for screening purposes.

The Wittig reaction employing polymer-supported ylides is particularly useful since the by-product phosphine oxide remains attached to the polymeric-support and hence can be completely removed by filtration. This transformation has been exploited by Ley *et al.* in a multi-step sequence to produce selected alkenes from aldehydes and ketones which, upon treatment with dimethyldioxirane, undergo clean conversions to the corresponding epoxides. In an ensuing epoxide ring opening reaction with various amines, the  $\beta$ -hydroxyamino compounds were obtained in high yields (Scheme 2.46) [72]. These relatively easily prepared systems are considered to be highly valuable structural motifs in many pharmaceutical products.

Polymer-supported perruthenate has also been used in two convergent pathways for the synthesis of isoxazolidines with each route employing different starting materials in order to create the maximum structural diversity [73]. In the first route secondary hydroxylamines, readily prepared from amines by *in situ* treatment with dimethyldioxirane, were oxidized directly to nitrones using polymer-supported perruthenate (PSP). Alternatively, primary alcohols were used as the

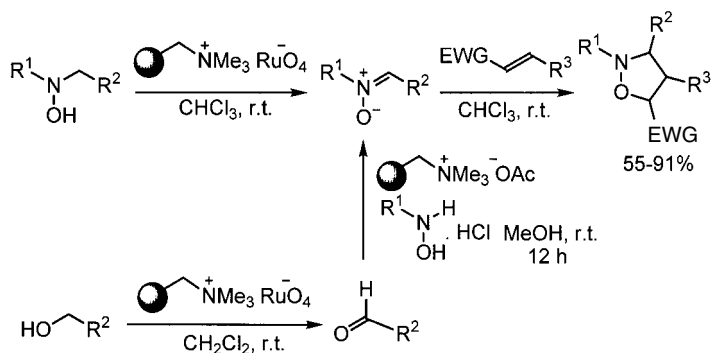


**Scheme 2.46** PSP oxidation of alcohols to aldehydes, versatile starting materials for chemical synthesis.

starting material which, upon oxidation with PSP, gave aldehydes. These were in turn condensed with primary hydroxylamines, promoted by polymer-bound acetate, to produce nitrones. The nitrones assembled using either method then underwent 1,3-dipolar cyclo-addition reactions with various alkenes to give the corresponding isoxazolidines (Scheme 2.46 and 2.47).

Under carefully controlled conditions the selective mono bromination of an electronically diverse range of acetophenone derivatives can be realized using the polymer-supported pyridinium perbromide reagent. The resultant  $\alpha$ -bromoketone



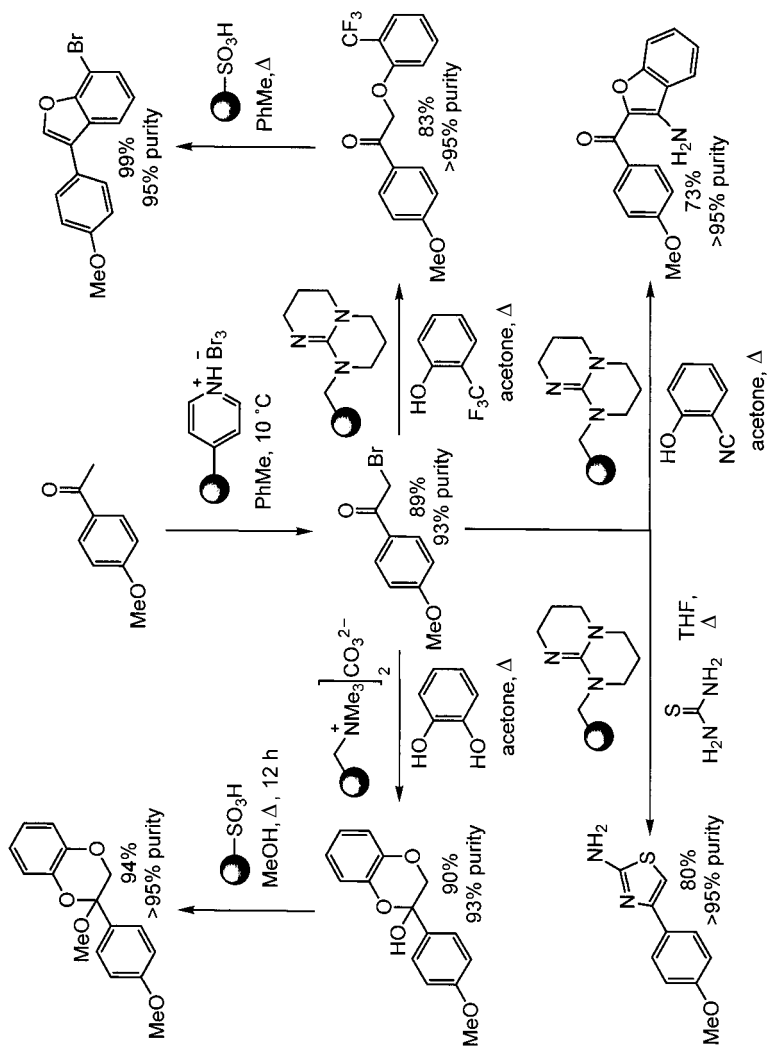


**Scheme 2.47** Preparation of isoxazolidines via 1,3-dipolar cyclo-addition.

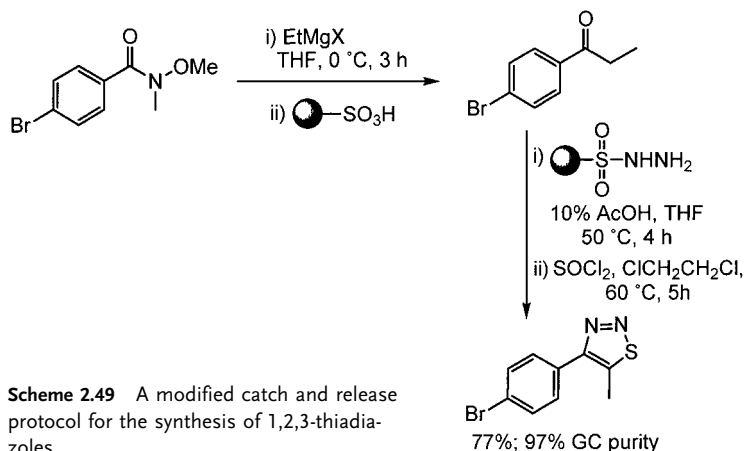
products are themselves very attractive precursors for synthetic programs, being readily converted into a many interesting heterocyclic compounds. For example, libraries of benzofurans have been prepared by two independent routes starting from these simple intermediates (Scheme 2.48) [74]. Hence the reaction of substituted phenols and  $\alpha$ -bromoketones in the presence of a solid-supported base such as PS-TBD affords the substitution product which, upon treatment with Amberlyst 15 cyclizes to the 3-arylbenzofurans. Alternatively, the reaction of an  $\alpha$ -bromoketone with 2-hydroxy benzonitrile under the same base catalyzed conditions leads directly to the 3-aminobenzofuran adduct. In another related study these same  $\alpha$ -bromoketones were treated with catechols in the presence of a carbonate resin to give rise to 1,4-benzodioxans (Scheme 2.48) [75]. The compounds could then be additionally modified via hemiacetal exchange with an alcohol in the presence of a sulfonic acid resin. A further application is the condensation of  $\alpha$ -bromoketones with thiourea in the presence of a polymer-supported guanidinium base (PS-TBU) to give 2-amino-4-phenyl-1,3-thiazole derivatives. All these compounds can be conveniently prepared in gram scale either as dedicated targets or as fragments for incorporation into other synthetic programs.

Novel ketones prepared from the addition of Grignard reagents to Weinreb amide derivatives have been used as the starting point for the synthesis of substituted thiadiazoles in yields ranging from 48 to 98% (Scheme 2.49) [76]. The organometallic reactions were worked-up by protonation with a sulfonic acid resin acting to both quench the tetrahedral intermediate (plus residual metalated species) and to remove the extruded Weinreb amine. The key synthetic feature of this sequence is the subsequent covalent capture of the newly formed ketone onto a sulfonyl hydrazine functionalized polystyrene followed by a ring forming Hund-Mori release reaction using thionyl chloride. In this way only substrates that undergo the desired reaction are released from the polymer, allowing isolation of the products in reasonably high purity 71–99% (by GC).

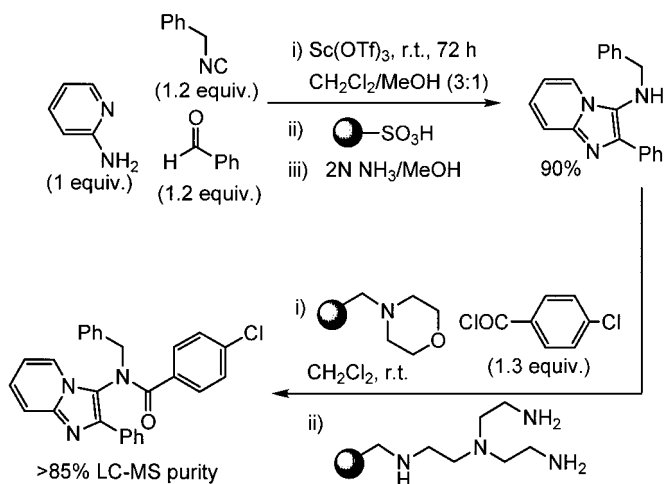
Multi-component condensation reactions offer tremendous scope for increasing diversity in combinatorial chemistry programs since, in a single reaction, structurally advanced compounds can be realized from very simple starting materials. In

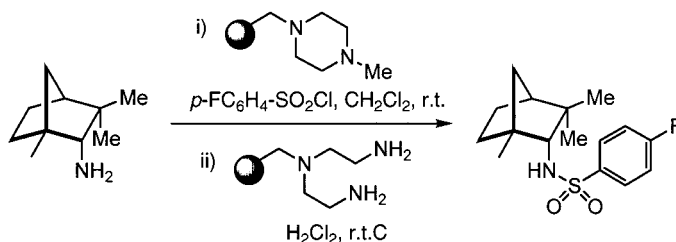


**Scheme 2.48** Multi-step synthesis of 3-arylbenzofurans, 1,4-benzodioxans and 2-amino-4-phenylthiazole derivatives.



this manner a new regioselective three-component coupling reaction involving a scandium triflate catalyzed condensation of an aldehyde, isonitrile and amine has been developed and applied to the parallel synthesis of 3-aminoimidazo[1,2a]-pyridines and pyrazines (Scheme 2.50) [77]. The products from these reactions were then captured onto a strongly acidic cation exchange resin, thereby removing them from contaminating impurities and unreacted aldehyde and isonitrile. The purified material was cleanly released from the resin by treatment with a solution of methanolic ammonia with isolated yields typically in the range of 75–95% and purities exceeding 85%. The 3-amino position could be additionally acylated in the





**Scheme 2.51** Derivatization of fenchylamines using immobilized reagents.

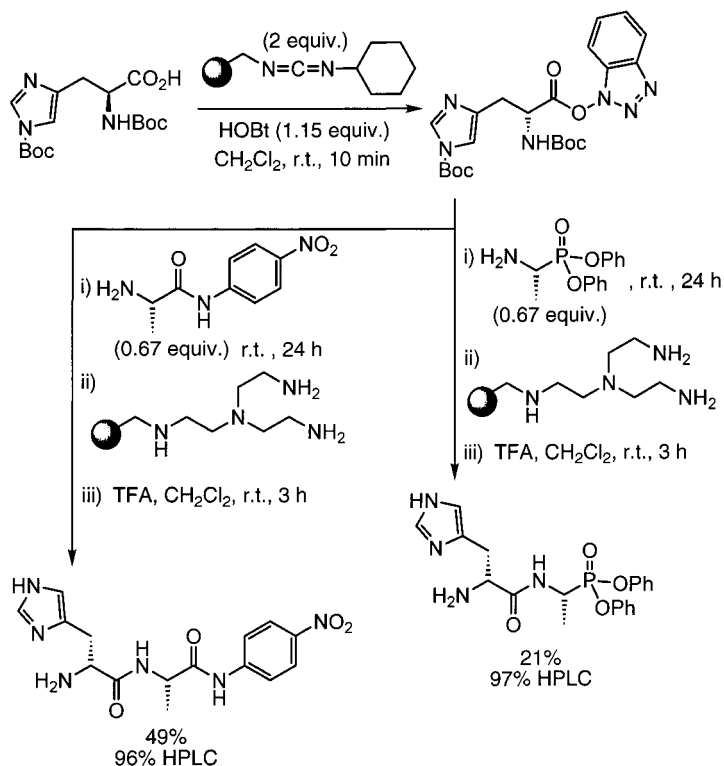
presence of a polymer-supported morpholine base with excess acid chloride being scavenged by a polymer-supported tris(2-aminoethyl)amine derivative.

A simple derivatization of optically pure *endo*-fenchylamines has been carried out using several aryl sulfonyl chlorides, catalyzed by an immobilized *N*-methyl piperazine (Scheme 2.51) [78]. The compound collection was purified by treatment with a polyamine resin in order to remove excess sulfonyl chloride and derived hydrolysis products. The resulting sulfonamide was used to establish a basic structure activity relationship for this class of amyloid  $\beta$  peptide inhibitors with the aim of developing a new drug for the treatment of Alzheimer's disease. Although this specific example is not particularly attractive because of the chemistries involved, it does demonstrate the changing philosophy towards the application of these methods in drug discovery programs.

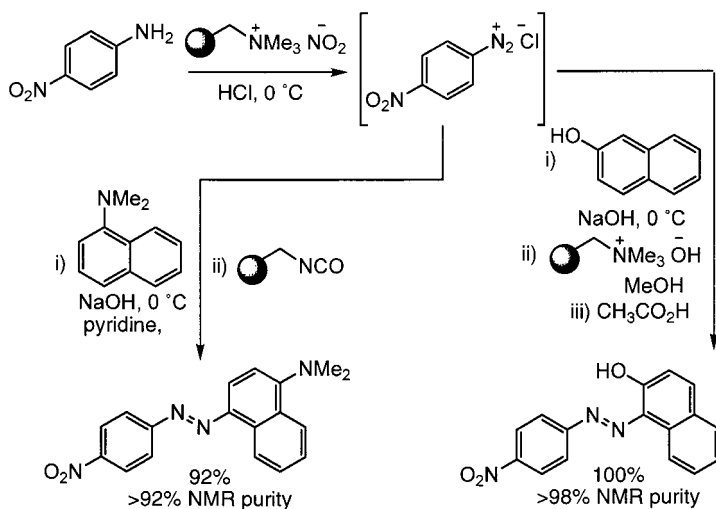
Supported reagents have found application in many areas of synthesis including the construction of small peptides, the traditional foundation stone of solid phase synthesis. For example a recent paper describes the preparation of dipeptide *p*-nitroanilide and phosphonate libraries by supported carbodiimide coupling and scavenger purification (Scheme 2.52) [79].

The clean and efficient production of azo dyes is a classical chemistry problem. The manufacture of this industrially important family of compounds is traditionally associated with the additional formation of large quantities of hazardous and colored waste. A method for the construction of both phenolic and amino azo dyes has been reported using a polymer-supported nitrite reagent to effect diazotization of aromatic amines (Scheme 2.53) [80]. Waste minimization and operational simplicity, along with improved separation technologies, are key advantages of polymer-supported reagents in this area.

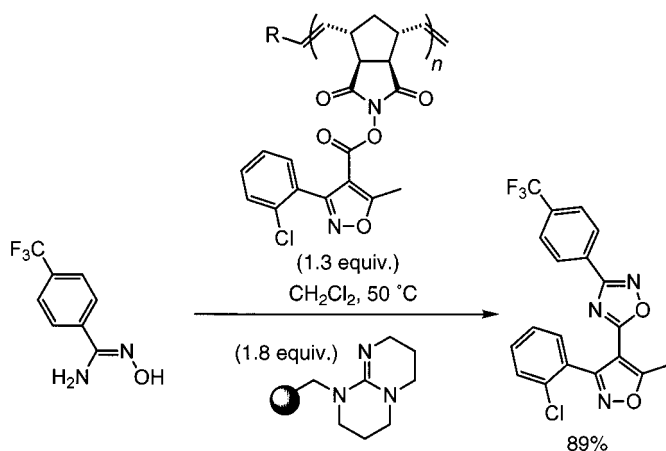
Barrett has developed a polymerization process for incorporating functionalized monomer units which possess either the desired reagent moiety or an easily derivatized group. Typically these reagent species are manufactured by a ruthenium catalyzed co-polymerization of an appropriately substituted alkene monomer and a strained olefin such as norbornene or 7-oxanorbornene. A number of such systems have been prepared and given the generic title of ROMPGELS. This polymerization process leads to supports with a range of physical properties, such as solubility characteristics caused by differing chain lengths and the degree of functionalization of the polymer. An interesting application of an insoluble variant has been described



Scheme 2.52 Peptide library generation using supported reagents.



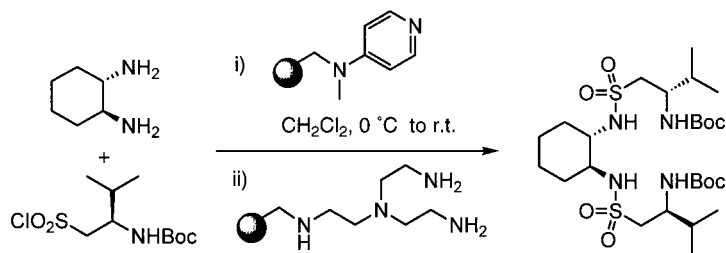
Scheme 2.53 General procedures for the construction of various azo dyes.



**Scheme 2.54** ROMPGEL polymers for organic synthesis.

for the chromatography-free one-pot synthesis of 1,2,4-oxadiazoles [81]. In this case a range of ROMPGEL supported active esters were prepared and reacted with amidoximes giving the *O*-acylation intermediates which then underwent base catalyzed dehydrative cyclization promoted by polymer-supported 1,5,7-triazabicyclo[4.4.0]dec-5-ene (PS-TBU) to yield the oxadiazoles in excellent yields (Scheme 2.54).

Supported reagents and scavengers have been principally used by medicinal chemists to expedite the work-up and purification of combinatorial libraries targeted at lead generation and lead optimization of biologically active compounds. Alternatively, solid phase extraction (SPE) techniques have also found application in the preparation of two new families of chiral Schiff bases used as ligands in transition metal-catalyzed enantioselective synthesis [82]. For example, a set of 1,2-diamines were reacted with a number of amino-acid derived sulfonyl chlorides catalyzed by polymer-bound dimethylaminopyridine (PS-DMAP), any excess sulfonyl chloride was subsequently removed with an polyamino scavenging resin (Scheme 2.55). The resulting disulfonamide ligand library (30 compounds) was screened for enantioselective induction in the  $\text{Ti}(\text{OiPr})_4$  mediated addition of  $\text{Et}_2\text{Zn}$  to a variety of aldehydes with good to excellent enantiomeric ratios being obtained.

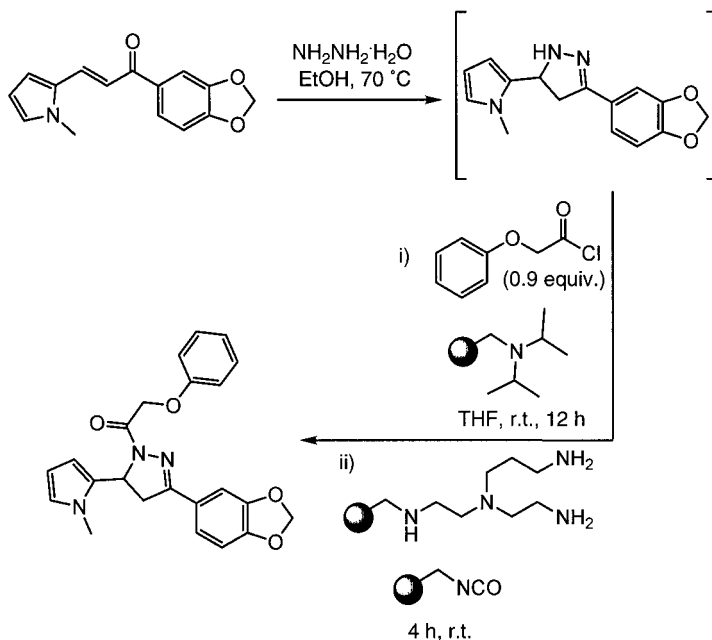


**Scheme 2.55** The combinatorial preparation of schiff bases as ligands for asymmetric catalysis.

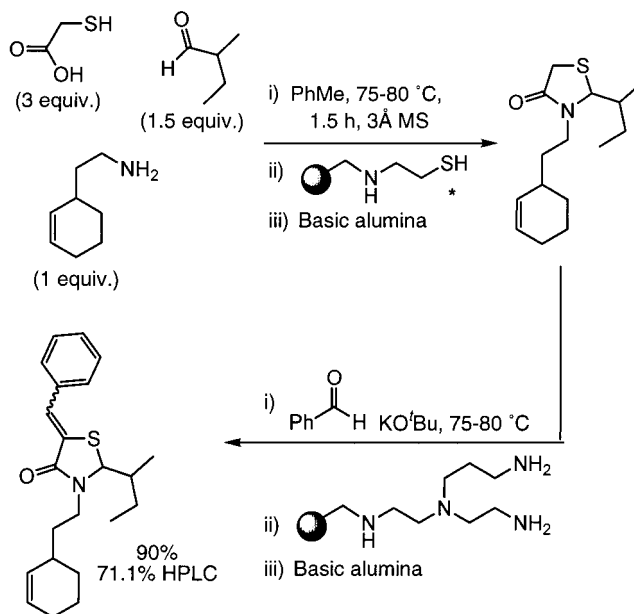
**Automated library synthesis using solid-supported reagents**

Recently, a procedure for the synthesis of substituted pyrazoles, employing solid-supported reagents, has been published (Scheme 2.56) [83]. This approach involves the direct treatment of chalcones with hydrazine monohydrate followed by *in situ* trapping of the unstable pyrazoline intermediates with various classes of electrophile (acid chlorides, chloroformates, isocyanates and sulfonyl chlorides). In the reactions where this combination of reagents generated hydrochloric acid, a polymer-bound diisopropylamine base was employed. The tandem sequestration of trace amounts of pyrazoline and excess electrophile was accomplished by applying a combination of polymer-supported isocyanate and polytrisamine resins to form in excess of 1500 derivatives, generated in a 96-well format. Several of the compounds prepared were identified as possessing biological activity although no specific mention of their therapeutic applications was designated.

A one pot formation and purification of a 5-arylidine 4-thiazolidinone library has also been reported using polymer scavenging as the principle method of purification. An automated synthesizer was employed to make a parallel array of 4080 4-thiazolidinones, prepared simultaneously from a 3-component condensation of mercaptoacetic acid with an amine and a carbonyl compound. Further structural decoration was then introduced using the 'libraries from libraries' principle where the core template was derivatized via an aldol reaction with a second carbonyl unit at the 5-methylene position (Scheme 2.57) [84]. After both synthetic steps,



**Scheme 2.56** Polymer-supported reagents for heterocycle formation.



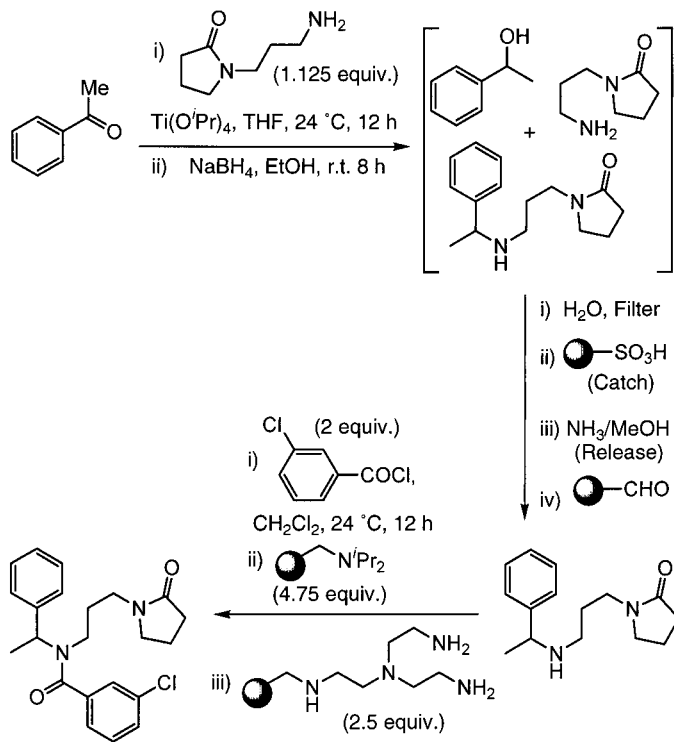
**Scheme 2.57** Three component condensation reaction using polymer supported scavenger purification \* alternatively the trisamine resin could be substituted for purification in this step.

the addition of basic alumina was used to remove trace amounts of baseline material by filtration, thereby increasing the overall purity of the products.

An extended library synthesis of simple amide analogs has been prepared and was conducted on an automated platform. The routine involved a combination of standard solution phase reagents and supported scavenging agents (Scheme 2.58) [85]. Initially, an array of 24 secondary amines was generated by a titanium(IV) isopropoxide mediated reductive amination procedure (3 ketones, 3 aldehydes and 4 amines) using a Trident<sup>TM</sup> synthesizer. These amines were then used in split array synthesis to generate sub-libraries of ureas, amides and sulfonamides. Various immobilized scavenger systems were employed to assist in the parallel work-up and purification of the different libraries including a catch and release technique for the separation of the desired amine component from contaminating alcohol by-products following the borohydride reduction step. Although this work involved the formation of relatively simple compounds it does aptly demonstrate the ease and effectiveness of employing supported reagents for the generation of chemical libraries involving automated purification strategies.

Poly(4-vinylpyridine), a readily available and inexpensive base, was used to facilitate the coupling of acyl and sulfonyl chlorides with a range of nitrogen nucleophiles (Scheme 2.59) [86]. Excess unreacted electrophilic components were scavenged using aminomethylpolystyrene and any remaining amine fragments were removed by a polymer-bound sulfonic acid. Alternatively, the acyl component

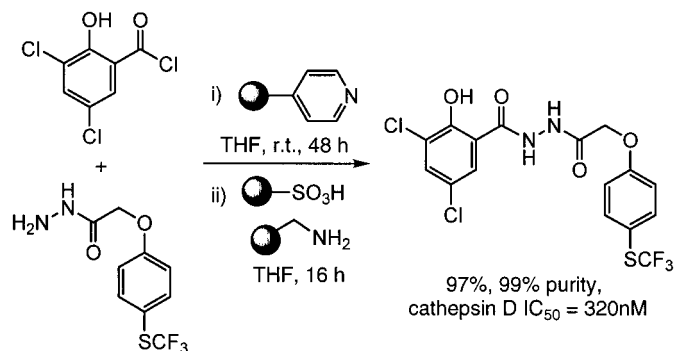




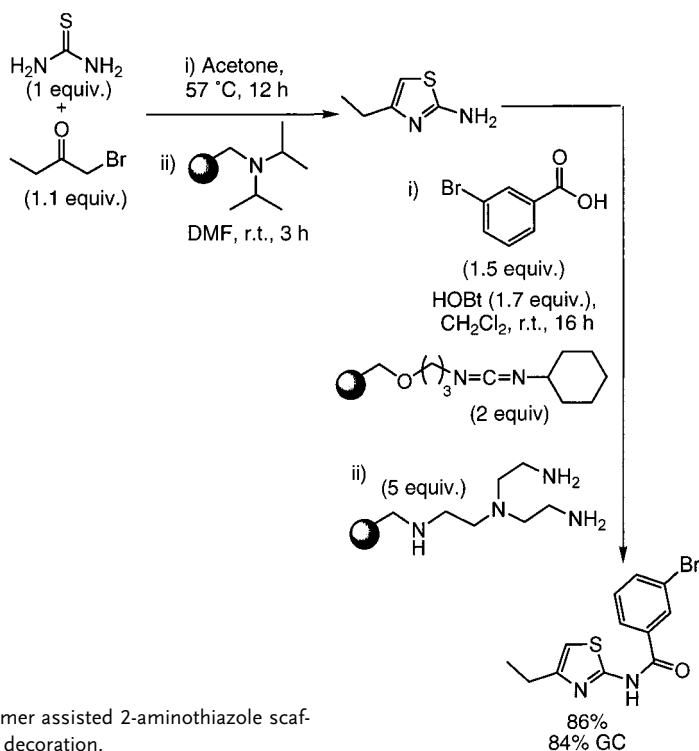
**Scheme 2.58** The automated preparation of urea, amide and sulfonamide libraries.

could be generated from a carboxylic acid by activation using either 1-ethyl-3-(3-dimethylaminopropyl)carbodiimide (EDC) or 2,4,6-triisopropylbenzenesulfonyl chloride. Both of these coupling agents and their by-products contain either a basic or acidic function which can be used as a handle for their sequestration under the above scavenging sequence. These methods have been successfully applied to the preparation of a 300-membered library of cathepsin D inhibitors with yields ranging from 60–100% and in greater than 90% purity. A new cathepsin D inhibitor with sub-micromolar activity was also identified from this study (Scheme 2.59).

Yun *et al.* used an automated parallel synthesizer (Quest 205 Organic Synthesizer) with large reaction vessels to carry out the large scale synthesis of 2-aminothiazole scaffolds for subsequent combinatorial decoration through polymer assisted transformations [87]. The reaction of thioureas and  $\alpha$ -bromoketones in acetone generated a thiazole hydrobromide monohydrate salt which could be cleanly isolated by precipitation and neutralization with an immobilized tertiary amine base (Scheme 2.60). The free thiazole was then coupled with a carboxylic acid via the activated ester intermediate prepared using a PS-carbodiimide and HOBt. Any excess acid remained bound to the resin and the HOBt could be removed using



**Scheme 2.59** Cathepsin D inhibitors prepared using solid-supported reagent technology.



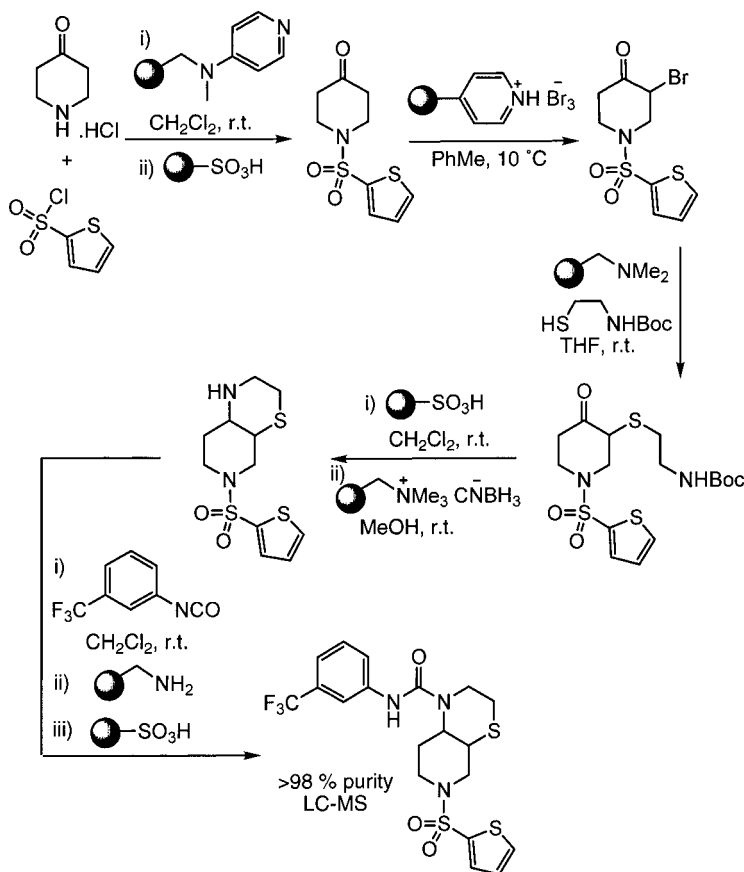
**Scheme 2.60** Polymer assisted 2-aminothiazole scaffold synthesis and decoration.

polymer-supported trisamine. An alternative procedure was also described using acid chlorides as the coupling partners, followed by scavenging again with polymer-supported trisamine.

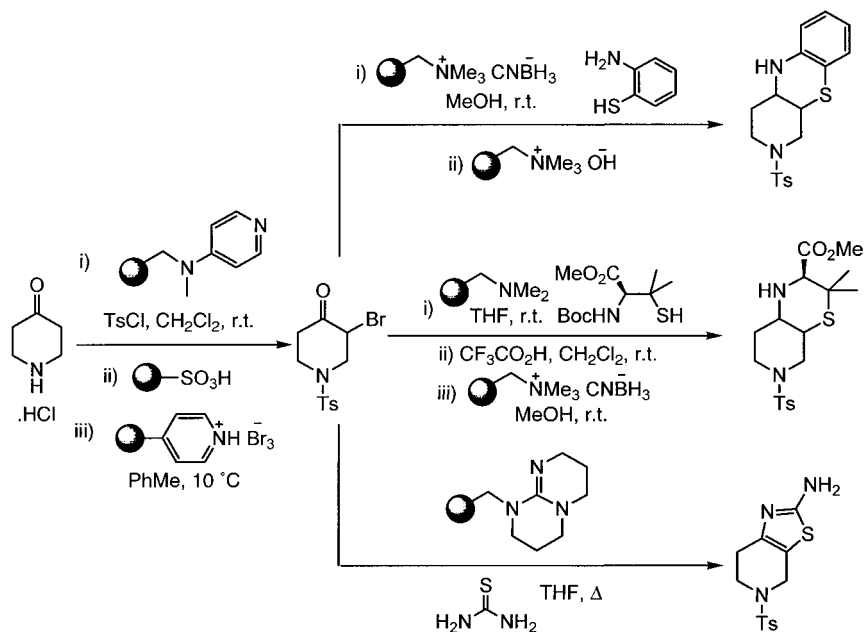
An orchestrated six-step reaction sequence using *seven* different supported reagents has been described for the synthesis of a piperidino-thiomorpholine library

(Scheme 2.61) [88]. *N*-sulfonylation followed by  $\alpha$ -bromination of commercially available 4-piperidone proved to be facile reactions which could be performed on a large scale. The subsequent nucleophilic substitution by an *N*-protected amino-thiol using Amberlyst 21 as the base was also successful. Cleavage of the Boc group with either Amberlyst 15 or trifluoroacetic acid (TFA) in dichloromethane yielded the corresponding imine directly which could be reduced with polymer-supported cyanoborohydride. The resulting thiomorpholine derivative could then be decorated by reaction with a selection of isocyanates or isothiocyanates and purified by previously described scavenging methods.

In addition, the intermediates from various stages of the reaction sequence can be incorporated into alternative reaction pathways allowing access to large number of heterocyclic compounds in a relatively short period of time (Scheme 2.62). Clearly, being able to change the core structure is as crucially important as changing the fin-



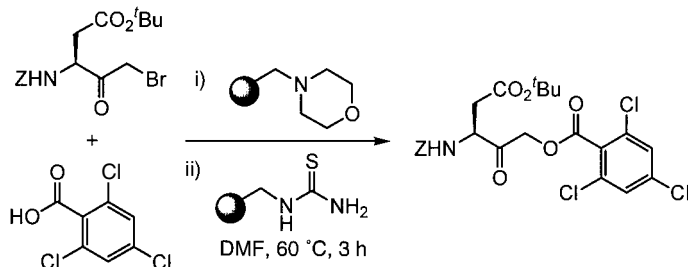
**Scheme 2.61** An orchestrated six-step library preparation of piperidino-thiomorpholine derivatives.



**Scheme 2.62** Additional compound collections from template decoration.

gertips of a molecule. This divergent approach also exemplifies the general versatility of a solution-phase synthesis using solid-supported reagents and hints at the tremendous opportunities that may be attained in drug discovery programs particularly in the area of establishing structure activity relationships (SARs). When combined with automation this route rapidly generated over 5000 product variants.

The application of multiple reaction parameters executed in a parallel array format has been used to expedite the identification of optimal conditions for the synthesis of a collection of almost 600 new interleukin- $1\beta$  converting enzyme inhibitors [89]. The reaction in question was the problematic conversion of a  $\beta$ -*tert*-butyl aspartic acid bromoethylketone to the corresponding acyloxyketone (Scheme 2.63). The study en-



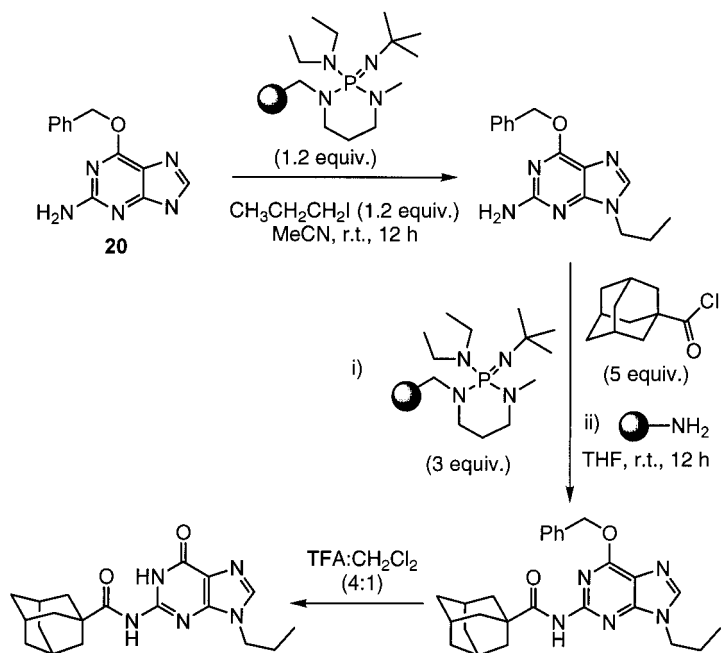
**Scheme 2.63** The conversion of  $\alpha$ -*tert*-butyl aspartic acid derivatives to the corresponding acyloxyketone.

abled the comparison of an extensive range of reagent combinations including many organic and inorganic acids and bases. In a few examples the sequential use of solid-supported reagents and scavenging agents was also pursued (Scheme 2.63). In total over 200 different reaction conditions were evaluated with the final optimized sequence being devised in just three to four days. Finally, to enable a generic purification strategy it was found necessary to develop a new polymer-supported thiourea in order to scavenge out any unreacted  $\alpha$ -bromoketone.

### Heterocyclic scaffold decoration

We have already seen a number of procedures for increasing compound diversity by coupling or decorating molecules with various smaller building blocks. What follows are three examples from the supported reagent literature which involve the dedicated creation of biologically interesting compound libraries by the systematic functionalization of a core heterocyclic template.

Schwesinger's phosphazene base 2-*tert*-butylamino-2-diethylamino-1,3-dimethylperhydro-1,3,2-diazaphosphorine (PS-BEMP has a  $\text{pK}_\text{B}$ =27.5 in MeCN) has been immobilized and shown to have immense utility in the *N*- and *O*-alkylation of many weakly acidic heterocycles. Kim *et al.* has made extensive use of this reagent in the multi-step synthesis of a small collection of guanines possessing potential antiviral activity [90]. The generic procedure involved the direct alkylation of the purine moiety (**20**) (Scheme 2.64), promoted by PS-BEMP, resulting in a mixture

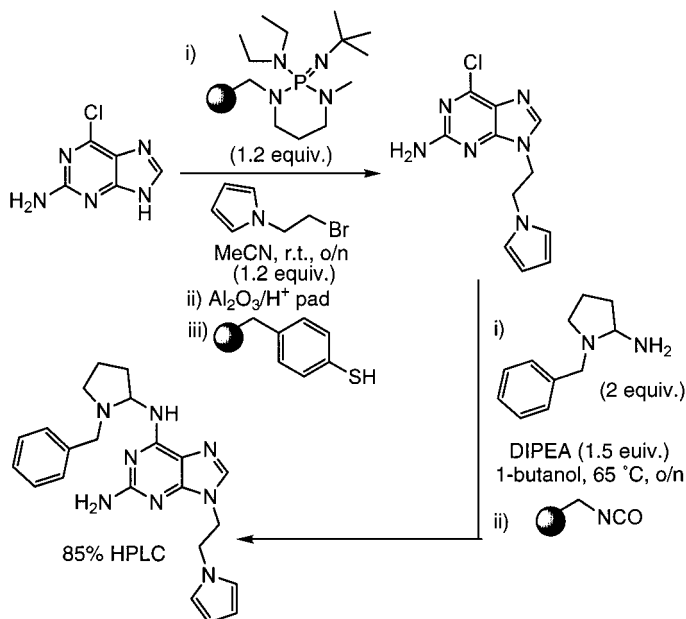


**Scheme 2.64** The clean and efficient *N*-alkylation of heterocyclic compounds.

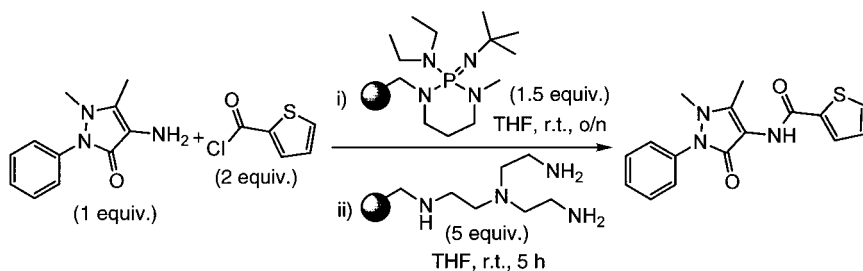
of the N7 and N9 substituted products. It was discovered that convenient separation of the desired N9 regioisomer could be achieved in moderate yields (30–75%) but with high overall purity (>99%) by simple filtration of the reaction mixture through a short plug of acidic aluminum oxide. Efficient acylation of the 2-amino functionality with various acid chlorides was again facilitated by PS-BEMP and scavenger clean-up, using a functionalized amino silicate. Finally, unmasking the amide group through TFA promoted cleavage of the benzyl protecting group gave the target compounds.

In an analogous manner the preparation of an eight by eight array of 6,9-disubstituted purines have also been synthesized (Scheme 2.65) [91]. The first sequence of manipulations duplicates the initial alkylation process described above. Hence starting from 2-amino-6-chloropurine a set of alkyl halides were reacted and the resulting N-9 isomers separated. If required, the addition of a thiophenol scavenging resin could be used to remove excess alkylating reagent. Each core template was then split and subjected to nucleophilic substitution of the chloro group with a selection of six different amines (primary and secondary) to yield the desired products. Any unreacted residual amine was trapped by the addition of an immobilized isocyanate scavenger. The use of PS-BEMP for the acylation of other weakly acidic heterocycles, in combination with a polymeric trisamine scavenger has also been reported (Scheme 2.66) [92].

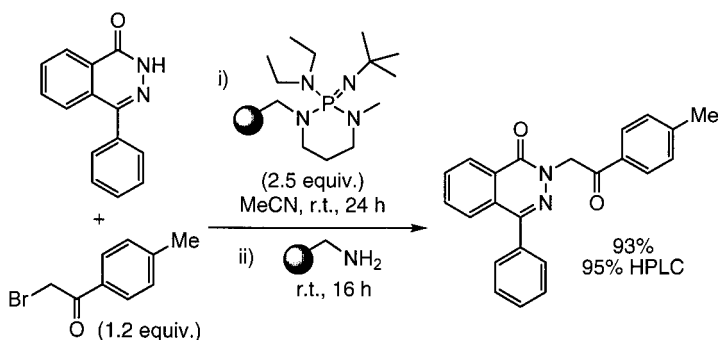
Similarly, Xu has applied a combination of supported bases and amine scavengers for the decoration of both phenolic compounds [93] and various alkaloids



**Scheme 2.65** Combinatorial decoration of 2-amino-6-chloropurine.



**Scheme 2.66** PS-BEMP as a versatile base in organic synthesis.



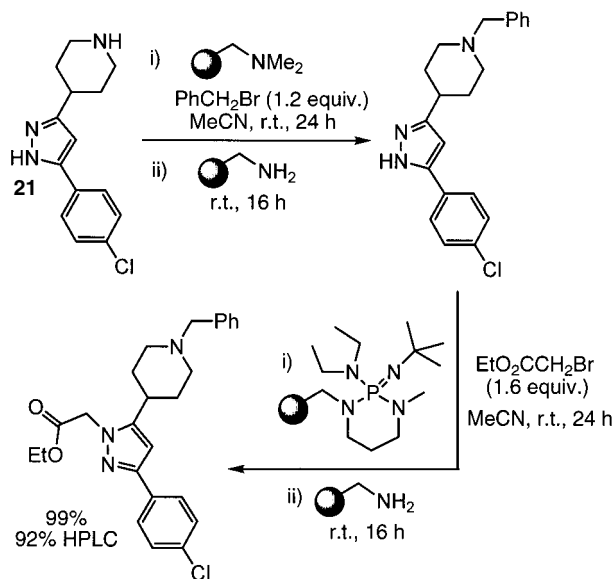
**Scheme 2.67** The use of a supported base and scavenger for alkylation of 4-phenyl-2H-phthalazin-1-one.

[94]. In a representative example alkylation of 4-phenyl-2H-phthalazin-1-one (Scheme 2.67) was achieved using PS-BEMP at ambient temperature in acetonitrile. Purification of the reaction mixture was realized by removal of the excess alkylating agent using an aminomethylpolystyrene scavenger.

In a later paper Xu and co-workers conducted an extensive evaluation of the  $pK_B$  characteristics of several polymeric systems and used this information to perform an elegant one-pot tandem manipulation of a piperidine substituted pyrazole (Scheme 2.68) [94]. The starting material (**21**) contains two distinct amino functionalities with significantly different acidities. This difference was used to selectively discriminate between the two groups during a *N*-alkylation sequence (Scheme 2.68). In this way regioselective addition to the piperidinyl nitrogen was achieved with a weak polymer-supported tertiary amine, whereas alkylation of the pyrazole nitrogen required the presence of PS-BEMP which is a much stronger base. At both stages a purification step was incorporated employing aminomethylpolystyrene to remove excess alkyl halide.

### Synthetic procedure involving extended sequences

The continuing synthetic challenge of assembling novel molecular architecture often requires the formation of new carbon-carbon bonds. One of the most efficient

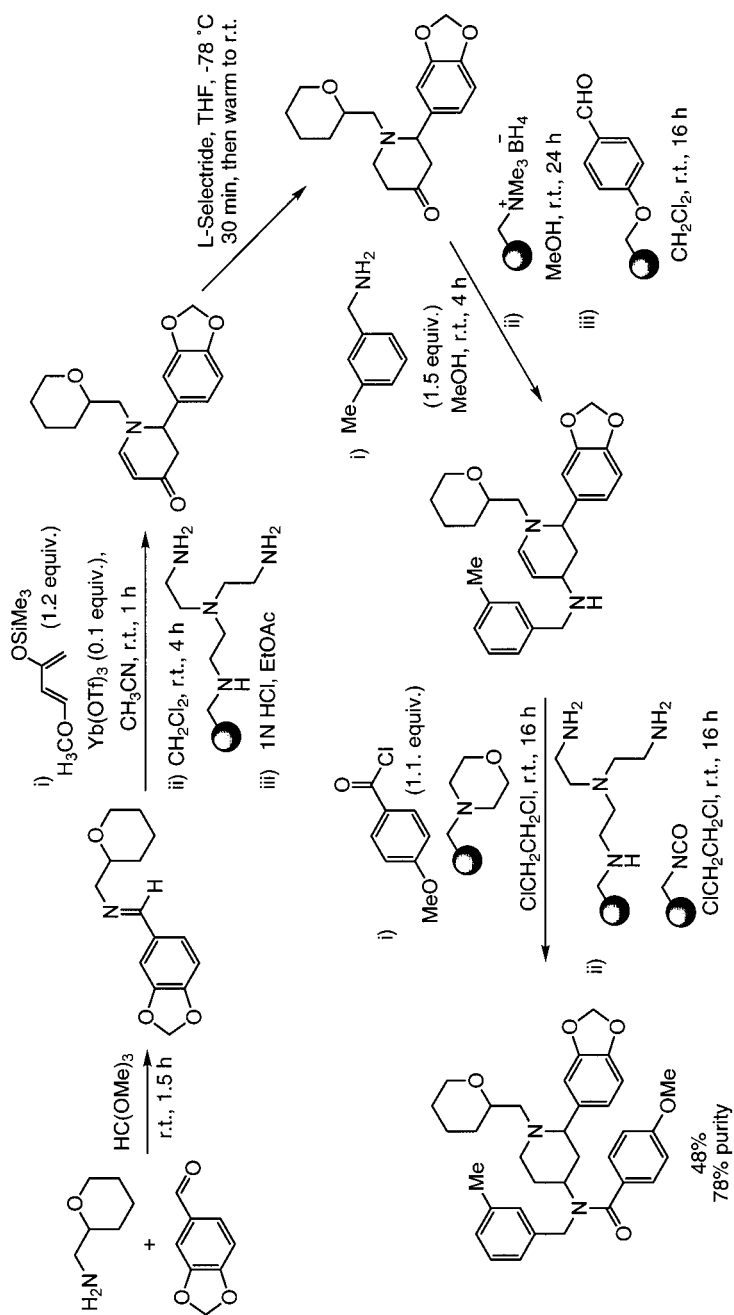


**Scheme 2.68** One pot tandem transformation of pyrazoles.

routes for the formation of new carbon-carbon bonds and for accessing unique functionalized heterocyclic scaffolds is the hetero-Diels-Alder reaction. In 1998, Creswell *et al.* created an acyl-aminopiperidine library based around a ytterbium triflate catalyzed hetero-Diels-Alder reaction of imines, formed *in situ* from aldehydes and amines, with the Danishefsky diene (Scheme 2.69) [95]. A polyamino scavenging resin was then used to remove any unreacted imine in addition to any by-products derived from decomposition of the diene. Acid hydrolysis of the pericyclic intermediate yielded the dihydropyridone which was chemoselectively reduced by *L*-selectride to obtain the 4-piperidone product. Next the ketone functionality was subjected to reductive amination using polymer-supported borohydride and a variety of amines. Scavenging the crude reaction mixture with a polymer-supported aldehyde trapped any excess primary amine. Acylation was completed using acid chloride in the presence of polymer-bound morpholine and a combination of electrophilic and nucleophilic scavengers for purification (Scheme 2.69).

A sequential multi-step sequence involving polymer-supported reagents and scavengers has also been developed for the preparation of tetra-substituted pyrrole scaffolds [96]. The synthetic route begins with the oxidation of commercially available benzylic alcohols to aldehydes using polymer-supported permanganate (Scheme 2.70). From these aldehyde systems the corresponding nitrostyrene derivatives were synthesized by a Henry reaction promoted by tetra alkyl ammonium hydroxide resin, Amberlite IRA 420, followed by elimination effected by trifluoroacetic anhydride and triethylamine. A work-up and purification scavenging protocol using aminomethylpolystyrene and acidic Amberlyst A-15 afforded the clean





Scheme 2.69 Extended synthesis of a functionalised piperidine library.

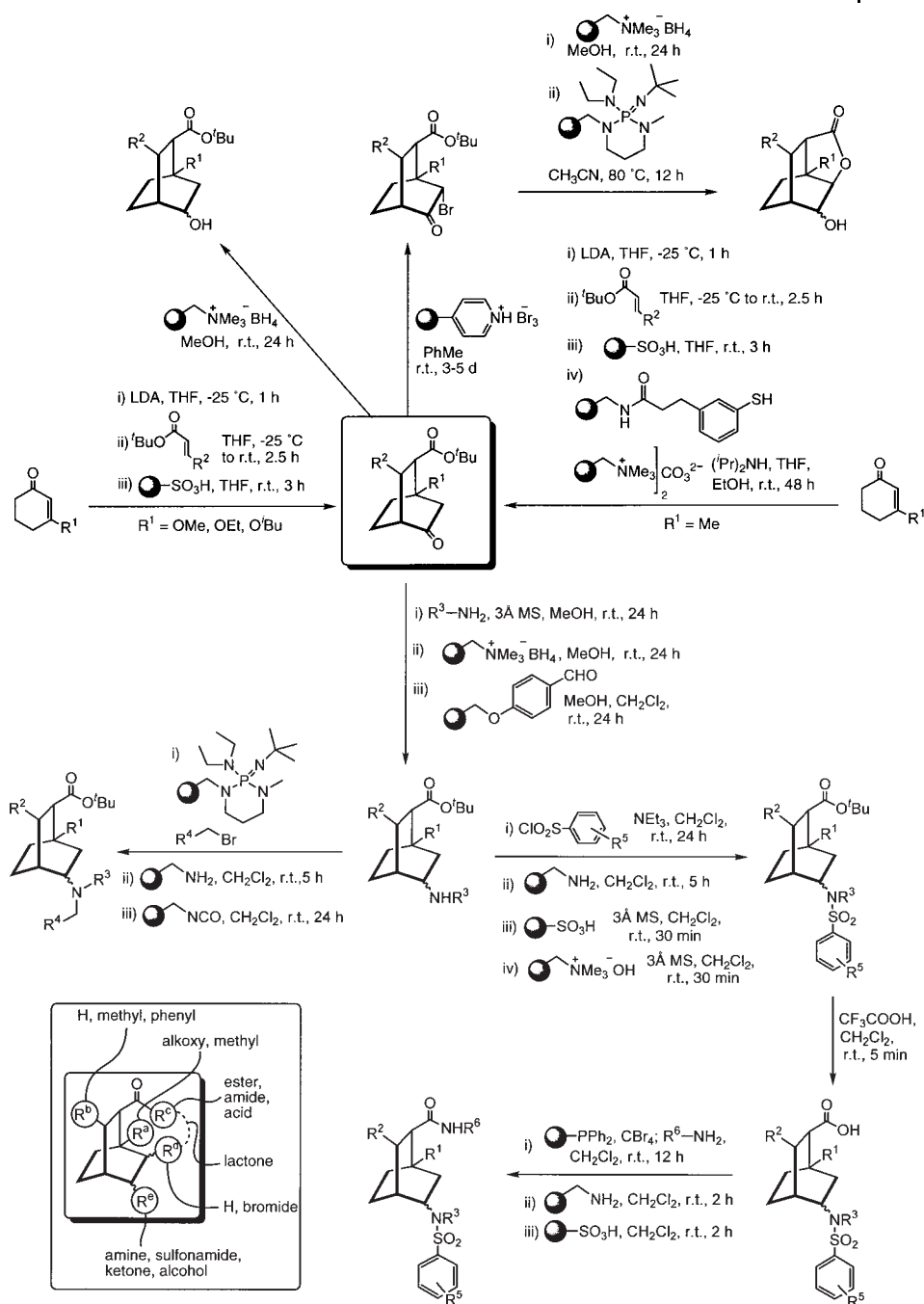


products. Construction of the pyrrole ring by a 1,3-dipolar cyclo-addition of *tert*-butyl isocyanate with the nitroalkenes in the presence of the polymer-supported guanidine base 1,5,7-triazabicyclo[4.4.0]dec-5-ene (PS-TBU) proceeded smoothly. These pyrrole products were then further elaborated by *N*-alkylation using a polymer-supported phosphazene base and various alkyl halides (excess halide was removed using aminomethylpolystyrene). Additional modification of the pyrrole products could be achieved by treatment with trifluoroacetic acid resulting in rapid cleavage of the *tert*-butyl esters followed by *in situ* decarboxylation to give the simplified compounds. This synthesis is also a clear demonstration of the power of these systems in multi-step operations and further illustrates the principal and importance of convergency in the synthesis of chemical libraries.

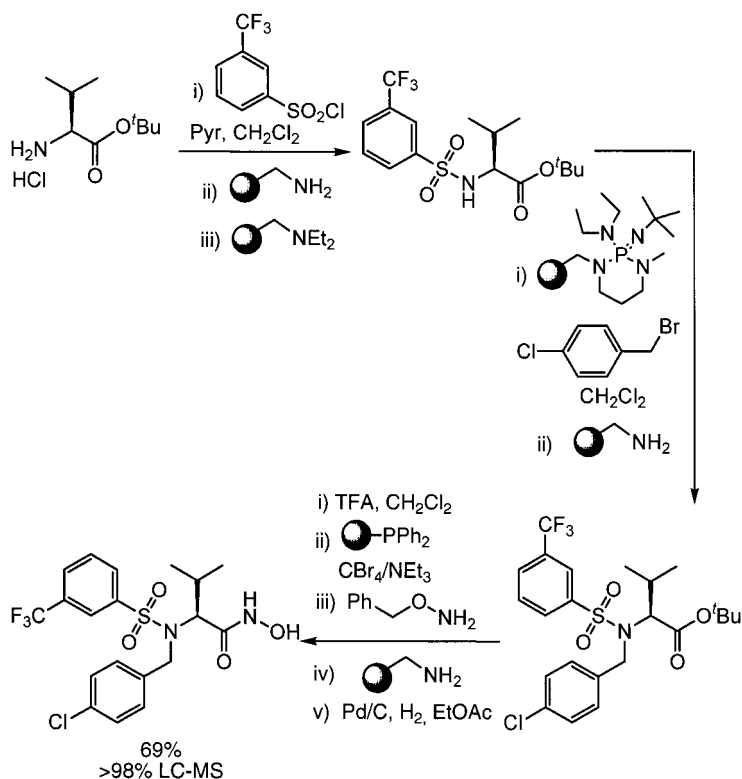
In another study a bicyclo[2.2.2]octane library was constructed using a tandem Michael addition of the enolates of 2-cyclohexenones with various substituted acrylates [97]. In this way it was possible to prepare a rigid scaffold, from readily available substrates, which could be further elaborated by transformation of the functional groups to give a large array of compounds (Scheme 2.71). A range of standard reactions including bromination, ketone reduction, lactonization, reductive amination, *N*-alkylation, sulfonylation and amide formation were all used to modify the structure at various positions on the bicyclic framework. What is noteworthy about these studies is how easily polymer-supported reagents and scavengers can be incorporated into such synthetic routes. This synthesis required minimal optimization and was a considerable improvement over an earlier route which had been developed with the substrate supported on a Wang resin [98].

The acceleration of lead structure development by combinatorial decoration of known biologically active templates, followed by substructure optimization, is a proven procedure for the identification of new drug candidates. This approach has been adopted for the preparation of an array of potential matrix metalloproteinase (MMP) inhibitors based on a hydroxamic acid skeleton [99] as identified from the literature [100]. The synthetic route employed a split and divert approach [101] starting from various L-amino acid *tert*-butyl esters scaffolds with diversity being added along the way by application of a total of seven polymer-supported reagents and scavengers (Scheme 2.72). The absence of conventional work-up or chromatographic purification at any stage during this program of work significantly reduced the time required to generate library members and suggests considerable potential for the way in which structure activity relationship studies, for example, could be carried out in the future.

Recently, Kirschning developed a general strategy for solution-phase glycosylation in the construction of glycoconjugates and oligosaccharides using polymer assisted reactions [102]. Several examples of sugars bearing anomeric substituted acetates were activated using a polymer-bound silyl triflate to act as glycosyl donors. The subsequent addition of a selection of structurally diverse alcohols including simple alkyl, benzyl, steroidal and carbohydrate-derived systems was successfully achieved in high yields and with remarkable stereochemical control. This powerful synthetic approach was also extended to the more advanced preparation of a deoxytrisaccharide unit (Scheme 2.73). The protected glycal starting material

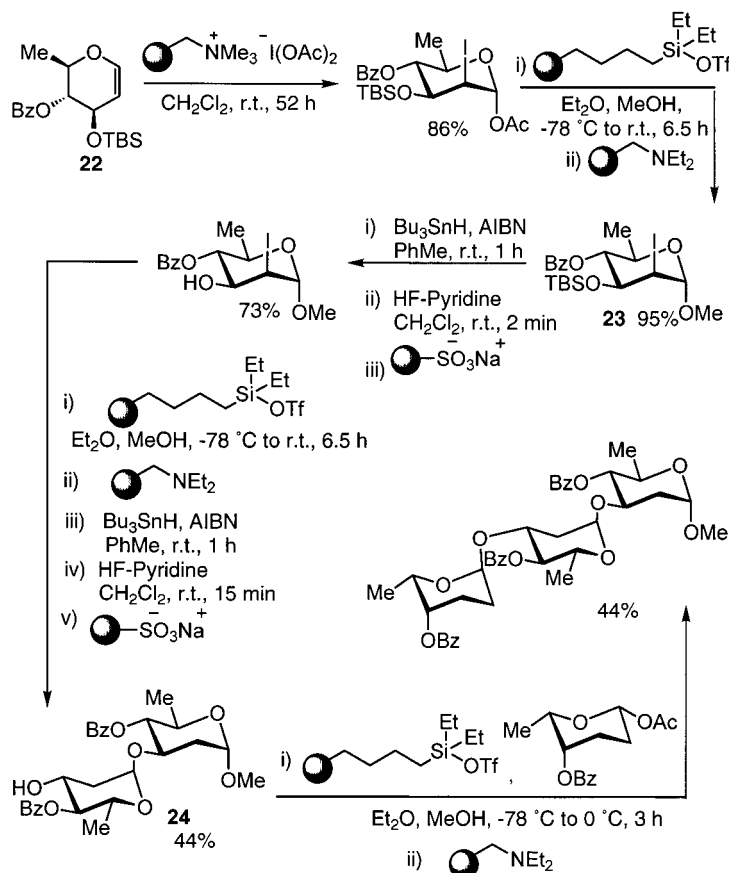


Scheme 2.71 Construction and decoration of rigid bicyclo[2.2.2]octanes.



**Scheme 2.72** Assembly of matrix metalloproteinase inhibitors using supported reagents.

(22) was transformed to the 2-iodoglycosyl acetate using a polymer-bound bis(acetoxy)iodate(I) complex. This intermediate was then progressed through a series of chemical modifications to give the methoxy substituted species (23). In addition, it was also incorporated as the corresponding coupling partner in the subsequent glycosidation reaction to afford the disaccharide (24). The prior sequence of reactions leading to the methyl glycoside (23) involved activation with a polymer-immobilized Lewis acid and reaction with methanol followed by neutralization with an immobilized triethylamine equivalent. Next, a radical dehalogenation using  $\text{Bu}_3\text{SnH/AIBN}$  preceded a facile *O*-desilylation with HF-Pyridine complex, which was worked-up by quenching with Amberlite A-200 ( $\text{Na}^+$  form). This simultaneously formed the sodium fluoride salt and was also found to be efficient at trapping out the pyridine. A third glycosidation sequence using a rhodinosyl acetate donor gave the trisaccharide product in a respectable yield. This synthetic approach was successful because its design efficiently integrated both classical solution phase reagents and polymer-supported species, demonstrating yet another



**Scheme 2.73** Preparation of glycoconjugates and oligosaccharides using polymer-assisted glycosylation reactions.

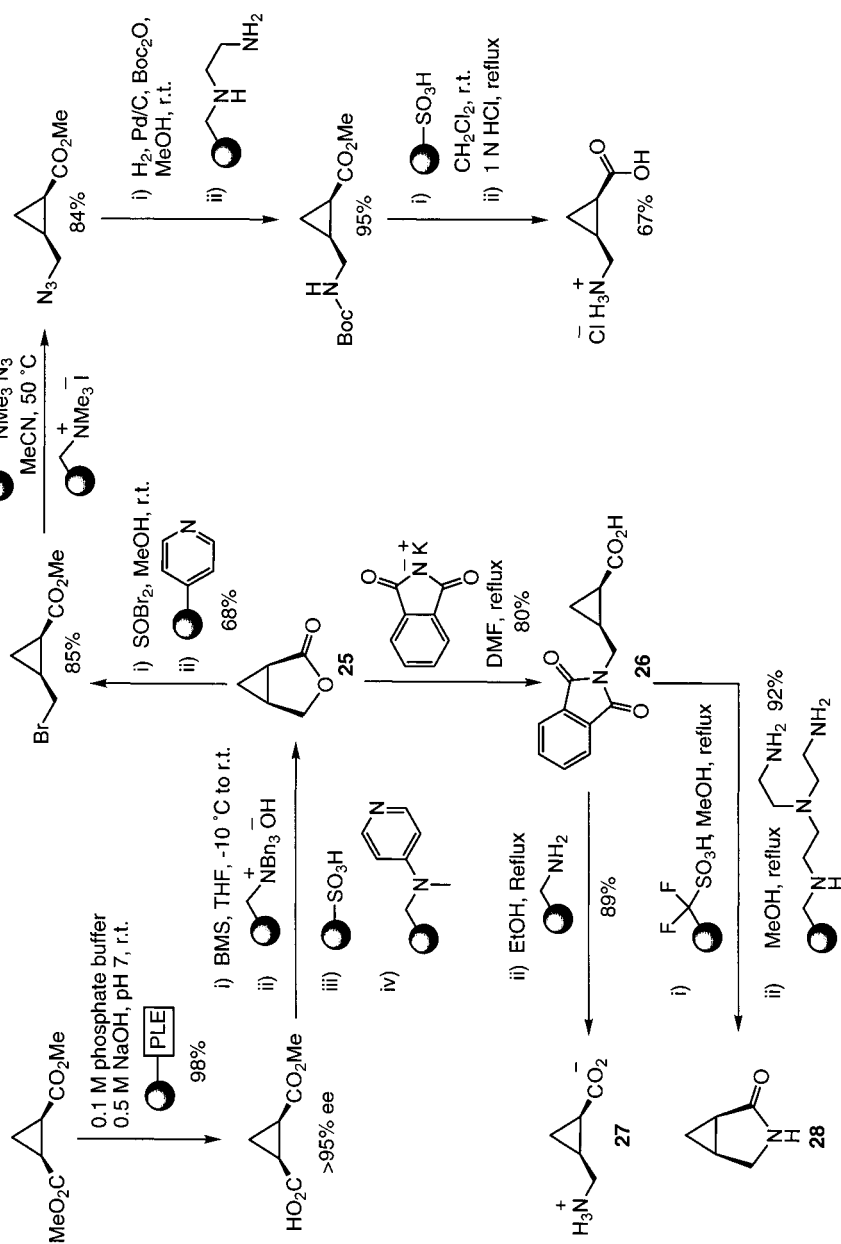
facet of using immobilized reagents in synthesis. We can expect many other applications in the future.

Classical routes for the stereospecific synthesis of multi-functional cyclopropane derivatives normally involve either an intramolecular cyclization or more frequently asymmetric carbene addition reactions. In an alternative approach combining the advantages of immobilized enzymes and solid-supported reagents a number of strained ring systems including cyclopropanes have been synthesized as  $\gamma$ -aminobutyric acid (GABA) neurotransmitter analogs [103]. In the example shown (Scheme 2.65), a Eupergit tethered pig liver esterase was used for the desymmetrization of a cyclopropane *meso*-diester, providing gram quantities of resolved starting materials for the synthesis. Reduction of the newly revealed carboxylic acid function using  $\text{BH}_3 \cdot \text{SMe}_2$  in THF gave the corresponding alcohol, which spontaneously cyclized to the lactone (25) (any uncyclized material was re-

moved using PS-DMAP). The reaction was then quenched with a small amount of water and the boronic acid salts scavenged with Amberlite IRA-743. At this point the sequence diverges enabling the preparation of several different frameworks. Direct transformation of the lactone (**25**) using excess thionyl bromide in methanol followed by neutralization with poly(4-vinylpyridine) afforded the bromide adduct in 85% yield. This material was then smoothly converted to the azide which was immediately reduced in the presence of Boc-anhydride to the protected amine derivative thus avoiding troublesome lactam formation. Simultaneous deprotection with catch and release purification and saponification of the methyl ester using Amberlyst 15 gave the GABA-analogue. Alternatively, ring opening of the lactone (**25**) with the potassium salt of phthalimide in refluxing DMF, provided high yields of the differentiated cyclopropane system (**26**). The phthalimide protecting group could be removed with either with aminomethyl polystyrene to give the Zwitterion (**27**) or, via ester formation and treatment with trisamine resin, to yield the lactam (**28**). This work constitutes the first example of using immobilized enzymes together with supported reagents and scavengers to prepare molecules in a multi-step mode.

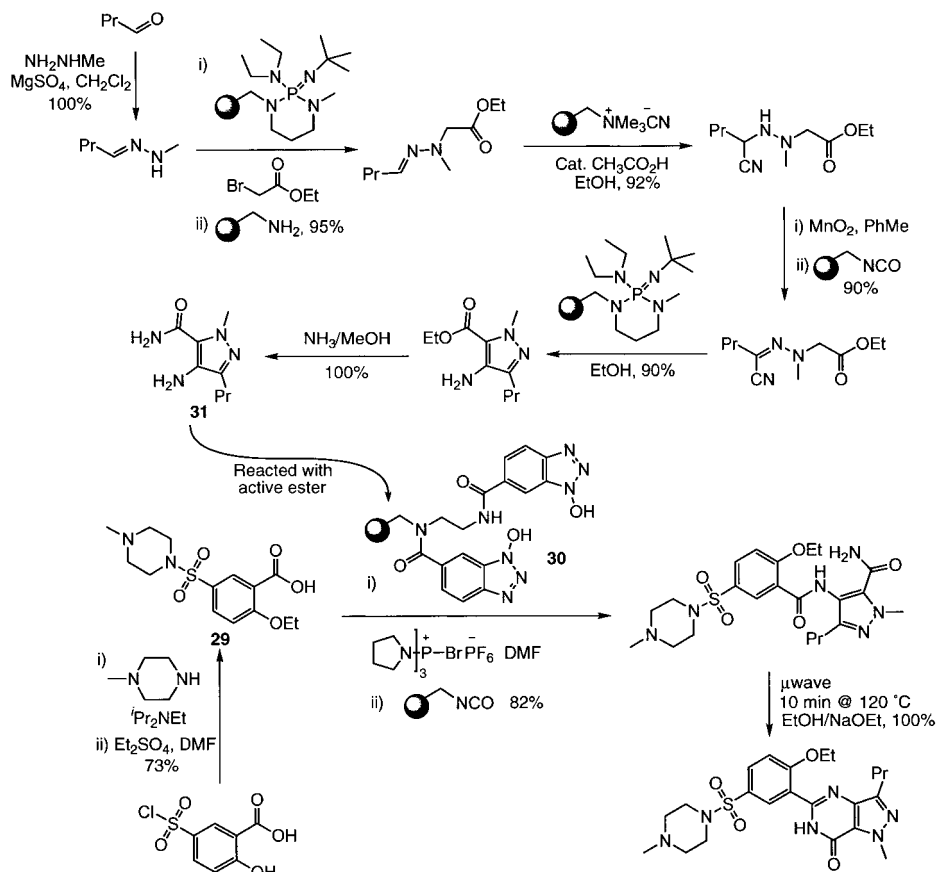
In an effort to demonstrate the power of these immobilized methods when applied to contemporary drug design, the synthesis of Pfizer's well known treatment for male erectile dysfunction, Sildenafil (Viagra<sup>TM</sup>) was completed by Ley *et al.* (Scheme 2.75) [33a]. A key feature of this work is that a convergent synthetic strategy was used. The reaction between the resin-bound activated ester (generated from (**29**) and (**30**)) and heterocyclic amine (**31**) formed the important amide bond with any excess amine being scavenged by polymer-supported isocyanate. The polymer-supported hydroxybenzotriazole used in the coupling step performed a dual function. This reagent facilitated the simultaneous activation of the acid (**29**) and also its purification from various impurities and by-products accumulated during its formation. Cyclodehydration was then effected using sodium ethoxide under microwave irradiation conditions to afford gram quantities of Sildenafil in excellent overall yield.

Salmeterol (Serevent<sup>®</sup>) is a potent and long acting  $\beta_2$  adrenoceptor agonist used as a bronchodilator for the prevention of bronchospasm in patients with asthma and chronic obstructive pulmonary disease. Although this molecule has been previously synthesized the routes employed have had a number of drawbacks including in a number of cases extensive chromatographic separation of diastereomeric mixtures. The route described in Scheme 2.76 circumvents these problem and facilitates the synthesis of this molecule without resorting to any chromatographic purification steps [104]. Only a single recrystallization was used to enhance the diastereomeric purity of an intermediate with all other transformations and purifications being performed using solid-supported reagents. An interesting transformation which is worth highlighting is the initial condensation of the starting phenolic material with an immobilized methyleneiminium salt. This reagent prepared from a polymer bound carbonate resin and the Eschenmoser's amine was found to be quite general for the *ortho*-aminomethylation of phenolic compounds.



Scheme 2.74 Rapid preparation of GABA analogs using a combination of immobilized enzymes and supported reagents.



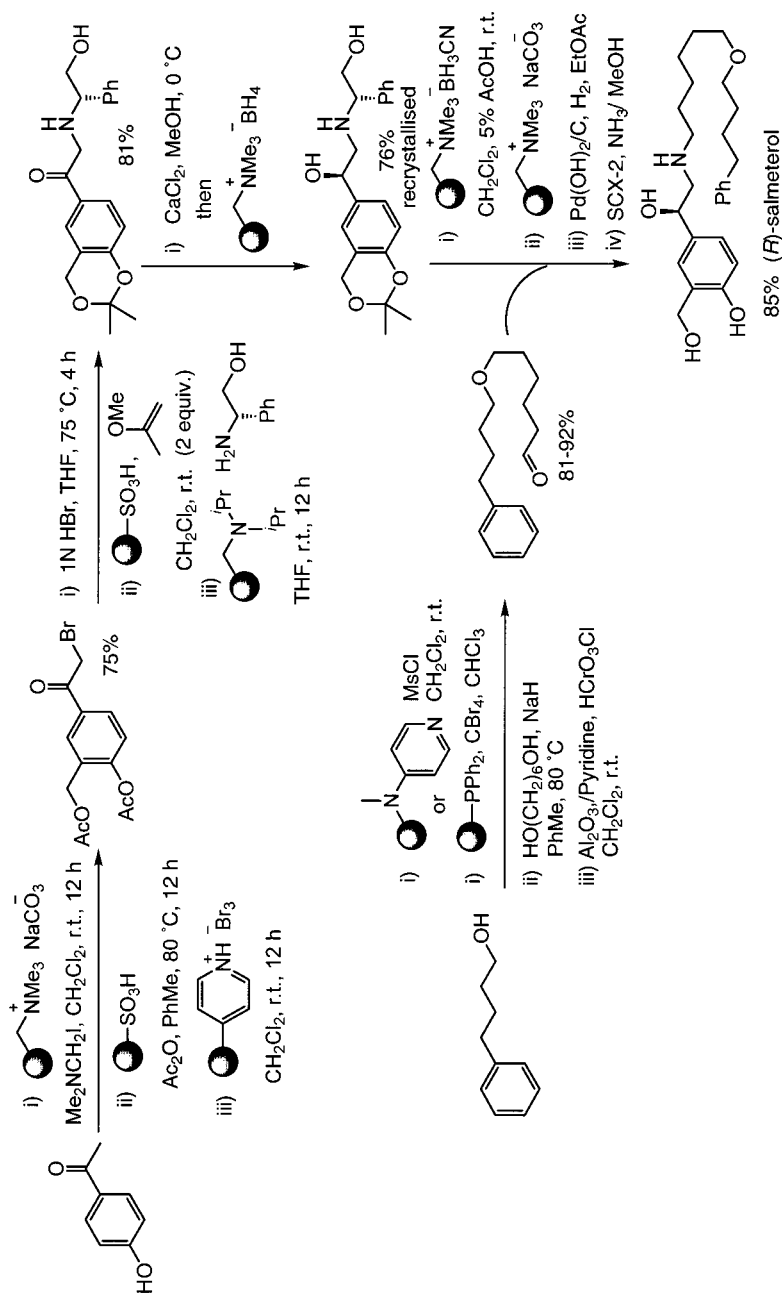


Scheme 2.75 Synthesis of Sildenafil (Viagra®).

## 2.2.4

## Natural Product Synthesis

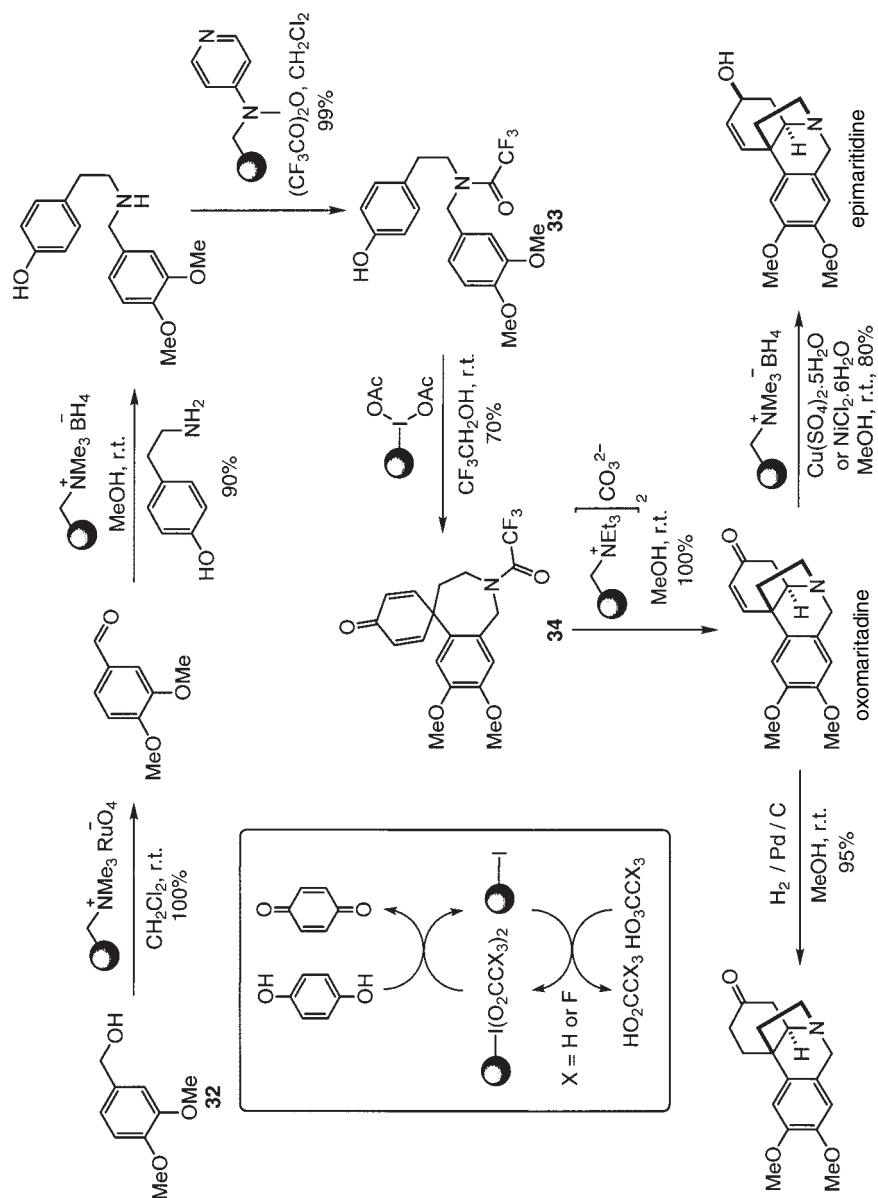
The concepts and philosophy of solid-supported reagents bridges many aspects of synthetic chemistry from simple library generation (as seen above) to more elaborate multi-step target orientated syntheses. The absence of conventional work-up and purification requirements, combined with the ease of optimization by a parallel process, means that the use of solid-supported reagents is certainly beneficial for the assembly of more complex structures. Additionally, the potential for scale up of reactions, so as to provide significant quantities of both intermediates and final products presents attractive opportunities. Accordingly we have investigated the synthesis of a number of natural products using solid-supported reagents to create efficient, durable routes that can also be easily adapted to the syntheses of natural product like variants. This is particularly important because these mole-

Scheme 2.76 Preparation of (*R*)-Salmeterol.

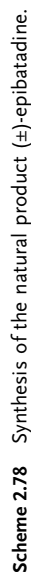
cules could produce a new access to cellular signaling compounds not directly available from natural sources.

The synthesis of the alkaloid ( $\pm$ )-epimaritidine has been achieved through a linear six step reaction sequence requiring only simple filtration of the spent solid supported reagents for purification, resulting in isolation of the product in an overall yield of 50% (Scheme 2.77) [105]. The first transformation of the synthesis applied the polymer-supported perruthenate reagent for oxidation of a readily available benzylic alcohol (**32**) to the corresponding aldehyde, which was then subjected to reductive amination with tyramine using an immobilized borohydride reagent. A selective trifluoroacetate protection of the newly formed secondary amino function afforded (**33**), again in gram quantities ready for the subsequent key bond forming intramolecular cyclization reaction. The oxidative phenolic coupling was efficiently conducted using polymer-supported diacetoxyiodobenzene [106] in trifluoroethanol and led directly to the desired *para-para* coupled spirodienone product (**34**) in 70% yield with no other products detected by LC/MS. An advantage of this polymer-supported variant is that the iodobenzene by-product remains attached to the resin and, following removal by filtration, may be conveniently recycled by treatment with peracetic acid, increasing the overall efficiency of this process (Scheme 2.77). Removal of the trifluoroacetate protecting group with polymer-supported carbonate in methanol was followed by a spontaneous intramolecular 1,4-addition to give ( $\pm$ )-oxomaritidine. This compound could in turn be stereoselectively reduced with polymer-supported borohydride in the presence of a catalytic quantity of nickel(II) chloride or copper(II) sulfate to yield ( $\pm$ )-epimaritidine. This short synthetic route allowed direct access to ( $\pm$ )-epimaritidine in multi-gram quantities, which has potential for further decoration in a combinatorial fashion to provide large numbers of analogous compounds for biological evaluation.

The power of these multi-step transformations using batches of supported reagents, has been similarly demonstrated by the synthesis of the potent analgesic ( $\pm$ )-epibatidine (Scheme 2.78) [107]. In this case, no less than *ten* polymer-bound reagents were used to effect the synthesis, resulting in isolation of the product in an overall yield of 32% and in >90% purity. Starting from the acid chloride (**35**) complete reduction with polymer supported borohydride afforded the benzylic alcohol which was easily re-oxidized to the corresponding pyridyl aldehyde (**36**). A number of oxidants were investigated for this process including polymer-supported versions of perruthenate (PSP), permanganate (PSM) and diacetoxyiodobenzene (DAIB) all of which were found to be extremely efficient with no over-oxidation to the corresponding carboxylic acid being observed. Alternatively, oxidants such as Magtrieve<sup>TM</sup> (magnetized CrO<sub>2</sub> filaments) and manganese dioxide were also suitable for this reaction, but reaction times were considerably longer. Next a base catalyzed Henry reaction between the aldehyde (**36**) and nitromethane promoted by Amberlite resin IRA-420 afforded the unstable nitro alcohol which was immediately dehydrated to the nitroalkene by derivatization with trifluoroacetic anhydride and base catalyzed elimination induced by an immobilized triethylamine derivative. In an important modification of this pathway, it was found that by encapsulating quantities of the polymer-supported reagents in sealed porous



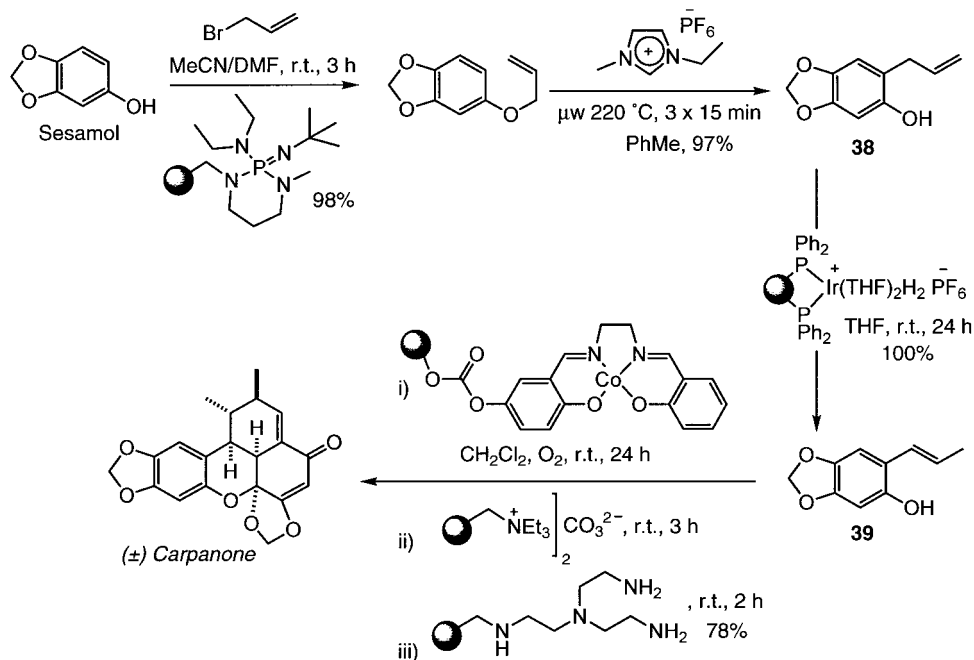
Scheme 2.77 Preparation of the natural products (±)-oxomaritidine and (±)-epimaritidine.



**Scheme 2.78** Synthesis of the natural product (±)-epibatidine.

pouches, the five step reaction sequence of acid chloride (**35**) to nitroalkene (**37**) could be carried out in a one-pot procedure. The reaction progress, as effected by the pouched reagents could be easily monitored by TLC or LC/MS. When the reaction was judged to have reached completion the pouch was removed, with washing, and the next set of bagged reagents was added, thus facilitating the filtrations between steps. Next, construction of the cyclohexyl ring system was carried out *via* a thermal Diels-Alder reaction between the *trans*-nitroalkene and a *tert*-butyldimethylsilyl (TBDMS) protected diene which reproducibly gave quantitative yields of the silicon protected adduct. Simple removal of any excess diene was achieved *in vacuo* followed by TFA-catalyzed hydrolysis of the silyl enol ether to afford exclusively the *cis* configured ketone (**38**). Reduction of the ketone functionality with supported borohydride gave a 7:1 diastereomeric ratio in favor of the all equatorial substituted cyclohexanol. In the subsequent conversion of the alcohol to the corresponding mesylate a reactive cocktail of dimethylaminomethyl polystyrene and mesyl chloride were discovered to be a particularly mild and effective combination. A selective reduction of the aliphatic nitro substituent, in the presence of both the mesylate and 2-chloropyridine, was carried out with an immobilized nickel boride generated *in situ* from nickel(II) chloride hexahydrate and polymer-supported borohydride. This led to the key synthetic reaction, a transannular displacement of the mesylate by the amino group. This reaction proceeded smoothly in the presence of PS-BEMP, with any impurities, including the uncyclized species derived from the minor alcohol diastereoisomer, being conveniently removed by scavenging with aminomethyl polystyrene. The final step of the synthesis, namely the epimerization of the *endo*-pyridyl to form ( $\pm$ )-epibatidine, required extensive optimization. The most effective conditions were determined to be extended heating by microwave irradiation, which not only accelerated the reaction, but also shifted the equilibrium in favor of the desired *exo* isomer. The amine product was then captured onto Amberlyst 15 and washed to remove any nonbasic impurities. Release from the resin was enabled by displacement with excess methanolic ammonia to yield a 3:1 (*exo:endo*) mixture of easily separable isomers.

The natural product ( $\pm$ )-carpanone, possess an attractive and relatively complex architecture that can be rapidly assembled from very basic starting materials [108]. We have recently reinvestigated the synthesis of this biologically interesting target using a combination of solid supported-reagents and scavengers in a multi-step process (Scheme 2.79) [20, 109]. The synthesis began from commercially available sesamol which was readily allylated in acetonitrile using allyl bromide and the polymer-supported phosphazene base, PS-BEMP. The aryl ether was then subjected to a microwave assisted Claisen rearrangement, conducted in a toluene-ionic liquid biphasic system. This gave a clean and selective conversion to the phenolic compound (**38**), which was converted to the key intermediate (**39**) by isomerization of the alkene using an immobilized version of Felkin's iridium catalyst. With large quantities of compound (**39**) in hand the dimerization and intramolecular Diels-Alder cascade to furnish carpanone was conducted using a highly efficient and easily recycled cobalt salen complex. The final product was isolated in 66% overall yield and greater than 90% purity following a rapid scavenging se-



**Scheme 2.79** Synthesis of carpanone.

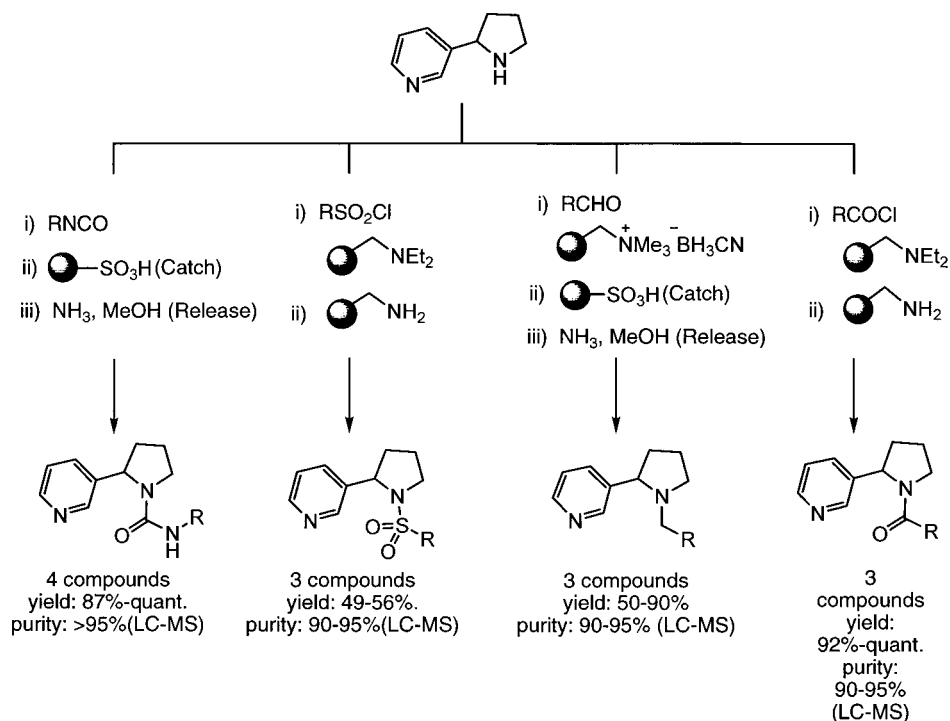
quence to remove any trace amounts of by-products or unreacted monomer starting material. Again all reactions could be carried out on a significant preparative scale.

The natural products nicotine and nornicotine have attracted considerable interest from medicinal chemists owing to their potent biological activity as ligands at the nicotinic acetylcholine receptors (nAChR). The pharmacological effects of these compounds on cognitive function and neuroprotection are particularly well documented and of continuing scientific interest [110]. It was therefore of value to develop a general synthetic procedure for the construction of these compounds that would also enable combinatorial changes to be made to the core structure in order to further investigate their biological function [111]. The route began with the reaction of the commercially available 1,3-dioxolane Grignard reagent with pyridine-3-carboxaldehyde which was then quenched by the addition of Amberlite IRC-50 carboxylic acid functionalized resin to give the addition product in 85% yield and >95% purity (Scheme 2.80). Traditional aqueous work-up of this reaction led to substantial amounts of the acetal cleavage product, therefore demonstrating a clear advantage of the application of polymer-supported quenching techniques. Direct conversion of the alcohol to the corresponding bromide was achieved in dichloromethane using carbon tetrabromide and polymer-supported triphenylphosphine in essentially quantitative yield. The bromide was then transformed to the azide using an azide ion exchange resin followed by reduction to



Starting from nornicotine, we were able to demonstrate the rapid construction of a small collection of nicotine derivatives using a range of readily available monomers (Scheme 2.81). In this way we were able to create compounds to probe



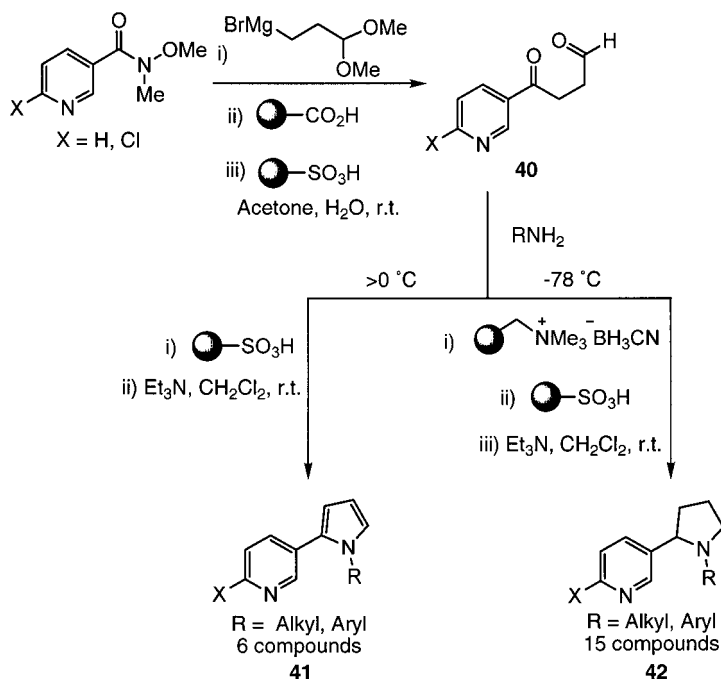


**Scheme 2.81** Combinatorial decoration of nornicotine core.

changes to the nitrogen of the pyrrolidine ring and to give compounds that may find application as chiral ligands/catalysts in organic synthesis.

Similarly, we were able to modify the initial synthetic route to prepare additional arrays of compounds with different heterocyclic cores (Scheme 2.82).

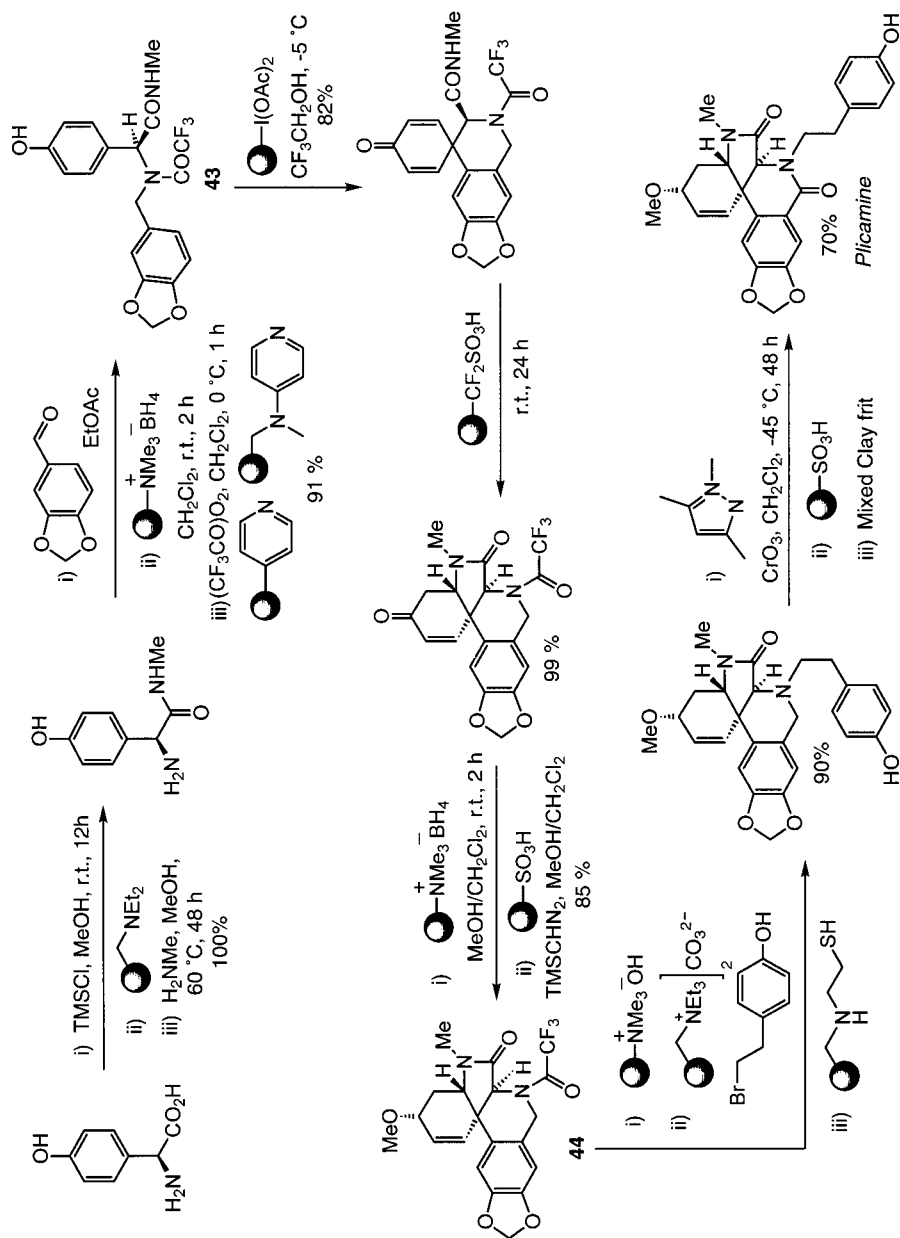
The synthesis of a recently isolated amaryllidaceae alkaloid (+)-plicamine was reported utilizing *twelve* immobilized systems (Scheme 2.83) [21]. This route not only constitutes the first synthesis of this molecule but was rapidly achieved using immobilized reagent methodology. Initially, optically pure 4-hydroxyphenyl glycine was converted to the corresponding methyl amide. Then, in a sequence reminiscent of the epimaritadine synthesis, reductive amination and *N*-protection as the trifluoroacetate gave compound (**43**) in 91% yield over the six-step sequence. The key synthetic transformation was the oxidative spiro-cyclization to form the 6,6-bicyclo skeleton which was immediately followed by an acid catalyzed conjugate addition to give the advanced isoquinolin[3,4-*c*]hydroindole system. Stereoselective 1,2-reduction of the  $\alpha,\beta$ -unsaturated carbonyl with supported borohydride, followed by *O*-alkylation using trimethylsilyl diazomethane and Amberlyst 15 resin gave the methoxy substituted compound (**44**). Unmasking the secondary amine by removal of the trifluoroacetate group using an Amberlyst hydroxide ion exchange resin permitted the attachment of the pendant side chain by an alkylation which



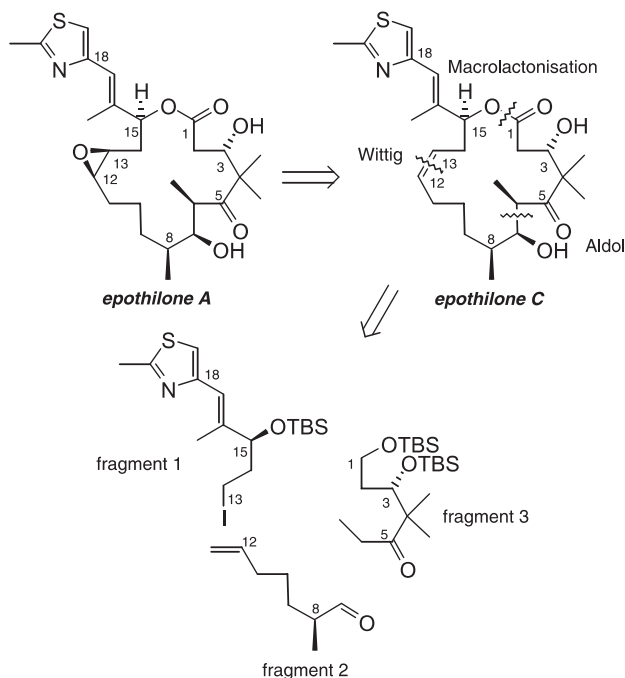
**Scheme 2.82** A short synthetic sequence to nicotine derivatives.

was carried out using an excess of the alkyl bromide and an immobilized carbonate base. An aminothiol resin was applied to remove residual alkyl bromide. The final amine to amide oxidation was carried out in solution and purified by a combination of solid phase extraction and scavenging resins. The complexity of plicamine as a target molecule nicely confirms the power and effectiveness of these new approaches as tools for use in organic synthesis. In addition this approach permitted the parallel synthesis of both enantiomeric forms and the generation of significant pools of intermediates for use in the construction of many unnatural analogs or natural product like compounds [21 a].

The prestigious epothilone family of natural products was chosen as a platform to fully demonstrate the wide utility and applicability of solid-supported reagents in modern organic synthesis. These highly cytotoxic polyketides were originally isolated in the early 1990s from the Soce90 strain of myxobacterium *Sorangium cellulosum*, extracted from soil samples collected on the banks of the Zambezi river in Africa in 1985. They have been shown to exhibit their biological activity by the same mechanism as the commercially successful natural product drug Taxol®. This discovery has generated excitement within the chemical and pharmaceutical world and led to the epothilones being investigated as possible successors to Taxol®. As a result, intensive chemical and biological programmes have been ongoing to further elucidate the extensive biological and structural profile of the nat-



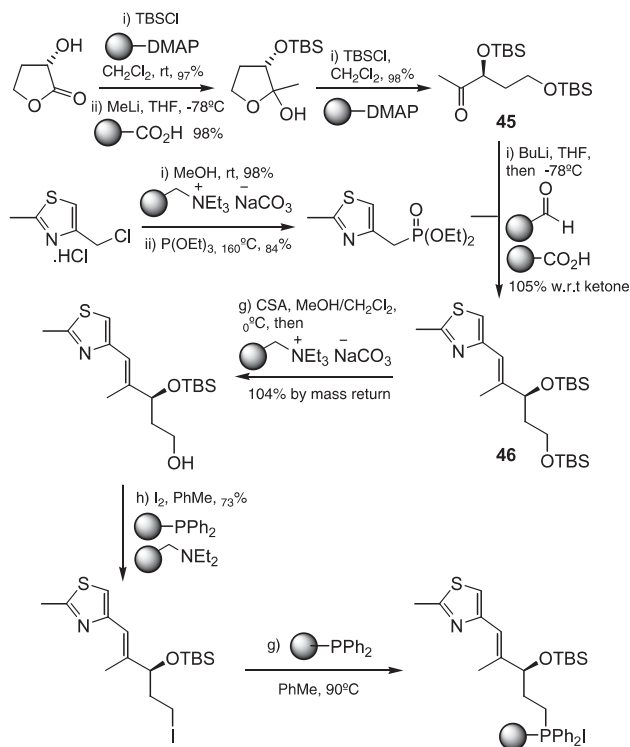
Scheme 2.83 Synthesis of the natural product (±)-plicamine.



**Fig. 2.5** Disconnection approach to the epothilone members A & C.

ural and synthetic analogue epothilones. Currently several major pharmaceutical companies are continuing drug discovery programmes with several analogues undergoing clinical trials as treatments for a variety of malignant tumour types. Accordingly, there have been many total syntheses of the epothilones reported from both academic and industrial research groups since the disclosure of their biological importance. However, all of these synthetic programmes have required silica gel chromatography to remove contaminating by-products after virtually every synthetic step. While this is acceptable for research laboratory investigations, such processes are not viable within larger scale production, nor are they appropriate for the high throughput preparation of libraries of analogues.

The total synthesis of epothilone C represented the most complex target attempted using these methodologies, so a highly diastereoselective and well planned synthesis was essential for success. The resulting strategy was built upon previously reported conventional syntheses but enabled the avoidance of the associated laborious work-up protocols and extensive chromatographic methods. The macrocyclic structure was assembled from three fragments (Fig. 2.5); fragments 2 and 3 were joined *via* a stereoselective aldol reaction, prior to unmasking an aldehyde at C-12, for a Wittig coupling to incorporate fragment 1 and install the *cis* configured olefin. Selective protecting group manipulation, followed by a macro-

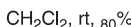


**Scheme 2.84** Synthesis of Fragment 1.

lactonisation finally yielded the total synthesis of cyclic natural product epothilone C and represented a formal synthesis of epothilone A [112].

Fragment 1 was generated *via* a convergent route beginning from *S*-( $-$ )- $\alpha$ -hydroxy- $\beta$ -butyrolactone which was readily protected as the TBS (tributyl silyl) ether using a polymer supported DMAP catalyst. Reduction of this intermediate with methyl lithium formed the lactol which was immediately trapped in the open chain form by a second TBS protection to give compound 45 (Scheme 2.84). The thiazole unit was then installed using methyl-2-methylthiazole phosphonate, in a Horner-Wadsworth-Emmons reaction to give fragment 46. An excess of the phosphonate anion with respect to the ketone was used to drive the olefination reaction to completion resulting in only the desired *trans*-trisubstituted olefin. The excess phosphonate could be conveniently scavenged using a polymeric benzaldehyde resin. Following selective deprotection of the primary TBS ether and conversion of the alcohol to the corresponding iodide, fragment 1 was then loaded onto polymer-supported triphenylphosphine as the phosphonium salt in readiness for coupling *via* a Wittig reaction.

Fragment 2 was prepared from (*R*)-( $-$ )-3-bromo-2-methyl-1-propanol by initial protection as the tetrahydropyranyl ether, followed by a Finkelstein halogen ex-



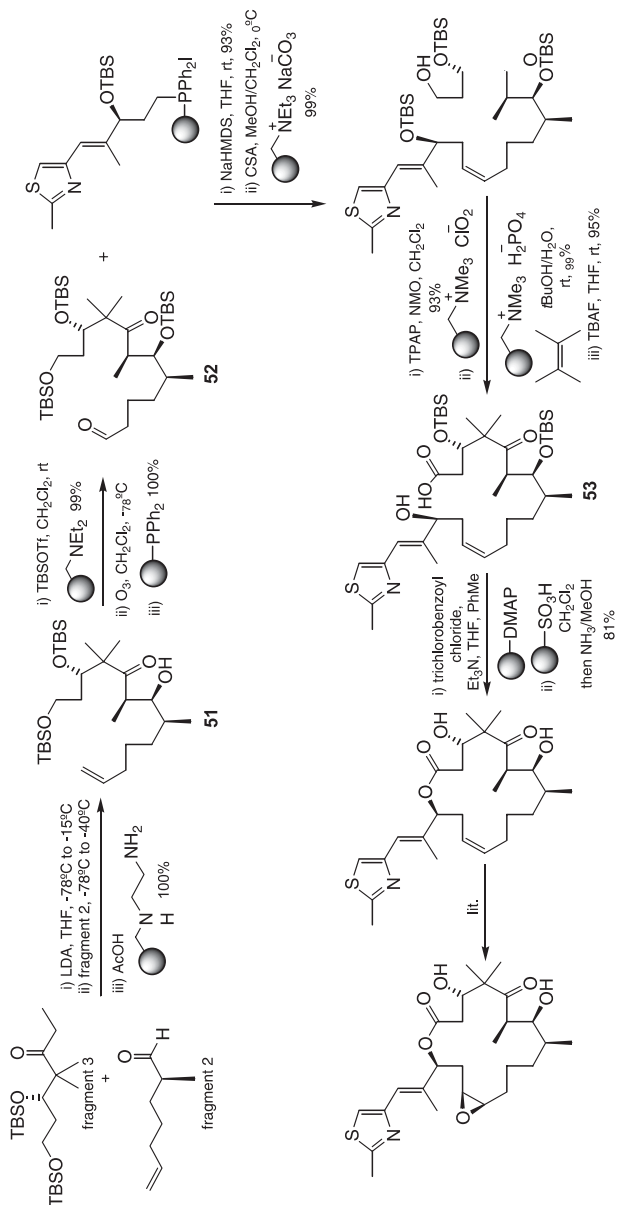
**Scheme 2.85** Synthesis of Fragment 2.



**Scheme 2.86** Synthesis of Fragment 3.

change reaction to furnish the primary iodide (Scheme 2.85). The subsequent copper(I) mediated carbon-carbon bond forming reaction with 3-butenyl magnesium bromide gave, after quenching with a polymeric carboxylic acid and amine resins, to scavenge the copper residues, the chain homologated product **47**. Simple deprotection and oxidation with an immobilised PCC reagent furnished fragment **2**.

The asymmetric center in fragment 3 was efficiently installed using Kiyooka's chiral Lewis acid promoted Mukaiyama aldol chemistry (Scheme 2.86). Commer-



Scheme 2.87 Coupling strategy.

cially available TMS silyl enol ether **48** was combined with readily accessible aldehyde **49**. Amberlite IRA-743 was used as a boron specific scavenging resin to remove residual boron by-products following the reaction. Protection of the hydroxyl was followed by TMSMeLi addition to the ester to furnish methyl ketone (**50**), alkylation of the methyl ketone then was applied to provide ethyl ketone fragment **3** in high yield and excellent enantioselectivity.

The coupling of the fragments begins with a substrate controlled stereoselective aldol reaction between fragments **2** and **3** to generate component **51**, establishing two new stereogenic centres (Scheme 2.87). In this reaction an excess of the aldehyde (fragment **2**) was used to force the reaction to completion giving a final diastereomeric ratio of greater than 13:1 for the required anti-Felkin Anh adduct. The reaction was easily worked-up by acetic acid quench, followed by diamine resin to scavenge the excess aldehyde and acid. A facile TBS protection of the aldol product **51** was followed by cleavage of the terminal olefin by ozonolysis, using polymer-supported triphenylphosphine to decompose the ozonide, cleanly providing aldehyde **52**. Treatment of the phosphonium salt of immobilised fragment **1** (Scheme 2.86) with sodium hexamethyldisilazane and addition of the aldehyde **52** installed the necessary *cis* olefin. Selective deprotection of the primary alcohol, followed by oxidation to the carboxylic acid was achieved by a two-step oxidation. A second selective deprotection of the allylic TBS then provided the hydroxy acid **53** in readiness for a macrolactonisation. The macrocyclization of the linear hydroxy acid under modified Yamaguchi conditions proceeded in good yield to furnish the required 16-membered lactone. Finally total deprotection was effected by a sulfonic acid resin which also acted to catch the product, allowing a catch and release purification procedure in the final step to yield natural product epothilone C. From this product oxidation of the *cis* olefin to the epoxide using a dioxirane reagent has been shown to proceed in high yield and with a good facial selectivity (5:1) to provide a formal synthesis of the second natural product, epothilone A [113].

This total synthesis has demonstrated the scope and utility of supported reagents and scavenging techniques within a multi-step context by stereoselectively providing epothilone C in 29 steps overall and with a longest linear sequence of only 17 steps from commercially available materials. It is envisaged that this will encourage the further integration of immobilized reagent and scavenging techniques alongside conventional methods for general application within synthesis programmes and drug discovery.

## 2.3

### Conclusion

The future of solid supported solution phase chemistry will continue to generate many exciting developments. Only in recent years have we truly perceived what might be possible to achieve with these systems in multi-step organic synthesis. Building upon this knowledge platform we believe it is certainly possible to use



these reagents in many more elaborate one-pot multi-reagent combinations, even with the aim of discovering new chemical reactions. However in order to achieve further progress we require the development of a larger tool-kit of supported reagents. As these new species will need to be catalytic or readily recyclable and available at a low cost, this will invariably mean that new polymers and support materials will have to be invented. There is also the need for greatly improved and more efficient scavenging and quenching agents to be manufactured in order to allow a wider range of chemistries to be carried out in a more efficient fashion.

As the true scope and versatility of the supported reagents are globally realized the development of automated reactors will become increasingly important. We believe that the compatibility of the solid phase reagents in automated reaction formats will allow rapid integration with existing reactors for both flow and batch processing. Other novel reactor packs, reagent chips or plug-in reagent cartridges will also become prominent in organic synthesis programs of the future. Another important consideration is the ability to link the product formation with real-time feedback of information which should lead to self-optimizing systems. The removal of the potentially contaminating reagents and other impurities *via* scavenging from the reaction stream will certainly simplify the analysis process.

Overall the area of solid supported reagents is flourishing as the tremendous advantages offered by these systems for enhanced synthesis becomes apparent. We are already seeing these reagent systems being integrated into many synthetic programs across all areas of chemistry from the early design and development experiments to large scale manufacturing. Undoubtedly this is a trend that will certainly increase with time.

## 2.4

### References

- 1 (a) S. V. LEY, I. R. BAXENDALE, *The chemical Record* **2002**, 2, 377. (b) S. V. LEY, I. R. BAXENDALE, G. BRUSOTTI, *et al.*, *Il Farmaco* **2002**, 57, 231. (c) I. R. BAXENDALE, S. V. LEY, *Nature Rev. (Drug Discovery)* **2002**, 2, 573. (d) B. CLAPHAM, T. S. REGER, K. D. JANDA, *Tetrahedron* **2001**, 57, 4637. (e) A. KIRSCHNING, H. MONENSCHIN, R. WITTEBERG, *Angew. Chem. Int. Ed.* **2001**, 40, 650. (f) D. C. SHERRINGTON, *J. Polym. Sci., Polym. Chem.* **2001**, 39, 2364. (g) S. V. LEY, I. R. BAXENDALE, R. N. BREAN, *et al.*, *J. Chem. Soc., Perkin Trans. 1* **2000**, 3815. (h) L. A. THOMPSON, *Curr. Opin. Chem. Biol.* **2000**, 4, 324. (i) S. Kobayashi, *Curr. Opin. Chem. Biol.* **2000**, 4, 338. (j) S. V. LEY, I. R. BAXENDALE, *The Development and Application of Supported Reagents for Multi-step Organic Synthesis in Supported Catalysts and their Applications*, (eds. D. C. SHERRINGTON, A. P. KYBETT), The Royal Society of Chemistry, Cambridge, **2001**, pp 9–18; ISBN 0-85404-880-4. (k) B. HALL, F. HAUNERT, J. SCOTT, *et al.*, *Preparation of Compounds Using Polymer Supported Reagents*, Patent WO 9958475, **1999**. (l) S. T. SHUTTLEWORTH, M. S. ALLIN, P. K. SHARMA, *Synthesis* **1997**, 1217.
- 2 (a) R. L. LETSINGER, M. J. KORNET, *J. Am. Chem. Soc.* **1963**, 85, 3045. (b) R. L. LETSINGER, S. B. HAMILTON, *J. Am. Chem. Soc.* **1959**, 81, 3009.
- 3 R. B. MERRIFIELD, *J. Am. Chem. Soc.* **1963**, 85, 2149.
- 4 (a) D. ORBECHT, J. M. VILLALGORDO, in *Solid-Supported Combinatorial and Parallel Synthesis of Small-Molecular-Weight Compound Libraries*, *Tetrahedron Organic Chemistry Series*, **1998**, Vol. 17, Pergamon, Elsevier Science, ISBN 0-08-043257-3. (b) P. SENECI, in *Solid-Phase*

- Synthesis and Combinatorial Technologies*, 2000, John Wiley & Sons, ISBN 0-471-33195-3.
- 5 D. P. CURRAN, *Angew. Chem. Int. Ed.* **1998**, 1175.
  - 6 C. SPANKA, P. WENTWORTH, K. D. JANDA, *Comb. Chem. High Throughput Scr.* **2002**, 5, 233.
  - 7 B. A. ADAMS, H. E. LEE., *J. Soc. Chem. Ind.* **1935**, 54.
  - 8 W. C. BAUMAN, **1949**, patent WO2466675.
  - 9 W. P. HOHENSTEIN, H. MARK, *J. Polym. Sci., A* **1946**, 127.
  - 10 S. SUSSMAN, *Ind. Eng. Chem.* **1946**, 38, 1228.
  - 11 F. HELFERRICH, McGraw-Hill, New York **1962** (Chapter 11), p. 519.
  - 12 M. J. ASTLE, *Ion Exchangers in Organic and Biochemistry*, Interscience, New York **1957**, (Chapter 36), p. 658.
  - 13 (a) M. H. BOLLI, S. V. LEY, *J. Chem. Soc., Perkin Trans. 1* **1998**, 2243. (b) S. V. MCKINLEY, J. W. RAKSHYS, *J. Chem. Soc. Chem. Commun.* **1972**, 134. (c) F. CAMPS, J. CASTELLS, M. J. FERNANDO, *et al.*, *Tetrahedron Lett.* **1971**, 1713.
  - 14 (a) S. V. LEY, M. H. BOLLI, B. HINZEN, *et al.*, *J. Chem. Soc., Perkin Trans. 1* **1998**, 2239. (b) B. HINZEN, R. LENZ, S. V. LEY, *Synthesis* **1998**, 977. (c) B. HINZEN, S. V. LEY, *J. Chem. Soc., Perkin Trans. 1* **1997**, 1907.
  - 15 S. V. LEY, A. W. THOMAS, H. FINCH, *J. Chem. Soc., Perkin Trans. 1* **1999**, 669.
  - 16 B. S. PEDERSON, S.-O. LAWESSON, *Bull. Soc. Chem. Belg.* **1977**, 86, 693.
  - 17 S. V. LEY, A. G. LEACH, R. I. STORER, *J. Chem. Soc., Perkin Trans. 1* **2001**, 358.
  - 18 K. C. NICOLAOU, S. PASTOR, S. BARLUENGA, *et al.*, *J. Chem. Soc., Chem. Commun.* **1998**, 1947.
  - 19 (a) A. K. BROSE, M. S. MANHAS, S. N. GANGULY, *et al.*, *Synthesis* **2002**, 1578. (b) A. LEW, P. O. KRUTZIK, M. E. HART, *et al.*, *J. Comb. Chem.* **2001**, 4, 95. (c) P. LINDSTROM, J. TIERNEY, B. WATHEY, *et al.*, *Tetrahedron* **2001**, 57, 9225.
  - 20 (a) I. R. BAXENDALE, A. L. LEE, S. V. LEY, *Synlett.* **2001**, 2004. (b) I. R. BAXENDALE, A. L. LEE, S. V. LEY, *Synlett.* **2001**, 1482.
  - 21 (a) I. R. BAXENDALE, S. V. LEY, M. NESSI, *et al.*, *Tetrahedron* **2002**, 58, 6285. (b) I. R. BAXENDALE, S. V. LEY, C. PIUTTI, *Angew. Chem. Int. Ed.* **2002**, 41, 2194.
  - 22 (a) ELLIS, W. KEIM, P. WASSERSCHIED, *J. Chem. Soc., Chem. Comm.* **1999**, 337. (b) H. WAFFENSCHMIDT, P. WASSERSCHIED, D. VOGT, *et al.*, *J. Catal.* **1999**, 186, 481. (c) H. WAFFENSCHMIDT, P. WASSERSCHIED, W. KEIM, Deutsche Patentanmeldung **1999**, 19901524.4. (d) T. WELTON, *Chem. Rev.* **1999**, 99, 2071. (e) M. FREEMANTLE, *Chem. Eng. News* **1998**, 76(13), 32. (f) K. R. SEDDON, *J. Chem. Technol. Biotechnol.* **1997**, 68, 351. (g) K. R. SEDDON, *Kinet. Catal.* **1996**, 37, 693. (h) S. V. VOLKOV, *Chem. Soc. Rev.* **1990**, 19, 21. (i) W. SUNDERMEYER, *Chemie in unserer Zeit* **1967**, 1, 150. (j) W. SUNDERMEYER, *Angew. Chem.* **1965**, 77, 241. (k) W. SUNDERMEYER, *Angew. Chem. Int. Ed.* **1965**, 4, 222.
  - 23 S. V. LEY, S. J. TAYLOR, *Bioorg. Med. Chem. Lett.* **2002**, 12, 1813.
  - 24 (a) P. HODGE, *Chem. Soc. Rev.* **1997**, 26, 417. (b) A. AKELAH, *J. Mater. Sci.* **1986**, 21, 2977.
  - 25 (a) M. A. KRAUS, A. PATCHORNIK, *Chemtech* **1979**, 119. (b) A. PATCHORNIK, M. A. KRAUS, *Pure Appl. Chem.* **1976**, 46, 183. (c) A. PATCHORNIK, *Chemtech* **1987**, 58.
  - 26 C. G. OVERBERGER, K. N. SANNES, *Angew. Chem Int. Ed.* **1974**, 13, 99.
  - 27 B. M. TROST, R. W. WARNER, *J. Am. Chem. Soc.* **1983**, 105, 5940.
  - 28 (a) P. HODGE, J. WATERHOUSE, *J. Chem. Soc., Perkin Trans. 1* **1983**, 2319. (b) C. C. LEZNOFF, *Acc. Chem. Res.* **1978**, 11, 327. (c) J. M. GOLDWASSER, C. C. LEZNOFF, *Can. J. Chem.* **1978**, 56, 1562. (d) T. M. FYLES, C. C. LEZNOFF, *Can. J. Chem.* **1976**, 54, 935. (e) T. M. FYLES, C. C. LEZNOFF, J. WEATHERSTON, *Can. J. Chem.* **1978**, 56, 1031. (f) J. M. J. FRECHET, L. J. NUYENS, *Can. J. Chem.* **1976**, 54, 926. (g) J. Y. WONG, C. MANNING, C. C. LEZNOFF, *Angew. Chem. Int. Ed.* **1974**, 13, 666. (h) C. C. LEZNOFF, J. Y. WONG, *Can. J. Chem.* **1973**, 51, 2452. (i) C. C. LEZNOFF, J. Y. WONG, *Can. J. Chem.* **1973**, 51, 3756. (j) C. C. LEZNOFF, J. Y. WONG, *Can. J. Chem.* **1972**, 50, 2892. (k) T. KUSAMA, H. HAYATSU, *Chem. Pharm. Bull. Jpn.* **1970**, 18, 319.

- 29 C. C. LEZNOFF, C. M. DIXIT, *Can. J. Chem.* **1977**, *55*, 3351.
- 30 G. A. CROSBY, N. M. WEINSHENKER, H.-S. UH, *J. Am. Chem. Soc.* **1975**, *97*, 2232.
- 31 (a) A. KIRSCHNING, H. MONENSCHIN, R. WITTENBURG, *Chem. Eur. J.* **2000**, *6*, 4445. (b) T. A. KEATING, R. W. ARMSTRONG, *J. Am. Chem. Soc.* **1996**, *118*, 2574. (c) J. M. J. FRECHET, L. J. NUYENS, *Can. J. Chem.* **1976**, *54*, 926. (d) J. Y. WONG, C. C. LEZNOFF, *Can. J. Chem.* **1973**, *51*, 2452. (e) C. C. LEZNOFF, J. Y. WONG, *Can. J. Chem.* **1972**, *50*, 2892. (f) I. T. HARRISON, S. HARRISON, *J. Am. Chem. Soc.* **1967**, *89*, 5723.
- 32 G. FAITA, A. PAIO, P. QUADRELLI, *et al.*, *Tetrahedron Lett.* **2000**, *41*, 1265.
- 33 (a) I. R. BAKENDALE, S. V. LEY, *Bioorg. Med. Chem. Lett.* **2000**, *10*, 1983. (b) Y. H. HU, S. BAUDART, J. A. PORCO, *J. Org. Chem.* **1999**, *64*, 1049.
- 34 J. REBEK, F. GAVINA, *J. Am. Chem. Soc.* **1974**, *96*, 7112.
- 35 J. REBEK JR., D. BROWN, S. ZIMMERMAN, *J. Am. Chem. Soc.* **1975**, *97*, 454.
- 36 A. WARSHAWSKY, R. KALIR, A. PATCHNORNIK, *J. Am. Chem. Soc.* **1978**, *100*, 4544.
- 37 C. V. PITTMAN, L. R. SMITH, *J. Am. Chem. Soc.* **1975**, *97*, 1749.
- 38 B. J. COHEN, M. A. KRAUS, A. PATCHORNIK, *J. Am. Chem. Soc.* **1977**, *99*, 4165.
- 39 G. CAINELLI, M. CONTENTO, F. MANESCALCHI, *et al.*, *J. Chem. Soc. Perkin Trans. 1* **1980**, 2516.
- 40 D. E. BERGBREITER, R. CHANDRAN, *J. Am. Chem. Soc.* **1985**, *107*, 4792.
- 41 J. M. J. FRECHET, P. DARLING, M. J. FARRALL, *J. Org. Chem.* **1981**, *46*, 1728.
- 42 M. BESSODES, K. ANTONAKIS, *Tetrahedron Lett.* **1985**, *26*, 1305.
- 43 N. HEBERT, A. BECK, R. B. LENNOX, *et al.*, *J. Org. Chem.* **1992**, *57*, 1777.
- 44 S. L. REGEN, M. KODOMARI, *J. Chem. Soc., Chem. Commun.* **1987**, 1428.
- 45 G. CARDILLO, M. ORENA, G. PORZI, *et al.*, *J. Chem. Soc., Chem. Commun.* **1982**, 1309.
- 46 G. CARDILLO, M. ORENA, S. SANDRI, *J. Org. Chem.* **1986**, *51*, 713.
- 47 J. CHOI, N. M. YOON, *Syn. Commun.* **1995**, *25*, 2655.
- 48 J. J. PARLOW, *Tetrahedron Lett.* **1995**, *36*, 1395.
- 49 (a) J. EAMES, M. WATKINSON, *Eur. J. Org. Chem.* **2001**, 1213. (b) L. A. THOMPSON, *Curr. Opin. Chem. Biol.*, **2000**, *4*, 324. (c) R. J. BOOTH, J. C. HODGES, *Acc. Chem. Res.* **1999**, *32*, 18. (d) J. C. HODGES, *Synlett.* **1999**, *1*, 152. (e) J. J. PARLOW, R. V. DEVRAJ, M. S. SOUTH, *Curr. Opin. Chem. Biol.* **1999**, *3*, 320. (f) D. L. FLYNN, R. V. DEVRAJ, W. NAING, *et al.*, *Med. Chem. Res.* **1998**, *8*, 219. (g) D. L. FLYNN, R. V. DEVRAJ, J. J. PARLOW, *Curr. Opinion Drug Disc. Dev.* **1998**, *1*, 41. (h) S. W. KALDOR, M. G. SIEGEL, *Curr. Opin. Chem. Biol.* **1997**, *1*, 101. (i) S. W. KALDOR, M. G. SIEGEL, J. E. FRITZ, *et al.*, *Tetrahedron Lett.* **1996**, *37*, 7193.
- 50 D. L. FLYNN, J. Z. CRICH, R. V. DEVRAJ, *et al.*, *J. Am. Chem. Soc.* **1997**, *119*, 4874.
- 51 J. J. PARLOW, B. L. CASE, M. S. SOUTH, *Tetrahedron* **1999**, *55*, 6785.
- 52 J. J. PARLOW, M. L. VAZQUEZ, D. L. FLYNN, *Bioorg. Med. Chem. Lett.* **1998**, *8*, 2391.
- 53 T. DEEGAN, O. W. GOODING, S. BAUDART, *et al.*, *Tetrahedron Lett.* **1997**, *38*, 4973.
- 54 K. FUKASE, T. YOSHIMURA, S. KOTANI, *et al.*, *Bull. Chem. Soc. Jpn.* **1994**, *67*, 473.
- 55 S. W. KALDOR, J. E. FRITZ, J. TANG, *et al.*, *Bioorg. Med. Chem. Lett.* **1996**, *6*, 3041.
- 56 R. J. BOOTH, J. C. HODGES, *J. Am. Chem. Soc.* **1997**, *119*, 4882.
- 57 J. J. PARLOW, D. A. MISCHKE, S. S. WOODARD, *J. Org. Chem.* **1997**, *62*, 5908.
- 58 M. S. SOUTH, T. A. DICE, J. J. PARLOW, *Biotechnol. Bioeng. (Comb. Chem.)* **2000**, *71*, 51.
- 59 M. S. SOUTH, B. L. CASE, T. A. DICE, *et al.*, *Comb. Chem. High Throughput Scr.* **2000**, *3*, 139.
- 60 C. F. STURINO, M. LABELLE, *Tetrahedron Lett.* **1998**, *39*, 5891.
- 61 G. W. STARKEY, J. J. PARLOW, D. L. FLYNN, *Bioorg. Med. Chem. Lett.* **1998**, *8*, 2385.
- 62 J. J. PARLOW, W. NAING, M. S. SOUTH, *et al.*, *Tetrahedron Lett.* **1997**, *38*, 7959.
- 63 J. J. PARLOW, D. L. FLYNN, *Tetrahedron* **1998**, *54*, 4013.
- 64 B. RAJU, J. M. KASSIR, T. P. KOGAN, *Bioorg. Med. Chem. Lett.* **1998**, *8*, 3043.
- 65 J. J. WEIDNER, J. J. PARLOW, D. L. FLYNN, *Tetrahedron Lett.* **1999**, *40*, 239.
- 66 I. R. HARDCASTLE, A. M. BARBER, J. H. MARRIOTT, *et al.*, *Tetrahedron Lett.* **2001**, *42*, 1363.

- 67 (a) B. HINZEN, R. LENZ, S.V. LEY, *Synthesis* **1998**, 977. (b) B. HINZEN, S.V. LEY, *J. Chem. Soc., Perkin Trans. 1* **1997** 1907.
- 68 F. HAUNERT, M.H. BOLLI, B. HINZEN, *et al.*, *J. Chem. Soc., Perkin Trans. 1* **1998**, 2235.
- 69 (a) F.C. COPP, P.J. ISLIP, J.E. TATESON, *Biochem. Pharmacol.* **1984**, 33, 339. (b) G.A. HIGGS, R.J. FLOWER, J.R. VANE, *Biochem. Pharmacol.* **1979**, 28, 1959.
- 70 I.R. BAXENDALE, S.V. LEY, W. LUMERAS, *et al.*, *Comb. Chem. High Throughput Scr.* **2002**, 5, 197.
- 71 S.V. LEY, M.H. BOLLI, B. HINZEN, *et al.*, *J. Chem. Soc., Perkin Trans. 1* **1998**, 2239.
- 72 M.H. BOLLI, S.V. LEY, *J. Chem. Soc., Perkin Trans. 1* **1998**, 2243.
- 73 B. HINZEN, S.V. LEY, *J. Chem. Soc., Perkin Trans. 1* **1998**, 1.
- 74 J. HABERMANN, S.V. LEY, R. SMITS, *J. Chem. Soc., Perkin Trans. 1* **1999**, 2421.
- 75 J. HABERMANN, S.V. LEY, J.J. SCICINSKI, J.S. SCOTT, *et al.*, *J. Chem. Soc., Perkin Trans. 1* **1999**, 2425.
- 76 Y.H. HU, S. BAUDART, J.A. PORCO, *J. Org. Chem.* **1999**, 64, 1049.
- 77 C. BLACKBURN, B. GUAN, P. FLEMING, *et al.*, *Tetrahedron Lett.* **1998**, 39, 3635.
- 78 G.M. RISHTON, D.M. RETZ, P.A. TEMPEST, *et al.*, *J. Med. Chem.* **2000**, 43, 2297.
- 79 K. SENTEN, P.V. VENKEN, G. BAL, *et al.*, *Tetrahedron Lett.* **2001**, 42, 9135.
- 80 M. CALDARELLI, I.R. BAXENDALE, S.V. LEY, *J. Green Chem.* **2000**, 43.
- 81 A.G.M. BARRETT, S.M. CRAMP, R.S. ROBERTS, *et al.*, *Comb. Chem. High Throughput Scr.* **2000**, 3, 131.
- 82 (a) I. CHATAIGNER, C. GENNARI, U. PIARULLI, *et al.*, *Angew. Chem. Int. Ed.* **2000**, 39, 916. (b) C. GENNARI, S. CECCARELLI, U. PIARULLI, *et al.*, *J. Org. Chem.* **1998**, 63, 5312.
- 83 U. BAUER, B.J. EGNER, I. NILSSON, *et al.*, *Tetrahedron Lett.* **2000**, 41, 2713.
- 84 S.E. AULT-JUSTUS, J.C. HODGES, M.W. WILSON, *Biotech. Bioeng. (Comb. Chem.)* **1998**, 61, 17.
- 85 S. BHATTACHARYYA, L. FAN, L. VO, *et al.*, *Comb. Chem. & High Throughput Scr.* **2000**, 3, 117.
- 86 J.S. CHEN, B.R. DIXON, J. DUMAS, *et al.*, *Tetrahedron Lett.* **1999**, 40, 9195.
- 87 Y.K. YUN, S.S. W. LEUNG, J.A. PORCO JR., *Biotechnol. Bioeng. (Comb. Chem.)* **2000**, 71, 9.
- 88 J. HABERMANN, S.V. LEY, J.S. SCOTT, *J. Chem. Soc. Perkin Trans. 1* **1998**, 3127.
- 89 J.S. WARMUS, T.R. RYDER, J.C. HODGES, *et al.*, *Bioorg. Med. Chem. Lett.* **1998**, 8, 2309.
- 90 W. MCCOMAS, L. CHEN, K. KIM, *Tetrahedron Lett.* **2000**, 41, 3573.
- 91 K. KIM, W. MCCOMAS, *Comb. Chem. High Throughput Scr.* **2000**, 3, 125.
- 92 K. KIM, K. LE, *Synlett.* **1999**, 1957.
- 93 W. XU, R. MOHAN, M.M. MORRISSEY, *Tetrahedron Lett.* **1997**, 38, 7337.
- 94 W. XU, R. MOHAN, M.M. MORRISSEY, *Bioorg. Med. Chem. Lett.* **1998**, 8, 1089.
- 95 M.W. CRESWELL, G.L. BOLTON, J.C. HODGES, *et al.*, *Tetrahedron* **1998**, 54, 3983.
- 96 M. CALDARELLI, J. HABERMANN, S.V. LEY, *J. Chem. Soc., Perkin Trans. 1* **1999**, 107.
- 97 (a) S.V. LEY, A. MASSI, *J. Comb. Chem.* **2000**, 2, 104. (b) S.V. LEY, A. MASSI, *J. Chem. Soc. Perkin Trans. 1* **2000**, 3645.
- 98 S.V. LEY, D.M. MYNETT, W. J. KOOT, *Synlett.* **1995**, 1017.
- 99 M. CALDARELLI, J. HABERMANN, S.V. LEY, *Bioorg. Med. Chem. Lett.* **1999**, 9, 2049.
- 100 M. WHITTAKER, P. BROWN, *Curr. Opin. Drug Discovery Dev.* **1998**, 1, 157.
- 101 J. HABERMANN, S.V. LEY, J.J. SCICINSKI, *J. Chem. Soc., Perkin Trans. 1* **1999**, 2425.
- 102 (a) A. KIRSCHNING, M. JESBERGER, A. SCHÖNBERGER, *Org. Lett.* **2001**, 3, 3623. (b) A. KIRSCHNING, M. JESBERGER, H. MONENSCHN, *Tetrahedron Lett.* **1999**, 40, 8999.
- 103 I.R. BAXENDALE, M. ERNST, W.-R. KRAHNERT, *et al.*, *Synlett.* **2002**, 1641–1644.
- 104 R.N. BREAN, S.V. LEY, P.A. PROCOPIOU, *Org. Lett.* **2002**, 4, 3793.
- 105 S.V. LEY, O. SCHUCHT, A.W. THOMAS, *et al.*, *J. Chem. Soc., Perkin Trans. 1* **1999** 1251.
- 106 S.V. LEY, A.W. THOMAS, H. FINCH, *J. Chem. Soc., Perkin Trans. 1* **1999**, 669–671.
- 107 J. HABERMANN, S.V. LEY, J.S. SCOTT, *J. Chem. Soc., Perkin Trans. 1* **1999**, 1253.
- 108 O.L. CHAPMAN, M.R. ENGEL, J.P. SPRINGER, *et al.*, *J. Am. Chem. Soc.* **1971**, 6696.

- 109 I. R. BAXENDALE, A. L. LEE, S. V. LEY, J. *Chem. Soc. Perkin Trans. 1* **2002**, 1850.
- 110 (a) V. KUMAR, K. SUGAYA, S. SAUNDERS, J. MECHANIC, *Drugs Today* **1996**, 32, 529. (b) M. F. SIDDIQUI, A. I. LEVEY, *Drugs Future* **1999**, 24, 417. (c) Z. G. GAO, W. Y. CUI, H. T. ZHANG, C. G. LIU, *Pharmacol. Res.* **1998**, 38, 101. (d) J. R. PAULY *Alzheimer's Disease Review* **1998**, 3, 28. (e) M. A. PRENDERGAST, W. J. JACKSON, A. V. TERRY, *et al.*, *Psychopharmacology* **1998**, 136, 50. (f) M. W. HOLLADAY, M. J. DART, J. K. LYNCH, *J. Med. Chem.* **1997**, 40, 4169. (g) M. W. DECKER, J. D. BRIONI, Neuronal Nicotinic Receptors: Potential Treatment of Alzheimer's Disease with Novel Cholinergic Channel Modulators. In *Pharmacological Treatment of Alzheimer's Disease: Molecular and Neurobiological Foundations*; J. D. BRIONI, M. W. DECKER eds. Wiley-Liss, New York, **1997**, 433. (h) J. D. BRIONI, M. W. DECKER, J. P. SULLIVAN, S. P. ARNERIC, *Adv. Pharmacol.* **1997**, 37, 1153. (i) I. A. McDONALD, N. COSFORD, J.-M. VERNIER, in *Annual Reports in Medicinal Chemistry*; J. A. BRISTOL ed. Academic Press, San Diego, CA **1995**, 30, 41. (j) J. L. GALZI, J. P. CHANGEUX, *Neuropharmacology* **1995**, 34, 563. (k) M. TOMIZAWA, H. OTSUKA, T. MIYAMOTO, *et al.*, *J. Pesticide Sci.* **1995**, 20, 57. (l) E. K. PERRY, C. M. MORRIS, J. A. COURT, *et al.*, *Neuroscience* **1995**, 64, 385. (m) A. AKAIKE, Y. TAMURA, T. YOKOTA, *et al.*, *Brain Res.* **1994**, 644, 181.
- 111 I. R. BAXENDALE, G. BRUSOTTI, M. MATSUOKA, *et al.*, *J. Chem. Soc. Perkin Trans. 1* **2002**, 143.
- 112 S. V. LEY, R. I. STORER, T. TAKEMOTO, P. S. JACKSON, S. V. LEY, *Angew. Chem. Int. Ed.* **2003**, in press.
- 113 K. C. NICOLAOU, S. NINKOVIC, F. SARBIA, *et al.*, *J. Am. Chem. Soc.* **1997**, 119, 7974.

## 3

**Organic Synthesis on Polymeric Supports**

CARMEN GIL, KERSTIN KNEPPER and STEFAN BRÄSE

## 3.1

**Introduction**

Over the past decade, the advances in High Throughput Screening (HTS) and combinatorial chemistry have revolutionized the approaches of chemists to the synthesis of large compound libraries with the advent of combinatorial chemistry, which is especially suitable for the initial stages of the drug discovery process [1–3]. In addition, this powerful technique has increasingly being applied to other areas of chemistry such as material sciences and the discovery of new catalysts [4].

In general, organic chemistry on polymeric supports, which is the major tool in combinatorial chemistry with the implementation of organic compounds, can be divided into three parts: the polymeric support, often a polystyrene resin; the product, and the linker which enables a suitable connection between the two parts (Fig. 3.1) [5].

A key aspect of any synthesis strategy on a polymeric support is the linkage element, which acts as a tether to the polymeric support. Ideally, the linker should be stable to all reaction conditions used in a synthesis sequence and should be cleaved quantitatively under conditions that do not degrade the desired target molecule [6]. In this overview the different kinds of linkers and the synthetic transformations that can be used on polymeric supports will be presented. At the end, synthetic strategies for the synthesis of heterocycles and natural products will be mentioned.

Synthesis methods on polymeric supports have been employed in the past for the preparation of synthetic oligonucleotides [7, 8] oligosaccharides [9, 10] and peptides [11]. The synthesis of oligopeptides and oligonucleotides is usually automated employing polymeric supports. Automated solid-phase synthesis of oligosaccharides has been described less often than other methods [12, 13]. The synthesis of these complex molecules requires the selection of the linker as a critical point, because the linker should be stable towards glycosylation conditions and protecting group manipulation. The other important point is that the cleavage conditions should not affect the structure of the obtained compound [14].

The use of polymer-supported synthesis in combinatorial chemistry has become increasingly important in drug discovery [15]. Therefore, an efficient synthetic

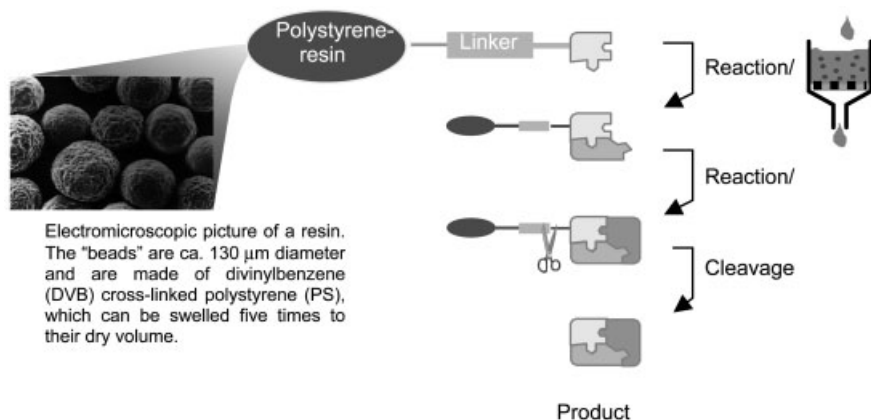


Fig. 3.1 General Scheme for synthesis on an insoluble polymeric support.

methodology has been developed using polymeric supports for targeting new molecules and natural products with desired properties which play an important role in pharmaceutical research [16, 17].

The use of polymeric materials for the rapid access of compound libraries in solution will be presented in chapter 5.

In general, both soluble and insoluble (solid) polymeric supports can be used for this purpose, however, nowadays insoluble polymeric supports are more frequently being used because they are easy to automate.

### 3.2

#### Linkers for Organic Synthesis on Polymeric Supports

The design of powerful new linker strategies is crucial to the advancement of technologies used for combinatorial chemistry on polymeric supports. They are usually derived from protecting groups known for solution-phase chemistry [6, 18].

The International Union of Pure and Applied Chemistry (IUPAC) defines linker as a "bifunctional chemical moiety attaching a compound to a solid support or soluble support which can be cleaved to release compounds from the support. A careful choice of the linker allows cleavage to be performed under appropriate conditions compatible with the stability of the compound and assay method" [19].

The proper choice of a suitable linker is a therefore a key consideration in the design of a solid-phase chemical route. Linkers have to be developed in order to be stable in the presence of reagents and to permit orthogonal cleavage under mild conditions. Often, cleavage conditions dictate the requirements for work-up and purification steps of the released compound. Different cleavage strategies have been developed such as photocleavable, safety catch and traceless linkers as mentioned in Section 3.2.2 [20].

## 3.2.1

## Linker Families

## 3.2.1.1 Benzyl-Type Linkers Including Trityl and Benzhydryl Linkers

As the pioneering development of Merrifield [21] and Wang [22] are based on the benzyl linker type, this type represents the starting point of modern linker development.

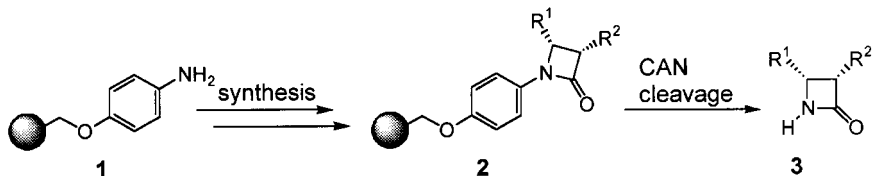
Benzyl-type linkers (Tab. 3.1) are the most common anchoring groups for various kinds of functionalities. Especially esters, amides, amines, alcohols and thiols can be immobilized by this linker family. They are typically cleaved by strong acids like trifluoroacetic acid, which affects a protonation and subsequent elimination of the solid-bound substrate. Strong acidolytic cleavage procedures are extremely hazardous and not generally applicable to multiple parallel syntheses, which limits their use. Two different approaches have been successfully applied to improve the acid lability linker types, which leads to the development of the Wang (7), SASRIN (9), Rink (12–15) and trityl (16) linkers. In 1973, Wang [3] described the *p*-alkoxybenzyl alcohol linker, which allows the cleavage of peptide acids from the solid supports using relatively mild acidic conditions. The addition of one or more alkoxy groups onto the Wang linker (7) furnishes the SASRIN resin (9) (super acid sensitive resin, 1% TFA cleavable) [23] and the HAL linker (10) (hypersensitive acid-labile, 0.1% TFA cleavable) [24], to render this linker more acid labile because of the increased stabilization of the carbocation formed upon cleavage.

The introduction of alkoxy groups onto the benzhydryl system leading to a system cleavable by HF was first reported by Walter in 1976 [25] while one additional alkoxy group leads to the Rink linker (12), introduced in 1987 [26]. As quite mild conditions are sufficient for the release of the library components, the Rink resin has effectively been applied to the synthesis of several small molecule libraries [27].

The immobilization of nucleophilic substrates such as acids, alcohols, thiols and amines is realized by the Trityl resin (16), which is reasonably acid sensitive [28–30].

A linker originally designed for solid-phase synthesis of peptides is the backbone amide linker (11) (BAL), this anchoring approach has now been extended to the combinatorial synthesis of diverse amide [31], hydroxamate [32], oligosaccharide [33] and heterocyclic small molecule libraries [34–36].


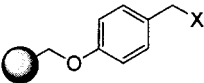
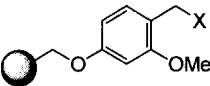
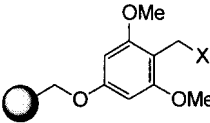
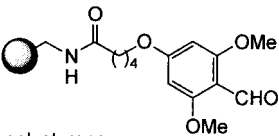
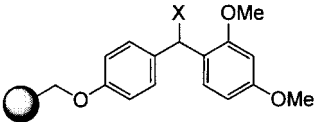
Recently a new linker of this category has been described. A novel benzyloxyaniline linker **1** that uses ceric ammonium nitrate (CAN) as a cleavage reagent, was described by Balasubramanian and Gordon (Scheme 3.1) [37].



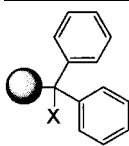
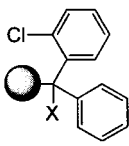
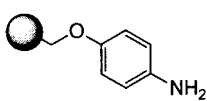
Scheme 3.1 CAN cleavage reaction by Balasubramanian et al. [37].



Tab. 3.1 Structures and properties of benzyl-type linkers including trityl and benzhydryl linkers.

Structure/Generic name of the resin	Cleavage conditions
 <p>Merrifield resin (X=Cl: 4 [21]); AM PS (Aminomethyl polystyrene) (X=NH<sub>2</sub>: 5); hydroxy methyl polystyrene (X=OH: 6)</p>	HF
 <p>Wang linker (X=OH: 7) [22] Boba resin (X=NH<sub>2</sub>: 8) [38]</p>	Cleavage of thiols: HF [39]; cleavage of esters: CF <sub>3</sub> SO <sub>3</sub> H [40]; 95% TFA [22]; H <sub>2</sub> O <sub>2</sub> [41]
 <p>SASRN (9) (Super Acid Sensitive Resin) [23]</p>	Cleavage of esters: 1% TFA, CH <sub>2</sub> Cl <sub>2</sub> , 20 °C, 5 min [23].
 <p>HAL (10) (Hyper-sensitive Acid-Labile) [24]</p>	Cleavage of esters: 0.1% TFA (CH <sub>2</sub> Cl <sub>2</sub> ), 25 °C, 1 h
 <p>polystyrene or PEG polystyrene</p> <p>BAL (Backbone Amide Linker) (11) [42]</p>	Cleavage of amides: TFA 50% CH <sub>2</sub> Cl <sub>2</sub> [43]
 <p>Rink acid (X=OH: 12); Rink amide (X=NH<sub>2</sub>: 13) [26, 44]; Rink chloride (X=Cl: 14); Rink triflate (X=OTf: 15)</p>	Cleavage of esters: 10% AcOH, CH <sub>2</sub> Cl <sub>2</sub> , 20 °C, 1.5 h; 1% TFA [26]; cleavage of amides: TFA [26] 20% TFA, CH <sub>2</sub> Cl <sub>2</sub> [45]

Tab. 3.1 (cont.)

Structure/Generic name of the resin	Cleavage conditions
 <p>Trityl (<b>16</b>) [28, 29]</p>	Cleavage of esters: 1%TFA/AcOH [46, 47]
 <p>2-Chlorotrityl (<b>17</b>)</p>	Cleavage of esters: (CF <sub>3</sub> ) <sub>2</sub> CHOH (HFIP) (20%), CH <sub>2</sub> Cl <sub>2</sub> [48]; AcOH/CF <sub>3</sub> CH <sub>2</sub> OH/CH <sub>2</sub> Cl <sub>2</sub>
 <p>Benzyloxylaniline (<b>18</b>) [37]</p>	Cleavage of secondary amides: CAN [37]

### 3.2.1.2 Allyl-Based Linkers

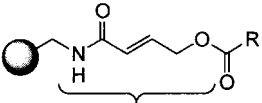
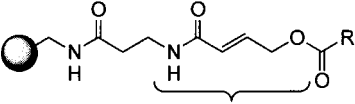
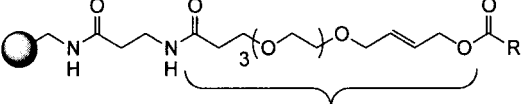
The group of allyl-based linkers was developed by Kunz et al. [49] Linkers of the general allyl type are particularly valuable, because they are removable under almost neutral conditions using palladium catalysis and are orthogonally stable towards the commonly used acid and base-labile protecting groups (Tab. 3.2).

New allylic anchors as the HYCRAM (**19**) (*hydroxycrotonylamide*) [50] and HYCRON (**21**) (*hydroxycrotyl-oligoethylene glycol-*n*-alkanoyl*) [51] linker have been developed, which exhibit excellent properties for the solid-phase synthesis of protected peptides and glycopeptides. A more flexible spacer was inserted in the HYCRON (**21**) linker between the anchor and the polymeric support in order to facilitate an efficient access to the Pd(0) complex during the detachment reaction.

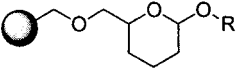
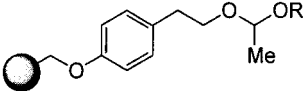
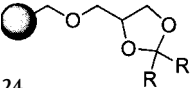
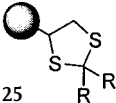
### 3.2.1.3 Ketal/Acetal-Based Linkers

Acetals and ketals are very important protecting groups in solution-phase synthesis, but only a few constructs have been used as linkers in solid-phase synthesis (Tab. 3.3). The THP-linker (**22**) (*tetrahydropyran*) was introduced by Ellman [54] in order to provide a linker allowing the protection of alcohols, phenols and nitrogen functionalities in the presence of pyridinium toluene sulfonate, and the resulting structures are stable towards strong bases and nucleophiles. Other acetal-linkers have also been used for the attachment of alcohols [55, 56]. Formation of diastereomers caused by the chirality of these linkers is certainly a drawback. Other ketal linkers like

Tab. 3.2 Structures of allyl-type linkers.

Structure	Reference
 19 HYCRAM	[49]
 20 HYCRAM with $\beta$ -Ala-AMPS	[49]
 21 HYCRON with $\beta$ -Ala-AMPS	[51–53]

Tab. 3.3 Structures of acetal and ketal-type linkers.

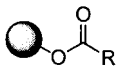
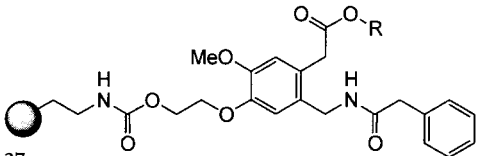
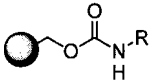
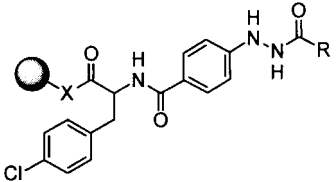
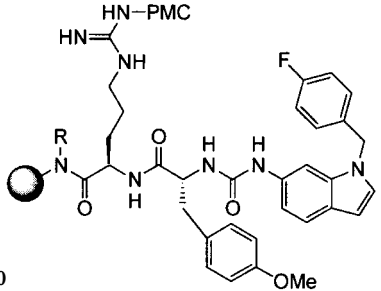
Structure	Comments/References
 22 THP resin (22)	Most common linker for alcohols [54]
 23 New linker for alcohols [55]	
 24 Common linker for ketones and aldehydes [57–60]	
 25 Linker for sterically hindered ketones [61]	

(24) were developed some twenty years ago by Leznoff in order to link aldehydes [57, 58] and ketones [59, 60]. A linker (25) [61] using dithianes is suitable for ketones.

### 3.2.1.4 Ester-, Amide- and Carbamate-Based Linkers

There are many examples that demonstrate the useful application of ester and amide moieties in solid-phase synthesis. They can be used in the benzyl and allyl

Tab. 3.4 Overview of some ester- amide-based linkers.

Structure	Structures achievable
 <p>26</p>	<p>Esters: cleavage with methoxide; Alcohols: cleavage by Grignard reagents [70, 71]</p>
 <p>27</p>	<p>Alcohols: cleavage with enzymes [72]</p>
 <p>28</p>	<p>Amines: cleavage with Pd(OAc)<sub>2</sub>, H<sub>2</sub> (45 psi) DMF, rt, 16 h [68]</p>
 <p>29</p>	<p>Amides, esters: cleavage with Cu(II) salts [73]</p>
 <p>30</p>	<p>Indoles: cleavage with TFA/<i>i</i>-Pr<sub>3</sub>SiH/ 1,2-ethane-dithiol/ H<sub>2</sub>O (9:1:4.5:4.5) 23 °C [67]</p>

linker type and also for the attachment of functional groups. This kind of linker (Tab. 3.4) was employed to attach saccharides to a polymeric support, as efficient solid-phase oligosaccharide synthesis requires a linker stable to all reaction conditions [62–65]. A new efficient process for the solid-phase preparation of fully substituted hydantoins has been developed by introducing a new cyclization/cleavage step with the formation of a very stable amide bond [66]. A secondary amide linker has been used to construct a library of indole-based peptide mimetics [67]. Benzyl carbamates are useful linkers for the synthesis of amines since they are readily cleavable by palladium salts [68]. Another carbamate linker allows the synthesis of guanidines in a traceless way [69].

### 3.2.1.5 Silyl Linkers

Some of the most widely used protecting groups in organic synthesis are the organosilyl groups. The silicon groups are mainly used for the protection of heteroatoms, but they can also be situated on carbon centers. The electronic and steric properties have been used in many applications for the design and use of new linker types. Cleavage can be effected by means of electrophiles such as protons, for example in TFA, or nucleophiles like fluoride ions which causes an element of orthogonality to various other linkers or protecting groups. Several applications using silicium derivatives on solid-phase have been reported leading to traceless linkers (Section 3.2.2.5) or silyl-based spacers. A silyl linker was used in Ellman's traceless synthesis of a benzodiazepine library [74]. The silicon-based linkers have been used to obtain arenes [75–88] and alkenes [89] in a traceless way. Other linkers featuring silyl fragments are the SAC linker (**35**) [90], the SAL linker (**34**) [91], the Pbs linker ("silico Wang linker") (**36**) [92], the Ramage silyl (**37**) [93], the SEM linker (**38**) [94] and silylated benzhydryl linkers (**39**) [95].

Silyl linkers (Tab. 3.5) have successfully been used for the synthesis of natural products [96, 97], oligosaccharides [98], oligonucleotides [99] and in peptide synthesis [100].

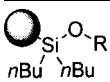
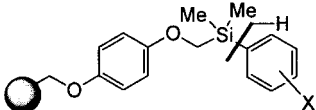
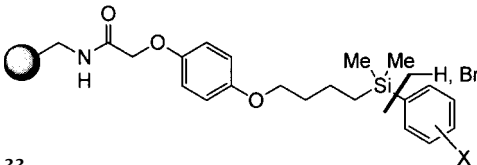
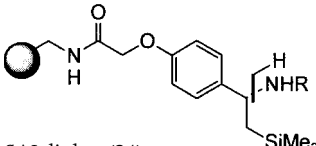
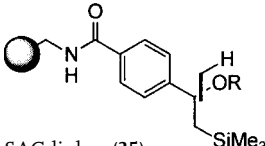
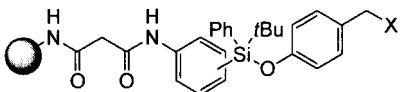
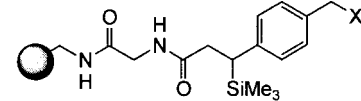
### 3.2.1.6 Boronate Linkers

Boronic acid linkers (Tab. 3.6) are useful for the attachment of diols, the protection of glycosides [105] or as precursors for the metal-mediated cleavage [106]. The boronates formed are sensitive to water and simple hydrolysis is sufficient for cleavage. Recently, Carreaux and Carboni developed a new boronate-based strategy for traceless solid-phase synthesis of aromatic compounds [107].

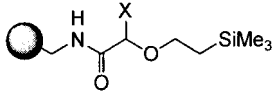
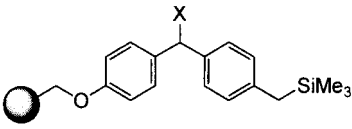
### 3.2.1.7 Sulfur-, Stannane- and Selenium-Based Linkers

Linkers based on sulfur, stannane and selenium chemistry are certainly some of the most flexible systems, because these elements can favorably be tailored for the use as fragile points of attachment.

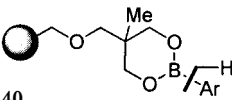
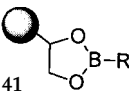
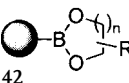
Tab. 3.5 Some silyl linkers.

Structure	Structures achievable
 <p>31</p>	Alcohols: cleavage with TBAF [101]
 <p>32</p>	Traceless linking of arenes [102]
 <p>33</p>	Traceless linking of arenes [103]
 <p>SAL linker (34)</p>	Amides: cleavage with 90% TFA, scavenger [91]
 <p>SAC linker (35)</p>	Acids: cleavage with TBAF [90]
 <p>Pbs linker ("silico Wang linker") (36)</p>	Carboxylic acids: cleavage with TBAF [92]
 <p>Ramage linker (37)</p>	Carboxylic acids: cleavage with TBAF [93, 104]

Tab. 3.5 (cont.)

Structure	Structures achievable
 <p>SEM linker (38)</p>	Alcohols: cleavage with TBAF [94]
 <p>39</p>	Esters: cleavage with TBAF or $\text{Cs}_2\text{CO}_3$ [95, 44]

Tab. 3.6 Boronate linkers.

Structure	Structures achievable
 <p>40</p>	Arenes: cleavage by $\text{Ag}^+$ [107]
 <p>41</p>	Biaryls by Suzuki cross-coupling [106]
 <p>42</p>	Diols [105]

The development of sulfone linkers, the exploration of sulfone based chemical transformations and cleavage strategies are an important objective in solid-phase organic synthesis. This kind of linker (Tab. 3.7) has been used with thioethers [108], sulfoxides [109], sulfones [110], sulfonic acids and their corresponding derivatives [111]. Because carbon-sulfur bonds can be cleaved under very mild conditions, some linkers have been based on this effect. They can be cleaved under reductive conditions [112, 113], photolytic conditions [114, 115] or with strong bases [116]. Various safety catch linkers have been developed based on the fact that thiols can be oxidized to sulfoxides and sulfones [112, 113].

Stannane based linkers (Tab. 3.8) are used for the Stille reaction (see below, section 3.3.2.1) on solid supports [119]. Nicolaou et al. developed polymer-bound alkenylstannanes to obtain the natural product (*S*)-zearalenone by an intramolecular Stille reaction and a cyclative cleavage [120].

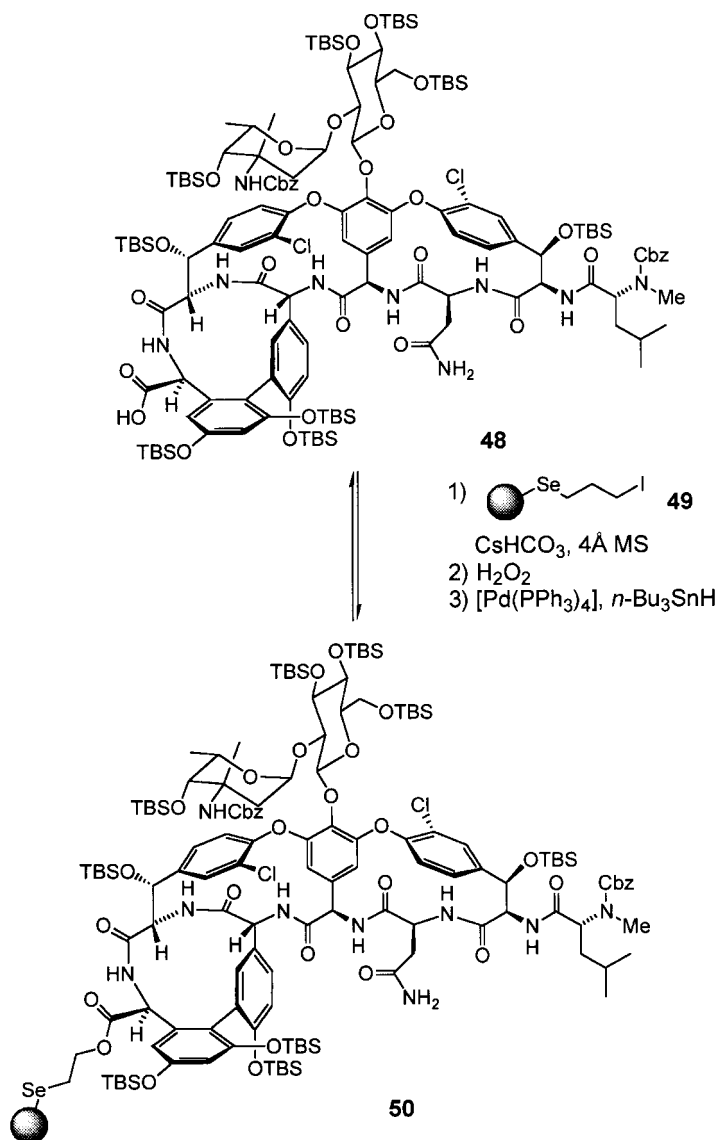
Tab. 3.7 Overview of sulfur linkers.

Structure	Structures achievable
<p>43</p>	Amides [117]
<p>44</p>	Carboxylic acids [118]
<p>45</p>	Linker for sterically hindered ketones [61]
<p>46</p>	Benzofurans: cleavage with bases [116]

Tab. 3.8 Stannane-based linker.

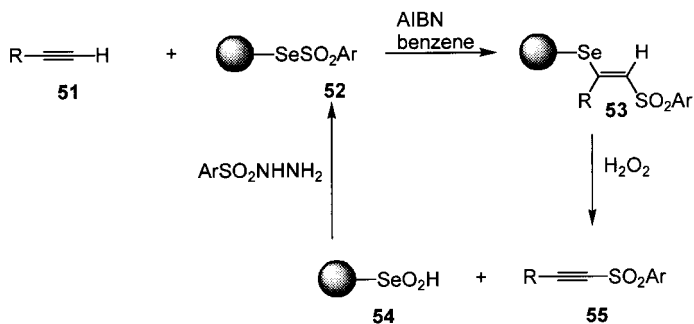
Structure	Structures achievable
<p>47</p>	Alkenes: cleavage with oxidants [120]





**Scheme 3.2** Solid-phase semi synthesis of Vancomycin (**48**) based on a new selenium linker [123, 124].

The preparation of solid-supported selenium resins and their application as linkers and reagents for solid-phase synthesis have been described [121, 122]. These reagents have proven to be useful for applications in solid-phase and combinatorial synthesis because of their versatility and ease of handling.



**Scheme 3.3** Polystyrene-supported selenosulfonates by Huang et al. [126].

**Tab. 3.9** Selenium-based linker.

Structure	Structures achievable
<p>56</p>	Alkenes [125]
<p>57</p>	Alkanes, alkenes [121, 122]

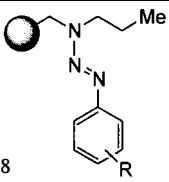
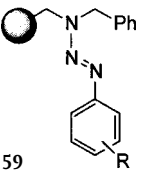
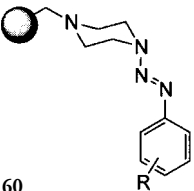
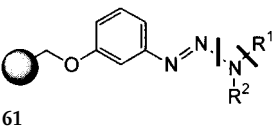
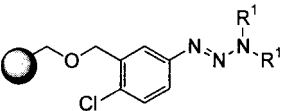
Recently, the semi-synthesis of Vancomycin (**48**) on solid supports was accomplished using an allylic linker (Scheme 3.2) [123, 124]. Polymer-bound chiral electrophilic selenium reagents have been developed and applied to stereoselective selenylation reactions of various alkenes (Tab. 3.9) [125].

The preparation of polystyrene-supported selenosulfonates and their application for the synthesis of acetylenic sulfones have been reported by Huang et al. (Scheme 3.3) [126].

#### 3.2.1.8 Triazene-Based Linkers

Triazenes are disguised diazonium ions which can be released under very mild acidic conditions. Inspired by the use of triazenes in natural product synthesis by Nicolaou et al. [127] and the pioneering work of Moore et al. [128, 129] and Tour et al. [130] in the synthesis of triazenes on a solid support and the final detachment to give iodoarenes, a whole set of triazene-based linkers has been developed (Tab. 3.10) [131]. The arene diazonium salts generated from the triazene linkers offer diverse opportunities for multifunctional cleavage. Two linkers based on tria-

Tab. 3.10 Overview of triazene-based linker.

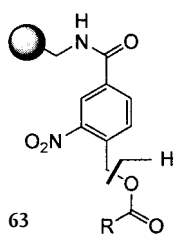
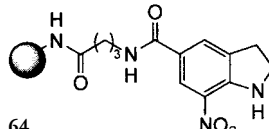
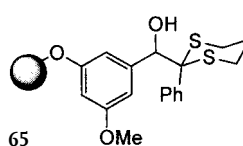
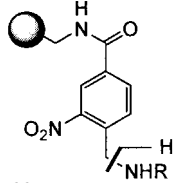
Structure	Structures achievable
 <p>58</p>	Iodoarenes [128]
 <p>59</p>	T1 resin: "traceless" linker [131–134], synthesis of phenols [135], biaryls, alkyl arenes [136, 137], azides [138], aromatic hydrazines, halides [cf. 128, 129, 139], ester, azo compounds, cinnolines [140], benzotriazoles [141]
 <p>60</p>	As above
 <p>61</p>	T2 resin: synthesis of substituted amines [142], amides (peptides) [143], (thio)ureas [143, 144], hydrazines, alcohols, esters [145, 146], guanidines [143], alkyl halides [145, 146], sulf-oximines
 <p>62</p>	T2* resin: as above [147, 148]; scavenger for amines and phenols

zene chemistry have been developed. While the T1 linker system (59) consists of 3,3-dialkyl-1-aryl triazenes bound to the support via the alkyl chain, the T2 linker family (61) is based on immobilized aryl diazonium salts. These diazonium-based linkers have been used to anchor primary and secondary amines. The resulting triazene moieties in the T1 and T2 linker are stable towards various chemical transformations and resist water, air and daylight.

## 3.2.1.9 Photocleavable Linkers

Photocleavable protecting groups have been used widely in carbohydrate chemistry, nucleotide and peptide synthesis. They have less frequently been used in the synthesis of small organic molecules. Photolytic cleavage offers a mild method of cleavage from the support, which is particularly attractive in combinatorial library screening. Although the original photo-labile supports have been employed in the peptide synthesis, their stability under acidic and basic conditions make them suitable for the synthesis of small organic molecule synthesis [149]. Rich and Gurwara developed the first photo-labile linker (**63**) (Tab. 3.11), which is an *o*-nitrobenzyl linker [150, 151]. Balasubramanian et al. described a new class of benzoin type photocleavable safety catch linkers (**65**) [152, 153].

Tab. 3.11 Photocleavable linkers.

Structure	Structures achievable
 <p><b>63</b></p>	Carboxylic acids [150]
 <p><b>64</b></p>	Carboxylic acids [154]
 <p><b>65</b></p>	Carboxylic acids [153]
 <p><b>66</b></p>	Amines [155]

Tab. 3.11 (cont.)

Structure	Structures achievable
<p>67</p>	Alcohols [156]
<p>68</p>	Methylarenes [157]

## 3.2.2

## Linker Strategies

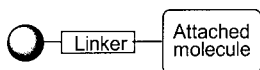
The proper choice of the solid support and the connected linker is important for the success of solid-phase organic synthesis. To date, the possibility of reactions on the resins have been limited by the number of linkers, because most of them were initially developed for peptide synthesis.

Usually, linkers are bifunctional molecules: one functionality is for connection to the solid support, and the other is a selective cleavable functional group. Because peptide synthesis was more or less the only application for solid-phase chemistry in its early days, most of the linkers were developed to supply amines or carboxylic acids after cleavage.

Nowadays, solid-phase synthesis has been used as a powerful tool in organic chemistry, especially to prepare small molecule libraries. New linkers to obtain different functionalities after cleavage have been developed. There are different linker strategies (Fig. 3.2), for example traceless linkers, multifunctional linkers, safety catch linkers, fragmentation/ cycloreversion cleavage linkers, cyclization cleavage linkers, which are useful methods for combinatorial solid-phase chemistry.

## 3.2.2.1 Safety Catch Linkers

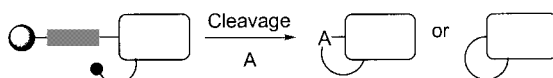
Among the successful linker strategies that are being developed specifically for solid-supported synthesis of small organic molecules, the safety catch principle has become one of the most important approaches. Safety catch linker strategies



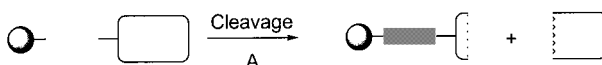
'Safety catch' linkers:



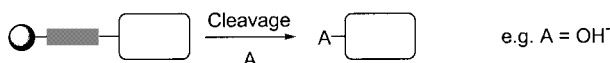
Cyclization-cleavage linkers:



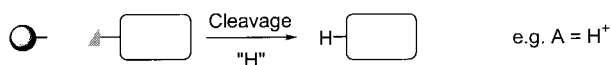
Fragmentation/ Cycloreversion-cleavage linkers:



Monofunctional linkers:



Traceless linkers:



Multifunctional linkers:

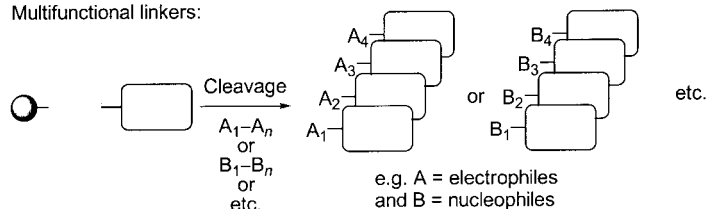


Fig. 3.2 Linker strategies for solid-phase chemistry [146].

in which a stable linkage is activated for cleavage by a discrete chemical modification have proven to be useful, because they are often compatible with a broad range of reactions (Table 3.12). The concept of safety catch linkers has been widely explored since the development of the sulfonamide linker (**69**) by Kenner et al. [158] The revision of the Kenner linker [159–162] and the development of novel types [163–166] is still a continuing process.

Tab. 3.12 Safety catch linkers.

Structure	Structures achievable
<p>69</p> <p>methylation</p>	Amides, carboxylic acids, hydrazides [158]
<p>70</p> <p>methylation</p>	Amides, Peptides [117, 167]
<p>71</p> <p>oxidation</p>	Amines [168]
<p>72</p> <p>reduction</p>	Esters [169]
<p>73</p> <p>deprotection</p>	Nucleic acids [170]

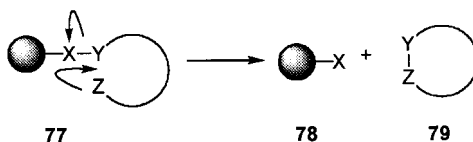
Tab. 3.12 (cont.)

Structure	Structures achievable
<p>74</p>	Alcohols; cleavage with enzymes [72]
<p>75</p>	Diketopiperazines [171]
<p>76</p>	Benzofurans; cleavage with bases [116]

### 3.2.2.2 Cyclative Cleavage (Cyclorelease Strategy)

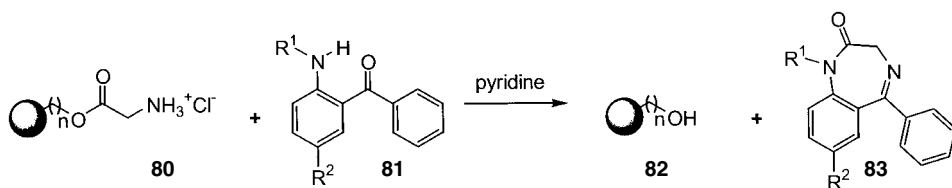
Cyclative-cleavage strategy is a process in which activation promotes the cleavage, while an intramolecularly located nucleophile, electrophile, radical or another group attacks, so that the product is released from the solid support (Scheme 3.4).

Therefore it has to be distinguished from traceless-cleavage. As the intramolecular step is in general faster than any intermolecular step, this strategy provides an additional purification step, because only cyclized structures are detached from the resin. The method of cyclative cleavage by nucleophilic displacement has been



**Scheme 3.4** General strategy for cyclative cleavage.





**Scheme 3.5** Synthesis of 1,4-benzodiazepin-2-ones (**83**) by cyclative cleavage [172].

frequently used since the synthesis of benzodiazepines was disclosed by Camps et al. in 1974 (Scheme 3.5) [172].

Since then this method has been used for the development of synthetic strategies for many kinds of heterocycles, such as hydantoins [173, 174] or diketopiperazines [175] as well as natural products [120] cyclic peptides [176] and macrocyclic lactones [108].

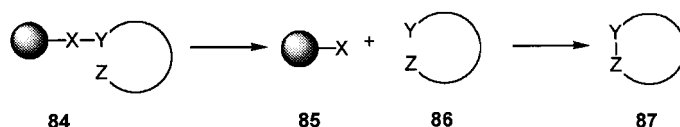
Besides nucleophilic attack, cyclative cleavage can be effected for example by Stille reactions [120], Wittig olefination reactions [177], Wittig-Horner [178, 179] or metathesis reactions [180–183]. For more details of C-C-bond formation, see Section 3.3.2.

### 3.2.2.3 Cleavage-Cyclization Cases

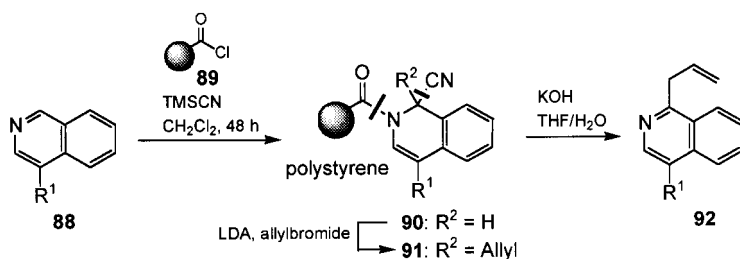
The cyclative-cleavage strategy is different to the cases in which the cyclization occurs in solution after the cleavage (Scheme 3.6). This is true for most acidic cleavage conditions: in these cases the uncyclized reactant is also found in the liquid-phase. Examples of this strategy are the synthesis of benzofurans [184], imidazoquinoxalinones [185, 186] and diketopiperazines [187].

### 3.2.2.4 Fragmentation Strategies

The fragmentation strategy is based on a similar concept to traceless solid-phase chemistry, like retrocycloaddition cleavage, cycloelimination or cyclofragmentation. These are synthetically useful reactions with wide scope for the construction of rigid templates of different ring sizes. Up to now only one example for the attachment of heteroatoms via addition/elimination strategy has been developed, by Kurth et al. (Scheme 3.7) [188, 189].



**Scheme 3.6** Cyclization after cleavage.



**Scheme 3.7** The addition/elimination strategy used by Kurth et al. [188].

### 3.2.2.5 Traceless Linkers

Solid-phase strategies associated with the construction of organic molecules and their functionalization are often limited by the nature of the anchoring group or the linker. Traceless linkers allow chemical transformations on the polymer bound molecules, which can be cleavage to the formation of a C-H bond on the seceding molecule and which enables the preparation of pure hydrocarbons (Table 3.13) [134, 190].

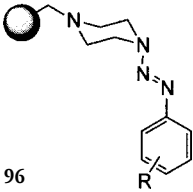
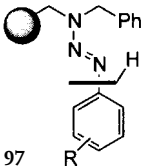
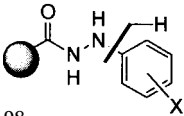
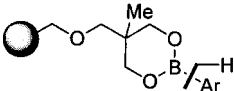
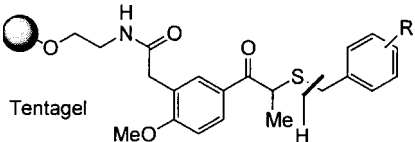
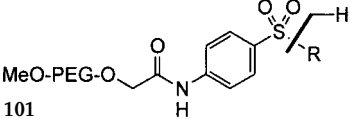
### 3.2.2.6 Multifunctional Cleavage

In contrast to traceless cleavage, which releases only hydrocarbon-like molecules, multifunctional cleavage provides additional diversity of functional compounds in

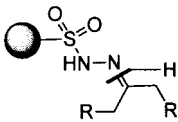
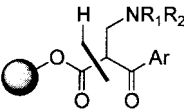
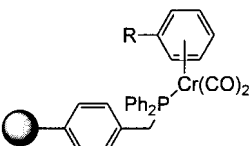
**Tab. 3.13** Traceless linkers.

Structure	Cleavage
<p>93</p>	Cleavage with fluoride; other dialkylsilyl-linker are known [75–77, 102, 103, 191], for arenes
<p>94</p>	Cleavage with TFA or bromine, for arenes [192, 193]
<p>95</p>	Cleavage with palladium/formate [194], other linkers [195] for arenes

Tab. 3.13 (cont.)

Structure	Cleavage
 <p>96</p>	T1 resin: cleavage with HCl/ THF, HSiCl <sub>3</sub> or DMF, for arenes [131–134]
 <p>97</p>	T1 resin: cleavage with HCl/THF or HSiCl <sub>3</sub> , for arenes [131]
 <p>98</p>	Cleavage for arenes [196]
 <p>99</p>	Cleavage by Ag <sup>+</sup> , for arenes [107]
 <p>Tentagel</p> <p>100</p>	Methylarenes: photolytic cleavage; other linkers for methylarenes [114, 115, 177]
 <p>MeO-PEG-O-CH<sub>2</sub>-C(=O)-NH-</p> <p>101</p>	Alkanes: cleavage with Na/Hg, other linkers for alkanes [112, 113, 120–122, 197]

Tab. 3.13 (cont.)

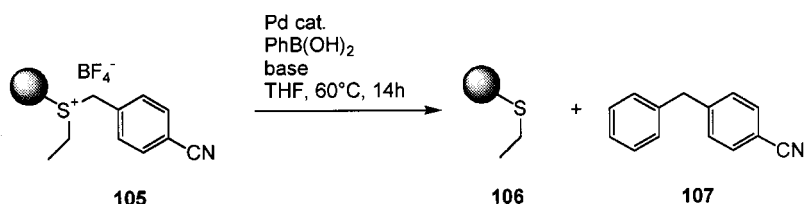
Structure	Cleavage
 <p>102</p>	Alkenes and alkanes: cleavage by reducing media or bases [198]
 <p>103</p>	Ketones: other linkers for carbonyl compounds [199, 200]
 <p>104</p>	Cleavage by oxidation [201]

a library. The number of new functionalities that it is possible to incorporate after cleavage, can multiply the number of compounds produced.

Examples for multifunctional cleavage are given by the use of sulfone-, silyl- or triazene-linkers [202]. Wagner et al. for example used a cleavage Suzuki reaction on a sulfonium-linker (**105**) (Scheme 3.8) [206].

### 3.2.2.7 Linkers for Asymmetric Synthesis

The search for new enantiopure molecules in industry have recently become more and more important especially in the pharmaceutical area. Until now there are only a few examples of asymmetric synthesis on solid supports. However, as the recovery of a polymer-supported chiral auxiliary by simple filtration techniques

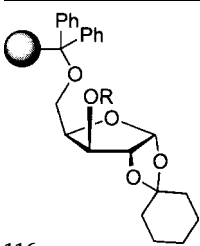
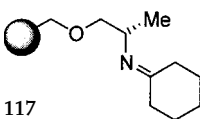
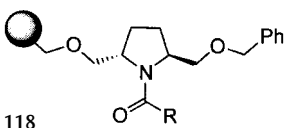
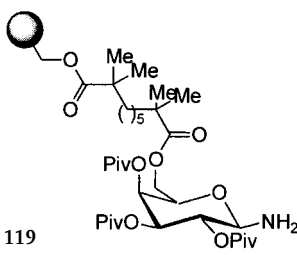
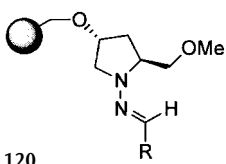
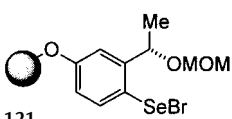
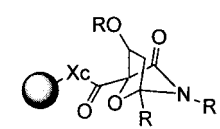


Scheme 3.8 Cleavage Suzuki reaction by Wagner et al. [206].

Tab. 3.14 Overview of multifunctional linkers.

Structure	Reaction for cleavage
<p>108</p>	Cross-metathesis [203]
<p>109</p>	Wittig reaction for the synthesis of alkenes [177]
<p>110</p>	Stille reaction (cross-coupling) for the synthesis of alkenes [120]
<p>111</p>	Nucleophile substitution of the T1 resin; synthesis of phenols, biaryls, alkyl arenes, azides, aromatic hydrazines, halides, ester, azo compounds; cinnolines, benzotriazoles [129–137, 140, 141]
<p>112</p>	Synthesis of alcohols, esters [134, 145, 146]
<p>113</p>	T2*-resin: as above [147]
<p>114</p>	Nucleophilic displacement, for the synthesis of Amines, thiols, halides, azides, acetates [204, 205] Other sulfur linker give alkenes by cleavage with palladium catalyst [206, 207] or heterocycles by cleavage with nucleophiles [208]
<p>115</p>	Metathesis cleavage gives alkenes [181, 206]

Tab. 3.15 Linkers for asymmetric synthesis.

Structure	Reaction
<p>116</p> 	Asymmetric synthesis of $\alpha$ -hydroxy acids [209, 210]
<p>117</p> 	Asymmetric $\alpha$ -alkylation of cyclohexanone [211, 212]
<p>118</p> 	Iodolactonisation of polymer-bound alkanes [213, 214]
<p>119</p> 	Stereoselective Ugi four-component condensation [215]
<p>120</p> 	Asymmetric synthesis of $\alpha$ -branched primary amines [216]
<p>121</p> 	Selenylation of alkenes [125]
<p>122</p> 	Diastereofacially selective 1,3-dipolar cycloaddition [217]

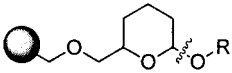
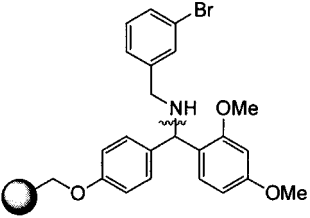
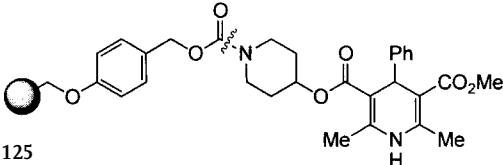
is a viable method, its recycling through the reaction sequence and the diversity of many reactions are clear advantages over solution-phase chemistry. The polymer-bound auxiliaries can be used in asymmetric synthesis including enolate alkylation chemistry, multicomponent reactions, cycloaddition and nucleophilic addition to carbon-heteroatom double bonds. For a review see Ref. [4].

### 3.2.3

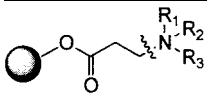
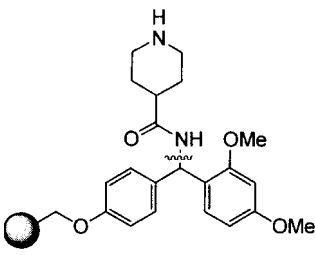
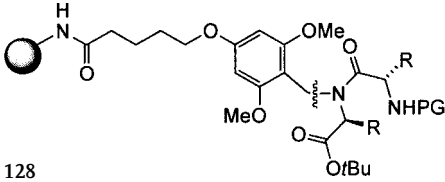
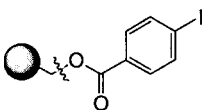
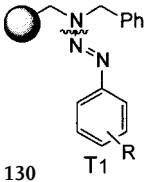
#### Linkers for Functional Groups

The requirement for diverse compound libraries by means of solid-phase synthesis led to the development of linkers for most functional groups found in organic synthesis. The number of linkers developed for a specific group also reflects the distribution of pharmacophoric groups present in natural products and other bioactive compounds. Tab. 3.16 gives an overview of examples of linkers for different functional groups.

Tab. 3.16 Some linkers for different functionalities.

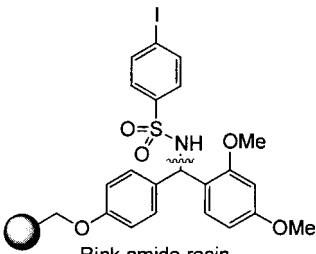
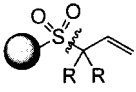
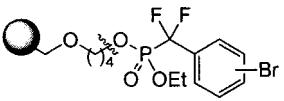
Structure	Linkers for different functional groups
 THP type linker 123	Alcohol [54, 218]
 Rink resin 124	Primary amine [27]
 125	Secondary amines [219]

Tab. 3.16 (cont.)

Structure	Linkers for different functional groups
 REM linker 126	Tertiary amines [220]
 Rink resin 127	Primary amides [221]
 128	Secondary amides [222]
 129	For carbonyl groups [70]
 130 T1	Diazonium salts and azides [138, 223]



Tab. 3.16 Some linkers for different functionalities.

Structure	Linkers for different functional groups
 <p>Rink amide resin</p> <p>131</p>	Sulfonamides [44]
 <p>132</p>	Alkenes [224]
 <p>NCPS</p> <p>133</p>	Phosphonates [225]

### 3.3

#### Organic Transformations on Polymeric Supports

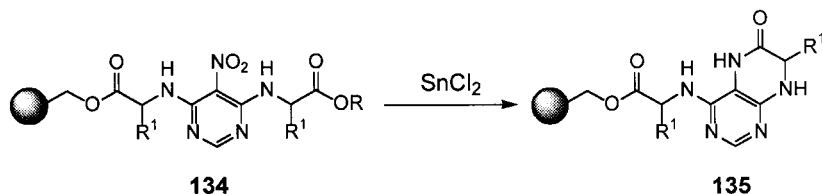
##### 3.3.1

##### Oxidation and Reduction Reactions

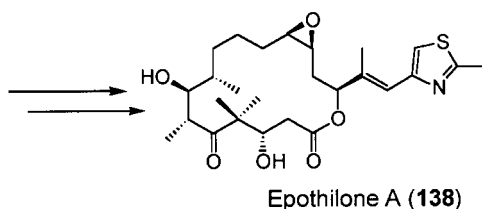
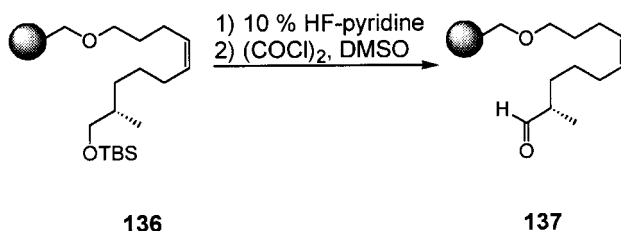
Oxidation and reduction reactions are very important processes in organic synthesis and they have been used for various transformations.

There are only few examples for oxidation reactions on solid supports, because most linkers or polymeric supports are sensitive towards some reagents suitable for classical transformations. Classical oxidation reagents are not soluble in most solvents used in the solid-phase organic synthesis step (but e.g. Scheme 3.10).

In contrast there are many examples for reduction processes on polymeric supports, because it is an especially useful transformation for aromatic nitro compounds in solid-phase chemistry. The reaction can be divided into two general classes: polymer-bound substrates and polymer-bound oxidant- and reductant-reagents.



**Scheme 3.9** Example of reduction in solid-phase for the synthesis of bicyclic pyrimidine (**135**) derivatives [236].



**Scheme 3.10** Oxidation step for the solid-phase synthesis of Epothilone A (**138**) [181].

However, oxidation processes like epoxidation or dihydroxylation reactions are important transformations in solid support chemistry, because they allow the synthesis of ketones [226], aldehydes [227, 228] and even sulfoxides and sulfones [229].

Reduction is used for carbonyl functionalities [71, 230] such as thioesters [231], amides [232], and carbamates [233], as well as for sulfur [234] and selenium [122] compounds. Recently, the synthesis of a potential carbohydrate vaccine is described via an reduction-oxidation sequence [235]. An efficient solid-phase synthesis of pyrimidine derivatives that involved reduction of the corresponding nitro derivatives was developed by Makara et al. in 2001 (Scheme 3.9) [236].

### 3.3.2

#### C-C Bond Formation Reactions

The formation of C-C bonds is of great importance for the synthesis of nonpeptidic small molecules. For this, there is an increasing interest in the development of solid-phase methodology for this kind of transformation. Well-known liquid-phase reactions have been successfully transferred to solid-supported chemistry.

### 3.3.2.1 Palladium-Catalyzed Reactions

Palladium-catalyzed coupling reactions are very efficient for the introduction of new carbon-carbon bonds onto molecules attached to solid support. The mild reaction conditions and compatibility with a broad range of functionalities and high reaction yields, have made this kind of transformation a very common tool for the combinatorial synthesis of small organic molecules. The literature for synthetic methods of palladium-catalyzed reactions on solid supports has recently been reviewed [237–239].

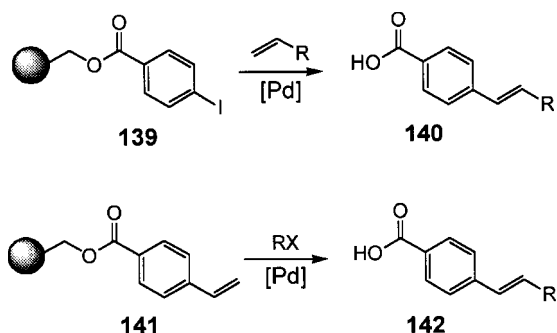
#### Heck reactions

C-C bond formation using the Heck reaction allows the introduction of functional groups to obtain new organic structures on solid supports. This reaction between an alkene with an alkenyl or an aryl halide has been widely employed in various intra- and inter-molecular versions on solid-phase because of the readily accessibility of starting materials. The Heck reaction was performed on immobilized aryl or alkenyl halides with soluble alkenes and vice versa (Scheme 3.11).

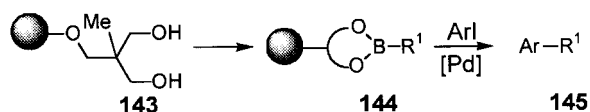
The intramolecular Heck reaction is useful for the construction of complex natural products [241] and for the synthesis of indoles [242] benzofurans [243] quinolines [244] and benzazepines [245].

#### Suzuki reactions

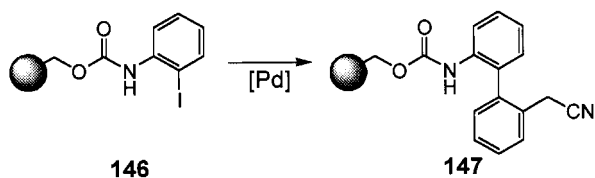
The palladium-catalyzed coupling of boronic acids with aryl and alkenyl halides, the Suzuki reaction, is one of the most efficient C-C cross-coupling processes used in reactions on polymeric supports. These coupling reactions requires only gentle heating to 60–80 °C and the boronic acids used are nontoxic and stable towards air and water. The mild reaction conditions have made this reaction a powerful and widely used tool in the organic synthesis. When the Suzuki reaction is transferred to a solid support, the boronic acid can be immobilized or used as a liquid reactant. Carboni and Carreaux recently reported the preparation of the macroporous support that can be employed to efficiently immobilize and transform functionalized arylboronic acids (Scheme 3.12) [107, 246, 247].



**Scheme 3.11** Heck reactions in solid-phase synthesis [240].



**Scheme 3.12** Solid supported boronic acids (144) as reagents for Suzuki couplings [107].



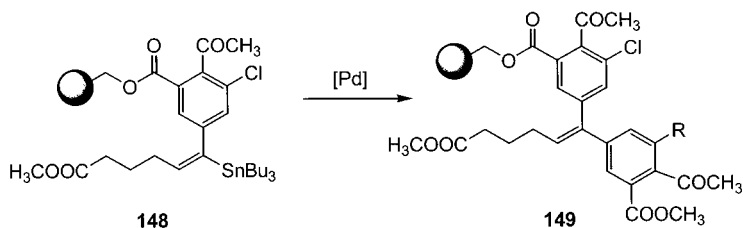
**Scheme 3.13** Solid-phase synthesis of biaryls (147) [249].

Solid-phase Suzuki reaction was first used in the preparation of biaryls [248]. One recent example is given by Baudoin et al. for the synthesis of biologically active biaryl compounds (Scheme 3.13) [249].

Recently, this methodology has been extended to the coupling of alkyl, allylic, 1-alkenyl and 1-alkynyl halides with 1-alkenyl and even alkyl boron reagents.

### Stille reactions

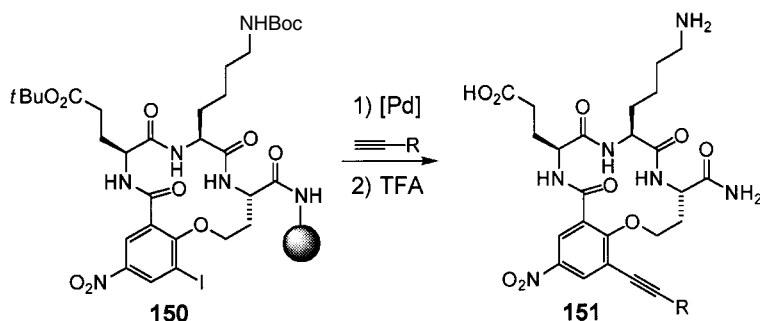
One of the first cross-coupling reactions performed on solid supports was the Stille reaction [250] which is a palladium-catalyzed reaction of a trialkylaryl or trialkylalkenyl stannane with an aromatic iodide, bromide or triflate. In contrast to the process in liquid-phase, the organotin reagent is easily removed from the solid-phase because of the subsequent washing processes. Immobilized aryl halides have been frequently coupled with aryl and alkenylstannanes, whereas stannanes attached to the solid support have been used less frequently for the Stille reaction. An example is the synthesis of a benzodiazepine library by Ellman et al. Recently, a Stille cross-coupling reaction has been employed in the synthesis of alkenyldiarylmethanes (ADAM) series of non-nucleoside HIV-1 Reverse Transcriptase Inhibitors (Scheme 3.14) [251].



**Scheme 3.14** Synthesis of ADAM by a Stille reaction [251].

**Sonogashira reactions**

The palladium-catalyzed arylation and alkenylation of terminal alkynes with aryl or alkenyl halides in presence of a copper(I) co-catalyst is called Sonogashira reaction. In the same way as in the other cross-coupling reactions described before, it is possible to immobilize the alkyne or the aromatic bromides, iodides or triflates on solid supports (Scheme 3.15).



**Scheme 3.15** Structural diversity in macrocyclic systems (**150**) via Sonogashira reaction [252].

This reaction and some variations have been successfully used for the synthesis of heterocycles as indoles [253] or for the preparation of precursors necessary for the synthesis of cinnolines by Richter reaction [140] as mentioned in Section 3.4.2.1.

**Other cross coupling reactions**

For purposes of completeness, palladium-catalyzed reactions for the synthesis of biaryls using zincates and arylhalides (Negishi Couplings) [254] or using silicon compounds [255, 256] need to be mentioned.

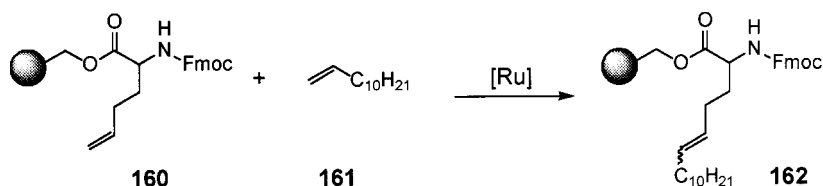
**3.3.2.2 Grignard and Similar Reactions**

Grignard reaction and similar transformations allow C-C bond formation without a palladium catalyst. Grignard reagents and organolithium compounds are very versatile carbanion sources used in the synthesis of acyclic, heterocyclic and carbocyclic compounds. The esters, ketones and aldehydes are more stable when the reaction takes place on solid supports than in the liquid-phase, because this immobilized components are not so sensitive towards water or oxygen. In the total synthesis of (S)-zearelenone (**155**) on solid supports the Grignard reaction is one of the key steps (Scheme 3.16) [120].

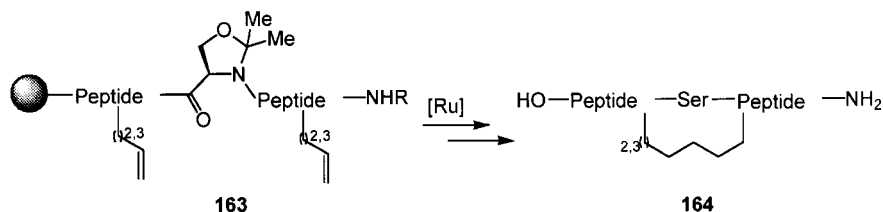
**3.3.2.3 Michael Reactions and 1,2-Addition Reactions**

The Michael addition has attracted enormous attention as one of the most important C-C bond-forming reactions in solution-phase organic synthesis. In general,





**Scheme 3.19** Linear cross-metathesis of unsaturated  $\alpha$ -amino acid derivatives [262].



**Scheme 3.20** Peptides (**164**) prepared by ring closing metathesis (RCM) in solid-phase [264].

tathesis, the linear elongation of an alkene (Scheme 3.19), the ring closing (RCM) and ring opening (ROM) metathesis.

The ring closing metathesis is used for the synthesis of heterocycles [263], analogs of peptides (Scheme 3.20) [264] and natural [181] in solid-phase organic chemistry.

The combination of ring opening and ring closing metathesis is used for the synthesis of polycyclic structures by Lee et al. [265]. The metathesis on solid-phase includes not only the chemical transformation of resin bound intermediates but as well as the cleavage of final products from the support [181].

### 3.3.3

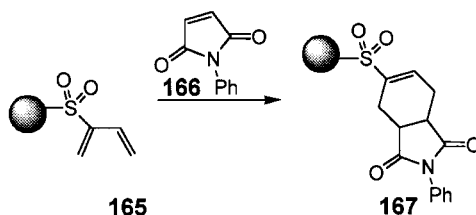
#### Cycloaddition Reactions

Isocyclic and heterocyclic compounds are very often synthesized by cycloaddition reactions. The most widespread reactions are the Diels-Alder reaction and the 1,3-dipolar cycloaddition.

##### 3.3.3.1 Diels-Alder Reactions

The Diels-Alder reaction is a [4+2]-cycloaddition to synthesize six-membered rings. It is a well-known reaction in combinatorial chemistry and there have been many examples in which this reaction has been described in solid-phase synthesis [266]. In solid-phase organic synthesis it is possible to immobilize the diene (Scheme 3.21) [267] or the dienophile [268].

Intramolecular Diels-Alder reactions have been widely used to prepare cyclic compounds [269].

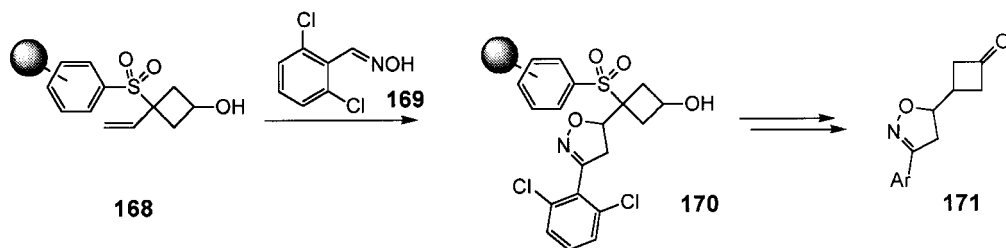


**Scheme 3.21** Diels-Alder cycloaddition for the synthesis of tetrahydroisindole (**167**) derivatives [267].

### 3.3.3.2 1,3-Dipolar Cycloaddition Reactions

The 1,3-dipolar cycloaddition reactions ([3+2]) are often used to synthesize five member aza- or azoxaheterocycles. Depending on the nature of the 1,3-dipoles employed in the transformation, different types of heterocycles such as isoxazoles [270], isoxazolines (Scheme 3.22) [110], hydantoins [271], pyrrolidines [272], indolizines [273] or pyrazoles [274] are obtained.

In addition to these reactions, less common cycloaddition reaction types like [2+2] [275] or [6+3] [276] cycloaddition have been employed for the ring formation on solid supports.

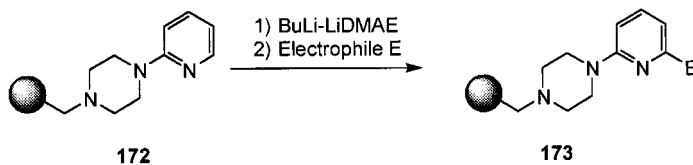


**Scheme 3.22** 1,3-Dipolar cycloaddition step for the solid-phase synthesis of isoxazolocyclobutanones (**171**) [110].

### 3.3.4

#### Organometallic Chemistry on Polymeric Supports

The organometallic reagents are very useful in solid-phase organic synthesis, as described in Section 3.3.2. Metal complexes [277] have found application too, as



**Scheme 3.23** Lithiation of pyridine derivatives (**172**) on a polymeric support [279].



linkers [201] and as cleavage reagents [107]. But the most important and most frequent use of metal complexes on solid supports is catalysis [278].

Asymmetric organocatalysis in solid-phase chemistry has been recently reviewed [280].

### 3.3.5

#### Multicomponent Reactions

The multicomponent reactions have been widely used in solid and solution-phase chemistry during the last years. Multicomponent reaction strategies offer significant advantages compared with conventional linear type syntheses. Three or more reactants come together in a one pot reaction to form new products that contain portions of all the components [281]. There are several well-known multicomponent reactions that have been used in combinatorial chemistry.

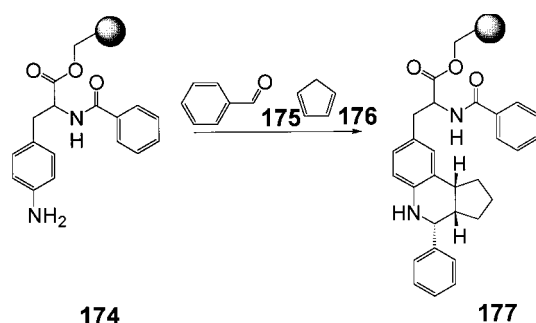
##### 3.3.5.1 Grieco Reactions

The Grieco reaction is a three component condensation of anilines, aldehydes and electron rich alkenes to form six-membered nitrogen-containing heterocycles. Kiseljov et al. for example synthesized a library of tetrahydroquinolines using this synthetic pathway (Scheme 3.24) [282].

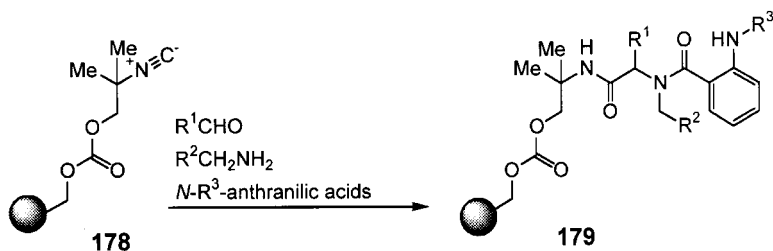
For the Grieco three component reaction it is also possible to connect the aldehyde [283] or the alkene [284] to the solid support.

##### 3.3.5.2 Ugi Reactions

The four component Ugi reaction is a condensation between a carboxylic acid, a ketone or an aldehyde, an amine and an isonitrile. Basically each of the reaction components can be attached to the resin. The Ugi reaction is employed for the synthesis of small molecule combinatorial libraries on solid supports. Recently a novel resin bound isonitrile has been used in the Ugi multicomponent reaction for synthesizing diversity libraries of diketopiperazines and benzodiazepindiones (Scheme 3.25) [285].



**Scheme 3.24** Grieco three-component reaction for the synthesis of tetrahydroisoquinolines (**177**) [282].



**Scheme 3.25** Ugi multicomponent reaction to form intermediates (**179**) for the synthesis of benzodiazepinediones [285].

### 3.3.6

#### Mannich Reactions

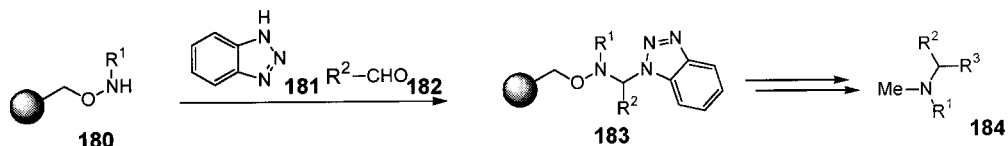
The Mannich reaction is a three component reaction in which an imine, that was formed from the condensation of an amine with an aldehyde, reacts with a component containing at least one hydrogen atom of pronounced reactivity. It is possible to immobilize every Mannich partner on solid supports. In combinatorial chemistry the Mannich reaction has been used for the generation of different libraries (Scheme 3.26).

##### 3.3.6.1 Hantzsch Reactions

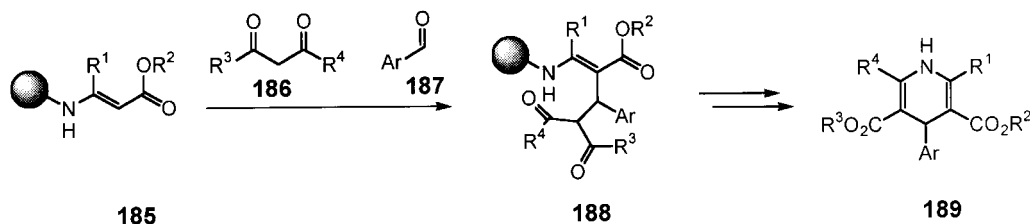
The Hantzsch reaction that allows the synthesis of pyridine derivatives, is a condensation involving two equivalents of a  $\beta$ -ketoester or a  $\beta$ -ketoamide, one equivalent of an aldehyde and ammonia. The Hantzsch reaction was used by Patel et al. for the synthesis of a 300 member dihydropyridine library (Scheme 3.27) [287].

##### 3.3.6.2 Biginelli Reactions

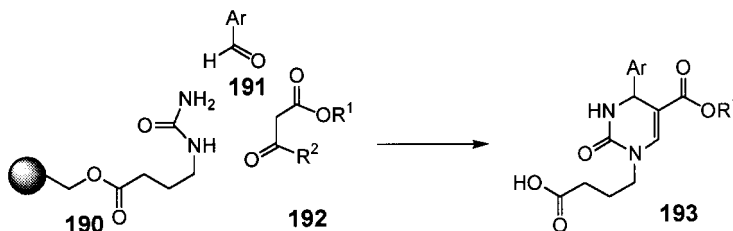
The Biginelli reaction is a cyclocondensation between ethylacetoacetate, an arylaldehyde and urea derivatives to obtain dihydropyrimidines. Transfer this reaction to the solid-phase chemistry, allow the preparation of libraries of this kind of products (Scheme 3.18) [288].



**Scheme 3.26** Intermediates synthesis for the synthesis of tertiary methylamines (**184**) via Mannich reaction [286].



**Scheme 3.27** Hantzsch reaction for the synthesis of dihydropyridine derivatives (**189**) [287].



**Scheme 3.28** Biginelli reaction to form dihydropyrimidines (**193**) [288].

### 3.4

#### Targets for Synthesis on Polymeric Supports

##### 3.4.1

##### Natural Products

Natural products have served as an important source for medical compounds and pharmaceutical leads over the last century. In fact, many approved therapeutics as well as drug candidates are derived from natural sources. Natural products play such a pivotal role in drug discovery because they offer a great diversity of chemical scaffolds for finding new lead compounds and can be considered as starting points for optimization programs. For this reason, there is now a great interest in the construction of structurally complex, natural products based libraries using solid-phase combinatorial synthesis techniques [289–291].

There are different strategies for making libraries wherein natural products skeletons have been constructed or immobilized on solid supports and subsequently derivatized:

1. Solid-phase target-oriented total synthesis of natural products;
2. Combinatorial derivatization for immobilized natural product skeletons;
3. Construction of natural product like libraries;
4. Adaptation of new synthetic methods for the solid-phase synthesis of combinatorial libraries.

## 3.4.1.1 Solid-phase Target-Oriented Total Synthesis of Natural Products

In the past few years the total synthesis of a number of quite complex natural products with many different structures have been achieved on solid supports (Fig. 3.3), for example Verrucine A and B (**195**, **196**) [292], Trypostatin B (**197**) [97] Epothilone A (**198**) [181] Deglycobleomycin A<sub>5</sub> (**194**) [293] and Oscillamide Y (**199**) [294].

The selenium linker has been used as starting point for a library of natural products and medicinal relevant molecules by Nicolaou et al. (Scheme 3.29) [295, 296].

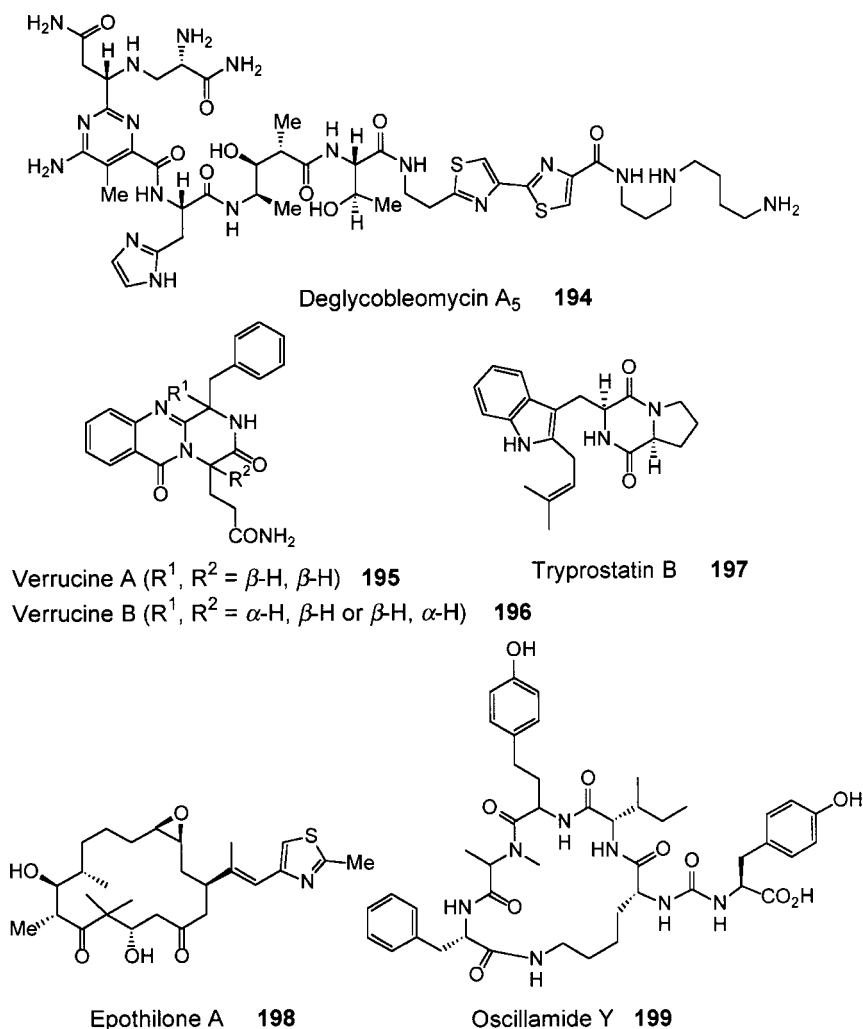
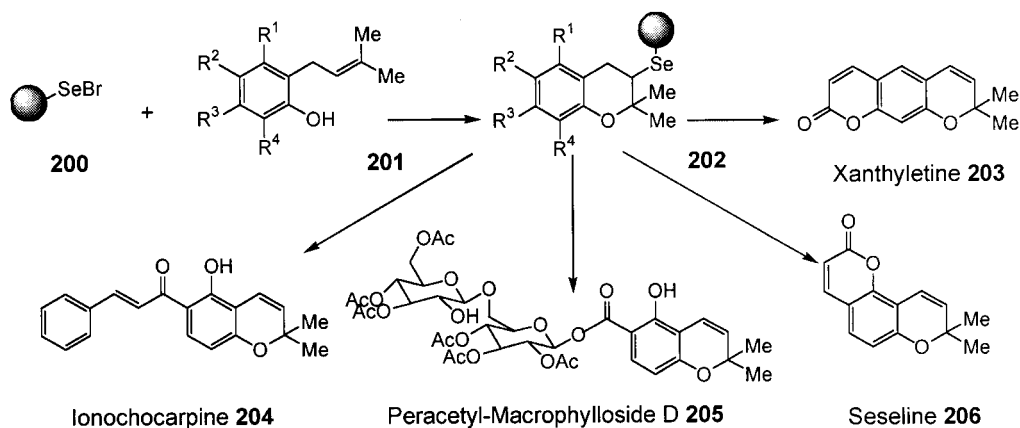


Fig. 3.3 Some natural products synthesized on polymeric supports.



**Scheme 3.29** The selenium linker (**200**) in the synthesis of benzopyran systems by Nicolaou et al. [295].

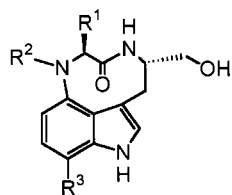
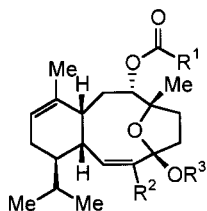
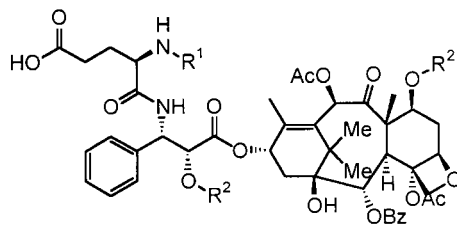
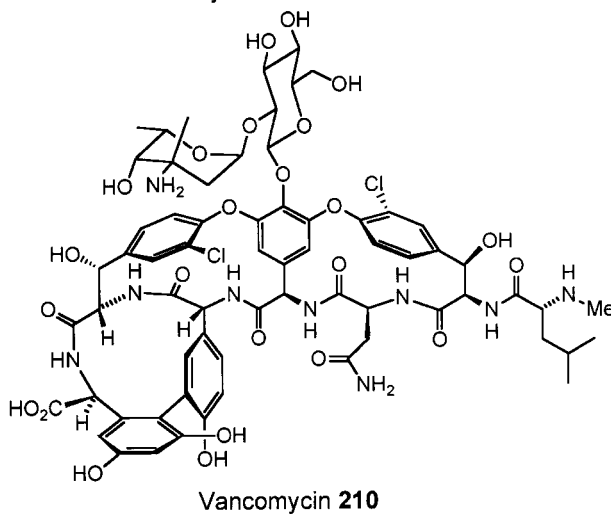
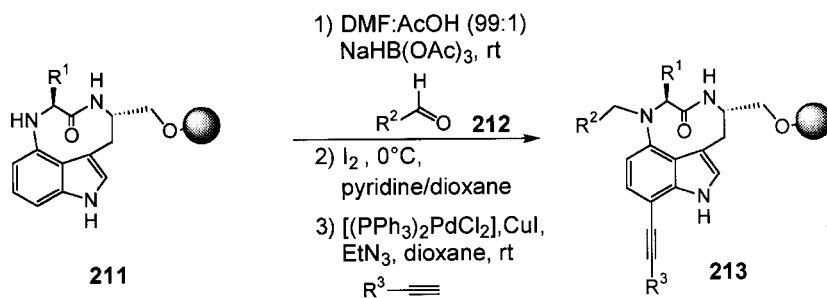
#### 3.4.1.2 Combinatorial Derivatization for Immobilized Natural Product Skeletons and Combinatorial Semi-synthesis

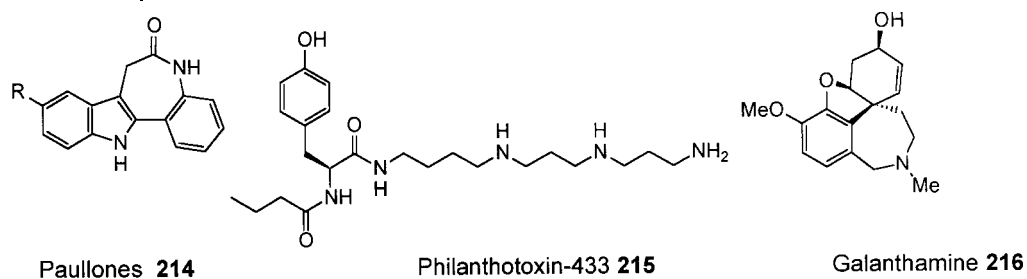
In this approach, the natural product skeleton is immobilized on the solid support to create libraries of analogs by introducing diversity. This strategy allows the generation of libraries, that can be useful for the high throughput screening in new drug developments. The advantage of this approach is based on the use of the preformed skeleton of the natural product that might be too complex to be synthesized on solid supports with the techniques now available.

Some research groups have derivatized biological active and very important natural products (Scheme 3.30) like Indolactam V (**207**) [297], Sarcodictyin (**208**) [298] Taxol (**209**) [299] and Vancomycin (**210**) [123]. For example, the solid-phase synthesis of Indolactam derivatives (**213**) with three points of diversity has been reported by Waldmann et al. in 1999 (Scheme 3.31) [297].

#### 3.4.1.3 Construction of Natural Product-Like Libraries

Because isolation of most of the natural products that are useful for industry is expensive, there is an increased need for new solid combinatorial synthesis to construct libraries of natural product-like compounds. A new strategy for the construction of these libraries was introduced by Nicolaou et al. [300], using the concept of privileged structures, a term originally introduced to describe structural motifs capable of interacting with a variety of unrelated molecular targets. Recently the synthesis of libraries of analogs for medicinal chemistry has been reported. For example the synthesis of biologically active biaryl lactams like Paulonones (**214**) [249] Philanthotoxin (**215**) analogs [301] and Galanthamine (**216**) like molecules [302] have been developed (Scheme 3.32).

Indolactam derivatives **207**Sarcodictyin derivatives **208**Taxol derivatives **209**Vancomycin **210****Scheme 3.30** Derivatives of natural product skeletons and combinatorial semi-synthesis products.**Scheme 3.31** Solid-phase synthesis of Indolactam derivatives (**213**) [297].



**Scheme 3.32** Prototypical structures for the synthesis of natural product-like libraries.

### 3.4.2

#### Adaptation of New Synthetic Methods for the Solid-phase Synthesis of Combinatorial Libraries

Finally the adaptation of newly discovered solution-phase methodologies for combinatorial use on solid supports needs to be described. As seen in Section 3.3, well-known liquid-phase reactions can also be employed in solid-phase for the generation of natural and natural like products [181, 241, 249, 252].

##### 3.4.2.1 Heterocycles

At first, combinatorial chemistry focused on peptide and nucleotide libraries synthesis, but because poor pharmacokinetical properties cause poor oral availability of this kind of molecule, there is increasing interest in the development of new methods to prepare small, drug-like molecules which obey Lipinski's rule of five [303]. Heterocyclic compounds can offer a high degree of structural diversity and have proven to be useful as therapeutic agents. For these, there are recent advances in the preparation of heterocycles on solid supports [304]. The examples reported in this section are organized by their ring size.

##### Three-membered heterocycles

There are only a few syntheses of three-membered heterocycles (Fig. 3.4) reported in solid-phase chemistry. Filigheddu et al. [305] described the synthesis of aziridines (**223**) (Scheme 3.33), which are important heterocycles in organic and medicinal chemistry.

##### Four-membered heterocycles

Although four-membered rings are highly strained and not very stable heterocycles, there are some examples (Fig. 3.5) for the preparation of heterocycles of this type on solid supports. Different  $\beta$ -lactams (**229–230**) have been synthesized employing different synthetic pathways [133, 275, 306–309] such as the addition of ketenes (Scheme 3.34) [306], or ester enolates to imines [133]. Also the synthesis of four-membered rings with two heteroatoms has been reported [310].

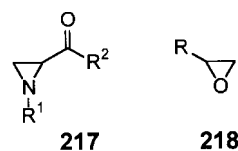
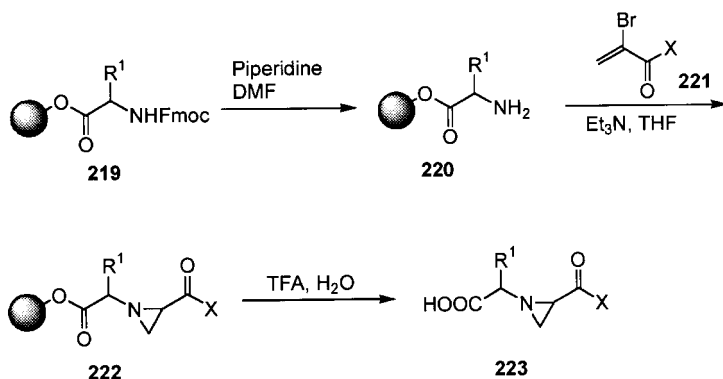


Fig. 3.4 Three-membered heterocycles obtained by solid-phase chemistry



Scheme 3.3 Solid-phase synthesis of aziridines (**223**) by Filigheddu et al. [305].

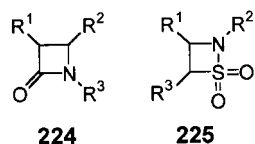


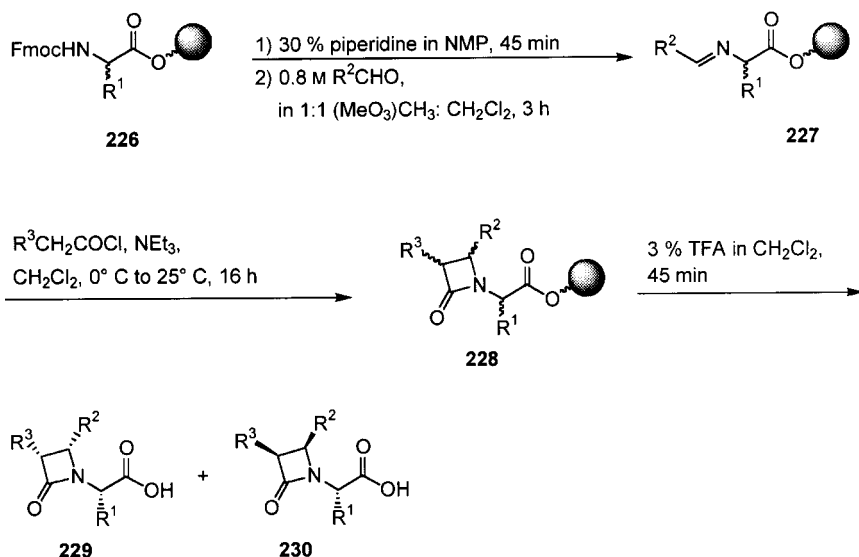
Fig. 3.5 Four-membered heterocycles obtained by solid-phase chemistry.

### Five-membered heterocycles

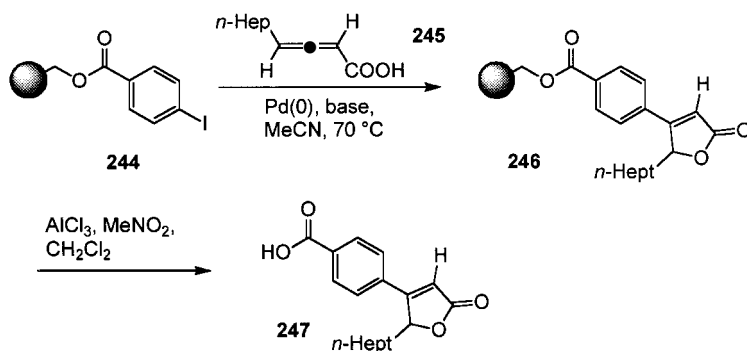
The preparation of five-membered rings in solid-phase organic chemistry has been reported in several publications. Versatile syntheses of these heterocycles with different numbers and kinds of heteroatoms have been described. The synthesis of five-membered rings containing one nitrogen atom (Fig. 3.6) as pyrrolidines (**231**) [311–316] pyrroles (**232**) [317–320] pyrrolidinones (**233**) [321–323] pyrrolinones (**234**) [324–326] 2,5-pyrrolidinediones (**235**) [327–329] 2,4-pyrrolidinediones (**236**) [330–332] 2,5-pyrrolinediones (**237**) [333] or heterocycles with one oxygen or one sulfur atom like tetrahydrofurans (**238**) [334–336] 2,5-dihydrofurans (**239**) [337], furans (**240**) [338, 339],  $\beta$ -lactones (**241**) [340–343], 2,5-dihydrofuranones (**242**) [344] (Scheme 3.35) and thiophenes (**243**) [345, 346] can be accomplished on solid supports.

In addition, solid-phase synthetic pathways to heterocycles with more than one heteroatom are very important.





Scheme 3.34 Polymer-supported synthesis of  $\beta$ -lactams (229–230) by Gallop et al. [306].



Scheme 3.35 Solid-phase synthesis of 2,5-dihydrofuranones (247) by Ma et al. [344].

For the heterocycles including two heteroatoms (Fig. 3.7), there are examples with two nitrogen atoms like pyrazoles (248) [347–349] pyrazolines (249) [350], pyrazolones (250) [351–353], hydantoin (251) [56, 354–356] (Scheme 3.36) and imidazoles (252) [357–360] or with one nitrogen and one oxygen like oxazoles (253) [361], isoxazoles (254) [45], isoxazolines (255) [362, 363], oxazolidines (256) [364], oxazolidinones (257) [365, 366] and isoxazolidines (258) [367] and with one nitrogen and one sulfur like thiazoles (259) [346, 368], thiazolidines (260) [369] and thiazolidinones (261) [370, 371].

Heterocycles containing three heteroatoms (Fig. 3.8), as triazoles (269) [372, 373], thiadiazoles (270) [374] and oxadiazoles (271) [375] have been described, too.

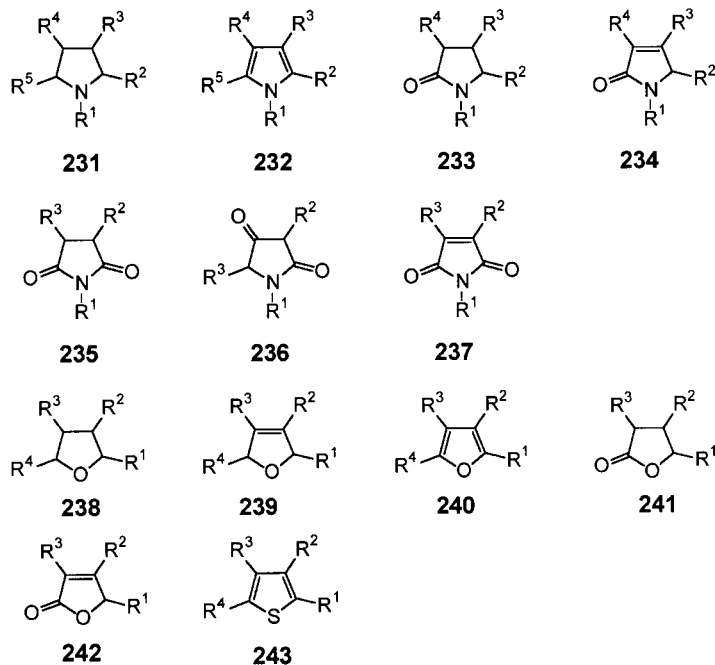


Fig. 3.6 Five-membered heterocycles with one heteroatom obtained by solid-phase chemistry.

### Six-membered heterocycles

As six-membered heterocycles are present in a number of natural products and biologically important molecules, solid-phase synthesis of these has been reported very often (Fig. 3.9). Solid-phase synthesis for nearly every six-membered ring including one nitrogen atom are known: piperidines (272) [376], tetrahydropyridines (273) [377, 378], dihydropyridines (274) [219, 379, 380], pyridines (275) [349, 381–386], (Scheme 3.37), piperidinones (276) [387], dihydropyridones (277–279) [313, 378, 388–390], pyridinones (280–281) [328, 329] and piperidindiones (282) [391] derivatives. In contrast, the synthesis of six-membered rings with one single oxygen is rarely described. Nevertheless, solid-phase synthesis of dihydropyrans (283–284) [392–394] and tetrahydropyrans (285) [335, 336] has been reported.

The synthesis of six-membered heterocycles with two nitrogen atoms like pyrimidines (292) [395–397], pyridazines (293) [398], pyrimidinones (294) [399, 400] dihydropyrimidines (295) [401], dihydropyrimidinediones (296) [402] ketopiperazines (297) [403–408], diketopiperazines (298) [409–416], piperazines (299) [417] have been covered in various publications. Diketomorpholines (300) [410, 412] and thiomorpholinones (301–302) [370, 418] are examples for six-membered heterocycles with one nitrogen and one oxygen or sulfur atom (Fig. 3.10).

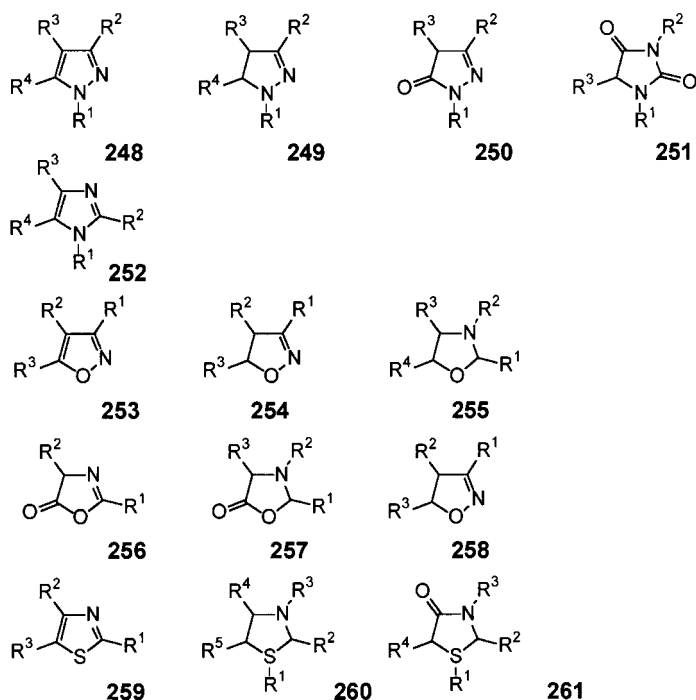
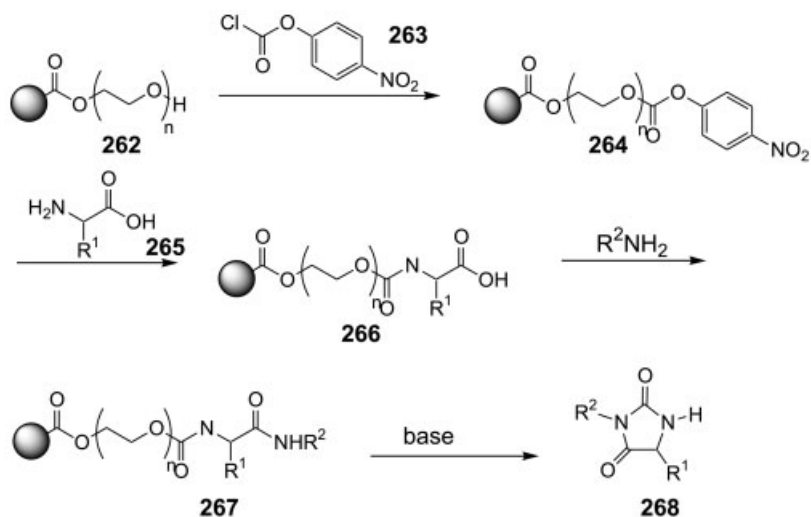


Fig. 3.7 Five-membered heterocycles with two heteroatoms obtained by solid-phase chemistry.



Scheme 3.36 Polymer-supported synthesis of hydantoin (**268**) by Frechet et al. [356].

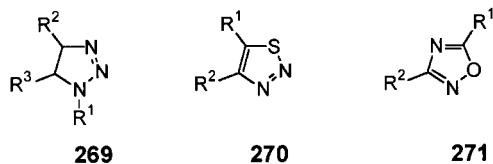


Fig. 3.8 Five-membered heterocycles with three heteroatoms obtained by solid-phase chemistry

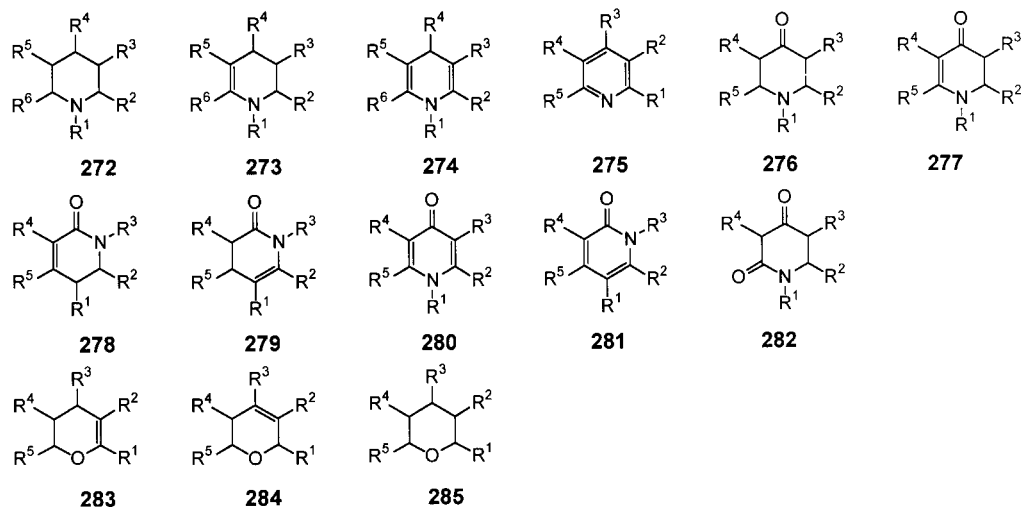
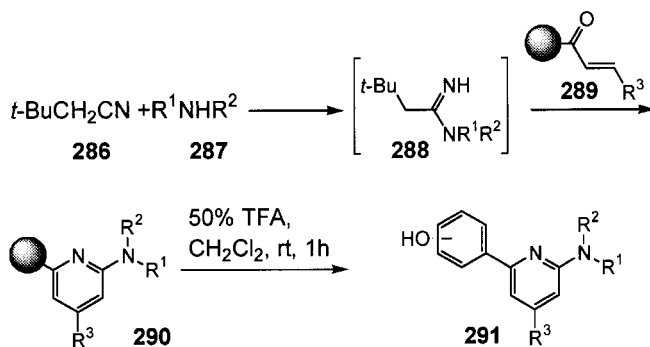


Fig. 3.9 Six-membered heterocycles with one heteroatom obtained by solid-phase chemistry.



Scheme 3.37 Solid-supported synthesis of diarylpyridines (**291**) by Katritzky et al [386].

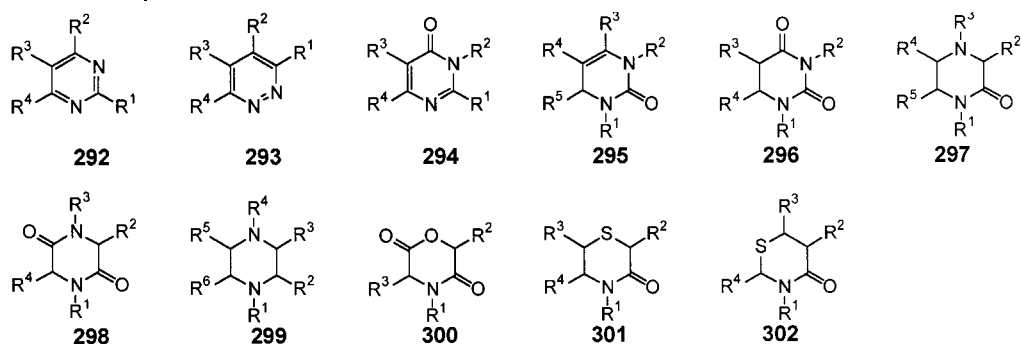


Fig. 3.10 Six-membered heterocycles with two heteroatoms obtained by solid-phase chemistry.

### Seven-membered heterocycles

The synthesis of seven-membered rings containing one or more heteroatoms has been described on solid supports (Fig. 3.11). This includes the synthesis of azepanes (**303**) [419], azepanones (**306**) [183, 420], tetrahydroazepinones (**305**) [180, 420], tetrahydroazepines (**304**) [421] perhydrodiazepinediones (**307**) [422, 423] and triazepanediones (**308**) (Scheme 3.38) [424].

### Benzoannulated nitrogen heterocycles

The recent impact of solid-phase synthesis on medically relevant benzoannulated nitrogen heterocycles has been recently reviewed [16], therefore in this section only recent publications are included. Benzoannulated heterocycles can be prepared efficiently through cyclization on solid supports employing classical heterocycle forming reactions such as the Fischer [425], the Bischler-Napieralski [426], Tsuge [427], Nenitzescu [428], and Richter [140] reactions. In addition, the

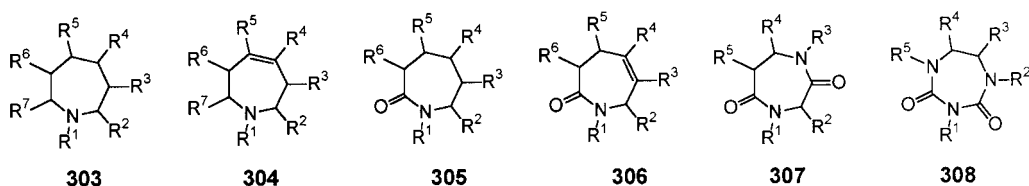
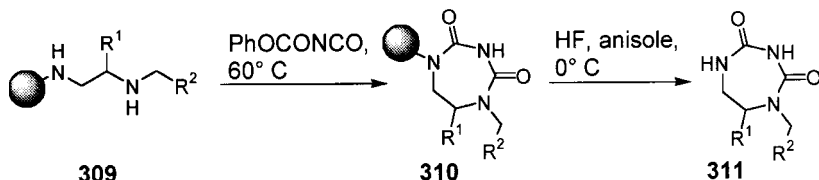


Fig. 3.11 Seven-membered heterocycles obtained by solid-phase chemistry.



Scheme 3.38 Solid-phase synthesis of triazepanediones (**311**) by Houghten et al. [424].

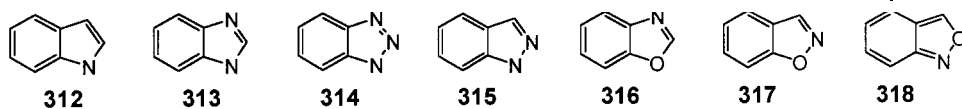
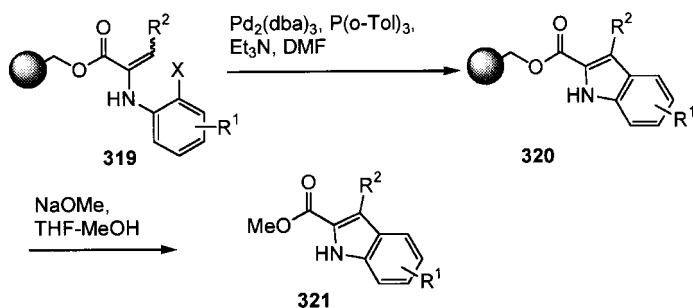


Fig. 3.12 Skeletons of five-membered benzoannulated nitrogen heterocycles.



Scheme 3.39 Polymer-supported synthesis of indoles (**321**) by Kondo et al. [430].

Heck [245, 429], Sonogashira [140] Wittig [177], Diels-Alder [263] and alkene metathesis reactions have been used.

Several five-membered benzoannulated heterocycles (Fig. 3.12) as indoles (**312**) [425, 430–432] (Scheme 3.39), benzimidazoles (**313**) [433–438], benzotriazoles (**314**) [141], indazoles (**315**) [439, 440], benzoxazoles (**316**) [441], isoxazoles (**317**) [442], and benzisoxazoles (**318**) [443] have been synthesized.

Six-membered heterocycles are part of many biologically interesting compounds (Fig. 3.13).

The solid-phase syntheses of quinolines (**322**) [283], isoquinolines (**323**) [444, 445], quinazolines (**324–325**) [446–448], cinnolines (**326**) [140], quinoxalines (**327**) (Scheme 3.40) [449–452], and benzothiazines (**328**) [453] have been reported.

There are many examples for seven-membered benzoannulated heterocycles that include benzazepines (**332**) [245, 454] benzothiazepines (**333**) [455, 456] and the very important pharmacological family of benzodiazepines (**334**) [285, 457, 458], which was the first class of small molecules synthesized on solid supports [459]. Benzoxazocines (**335**) [460] are examples for benzoannulated eight-membered heterocycles obtained on solid supports (Fig. 3.14).

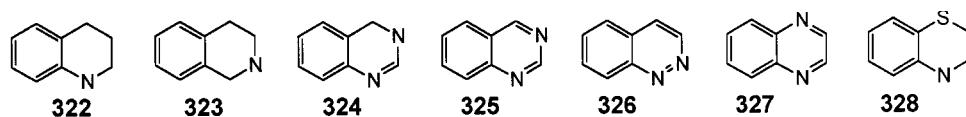
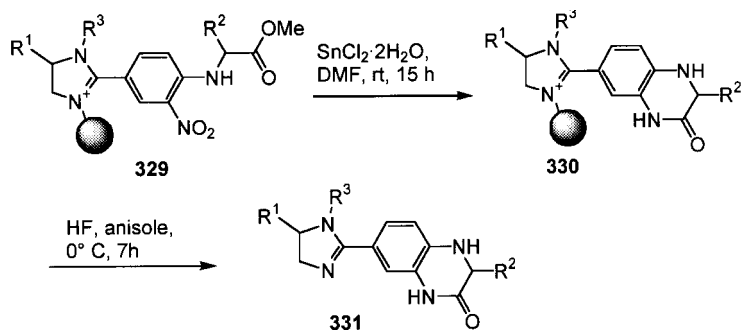
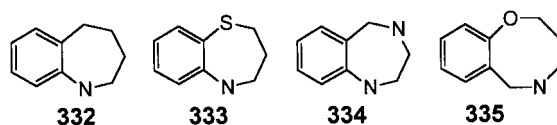


Fig. 3.13 Skeletons of six-membered benzoannulated nitrogen heterocycles.



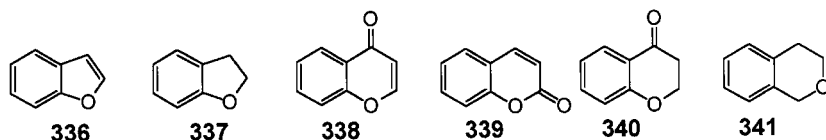
**Scheme 3.40** Solid-supported synthesis of dihydroimidazolyldihydroquinoxalines (**331**) by Houghten et al. [452].



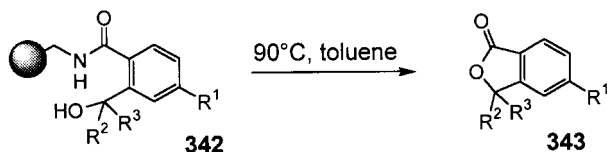
**Fig. 3.14** Skeletons of seven- and eight-membered benzoannelated nitrogen heterocycles.

### Benzoannelated oxygen heterocycles

In contrast to the benzoannelated nitrogen heterocycles, only a few kinds of benzoannelated systems without nitrogen have been described (Fig. 3.15). Five-membered rings such as benzo[b]furans (**336**) [184, 461] and hydrobenzo[b]furans (**337**) (Scheme 3.41) [337, 462, 463] and six-membered rings like 4*H*-1-benzopyran-4-ones (4-chromones) (**338**) and 2*H*-1-benzopyran-2-ones (coumarines) (**339**) [96, 464, 465] 2,3-dihydro-4*H*-1-benzopyran-4-ones (chroman-4-ones) (**340**) [466] and 3,4-dihydro-1*H*-2-benzopyrans (isochromans) (**341**) [444] have been reported.



**Fig. 3.15** Skeletons of five- and six-membered benzoannelated oxygen heterocycles.



**Scheme 3.41** Solid-phase synthesis of hydrobenzofurans (**343**) by Garibay et al. [463].

## 3.5

**Conclusion, Summary and Outlook**

Solid-phase organic chemistry has become a very important tool for the synthesis of small molecules, heterocycles and natural products over recent years. The solid-phase synthesis of heterocycles that have been reported to date, illustrate several different approaches to the challenge of preparing libraries of bioactive products. The impressive pharmacological activities of some heterocycles, such as hydantoin, benzodiazepines or indoles, have led to several synthetic approaches to heterocycles being reported. Also, natural products have been an important source of medicinal compounds and pharmaceutical leads. For this there are many research groups involved in the development of solid-phase organic synthesis techniques for the construction of natural product skeletons. In order to expand the scope of functional groups and reactions that can be adapted to the solid phase, there is a continuing need for the development of new linking and synthetic strategies. Various new types of linkers have emerged, especially for the synthesis of small molecules on solid supports. To select the best linking strategy for the solid-phase synthesis of a particular heterocycle or natural product, several factors, such as the stability of the linker to the reaction conditions and the stability of the target compounds towards cleaving conditions, have to be taken into account. Another important point is the transformation of well-known solution-phase organic reactions to the solid phase, and the development of new kinds of reaction. In this chapter we have given an overview of the different linkers and reactions that have been reported on solid supports. Although the syntheses of many heterocycles and natural products in solid-phase chemistry have been described, this area continues to grow. We expect that in the future ample new linkers and reactions will be developed in solid-phase organic chemistry.

## 3.6

**List of Abbreviations**

Ac	Acetyl
ADAM	Alkenyldiarylmethanes
AIBN	2,2'-Azobisisobutyronitrile
Alloc	N-Allyloxycarbonyl
AMPS	Aminomethyl polystyrene
BAL	Backbone Amide Linker
BHA	Benzhydramine
Bz	Benzoyl
CAN	Ceric Ammonium Nitrate
Cbz	Benzylloxycarbonyl
DMAE	Dimethylaminoethoxide
DMF	N,N-Dimethylformamide
DMSO	Dimethylsulfoxide



E	Electrophile
Fmoc	Fluorenylmethyloxycarbonyl
HAL	Hypersensitive Acid-Labile
HFIP	Hexafluoroisopropanol
HYCRAM	Hydroxycrotonylamide
HYCRON	Hydroxycrotyl-oligoethylene glycol- <i>n</i> -alkanoyl
HTS	High Throughput Screening
IUPAC	International Union of Pure and Applied Chemistry
LDA	Lithium diisopropylamide
MOM	Methoxymethyl
MS	Molecular Sieves
NCPS	Soluble noncellulose polysaccharides
NMP	1-Methylpyrrolidin-2-one
Nu	Nucleophile
PbS	<i>N</i> -(3 or 4)-[[4-(Hydroxymethyl)phenoxy]- <i>tert</i> -butyl-phenylsilyl]phenyl pentanedionic acid monoamide
PEG	Polyethylene glycol
Piv	Pivaloyl
RCM	Ring Closing Metathesis
REM	Polymer-bound benzyl acrylate: <i>RE</i> generated Michael acceptor) resin
ROM	Ring Opening Metathesis
SAC	Silyl Acid Linker: 4-[1-Hydroxy-2-(trimethylsilyl)ethyl]-benzoic acid
SAL	Silyl Amide Linker: 4-[(1-Amino)-2-(trimethylsilyl)ethyl]-phenoxyacetic acid
SASRIN	Super Acid Sensitive Resin
SEM	2-Trimethylsilylethoxymethyl
SPOS	Solid-phase Organic Synthesis
TBAF	Tetrabutylammonium fluoride
TBS	Tertbutyldimethylsilyl
Tf	Trifluoromethylsulfonyl
TFA	Trifluoroacetic acid
THF	Tetrahydrofuran
THP	Tetrahydropyran
TMS	Trimethylsilane
Tol	Tolyl

## 3.7

## References

- 1 L.A. THOMPSON, *Curr. Opin. Chem. Biol.* **2000**, 4, 324–337.
- 2 W.A. WAR, *J. Chem. Inf. Comput. Sci.* **1997**, 37, 134–140.
- 3 B. LOU, *Drug Discov. Today*, **2001**, 6, 1288–1294.
- 4 J. H. KIRCHHOFF, M.E.P. LORMANN, S. BRÄSE, *Chimica Oggi* **2001**, 19, 28–33.
- 5 A.R. BROWN, P.H.H. HERMKENS, H.C.J. OTTENHEIJM, D.C. REES, *Synlett* **1998**, 817–827.
- 6 F. GUILLIER, D. ORAN, M. BRADLEY, *Chem. Rev.* **2000**, 100, 2091–2157.
- 7 R.T. PON, S. YU, Y.S. SANGHVI, *J. Org. Chem.* **2002**, 67, 856–864.
- 8 V. VERMA, F. ECKSTEIN, *Annu. Rev. Biochem.* **1998**, 67, 99–134.
- 9 A. BARTOLOZZI, P.H. SEEBERGER, *Curr. Opin. Struct. Biol.* **2001**, 11, 587–592.
- 10 D. CRICH, M. SMITH, *J. Am. Chem. Soc.* **2002**, 124, 8867–8869.
- 11 M. GOODMAN, C. ZAPF, Y. REW, *Biopolymers* **2001**, 60, 229–245.
- 12 P.H. SEEBERGER, W.-C. HAASE, *Chem. Rev.* **2000**, 100, 4349–4393.
- 13 O.J. PLANTE, E.R. PALMACCI, P.H. SEEBERGER, *Science* **2001**, 291, 1523–1527.
- 14 X. WU, M. GRATHWOHL, R.R. SCHMIDT, *Org. Lett.* **2001**, 3, 747–750.
- 15 R.A. FECIK, K.E. FRANK, E.J. GENTRY, *et al.*, *Med. Res. Rev.* **1998**, 18, 149–185.
- 16 S. BRÄSE, C. GIL, K. KNEPPER, *Bioorg. Med. Chem.* **2002**, 10, 2415–2437.
- 17 P. ARYA, R. JOSEPH, D.T.H. CHOU, *Chem. Biol.* **2002**, 9, 145–156.
- 18 J. BACKES, J.A. ELMAN, *Curr. Opin. Chem. Biol.* **1997**, 1, 86–93.
- 19 D. MACLEAN, J.J. BALDWIN, V.T. IVANOV, *et al.*, *Pure Appl. Chem.* **1999**, 71, 2349–2365.
- 20 S. BRÄSE, S. DAHMEN, *Handbook of Combinatorial Chemistry*, K.C. NICOLAOU, R. HANKO, W. HARTWIG, eds., Wiley-VCH, Weinheim, **2002**, 59–169.
- 21 R.B. MERRIFIELD, *J. Am. Chem. Soc.* **1963**, 85, 2149–2154.
- 22 S.-S. WANG, *J. Am. Chem. Soc.* **1973**, 95, 1328–1333.
- 23 M. MERGLER, R. TANNER, J. GOSTELI, *et al.*, *Tetrahedron Lett.* **1988**, 29, 4005–4008.
- 24 F. ALBERICIO, G. BARANY, *Tetrahedron Lett.* **1991**, 32, 1015–1018.
- 25 R.C. ORLOWSKI, R. WALTER, D. WINKLER, *J. Org. Chem.* **1976**, 41, 3701–3705.
- 26 H. RINK, *Tetrahedron Lett.* **1987**, 28, 3787–3790.
- 27 R.S. GARIGIPATI, *Tetrahedron Lett.* **1997**, 38, 6807–6810.
- 28 J.M.J. FRECHET, L. NUYENS, *Can. J. Chem.* **1976**, 54, 926–934.
- 29 T.M. FYLES, C.C. LEZNOFF, *Can. J. Chem.* **1976**, 54, 935–942.
- 30 N. THIERIET, F. GUIBE, F. ALBERICIO, *Org. Lett.* **2000**, 2, 1815–1817.
- 31 D.S. YAMASHITA, X. DONG, H.-J. OH, *et al.*, *J. Comb. Chem.* **1999**, 1, 207–215.
- 32 K. NGU, D.V. PATEL, *J. Org. Chem.* **1997**, 62, 7088–7089.
- 33 L. PETERSEN, K.J. JENSEN, *J. Chem. Soc. Perkin Trans. I* **2001**, 2175–2182.
- 34 J. GIOVANNONI, G. SUBRA, M. AMBLARD, *et al.*, *Tetrahedron Lett.* **2001**, 42, 5389–5392.
- 35 J. JIN, T.L. GRAYBILL, M.A. WANG, *et al.*, *J. Comb. Chem.* **2001**, 3, 97–101.
- 36 S. CAIX-HAUMESSER, I. HANNA, J.-Y. LALLEMAND, *et al.*, *Tetrahedron Lett.* **2001**, 42, 37213–723.
- 37 K.H. GORDON, S. BALASUBRAMANIAN, *Org. Lett.* **2001**, 3, 53–56.
- 38 S. KOBAYASHI, Y. AOKI, *Tetrahedron Lett.* **1998**, 39, 7345–7348.
- 39 D.R. ENGLEBRETSSEN, B.G. GARNHAM, D.A. BERGMAN, *et al.*, *Tetrahedron Lett.* **1995**, 36, 8871–8874.
- 40 G. BARANY, R.B. MERRIFIELD, IN *The Peptides* (eds.: E. GROSS, J. MEIENHOFER), Academic Press, New York **1979**.
- 41 G.-s. LU, S. MOJSOV, J.P. TAM, R.B. MERRIFIELD, *J. Org. Chem.* **1981**, 46, 3433–3436.
- 42 K.J. JENSEN, J. ALSINA, M.F. SONGSTER, *et al.*, *J. Am. Chem. Soc.* **1998**, 120, 5441–5452.
- 43 C.T. BUI, F.A. RASOUL, F. ERCOLE, *et al.*, *Tetrahedron Lett.* **1998**, 39, 9279–9282.
- 44 K.A. BEAVER, A.C. SIEGMUND, K.L. SPEAR, *Tetrahedron Lett.* **1996**, 37, 1145–1148.

- 45 A. L. MARZINZIK, E. R. FELDER, *Tetrahedron Lett.* **1996**, 37, 1003–1006.
- 46 K. BARLOS, D. GATOS, J. KALLITSIS, *et al.*, *Liebigs Ann. Chem.* **1988**, 1079–1081.
- 47 K. BARLOS, D. GATOS, J. KALLITSIS, *et al.*, *Tetrahedron Lett.* **1989**, 30, 3943–3946.
- 48 K. BARLOS, O. CHATZI, D. GATOS, *et al.*, *Int. J. Pept. Protein Res.* **1991**, 37, 513–520.
- 49 H. KUNZ, B. DOMBO, *Angew. Chem. Int. Ed. Engl.* **1988**, 12, 711–712; *Angew. Chem.* **1988**, 100, 732–734.
- 50 C. SCHUMANN, L. SEYFARTH, G. GREINER, *et al.*, *J. Pept. Res.* **2000**, 55, 428–435.
- 51 O. SEITZ, H. KUNZ, *J. Org. Chem.* **1997**, 62, 813–826.
- 52 O. SEITZ, *Tetrahedron Lett.* **1999**, 40, 4161–4164.
- 53 O. SEITZ, H. KUNZ, *Angew. Chem. Int. Ed.* **1995**, 34, 803–805; *Angew. Chem.* **1995**, 107, 901–904.
- 54 L. A. THOMPSON, J. A. ELLMAN, *Tetrahedron Lett.* **1994**, 35, 9333–9336.
- 55 S.-E. YOO, Y.-D. GONG, M.-Y. CHOI, *et al.*, *Tetrahedron Lett.* **2000**, 41, 6415–6418.
- 56 G. T. WANG, S. LI, N. WIDEBURG, G. A. KRAFFT, *et al.*, *J. Med. Chem.* **1995**, 38, 2995–3002.
- 57 C. C. LEZNOFF, J. Y. WONG, *Can. J. Chem.* **1973**, 51, 3756–3764.
- 58 C. C. LEZNOFF, S. GREENBERG, *Can. J. Chem.* **1976**, 54, 3824–3829.
- 59 Z. H. XU, C. R. MCARTHUR, C. C. LEZNOFF, *Can. J. Chem.* **1983**, 61, 1405–1409.
- 60 R. MALTAIS, M. BERUBE, O. MARION, *et al.*, *Tetrahedron Lett.* **2000**, 41, 1691–1694.
- 61 C. M. HUWE, H. KÜNZER, *Tetrahedron Lett.* **1999**, 40, 683–686.
- 62 F. ROUSSEL, M. TAKHI, R. R. SCHMIDT, *J. Org. Chem.* **2001**, 66, 8540–8548.
- 63 T. ZHU, G.-J. BOONS, *Chem. Eur. J.* **2001**, 7, 2382–2398.
- 64 F. ROUSSEL, L. KNERR, R. R. SCHMIDT, *Eur. J. Org. Chem.* **2001**, 2067–2073.
- 65 N. DRINNAN, M. L. WEST, M. BROADHURST, *et al.*, *Tetrahedron Lett.* **2001**, 42, 1159–1162.
- 66 M. LAMOTHE, M. LANNUZEL, M. PEREZ, *J. Comb. Chem.* **2002**, 4, 73–78.
- 67 H.-C. ZHANG, D. F. MCCOMSEY, K. B. WHITE, *et al.*, *Bioorg. Med. Chem. Lett.* **2001**, 11, 2105–2109.
- 68 J. R. HAUSKE, P. DORFF, *Tetrahedron Lett.* **1995**, 36, 1589–1592.
- 69 C. W. ZAPF, C. J. CREIGHTON, M. TOMIOKA, *et al.*, *Org. Lett.* **2001**, 3, 1133–1136.
- 70 Y. KONDO, T. KOMINE, M. FUJINAMI, *et al.*, *J. Comb. Chem.* **1999**, 1, 123–126.
- 71 L. F. TIETZE, A. STEINMETZ, *Angew. Chem. Int. Ed.* **1996**, 35, 651–652; *Angew. Chem.* **1996**, 108, 682–683.
- 72 U. GRETHER, H. WALDMANN, *Angew. Chem. Int. Ed.* **2000**, 39, 1629–1632; *Angew. Chem.* **2000**, 112, 1688–1691.
- 73 C. R. MILLINGTON, R. QUARREL, G. LOWE, *Tetrahedron Lett.* **1998**, 39, 7201–7204.
- 74 F. X. WOOLARD, J. PAETSCH, J. A. ELLMAN, *J. Org. Chem.* **1997**, 62, 6102–6103.
- 75 Y. HAN, S. D. WALKER, R. N. YOUNG, *Tetrahedron Lett.* **1996**, 37, 2703–2706.
- 76 T. L. BOEHM, H. D. H. SHOWALTER, *J. Org. Chem.* **1996**, 61, 6498–6499.
- 77 C. A. BRIEHN, T. KIRSCHBAUM, P. BÄUERLE, *J. Org. Chem.* **2000**, 65, 352–359.
- 78 Y. HU, J. J. A. PORCO, *Tetrahedron Lett.* **1998**, 39, 2711–2714.
- 79 K. A. NEWLANDER, B. CHENERA, D. F. VEBER, *et al.*, *J. Org. Chem.* **1997**, 62, 6726–6732.
- 80 Y. H. HU, J. A. PORCO, J. W. LABADIE, *et al.*, *J. Org. Chem.* **1998**, 63, 4518–4521.
- 81 N. D. HONE, S. G. DAVIES, N. J. DEVEREUX, *et al.*, *Tetrahedron Lett.* **1998**, 39, 897–900.
- 82 R. MALTAIS, M. R. TREMBLAY, D. POIRIER, *J. Comb. Chem.* **2000**, 2, 604–614.
- 83 S. D. BROWN, R. W. ARMSTRONG, *J. Org. Chem.* **1997**, 62, 7076–7077.
- 84 R. H. CRABTREE, *Chem. Commun.* **1999**, 1611–1616.
- 85 Y. LEE, R. B. SILVERMAN, *J. Am. Chem. Soc.* **1999**, 121, 8407–8408.
- 86 S. CURTET, M. LANGLOIS, *Tetrahedron Lett.* **1999**, 40, 8563–8566.
- 87 A. STUDER, S. HADIDA, R. FERRITTO, *et al.*, *Science* **1997**, 275, 823–826.
- 88 A. STUDER, P. JEGER, P. WIPF, D. P. CURRAN, *J. Org. Chem.* **1997**, 62, 2917–2924.
- 89 M. SCHUSTER, N. LUCAS, S. BLECHERT, *Chem. Commun.* **1997**, 823–824.
- 90 H. G. CHAO, M. S. BERNATOWICZ, P. D. REISS, *et al.*, *J. Am. Chem. Soc.* **1994**, 116, 1746–1752.

- 91 H. CHAO, M. S. BERNATOWICZ, G. R. MATSUDA, *J. Org. Chem.* **1993**, *58*, 2640–2644.
- 92 D. G. MULLEN, G. BARANY, *J. Org. Chem.* **1988**, *53*, 5240–5248.
- 93 R. RAMAGE, C. A. BARRON, S. BIDECKI, *et al.*, *Tetrahedron Lett.* **1987**, *28*, 4105–4108.
- 94 W. J. KOOT, *J. Comb. Chem.* **1999**, *1*, 467–473.
- 95 A. ROUTLEDGE, H. T. STOCK, S. L. FLITSCH, *et al.*, *Tetrahedron Lett.* **1997**, *38*, 8287–8290.
- 96 L. S. HARIKRISHNAN, H. D. H. SHOWALTER, *Tetrahedron* **2000**, *56*, 515–519.
- 97 B. WANG, L. CHEN, K. KIM, *Tetrahedron Lett.* **2001**, *42*, 1463–1466.
- 98 A. MATSUDA, T. DOI, H. TANAKA, T. TAKAHASHI, *Synlett* **2001**, 1101–1104.
- 99 A. KOBORI, K. MIYATA, M. USHIODA, *et al.*, *Chem. Lett.* **2002**, 16–17.
- 100 B. H. LIPSHUTZ, Y.-J. SHIN, *Tetrahedron Lett.* **2001**, *42*, 5629–5633.
- 101 L. A. THOMPSON, F. L. MOORE, Y. C. MOON, *et al.*, *J. Org. Chem.* **1998**, *63*, 2066–2067.
- 102 B. CHENERA, J. A. FINKELSTEIN, D. F. VEBER, *J. Am. Chem. Soc.* **1995**, *117*, 11999–12000.
- 103 M. J. PLUNKETT, J. A. ELLMAN, *J. Org. Chem.* **1995**, *60*, 6006–6007.
- 104 R. RAMAGE, C. A. BARRON, S. BIELECKI, *et al.*, *Tetrahedron* **1992**, *48*, 499–514.
- 105 J. M. J. FRECHET, L. J. NUYENS, E. SEYMOUR, *J. Am. Chem. Soc.* **1979**, *101*, 432–436.
- 106 W. LI, K. BURGESS, *Tetrahedron Lett.* **1999**, *40*, 6527–6530.
- 107 C. POURBAIX, F. CARREAUX, B. CARBONI, *et al.*, *Chem. Commun.* **2000**, 1275–1276.
- 108 E. LA PORTA, U. PIARULLI, F. CARDULLO, *et al.*, *Tetrahedron Lett.* **2002**, *43*, 761–766.
- 109 C. ROLLAND, G. HANQUET, J.-B. DUCEP, *et al.*, *Tetrahedron Lett.* **2001**, *42*, 7563–7566.
- 110 W.-C. CHENG, M. WONG, M. M. OLMESTEAD, *et al.*, *Org. Lett.* **2002**, *4*, 741–744.
- 111 T. KANEMITSU, C.-H. WONG, O. KANIE, *J. Am. Chem. Soc.* **2002**, *124*, 3591–3599.
- 112 K. W. JUNG, X. Y. ZHAO, K. D. JANDA, *Tetrahedron* **1997**, *53*, 6645–6652.
- 113 K. W. JUNG, X. Y. ZHAO, K. D. JANDA, *Tetrahedron Lett.* **1996**, *37*, 6491–6494.
- 114 I. SUCHOLEIKI, *Tetrahedron Lett.* **1994**, *35*, 7307–7310.
- 115 J. R. HORTON, L. M. STAMP, A. ROUTLEDGE, *Tetrahedron Lett.* **2000**, *41*, 9181–9184.
- 116 K. C. NICOLAOU, S. A. SNYDER, A. BIGOT, *et al.*, *Angew. Chem. Int. Ed.* **2000**, *39*, 1093–1096; *Angew. Chem.* **2000**, *112*, 1135–1138.
- 117 H. S. OVERKLEEF, P. R. BOS, B. G. HEKING, *et al.*, *Tetrahedron Lett.* **2000**, *41*, 6005–6009.
- 118 D. L. MARSHALL, I. E. LIENER, *J. Org. Chem.* **1970**, *35*, 867–868.
- 119 H. KUHN, W. P. NEUMANN, *Synlett* **1994**, 123–124.
- 120 K. C. NICOLAOU, N. WINSSINGER, J. PASTOR, *et al.*, *Angew. Chem. Int. Ed.* **1998**, *37*, 2534–2537; *Angew. Chem.* **1998**, *110*, 2677–2680.
- 121 K. C. NICOLAOU, J. PASTOR, S. BARLUENGA, *et al.*, *Chem. Commun.* **1998**, 1947–1948.
- 122 T. RUHLAND, K. ANDERSEN, H. PEDERSEN, *J. Org. Chem.* **1998**, *63*, 9204–9211.
- 123 K. C. NICOLAOU, N. WINSSINGER, R. HUGHES, *et al.*, *Angew. Chem. Int. Ed.* **2000**, *39*, 1984–1989; *Angew. Chem.* **2000**, *112*, 1126–1130.
- 124 K. C. NICOLAOU, S.-Y. CHO, R. HUGHES, *et al.*, *Chem. Eur. J.* **2001**, *7*, 3798–3823.
- 125 L. UEHLIN, T. WIRTH, *Org. Lett.* **2001**, *3*, 2931–2933.
- 126 H. QIAN, X. HUANG, *Tetrahedron Lett.* **2002**, *43*, 1059–1061.
- 127 K. C. NICOLAOU, C. N. C. BODDY, S. BRÄSE, *et al.*, *Angew. Chem.* **1999**, *111*, 2230–2287; *Angew. Chem. Int. Ed.* **1999**, *38*, 2097–2152.
- 128 J. C. NELSON, J. K. YOUNG, J. S. MOORE, *J. Org. Chem.* **1996**, *61*, 8160–8168.
- 129 J. K. YOUNG, J. C. NELSON, J. S. MOORE, *J. Am. Chem. Soc.* **1994**, *116*, 10841–10842.
- 130 L. JONES, J. S. SCHUMM, J. M. TOUR, *J. Org. Chem.* **1997**, *62*, 1388–1410.
- 131 S. BRÄSE, D. ENDERS, J. KÖBBERLING, *et al.*, *Angew. Chem. Int. Ed.* **1998**, *37*, 3413–3415; *Angew. Chem.* **1998**, *110*, 3614–3616.
- 132 M. LORMANN, S. DAHMEN, S. BRÄSE, *Tetrahedron Lett.* **2000**, *41*, 3813–3816.
- 133 S. SCHUNK, D. ENDERS, *Org. Lett.* **2000**, *2*, 907–910.

- 134 S. BRÄSE, S. DAHMEN, *Chem. Eur. J.* **2000**, *6*, 1899–1905.
- 135 M. LORMANN, S. BRÄSE, UNPUBLISHED.
- 136 S. BRÄSE, M. SCHROEN, *Angew. Chem. Int. Ed.* **1999**, *38*, 1071–1073; *Angew. Chem.* **1999**, *111*, 1139–1142.
- 137 A. DE MEIJERE, H. NÜSKE, M. ES-SAYED, *et al.*, *Angew. Chem. Int. Ed.* **1999**, *38*, 3669–3672; *Angew. Chem.* **1999**, *111*, 3881–3884.
- 138 F. AVEMARIA, V. ZIMMERMANN, S. BRÄSE, *J. Comb. Chem.* **2003**, submitted.
- 139 S. BRÄSE, M. LORMANN, J. HEUTS, unpublished.
- 140 S. BRÄSE, S. DAHMEN, J. HEUTS, *Tetrahedron Lett.* **1999**, *40*, 6201–6203.
- 141 M. E. P. LORMANN, C. H. WALKER, S. BRÄSE, *Chem. Commun.* **2002**, 1296–1297.
- 142 S. BRÄSE, J. KÖBBERLING, D. ENDERS, *et al.*, *Tetrahedron Lett.* **1999**, *40*, 2105–2108.
- 143 S. BRÄSE, S. DAHMEN, M. PFEFFERKORN, *J. Comb. Chem.* **2000**, *2*, 710–717.
- 144 S. DAHMEN, S. BRÄSE, *Org. Lett.* **2000**, *2*, 3563–3565.
- 145 a) C. PILOT, MAÎTRISE DE CHIMIE **1999**, RWTH Aachen/Université Strasbourg. b) C. PILOT, S. DAHMEN, F. LAUTERWASSER, *et al.*, *Tetrahedron Lett.* **2001**, *42*, 9179–9181.
- 146 S. BRÄSE, *Chimica Oggi* **2000**, *18(9)*, 14–18.
- 147 S. DAHMEN, S. BRÄSE, *Angew. Chem. Int. Ed.* **2000**, *39*, 3681–3683; *Angew. Chem.* **2000**, *112*, 3827–3830.
- 148 N. VIGNOLA, S. DAHMEN, D. ENDERS, *et al.*, *Tetrahedron Lett.* **2001**, *42*, 7833–7836.
- 149 C. G. BOCHET, *J. Chem. Soc., Perkin Trans I*, **2002**, 125–142.
- 150 D. H. RICH, S. K. GURWARA, *J. Am. Chem. Soc.* **1975**, *97*, 1575–1579.
- 151 D. H. RICH, S. K. GURWARA, *J. Chem. Soc. Chem. Commun.* **1973**, 610–611.
- 152 H. B. LEE, S. BALASUBRAMANIAN, *J. Org. Chem.* **1999**, *64*, 3454–3460.
- 153 M. CANO, M. LADLOW, S. BALASUBRAMANIAN, *J. Org. Chem.* **2002**, *67*, 129–135.
- 154 K. C. NICOLAOU, B. S. SAFINA, N. WINSINGER, *Synlett* **2001**, 900–903.
- 155 R. P. HAMMER, F. ALBERICIO, E. GIRALT, *et al.*, *Int. J. Pept. Protein Res.* **1990**, *28*, 31–45.
- 156 R. GLATTHAR, B. GIESE, *Org. Lett.* **2000**, *2*, 2315–2317.
- 157 F. W. FORMAN, I. SUCHOLEIKI, *J. Org. Chem.* **1995**, *60*, 523–528.
- 158 G. W. KENNER, J. R. McDERMOTT, R. C. SHEPPARD, *J. Chem. Soc. Chem. Commun.* **1971**, 636–637.
- 159 B. J. BACKES, J. A. ELLMAN, *J. Am. Chem. Soc.* **1994**, *116*, 11171–11172.
- 160 B. J. BACKES, J. A. ELLMAN, *J. Org. Chem.* **1999**, *64*, 2322–2330.
- 161 B. J. BACKES, A. A. VIRGILIO, J. A. ELLMAN, *J. Am. Chem. Soc.* **1996**, *118*, 3055–3056.
- 162 D. MACLEAN, R. HALE, M. CHEN, *Org. Lett.* **2001**, *3*, 2977–2980.
- 163 C. L. BEECH, J. F. COOPE, G. FAIRLEY, *et al.*, *J. Org. Chem.* **2001**, *66*, 2240–2245.
- 164 D. ORAIN, M. BRADLEY, *Tetrahedron Lett.* **2001**, *42*, 515–518.
- 165 G. T. BOURNE, S. W. GOLDING, R. P. McGEARY, *et al.*, *J. Org. Chem.* **2001**, *66*, 7706–7713.
- 166 D. FATTORI, O. KINZEL, P. INGALLINELLA, *et al.*, *Bioorg. Med. Chem. Lett.* **2002**, *12*, 1143–1147.
- 167 R. QUADERER, D. HILVERT, *Org. Lett.* **2001**, *3*, 3181–3184.
- 168 Z. TIMAR, T. GALLAGHER, *Tetrahedron Lett.* **2000**, *41*, 3173–3176.
- 169 M. PATEK, M. LEBL, *Tetrahedron Lett.* **1991**, *32*, 3891–3894.
- 170 M. H. LYTTLE, D. HUDSON, R. M. COOK, *Nucl. Acid Res.* **1996**, *24*, 2793–2798.
- 171 F. BERST, A. B. HOLMES, M. LADLOW, *et al.*, *Tetrahedron Lett.* **2000**, *41*, 6649–6653.
- 172 F. CAMPS, J. CASTELLS, J. PI, *Ann. Quim.* **1974**, *70*, 848–849.
- 173 F. ALBERICIO, J. GARCIA, E. L. MICHELOTI, *et al.*, *Tetrahedron Lett.* **2000**, *41*, 3161–3163.
- 174 J. MATTHEWS, R. A. RIVERO, *J. Org. Chem.* **1997**, *62*, 6090–6092.
- 175 A. GOLEBIOWSKI, S. R. KLOPFENSTEIN, J. J. CHEN, *et al.*, *Tetrahedron Lett.* **2000**, *41*, 4841–4844.
- 176 C. ROSENBAUM, H. WALDMANN, *Tetrahedron Lett.* **2001**, *42*, 5677–5680.
- 177 I. HUGHES, *Tetrahedron Lett.* **1996**, *37*, 7595–7598.
- 178 K. C. NICOLAOU, J. PASTOR, N. WINSINGER, *et al.*, *J. Am. Chem. Soc.* **1998**, *120*, 5132–5133.
- 179 C. R. JOHNSON, B. R. ZHANG, *Tetrahedron Lett.* **1995**, *36*, 9253–9256.

- 180 J. H. VAN MAARSEVEEN, J. A. J. DEN HARTOG, V. ENGELN, *et al.*, *Tetrahedron Lett.* **1996**, 37, 8249–8252.
- 181 K. C. NICOLAOU, N. WINSSINGER, J. PASITOR, *et al.*, *Nature* **1997**, 387, 268–272.
- 182 J. U. PETERS, S. BLECHERT, *Synlett* **1997**, 348–350.
- 183 A. D. PISCOPIO, J. F. MILLER, K. KOCH, *Tetrahedron* **1999**, 55, 8189–8198.
- 184 E. J. GUTHRIE, J. MACRITCHIE, R. C. HARTLEY, *Tetrahedron Lett.* **2000**, 41, 4987–4990.
- 185 A. MAZUROV, *Tetrahedron Lett.* **2000**, 41, 7–10.
- 186 A. MAZUROV, *Bioorg. Med. Chem. Lett.* **2000**, 10, 67–70.
- 187 S. BRÄSE, R. LAZNY, UNPUBLISHED.
- 188 B. K. LORSBACH, R. B. MILLER, M. J. KURTH, *J. Org. Chem.* **1996**, 61, 8716–8717.
- 189 B. A. LORSBACH, J. T. BAGDANOFF, R. B. MILLER, *et al.*, *J. Org. Chem.* **1998**, 63, 2244–2250.
- 190 P. BLANEY, R. GRIGG, V. SRIDHARAN, *Chem. Rev.* **2002**, 102, 2607–2624.
- 191 K. J. LEE, K. D. JANDA, *Can. J. Chem.* **2001**, 79, 1556–1561.
- 192 M. J. PLUNKETT, J. A. ELLMAN, *J. Org. Chem.* **1997**, 62, 2885–2893.
- 193 A. C. SPIVEY, C. M. DIAPER, H. ADAMS, *et al.*, *J. Org. Chem.* **2000**, 65, 5253–5263.
- 194 S. J. JIN, D. P. HOLUB, D. J. WUSTROW, *Tetrahedron Lett.* **1998**, 39, 3651–3654.
- 195 Y. PAN, C. P. HOLMES, *Org. Lett.* **2001**, 3, 2769–2771.
- 196 F. STIEBER, U. GREYER, H. WALDMANN, *Angew. Chem. Int. Ed.* **1999**, 38, 1073–1077; *Angew. Chem.* **1999**, 111, 1142–1145.
- 197 Z. LI, B. A. KULKARNI, A. GANESAN, *Bio-technol. Bioeng.* **2000**, 71, 104–106.
- 198 H. KAMOGAWA, A. KANZAWA, M. KADOYA, *et al.*, *Bull. Chem. Soc. Jpn.* **1983**, 56, 762–765.
- 199 P. GARIBAY, J. NIELSEN, T. HOEG-JENSEN, *Tetrahedron Lett.* **1998**, 39, 2207–2210.
- 200 F. MCKERLIE, D. J. PROCTER, G. WYNNE, *Chem. Commun.* **2002**, 584–585.
- 201 J. H. RIGBY, M. A. KONDRATENKO, *Org. Lett.* **2001**, 3, 3683–3686.
- 202 F. ZARAGOZA, *Angew. Chem. Int. Ed.* **2000**, 39, 2077–2079; *Angew. Chem.* **2000**, 112, 2158–2159.
- 203 S. C. SCHÜRER, S. BLECHERT, *Synlett* **1998**, 166–168.
- 204 J. K. RUETER, S. O. NORTEY, E. W. BAXTER, *et al.*, *Tetrahedron Lett.* **1998**, 39, 975–978.
- 205 J. A. HUNT, W. R. ROUSH, *J. Am. Chem. Soc.* **1996**, 118, 9998–9999.
- 206 C. VANIER, F. LORGÉ, A. WAGNER, *et al.*, *Angew. Chem. Int. Ed.* **2000**, 39, 1679–1683; *Angew. Chem.* **2000**, 112, 1745–1749.
- 207 W. C. CHENG, C. HALM, J. B. EVARTS, M. *et al.*, *J. Org. Chem.* **1999**, 64, 8557–8562.
- 208 K. C. NICOLAOU, P. S. BARAN, Y. L. ZHONG, *J. Am. Chem. Soc.* **2000**, 122, 10246–10248.
- 209 M. KAWANA, S. EMOTO, *Tetrahedron Lett.* **1972**, 13, 4855–4858.
- 210 M. KAWANA, S. EMOTO, *Bull. Chem. Soc. Jpn.* **1974**, 47, 160–165.
- 211 P. M. WORSTER, C. R. MCARTHUR, C. C. LEZNOFF, *Angew. Chem. Int. Ed. Engl.* **1979**, 18, 221; *Angew. Chem.* **1979**, 91, 255.
- 212 C. R. MCARTHUR, P. M. WORSTER, J.-L. JIANG, C. C. LEZNOFF, *Can. J. Chem.* **1982**, 60, 1836–1841.
- 213 H. S. MOON, N. E. SCHORE, M. J. KURTH, *J. Org. Chem.* **1992**, 57, 6088–6089.
- 214 H. S. MOON, N. E. SCHORE, M. J. KURTH, *Tetrahedron Lett.* **1994**, 35, 8915–8918.
- 215 K. OERTEL, G. ZECH, H. KUNZ, *Angew. Chem. Int. Ed.* **2000**, 39, 1431–1433; *Angew. Chem.* **2000**, 112, 1489–1491.
- 216 D. ENDERS, J. H. KIRCHHOFF, J. KÖBBERLING, *et al.*, *Org. Lett.* **2001**, 3, 1241–1244.
- 217 S. S. SAVINOV, D. J. AUSTIN, *Org. Lett.* **2002**, 4, 1419–1422.
- 218 S. E. YOO, J. S. SEO, K. Y. YI, *et al.*, *Tetrahedron Lett.* **1997**, 38, 1203–1206.
- 219 J. G. BREITENBUCHER, G. FIGLIOZZI, *Tetrahedron Lett.* **2000**, 41, 4311–4315.
- 220 A. R. BROWN, D. C. REES, Z. RANKOVIC, *et al.*, *J. Am. Chem. Soc.* **1997**, 119, 3288–3295.
- 221 Y. WANG, T.-N. HUANG, *Tetrahedron Lett.* **1999**, 40, 5837–5840.
- 222 J. ALSINA, T. S. YOKUM, F. ALBERICIO, *et al.*, *J. Org. Chem.* **1999**, 64, 8761–8769.
- 223 M. LORMANN, S. BRÄSE, H. VOGT, *Proceedings of ECSOC-4, The Third International Electronic Conference on Synthetic Organic Chemistry*, <http://www.mdpi.org/ec-soc-4.htm>, Scope and Limitation of a Tin

- Promoted Amidation on Solid phase: A New Monitoring for the T1 Triazene Linker, September 1–30, 2000.
- 224 C. E. J. HALM, M. J. KURTH, *Tetrahedron Lett.* **1997**, 38, 7709–7712.
- 225 G. HUM, J. GRZYB, S. D. TAYLOR, *J. Comb. Chem.* **2000**, 2, 234–242.
- 226 U. REISER, J. JAUCH, *Synlett* **2001**, 1, 9092.
- 227 P. PAGE, M. BRADLEY, I. WALTERS, *et al.*, *J. Org. Chem.* **1999**, 64, 794–799.
- 228 O. MELNYK, J.-S. FRUCHART, C. GRANDJEAN, *et al.*, *J. Org. Chem.* **2001**, 66, 4153–4160.
- 229 E. G. MATA, *Tetrahedron Lett.* **1997**, 38, 6335–6338.
- 230 T. MASUDA, J. K. STILLE, *J. Am. Chem. Soc.* **1978**, 10, 268–272.
- 231 S. KOBAYASHI, I. HACHIYA, S. SUZUKI, M. MORIWAKI, *Tetrahedron Lett.* **1996**, 37, 2809–2812.
- 232 A. NEFZI, J. M. OSTRESH, J.-P. MEYER, *et al.*, *Tetrahedron Lett.* **1997**, 38, 931–934.
- 233 G. LIU, J. A. ELLMAN, *J. Org. Chem.* **1995**, 60, 7712–7713.
- 234 G. HUMMEL, O. HINDSGAUL, *Angew. Chem. Int. Ed. Engl.* **1999**, 38, 1782–1784; *Angew. Chem.* **1999**, 111, 1900–1902.
- 235 M. C. HEWITT, P. H. SEEBERGER, *J. Org. Chem.* **2001**, 66, 4233–4243.
- 236 G. M. MAKARA, W. E. Y. MA, E. WINTNER, *J. Org. Chem.* **2001**, 66, 5783–5789.
- 237 C. J. ANDRES, D. L. WHITEHOUSE, M. S. DESPHANDE, *Curr. Opin. Chem. Biol.* **1998**, 2, 353–362.
- 238 R. FRANZÉN, *Can. J. Chem.* **2000**, 78, 957–962.
- 239 S. BRÄSE, J. KÖBBERLING, N. GRIEBENOW IN *Handbook of Palladium Chemistry*, E.-i. Negishi, ed., Wiley, New York **2002**, 3031–3128.
- 240 K.-L. YU, M. S. DESHPANDE, D. M. VYAS, *Tetrahedron Lett.* **1994**, 35, 8919–8922.
- 241 M. HIROSHIGE, J. R. HAUSKE, P. J. ZHOU, *J. Am. Chem. Soc.* **1995**, 117, 11590–11591.
- 242 W. Y. YUN, R. MOHAN, *Tetrahedron Lett.* **1996**, 37, 7189–7192.
- 243 H. C. ZHANG, B. E. MARYANOFF, *J. Org. Chem.* **1997**, 62, 1804–1809.
- 244 S. BERTEINA, S. WENDEBORN, A. DE MESMAEKER, *Synlett* **1998**, 1231–1233.
- 245 G. L. BOLTON, J. C. HODGES, *J. Comb. Chem.* **1999**, 1, 130–133.
- 246 C. POURBAIX, F. CARREAX, B. CARBONI, *Org. Lett.* **2001**, 3, 803–805.
- 247 M. GRAVEL, K. A. THOMPSON, M. ZAK, *et al.*, *J. Org. Chem.* **2002**, 67, 3–15.
- 248 R. FRETTE, R. W. FRIESEN, *Tetrahedron Lett.* **1994**, 35, 9177–9180.
- 249 O. BAUDOIN, M. CESARIO, D. GUÉNARD, *et al.*, *J. Org. Chem.* **2002**, 67, 1199–1207.
- 250 M. S. DESPHANDE, *Tetrahedron Lett.* **1994**, 35, 5613–5614.
- 251 G. XU, T. L. LOFTUS, H. WARGO, *et al.*, *J. Org. Chem.* **2001**, 66, 5958–5964.
- 252 C. PARK, K. BURGESS, *J. Comb. Chem.* **2001**, 3, 257–266.
- 253 M. D. COLLINI, J. W. ELLINGBOE, *Tetrahedron Lett.* **1997**, 38, 7963–7966.
- 254 S. MARQUAIS, M. ARLT, *Tetrahedron Lett.* **1996**, 37, 5491–5494.
- 255 F. HOMSI, K. HOSOI, K. NOZAKI, *et al.*, *J. Organomet. Chem.* **2001**, 624, 208–216.
- 256 F. HOMSI, K. NOZAKI, T. HIYAMA, *Tetrahedron Lett.* **2000**, 41, 5869–5872.
- 257 X. OUYANG, R. W. ARMSTRONG, M. M. MURPHY, *J. Org. Chem.* **1998**, 63, 1027–1032.
- 258 C. P. BALL, A. G. M. BARRETT, D. COMPERE, *et al.*, *J. Chem. Soc. Chem. Commun.* **1998**, 2019–2020.
- 259 T. RUHLAND, H. KÜNZER, *Tetrahedron Lett.* **1996**, 2757–2760.
- 260 M. SCHUSTER, J. PERNERSTORFER, S. BLECHERT, *Angew. Chem. Int. Ed. Engl.* **1996**, 35, 1979–1980; *Angew. Chem.* **1996**, 35, 2111–2112.
- 261 T. GROTH, M. MELDAL, *J. Comb. Chem.* **2001**, 3, 34–44.
- 262 S. C. G. BIAGINI, S. E. GIBSON, S. P. KEEN, *J. Chem. Soc. Perkin Trans. 1* **1998**, 2485–2499.
- 263 D. A. HEERDING, D. T. TAKATA, C. KWON, *et al.*, *Tetrahedron Lett.* **1998**, 39, 6815–6818.
- 264 N. SCHMIEDEBERG, H. KESSLER, *Org. Lett.* **2002**, 4, 59–62.
- 265 D. LEE, J. K. SELLO, S. L. SCHREIBER, *Org. Lett.* **2000**, 2, 709–712.
- 266 R. E. SAMMELSON, M. J. KURTH, *Chem. Rev.* **2001**, 101, 137–202.
- 267 W. C. CHENG, M. M. OLMSTEAD, M. J. KURTH, *J. Org. Chem.* **2001**, 66, 5528–5533.
- 268 B. A. BURKETT, C. L. L. CHAI, *Tetrahedron Lett.* **1999**, 40, 7035–7038.

- 269 K. PAULVANNAN, T. CHEN, J. W. JACOBS, *Synlett* **1999**, 1609–1611.
- 270 Y. PEI, H. MOOS, *Tetrahedron Lett.* **1994**, 35, 5825–5828.
- 271 K.-H. PARK, J. EHLE, H. SPORRI, *et al.*, *J. Comb. Chem.* **2001**, 3, 171–176.
- 272 E. J. KANTOROWSKI, M. J. KURTH, *Mol. Div.* **1996**, 2, 207–216.
- 273 D. A. GOFF, *Tetrahedron Lett.* **1999**, 40, 8741–8745.
- 274 K. I. WASHIZUKA, K. NAGAI, S. MINAKATA, *et al.*, *Tetrahedron Lett.* **2000**, 41, 691–695.
- 275 R. SINGH, J. M. NUSS, *Tetrahedron Lett.* **1999**, 40, 1249–1252.
- 276 B. C. HONG, Z. Y. CHEN, W. H. CHEN, *Org. Lett.* **2000**, 17, 2647–2648.
- 277 K. HEINZE, *Chem. Eur. J.* **2001**, 7, 2922–3932.
- 278 S. DAHMEN, S. BRÄSE, *Synthesis* **2001**, 1431–1449.
- 279 P. GROS, F. LOUËRAT, Y. FORT, *Org. Lett.* **2002**, 4, 1759–1761.
- 280 P. I. DALKO, L. MOISAN, *Angew. Chem. Int. Ed. Engl.* **2001**, 40, 3726–3748; *Angew. Chem.* **2001**, 113, 3840–3864.
- 281 R. W. ARMSTRONG, A. P. COMBS, P. A. TEMPEST, *et al.*, *Acc. Chem. Res.* **1996**, 29, 123–131.
- 282 A. S. KISELYOV, L. SMITH, R. W. ARMSTRONG, *Tetrahedron* **1998**, 54, 5089–5096.
- 283 D. W. ZHANG, A. S. KISELYOV, *Synlett* **2001**, 1173–1175.
- 284 A. S. KISELYOV, L. SMITH, A. VIRGILIO, *et al.*, *Tetrahedron* **1998**, 54, 7987–7996.
- 285 A. L. KENNEDY, A. M. FRYER, J. A. JOSEY, *Org. Lett.* **2002**, 4, 1167–1170.
- 286 P. BLANEY, R. GRIGG, Z. RANKOVIC, *et al.*, *Tetrahedron Lett.* **2000**, 41, 6639–6642.
- 287 M. F. GORDEEV, D. V. PATEL, B. ENGLAND, *et al.*, *Bioorg. Med. Chem.* **1998**, 6, 833–889.
- 288 C. O. KAPPE, *Acc. Chem. Res.* **2000**, 33, 879–888.
- 289 D. G. HALL, S. MANKU, F. WANG, *J. Comb. Chem.* **2001**, 3, 125–150.
- 290 K. C. NICOLAOU, J. A. PFEFFERKORN, *Biopolymers (Peptide Science)* **2001**, 60, 171–193.
- 291 A. GANESAN, *Pure Appl. Chem.* **2001**, 73, 1033–1039.
- 292 H. WANG, M. M. SIM, *J. Nat. Prod.* **2001**, 64, 1497–1501.
- 293 K. L. SMITH, Z.-F. TAO, S. HASHIMOTO, *et al.*, *Org. Lett.* **2002**, 4, 1079–1082.
- 294 I. R. MARSH, M. BRADLEY, S. J. TEAGUE, *J. Org. Chem.* **1997**, 62, 6199–6203.
- 295 K. C. NICOLAOU, J. A. PFEFFERKORN, H. J. MITCHELL, *et al.*, *J. Am. Chem. Soc.* **2000**, 122, 9954–9967.
- 296 K. C. NICOLAOU, G.-Q. CAO, J. A. PFEFFERKORN, *Angew. Chem. Int. Ed.* **2000**, 39, 739–743; *Angew. Chem.* **2000**, 112, 755–759.
- 297 B. MESEGUER, D. ALONSO-DÍAZ, N. GRIEBENOW, *et al.*, *Angew. Chem. Int. Ed.* **1999**, 38, 2902–2906; *Angew. Chem.* **1999**, 111, 3083–3087.
- 298 K. C. NICOLAOU, N. WINSSINGER, D. VOURLOUMIS, *et al.*, *J. Am. Chem. Soc.* **1998**, 120, 10814–1826.
- 299 X.-Y. XIAO, Z. PARANDOOSH, M. P. NOVA, *J. Org. Chem.* **1997**, 62, 6029–6033.
- 300 K. C. NICOLAOU, J. A. PFEFFERKORN, A. J. ROECKER, *et al.*, *J. Am. Chem. Soc.* **2000**, 122, 9939–9953.
- 301 K. STRØMGAAARD, T. J. BRIER, K. ANDERSEN, *et al.*, *J. Med. Chem.* **2000**, 43, 4526–4533.
- 302 H. E. PELISH, N. J. WESTWOOD, Y. FENG, *et al.*, *J. Am. Chem. Soc.* **2001**, 123, 6740–6741.
- 303 C. A. LIPINSKI, F. LOMBARDO, B. W. DOMINY, *et al.*, *Adv. Drug Deliv. Rev.* **1997**, 23, 3–25.
- 304 R. G. FRANZÉN, *J. Comb. Chem.* **2000**, 2, 195–214.
- 305 S. N. FILIGHEDDU, S. MASALA, M. TADDEI, *Tetrahedron Lett.* **1999**, 40, 650–36506.
- 306 B. RUHLAND, A. BHANDARI, E. M. GORDON, *et al.*, *J. Am. Chem. Soc.* **1996**, 118, 253–254.
- 307 B. RUHLAND, A. BOMBRUN, M. A. GALLOP, *J. Org. Chem.* **1997**, 62, 7820–7826.
- 308 J. PITLIK, C. A. TOWNSEND, *Bioorg. Med. Chem. Lett.* **1997**, 7, 3129–3134.
- 309 B. A. KULKARNI, A. GANESAN, *J. Comb. Chem.* **1999**, 1, 373–378.
- 310 M. F. GORDEEV, E. M. GORDON, D. V. PATEL, *J. Org. Chem.* **1997**, 62, 8177–8181.
- 311 S. P. HOLLINSHEAD, *Tetrahedron Lett.* **1996**, 37, 9157–9160.
- 312 W. H. PEARSON, R. B. CLARK, *Tetrahedron Lett.* **1997**, 38, 7669–7672.



- 313 J. J. N. VEERMAN F. P. J. T. RUTJES, J. H. VAN MAARSEVEEN, *et al.*, *Tetrahedron Lett.* **1999**, 40, 6079–6082.
- 314 R. C. D. BROWN, M. FISCHER, *Chem. Commun.* **1999**, 1547–1548.
- 315 P. KAROYAN, A. TRIOLO, R. NANNICINI, *et al.*, *Tetrahedron Lett.* **1999**, 40, 71–74.
- 316 H. A. DONDAS, R. GRIGG, W. S. MACLACHLAN, *et al.*, *Tetrahedron Lett.* **2000**, 41, 967–970.
- 317 A. M. M. MJALLI, S. SARSHAR, T. J. BAIGA, *Tetrahedron Lett.* **1996**, 37, 2943–2946.
- 318 A. M. STROCKER, T. A. KEATING, P. A. TEMPEST, *et al.*, *Tetrahedron Lett.* **1996**, 37, 1149–1152.
- 319 A. W. TRAUTWEIN, G. JUNG, *Tetrahedron Lett.* **1998**, 37, 8263–8266.
- 320 A. W. TRAUTWEIN, R. D. SUBMUTH, G. JUNG, *Bioorg. Med. Chem. Lett.* **1998**, 8, 2381–2384.
- 321 G. C. B. HARRIMAN, *Tetrahedron Lett.* **1997**, 38, 5591–5594.
- 322 J. ZHANG, A. JACOBSON, J. R. RUSCHE, *et al.*, *J. Org. Chem.* **1999**, 64, 1074–1076.
- 323 C. HULME, L. MA, M. P. CHERRIER, *et al.*, *Tetrahedron Lett.* **2000**, 41, 1883–1887.
- 324 J. MATTHEWS, R. A. RIVERO, *J. Org. Chem.* **1998**, 63, 4808–4810.
- 325 B. A. KULKARNI, A. GANESAN, *Tetrahedron Lett.* **1998**, 39, 4369–4372.
- 326 P. C. MILLER, T. J. OWEN, J. M. MOLYNEAUX, *et al.*, *J. Comb. Chem.* **1999**, 1, 223–234.
- 327 S. HANESSION, R. Y. YANG, *Tetrahedron Lett.* **1996**, 37, 5835–5838.
- 328 A. R. FAR, T. T. TIDWELL, *J. Org. Chem.* **1998**, 63, 8636–8637.
- 329 J. M. ALVAREZ-GUTIERREZ, A. NEFZI, R. A. HOUGHTEN, *Tetrahedron Lett.* **2000**, 41, 609–612.
- 330 A. L. SMITH, G. I. STEVENSON, C. J. SWAIN, *et al.*, *Tetrahedron Lett.* **1998**, 39, 8317–8320.
- 331 C. POTHION, J. A. FEHRENTZ, A. AUMELAS, *et al.*, *Tetrahedron Lett.* **1996**, 37, 1027–1030.
- 332 T. T. ROMOFF, L. MA, Y. WANG, *et al.*, *Synlett* **1998**, 1341–1342.
- 333 D. R. BARN, J. R. MORPHY, *J. Comb. Chem.* **1999**, 1, 151–156.
- 334 A. ROUTLEDGE, C. ABELL, S. BALASUBRAMANIAN, *Synlett* **1997**, 61–62.
- 335 X. BEEBE, C. L. CHIAPPARI, M. M. OLMSTEAD, *et al.*, *J. Org. Chem.* **1995**, 60, 4204–4212.
- 336 X. BEEBE, N. E. SCHORE, M. J. KURTH, *J. Org. Chem.* **1995**, 60, 4196–4203.
- 337 M. ROTTLANDER, P. KNOCHEL, *J. Comb. Chem.* **1999**, 1, 181–183.
- 338 D. L. WHITEHOUSE, K. H. NELSON, S. N. SAVINOV, *et al.*, *Bioorg. Med. Chem. Lett.* **1998**, 6, 1273–1282.
- 339 M. R. GOWRAVARAM, M. A. GALLOP, *Tetrahedron Lett.* **1997**, 38, 6973–6976.
- 340 S. KOBAYASHI, T. WAKABAYASHI, M. YASUDA, *J. Org. Chem.* **1998**, 63, 4868–4869.
- 341 C. LE HETET, M. DAVID, F. CARREAUX, *et al.*, *Tetrahedron Lett.* **1997**, 38, 5153–5156.
- 342 Y. WATANABE, S. ISHIKAWA, G. TAKAO, *et al.*, *Tetrahedron Lett.* **1999**, 40, 3411–3414.
- 343 N. GOUAULT, J. F. CUPFI, A. SAULEAU, *et al.*, *Tetrahedron Lett.* **2000**, 41, 7293–7297.
- 344 S. MA, D. DUAN, Z. SHI, *Org. Lett.* **2000**, 2, 1419–1422.
- 345 H. STEPHENSEN, F. ZARAGOZA, *J. Org. Chem.* **1997**, 62, 6090–6097.
- 346 F. ZARAGOZA, *Tetrahedron Lett.* **1996**, 37, 6213–6216.
- 347 S. P. WATSON, R. D. WILSON, D. B. JUDD, *et al.*, *Tetrahedron Lett.* **1997**, 38, 9065–9068.
- 348 R. D. WILSON, S. P. WATSON, S. A. RICHARDS, *Tetrahedron Lett.* **1998**, 39, 2827–2830.
- 349 P. GROSCHKE, A. HOLTZEL, T. B. WALK, *et al.*, *Synthesis* **1999**, 1961–1970.
- 350 L. O. LYGSO, J. NIELSEN, *Tetrahedron Lett.* **1998**, 39, 5845–5848.
- 351 L. F. TIETZE, A. STEINMETZ, *Synlett* **1996**, 667–668.
- 352 L. F. TIETZE, A. STEINMETZ, F. BALKENHOHL, *Bioorg. Med. Chem. Lett.* **1997**, 7, 1303–1306.
- 353 S. KOBAYASHI, T. FURUTA, K. SUGITA, *et al.*, *Tetrahedron Lett.* **1999**, 40, 1341–1344.
- 354 P. Y. CHONG, P. A. PETILLO, *Tetrahedron Lett.* **1999**, 40, 2493–2496.
- 355 A. NEFZI, M. GIULIANOTTI, L. TRUONG, *J. Comb. Chem.* **2002**, 4, 175–178.
- 356 R. KITA, F. SVEC, J. M. J. FRECHET, *J. Comb. Chem.* **2001**, 3, 564–571.
- 357 C. ZHANG, E. J. MORAN, T. F. WOIWODE, *et al.*, *Tetrahedron Lett.* **1996**, 37, 751–754.
- 358 M. T. BILODEAU, A. M. CUNNINGHAM, *J. Org. Chem.* **1998**, 63, 2800–2801.

- 359 Y. YU, J. M. OSTRESH, R. A. HOUGHTEN, *J. Org. Chem.* **2002**, 67, 3138–3141.
- 360 A. NEFZI, M. A. GIULIANOTTI, R. A. HOUGHTEN, *J. Comb. Chem.* **2001**, 3, 68–70.
- 361 B. A. KULKARNI, A. GANESAN, *Tetrahedron Lett.* **1999**, 40, 5633–5636.
- 362 B. B. SHANKAR, D. Y. YANG, S. GIRTON, *et al.*, *Tetrahedron Lett.* **1998**, 39, 2447–2448.
- 363 J.-F. CHENG, A. M. M. MJALLI, *Tetrahedron Lett.* **1998**, 39, 939–942.
- 364 M. R. TREMBLAY, P. WENTWORTH, G. E. LEE, *et al.*, *J. Comb. Chem.* **2000**, 2, 698–709.
- 365 H. P. BUCHSTALLER, *Tetrahedron* **1998**, 54, 3465–3470.
- 366 P. TEN HOLTE, L. THIJS, B. ZWANENBURG, *Tetrahedron Lett.* **1998**, 39, 7407–7410.
- 367 W. J. HAAP, D. KAISER, T. B. WALK, *et al.*, *Tetrahedron* **1998**, 54, 3705–3724.
- 368 P. C. KEARNEY, M. FERNANDEZ, J. A. FLYGARE, *J. Org. Chem.* **1998**, 63, 196–209.
- 369 M. PATEK, B. DRAKE, M. LEBL, *Tetrahedron Lett.* **1995**, 36, 2227–2230.
- 370 C. P. HOLMES, J. P. CHINN, G. C. LOOK, *et al.*, *J. Org. Chem.* **1995**, 60, 7328–7333.
- 371 M. C. MUNSON, A. W. COOK, J. A. JOSEY, *et al.*, *Tetrahedron Lett.* **1998**, 39, 7223–7226.
- 372 F. ZARAGOZA, S. V. PETERSEN, *Tetrahedron* **1996**, 52, 10823–10826.
- 373 C. W. TORNØE, C. CHRISTENSEN, M. MELDAL, *J. Org. Chem.* **2002**, 67, 3057–3064.
- 374 Y. HU, S. BAUDART, J. A. PORCO JR. *J. Org. Chem.* **1999**, 64, 1049–1051.
- 375 N. HEBERT, A. L. HANNAH, S. C. SUTTON, *Tetrahedron Lett.* **1999**, 40, 8547–8550.
- 376 K. ROSSEN, J. SAGER, L. M. DiMICHELE, *Tetrahedron Lett.* **1997**, 38, 3183–3186.
- 377 W. ZHANG, W. XIE, J. FANG, *et al.*, *Tetrahedron Lett.* **1999**, 40, 7929–7933.
- 378 M. W. CRESWELL, G. L. BOLTON, J. C. HODGES, *et al.*, *Tetrahedron* **1998**, 54, 3983–3998.
- 379 M. F. GORDEEV, D. V. PATEL, B. P. ENGLAND, *et al.*, *Bioorg. Med. Chem. Lett.* **1998**, 6, 883–889.
- 380 M. F. GORDEEV, D. V. PATEL, E. M. GORDON, *J. Org. Chem.* **1996**, 61, 924–928.
- 381 M. F. GORDEEV, D. V. PATEL, J. WU, *et al.*, *Tetrahedron Lett.* **1996**, 37, 4643–4646.
- 382 I. C. COTTERILL, A. Y. USYATINSKY, J. M. ARNOLD, *et al.*, *Tetrahedron Lett.* **1998**, 39, 1117–1120.
- 383 G. R. PABST, K. SCHMID, J. SAUER, *Tetrahedron Lett.* **1999**, 39, 6691–6694.
- 384 D. G. POWERS, D. S. CASEBIE, D. FOKAS, *et al.*, *Tetrahedron* **1998**, 54, 4085–4096.
- 385 S. TADESSE, A. BHANDARI, M. A. GALLOP, *J. Comb. Chem. Chem.* **1999**, 1, 184–187.
- 386 A. R. KATRITZKY, L. SERDYUK, C. CASSAING, *et al.*, *J. Comb. Chem.* **2000**, 2, 182–185.
- 387 A. BARCO, S. BENETTI, C. DE RISI, *et al.*, *Tetrahedron Lett.* **1998**, 39, 7591–7594.
- 388 K. PAULVANNAN, T. CHEN, *J. Org. Chem.* **2000**, 65, 6160–6166.
- 389 A. S. WAGMAN, L. WANG, J. M. NUSS, *J. Org. Chem.* **2000**, 65, 9103–9113.
- 390 Y. WANG, S. R. WILSON, *Tetrahedron Lett.* **1997**, 38, 4021–4024.
- 391 W. CHAI, W. V. MURRAY, *Tetrahedron Lett.* **1999**, 40, 7185–7188.
- 392 L. F. TIETZE, T. HIPPE, A. STEINMETZ, *Synlett* **1996**, 1043–1044.
- 393 S. LECONTE, G. DUJARDIN, E. BROWN, *Eur. J. Org. Chem.* **2000**, 639–643.
- 394 A. D. PISCOPIO, J. F. MILLER, K. KOCH, *Tetrahedron Lett.* **1997**, 38, 7143–7146.
- 395 D. OBRECHT, C. ALBRECHT, A. GRIEDER, *et al.*, *Helv. Chim. Acta* **1997**, 80, 65–72.
- 396 T. MASQUELIN, D. SPRENGER, R. BAER, *et al.*, *Helv. Chim. Acta* **1998**, 81, 646–660.
- 397 A. L. MARZINZIK, E. R. FELDER, *J. Org. Chem.* **1998**, 63, 723–727.
- 398 J. S. PANEK, B. ZHU, *Tetrahedron Lett.* **1996**, 37, 8151–8154.
- 399 E. NIZI, M. BOTTA, F. CORELLI, *et al.*, *Tetrahedron Lett.* **1998**, 39, 3307–3310.
- 400 B. C. HAMPER, K. Z. GAN, T. J. OWEN, *Tetrahedron Lett.* **1999**, 40, 4973–4976.
- 401 P. WIPF, A. CUNNINGHAM, *Tetrahedron Lett.* **1995**, 36, 7819–7822.
- 402 S. KOŁODZIEJ, B. C. HAMPER, *Tetrahedron Lett.* **1996**, 37, 5277–5280.
- 403 D. A. GOFF, R. N. ZUCKERMANN, *Tetrahedron Lett.* **1996**, 37, 6247–6250.
- 404 C. HULME, J. PENG, G. MORTON, *et al.*, *Tetrahedron Lett.* **1998**, 39, 7227–7230.
- 405 T. VOJKOVSKY, A. WEICHSSEL, M. PATEK, *J. Org. Chem.* **1998**, 63, 3162–3163.
- 406 D. GOFF, *Tetrahedron Lett.* **1998**, 39, 1473–1476.

- 407 N. MOHAMED, U. BHATT, G. JUST, *Tetrahedron Lett.* **1998**, 39, 8213–8216.
- 408 K. SHREDER, L. ZHANG, J.-P. GLEESON, *et al.*, *J. Comb. Chem.* **1999**, 1, 383–387.
- 409 J. KOWALSKI, M.A. LIPTON, *Tetrahedron Lett.* **1996**, 37, 5839–5840.
- 410 B.O. SCOTT, A.C. SIEGMUND, C.K. MARLOWE, *et al.*, *Mol. Div.* **1996**, 1, 125–134.
- 411 V.S. GOODFELLOW, C.P. LAUDEMAN, J.I. GERRITY, *et al.*, *Mol. Div.* **1996**, 2, 97–102.
- 412 A.K. SZARDENINGS, T.S. BURKOTH, H.H. LU, *et al.*, *Tetrahedron* **1997**, 53, 6573–6593.
- 413 A.K. SZARDENINGS, D. HARRIS, S. LAM, *et al.*, *J. Med. Chem.* **1998**, 41, 2194–2200.
- 414 M. DEL FRESNO, J. ALSINA, M. ROYO, *et al.*, *Tetrahedron Lett.* **1998**, 39, 2639–2642.
- 415 W.R. LI, S.Z. PENG, *Tetrahedron Lett.* **1998**, 39, 7373–7376.
- 416 R.A. SMITH, M.A. BOBKO, W. LEE, *Bioorg. Med. Chem. Lett.* **1998**, 8, 2369–2374.
- 417 A. NEFZI, M.A. GIULIANOTTI, R.A. HOUGHTEN, *Tetrahedron Lett.* **1999**, 40, 8539–8542.
- 418 A. NEFZI, M.A. GIULIANOTTI, R.A. HOUGHTEN, *Tetrahedron Lett.* **1998**, 39, 3671–3674.
- 419 L. GAUZY, Y. LE MERRER, J.C. DEPEZAY, *Tetrahedron Lett.* **1999**, 40, 6005–6008.
- 420 A.D. PISCOPIO, J.F. MILLER, K. KOCH, *Tetrahedron Lett.* **1998**, 39, 2667–2670.
- 421 J. PERNERSTORFER, M. SCHUSTER, S. BLECHERT, *Synthesis* **1999**, 138–144.
- 422 A. NEFZI, J.M. OSTRESH, R.A. HOUGHTEN, *Tetrahedron Lett.* **1997**, 38, 4943–4946.
- 423 V. KRCHŇÁK, A.S. WEICHSEL, *Tetrahedron Lett.* **1997**, 38, 7299–7302.
- 424 Y. YU, J.M. OSTRESH, A.R. HOUGHTEN, *Org. Lett.* **2001**, 3, 2797–2799.
- 425 L.C. COOPER, G.G. CHICCHI, K. DINNELL, *et al.*, *Bioorg. Med. Chem. Lett.* **2001**, 11, 1233–1236.
- 426 L.W.D.F. MEUTERMANS, P.F. ALEWOOD, *Tetrahedron Lett.* **1995**, 36, 7709–7712.
- 427 A.J. BICKNELL, N.W. HIRD, S.A. READSHAW, *Tetrahedron Lett.* **1998**, 39, 5869–5872.
- 428 D.M. KETCHA, L.J. WILSON, D.E. PORTLOCK, *Tetrahedron Lett.* **2000**, 41, 6253–6257.
- 429 Y. WANG, T.N. HUANG, *Tetrahedron Lett.* **1998**, 39, 9605–9608.
- 430 K. YAMAZAKI, Y. KONDO, *Chem. Commun.* **2002**, 210–211.
- 431 C. MACLEOD, R.C. HARTLEY, D.W. HAMPRECHT, *Org. Lett.* **2002**, 4, 75–78.
- 432 K.C. NICOLAOU, A.J. ROECKER, J.A. PFEFFERKORN, *et al.*, *J. Am. Chem. Soc.* **2000**, 122, 2966–2967.
- 433 Y.C. CHI, C.M. SUN, *Synlett* **2000**, 591–594.
- 434 J.P. KILBURN, J. LAU, R.C.F. JONES, *Tetrahedron Lett.* **2000**, 41, 5419–5421.
- 435 A. MAZUROV, *Bioorg. Med. Chem. Lett.* **2000**, 10, 67–70.
- 436 Z. WU, P. REA, G. WICKHAM, *Tetrahedron Lett.* **2000**, 41, 9871–9874.
- 437 D. TUMELTY, K. CAO, C.P. HOLMES, *Org. Lett.* **2001**, 3, 83–86.
- 438 V. KRCHÁK, J. SMITH, J. VÁGNER, *Tetrahedron Lett.* **2001**, 42, 1627–1630.
- 439 B. YAN, H. GSTACH, *Tetrahedron Lett.* **1996**, 37, 8325–8328.
- 440 P. LOPEZ-CREMADES, P. MOLINA, E. ALLER, *et al.*, *Synlett* **2000**, 1411–1414.
- 441 X. BEEBE, D. WODKA, T.J. SOWIN, *J. Comb. Chem.* **2001**, 3, 360–366.
- 442 S.D. LEPORE, M.R. WILEY, *J. Org. Chem.* **1999**, 64, 4547–4550.
- 443 H. STEPHENSEN, F. ZARAGOZA, *Tetrahedron Lett.* **1999**, 40, 5799–5802.
- 444 D. CRAIG, M.J. ROBSON, S.J. SHAW, *Synlett* **1998**, 1381–1383.
- 445 K. RÖLFING, M. THIEL, H. KÜNZER, *Synlett* **1996**, 10361038.
- 446 J.M. COBB, M.T. FIORINI, C.R. GODDARD, *et al.*, *Tetrahedron Lett.* **1999**, 40, 1045–1046.
- 447 J. ZHANG, J. BARKER, L. BOLIANG, *et al.*, *Tetrahedron Lett.* **2001**, 42, 8405–8408.
- 448 S. MAKINO, E. NAKANISHI, T. TSUJI, *Tetrahedron Lett.* **2001**, 42, 1749–1752.
- 449 B. ATRASH, M. BRADLEY, R. KOBYLECKI, *et al.*, *Angew. Chem. Int. Ed. Engl.* **2001**, 40, 938–941; *Angew. Chem.* **2001**, 113, 964–967.
- 450 V. KRCHŇÁK, J. SMITH, J. VÁGNER, *Tetrahedron Lett.* **2001**, 42, 2443–2446.
- 451 Z. WU, N.J. EDE, *Tetrahedron Lett.* **2001**, 42, 8115–8118.
- 452 A.N. ACHARYA, J.M. OSTRESH, R.A. HOUGHTEN, *Tetrahedron* **2002**, 58, 221–225.
- 453 C.L. LEE, K.P. CHAN, Y. LAM, *et al.*, *Tetrahedron Lett.* **2001**, 42, 1167–1169.

- 454 X. OUYANG, N. TAMAYO, A. S. KISELYOV, *Tetrahedron* **1999**, 55, 2827–2834.
- 455 M. K. SCHWARZ, D. TUMELTY, M. A. GALLOP, *J. Org. Chem.* **1999**, 64, 2219–2231.
- 456 A. NEFZI, N. A. ONG, M. A. GIULIANOTTI, *et al.*, *Tetrahedron Lett.* **1999**, 40, 4939–4942.
- 457 A. KAMAL, G. S. K. REDDY, K. L. REDDY, *Tetrahedron Lett.* **2001**, 42, 6969–6971.
- 458 G. BHALAY, P. BLANEY, V. H. PALMER, *et al.*, *Tetrahedron Lett.* **1997**, 38, 8375–8378.
- 459 B. A. BUNIN, J. A. ELLMAN, *J. Am. Chem. Soc.* **1992**, 114, 10997–10998.
- 460 X. OUYANG, A. S. KISELYOV, *Tetrahedron* **1999**, 55, 8295–8302.
- 461 J. HABERMANN, S. V. LEY, R. SMITS, *J. Chem. Soc. Perk. Trans. I* **1999**, 17, 2421–2423.
- 462 P. GARIBAY, P. H. TOY, T. HOEG-JENSEN, *et al.*, *Synlett* **1999**, 1438–1440.
- 463 P. GARIBAY, P. VEDSØ, M. BEGTRUP, *et al.*, *J. Comb. Chem.* **2001**, 3, 332–340.
- 464 A. S. BHAT, J. L. WHETSTONE, R. W. BRUEGGEMEIER, *J. Comb. Chem.* **2000**, 2, 597–599.
- 465 B. T. WATSON, G. E. CHRISTIANSEN, *Tetrahedron Lett.* **1998**, 39, 6087–6090.
- 466 J. J. BALDWIN, *Mol. Diversity* **1996**, 2, 81–88.

## 4

**Solid-Phase Bound Catalysts: Properties and Applications**

THOMAS FRENZEL, WLADIMIR SOLODENKO and ANDREAS KIRSCHNING

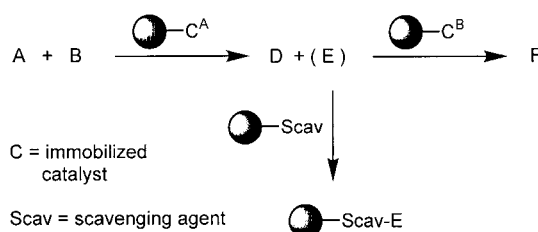
## 4.1

**Introduction**

It all started with Bruce Merrifield [1] who introduced solid supports, particularly cross-linked polystyrene as insoluble matrices to organic synthesis [2]. The solid-phase technique totally changed polypeptide and polynucleotide synthesis and in the early 1990s it set the stage for combinatorial chemistry [3]. In this context, the utilization of functional polymers as reagents [4] and catalysts [5] has flourished only sluggishly. It is not the substrate which remains attached to the solid support during a multi-step synthesis until it is finally cleaved from the support, but instead, the immobilized reagent or catalyst promotes a chemical transformation of a substrate which is present in solution (Scheme 4.1). Thus, a catalytically promoted reaction may yield product D from starting compounds A and B. If a by-product is formed or one of the starting materials was employed in excess a scavenging reagent can be introduced for the purpose of purification [6]. Furthermore, a multi-step sequence becomes feasible if the product is directly converted into product F using a second solid-supported catalyst. This solution-phase concept is very familiar to organic chemists, as reactions can be monitored using known analytical techniques like thin layer chromatography.

In the 1970s and 1980s, however, it was believed that the key to wider use of solid-phase supported reagents and catalysts is their adoption in industry for fine chemical and pharmaceutical manufacturing on a large scale. In fact, this restricted view hampered their wide use [7]. The dramatic developments in the need for compound library preparation in pharmaceutical and agrochemical industries have finally removed functionalized supports from their academic corner and helped “reinvent” them for industrial purposes and applications.

Among functionalized supports, immobilized catalysts will play a far greater role in future applications compared with polymer-bound reagents. This field is only recently experiencing intense research efforts, particularly since chiral ligand systems for asymmetric transformations using homogeneous transition metal catalysts have been developed and widely applied in research laboratories. Their immobilization will allow their efficient use in preparing compound libraries with enhanced structural complexity compared with what is still being published by



**Scheme 4.1** The concept of polymer-assisted solution phase synthesis with immobilized catalysts.

high throughput synthesis laboratories. Furthermore, these immobilized homogeneous catalysts will become attractive tools for drug synthesis and fine chemicals. In contrast, stoichiometrically applied solid-phase bound reagents will most likely see selective use in pharmaceutical research, in the derivatization of biologically relevant molecules and for certain transformations in fine chemical synthesis such as selective and efficient oxidations.

Indeed, immobilization of catalysts to a solid phase involves various advantages over conventional solution-phase chemistry:

1. The ease of separation of the supported species from a reaction mixture by filtration and washing;
2. Reuse of a catalyst after regeneration;
3. Their adaptability to continuous flow processes and hence use in automated synthesis;
4. The reduced toxicity and odor of supported species compared with low molecular weight species;
5. Chemical differences, such as prolonged activity or altered selectivity of a catalyst in supported form compared with its soluble analog.

Furthermore, polymer-assisted solution-phase syntheses also show several advantages over Merrifield-type syntheses. Except for some industrially employed heterogeneous catalysts the requirement of high loading capacities for the solid supports is not necessarily of prime importance for immobilized catalysts. Because not every site needs to react, lower loadings are acceptable. The recovered catalyst is often available for immediate reuse. A discussion on immobilized catalysts should also include a brief listing of obstacles associated with their use, particular in comparison to their soluble analogs:

1. Higher costs;
2. Lower reactivities caused by diffusional limitations;
3. Greater difficulty of structural analysis of the supported species;
4. The inability to separate solid-supported impurities.

From this discussion it becomes clear that the community of academic and industrial chemists sees great future prospects particularly for solid-phase bound transition metal catalysts despite the fact that it is a very young field and that not all expectations have been fulfilled so far. A major problem is that transition metals are often not bound irreversibly, and their complexes are not as stable as they were

once thought to be. Still, they combine the best of both worlds: heterogeneous and homogeneous catalysis.

## 4.2

### The Solid Support

A key element of solid-phase-assisted chemistry, which has been underscored by most chemists, is the support itself. However, it is evident from the discussion so far that the supports used are still far from ideal in several respects and that there is considerable scope to prepare improved supports [8]. Indeed, this has become a very active interdisciplinary area of research. Many reviews have been devoted to the various supports employed in solid-phase-assisted synthesis [9, 10] together with some reviews devoted to the physical properties of resins [11].

#### 4.2.1

##### Polymer Supports

Two aspects of solid-supported synthesis using immobilized catalysts are particularly important: on one hand, one has to elaborate the optimum approach for the attachment of the catalytically active species, on the other, the chemical and physical properties of the solid phase need to be well chosen to achieve the best results. In most cases a discussion of the former aspect is identical for both a polymeric and inorganic support. Thus, attachment of chemical functionality (a ligand or a metal) to polymeric supports has been realized by physical adsorption or by chemical bonding. The former technique is sometimes unsatisfactory. Dissociation can occur too easily and hence this method is particularly unsuitable for column or cyclic applications. Chemical attachment has been achieved by ionic, coordinative interactions and in an increasing number of cases by covalent bonding. The former mode of attachment is mainly found in ion-exchange resins and is highly attractive for generating rare earth-derived catalysts (see above). These catalysts are very easily regenerated as most of them only require treatment with an excess of the ionic reactant for generation. In contrast, ligands that will bind the catalytically active metal center are preferentially loaded to polymeric support by covalent attachment. It should be noted that the discussion of attachment covers in most cases both a polymeric and an inorganic support.

With respect to the polymeric backbone, two approaches exist for the preparation of functional polymers, the polymerization or copolymerization of monomers which carry the desired functionality, and secondly the chemical modification of preformed polymers. The former concept, the polymerization of prefunctionalized monomers, was often tested in the 'early days' of polymer-assisted syntheses, e. g. in the preparation of polymers containing pyridine [12] or quinone [13] residues, and benzaldehyde [14] or phosphine [15] functionalities. Although the latter approach demands that the synthetic organic chemist acquires profound knowledge of polymers and polymerization, this strategy can have advantages because

most supports employed today are still far from ideal. A recent example was disclosed by Masaki *et al.* who reported the copolymerization of ethylene glycol dimethylacrylate (EGDMA) with dicyanoketene acetal homodimer to provide a polymer-supported  $\pi$ -acid [16]. In conjunction with olefin metathesis polymerization, the first concept has recently seen a renaissance [17]. However, it is mainly the second approach that has been exploited in the preparation of polymer-bound catalysts. Cross-linked poly(styrene-co-divinylbenzene) resins (1% or 2% cross-linking) are widely used as functionalized polymers because of their stability, reasonably high loading capacity ( $>1 \text{ mmol g}^{-1}$ ), and good swelling characteristics. Important features of polystyrenes are their compatibility with a variety of nonprotic solvents and that many functionalized analogs are commercially available. Recently, Bradley and coworkers conducted a detailed and thorough study on the impact the degree of cross-linking in polystyrenes exerts on the “synthetic properties” of the polymer [18]. Thus, 0.3% cross-linked polymers swell to almost nine times their dry volume in chloroform. Rate enhancement of up to 500% was observed for cleavage reactions from resins with cross-linking between 6% and 0.3%. However the purity of the cleaved products (e.g. peptides like Kawaguchi-peptin B) decreased with decreasing cross-linking. These results are in accordance with earlier observations [9e, 19]. In many cases, reactions carried out under homogeneous conditions are the same in terms of efficiency and selectivity as reactions of polymer-supported species. This statement loses some of its generality when considering that as much as 99% of functional groups are within a polymer bead of diameter of ca 100  $\mu\text{m}$ . Thus, most of the reactive reactants in solution will have to enter into the beads to react in a gel phase. Swelling of the polymers with organic solvents is one method of choice for gaining better access to the reactive sites of the polymer prior to its use [18]. However, in this context it is important to recall that the extent of swelling decreases markedly as the percentage of cross-linking increases from 1% to 2% and even higher values. The choice of reaction solvent is therefore crucial in polymer-supported reactions and the best solvent may not be the same as the one commonly applied in the analogous reaction using low molecular mass reactants. Still, the diffusion of the soluble substrate into the active sites in beads is rate-limiting and therefore, in some cases, this can result in the supported catalyst displaying a pronounced size selectivity [9e, 19, 20]. The differences are caused by the fact that a more bulky molecule diffuses more slowly to the reactive sites in the beads. Another effect that needs consideration arises when the polarity of the microenvironment within the beads differs significantly from that of the solvent outside. This difference can either facilitate or distract a low molecular mass reactant from approaching the active sites.

Generally, it is believed that attaching reactive species to a polymer support leads to site isolation. But in fact, many examples are known which clearly indicate that functional groups on a bead do interact with each other [9e, 21]. A typical loading of functional groups on a polystyrene-based support is around  $1 \text{ mmol g}^{-1}$ . This results in a concentration of reactive groups of around  $0.33 \text{ mol dm}^{-3}$  provided that the reaction solvent is able to swell the polymer by a factor of 3. One strategy to circumvent the ease of site-site interaction is by increasing the percentage of cross-linking



which is expected to reduce chain mobility. It is also important to note that the supported substrate molecule can act as a flexible spacer group which facilitates site-site interactions. In this respect, the strategy of polymer-supported catalysts has clearly advantages over the construction of molecules on a polymer support, as high loading capacities are not required. It is noteworthy that for some processes the site-site interaction can play an important role. For example, the positive correlation between the rate of the reaction and the probability of catalyst interaction on the support surface was observed for the hydrolytic kinetic resolution of terminal epoxides using immobilized cobalt–salen complexes. The authors suggest a cooperative mechanism for this reaction implying that two catalytic units interact simultaneously with one substrate molecule [22]. Recently, microencapsulation technique appeared on the scene of immobilized catalysts [23]. One of the earliest synthetic uses of these materials was described by Reetz and Lohmer who showed that the Heck reaction can be performed in the absence of phosphane ligands [23a]. Also triphenylphosphine palladium can be immobilized by this way. Polystyrene and the catalysts are dissolved in a suitable solvent like cyclohexane and precipitation is slowly initiated by cooling to 0 °C. This procedure finally results in microcapsules which physically envelop the catalysts. The attachment is further enhanced by electronic  $\pi$ -interaction between the benzene rings of the polymer and vacant orbitals of the catalyst [23b–d].

Some of the restrictions in accessing active sites may also be overcome by using macroporous or macroreticular polymers [24]. These polymers are usually prepared by suspension polymerization in the presence of a porogen to afford 20–40% cross-linked polystyrene beads. Typically, such beads have a rigid porous structure and commonly do not swell in most organic solvents. Some commercial macroporous polymeric supports, in particular certain anion-exchange resins, are ideally suited for making anions available for reactions in nonaqueous solvents [25]. For example, the periodate form of such resins cleaves diols in a wide range of different solvents like ethanol, chloroform, diethyl ether, benzene and even water [26]. Another advantage of macroporous resins is their dimensional stability which makes them ideally suited for column applications where better solvent flow rates can be achieved than would be the case with gel polymers.

Contrary to the use of cross-linked polystyrenes and the concept of macropores, non-cross-linked polystyrene copolymer supports have been introduced to overcome restrictions to access active sites [27]. These polymers are soluble in most organic solvents but precipitate in cold methanol or other solvents [28, 29]. This development is in line with the use of other soluble polymers and in particular soluble poly(ethylene glycol) (PEG) [30] in polymer-supported synthesis. In many cases, these soluble supports truly behave like reactants in homogenous reactions [31]. Major disadvantages of PEG-ethers are (a) that they are highly hygroscopic and (b) typically have low loading capacities (0.2 mmol g<sup>-1</sup>). Often, large amounts of solvent are required to quantitatively precipitate the soluble polymer. The latter drawback makes their employment in automated parallel synthesis very cumbersome.

The merging of the properties of cross-linked polystyrene and soluble PEG is achieved in so called tentagels. Here, the hydrophobic properties of cross-linked

polystyrenes have been substantially offset by carrying out graft polymerization of ethylene oxide inside the beads [32]. Tentagels and related AgroGels show low loading capacities (about  $0.2 \text{ mmol g}^{-1}$ ) which makes them difficult to use in stoichiometric transformations. However, they are very well suited for catalytic applications. Another way forward is to investigate beads prepared using longer more flexible cross-linking agents than divinyl benzene. Such networks are likely to be superior in terms of accessibility compared with the common polystyrene beads [33]. Bradley and coworkers have further developed the concept of tentagels by grafting various branched dendrimers like polyamines (PAMAM) onto polystyrene backbones in order to amplify resin loading sites [34].

Functionalized hyperbranched polymers see increasing relevance in solid-phase-assisted synthesis [35]. Bergbreiter and coworkers devised new polymer supports by hyperbranching crafting chemistry. Here polyethylene was the starting point which was functionalized after chromium(VI) oxidation [36]. An even simpler branching concept was reported by Frey and Haag. They described the controlled synthesis of well-defined hyperbranched polyglycerols [37] which, like related polymers [38], have very high loadings ( $4\text{--}8.8 \text{ mmol g}^{-1}$ ) and are superior to dendrimers in terms of preparative accessibility. As pointed out by the authors, reagents or catalysts attached to these soluble polymeric supports may conveniently be used in continuous reactors using membrane techniques. Amphiphilic polymers prepared by esterification of polyglycerol scaffolds with palmitoyl chloride are able to solubilize  $\text{PdCl}_2$  and finally afford nanoparticles of Pd within these amphiphilic hyperbranched polyglycerols. These clusters show catalytic activity in hydrogenation reactions [39].

Typical examples of some catalysts which are attached to different polymeric supports discussed here are listed in Fig. 4.1.

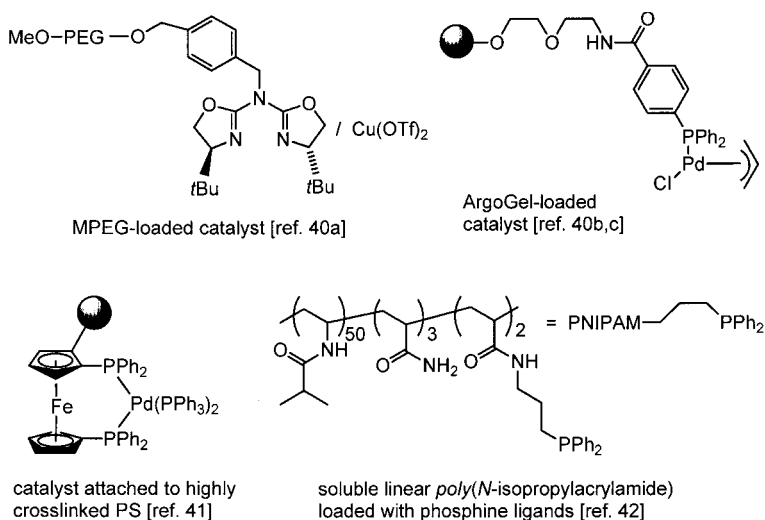


Fig. 4.1 Selected examples of polymer supports for the immobilization of catalysts.

Finally, the question needs to be raised what is the best polymer support for immobilization of catalysts thereby retaining the full activity and selectivity as is known for the solution-phase catalysts. So far not enough data have been accumulated to provide a simple recipe. Sherrington and coworkers carried out a detailed study on resin-supported Pt catalysts and found that the most active and stable polymer catalysts have highest surface area ( $550 \text{ m}^2 \text{ g}^{-1}$ ) along with the lowest ligand and Pt contents ( $0.25 \text{ mmol g}^{-1}$ ). These are conditions under which maximum accessibility to potential metal complex catalytic sites and discrete isolated ligand-Pt species are guaranteed [43].

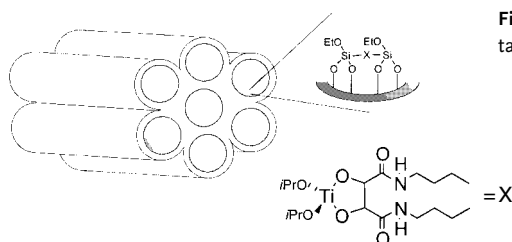
#### 4.2.2

##### Inorganic Supports

Although this book is dedicated to polymeric supports we felt that for the purpose of comparison and completeness it is important to include a brief chapter on inorganic supports. Inorganic materials are increasingly used in heterogenization techniques and show some altered properties compared with polymers. Indeed, dramatic improvements in the design of ideal supports for catalysts have recently been observed in the field of inorganic materials [10]. In general, inorganic supports do not tend to swell, which makes them ideal supports for use in continuous reactors. Indeed, mesoporous phases based on zeolites, glass and metal oxides, of which MCM-41 is the most prominent member, have appeared as highly promising supports in solid-phase-assisted synthesis, [44] mainly as catalysts [5f, 45]. These materials using surfactant micellar structures as templates have very high surface area ( $>1000 \text{ m}^2 \text{ g}^{-1}$ ). Techniques have been developed that allow construction of pores of highly defined size [46]. They are composed of an ordered pore structure which is mostly an hexagonally packed array of inorganic tubules ranging from 20–100 Å in diameter. Remarkably, they show an extremely narrow pore size distribution and the pore diameter can be adjusted from 2 to 15 nm. In some cases pore tailoring methods have been developed by which the pore-opening sizes of MCM-41 materials can be finely tuned without significant loss in pore volume and surface area [47]. Co-condensation of reactive species during the mesopore synthesis is a method to incorporate functionality into the walls of the channel system [48]. In this way, organometallic complexes can be attached which lead to immobilized catalysts that were originally designed for homogeneous catalysis (Fig. 4.2) [49, 50]. Reactions [51] that have so far been conducted with these novel catalysts are the Heck reaction [52], epoxidations [53], C–H activation [54], and Ziegler–Natta polymerization [55].

Along this line, sol–gel materials based on  $\text{SiO}_2$  find increasing use in solid-phase assisted synthesis. The sol–gel synthesis creates well ordered porous glasses which retain a rigid and exposed surface area ( $300\text{--}1000 \text{ m}^2 \text{ g}^{-1}$ ) [56]. Gelation occurs after a sol is cast into a mold so that the monolithic samples can be tailored to a desired size or shape [57].

Recently, the first stable organic analog of a zeolite was prepared [58] which showed catalytic properties in the base-catalyzed Knoevenagel condensation. In



**Fig. 4.2** MCM-41-type zeolites and attachment of organic ligands.

their remarkable work the authors employed lyotropic liquid crystals, which are organized in hexagonal channels in an aqueous environment. Depending on the amount of water used an inverted supramolecular structure is formed with the polar carboxylates directed into the channel with counteranions densely packed. These conglomerates were cross-linked in the presence of divinyl benzene which froze the cylindrical hexagon.

Composites of inorganic and organic material are emerging in this field like tailored palladium containing silica spheres. Here palladium containing silica spheres are tailored by a multi-step procedure consisting of the preparation of ion exchange resin–silica composites, Pd ion exchange, and finally calcination [59]. Sol–gel preparations of macroporous silica gel films by templating with polystyrene microspheres have been described which are composed of thin macroporous silicate films with controllable porosity for catalysis and chemical sensing related applications [60].

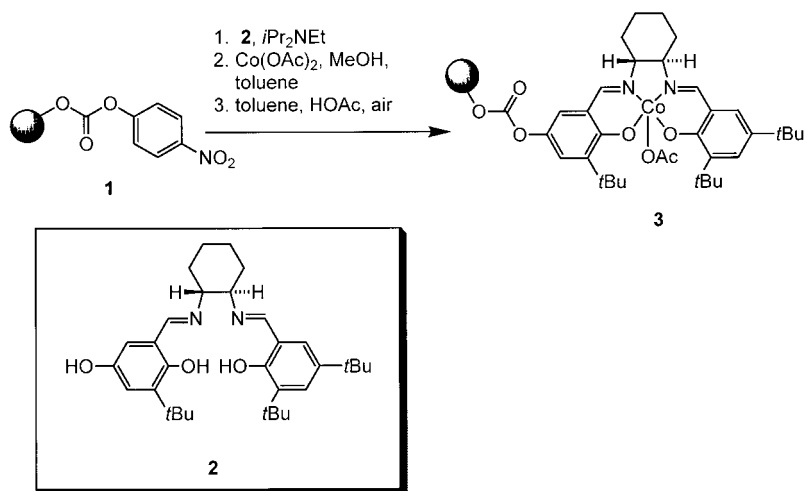
#### 4.2.3

#### Selected Examples for Attachment of Ligands to Solid Supports

The preparation of solid-phase bound homogeneous catalysts is often accompanied with multi-step synthesis on the chosen support. This implies that the linkers have to be well chosen, as is known from solid-phase synthesis [3, 4]. To give a demonstration of this “extra work” some examples of attachment of important chiral catalysts are given in this section.

A very important class of versatile chiral ligands is the group of salen ligands (e.g. ligand **(2)** as depicted in Scheme 4.2) first reported by Jacobsen and co-workers [61]. Depending on the number and nature of substituents attached to the phenyl rings as well as the choice of metal very effective chiral catalysts for the epoxidation of alkenes, the kinetic resolution of oxiranes in the presence of nucleophiles as well as enantioselective Diels–Alder reactions are obtained [62]. Jacobsen's group also developed a general method for the covalent attachment of salen complexes **(3)** to two types of supports, namely polystyrene **(1)** and silica (Scheme 4.2) [22]. The systems have shown to be efficient and highly enantioselective catalysts for the hydrolytic kinetic resolution of terminal epoxides. The supported catalysts are recyclable without loss of activity and selectivity.

Another chiral ligand which plays an increasingly important role in asymmetric catalysis is TADDOL (*a, a', a', a'*-tetraaryl-1,3-dioxolane-4,5-dimethanol) [63]. Various attempts have been made to immobilize this chiral system to various solid sup-



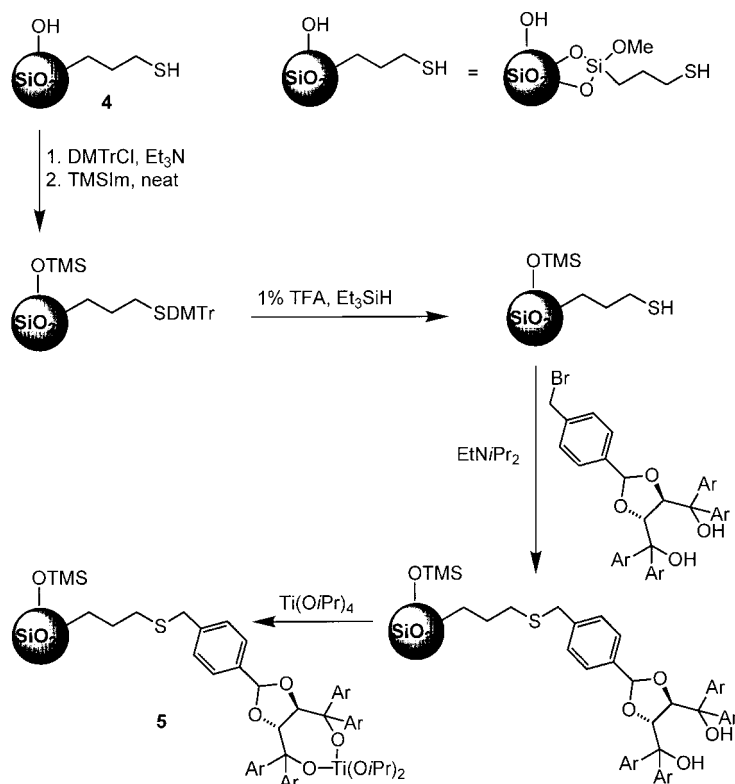
**Scheme 4.2** Preparation of a polymer-bound salen complex.

ports [64]. A comprehensive paper was recently disclosed by Seebach and Heckel which thoroughly describes the preparation and characterization of TADDOL derivatives (**5**) containing different aryl groups which were immobilized via a thioether linkage on hydrophobic controlled-pore glass-silica gel (**4**) (Scheme 4.3) [65]. This inorganic material has the advantage that it is a rigid support that offers an openly accessible pore structure in all possible solvents and in a wide temperature and pressure range. In addition, they employed it in enantioselective heterogeneous catalysis thereby comparing it with the soluble analogs.

Alternatively, polystyrene-based solutions were developed. Best results for immobilization were found when TADDOL derivatives (**6**) and (**7**) containing phenolic hydroxy groups were prepared in solution and anchored to Merrifield resin (Scheme 4.4) [66]. The authors managed to couple (**7**) to PS-DVB polymers with different loading and cross-linking degrees as well as on polyethylene polymer which contained polyvinylbenzyl chloride chains (SMOP-3-resins).

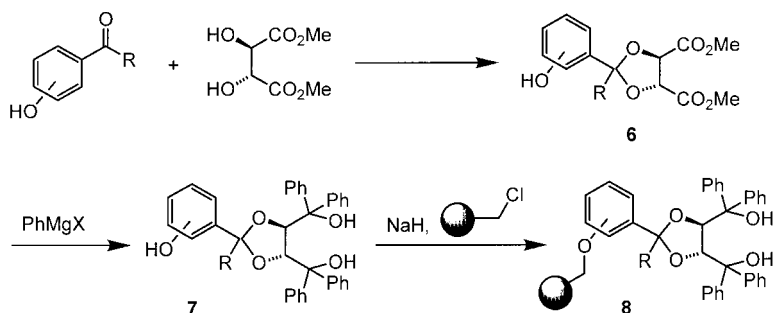
Additionally, TADDOL derivative (**9**) which contained an additional styrene group was first prepared in solution and then underwent bulk polymerization in the presence of various porogenic agents in order to obtain solid-phase-bound catalyst (**10**) with the desired porosity (Scheme 4.5) [67].

So far, few data are available which allow the comparison of differences in efficacy and selectivity of one catalytic system attached to different supports. As far as the TADDOLate complexes are concerned, no clear rules can be drawn. Polystyrene-based catalysts derived from (**8**) and (**10**) show similar enantioselectivities and reaction rates. Differences appear, however, when comparing them with a polystyrene-embedded dendritic ligand system, generated by co-polymerization from TADDOL-derivative (**32**) (Scheme 4.18) which is described in Section 4.3.2.1. Recyclability seems to be easier for the dendritic catalyst and the enantioselectivity,

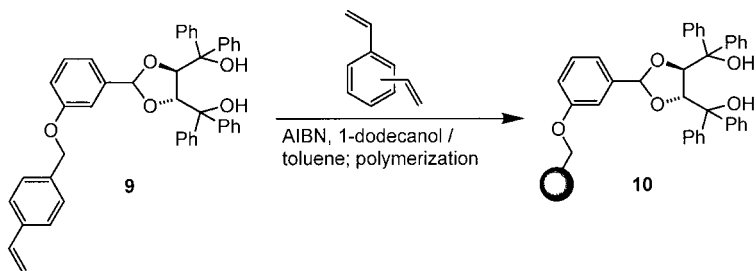


**Scheme 4.3** Preparation of a TADDOLate-complex bound to controlled-pore-glass-silica.

which is comparable, does decrease to a lesser extent for each run compared with (8) and (10). However, reactions employing the (32)-derived catalyst (refer to scheme 4.18) proceed at a lower reaction rate. Interestingly, Altava and coworkers reported that the TADDOLates give opposite stereoselectivity in Diels–Alder cycloaddition reactions depending on whether the catalyst is prepared by grafting TADDOL-derivatives to polystyrene or by copolymerization of styrene modified by the ligand [67]. CPG-supported TADDOLate (Scheme 4.3) is supposed to be the most inert support that offers an accessible pore structure in all possible solvents and in a wide temperature and pressure range. It will need a lot of further fundamental research until general and applicable recipes for the best solid phase/linker/catalyst combinations can be given.



**Scheme 4.4** Attachment of TADDOL to polystyrene by grafting.



**Scheme 4.5** Attachment of TADDOL to polystyrene by polymerization of functionalized styrene.

### 4.3

#### Applications in Catalysis

This report presents only a selection of recent applications with solid-phase bound catalysts; for additional examples the reader is referred to the excellent review by Janda and coworkers [5 b].

##### 4.3.1

#### Polymer Supported Oxidations

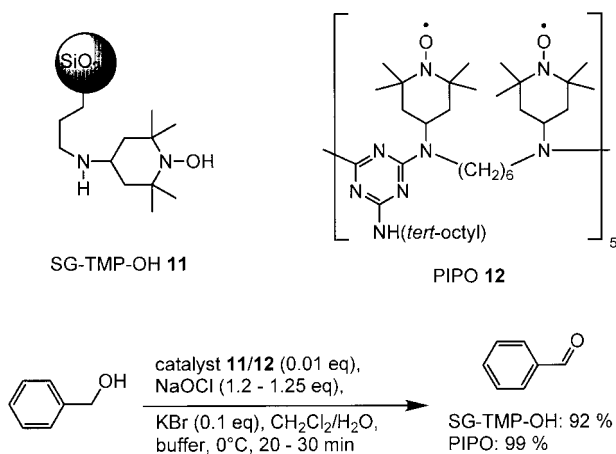
Oxidations of various organic functional groups such as alcohols or alkenes are some of the most important transformations in organic chemistry. Unfortunately, their use is sometimes restricted by poor selectivities or the need for transition metals and other species, which might be toxic or difficult to remove during work-up. Therefore, numerous attempts have been made to immobilize oxidants on a solid support [4], and these are compiled in the following.

## 4.3.1.1 Oxidation of Alcohols

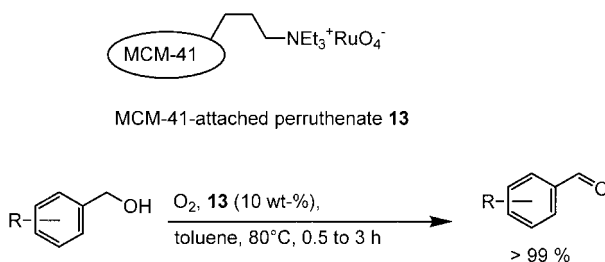
Some successful attempts to immobilize catalysts for the oxidation of alcohols to carbonyl compounds involve the attachment of TEMPO-derivatives to a solid phase. Bolm *et al.* were the first to immobilize 1-hydroxy-2,2,6,6-tetramethylpiperidine to modified silica gel (SG-TMP-OH) (**11**) and applied in the oxidation of multifunctional alcohols [68]. Other groups further investigated the use of polymer-supported TEMPO [69]. This system allowed the oxidation of alcohols to aldehydes and ketones, respectively, using bleach to regenerate the immobilized nitroxyl radical (Scheme 4.6).

In another approach, a polymer-bound TEMPO-species, referred to as PIPO (polyamine immobilized piperidinyl oxyl), was derived by oxidation of commercially available Chimasorb 944, an oligomeric sterically hindered amine. Together with bleach as co-oxidant PIPO (**12**) afforded aldehydes and ketones in short reaction times and with yields from 80 to > 99% (Scheme 4.6) [70].

Ley *et al.* performed oxidations of activated (benzylic, allylic) alcohols by employing polymer-attached perruthenate catalysts and oxygen as oxidant. Triethylammo-



**Scheme 4.6** Solid-phase supported TEMPO-species.



**Scheme 4.7** Solid-phase supported perruthenate.



nium perruthenate derivatives were immobilized within the internal pore system of MCM-41 (**13**) (Scheme 4.7) [71].

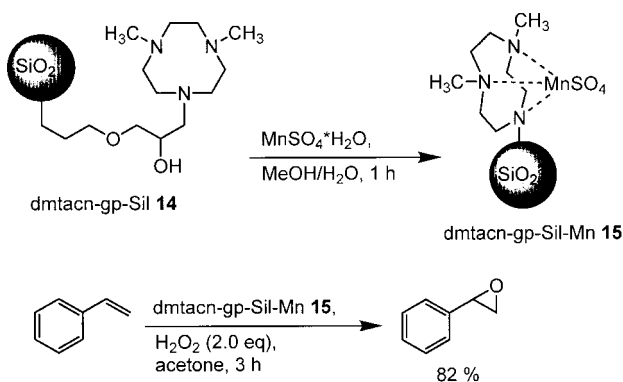
In this context, it was shown that polymer-supported triphenylphosphine as a ligand for metal-based oxidation is an alternative catalytic system [72].

#### 4.3.1.2 Epoxidation of Alkenes

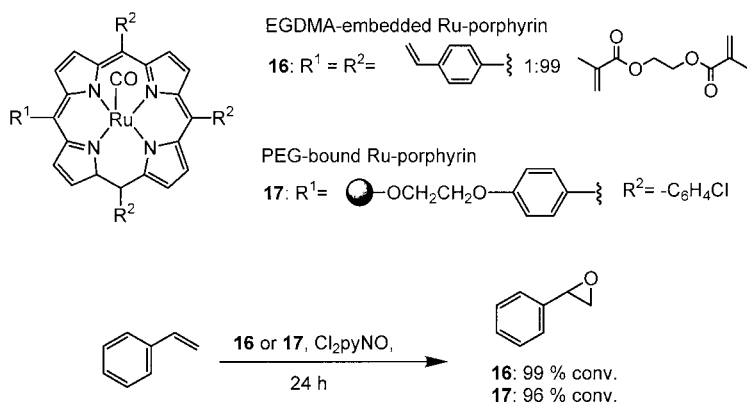
Epoxidation of alkenes are particular powerful and well-established stereospecific methods for synthetic chemistry. Numerous efforts have been conducted to establish solid-supported oxidants for this purpose. By attaching 1,4-dimethyl-1,4,7-triazacyclononane (dmtacn) via a 3-glycidyloxypropyl linker to silica, Jacobs *et al.* created an immobilized ligand (**14**) (dmtacn-gp-Sil) that was capable of coordinating manganese. The resulting complex (**15**) catalyzes the epoxidation of terminal and disubstituted olefins under mild conditions using  $\text{H}_2\text{O}_2$  as oxidant. Yields varied from 58 to 82% (Scheme 4.8). Interestingly, when disubstituted olefins were used, yields decreased and vicinal *cis*-diols were formed as by-products to some degree [73].

Other examples involve the immobilization of ruthenium porphyrin catalysts [74]. While Severin *et al.* generated insoluble polymer-embedded catalysts **16** by co-polymerizing porphyrin derivatives with ethylene glycol dimethacrylate (EGDMA) [74a], Che *et al.* linked the ruthenium–porphyrin unit to soluble polyethylene glycol (PEG) **17** [74b]. Both immobilized catalysts were employed in a variety of olefin epoxidations with 2,6-dichloropyridine *N*-oxide ( $\text{Cl}_2\text{pyNO}$ ), providing similar conversions of up to 99% and high selectivities (Scheme 4.9).

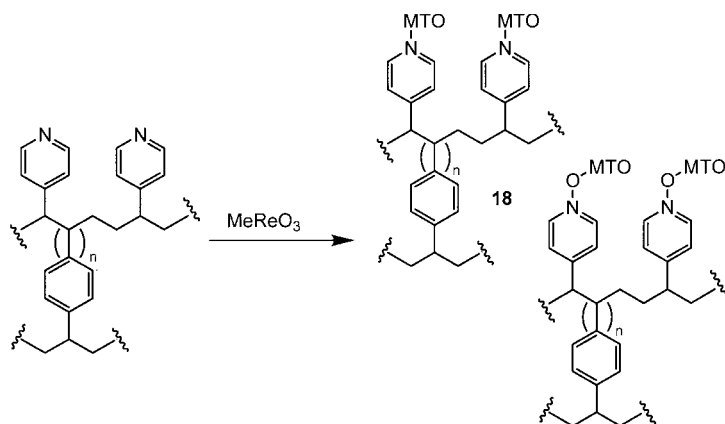
Methylrheniumtrioxide (MTO) can straightforwardly be immobilized using copolymers consisting of polystyrene and polyvinyl pyridine. The authors proposed two possible structures **18** shown in Scheme 4.10. In the presence of  $\text{H}_2\text{O}_2$  these catalysts are efficient and selective heterogeneous catalysts for the epoxidation of alkenes. It was shown that their activity is maintained for at least five recycling experiments [23d]. In analogy to this work, bipyridyl-functionalized mesoporous silica can be employed for the immobilization of MTO [75].



**Scheme 4.8** Silica-supported 1,4-dimethyl-1,4,7-triazacyclononane in epoxidations of alkenes.



**Scheme 4.9** Polymer-supported porphyrines in epoxidations of alkenes.

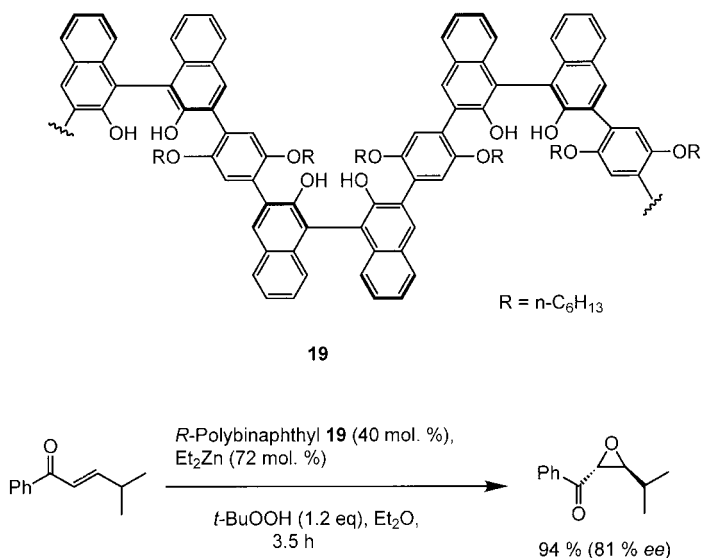


**Scheme 4.10** Polymer-bound methylrhenium trioxide.

One of the first attempts to extend polymer-assisted epoxidations to asymmetric variants were disclosed by Sherrington *et al.* The group employed chiral poly(tartrate ester) ligands in Sharpless epoxidations utilizing  $\text{Ti}(\text{O}i\text{Pr})_4$  and  $t\text{BuOOH}$ . However, yields and degree of stereoselection were only moderate [76]. In contrast to most concepts, Pu and coworkers applied chiral polymers, namely polymeric binaphthyl zinc to effect the asymmetric epoxidation of  $\alpha,\beta$ -unsaturated ketones in the presence of *tert*-butyl hydroperoxide (Scheme 4.11).

The soluble catalytic species was generated *in situ* by reaction of the polybinaphthyl resin (**19**) with diethylzinc prior to addition of the unsaturated ketone and  $t\text{BuOOH}$  (Scheme 4.11). After completion of the reaction, the soluble polymer had to be precipitated by addition of methanol. Yields were reported in the range between 67 to 95% [77].

Most publications regarding this field are based on immobilized chiral salen ligands [62] which are coordinated with manganese [45 a, 78–82] or chromium [83]

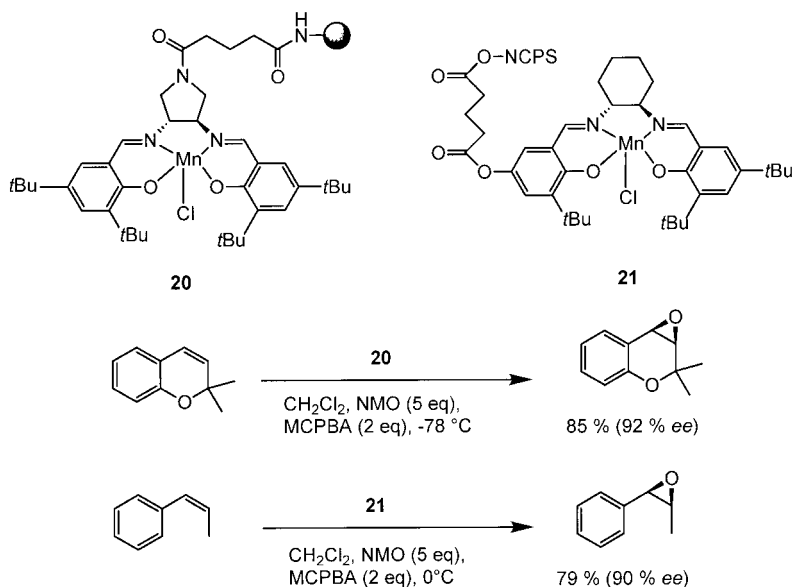


**Scheme 4.11** Polybinaphthyl resin as catalyst in asymmetric epoxidations of enones.

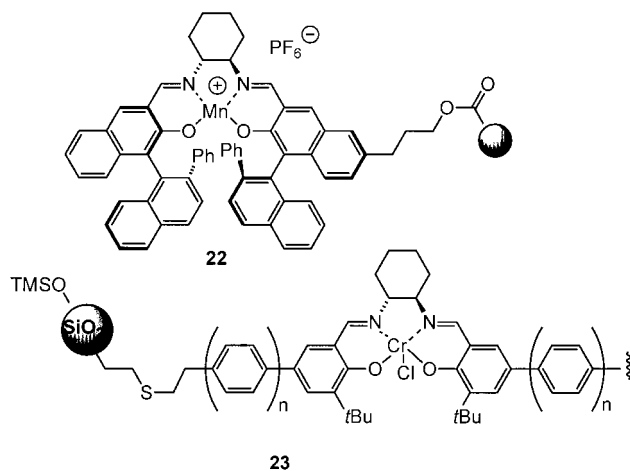
(also refer to Scheme 4.2). Song and Janda both reported manganese salen complexes that were covalently attached via different linkers and positions to a selection of polymers and showed catalytic activity in Jacobsen epoxidations utilizing NMO (*N*-methyl-morpholin-*N*-oxide) and MCPBA (*m*-chloroperbenzoic acid) as co-oxidants. While Song *et al.* employed an insoluble amino functionalized polymer (**20**) and obtained yields up to 85% with *ee*'s in the range from 68 to 92% (Scheme 4.12), [78] Janda *et al.* got best results with soluble non-cross-linked polystyrene (NCPS) as scaffold (**21**), affording yields of up to 79% and *ee*'s up to 90% (Scheme 4.12) [79]. As a major drawback, both reported partial decomposition of the polymeric catalyst under the reaction conditions.

Similar results were reported by Kim *et al.* [45a] and Che *et al.*, [83] who both employed salen complexes attached to zeolite MCM-41. Similarly, Seebach and co-workers generated dendritic elongated salen derivatives that could be embedded in polystyrene by co-polymerization [80].

The unsymmetrical analog of a Katsuki-type salen ligand was attached to Merrifield's resin (1% cross-linked) yielding a catalyst (**22**) (Fig. 4.3) which showed good efficiency and selectivity in the asymmetric epoxidation of 1,2-dihydronaphthalene with good performance after several recycling steps [81]. Related complexes (**23**) immobilized on silica were recently disclosed by Seebach and coworkers (Fig. 4.3) [82].



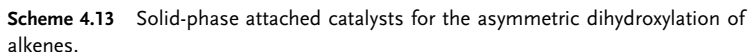
**Scheme 4.12** Polymer-bound salen-complexes in asymmetric epoxidations of styrenes.



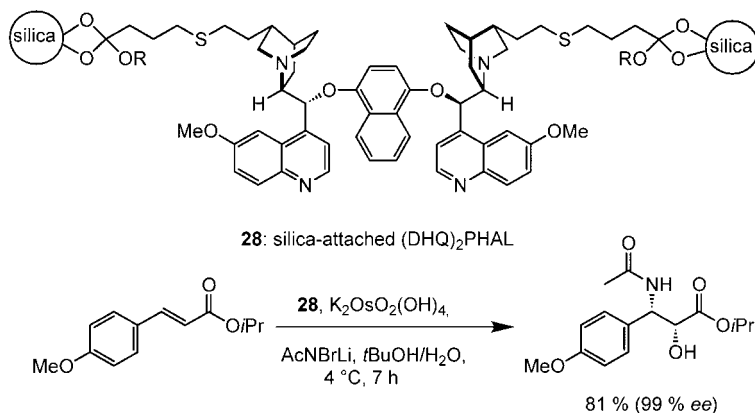
**Fig. 4.3** Polymer-bound salen complexes (**22**) and (**23**).

#### 4.3.1.3 Dihydroxylation and Aminohydroxylation of Alkenes

Dihydroxylations and aminohydroxylations of alkenes are important reactions in organic synthesis in order to introduce 1,2-functionalization into simple unsaturated precursors. Since these transformations mostly involve toxic osmium tetroxide or valuable chiral ligands, attempts to immobilize those reagents are especially appealing.



Janda, Bolm and Zhang generated soluble polymer-bound catalysts for the asymmetric dihydroxylation by attaching cinchona alkaloid derivatives to polyethylene glycol monomethyl ether (MeO-PEG) [84–87]. Since these polymeric catalysts like **(24)** are soluble in many common solvents they are often as effective as their small homogenous counterparts. Janda *et al.* prepared catalyst **(24)** in which two dihydroquinidine (DHQD) units were linked together by phthalazine and finally were attached to MeO-PEG via one of the bicyclic ring system moieties (Scheme



**Scheme 4.14** Aminohydroxylation of  $\alpha$ ,  $\beta$ -unsaturated esters by silica-attached (DHQ)<sub>2</sub>PHAL.

4.13) [85]. Similar MeO-PEG-bound DHQD ligand systems were generated by Bolm [86] and Zhang [87] and also showed very good activity and selectivity under Sharpless dihydroxylation conditions.

Other functionalized supports that are able to serve in the asymmetric dihydroxylation of alkenes were reported by the groups of Sharpless (catalyst **25**) [88], Salvadori (catalyst **26**) [89–91] and Crudden (catalyst **27**) (Scheme 4.13) [92]. Commonly, the oxidations were carried out using  $\text{K}_3\text{Fe}(\text{CN})_6$  as secondary oxidant in acetone/water or *tert*-butyl alcohol/water as solvents. For reasons of comparison, the dihydroxylation of *trans*-stilbene is depicted in Scheme 4.13. The polymeric catalysts could be reused but had to be regenerated after each experiment by treatment with small amounts of osmium tetroxide. A systematic study on the role of the polymeric support and the influence of the alkoxy or aryloxy group in the C-9 position of the immobilized cinchona alkaloids was conducted by Salvadori and coworkers [89–91]. Co-polymerization of a dihydroquinidine phthalazine derivative with hydroxyethylmethacrylate and ethylene glycol dimethacrylate afforded a functionalized polymer (**26**) with better swelling properties in polar solvents and hence improved performance in the dihydroxylation process [90].

Grafting a modified cinchona alkaloid to hexagonal mesoporous molecular sieve SBA-15 afforded catalyst (**27**) with excellent activity. 1-Phenyl-1-propene was converted to the corresponding diol in 98% yield (98% ee), while *trans*-stilbene yielded the desired product in 97% yield (99% ee) [92]. Other examples in this field are the utilization of microencapsulated osmium tetroxide by Kobayashi [93] and the application of continuous dihydroxylation runs in chemzyme membrane reactors described by Wöltinger [94].

Finally, osmium tetroxide-loaded, immobilized DHQ-ligand system (**28**) disperses activity in the asymmetric aminohydroxylation of *trans*-cinnamate derivatives (Scheme 4.14) [95]. Here, the reagent system AcNHBr/LiOH was employed as nitrogen source. The immobilized catalyst could entirely be removed by filtra-

tion without loss of activity in consecutive runs. With analogous insoluble organic polymeric phases only moderate *ee*'s were achieved [96].

#### 4.3.2

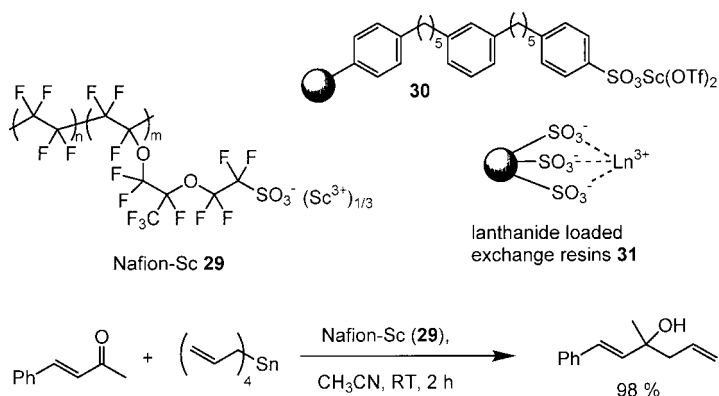
##### Lewis Acid-Mediated Reactions

Lewis acids have served as catalysts in numerous fields of organic synthesis. By temporary coordination to basic sites substrates can be activated resulting in enhanced reaction rates. Immobilization of Lewis acids to a solid support has been carried out in order to overcome work-up problems, for complexing ligands or for generating distinct reaction environments.

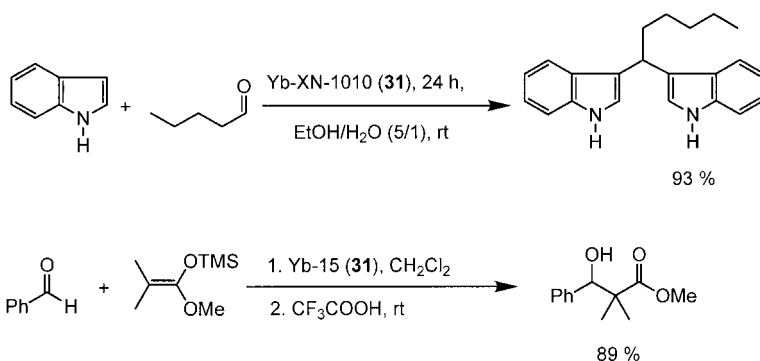
##### 4.3.2.1 Addition Reactions to Carbonyl Compounds

By treating Nafion (NR-50), a perfluorinated acidic ion exchanger based on sulfonic acid groups, with scandium(III) chloride hexahydrate Kobayashi *et al.* generated a solid scandium-derived catalyst (**29**) (Nafion-Sc) that proved to be effective in allylation reactions of carbonyl compounds with tetraallyltin (Scheme 4.15). Since the catalyst is stable in both organic solvents and water, even unprotected carbohydrates could be transformed directly in aqueous solvents. The resulting homoallylic alcohols were separated by simple filtration [97].

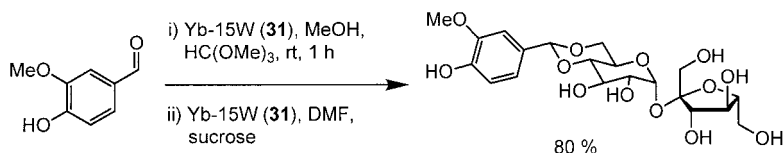
A modified rare earth catalyst (**30**) which is based on a polystyrene backbone as depicted in Scheme 4.15 can be applied even in neat water. It is attached via a hydrophobic oligomeric linker which creates a nonpolar reaction environment and acts as a surfactant for the substrates. The reaction of 4-phenyl-2-butanone with tetraallyltin in water using 1.6 mol% of the scandium catalyst (**30**) afforded the corresponding homoallyl alcohol in a yield of 95%. Interestingly, when using other solvents (dichloromethane, acetonitrile, benzene, ethanol, DMF) the yields decreased drastically, indicating a much higher reaction rate in water [98].



**Scheme 4.15** Polymer-bound Lewis acid in allylation of enones.



**Scheme 4.16** Synthetic applications of immobilized lanthanide-based Lewis acids.



**Scheme 4.17** Immobilized lanthanide-based Lewis acid (**31**) as tool for selective protection strategies of 1,3-diols.

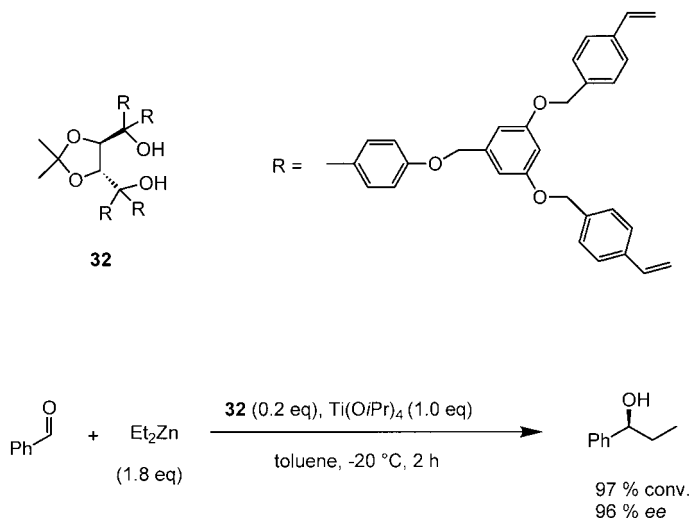
Wang *et al.* investigated the catalytic behavior of cation exchange resin supported lanthanide(III) salts of the general structure (**31**) (Scheme 4.15), prepared from Dowex, Amberlite, Amberlyst and other resins [99]. It turned out that Amberlyst XN-1010 and Amberlyst 15 complexed best with lanthanides(III). Thus, among others, electrophilic substitution of indole with hexanal and Mukayama-type aldol reaction of benzaldehyde with ketene silyl acetal proceeded in excellent yields under catalytic conditions (Scheme 4.16).

The latter reaction could be repeated ten times without loss of activity of Yb-XN-1010. Similar results were obtained with ytterbium(III) loaded Amberlyst 15W resin in a two-step one-pot procedure first involving the formation of the active dimethyl acetal from a benzaldehyde derivative which was followed by *in situ* protection of sucrose (Scheme 4.17) [100].

Likewise thioacetals have been prepared in yields between 60 to >99% by treatment of aldehydes or ketones with 1,2-ethanethiol in the presence of Zeolite HSZ-360, a dealuminated Y-Zeolite [101]. Many other functional groups like alkenes, tetrahydropyranyl and nitriles are tolerated under the mild reaction conditions.

As has been described in Section 4.2.3, immobilized TADDOL-derivatives are particularly important catalytic species which can be applied to asymmetric synthesis in many ways. Seebach *et al.* developed a dendritic elongated TADDOL-derivative (**32**) that could be embedded in polystyrene by copolymerization (Scheme 4.18). Upon treatment with  $\text{Ti}(\text{O}i\text{Pr})_4$  the chiral polymeric diisopropoxy-Ti-TAD-





**Scheme 4.18** TADDOL-mediated asymmetric alkylation of benzaldehyde.

DOLate was formed which was tested in the Lewis acid catalyzed enantioselective addition of diethylzinc to benzaldehyde. The authors note that the catalyst can be recovered by simple filtration and was active for at least more than twenty runs (refer also to Section 4.2.3) [102].

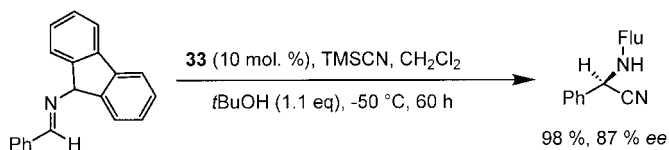
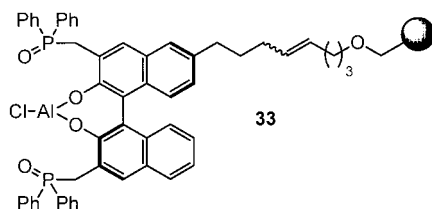
Other examples involved the use of chiral Schiff base-zinc complexes as catalysts [33a] and polymer-supported chiral *N*-tritylaziridino alcohols as catalysts. The stereoselectivity was reported to be up to 97% *ee* for aliphatic and up to 96% *ee* for aromatic aldehydes [103].

#### 4.3.2.2 Addition Reactions to Imines

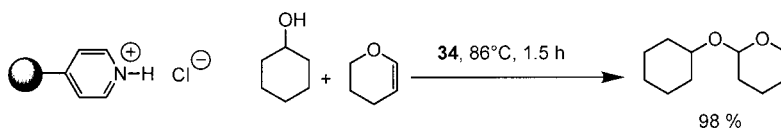
Amberlyst 15 DRY, a sulfonic cation exchange resin with a large surface area, was found to catalyze the imino aldol reaction of imines with ketene silyl acetals to provide racemic  $\beta$ -amino esters in yields up to 99% [104].

Shibasaki *et al.* developed a polymer-supported bifunctional catalyst (**33**) in which aluminum was complexed to a chiral binaphthyl derivative containing also two Lewis basic phosphine oxide-functionalities. The binaphthyl unit was attached via a non-coordinating alkenyl linker to the Janda Jel-polymer, a polystyrene resin containing flexible tetrahydrofuran-derived cross-linkers and showing better swelling properties than Merifield resins (Scheme 4.19) [105]. Catalyst (**33**) was employed in the enantioselective Strecker-type synthesis of imines with TMSCN.

The polymer-bound catalyst was recyclable by filtration and showed just slightly decreased activity when reused. Catalyst (**33**) also promotes asymmetric Reissert-type reactions [106].



**Scheme 4.19** Asymmetric Strecker-type synthesis of  $\alpha$ -amino nitriles.



Reillex 425 - HCl **34**

**Scheme 4.20** Protonated polyvinyl pyridine – a mild solid acid for THP-ether formation.

#### 4.3.2.3 Addition Reactions to Carbon–Carbon Double Bonds

Amberlyst 15 resin was found to catalyze the addition of primary alcohols to olefins. The activity displayed was higher than for soluble anhydrous *p*-toluenesulfonic acid. The addition of methanol or *n*-butanol to isobutene is well-established as an industrial process [7].

A number of efforts have been devoted to the simplified, acid catalyzed reaction between dihydropyran and alcohols to form THP-ethers. Thus, employing the hydrochloride salt of Reillex 425 (**34**) [a cross-linked macroreticular poly(4-vinylpyridine) resin] the tetrahydropyranylation even of hindered alcohols proceeds under mild conditions in high yields without side-reactions (Scheme 4.20) [107].

In an alternate approach sulfuric acid adsorbed on silica (3% H<sub>2</sub>SO<sub>4</sub> on Merck Kieselgel 60, 70–230 mesh) was employed to promote the formation of THP-ethers [108].

Simple ways to catalyze nitrations and sulfonylations of aromatic compounds are of great interest since these reactions are carried out industrially on large scale. Clays and zeolites with defined pore structures and channels as acidic catalysts have been utilized in nitrations [109] and Friedel–Crafts sulfonylations [110].

#### 4.3.2.4 Cycloaddition Reactions

Lewis acids can be efficiently used to increase the reactivity of reactants in cycloaddition reactions. At the same time improved regio- and stereoselectivities can be achieved.

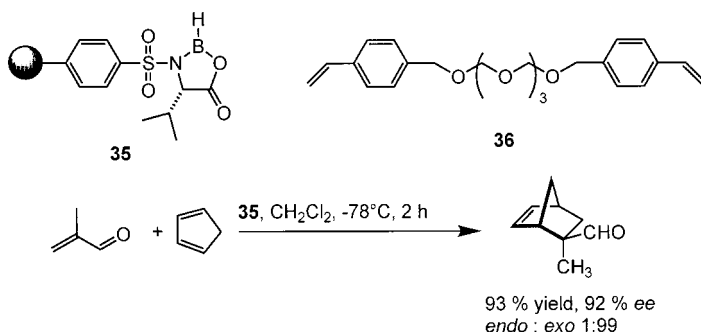
Thus, an achiral promoter for the Cr(0)-mediated [6+2] cycloaddition was recently disclosed by Rigby. Here, Cr(0) is attached to the polymeric backbone via immobilized triphenylphosphine [111].

Itsuno *et al.* demonstrated that the Diels–Alder reaction can be catalyzed by use of polystyrene-based polymers (**35**) which are cross-linked with oligo(oxyethylene) chains (**36**) and functionalized with oxazaborolidinone units (Scheme 4.21) [112].

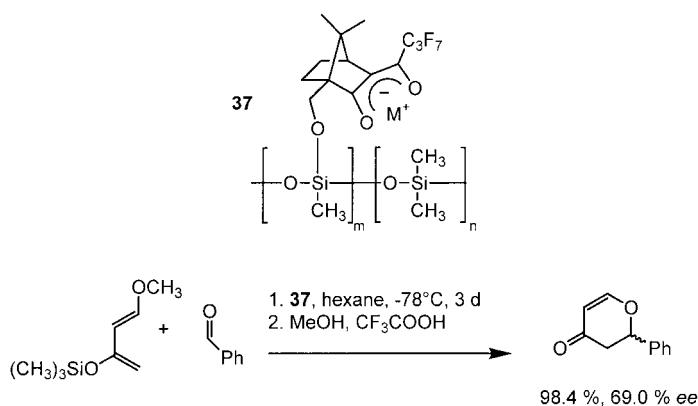
Asymmetric Diels–Alder reactions have also been achieved in the presence of poly(ethylene glycol)-supported chiral imidazolidin-4-one [113] and copper-loaded silica-grafted bis(oxazolines) [114]. Polymer-bound, camphor-based polysiloxane-fixed metal 1,3-diketonates (chirasil-metals) (**37**) have proven to catalyze the hetero Diels–Alder reaction of benzaldehyde and Danishefsky's diene. Best catalysts were obtained when oxovanadium(IV) and europium(III) were employed as coordinating metals. Despite excellent chemical yields the resulting pyran-4-ones were reported to be formed with only moderate stereoselectivity (Scheme 4.22). The polymeric catalysts are soluble in hexane and could be precipitated by addition of methanol. Interestingly, the polymeric oxovanadium(III)-catalysts invoke opposite enantioselectivities compared with their monomeric counterparts [115].

Immobilization of TADDOL-derivatives to silica and treatment with various titanium(IV) salts furnished a catalytic system (**38**) which was utilized in [2+3] cycloadditions of diphenylnitron and acylated oxazolidinone to yield oxazolines (Scheme 4.23) [65]. It is noteworthy that the ligand X has an impact on the outcome of this cycloaddition. While the dichloro catalyst affords the *exo*-adduct in good yield and with a high stereoselectivity, the corresponding tosyloxy catalyst preferentially affords the *endo*-cycloadduct. The efficiency of the process is comparable to those obtained with the analogous soluble catalysts. The catalyst, however, had to be recycled prior to each experiment.

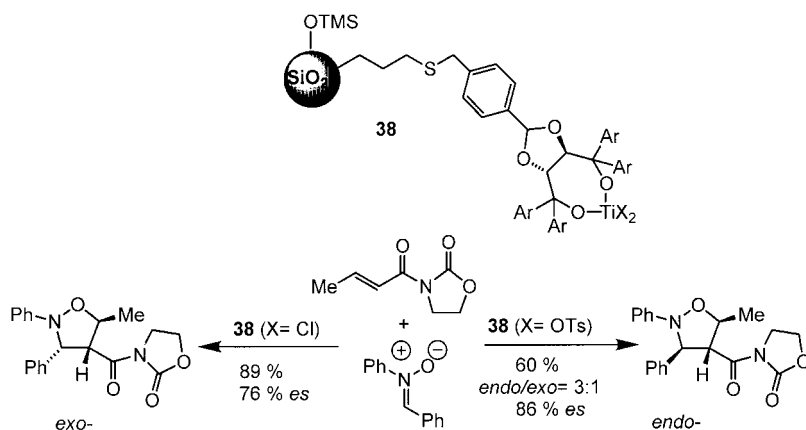
Nitrones also undergo 1,3-dipolar cycloadditions with alkenes to furnish the corresponding isoxazolidines in a diastereo- and enantioselective manner when the



**Scheme 4.21** Polymer-bound oxazaborolidinone in Diels–Alder cycloadditions.



**Scheme 4.22** Camphor-based polysiloxane-fixed metal diketonates in Diels–Alder cycloadditions.



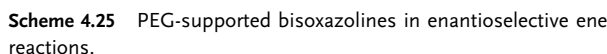
**Scheme 4.23** [2+3]-Cycloadditions mediated by CPG-attached TADDOLate. Role of X in view of diastereoselectivity.

reaction was catalyzed by the chiral polymer (**39**) which was built up from monomeric binaphthyl units. In the presence of  $\text{AlMe}_3$ , a powerful polymeric but soluble Lewis acid was generated *in situ*. The reaction was terminated by addition of methanol (Scheme 4.24). The activity of the polymeric catalyst turned out to be almost identical to its monomeric counterpart and decreased just slightly when the catalyst was reused [116].

Likewise, PEG-supported bisoxazoline (**40**) can be used as a ligand for copper-mediated enantioselective reactions such as cyclopropanations of alkenes, [2+4] cycloadditions as well as ene reactions. Best results were obtained in case of the latter reactions as products were formed in yields up to 96% and *ee*'s up to 95% (Scheme 4.25) [117].



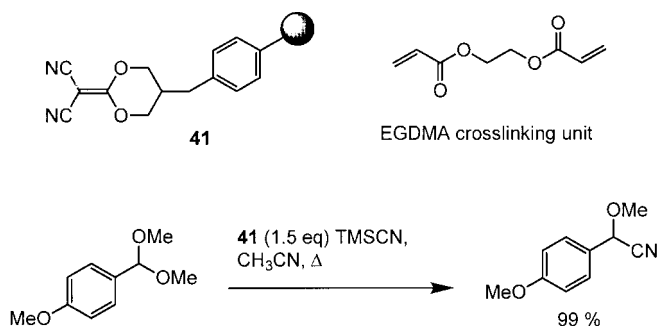
**Scheme 4.24** [2+3]-Cycloadditions mediated by polybinaphthyl resins.



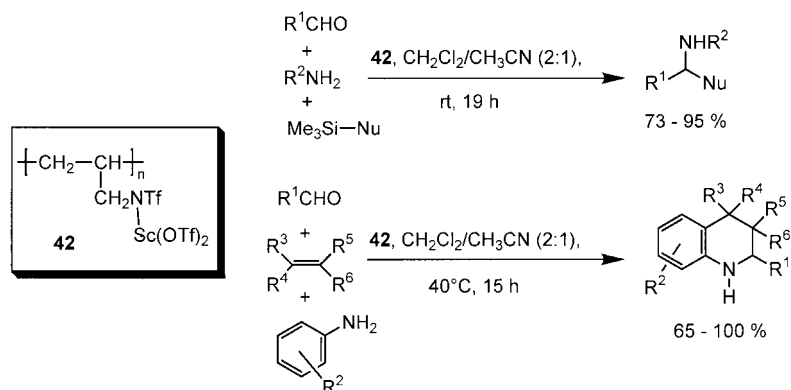
#### 4.3.2.5 Miscellaneous Applications

Copolymerization of polystyrene-bound dicyanoketene acetal (DCKA) and ethylene glycol dimethacrylate (EGDMA) yielded a polymer (**41**) with high  $\pi$ -acidity. It was found to be an effective and completely recyclable catalyst in the high yielding carbon-carbon bond-forming reaction of dimethylacetals with silylated nucleophiles (Scheme 4.26) [118].

Kobayashi *et al.* developed the polymeric scandium(III)-catalyst (**42**) (PA-Sc-TAD) which promotes the three-component coupling reactions of aldehydes and aromatic amines with either alkenes to generate quinolines or silylated nucleophiles to form  $\beta$ -amino ketones, esters and nitriles. This methodology turned out to be highly efficient with regard to automated high throughput synthesis (Scheme 4.27) [119].



**Scheme 4.26** Polystyrene-bound dicyanoketen acetal – solid with high  $\pi$ -acidity for the activation of acetals.



**Scheme 4.27** Multicomponent reactions using polymeric  $\text{Sc(III)}$ -catalyst (**42**).

#### 4.3.3

#### Transition Metal Catalysts

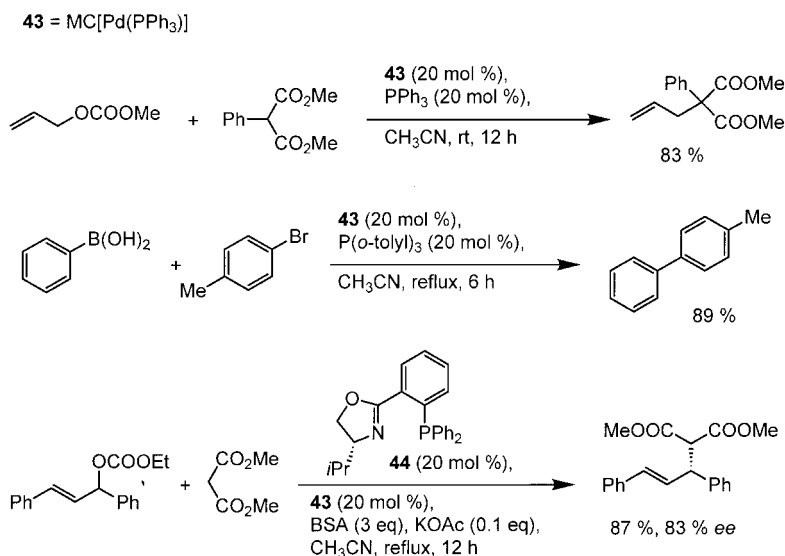
Transition metal catalysts play an important role in modern organic chemistry promoting a number of fundamental reactions such as carbon-carbon, carbon-nitrogen, carbon-hydrogen, and carbon-oxygen bond formation. The immobilization of the catalytic active transition metal complexes onto suitably stable solid supports is of great interest from the economical as well as the ecological point of view since it allows efficient catalyst recovery and reuse, thereby minimizing both catalyst cost and contamination of the reaction products. A growing number of publications on the preparation of polymer-supported catalysts has been discussed in the reviews [4d, 5b, 120]; in fact the last review appeared in 2001. In this section we consider some of the most recent results published during the last two years and thus illustrating the main trends in this area.

## 4.3.3.1 Palladium-catalyzed Coupling Reactions

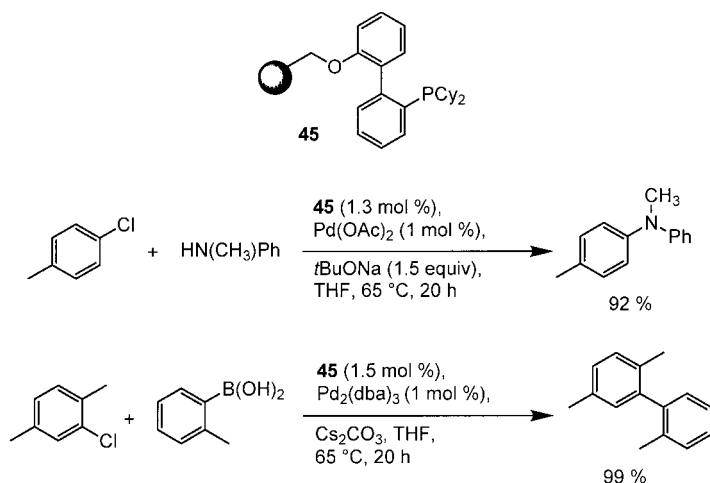
A new method for immobilizing catalysts is based on physical envelopment by polymers (see also Section 4.2.1 and refs. 23a and 39). This strategy was used by Kobayashi *et al.* who prepared a recoverable and reusable polystyrene-supported palladium catalyst from  $\text{Pd}(\text{PPh}_3)_4$  applying a simple microencapsulation procedure [23b]. The encapsulated Pd-species supposedly was  $\text{Pd}(\text{PPh}_3)_2$  and the resulting catalyst (**43**) {MC [ $\text{Pd}(\text{PPh}_3)_2$ ]; MC=microencapsulated} was used in the allylation of C-nucleophiles with allylic carbonates and allylic acetates as well as in the Suzuki cross-coupling reactions of boronic acids with aryl bromides (Scheme 4.28). In order to proceed smoothly, all these reactions required an additional external ligand such as triphenylphosphine or tri-*o*-tolylphosphine. In the presence of the chiral isoxazoline-derived ligand (**44**), allylation products were accessible in good yield and enantiopurity (Scheme 4.28).

Buchwald has shown that, in combination with palladium(II) acetate or  $\text{Pd}_2(\text{dba})_3$  [tris(dibenzylideneacetone)dipalladium], the Merrifield resin-bound electron-rich dialkylphosphinobiphenyl ligand (**45**) (Scheme 4.29) forms the active polymer-supported catalysts for amination and Suzuki reactions [121]. Inactivated aryl iodides, bromides, or even chlorides can be employed as substrates in these reactions. The catalyst derived from ligand (**45**) and a palladium source can be recycled for both amination and Suzuki reactions without addition of palladium.

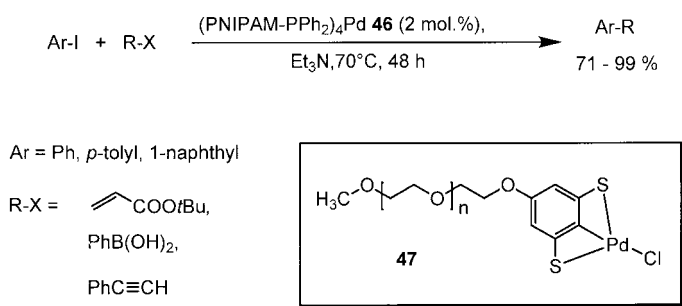
Bergbreiter reported that poly(*N*-isopropylacrylamide)-bound phosphine ligands (PNIPAM-resins) coordinated with the  $\text{Pd}(0)$  moieties afford efficient catalysts (**46**) for the Heck, Suzuki and  $\text{sp-sp}^2$  cross-coupling reactions (Scheme 4.30) [122].



Scheme 4.28 Applications of microencapsulated  $\text{Pd}(0)$ -catalyst.



**Scheme 4.29** Pd(0)-mediated Buchwald–Hartwig and Suzuki cross-coupling reactions.



**Scheme 4.30** Immobilized Pd-catalysts (**46**) and (**47**) in Heck and Suzuki cross-coupling reactions.

The reactions were carried out at 70 °C in the so called thermomorphic solvent system (heptane/90% aqueous EtOH) which undergoes phase separation after cooling to room temperature. Alternatively, air-stable tridentate sulfur–carbon–sulfur (SCS)-Pd(II) catalysts (**47**) bound to PNIPAM or polyethyleneglycol were also prepared and used in the Heck and Suzuki reactions under thermomorphic conditions.

Other important examples of immobilized palladium catalysts (**48**)–(**50**) which were employed in Heck, Suzuki–Miyaura and allylic alkylation reactions are summarized in Fig. 4.4 [123]. Catalyst (**49**) is particularly noteworthy as it is a recyclable amphiphilic resin-supported P,N-chelating Pd-complex which performs asymmetric allylic alkylations in water.



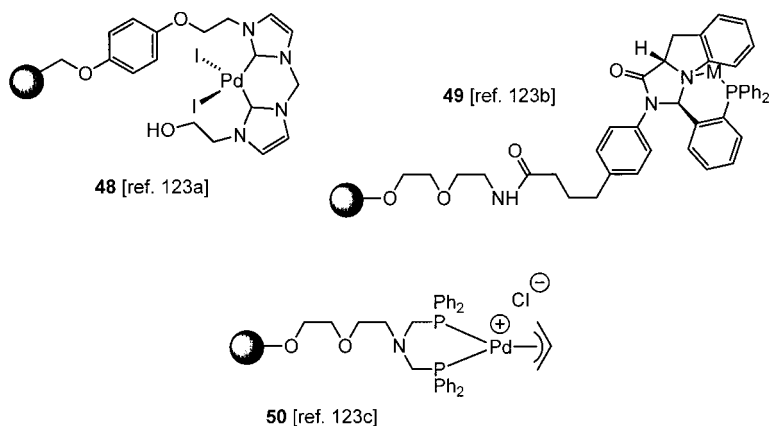


Fig. 4.4 Polymer-bound palladium catalysts (48–50).

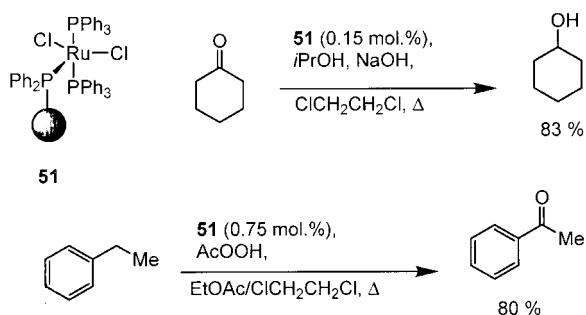
#### 4.3.3.2 Olefin Metathesis

The formation of carbon-carbon bonds using olefin metathesis methodology is a powerful technique in fine organic synthesis and polymer chemistry. The increasing importance of these reactions is reflected by the numerous publications over the last few years. Many of these publications deal with the design and application of polymer-supported olefin metathesis catalysts with the aim to overcome the common drawbacks of the homogeneous catalysts: low thermal stability and difficulties associated with their recovery from the reaction mixtures. The modern state of art in this important field is described in chapter 11 of this volume.

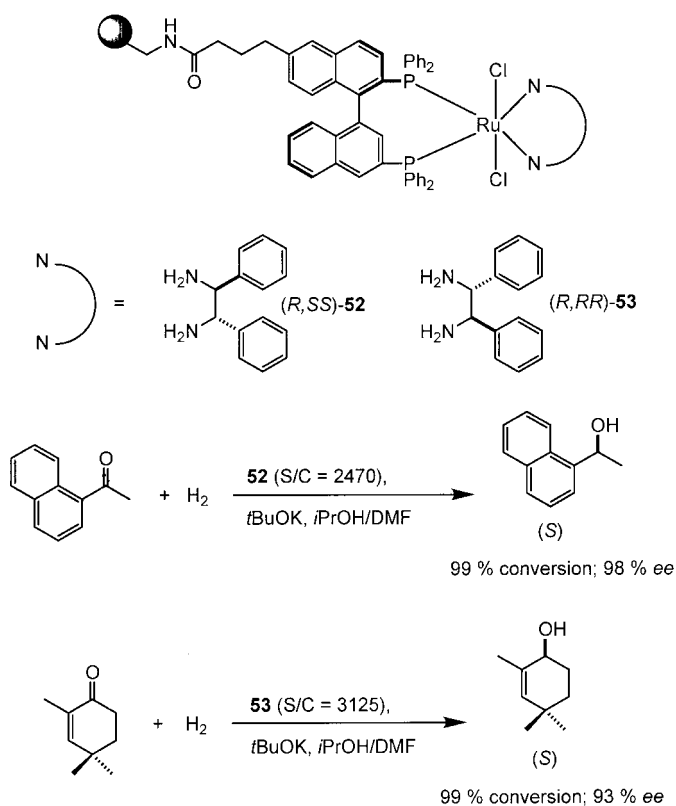
#### 4.3.3.3 Transition Metal-catalyzed Hydrogenation and Hydroformylation

Ruthenium complexes are able to dehydrogenate alcohols and to deliver the hydrides to a ketone thus acting as transfer hydrogenation catalysts. Leadbeater used the commercially available “polymer-supported triphenylphosphine” for the preparation of the immobilized ruthenium complex (**51**) (Scheme 4.31) [124]. In the presence of the catalyst, the selective hydrogen transfer from propan-2-ol to various ketones occurs quickly, providing the corresponding alcohols. In addition, catalyst (**51**) was also active in the oxidation of several alcohols and hydrocarbons using *tert*-butyl hydroperoxide as co-oxidant to yield the corresponding carbonyl products. The activity of catalyst (**51**) is in the range of soluble analogs. However, it is air-stable and can be reused repeatedly.

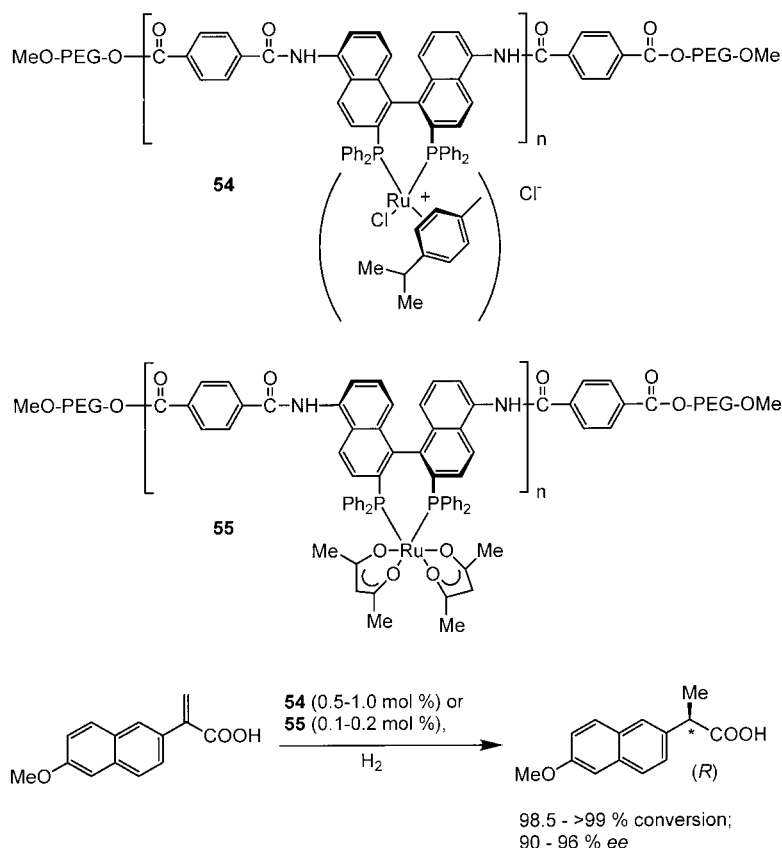
(*R*)-BINAP/1,2-diphenylethylenediamine ruthenium(II) complexes covalently attached to polystyrene (Scheme 4.32) promote the asymmetric hydrogenation of aromatic ketones and of  $\alpha$ ,  $\beta$ -unsaturated ketones [125]. The catalysts (**52**) and (**53**) were reused at high substrate/catalyst molar ratio (S/C) of 2470 in 14 experiments. Remarkably, the enantiopurity of the products remained high after each run, constantly being in the range of 97 to 98% *ee*.



**Scheme 4.31** Polymer-bound catalyst (**51**) in hydrogen transfer reactions.



**Scheme 4.32** BINAP-based polymer-bound catalysts for the asymmetric reduction of ketones.

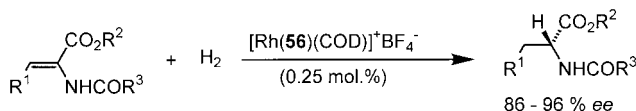
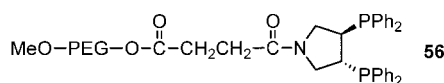


**Scheme 4.33** PEG-supported BINAP-ligand in asymmetric reductions of electron deficient alkenes.

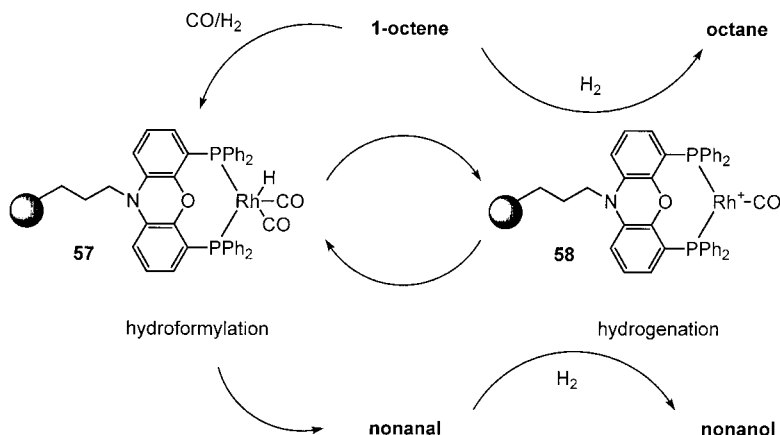
Soluble polymer-supported (*R*)-BINAP ligands were employed for the preparation of the Ru<sup>II</sup>-bearing catalysts (**54**) and (**55**) which are shown in Scheme 4.33 [126]. Both these catalysts exhibited high activity and enantioselectivity in the asymmetric hydrogenation of 2-(6'-methoxy-2'-naphthyl)propenoic acid.

The same soluble MPEG-resin was used for the immobilization of (3*R*,4*R*)-3,4-bis(diphenylphosphino)pyrrolidine ligand (**56**) (Scheme 4.34). The rhodium(I) catalyst was generated in situ from ligand (**56**) and [Rh(COD)<sub>2</sub>]<sup>+</sup>BF<sub>4</sub><sup>-</sup> and was found to be active in the asymmetric hydrogenation of prochiral enamides [126].

The rhodium complex with bis(diphenylphosphino)phenoxazine was immobilized on silica using the sol-gel technique or by a direct grafting to commercially available silica [127]. Under standard hydroformylation conditions (CO/H<sub>2</sub> atmosphere), a neutral hydridic complex (**57**) and cationic species (**58**) (Scheme 4.35) coexist on the support and act as a hydroformylation/hydrogenation sequence catalyst, giving selectively 1-nonanol from 1-octene: 98% of 1-octene were converted to mainly linear nonanal which was subsequently hydrogenated to 1-nonanol. The



**Scheme 4.34** Application of PEG-supported ligand (**56**) for the synthesis of enantio-enriched  $\alpha$ -amino acids.



**Scheme 4.35** Multifunctional properties of solid-phase-bound catalysts.

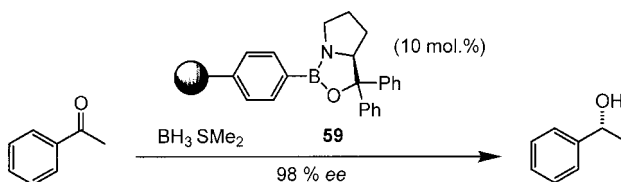
addition of 1-propanol suppresses completely the reduction reaction, and the system acts as a hydroformylation catalyst, which produces 1-nonanal with an overall selectivity of 93%. Under hydrogen atmosphere the system is switched to the hydrogenation mode and shows complete hydrogenation of 1-octene and 1-nonanal to octane and 1-nonanol, respectively. The immobilized catalyst is recyclable, and the desired catalyst mode can be easily turned on by simple changes in the reaction conditions. It enables selective reactions for different important catalytic processes using only one catalyst system.

#### 4.3.4

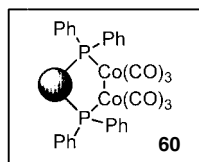
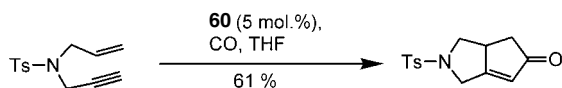
##### Miscellaneous

Various polymer-bound (polystyrene-bound) oxazaborolidine catalysts for the reduction of secondary alcohols were reported [128]. These can simply be prepared by condensation of the resin-bound boronic acid with chiral 1,2-amino alcohols. The best results as far as enantioselectivity is concerned were obtained with oxazaborolidine (**59**) (Scheme 4.36).

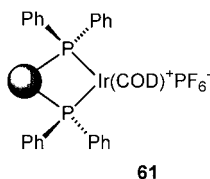
The reuse of the chiral catalyst is highly dependent on workup since the activity of (**59**) dramatically decreases if hydrolytic quench is not avoided.



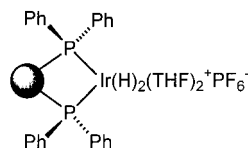
**Scheme 4.36** Polymer-bound oxazaborolidine catalysts (**59**).



**Scheme 4.37** The Pauson-Khand reaction using polymer-bound catalyst (**60**).



**61**



**62**

**Fig. 4.5** Polymer-supported iridium catalysts (**61**) and (**62**) for the isomerization of olefinic double bonds.

The Pauson-Khand reaction involves the annulation of an alkene, an alkyne and carbon monoxide to yield cyclopentenones. Recently, it was shown that in this respect polymer-bound species (**60**) is an effective catalyst which may be generated by heating  $\text{Co}_2(\text{CO})_8$  with polystyrene-bound phosphine (Scheme 4.37) [129].

The preparation of polymer-supported iridium catalysts (**61**) and (**62**) for the stereoselective isomerization of double bonds using polystyrene based immobilized triphenyl phosphine were recently reported by Ley and coworkers (Fig. 4.5). The immobilized catalyst is potentially useful for deprotection strategies of allyl ethers [130].

#### 4.4

#### Outlook

There is a renewed interest in the immobilization of catalysts on solid supports, because high throughput synthesis and combinatorial chemistry demand techniques which allow simple purification. Furthermore, the last two decades have seen the birth of many new highly efficient and selective homogeneous catalysts especially in asymmetric synthesis. However, the adaption of solution-phase techniques to the solid-phase cannot straightforwardly be achieved. Apart from altering known catalysts to the needs and requirements of the solid support in order to achieve similar efficiencies and selectivities as in the solution phase, organic chemists should not ignore the solid phase. Important aspects to consider include the search for appropriate linkers and for the optimized loading of individual catalysts, the ideal architecture and cross-linking of polymers as well as polarity of the solid support. The use of recyclable solid-phase bound catalysts is one important tool within the emerging concepts of sustainability within chemistry. It is hoped that reports like the present one will inspire many more chemists to merge the art of chemistry with new technologies for applications in research and industrial applications.

Finally, we apologize to those investigators whose work could not be summarized herein.

While this manuscript was under preparation, a considerable number of examples of solid-phase-attached catalysts appeared in the literature which is a clear indication for the dynamic character of this field. These include catalysts based on palladium [131, 132], nickel [133] and rhodium [134] as well applications in hydrogenations including transfer hydrogenations [135, 136] and oxidations [137]. In addition various articles have appeared that are dedicated to immobilized chiral ligands for asymmetric synthesis such as chiral binol [138], salen [139], and bisoxazoline [140] cinchona alkaloid derived [141] complexes.

#### 4.5

#### Acknowledgments

Our contributions in this field were supported by the Fonds der Chemischen Industrie. We thank G. Dräger, M. Jesberger, G. Sourkouni-Argirusi, N. Merayo, E. Kunst, N. Hoffmann, J. Jaunzems, and A. Schönberger for expert preparative contributions. Furthermore, we thank CHELONA GmbH (Potsdam, Germany), Solvay Pharmaceuticals (Hannover, Germany), Bayer AG (Leverkusen, Germany) as well as Novabiochem (Switzerland) for financial and technical assistance.

## 4.6

## References

- 1 R. B. MERRIFIELD, *J. Am. Chem. Soc.* **1963**, 85, 2149–2154.
- 2 a) F. Z. DÖRWALD, *Organic Synthesis on Solid Support*, Wiley VCH, Weinheim **2000**; b) N. K. TERRETT, *Combinatorial Chemistry*, Oxford University Press **1998**; c) D. OBRECHT, J. M. VILLALGORDO, *Solid-supported combinatorial and parallel synthesis of small-molecular-weight compound libraries*, Pergamon, Elsevier Science Ltd, Oxford, **1998**; d) S. R. WILSON, A. W. CZARNIK, *Combinatorial Chemistry, Synthesis, Application*, Wiley, New York **1997**.
- 3 a) D. HUDSON, *J. Comb. Chem.* **1999**, 1, 333–360 and 403–457; b) D. E. BERGBREITER, *Med. Res. Rev.* **1999**, 19, 439–450; c) S. F. OLIVER, C. ABELL, *Curr. Opin. Chem. Biol.* **1999**, 3, 299–306; d) J. S. FRÜCHTEL, G. JUNG, *Angew. Chem.* **1996**, 108, 19–46; *Angew. Chem. Int. Ed. Engl.* **1996**, 35, 17–42; e) F. BALKENHOL, C. VON DEM BUSSCHE-HÜNNFELD, A. LANSKY, *et al.*, *Angew. Chem.* **1996**, 108, 2437–2488; *Angew. Chem. Int. Ed. Engl.* **1996**, 35, 2288–2337; f) L. A. THOMPSON, J. A. ELLMAN, *Chem. Rev.* **1996**, 96, 555–600.
- 4 Reviews on polymer-supported reagents: a) A. KIRSCHNING, H. MONENSCHIN, R. WITTENBERG, *Angew. Chem.* **2001**, 113, 670–701; *Angew. Chem. Int. Ed. Engl.* **2001**, 40, 650–679; b) S. V. LEY, I. R. BAXENDALE, R. N. BREAM, *et al.*, *J. Chem. Soc., Perkin Trans. I* **2000**, 3815–4195; c) D. H. DREWRY, D. M. COE, S. POON, *Med. Res. Rev.* **1999**, 19, 97–148; d) S. J. SHUTTLEWORTH, S. M. ALLIN, P. K. SHARMA, *Synthesis* **1997**, 1217–1239; e) C. U. PITTMAN, JR., *Polym. News* **1998**, 23, 416–418; f) S. W. KALDOR, M. G. SIEGEL, *Curr. Opin. Chem. Biol.* **1997**, 1, 101–106.
- 5 For reviews on solid-supported catalysts refer to ref. 4 and a) O. SEITZ, *Nachr. Chem. Techn. Lab.* **2001**, 1419–1423; b) B. CHAPHAM, T. S. REGER, K. D. JANDA, *Tetrahedron* **2001**, 57, 4637–4662; c) B. JANDELEIT, D. J. SCHAEFFER, T. S. POWERS, *et al.*, *Angew. Chem.* **1999**, 111, 2648–2689; *Angew. Chem. Int. Ed. Engl.* **1999**, 38, 2476–2514; d) E. LINDNER, T. SCHNELLER, F. AUER, *et al.*, *Angew. Chem.* **1999**, 111, 2288–2309; *Angew. Chem. Int. Ed. Engl.* **1999**, 38, 2154–2174; e) J. H. CAMERON in *Solid state organometallic chemistry: Methods and applications*, (Eds.: M. GIELEN, R. WILLEM, B. WRACKMEYER), Wiley, Chichester **1999**, p. 473–519; f) J. H. CLARK, D. J. MACQUARRIE, *Chem. Soc. Rev.* **1996**, 303–310; g) D. C. BAILEY, S. H. LANGER, *Chem. Rev.* **1981**, 81, 109–148.
- 6 For scavenger techniques refer to refs. 4 and 5 and particularly to: J. J. PARLOW, R. V. DEVRAJ, M. S. SOUTH, *Curr. Opin. Chem. Biol.* **1999**, 3, 320–336.
- 7 Acidic ion-exchange resins are in industrial large scale use, e. g. as catalysts for the addition of methanol to isobutylene to form methyl *tert*-butyl ether. F. ANCILLOTTI, M. M. MAURI, E. PESCAROLLO, *J. Catal.* **1977**, 46, 49–57 and references cited herein.
- 8 X. GUO, A. WEISS, M. BALLAUFF, *Macromolecules*, **1999**, 32, 6043–6046.
- 9 Reviews on properties of polymers in conjunction with solid-phase synthesis: a) A. R. VAINO, K. D. JANDA, *J. Comb. Chem.* **2000**, 2, 579–596; b) E. R. FELDER in *Combinatorial Chemistry and Technology: Principles, Methods and Applications*, Marcel Dekker Inc. (Eds.: S. MIERTUS, G. FASSINA) **1999**, 35–51; c) B. RENNEBERG, J. W. LABADIE, *Chim. Oggi* **1999**, 17, 7–9; d) D. C. SHERRINGTON, *Chem. Commun.* **1998**, 2275–2286; e) P. HODGE, *Chem. Soc. Rev.* **1997**, 26, 417–424; f) J. W. LABADIE, *Curr. Opin. Chem. Biol.* **1998**, 2, 346–352.
- 10 Selected reviews on inorganic supports in conjunction with solid-phase synthesis: a) R. S. VARMA, *Tetrahedron* **2002**, 58, 1235–1255; b) S. E. SEN, S. M. SMITH, K. A. SULLIVAN, *Tetrahedron* **1999**, 55, 12657–12698; c) J. Y. YING, C. P. MEHNERT, M. S. WONG, *Angew. Chem.* **1999**, 111, 58–82; *Angew. Chem. Int. Ed.* **1999**, 38, 56–77; d) S. BIZ, M. L. OCELLI, *Cat. Rev. Sci. Engl.* **1998**, 40, 329–407; e) K. MOLLER, T. BEIN, *Chem. Mat.* **1998**, 10, 2950–2963; f) A. CORMA, *Top. Curr. Cat.* **1997**, 4, 249–260; g) C. J. BRINKER, *Curr. Opin. Sol. Sta. Mat. Sci.* **1996**, 1, 798–805; h) N. K. RAMAN, M. T.

- ANDERSON, C. J. BRINKER, *Chem. Mat.* **1996**, *8*, 1682–1701; i) D. M. ANTONELLI, J. Y. YING, *Curr. Opin. Coll. Int. Sci.* **1996**, *1*, 523–529; j) X. S. ZHAO, G. Q. LU, G. J. MILLAR, *Ind. Eng. Chem. Res.* **1996**, *35*, 2075–2090; k) P. BEHRENS, *Angew. Chem.* **1996**, *108*, 561–564; *Angew. Chem. Int. Ed. Engl.* **1996**, *35*, 515–518; l) C. E. SONG, S.-G. LI, *Chem. Rev.* **2002**, *102*, 3495–3524.
- 11 a) B. YAN, *Comb. Chem. High Throughput Screening* **1998**, *1*, 215–229; b) J. M. J. FRÉCHET, G. D. DARLING, S. ITSUNO, P.-Z. LU, M. V. DE MEFTAH, W. A. ROLLS JR., *Pure Appl. Chem.* **1988**, *60*, 353–364.
  - 12 a) J. M. J. FRÉCHET, M. J. FARRALL, L. NUYENS, *J. Macromol. Sci. Chem.* **1977**, *A11*, 507–514; b) J. M. J. FRÉCHET, J. WARRNOCK, M. J. FARRALL, *J. Org. Chem.* **1978**, *43*, 2618–2621; c) J. A. GREIG, D. C. SHERRINGTON, *Polymer* **1978**, *19*, 163–172.
  - 13 a) G. MANECKE, G. RAMLOW, *J. Polym. Sci. Part C* **1969**, *22*, 957–963; b) G. MANECKE, C.-S. RÜHL, G. WEHR, *Makromol. Chem.* **1972**, *154*, 121–128; c) G. MANECKE, W. STORCK, *Angew. Chem.* **1962**, *74*, 903–904.
  - 14 H. KAMOGAWA, S. ODABE, M. NANANAWA, *Bul. Chem. Soc. Jpn.* **1976**, *49*, 1917–1919.
  - 15 a) S. V. MCKINLEY, J. W. RAKSHYS, *Chem. Commun.* **1972**, 134–135; b) C. U. PITTMAN, JR., R. M. HANES, *Ann. N. Y. Acad. Sci.* **1974**, *239*, 76–87; c) H. M. RELLES, R. W. SCHLUENZ, *J. Am. Chem. Soc.* **1974**, *96*, 6469–6475; d) W. HEITZ, R. MICHELS, *Angew. Chem.* **1972**, *84*, 296–297; *Angew. Chem. Int. Ed.* **1972**, *11*, 298–299.
  - 16 a) N. TANAKA, Y. MASAKI, *Synlett.* **1999**, 1960–1962. b) Y. MASAKI, N. TANAKA, T. MIURA, *Tetrahedron Lett.* **1998**, *39*, 5799–5802. c) N. TANAKA, Y. MASAKI, *Synlett.* **2000**, 406–408.
  - 17 Refer to chapter 8 of this volume.
  - 18 S. RANA, P. WHITE, M. BRADLEY, *J. Comb. Chem.* **2001**, *3*, 9–15.
  - 19 a) D. C. SHERRINGTON in *Polymer-supported Reactions in Organic Synthesis* (Eds.: P. HODGE, D. C. SHERRINGTON), Wiley **1980**, 1–82; b) W. HEITZ, *Adv. Pol. Sci.* **1977**, *23*, 1–23; c) J. I. CROWLEY, H. RAPOPORT, *Acc. Chem. Res.* **1976**, *9*, 135–144.
  - 20 R. H. GRUBBS, L. C. KROLL, *J. Am. Chem. Soc.* **1971**, *93*, 3062–3063.
  - 21 a) W. T. FORD in *Polymeric Reagents and Catalysts*, (Ed.: W. T. FORD), ACS Symp. Ser. No 308, Washington DC, **1986**, chapter 11; b) M. EDA, M. J. KURTH, *Chem. Commun.* **2002**, 723–724; c) A. BASSO, M. BRADLEY, *Tetrahedron Lett.* **2003**, *44*, 2699–2702.
  - 22 a) D. A. ANNIS, E. N. JACOBSEN, *J. Am. Chem. Soc.* **1999**, *121*, 4147–4154; b) S. PEUKERT, E. N. JACOBSEN, *Org. Lett.*, **1999**, *1*, 1245–1248.
  - 23 a) M. T. REETZ, G. LOHMER, *Chem. Commun.* **1996**, 1921–1922; b) R. AKIYAMA, S. KOBAYASHI, *Angew. Chem.* **2001**, *113*, 3577–3579; *Angew. Chem. Int. Ed.* **2001**, *40*, 3469–3471; c) S. KOBAYASHI, S. NAGAYAMA, *J. Am. Chem. Soc.* **1998**, *120*, 2985–2986; d) R. SALADINO, V. NERI, A. R. PELLICIA, *et al.*, *J. Org. Chem.* **2002**, *67*, 1323–1332; e) K. KÖHLER, R. G. HEIDENREICH, J. G. E. KRAUTER, *et al.*, *Chem. Eur. J.* **2002**, *8*, 622–631; f) Y. NIU, R. M. CROOKS, *J. Am. Chem. Soc.* **2001**, *123*, 6840–6846; g) S. KOBAYASHI, R. AKIYAMA, *Chem. Commun.* **2003**, 449–460.
  - 24 a) F. SVEC, J. M. J. FRÉCHET, *Science* **1996**, *273*, 205–211; b) F. SVEC, J. M. J. FRÉCHET, *Ind. Eng. Chem. Res.* **1999**, *38*, 34–48.
  - 25 The influence of the nature of the polymer support on the oxidation power of complex chromates was investigated by: T. BRUNELET, C. JOUITTEAU, G. GELBARD, *J. Org. Chem.* **1986**, *51*, 4016–4022.
  - 26 C. R. HARRISON, P. HODGE, *J. Chem. Soc., Perkin Trans I* **1982**, 509–511.
  - 27 D. E. BERGBREITER in *Polymeric reagents and catalysts* (Ed.: W. T. FORD), ACS Symposium Series 308, Washington DC, **1986**, 17–41.
  - 28 E. J. ENHOLM, J. P. SCHULTE II, *Org. Lett.* **1999**, *1*, 1275–1277.
  - 29 K. J. LEE, A. ANGULO, P. GHAZAL, K. D. JANDA, *Org. Lett.* **1999**, *1*, 1859–1862.
  - 30 a) M. MUTTER, H. HAGENMAIER, E. BAYER, *Angew. Chem.* **1971**, *83*, 883–884; *Angew. Chem. Int. Ed. Engl.* **1971**, *10*, 811–812; b) E. BAYER, M. MUTTER, *Nature* **1972**, *237*, 512–513.
  - 31 Reviews on soluble polymer supports: a) P. WENTWORTH, JR., K. D. JANDA, *Chem. Commun.* **1999**, 1917–1924; b) D. J. GRAVERT, K. D. JANDA, *Chem. Rev.* **1997**, *97*, 489–509; c) K. E. GECKELER, *Adv.*



- Polym. Sci. **1995**, 121, 31–79; d) J. M. HARRIS in *Polyethylene Glycol Chemistry: Biotechnology and Biomedical Applications*, (Ed.: J. M. HARRIS), Plenum Press, New York, **1992**; 326–371.
- 32 E. BAYER, *Angew. Chem.* **1991**, 103, 117–133; *Angew. Chem., Int. Ed.* **1991**, 30, 113–129.
  - 33 a) S. ITSUNO, Y. SAKURAI, K. ITO, *et al.*, *J. Org. Chem.* **1990**, 55, 304–310; b) K. S. KUMAR, V. N. R. PILAI, *Tetrahedron* **1999**, 55, 10437–10446.
  - 34 a) A. BASSO, B. EVANS, N. PEGG, *et al.*, *Tetrahedron Lett.* **2000**, 41, 3763–3767; b) V. SWALI, N. J. WELLS, G. J. LANGLEY, *et al.*, *J. Am. Chem. Soc.* **1997**, 62, 4902–4903; c) N. J. WELLS, A. BASSO, M. BRADLEY, *Biopolymers (Peptide Science)* **1998**, 47, 381–396; d) A. FROMONT, M. BRADLEY, *Chem. Commun.* **2000**, 283–284; e) S. LEBRETON, N. NEWCOMBE, M. BRADLEY, *Tetrahedron Lett.* **2002**, 43, 2475–2478 and 2479–2482.
  - 35 R. HAAG, *Chem. Eur. J.* **2001**, 7, 327–335.
  - 36 D. E. BERGBREITER, G. TAO, A. M. KIPPENBERGER, *Org. Lett.* **2000**, 2, 2853–2855.
  - 37 a) A. SUNDER, R. MÜHLHAUPT, R. HAAG, *et al.*, *Adv. Mat.* **2000**, 12, 235–239; b) A. SUNDER, R. HANSELMANN, H. FREY, *et al.*, *Macromolecules* **1999**, 32, 4240–4246; c) R. HAAG, J.-F. STUMBÉ, A. SUNDER, *J. Am. Chem. Soc.* **2000**, 112, 2954–2955; d) A. SUNDER, R. MÜHLHAUPT, R. HAAG, *et al.*, *Macromolecules* **2000**, 33, 253–254.
  - 38 A. B. KANTCHEV, J. R. PARQUETTE, *Tetrahedron Lett.* **1999**, 40, 8049–8052.
  - 39 S. MECKING, R. THOMANN, H. FREY, *et al.*, *Macromolecules*, **2000**, 33, 3958–3960.
  - 40 a) M. GLOS, O. REISER, *Org. Lett.* **2000**, 2, 2045–2048; b) Y. UOZOMI, H. DANJO, T. HAYASHI, *J. Org. Chem.* **1999**, 64, 3384–3388; c) Y. UOZOMI, H. DANJO, T. HAYASHI, *Tetrahedron Lett.* **1998**, 39, 8303–8306; d) H. DANJO, D. TANAKA, T. HAYASHI, *et al.*, *Tetrahedron* **1999**, 55, 14341–14352.
  - 41 J. K. STILLE, H. SU, D. H. HILL, *et al.*, *Organometallics* **1991**, 10, 1993–2000.
  - 42 D. E. BERGBREITER, B. L. CASE, Y.-S. LIU, *et al.*, *Macromolecules* **1998**, 31, 6053–6062.
  - 43 D. C. SHERRINGTON, presented at the ACS Conference on Polymers and Organic Chemistry 2002, UCSD, San Diego (U.S.A.), July 14–18, 2002.
  - 44 a) D. C. LOCKE, *J. Chrom. Sci.* **1973**, 11, 120–128; b) J. J. KIRKLAND, J. DESTEFANO, *J. Chrom. Sci.* **1970**, 8, 309–314; c) W. PARR, K. GROHMANN, *Tetrahedron Lett.* **1971**, 2633–2636; d) W. PARR, K. GROHMANN, *Angew. Chem.* **1972**, 84, 266; *Angew. Chem. Int. Ed. Engl.* **1972**, 11, 314; e) R. EBY, C. SCHUERCH, *Carbohydr. Res.* **1975**, 39, 151–155; f) L. A. CARPINO, E. M. E. MANSOUR, C. H. CHENG, *et al.*, *J. Org. Chem.* **1983**, 48, 661–665; g) L. A. CARPINO, E. M. E. MANSOUR, J. KNAPCZYK, *J. Org. Chem.* **1983**, 48, 666–669; h) J. H. CLARK, S. J. TAVENER, S. J. BARLOW, *J. Mat. Chem.* **1995**, 5, 827–830.
  - 45 a) G.-J. KIM, J.-H. SHIN, *Tetrahedron Lett.* **1999**, 40, 6827–6830; b) I. C. CHISEM, J. RAFELT, M. T. SHIEH, *et al.*, *Chem. Commun.* **1998**, 1949–1950; c) J. CHISEM, I. C. CHISEM, J. S. RAFELT, *et al.*, *Chem. Commun.* **1997**, 2203–2204; d) J. H. CLARK, D. J. MACQUARRIE, *Chem. Soc. Rev.* **1996**, 303–310.
  - 46 a) D. M. ANTONELLI, J. Y. YING, *Angew. Chem.* **1996**, 108, 461–464; *Angew. Chem. Int. Ed. Engl.* **1996**, 35, 426–430; b) D. M. ANTONELLI, A. NAKAHIRA, J. Y. YING, *Inorg. Chem.* **1996**, 35, 3126–3136; c) D. M. ANTONELLI, J. Y. YING, *Angew. Chem.* **1995**, 107, 2202–2206; *Angew. Chem. Int. Ed. Engl.* **1995**, 34, 2014–2017; d) C. T. KRESGE, M. E. LEONOWITZ, W. J. ROTH, *et al.*, *Nature* **1992**, 359, 710–712; e) J. S. BECK, J. C. VARTULI, W. J. ROTH, *et al.*, *J. Am. Chem. Soc.* **1992**, 114, 10834–10843.
  - 47 X. SONG ZHAO, G. Q. (MAX) LU, X. HU, *Chem. Commun.* **1999**, 1391–1392.
  - 48 a) D. S. SHEPARD, W. ZHOU, T. MASCHMEYER, *et al.*, *Angew. Chem.* **1998**, 110, 2847–2851; *Angew. Chem. Int. Ed. Engl.* **1998**, 37, 2719–2723; b) S. INAGAKI, S. GUAN, Y. FUKUSHIMA, *et al.*, *J. Am. Chem. Soc.* **1999**, 121, 9611–9614.
  - 49 a) C. LIU, X. YE, Y. WU, *Catal. Lett.* **1996**, 36, 263–266; b) J. F. DIAZ, K. J. BALKUS, JR., F. BEDIQUI, *et al.*, *Chem. Mat.* **1997**, 9, 61–67; c) S. O'BRIAN, J. TUDOR, S. BARLOW, *et al.*, *Chem. Commun.* **1997**, 36, 641–642.
  - 50 S. XIANG, Y. ZHANG, Q. XIN, *et al.*, *Angew. Chem.* **2002**, 114, 849–852; *Angew. Chem. Int. Ed.* **2002**, 41, 821–824.

- 51 MCM-41 has been employed as an acidic solid support for deprotection of the triethylsilyl group: A. ITOH, T. KODAMA, Y. MASAKI, *Synlett*. **1999**, 357–359.
- 52 C. P. MEHNERT, J. Y. YING, *Chem. Commun.* **1997**, 2215–2216.
- 53 a) C.-J. LIU, W.-Y. YU, S.-G. LI, *et al.*, *J. Org. Chem.* **1998**, 63, 7364–7369; b) P. SUTRA, D. BRUNEL, *Chem. Commun.* **1996**, 2485–2486; c) Y. V. S. RAO, D. E. DE VOS, T. BEIN, *et al.*, *Chem. Commun.* **1997**, 355–356; d) C.-J. LIU, S.-G. LI, W.-Q. PANG, *et al.*, *Chem. Commun.* **1997**, 65–66.
- 54 a) T. MASCHMEYER, R. D. OLDROYD, G. SANKAR, *et al.*, *Angew. Chem.* **1997**, 109, 1713–1716; *Angew. Chem. Int. Ed. Engl.* **1997**, 36, 1639–1642; b) W. ZHANG, J. WANG, P. T. TANEV, *et al.*, *Chem. Commun.* **1996**, 979–980.
- 55 a) Y. S. KO, T. K. HAN, J. W. PARK, *et al.*, *Macromol. Rapid Commun.* **1996**, 17, 749–750; b) J. TUDOR, D. O'HARE, *Chem. Commun.* **1997**, 603–604.
- 56 C. J. BRINKLER, G. W. SCHERER, *Sol-Gel Science: The Physics and Chemistry of Sol-Gel Processing*. Academic Press, San Diego, CA, **1990**.
- 57 J. S. KINGSBURY, S. B. GARBER, J. M. GIFTOS, *et al.*, *Angew. Chem.* **2001**, 113, 4381–4386; *Angew. Chem. Int. Ed.* **2001**, 40, 4251–4256.
- 58 S. A. MILLER, E. KIM, D. H. GRAY, *et al.*, *Angew. Chem.* **1999**, 111, 3206–3210; *Angew. Chem. Int. Ed. Engl.* **1999**, 38, 3022–3026.
- 59 L. TOSHEVA, J. STERTE, *Chem. Commun.* **2001**, 1112–1113.
- 60 A. N. KHRAMOV, M. M. COLLINSON, *Chem. Commun.* **2001**, 767–768.
- 61 E. N. JACOBSEN, In *Catalytic Asymmetric Synthesis*, (Ed.: I. OJIMA), VCH Weinheim, **1993**, Chapter 4.2.
- 62 Reviews: a) M. BANDINI, P. G. COZZI, A. UMANI-RONCHI, *Chem. Commun.* **2002**, 919–927; b) T. KATSUKI, *Adv. Synth. Catal.* **2002**, 344, 131–147.
- 63 D. SEEBACH, A. K. BECK, A. HECKEL, *Angew. Chem.* **2001**, 113, 96–142; *Angew. Chem. Int. Ed.* **2001**, 40, 92–138.
- 64 a) D. SEEBACH, R. E. MARTI, T. HINTERMANN, *Helv. Chim. Acta* **1996**, 79, 1710–1740; b) P. J. COMINA, A. K. BECK, D. SEEBACH, *Org. Proc. Res. Dev.* **1998**, 2, 18–26; c) B. ALTAVA, M. I. BURGUETE, S. V. LUIS, *et al.*, *Tetrahedron* **1994**, 50, 7535–7542; d) J. IRURRE, A. FERNANDEZ-SERRAT, F. ROSANAS, *Chirality*, **1997**, 9, 191–197; e) J. IRURRE, A. FERNANDEZ-SERRAT, M. ALTAYO, *et al.*, *Enantiomer*, **1998**, 3, 103–120.
- 65 A. HECKEL, D. SEEBACH, *Chem. Eur. J.* **2002**, 8, 559–572.
- 66 P. ALTAVA, M. I. BURGUETTE, B. ESCUDER, *et al.*, *J. Org. Chem.* **1997**, 62, 3126–3134.
- 67 B. ALTAVA, M. I. BURGUETE, J. M. FRAILE, *et al.*, *Angew. Chem.* **2000**, 112, 1563–1566; *Angew. Chem. Int. Ed.* **2000**, 39, 1503–1506.
- 68 C. BOLM, T. FEY, *Chem. Commun.* **1999**, 1795–1796.
- 69 S. WEIK, G. NICHOLSON, G. JUNG, *et al.*, *Angew. Chem.* **2001**, 113, 1489–1492; *Angew. Chem. Int. Ed.* **2001**, 40, 1436–1439.
- 70 A. DIJKSMAN, I. W. C. E. ARENDS, R. A. SHELDON, *Chem. Commun.* **2000**, 271–272.
- 71 A. BLELOCH, B. F. G. JOHNSON, S. V. LEY, *et al.*, *Chem. Commun.* **1999**, 1907–1908.
- 72 a) N. E. Leadbeater, K. A. Scott, *J. Org. Chem.* **2000**, 65, 4770–4772; b) C.-H. JUN, H.-S. HONG, C.-W. HUH, *Tetrahedron Lett.* **1999**, 40, 8897–8900.
- 73 D. E. DE VOS, S. DE WILDEMAN, B. F. SELS, *et al.*, *Angew. Chem.* **1999**, 111, 1033–1036; *Angew. Chem. Int. Ed.* **1999**, 38, 980–983.
- 74 a) O. NESTLER, K. SEVERIN, *Org. Lett.* **2001**, 3, 3907–3909; b) J.-L. ZHANG, C. M. CHE, *Org. Lett.* **2002**, 4, 1911–1914.
- 75 C. D. NUNES, M. PILLINGER, A. A. VALENTE, *et al.*, *Eur. J. Inorg. Chem.* **2002**, 1100–1107.
- 76 L. CANALI, J. K. KARJALAINEN, D. C. SHERINGTON, *et al.*, *Chem. Commun.* **1997**, 123–124.
- 77 a) H.-B. YU, X.-F. ZHENG, Z.-M. LIN, *et al.*, *J. Org. Chem.* **1999**, 64, 8149–8155; b) M. JOHANNSEN, K. A. JORGENSEN, X.-F. ZHENG, *et al.*, *J. Org. Chem.* **1999**, 64, 299–301.
- 78 C. E. SONG, E. J. ROH, B. M. YU, *et al.*, *Chem. Commun.* **2000**, 615–616.
- 79 T. S. REGER, K. D. JANDA, *J. Am. Chem. Soc.* **2000**, 122, 6929–6934.
- 80 H. SELLNER, J. K. KARJALAINEN, D. SEEBACH, *Chem. Eur. J.* **2001**, 7, 2873–2887.

- 81 K. SMITH, C.-H. LIU, *Chem. Commun.* **2002**, 886–887.
- 82 A. HECKEL, D. SEEBACH, *Helv. Chim. Acta* **2002**, 85, 913–926.
- 83 X.-G. ZHOU, X.-Q. YU, J.-S. HUANG, *et al.*, *Chem. Commun.* **1999**, 1789–1790.
- 84 H. HAN, K.D. JANDA, *J. Am. Chem. Soc.* **1996**, 118, 7632–7633.
- 85 H. HAN, K.D. JANDA, *Tetrahedron Lett.* **1997**, 38, 1527–1530.
- 86 C. BOLM, A. GERLACH, *Angew. Chem.* **1997**, 109, 773–775; *Angew. Chem. Int. Ed.* **1997**, 36, 741–743.
- 87 Y.-Q. KUANG, S.-Y. ZHANG, L.-L. WEI, *Tetrahedron Lett.* **2001**, 42, 5925–5927.
- 88 B.M. KIM, K.B. SHARPLESS, *Tetrahedron Lett.* **1990**, 31, 3003–3006.
- 89 A. PETRI, D. PINI, P. SALVADORI, *Tetrahedron Lett.* **1995**, 36, 1549–1552.
- 90 P. SALVADORI, D. PINI, A. PETRI, *J. Am. Chem. Soc.* **1997**, 119, 6929–6930.
- 91 P. SALVADORI, D. PINI, A. PETRI, *Synlett.* **1999**, 8, 1181–1190.
- 92 I. MOTORINA, C.M. CRUDDEN, *Org. Lett.* **2001**, 3, 2325–2328.
- 93 S. KOBAYASHI, T. ISHIDA, R. AKIYAMA, *Org. Lett.* **2001**, 3, 2649–2652.
- 94 J. WÖLTINGER, H. HENNIGES, H.-P. KRIMMER, *et al.*, *Tetrahedron Asym.* **2001**, 12, 2095–2098.
- 95 C.E. SONG, C.R. OH, S.W. LEE, *et al.*, *Chem. Commun.* **1998**, 2435–2436.
- 96 A. MANDOLI, D. PINI, A. AGOSTINI, *et al.*, *Tetrahedron Asym.* **2000**, 11, 4039–4042.
- 97 S. KOBAYASHI, S. NAGAYAMA, *J. Org. Chem.* **1996**, 61, 2256–2257.
- 98 S. NAGAYAMA, S. KOBAYASHI, *Angew. Chem.* **2000**, 112, 578–581; *Angew. Chem. Int. Ed.* **2000**, 39, 567–569.
- 99 L. YU, D. CHEN, J. LI, P.G. WANG, *J. Org. Chem.* **1997**, 62, 3575–3581.
- 100 S. PORWANSKI, P. SALANSKI, G. DESCOTES, *et al.*, *Synthesis* **2000**, 525–528.
- 101 R. BALLINI, L. BARBONI, R. MAGGI, *et al.*, *Synth. Comm.* **1999**, 29, 767–772.
- 102 H. SELLNER, D. SEEBACH, *Angew. Chem.* **1999**, 111, 2039–2041; *Angew. Chem. Int. Ed.* **1999**, 38, 1918–1920.
- 103 P.T. HOLTE, J.-P. WIJGERGANGS, L. THIJS, *et al.*, *Org. Lett.* **1999**, 1, 1095–1097.
- 104 M. SHIMIZU, S. ITOHARA, E. HASE, *Chem. Commun.* **2001**, 2318–2319.
- 105 H. NOGAMI, S. MATSUNAGA, M. KANAI, *et al.*, *Tetrahedron Lett.* **2001**, 42, 279–283.
- 106 M. TAKAMURA, K. FUNABASHI, M. KANAI, *et al.*, *J. Am. Chem. Soc.* **2001**, 123, 6801–6808.
- 107 R.D. JOHNSTON, C.R. MERSTON, P.E. KRIEGER, *et al.*, *Synthesis* **1988**, 393–394.
- 108 F. CHAVEZ, R. GODINEZ, *Synth. Commun.* **1992**, 22, 159–164.
- 109 B.M. CHOUDARY, M. SATEESH, M.L. KANTAM, *et al.*, *Chem. Comm.* **2000**, 25–26.
- 110 B.M. CHOUDARY, N.S. CHOWDARI, M.L. KANTAM, *et al.*, *Tetrahedron Lett.* **1999**, 40, 2859–2862.
- 111 J.H. RIGBY, M.A. KONDRATENKO, C. FIEDLER, *Org. Lett.* **2000**, 24, 3917–3919.
- 112 K. KAMAHORI, K. ITO, S. ITSUNO, *J. Org. Chem.* **1996**, 61, 8321–8324.
- 113 M. BENAGLIA, G. CELENTANO, M. CINQUINI, *et al.*, *Adv. Synth. Catal.* **2002**, 344, 149–152.
- 114 D. RECHAVI, M. LEMAIRE, *Org. Lett.* **2001**, 3, 2493–2496.
- 115 F. KELLER, H. WEINMANN, V. SCHURIG, *Chem. Ber.* **1997**, 130, 879–885.
- 116 K.B. SIMONSEN, K.A. JORGENSEN, Q.-S. HU, *et al.*, *Chem. Comm.* **1999**, 811–812.
- 117 R. ANNUNZIATA, M. BENAGLIA, M. CINQUINI, *et al.*, *J. Org. Chem.* **2001**, 66, 3160–3166.
- 118 N. TANAKA, Y. MASAKI, *Synlett.* **1999**, 8, 1277–1279.
- 119 a) S. KOBAYASHI, S. NAGAYAMA, T. BUSUJIMA, *Tetrahedron Lett.* **1996**, 51, 9221–9224; b) S. KOBAYASHI, S. NAGAYAMA, *J. Am. Chem. Soc.* **1996**, 118, 8977–8978.
- 120 S.J. SHUTTLEWORTH, S.M. ALLIN, R.D. WILSON, *et al.*, *Synthesis* **2000**, 1035–1074.
- 121 C.A. PARRISH, S.L. BUCHWALD, *J. Org. Chem.* **2001**, 66, 3820–3827.
- 122 D.E. BERGBREITER, P.L. OSBURN, A. WILSON, *et al.*, *J. Amer. Chem. Soc.* **2000**, 122, 9058–9064.
- 123 a) J. SCHWARZ, V.P.W. BÖHM, M.G. GARDINER, *et al.*, *Chem. Eur. J.* **2000**, 6, 17773–1780; b) Y. UOZUMI, K. SHIBATONI, *J. Am. Chem. Soc.* **2001**, 123, 2919–2920; c) Y. UOZUMI, Y. NAKAI, *Org. Lett.*, **2002**, 4, 2997–3000.
- 124 N.E. LEADBEATER, *J. Org. Chem.* **2001**, 66, 2168–2170.
- 125 T. OHKUMA, H. TAKENO, Y. HONDA, *et al.*, *Adv. Synth. Cat.* **2001**, 343, 369–375.

- 126 Q.-H. FAN, G.-J. DENG, C.-C. LIN, *et al.*, *Tetrahedron Asymm.* **2001**, 12, 1241–1247.
- 127 A. J. SANDEE, J. N. H. REEK, P. C. J. KAMMER, *et al.*, *J. Am. Chem. Soc.* **2001**, 123, 8468–8476.
- 128 C. FRANOT, G. B. STONE, P. ENGELI, *et al.*, *Tetrahedron Asymm.* **1995**, 6, 2755–2766.
- 129 A. C. COMELY, S. E. GIBSON, N. J. HALES, *Chem. Commun.* **2000**, 305–306.
- 130 I. R. BAXENDALE, A.-L. LEE, S. V. LEY, *Synlett.* **2002**, 516–518.
- 131 Review: D. J. MACQUARRIE, *Platinum Metals Rev.* **2001**, 45, 102–110.
- 132 a) Y. LI, X. M. HONG, D. M. COLLARD, M. A. EL-SAYED, *Org. Lett.* **2002**, 2, 2385–2388; b) B. M. CHOUDHARY, S. MADHI, N. S. CHOWDARI, M. L. KANTAM, B. SREEDHAR, *J. Am. Chem. Soc.* **2002**, 124, 14127–14136; c) K. MUKHOPADHYAY, B. R. SAKAR, R. V. CHOUDHARI, *J. Am. Chem. Soc.* **2002**, 124, 9692–9693; d) Y. M. A. YAMADA, K. TAKEDA, H. TAKAHASHI, S. IKEGAMI, *Tetrahedron Lett.* **2003**, 44, 2379–2382; e) R. AKIYAMA, S. KOBAYASHI, *J. Am. Chem. Soc.* **2003**, 125, 3412–3413; f) V. KOGAN, Z. AIZENSHTAT, R. POPOVITZ-BIRO, R. NEUMANN, *Org. Lett.* **2002**, 4, 3529–2532; g) C. BALEIZAO, A. CARMO, H. GARCÍA, A. LEYVA, *Chem. Commun.* **2003**, 606–607; h) V. CHANDRASEKHAR, A. ATHIMOOLAM, *Org. Lett.* **2002**, 4, 2113–2116; i) Y. UOZUMI, T. RIMURA, *Synlett* **2002**, 2045–2048; j) D. E. BERGBREITER, A. M. KIPPENBERGER, G. TAO, *Chem. Commun.* **2002**, 2158–2159; k) C. E. SONG, J. W. YANG, E. J. ROH, S.-G. LEE, J. H. AHN, H. HAN, *Angew. Chem.* **2002**, 4004–4010; l) C. A. PARRISH, S. L. BUCHWALD, *J. Org. Chem.* **2001**, 66, 3820–3827; m) K. OKUBO, M. SHIRAI, C. YOKOYAMA, *Tetrahedron Lett.* **2002**, 43, 7115–7118; n) L. TOSHEVA, J. STERTE, *Chem. Commun.* **2001**, 1112–1113; o) A. HEBEL, R. HAAG, *J. Org. Chem.* **2002**, 67, 9452–9455.
- 133 S. TASLER, B. H. LIPSHUTZ, *J. Org. Chem.* **2003**, 68, 1190–1199; b) B. H. LIPSHUTZ, S. TASLER, W. CHRISMAN, B. SPLITHOFF, B. TESCHE, *J. Org. Chem.* **2003**, 68, 1177–1189.
- 134 Y. UOZUMI, M. NAKAZONO, *Synlett* **2002**, 344, 274–277.
- 135 Reviews: a) M. STUDER, H.-U. BLASER, C. EXNER, *Adv. Synth. Catal.* **2003**, 345, 45–65; b) A. TUNGLER, T. TARNAI, L. HEGEDUS, K. FODOR, *Platinum Metals Rev.* **1998**, 42, 108–115; c) C. SALUZZO, M. LEMAIRE, *Adv. Synth. Catal.* **2002**, 344, 915–928.
- 136 a) Y. KAYAKI, Y. SHINOKAWATOKO, T. IKARIYA, *Adv. Synth. Catal.* **2003**, 345, 175–179; b) E. ARSTAD, A. G. M. BARRETT, L. TEDESCHI, *Tetrahedron Lett.* **2003**, 44, 2703–2707.
- 137 a) Y. M. A. YAMADA, H. TABATA, H. TAKAHASHI, S. IKEGAMI, *Synlett* **2002**, 2031–2034; b) J. W. YANG, H. HAN, E. J. ROH, S.-G. LEE, *Org. Lett.* **2002**, 4, 4685–4688; c) J.-L. ZHANG, C.-M. CHE, *Org. Lett.* **2002**, 4, 1911–1914; d) G. V. NIZOVA, C. BOLM, S. CECCARELLI, C. PAVAN, G. B. SHUI'PIN, *Adv. Synth. Catal.* **2002**, 344, 899–905; e) M. BENAGLIA, T. DANELLI, F. FABRIS, D. SPERANDIO, G. POZZI, *Org. Lett.* **2002**, 4, 4229–4232; f) N. AL-HAQ, A. C. SULLIVAN, J. R. H. WILSON, *Tetrahedron Lett.* **2003**, 44, 769–771; g) E. BRULÉ, Y. R. DE MIGUEL, *Tetrahedron Lett.* **2002**, 43, 8555–8558.
- 138 S. HERRES, P. HESEMANN, J. J. E. MOREAU, *Eur. J. Org. Chem.* **2003**, 99–105.
- 139 S. XIANG, Y. ZHANG, Q. XIN, C. LI, *Chem. Commun.* **2002**, 2696–2697.
- 140 a) A. CORMA, H. GARCÍA, A. MOUSSAIF, M. J. SABATER, R. ZNIBER, A. REDOUANE, *Chem. Commun.* **2002**, 1058–1086; b) H. HOCKE, Uozumi, *Synlett* **2002**, 2049–2053.
- 141 a) T. DANELLI, R. ANNUNZIATA, M. BENAGLIA, M. CINQUINI, F. COZZI, G. TOCCO, *Tetrahedron Asymmetry* **2003**, 14, 461–467; b) B. M. CHOUDHARY, N. S. CHOWDARI, K. JYOTHI, S. MADHI, M. L. KANTAM, *Adv. Synth. Catal.* **2002**, 344, 503–506.

## 5

**Soluble Polymers as Catalyst and Reagent Platforms:  
Liquid-phase Methodologies**

TOBIN J. DICKERSON, NEAL N. REED and KIM D. JANDA

## 5.1

**Introduction**

The use of polymeric supports in organic synthesis has become common practice, especially following the rapid development of combinatorial chemistry. Starting with the introduction of solid-phase peptide synthesis by Merrifield [1], insoluble supports such as lightly cross-linked polystyrene have been implemented in a wide range of synthetic methodologies [2–4]. Primarily, the uses of these polymers in synthesis have fallen into one of two areas: (a) the use of the polymer as a support for reactants or (b) the use of the polymer as a support for reagents and catalysts during a reaction. Both of these methods allow rapid product purification and the ability to drive a given reaction to completion through the use of an excess of reagents. However, despite the well-known advantages of insoluble supports, there are several shortcomings in the use of these resins because of the heterogeneous nature of the reaction conditions. Several laboratories have explored alternative methodologies to restore homogeneous reaction conditions resulting from a number of problems associated with insoluble polymer supports, including nonlinear kinetic behavior, unequal distribution and/or access to the chemical reaction, solvation problems associated with the nature of the support, and synthetic difficulties in transferring standard organic reactions to the solid phase. By replacing insoluble cross-linked resins with *soluble* polymer supports, the familiar reaction conditions of classical organic chemistry are reinstated, yet product purification is still facilitated through application of macromolecular properties. This methodology, termed liquid-phase synthesis, in essence avoids the difficulties of solid-phase synthesis while preserving many of its advantages.

Initially, the term “liquid-phase” synthesis was used to contrast the differences between solid-phase peptide synthesis and a method of synthesis on soluble polyethylene glycol (PEG) [5, 6]. Although “soluble polymer-supported” synthesis is less ambiguous than “liquid-phase” synthesis, the latter term is more prevalent in the literature. In-keeping with previous reviews [7–12], the phrases “classical” or “solution” synthesis will be used to describe homogeneous reaction schemes that do not employ polymer supports while “liquid-phase” synthesis will be reserved

for methodologies incorporating a soluble macromolecular carrier to facilitate product isolation.

In recent years, the use of soluble polymer supported reagents and catalysts has gained significant attention as an alternative to traditional solid-phase synthesis. Inherent to library generation on solid support are two nondiversity-building steps: attachment and cleavage. Frequently, these procedures are not advantageous and as a result, parallel libraries are commonly generated in solution. To facilitate synthesis, polymer-supported reagents and catalysts have found frequent use in the preparation and purification of these solution-phase libraries [13–17]. However, the catalytic activity and/or stereoselectivity of these polymer-supported catalysts does not always correlate with their solution-phase counterparts. Subtle variations in the polymeric backbone can have profound implications in the activity of a support-bound catalyst. Also, in the case of solid-supported catalysts, many of the drawbacks of solid-supported organic synthesis are still present (e.g. inherent heterogeneity of reactions, inaccessibility of reagents to the catalyst). In order to combine some of the advantages of solution-phase chemistry with insoluble-polymer immobilized reagents and catalysts, soluble polymers have received significant attention as an alternative polymer support. This article will focus on the implementation of methodologies for soluble-polymer supported catalysts and reagents in organic synthesis.

## 5.2

### Overview of Soluble Polymers in Organic Synthesis

#### 5.2.1

##### Properties of Soluble Polymeric Supports

In order for a polymer to be useful as a soluble support for a catalyst or reagent, the polymer must (1) be commercially available or rapidly and conveniently prepared, (2) demonstrate good mechanical and chemical stability, (3) provide appropriate functional groups for easy attachment of organic moieties and (4) exhibit high solubilizing power in order to dissolve molecular entities with low solubilities and permit the development of a general synthetic methodology independent of the physicochemical properties of target compounds.

Additionally, it should be realized that polymer supports purchased or prepared in the laboratory do not exist as one discrete molecular weight, but instead consist of macromolecules with variable sizes. Polymer properties are known to vary with chain length, and as such, the molecular weight range of the support should be narrow, that is, the polydispersity should approach unity. Soluble supports in general should have molecular weights high enough to be solid or crystalline at room temperature and yet not excessively high that solubility and loading capacity are reduced to impractical levels.

Furthermore, the polymeric carrier must be robust enough to withstand the reaction conditions used in solution-phase synthesis. Consequently, most soluble

supports used in liquid-phase synthesis possess hydrocarbon or alkyl ether backbone structures because they are inherently stable to standard reaction conditions. The properties of the macromolecular carrier, as well as the possible sites of attachment, are determined by variation of both the terminal and pendant functional groups of these two core backbone structures. If the conditions of polymerization and choice of monomer allow for suitable polymer functionalization, anchoring of the initial synthetic structure may be made directly to the support for liquid-phase synthesis. However, a linking group is often employed to impart anchor stability throughout synthesis, to improve accessibility to reagents, and to allow for product cleavage under specific, and generally orthogonal, conditions.

Polymers chosen for liquid-phase synthesis must also provide a reasonable compromise between loading capacity and solubilizing power. The loading capacity of a polymer support is a measure of the number of anchoring sites per gram of polymer and is expressed in units of millimoles per gram ( $\text{mmol g}^{-1}$ ). High loading capacities are advantageous to reduce the total expenditure for polymer supports and to allow manageable amounts of material in medium- or large-scale applications. Solubilizing power refers to the ability of the macromolecular carrier to maintain a homogeneous solution of the polymer-bound organic moiety; this property is especially important in cases where the unbound moiety is insoluble in the reaction medium. High solubilizing power is desirable to ensure homogeneous reactions and high yields throughout the synthetic scheme. Generally, solubilizing power decreases as loading capacity increases because as the polymer is further loaded, the solubility properties of the polymer–organic moiety conjugate are increasingly determined by the properties of the attached compounds. Thus, it is critical to achieve a balance between polymer loading and solubilizing power that limits solubility changes while still providing an economic and manageable synthesis.

Finally, polymers with a high loading capacity can experience complications caused by the influence of neighboring anchoring sites. The presence of multiple compounds attached to a polymer support may result in nonequivalent reactivity of bound moieties caused by unequal distribution along the polymer backbone. In some situations, excess reagents or longer reaction times may be required for reaction of attached compounds on heavily laden polymers; however, other reactions may require linkage exclusively to polymer termini to provide adequate accessibility to polymer-bound reagents or enzymes.

### 5.2.2

#### Methods for Separating Polymers from Reaction Mixtures

Traditionally, soluble polymers have received less attention as polymeric supports than their insoluble counterparts. A perceived problem with the use of soluble polymers rested in the ability to isolate the polymer from all other reaction components. Yet, in practice this separation is not difficult and several methods have capitalized on the macromolecular properties of the soluble support to achieve product separation in liquid-phase synthesis. Most frequently the homogeneous

polymer solution is simply diluted with an appropriate solvent that induces precipitation of the support. Analogous to solid-phase synthesis, the resulting heterogeneous mixture is filtered to isolate the polymer-product conjugate while excess reagents and impurities are rinsed away. Some polymers may be recrystallized to minimize the formation of inclusion complexes during precipitation, and the proper choice of solvents and temperature must be made to achieve satisfactory recovery and purification [18, 19].

Although precipitation/crystallization is the fastest and most common mode of product separation, other methods have been used to isolate soluble polymeric supports from low molecular weight impurities. Dialysis using a semipermeable membrane has achieved polymer purification [20]. This methodology becomes less time-consuming in ultrafiltration, also called diafiltration or membrane filtration, when pressure gradients speed the separation of polymer from the reaction supernatant using a membrane. Additionally, centrifugation methods allow convenient isolation of biomolecules and could be applied to more general polymer separations. Gel permeation chromatography and adsorption chromatography have also been demonstrated as means to remove excess reagents and byproducts away from polymeric products [9].

These macromolecule-based purification methods isolate polymer-bound products from soluble impurities, but do not generally purify the product from other polymer-bound byproducts. Such byproducts arise from incomplete reactions or side reactions; and in classical solution chemistry, similar byproducts are removed during product purification at each step of a multi-step synthesis. Support-based methodologies, while removing the multiple, laborious purification steps of a classical synthesis, generally do not provide a method for the purification of intermediates. Instead, these methodologies demand that reaction conditions be optimized such that reactions are driven to completion to avoid a complicated final mixture of products. However, some developed liquid-phase methods achieve high purity of products without quantitative reaction yields [21–26].

### 5.2.3

#### **Analytical Methods in Liquid-phase Synthesis**

A frequent complication in the use of an insoluble polymeric support lies in the on-bead characterization of intermediates. Although techniques such as MAS  $^1\text{H}$  NMR, gel-phase  $^{13}\text{C}$  NMR, and single bead IR have had a tremendous effect on the rapid characterization of solid-phase intermediates [27–30], the inherent heterogeneity of solid-phase systems precludes the use of many traditional analytical methods. Liquid-phase synthesis does not suffer from this drawback and permits product characterization on soluble polymer supports by routine analytical methods including UV/visible, IR, and NMR spectroscopies as well as high resolution mass spectrometry. Even traditional synthetic methods such as TLC may be used to monitor reactions without requiring preliminary cleavage from the polymer support [10, 18, 19]. Moreover, aliquots taken for characterization may be returned to the reaction flask upon recovery from these nondestructive



analytical methods. Chemical methods such as titration and derivatization can also be routinely performed and allow for subsequent characterization in the presence of the bound soluble support. Other traditional analytical methods used to monitor amide bond formation have been performed on polyethylene glycol [31], however, unreliable results have been demonstrated using certain methods [32]. Circular dichroism (CD) measurements have also been shown to be feasible on polyethylene glycol-bound peptides [33]. Two peptides, substance P and a hydrophobic peptide corresponding to myoglobin sequence 66–73 were synthesized and CD data reported the formation of secondary structures and the influence of peptide protecting groups on structure. The polyethylene glycol support did not interfere because its UV cutoff is 190 nm, and the solubilizing power of the polymer support allowed solution measurements in solvents which the free peptide displayed limited solubility.

#### 5.2.4

##### Listing of Polymers

Soluble polymers that have been used in liquid-phase methodologies are listed in Fig. 5.1 [3, 7, 8, 34, 35]. Polyethylene glycol and non-cross-linked polystyrene are some of the most often used polymeric carriers for organic synthesis and have found frequent use in the preparation of soluble polymer-supported catalysts and reagents; consequently, a brief discussion of these polymers is warranted.

##### 5.2.4.1 Polyethylene Glycol (PEG)

Polyethylene glycol (PEG), polyethylene oxide (PEO), polyoxyethylene (POE), and polyoxirane all refer to the same linear polymer formed from the polymerization of ethylene oxide. By convention, PEG usually indicates the polyether of molecular weight less than 20 000; PEO signifies polymers of higher molecular weights, and POE and polyoxirane have been applied to polymers of a wide range of molecular weights [19]. Throughout this review, the term PEG will be used since polyethylene glycols of 2000 to 20 000 molecular weight are utilized as supports in organic synthesis. These limits have been set by the physical properties of the polymer, that is, within this molecular weight range PEG is both crystalline and has an acceptable loading capacity (1 to 0.1 mmol g<sup>-1</sup>); lower molecular weight PEG exists as a liquid or wax at room temperature, and higher molecular weight PEG has a low loading capacity. Macromolecular size will be reported in this review using the notation PEG<sub>6000</sub> to represent polyethylene glycol of molecular weight 6000. It should again be emphasized that polymers do not exist as a singular molecular weight species, but as a distribution of molecular weights, although the polydispersity of commercial PEG is reasonably narrow [19].

Depending on polymerization conditions, PEG termini may consist of hydroxyl groups or may be selectively functionalized. Commercially available PEG is produced through anionic polymerization of ethylene oxide to yield a polyether struc-

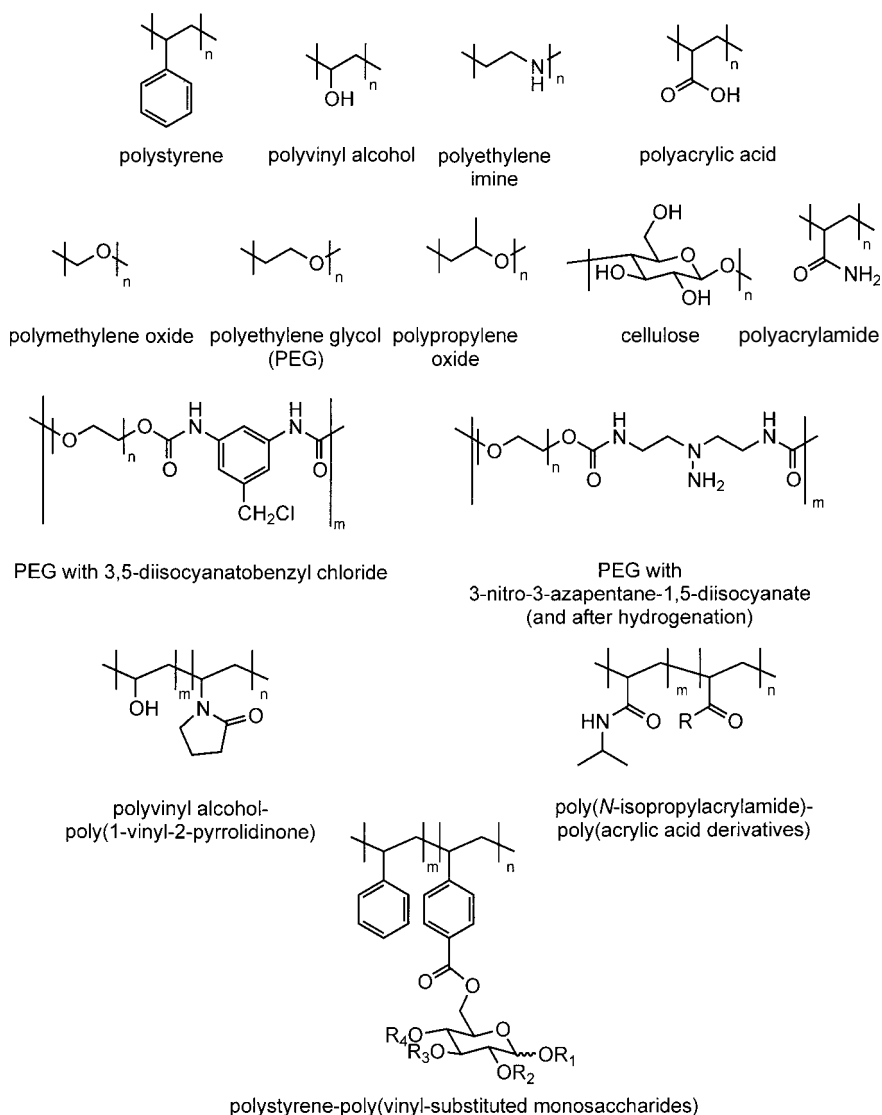


Fig. 5.1 Soluble polymers used as supports for liquid-phase synthesis.

ture possessing either hydroxyl groups at both ends, or a methoxy group at one end and a hydroxyl group at the other. Further development of this method also allows the preparation of PEG which possesses a benzyl, *tert*-butyldimethylsilyl, or tetrahydropyranyl ether on one end and a free hydroxyl group at the other [36]. In this review, PEG will be used to represent polyethylene glycol with hydroxyl functionalities at both ends. Similarly, MeO-PEG (polyethylene glycol monomethyl ether) will indicate the polyether terminated by a methoxy group at one end and a

free hydroxyl at the other. The polymer MeO-PEG is considered monofunctional because the methoxy group of MeO-PEG typically remains unchanged throughout chemical manipulations; and for identical chain lengths, the loading capacity of PEG is twice that of MeO-PEG as two hydroxyl groups serve as anchoring sites on PEG.

Employed as a protecting group, polyethylene glycol exhibits solubility in a wide range of solvents including DMF, dichloromethane, toluene, acetonitrile and water. PEG is insoluble in hexane, diethyl ether, *tert*-butyl methyl ether, isopropyl alcohol [37], and cold ethanol and these solvents have been used to induce PEG precipitation for purification. Careful precipitation conditions or cooling of polymer solutions in alcoholic solvents yields crystalline PEG, because the helical structure of the polymer produces a strong propensity to crystallize [19]. Purification by crystallization of the polymeric support is therefore feasible at each reaction step provided that the polymer backbone remains unaltered during the synthesis. Additionally, the solubilizing power of PEG not only permits homogeneous reactions conditions, but also allows individual reaction steps to be monitored without requiring cleavage from the polymer support. The characterization of PEG-immobilized organic moieties is often identical to solution-phase small molecule characterization as the polymer does not interfere with spectroscopic or chemical methods of analysis. In the case of MeO-PEG, the single methoxy group ( $\delta = 3.38$  ppm; ethyl protons of PEG backbone  $\delta = 3.64$  ppm in  $\text{CDCl}_3$ ) [38] can be used as an internal integration standard, allowing for easy monitoring of chemical reactions by  $^1\text{H}$  NMR spectroscopy [39].

#### 5.2.4.2 Non-cross-linked Polystyrene

Although polyethylene glycol has found widespread use in both liquid-phase synthesis and as a scaffold for liquid-phase reagents and catalysts, it is not without drawbacks. Under standard low temperature conditions used in synthesis ( $-78^\circ\text{C}$  in THF), PEG has very limited solubility. Additionally, PEG also poses a problem during the removal of excess organometallic reagents and inorganic materials caused by its water solubility. Furthermore, the polyether backbone of PEG has known lability to strong base, complicating the use of organometallic reagents. To compensate for this other polymeric supports, such as non-cross-linked polystyrene (NCPS), have been employed in liquid-phase methodologies. As is true for many other polymeric support-based methodologies, NCPS was first demonstrated to be useful in peptide synthesis [40, 41]. The utility has been further extended in a variety of publications detailing synthetic transformations of compounds immobilized on NCPS [42–48].

Non-cross-linked polystyrene is readily prepared from inexpensive materials using standard conditions and the functional group content of the polymer easily controlled by the stoichiometry of each monomer present in the monomer feed. As with PEG, the functional group content can be readily quantified using simple  $^1\text{H}$  NMR analysis. The polymer has remarkable solubility properties that are extremely useful to organic chemists. It is soluble in THF, dichloromethane, chloro-

form, benzene and ethyl acetate even at low temperatures ( $-78^{\circ}\text{C}$ ) and is insoluble in water and methanol. It is this solubility profile that allows the implementation of solvent extraction techniques commonly used in classical organic synthesis [7, 18, 42–46]. Consequently, after completion of a homogeneous reaction, the polymer-bound compounds can be diluted with dichloromethane or ethyl acetate and the organic layer subjected to an aqueous extraction. Methanol can then be used to precipitate the polymer and its uniquely bound compound as a solid, leaving behind any solution-phase products that can be separated by filtration. Finally, as NCPS is a soluble polymer, NMR analysis can be accomplished of any polymer-bound intermediates in a nondestructive manner [42–48] without the need for specialized NMR techniques or equipment.

### 5.3

#### PEG-supported Catalysts

Many different soluble polymers have been used as supports for catalyst immobilization. Since solvation of otherwise insoluble catalysts can frequently be accomplished by attachment to a soluble polymer, these supports have found significant use in the immobilization of classical solution phase catalysts. Here, we will only survey polyethylene glycol (PEG) as a soluble polymeric support for catalysis. The use of other types of soluble polymers (e.g., polyethylene, non-cross-linked polystyrene) has been reviewed elsewhere [49].

#### 5.3.1

##### Hydrogenation Catalysts

The earliest disclosure of a catalyst on a soluble-polymer support was made by Bayer and Schurig, who reported the preparation of several soluble hydrogenation catalysts [50]. Although these catalysts included MeO-PEG-supported hydrogenation catalysts, only results using NCPS were described. Another early application of soluble polymers as a catalyst support was reported by Whitesides [51]. Here, a series of water-soluble phosphines, including a MeO-PEG supported bis(phosphine), were prepared for rhodium-catalyzed hydrogenation of various olefins in water. It was hypothesized that by appending MeO-PEG onto the ligand, the solubility of the phosphine ligand would be increased. Water solubility was also achieved by forming various salts, and these proved more practical than the MeO-PEG catalyst since the observed number of turnovers (27) for the MeO-PEG bis(phosphine) was among the lowest reported in the series of catalysts surveyed.

In 1993 Bergbreiter prepared two soluble polymer-supported phosphines that exhibited an inverse temperature-dependent solubility in water [52]. Although PEG-supported phosphine undergoes a phase-separation from water at  $95\text{--}100^{\circ}\text{C}$ , the PEO-poly(propylene oxide)-PEO supported catalyst was superior as it is soluble at low temperatures and phase-separates at a more practical  $40\text{--}50^{\circ}\text{C}$ . Treatment of a diphenylphosphinoethyl-terminated PEO-PPO-PEO triblock copolymer

with  $(\text{Ph}_3\text{P})_3\text{RhCl}$  provided a catalyst that was used in the aqueous hydrogenation of allyl alcohol. This hydrogenation proceeded smoothly at  $0^\circ\text{C}$ , but stopped upon warming to  $40\text{--}50^\circ\text{C}$  and produced a dispersion of clear oily droplets. This effect was reversible, and cooling the reaction mixture allowed hydrogen uptake to continue. Furthermore, this behavior was observed through a series of four heating and cooling cycles. Bergbreiter termed these “smart ligands” since they control catalytic activity as a function of temperature.

Asymmetric hydrogenation catalysts such as BINAP have received significant attention, and MeO-PEG supported (*R*)-BINAP and (3*R*, 4*R*)-Pyrphos ligands have also been prepared and shown to be effective in  $\text{Ru}^{\text{II}}$ - and  $\text{Rh}^{\text{I}}$ -catalyzed asymmetric hydrogenations [53]. High enantioselectivity was observed (86–96%) and furthermore, these catalysts were found to be easily recyclable with little loss of catalytic activity. A second approach to MeO-PEG-immobilized BINAP was reported by Guerreiro *et al.* [54] MeO-PEG<sub>5000</sub> was treated with glutaric anhydride, then acylated with (*R*)-diaminomethyl-BINAP to afford a soluble chiral ligand. Treatment of the ligand with  $\text{Ru}(\text{COD})(\eta^3(\text{CH}_2)_2\text{CCH}_3)_2$  *in situ* provided the active catalyst. Hydrogenation of methyl acetoacetate in methanol at  $50^\circ\text{C}$  yielded the desired product in 99% *ee*, which could then be easily purified by precipitation of the catalyst from diethyl ether. This catalyst could be easily recycled for at least four times without any apparent loss of activity.

### 5.3.2

#### Chinchona Alkaloid Ligands for the Sharpless AD Reaction

The Sharpless osmium-catalyzed asymmetric dihydroxylation (AD) reaction [55, 56] has immense synthetic utility, and large efforts have been devoted towards the development of polymer-supported chinchona alkaloid ligands for this reaction [57]. The first use of a chinchona alkaloid ligand appended to a soluble polymeric support was demonstrated by Han and Janda in 1996 [58]. MeO-PEG<sub>5000</sub> was attached through a glutarate linker to dihydroquinidine (DHQD) *via* the chiral secondary alcohol to give ligand (**1a**) (Fig. 5.2). In the Sharpless AD reaction of stilbene using *N*-methylmorpholine-*N*-oxide as the stoichiometric oxidant, ligand (**1a**) gave higher *ee* values (88%) and similar yields (89%) compared with an insoluble polyacrylonitrile-supported DHQD (82% *ee*, 87% yield). Styrene, *trans*- $\beta$ -methylstyrene, and *trans*-dec-5-ene were also epoxidized under the same conditions (Tab. 5.1). Precipitation allowed for excellent recovery and five cycles of catalyst use and recovery were demonstrated with no apparent loss of activity. Importantly, this work showed that a chiral ligand could be immobilized onto a soluble polymer, giving rates similar to existing catalysts while allowing facile recovery of the catalyst.

This initial publication was rapidly followed by development of a second generation catalyst (**2**) (Fig. 5.2) [59]. Based on an earlier report [60], MeO-PEG modified phthalazine [(DHQD)<sub>2</sub>PHAL] ligand (**2**) was synthesized from MeO-PEG-NH<sub>2</sub> and found to be soluble in both *t*-butanol/water and acetone/water mixtures, allowing for homogeneous AD reactions. Furthermore, in terms of time and enantioselectivity, the soluble polymer-bound catalyst was as efficient as the classical solution-phase alkaloid.

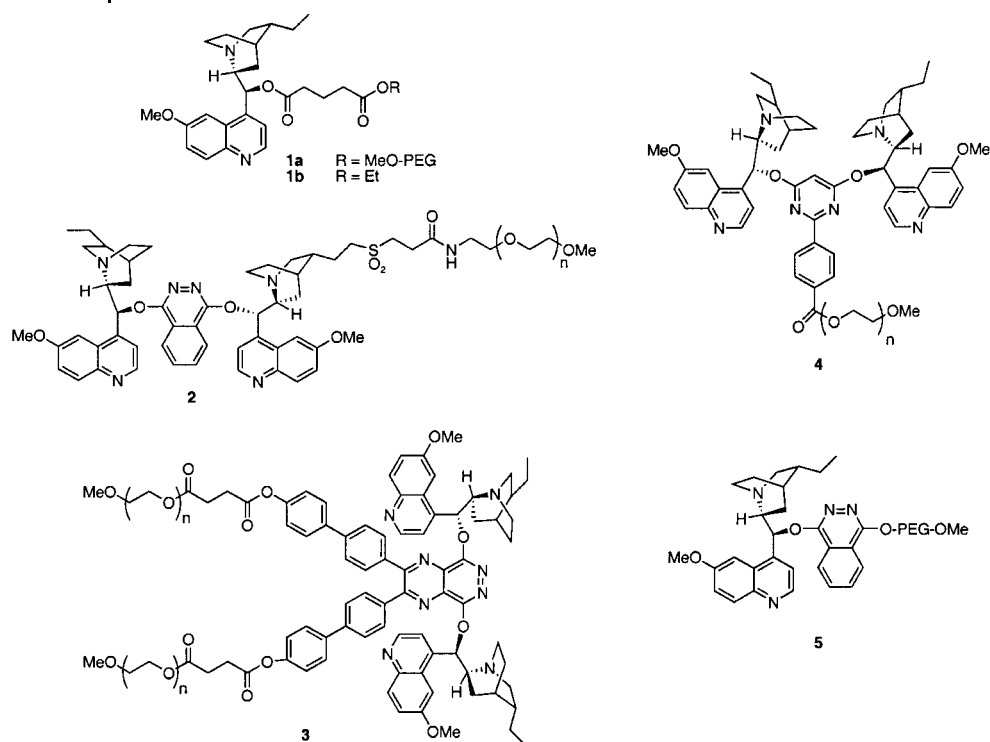


Fig. 5.2 PEG-supported Chinchona ligands.

Han and Janda also took advantage of the solubility of PEG-supported catalyst (**2**) to perform *multipolymer* AD reactions, effecting dihydroxylation on polymer-supported olefins [61]. Four polymeric supports for the olefin were investigated: Tentagel-; Wang-; Merrifield-; and MeO-PEG-supported *trans*-cinnamic acid. The use of *N*-methylmorpholine-*N*-oxide in *t*-butanol/water gave excellent results for the Tentagel- and MeO-PEG-supported cinnamates, while  $K_3[Fe(CN)_6]$  in acetone/water was needed for the Wang- and Merrifield-supported cinnamates.

Soon after Janda's initial publication [58], Bolm and Gerlach reported MeO-PEG-supported chinchona alkaloids for the Sharpless AD reaction [62]. Two catalysts were described, MeO-PEG-supported diphenylpyrazinopyridazine (DPP) (**3**) and pyrimidine (PYR) (**4**) ligands using both DHQD and DHQ for the chiral ligand (Fig. 5.2; only the DHQ derivative is shown). Enantioselectivity was observed comparable to that reported for the original DHQD and DHQ systems. Additionally, it was also noted that changing the linkage to the polymer from an ester to an ether eliminated hydrolysis of the ligand during the basic reaction conditions, allowing reuse of the catalyst without the loss of enantioselectivity observed with the pyridazine ester linkage [63]. A further improvement to this reagent using an anthraquinone core has also been reported [64].

**Tab. 5.1** Comparison of catalytic asymmetric dihydroxylation using MeO-PEG supported ligand **1a** and solution ligand **1b**.

Entry	Ligand	Olefin	Reaction Time (h)	Yield (%)	ee (%)
1	<b>1a</b>	<i>trans</i> -stilbene	5	89	88
2	<b>1b</b>	<i>trans</i> -stilbene	5	89	88
3	<b>1a</b>	styrene	5	80	60
4	<b>1b</b>	styrene	5	80	60
5	<b>1a</b>	<i>trans</i> - $\beta$ -methylstyrene	5	80	84
6	<b>1b</b>	<i>trans</i> - $\beta$ -methylstyrene	5	80	85
7	<b>1a</b>	<i>trans</i> -dec-5-ene	10	62	42
8	<b>1b</b>	<i>trans</i> -dec-5-ene	10	65	43

The latest entry into soluble-polymer supported chinchona catalysts was a recent report by Zhang and coworkers [65]. Using MeO-PEG<sub>5000</sub> as the soluble support, two different convenient two-step procedures to synthesize DHQD-PHAL-PEG-OMe (**5**) were developed to avoid the complicated synthetic manipulations in previous soluble polymer-bound chinchona ligands (Fig. 5.2) [59, 62]. This ligand gave >90% yields and 96–99% *ee* for the dihydroxylation of stilbene using K<sub>3</sub>Fe(CN)<sub>6</sub> as the stoichiometric oxidant and was recycled six times without apparent loss of activity.

### 5.3.3

#### Phase-transfer Catalysts

While poly(ethylene glycol) is well known for its ability to act as a phase-transfer catalyst [66] the first report of a derivatized PEG with quaternary ammonium end-groups for phase-transfer catalysis was reported in 1991 by Grinberg and Shaubi [67]. Treatment of PEG-dibromide with tributylamine or tributyl phosphine afforded the PEG-supported ammonium or phosphonium salts (**6**) and (**7**), respectively. Hydroxy-ammonium PEG quaternary salts (**8**) and (**9**) also were prepared in a similar manner from what was reported to be monobrominated-PEG (Fig. 5.3). It should be noted that the conditions used to form the monobrominated PEG would be expected to produce a statistical mixture of monobrominated-PEG (50%), dibrominated-PEG (25%) and PEG-diol (25%) which is indistinguishable by <sup>1</sup>H NMR and elemental analysis from pure monobrominated PEG; however, this issue was not addressed. The catalytic activity of these compounds were then examined in the dehydrobromination of bromo-(2-bromoethyl)benzene and dibromo-(2-bromoethyl)benzene to afford bromostyrene and dibromostyrene, respectively. While no mention was made of the catalytic activity of (**7**), it was shown that the four remaining catalysts were more effective in dehydrohalogenation reactions than either PEG or tetrabutylammonium bromide alone, suggesting that both the polymer backbone and covalently bound catalyst play a significant role in

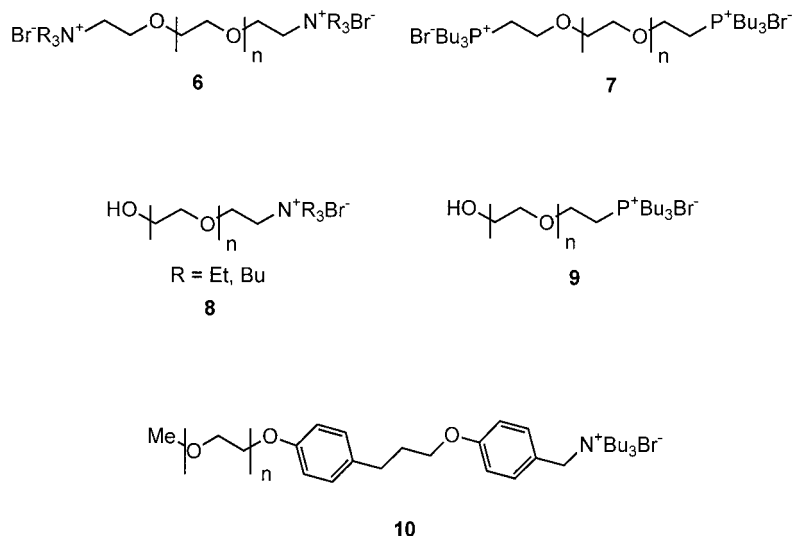


Fig. 5.3 PEG-based phase transfer catalysts.

the observed catalysis. Additionally, the hydroxy-ammonium salt catalysts (**8**) and (**9**) were more effective than PEG-supported ammonium salt (**6**).

In an extension of this work, the reuse of the polymeric catalyst was addressed and several new PE-poly(alkene) glycol copolymers were prepared [68]. Commercially available oxidized polyethylene ( $\text{CO}_2\text{H}$  terminated, both high and low molecular weight) was converted to the acid chloride and reacted with Jeffamine D or Jeffamine EDR, and subsequently converted to the tributylammonium bromide salt with butyl bromide. These new quaternary salts were shown to catalyze the nucleophilic substitution of 1,6-dibromohexane with sodium cyanide or sodium iodide. While none of the polymeric quaternary salts catalyzed the reaction as well as tetrabutylammonium bromide, the temperature-dependent solubility of the polymers allowed removal of the polymer by simple filtration.

In 2000, Benaglia and coworkers reported preparation of MeO-PEG supported quaternary ammonium salt (**10**) and examined the catalytic efficiency in a series of phase-transfer reactions (Fig. 5.3) [69]. The reactions occurred at lower temperatures and with shorter reaction times than with comparable insoluble 2% cross-linked polystyrene-supported quaternary ammonium salts, although yields varied with respect to classical solution phase quaternary ammonium salt catalyzed reactions. It was observed that yields dropped with a shorter linker, and that PEG alone was not responsible for the extent of phase-transfer catalysis. While the catalyst was recovered in good yield by precipitation, it contained an undetermined amount of sodium hydroxide, although the presence of this byproduct was found to have no effect on the recyclability of the catalyst.



## 5.3.4

**Epoxidation Catalysts**

Soluble polymer-bound catalysts for epoxidation reactions have also been explored, with a complete study into the nature of the polymeric backbone performed by Janda [70]. Chiral (salen)-Mn complexes were appended to MeO-PEG, NCPS, JandaJel™ and Merrifield resin via a glutarate spacer. It was found that for the Jacobsen epoxidation of *cis*- $\beta$ -methylstyrene, the enantioselectivities for each polymer-supported catalyst were comparable (86–90%) to commercially available Jacobsen catalyst (88%). Both soluble polymer-supported catalysts could be used twice before a decline in yield and enantioselectivity was observed. However, neither soluble polymer support proved as suitable as the insoluble JandaJel-supported (salen)-Mn complex for the epoxidation because residual impurities during precipitation and leaching of Mn from the complex, resulted in lowered yields.

Flood and coworkers utilized diamino-PEG<sub>3350</sub>-supported poly-L-leucine to catalyze the Julia-Colonná asymmetric epoxidation of enones [71]. Four catalysts were prepared with polyleucine content of 3.9, 7.5, 11.6 and 12.2 units long (average chain lengths). To measure the efficiencies of these catalysts, chalcone was epoxidized to chalcone epoxide using a THF solution of H<sub>2</sub>O<sub>2</sub> giving the product in 95–98% *ee*. The conversion to chalcone epoxide was better for the catalysts containing 3.9 and 7.5 leucine units (80%) than the catalysts with longer leucine chains (11.6: 63%; 12.2: 58%). Finally, it was determined using FT-IR that these catalysts contain a  $\alpha$ -helical structure and it is the nature of this secondary structure which leads to the observed enantioselectivity. This was supported experimentally by the preparation of an additional catalyst containing an average of 1.8 leucine units that gave chalcone epoxide in only 5% *ee*.

## 5.3.5

**Carbon–Carbon Bond-forming Catalysts**

Bis(oxazolines) have proven to be versatile ligands and a MeO-PEG-supported bis(oxazoline) ligand (**11**) for a soluble copper (I) catalyst was reported by Glos and Reiser (Fig. 5.4) [72]. The soluble-polymer supported ligand was prepared by attaching an aza-bis(oxazoline) to MeO-PEG containing a benzylidene linker. The active copper (I) complex was generated *in situ* using copper (II) triflate (1 mol%), the ligand (2.2 mol%) and phenylhydrazine. This catalyst was used for the cyclopropanation of 1,1-diphenylethylene and gave higher yields and better enantioselectivities than the classical solution phase analogues (78% yield, 90% *ee* for the MeO-PEG bound catalyst versus 49% yield, 56% *ee* for a solution phase ligand). The catalyst was reused in the cyclopropanation reaction nine times with nearly identical results before loss of activity was observed, however, the catalyst was regenerated by addition of phenylhydrazine to restore activity.

PEG-supported bis(oxazoline) ligands (**12**) were prepared and tested as ligands in homogeneous Cu-catalyzed asymmetric transformations (Fig. 5.4) [73]. The Diels–Alder reaction proceeded in poor *ee*, while cyclopropanation and ene reac-

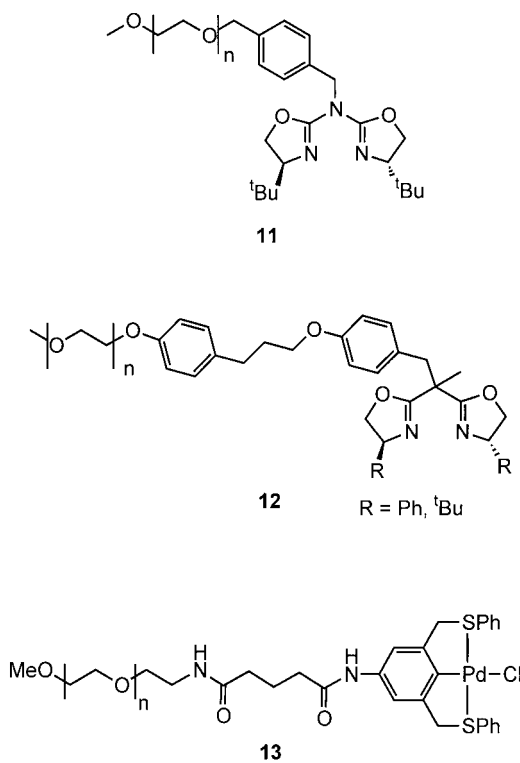
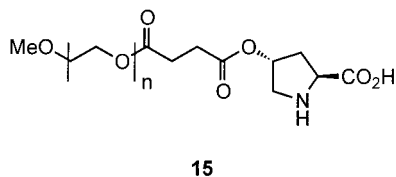
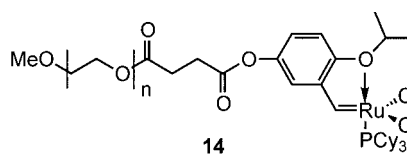


Fig. 5.4 Bidentate ligands for carbon–carbon bond formation.

tions proceeded in good yield and good to excellent enantioselectivity, with ene reactions also displaying good diastereomeric excess as well. The catalysts were recovered by precipitation and regenerated, although a slight reduction in yield and *ee* was noted.

In conjunction with the development of low molecular weight “pincer” type S–C–S tridentate ligands for Pd(II)-catalyzed Heck reactions, the MeO-PEG supported catalyst (**13**) was also prepared [74, 75]. The SCS ligand was connected to MeO-PEG<sub>5000</sub> via an aryl ether linkage. After treating the ligand with Pd(PhCN)<sub>2</sub>Cl<sub>2</sub>, it was found that this catalyst slowly decomposed during the Heck reaction, giving a black precipitate of Pd<sup>0</sup>. Changing the aryl ether linkage to a more robust acetamido linker proved successful, and the new catalyst was shown to be stable and recyclable with no apparent loss of activity (Fig. 5.4). Using 0.1 mol% of the catalyst with triethylamine in DMF at 115 °C, the Heck reaction of iodophenol and styrene to form stilbene and reaction of iodophenol with methyl acrylate to form methyl cinnamate went to completion within seven hours. Precipitation of the catalyst and extractive work-up provided the pure Heck coupling products. The reactions were repeated three times with no deactivation of the catalyst observed.

**Fig. 5.5** PEG-supported catalysts for carbon–carbon bond formation.



Olefin metathesis has emerged as a powerful synthetic methodology, especially with the development of powerful catalysts such as the Schrock molybdenum alkylidene [76] and the Grubbs-type ruthenium alkylidenes [77–79]. However, attempts to immobilize the Grubbs catalyst on insoluble polymers have been met with limited success [80–82]. Poly(ethylene glycol) monomethyl ether (MeO-PEG<sub>5000</sub>) was coupled to a substituted styrene using a succinate linker to provide, after treatment with a ruthenium alkylidene, MeO-PEG supported Grubbs-type catalyst (**14**) (Fig. 5.5) [83]. This catalyst was used for the ring-closing metathesis reaction of a number of dienes and demonstrated excellent conversions (>92%) for all studied examples and only a slight decrease in catalytic activity after repeated use.

Recently, small organic molecule asymmetric catalysts have seen extensive use in synthesis. Primarily, these catalyst have used amine functionalities to impart either a lowering of the LUMO of one of the substrates [84], or nucleophilic catalysis mechanisms. Indeed, compounds such as proline catalyze a variety of processes including the aldol reaction via an enamine-based process [85–87]. A soluble polymer-supported L-proline aldol catalyst was recently reported by Benaglia in which 4-hydroxyproline was attached to MeO-PEG<sub>5000</sub> through a succinate spacer to generate catalyst (**15**) (Fig. 5.5) [88]. Catalyst (**15**) served as an efficient aldol catalyst for the reaction of acetone or hydroxyacetone with various aldehydes giving aldol addition products in comparable yield and *ee* to proline-catalyzed reactions. Reuse of the catalyst was demonstrated, and after two cycles, only a slight loss of catalytic activity was observed, with no apparent reduction of enantioselectivity.

## 5.4

### Soluble Polymer-supported Reagents

Soluble polymer-supported reagents have both advantages and disadvantages compared with insoluble macromolecular reagents. The most obvious advantage of either form of reagent is the ease of separation from solution-phase components. However, a potential disadvantage unique to soluble polymer-supported reagents derives from the higher molecular weight of the polymer relative to a traditional reagent. Essentially, the number of equivalents of reagent per gram of polymer can become a pronounced liability, especially when working with larger scale synthetic applications. A loading capacity in the range of 1 to 0.1 mmol g<sup>-1</sup> may not provide the required number of equivalents of reagent without using extraordinary amounts of polymer-bound reagent. This drawback is not as prevalent with soluble polymer-supported catalysts as multiple equivalents of the catalyst are generally not required.

#### 5.4.1

##### Phosphine Reagents

Soluble polymer variants of triphenylphosphine have found significant attention and several applications of these reagents have been demonstrated. This reagent has widespread use in organic chemistry in reactions such as the Staudinger reduction, Mitsunobu reaction, Wittig reaction, and halogenation of alcohols. The key advantage to the use of these reagents is the ease in which they allow the phosphine oxide byproduct to be separated away from the rest of the reaction mixture.

The first publication of a soluble polymer-supported phosphine was reported in 1983 [89]. In this work, non-cross-linked polystyrene was used as the polymeric support for the formation of poly(styryldiphenylphosphine) (**16**) with a loading of 2.7–3.0 mmol phosphine per gram polymer (Fig. 5.6). Interestingly, the efficiency of the soluble polymer-supported phosphine was found to be comparable to divinylbenzene cross-linked poly(styryldiphenylphosphine) in the formation of alkyl chlorides from an alcohol and carbon tetrachloride; however, upon prolonged storage the polymeric reagent appeared to cross-link and become insoluble. The starting linear polystyrene was soluble under the reaction conditions, yet upon completion, the polymer precipitated allowing purification by filtration. It was postulated that the depleted polymeric reagent contained both the corresponding phosphine oxide as well as chloro- or dichloromethylphosphonium salts derived from the starting polymer. Through the use of a kinetic study of the conversion of benzyl alcohol or 3-phenylpropanol to the corresponding chlorides, Hodge demonstrated that the soluble polymer-supported phosphine was only slightly less reactive than a similar divinylbenzene cross-linked insoluble polymer-supported phosphine. A further refinement of a triphenylphosphine reagent on NCPS (**17**) has been reported for a Staudinger/aza-Wittig process with superior results observed relative to an insoluble-polymer variant of the reagent [90]. In a later study, this second-generation reagent was implemented in the Mitsunobu reaction and the synthesis

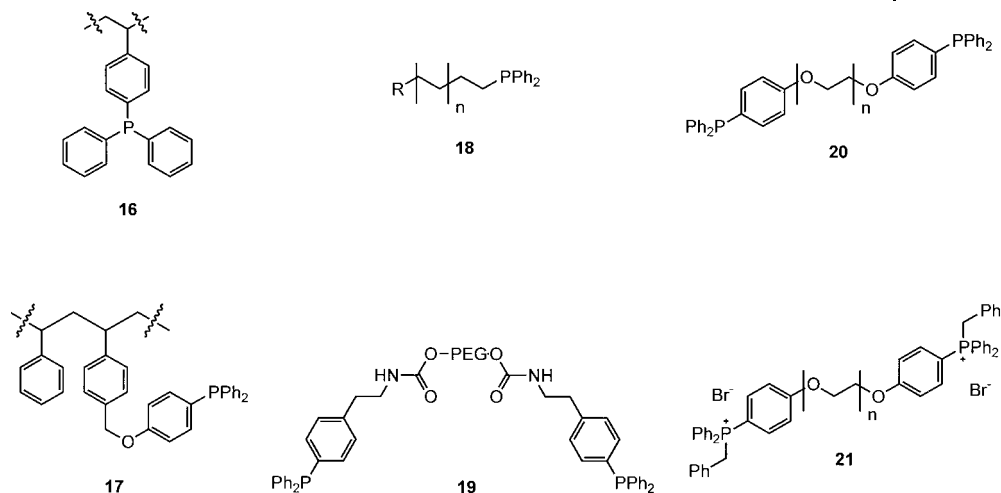


Fig. 5.6 Soluble polymer-supported phosphine reagents.

of *E*-trisubstituted alkenes from Baylis–Hillman adducts *via* a highly regioselective  $S_N2'$  Mitsunobu reaction [91]. Interestingly, the use of the soluble polymer-bound reagent showed significantly higher regioselectivity in this reaction as compared with triphenylphosphine, possibly because of increased steric bulk present in the NCPS-supported phosphine.

A polyethylene backbone has also been demonstrated as a suitable support for the immobilization of a diphenylphosphine reagent (**18**) (Fig. 5.6) [92]. Here, linear polyethylene was prepared via an anionic polymerization process and the polymer capped with chlorodiphenylphosphine. This reagent also showed good activity in the synthesis of alkyl chlorides from alcohols displaying comparable results to insoluble polystyrene-bound phosphine reagents. Furthermore, (**19**) could be recycled by reduction of any present phosphine oxide moieties with trichlorosilane, albeit with reduced activity. After one cycle of reaction and then regeneration, the recycled reagent only retained 65% of the activity of the fresh reagent. This is in agreement with previously observed results by Hodge in which insoluble divinylbenzene cross-linked diphenylphosphine only retained 40% of original activity upon regeneration using trichlorosilane. This reduction in the active reagent was hypothesized to be a result of reactions in which halogenated phosphonium salts form as unwanted and unreducible by-products [89].

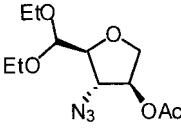
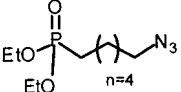
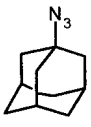
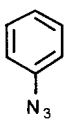
In 1997, Janda reported a polyethylene glycol variant of soluble-polymer supported diphenylphosphine [93]. This reagent (**19**) (Fig. 5.6) was synthesized on dihydroxy-PEG<sub>3400</sub> and this support was found to satisfy two key requirements. The polymer was of low enough molecular weight to allow acceptable loading while still affording both excellent solubility in certain solvents (i.e.,  $H_2O$ , DMSO, DMF,  $CH_2Cl_2$ , toluene, benzene, and warm THF) as well as high polymer recovery (>97%) when precipitated from an appropriate solvent. Synthetically, it was dis-

covered to be advantageous to first synthesize the triarylphosphine derivative followed by loading of this molecule onto the polymer since significant decomposition of the PEG support was observed if the synthetic steps were reversed. Polymer loadings were excellent (0.5 mmol phosphine per gram of polymer) and determined by both  $^1\text{H}$  NMR spectroscopy and *p*-nitrophenol release during polymer loading.

The utility of the polyethylene glycol-supported triarylphosphine reagent was shown in two reactions. First, the reagent was used in the chemoselective reduction of azides, the Staudinger reaction [94, 95]. Although the demonstration of a polystyrene-bound reagent in this reaction had been shown [96], no soluble polymer approach has been disclosed. A variety of alkyl and aryl azides were subjected to the conditions of the Staudinger reaction using both the soluble polymer-supported phosphine and an insoluble polystyrene-bound phosphine. Reaction times were observed to be shorter in all cases for the PEG-supported reagent, and in one case, no reaction was observed for the polystyrene-supported phosphine thus highlighting the importance of this liquid-phase methodology (Tab. 5.2).

The second reaction utilized with this reagent was the Mitsunobu reaction [97], a reaction known to require chromatographic purification to obtain pure product because side-products are formed. An insoluble polymer approach to this problem is known [98], however, the nature of the support means that the reaction is inherently heterogeneous (see above). The reaction between phenol and a series of alco-

Tab. 5.2 Comparative Staudinger reactions using **19** and polystyrene- $\text{PPh}_3$  with the listed azides.

Azide	19		Polystyrene- $\text{PPh}_3$	
	Yield (%)	<i>t</i> (h)	Yield (%)	<i>t</i> (h)
	95	2	–	No reaction
	98	1.5	82	8
	91	4.5	95	11
	90	3	94	3.5

hols in the presence of reagent (**19**) and diethylazodicarboxylate (DEAD) was performed and each gave the respective Mitsunobu etherification product in excellent yield. As was observed for the Staudinger reductions, reactions using the soluble polymeric reagent proceeded faster than reactions using the corresponding insoluble polymer-supported triphenylphosphine. Furthermore, ether formation was observed in the case of benzyl alcohol only when using the PEG-supported reagent.

In a continuation of their initial study, Janda and Wentworth disclosed an optimized version of the polyethylene glycol-supported triarylphosphine reagent (**20**) (Fig. 5.6) [99]. In the previous report, the carbamate linkage used has known susceptibility to base, Lewis acid, and metalating agents. A more stable attachment was devised that would more closely resemble that of the polymer backbone. Here, the phosphine was attached to the polymer backbone using a more stable aryl ether linkage rather than a urethane linker. The reagent was prepared through a very concise synthesis starting from *p*-bromophenol in 85% yield over three steps. The unsupported reagent was then loaded onto PEG<sub>3400</sub> via displacement of the mesylate moieties of the polymer. Interestingly, the preparation of the dimesylate was accomplished by heating PEG<sub>3400</sub> in a neat solution of methanesulfonyl chloride without the need for a scavenger base. Upon generation of reagent (**20**), it was determined by <sup>31</sup>P NMR spectroscopy that less than 2% phosphorus oxidation had occurred. Furthermore, the reagent was found to be stable to air exposure for prolonged periods of time (2–3 weeks) with little oxidation of the phosphine moiety (<5%).

To test the ability of this second generation reagent to perform as a substitute for triphenylphosphine, it was first used in the decomposition of ozonides. Triphenylphosphine is an important alternative to standard methods for the decomposition of these types of compounds as it is not only a very mild reaction, but also avoids the use of malodorous reagents and high-boiling-point byproducts that are present in other methods [100]. Unfortunately, when triphenylphosphine is used in solution, the removal of excess reagent and triphenylphosphine oxide can cause significant problems. As an alternative, solid-supported triphenylphosphine has been reported as an acceptable alternative to PPh<sub>3</sub> in the generation of aldehydes [101]. A series of alkenes were exposed to ozone and the resulting ozonides treated with PEG-supported triarylphosphine reagent (**20**). For comparison, ozonides were treated with triphenylphosphine as well as a commercially available polystyrene-immobilized triphenylphosphine resin. Isolation of (**20**) following the completion of the reaction was performed by simple precipitation and consistently removed >99% of the polymer byproduct. Also, in almost all studied cases, the produced aldehydes were obtained in highest yield with the soluble polymer reagent (Tab. 5.3). The regeneration of the phosphine reagent from the corresponding phosphine oxide was also studied [99]. A number of standard methods for the reduction of phosphine oxides were tested including polymethylhydrosiloxane (PMHS) [102], trichlorosilane [103], and alane (AlH<sub>3</sub>) [104]. Of the methods tested only alane gave satisfactory results for the regeneration of (**20**) as determined by <sup>31</sup>P NMR. Upon reduction, the polymer could be isolated in 75% yield by precipi-

**Tab. 5.3** Direct comparison of ozonide hydrolysis between solution-phase, solid-phase and liquid-phase triphenylphosphine.

Entry	Alkene	Product	Yield (%)		
			<i>PPh</i> <sub>3</sub>	●- <i>PPh</i> <sub>3</sub>	20
1			94	58	98
2			80	73	92
3			84	60	97
4			51	56	77
5			72	62	63

tation into degassed diethyl ether. The incomplete recovery of polymer was attributed to the presence of aluminum salts that could either prevent precipitation by complexing the polymeric support or cause hydrolysis of the polymer backbone during phosphine reduction.

The use of polymeric supports to aid in the Wittig olefination reaction are well-documented [105–110]. Polymer-bound phosphonium salts have the advantage of being readily separated from a reaction mixture once converted to their respective phosphine oxides. Furthermore, these oxides can then be readily recycled by reduction of the phosphine oxide by standard methods. Divinylbenzene cross-linked polystyrene has been the most common polymeric carrier used, and there has been significant success in the use of these reagents. However, soluble polymers have also been shown useful as supports for Wittig reagents. Hodge reported the use of a diphenylphosphinylated non-cross-linked polystyrene support ( $M_w = 100\,000$ ) for use as a Wittig reagent [111]. This reagent contained approximately 2.7 mmol of phosphine per gram of polymer and could be readily converted to the corresponding phosphonium salt via reaction with either benzyl chloride or 2-bromomethylnaphthalene. A series of ketones were tested as substrates for the soluble polymeric reagent, in addition to 1% and 8% divinylbenzene cross-linked polystyrene reagents. Since the bases used in these experiments were only soluble under aqueous conditions, a phase-transfer catalyst was necessary in the case of



the insoluble polymeric supports. However, no phase-transfer catalyst was necessary with the soluble polymeric reagent, reportedly because of the known ability of soluble polymeric supports to function as phase-transfer reagents [66]. Isolation of the alkene products from the soluble polymer was accomplished by precipitation of the linear poly(styryldiphenylphosphine oxide) using methanol.

Organic chemistry performed in water has attracted significant effort in recent years because of both the ready availability and environmental compatibility of water relative to organic solvents [112, 113]. Examples of aqueous Wittig reactions are known [114, 115], however, none of these employ polymeric reagents. The physical properties of the PEG backbone are such that a PEG-supported phosphonium reagent could have excellent solubility in water. Janda and Wentworth reported the preparation of polyethylene glycol-supported phosphonium reagent (**21**) in 81% yield by a treating PEG-immobilized phosphine (**20**) with benzyl bromide (Fig. 5.6) [99]. Reagent (**21**) was used in the Wittig olefination to prepare a series of stilbene derivatives in aqueous sodium hydroxide solution. All products were obtained in good to excellent yield by partitioning the stilbene products into  $\text{CH}_2\text{Cl}_2$ , followed by precipitation of the polymer-bound phosphine oxide by-product in diethyl ether. Furthermore, unlike previous reports which stated the *E:Z* ratio could be affected by product isolation conditions [116], this methodology allows for full extraction of both isomeric stilbenes without concern for phosphine oxide contamination, which is removed by precipitation and filtration. The scope of this reaction was further explored by varying both the base strength and temperature of the reaction. It was found that by increasing the base strength from 1 to 2 M sodium hydroxide, neither the yield of stilbene nor the ratio of geometric isomers was affected. However, elevation of the reaction temperature did give improved reaction yields as well as an expected increase in the *E:Z* ratio.

#### 5.4.2

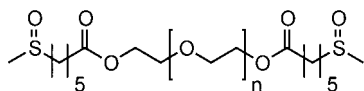
##### Oxidants

A variety of groups have reported the preparation and use of oxidizing agents in which a polymeric backbone is used to either ionically or covalently bind the oxidant. Oxidation reagents that have been immobilized onto soluble polymeric supports have also been studied. For example, Schuttenberg reported the use of *N*-chlorinated nylon polymers as a soluble reagent for the oxidation of primary and secondary alcohols as well as the oxidation of sulfides to sulfoxides [117]. These polymers contained a high loading of *N*-chloro moieties, facilitating the ability of the polymer to serve as a reagent. The oxidant was prepared by chlorination of linear polyamides using either *tert*-butyl hypochlorite, chlorine monoxide or hypochlorous acid in carbon tetrachloride. Using Nylon 66 and *tert*-butyl hypochlorite as the oxidant, these reactions were complete in three hours at 15 °C and converted 94% of the original *N*-H bonds to *N*-Cl bonds. Interestingly, the new polyamide reagent had markedly different solubility properties relative to the parent polymer. Although the starting polyamide was relatively insoluble in many solvents, the new polymer was readily soluble in chloroform, benzene, and toluene.

This new solubility was hypothesized to be caused by diminished hydrogen bonding as most N–H hydrogen bond donors had now been converted to N–Cl bonds. When used as an oxidant, the polymeric reagent would then be converted back into the starting polyamide, which had poor solubility in the reaction solvent. Therefore, upon completion of the reaction, the reagent could be filtered away from the products and regenerated by treatment with *tert*-butyl hypochlorite or hypochlorous acid. A range of secondary alcohols were oxidized to the corresponding ketone at 35 °C typically in 24 hours using the nylon-based reagent in good to excellent yield as measured by gas chromatography. A series of primary alcohols and sulfides were also oxidized, however significant variability was seen in the products. Attempts at performing asymmetric oxidations of sulfides using a chiral *N*-chloro nylon derived from (–)-poly-*S*-(–)-4-methylazetidin-2-one were also described, but the sulfoxides obtained were optically inactive.

The Swern oxidation is among the most valuable and widely used reactions in synthetic organic chemistry [118]. Although highly effective, its main drawback rests in the production of the noxious, volatile byproduct, dimethyl sulfide. A number of solutions to this problem have been reported, including the use of modified dimethylsulfoxide reagents in the Swern oxidation [119]. A soluble polymer approach to the Swern oxidation has also been reported [120]. Here, 6-(methylsulfinyl)hexanoic acid was attached to PEG<sub>2000</sub> under standard conditions to allow for optimal loading while still retaining high polymer recoveries after precipitation of the reagent. The sulfinyl ether was then oxidized to the corresponding sulfoxide reagent (**22**) using sodium metaperiodate (Fig. 5.7). Initial studies were conducted using insoluble polymeric supports such as Merrifield resin, but although the reagent performed acceptably, regeneration of the reagent was accompanied by a loss in oxidation capacity from 92% to 78%. A series of alcohols were explored and a comparison was made between the PEG-sulfoxide reagent, 6-(methylsulfinyl)hexanoic acid, and literature yields obtained under standard Swern conditions. In all tested cases, yields were comparable to both previously reported reagents demonstrating the utility of this reagent. The recyclability of the PEG-supported sulfoxide was also tested. After performing the oxidation of *endo*-borneol under limiting conditions using a slight excess of sulfoxide reagent, the recovered reagent was re-oxidized with sodium metaperiodate. The desired reagent was regenerated in excellent yield (91%) and reused for five oxidation/regeneration cycles with no apparent loss of oxidation capacity.

Hypervalent iodine reagents have become extremely valuable tools in organic chemistry [121]. Reagents such as the Dess–Martin periodinane have received immense attention because of its efficiency and mild reaction conditions. The precursor to the Dess–Martin periodinane, *o*-iodoxybenzoic acid (IBX) has also be-

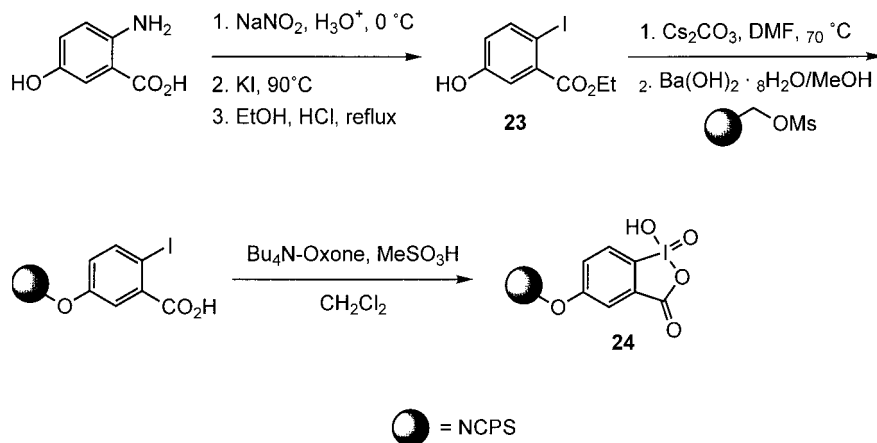
**22****Fig. 5.7** PEG-supported Swern oxidant.

come popular as a reagent and has been implemented in various synthetic methodologies [122]. In some cases, IBX is a preferred reagent as it is shelf-stable, conveniently handled, and exhibits greater selectivity in its oxidation potential relative to the Dess–Martin periodinane [123, 124]. However, IBX is notoriously insoluble, and reactions which use IBX as an oxidant are frequently performed as heterogeneous slurries of the reagent. Insoluble polymer-supported hypervalent iodine species have been reported by Ley [125], this reagent, polystyrene(diacetoxyiodo)benzene, was immobilized on divinylbenzene cross-linked polystyrene and successfully used in the oxidation of a variety of substrates. Recently, Janda and co-workers have reported a soluble polymer-supported version of IBX that has the advantage of being soluble in a greater range of solvents [126]. This reagent was prepared by first synthesising the appropriate *m*-hydroxyiodobenzoic acid precursor (**23**) (Scheme 5.1). Loading of this compound onto NCPS, followed by ester hydrolysis and oxidation of the iodine from I(III) to I(V) led to NCPS-supported reagent (**24**). Although PEG was also explored as a possible soluble support for this reagent, difficulties in purifying the PEG-immobilized reagent from Oxone<sup>TM</sup> salts led the researchers to drop this support from the study. Using two equivalents of NCPS supported-IBX, it was demonstrated that the conversion of benzyl alcohol to benzaldehyde proceeded in quantitative yield after only one hour in methylene chloride. In comparison, a macroporous polystyrene-supported IBX reagent required four hours to achieve quantitative conversion, and a gel-type polystyrene-supported reagent only gave 75% conversion even after extended reaction times.

#### 5.4.3

#### Reducing Agents

Polymer-bound reducing agents have received significantly less attention, presumably because main group metal hydride complexes predominate as reducing



**Scheme 5.1** Synthesis of NCPS-supported IBX.

agents. However, there have been a few approaches to soluble polymer-supported reducing agents. One example of a soluble polymeric metal hydride is linear poly(vinylpyridine) used as a matrix to bind borane [127]. This polymer-borane complex was shown to behave much like pyridine-borane in the reduction of carbonyl moieties to hydroxyl groups. Compounds such as benzaldehyde, *p*-chlorobenzaldehyde and cyclopentanone were shown to be reduced to the corresponding alcohols by the polymeric reagent in comparable yield to that of pyridine-borane. Furthermore, in the case of benzophenone, the alcohol product was obtained in 40% yield with the polymeric reagent, while pyridine-borane showed no visible reduction of the ketone functional group.

Radical anion species derived from the reaction of an alkali metal with aromatic moieties have been reported on insoluble polymeric supports [128, 129]. Similar soluble polymer-based reagents have also been developed using either poly(vinyl-naphthalene) and polyacenaphthalene as the polymeric support [130]. Alkali metal derivatives of poly(vinyl-naphthalene) were reported to include the dilithium salt, sodium salt, and potassium salt. Each was prepared by reaction of a solution of the soluble polymer with the appropriate alkali metal at room temperature for 24 hours. The polymeric lithium derivative was found to quantitatively react with organic halides such as benzyl chloride, butyl bromide and allyl chloride. However, it displayed no reaction with iodobenzene or other halogenated arenes or with cyclohexyl chloride. This discrepancy in reactivity was hypothesized to be caused by the cyclic structure of the failed substrates, presumably from steric hindrance with the naphthalene-based backbone. Yet, reagents derived from a polyacenaphthalene did react with these cyclic halides and this was rationalized as being a result of the greater flexibility and resultant diminished steric hindrance of the naphthalene groups in the polymeric backbone. It is difficult to assess if this is a general phenomenon with soluble polymer-supported alkali radical anions as a thorough study of the poly(vinyl-naphthalene) support was not conducted.

An atypical approach to the use of a soluble-polymeric reducing agent was described by Smith for the generation of colloidal dispersions of red, amorphous selenium [131]. An aqueous solution of polyacrylic acid was treated with hydrazine hydrate followed by selenious acid to yield stable red dispersions of amorphous selenium. These reactions are performed at sufficiently dilute concentrations such that each polyacrylate is viewed as discrete and noninteracting. As a solution of selenious acid is added to the polymer, the selenious acid molecules that are spatially close to a given hydrazone polyacrylate macromolecule are reduced to selenium atoms. These atoms were reported to aggregate in a single hydrophobic particle that remains bound to the acrylate backbone. Importantly, only 75% of the pendant acid groups were neutralized by added hydrazine to insure that the polymeric reagent would contain a small amount of residual acid. These acidic moieties presumably serve to catalyze the reduction of the selenious acid by the polymeric reagent.

## 5.4.4

**Microgel-supported Reagents**

The use of microgel-supported reagents for organic synthesis have unique advantages not present in other soluble polymeric reagents. Microgels are intramolecularly cross-linked molecules that form a stable solution in many solvents. Analogous to soluble polymers, microgel polymers are soluble in THF, toluene, methylene chloride, and DMF but insoluble in hexane and methanol. Unlike soluble polymers however, microgel solutions also possess low viscosity even at high concentrations of polymer [132]. Explorations into the uses of microgels in organic synthesis have only started [133, 134], however it is anticipated that they will offer many of the advantages of soluble polymeric reagents without suffering from low loading capacities. Currently, these polymers are not commercially available but their preparation is readily accomplished with minimal effort.

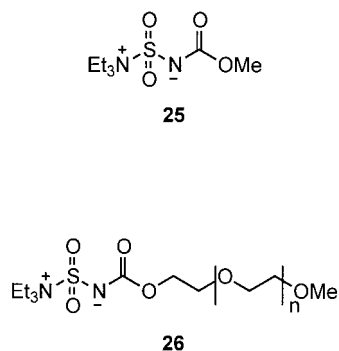
Many soluble polymeric reagents suffer from low loading capacities relative to insoluble supports because of the nature of their backbone structures. For example, in the range of usable molecular weights (*vide supra*), polyethylene glycol has a maximum loading capacity of approximately  $1.0 \text{ mmol g}^{-1}$  as the only sites of functionality are the two ends of the linear polymer chain [135]. However, microgel-based reagents would not suffer from this drawback as they can be prepared at identical loadings to that of insoluble polymer-bound reagents.

Janda and co-workers have recently reported the preparation and use of two microgel-supported reagents, a polyamine-based scavenging reagent and borohydride reducing agent [136]. These polymers are prepared in a manner similar to insoluble cross-linked polystyrene resins, however, monomer concentrations are held at very low concentrations and consequently the polymerization must be performed over extended periods of time. Both reagents were prepared from a chloromethyl functionalized microgel using previously reported conditions for insoluble polymeric reagents. The effectiveness of the polyamine reagent (loading level:  $0.84 \text{ mmol amine per gram}$ ) was demonstrated in the scavenging of excess phenyl isocyanate from the reaction of the isocyanate and *sec*-butyl amine. Upon addition of a slight excess of the reagent and precipitation of the microgel with methanol, the desired product was obtained in quantitative yield and 97% purity. For a similar reaction using an insoluble polymer-supported reagent, not only were more equivalents of reagent necessary, but also longer reaction times [137]. The borohydride reagent (loading level:  $0.44 \text{ mmol borohydride per gram}$ ) was explored in the context of the reduction of 4-chlorobenzaldehyde to the corresponding alcohol. Using an excess of borohydride reagent (1.1 eq) complete reduction of the carbonyl moiety was observed and the spent reagent precipitated from the reaction mixture using hexane. Further explorations into the utility of microgels as scaffolds for polymer-supported reagents is clearly needed as these polymers display many of the advantages of liquid-phase chemistry while limiting its shortcomings.

## 5.4.5

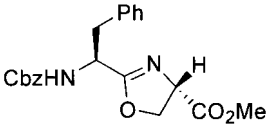
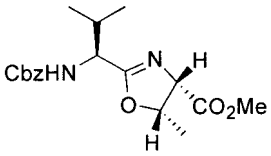
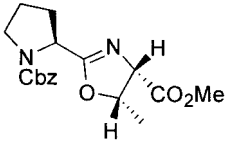
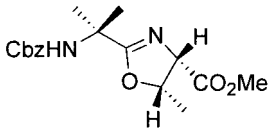
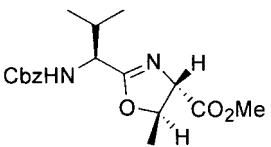
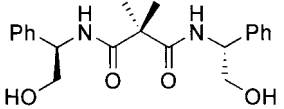
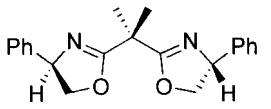
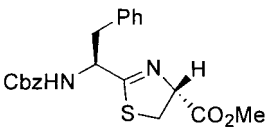
**Miscellaneous Reagents**

A variety of synthetically useful soluble-polymer supported reagents have been developed to capitalize on the inherent advantages of liquid-phase synthesis. One example of this is the MeO-PEG-immobilized version of the Burgess reagent [138] reported by Wipf in 1996 [139]. The Burgess reagent (methyl *N*-(triethylammonium-sulfonyl)carbamate) (**25**) has been shown to be extremely useful in the preparation of varied heterocyclic structures such as oxazolines and thiazolines with high stereochemical purity (Fig. 5.8) [140, 141]. However, the reagent has known susceptibility to oxidation, moisture and temperature. Even with appropriate precautions taken, the reagent still possesses a limited shelf-life and should be freshly prepared for each use. Wipf successfully coupled chlorosulfonyl isocyanate with either dry MeO-PEG<sub>750</sub> or MeO-PEG<sub>2000</sub> followed by treatment with triethylamine to generate PEG-bound reagent (**26**) (Fig. 5.8). Interestingly, prior attempts to couple the reagent to modified Merrifield resin failed. Cyclodehydrations proceeded smoothly and in superior yields with PEG-supported Burgess reagent (**26**) (Tab. 5.4) compared with (**25**). Furthermore, considerable reactivity was retained even after extended storage of the reagent at or below room temperature. Upon completion of the reaction, the polymer was readily removed by filtration through a plug of silica gel. When chiral substrates were used for cyclodehydration reactions, little epimerization or elimination was observed, and furthermore, it was demonstrated that the reaction was stereospecific. In a remarkable example of the utility of this reagent, sensitive oxazolines could be generated in high yields (88%) using the MeO-PEG<sub>2000</sub> supported reagent, whereas the reported maximum yield for this reaction was nearly three-fold less. A further example of the utility of PEG-supported Burgess reagent has been shown in the cyclodehydration of a range of substituted 1,2-diacylhydrazines [142]. Using reagent (**26**) in conjunction with single-mode microwave heating 1,3,4-oxadiazoles were provided in excellent yields (>70%) and purity (>89%) as determined by HPLC. It was also discovered that transformations involving protected threonine, tyrosine and serine derivatives



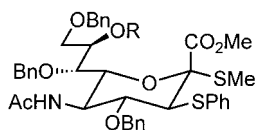
**Fig. 5.8** Burgess reagent and PEG-supported Burgess reagent.

Tab. 5.4 Cyclodehydration of hydroxyamides and thioamides with polymeric Burgess reagent **26**.

Entry	Hydroxyamide	Azole	Yield (%)
1	Cbz-Phe-Ser-OMe		88
2	Cbz-Val-Thr-OMe		90
3	Cbz-Pro-Thr-OMe		85
4	Cbz-Aib-Thr-OMe		88
5	Cbz-Val-αThr-OMe		76
6			80
7	Cbz-Phe-ψ(CSNH)Ser-OMe		98

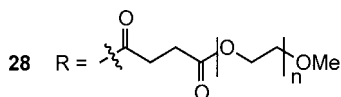
required a larger excess of reagent, longer irradiation times, and the addition of the reagent in two lots.

Soluble polymeric reagents for use in carbohydrate chemistry have also been developed. Sialic acid (NeuAc) is frequently found as a nonreducing end terminal residue in oligosaccharides, and a MeO-PEG<sub>5000</sub>-immobilized reagent has been synthesized to facilitate its introduction into a growing oligosaccharide chain [143]. In order to guarantee nearly complete stereocontrol over the glycosylation



**Fig. 5.9** PEG-supported thioglycoside for carbohydrate synthesis.

**27** R = H

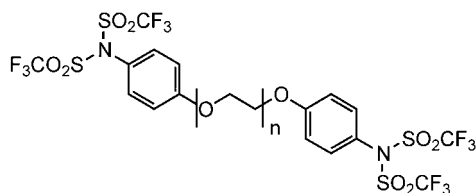


reaction independent of reaction conditions, thioglycoside (**27**) was chosen as a suitable auxiliary in the preparation of reagent (**28**) (Fig. 5.9). Model glycosylations were performed with a galactose derivative using standard conditions for thioglycoside activation and the desired disaccharide product was obtained in good yield (65–70%) after cleavage from the soluble polymer. A less reactive glycoside acceptor was also investigated and yielded the desired disaccharide product, albeit in reduced yield (50–60%).

As an improvement upon solution-phase triflating agent (**29**), PEG-derivative (**30**) was reported by Janda and Wentworth for use in the high-throughput synthesis of aryl and enol triflates (Fig. 5.10) [144]. Aryl and enol triflates have been utilized in a variety of organometallic cross-coupling reactions, however, triflates are inherently unstable and the preparation of these types of compounds can be complicated by classical solution-phase purification techniques. Soluble polymer-supported reagent (**30**) was synthesized from PEG<sub>3400</sub>-dimesylate in greater than 98% yield over three steps. Loading of the reagent was determined to be quantitative (*ca.* 0.6 mmol triflate per gram polymer) by <sup>1</sup>H NMR and purity of the bis(*N*-trifli-



**29**



**30**

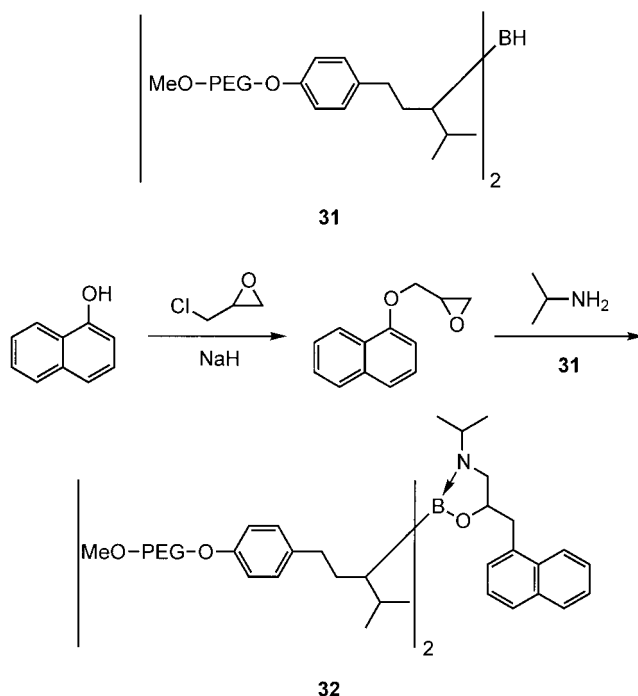
**Fig. 5.10** Classical triflimide reagent PEG-based triflimide.



mide) was determined by  $^{19}\text{F}$  NMR. As was previously observed with the PEG-Burgess reagent [139], **(30)** was found to be very stable on standing in air, unlike the corresponding classical solution-phase reagent. A range of aromatic alcohols was subjected to standard triflate formation conditions and all products were formed in excellent yields and purity. Furthermore, the soluble polymeric reagent was also used in the trapping of kinetic enolates to form vinyl triflates in superior yield to the classical triflimide reagent. The ability of **(30)** to be recycled was also examined and it was found that the triflimide reagent could be quantitatively recovered and regenerated with no apparent loss of activity.

In a soluble polymer strategy comparable to resin-capture [145], Janda reported a MeO-PEG<sub>5000</sub>-supported dialkyl borane reagent **(31)** that was used in the purification of a solution-phase library of  $\beta$ -amino alcohols [146]. Purification was achieved by simply adding **(31)** to the crude reaction mixture followed by subsequent precipitation of the polymer with diethyl ether to give polymer-supported 1,3,2-oxazaborolidine **(32)** (Scheme 5.2). The  $\beta$ -amino alcohol product could then be released from the soluble support by treatment with acid. In a two-step synthetic strategy that is readily amendable to automation, the isolation of a small library of  $\beta$ -amino alcohols was accomplished with all compounds obtained in >80% purity.

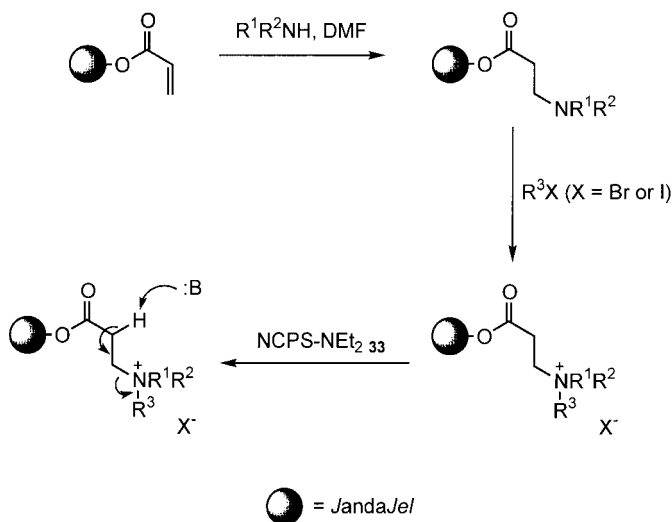
Thioacetals and thioketals have significant synthetic potential for use in organic chemistry but are often neglected because of their unpleasant odor. A polymeric reagent for the preparation of ketones *via* 1,3-dithianes has been reported using



**Scheme 5.2** PEG-supported boranes for  $\beta$ -amino alcohol purification.

NCPS as a soluble support [147]. Using this reagent, a number of aldehydes were converted to the 1,3-dithiane immobilized compound in the presence of boron trifluoride etherate. These types of compounds have umpolung reactivity as a carb-anionic species and can be readily generated and then alkylated with alkyl halides to produce ketones. Treatment of the polymer-supported 1,3-dithianes with *n*-butyl lithium followed by treatment with various alkyl halides generated polymer-bound thioketals which could be released upon oxidative treatment with either periodic acid or mercury (II) perchlorate trihydrate. These reagents were further studied and a series of six polymers were synthesized ranging the amount of dithiol monomer from 10% to 50% to determine if each new polymer could serve as an acceptable reagent for dithiane formation [148]. The six polymers were compared in the alkylation of a dithiane resulting from benzaldehyde. Polymers with lower contents of the active monomer showed identical yields of 1-phenyl-1-heptanone while soluble polymers with higher proportions of active monomer (i.e. 40–50%) showed a slightly decreased yield of product. Based upon this decreased yield, the authors proposed a 1:1 mixture of active monomer and styrene in the monomer feed as an upper limit for the formation of usable reagent.

In an interesting multipolymer application of a REM (*Re*generated Michael ac-ceptor) resin, Janda reported the use of NCPS-supported soluble reagent (**33**) to cleave tertiary amines from an insoluble support (Scheme 5.3) [149]. This type of resin was developed by Rees and co-workers and has been used in the preparation of tertiary amines by sequential Michael addition, quaternization, and resin cleavage processes [150]. In the initial reports demonstrating the use of REM resins, purification of the amine products required either liquid–liquid extraction techniques or chromatography. Therefore, the use of a polymeric cleavage reagent



**Scheme 5.3** Multipolymer approach to cleavage of REM resin.

in conjunction with the insoluble REM resin would allow the rapid synthesis and purification of a variety of tertiary amines. Previous multipolymer strategies are known for cleavage of REM resins using a basic ion-exchange resin [151]. However, the insoluble nature of the cleavage reagent precluded the recycling of the REM resin as the two insoluble polymers could not be separated. In Janda's approach, the NCPS-supported reagent (**33**) was used to cleave a small library of tertiary amines from a JandaJel-REM resin in modest to good yield and in high purity (Scheme 5.3). Furthermore, (**33**) could be recovered and recycled after use by precipitation of the polymer from methanol.

Organostannane reagents have found widespread use for the free radical formation of carbon–carbon bonds. An allylstannane reagent synthesized on a soluble NCPS support has been developed and utilized in the formation of carbon–carbon bonds with alkyl halides [152]. The reagent (**34**) was prepared by derivatization of a chloromethyl-functionalized NCPS soluble polymer and high loadings (up to 3.3 mmol stannane per gram polymer) were achieved (Fig. 5.11). It was found that above 3.3 mmol g<sup>-1</sup> loading, the polymer became gelatinous and no longer readily precipitated from cold methanol. A series of structurally diverse alkyl halides were tested with allylstannane reagent (**34**) and all gave the desired allyl products in modest to good yields. Interestingly, a hindered tertiary bromide did not react with allyltributyltin but does react with NCPS-reagent (**34**). Furthermore, regioselectivity was observed in the allylation of dihalides, with a strong preference for an electron-deficient radical. This type of regioselectivity is unparalleled among other allylstannane organometallic reagents. Presumably, chelation to the oxygen of the linker, (Fig. 5.11) causes the allylstannane to become electron-rich and have a marked preference for electron poor-radicals. Enholm later reported another organotin reagent on NCPS (**35**) for use in the reduction of alkyl halides (Fig. 5.11) [153]. Typically, insoluble polymer-supported organotin reagents require multiple equivalents of reagent and prolonged reaction times when reducing alkyl halides, because of the heterogeneous nature of the reaction. In this report, a vari-

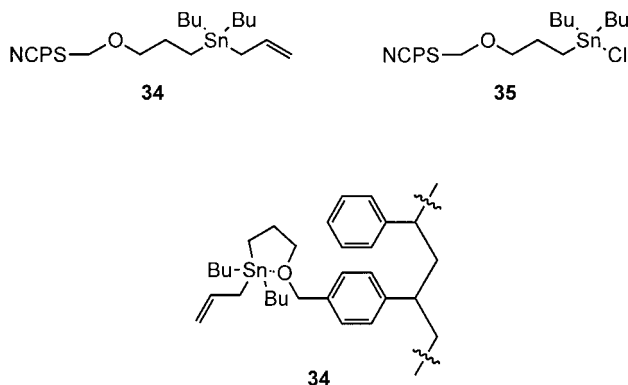


Fig. 5.11 NCPS-supported stannane reagents.

ant of the procedure developed by Corey and Suggs for catalytic use of a tin reagent in the presence of sodium borohydride was used [154]. A NCPS-supported dibutyltin chloride was prepared and used in the reduction of a variety of alkyl halides. Reductions were successfully accomplished in good yield with primary, secondary, and tertiary halides with most reactions going to completion within 2.5 hours. Furthermore, many reactions could be performed using only 0.01 equivalents of the polymer-bound reagent and excess sodium borohydride.

## 5.5

### Conclusions

The use of soluble polymers provides an alternative platform for organic synthesis by incorporating beneficial aspects of both solution-phase and solid-phase chemistry. By establishing homogeneous reaction conditions while still facilitating product separation, soluble polymer-supported methodologies have demonstrated utility in a variety of areas including peptide synthesis, small molecule organic synthesis, polymer-supported reagents, and polymer-supported catalysts. Although great strides have been made in the use of soluble polymers as supports for recoverable reagents and catalysts, considerable research remains to be done.

It has been recognized that the nature of the macromolecular support plays a significant role in solid-phase organic synthesis [155]. Compatibility problems between reagent or substrate and the polymer support can greatly limit the applications of a given support. To overcome these limitations, soluble polymer-supported reagents and catalysts have been utilized. Furthermore, in the case of substrates that possess limited solubility, covalent attachment to a soluble support would allow their use in a previously inaccessible range of synthetic applications. The refinement of current liquid-phase methodologies, coupled with the development of new soluble polymeric supports tailored for organic synthesis combine to make soluble polymers an increasingly valuable tool for synthetic chemists.

## 5.6

### Acknowledgements

This work was supported in part by the National Institutes of Health (GM-56164), The Scripps Research Institute, and The Skaggs Institute for Chemical Biology.

## 5.7

## References

- 1 MERRIFIELD, R. B. J. *Am. Chem. Soc.* 1963, 85, 2149.
- 2 THOMPSON, L. A.; ELLMAN, J. A. *Chem. Rev.* 1996, 96, 555.
- 3 TOY, P.; JANDA, K. D. *Acc. Chem. Res.* 2000, 33, 546.
- 4 SEEBERGER, P. H.; HAASE, W.-C. *Chem. Rev.* 2000, 100, 4349.
- 5 MÜTTER, M.; HAGENMAIER, H.; BAYER, E. *Angew. Chem., Int. Ed. Engl.* 1971, 10, 811.
- 6 BAYER, E.; MÜTTER, M. *Nature (London)* 1972, 237, 512.
- 7 GRAVERT, D. J.; JANDA, K. D. *Chem. Rev.* 1997, 97, 489.
- 8 WENTWORTH, P., JR.; JANDA, K. D. *Chem. Commun.* 1999, 1917.
- 9 GECKELER, K. E. *Adv. Polym. Sci.* 1995, 121, 31.
- 10 MÜTTER, M.; BAYER, E. In *The Peptides*; Academic Press: New York, 1979; Vol. 2, p 285.
- 11 GECKELER, K.; PILLAI, V. N. R.; MÜTTER, M. *Adv. Polym. Sci.* 1980, 39, 65.
- 12 PILLAI, V. N. R.; MÜTTER, M. In *Topics in Current Chemistry*; BOSCHKE, F. L., ed.; Springer-Verlag: New York, 1982; Vol. 106, p 119.
- 13 SHUTTLEWORTH, S. J.; ALLIN, S. M.; SHARMA, P. K. *Synthesis* 1997, 1217.
- 14 SHUTTLEWORTH, S. J.; ALLIN, S. M.; WILSON, *et al.*, *Synthesis* 2000, 1035.
- 15 AKELAH, A.; SHERRINGTON, D. C. *Chem. Rev.* 1981, 81, 557.
- 16 AKELAH, A.; SHERRINGTON, D. C. *Polymer* 1983, 24, 1369.
- 17 LEY, S. V.; BAXENDALE, I. R.; BREAM, R. N.; *et al.*, *J. Chem. Soc., Perkin Trans. 1* 2000, 3815.
- 18 HAN, H.; WOLFE, M. M.; BRENNER, S.; *et al.*, *Proc. Natl. Acad. Sci. USA* 1995, 92, 6419.
- 19 HARRIS, J. M. In *Poly(Ethylene Glycol) Chemistry: Biotechnical and Biomedical Applications*; HARRIS, J. M. ed.; Plenum Press: New York, 1992; p 2.
- 20 KÖSTER, J. *Tetrahedron Lett.* 1972, 1535.
- 21 FRANK, H.; MEYER, H.; HAGENMAIER, H. In *Peptides: Chemistry, Structure, and Biology*; Proc. Fourth Am. Pep. Symp.; Ann Arbor Science: Ann Arbor, 1975; p 439.
- 22 FRANK, H.; HAGENMAIER, H. *Experientia* 1975, 31, 131.
- 23 HEUSEL, G.; BOVERMANN, G.; GÖHRING, W.; *et al.*, *Angew. Chem., Int. Ed. Engl.* 1977, 16, 642.
- 24 FRANK, H.; MEYER, H.; HAGENMAIER, H. *Chem.-Ztg.* 1977, 101, 188.
- 25 FRANK, H.; HAGENMAIER, H.; BAYER, E.; *et al.*, In *Peptides: Chemistry, Structure, and Biology*; Proc. Fifth Am. Pep. Symp.; Wiley: New York, 1977; p 514.
- 26 SELIGER, H.; GÖLDNER, E.; KITTEL, I.; *et al.*, *Fresenius J. Anal. Chem.* 1995, 351, 260.
- 27 SHAPIRO, M. S.; GOUNARIDES, J. S. *Progress in Nuclear Magnetic Resonance Spectroscopy* 1999, 35, 153.
- 28 YAN, B.; LI, W.; LIU, L. *Recent Res. Dev. Org. Chem.* 1998, 2, 381 and references therein.
- 29 GALLOP, M. A.; FITCH, W. L. *Curr. Opin. Chem. Biol.* 1997, 1, 94.
- 30 YAN, B. *Acc. Chem. Res.* 1998, 31, 621 and references therein.
- 31 HAGENMAIER, H.; MÜTTER, M. *Tetrahedron Lett.* 1974, 767.
- 32 BAYER, B.; MÜTTER, M.; HOLZER, G. In *Peptides: Chemistry, Structure, and Biology*; Proc. Fourth Am. Pep. Symp.; Ann Arbor Science: Ann Arbor, 1975; p 456.
- 33 MÜTTER, M.; MÜTTER, H.; UHMANN, R.; *et al.*, *Biopolymers* 1976, 15, 917.
- 34 WENTWORTH, P., JR. *TIBTECH*, 1999, 17, 448.
- 35 BERGBREITER, D. E. *Med Res. Rev.* 1999, 19, 439.
- 36 REED, N. N.; JANDA, K. D. *J. Org. Chem.* 2000, 65, 5843.
- 37 ZHAO, X.-Y.; METZ, W. A.; SIEBER, F.; *et al.*, *Tetrahedron Lett.* 1998, 39, 8433.
- 38 BERGBREITER, D. E.; HU, H.-P.; HEIN, M. D. *Macromolecules* 1994, 27, 157.
- 39 ANNUNZIATA, R.; BENAGLIA, M.; CINQUINI, M.; *et al.*, *Chem. Eur. J.* 2000, 6, 133.
- 40 NARITA, M.; HIRATA, M.; KUSANO, K.; *et al.*, In *Peptide Chemistry*; Yonehara, H., ed.; Protein Research Foundation: Osaka, 1979; pp 107–112.

- 41 NARITA, M. *Bull. Chem. Soc. Jpn.* **1978**, *51*, 1477.
- 42 CHEN, S.; JANDA, K.D. *J. Am. Chem. Soc.* **1997**, *119*, 8724.
- 43 CHEN, S.; JANDA, K.D. *Tetrahedron Lett.* **1998**, *39*, 3943.
- 44 LEE, K.J.; ANGULO, A.; GHAZAL, P.; *et al.*, *Org. Lett.* **1999**, *1*, 1859.
- 45 MANZOTTI, R.; TANG, S.-Y.; JANDA, K.D. *Tetrahedron* **2000**, *56*, 7885.
- 46 LOPEZ-PELEGRIN, J.A.; JANDA, K.D. *Chem. Eur. J.* **2000**, *6*, 1917.
- 47 ENHOLM, E.J.; SCHULTE, J.P. II. *Org. Lett.* **1999**, *1*, 1275.
- 48 ENHOLM, E.J.; GALLAGHER, M.E.; JIANG, S.; *et al.*, *Org. Lett.* **2000**, *2*, 3355.
- 49 BERGBREITER, D.E. *Chem Rev.* **2002**, *102*, 3345.
- 50 BAYER, E.; SCHURIG, V. *Angew. Chem., Int. Ed. Engl.* **1975**, *14*, 493.
- 51 NUZZO, R.G.; FEITLER, D.; WHITESIDES, G.M. *J. Am. Chem. Soc.* **1979**, *101*, 3683.
- 52 BERGBREITER, D.E.; ZHANG, L.; MARIAGNANAM, V.M. *J. Am. Chem. Soc.* **1993**, *115*, 9295.
- 53 FAN, Q.-H.; DENG, G.-J.; LIN, C.-C.; *et al.*, *Tetrahedron: Asymmetry* **2001**, *12*, 1241.
- 54 GUERREIRO, P.; RATOVELOMANANA-VIDAL, V.; GENT, J.-P.; *et al.*, *Tetrahedron Lett.* **2001**, *42*, 3423.
- 55 WILLIAMS, J.M.J. *Catalysis in Asymmetric Synthesis*; Sheffield Academic Press Ltd: UK, 1999; pp 69-77.
- 56 KOLB, H.C.; VANNIEUWENHZE, M.S.; SHARPLESS, K.B. *Chem. Rev.* **1994**, *94*, 2483.
- 57 KIM, B.M.; SHARPLESS, K.B. *Tetrahedron Lett.* **1990**, *31*, 3003.
- 58 HAN, H.; JANDA, K.D. *J. Am. Chem. Soc.* **1996**, *118*, 7632.
- 59 HAN, H.; JANDA, K.D. *Tetrahedron Lett.* **1997**, *38*, 1527.
- 60 SHARPLESS, K.B.; AMBERG, W.; BENNANI, Y. L.; *et al.*, *J. Org. Chem.* **1992**, *57*, 2768.
- 61 HAN, H.; JANDA, K.D. *Angew. Chem., Int. Ed. Engl.* **1997**, *36*, 1731.
- 62 BOLM, C.; GERLACH, A. *Angew. Chem., Int. Ed. Engl.* **1997**, *36*, 741.
- 63 BOLM, C.; GERLACH, A. *Eur. J. Org. Chem.* **1998**, *21*.
- 64 BOLM, C.; MAISCHAK, A. *Synlett* **2001**, 93.
- 65 KUANG, Y.-Q.; ZHANG, S.-Y.; WEI, L.-L. *Tetrahedron Lett.* **2001**, *42*, 5925.
- 66 KIMURA, Y.; REGEN, S.L. *J. Org. Chem.* **1982**, *42*, 2493.
- 67 GRINBERG, S.; SHAUBI, E. *Tetrahedron* **1991**, *47*, 2895.
- 68 GRINBERG, S.; KAS'YANOV, V.; SRINIVAS, B. *Reactive & Functional Polymers* **1997**, *34*, 53.
- 69 ANNUNZIATA, R.; BENAGLIA, M.; CINQUINI, M.; *et al.*, *Org. Lett.* **2000**, *2*, 1737.
- 70 REGER, T.S.; JANDA, K.D. *J. Am. Chem. Soc.* **2000**, *122*, 6929.
- 71 FLOOD, R.W.; GELLER, T.P.; PETTY, S.A.; *et al.*, *Org. Lett.* **2001**, *3*, 683. For a recent study on the effect of the primary structure of the polypeptide catalyst on the enantioselectivity of the reaction see: BENTLEY, P.A.; FLOOD, R.W.; ROBERTS, S.M.; *et al.*, *Chem Commun.* **2001**, 1616.
- 72 GLOS, M.; REISER, O. *Org. Lett.* **2000**, *2*, 2045.
- 73 ANNUNZIATA, R.; BENAGLIA, M.; CINQUINI, M.; *et al.*, *J. Org. Chem.* **2001**, *66*, 3160.
- 74 BERGBREITER, D.E.; OSBURN, P.L.; LIU, Y.-S. *J. Am. Chem. Soc.* **1999**, *121*, 9531.
- 75 BERGBREITER, D.E.; OSBURN, P.L.; WILSON, A.; *et al.*, *J. Am. Chem. Soc.* **2000**, *122*, 9058.
- 76 SCHROCK, R.R.; MURDZEK, J.S.; BAZAN, G.C.; *et al.*, *J. Am. Chem. Soc.* **1990**, *112*, 3875.
- 77 NGUYEN, S.T.; GRUBBS, R.H.; ZILLER, J.W. *J. Am. Chem. Soc.* **1993**, *115*, 9858.
- 78 SCHWAB, P.; FRANCE, M.B.; ZILLER, J.W.; *et al.*, *Angew. Chem., Int. Ed. Engl.* **1995**, *34*, 2039.
- 79 SCHWAB, P.; GRUBBS, R.H.; ZILLER, J.W. *J. Am. Chem. Soc.* **1996**, *118*, 100.
- 80 NGUYEN, S.T.; GRUBBS, R.H. *J. Organomet. Chem.* **1995**, *497*, 195.
- 81 AHMED, M.; BARRETT, A.G.M.; BRADDOCK, D.C.; *et al.*, *Tetrahedron Lett.* **1999**, *40*, 8657.
- 82 KINGSBURY, J.S.; GARBER, S.B.; GIFTOS, J.M.; *et al.*, *Angew. Chem., Int. Ed. Engl.* **2001**, *40*, 4251.
- 83 YAO, Q. *Angew. Chem., Int. Ed. Engl.* **2000**, *39*, 3896.
- 84 PARAS, N.A.; MACMILLAN, D.W.C. *J. Am. Chem. Soc.* **2001**, *123*, 4370 and references therein.
- 85 LIST, B.; LERNER, R.A.; BARBAS, C.F. J. *Am. Chem. Soc.* **2000**, *122*, 2395.

- 86 SAKTHIVEL, K.; NOTZ, W.; BUI, T.; *et al.*, *J. Am. Chem. Soc.* **2001**, 123, 5260.
- 87 DICKERSON, T.J.; JANDA, K.D. *J. Am. Chem. Soc.* **2002**, 124, 3220.
- 88 BENAGLIA, M.; CELENTANO, G.; COZZI, F. *Adv. Synth. Catal.* **2001**, 343, 171.
- 89 HARRISON, C.R.; HODGE, P.; HUNT, B.J.; *et al.*, *J. Org. Chem.* **1983**, 48, 3721.
- 90 CHARETTE, A.B.; BOEZIO, A.A.; JANES, M.K. *Org. Lett.* **2000**, 2, 3777.
- 91 CHARETTE, A.B.; JANES, M.K.; BOEZIO, A.A. *J. Org. Chem.* **2001**, 66, 2178.
- 92 BERGBREITER, D.E.; BLANTON, J.R. *J. Chem. Soc., Chem. Commun.* **1985**, 337.
- 93 WENTWORTH, P., JR.; VANDERSTEEN, A.M.; JANDA, K.D. *Chem. Commun.* **1997**, 759.
- 94 STAUDINGER, H. *Helv. Chim. Acta.* **1919**, 2, 635.
- 95 COOPER, R.D.G. *Pure Appl. Chem.* **1987**, 59, 485.
- 96 HOLLETZ, T.; CECHE, D. *Synthesis* **1994**, 789.
- 97 MITSUNOBU, O. *Synthesis* **1980**, 1.
- 98 KRCHNAK, V.; FLEGELOVA, Z.; WEICHSEL, A.S.; *et al.*, *Tetrahedron Lett.* **1995**, 36, 6193.
- 99 SIEBER, F.; WENTWORTH, P., JR.; TOKER, J.D.; *et al.*, *J. Org. Chem.* **1999**, 64, 5188.
- 100 FEISER, M.; FEISER, L.F. IN *Reagents for Organic Synthesis*; Mir, Moscow: USSR, 1978; pp 1238–1239.
- 101 FERRABOSCHI, P.; GAMBERO, C.; AZADANI, M.N.; *et al.*, *Synth. Commun.* **1986**, 16, 667.
- 102 LIPOWITZ, J.; BOWMAN, S.A. *J. Org. Chem.* **1973**, 38, 162.
- 103 HORNER, L.; BALZER, W.D. *Tetrahedron Lett.* **1965**, 3, 1157.
- 104 GRIFFIN, S.; HEATH, L.; WYATT, P. *Tetrahedron Lett.* **1998**, 39, 4406.
- 105 MCKINLEY, S.V.; RAKSHYS, J.W.; *J. Chem. Soc., Chem. Commun.* **1972**, 134.
- 106 HEITZ, W.; MICHELS, R. *Angew. Chem., Int. Ed. Engl.* **1972**, 11, 298.
- 107 HEITZ, W.; MICHELS, R. *Justus Liebigs Ann. Chem.* **1973**, 227.
- 108 CLARKE, S.D.; HARRISON, C.R.; HODGE, P. *Tetrahedron Lett.* **1980**, 21, 1375.
- 109 HODGE, P.; WATERHOUSE, J. *Polymer* **1981**, 22, 1153.
- 110 BERNARD, M.; FORD, W.T. *J. Org. Chem.* **1983**, 48, 326.
- 111 HODGE, P.; HUNT, B.J.; KHOSHDEL, E.; *et al.*, *Nouv. J. Chim.* **1982**, 6, 617.
- 112 LI, C.-J.; CHAN, T.-H. IN *Organic Reaction in Aqueous Media*; John Wiley & Sons: New York, 1997.
- 113 LI, C.-J. *Chem. Rev.* **1993**, 93, 2023.
- 114 BUTCHER, M.; MATHEWS, R.J.; MIDDLETON, S. *Aust. J. Chem.* **1973**, 26, 2067.
- 115 BROOS, R.; TAVERNIER, D.; ANTEUNIS, M. *J. Chem. Educ.* **1978**, 55, 813.
- 116 RUSSELL, M.G.; WARREN, S. *Tetrahedron Lett.* **1998**, 39, 7995.
- 117 SCHUTTENBERG, H.; KLUMP, G.; KACZMAR, U.; *et al.*, *J. Macromol. Sci. Chem.* **1973**, A7, 1085.
- 118 MANCUSO, A.J.; SWERN, D. *Synthesis* **1981**, 165.
- 119 LIU, Y.; VEDERAS, J.C. *J. Org. Chem.* **1996**, 61, 7856.
- 120 HARRIS, J.M.; LIU, Y.; CHAI, S.; *et al.*, *J. Org. Chem.* **1998**, 63, 2407.
- 121 WIRTH, T.; HIRT, U.H. *Synthesis* **1999**, 1271.
- 122 NICOLAOU, K.C.; MONTAGNON, T.; BARAN, P.S.; *et al.*, *J. Am. Chem. Soc.* **2002**, 124, 2245.
- 123 FRIGERIO, M.; SANTAGOSTINO, M. *Tetrahedron Lett.* **1994**, 35, 8019.
- 124 FRIGERIO, M.; SANTAGOSTINO, M.; SPUTORE, S.; *et al.*, *J. Org. Chem.* **1995**, 60, 7272.
- 125 LEY, S.V.; THOMAS, A.W.; FINCH, H. *J. Chem. Soc. Perkin Trans. 1* **1999**, 669.
- 126 REED, N.N.; DELGADO, M.; HEREFORD, K.; *et al.*, *Bioorg. Med. Chem. Lett.* **2002**, in press.
- 127 HALLENSLEBEN, M.L. *J. Polym. Sci., Polymer Symposia* **1974**, 47, 1.
- 128 BERGBREITER, D.E. IN *Metal-Containing Polymeric Systems*, SHEATS, J.E.; CARRAHER, C.E., JR.; PITTMAN, C.U., JR., eds.; Plenum Press: New York, 1985, pp 405–424.
- 129 BERGBREITER, D.E.; BLANTON, J.R.; CHEN, B. *J. Org. Chem.* **1983**, 48, 5366 and references therein.
- 130 AVNY, Y.; MAROM, G.; ZILKHA, A. *Eur. Polym. J.* **1971**, 7, 1037.
- 131 SMITH, T.W.; CHEATHAM, R.A. *Macromolecules* **1980**, 13, 1203.
- 132 STACEY, K.A.; WEATHERHEAD, R.H.; WILLIAMS, A. *Makromol. Chem.* **1980**, 181, 2517.

- 133 SCHUNICHT, C.; BIFFS, A.; WULFF, G. *Tetrahedron* **2000**, 56, 1693.
- 134 SPANKA, C.; CLAPHAM, B.; JANDA, K.D. *J. Org. Chem.* **2002**, 67, 3045.
- 135 For examples of methods to increase the loading of PEG, see: a) BENAGLIA, M.; ANNUNZIATA, R.; CINQUINI, M.; *et al.*, *J. Org. Chem.* **1998**, 63, 8328. b) REED, N.N.; JANDA, K.D. *Org. Lett.* **2000**, 2, 1311.
- 136 SHIMOMURA, O.; CLAPHAM, B.; SPANKA, C.; *et al.*, *J. Comb. Chem.* **2002**, in press.
- 137 BOLTON, G.L.; HODGES, J.C. *J. Am. Chem. Soc.* **1997**, 119, 4882.
- 138 ATKINS, G.M.; BURGESS, E.M. *J. Am. Chem. Soc.* **1968**, 90, 4744.
- 139 WIPF, P.; VENKATRAMAN, S. *Tetrahedron Lett.* **1996**, 37, 4659.
- 140 WIPF, P.; MILLER, C.P. *Tetrahedron Lett.* **1992**, 33, 907.
- 141 WIPF, P.; MILLER, C.P. *J. Org. Chem.* **1993**, 58, 1575.
- 142 BRAIN, C.T.; PAUL, J.M.; LOONG, Y.; *et al.*, *Tetrahedron Lett.* **1999**, 40, 3275.
- 143 KONONOV, L.O.; ITO, Y.; OGAWA, T. *Tetrahedron Lett.* **1997**, 38, 1599.
- 144 WENTWORTH, A.D.; WENTWORTH, P. JR.; MANSOOR, U.F.; *et al.*, *Org. Lett.* **2000**, 2, 477.
- 145 KEATING, T.A.; ARMSTRONG, R.W. *J. Am. Chem. Soc.* **1996**, 118, 2574.
- 146 HORI, M.; JANDA, K.D. *J. Org. Chem.* **1998**, 63, 889.
- 147 BERTINI, V.; LUCCHESINI, F.; POCCHI, M.; *et al.*, *Tetrahedron Lett.* **1998**, 39, 9263.
- 148 BERTINI, V.; LUCCHESINI, F.; POCCHI, M.; *et al.*, *J. Org. Chem.* **2000**, 65, 4839.
- 149 TOY, P.H.; REGER, T.S.; JANDA, K.D. *Org. Lett.* **2000**, 2, 2205.
- 150 MORPHY, J.R.; RANKOVIC, Z.; REES, D. *Tetrahedron Lett.* **1996**, 37, 3209.
- 151 OUYANG, X.; ARMSTRONG, R.W.; MURPHY, M.M. *J. Org. Chem.* **1998**, 63, 1027.
- 152 ENHOLM, E.J.; GALLAGHER, M.E.; MORAN, K.M.; *et al.*, *Org. Lett.* **1999**, 1, 689.
- 153 ENHOLM, E.J.; SCHULTE, J.P. III *Org. Lett.* **1999**, 1, 1275.
- 154 COREY, E.J.; SUGGS, J.W. *J. Org. Chem.* **1975**, 40, 2554.
- 155 VAINO, A.R.; JANDA, K.D. *J. Comb. Chem.* **2000**, 2, 579.



## 6

**Polymers for Micellar Catalysis**

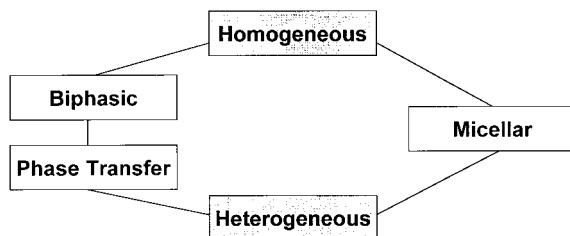
OSKAR NUYKEN, RALF WEBERSKIRCH, THOMAS KOTRE, DANIEL SCHÖNFELDER  
and ALEXANDER WÖRNDLE

## 6.1

**Introduction**

Micellar catalysis has been a subject of intensive research for over 30 years. This is based on the realization that many biochemical processes take place in a micro-heterogeneous system composed of organic phases and aqueous phases. Moreover, the general analogy of micellar to enzymatic catalysis with respect to its kinetics, globular structure and micro-environmental effect were major reasons to study the catalytic effect of micelles in hydrolysis and nucleophilic substitution reactions [1]. With many advances in metal–organic chemistry, new techniques in catalyst design and significant new developments in polymer design and synthesis, micellar catalysis has experienced a revival in recent years. The aim of this chapter is to summarize some of the recent developments in the use of different amphiphilic polymers for metal-catalyzed cross-coupling reactions in micelles.

Metal-catalyzed cross-coupling reactions have attracted enormous interest in academia and industry as one of the most versatile synthetic methodologies, that give access to wide variety of organic compounds, such as pharmaceuticals, fine chemicals and polymers [2]. In spite of the numerous advantages that can be associated with homogeneous catalysis, the heterogeneous variant is absolutely dominant for catalytic applications in industrial processes [3]. This ranking is mainly ascribed to easier product and catalyst separation as well as the possibility of catalyst recycling in heterogeneous catalysis [4]. Although homogeneous catalysis generally shows higher activity and selectivity, better reproducibility and milder reaction conditions, it is the lack of catalyst recycling that makes this technique inferior for industrial applications [5, 6]. From an industrial point of view, two important goals have to be realized in the near future that will make catalytic reactions even more attractive: (i) the use of water as the preferred solvent for economical, physiological and safety-related process engineering reasons and (ii) easy separation of the catalyst from the product, allowing catalyst recycling and preparation of metal-free products. Among the efforts to combine the advantages of homogeneous and heterogeneous catalysis and to perform catalytic transformations in water as solvent, the methodology of liquid multiphase catalysis is an attractive and very promising approach [7]. In such systems the catalyst is dissolved in one of the two

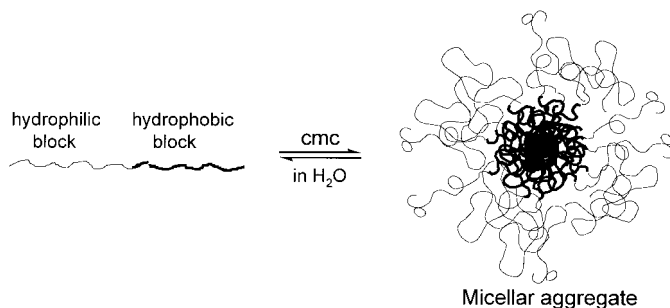


**Scheme 6.1** Different possibilities of heterogenization by applying biphasic, phase transfer or micellar conditions.

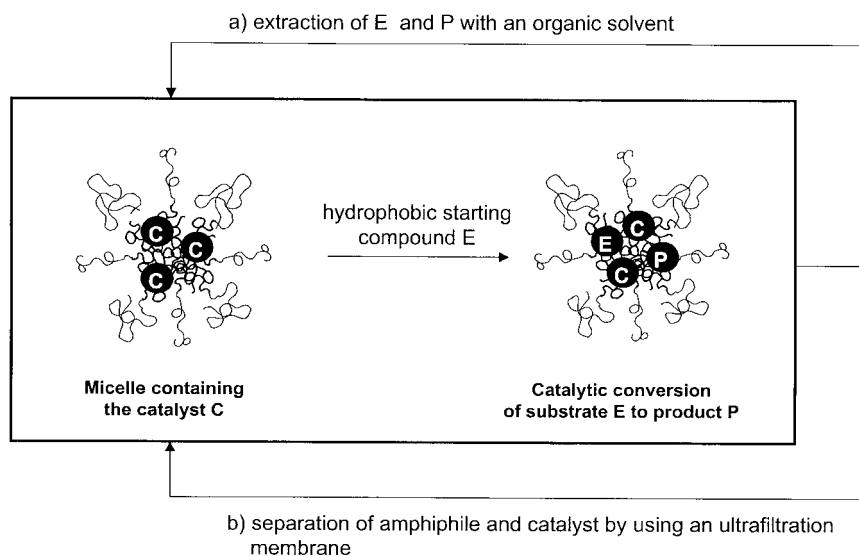
immiscible phases, while the substrate(s) and the product(s) are soluble in the other phases. Aqueous biphasic catalysis is a special case of liquid-liquid two-phase catalysis. The aqueous solution contains the water-soluble catalyst, whereas the substrate(s) and product(s) are used as neat liquids or dissolved in water-immiscible solvents (Scheme 6.1) [8]. Important examples for catalysis in biphasic or phase transfer liquid-liquid systems are the Shell Higher Olefin Process (SHOP) [9], which are used industrially, and the hydroformylation process of Ruhrchemie–Rhône Poulenc [10].

However, biphasic catalysis, such as the above-mentioned process, is limited by the solubility of the reaction compounds in the aqueous phase. Hence, only compounds with sufficient water solubility are suitable for biphasic catalytic application. More hydrophobic substrates cannot diffuse to the catalytic active species, which is solubilized in the aqueous phase, and the reaction cannot take place.

Micellar catalysis is an improvement of the biphasic concept, which solves the problem of catalytic transformation of hydrophobic substrates. Micelles and micellar analogous structures offer even more advantages. The catalytic transformation of hydrophobic substrates can be performed in neat aqueous phase and the catalyst, solubilized in the micelles either by covalent linkage or only dissolved in the micellar core, can be recycled and re-used again [11]. The principle is illustrated in Fig. 6.1. First of all, an amphiphile is needed, which can be of low molecular



**Fig. 6.1** Self-organization of amphiphilic block polymers in water (cmc = critical micelle concentration).



**Fig. 6.2** The principle of micellar catalysis and the recycling of the catalytic active micelles by (a) using an extracting solvent or (b) an ultrafiltration membrane.

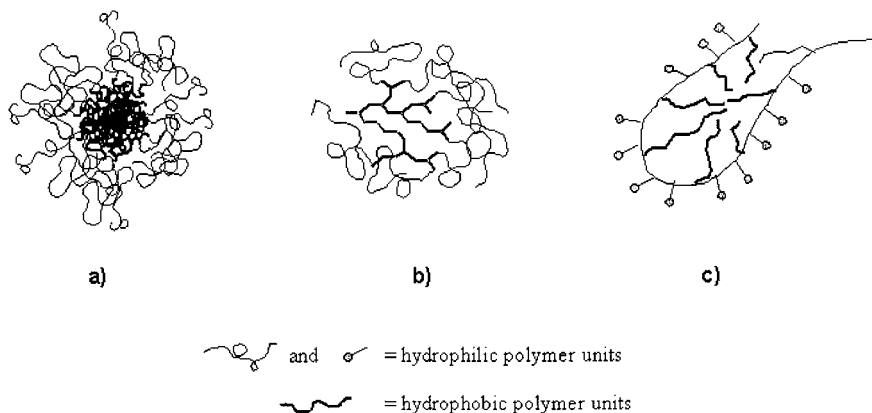
weight or of polymeric nature. In water the amphiphilic molecules associate to form micellar structures. The hydrophobic part of the molecules thereby forms the interior of the micelles and the hydrophilic part is exposed to the aqueous phase and guarantees water-solubility [12, 13].

The catalytic principle of micelles as depicted in Fig. 6.2, is based on the ability to solubilize hydrophobic compounds in the micellar interior so the micelles can act as reaction vessels on a nanometer scale, as so-called nanoreactors [14, 15]. The catalytic complex is also solubilized in the hydrophobic part of the micellar core or even bound to it. Thus, the substrate (S) and the catalyst (C) are enclosed in an appropriate environment. In contrast to biphasic catalysis no transport of the organic starting material to the active catalyst species is necessary and therefore no transport limitation of the reaction will be observed. As a consequence, the conversion of very hydrophobic substrates in pure water is feasible and all the advantages mentioned above, which are associated with the use of water as medium, are given. Often there is an even higher reaction rate observed in micellar catalysis than in conventional monophasic catalytic systems because of the smaller reaction volume of the micellar reactor and the higher reactant concentration, respectively. This enhanced reactivity of encapsulated substrates is generally described as micellar catalysis [16, 17]. Due to the similarity to enzyme catalysis, micelle and enzyme catalysis have sometimes been correlated in literature [18].

For catalyst recycling three different methods are possible. The first approach is based on an ultrafiltration membrane for separating the amphiphiles and the catalytic complex from the products and nonconverted starting compounds [19]. Here

the polymeric structure and the high molecular mass of the amphiphile are of great advantage for separation using a nanofiltration membrane. The separation principle of the second method is generally similar to that applied in biphasic catalysis. In this case, the products can be extracted by adding an organic solvent to the reaction mixture. The amphiphiles are still aggregated in the aqueous phase to the catalyst containing micelles and are not extracted by the organic solvent. So the catalytically active aqueous phase can be separated from the organic phase and also be reused for further catalytic cycles. Furthermore, Bergbreiter and co-workers described so-called “smart” polymeric ligands, which exhibit inverse temperature behavior in water, meaning that the polymeric ligand precipitates out from solution above a certain temperature, known as the lower critical solution temperature (LCST). Two examples of such polymers are poly(alkene oxide) copolymers and poly(*N*-alkylacrylamides). They are soluble at lower temperatures and precipitate at higher temperature, thereby allowing easy separation of the polymeric catalyst from the products [20].

Many micellar catalytic applications using low molecular weight amphiphiles have already been discussed in reviews and books and will not be the subject of this chapter [1]. We will rather focus on the use of different polymeric amphiphiles, that form micelles or micellar analogous structures and will summarize recent advances and new trends of using such systems for the catalytic synthesis of low molecular weight compounds and polymers, particularly in aqueous solution. The polymeric amphiphiles discussed herein are block copolymers, star-like polymers with a hyperbranched core, and polysoaps (Fig. 6.3).



**Fig. 6.3** Different types of micelles and micelle analogous structures: a) amphiphilic block copolymers, b) star-like polymers with a hyperbranched core, c) polysoaps.

## 6.2

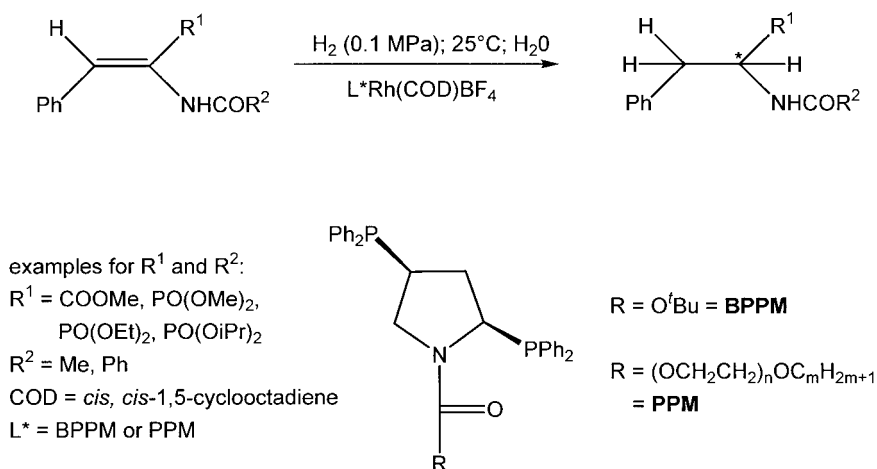
## Amphiphilic Block Copolymers for Micelle Formation

In the past decade there has been considerable progress in the development of synthetic strategies to prepare amphiphilic block copolymers with different architectures, solubility and functionality. In addition to the more classical routes to block copolymer synthesis by living anionic polymerization [21], new methods such as the living cationic polymerization [22], controlled radical polymerization [23], group-transfer [24] and ring-opening metathesis polymerization [25] have been intensively investigated and now allow for a wide variety of different block copolymers which are summarized in some excellent reviews [26].

## 6.2.1

## Transition Metal Catalysts Solubilized in Micellar Aggregates

The first type of micellar catalysis discussed in this chapter is most similar to the application of low-molecular weight amphiphiles for catalysis. The system is very simple and consists of a polymeric amphiphile as well as a hydrophobic catalyst, which is only solubilized in the micelle and not covalently bound to the amphiphilic polymer. The most important reason for using polymers based on poly(propylene oxide)-*block*-poly(ethylene oxide), instead of low molecular weight amphiphiles, is the possibility of polymer/catalyst recycling by using an ultrafiltration membrane. The field of research was predominantly investigated by the group of G. Oehme in Rostock, Germany [4, 27, 28]. As a model reaction, they chose the asymmetric hydrogenation of unsaturated amino acid derivatives catalyzed by rhodium(I) complexes (Scheme 6.2).



**Scheme 6.2** Asymmetric hydrogenation of unsaturated amino acid derivatives as a model reaction for micellar catalysis using amphiphilic block copolymers.

The chiral ligand was in all cases (2*S*,4*S*)-*N*-*tert*-butoxycarbonyl-4-diphenylphosphino-2-diphenylphosphinomethylpyrrolidine (BPPM) and the catalyst was formed in an *in situ* system of  $[\text{Rh}(\text{COD})_2]^+\text{BF}_4^-$ . The asymmetric hydrogenation is well investigated in organic solvents like methanol, but the presence of water usually causes loss of activity and enantioselectivity because of the low solubility of both the catalyst and the substrate in water [27, 29]. The addition of low-molecular surfactants or commercially available polymeric amphiphiles increases the activity (here given as time of consumption of half the stoichiometric volume of hydrogen,  $t/2$ ) as well as the enantioselectivity [4]. Tab. 6.1 summarizes selected experiments with different polymeric amphiphiles.

It turned out that for all the polymeric amphiphiles of the  $(\text{EO})_n\text{-(PO)}_m\text{-(EO)}_n$  type there was an increase in enantioselectivity compared with the reaction without amphiphile. Moreover, the ratio of the length of the  $(\text{PO})_m$  block compared with the  $(\text{EO})_n$  block seemed to determine enantioselectivity and activity and not the cmc (critical micelle concentration). A  $(\text{PO})_m$  block length of 56 units works best with different length of the  $(\text{EO})_n$  block in this type of hydrogenation [30]. For the work-up of the experiments, G. Oehme *et al.* used the extraction method, but initial experiments failed and the catalyst could not be recycled that way. To solve this problem the authors applied a membrane reactor in combination with the amphiphile  $(\text{EO})_{37}\text{-(PO)}_{56}\text{-(EO)}_{37}$  (Tab. 6.1, entry 9) [31]. By doing so, the polymer/Rh-catalyst was retained and could be reused several times without loss of activity and enantioselectivity by more than 99%.

Two approaches have been studied in the past to avoid metal leaching, either by metal colloids stabilized in micellar core or catalyst bound to the micellar structures and will therefore discussed in the following sections.

**Tab. 6.1** Selected hydrogenation experiments with polymeric amphiphiles (experimental data are listed in Scheme 6.2,  $\text{R}_1=\text{COOMe}$ ,  $\text{R}_2=\text{Me}$ ).

Surfactant	$t/2$ (min)	Optical yield (% ee <i>R</i> )	Ref.
1. none (pure water)	90	78	5
2. none (pure methanol)	2	90	5
3. SDS	6	94	5
4. Brij 35 <sup>a)</sup>	4	94	31
5. Brij 56 <sup>b)</sup>	7	95	5
6. $(\text{EO})_5\text{-(PO)}_{56}\text{-(EO)}_5$ <sup>c)</sup>	7	93	32
7. $(\text{EO})_{17}\text{-(PO)}_{56}\text{-(EO)}_{17}$ <sup>c)</sup>	3	91	32
8. $(\text{EO})_{27}\text{-(PO)}_{56}\text{-(EO)}_{27}$ <sup>c)</sup>	4	92	32
9. $(\text{EO})_{37}\text{-(PO)}_{56}\text{-(EO)}_{37}$ <sup>c)</sup>	5	90	32
10. $(\text{EO})_{132}\text{-(PO)}_{56}\text{-(EO)}_{132}$ <sup>c)</sup>	6	92	32

a) Poly(oxyethylene)(23)dodecylether.

b) Poly(oxyethylene)(10)hexadecylether.

c)  $(\text{EO})_n\text{-(PO)}_m\text{-(EO)}_n$ : poly(oxyethylene)-*block*-poly(oxypropylene)-*block*-poly(oxyethylene) triblock copolymers.

## 6.2.2

**Metal Colloids Stabilized in Micellar Aggregates**

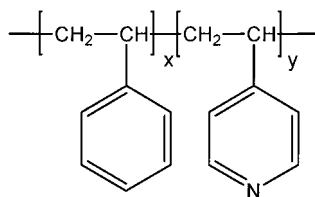
Metal nanoparticles have received much attention in the past because their unique electronic structure makes them interesting materials for nanoelectronics, optics and catalysis [33]. A large body of work has already been published on the preparation [34] and characterization [35] of such particles and will not be the subject of this section.

The major disadvantages of colloidal catalysts studied so far can be attributed to problems in controlling the metal colloid formation (control of particle size, particle size distribution, structure of metal colloids) and stabilization of the prepared particles, which are not yet completely solved. But it is exactly the stability of the nanoparticles, that is decisive for long-term usage during catalytic processes. Moreover for catalytic application, it is extremely important to preserve the large surface of such colloidal systems.

A promising strategy towards stable and catalytically active metal colloids is their preparation inside the core of micelles formed by amphiphilic block copolymers. This strategy offers a number of advantages: (i) micelles represent a nanostructured environment which can be exactly tailored by block copolymer synthesis; (ii) polymers act as effective steric stabilizer [36]; (iii) metal leaching might be avoided; (iv) micelles allow control over particle size, size distribution and particle solubility [37] and (v) micelles are also supposed to effect catalytic activity and selectivity [38].

Application of amphiphilic block copolymers for nanoparticle formation has been developed by several research groups. R. Schrock *et al.* prepared nanoparticles in segregated block copolymers in the solid state [39]; A. Eisenberg *et al.* used ionomer block copolymers and prepared semiconductor particles (PdS, CdS) [40]; M. Möller *et al.* studied gold colloids in thin films of block copolymers [41]. M. Antonietti *et al.* studied noble metal nanoparticle stabilized in block copolymer micelles for the purpose of catalysis [36]. Initial studies were focused on the use of poly(styrene)-*block*-poly(4-vinylpyridine) (PS-*b*-P4VP) copolymers prepared by anionic polymerization and its application for noble metal colloid formation and stabilization in solvents such as toluene, THF or cyclohexane (Fig. 6.4) [42].

Several routes have been developed to control the formation of nanoparticles in block copolymer systems. They include several steps: (i) preparation of block copolymers; (ii) loading of the precursor polymer; (iii) micellization; (iv) chemical



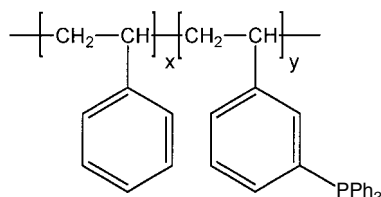
**Fig. 6.4** Chemical structure of poly(styrene)-*block*-poly(4-vinylpyridine) (PS-*b*-P4VP)

reduction, nucleation and growth process. Loading of the micelles can be done either by binding the transition metal ions to the monomer, or directly to the block copolymer, which is the most common method. A third possibility is based on the direct loading of the micellar core with a transition metal (e.g.  $\text{Pd}(\text{OAc})_2$  or  $\text{Cd}(\text{ClO}_4)_2$ ). Reduction of the noble metal salt relies on adjustment of the reactivity of the reducing agent to the redox potential of the metal. Commonly used reducing agents are  $\text{LiAlH}_4$ ,  $\text{NaBH}_4$ ,  $\text{LiBEt}_3\text{H}$ , alkyl silanes, hydrides and hydrogen. The primary formed metal atoms subsequently aggregate to form nanoparticles by nucleation and growth processes. Depending on the method used, one or more metal colloids can be formed within the micellar micro-domains. This preparation method results in hybrid materials which possess the desired solution properties of the block copolymers on the one hand, and the catalytic activity of metal colloids on the other. The size of the prepared colloid particles can be controlled by the micelle size, the molar ratio of metal salt to 4-vinylpyridine units and especially the type of reducing agent used. First experiments with such micellar Pd particles for the hydrogenation of cyclohexane indicated similar activity compared with commercial catalysts [36]. In a more detailed study results reported for the hydrogenation of cyclohexene were ~33% yield after 30 min hydrogenation. Cyclohexane yield is dependent on the type of reducing agent, ranging from 32.7% for superhydride ( $\text{LiBEt}_3\text{H}$ ), 1% for  $\text{N}_2\text{H}_4 \cdot \text{H}_2\text{O}$  and 45.5% for superhydride (deposited on  $\text{Al}_2\text{O}_3$ ). Moreover, the use of bimetallic colloids ( $\text{Au}/\text{Pd}=1/4$ ) increased the catalytic activity by a factor of 2. All results indicated better selectivity, activity and long term stability compared with commercial Pd on activated carbon [43]. In order to increase the long term stability of the catalyst, the micellar stabilized colloids were deposited on  $\text{Al}_2\text{O}_3$ . The resulting systems were used for selective hydrogenation of the triple bond in dehydrolinalool to a double bond in linalool, a fragrant substance of terpenic series [44]. The PS-*b*-P4VP/ $\text{Al}_2\text{O}_3$  system exhibited high reactivity and selectivity, which was explained by the hydrogenation of the triple bond with very small Pd particles surrounded by 4VP units. The  $\text{Al}_2\text{O}_3$ -supported system was also studied in the hydrogenation of cyclohexene. The catalytic activity was unaffected after five cycles in hydrogenation, while commercial Pd/C catalyst showed a loss in activity already after three cycles.

A second reaction that was studied with PS-*b*-P4VP stabilized Pd colloids was the Heck reaction [45]. Catalytic reactions were performed at 140 °C in the presence of tris(*n*-butylamines) as a base. It was found that the catalytic activity was at least as high as that of the standard Heck catalyst  $\text{Pd}(\text{OAc})_2/\text{TOP}$  (*tri-o*-tolylphosphine) system. Turnover numbers as high as 56 600 mol of product per mol. catalyst were obtained. The efficiency is dependent on the relative amount of catalyst, the micelle size, type and dispersity of the metal. Smaller micelles and ultra-fine Pd particle distribution within the micelles were the essential criteria for high catalytic activity. The reaction worked well for activated arylbromides, however, deactivated arylbromides and arylchlorides gave poor results. The advantages of these stabilized colloids are the increased lifetime compared with other catalysts, avoiding of “Pd black” formation during the reaction and the application of “simple” solvents, such as toluene.



**Fig. 6.5** Chemical structure of polystyrene-*block*-poly(*m*-vinyltriphenylphosphine) (PS-*b*-PPH)



Another possible strategy towards colloids stabilized by micellar systems is the use of nonamphiphilic block copolymers containing metal binding ligands in only one of the blocks. For example, a poly(styrene)-*block*-poly(*m*-vinyltriphenylphosphine) (PS-*b*-PPH) was examined with respect to its colloid formation properties (Fig. 6.5) [46].

Therefore, a polymer consisting of a relatively short triphenylphosphine block and long polystyrene block (good solubilization) was prepared by anionic polymerization and complexed with Pd in the form of  $(PPh_3)PdCl_2$  or  $(CH_3CN)_2PdCl_2$  in THF as solvent. The complexation of the triphenylphosphine groups of these polymers induced a micellization of the system and no polymer gels were formed. Afterwards Pd-colloids were prepared by reduction of the complexes, e.g. with  $LiAlH_4$ , superhydride ( $LiBEt_3H$ ) or  $N_2H_4 \cdot H_2O$ .

The morphology of the colloids obtained is again controlled by the strength of the reducing agent. A strong reducing agent led to many small particles per micelle, whereas a weak one gave only one particle per micelle. The aggregate structure was found to depend strongly on the composition of the initial diblock copolymer and the type of Pd compound used. It can vary between spherical aggregates, presumably multilamellar vesicles, disk-like micelles and unilamellar vesicles.

The concept of induced micellization as described above can also be transferred to aqueous systems. Water as the reaction medium of choice has a number of advantages in a wide field of various catalytic reactions such as hydrogenation, oxidation or gas-shift reaction [47]. This becomes possible by the use of so-called “double-hydrophilic” block copolymers, where both blocks are soluble in water, but only one block can coordinate to metal ions. One example for such a polymer is linear or branched poly(ethyleneimine)-*block*-poly(ethyleneoxide) (PEI-*b*-PEO), where only the PEI-block is able to coordinate to metal ions as Pd, Pt, Rh or Au [48]. Such systems are able to form stable colloids with efficient control of particle growth and stabilization. The branched PEI-*b*-PEO with their higher molecular weight and steric demands are better stabilizing systems for metal colloids compared with the linear ones. The use of “double-hydrophilic” block copolymers for stabilizing metal colloids is promising for the development of new catalytic systems operating in water as solvent.

A. Mayer *et al.* examined poly(dimethylsiloxane)-*block*-poly(ethylene oxide) (PDMS-*b*-PEO), poly(styrene)-*block*-poly(ethylene oxide) (PS-*b*-PEO), polystyrene-*block*-poly(methacrylic acid) (PS-*b*-PMAA) as amphiphilic block copolymers with regard to their properties in stabilizing colloidal metal nanoparticles [37, 49]. All three polymers are successfully used to stabilize various transition metal colloids

exhibiting very small particle sizes and narrow size distributions that depended on the reducing method and the solvent as well as on the metal precursor used. PDMS-*b*-PEO has an advantage because of its reducing character, which allows the metal colloid formation at room temperature without the addition of a further reducing agent.

Pd- and Pt-nanoparticles protected by PS-*b*-PMAA were used to perform catalytic hydrogenations of cyclohexene in ethanol as solvent. It could be shown that such colloids are catalytically active and thus interesting for the development of catalysts tailored for special reactions.

In summary, the examples given above demonstrate that immobilization of metal salts in a block copolymer micellar system followed by a reduction step is a suitable method to synthesize stable colloids with small particle sizes and narrow size distributions. Moreover, such systems are very interesting for catalytic applications because they offer the possibility of designing tailored catalysts for special demands and can be easily tuned by the choice and combination of different polymer block types and lengths, different types of the metal precursor and of the reduction method used. Additional introduction of further functionalities such as charges or chiral groups could make these catalyst systems even more versatile and effective.

### 6.2.3

#### Catalysts Covalently Bound to the Amphiphilic Block Copolymer

A second approach that should allow for catalyst recycling is based on amphiphilic block copolymers, where the catalyst is covalently bound to the hydrophobic block. The groups of G. Oehme in Rostock and O. Nuyken in Munich are working on such systems that are sometimes described as metallosurfactants. The appending polymers without the catalyst are called macroligands or amphiphilized ligands [4, 50].

##### 6.2.3.1 Phosphine-Functionalized Amphiphiles for Rhodium-Catalyzed Hydrogenation

G. Oehme *et al.* utilize commercially available polyoxyethylene ethers of the Brij-type which are functionalized with a chiral phosphine unit attached to the hydrophilic polyether group of the amphiphile [4]. The hydrophobic tail is composed of a dodecyl group (see Scheme 6.2). As a model reaction they investigated the asymmetric hydrogenation of unsaturated amino acid derivatives as mentioned above (Scheme 6.2, cf. section 6.2.1) [4, 27]. Tab. 6.2 summarizes selected results obtained in the hydrogenation reaction with an *in situ* formed rhodium(I) complex of the amphiphilized ligand in comparison to the analogously formed BPPM complex.

In methanol as solvent, the results are comparable with respect to activity and enantioselectivity (Tab. 6.2, entry (1)) whereas in water the complex of the amphiphilic ligand shows a significant increase in activity and enantioselectivity compared with the BPPM complex (entry (2)). The values obtained for mixed micelles

**Tab. 6.2** Selected hydrogenation experiments with amphiphilized PPM and BPPM (experimental data are listed in Scheme 6.2,  $R_1 = \text{COOMe}$ ,  $R_2 = \text{Me}$ , amphiphilized PPM:  $n = 23$ ,  $m = 12$ ).

Solvent and type of ligand		<i>t</i> /2 (min)	optical yield (% ee)	Ref.
1.	methanol			5
.	. amphiphilized PPM	4	94	
.	. BPPM	2	93	
2.	water			5
.	. amphiphilized PPM	13	91	
.	. BPPM	90	78	
3.	water (SDS <sup>a)</sup> )			5
.	. amphiphilized PPM	7	96	
.	. BPPM	6	94	
4.	water (1 <sup>a, b)</sup> )			5
.	. amphiphilized PPM	8	94	
.	. BPPM	12	96	

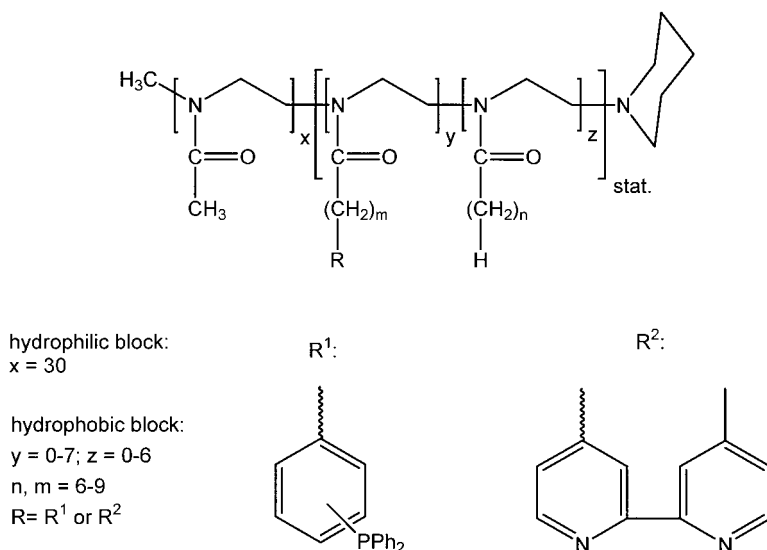
a) As auxiliary amphiphile.

b) 1 as non-functionalized co-surfactant = amphiphilized PPM,  $n = 12$  (see Scheme 6.2) without  $-\text{PPh}_2$  groups.

are generally higher than the corresponding results for pure micelles consisting of only one type of amphiphile (entries (3) and (4)). This trend can be traced back to an 'embedding effect' of the auxiliary amphiphiles: a micellar system formed by amphiphilic complexes leads to an extreme concentration of active centers near the surface of the micelles and probably limits the accessibility. This should be overcome by mixing with nonfunctionalized surfactants. Entries (3) and (4) display this embedding effect as evident in an enhancement of activity and enantioselectivity [5, 27]. Furthermore, the use of mixed micelles has an additional advantage: the concentration of the catalytic system could be decreased significantly without loss of enantioselectivity. However, the activity of such a system is naturally smaller [27].

#### 6.2.3.2 Triphenylphosphine-Functionalized Amphiphiles for Rhodium-Catalyzed Hydroformylation and Palladium-Catalyzed Heck Coupling Reaction

The second group working in this field of research (the group of O. Nuyken) has specialized in this type of micellar catalysis. They used amphiphilic poly(2-oxazoline) block copolymers bearing triphenylphosphine or 2,2'-bipyridine moieties respectively as ligand-functionalized block copolymers (Scheme 6.3). In aqueous media these polymers form functionalized micelles with transition metal binding sites located in the hydrophobic core, thereby forming a catalytically active nanoreactor. These ligand-functionalized polymers were used in different catalytic applications, such as hydroformylation and Heck coupling reaction, as well as polymerization reactions like copper- and ruthenium-catalyzed ATRP (cf. Section 6.2.3.3).

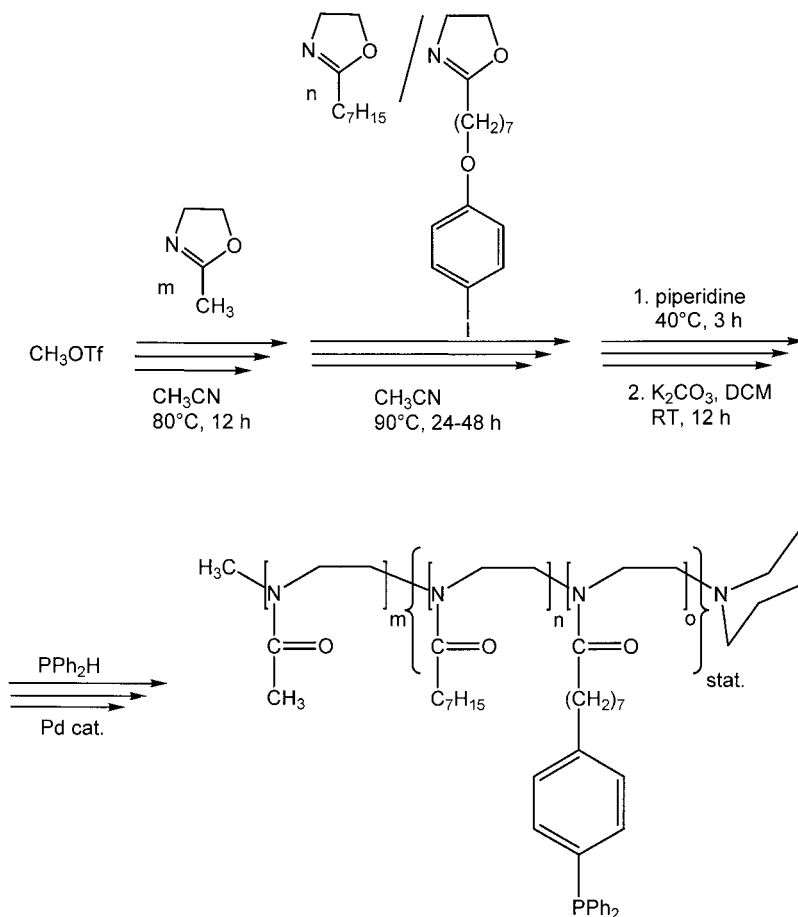


**Scheme 6.3** Amphiphilic poly(2-oxazoline) block copolymers bearing triphenylphosphine and bipyridine moieties respectively as polymeric macroligands for micellar catalysis.

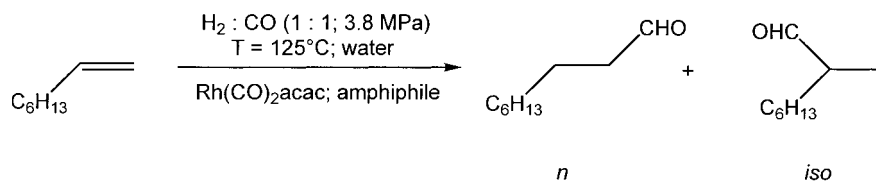
The synthesis of triphenylphosphine-functionalized amphiphiles is shown in Scheme 6.4 [50]. The triphenylphosphine moieties were selectively introduced into the hydrophobic block by a polymer-analogous Pd-catalyzed P-C coupling reaction. The corresponding polymer precursor was prepared by living cationic polymerization of 2-methyl-2-oxazoline forming the hydrophilic part and statistical copolymerization of 2-alkyl-2-oxazoline and iodoaryloxyalkyl-2-oxazoline for the functionalized hydrophobic segment. This route allows direct control of the number of ligand functions by the ratio of the two hydrophobic monomers.

In the first set of experiments O. Nuyken *et al.* studied the rhodium-catalyzed hydroformylation of 1-octene to its corresponding *n*-aldehyde (Scheme 6.5) [51–53]. The active catalyst species was formed *in situ* by mixing the appropriate amount of polymeric macroligand, Rh(CO)<sub>2</sub>acac and 1-octene in water. The results are summarized in Tab. 6.3.

The rhodium-catalyzed hydroformylation proceeded in the presence of the polymeric macroligand in good yield (78–84%). The *n*:*iso* selectivities were typical for rhodium based catalyst systems in the range of 76:24 to 82:18. Notable is the high catalytic efficiency of the system with turn over numbers (TON) ranging from 5560 to 7400 and turn over frequencies (TOF) ranging from 1850 h<sup>-1</sup> to 2480 h<sup>-1</sup> after 3 h reaction time. In comparison with other values reported in literature, these are the highest reported numbers for hydroformylation of 1-octene in water in the presence of amphiphilic ligands or water soluble ligand systems [53]. To prove the recycling of the polymeric catalyst, the authors used ligand (3) (Tab. 6.3, entry (3)) for three runs in a row and methyl-*tert*-butylether as extractive



**Scheme 6.4** Synthesis of triphenylphosphine-functionalized amphiphilic poly(2-oxazoline)s [50].



**Scheme 6.5** Hydroformylation of 1-octene as a model reaction for micellar catalysis using triphenylphosphine-functionalized poly(2-oxazoline)s as macroligands.

**Tab. 6.3** Selected hydroformylation experiments with polymeric amphiphiles (experimental data are listed in Scheme 6.5, reaction time=3 h).

Macroligand <sup>a)</sup>	Yield (%)	<i>n</i> : <i>iso</i>	TON	TOF (h <sup>-1</sup> )
1 x=27, y=2, z=4, m=n=9	82	76:24	7400	2480
2 x=28, y=4, z=3, m=n=9	78	81:19	5560	1850
3 x=33, y=7, z=0, m=n=9	84	82:18	7200	2400

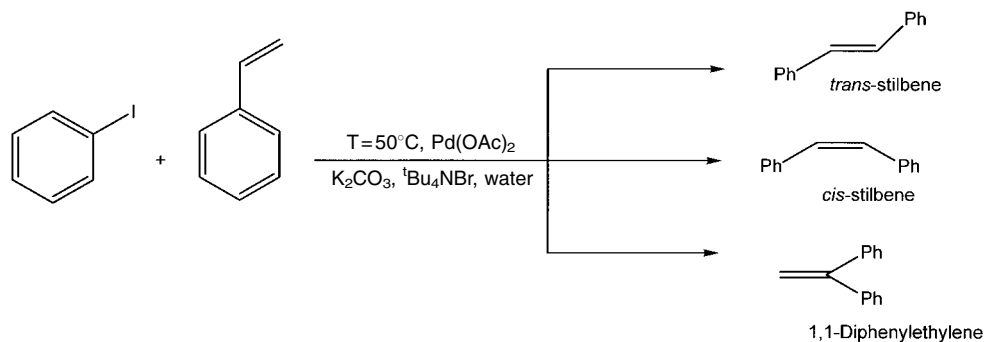
a) Scheme 6.3, R=R<sub>1</sub>.**Tab. 6.4** Recycling experiments and subsequent reuse of the polymeric catalyst (macroligand 3, Table 6.3, reaction time=3 h).

Run	Conversion (%)	Yield (%) <sup>a)</sup>	<i>n</i> : <i>iso</i>
1	96	89	4:1
2	96	89	4:1
3	95	88	4:1

a) Based on GC analysis.

solvent. The conversion of 1-octene was still almost quantitative, the yield of the product remained at 89% and the *n*:*iso* selectivity did not change from 80:20 for any of the experiments (Tab. 6.4).

In the second series of experiments, O. Nuyken *et al.* investigated the Heck reaction of iodobenzene with styrene as a model for the numerous palladium-catalyzed coupling reactions (Scheme 6.6) [54]. In the literature only a few Heck coupling reactions of hydrophobic substrates in aqueous solution are known. The most detailed study has been performed by Jeffery *et al.* on the model reaction of iodobenzene with methylacrylate in the presence of tetrabutylammonia salts. Product yield was at least 95% after 2 h reaction time at 50 °C in pure aqueous solution [55], however more

**Scheme 6.6** Heck coupling of iodobenzene and styrene as a model reaction for micellar catalysis using triphenylphosphine-functionalized poly(2-oxazoline)s as macroligands

**Tab. 6.5** Selected Heck coupling experiments with polymeric amphiphiles (experimental data are listed in Scheme 6.6, reaction time = 7 h).

Macroligand	<i>trans</i> -stilbene (%) <sup>a)</sup>	1,1-diphenylethylene (%) <sup>a)</sup>	<i>cis</i> -stilbene (%) <sup>a)</sup>
1 x=27, y=2, z=4, m=n=9	62.5	2.1	<0.5
2 x=28, y=4, z=3, m=n=9	41.7	1.7	<0.5
3 x=33, y=7, z=0, m=n=9	52.6	1.7	<0.5

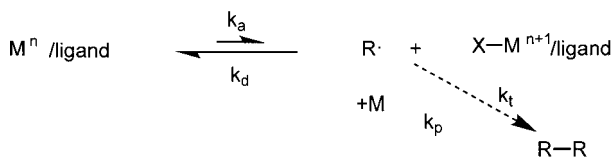
a) Based on GC analysis.

hydrophobic substrates seemed to require higher temperatures and longer reaction times [56]. Similar to these experiments, the active catalyst species was preformed by mixing the amphiphilic block copolymer with Pd(OAc)<sub>2</sub> in dichloromethane overnight and subsequent evaporation of the solvent afterwards. Using this preformed catalyst the catalytic reaction was carried out under mild conditions at 50 °C in aqueous solution in the presence of tetrabutylammoniumbromide as phase transfer reagent for the inorganic base potassium carbonate.

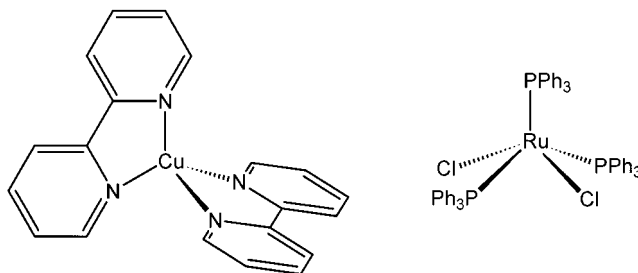
After an induction period of approximately 1 h the reaction started. Gas chromatographic analysis indicated 80% yield of *trans*-stilbene after 14 h reaction time based on iodobenzene. Considering the mild reaction conditions, this is a particularly remarkable result. As side products 1,1-diphenylethylene and *cis*-stilbene were identified in very low amounts of 2.8% and 0.7% respectively (after 14 h reaction time). Furthermore, catalytic activity depends strongly on the structure of the macroligand used (Tab. 6.5) [57].

### 6.2.3.3 ATRP of Methyl Methacrylate in the Presence of an Amphiphilic, Polymeric Macroligand

ATRP is a transition metal-catalyzed “living”, controlled radical polymerization that allows the synthesis of well-defined polymers showing narrow molecular weight distributions with preservation of functional end groups [58] and is less sensitive towards impurities, especially traces of water, compared with other typical ionic polymerization methods. Major drawbacks of ATRP in bulk or solution are the low polymerization rates and the difficulties in catalyst separation, which up to date prevent its application on an industrial scale. Both these drawbacks might be overcome by performing ATRP in aqueous micellar systems. Covalent binding of the metal-ligand to the surfactants allows separation of the catalyst from the resulting polymer. Moreover, separation of the reaction mixtures into micelles as nanoreactors might permit a higher number of radicals to be active compared with conventional ATRP in solution without an increase of termination. Similar to other “living” radical polymerization methods, ATRP is also based on controlling the number of active, free radicals in the reaction mixture [59]. This control is achieved by the following equilibrium between an inactive, “dormant” species RX and an active radical species.



**Scheme 6.7** Equilibrium between “dormant” and active species.



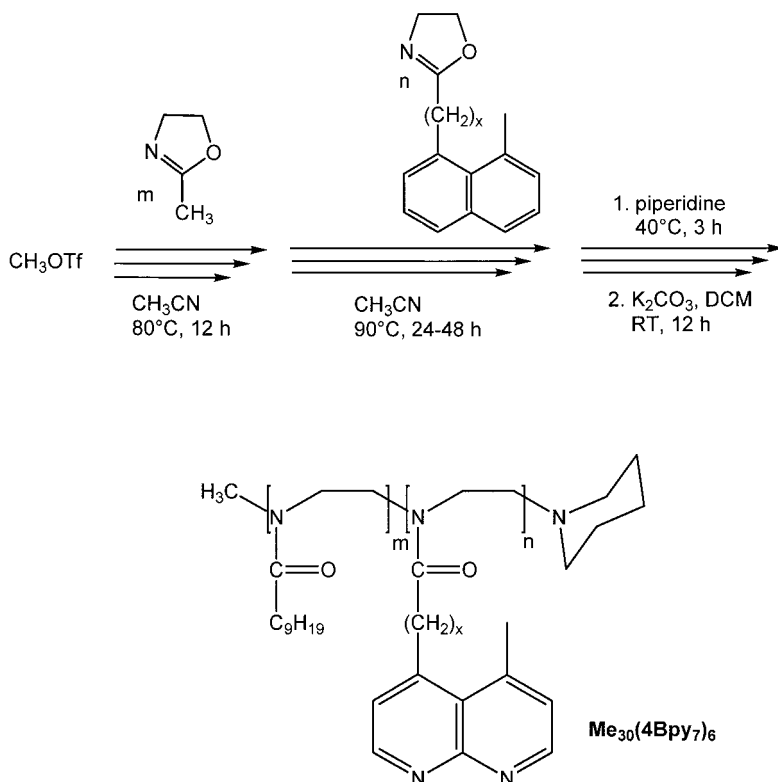
**Fig. 6.6** Typical Cu(I) and Ru(II)-complexes used for ATRP.

In this equilibrium, the number of the dormant species is much higher than the number of active species, which provides the above-mentioned control. Low radical concentration depresses chain propagation much less than termination (radical combination or disproportionation). In recent years, complexes of several different metals have been used successfully for ATRP of various monomers, whereby Cu(I) [60] and Ru(II)-complexes [61] proved to be the most promising ones. In Fig. 6.6 two examples of such complexes are shown [58].

Much research has already been devoted in the past couple of years to (i) the immobilization of ATRP active metal catalysts on various supports to allow for catalyst separation and recycling and (ii) ATRP experiments in pure water as the solvent of choice [62]. A strategy to combine these two demands with an amphiphilic block polymer has recently been presented. Two types of polymeric macroligands where the ligand was covalently linked to the amphiphilic poly(2-oxazoline)s were prepared. In the case of ruthenium, the triphenylphosphine-functionalized poly(2-oxazoline)s described in section 6.2.3.2 were used, whereas in the case of copper as metal, 2,2'-bipyridine functionalized block copolymers were prepared via living cationic polymerization [63] of 2-methyl-2-oxazoline and a bipyridine-functionalized monomer as shown in Scheme 6.8.

Complex formation takes place in an organic solvent or in a water/monomer mixture by reaction of the macroligand with a metal compound (e.g. a Cu(I)-halide). It is supposed that the conditions in the reaction mixture are comparable to those in conventional emulsion polymerization, where monomer droplets stabilized by surfactant molecules coexist with monomer swollen micelles [64]. Reaction sites are presumably the hydrophobic core of the micelles and the monomer droplets as well. Initial results of the micellar-catalyzed ATRP of methyl methacry-



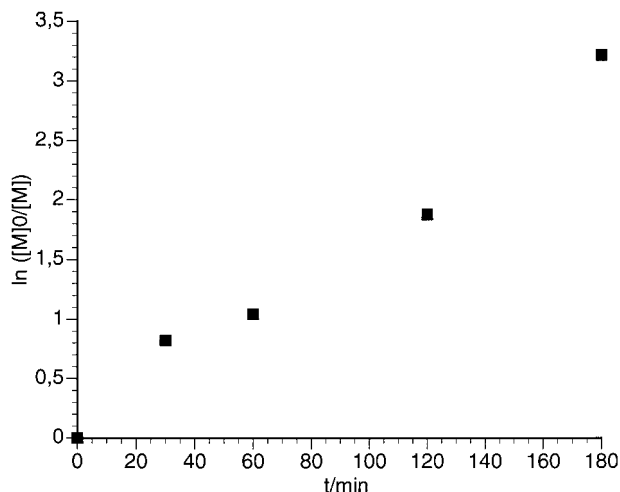


**Scheme 6.8** Synthesis of 2,2'-bipyridine-functionalized poly(2-oxazoline)s [61].

late (MMA) with the copper-bipyridine system indicated that polymers with polydispersities ranging from 1.2 to 1.6 could be obtained. A kinetic study revealed a first-order reaction suggesting a constant number of radicals throughout the whole polymerization time, which is in agreement with the expected behavior of a living/controlled polymerization mechanism, see Fig. 6.7.

Polymerization conditions with temperatures of 60 °C were mild compared with conventional ATRP in solution, where typically temperatures around 100 °C are applied. Despite these mild conditions, high polymerization rates and high conversion within only 3 h were achieved. Moreover, it could be demonstrated that the catalyst, being covalently bound to the surfactant, can easily be removed by filtering off the latex and subsequent washing with methanol. By this procedure the copper content of the resulting PMMA was reduced from the theoretical value of 0.73% to 0.06% and the polymer appeared colorless while the washing fraction was colored [65].

The ruthenium–triphenylphosphine system was also tested under very mild conditions [66]. At room temperature, quantitative monomer conversion was achieved within only 24 h. At 40 °C, polymers with well-controlled molar masses



**Fig. 6.7** First-order kinetic plot for ATRP experiments with MMA in the presence of macroligand  $\text{Me}_{30}(\text{4Bpy7})_6$ .

(deviations <10% from calculated value) and polydispersities of 1.4 were formed quantitatively within less than 24 h. However the preservation of the halide end-groups reached only 46%. This is most probably caused by the loss of halide functions, which has also been reported for several other aqueous systems [67]. The polymers formed were isolated by extraction of the reaction emulsion with large amounts of toluene. Following this procedure, colorless polymers were obtained. The metal contents of these polymers have not yet been examined but as small amounts of ruthenium lead to strongly colored substances, this suggests a very low metal content of the polymers formed. After extraction, the catalyst was used in a subsequent polymerization with a fresh feed of monomer. Catalyst activity was preserved through recycling and the control of the polymerization was still good (PDI: 1.5), while the molar mass was 50% higher than expected.

### 6.3

#### Amphiphilic Polymers Forming Micelle Analogous Structures

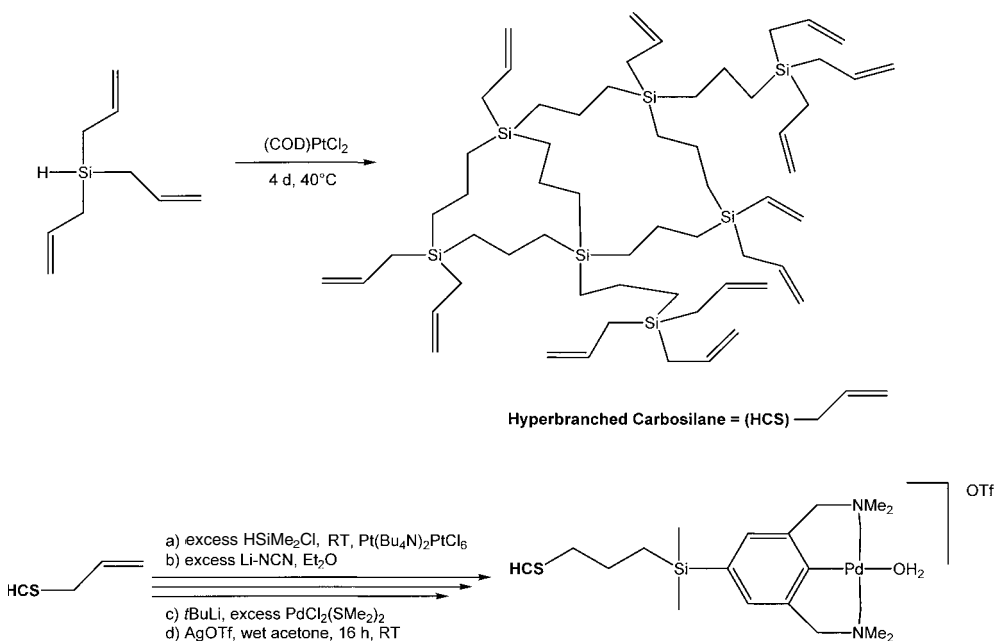
As an extension of the perspective of micelle formation by amphiphilic block copolymers the following part will focus on two other types of polymers. The micellar structures that will be discussed are (i) micelles and inverse micelles based on a hyperbranched polymers and (ii) polysoaps, that are copolymers composed of hydrophilic and amphiphilic or hydrophobic monomers. Whereas the first class of polymers is still very new and only few examples exist of the synthesis and application of such structure in catalysis, the synthesis and aggregation characteristics of polysoaps has already been intensively discussed in the literature.

## 6.3.1

**Amphiphilic Star Polymers with a Hyperbranched Core**

In the search to develop new materials for immobilization of homogeneous transition metal catalyst to facilitate catalyst-product separation and catalyst recycling, the study of dendrimers and hyperbranched polymers for application in catalysis has become a subject of intense research in the last five years [68], because they have excellent solubility and a high number of easily accessible active sites. Moreover, the pseudo-spherical structure with nanometer dimensions opens the possibility of separation and recycling by nanofiltration methods. Although dendrimers allow for controlled incorporation of transition metal catalysts in the core [69] as well as at the surface [70], a serious drawback of this approach is the tedious preparation of functionalized dendrimers by multi-step synthesis.

In contrast to dendrimers, hyperbranched polymers with high molecular weights can be obtained on a large scale in a one-step procedure from  $AB_n$ -type monomers [71]. The first example of using hyperbranched polymers in catalysis has been reported by H. Frey and G. van Koten [72]. They prepared hyperbranched carbosilane polymers starting from triallylsilane in a Pt-catalyzed polyaddition reaction. In a multi-step post-analog modification, terminal double bonds were modified with NCN ligands  $[C_6H_3(CH_2NMe_2)-2,6]^-$  to give catalytically active polymers in the presence of  $[PdCl_2(SMe_2)_2]$  (Scheme 6.9). These polymers were

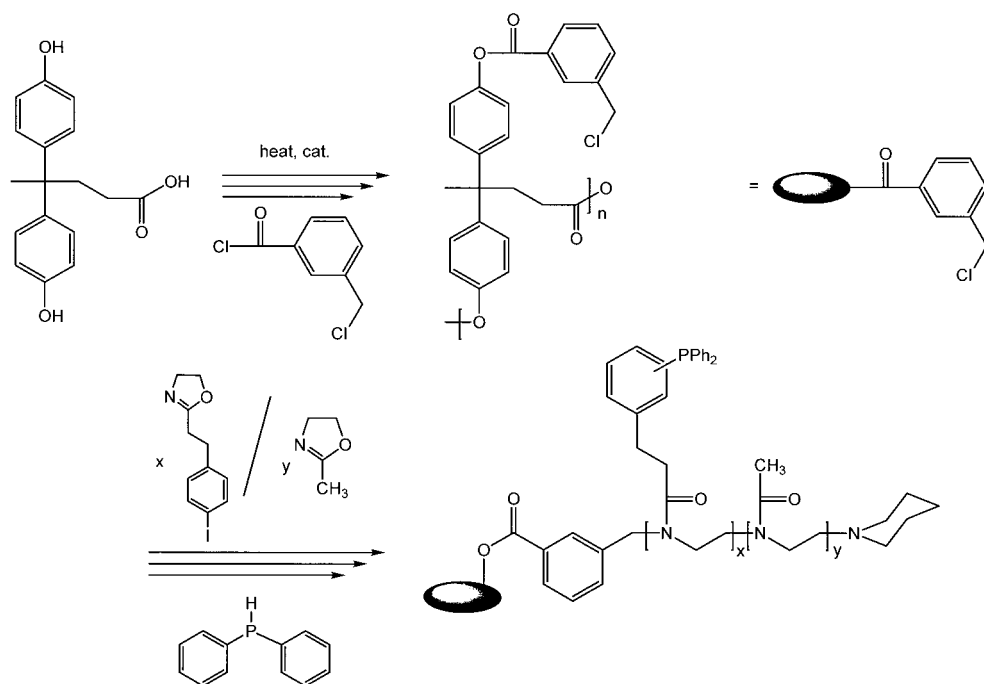


**Scheme 6.9** Synthesis of the catalytic, hyperbranched polytriallylsilane Pd(II) complex.

successfully tested in the aldol-condensation of benzaldehyde with methyl isocyanate in dichloromethane as a solvent and gave quantitative yields after 24 h reaction with a TOF number (per Pd center per hour, during the first hour) of 19 compared with 37 for the nonpolymer supported catalyst.

More recently, the scope of using hyperbranched polymers as soluble supports in catalysis has been extended by the synthesis of amphiphilic star polymers bearing a hyperbranched core and amphiphilic diblock graft arms. This approach is based on previous work, where the authors reported the synthesis of a hyperbranched macroinitiator and its successful application in a cationic “grafting-from” reaction of 2-methyl-2-oxazoline to obtain water-soluble, amphiphilic star polymers [73]. Based on this approach, Nuyken *et al.* prepared catalytically active star polymers where the transition metal catalysts are located at the core-shell interface. The synthesis is outlined in Scheme 6.10.

Starting from a hyperbranched polyester based on 4,4'-bis(hydroxyphenyl)valeric acid, terminal  $-OH$  groups were derivatized to yield the hyperbranched macroinitiator. The ligand precursor was introduced as the first block in the grafting from reaction, followed by 2-methyl-2-oxazoline polymerization to give the second block and allow for water-soluble polymers. The triphenylphosphine-functionalized amphiphilic star block copolymer was obtained after transformation of the iodoaryl

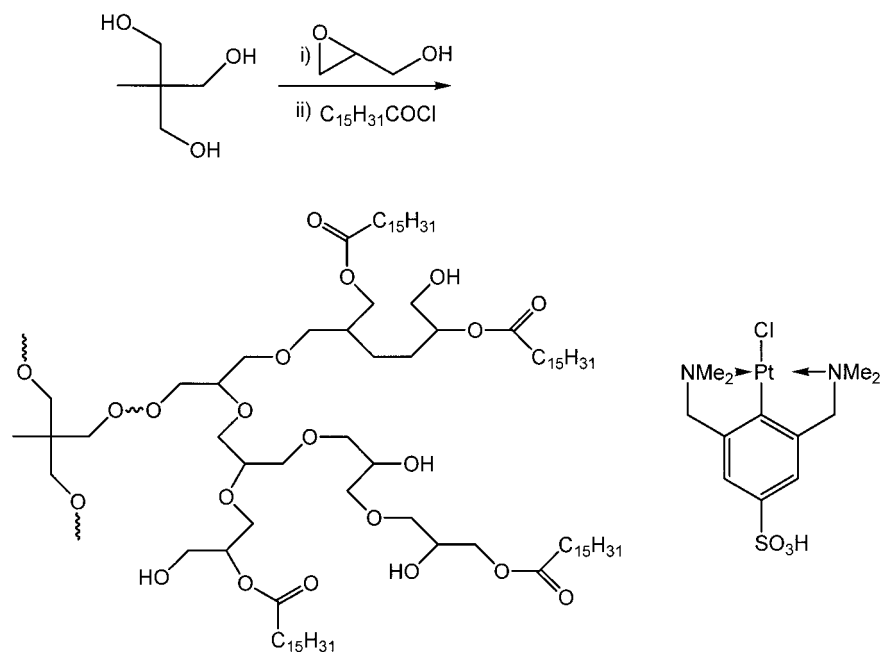


**Scheme 6.10** Synthesis of the amphiphilic star polymers with a hyperbranched core and amphiphilic diblock graft arms [69].

precursor in a Pd-catalyzed reaction with diphenyl phosphine and was applied in two test reactions.

In a first test reaction, the polymer support was used for the hydroformylation of 1-octene in water in the presence of  $\text{Rh}(\text{CO})_2\text{acac}$ . Within a reaction time of 10 h at  $120^\circ\text{C}$  and a  $\text{H}_2/\text{CO}$  (1:1) pressure of 5 MPa, conversion of up to 94% was obtained. The *n*:*iso* ratio was 3:1, sometimes reaching 9:1. The quantities of 3- and 4-nonanal resulting from olefin isomerization, were below 5% [74]. The versatility of the polymer support was further demonstrated with the Heck reaction of styrene and iodobenzene in the presence of  $\text{Pd}(\text{OAc})_2$  as the metal catalyst. The reaction was again performed in pure water at  $50^\circ\text{C}$  and product yield of up to 80% was obtained after 20 h reaction time [75].

Recently, Mecking *et al.* reported the synthesis of inverse micelles based on a hyperbranched polyglycerol polymer. Terminal  $-\text{OH}$  groups were modified with palmitoyl chloride and gave a polymeric catalyst soluble in organic solvents with hydrophilic core to immobilize water-soluble guest molecules such as  $\text{PdCl}_2$  or  $\text{Pd}(\text{OAc})_2$ . After reduction, Pd nanoparticles in the range of 5.2 nm were obtained. Particle size could be controlled by the ratio of  $-\text{OH}$  groups to Pd. Hydrogenation of cyclohexene in toluene gave a TON of 20 000 corresponding to a TOF of  $700 \text{ h}^{-1} \text{ atm}(\text{H}_2)^{-1}$  at 75% cyclohexene conversion. The catalyst was easily separated from the product by vacuum distillation and/or dialysis or membrane filtration [76].



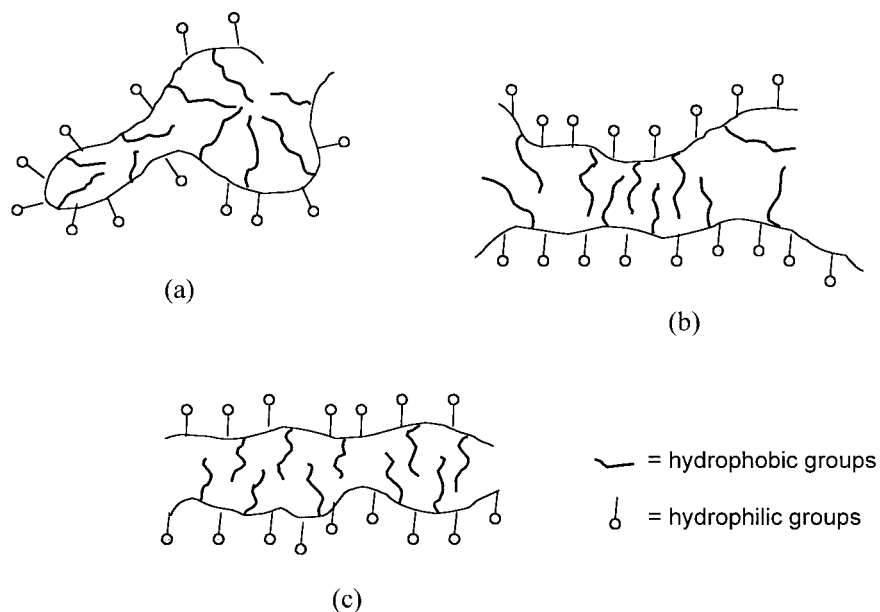
**Scheme 6.11** Synthesis of hyperbranched polyglycerol polymers with terminal palmitoyl groups.

The same hyperbranched polyglycerol modified with hydrophobic palmitoyl groups was used for a noncovalent encapsulation of hydrophilic platinum Pincer [77]. In a double Michael addition of ethyl cyanoacetate with methyl vinyl ketone, these polymer supports indicated high conversion (81 to 59%) at room temperature in dichloromethane as a solvent. The activity was still lower compared with the noncomplexed Pt catalyst. Product catalyst separation was performed by dialysis allowing the recovery of 97% of catalytic material. This is therefore an illustrative example for the possible application of such a polymer/catalyst system in continuous membrane reactors.

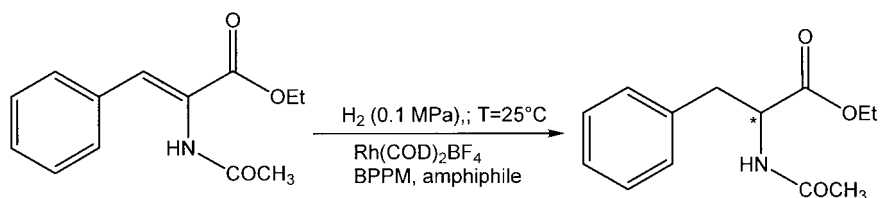
### 6.3.2

#### Polysoaps

A second interesting class of amphiphilic polymers is the polysoaps or “micellar polymers” as they are often referred to. Such polymers are composed of hydrophilic and hydrophobic fragments leading to various molecular architectures that have been discussed in detail by A. Laschewsky [78]. The precise structure of the resulting micelles, that is, whether they are intra- or intermolecular assemblies, is still subject to discussion because the polymer structure is so versatile. Possible micellar structures are depicted in Fig. 6.8. The most interesting feature of such polymers with respect to their application in catalysis is (i) their remarkable abil-



**Fig. 6.8** Possible shapes of “polymeric micelles” formed by polysoaps. (a) “local micelle” (b) “regional micelle” (c) “molecular micelle”.



**Scheme 6.12** Asymmetric hydrogenation of cinnamic acid acetamides.

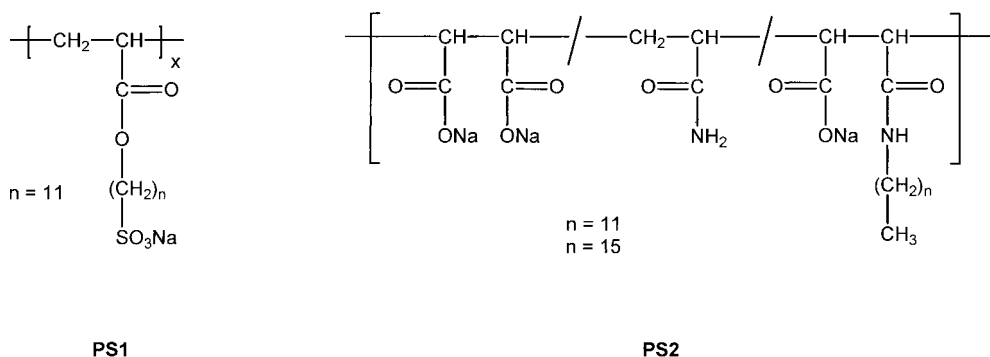
ity to solubilize hydrophobic guest molecules in their hydrophobic domains and (ii) their high molecular weight which permits separation from the product by membrane filtration. Moreover, the presence of hydrophobic micro-domains in the compact conformation of polysoaps may lead to rate enhancements because of a specific micro-environmental effect and an accumulation of reactants in the pseudophase.

Although much work has already been devoted to the use of polysoaps in micellar catalysis application, in particular as models for esterases [79] and systems for photochemical catalyzed reactions [80], only a few reports have appeared on the use of such polymer supports in transition metal catalysis.

Thus, G. Oehme *et al.* employed two types of polysoaps in the micellar catalytic asymmetric hydrogenation of cinnamic acid acetamides as amino acid precursors [81, 82].

The first type is a standard polysoap derived from a polymerizable surfactant leading to poly(sodium 11-acryloyloxyundecane-1-sulfonate) PS1 whereas the second polysoap is an alternating copolymer of maleic acid anhydride and acrylamide leading to a polymer with carboxylic acid groups and hydrophobic *n*-alkylamide groups PS2 (see Fig. 6.9). The organometallic catalyst was not covalently bound to the polysoaps in the catalytic experiments.

Hydrogenation was less fast in the presence of polysoap PS1 and PS2 compared with SDS which has been explained by diffusion limitation of the polymer-



**Fig. 6.9** Two examples for linear polysoaps used in the asymmetric hydrogenation [76].

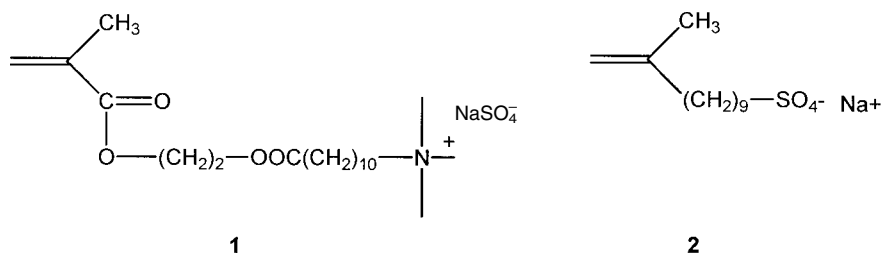


Fig. 6.10 Two examples for polymerizable surfactants [77].

ized structures. However, the high enantiomeric excess values (ee) of up to 94% indicate the formation of a favorable micro-environment in the presence of PS1 and PS2 [81].

More defined polysoaps have been prepared by ionic surfactants with polymerizable head groups, either in the hydrophilic head region or the hydrophobic tail (Fig. 6.10). Best results were obtained by a photo-induced polymerization in water in concentrations slightly above the cmc in the presence of AIBN or  $\text{K}_2\text{S}_2\text{O}_8/\text{Na}_2\text{S}_2\text{O}_5$  as initiators with molecular weight  $M_w$  ranging from  $1200 \text{ g mol}^{-1}$  to  $6900 \text{ g mol}^{-1}$ . Higher surfactant concentration resulted in incomplete polymerization [82].

In most cases the enantiomeric excess (ee) in the presence of the polymerized micelles were higher compared with the monomeric counterpart. The catalytic efficiency is mainly controlled by the solubilization capacity of the amphiphiles. Results however are quite different as can be seen from the data summarized in Tab. 6.6. A major limitation of these polymerized micelles is their low molecular weight that makes it almost impossible to separate them from the products by nanofiltration methods.

Tab. 6.6 Selected examples for the hydrogenation of (Z) methyl  $\alpha$ -acetoimidocinnamate in water according to Scheme 6.11.

Amphiphile	Molar ratio amphiphile:Rh	Enantiomeric excess (ee) (%)	Half time of hydrogenation ( $t_{1/2} \text{ min}^{-1}$ )	Ref.
SDS	50:1	94	3.5	81
1	20:1	85	6	81
2 (C12)	20:1	94	960	81
2 (C16)	20:1	93	270	81
3 (monomer)	20:1	83	50	82
3 (poly)	20:1	87	26	82
4 (monomer)	20:1	89	16	82
4 (poly)	20:1	94	13	82



## 6.4

## Summary and Outlook

The past five years have seen a revival in the use of amphiphilic block copolymers as support materials for homogenous transition metal catalysis. The unique properties of amphiphilic polymers, which allow solubilization of hydrophobic substrates in pure water, will make them increasingly useful in the field of polymer-supported chemistry, where the driving force today is environmentally-friendly production of fine chemicals, pharmaceuticals and polymers as well as long-term stability of the catalyst system. We believe that amphiphilic polymers, such as block copolymers, star polymers and polysoaps, will render very promising polymer support catalysts in the future, following significant improvement in catalyst design and control over polymer architecture.

## 6.5

## References

- 1 For example see: a) J. H. FENDLER, E. J. FENDLER, *Catalysis in Micellar and Macromolecular Systems*, Academic Press, New York, 1975 and references therein; b) L. S. RONSTED, C. A. BUNTON, J. H. YAO, *Curr. Opin. Coll. Interf. Sci.* **1997**, 2, 622–628.
- 2 a) S. G. DAVES; S. I. MURAHASHI, *Transition Metal Catalyzed Reactions*, Blackwell Science, Oxford, 1998; b) F. DIEDERICH, P. J. STANG, *Metal-Catalyzed Cross Coupling Reactions*, Wiley-VCH, New York, 1998; c) K. FAGNOU, M. LAUTENS, *Angew. Chem. Int. Ed.* **2002**, 41, 26–47; d) B. M. TROST, *Science* **1991**, 254, 1471–1477; e) G. KISS, *Chem. Rev.* **2001**, 101, 3435–3456; f) N. MIYAURA, A. SUZUKI, *Chem. Rev.* **1995**, 95, 2457–2483; g) R. C. LAROCK, *J. Organomet. Chem.* **1999**, 576, 111–124.
- 3 B. CORNILS, W. A. HERRMANN (eds.), *Aqueous-Phase Organometallic Catalysis*, Wiley-VCH, Weinheim, 1998.
- 4 W. A. HERRMANN, B. CORNILS, *Angew. Chem.* **1997**, 109, 1074–1095; *Angew. Chem. Int. Ed. Engl.* **1997**, 36, 1049–1067.
- 5 G. OEHME, I. GRASSERT, S. ZIEGLER, *et al.*, *Catal. Today* **1998**, 42, 459.
- 6 A. BEHR, W. KEIM, *Erdöl Erdgas Kohle Petrochem.* **1987**, 103, 126.
- 7 a) J. MANASSEN, in: *Catalysis. Progress in Research*, F. BASALO, R. L. BURWELL, JR., Plenum Press, London, 1973. b) Y. DROR, J. MANASSEN, *J. Mol. Cat.* **1976**, 77, 219.
- 8 a) W. A. HERRMANN, C. W. KOHLPAINTER, *Angew. Chem.* **1993**, 105, 1588–1608; *Angew. Chem. Int. Ed. Engl.* **1993**, 32, 1524–1544; b) F. JOÓ, Z. TÓTH, *J. Mol. Catal.* **1980**, 8, 369–388.
- 9 E. WIEBUS, B. CORNILS, *Chem. Ing. Technol.* **1994**, 66, 916–923.
- 10 D. VOGT, in B. CORNILS, W. A. HERRMANN (eds.), *Applied Homogenous Catalysis with Organometallic Compounds*, Vol. 1, Wiley-VCH, Weinheim, 1996.
- 11 G. PAPADOGLIANAKIS, R. A. SHELDON, in B. CORNILS, W. A. HERRMANN (eds.), *Aqueous-Phase Organometallic Catalysis*, Wiley-VCH, Weinheim, 1998.
- 12 G. OEHME, in B. CORNILS, W. A. HERRMANN (eds.), *Aqueous-Phase Organometallic Catalysis*, Wiley-VCH, Weinheim, 1998.
- 13 J.-H. FUHRHOP, J. KÖNING, *Membranes and Molecular Assemblies: The Syntkinetic Approach*, The Royal Society of Chemistry, Cambridge, 1994.
- 14 S. D. CHRISTIAN, J. F. SCAMEHORN (eds.), *Solubilization in Surfactant Aggregates*, Marcel Dekker, New York, 1995.
- 15 M. ANTONIETTI, K. LANDFESTER, Y. MASTAI, *Israel J. Chem.* **2001**, 41, 1–5.
- 16 H. MORAWETZ, *Adv. Catal.* **1969**, 20, 341–371.
- 17 C. A. BUNTON in M. GRÄTZEL, K. KALYANASUNDARAM (eds.), *Kinetics and Catalysis*

- in *Microheterogeneous Systems*, Marcel Dekker, New York, 1991.
- 18 Y. MURAKAMI, J. KIKUCHI, Y. HISEADA, *et al.*, *Chem. Rev.* **1996**, 96, 721.
  - 19 a) Y. CHOI, S.-B. LEE, D.-J. LEE, *et al.*, *J. Membr. Sci.* **1998**, 148, 185–194; b) T. DWARS, J. HABERLAND, I. GRASSET, *et al.*, *J. Mol. Catal. A: Chem.* **2001**, 168, 81–86.
  - 20 a) D. E. BERGBREITER, L. ZHANG, V. M. MARIAGNANAM, *J. Am. Chem. Soc.* **1993**, 115, 9295–9296; b) D. E. BERGBREITER, V. M. MARIAGNANAM, L. ZHANG, *Adv. Mater.* **1995**, 7, 69–71. c) D. E. BERGBREITER, J. W. CARAWAY, *J. Am. Chem. Soc.* **1996**, 118, 6092–6093.
  - 21 M. SZWARC, M. LEVY, R. MILKOWICH, *J. Am. Chem. Soc.* **1957**, 78, 2656–2657.
  - 22 M. MIYAMOTO, M. SAWAMOTO, T. HIGASHIMURA, *Macromolecules* **1984**, 17, 265–268.
  - 23 M. K. GEORGES, R. P. N. VEREIGIN, P. M. KAZMEIER, *et al.*, *Macromolecules* **1994**, 27, 7228–7229.
  - 24 O. W. WEBSTER, W. R. HERTLER, D. Y. SOGAH, *et al.*, *J. Am. Chem. Soc.* **1983**, 105, 5706–5708.
  - 25 R. H. GRUBBS, W. TUMAS, *Science* **1989**, 243, 907–915.
  - 26 For example: a) S. FÖRSTER, M. ANTONIETTI, *Adv. Mater.* **1998**, 10, 195–217; b) M. PITSIKALIS, S. PISPAS, J. W. MAYS, *et al.*, *Adv. Polym. Sci.* **1998**, 135, 1–137.
  - 27 I. GRASSET, U. SCHMIDT, S. ZIEGLER, *et al.*, *Tetrahedron Assym.* **1998**, 9, 4193–4202.
  - 28 G. OEHME, I. GRASSET, E. PAETZOLD, *et al.*, *Coord. Chem. Rev.* **1999**, 185–186, 585–600.
  - 29 L. LECOMTE, D. SINOU, J. BAKOS, *et al.*, *J. Organomet. Chem.* **1989**, 370, 277–284.
  - 30 T. DWARS, J. HABERLAND, I. GRASSET, *et al.*, *J. Mol. Catal. A* **2001**, 168, 81–86.
  - 31 a) F. ROBERT, G. OEHME, I. GRASSET, *et al.*, *J. Mol. Catal. A* **2000**, 156, 127–132; b) I. GRASSET, G. OEHME, *J. Organomet. Chem.* **2001**, 621, 158–165.
  - 32 K. DREXLER, R. MEISEL, I. GRASSET, *et al.*, *Macromol. Chem. Phys.* **2000**, 201, 1436–1441.
  - 33 a) A. HENGLEIN, *Chem. Rev.* **1989**, 89, 1861–1873; b) S. OGGAWA, Y. HAYASHI, N. KOBAYASHI, *et al.*, *Jpn. J. Appl. Phys.* **1994**, 33, 331–333; c) L. N. LEWIS, *Chem. Rev.* **1993**, 93, 2693–2730.
  - 34 a) H. BÖNNEMANN, R. H. RICHARDS, *Eur. J. Inorg. Chem.* **2001**, 2455–2480; b) M. KRÁLÍK, A. BIFFIS, *J. Mol. Catal. A: Chem.* **2001**, 177, 113–138.
  - 35 B. CORAIN, K. JERÁBEK, M. ZECCA, *J. Mol. Catal. A: Chem.* **2001**, 177, 3–20; b) G. A. SOMORJAI, *Introduction to Surface Chemistry and Catalysis*, Wiley, New York, 1994.
  - 36 D. H. NAPPER, *Polymeric Stabilization of Colloidal Dispersions*, Academic Press, London, 1983.
  - 37 A. B. R. MAYER, J. E. MARK, *Coll. Polym. Sci.* **1997**, 275, 333–340.
  - 38 M. ANTONIETTI, E. WENZ, L. BRONSTEIN, *et al.*, *Adv. Mater.* **1995**, 7, 1000–1005.
  - 39 a) Y. C. N. CHAN, R. R. SCHROCK, R. E. COHEN, *Chem. Mater.* **1992**, 4, 24–27; b) V. SANKARAN, J. YUE, R. E. COHEN, *et al.*, *Chem. Mater.* **1993**, 5, 1133–1142.
  - 40 a) M. MOFFITT, A. EISENBERG, *Chem. Mater.* **1995**, 7, 1178–1784. b) M. MOFFITT, L. McMAHOM, V. PESSER, A. EISENBERG, *Chem. Mater.* **1995**, 7, 1185–1192.
  - 41 a) J. P. SPATZ, A. RÖSCHER, M. MÖLLER, *Adv. Mater.* **1996**, 8, 337–340; b) J. P. SPATZ, S. SHEIKO, M. MÖLLER, *Macromolecules* **1996**, 29, 3220–3226.
  - 42 a) M. ANTONIETTI, S. HEINZ, C. ROSENBAUER, *et al.*, *Macromolecules* **1994**, 27, 3276–3281; b) S. FÖRSTER, M. ZISENIS, E. WENZ, *et al.*, *J. Chem. Phys.* **1996**, 104, 9956–9970.
  - 43 M. SEREGINA, L. BRONSTEIN, O. PLATONOVA, *et al.*, *Chem. Mat.* **1997**, 9, 923–931.
  - 44 a) E. SULMAN, Y. BODROVA, V. MATVEEVA, *et al.*, *Appl. Catal. A* **1999**, 176, 75–81; b) L. BRONSTEIN, D. CHERNYSHOV, I. VOLKOV, *et al.*, *J. Catal.* **2000**, 196, 302–314; c) E. SULMAN, V. MATVEEVA, A. USANOV, *et al.*, *J. Mol. Catal. A* **1999**, 146, 265–269.
  - 45 S. KLINGELHÖFER, W. HEITZ, A. GREINER, *et al.*, *J. Am. Chem. Soc.* **1997**, 119, 10116–10120.
  - 46 D. CHERNYSHOV, L. BRONSTEIN, H. BÖRNER, *et al.*, *Chem. Mater.* **2000**, 12, 114–121.
  - 47 a) D. J. DARENSBOURG, F. JOO, M. KANISTO, *et al.*, *Inorg. Chem.* **1994**, 33, 200–208; b) S. GANGULY, D. M. ROUNDHILL, *Organometallics* **1993**, 12, 4825–4832; c) B. S. L. NETO, K. H. FORD, A. J. PARDEY, *et al.*, *Inorg. Chem.* **1991**, 30, 3837–3842.

- 48 a) S. SIDOROV, L. BRONSTEIN, P. VALET-SKY, *et al.*, *J. Coll. Interf. Sci.* **1999**, *212*, 197–201; b) L. M. BRONSTEIN, S. N. SIDOROV, A. Y. GOURKOVA, *et al.*, *Inorg. Chim. Acta* **1998**, *280*, 348–354.
- 49 A. B. R. MAYER, J. E. MARK, *Coll. Polym. Sci.* **1997**, *275*, 333–340.
- 50 P. PERSIGHEHL, R. JORDAN, O. NUYKEN, *Macromolecules* **2000**, *33*, 6977–6981.
- 51 P. PERSIGHEHL, PhD thesis, TU München, **2000**.
- 52 O. NUYKEN, P. PERSIGHEHL, R. WEBERSKIRCH, *Macromol. Symp.* **2002**, *177*, 163–173.
- 53 P. PERSIGHEHL, O. NUYKEN, R. WEBERSKIRCH, *manuscript in preparation*.
- 54 a) H. DING, B. E. HANSON, T. BARTIK, *et al.*, *Organometallics* **1994**, *13*, 3761–3763; b) I. TTH, I. GUO, B. E. HANSON, *J. Mol. Cat. A* **1997**, *116*, 217–229; c) H. CHEN, Y. Z. LI, J. R. CHEN, *et al.*, *J. Mol. Cat. A* **1999**, *149*, 1–6.
- 55 a) T. JEFFERY, *Tetrahedron Lett.* **1994**, *35*, 3051–3054; b) T. JEFFERY, *Tetrahedron* **1996**, *52*, 10113–10130.
- 56 H. ZAO, M. Z. CAI, C. Y. PENG, *et al.*, *J. Chem. Research (S)* **2002**, *1*, 28–29.
- 57 a) D. SCHÖNFELDER, Diploma Thesis, TU München, **2001**; b) D. SCHÖNFELDER, R. WEBERSKIRCH, O. NUYKEN, *manuscript in preparation*.
- 58 a) K. MATYJASZEWSKI, J. XIA, *Chem. Rev.* **2001**, *101*, 2921–2990; b) M. KAMIGAITO, T. ANDO, M. SAWAMOTO, *Chem. Rev.* **2001**, *101*, 3689–3745.
- 59 a) K. MATYJASZEWSKI, *Macromol. Symp.* **1996**, *111*, 47–61; b) H. FISCHER, *Macromolecules* **1997**, *30*, 5666–5672.
- 60 a) J. S. WANG, K. MATYJASZEWSKI, *J. Am. Chem. Soc.* **1995**, *117*, 5614–5615; b) J. S. WANG, K. MATYJASZEWSKI, *Macromolecules* **1995**, *28*, 7901–7910.
- 61 M. KATO, K. KAMIGAITO, M. SAWAMOTO, *Macromolecules* **1995**, *28*, 1721–1723.
- 62 J. QIU, B. CHARLEUX, K. MATYJASZEWSKI, *Prog. Polym. Sci.* **2001**, *26*, 2083–2134.
- 63 a) T. KAGIYA, S. NARISAWA, T. MAEDA, *et al.*, *J. Polym. Sci., Polym. Lett. Ed. B4* **1966**, *441–447*; b) K. AOI, M. K. OKADA, *Prog. Polym. Sci.* **1996**, *21*, 151–208.
- 64 a) G. ODIAN, *Principles of Polymerization*, Wiley-Interscience Publication, New York, 1981; b) R. ARSHADY, *Coll. Polym. Sci.* **1992**, *270*, 717.
- 65 a) T. KOTRE, DIPLOMA THESIS, TU MÜNCHEN, **2001**; b) T. KOTRE, R. WEBERSKIRCH, O. NUYKEN, *manuscript in preparation*.
- 66 a) N. STÖCKEL, PhD thesis, TU München, **2002**; b) DE 10142908 (2001), BASF AG; Erf. O. NUYKEN, R. JORDAN, N. STÖCKEL.
- 67 S. JOUSSET, J. QIU, K. MATYJASZEWSKI, *Macromolecules* **2001**, *34*, 6641–6648.
- 68 a) G. E. OOSTEROM, J. N. H. REEK, P. C. J. KAMER, *et al.*, *Angew. Chem. Int. Ed. Engl.* **2001**, *40*, 1828–1849; *Angew. Chem.* **2001**, *113*, 1878–1901; b) R. M. CROOKS, M. ZHAO; L. SUN; *et al.*, *Acc. Chem. Res.* **2001**, *34*, 181–190; D. ASTRUC, F. CHAR-DAC, *Chem. Rev.* **2001**, *101*, 2991–3023.
- 69 For example: a) P. BHYRAPPA, J. K. YOUNG, J. S. MOORE, *et al.*, *J. Am. Chem. Soc.* **1996**, *118*, 5708–5711; b) C. C. MAK, H. F. CHOW, *Macromolecules* **1997**, *30*, 1228–1230; c) H. SELNER, D. SEEBACH, *Angew. Chem. Int. Ed. Engl.* **1999**, *38*, 1918–1920; *Angew. Chem.* **1999**, *111*, 2039–2041; d) A. W. KLEIJ, R. A. GOSSAGE, T. B. H. JASTRZESKI, *et al.*, *Angew. Chem. Int. Ed. Engl.* **2000**, *39*, 176–178; *Angew. Chem.* **2000**, *112*, 179–181.
- 70 For example: a) M. T. REETZ, C. LOHMER, R. SCHWICKHARDI, *Angew. Chem. Int. Ed. Engl.* **1997**, *36*, 1526–1529; b) P. DANI, T. KARLEN, E. A. GOSSAGE, *et al.*, *J. Am. Chem. Soc.* **1997**, *119*, 11317–11318; c) G. VAN KOTEN, J. T. B. H. JASTRZESKI, *J. Mol. Catal. A Chem.* **1999**, *146*, 317–323.
- 71 a) C. J. HAWKER, R. LEE, J. M. J. FRÉCHET, *J. Am. Chem. Soc.* **1991**, *113*, 4583–4588; b) Y. H. KIM, O. W. WEBSTER, *Macromolecules* **1992**, *25*, 5561–5572; S. R. TURNER, F. WALTER, B. I. VOIT, T. H. MOUREY, *Macromolecules* **1994**, *27*, 1611–1616.
- 72 a) C. SCHLENK, A. W. KLEIJ, H. FREY *et al.* *Angew. Chem. Int. Ed. Engl.* **2000**, *39*, 3445–3447; *Angew. Chem.* **2000**, *112*, 3587–3589; b) C. SCHLENK, A. W. KLEIJ, H. FREY *et al.*, *Angew. Chem. Int. Ed. Engl.* **2000**, *39*, 3736.
- 73 R. WEBERSKIRCH, R. HETTICH, O. NUYKEN, *et al.*, *Macromol. Chem. Phys.* **1999**, *200*, 863–873.
- 74 N. WEST, PhD thesis, TU München, **2000**.
- 75 a) A. WÖRNDLE, Diploma thesis, TU München, **2001**; b) A. WÖRNDLE, M. WAGNER, R. WEBERSKIRCH, *manuscript in preparation*.

- 76 S. MECKING, R. THOMANN, H. FREY, *et al.*, *Macromolecules* **2000**, 33, 3958–3960.
- 77 M.Q. SLAGT, S.E. STIRIBA, R.J.M. KLEIN GEBBINK, H. KAUTZ, H. FREY, G. VAN KOTEN, *Macromolecules* **2002**, 35, 5734–5737.
- 78 a) P. ANTON, P. KÖBERLE, A. LASCHWESKY, *Macromol. Chem.* **1993**, 194, 1–27; b) A. LASCHEWSKY, *Adv. Polym. Sci.* **1995**, 124, 1–86.
- 79 a) T. OKUBO, N. ISE, *Adv. Polym. Sci.* **1977**, 25, 135–181; b) B. BOYER, G. LAMATY, A. LEYDET, *et al.*, *New J. Chem* **1992**, 16, 887–892.
- 80 a) D.M. GRAVETT, J.E. GUILLET, *Macromolecules* **1995**, 28, 274–280; b) J.E. GUILLET, N.A.D. BURKE and M. NOWAKOWSKA, *Macromol. Symp.* **1997**, 118, 527–543.
- 81 H.N. FLACH, I. GRASSERT, G. OEHME, *Macromol. Chem. Phys.* **1994**, 195, 3289–3301.
- 82 H. FUHRMANN, I. GRASSERT, T. SCHAREINA, *et al.*, *Macromol. Chem. Phys* **2001**, 202, 426–434.

## 7

## Dendritic Polymers as High-Loading Supports for Organic Synthesis and Catalysis

RAINER HAAG and SEBASTIAN ROLLER

## 7.1

### Introduction

Polymeric supports have revolutionized organic synthesis in the last decade and have become a major driving force for lab automation and parallelization of chemical reactions in general. Solid-phase synthesis on modified polystyrene microbeads, which was originally introduced by Merrifield [1], still remains the major focus in this area (refer to other chapters in this book) [2, 3]. Although highly successful, solid-phase synthesis exhibits a number of problems, most notably the limited swelling behavior of the polymer beads in many organic solvents, i.e. protic solvents, the biphasic reaction behavior and the low concentration of functional groups (typically  $\leq 1.5$  mmol substrate per gram polymeric support). Therefore, some of these traditional polymeric supports are of limited use for preparative organic synthesis and catalysis. In the last decade a rapidly increasing number of high-loading polymeric supports has been reported [2, 4, 5]. In this chapter, the class of dendritic polymers, which has developed its own profile because of their unique properties both in a soluble (non-cross-linked) form [4] or as insoluble (cross-linked) hybrid polymers [6] (Fig. 7.1) will be described, focussing on the special features of high-loading dendritic polymeric architectures, their separation from reaction mixtures and applications in organic synthesis as well as catalysis. The formation and application of catalytically-active nanoparticles using dendritic polymer templates (see Chapter 6), monovalent transformations at the focal unit of dendritic polymers, dendritic initiators or cross-linkers will not be covered in this Chapter.

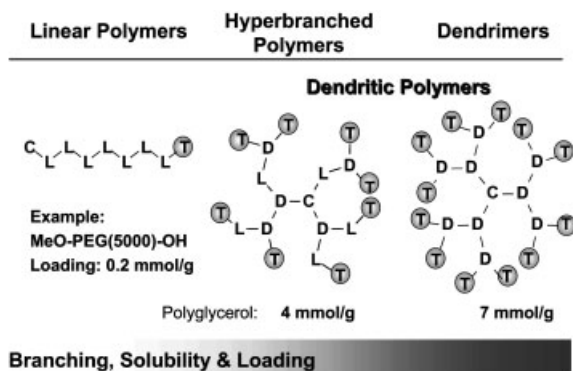
## 7.2

### General Aspects of Dendritic Polymers and Solid-phase Hybrid Polymers

## 7.2.1

#### Special Properties of Soluble Dendritic Polymeric Supports

Many drawbacks of conventional polymeric supports, such as limited solubilities/swellabilities in many organic solvents, limited site accessibility and poor loading



**Fig. 7.1** Schematic representation of linear versus dendritic polymers: linear (left) and hyperbranched (middle) polymers, perfect dendrimer (right). The amount of terminal groups is indicated below each structure. These architectures can also be attached to a cross-linked polymer bead to obtain a high-loading hybrid material.

capacities can be overcome by the use of branched polymer architectures [4]. An extreme example of tree-like branching is shown by the perfectly branched dendrimers (Fig. 7.1) [7–9]. These well-defined macromolecules are soluble in many organic solvents (mostly dependent on their end functionalities) and possess a maximum capacity of functional groups in their periphery. Their fully-branched, globular topology dictates their relatively low viscosity in solution and low glass transition temperatures in bulk. However, their high price and the limited chemical stability of the commercially available polyamine or polyamine dendrimers might be the reason for their limited use as supports in organic synthesis [10]. Despite these problems, polyamine and polycarbosilane dendrimers have been successfully used as high-loading supports in organic synthesis and catalysis (see Sections 7.3, 7.4, 7.5).

In contrast to perfect dendrimers, hyperbranched polymers are easily available in one reaction step on a large scale [11]. They contain dendritic, linear and terminal monomer units in their skeleton and hence can be considered as intermediates between linear polymers (degree of branching  $DB=0\%$ ) and dendrimers ( $DB=100\%$ ) with an approximate  $DB$  between 50 and 75% (Fig. 7.1) [12]. In some cases, however, the use of these commercial materials as supports for organic synthesis is limited because of the chemical stability of the respective polymer backbone (e.g. polyamines, polyesters) and the broad molecular weight distributions ( $>1.5$ ), i.e. for size-dependent separation techniques. Nevertheless, hyperbranched polymers show properties comparable to perfect dendrimers due to their high degree of branching and globular shape. Also, the potential loading capacity of these statistically branched dendritic structures is comparable with that of perfect dendrimers (5–23 mmol g<sup>-1</sup>). Even though the number of terminal groups is reduced to about 50–75% (compare Fig. 7.1) selective functionalization is possible [13]. Therefore, hyperbranched polymers can serve as easily accessible alternatives to

the perfect dendrimers for many applications, i.e. as high-loading polymeric supports in organic synthesis and catalysis [14].

### 7.2.2

#### Methods for Separating Dendritic Polymer Supports from Reaction Mixtures

This section will cover selected techniques for the separation of dendritic polymeric supports from low molecular weight compounds (e.g. impurities, products and reagents). It is generally believed that soluble polymeric supports, neglecting their advantages (e.g. homogeneous reaction conditions, standard analytical techniques and high-loading capacities), are difficult to separate from the reaction mixture. However, several techniques for the separation of soluble polymers from low molecular weight compounds were evaluated and extensively reviewed, recently (Tab. 7.1) [4, 15–17]. There are various methods that separate macromolecules by size (preparative SEC, dialysis and membrane filtration) [18–20]. Most of them are suitable for automation, yet little effort has been directed to multiparallel automation in this area, compared with the progress in solid-phase synthesis. Furthermore, other separation techniques, such as precipitation, phase separation and filtration through a silica cartridge were reported [15]. However, the application of these techniques to solution-phase synthesis depends on the physicochemical properties of each individual polymer. In addition, these techniques are more sensitive to the change of functionalities on the polymeric support during the synthesis. Therefore the use of soluble polymeric supports in organic synthesis and catalysis requires the careful selection of an appropriate separation technique.

For efficient and fast separations by size (hydrodynamic volume) homogeneous polymeric supports should have medium molecular weights (5000–50 000 g mol<sup>-1</sup>) and narrow molecular weight distributions (<1.5). In addition, macromolecules with a persistent three dimensional structure (e.g. highly branched polymers) are more suitable than a linear polymer structures. Apart from the polymer shape (e.g. hydrodynamic volume), size-based purification is general since it does not rely on other physicochemical differences between support-bound compounds, reagents or catalysts (e.g. polarity). In the following, three of the most general separation techniques for dendritic polymers are described briefly.

Size exclusion chromatography (SEC), also known as gel permeation chromatography (GPC), was used for the separation and fractionation of macromolecules on an analytical and preparative scale [17]. The separation occurs predominantly by the hydrodynamic volume of the macromolecules in solution, however, in some cases the polarity of the molecules can also influence the retention times. Like HPLC, the SEC technique is generally very reproducible with regard to its elution times (typically <1 h) and hence can be used for automated synthesis. But because the cost for an automated SEC system is high, it must be considered as a serial separation technique. In addition, larger scale separations >100 mg, usually require repetitive injection of small aliquots.

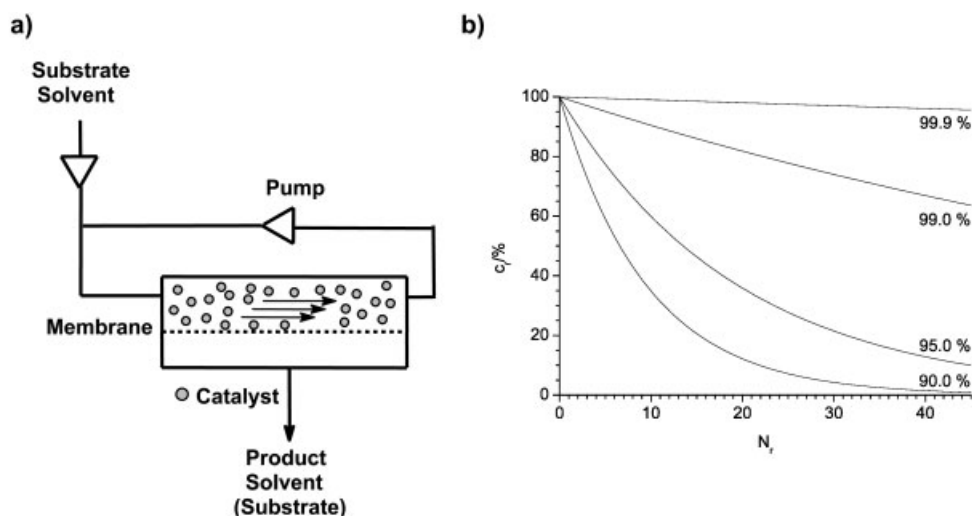
Dialysis, on the other hand, is a fairly well-established technique for the purification of soluble polymers and is also suitable for larger quantities [20]. Original-

**Tab. 7.1** Separation techniques for homogeneous polymeric supports.

<i>Parameter</i>	<i>Dialysis</i>	<i>Ultrafiltration</i>	<i>SEC</i>	<i>Precipitation/Filtration</i>	<i>Liquid Phase-Separation</i>
Separation by MW of polymer	Hydrodynamic volume > 1000 g mol <sup>-1</sup>	Hydrodynamic volume > 1000 g mol <sup>-1</sup>	Hydrodynamic volume –	Solubility > 3000 g mol <sup>-1</sup>	Solubility –
Typical sample volume	10 mL–1 L	1–100 mL	< 1 mL	1–100 mL	10 mL–1 L
Commercially available	Yes	Yes	Yes	–	–
Suitable for automation	Yes	Yes	Yes	No	Yes
Suitable for high-throughput	No	Yes	Yes	No	Yes
Limitations	Unsuitable for final cleavage step	–	–	Problematic in multistep syntheses	Different solubilities required



ly, dialysis was mostly used for the separation of biopolymers in aqueous media, because the membrane materials were incompatible with organic solvents. But nowadays, improved membrane materials permit dialysis to be performed in nearly any organic solvent. Typical molecular weight cut-offs (MWCO) are: 1000, 5000 and 20 000 g mol<sup>-1</sup> (based on linear polymer standards in water). In organic solvents, however, the MWCO can slightly vary because of the different swellability of the membrane materials in different solvents. Recently, multiparallel dialysis was introduced as a separation technique for dendritic polymers on a multi-gram scale [21]. A fundamental advantage of this technique is the separation of large quantities, which can be as large as 10 mmol of substrate in multiparallel approaches. Hence this method is attractive for the preparation of smaller libraries (10–100 compounds) on a relatively large scale. The limitations of this technique are the relatively long separation times (typically 12–36 h) and in some cases incompatibility with membrane materials e.g. separation of highly reactive or ionic compounds. Also, dialysis is unsuitable for the final cleavage step of a multi-step polymer supported synthesis because the cleaved low molecular weight compound would be diluted into a large amount of solvent when diffusing through the membrane. In this case, ultrafiltration (UF) can be used advantageously. UF is a very efficient and frequently used membrane separation technique for soluble macromolecules [18]. Like dialysis, it can be employed for the separation of low molecular weight compounds from soluble polymeric supports providing much shorter separation times (ca. 1–3 h) on the application of pressure (3–30 bar). For efficient separations, it is necessary to use stirred UF-cells in order to avoid clogging of the membrane. Membrane materials (organic and inor-



**Fig. 7.2** a) Schematic representation of a continuous flow membrane reactor and b) theoretical relative concentrations of (dendritic)

catalysts ( $C_r$ ) with different retention factors versus the Number of runs ( $N_r$ ) in a continuous process.

ganic) with high chemical stability and compatibility to most organic solvents [22] and chemically stable UF-units for pressures up to 6 bar are commercially available. For higher pressures and continuous flow membrane reactors it is necessary to use HPLC-type fluidics to avoid gas bubbles in the system (Fig. 7.2a). Because the automated systems are expensive, UF must still be considered as a serial separation technique.

Ultrafiltration has been used for the separation of dendritic polymeric supports in multi-step syntheses as well as for the separation of dendritic polymer-supported reagents [4, 21]. However, this technique has most frequently been employed for the separation of polymer-supported catalysts (see Section 7.5) [18]. In the latter case, continuous flow UF-systems, so-called membrane reactors, were used for homogeneous catalysis, with catalysts complexed to dendritic ligands [23–27]. A critical issue for dendritic catalysts is the retention of the catalyst by the membrane (Fig. 7.2b, see also Section 7.5).

### 7.2.3

#### Dendritic Hybrid Polymers as High-Loading Solid-phase Supports

A general disadvantage of solid-phase supports for preparative organic synthesis is the low loading capacity of the commonly used resins [2, 3]. Often, large quantities of resin are required in order to obtain substantial amounts of products ( $>100 \mu\text{mol}$ ). Only in very few cases high-loading Merrifield resins ( $4 \text{ mmol g}^{-1}$ ) were used successfully and the scale-up of reactions was possible directly on the resin [28]. The alternative approach, the copolymerization of monomers which carry the desired functionality, was often tested in the “early days” of polymer-supported synthesis and only recently became more attractive [29]. This strategy can be advantageous since it generates a tailor-made functional polymer. However, this approach is limited by the number of comonomers suitable for radical suspension polymerization and the amount of comonomer incorporation, leading to loading capacities typically below  $3 \text{ mmol g}^{-1}$ . A general problem of polystyrene-based solid supports is the poor swelling in highly polar and protic solvents and hence the slow diffusion of reagents into the beads. In many cases, modification of the unpolar surface with PEG chains becomes necessary to enhance the solution-phase character of the reaction, especially for reactions in protic solvents and water. A disadvantage arising from the grafting of monofunctional PEG chains onto the PS microbead is certainly the poor loading capacity obtained for the PEGylated resins ( $\sim 0.2\text{--}0.6 \text{ mmol g}^{-1}$ ) [2].

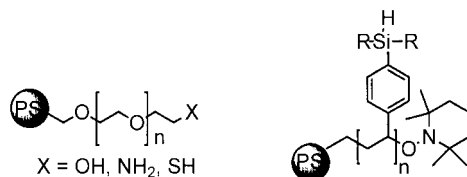


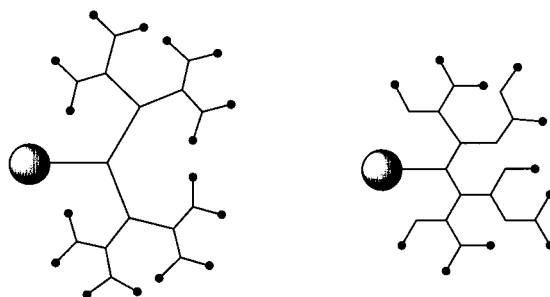
Fig. 7.3 Monofunctional (e.g. Tentagel) versus polyfunctional (e.g. ‘Rastasilane’) linear hybrid polymers.

Several approaches have been made to overcome this drawback, for example by grafting polyfunctional linear polymer chains onto the polystyrene resin (Fig. 7.3). A recent approach towards high-loading solid-phase supports uses cross metathesis between vinyl polystyrene beads and norbornene derivatives [30]. This resin shows high loading capacities (up to  $3.0 \text{ mmol g}^{-1}$ ), but the degree of swelling is lower compared with conventional resins. A second example for linear graft-polymers is based on a high-loading silyl-functionalized PS-hybrid resin, so-called 'Rasta Silane' [31]. Rasta resins are characterized by high loading levels between  $1.6$  and  $3.8 \text{ mmol g}^{-1}$  with regard to the silicon linker. An extreme of high-loading solid-phase supports was recently reported for cross-linked polyethylenimine ( $15 \text{ mmol g}^{-1}$ ) [32]. But it is not yet clear whether the loading capacity and the limited chemical stability of these polyamines will be suitable for broad application in organic synthesis other than e.g. as scavengers.

Another approach to high-loading resins are polystyrene-dendrimer hybrids (Fig. 7.4) [6]. The dendritic spacer molecules provide a rapid and efficient method of increasing the loading capacity and improving the swelling properties of the beads significantly. Again the coupling of highly-branched polymers onto the polystyrene resins would offer much easier access to dendritic hybrid materials compared with the tedious stepwise synthesis of perfectly dendronized solid-phase materials. Several applications of these dendritic high-loading hybrid materials in organic synthesis and catalysis were described (see Sections 7.3–7.5).

For the synthesis of perfectly dendronized solid-phase polymers (Fig. 7.4) various dendritic structures were prepared based on amide connections [6]. For example, the naturally occurring amino acid lysine was used as a building block in creating a dendritic scaffold [33]. The synthesis of symmetrical tri-branching dendrimers on aminomethyl polystyrene macrobeads was also described in literature [34]. Recently, aryl ether dendrimers were prepared on hydroxymethyl polystyrene using a Mitsunobu reaction with 3,5-bis(acetoxymethyl)phenol [35].

Finally, first attempts were made to extend the concept of soluble hyperbranched polymers to dendronized solid-phase materials. Recently, the first dendronized solid phase, accessible in only one reaction step was reported (Fig. 7.4) [36]. The coupling of hyperbranched polyglycerol to Merrifield resin yields a new type of high-loading solid-phase hybrid material with loading capacities of ca.  $3 \text{ mmol g}^{-1}$  and good swelling properties even in protic solvents (see also Section 3.4).



**Fig. 7.4** Perfectly dendronized (left) and hyperbranched (right) hybrid polymers.

In general, dendronized solid-phase supports show loading capacities in the range of 1–5 mmol g<sup>-1</sup> which could theoretically be as high as ~ 7 mmol g<sup>-1</sup>. However, these beads are then very sensitive to osmotic shock, caused by the large expansion of the network structure. It is noteworthy that the loading per gram of the dendritic solid-phase resin does not increase substantially with each generation because of the mass of the attached linker. However, the loading per bead increases exponentially from one generation to the next. In some cases [34], a single dendronized PS-macro bead provides the amount of compound necessary for <sup>1</sup>H NMR(!) in a one-bead-one-compound screening approach. Therefore these hybrid materials are useful for combinatorial split and mix synthesis. In addition, when using polar dendrons the swelling ability in polar solvents like MeOH, DMSO, and water in some cases increases significantly.

### 7.3

#### Dendritic Polymer-supported Organic Synthesis

##### 7.3.1

##### Perfect Dendrimers as Supports in Organic Synthesis

In 1996, Kim and coworkers reported for the first time on the use of a polyamidoamine (PAMAM) dendrimer [G1] as a soluble support for organic synthesis (Fig. 7.5) [37]. Advantages of PAMAM are its commercial availability and its high symmetry, which provides uniform site accessibility (in lower generations) and facilitates NMR interpretation. By attaching 4-hydroxymethylbenzoic acid (HMB) to

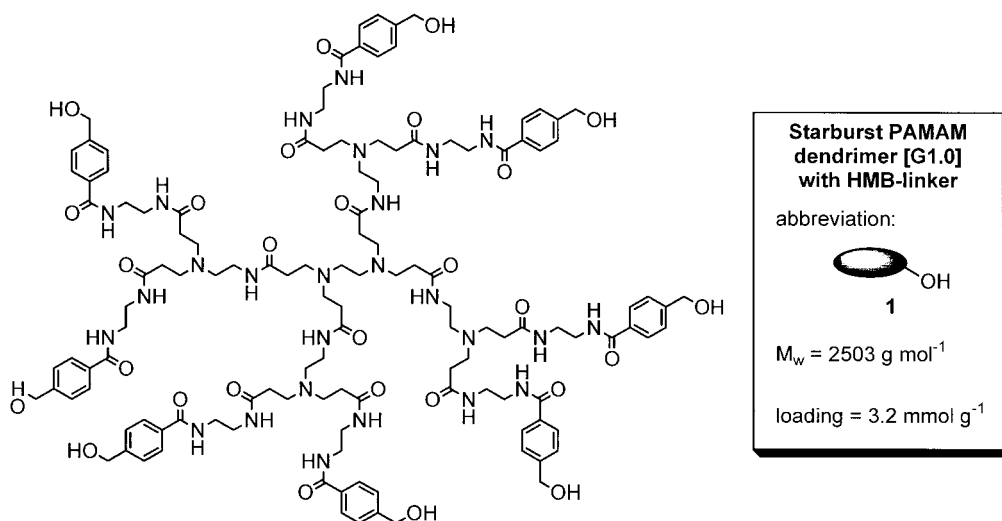


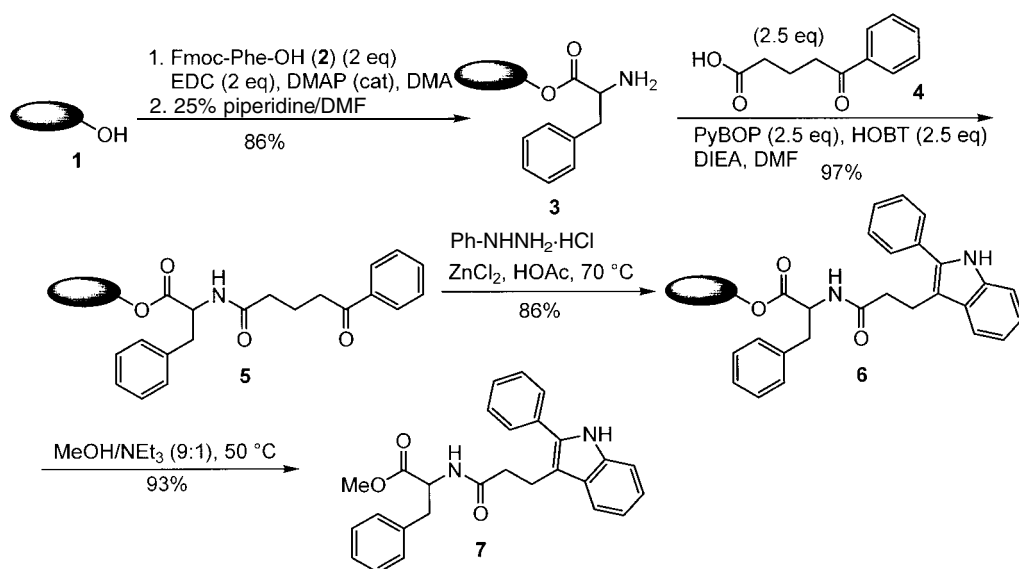
Fig. 7.5 PAMAM-Dendrimer with HMB-linker.

the amine groups of the dendrimer periphery, the support was equipped with a base-labile linker unit to obtain the soluble oligobenzylalcohol (**1**).

This dendritic support (**1**) was used to generate a library of indole derivatives with three centers of diversity following the Fischer protocol and the split and mix strategy. One example of this sequence is outlined in Scheme 7.1.

The first step was an immobilization of the Fmoc-protected amino acid (**2**) on the dendritic support (**1**). After deprotection, the amine functionality of (**3**) was acylated by benzoylbutyric acid (**4**) using a conventional coupling protocol. Cyclization to the indol could be performed with phenylhydrazine hydrochloride in glacial acetic acid containing 0.5 M  $\text{ZnCl}_2$  at higher temperatures. The release of the final indol compound was achieved with  $\text{MeOH}/\text{NEt}_3$  (9:1), yielding the corresponding methyl esters (**7**) and regenerated support (**1**). All intermediates were analysed by  $^1\text{H}$  NMR and electrospray mass spectrometry. Workup was performed within 15 minutes either *via* SEC, or by removal of solvent followed by treatment with MeCN and filtration of the insoluble dendrimer. SEC could also be used for purification during library generation using the split and mix procedure. All supported compounds were eluted as a single band because of their similar sizes. Products of excellent purities (84–99%, HPLC,  $^1\text{H}$  NMR) were received in yields higher than 90%. The reuse of the recovered support was not investigated.

Van Koten and coworkers functionalized  $\text{Me}_2\text{SiCl}$  terminated generation 0 and 1 carbosilane dendrimers with 4-(hydroxymethyl)phenyl groups (Fig. 7.6) [38]. Since this backbone is stable against many organometallic compounds, these linkers could be introduced by means of organolithium or Grignard reagents to give the dendritic support (**8**).



**Scheme 7.1** Fischer indol synthesis on a PAMAM dendrimer support.

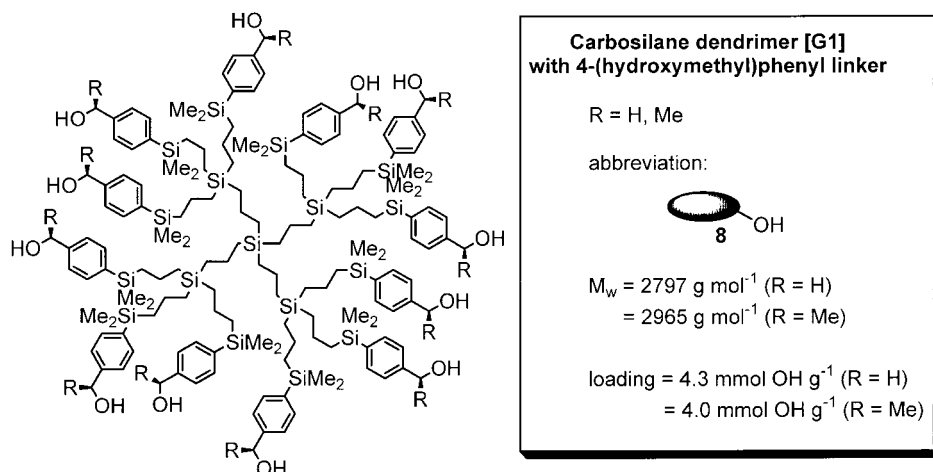
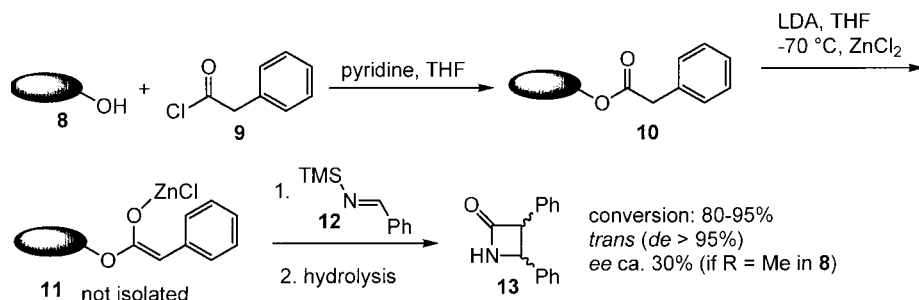


Fig. 7.6 Carbosilane dendrimer with 4-(hydroxymethyl)phenyl linker.

To demonstrate the applicability of this support in organic synthesis, the authors immobilized a (*p*-bromophenyl)acetic acid which was then transformed into the corresponding biaryl by means of the Suzuki cross-coupling reaction with *p*-methylphenylboronic acid. Quantitative NaOH cleavage of the ester linkage yielded the released biaryl, of which no purity was mentioned.

The different carbosilane dendrimer supports (generation 0, 1; R = H, Me) were then used for the synthesis of the  $\beta$ -lactam (**13**). As shown in Scheme 7.2, the first step was again an immobilization of a carboxylic acid *via* ester bond formation. Treatment with LDA and  $\text{ZnCl}_2$  yielded *in situ* the corresponding zinc ester enolate (**11**) which reacts with *N*-(trimethylsilyl)phenylimine (**12**) to form the final four membered lactam ring (**13**). The last reaction step includes several intermediates. The last one is a supported  $\beta$ -amino ester which undergoes spontaneous



Scheme 7.2  $\beta$ -Lactam formation on a dendritic carbosilane support.

ring closure under concomitant split off from the dendritic support (cyclative cleavage [15]).

Lactams were obtained in 80–95% conversion with high *trans*-selectivity (*de* > 95%) but only moderate enantioselectivity (*ee* ca. 30%). The stereoinduction results from the relatively remote stereocentres located at the linker units. For support recovery the authors performed nanofiltration experiments and it was found that the recovered dendrimers could be easily reused as substrate carriers.

To synthesize diverse analog products in a combinatorial way, the authors provided the support with two different acid moieties which then were transformed with a 1:1 mixture of two different imine derivatives to receive four different  $\beta$ -lactams in equal amounts (overall yields 85%).

A dendrimer containing a dye as core was synthesized by Zhang and coworkers (Fig. 7.7) [39, 40]. The *boc*-protected amine endgroups of this [G1] dendrimer were equipped with a 4-(hydroxymethyl)phenoxy acetic acid (HMPA) linker performing several reaction steps to obtain the red colored dendritic support (**14**).

Two substrates for Suzuki couplings were immobilized exposing the support (**14**) to *o*- or *p*-iodobenzoyl chloride. After purification on a Sephadex LH-20 SEC

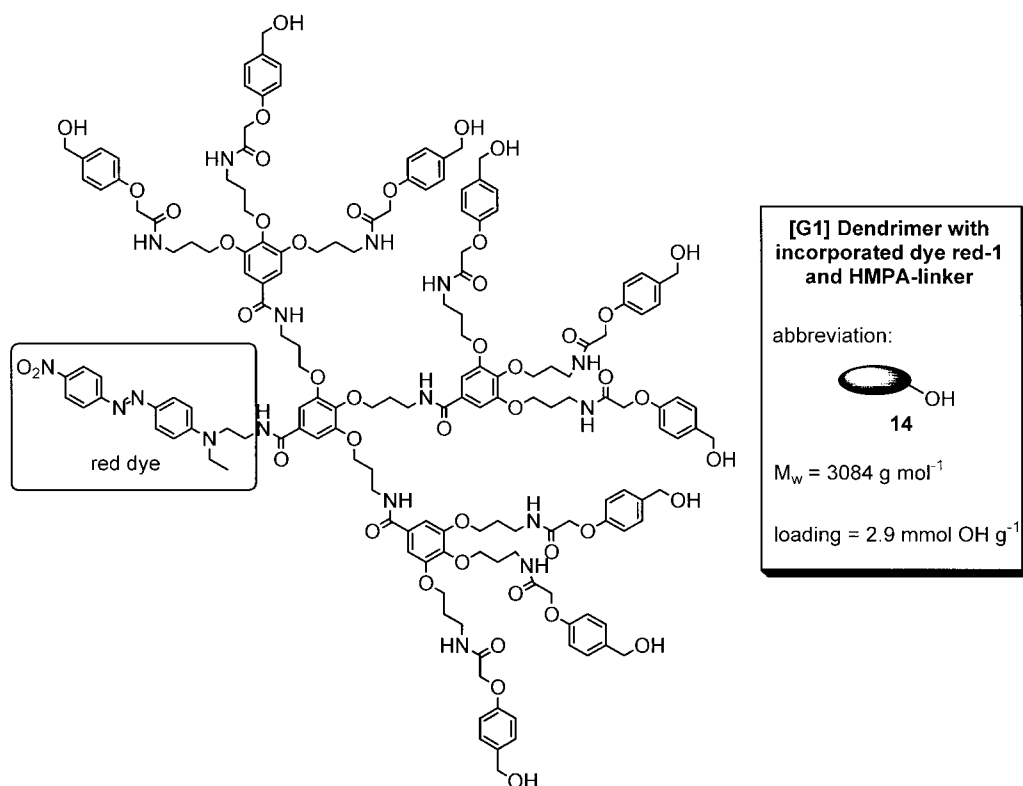


Fig. 7.7 Dendrimer with incorporated dye and HMPA-linker.

column Suzuki reactions with six commercial available boronic acids were performed. Work-up contained extraction with AcOEt and washing with water to eliminate inorganic salts. Purification was performed *via* SEC and simplified by the color indication of the dendritic support and took less than 30 min (for each compound). All products were characterized using conventional analytical methods (e.g. TLC). After ester cleavage the reaction mixture was worked up *via* a precipitation/filtration/extraction protocol to yield the biaryl products as white solids.

### 7.3.2

#### Hyperbranched Polymeric Supports in Organic Synthesis

Haag and coworkers recently introduced hyperbranched polyglycerol (PG) (**15**) as a soluble high-loading polymeric support (Fig. 7.8) [21]. This aliphatic polyetherpolyol could be obtained in a one step ring-opening polymerization of glycidol commencing from multifunctional starter molecules [41, 42].

The PG-support has a high loading capacity ( $13.5 \text{ mmol OH g}^{-1}$ ) and contains two kinds of functionalities: linear monohydroxy and terminal dihydroxy groups, which can be modified selectively and serve as linkers for the immobilization of diverse organic compounds [4, 21]. It was possible, for example, to attach carbonyl compounds directly to polyglycerol *via* acetal formation and split them off again after one or several modifications (Scheme 7.3). Polyglycerol was found to be soluble in many polar organic solvents and its aliphatic polyether skeleton is highly stable against a wide range of reaction conditions. Simple separation techniques like dialysis, ultrafiltration, precipitation, and liquid-liquid extraction were investigated for this support [4, 15].

Transformations on this support included the synthesis of aminoketones from supported chloroketones as well as biarylaldehydes after Suzuki cross-coupling reactions of supported bromo-benzaldehydes [21]. This dendritic polyglycerol was

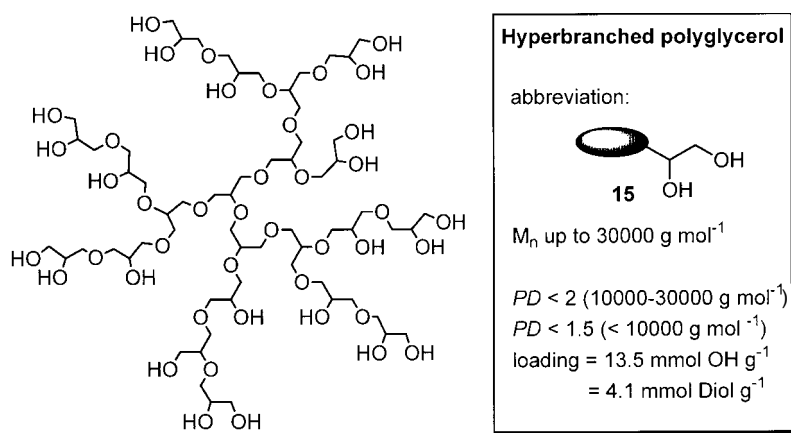
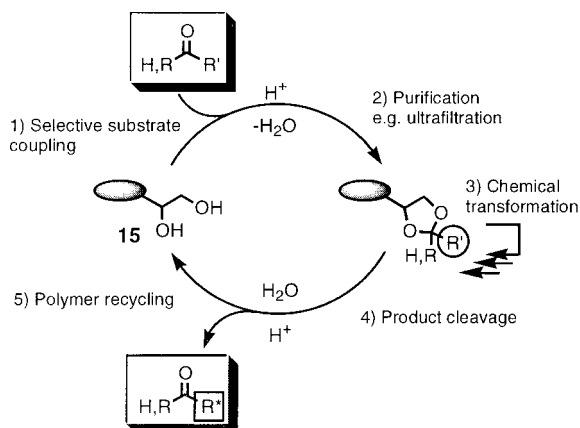


Fig. 7.8 Hyperbranched polyglycerol.



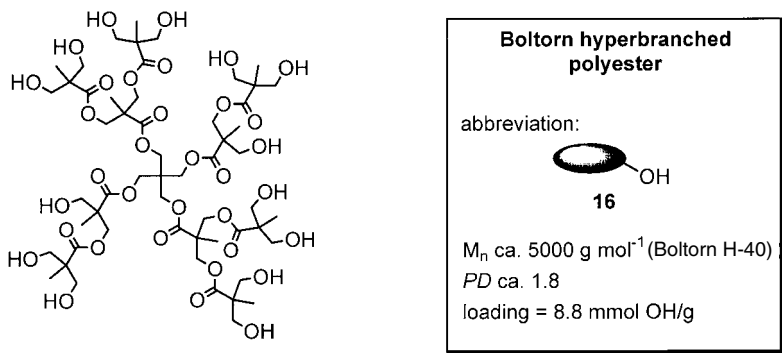


**Scheme 7.3** Immobilization, modification, and release of a carbonyl compound employing a polyglycerol support.

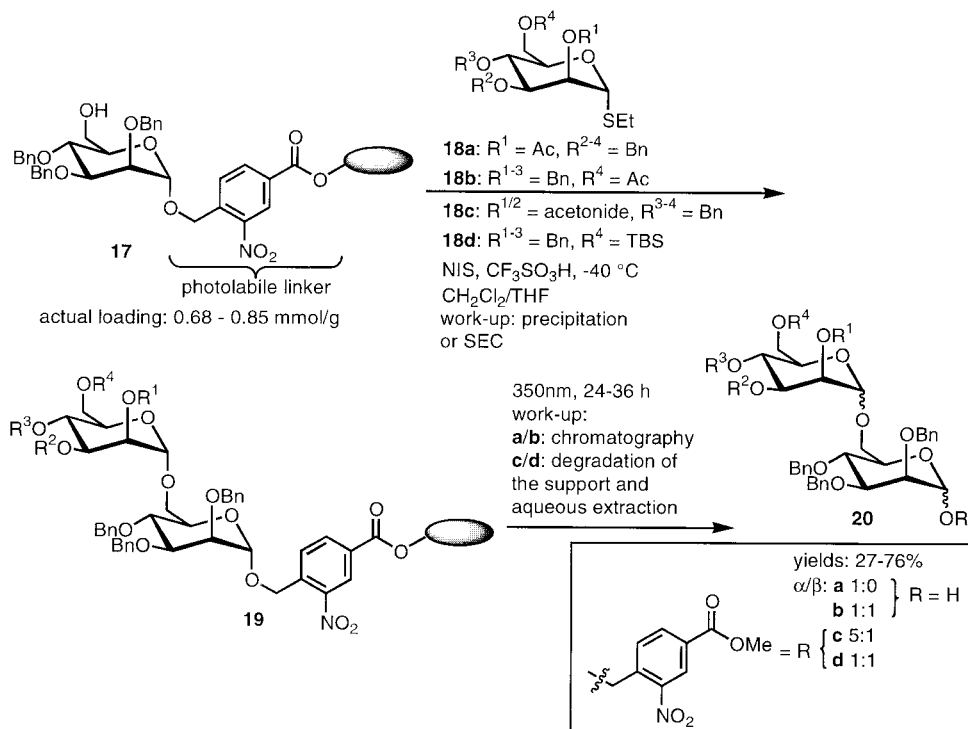
also used as support for reagents (see section 7.4). Multi-step syntheses of drug candidates were also performed on the polyglycerol support [43].

Parquette *et al.* reported on a disaccharide synthesis on a hyperbranched polyester support (Boltorn hyperbranched polymer) (**16**) (Fig. 7.9) [44]. This polymer was obtained in a one-step synthesis and offers low cost, high-loading capacities (8.8 mmol OH-groups g<sup>-1</sup>), and the intermediates were soluble in most aprotic solvents.

The authors designed a photolabile *o*-nitrobenzylalcohol linker group to which a mannosyl acceptor is coupled. Overall, seven reaction steps were performed before immobilization on the polymeric support. The latter was realized *via* EDCI-coupling. A partially loaded (40%) Boltorn polymer was generated to provide an intermediate substrate loading on the support (Scheme 7.4). The remaining OH-functionalities were protected by means of acetyl chloride. Higher loading levels were not investigated. After deprotection of the 6-hydroxy group with HF/pyridine



**Fig. 7.9** Boltorn hyperbranched polymer.



**Scheme 7.4** Disaccharide synthesis using a hyperbranched polymer (Boltorn polymer) as a soluble support.

and adjacent aqueous extraction work-up the actual loading of the immobilized substrate (**17**) was determined by  $^1\text{H}$  NMR to be 0.68–0.85 mmol  $\text{g}^{-1}$  because of the significant increase in molecular weight upon the loading step. Glycosylation reactions were realized with four different thioglycoside donors and work-up was carried out *via* precipitation from methanol or SEC. Generally speaking, membrane-based separation techniques are complicated by the relative broad molecular weight distribution ( $>1.8$ ) of these dendritic polyesters.

Two different kinds of cleavage protocols were investigated. The first was a light induced photo-release reaction followed by a chromatographic work-up. Also, reaction monitoring was performed by MALDI/TOF/MS since the LASER cleaves the disaccharide from the support. The second is a hydrolytic cleavage reaction under degradation of the polymeric support and subsequent aqueous extraction to yield the pure product. The disaccharides (**20**) were obtained in yields of 27–76%.

Both strategies are tainted with disadvantages: the first contains a conventional chromatographical purification and therefore does not profit from the actual benefits of polymer supported synthesis; the second makes use of aqueous extraction, which is only possible after degradation of the polymeric support. The latter step

is caused by the instability of the polymer backbone against nucleophiles and thus, this support has only a narrow spectrum of applications.

### 7.3.3

#### Other Soluble Multivalent Supports in Organic Synthesis

Cozzi and coworkers reported on the generation of soluble dendronized PEG supports with an expanded functional group capacity by combining the basic principles of dendrimer chemistry with that of PEG polymers [45]. They synthesized five different tetravalent PEG derivatives (**21a–e**) each of them containing interesting linking functionalities (Fig. 7.10).

To demonstrate the feasibility of organic synthesis using this support, the authors immobilized a *N*-Boc protected glycine (**22**) on the support (Scheme 7.5). After deprotection imine formation readily occurs with an excess of benzaldehyde. The product was then subjected to a Staudinger reaction with phenoxyacetylchloride to yield the polymer supported  $\beta$ -lactam (**26**) which could be released to give the  $\beta$ -lactam (**27**) with TEA in methanol.

The tetraol (**21c**) could be recovered and recycled and throughout the reaction sequence the modified polymer support retained its usual solubility/insolubility properties.

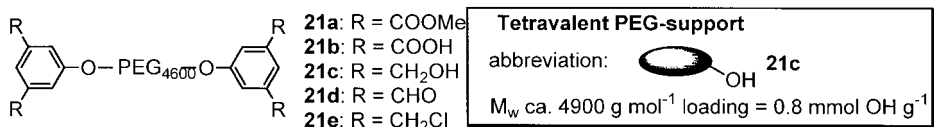
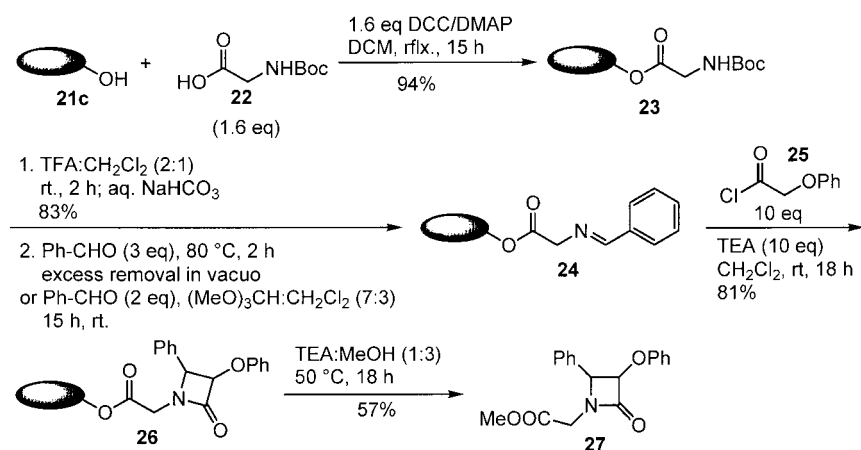


Fig. 7.10 Tetravalent PEG-support.



Scheme 7.5  $\beta$ -Lactam formation on a tetravalent PEG support.

It should be noted, that this strategy provides only a slight improvement over the linear PEG(4600)-supports with a loading capacity of  $0.4 \text{ mol g}^{-1}$ . Especially the difference between a [G0] and a [G1] (loading ca.  $1 \text{ mmol g}^{-1}$ ) dendron does not justify the synthetic effort.

Kim and coworkers reported on the generation of a 48-fold library of di- and tri-substituted guanidines using a soluble, tetravalent support (**27**) [46]. These PEG-based oligomers are soluble in a wide range of solvents and show good chemical stabilities as well as good  $^1\text{H}$  NMR properties. Different supports with molecular weights of 2–26 kDa and a varying number of PEG-arms (4–32) were investigated. The smaller species (2.5–5 kDa) were found to offer advantages in characterizability, while maintaining sufficient size to be readily separated from small molecules. For this study the four-armed PEG oligomer Sunbright PTE-2000 was employed after conversion to the tetraamine and coupling of four Rink [47] linkers to give the support (**27**) with an average molecular weight of about 3.2 kDa (Fig. 7.11). Automated parallel SEC (four columns) was used as a relatively fast work-up technique for small scales ( $< 100 \text{ mg}$ ) and support recovery was around 95%.

In the first step of the synthesis an excess of Fmoc-protected  $\omega$ -amino acid (**28**) was coupled to the support (**27**) via DIC-coupling (Scheme 7.6). After deprotection the immobilized substrate was exposed to an excess of an isothiocyanate (**30**) to yield the corresponding thiourea (**31**). Guanidine formation could either be performed in a single step using an excess of a primary or secondary amine (**32**) and  $\text{HgCl}_2$  or in two steps via the methyl isothiurea. TFA-cleavage yielded the final di- or trisubstituted guanidines (**34**) as TFA-salts (yields: 11–77%, purities up to 95%), which were lyophilized from MeCN/ $\text{H}_2\text{O}$ . To generate a library, two different or nine  $\omega$ -amino acids (in latter case the sequence starts with the thiourea formation step), four isothiocyanates, and four amines were employed. A disadvantage of this approach is the significant polymerization of the support during the cleavage reaction because of cross-linking of the Rink linkers.

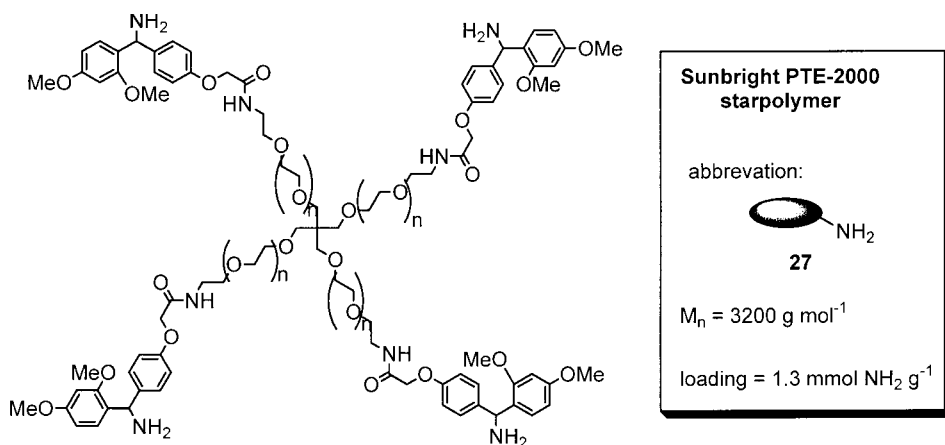
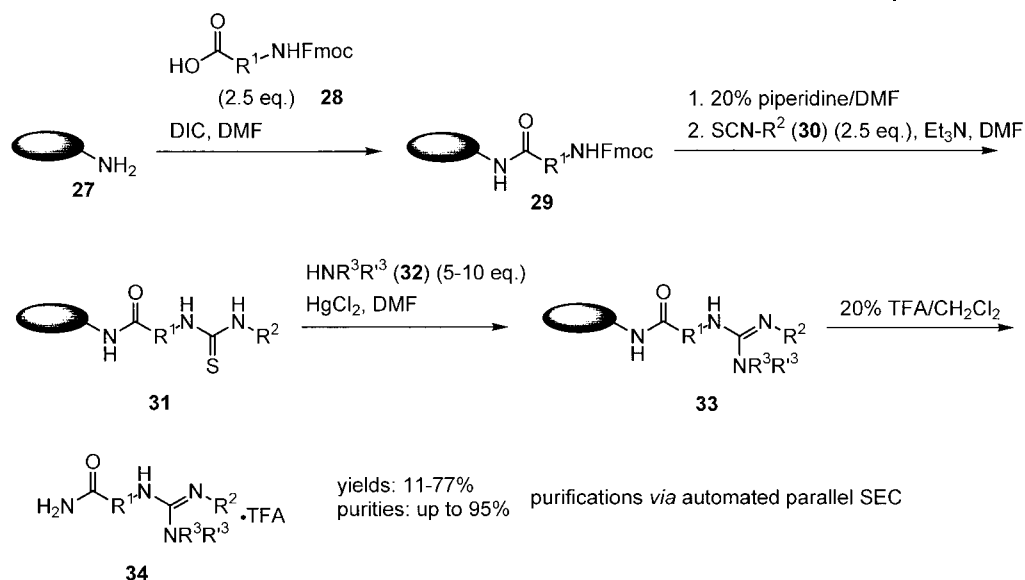


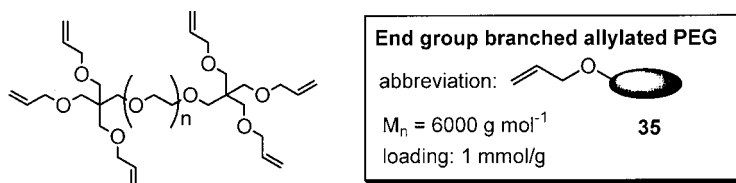
Fig. 7.11 Sunbright starpolymer.



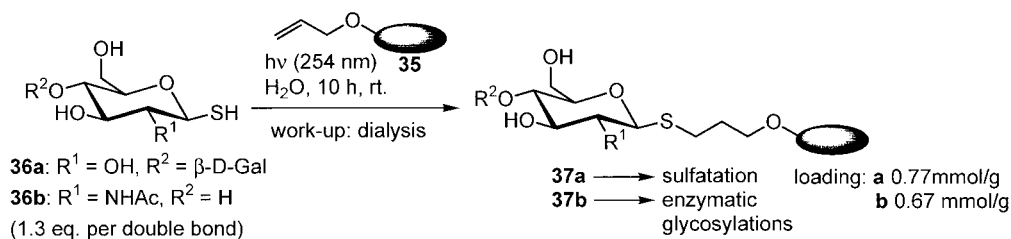
**Scheme 7.6** Synthesis of di- and trisubstituted guanidines on a modified four-arm PEG-support.

Enzymatic solid-phase synthesis raises several problems, such as accessibility to the interior of the solid matrix of the enzyme, or for chemo-enzymatic synthesis, compatibility of the support with both aqueous and organic solvents [48]. In this connection, Le Narvor and coworkers reported on an end-group branched PEG-6000 derivative (**35**) as a soluble support for oligosaccharide enzymatic synthesis (Fig. 7.12) [49]. Its loading capacity amounts to  $1 \text{ mmol g}^{-1}$  and in this respect has no advantages compared with conventional solid-phase supports. The support (**35**) was obtained in three steps in 80% yield and >95% conversion of the hydroxy-groups emanating from pentaerythritol. Purification was performed via dialysis. The allylic linker functionalities allowed for thiol-substrate coupling via smooth, high yielding, radical addition. The loaded support was stable against a wide range of reaction conditions and product cleavage could be induced by thiophilic reagents or electrochemical protocols.

The authors immobilized 1-thiolactose (**36a**) and 2-acetamido-2-deoxy-1-thio- $\beta$ -D-glucopyranoside (**36b**) on the hexavalent support by means of irradiation



**Fig. 7.12** End group branched allylated PEG.



**Scheme 7.7** Immobilization of a thiol-group containing sugar substrate on a hexavalent PEG-derivative for sulfatation and enzymatic glycosylation reactions.

(Scheme 7.7). Workup was performed *via* dialysis. The loading was determined by mercury(II) trifluoroacetate cleavage or electrohydrolysis: the recovery of (**36a**) was  $0.77 \text{ mmol g}^{-1}$  (support) and of (**36b**)  $0.67 \text{ mmol g}^{-1}$  (support).

The immobilized lactose (**37a**) was employed in sulfatation reactions using  $\text{SO}_3\text{-NEt}_3$  complex. After mercury(II) trifluoroacetate cleavage, a 2.7:1 mixture of 3'-sulfated lactose and lactose was isolated and separated using anionic exchange resin.

(**37b**) was exposed to enzymatic glycosylations to obtain *N*-acetyllactosamine (230 mg per gram of support). Reaction monitoring was performed using  $^1\text{H}$  NMR analysis or TLC after chemical cleavage of an aliquot. The reaction could be driven to completion performing a dialysis step in between and subsequent addition of fresh enzymes. The authors also synthesized the trisaccharide Lewis<sup>x</sup> on this support.

#### 7.3.4

#### Dendronized Solid-phase Supports for Organic Synthesis

In the late 1980s Tam used a dendronized solid-phase resin to generate a multiple antigen peptide system (MAP) with an octa-branching core matrix consisting of a heptalysine [50]. The branched peptide oligolysine was removed from the cross-linked polystyrene resin support *via* HF- or trifluoromethanesulfonic acid cleavage to receive the MAP in 85–93% yield which required further work-up steps including extraction and dialysis.

In 1997, Bradley and coworkers reported on the synthesis of a Tentagel-based PAMAM-dendronized resin which shows good water compatibility [51]. They built up generation 4.0 (loading:  $2.8 \text{ mmol g}^{-1}$ ; 9.6 nmol per bead) from generation 3.0 dendrimers (loading:  $2.3 \text{ mmol g}^{-1}$ ; 5–6 nmol per bead), in the course of which the loading per bead doubled, whereas the loading per gram only increased by  $0.5 \text{ mmol g}^{-1}$  because of the concomitant mass increase. The authors employed the generation 3.0 solid-phase supported dendrimer (**38**) for the synthesis of a dipeptide using a HMPB-linker [52] and Fmoc chemistry (Fig. 7.13).

This dual linker approach allowed selective cleavage of the peptide from the dendrimer using 1% TFA/ $\text{CH}_2\text{Cl}_2$  without cleaving the dendrimer from the resin. Proceeding from the Tentagel resin the final product was obtained in 44% yield

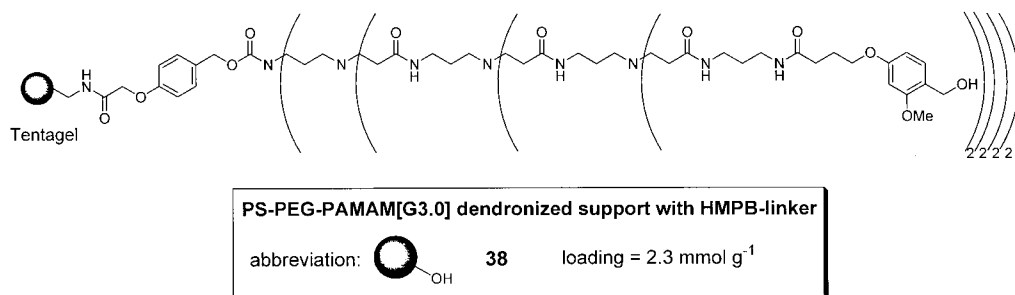


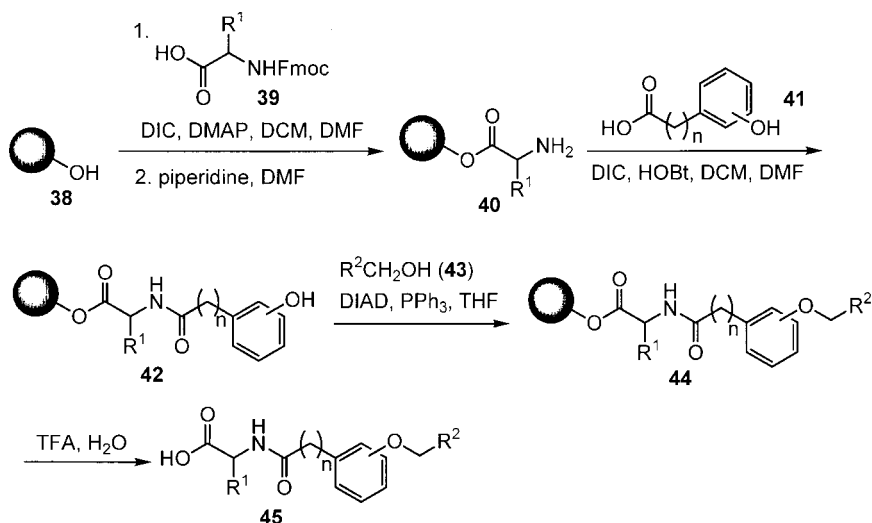
Fig. 7.13 PS-PEG-PAMAM dendronized support with HMPB-linker.

and >95% purity (HPLC) after 13 reaction steps. For synthetic applications the authors recommend the usage of the generation 3.0 resins because of the insignificant higher loading capacity of the generation 4.0 resins and the reduced likelihood of interstrand side reactions as well as reduced steric encumbrance.

In a further work the authors reported the preparation of high-loading PS-PEG-PAMAM resin beads such that a single bead gives sufficient material for NMR characterization, mass spectrometry, and repeated conventional HPLC analysis to make single bead/single compound combinatorial synthesis possible [53]. These high-loading beads (32 nmol per bead) were observed to be exceptionally robust, compatible with a wide range of solvents, stable to prolonged storage, and easy to handle for both synthesis and single-bead manipulations. A tripeptide was synthesized on the support and product analysis was made with the amount of material of only one bead. The cleavage reaction was carried out within a NMR-tube employing 1% F<sub>3</sub>CCOOD in CDCl<sub>3</sub> giving a high quality <sup>1</sup>H NMR spectrum. Afterwards, 25% of the NMR sample was analyzed by reversed-phase HPLC and ESMS. The amount of beads per gram was approximately 34 500, which was acceptable for split and mix library applications. After this aptitude test a library of 20 hexapeptides was generated and analyzed after single-bead cleavage.

Analogous PS-PEG-PAMAM [G3] resins with loading capacities of 4.0 nmol per bead (commencing from 160 μm TentaGel beads) were used in Mitsunobu reactions to generate a library of aryl ethers (**45**) (Scheme 7.8) [54]. In the first step, a Fmoc-protected amino acid (**39**) was coupled to the HMPB-linker of the hybrid support. After deprotection, a hydroxyphenyl carboxylic acid (**41**) was immobilized *via* amide formation. Both initial coupling steps were performed under standard coupling conditions. A conventional Mitsunobu step yielded a polymer supported *N*-(alkoxyphenyl)alkanoylated amino acid (**44**) which could be released by means of TFA cleavage to yield (**45**).

A number of different reaction conditions were investigated for the Mitsunobu reaction and DIAD/PPh<sub>3</sub> proved to be the most efficient combination of reagents. The dendronized support was then compared with the conventional TentaGel resin keeping the scaffold on the resin constant (glycine and 4-hydroxyphenylacetic acid) and employing four different alcohols. Much better yields were obtained



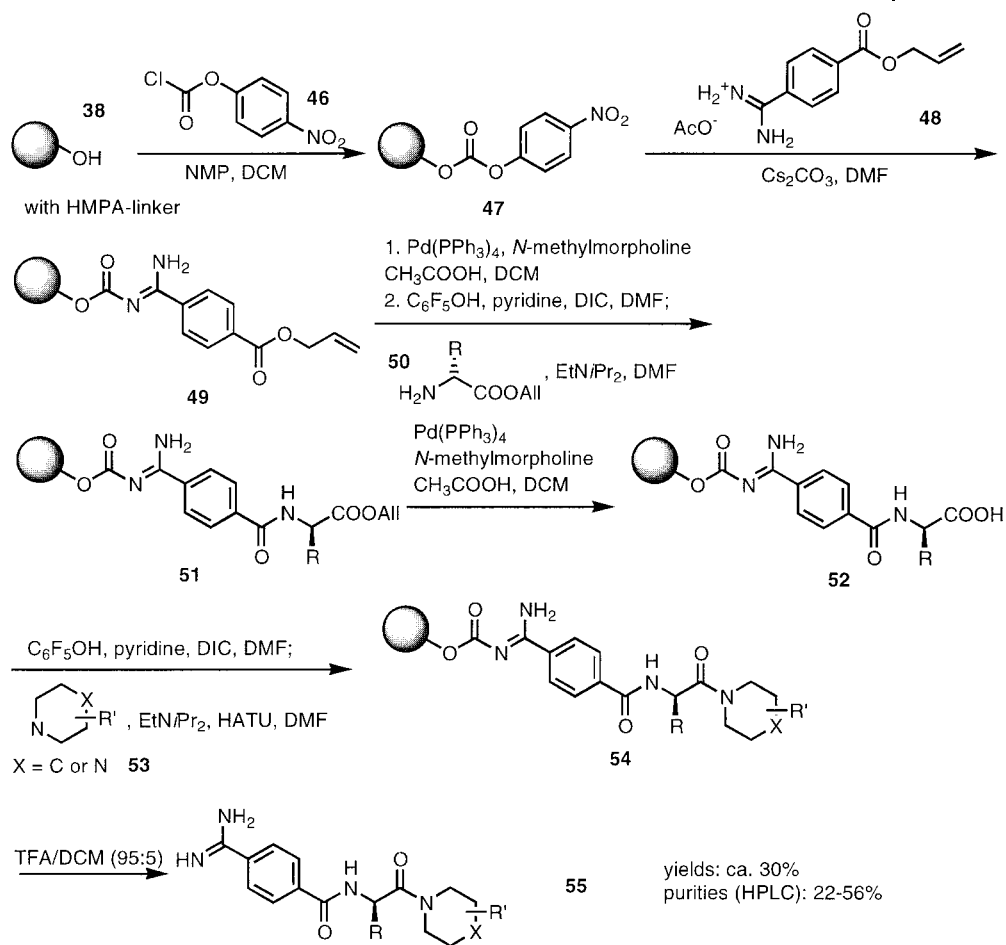
**Scheme 7.8** Generating a library of aryl ethers on a Tentagel-PAMAM hybrid support.

with the dendrimer resin (67–100%) as compared with TentaGel (0–91%) although the purity was high in all cases. A small library of ary ethers was then synthesized in a semi-automated fashion on an Argonaut QUEST 210 by varying the hydroxyphenyl acid and the alcohol. Good yields (62–88%, NMR *via*  $d_5$ -DMSO quantification) and purities (67–100%, HPLC) were obtained for the tested substrate combinations. Additionally, the products were analyzed by single-bead MS.

These dendronized TentaGel resins were also used in a further work to generate a library of amidines [55]. Many amidine-based molecules are known to be antagonists of the fibrinogen-GP IIb-IIIa interaction, therefore useful in the treatment of thrombotic diseases. For the synthesis the generation 2.0 and 3.0 dendritic wedges were equipped with HMPA-linkers, which were converted to the active carbonates (**47**) with *p*-nitrophenylchloroformate (**46**) (Scheme 7.9). After introduction of the amidine moiety (**48**) in the presence of  $Cs_2CO_3$  the selective removal of the allyl protecting group occurred under mild, neutral conditions, with *N*-methylmorpholine/acetic acid and  $Pd(PPh_3)_4$  in DCM. The best results for the coupling of five different amino acids (**50**) to the deprotected carboxyl functionality were obtained applying the active ester strategy with pentafluorophenol. Deprotection of the allyl-protected amino acids (**51**) and activation of the carboxyl groups was performed under the same conditions as mentioned above. The authors introduced three different piperidine derivatives (**53**) and after TFA-cleavage products (**55**) with approximately 30% overall yields and purities of 22 to 56% (HPLC) were obtained.

Following this synthetic route two known active compounds of this substance class (Ro44-9883 and TAK-029) were synthesized. The overall isolated yields were comparable with those obtained in solution but this route did not require isolation and purification of the intermediates.





**Scheme 7.9** Synthesis of a library of amidine-based GP IIb-IIIa antagonists on a dendronized solid support.

Chan and coworkers reported on the synthesis of an aminomethylpolystyrene resin (**56**) dendronized with triamine triple branched building blocks (1st and 2nd generation) which can be provided with Rink [47] linker groups (Fig. 7.14) [33]. Although the loading per gram ([G1]: 0.9 mmol g<sup>-1</sup>; [G2]: 1.17 mmol g<sup>-1</sup>) of the resin did not increase substantially because of the mass of the compound attached to the resin, the loading per reaction bead increased exponentially from one generation to the next. The support showed good swelling properties in dichloromethane.

The authors used this dendronized resin support (generation 1 and 2) (**56**) for the synthesis of 2-naphthalenesulfonamide (**57**) and *N*-phenylacetyl-L-phenylalaninamide (**58**). Compound (**57**) was prepared *via* support-deprotection, coupling with 2-naphthalenesulfonylchlorid in the presence of DIPEA and subsequent

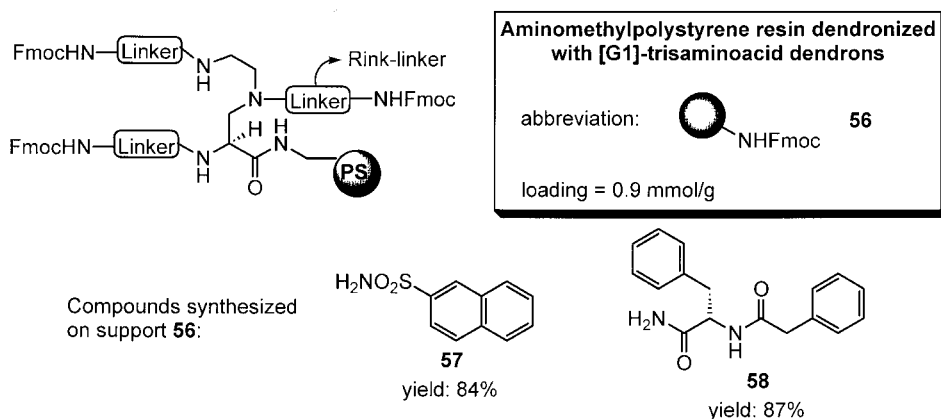


Fig. 7.14 Dendronized aminomethylpolystyrene resin.

TFA-induced cleavage in the course of which the dendrimer core remained intact. 2-Naphtalenesulfonamide (**57**) was obtained in 84% yield. Compound (**58**) was obtained *via* support-deprotection and immobilization of a Fmoc protected amino acid by means of HATU coupling. The supported substrate was deprotected and acylated with phenylacetic acid using standard coupling protocols. The final step was the product cleavage, which delivered the phenylalaninamide (**58**) in 87% yield.

Employing the second generation dendron the yield increased for both products to nearly quantitative values. The authors did not report on the purity of the synthesized compounds.

The use of a Fréchet-type aryl-ether dendronized solid support (**59**) for the synthesis of a hexapeptide was reported by Bradley and coworkers [35]. These dendrons were introduced to find an alternative to PAMAM dendrimers which are not stable against strong reducing agents and bases. The loading capacity of the solid support increased during the dendronization from  $0.82 \text{ mmol g}^{-1}$  ( $0.44 \text{ nmol}$  per bead) (starting resin hydroxymethylpolystyrene) to the sevenfold value of  $2.85 \text{ mmol g}^{-1}$  ( $3 \text{ nmol}$  per bead) ([G3]-dendrons). The swelling properties in diverse solvents were investigated. After dendronization the support was equipped with a Wang linker group by means of Mitsunobu reaction with methyl-4-hydroxybenzoate and adjacent  $\text{LiAlH}_4$ -reduction. The final loading of the dendrimer-Wang resin (**59**) was found to be  $2.2 \text{ mmol g}^{-1}$  ( $2.3 \text{ nmol}$  per bead) (Fig. 7.15).

The authors investigated the utility of the dendritic resin (**59**) by synthesizing the hexapeptide Leu-Enkephaline-Lys. Cleavage was performed with 95% TFA/water and the final product was isolated in 66% yield.

A very similar approach to the same solid-phase supported dendrimers was reported by Portnoy and coworkers by means of iterative Mitsunobu/reduction steps starting with a Wang resin [56]. They used [G1] (loading  $0.62 \text{ mmol g}^{-1}$ ) to [G3] (loading  $0.32 \text{ mmol g}^{-1}$ ) dendrimers for synthetic applications. The synthesis of a tripeptide was carried out without previous linker introduction to yield a dendri-

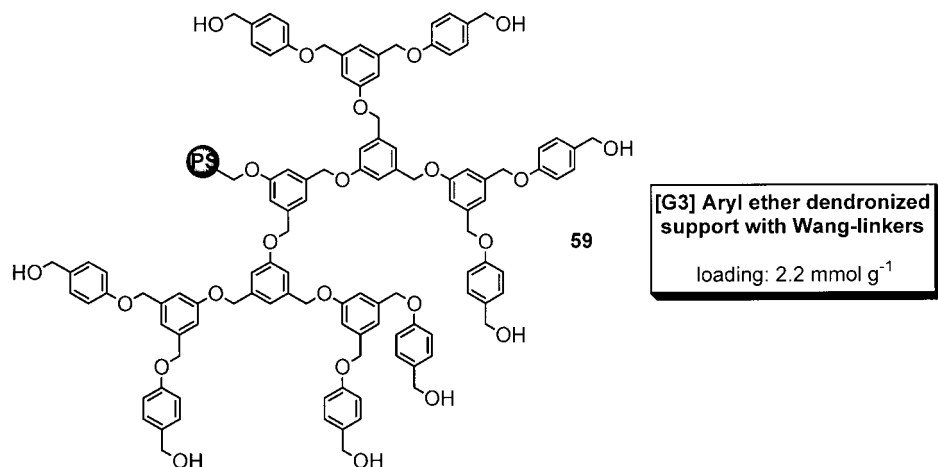


Fig. 7.15 Aryl ether dendronized support with Wang-linkers.

mer-peptide construct as final product in 83–85% yield after TFA-cleavage. In another experiment a Heck reaction was performed: iodophenol which was immobilized *via* Mitsunobu reaction was coupled with methyl acrylate in quantitative conversion. After TFA-cleavage the purities of the dendrimer-bound reaction products were not specified.

In an earlier work of the Bradley research group the synthesis of a tribranching symmetrical dendrimer on the solid phase with an 18-fold amplification of resin loading per bead was reported [34]. Starting point for synthetic applications was an aminomethyl polystyrene resin (bead diameter 400–500  $\mu\text{m}$ ) loaded with a polyamine scaffold which was dendronized with tris-based building blocks (Fig. 7.16). Generation 1 had a loading of 116 nmol per bead, while generation 2.0 had a loading of 230 nmol per bead. HMPB linker units were attached to the peripheral amino groups to obtain support (**60**). These new resins showed better swelling properties in polar solvents than the starting polymers and were well suited for the single bead/single compound concept, since a single bead contained more than sufficient compound for conventional analysis, including NMR. The large beads which were used for organic synthesis applications were found to be not as robust as smaller ones (250–300  $\mu\text{m}$ ) and much more sensitive to fast changes of solvent polarity (osmotic shock) and mechanical influence. Therefore the authors gave preference to the smaller generation 2.0 (36 nmol per bead) or 3.0 (100 nmol per bead) beads for synthetic applications.

Evaluation of this support for organic chemistry included peptide chemistry (synthesis of Fmoc-Val-Phe-Ala-OH) and a Suzuki coupling of immobilized 4-iodobenzoic acid with 4-methylbenzene boronic acid coupled under standard conditions.

A first example of a polystyrene dendronized with a hyperbranched polymer was recently reported by Stumbé and Haag [36]. They synthesized a polystyrene-polyglycerol hybrid support (**61**) by coupling a hyperbranched polyglycerol (**15**)

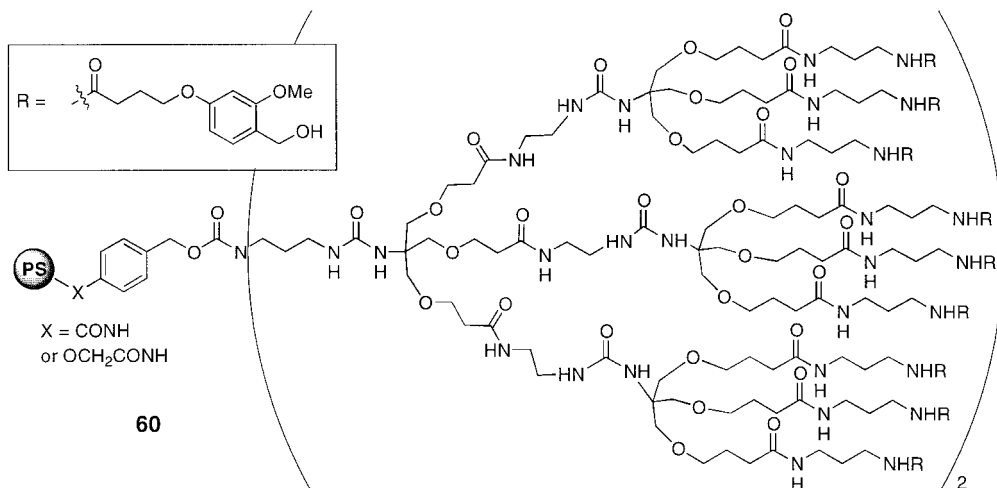


Fig. 7.16 Aminomethylpolystyrene dendronized with tris-based dendrons.

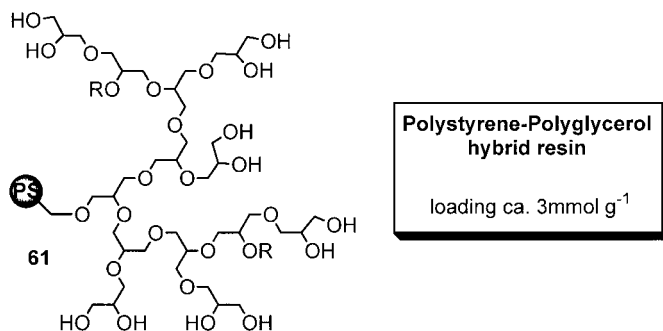


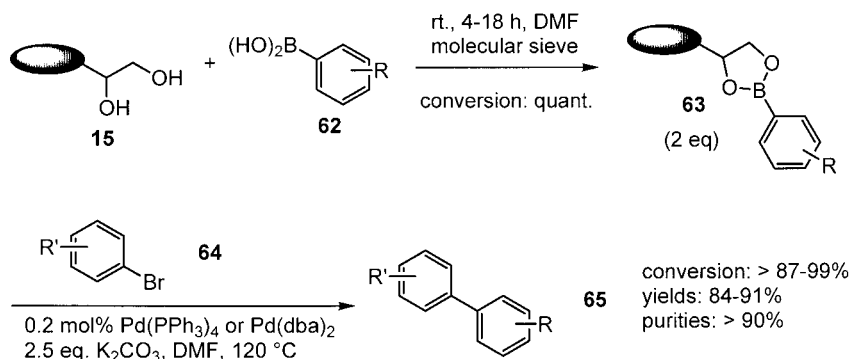
Fig. 7.17 Polystyrene-Polyglycerol hybrid resin.

onto a Merrifield resin (Fig. 7.17). This support showed high loading capacities (ca. 3 mmol g<sup>-1</sup>), good swelling properties (e.g. in methanol) and is currently under investigation for synthetic applications.

#### 7.4

##### Dendritic Polymer-supported Reagents and Scavengers

Recently, Hebel and Haag reported on the immobilization of aryl boronic acids (**62**) on a dendritic polyglycerol support (**15**) (Fig. 7.8,  $M_n = 8000 \text{ g mol}^{-1}$ ) (Scheme 7.10) [57]. This commercially available support was directly used and no additional



**Scheme 7.10** Polyglycerol boronic esters as high-loading soluble reagents for Suzuki cross-coupling reactions.

linker synthesis was necessary. In most cases the coupling occurred at room temperature and the conversion could be driven to completion (> 95%, <sup>13</sup>C NMR) with small amounts of molecular sieves. No further purification was required. The immobilized compounds were then exposed to Pd-catalyzed Suzuki cross-coupling reactions. For this purpose, an excess of (63) was treated with an aryl bromide (64) and potassium carbonate in DMF at 120 °C for 18 hours.

In contrast to solid-phase Suzuki coupling, very low amounts of the Pd-catalyst (0.2 mol%) were sufficient and high conversions (87–99%) to biaryls (65) were obtained to yield relatively pure products (> 90%, GC/MS, <sup>1</sup>H NMR) after ultrafiltration. In some cases most of the polymer supported boronic compound precipitated during the reaction and therefore no further purification was required. Nonetheless, quantitative removal of catalyst traces was not yet possible with either work-up protocol.

Janda and coworkers reported on the synthesis of octavalent PEG-based star polymers containing a triphosphatriazine core unit (Fig. 7.18) [58]. These molecules are not dendritic but can also serve as soluble supports with a slightly higher loading than PEG itself. They were found to show similar precipitation properties than conventional PEG supports. The non-carbon-containing core unit leads to another advantage compared with other PEG star polymers: no additional signals occur in <sup>1</sup>H or <sup>13</sup>C NMR spectra and interfere with NMR characterization of substrates attached to the star termini. This support gives <sup>1</sup>H and <sup>13</sup>C NMR spectra nearly identical to those of linear PEG. Additionally, the triphosphatriazine core unit is of low cost and bears remarkable stability.

A PEG-star supported triphenylphosphine analog (66) was synthesized and employed in Mitsunobu reactions. Four phenolethers were prepared within 3–18 h reaction time and 68–93% yield. Upon completion of the reactions, the formed polymer supported triphenylphosphine oxide was isolated by precipitation from diethyl ether in > 85% yield. The reagent could be recycled by means of alane reduction (73%).

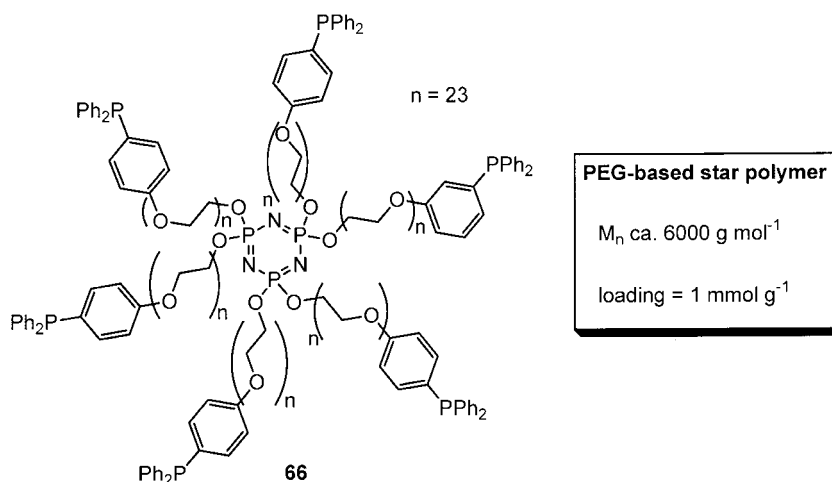


Fig. 7.18 PEG-based star polymer.

Rico-Lattes and coworkers investigated the chiral induction of dendrimer-bound D-gluconolactone sugar groups during the reduction of prochiral ketones with sodium borohydride [59, 60]. D-Glucono-1,5-lactone was coupled to PAMAM [G1], [G2], [G3], and [G4] dendrimers to receive gluconamide PAMAM dendrimers. The properties of these supports were tested under both heterogeneous and homogeneous reaction conditions.

A variety of prochiral ketones was exposed to the heterogeneous reduction protocol using [G3] dendritic supports to obtain the corresponding alcohols with yields of 45–97% and  $\epsilon$  values of 25–100%. Good results were even obtained employing linear alkyl ketones.

Marsh and coworkers described the synthesis and applications of high-loading dendritic scavenger resins to remove both nucleophiles and acids [61]. Wang resin was dendronized with triazine based wedges. To remove protons from reaction mixtures [G1] dendritic units containing morpholine endgroups were used (Fig. 7.19) (67). The removal of nucleophiles was performed employing a [G1] dichlorotriazin resin (68). However, the loading capacity of both resins was not mentioned.

The acylation of benzylamine with 4-chlorobenzoyl chloride served as a model reaction to evaluate the efficacy of both of these resins. After removal of both protons and amines the corresponding amide was obtained in 77% yield contaminated with less than 1% benzylamine and acid chloride. The transformation was also performed with commercially available scavenger resins PS-NCO and/or PS-NMM to obtain comparable results, but only approximately half the mass and volume of dendronized resin was required to achieve similar scavenging efficiency.

Both resins were also examined in a second test reaction, the tosylation of a primary amine, to receive analogous results compared with the commercially available resins. The authors did not report on the re-isolation, regeneration, and re-use of their dendronized scavenger resins.

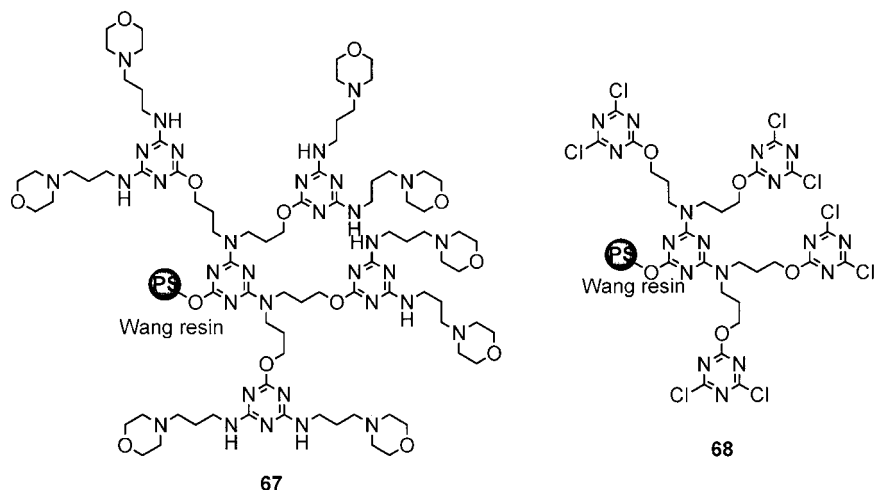


Fig. 7.19 Wang-resins dendronized with triazine-based wedges as scavengers.

Williams and coworkers used a [G4]-PAMAM dendrimer as a scavenger in the reactions of an arylpiperazine with slight excesses of three different electrophiles (an isocyanate, a sulfonyl chloride, and a benzyl halide) [62]. After TLC had indicated that all amine substrate had reacted the dendritic scavenger was added. Solvent removal, adding of chloroform, and filtration of the insoluble dendrimer afforded the products in high yields (87–99%) and purities (>95%, HPLC).

## 7.5

### Dendritic Polymers as High-Loading Supports for Catalysts

#### 7.5.1

##### Dendritic Polymeric Supports in Homogeneous Catalysis

In this section recent developments of dendritic polymers as high-loading supports for catalysts will be described. The formation of catalytically active metal nanoparticles using dendritic polymer templates (see Chapter 6) and monovalent catalysis at the focal unit of dendritic polymers will not be covered in this section. Instead of giving a comprehensive overview of dendritic catalysts [63–67], we will highlight the unique properties of these systems and point out advantages and disadvantages in some specific cases. A listing of high-loading dendritic catalysts is presented in Tab. 7.2, which is organized in the following way: soluble dendritic polymers by ligand class with a subdivision of asymmetric catalysis and heterogeneous solid-phase catalysis.

Homogeneous catalysis with a dendrimer supported catalyst was introduced by van Koten *et al.* in 1994 [68] and since then has rapidly expanded [5, 64–67]. The advantage of dendrimers over linear or irregular polymeric supports is their well-

defined molecular structure. Therefore the design of dendritic catalysts is not based on stochastic, but on individual, structurally defined molecules. However, the interaction of the many catalytically active centers is complex and can not yet be predicted. Another major drawback of these perfect dendritic catalyst supports is the tedious, generation-wise synthesis of dendrimer scaffolds. Therefore, in many cases only G0 and/or G1 of the catalytic systems are described, which are not yet real macromolecules. Recently, it was demonstrated that highly branched dendritic polymers, i.e. hyperbranched polymers (see below), show similar behavior as perfect dendritic supports in homogeneous catalysis and require similarly low amounts of catalyst compared with the unsupported system [69].

Generally these globular dendritic architectures offer several advantages over other kinds of organic polymers, such as the full exposure of the catalytic centers to the environment. In contrast to linear or cross-linked polymeric supports, which can partially hide catalytic centers, the functional groups are located on the surface of the dendritic nanoparticle and diffusional limitations are less relevant. Furthermore the close proximity of the catalytic centers on the surface of the dendritic polymer can enhance the catalytic activity by multiple complexation or even cooperativity. This behavior is described as “positive” dendritic effect. However, in some cases a “negative” dendritic effect was observed, which is caused by an undesired interaction or electron transfer between the neighboring catalytic centers on the surface of the dendrimer [70].

Two other advantages of dendritic polymer supported catalysts are often mentioned: (1) their higher stability towards decomposition and (2) the possibility of efficient recycling, which can be used for a continuous process (see also Section 2). Deactivation of catalysts is a general problem, e.g. for palladium, which is reduced to Pd(0) to give large metallic particles. It is evident that diffusion and entropic effects make the encounter rate of such processes much higher for small molecules than for macromolecules. The potential recycling of dendritic polymer supported catalysts is still problematic, i.e. if using membrane separation techniques. High molecular weights ( $> 3000 \text{ g mol}^{-1}$ ) are required in order to get good retention of the dendritic catalyst. For example a retention of  $> 99.9\%$  is necessary to retain  $> 98\%$  of catalyst after 10 reaction cycles (compare Fig. 7.2b). The current retentions of most dendritic catalysts are in the range of 85–97% and are disastrous for continuous processes. However, improvement of membrane technology as well as the use of easily accessible dendritic polymers with higher molecular weights (5000–10 000  $\text{g mol}^{-1}$ ) and low molecular weight distributions ( $< 1.5$ ) will further increase the potential of dendritic supports for homogeneous catalysis.

#### 7.5.1.1 Selected Examples for Dendritic Polymer-supported Catalysis (see Tab. 7.2)

An instructive example for a “positive” dendritic effect was reported by Reetz *et al.* [71]. The authors described a poly(propylenimine) dendrimer, with diphenylphosphine groups in the periphery (Fig. 7.20). A dendritic  $[\text{PdMe}_2]$ -complex was tested as an efficient catalyst in the Heck reaction of bromobenzene and styrene to yield stilbene (85–90% conversion). The separation technique originally investigated for



the dendritic complex was precipitation with diethyl ether to recover the Pd-containing dendrimer in 98% yield. It is noteworthy that the activity (TON) of the dendritic catalyst was three times higher than that of the monomeric catalyst with respect to the individual metallic centers and did not decrease significantly upon recycling. Unlike the unsupported catalytic system, the dendritic catalysts did not decompose to elemental palladium, which was explained by the higher thermal stability of the dendritic complex. Another application for these dendritic phosphine ligands are Rh-catalyzed hydroformylation reactions. In addition, the use of these dendrimer supported catalysts in combination with a continuous membrane reactor has been reported [25].

An extension of these dendritic phosphine ligands for Pd-catalyzed allylic amination was recently described using a thermomorphic system for separation [72]. In this case an active dendritic Pd<sup>0</sup>-species could be generated by hydrazine reduction and subsequently used in a DMF/heptane mixture at 75 °C for the stereoselective allylic amination. After completion of the reaction and cooling to room temperature, the catalysts can be recovered by simple phase separation.

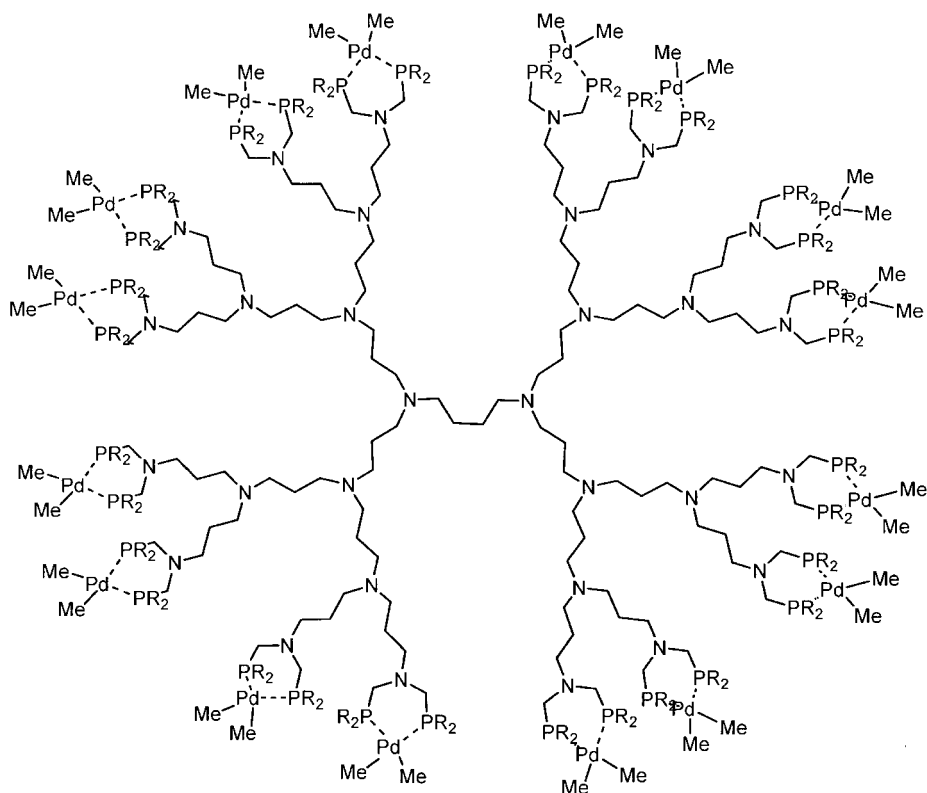


Fig. 7.20 [G3] PPI-Dendrimer with [PdMe<sub>2</sub>]-phosphine complex (R=Phenyl).

The use of soluble dendrimers with phosphine ligands experienced a rapid growth and was also transferred to several other dendrimer scaffolds [64–66]. Many reactions, such as hydrogenation, hydrovinylation, Stille coupling, Knoevenagel condensation and Michael addition were reported (Tab. 7.2) [73, 74].

A very well studied example of a “negative” dendritic effect is the Kharasch reaction (e.g. the addition of  $\text{CCl}_4$  to methyl methacrylate by an atom transfer-radical reaction) with dendritic Ni-complexes [70]. In their initial paper, van Koten *et al.* reported a [G0] and [G1] carbosilane dendrimer with a pincer ligand forming the Ni-complex (Fig. 7.21) [68]. For these low generation dendrimers no rate acceleration was observed. However, the activity (initial turn over rate) and the obtained conversions of the catalyst with 4 or 12 Ni-sites, respectively, were already reduced by a factor 1.5 as compared with the monomeric complex. In further studies the authors demonstrate that higher generations (i.e. [G2]) showed an even more pronounced negative dendritic effect, which originates in a fast deactivation of the dendritic catalyst beyond generation [G0] [75]. The deactivation is caused by the irreversible formation of catalytically inactive Ni(III) sites on the periphery of the dendrimer. This hypothesis was further supported by model studies as well as ESR measurements. Nonetheless the activity and separation properties of the [G0]-complex make it synthetically useful and its membrane retention was already 97.4% with a nanofiltration membrane (Koch MPF-50).

More recently pincer-ligands were also used in combination with a hyperbranched carbosilane polymer to form a dendritic Pd-complex, which was applied to an aldol condensation [69]. The obtained yield and catalytic activity of the dendritic complex was only slightly lower than for the monomeric complex. However, the hyperbranched carbosilane polymer showed a very broad molecular weight distribution of 5.2, initially, which is not suitable for continuous processes with membrane separation. After dialysis ( $\text{MWCO } 1000 \text{ g mol}^{-1}$ ) about 70% of the dendritic ligand with a molecular weight distribution of 1.8 could be obtained and was used for catalysis to give >95% conversion with 0.8 mol% of dendritic catalyst. The recycling of the dendritic catalyst, however was not studied in this case. Nonetheless, this example indicates that dendritic polymers with average molecular weights  $\geq 5000 \text{ g mol}^{-1}$  and narrow molecular weight distributions ( $< 1.5$ ) can potentially substitute perfect dendrimers as high-loading dendritic supports for catalysts. However, only few examples of well-defined hyperbranched polymers are known and only some are commercially available (see also Section 7.2.1) [11, 14].

A very successful example for the use of dendritic polymeric supports in asymmetric synthesis was recently described by Breinbauer and Jacobsen [76]. PAMAM-dendrimers with [Co(salen)]complexes were used for the hydrolytic kinetic resolution (HKR) of terminal epoxides. For such asymmetric ring opening reactions catalyzed by [Co(salen)]complexes, the proposed mechanism involves cooperative, bimetallic catalysis. For the study of this hypothesis, PAMAM dendrimers of different generation [G1–G3] were derivatized with a covalent salen ligand through an amide bond (Fig. 7.22). The separation was achieved by precipitation and SEC. The catalytically active [Co<sup>III</sup>(salen)]dendrimer was subsequently obtained by quantitative oxidation with elemental iodine (Fig. 7.22).

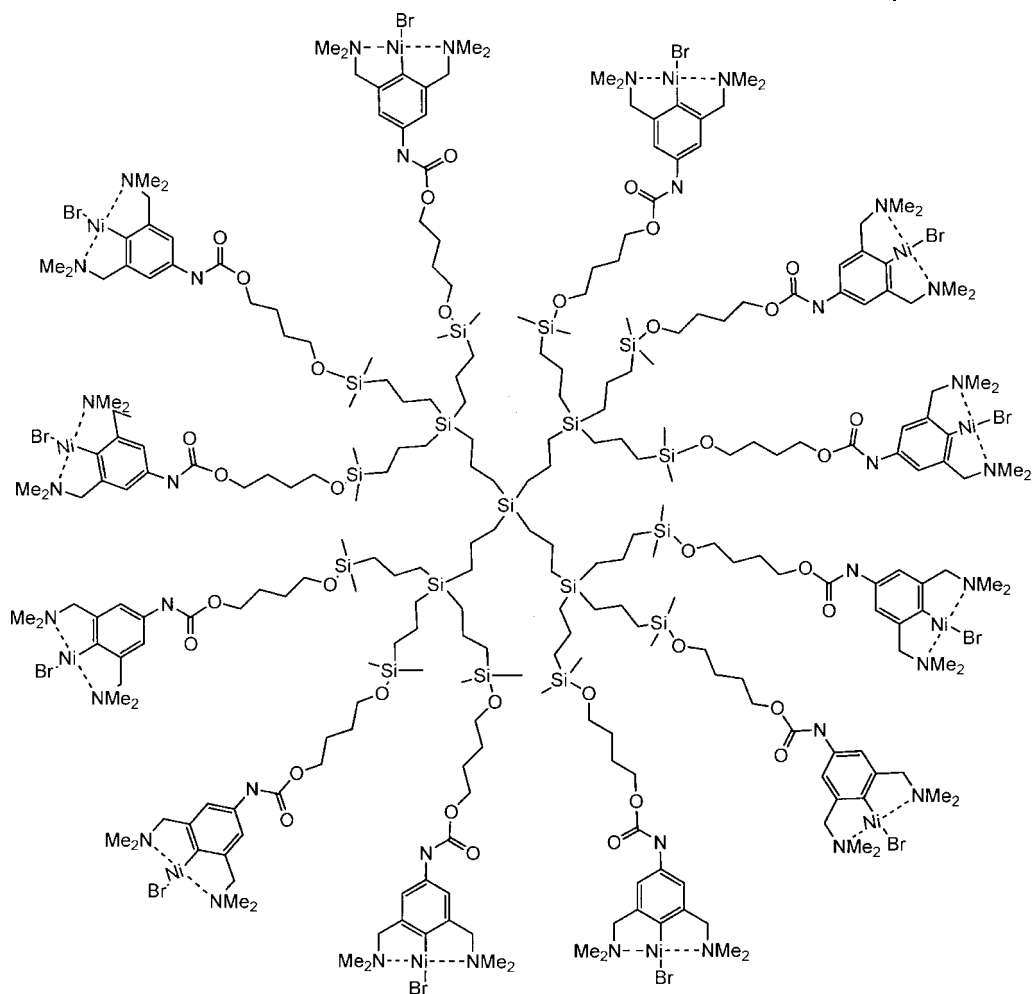


Fig. 7.21 [G1] Carbosilan dendrimer with pincer ligands (Ni<sup>II</sup>-complex).

In order to assess whether intramolecular cooperativity could occur within the dendrimeric [Co(salen)]catalyst the HKR of racemic 1-cyclohexyl-1,2-ethenoxide was studied at low catalyst concentrations ( $2 \times 10^{-4}$  M). Under these conditions the monomeric [Co(salen)] complex showed no conversion at all, while the dendritic [G2]-[Co(salen)]catalyst gave an impressive enantiomeric excess of 98% *ee* of the epoxide at 50% conversion. Further catalytic studies for the HKR with 1,2-hexenoxide revealed that the dendritic catalysts are significantly more active than a dimeric model compound. However, the [G1]-complex represents already the maximum (100%) in relative rate per Co-salen unit, which was lower for higher generations [G2] (66%) and [G3] (45%).

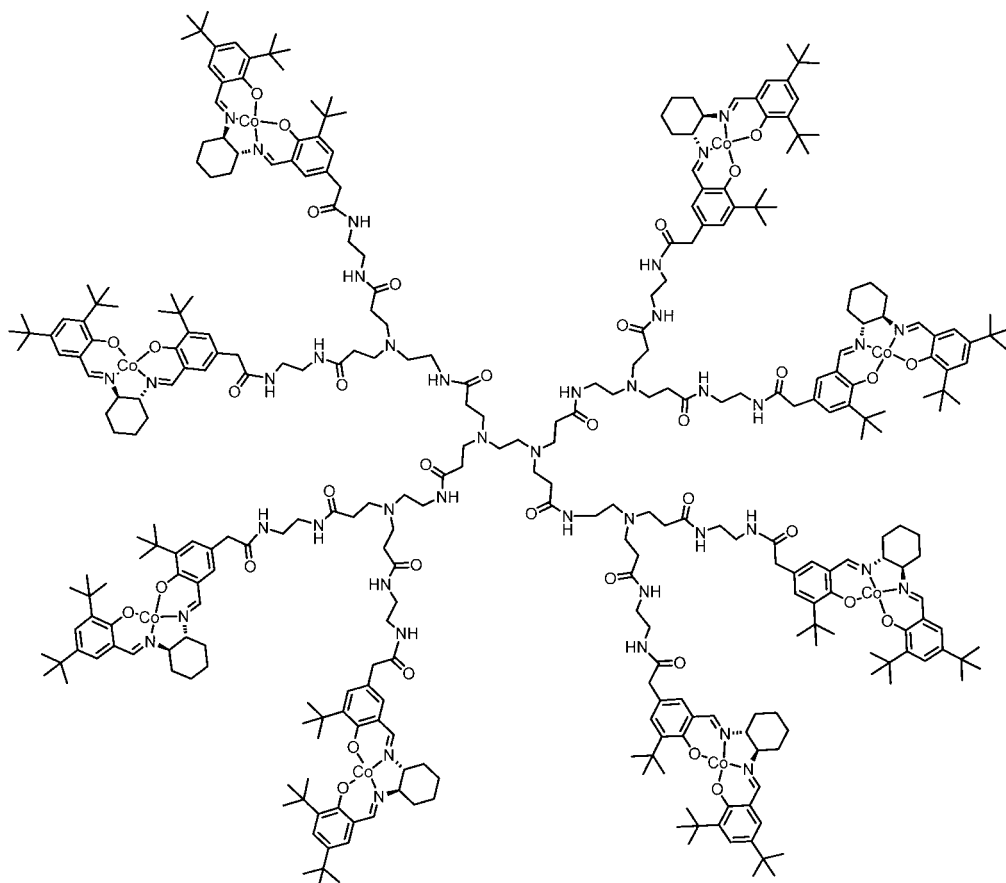


Fig. 7.22 [G2] PAMAM-dendrimer with [Co(salen)] complex.

### 7.5.2

#### Dendritic Polymeric Supports in Heterogeneous Catalysis

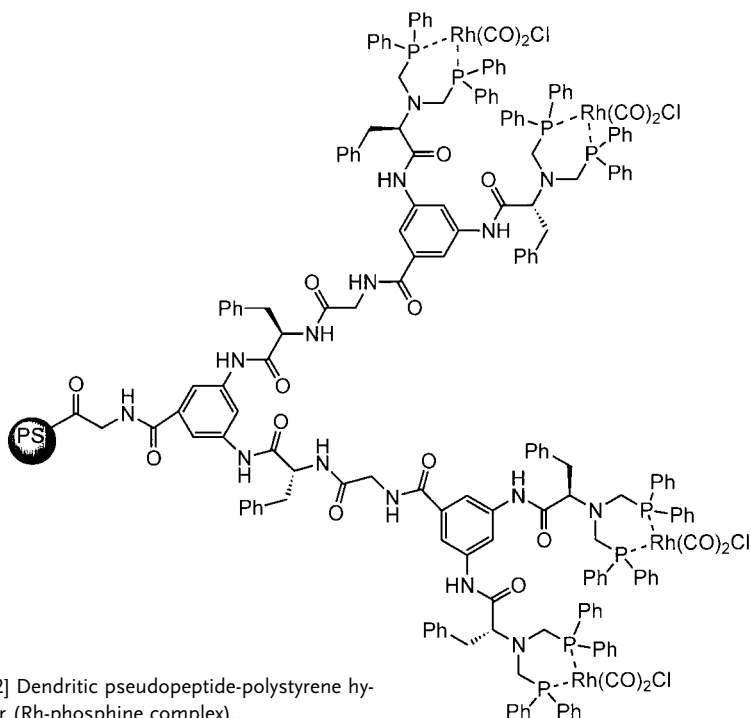
High-loading dendritic solid-phase resins were also used as supports for catalysts. Even though the solid-phase beads are heterogeneous, the reaction rate of catalytic reactions can be similarly high as compared with homogenous monomeric systems [77]. Arya and coworkers reported on the solid-phase synthesis of Rh-complexed PAMAM-diphosphonated dendrimers anchored onto silica and their application in the hydroformylation of olefins [78]. The heterogeneous catalyst was recycled and reused without significant loss of selectivity and activity. A similar approach was then carried out using polystyrene beads and pseudopeptide-based building blocks to form the dendritic skeleton [79, 80]. Again the formation of a rhodium complex with dendritic phosphine ligands was achieved (Fig. 7.23). Different dendrimer

Tab. 7.2 Application of dendritic polymer-supported catalysts.

Ligand	Dendritic Scaffold	Metal	Reaction	Metal/Substrate	Conversion (%)	Recovery Method	Comment	Refs.
Pincer ligand	Carbosilane Dendrimer G0–G2	Ni	Kharasch reaction (atom transfer radical reaction)	0.03 mol%	1–79	Ultrafiltration	Negative dendritic effect for [G1,G2]	68, 70, 75
Pincer ligand	Hyperbranched Carbosilane G0	Pd	Aldol condensation	0.8 mol%	>95	Membrane separation suggested	No dendritic effect	69
PPh <sub>2</sub> P,N,P-Ligand	Polyamine PPI	Pd Rh Ir	Heck Hydroformylation (prelim. results) Hydrogenation	2 mol%	85–90	Precipitation, Continuous flow membrane reactor	Positive dendritic effect, little deactivation	25, 71
PPh <sub>2</sub> P,N,P-Ligand	Polyamine PPI	Pd		–	–	Not specified	Positive dendritic effect from complexation	83
PPh <sub>2</sub> P,N,P-Ligand	Polyamine PPI G1–G4	Pd(0)	Allylic Amination	0.3 mol%	>99	Thermomorphing separation	Increasing selectivity at higher generations	72
PPh <sub>2</sub>	Carbosilane Dendrimer G0	Pd	Hydrovinylation	0.01–0.05 mol%	68–99.9	Continuous membrane reactor	Negative dendritic effect	27
PPh <sub>2</sub>	Phosphorous-based	Pd, Pt Rh, Ru	Stille Coupling Knoevenagel Michael Addition	0.41 mol%	79–95	Recycling possible	Positive dendritic effect	73, 74
PPh <sub>2</sub>	Silane/Phosphorous-based	Rh Ru	Hydrogenation	0.5 mol%	Not specified	Extraction and recrystallization	No dendritic effect	84
PPh <sub>2</sub> P,Si,P-Ligand	Carbosilane Dendrimer [G1]	Pd Rh	Allylic Alkylation Hydroformylation	0.01–0.05 mol%	68–99.9	Continuous membrane reactor	Positive dendritic effect	26, 85
N,O-Ligand	Carbosilane [G1]	Ru	RCM		20	Nanofiltration Koch MPF-60		86

Tab. 7.2 (cont.)

Ligand	Dendritic Scaffold	Metal	Reaction	Metal/Substrate	Conversion (%)	Recovery Method	Comment	Refs.
O, Carbene-Ligand	Carbosilane [G0]	Ru	RCM	5 mol%	87–99	Column chromatography	Loss of Ru after recycling	87
O,O,O-Ligand	Carbosilane [G0]	Polyoxometal	Oxidation of thioethers	1.7 mol%	Not specified	Precipitation/Filtration		88
<b>High-Loading Dendritic Catalysts in Asymmetric Synthesis</b>								
Salen	PAMAM	Co	Asymmetric resolution of epoxides	0.027 mol%	50 (100)	SEC	Positive dendritic effect, cooperativity, excellent ees > 98%	76
TADDOL	Fréchet type	Ti	Enantioselective nucleophilic additions to aldehydes	20 mol%	Not specified	Column chromatography		89
Chiral ferrocenyl phosphine (Josiphos)	Amide/Carbosilane, different cores	Rh	Asymmetric hydrogenation	Not specified	Not specified	Ultrafiltration	High ees (98%) No dendritic effect	90, 91
Ephedrine	PAMAM	Zn	Asymmetric diethylzinc addition	50 mol%			Moderate ees due to flexible scaffold	92
Ephedrine	Polyphenylene	Zn	Asymmetric diethylzinc addition	3.3 mol%	32–70%	Recovery possible	High ees 77–86% due to rigid scaffold	93
<b>High-Loading Dendritic Solid Phase Catalysts</b>								
Dendritic Amine	Cross-linked PPI dendrimers	ScOTf	Aldol, Diels–Alder	7 mol%	73–89%	Filtration	No dendritic effect but high reactivity	94
Diphenyl-phosphine	PS-Peptide-Dendron [G1–G3]	Rh	Hydroformylation	Not specified	G1 42–85% G2 > 99% G3 99%	Filtration	Positive dendritic effect	79, 80
Diphenyl-phosphine	PS-Peptide-Dendron on Silica G0–G4	Rh	Hydroformylation	0.1 mol%	G2 96–99	Filtration	Positive dendritic effect	78



**Fig. 7.23** [G2] Dendritic pseudo-peptide-polystyrene hybrid polymer (Rh-phosphine complex).

generations were prepared and tested as catalysts for the hydroformylation reaction of several olefins. For the hydroformylation of styrene, the PS [G2] dendrimer (Fig. 7.23) showed higher conversions and selectivities (94% branched isomer) than the first generation and its activity did not decrease for up to five cycles. The origin of this increased reactivity might be attributed to the higher density of ligands on the outer core and cooperative effects, and once again would be an example for a positive dendritic effect. However, it should be noted that many catalytic reactions using palladium in combination with solid-phase supports require very large amounts (1–100 mol%) of catalyst following deactivation [81, 82].

## 7.6

### Conclusions

Dendritic polymeric supports or hybrids of these with solid-phase resins are among the most promising candidates for new high-loading supports in organic synthesis and catalysis. However, every new polymeric support has to compete with the current bench mark, the so-called Merrifield resin and its derivatives.

Therefore new high-loading supports should:

1. be easily accessible in large quantities;
2. have a loading capacity > 1.5 mmol linker per gram polymer;
3. contain reactive groups, which are conveniently functionalized by standard solution phase chemistry;
4. be chemically and mechanically stable; and
5. be easy to separate by standard laboratory techniques.

For ecological and financial reasons new polymeric supports should also allow mmol-scale synthesis and the complete recycling of the support after each transformation.

None of the previously mentioned high-loading dendritic supports is perfect, however, some (i.e. polyamides, polysilanes and polyethers) are chemically more robust than for example polyesters or polyamines. For multi-step organic synthesis in a parallel format, hybrid resins are especially attractive because they can combine several materials properties (e.g. good swelling properties, high loading capacities) and allow the full characterization of the product by standard analytical techniques (including  $^1\text{H}$  NMR) after cleavage from a single microbead. For homogeneous catalysis on the other hand, soluble dendritic polymers are the most promising candidates. In some cases the high density of catalytically active centers can result in a positive dendritic effect because of additional stabilization, chelate formation and cooperative catalysis. However, for continuous flow membrane separation higher retentions (> 99.9%) are required, which can only be achieved by further optimization of the dendritic polymer size (molecular weight distribution) and the membrane material.

Another important criterion for high-loading dendritic polymeric supports certainly is the possibility of intramolecular cross-reactions in these highly functional supports. However, site isolation in dendritic polymer derivatives with a degree of branching between 50–75% is less problematic, because of the randomized 3D-orientation and lower concentration of the terminal groups as compared with a perfectly branched dendrimers or high-loading linear polymers, such as polyvinyl alcohol. Nevertheless, it is necessary to find an optimum between accessibility, flexibility and loading of functional groups in these dendritic polymer scaffolds.

Whether or not a new polymeric support is suitable for general application in organic synthesis and catalysis can only be determined by application in diverse chemical syntheses. At present these investigations are in a too early stage to give a qualified answer to this question. But the width of successful synthetic as well as catalytic applications carried out on these high-loading dendritic supports show interesting effects and indicate a large potential for the future.

## 7.7

### Acknowledgements

The authors would like to thank their coworkers and colleagues, which are mentioned in the papers, for their contribution. They are especially indebted to Prof.



Rolf Mülhaupt for his generous support, the Deutsche Forschungsgemeinschaft, the Fonds der Chemischen Industrie, the Otto-Röhm-Gedächtnisstiftung and Bayer AG for financial support.

## 7.8

### Abbreviations

Bn	benzyl
Boc	<i>tert.</i> butyloxycarbonyl
EDC	1-ethyl-3-(3-dimethylaminopropyl)carbodiimide
DCM	dichloromethane
<i>de</i>	diastereomeric excess
DIC	<i>N,N'</i> -diisopropylcarbodiimide
DIEA	diisopropylethylamine
DIPEA	diisopropylethylamine
DMA	dimethyl acetamide
DMAP	4-( <i>N,N</i> -dimethylamino)pyridine
DMF	dimethyl formamide
EDCI	<i>N'</i> -(3-dimethylaminopropyl)- <i>N</i> -ethylcarbodiimide
<i>ee</i>	enantiomeric excess
Fmoc	9-fluorenylmethoxycarbonyl
HATU	<i>O</i> -(7-azabenzotriazol-1-yl)- <i>N,N,N'</i> -tetramethyluronium hexafluorophosphate
HMB	4-hydroxymethylbenzoic acid
HMPA	4-(hydroxymethyl)phenoxyacetic acid
HMPB	4-(4'-hydroxymethyl-3'-methoxy)phenoxybutyric acid
HOBt	1-hydroxybenzotriazole
HPLC	high performance liquid chromatography
<i>PD</i>	polydispersity
PEG	poly(ethyleneglycol)
PG	polyglycerol
PS	polystyrene
PyBOP	benzotriazole-1-yl-oxy-tris-pyrrolidino-phosphonium hexafluorophosphate
TBS	<i>tert</i> -butyldimethylsilyl
TBTU	<i>O</i> -(1 <i>H</i> -benzotriazol-1-yl)-1,1,3,3-tetramethyluronium tetrafluoroborate
TEA	triethylamine
TFA	trifluoroacetic acid
TLC	thin layer chromatography
Tris	tris(hydroxymethyl)aminomethane

## 7.9

## References

- 1 R. B. MERRIFIELD, *J. Am. Chem. Soc.* **1963**, *85*, 2149–2154.
- 2 R. HAAG, A. HEBEL, J.-F. STUMBÉ, IN *Handbook of Combinatorial Chemistry* (eds. R. HANKO, K. C. NICOLAOU, W. HARTWIG), Wiley-VCH, Weinheim, **2002**, pp. 24–58.
- 3 F. ZARAGOSA-DÖRWALD, *Organic Synthesis on Solid Phase*, Wiley-VCH, Weinheim, **2000**.
- 4 R. HAAG, *Chem. Eur. J.* **2001**, *7*, 327–335; and references therein.
- 5 R. J. M. KLEIN GEBBINK, C. A. KRUTHOF, G. P. M. VAN KLINK, *et al.*, *Reviews in Molecular Biotechnology* **2002**, *90*, 183–193.
- 6 S. LEBRETON, S. MONAGHAN, M. BRADLEY, *Aldrichim. Acta* **2001**, *34*, 75–83.
- 7 G. R. NEWKOME, C. N. MOOREFIELD, F. VÖGTLE, *Dendritic Molecules: Concepts, Syntheses, Perspectives*, 2nd edn., Wiley-VCH, Weinheim, **2001**.
- 8 M. FISCHER, F. VÖGTLE, *Angew. Chem.* **1999**, *111*, 934–955; *Angew. Chem. Int. Edn.* **1999**, *38*, 884–905.
- 9 A. W. BOSMAN, H. M. JANSSEN, E. W. MEIJER, *Chem. Rev.* **1999**, *99*, 1665–1688.
- 10 Commercially available dendrimers are: polyamine dendrimers (Astramol®, DSM) and polyamidoamine dendrimers (Starburst®, Dendritec).
- 11 H. FREY, R. HAAG, in *Encyclopedia of Materials, Science and Technology* (eds. K. H. J. BUSCHOW, R. H. CAHN, M. C. FLEMINGS, *et al.*), Elsevier Science Ltd., Oxford, **2001**, pp. 3997–4000.
- 12 A. SUNDER, J. HEINEMANN, H. FREY, *Chem. Eur. J.* **2000**, *6*, 2499–2505.
- 13 R. HAAG, J.-F. STUMBÉ, A. SUNDER, *et al.*, *Macromolecules* **2000**, *33*, 8158–8166.
- 14 Commercially available hyperbranched polymers are Polyglycerol (aliphatic polyether polyol) and Polyethylenimine (aliphatic polyamine) both from Hyperpolymers, Boltorn (aliphatic polyesters) from Perstorp and Hybrane (aromatic polyester amide) from DSM.
- 15 C. C. TZSCHUCKE, C. MARKERT, W. BANNWARTH, S. ROLLER, A. HEBEL, R. HAAG, *Angew. Chem.* **2002**, *114*, 4136–4173; *Angew. Chem. Int. Ed.* **2002**, *41*, 3694–4001, and refs. cited
- 16 D. J. GRAVERT, K. D. JANDA, *Chem. Rev.* **1997**, *97*, 489–509.
- 17 K. E. GECKELER, *Adv. Polymer Sci.* **1995**, *121*, 31–79.
- 18 U. KRAGL, T. DWARS, *TRENDS Biotechnol.* **2001**, *19*, 442–449.
- 19 D. PAUL, *Chem. unserer Zeit* **1998**, *32*, 197–205.
- 20 H. DETERMANN, K. LAMPERT, *Mitt. Dtsch. Pharmaz. Ges.* **1970**, *40*, 117–134.
- 21 R. HAAG, A. SUNDER, A. HEBEL, S. ROLLER, *J. Comb. Chem.* **2002**, *4*, 112–119.
- 22 E. STAUDE, *Membranen und Membranprozesse*, VCH, Weinheim, **1992**.
- 23 S. LAUE, L. GREINER, J. WÖLTINGER, *et al.*, *Adv. Synth. Catal.* **2001**, *343*, 6–7.
- 24 H. P. DIJKSTRA, G. P. M. VAN KLINK, G. VAN KOTEN, *Acc. Chem. Res.* **2002**, *35*, 798–810.
- 25 N. BRINKMANN, D. GIEBEL, G. LOHMER, *et al.*, *J. Catalysis* **1999**, *183*, 163–168.
- 26 D. DEGROOT, E. B. EGGELING, J. C. D. WILDE, *et al.*, *Chem. Commun.* **1999**, 1823–1824.
- 27 N. J. HOVESTAD, E. B. EGGELING, H. J. HEIDBUCHEL, *et al.*, *Angew. Chem.* **1999**, *111*, 1763–1765; *Angew. Chem. Int. Ed. Engl.* **1999**, *38*, 1655–1658.
- 28 For an example see: S. P. RAILLARD, G. JI, A. D. MANN, T. A. BAER, *Organic Process Research & Development* **1999**, *3*, 177–183.
- 29 D. C. SHERRINGTON, *Chem. Commun.* **1998**, 2275–2286.
- 30 A. G. M. BARRETT, S. M. CRAMP, R. S. ROBERTS, *Org. Lett.* **1999**, *1*, 1083–1086.
- 31 C. W. LINDSLEY, J. C. HODGES, G. F. FILZEN, *et al.*, *J. Comb. Chem.* **2000**, *2*, 550–559.
- 32 J. RADEMAN, M. BARTH, *Angew. Chem.* **2002**, *114*, 3087–3090; *Angew. Chem. Int. Ed.* **2002**, *41*, 2975–2978.
- 33 A. MAHAJAN, S. R. CHHABRA, W. C. CHAN, *Tetrahedron Lett.* **1999**, *40*, 4909–4912.
- 34 C. FROMONT, M. BRADLEY, *Chem. Commun.* **2000**, 283–284.
- 35 A. BASSO, B. EVANS, N. PEGG, *et al.*, *Chem. Commun.* **2001**, 697–698.

- 36 J.-F. STUMBÉ, R. HAAG, *Entropie* **2001**, 37, 27–31.
- 37 R. M. KIM, M. MANNA, S. M. HUTCHINS, *et al.*, *Proc. Natl. Acad. Sci. USA* **1996**, 93, 10012–10017.
- 38 N. J. HOVESTAD, A. FORD, J. T. B. H. JASTRZEBSKI, *et al.*, *J. Org. Chem.* **2000**, 65, 6338–6344.
- 39 J. ZHANG, G. DRUGEON, N. L'HERMITE, *Tetrahedron Lett.* **2001**, 42, 3599–3601.
- 40 J. ZHANG, J. ASZODI, C. CHARTIER, *et al.*, *Tetrahedron Lett.* **2001**, 42, 6683–6686.
- 41 A. SUNDER, R. HANSELMANN, H. FREY, *et al.*, *Macromolecules* **1999**, 32, 4240–4246.
- 42 A. SUNDER, R. MÜLHAUPT, R. HAAG, *et al.*, *Adv. Mater.* **2000**, 12, 235–239.
- 43 S. ROLLER, DIPLOMARBEIT, UNIVERSITÄT FREIBURG, **2002**.
- 44 A. B. KANTCHEV, J. R. PARQUETTE, *Tetrahedron Lett.* **1999**, 40, 8049–8053.
- 45 M. BENAGLIA, R. ANNUNZIATA, M. CINQUINI, *et al.*, *J. Org. Chem.* **1998**, 63, 8628–8629.
- 46 J. CHANG, O. OYELARAN, C. K. ESSER, *et al.*, *Tetrahedron Lett.* **1999**, 40, 4477–4480.
- 47 H. RINK, *Tetrahedron Lett.* **1987**, 28, 3787–3790.
- 48 J. KRESS, R. ZANALETI, A. AMOUR, *et al.*, *Chem. Eur. J.* **2002**, 8, 3769–3772.
- 49 A. LUBINEAU, A. MALLERON, C. LE NARVOR, *Tetrahedron Lett.* **2000**, 41, 8887–8891.
- 50 J. P. TAM, *Proc. Natl. Acad. Sci. USA* **1988**, 85, 5409–5413.
- 51 V. SWALI, N. J. WELLS, G. J. LANGLEY, *et al.*, *J. Org. Chem.* **1997**, 62, 4902–4903.
- 52 I. R. MARSH, H. SMITH, M. BRADLEY, *Chem. Commun.* **1996**, 941–942.
- 53 N. J. WELLS, M. DAVIES, M. BRADLEY, *J. Org. Chem.* **1998**, 63, 6430–6431.
- 54 A. BASSO, B. EVANS, N. PEGG, *et al.*, *Tetrahedron Lett.* **2000**, 41, 3763–3767.
- 55 A. BASSO, N. PEGG, B. EVANS, *et al.*, *Eur. J. Org. Chem.* **2000**, 3887–3891.
- 56 A. DAHAN, M. PORTNOY, *Macromolecules* **2003**, 36, 1034–1038.
- 57 A. HEBEL, R. HAAG, *J. Org. Chem.* **2002**, 67, 9452–9455.
- 58 N. N. REED, K. D. JANDA, *Org. Lett.* **2000**, 2, 1311–1313.
- 59 A. R. SCHMITZER, S. FRANCESCHI, E. PEREZ, *et al.*, *J. Am. Chem. Soc.* **2001**, 123, 5956–5961.
- 60 A. SCHMITZER, E. PEREZ, I. RICO-LATTES, *et al.*, *Tetrahedron Lett.* **1999**, 40, 2947–2950.
- 61 A. MARSH, S. J. CARLISLE, S. C. SMITH, *Tetrahedron Lett.* **2001**, 42, 493–496.
- 62 L. WILLIAMS, S. M. NESSET, in *Fourth International Electronic Conference on Synthetic Organic Chemistry (ECSOC-4)*, **2000**.
- 63 D. E. BERGBREITER, *Chem. Rev.* **2002**, 102, 3345–3384.
- 64 D. ASTRUC, F. CHARDAC, *Chem. Rev.* **2001**, 101, 2991–3023.
- 65 R. KREITER, A. W. KLEIJ, R. J. M. K. GEBBINK, *et al.*, *Top. Curr. Chem.* **2001**, 217, 163–199.
- 66 G. E. OOSTEROM, J. N. H. REEK, P. C. J. KAMMER, *et al.*, *Angew. Chem.* **2001**, 113, 1878–1901; *Angew. Chem. Int. Ed.* **2001**, 40, 1828–1849.
- 67 H. BRUNNER, *J. Organomet. Chem.* **1995**, 500, 39–46.
- 68 J. W. J. KNAPEN, A. W. V. D. MADE, J. C. D. WILDE, *et al.*, *Nature* **1994**, 372, 659–663.
- 69 C. SCHLENK, A. W. KLEIJ, H. FREY, *et al.*, *Angew. Chem.* **2000**, 112, 3587–3589; *Angew. Chem. Int. Ed. Engl.* **2000**, 39 (19), 3445–3447.
- 70 A. W. KLEIJ, R. A. GOSSAGE, J. T. B. H. JASTRZEBSKI, *et al.*, *Angew. Chem.* **2000**, 112, 179–182; *Angew. Chem. Int. Ed. Engl.* **2000**, 39, 176–178.
- 71 M. T. REETZ, G. LOHMER, R. SCHWICKARDI, *Angew. Chem.* **1997**, 109, 1559–1162; *Angew. Chem. Int. Ed. Engl.* **1997**, 36, 1526–1529.
- 72 T. MIZUGAKI, M. MURATA, M. OOE, *et al.*, *Chem. Commun.* **2002**, 52–53.
- 73 V. MARAVAL, R. LAURENT, A.-M. CAMINADE, *et al.*, *Organometallics* **2000**, 19, 4025–4029.
- 74 M. BARDAJI, M. KUSTOS, A.-M. CAMINADE, *et al.*, *Organometallics* **1997**, 16, 403.
- 75 A. W. KLEIJ, R. A. GOSSAGE, R. J. M. K. GEBBINK, *et al.*, *J. Am. Chem. Soc.* **2000**, 122, 12112–12124.
- 76 R. BREINBAUER, E. N. JACOBSEN, *Angew. Chem.* **2000**, 112, 3750–3753.
- 77 T. S. REGER, K. D. JANDA, *J. Am. Chem. Soc.* **2000**, 122, 6929–6934.
- 78 S. C. BOURQUE, F. MALTAIS, W.-J. XIAO, *et al.*, *J. Am. Chem. Soc.* **1999**, 121, 3035–3038.

- 79 P. ARYA, N. V. RAO, J. SINGKHONRAT, *J. Org. Chem.* **2000**, 65, 1881–1885.
- 80 P. ARYA, G. PANDA, N. V. RAO, *et al.*, *J. Am. Chem. Soc.* **2001**, 123, 2889–2890.
- 81 Y. R. D. MIGUEL, E. BRULÉ, R. G. MARGUE, *J. Chem. Soc., Perkin Trans. I* **2001**, 3085–3094.
- 82 S. DAMMEN, S. BRÄSE, *Synthesis* **2001**, 1431.
- 83 T. MIZUGAKI, M. OOE, K. EBITANI, *et al.*, *J. Mol. Cat. A: Chem.* **1999**, 145, 329.
- 84 M. PETRUCCI-SAMIJA, V. GUILLEMETTE, M. DASGUPTA, *et al.*, *J. Am. Chem. Soc.* **1999**, 121, 1968–1969.
- 85 D. DEGROOT, P. G. EMMERINK, C. COUCKE, *et al.*, *Inorg. Chem. Commun.* **2000**, 3, 711.
- 86 P. WIJKENS, J. T. B. H. JASTRZEBSKI, P. A. V. SCHAAF, *et al.*, *Org. Lett.* **2000**, 2, 1621–1624.
- 87 S. B. GARBER, J. S. KINGSBURY, B. L. GRAY, *et al.*, *J. Am. Chem. Soc.* **2000**, 122, 8168–8179.
- 88 H. ZENG, G. R. NEWKOME, C. L. HILL, *Angew. Chem.* **2000**, 112, 1842–1844; *Angew. Chem. Int. Ed.* **2000**, 39, No. 10, 1771–1774.
- 89 D. SEEBACH, R. E. MARTI, T. HINTERMANN, *Helv. Chim. Acta* **1996**, 79, 1710–1740.
- 90 R. SCHNEIDER, C. KÖLLNER, I. WEBER, *et al.*, *Chem. Commun.* **1999**, 2415–2416.
- 91 C. KÖLLNER, B. PUGIN, A. TOGNI, *J. Am. Chem. Soc.* **1998**, 120, 10274–10275.
- 92 T. SUZUKI, Y. HIROKAWA, K. OHTAKE, *et al.*, *Tetrahedron: Asymmetry* **1997**, 8, 4033–4040.
- 93 I. SATO, T. SHIBATA, K. OHTAKE, *et al.*, *Tetrahedron Lett.* **2000**, 41, 3123–3126.
- 94 M. T. REETZ, D. GIEBEL, *Angew. Chem.* **2000**, 112, 2615–2617; *Angew. Chem. Int. Ed.* **2000**, 39, 2498–2501.

Note added in proof:

A remarkable dendritic effect in the Heck arylation of olefins by a dendrimer supported Pd-catalyst has recently reported by PORTNOY *et al.*: A. DAHAN, M. PORTNOY, *Org. Lett.* **2003**, 5, 1197–1200.

## 8

# Metathesis-Based Polymers for Organic Synthesis and Catalysis

MICHAEL R. BUCHMEISER

### 8.1

#### Introduction

The almost dramatic improvements in homogeneous catalysis have re-initiated intense research in the area of molecular heterogeneous catalysis. Taking advantage of the ongoing developments in key areas such as macromolecular and organometallic chemistry, efforts currently focus on the synthesis of catalytic supports that not only possess a well-defined and stable surface chemistry but also mimic the homogeneous analog. Such high definitions are nowadays basic requirements in heterogeneous catalysis since they allow the correlation of catalytic data obtained by heterogeneous catalysis with those retrieved under homogeneous conditions. Standard functionalization procedures of organic supports often used divergent synthetic approaches that entailed step-by-step transformations of surface-bound functional groups. As a result, ill-defined systems were obtained because such polymer transformations do not usually proceed quantitatively. Not surprisingly, catalyst poisoning and unwanted side reactions were associated with the use of these supports. The same applies to the area of polymer-supported organic reactions, nowadays under intense investigation in view of current applications in solid-phase synthesis, high-throughput screening and combinatorial chemistry. In this Chapter, the significant achievements in metathesis-based chemistry that have been made recently in the areas of homogeneous and heterogeneous catalysis, as well as in solid-phase synthesis, will be outlined and discussed in detail.

### 8.2

#### Polymeric Catalytic Supports Prepared by ROMP

##### 8.2.1

##### Precipitation Polymerization-based Techniques

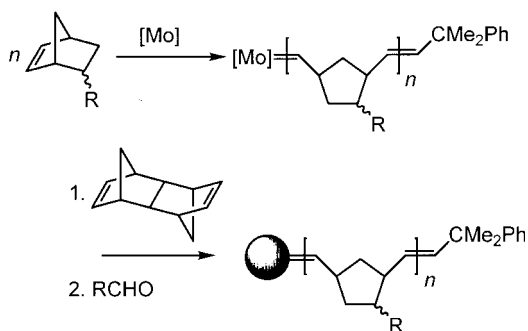
In order to fulfill the state of the art criteria of modern molecular heterogeneous catalysis, a conceptually new approach based on metathesis polymerization, that allows the synthesis of such supports by convergent synthetic route, starting from

functional monomers, has been developed. When well-defined initiators such as Schrock (typically of the general formula  $\text{Mo}(N\text{-}2,6\text{-R}_2\text{-C}_6\text{H}_3)(\text{CHCMe}_2\text{Ph})(\text{OR}')_2$ ) ( $\text{R}=\text{Me}$ ,  $i\text{-Pr}$ ,  $\text{R}'=\text{tert.-Bu}$ ,  $\text{CMe}(\text{CF}_3)_2$ , etc) or first and second generation Grubbs initiators ( $\text{Cl}_2\text{Ru}(\text{CHPh})(\text{PR}_3'')_2$ ,  $\text{Cl}_2\text{Ru}(\text{CHPh})(\text{NHC})(\text{PR}_3'')$ , ( $\text{R}''=\text{Ph}$ , cyclohexyl,  $\text{NHC}=\text{a } N\text{-heterocyclic carbene}$ ) are used [1–7], one gains access to a broad variety of polymeric architectures. In addition to the existing metathesis-based polymerization techniques ring-opening metathesis polymerization (ROMP), acyclic diene polymerization (ADMET) and 1-alkyne polymerization [5], ring-opening metathesis precipitation polymerization is an attractive technique for the synthesis of complex cross-linked architectures for various reasons. On the one hand, it comprises the possibility of polymerizing *functional monomers*, an almost unique property in view of the almost unlimited types of functional groups that may be introduced; on the other, the controlled, “living” polymerization mechanism [8] allows a highly flexible yet reproducible polymerization set-up in terms of molecular weights ( $M_w$ ,  $M_n$ ), polydispersity (PDI) and end groups.

Originally, ring-opening metathesis precipitation polymerization was developed for the synthesis of high-capacity cation exchange supports [9]. The synthetic concept is based on a living polymerization of a functional monomer, followed by addition of a cross-linker. By this approach, the functional group (i.e. the ligand) can be introduced without any change in its chemical nature, geometry or chirality. The living polymerization system must fulfill the criteria of a class VI living system according to Matyjaszewsky [10] for both the monomer and the cross-linker in order to obtain quantitative conversion and incorporation of the functional monomer into the support. The solvent system was designed so that the linear polymer chains precipitate *during* polymerization, prior to addition of the cross-linker. Depending on the polarity of the monomer,  $\text{CH}_2\text{Cl}_2$  or mixtures of  $\text{CH}_2\text{Cl}_2$  and diethyl ether were found to be appropriate. Upon addition of the cross-linker (e.g. 1,4,4a,5,8,8a-hexahydro-1,4,5,8-*exo-endo*-dimethanonaphthalene, DMN-H6), irregularly shaped polymer beads with a mean diameter of 40–60  $\mu\text{m}$  were prepared (Scheme 8.1) [11–15].

At the end of the reaction, the beads can be filtered off and used without sieving. Their size is ideal for their convenient removal at the end of any reaction by means of filtration. The molybdenum-based initiator can be removed quantitatively in a Wittig-type reaction by adding an aldehyde (e.g. ferrocene aldehyde) [1] and subsequently washing with aqueous base. As a consequence of the entire polymerization set-up and sequence, the linear polymer chains built from the functional monomer are located at the surface (or at least at the outer shell) of the beads. Degrees of polymerization up to 50 were found appropriate for these “tentacles. Upon addition of polar solvents such as THF or  $\text{CH}_2\text{Cl}_2$ , the beads show considerable swelling (20–65%), which directly translates into the data for the specific surface area ( $\sigma$ ). Thus, BET measurements of the dry material reveal values for  $\sigma \leq 30 \text{ m}^2 \text{ g}^{-1}$ , whereas inverse size exclusion chromatography (ISEC) [16, 17] in THF indicated specific surface areas of  $90 \text{ m}^2 \text{ g}^{-1}$ . Driven by the encouraging results obtained with dicarboxylate-based materials prepared by this concept, a variety of different dipyridyl-, respectively bis(pyrimidyl)-derivatized

**Scheme 8.1** Synthesis of cross-linked polymer beads via ring-opening metathesis precipitation polymerization.  $[\text{Mo}] = \text{Mo}(\text{N}-2,6\text{-i-Pr}_2\text{-C}_6\text{H}_3)(=\text{CHCMe}_2\text{Ph})(\text{OCMe}(\text{CF}_3)_2)_2$



supports have been prepared from norborn-2-ene- (NBE-) derived monomers containing ligands (1–6) [12–14, 18]. An overview over these ligands including applications is given in Tab. 8.1.

Typical amounts of the ligands immobilized onto the cross-linked support were in the range of  $0.03\text{--}1.0\text{ mmol g}^{-1}$ . Loading of these ligands with Pd (II) results in highly active supports for Pd-mediated C–C coupling reactions. The tentacle-type structure resulted in large amounts of functional groups being located at the surface. This ensured a fast mass transfer within the interphase [19]. In addition, the high selectivity of this ligand for Pd (II) [11] and its thermal and oxidative stability makes these supports attractive. Furthermore, the synthesis of monomeric, soluble analogs allows mechanistic correlations. Both the monomeric and the Pd-loaded supports were successfully used in Heck, Sonogashira-Hagihara and Suzuki-type couplings of aryl iodides and bromides as well as in the *N*-arylation of amines. The heterogeneous systems can be reused and are characterized by high turn-over numbers (TONs), typically in the range of  $10\,000\text{--}500\,000$ . In terms of stoichiometry, the amounts of Pd can be reduced to less than  $0.0003\text{ mol\%}$ , which illustrates the efficiency of these systems.

## 8.2.2

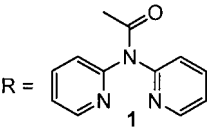
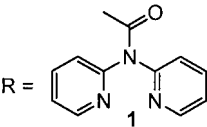
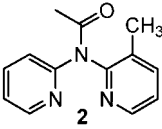
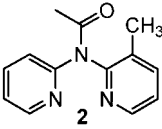
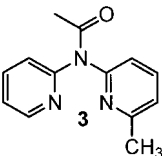
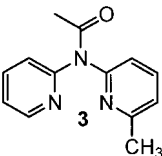
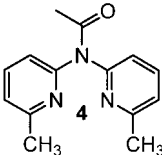
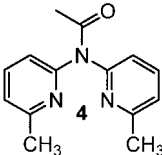
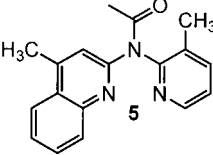
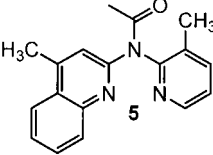
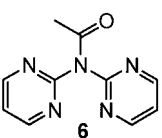
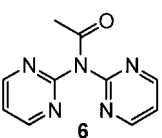
### Grafting Techniques

#### 8.2.2.1 Grafted Supports for Heck Reactions

As outlined above, *N,N*-dipyrid-2-ylnorborn-2-en-5-ylcarbamide can be polymerized in a living manner using well-defined Schrock initiators [11]. Thus, a class VI living system [10] is accomplished with  $\text{Mo}(\text{N}-2,6\text{-i-Pr}_2\text{-C}_6\text{H}_3)(\text{CHCMe}_2\text{Ph})(\text{CMe}(\text{CF}_3)_2)_2$ . Using norborn-2-ene surface functionalized silica, this monomer can be grafted thereon using a “grafting from” approach. In a first step, methyl-endcapped silica was reacted with the initiator. The surface-immobilized initiator was then used to generate tentacles of poly-*(N,N*-dipyrid-2-ylnorborn-2-en-5-ylcarbamide) with a controlled degree of polymerization (*DP*), typically  $<50$  (Scheme 8.2).

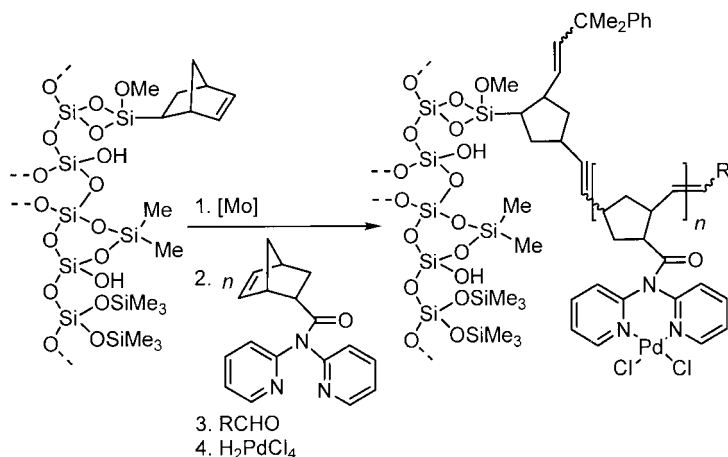
It is worth mentioning that the careful endcapping of silica with a mixture of  $\text{ClSiMe}_3$  and  $\text{Cl}_2\text{SiMe}_2$  eliminates any initiator deterioration caused by the interac-

Tab. 8.1 Overview over pyrid-2-yl- and pyrimid-2-yl-ligands used for immobilization.

Ligand (NBE-R)	Coupling reaction
 R = 	Heck Sonogashira-Hagihara
 R = 	Heck
 R = 	Heck
 R = 	Heck
 R = 	Heck
 R = 	Heck Sonogashira-Hagihara Suzuki

tion with the silanol groups. In addition, complete reaction of the initiator with the support as evidenced by the absence of any soluble polymer, was observed [20]. Not surprising,  $\text{Cl}_2\text{Ru}(\text{CHPh})(\text{PCy}_3)_2$  was not capable of polymerizing *N,N*-dipyrid-2-yl-norborn-2-en-5-ylcarbamide or its 7-oxa-analog because there is an irreversible coordination of the ligand to the ruthenium core. Pd-loading of the supports was simply accomplished by reaction with  $\text{H}_2\text{PdCl}_4$ . Within a few hours, a quantitative reaction was observed resulting in slightly yellow-colored supports. Values of 0.28 mmol and 0.08 mmol Pd  $\text{g}^{-1}$ , respectively, were achieved. The corresponding supports were



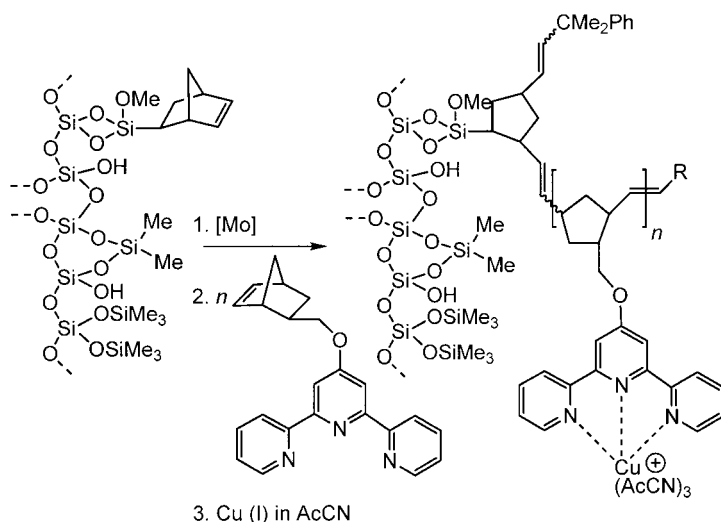


**Scheme 8.2** Surface-grafting of N,N-dipyrid-2-ylnorborn-2-en-5-ylcarbamide on silica.

again successfully used in a variety of Heck reactions including slurry reactions under standard as well as under microwave conditions. Removal of the support was again accomplished by filtration. In particular the use of microwave lead to a drastic reduction of reaction times, which is of particular interest for applications in high-throughput screening (HTS). TOFs were typically in the range of  $0.1\text{--}0.3\text{ s}^{-1}$ . Alternatively, silica-based materials were used as reaction columns as employed in HTS machines. Such columns can be loaded with the substrates of interest, and, after complete reaction, simply eluted with a suitable solvent, leaving the catalyst behind, and analyzed by a high throughput method, e.g. GC/MS. Quantitative conversion was achieved with iodoarenes, while even activated bromarenes require prolonged reaction times. Finally, catalyst-filled cartridges were created where the surface-derivatized silica was packed into stainless steel columns. These devices were used in reactions as flow-through columns. As for monolith-based supports (*see below*), a constant conversion of iodobenzene with styrene (70–80%) was observed over several hours. TOFs were in the range of  $0.06\text{--}0.07\text{ s}^{-1}$ . Nevertheless, this value was clearly lower than that obtained with monolithic columns, illustrating the superiority of the latter ones (*see below*). In all these experiments, irrespective of the application, only minor amounts of Pd, typically less than 2.5%, were leached into the reaction mixture [21].

#### 8.2.2.2 Grafted Supports for ATRP

4'-(Norborn-2-en-5-ylmethylenoxy)terpyridine can be polymerized by ROMP. The polymerization fulfilled the requirement of a class V living system [10]. The corresponding surface-grafted support was prepared applying a grafting-from approach as described above (Scheme 8.3) [20].



**Scheme 8.3** Surface grafting of 4'-(norborn-2-en-5-ylmethylenoxy)terpyridine on silica.

Briefly, norbornene-derivatized silica was first reacted with  $\text{Mo}(N\text{-}2,6\text{-}i\text{-Pr}_2\text{-C}_6\text{H}_3)(\text{CHCMe}_2\text{Ph})(\text{OCMe}(\text{CF}_3)_2)_2$ , followed by 4'-(norborn-2-en-5-ylmethylenoxy)terpyridine). Loading with Cu (I) afforded the desired ATRP support [18, 22–24]. Typical metal loadings were in the range of  $15 \text{ mmol g}^{-1}$ . Polystyrene (PS) obtained with these supports under ATRP-conditions showed comparably low polydispersities ( $\text{PDI}=1.55\text{--}1.77$ ). The ATRP system consisted of a metal center with one terpyridyl and presumably three acetonitrile ligands, which were at least in part substituted by monomer. Consequently, in contrast to standard systems [25], the equilibrium  $\text{M}^{n+}/\text{M}^{n+1}$  in this type of reaction did not require conformational changes or dissociation of a terpyridyl ligand. Therefore, polymerization proceeded comparably fast within two hours. Unfortunately, presumably because equilibria involving the dormant species were unfavorable, polymer yields were low ( $<35\%$ ).

### 8.2.2.3 Grafted Supports for Ring-closing Metathesis (RCM) and Related Reactions

The capability of ROMP of polymerizing even complex functional monomers was demonstrated by the fact that the cationic NHC-precursor 1,3-di(1-mesityl)-4-[[[bicyclo[2.2.1]hept-5-en-2-ylcarbonyl]oxy]methyl]-4,5-dihydro-1H-imidazol-3-ium tetrafluoroborate can be polymerized using both ruthenium and molybdenum-based initiators. Thus, reaction of this monomer with  $\text{Cl}_2\text{Ru}(\text{CHPh})(\text{PCy}_3)_2$  in methylene chloride at  $45^\circ\text{C}$  resulted in complete consumption of the initiator and formation of an oligomer with a  $\text{DP}$  of 7. Alternatively, polymerizations with the Schrock initiator  $\text{Mo}(N\text{-}2,6\text{-}i\text{-Pr}_2\text{-C}_6\text{H}_3)(\text{CHCMe}_2\text{Ph})(\text{OCMe}(\text{CF}_3)_2)_2$  [26] were performed in methylene chloride at ambient temperature. The theoretical  $\text{DP}$  of 7 was in excellent accordance with a  $\text{DP}$  of  $7 \pm 1$  found *via* endgroup analysis using

$^1\text{H}$  NMR. An endgroup suitable for oligomer grafting on silica was introduced by reacting the living polymer with an excess of  $\omega$ -(triethoxysilyl)propylisocyanate (Scheme 8.4).

Next, telechelic oligo-(1,3-di(1-mesityl)-4-[[bicyclo[2.2.1]hept-5-en-2-ylcarbonyl-oxy]methyl]-4,5-dihydro-1*H*-imidazol-3-ium tetrafluoroborate) was reacted with silica. Reaction of the grafted supports with KO-*t*Bu in THF at  $-30^\circ\text{C}$  yielded the free carbene which was subsequently reacted with  $\text{Cl}_2\text{Ru}(\text{CHPh})(\text{PCy}_3)_2$  to yield the immobilized second generation Grubbs catalyst [27]. The ruthenium content of the solution as measured by inductively coupled plasma-optical emission spectroscopy (ICP/OES) revealed catalyst loadings of 0.1–0.5 wt%. RCM carried out with diethyldiallylmalonate (DEDAM) as a benchmark gave TONs  $\leq 80$  for a stirred batch. No catalyst bleeding was observed, thus offering access to virtually metal free products.

#### 8.2.2.4 Other Grafted Supports

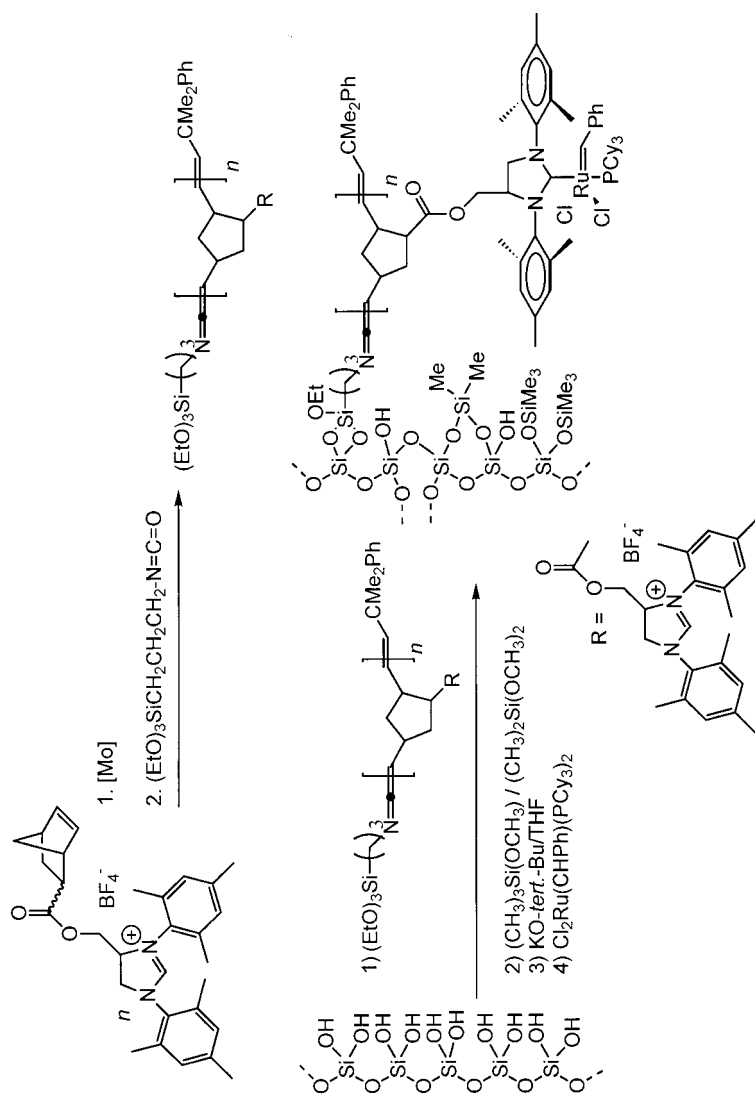
Barrett and coworkers reported on the synthesis of ROMP spheres for use in combinatorial chemistry [28]. These were synthesized by reaction of vinyl-PS-DVB with a low degree of cross-linking with  $\text{Cl}_2\text{Ru}(\text{=CHPh})(\text{PCy}_3)_2$  to form the immobilized catalytic species. Finally, reaction with norborn-2-en-5-ylmethyl 4-bromobenzoate gave the corresponding support with loadings up to 3 mmol of functional monomer per gram resin (Scheme 8.5). Swelling properties were similar to those materials prepared by ring-opening metathesis precipitation polymerization.

### 8.2.3

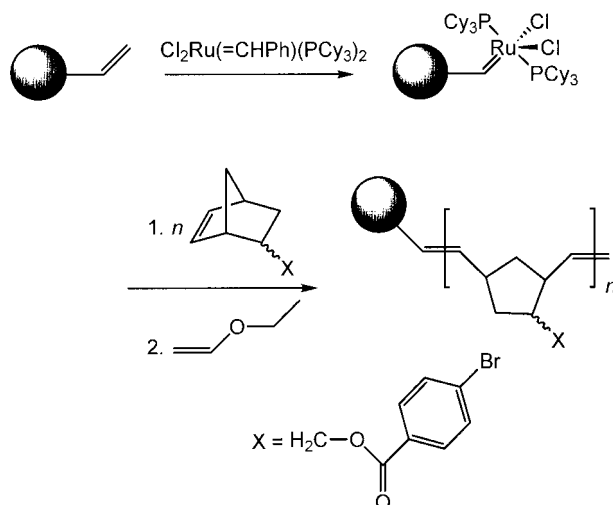
#### Coating Techniques

##### 8.2.3.1 Heck Supports Based on Coated Silica

Coating techniques offer a straightforward access to cheap materials. These materials are generally prepared by depositing a more or less homogeneous polymer layer on the support of choice. Though such surface-coated materials are easy to make and in addition highly stable versus acids or bases, the inhomogeneous polymer distribution [29–31] as well as the restricted access to the catalytic centers in particular in the case where these are located within micro- and mesopores certainly present an impediment. In order to investigate the general applicability of these coating techniques to the synthesis of metathesis-based heterogeneous catalytic supports, poly-(*N,N*-dipyrid-2-ylnorborn-2-en-5-ylcarbamide) was prepared and deposited onto silica applying standard coating techniques [32]. Loading with Pd resulted in a support containing 0.02 mmol Pd. In general, the amounts of metal immobilized on silica were sufficiently high for any of the applications of interest. Slurry-type Heck-type reactions were successfully carried out under both standard and microwave conditions. In addition, these materials can be filled in cartridges and used in form of reaction columns [21].



**Scheme 8.4** Grafting of isocyanate-telechelic poly(1,3-di(1-mesityl)-4-[(bicyclo[2.2.1]hept-5-en-2-ylcarbonyl)oxy]methyl)-4,5-dihydro-1H-imidazol-3-ium tetrafluoroborate) on silica and generation of the immobilized second generation Grubbs catalyst.



**Scheme 8.5** Synthesis of ROMP-spheres used for combinatorial chemistry.

#### 8.2.3.2 ATRP Supports Based on Coated Silica

Similar to the synthesis of Heck supports, silica was treated with solutions of poly(4'-(norborn-2-en-5-ylmethylenoxy)terpyridine) under evaporative conditions. Reaction with  $\text{CuBr} \times \text{Me}_2\text{S}$  and  $\text{Cu}(\text{OAc})_2 \times \text{H}_2\text{O}$ , respectively, gave the corresponding Cu-loaded supports. As observed for grafted ATRP supports, the monografted initiator resulted in comparably fast polymerizations. Using this system, PS was prepared up to a  $M_w$  of 80000. Again, polymer yields were in the range of 35%. The polymers are virtually metal-free, determined by atom absorption spectroscopy (AAS), which revealed a metal content of less than  $100 \text{ ng g}^{-1}$  [18, 22–24].

#### 8.2.3.3 RCM Supports Based on Coated Silica

Complementary to the above-mentioned grafting approach, coating techniques [32] using oligo-(1,3-di(1-mesityl)-4-[[bicyclo[2.2.1]hept-5-en-2-ylcarbonyl]oxy]methyl)-4,5-dihydro-1H-imidazol-3-ium tetrafluoroborate) where applied, leading to a surface-derivatized silica 60 containing 0.09 mmol of NHC precursor. Conversion into the initiator was carried out as described for the grafted analog, resulting in a support containing  $4.1 \mu\text{mol}$  ruthenium per gram. Good results were obtained with these coated supports in the RCM of DEDAM, 1,7-octadiene and diallylether. Thus, TONs were 210, 55 and 16, respectively, for these compounds under batch conditions. In all cases, ruthenium measurements by means of ICP/OES revealed quantitative retention of the original amount of ruthenium at the support within experimental error, thus offering an attractive access to metal free products [27].

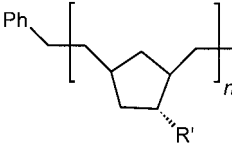
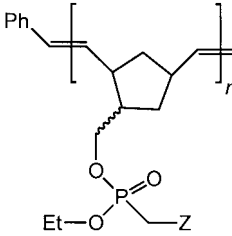
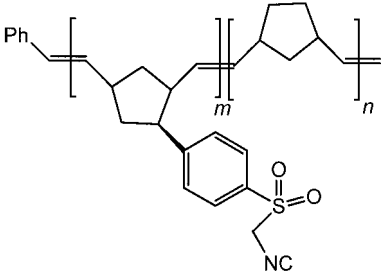
## 8.3

## ROMPgels and Other Functional Metathesis-based Polymers

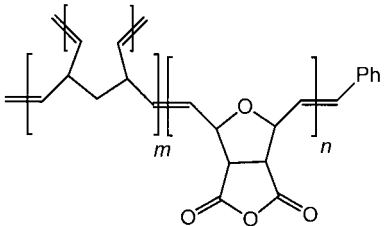
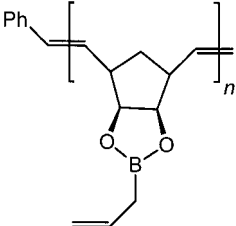
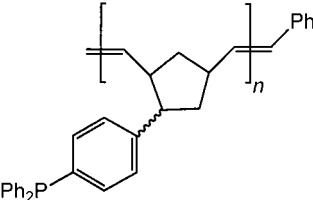
A variety of linear or cross-linked norborn-2-en-5-yl-derived polymers was prepared by Barrett [33–38], Bolm [39–41] and Buchmeiser *et al.* [21]. Barrett created the term “ROMPgels” for linear polymers, which swell, but do not dissolve, in certain solvents because solubility restrictions are governed by the nature of the functional monomer used. “ROMPgels” have been prepared with a variety of different functional groups including phosphines [33], allylboronates [34], a polymeric Tosmic reagent [36], naphthalenes and biphenyls [38], alkylphosphonates [37], as well as anhydrides [35]. The latter was used as a scavenger for excess reagent. These functional polymers are summarized in Tab. 8.2, together with the corresponding application. In some cases, cross-linking was performed in order to obtain insoluble supports.

Similar to anhydride-bearing polymers, the synthesis of a poly(norborn-2-en-5-yl-methanol)-derived system, polymerized by a Grubbs catalyst after scavenging excess of reagent, was reported by Hanson (Tab. 8.3) [42, 43].

Tab. 8.2 Different types of ROMPgels introduced by Barrett *et al.*

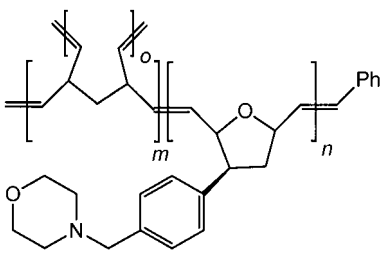
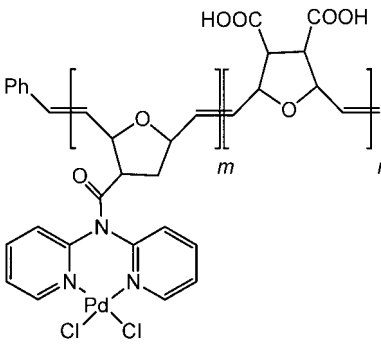
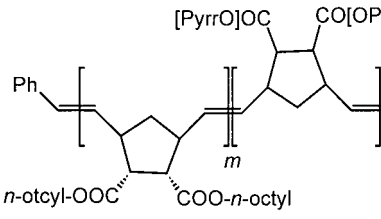
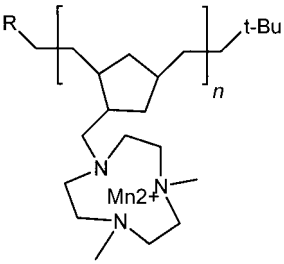
Polymer	Reaction (mode)
	Reductive lithiation R' = biphen-4-yl, naph-2-yl (homogeneous)
	Horner-Emmons Z = CO <sub>2</sub> Et, CN (heterogeneous)
	Oxazole synthesis – Tosmic route (heterogeneous)

Tab. 8.2 (cont.)

Polymer	Reaction (mode)
	Scavenger (heterogeneous)
	Allylboration DMN-H6-crosslinked (heterogenous)
	Halide synthesis reduction of ozonides isomerization reactions Staudinger reaction (heterogeneous)

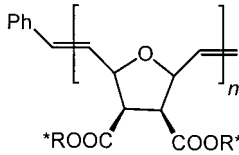
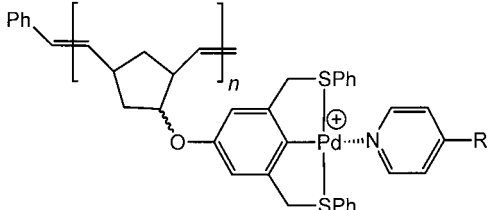
Catalytically active supports were described by Bolm and Buchmeiser *et al.* Bolm reported on the successful use of a ROMP-derived polymeric 1,4,7-triazacyclononane, which was used as a carrier in the Mn(II)-catalyzed epoxidation of alkenes as well as on polymeric, ROMP-derived chiral hydroxymethylpyridines and prolinols for asymmetric catalysis (Tab. 8.3) [39–41]. First and second generation Grubbs-type initiators were used throughout. In most cases, soluble polymers were prepared, which possess the enormous advantage that reactions can be carried out under homogeneous conditions without losing access to polymer separation, which is usually carried out by precipitation with methanol. Based on our results with dipyridylamido-Pd(II) systems for Heck couplings, a block-copolymer consisting of a poly(dicarboxylic acid) and a poly(dipyridylamido-Pd(II)) block was prepared by Buchmeiser *et al.* The latter was introduced by polymerizing the corresponding Pd (II) complex, *N,N*-bis(pyrid-2-yl)norborn-2-en-5-ylcarbamide PdCl<sub>2</sub>. Though polymerization of both the free ligand and the Pd (II) complex can be accomplished using a Schrock catalyst, poly(*N,N*-bis(pyrid-2-yl)norborn-2-en-5-ylcarbamide PdCl<sub>2</sub>) can also be prepared using a first generation Grubbs catalyst. In principle, the use of such a “ready to go” system eliminates any polymer transfor-

Tab. 8.3 ROMPgels and catalytic supports described by Hanson *et al.* and Bolm *et al.*

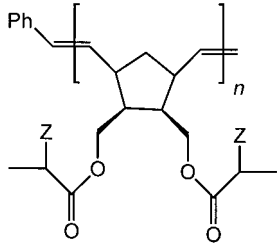
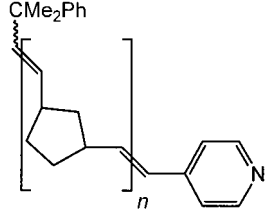
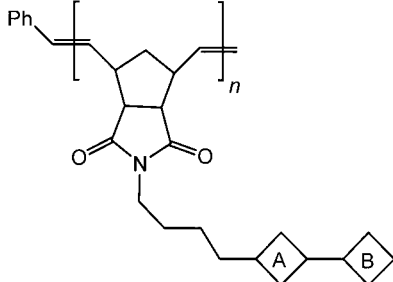
Polymer	Reaction (mode)
	Scavenger (heterogeneous)
	Heck (biphasic)
	Asymmetric catalysis (homogeneous)
	Alkene epoxidation (homogeneous)



Tab. 8.3 (cont.)

Polymer	Reaction (mode)
	Asymmetric catalysis (homogenous) R* = chiral ligand
	Heck reactions (homogeneous)

Tab. 8.4 Catalytically active ROMP-derived polymers reported by Enholm *et al.* and Nomura *et al.*

Polymer	Reaction (mode)
	Free radical allylation free radical reduction (homogeneous)
	Ru-catalyzed reduction (homogeneous)
	Diastereoselective radical cyclizations A = stereocontrol element B = substrate (homogeneous)

mation and provides maximum knowledge on the actual catalytic species. In terms of application, the corresponding block-copolymers were successfully used in biphasic Heck reactions [21]. A similar approach was reported by Weck *et al.*, using a terminally palladated S–C–S pincer complex (Tab. 8.3) [44]. Enholm *et al.* carried out free radical allylations and reductions on soluble ROMP-derived supports. The same group reported on diastereoselective radical cyclizations using a chiral ROMP-derived support (Tab. 8.4).

Taking advantage of the living character of ROMP, telechelic poly-NBE with a 4-pyridyl end group was prepared by Nomura *et al.* and successfully used in the homogeneous ruthenium-catalyzed catalytic reduction of 2-phenylacetaldehyde (Tab. 8.4) [45].

## 8.4

### Monolithic Catalytic Supports

Monolithic separation media evolved as a successful “joint-venture” between material and separation science. Based on theoretical reflections, the common idea was to produce a support with a high degree of continuity that would meet the requirements for fast, yet highly efficient separations [46, 47]. The first experiments into this direction were carried out in the 1960s and 1970s [48, 49], yet it took some 20 years to adapt this new technology to the area of heterogeneous catalysis. In the process of their evolution, these supports, usually referred to as monolithic supports, continuous beds or rigid rods [49], were successfully used in liquid chromatography including micro-separation techniques [50–56], capillary electrochromatography as well as solid-phase extraction (SPE) [57], focusing on medium and high molecular mass biopolymers [58], and even on low molecular mass analytes [59–62]. Quite recently, i. e. in 2001, Buchmeiser *et al.* developed a ROMP-based synthesis for these types of materials [63–67] and described the use of these supports in heterogeneous catalysis [21, 68].

#### 8.4.1

##### Basics and Concepts

Generally speaking, the term “monolith” applies to any single-body structure containing interconnected repeating cells or channels. Such materials may either be metallic or prepared from inorganic mixtures, e.g. by a sintering process to form ceramics [69], or from organic compounds, e.g. by a cross-linking polymerization [70]. In this chapter, the term “monolith” or “rigid rod” will comprise cross-linked, organic materials, which are characterized by a defined porosity and which support interactions/reactions between this solid and the surrounding liquid phase. Besides the advantages such as lower backpressure and enhanced mass transfer [71, 72], these materials demonstrate ease of fabrication and many possibilities in structural alteration.

A considerable variety of functionalized and nonfunctionalized monolithic materials based on either organic or inorganic polymers are already available. While in-

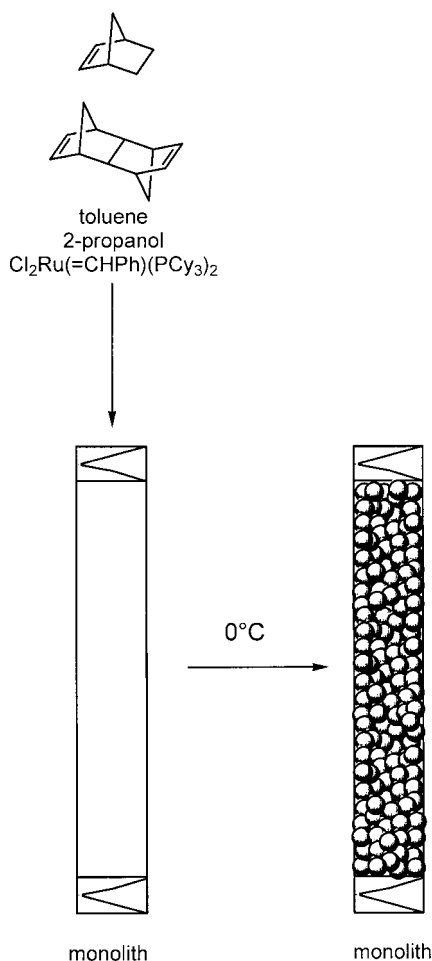
organic monoliths are usually based on silica and may conveniently be prepared *via* sol-gel techniques [59–62], organic continuous beds are mostly prepared from methacrylates or poly(styrene-*co*-divinylbenzene) [70, 73–76], almost exclusively by free radical polymerization. A profound insight into the technology of both sol-gel and free radical polymerization-based monoliths may be found in books particularly dedicated to this subject [77]. Despite the comparably poor control over free radical polymerization-based systems, the porosity and microstructure of monolithic materials have successfully been varied [70]. In contrast to the free radical process, Buchmeiser *et al.* confirmed the general applicability of a transition metal-based polymerization technique such as ROMP to the synthesis of high-performance monolithic separation media [64]. In fact this was accomplished by generating a continuous matrix by ring-opening metathesis copolymerization of suitable monomers with a cross-linker, in the presence of porogenic solvents within a device (column).

#### 8.4.2

##### Manufacture of Metathesis-based Monolithic Supports

The choice of a suitable initiator represents an important step in creating a well-defined polymerization system in terms of initiation efficiency and control over propagation. Only in the case where quantitative and fast initiation occurs, can the entire system be designed on a *stoichiometric basis*. This is of enormous importance, since for control of microstructure, the composition of the entire polymerization mixture needs to be varied within small increments. The catalyst needs to be carefully selected from both chemical and practical points of view. Generally, Schrock and Grubbs systems, both highly active in the ROMP of strained functionalized olefins, can be used. Since the preparation and in particular derivatization of ROMP-based rigid rods requires some handling that can hardly be performed under an inert atmosphere, the less oxygen-sensitive and less reactive ruthenium-based Grubbs-type initiators were used. Since  $\text{Cl}_2(\text{PPh}_3)_2\text{Ru}(=\text{CHPh})$  turned out to be too unreactive,  $\text{Cl}_2(\text{PCy}_3)_2\text{Ru}(=\text{CHPh})$  was used. In order to avoid any uncontrolled, highly exothermic reactions, second generation Grubbs catalyst were not used. Among the possible combinations of monomers and cross-linkers such as NBE, norbornadiene (NBDE), dicyclopentadiene (DCPD), 1,4,4a,5,8,8a-hexahydro-1,4,5,8-*exo-endo*-dimethanonaphthalene (DMN-H6), tris(norborn-2-en-5-yl-methylenoxy)methylsilane  $((\text{NBE}-\text{CH}_2\text{O})_3\text{SiCH}_3)$  and 1,4a,5,8,8a,9,9a,10,10a-decahydro-1,4,5,8,9,10-trimethanoanthracene, the copolymerization of NBE with DMN-H6 or  $(\text{NBE}-\text{CH}_2\text{O})_3\text{SiCH}_3$  in the presence of two porogenic solvents, e.g. 2-propanol and toluene, with  $\text{Cl}_2(\text{PCy}_3)_2\text{Ru}(=\text{CHPh})$  worked best (Scheme 8.6).

Scheme 8.6 Monolith synthesis.



## 8.4.3

**Microstructure of Metathesis-based Rigid Rods**

In order to understand monolithic supports and the effects of polymerization parameters, a brief description of the general construction of a monolith in terms of microstructure, backbone and relevant abbreviations is given in Fig. 8.1 [63, 64]. As can be deduced therefrom, monoliths consist of interconnected microstructure-forming microglobules, which are characterized by a certain diameter ( $d_p$ ) and microporosity ( $\varepsilon_p$ ). In addition, the monolith is characterized by an inter-microglobule void volume ( $\varepsilon_z$ ), which is mainly responsible for the backpressure at a certain flow rate. The sum of  $\varepsilon_p$  and  $\varepsilon_z$  directly translates into the total porosity  $\varepsilon_t$ .

The volume fractions of both micropores and voids (intermicroglobule porosity) represent the total porosity ( $\varepsilon_t$ ). This value, indicating a percentage of pores in the

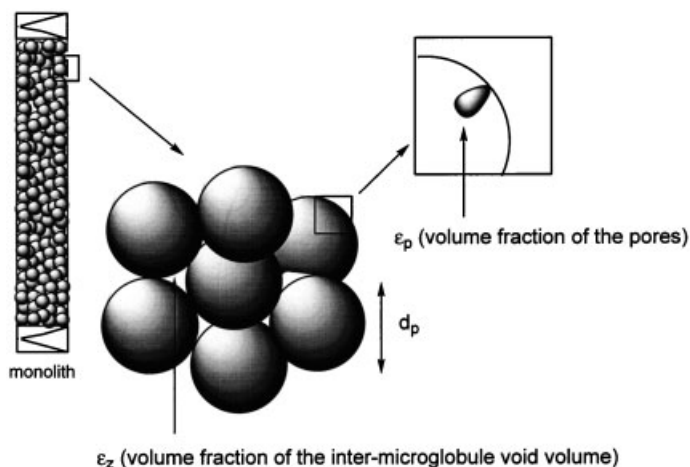


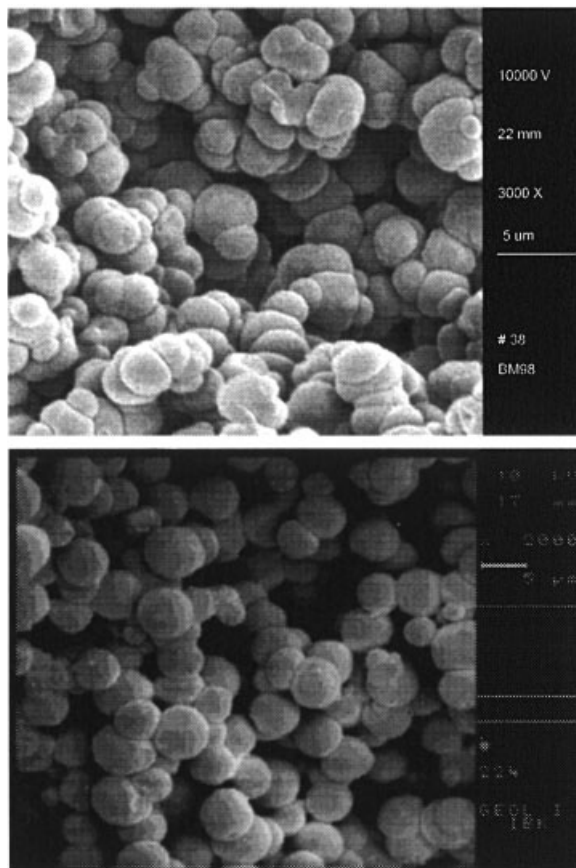
Fig. 8.1 General construction of a monolith.

monolith, together with the pore size distribution that can be calculated from inverse size exclusion chromatography (ISEC) data [17] or from mercury intrusion [78], on the one hand directly translates into a total pore volume  $V_p$ , expressed in  $\text{mL g}^{-1}$ , and on the other hand allows calculation of the specific surface area  $\sigma$ , expressed in  $\text{m}^2 \text{g}^{-1}$ . In order to design monolithic supports for different tasks, the influence of all variables, i. e. components of the polymerization mixture (NBE, DMN-H6 or  $(\text{NBE-CH}_2\text{O})_3\text{SiCH}_3$ ), solvents, free phosphine, initiator, and temperature on microstructure formation was investigated. The relative ratios of all components, i. e. NBE, DMN-H6, porogens and catalyst, allowed broad variations in the microstructure of the monolithic material including structures ideal for heterogeneous catalysis. In summary, the volume fraction of the interglobular void volume ( $\epsilon_z$ ) and total porosity ( $\epsilon_t$ ) were varied within a range of 0–50% and 50–80%, respectively. Fig. 8.2 illustrates some of the microstructures that were generated.

#### 8.4.4

##### Functionalization, Metal Removal and Metal Content

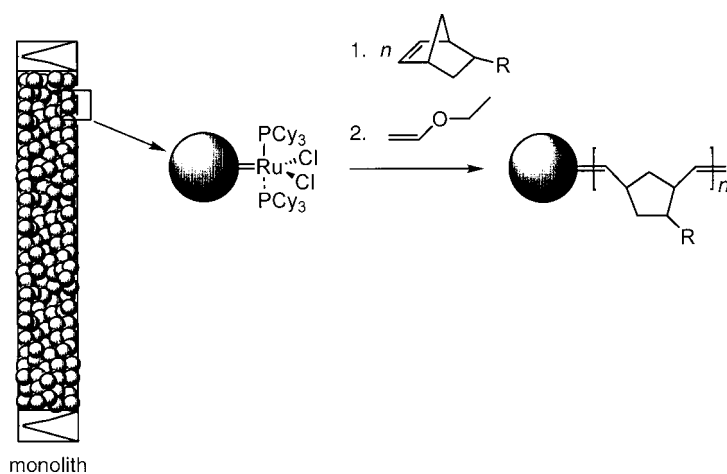
Using the ROMP-based protocol, functionalization can be achieved conveniently. In particular the “living” character [10, 79] of ruthenium-catalyzed polymerizations [80–83] and the high tolerance of the catalytic system towards different functional monomers made the ROMP approach very attractive. In fact, the active ruthenium-sites could be used for derivatization after rod-formation was complete. Investigations revealed that more than 98% of the initial amount of initiator was located at the microglobule surface after microstructure formation [68]. Using the initiator covalently bound to the surface, functional monomers were grafted onto the monolith surface by simply passing solutions thereof through the mold (Scheme 8.7) [63, 64].



**Fig. 8.2** Representative microstructures of monoliths used in heterogeneous catalysis.

Since no cross-linking can take place, again tentacle-like polymer chains attached to the surface were formed. In addition, microglobules were designed in a way that their pore size was  $<1.2$  nm, which basically restricted functionalization to their surface [67]. The degree of this graft polymerization of functional monomers varies within almost two orders of magnitude, depending on their ROMP activity. This approach offered multiple advantages. First, the structure of the “parent” monolith is not affected by the functional monomer and can be optimized regardless of the functional monomer used later. Secondly, solvents other than the porogens (e.g. methylene chloride, DMF) may be used for the *in situ* derivatization, depending on the solubility of the monomer. An overview over the different monomers that have already been grafted is given in Tab. 8.5.

Finally, when dealing with transition metal-catalyzed polymerizations, the efficiency of *metal removal* from the monolith after polymerization needs to be addressed. Investigations revealed that the remaining ruthenium concentrations



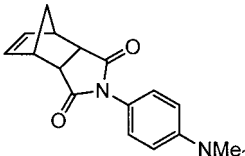
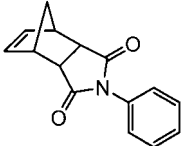
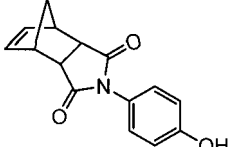
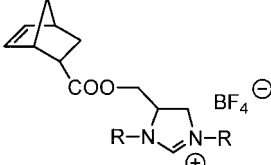
**Scheme 8.7** Surface-functionalization of a monolith.

**Tab. 8.5** Functional monomers used for surface-grafting of monolithic supports.

Monomer	mmol g <sup>-1</sup>
	0.2
	0.14
	0.03
	—

X = O, CH<sub>2</sub>

Tab. 8.5 (cont.)

Monomer	mmol g <sup>-1</sup>
	0.26
	0.22
	0.06
	0.002

after capping with ethylvinyl ether were below 10  $\mu\text{g g}^{-1}$ , corresponding to a metal removal of more than 99.8%.

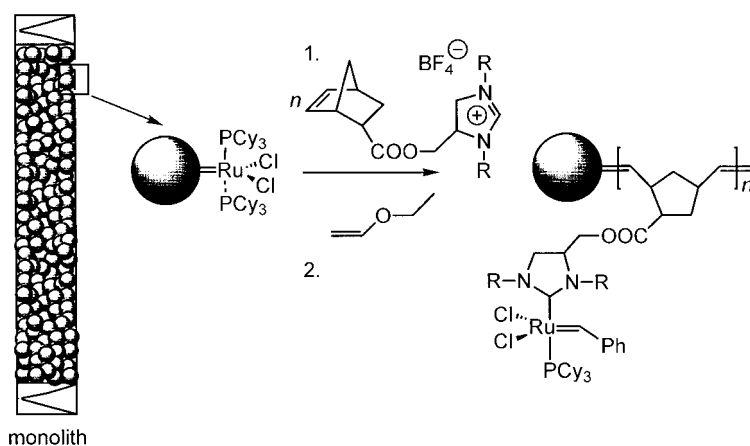
#### 8.4.5

#### Applications of Functionalized Metathesis-based Monoliths in Catalysis

##### 8.4.5.1 Grafted Supports for Ring-closing Metathesis (RCM) and Related Reactions

In heterogeneous catalysis, one wants to combine the general advantages of homogeneous systems such as high definition, activity, etc. with the advantages of heterogeneous catalysis such as increased stability, ease of separation, and recycling. So far, monolithic catalytic media have basically been restricted to metal oxides, porous metals and certain polysaccharides [84]. The first successful use of metathesis-based monolithic media for heterogeneous catalysis was accomplished by using these supports as carriers for Grubbs-type initiators based on *N*-heterocyclic carbenes (NHC-ligands) [85, 86]. In order to generate a sufficient porosity, monoliths with a suitable microporosity (40%) and microglobule diameter ( $1.5 \pm 0.5 \mu\text{m}$ ) were synthesized. Consecutive *in situ* derivatization was successfully accomplished using a mixture of norborn-2-ene and 1,3-di(1-adamantyl)-4-[[bi-



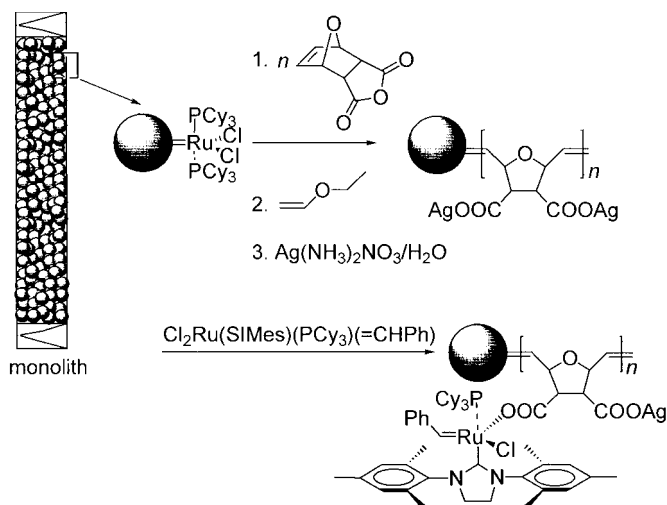


**Scheme 8.8** Synthesis of a monolith-supported second generation catalyst immobilized via the NHC-ligand. R=adamantyl, mesityl.

cyclo[2.2.1]hept-5-en-2-yl-carbonyl]oxy]methyl]-4,5-dihydro-1*H*-imidazol-3-ium tetrafluoroborate in methylene chloride (Scheme 8.8) [68].

The use of norborn-2-ene drastically enhanced grafting yields for the functional monomer. Using this setup, tentacles of copolymer with a degree of oligomerization of 2–5 of the functional monomer were generated. The free NHC necessary for catalyst formation was simply generated using a strong base such as 4-dimethylaminopyridine (DMAP). In a last step, excess base was removed by extensive washing and the catalyst was immobilized/formed by passing a solution of  $\text{Cl}_2\text{Ru}(\text{CHPh})(\text{PCy}_3)_2$  over the rigid rod. Loadings of up to 1.4% of Grubbs-catalyst on NHC base were achieved. Monolith-immobilized metathesis catalysts prepared by this approach showed high activity in various metathesis-based reactions such as ROMP and RCM. The *cis/trans* ratios of polymers (90%) exactly corresponded to the ones found with analogous homogeneous systems. The use of chain-transfer agents (CTAs, e.g. *cis*-1,4-diacetoxybut-2-ene, diethyldiallylmalonate, 2-hexene) allowed the regulation of molecular mass, in particular in the case of cyclooctene. The presence of CTAs additionally enhanced the lifetime of the catalytic centers by reducing the average lifetime of the ruthenium methylidenes, thus allowing the prolonged use of these systems. Additionally, both the tentacle-type structure and the designed microstructure of the support reduced diffusion to a minimum. In a benchmark reaction with DEDAM, these properties directly translated into high average turn-over frequencies (TOFs) of up to  $0.5 \text{ s}^{-1}$ , thus exceeding even the homogeneous analog ( $\text{TOF} = 0.07 \text{ s}^{-1}$ ;  $45^\circ\text{C}$ ) [87].

Alternatively, monolith-supported second generation Grubbs catalysts containing unsaturated (e.g. IMes) or saturated (e.g. SIMes) NHCs [5] can be prepared by a synthetic protocol summarized in Scheme 8.9. Surface-derivatization of a monolith was carried out with 7-oxanorborn-2-enedicarboxylic anhydride followed by conversion of the grafted poly(anhydride) into the corresponding poly-silver salt.



**Scheme 8.9** Synthesis of a monolith-supported second-generation catalyst immobilized via a carboxylate ligand.

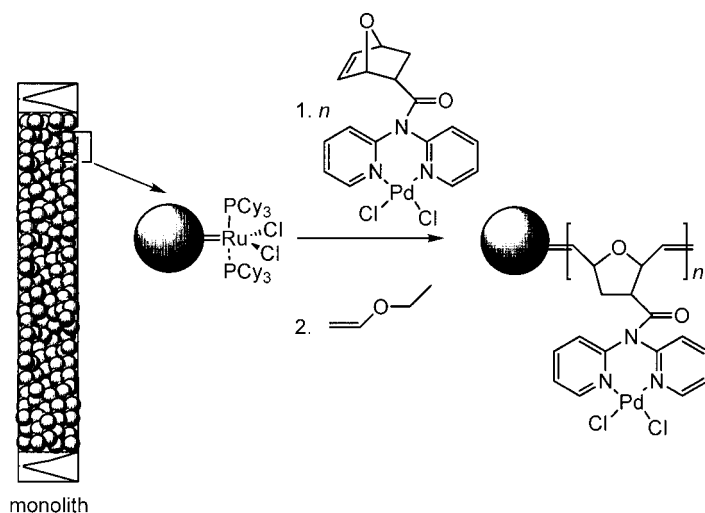
This silver salt was used for the halogen exchange with a broad variety of second generation Grubbs catalysts, leading to the catalytic species shown in Scheme 8.9. In the benchmark reaction with DEDAM, TONs up to 830 were achieved [88].

All monolith-based catalytic systems summarized here were successfully used as pressure stable catalytic reactors. Bleeding was virtually suppressed, leading even in RCM to basically ruthenium-free products with a ruthenium-content far below 0.1%.

#### 8.4.5.2 Poly-(*N,N*-dipyrid-2-yl-7-oxanorborn-2-en-5-ylcarbamido · $\text{PdCl}_2$ )-grafted Monolithic Supports for Heck Reactions

As outlined for the synthesis of heterogeneous metathesis catalysts, a grafting-from approach was used for the immobilization of dipyridylamide ligands. A completely new approach was elaborated for monolith-functionalization with ruthenium and pyridyl ligands, because they are incompatible. Since the lone pair needed to be prevented from coordinating to the ruthenium core, the preformed complex, *N,N*-dipyrid-2-yl-7-oxanorborn-2-en-5-ylcarbamido palladium dichloride, was grafted onto a monolith using norborn-2-ene as a comonomer (Scheme 8.10).

Grafted monoliths contained  $7\text{ }\mu\text{mol}$  (0.07%) Pd. In a model reaction between styrene and iodobenzene, TOFs of  $1.2\text{--}1.6\text{ s}^{-1}$  were found. These figures clearly exceed those obtained with supports prepared by ring-opening metathesis precipitation polymerization, which gave TOFs of  $0.35\text{ s}^{-1}$  in identical reactions [12]. Pd-leaching was generally low (2.2% total over 10 h). Alternatively, if used as a cartridge, amounts of reactants typical in combinatorial chemistry (50–100 mg in total) were converted in satisfactory yields (<80%) [21].



**Scheme 8.10** Synthesis of a monolith-supported Pd-catalyst.

#### 8.4.5.3 Poly-(*N,N*-dipyrid-2-yl-7-oxanorborn-2-en-5-ylcarbamido · PdCl<sub>2</sub>)-coated Monolithic Supports for Heck Reactions

Alternatively, a coating procedure using poly(*N,N*-di(pyrid-2-yl)norborn-2-ene-5-ylcarbamide) followed by reaction with H<sub>2</sub>PdCl<sub>4</sub> was developed and found applicable to the modification of monolithic supports. Monolithic supports were surface-coated with poly(*N,N*-di(pyrid-2-yl)norborn-2-ene-5-ylcarbamide) [63, 64, 67, 68]. Subsequent loading with Pd (II) resulted in supports containing 0.031 mmol (0.33%) Pd. Such supports were used in form of closed cartridges for HTS or as flow through reactors. Model reactions between iodobenzene and styrene were carried out in tributylamine without any additional solvent using a flow-through setup. At temperatures of 140 °C and 170 °C respectively, solvent-free mixtures of iodobenzene, styrene and NBU<sub>3</sub> were constantly converted into stilbene over a period of three hours. Constant TOFs of 0.3–0.4 s<sup>-1</sup> were found [21], which are comparable to those obtained with supports prepared by ring-opening metathesis precipitation polymerization (TOF=0.35 s<sup>-1</sup>) [12].

## 8.5

### Conclusion, Summary and Outlook

Metathesis-based reactions have gained a strong place among the most important C–C coupling reactions. Furthermore, metathesis-based polymerization techniques have become one of the most powerful, if not the most powerful, techniques for the synthesis of functionalized inorganic and organic supports for an almost unlimited variety of reactions. In view of the ongoing developments in catalyst design, mechanistic understanding and materials science, one can in fact expected a lot of additional significant contributions to organic synthesis and catalysis in future.

## 8.6

## Acknowledgement

Our work was supported by grants of the *Austrian Science Fund* (projects P-12963-GEN, START Y-158), the *österreichische Nationalbank* (project 789), the *University of Innsbruck*, the *Industriellenvereinigung Tirol* and the *European Commission* (contracts F14W-CT96-0019 and FIS 1999-00130). I wish to thank all my students and post-graduate students involved in the work described in this Chapter for their dedication and enthusiasm.

## 8.7

## References

- 1 R. R. SCHROCK, *Acc. Chem. Res.* **1986**, *19*, 342–368.
- 2 T. M. TRNKA, R. H. GRUBBS, *Acc. Chem. Res.* **2001**, *34*, 18–29.
- 3 R. R. SCHROCK, in *Ring-Opening Polymerization*, (ed. D. J. BRUNELLE), Hanser, Munich, **1993**, p. 129.
- 4 R. R. SCHROCK, *Polyhedron* **1995**, *14*, 3177–3195.
- 5 M. R. BUCHMEISER, *Chem. Rev.* **2000**, *100*, 1565–1604.
- 6 R. R. SCHROCK, *Chem. Rev.* **2002**, *102*, 14–179.
- 7 R. R. SCHROCK, *J. Chem. Soc., Dalton Trans.* **2001**, 2541–2550.
- 8 T. R. DARLING, T. P. DAVIS, M. FRYD *et al.*, *J. Polym. Sci. A: Polymer Chem.* **2000**, *38*, 1706–1708.
- 9 M. R. BUCHMEISER, N. ATZL, G. K. BONN, *J. Am. Chem. Soc.* **1997**, *119*, 9166–9174.
- 10 K. MATYJASZEWSKI, *Macromolecules* **1993**, *26*, 1787–1788.
- 11 F. SINNER, M. R. BUCHMEISER, R. TESSADRI, *et al.*, *J. Am. Chem. Soc.* **1998**, *120*, 2790–2797.
- 12 M. R. BUCHMEISER, K. WURST, *J. Am. Chem. Soc.* **1999**, *121*, 11101–11107.
- 13 J. SILBERG, T. SCHAREINA, R. KEMPE, *et al.*, *J. Organomet. Chem.* **2000**, *622*, 6–18.
- 14 M. R. BUCHMEISER, T. SCHAREINA, R. KEMPE, *et al.*, *J. Organomet. Chem.* **2001**, *634*, 39–46.
- 15 M. R. BUCHMEISER, *Bioorg. Med. Chem. Lett.* **2002**, *12*, 1837–1840.
- 16 I. HALÁSZ, K. MARTIN, *Ber. Bunsenges. Phys. Chem.* **1975**, *79*, 731–732.
- 17 I. HALÁSZ, K. MARTIN, *Angew. Chem.* **1978**, *90*, 954–961; *Angew. Chem. Int. Ed.* **1978**, *17*, 901–909.
- 18 M. R. BUCHMEISER, R. KRÖLL, K. WURST, *et al.*, in *Makromol. Symp. (Tailormade Polymers)*, Vol. 164 (eds. H.-J. P. ADLER, K.-F. ARNDT, D. KUCKLING, *et al.*), **2001**, pp. 187–196.
- 19 E. LINDNER, T. SCHNELLER, F. AUER, *et al.*, *Angew. Chem.* **1999**, *111*, 2288–2309; *Angew. Chem. Int. Ed.* **1999**, *38*, 2154–2174.
- 20 M. R. BUCHMEISER, F. SINNER, M. MUPA, *et al.*, *Macromolecules* **2000**, *33*, 32–39.
- 21 M. R. BUCHMEISER, S. LUBBAD, M. MAYR, *et al.*, *Inorg. Chim. Acta* **2003**, in press.
- 22 U. S. SCHUBERT, C. S. ESCHBAUMER, C. SCHWAIG, *et al.*, *German Pat. Appl. DE 100 13 305.3–44* (170300)
- 23 R. KRÖLL, C. ESCHBAUMER, U. S. SCHUBERT, *et al.*, *Macromol. Chem. Phys.* **2001**, *202*, 645–653.
- 24 U. S. SCHUBERT, C. H. WEIDL, C. ESCHBAUMER, *et al.*, *Polym. Mater. Sci. Eng.* **2001**, *84*, 514–515.
- 25 K. MATYJASZEWSKI, J. XIA, *Chem. Rev.* **2001**, *101*, 2921–2990.
- 26 J. H. OSKAM, H. H. FOX, K. B. YAP, *et al.*, *J. Organomet. Chem.* **1993**, *459*, 185–197.
- 27 M. MAYR, M. R. BUCHMEISER, K. WURST, *Adv. Synth. Catal.* **2002**, *355*, 712–719.
- 28 A. G. M. BARRETT, S. M. CRAMP, R. S. ROBERTS, *ORG. LETT.* **1999**, *1*, 1083–1086.
- 29 A. KURGANOV, O. KUZMENKO, V. A. DAVANKOV, *et al.*, *J. Chromatogr.* **1990**, *506*, 391–400.

- 30 M. HANSON, B. ERAY, K. UNGER, *et al.*, *Chromatographia* **1993**, 35, 403.
- 31 M.R. BUCHMEISER, *J. Chromatogr. A* **2001**, 918/2, 233–266.
- 32 M.R. BUCHMEISER, M. MUPA, G. SEEBER, *et al.*, *Chem. Mater.* **1999**, 11, 1533–1540.
- 33 E. RSTAD, A.G.M. BARRETT, B.T. HOPKINS, *et al.*, *Org. Lett.* **2002**, 4, 1975–1977.
- 34 T. ARNAULD, A.G.M. BARRETT, R. SEIFRIED, *Tetrahedron Lett.* **2001**, 42, 7899–7901.
- 35 T. ARNAULD, A.G.M. BARRETT, S.M. CRAMP, *et al.*, *Org. Lett.* **2000**, 2, 2663–2666.
- 36 A.G.M. BARRETT, S.M. CRAMP, A.J. HENNESSY, *et al.*, *Org. Lett.* **2001**, 3, 271–273.
- 37 A.G. BARRETT, S.M. CRAMP, R.S. ROBERTS, *et al.*, *Org. Lett.* **1999**, 1, 579–582.
- 38 T. ARNAULD, A.G.M. BARRETT, B.T. HOPKINS, *Tetrahedron Lett.* **2002**, 43, 1081–1083.
- 39 C. BOLM, C.L. DINTNER, A. SEGER, *et al.*, *J. Org. Chem.* **1999**, 64, 5730–5731.
- 40 A. GRENZ, S. CECCARELLI, C. BOLM, *Chem. Commun.* **2001**, 1726–1727.
- 41 C. BOLM, C. TANYELI, A. GRENZ, *et al.*, *Adv. Synth. Catal.* **2002**, 344, 649–656.
- 42 J. D. MOORE, A.M. HARNED, J. HENLE, *et al.*, *Org. Lett.* **2002**, 4, 1847–1849.
- 43 A.M. HARNED, P.R. HANSON, *Org. Lett.* **2002**, 4, 1007–1010.
- 44 J.M. POLLINO, M. WECK, *Org. Lett.* **2002**, 4, 753–756.
- 45 K. NOMURA, H. OGURA, Y. IMANISHI, *J. Mol. Catal. A: Chem.* **2002**, 185, 311–316.
- 46 N.B. AFEYAN, N.F. GORDON, I. MAZSAROFF, *et al.*, *J. Chromatogr.* **1990**, 519, 1.
- 47 N.B. AFEYAN, S.P. FULTON, F.E. REGNIER, *J. Chromatogr.* **1991**, 544, 267–279.
- 48 M. KUBIN, P. SPACEK, R. CHROMECEK, *Collect. Czech. Chem. Commun.* **1967**, 32, 3881–3887.
- 49 L. C. HANSEN, R.E. SIEVERS, *J. Chromatogr.* **1974**, 99, 123–133.
- 50 K. HOSOYA, H. OHTA, K. YOSHIZOKA, *et al.*, *J. Chromatogr. A* **1999**, 853, 11–20.
- 51 A. MARUSKA, C. ERICSON, A. VÉGVÁRI, *et al.*, *J. Chromatogr. A* **1999**, 837, 25–33.
- 52 I. GUSEV, X. HUANG, C. HORVÁTH, *J. Chromatogr. A* **1999**, 855, 273–290.
- 53 Q. TANG, B. XIN, M.L. LEE, *J. Chromatogr. A* **1999**, 837, 35–50.
- 54 R. ASIAIE, X. HUANG, D. FARNAN, *et al.*, *J. Chromatogr. A* **1998**, 806, 251–263.
- 55 E.C. PETERS, M. PETRO, F. SVEC, *et al.*, *Anal. Chem.* **1997**, 69, 3646–3649.
- 56 E.C. PETERS, M. PETRO, F. SVEC, *et al.*, *Anal. Chem.* **1998**, 70, 2288–2295.
- 57 S. XIE, F. SVEC, J.M.J. FRÉCHET, *Chem. Mater.* **1998**, 10, 4072–4078.
- 58 J.A. GERSTNER, R. HAMILTON, S.M. CRAMER, *J. Chromatogr.* **1992**, 596, 173–180.
- 59 N. TANAKA, H. NAGAYAMA, H. KOBAYASHI, *et al.*, *J. High Resol. Chromatogr.* **2000**, 23, 111–116.
- 60 F. RABEL, K. CABRERA, D. LUBDA, *Int. Lab.* **2001**, 01/02, 23–25.
- 61 K. CABRERA, K. SINZ, D. CUNNINGHAM, *Int. Lab. News* **2001**, 02, 12–13.
- 62 K. CABRERA, D. LUBDA, H.-M. EGGENWEILER, *et al. nishi*, *J. High Resol. Chromatogr.* **2000**, 23, 93–99.
- 63 F. SINNER, M.R. BUCHMEISER, *Macromolecules* **2000**, 33, 5777–5786.
- 64 F. SINNER, M.R. BUCHMEISER, *Angew. Chem.* **2000**, 112, 1491–1494; *Angew. Chem. Int. Ed.* **2000**, 39, 1433–1436.
- 65 B. MAYR, R. TESSADRI, E. POST, *et al.*, *Anal. Chem.* **2001**, 73, 4071–4078.
- 66 S. LUBBAD, B. MAYR, C.G. HUBER, *et al.*, *J. Chromatogr. A* **2002**, 959, 121–129.
- 67 S. LUBBAD, M.R. BUCHMEISER, *MACROMOL. RAPID COMMUN.* **2002**, 23, 617–621.
- 68 M. MAYR, B. MAYR, M.R. BUCHMEISER, *Angew. Chem.* **2001**, 113, 3957–3960; *Angew. Chem. Int. Ed.* **2001**, 40, 3839–3842.
- 69 G. ERTL, H. KNÖZINGER, J. WEITKAMP, Wiley-VCH, Weinheim, **1999**.
- 70 E.C. PETERS, F. SVEC, J.M.J. FRÉCHET, *Adv. Mater.* **1999**, 11, 1169–1181.
- 71 A.E. RODRIGUES, *J. Chromatogr. B* **1997**, 699, 47–61.
- 72 Y. XU, A.I. LIAPIS, *J. Chromatogr. A* **1996**, 724, 13–25.
- 73 D. SYKORA, F. SVEC, J.M.J. FRÉCHET, *J. Chromatogr. A* **1999**, 852, 297–304.
- 74 C. VIKLUND, F. SVEC, J.M.J. FRÉCHET, *et al.*, *Chem. Mater.* **1996**, 8, 744–750.
- 75 C. VIKLUND, E. PONTÉN, B. GLAD, *et al.*, *F. Svec, Chem. Mater.* **1997**, 9, 463–471.
- 76 Q.C. WANG, F. SVEC, J.M.J. FRÉCHET, *Anal. Chem.* **1993**, 65, 2243–2248.

- 77 Monolithic Separation Media (eds. T.B. TENNIKOVA, Z. DEYL, F. SCVEC), Elsevier, Amsterdam, **2001**.
- 78 C.A. LEON Y LEON, M.A. THOMAS, *GIT Lab.J.* **1997**, 2, 101–104.
- 79 M. SZWARC, *Makromol. Chem. Rapid Commun.* **1992**, 13, 141–145.
- 80 S. PENCZEK, P. KUBISA, R. SZYMANSKI, *Makromol. Chem. Rapid. Commun.* **1991**, 12, 77–80.
- 81 A.F. JOHNSON, M.A. MOHSIN, Z.G. MESZENA, *et al.*, *J. M. S.-Rev. Macromol. Chem. Phys.* **1999**, C39, 527–560.
- 82 M. SZWARC, *J. Polym. Sci. A Polym. Chem.* **1998**, 36, ix–xv.
- 83 O.W. WEBSTER, *Science* **1991**, 251, 887–892.
- 84 M.P. NANDAKUMAR, E. PILSSON, P.-E. GUSTAVSSON, *et al.*, *Bioseparation* **2001**, 9, 193–202.
- 85 M. SCHOLL, S. DING, C.W. LEE, *et al.*, *Org. Lett.* **1999**, 1, 953–956.
- 86 M. SCHOLL, T.M. TRNKA, J.P. MORGAN, *et al.*, *Tetrahedron Lett.* **1999**, 40, 2247–2250.
- 87 S.C. SCHÜRER, S. GESSLER, N. BUSCHMANN, *et al.*, *Angew. Chem.* **2000**, 112, 4062–4065; *Angew. Chem. Int. Ed.* **2000**, 39, 3898–3901.
- 88 M.R. BUCHMEISER, O. NUYKEN, J. KRAUSE, *Austrian Patent Application, patents pending*, **2002**.

## 9

**New Strategies in the Synthesis of Grafted Supports**

RAINER JORDAN

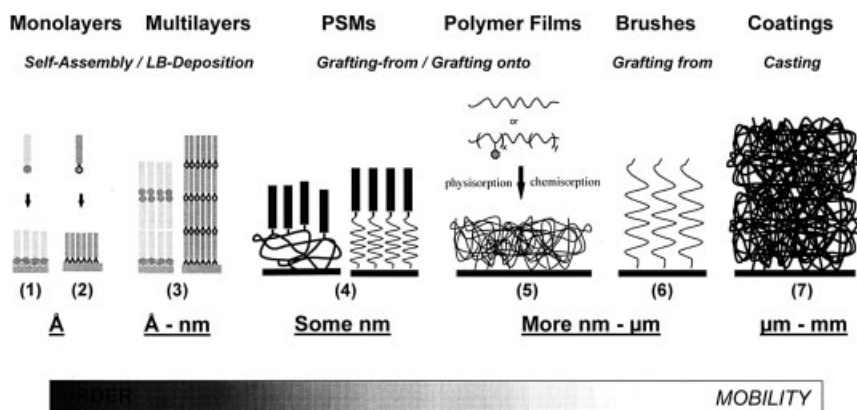
## 9.1

**Introduction and Scope**

The deposition of thin layers of organic compounds onto solids results in materials with the physical bulk property of the solid and the properties of the organic compound forming a new interface. The behavior of the resulting material, however, can not only be described by the mere addition of the physical and chemical properties of the solid and the deposited organic compound but the *morphology* and *dynamic behavior* of the thin layer has to be taken into account. Adsorption, wetting, adhesion and friction are strictly confined to the interface and are the origins of the macroscopic behavior of the new composite material. Rationalization of this simple fact resulted in the development of well-defined surface coatings, where the organic compound is not merely *deposited* onto the solid but *assembled*. The assembly of organic compounds into a defined layer requires firstly, a detailed knowledge of the physical properties (roughness, curvature, porosity, etc) and chemical properties (surface chemistry) of the support, ideally down to the dimension of the molecules which are to be assembled and secondly, to take into account the *interplay of order and mobility* within the layer. This is determined by the shape as well as size or molar mass of the molecules and their possible interactions along the phase boundaries. To illustrate the second point, Fig. 9.1 gives some examples of organic coatings, starting from monomolecular layers with a thickness of a few angstroms, to polymer coatings of several micrometers.

It is beyond the scope of this Chapter to discuss all kinds of various coating techniques, properties of the supports, properties of the coatings and the various fields of application of the composites in catalysis, separation techniques, materials science, colloid science, sensor technology, biocompatible materials, biomimetic materials, optics etc. The scope had to be restricted to the fundamental properties of ultrathin organic layers on solid supports followed by some examples, outlining the benefit of the tailored functional surfaces such as SAM and polymer brushes for catalysis.

Taking Fig. 9.1 as a guideline, the formation and properties of monomolecular layers formed by self-assembly is discussed, followed by slightly thicker layers in which mesogenic (order-inducing) units are combined with flexible polymers and



**Fig. 9.1** A schematic illustration of surface coatings with their typical thickness ranging from angstroms to micrometers. Selected are monomolecular layers fabricated by the transfer of Langmuir–Blodgett (LB) films onto solid substrates (1); self-assembled monolayers (SAMs) (2); multilayers thereof (3); polymer-

supported (alkyl) monolayers (PSMs) (4); physisorbed or chemisorbed polymer coatings (5); polymer brushes (6) and polymer layers fabricated by macroscopic casting techniques (7) along with possible ways of their fabrication and characteristic layer dimensions.

finally, new aspects in the preparation and properties of so called polymer brushes are presented. The latter will form a central subject of this Chapter, since new synthetic strategies have very recently been developed which enable the preparation of surface grafted polymer coatings of defined morphology and polymer architectures. By this, responsive functional coatings can be fabricated, being at the fine boundary between order and mobility.

## 9.2

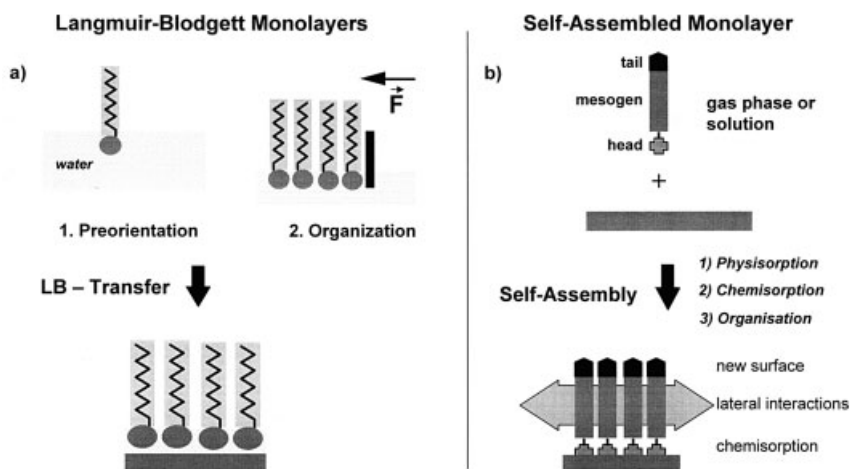
### Self-assembled Monolayers

#### 9.2.1

##### Two Dimensional Self-assembly

Highly ordered monomolecular layers on a solid substrate were originally prepared by the so-called Langmuir–Blodgett (LB) technique. Surfactant molecules are spread at the air-water interface and pre-assemble themselves by orienting the hydrophilic (polar or charged) head group towards the water and the hydrophobic tail towards the gas phase. The degree of order in this assembly can be increased by successive reduction of the available cross-sectional area for each molecule, simply by pushing the molecules together macroscopically by a movable barrier of an LB trough. During compression, the monolayer undergoes phase transition in two dimensions; analog to phase transitions in three dimensions: from the ‘gas-analog’ to the ‘liquid-analog’ up to the ‘solid-analog’ state. The phase transitions





**Fig. 9.2** Preparation of oriented monomolecular layers of surface active molecules on a solid support by (a) the Langmuir-Blodgett

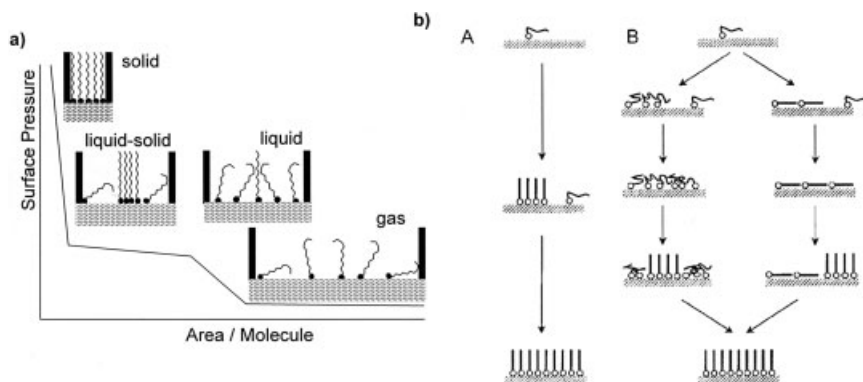
technique and consecutive transfer and (b) self-assembly

in the compression isotherms (lateral pressure,  $\Pi$ , versus area per molecule) and corresponding molecular ordering are depicted in Fig. 9.3. With this technique, highly organized monolayers can be prepared at the air–water interface having their hydrophobic moieties, typically *n*-alkyl tails, in a 2D crystalline analog state. Such layers can be deposited onto a solid substrate by controlled dipping of the substrate through the interface. The major drawback of monomolecular films prepared in this manner is the limited chemical and physical stability of the monolayer caused by its lack of strong specific (covalent) interactions, and the relatively tedious preparation, which limits the shape, surface topography and dimension of the substrate. Despite these drawbacks, it has to be noted that the LB-technique is not obsolete but still a very valuable tool for the study of amphiphilic compounds and the preparation of two-dimensional arrangements.

Monomolecular layers of the same quality in terms of the degree of order can also be prepared by *self-assembly*. Molecules forming self-assembled monolayers (SAMs) are characterized by three features: (1) A surface active *head group*, able to specifically bind to the substrate, (2) a suitable *mesogenic unit* to ensure favorable lateral intramolecular interactions and (3), a *tail group* which ultimately defines the surface physics and chemistry of the resulting SAM (Fig. 9.2). Since it is *self-assembly* the preparation is rather simple: The molecules assemble themselves from the gas phase or from a solution onto the substrate. With the right choice of head group, mesogen and tail group well-defined monolayers can be prepared.

Interestingly, in both approaches the two-dimensional arrangement undergoes sooner or later similar ‘phase transitions’ as illustrated in Fig. 9.3.

While for LB-layers, the molecules have to be organized by means of compression prior to deposition of the monolayer at the air–water interface, the self-organization process into SAMs follows similar pathways by itself. This requires suffi-



**Fig. 9.3** (a) Typical pressure-area ( $\Pi$ -A) isotherm with phase transition during compression of a monomolecular film of a surfactant along with a schematic depiction of the molecules. Depending on the mesogen, coexistence phases (e.g. liquid-solid coexistence phases) can be observed in form of a plateau in the  $\Pi$ -A isotherm. (b) Scheme of possible pathways of the formation of SAMs. Depend

ing on the concentration of surfactant molecules and the temperature, the growth proceeds via (A) first a 2D-vapor phase to a solid-vapor coexistence, to the final solid phase, or (B) through various intermediate coexistence phases (Reprinted with permission, from the Annual Review of Physical Chemistry, Volume 52 ©2001 by Annual Reviews [www.AnnualReviews.org](http://www.AnnualReviews.org)).

cient mobility of the molecules on the solid substrate before the formation of the final SAM. Ulman pointed out that the energy gain of the system during self-assembly (physisorption and especially chemisorption) can be compared with the pressure applied with the barrier of an LB-trough, to increase the order in the LB-monolayer at the air-water interface [5].

By now a broad range of SAMs on various substrates are available. For an overview on SAM systems several comprehensive reviews [1–4] as well as the reference book by A. Ulman are available [5]. In Tab. 9.1 a list of examples is given [5, 6, 33].

The process of formation of SAMs on the various substrates strongly depends on the nature of all three moieties of the surface active molecule. If a suitable mesogen is chosen, the affinity of the head group toward the substrate determines the kinetics of the physisorption and chemisorption as well as the stability of the resulting layer.

Among the SAM systems listed in Tab. 9.1, those based on silanes on silica and thiols on (noble) metals represent the majority of the reported accounts. In the following some specific properties of these two systems will be outlined.

### 9.2.2

#### Self-assembled Monolayers of Alkanethiols

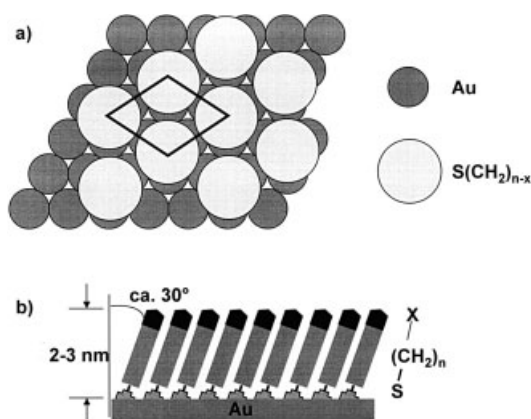
SAMs of alkanethiols on gold are the by far the most studied systems. For detailed descriptions of their growth and structural features, the recent reviews by F. Schreiber [4] and D.K. Schwarz [33] are highly recommended. It is believed that the thiol reacts with the gold substrate according to the following equation [5]:

**Tab. 9.1** Selected examples of substrates and surface active molecules suitable for the formation of SAMs.

<b>Substrate</b>	<b>Ligand or Precursor</b>	<b>Binding</b>	<b>Reference</b>
Au	RSH, (aliphatic thiols)	RS–Au	2–4, 7
Au	ArSH (aromatic thiols)	ArS–Au	4, 8–12
Au	RSSR' (disulfides)	RS–Au	2–4, 13
Au	RSR' (sulfides)	RS–Au	2–4, 14
Au	RSO <sub>2</sub> H	RSO <sub>2</sub> –Au	15
Au	R <sub>3</sub> P	R <sub>3</sub> P–Au	16
Ag	RSH, ArSH	RS–Ag	2, 4, 17
Ag	ArSH	ArS–Ag	8, 11, 12
Cu	RSH, ArSH	RS–Cu	2, 18
Pd	RSH, ArSH	RS–Pd	2, 19
Pt	RNC	RNC–Pt	2, 20
Pt	ROH, amides	RO–Pt	21
GaAs	RSH	RS–GaAs	22
GaAs	RSSR; RCOOH	RS–GaAs; RCOO//GaAs	23
InP	RSH	RS–InP	24
SiO <sub>2</sub> , glass	RSiCl <sub>3</sub> , RSi(OR') <sub>3</sub>	R–Si–O–Si	2, 3, 25, 46–48, 53, 59
Si/Si–H	(RCOO) <sub>2</sub> (neat)	R–Si	26
Si/Si–H	RCH=CH <sub>2</sub>	RCH <sub>2</sub> CH <sub>2</sub> –Si	27
Si/Si–Cl	RLi, RMgX	R–Si	28
Metal oxides	RCOOH	RCOO//MO <sub>n</sub>	29
Metal oxides	RCONHOH	RCONHOH//MO <sub>n</sub>	30
ZrO <sub>2</sub>	RPO <sub>3</sub> H <sub>2</sub>	RPO <sub>3</sub> <sup>2-</sup> //Zr <sup>4+</sup>	31
In <sub>2</sub> O <sub>3</sub> /SnO <sub>2</sub> (ITO)	RPO <sub>3</sub> H <sub>2</sub>	RPO <sub>3</sub> <sup>2-</sup> //M <sup>n-</sup>	32



Although the chemical reaction appears to be quite simple and the system have been studied for decades, the given reaction equation is still a working model. In particular, the fate of the hydrogen during and after the reaction is not fully understood. Because the final SAMs formed from thiols and disulfides are similar, it has been assumed that the chemisorption process follows a similar reaction pathway in both cases. Fig. 9.4 outlines some structural features of this system. The three aspects that determine the final molecular packing parameter of the SAM are first, the interaction between the thiolate and the crystalline Au(111) surface; second, the intramolecular forces in the two-dimensional assembly; and third, the interactions among the terminal functional groups [34–37]. The thiolates on Au(111) are tilted approx. 34° from the surface normal and the unit cells of the C–C–C planes are defined by two all-*trans* zig-zag chains twisted in different directions [38]. For further details on the monolayer structure on gold as depicted in Fig. 9.4 [39–42] and silver (Ag(111)) please refer to the original accounts [34, 43, 44] or the comprehensive review by Schreiber [4].



**Fig. 9.4** Structural features of a SAM of an alkanethiol formed on a Au(111) surface with a) a  $(\sqrt{3} \times \sqrt{3})R30^\circ$  structure in which the thiolates display a S–S distance of 4.99 Å. (modified from ref. 5) b) This results in a tilt of the alkanethiolate molecular axis of approx.  $30^\circ$  with respect to the surface normal to reestablish the vdW interchain interactions of the alkyl mesogen (modified from ref. [6]).

### 9.2.3

#### Self-assembled Monolayers of Silanes

In contrast to LB-monolayers, SAMs were from the very beginning of their development not only model systems for the study of interfacial phenomena but were readily used in technological applications. One example is the use of monomolecular coatings for chromatographic stationary phases. As mentioned, SAMs can be formed on substrates with various shapes or morphologies especially porous and nonporous amorphous silica. Silica gel is a common stationary phase in chromatography and its controlled modification using alkyl silanes were developed at an early date, for the preparation of reversed-phase (RP) stationary phases used in high performance liquid chromatography (HPLC). In this field, detailed knowledge of the surface chemistry of silica and the proper reaction conditions of the silanization procedure were soon developed. By the mid-1970s RP silica packings for HPLC became commercially available, which carried bonded *n*-octyl and *n*-octadecyl groups at the surface [45]. Protocols that were developed for the preparation of RP-stationary phases, are readily applicable to the preparation of SAMs on planar silica substrates. An RP-coating, especially RP-18, and a SAM of *n*-octadecyltrichlorosilane [46] are closely related, if, in many cases, not the very same thing.

For the surface modification of silica, the reactive surface group is the silanol group which can be reacted with a mono- or polyfunctional alkoxy- or chlorosilane:



The surface chemistry of SAMs of silanes on planar substrates such as oxidized silicon wafers is comparable to the chemistry of silica gel, with the absence of a porous structure [47].

The maximum surface density of the reactive silanol groups in a fully hydrated state is  $8\text{--}9 \mu\text{mol m}^{-2}$  (or  $\sim 5 \text{ SiOH nm}^{-2}$ ). This can be achieved by a hydrothermal activation of silica gel [48, 49] or, for planar substrates, a solution with hydrogen

peroxide/sulfuric acid ('piranha') or ideally a modified cleaning procedure used for silicon/silicon dioxide wafers ('RCA-method') [50, 51]. The different treatments for planar silica surfaces and silica gel particles are necessary because of their different specific surface areas and practical issues of handling the 'substrate'. It was found that the RCA method yields highly active, homogeneous surfaces and most importantly, they are of reproducible quality without a significant change of the surface roughness. The hydrothermal treatment of (porous) silica gel was optimized in terms of reactivity and maintaining the specific pore structure (specific surface area) and particle morphology.

It is not easy to obtain SAMs of trifunctional silanes on planar silica or silica gel particles. During the development of (RP-) stationary phases, several protocols were established, including modifications in aqueous systems [52]. For polyfunctional silanes, a hydrolysis and polycondensation reaction easily results in the formation of undefined three-dimensional polysiloxanes bound to the silica surface [47]. For the modification of porous silica, it was found that the uncontrolled grafting of oligo- or polysiloxanes from aqueous solution altered the pore structure and accessible surface area by clogging the pores. On planar substrates, the adsorbed polysiloxanes increased the surface roughness, and irregular coatings were observed using scanning electron microscopy (SEM) or scanning probe microscopy (SPM). To form a defined two-dimensional SAM, great care should be taken to avoid polymerization of the silane compound in the solution and the consecutive physisorption/chemisorption of siloxane oligomers [53]. Besides thorough purification of the silane compound, anhydrous reaction conditions for the silanization are required. By this method, the hydrolysis and condensation reaction of the silane is confined to the interface because only the thin layer of surface water on the silica is used for the silanization reaction. For the most popular silane compounds, the different reactivity follows the trend:  $\equiv \text{SiCl} > \equiv \text{Si}(\text{OCH}_3)_3 > \equiv \text{Si}(\text{OC}_2\text{H}_5)_3$ . In the two-step process of hydrolysis of the silane to the silanol species and the condensation (silanols to siloxane), the reaction-determining step is the rate of hydrolysis [54]. However, for polyfunctional silanes, hydrolysis and condensation overlap. Under defined reaction conditions, the reaction between the surface hydroxyl groups of the silica and the silane compound follows a distinct stoichiometry, which can be expressed by the number of surface hydroxyl groups that react with the organosilane. For monofunctional silanes this ratio is unity. For bifunctional and trifunctional reagents it varies between 1 and 2, depending on the cross-sectional area of the molecule. The stoichiometry is discussed in detail in Ref. [48]. Possible reaction pathways of mono- to trifunctional silane with surface hydroxyl groups are outlined by E. Bayer *et al.* [55]. Grafting densities can be increased by using various amines as a catalyst and base [56]. Although Wirth *et al.* [57] defined the bonding of trifunctional silanes as self-assembly, only if the grafting density approaches  $8 \mu\text{mol m}^{-2}$  (equal to  $2.2 \text{ nm}^2$  per molecule), whereas the ligand density for conventional RP-packings are in the range of  $\sim 5 \mu\text{mol m}^{-2}$ , it is doubtful whether most of the reported silane-based SAMs satisfy this extremely high ligand density criterion. Complete stoichiometric saturation of all silanol groups with ligands is sterically impossible. In several studies it was pointed

out that in the ordered SAMs of alkyl silanes, not all ligands are bonded to the surface but that a laterally cross-linked monomolecular layer covers the surface and chemical bonding occurs with 1 out of 5 silane molecules [58]. Studies from Silberzahn *et al.* [59] lead to the same view [47, 48], and it was argued that even full cross-linking is sterically hindered [60]. The structural features of silane-based SAMs are discussed in detail in Refs. [4, 5, 33]. Compared with the SAM formed by alkanethiols on gold, silane-based SAMs do not display the same degree of lateral long-range molecular order. This is because the SAMs of silanes are a two-dimensional polysiloxane networks with focal pinning points to the amorphous silica substrate, whereas in alkanethiol monolayers, the crystalline metal surface directs the epitaxial arrangement of the monolayer. The morphological picture that arises for SAMs of polyfunctional (trialkoxo- or trichloro-) silane compounds is depicted in Fig. 9.5.

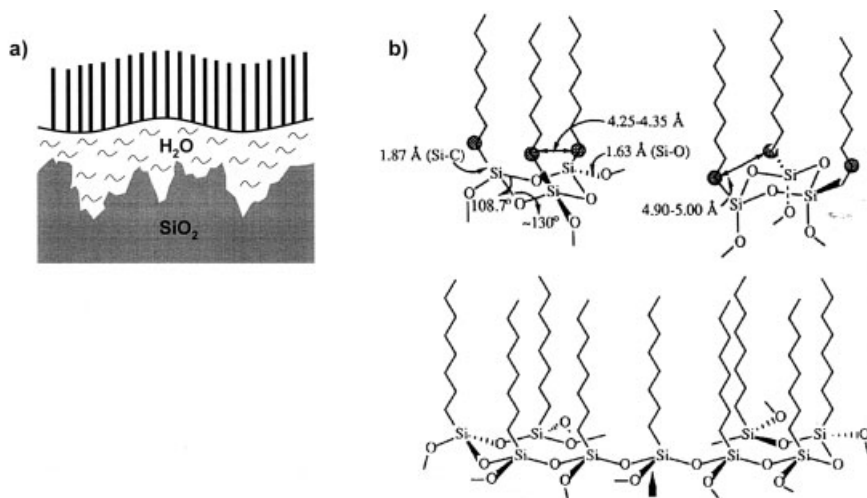
This distinct difference between SAMs of silanes on silica and e.g. thiols on gold leads to the consequence that ordered SAMs of silanes require an effective mesogen for lateral intralayer interactions to overcome the steric difficulties of the polysiloxane network. The behavior of silanes at an air-water interface, studied by the LB-technique during compression and during formation of the two-dimensional polysiloxane network layer, is a helpful tool for the investigation of the morphology of a SAM formed by self-assembly on a silica surface using the surface water layer. Hence, reports of surface modifications using silane compounds with, for example, short *n*-alkyl moieties as the order-inducing unit do often not meet the criteria of a SAM in terms of the morphology, degree of order and, in consequence, behavior of a defined surface coating.

#### 9.2.4

#### Self-assembled Monolayers for Surface Engineering

The intriguing aspect of SAM systems is the direct control of surface properties by the choice of the distal (tail) group of the molecules forming the new interface. The surface properties can be tailored more or less independently from the original substrate since surface properties are dominated by the outermost 5–10 Å of the organic material [61]. A variety of surfaces with specific interactions can be produced with fine structural control [62]. Jarzebinska *et al.* [63] compared composite polymer coatings containing nickel catalyst for the catalytic reduction of carbon dioxide with surface coatings prepared by the Langmuir-Blodgett technique using glassy carbon electrodes, as well as self-assembly on metals. They found a significantly higher catalytic activity of surfaces prepared by LB and especially with the organized self-assembled monolayers.

In addition, these thin films have been important in studies of electron transfer, relevant for catalytic systems [64], molecular recognition [65], biomaterial interfaces [66], cell growth [67], crystallization [68], adhesion [69], and many other aspects [70]. SAMs provide ideal model systems, because fine control of surface functional group concentration is possible by preparing mixed SAM systems of two or more compounds, evenly distributed over the surface [71, 72], as two- or



**Fig. 9.5** a) Schematic view of a SAM of trifunctional silanes on a silica surface according to Silberzahn *et al.* (modified from ref. [59]) along with b) A siloxane trimer with possible conformations of the alkyl chains in the equatorial (upper, left) and axial (upper, right) positions allowing a connection with a substrate. A schematic description of a polysiloxane at the monolayer-substrate surface (down). The arrow points to an equatorial Si-O bond that can be connected either to another polysiloxane chain or to the surface.

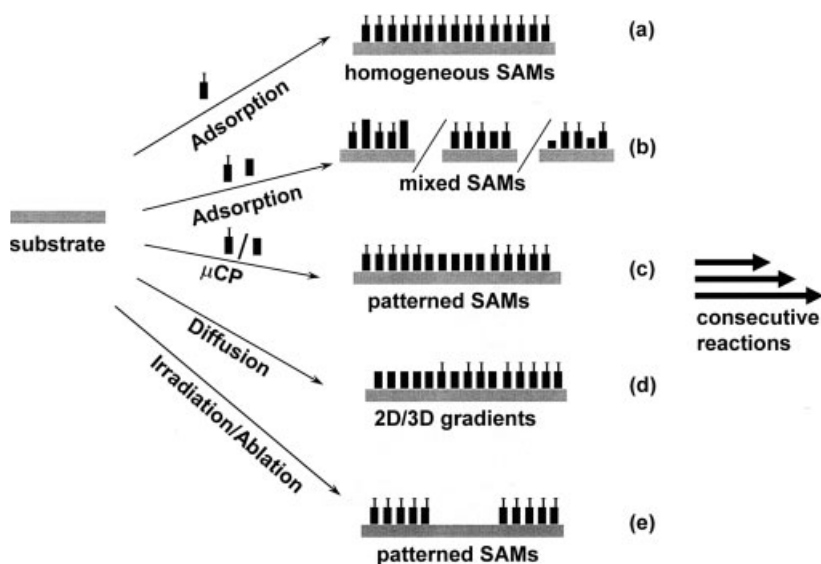
The dotted line on the left is a bond in a possible precursor trimer. X-ray data suggest an area of  $21 \pm 3 \text{ \AA}^2$  per alkyl chain, with a thickness of  $25 \pm 2 \text{ \AA}$ . FTIR spectroscopy suggest that the alkyl chains in *n*-octadecyltrichlorosilane SAMs are perpendicular to the surface (Reprinted with permission from: [5] A. Ulman, *Introduction to Thin Organic Films: From Langmuir-Blodgett to Self-Assembly*, Academic Press, Boston, 1991. p. 257 and 258. © Copyright 1991 Academic Press/Elsevier Science)

three-dimensional gradients [73] or as patterned mixed monolayers as prepared by  $\mu$ CP [6].

$\omega$ -functionalized SAMs are frequently used for the controlled attachment of catalytic sites onto a substrate surface, which otherwise do not offer the proper chemistry or which have to be shielded from the catalyst in order to enable specific reactions. In biocatalysis, tailored SAM systems are especially useful as intermediate coatings to attach enzymes in a defined way [74–76].

Fig. 9.6 outlines the possibilities of using SAMs for the study and application of physical and chemical surface engineering on the molecular scale.

In many supported catalytic systems, it is nearly impossible to determine either the specific species, responsible for the observed catalytic activity, or the mechanistic pathway of the reaction. Using a defined SAM system in which careful molecular design is followed by controlled deposition into a solid-supported catalyst of known morphology, surface coverage, mode of binding and molecular orientation, allows direct correlation of an observed catalytic activity with the structure on the molecular scale. SAM and LB-systems allow detailed and meaningful studies of established surface bound catalysts to understand their behavior in heterogeneous



**Fig. 9.6** Tailored SAMs for surface engineering provides the control of the surface physical properties, chemical reactivity and heterogeneity on the molecular level. a) Self-assembly of one kind of surface active compound results in homogeneous monolayers. b) Adsorption of two components give rise to mixed SAMs, combining the physical and

chemical properties of both terminal functionalities into one layer, thus varying the reactivity by dilution or screening. c) Patterned two component SAM by, for example micro contact printing ( $\mu$ CP) or post-deposition irradiation such as chemical lithography. d) Patterned SAMs prepared by partial photoablation.

environments. Recently, this approach was followed by Talham *et al.* [77]. They investigated the effect of a controlled surface immobilization of manganese tetraphenylporphyrin as an oxidation catalyst. A combination of LB and self-assembly was used for controlled binding of the catalytic active site. The metalloporphyrin monolayer showed enhanced catalytic activity, which could be attributed to the influence of a combination of enhanced catalytic lifetime and the altered conformation that the catalytic species adopts when confined to the defined surface. Similarly, Töllner *et al.* [78] used the LB-technique to assemble monolayers of amphiphilic rhodium bipyridine complexes. The LB-monolayers were found to have largely enhanced the catalytic efficiency with respect to an analog system in solution.

Besides the morphology, the free surface energy of a given surface determines the accessibility of catalytic active sites in heterogeneous catalysis (wettability). SAM surfaces can be produced to have free surface energies that span the range from “Teflon-like” surfaces (surface  $\text{CF}_3$  groups) to very high-energy surfaces (surface OH or COOH groups), e.g., surface tensions of 10–70 dyne  $\text{cm}^{-1}$ . For example, when the acidic protons in highly hydrophilic surfaces, such as  $-\text{OH}$ ,  $-\text{CONH}_2$ , and  $-\text{CO}_2\text{H}$  surfaces [79], are substituted by methyl groups [80], the surfaces become more hydrophobic, thus showing the sensitivity of wetting to the SAM surface functionality.



## 9.2.5

**Surface Reconstruction: A Dynamic View of Self-assembled Monolayer Systems**

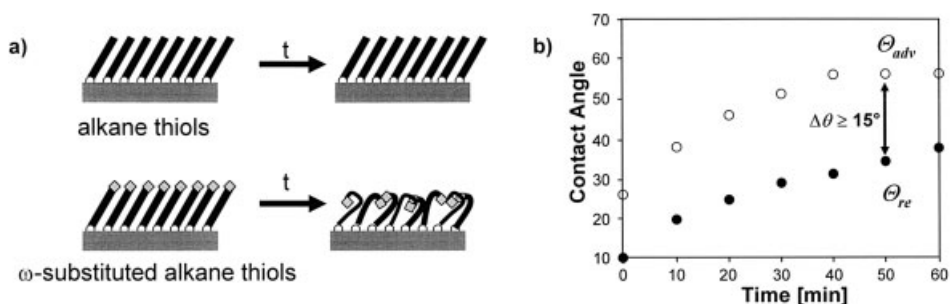
Although SAMs of alkanethiols can in principle be described as well packed, quasi-crystalline assemblies, the shortcoming of the flexible *n*-alkyl mesogen is that for example an increase of temperature or change in the polarity at the interface results in surface-*gauche* defects, and thus surface disorder. Studies of sum-frequency vibration spectroscopy show that the structure of a surface is clearly perturbed when it interacts strongly with another condensed phase [81], hence structural perturbations need to be considered. This is especially serious for very polar surface groups, such as OH [82], where the disorder introduced may be significant [83] and not confined to the outermost surface [81]. Thus, one cannot neglect surface reorganization during exposure to environments of various polarity during wetting or adhesion experiments or during chemical conversion involving the  $\omega$ -functionality. Recalling our introductory Fig. 9.1, even in monomolecular films, the game of order and mobility is already on.

Ulman *et al.* discussed the static and dynamic wetting behavior of pure 11-hydroxyundecane-1-thiol (HUT) and mixed HUT *n*-dodecanethiol in great detail [72] and found significant surface reconstruction in such monolayers. The time evolution of the minimization of surface free energy related to exposure towards air and the water contact angle hysteresis is depicted in Fig. 9.7 along with a schematic drawing.

Siepmann *et al.* [84] carried out Monte Carlo simulations of CH<sub>3</sub>-terminated SAMs under the influence of compressive stress. It was found that the monolayers relax almost elastically after the stress is removed. Their observation was that under pressure, surface-*gauche* defects developed in 40% of the chains. These defects result in the exposure of CH<sub>2</sub> groups at the surface, which, for  $\omega$ -substituted alkyl chains with polar groups, caused a significant decrease in surface free energy. In the case where stabilizing surface H-bonding interactions are enhanced by surface reorganization, the latter may not be reversible [81]. In consequence, especially polar  $\omega$ -functionalities are no longer accessible. This is a major limitation for the application of SAMs as reference or model systems for the study of interfacial phenomena or as intermediate binding systems for the immobilization of catalytic active sites.

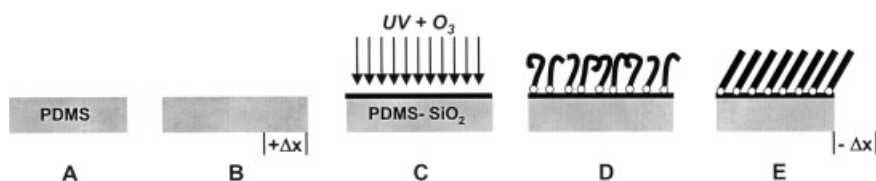
Recently, Genzer and coworkers [85] presented an interesting new approach for the preparation of stable silane-based SAM systems. As a substrate, cross-linked polydimethylsiloxane (PDMS) was oxidized by UV/ozone treatment to yield a thin silicon dioxide surface. The surface was then treated with fluorinated alkyltrichlorosilanes from the gas phase while being mechanically stretched by a certain length  $\Delta x$ . After modification, the elastomer was allowed to relax resulting in a mechanically assembled monolayer (MAM) at the surface (Fig. 9.8).

The MAMs were found to be closely packed. NEXAFS and FTIR spectroscopy studies revealed that the molecular tilting angles relative to the surface normal varied from 4° to 21° as a function of  $\Delta x$ . In wetting studies it was found that the highest water contact angles (~131°) with the lowest contact angle hysteresis



**Fig. 9.7** a) Highly polar surfaces of SAMs of *n*-alkylthiols undergo surface reconstruction when exposed to air to minimize the surface free energy. b) Advancing and receding water

contact angles on SAMs of HUT  $[\text{HO}(\text{CH}_2)_{11}\text{SH}]$  SAMs on Au(111) (modified from ref. [82]).



**Fig. 9.8** Schematic illustration of the preparation of mechanically assembled monolayers (MAMs). (A) A cross-linked PDMS film is (B) mechanically stretched by  $\Delta x$  (C), oxidized by UV/ozone treatment to yield a thin  $\text{SiO}_2$  sur-

face layer which was used to assemble SAMs of fluorinated trichlorosilanes (D). Release of the strain of the PDMS substrate resulted in further increase of the molecules/surface area in a so-called MAM (E). (modified from [85a]).

could be obtained at  $\Delta x \sim 70\%$  resulting in an optimal molecular dense packing. From hysteresis measurements and long-term stability studies it was concluded that the surface reconstruction in MAMs is significantly suppressed by the extremely high packing density. In principle, the MAM approach of Genzer *et al.* [85] can be viewed as an analog of the preparation of ordered LB films at the air–water interface subsequent to the self-assembly step.

#### 9.2.6

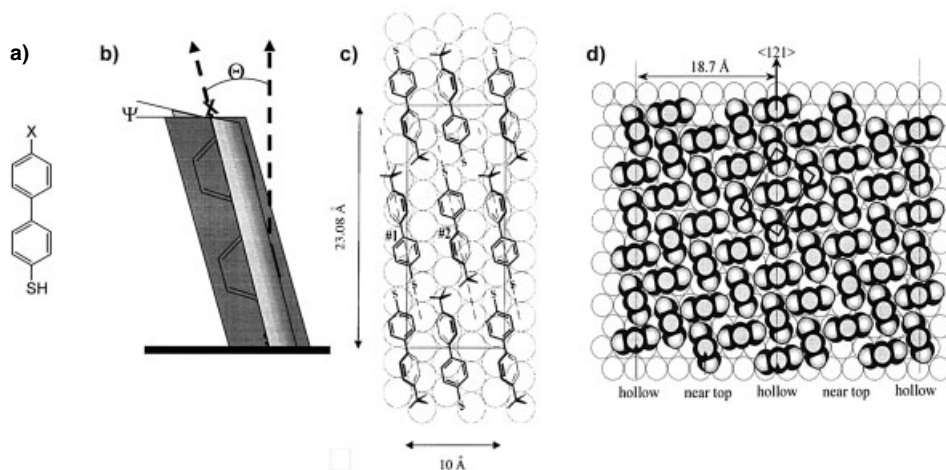
##### Self-assembled Monolayers of Rigid Mercaptobiphenyls

Another, more direct approach to overcome the problem of surface reconstruction, is the variation of the mesogenic unit of the surface active molecule. Instead of using flexible *n*-alkyl moieties with high conformational freedom, SAMs formed from molecules featuring a rigid mesogen in which conformational disorder has been eliminated as completely as possible should be suitable for the preparation

of reference systems for the study of interfacial phenomena. Very early, systems were under study containing aromatic units.

Several groups investigated aromatic thiol systems for the formation of rigid, conjugated SAM systems [86–94] and it soon became clear that among the discussed systems, mercaptobiphenyls and 4'-substituted-4-mercaptobiphenyls are promising candidates and currently the most intensively studied thiol-based SAM systems.

Rubinstein and coworkers were the first to investigate SAMs made of 4,4'-methyl-mercaptobiphenyls (MMB) on gold [87]. In recent investigations of the structure and growth of the 4'-methyl substituted mercaptobiphenyls using grazing-incidence X-ray diffraction (GIXD) and low-energy atom diffraction (LEAD) [95], a low-coverage ('lying-down' or 'striped') phase and a high-coverage ('standing-up') phase was found (Fig. 9.9), similar to the phase evolution of a comparable *n*-decanethiol. In the standing-up phase a commensurate hexagonal ( $\sqrt{3} \times \sqrt{3}$ )R30° structure was found, analogous to alkane thiols. However, the tilt angle of about 14° of the molecular axis with respect to the surface normal was found to be significantly smaller than for alkanethiols. It was concluded that for biphenyls, it is not necessary to tilt as strongly as *n*-alkanes to maximize the lateral intermolecular (van der Waals or  $\pi$ - $\pi$ ) interactions. This results in the picture of a closely packed SAM of mercaptobiphenyls with the molecules standing almost normal to the substrate surface. The generally low tilt angles were also found in studies using ellipsometry and ER-FTIR spectroscopy performed on different 4'-substituted-4-mercaptobiphenyls [10–12, 96–99]. These findings were



**Fig. 9.9** a) General molecular structure of 4-substituted-4'-mercaptobiphenyl. b) Eulerian angles defining the orientation of the molecule with respect to the surface normal. c) Proposed structure for the low coverage 'striped' phase of MMB (Reprinted with permission from: [4] F. Schreiber *Prog. Surf. Sci.*

**2000**, 65, 151–256 © Copyright 2000 Elsevier Science). d) Proposed structure of 4-chloro-4'-mercaptobiphenyl SAM (Reprinted with permission from: [10] J. F. Kang, A. Ulman, S. Liao, et al., *Langmuir* **2001**, 17, 95–106. © Copyright 2001 American Chemical Society).

further corroborated by recently performed detailed studies using X-ray photoelectron spectroscopy (XPS) and near-edge X-ray absorption fine structure spectroscopy (NEXAFS) [100, 101]. By comparing the alkanethiols with aromatic thiols on gold and silver, it was found that in the aromatic SAMs, the balance between the head group/substrate interactions and the intermolecular forces is shifted towards the intermolecular forces [101].

In conclusion, the overall picture arises that a biphenyl is a suitable if not ideal mesogen for the formation of highly ordered SAM systems if compared with aliphatic thiols. This is also reflected by the significantly higher thermal stability (melting temperature,  $T_M \geq 140^\circ\text{C}$  for MMB as compared with  $T_M \sim 100^\circ\text{C}$  for *n*-decanethiol) of mercaptobiphenyl SAMs [95].

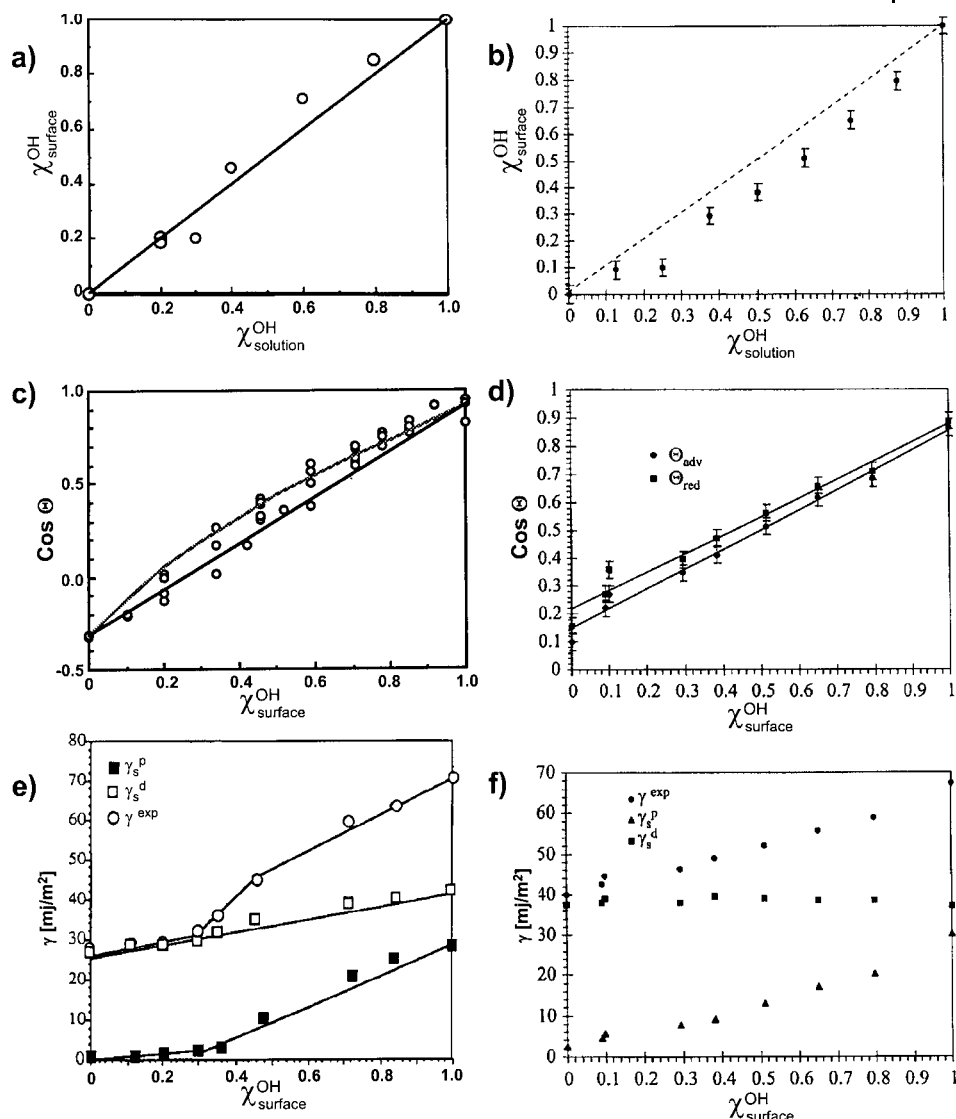
However, silane-based SAMs were found to be thermally stable up to a temperature of  $467^\circ\text{C}$  (C–C decomposition [102]). Detectable changes with surface probe microscopy and in terms of wetting behavior were reported to appear at around  $125^\circ\text{C}$  [103].

Besides the elimination of conformational freedom in the mesogen by switching from an aliphatic to an aromatic system, several other aspects have to be considered. First, the electronic nature of the molecule is entirely different. Because of the conjugation, the 4'-substitution has a strong influence upon the reactivity of the thiol head group. Electron donating or withdrawing substituents changes the acidity of the thiol. Second, asymmetric 4',4'-substituents induce a molecular dipole moment which should have a significant impact upon the formation as well as the stability of the corresponding SAM. Third, the polarity and polarizability of the molecule and the SAM is different, thus changing the surface potential as well as the optical properties of the SAM.

Kang *et al.* first studied the wetting properties of 4'-methyl- (MMB) and 4'-hydroxy-4-mercaptopbiphenyls (HMB) as an analog system for the aliphatic HUT/DDT mixed monolayer [97]. In Fig. 9.10 the results of analog wetting experiments for the two systems are compared.

For both cases, mixed monolayers can be prepared without a significant preferential adsorption of one compound (Fig. 9.10a,b). The plot of  $\cos \theta$  against the surface OH concentration (Fig. 9.10c,d) reveals an overall higher free surface energy of the biphenyl system, caused by the polar/polarizable biphenyl group. For example, the advancing contact angle of an HMB SAM is  $30^\circ$ , while that of HUT is about  $15^\circ$ . Although both surfaces feature OH terminal groups, the impact of the mesogen is significant. Both systems follow more or less the Cassie equation [104]. However, the water contact angle hysteresis for the HMB/MMB system, at  $5^\circ$ , is unusually small. Referring to the plot in Fig. 9.7 in aliphatic systems (pure HUT monolayer) a hysteresis of about  $15^\circ$  is usually observed. Additionally, while the aliphatic system undergoes dramatic changes with time of exposure to ambient air, the HMB/MMB system was found to show constant water contact angles for at least 1 month storage under nitrogen. This difference accounts for the fact that in the biphenyl system, the surface reconstruction is eliminated.

By the geometric-mean method [106] the total surface free energy ( $\gamma_s^{\text{exp}}$ ), the polar ( $\gamma_s^{\text{p}}$ ) and dispersive component ( $\gamma_s^{\text{d}}$ ) of both systems were calculated (Fig. 9.10e,f).



**Fig. 9.10** Comparison of the formation and wetting behavior of the aliphatic HUT/DDT (a, c, e) and the aromatic HMB/MMB (b, d, f) mixed monolayer system on Au(111). (a, b) Composition of the solution and surface composition of the resulting SAM. (c, d) Plot of the  $\cos \Theta = (\gamma_{\text{sv}} - \gamma_{\text{sl}}) / \gamma_{\text{lv}}$  of the advancing (and additionally in d) receding) water contact angle as a function of the surface OH concentration. The straight line represents the Cassie equation [104], in c) the grey line is calculated after the equation from Israelachvili [105] describing the contact angle on heterogeneous surfaces. (e, f)

Plots of the total surface free energy ( $\gamma_s^{\text{exp}}$ ), polar ( $\gamma_s^{\text{p}}$ ) and dispersive component ( $\gamma_s^{\text{d}}$ ) of both systems as a function of the surface composition. (b, d modified from ref. [97]); (a, c, e Reprinted with permission from: [62] A. Ulman, S. D. Evans, Y. Shnidman, *et al.*, *J. Am. Chem. Soc.* **1991**, 113, 1499–1506. © Copyright 1991 American Chemical Society; [72] A. Ulman, S. D. Evans, Y. Shnidman, *et al.*, *Adv. Coll. Interf. Sci* **1992**, 39, 175–224. © Copyright 1992 Elsevier Science; [97] J. F. Kang, R. Jordan, A. Ulman, *Langmuir* **1998**, 14, 3983–3985. © Copyright 1998 American Chemical Society).

While the aliphatic HUT/DDT system displays an abrupt change in the polar surface free energy component at about 30% OH and a wetting transition onset occurs at about the same concentration, for the biphenyl system,  $\gamma_s^p$  grows almost linearly and the dispersive component remains constant with increasing surface OH concentration and no wetting transition is observable.

The outlined properties make the biphenyl system ideal for the study of interfacial phenomena and applications as stable intermediate binding sites for catalytic systems.

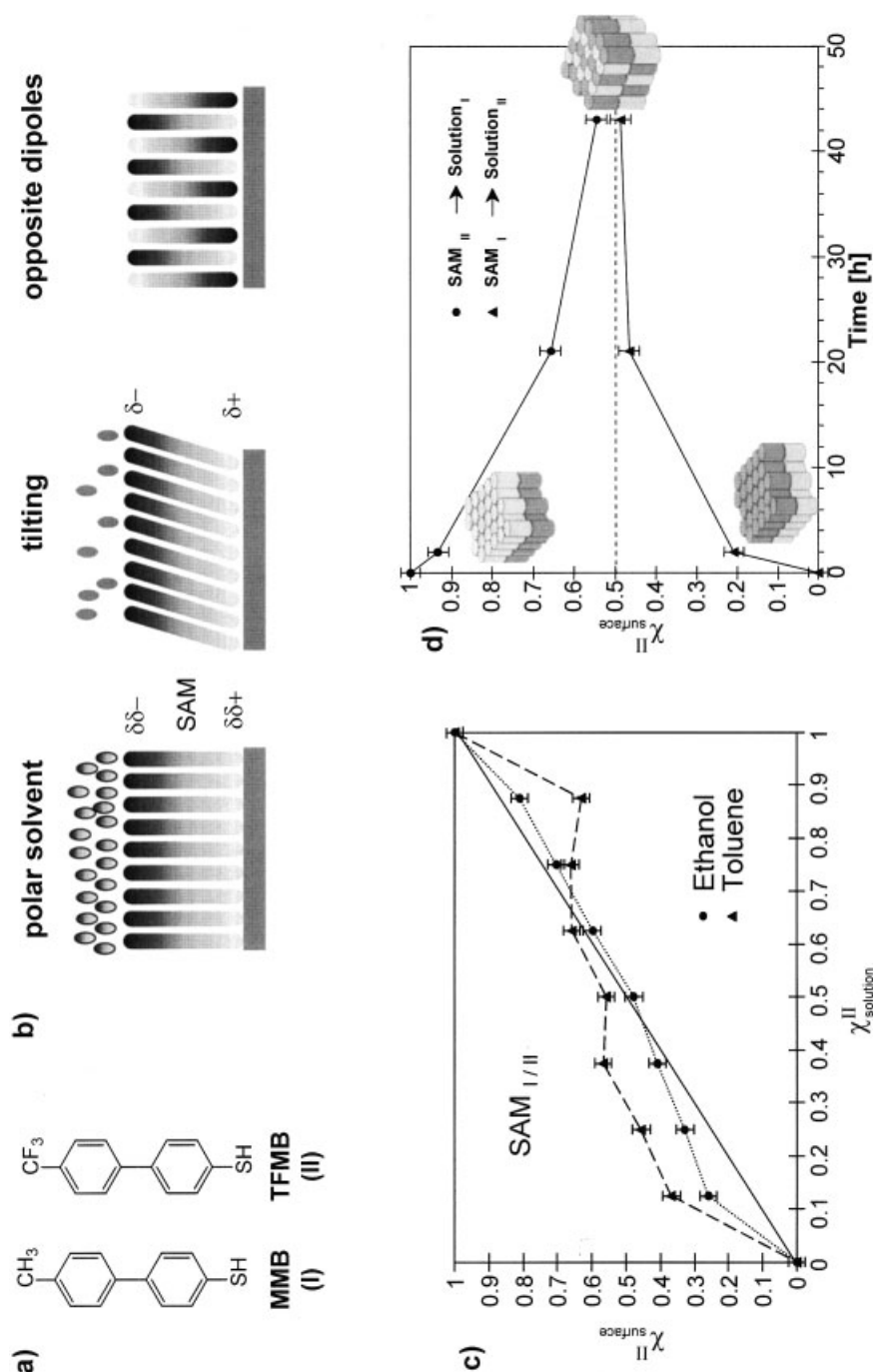
#### 9.2.6.1 Self-Assembly of Dipoles

The impact of the dipole moment in mercaptobiphenyls induced by the 4'-substitution and the polarity of the solvent upon adsorption kinetics, formation and stability was found to be much more significant than for analog aliphatic thiols [10, 96, 98]. For example, the formation of pure and mixed SAMs of MMB and 4'-trifluoromethyl-4-mercaptobiphenyl (TFMB) from different solvents were studied by means of ellipsometry, ER-FTIR spectroscopy and wetting experiments [96]. Varying the polarity of the solvent (ethanol and toluene) it was found that the stabilization of the polar SAM of TFMB leads either to an increasing tilt angle of the biphenyls to reduce the total dipole moment of the layer or to a SAM of upright standing TFMB which is stabilized by dipolar interactions with polar solvent molecules (Fig. 9.11). The study of mixed SAMs of TFMB and MMB of various solution compositions in the less polar toluene indicated a driving force to reach an equally mixed SAM. This could be explained by the fact that the two components have molecular dipoles in the opposite direction when assembled on the surface. In fact, the experiment where pure SAMs of either MMB or TFMB were submerged in a solution of the other component resulted in mixed SAMs of MMB/TFMB of approximately the same composition (Fig. 9.11).

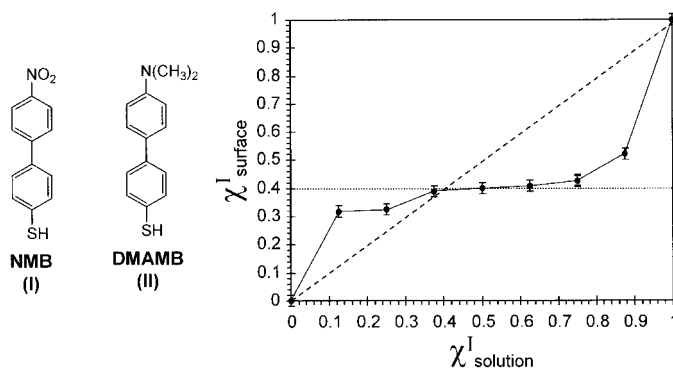
The above-mentioned experiments clearly show that the molecular dipoles of the assembling units direct the morphology and composition of the resulting assembly. The driving force for the mixing should therefore increase with increasing difference of the molecular dipole moments of the two components. This was demonstrated in the study of pure and mixed monolayers of the highly polar 4'-nitro-4-mercaptobiphenyl (NMB) and 4'-dimethylamino-4-mercaptobiphenyl (DMAMB) [98].

When mixed SAMs of NMB and DMAMB were prepared in toluene, the surface  $\text{NO}_2$  concentration, as determined by external reflection FTIR spectroscopy, displays a plateau at about 40%. If one assumes that the equilibrium concentration of the two components in the mixed SAM, in a nonpolar solvent, is driven by the formation of a two-dimensional assembly with zero net dipole moment, the results can be explained by using the Hammett equation.

Such control of surface functionalities, surface chemical potential, and surface dipole is not possible in mixed SAMs of  $\omega$ -functionalized saturated *n*-alkanethiols, since dipolar interaction of surface functionalities will result in surface reorganization [95, 99–101].



**Fig. 9.11** a) Chemical structures of MMB and TFMB. b) Possibilities to reduce the total dipole moment in a SAM of mercaptophenyls by interactions with a polar solvent, tilt or assembly of opposite dipoles in mixed monolayers. c) Surface versus solution composition found for MMB and TFMB mixed systems in polar (ethanol) and less polar (toluene) solutions illustrating the effect of the assembling dipoles. d) The opposite molecular dipoles of MMB and TFMB proved to be sufficient to induce ligand exchange in order to reach an equilibrium situation in the surface composition (modified from ref. [96]).



**Fig. 9.12** Chemical structure of NMB (I) and DMAMB (II). Composition of mixed monolayers of I and II versus the composition of the solution (modified from ref. [98]).

As already indicated in Fig. 9.9 and 9.12, the induced molecular dipole by 4'-substituent should have a significant impact upon the tilt angle of the bonded molecule. This was examined in great detail using ER-FTIR spectroscopy of SAMs of several 4'-substituted-4-mercaptobiphenyls on Au(111) and Ag(111) [10].

The impact of the choice of the substrate to be either gold or silver upon a different molecular orientation of rigid moieties within a SAM was recently demonstrated by Somashekarappa and Sampath [107]. They studied the impact of the different orientation of 2,9,6,23-tetraamino cobalt phthalocyanine bound as a SAM onto silver or gold upon their behavior in electrocatalysis. It was found that the different tilt of the phthalocyanine macrocycles and the consequently different accessibility of the metal surfaces and catalytic center results in a different reaction pathway and oxidation products.

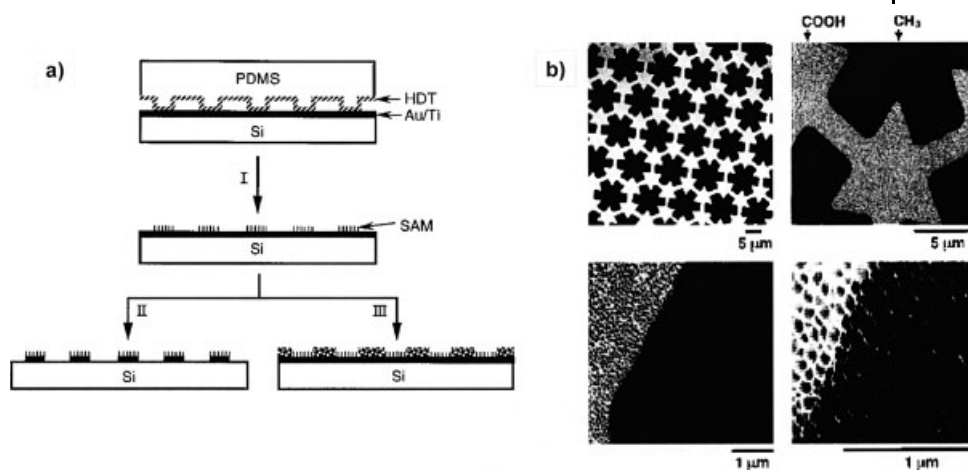
### 9.2.7

#### Patterned Self-assembled Monolayers

The formation of mixed SAMs composed of two components provides unique possibilities in the control of the physical and chemical surface properties. Besides homogeneously mixed SAMs, a directed deposition of the components results in surfaces of controlled heterogeneity. One example reported by Liedberg *et al.*, forming SAM gradients (Fig. 9.6d) by controlled diffusion has already been mentioned [73].

In Fig. 9.6c) and e), patterned SAM systems are schematically outlined. They can be prepared by lithographic tools using UV, electron beam, scanning probe and focused ion beam lithography, simply by decomposing or desorbing a SAM formed in selected areas using a mask or focused beams [108]. Although these techniques are limited by the wavelength of the irradiation used, significantly smaller features can be prepared because the thickness of the resist material is significantly reduced to the thickness of a monomolecular layer and hence, broad-





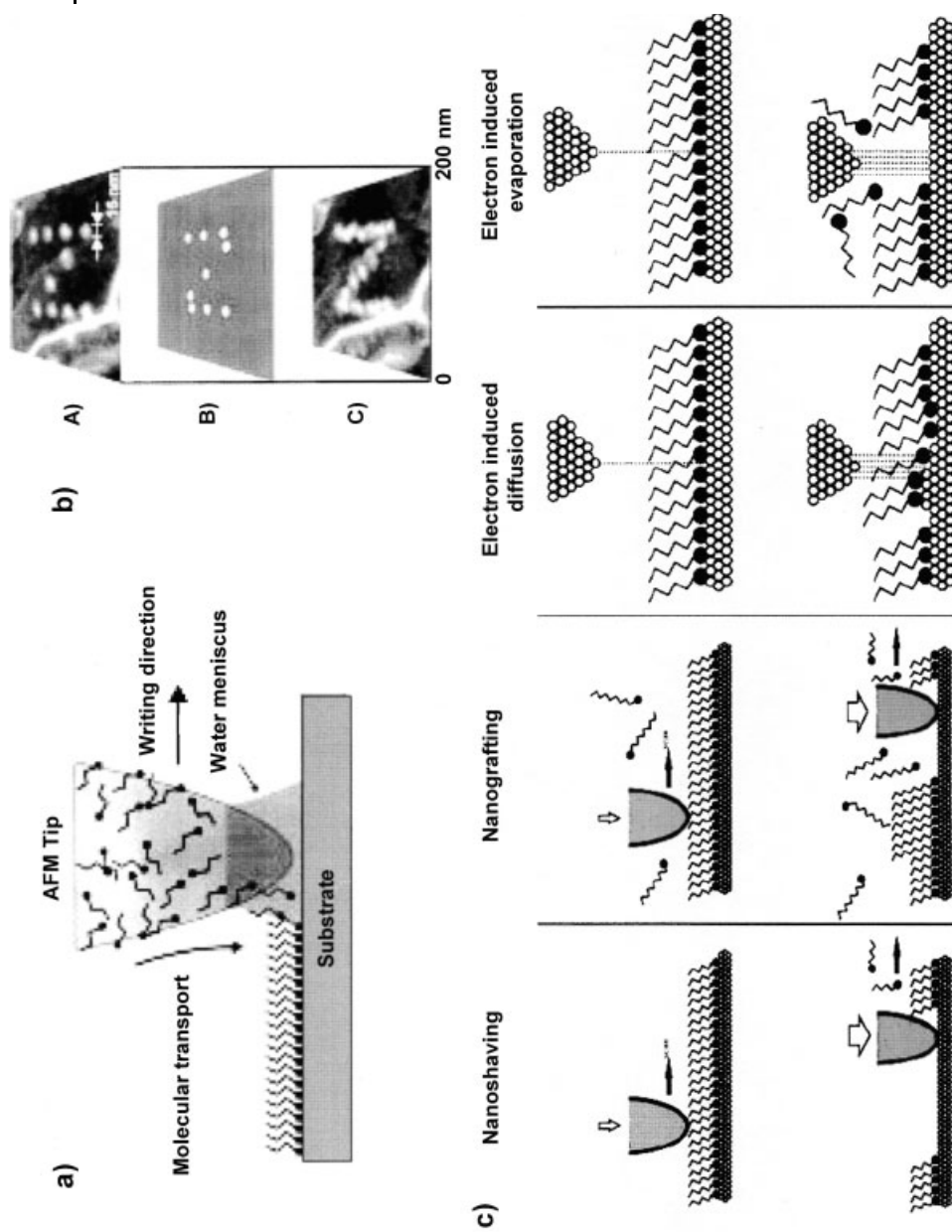
**Fig. 9.13** a) Preparation of laterally structured SAMs by the microcontact printing ( $\mu$ CP) technique. A structured PDMS stamp is 'inked' with self-assembling molecules (hexadecanethiols; HDT) and placed onto a planar substrate (gold). SAM formation occurs within seconds at the areas of contact (I). The structure can be further processed by etching (II) or deposition of a second SAM (III) onto

the remaining free substrate surface. b) Example of a structured SAM of HDT (dark) and  $\text{HS}-(\text{CH}_2)_{15}-\text{COOH}$  (bright) at for different magnifications, visualized by lateral force microscopy (LFM). (Reprinted with permission from: [6] Y. Xia, G. M. Whitesides, *Angew. Chem.* **1998**, *110*, 568–594; *Angew. Chem. Int. Ed.* **1998**, *37*, 550–575. © Copyright 1998 Wiley-VCH).

ening of the inscribed structures during irradiation and development of the patterns as known in common polymeric photoresist materials is negligible.

An alternative way to a partial decomposition of a SAM is the laterally *directed* deposition of a SAM at desired loci. Whitesides and coworkers developed the so-called soft lithography or microcontact printing ( $\mu$ CP) technique [6]. From elastomeric PDMS, a stamp with a defined relief is formed by casting and cross-linking PDMS on a master, 'inked' with a thin layer of surface active molecules (thiols or silanes) and placed on an appropriate substrate (gold, silicon dioxide etc.). At the areas of mechanical contact, a SAM is formed and the original structure of the stamp is positively transferred onto the substrate. The SAM has restricted formation because of the rapid physisorption/chemisorption of the thiol with the gold substrate, with locally high concentrations and the 'autophobicity' of the resulting SAM [109]. The remaining uncovered areas of the substrate can either be modified by deposition of another SAM from solution or further manipulated (for example etched). The procedure is outlined in Fig. 9.13. It was found that the quality of Au/thiolate SAMs formed by  $\mu$ CP is comparable to SAMs prepared by solution deposition [110].

The feature sizes that can be realized by  $\mu$ CP are typically within the range of several micrometers whereas recently, Michel *et al.* reported a resolution of approx. 100 nm [111].



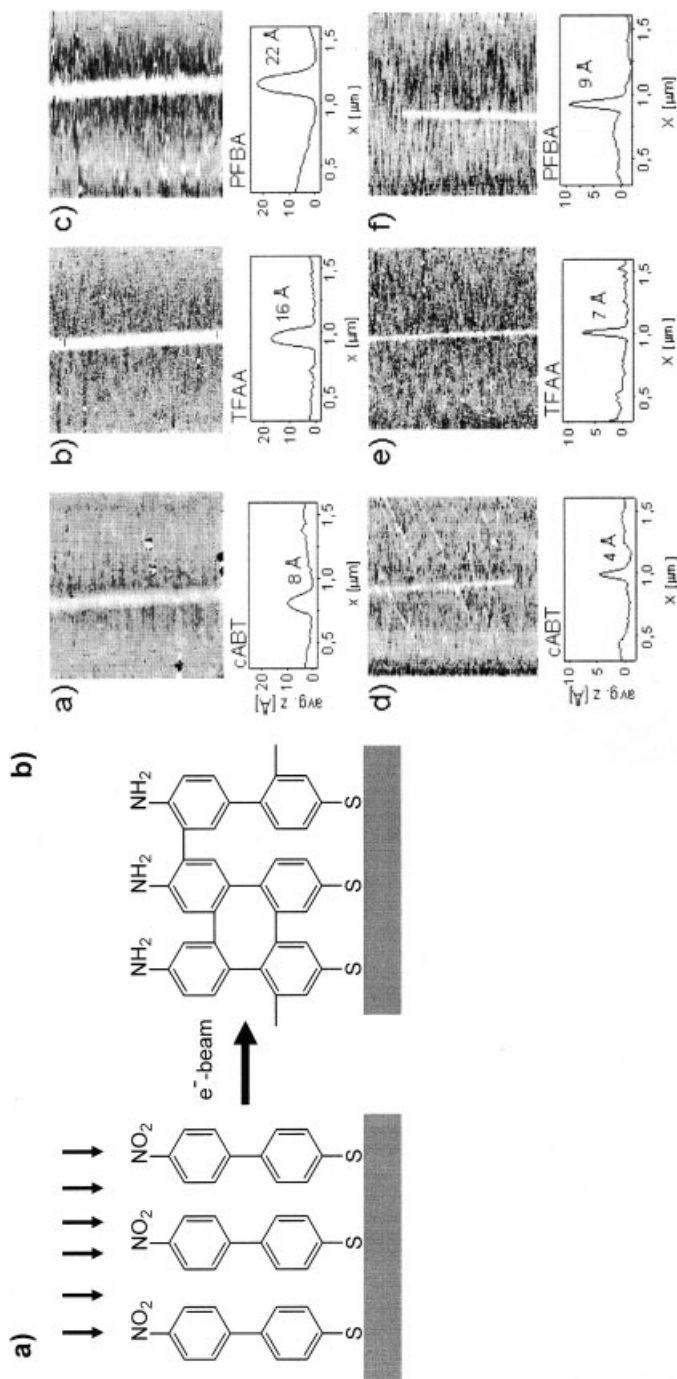
For direct patterning on the nanometer scale, scanning probe microscopy (SPM) based techniques such as 'dip-pen-nanolithography' (DPN), [112–114] 'nanografting', 'nanoshaving' or scanning tunneling microscopy (STM) based techniques such as electron induced diffusion or evaporation have recently been developed (Fig. 9.14) [115, 116]. The SPM based methods, allows the deposition of assemblies into restricted areas with 15 nm linewidths and 5 nm spatial resolution. Current capabilities and future applications of DPN are discussed in Ref. [117].

Patterned SAMs with feature sizes of comparable dimension can also be obtained by using electron beam irradiation. The smallest structures that have been generated with this technique into SAMs of *n*-octadecylsilane had a size of 5–6 nm [118]. Grunze and Götzhäuser applied e-beam nanolithography and proximity printing on aliphatic and aromatic thiol SAMs on gold [119]. While irradiation of SAMs of aliphatic thiols results in partial decomposition and cross-linking, inducing high disorder by *gauche*-defects within the irradiated areas, irradiation of SAMs of mercaptobiphenyls (MB) yielded an intact and most interestingly highly cross-linked monolayer. The observed cross-linking of mercaptobiphenyls SAMs in the irradiated areas improved the mechanical and chemical stability of the SAM which was found to resist a consecutive wet-etching procedure much better than the original MB SAM.

Based on this system an intriguing twist of nanolithography was developed by the same group, the so-called *chemical (nano)lithography* [120, 121]. The name was chosen, since electron irradiation of SAMs of 4-nitro-4'-mercaptobiphenyl (NMB) results in selective and quantitative reduction of the nitro functionalities to amino groups [122], while the aromatic biphenyl layer is dehydrogenated and cross-linked (Fig. 9.15 a). Hence, local irradiation of SAMs can be used for the chemically selective binding of functional entities using the terminal amino group. In contrast to the above-mentioned techniques based on SPM and mechanical interactions, chemical lithography is not restricted to any length scale since the use of electron flood guns in combination with adequate stencil masks allows an efficient patterning of large areas. For high resolution patterning, electron beams can be focused to nanometer sized spots, and the resolution is only limited by secondary electrons that are generated during irradiation. The smallest chemical nanostructures so far had lateral dimensions of ~20 nm (Fig. 9.15 b) [120, 121].

**Fig. 9.14** a) Principle of dip-pen nanolithography (DPN) and b) example of direct writing and positioning precision using DPN. b) Schematic diagram with lateral force microscopy (LFM) images of patterning and aligning multiple nanostructures via DPN. A) A pattern of 15 nm diameter 16-mercaptohexadecanoic acid (MHA) dots on Au(111) B) Projected second set of dots. C) Image after a second pattern of MHA nanodots. (Reprinted

with permission from: [117] C.A. Mirkin, S. Hong, L. Demers, *CHEMPHYSICHEM* **2001**, 2, 37–39. © Copyright 2001 Wiley-VCH). c) Schematic outline of SPM and STM based nanolithography techniques. The imaging (top) and manipulation modes (bottom) are illustrated. (Reprinted with permission from: [115] G.Y. Liu, S. Xu, Y. Qian, *Acc. Chem. Res.* **2000**, 33, 457–466. © Copyright 2000 American Chemical Society).



**Fig. 9.15** a) Principle of chemical nanolithography. Exposure of NMB results in the conversion to a cross-linked SAM of AMB (= cross-linked aminophenylthiol; cABT). b) AFM images and averaged height profiles of lines that were written with a focused electron beam into a NMB monolayer. a–c) 100 nm lines after electron exposure (a) and immobilization of trifluoro acetic acid anhydride (TFAA) (b) and perfluoro butyric acid anhydride (PFBA) (c). d–f) 20 nm lines after electron exposure (d) and immobilization of TFAA (e) and PFBA (f) (Reprinted with permission from: [120] A. Götzhäuser, W. Eck, W. Geyer, *et al.*, *Adv. Mater.* **2001**, 13, 806–809. © Copyright 2001 Wiley-VCH).

The preparation and application of SAM systems patterned by STM and their use in catalysis was demonstrated by Wittstock and Schuhmann [123]. The patterning (local desorption) of SAMs from alkane thiols on gold was performed by scanning electrochemical microscopy (SECM), followed by the assembly of an amino-derivatized disulfide and coupling of glucose oxidase to form a catalytically active pattern of the enzyme. The enzymatic activity could be monitored/imaged by SECM.

A different approach was followed by Blackledge *et al.* [124]. They used the catalytic activity of a palladium coated SPM-tip to selectively generate a pattern into different  $\omega$ -functionalized SAMs.

### 9.2.8

#### Self-assembled Monolayers as Tailored Functional Surfaces in Two and Three Dimensions

Since virtually any functional group can be introduced in SAMs as the tail group, SAM systems became a working platform for the study of surface confined reactions involving specific chemical reactions of small molecules [125], synthetic oligomers and polymers (see for example [6] as well as following paragraphs), peptides, proteins [126] and DNA [127], controlled deposition of functionalized nanoparticles [128–130], formation of surface confined heterostructures [4, 6] and control of cell adhesion [131, 132]. The combination of laterally structured SAMs with two or more different surface functionalities, the steric control of surface confined reactions and the broad range of characterization and detection methods of thin films resulted in numerous studies of SAM systems for directed (hierarchical) self-assembly of molecules and small objects as well as applications in sensor technology [133].

Specific, surface confined reactions not only directly involve catalysis but also the built-up of *self-assembled multilayers* (see Fig. 9.1 (3)) with  $\omega$ -functionalities for more complex (bio-) catalytic systems such as proteins or the directed deposition of active metals. Furthermore, SAM on flat substrates can be used for the study and development of, e.g. catalytic systems, but are not useful for large scale applications because they have very limited specific surface. Here, nanoparticle systems covered with 3D-SAMs are the ideal solution of combining the advantages of high surface area, defined surface composition and accessibility of proximal active catalytic centers.

Auer *et al.* [134] presented an example for multilayer formation and controlled deposition of functionalized nanoparticles on SAM of mercaptohexadecanoic acid (MHA) using electrostatic interactions. As a pH-sensitive switchable linker between the SAM of MHA and negatively charged gold nanoparticles, bis-benzamidine bolaamphiphiles having different alkyl spacers were used [135]. This strategy resulted in a potentially tunable and switchable property of the entire assembly. For example, the kinetics of adsorption as well as the final particle layer thickness can be controlled by the kind of bis-benzamidine used as the linker (Fig. 9.16).

Nanoparticles bearing a so-called three-dimensional self-assembled monolayer (3D-SAM) [136] coating or shell are ideal construction units for programmed, hierarchical self-assembly of larger objects [137]. Several research groups have successfully assembled functionalized nanoparticles into large nanocrystalline arrays



using hydrophobic or electrostatic interactions, as well as chemical bridging [138] or even biologically inspired specific interactions using the biotin-streptavidin system [139] (see Fig. 9.17).

The preparation and study of nanoparticles has attracted a remarkable academic and industrial research effort because of their potential applications, ranging from fundamental studies in quantum physics, fabrication of composite materials, information storage/optoelectronics, immunoassays, to catalysts. The precise control of size and chemical behavior (stability *and* reactivity) by means of the synthesis itself is still one of the main targets because the direct correlation of the new intriguing properties with the particle size which is just between a molecule and a bulk material [140].

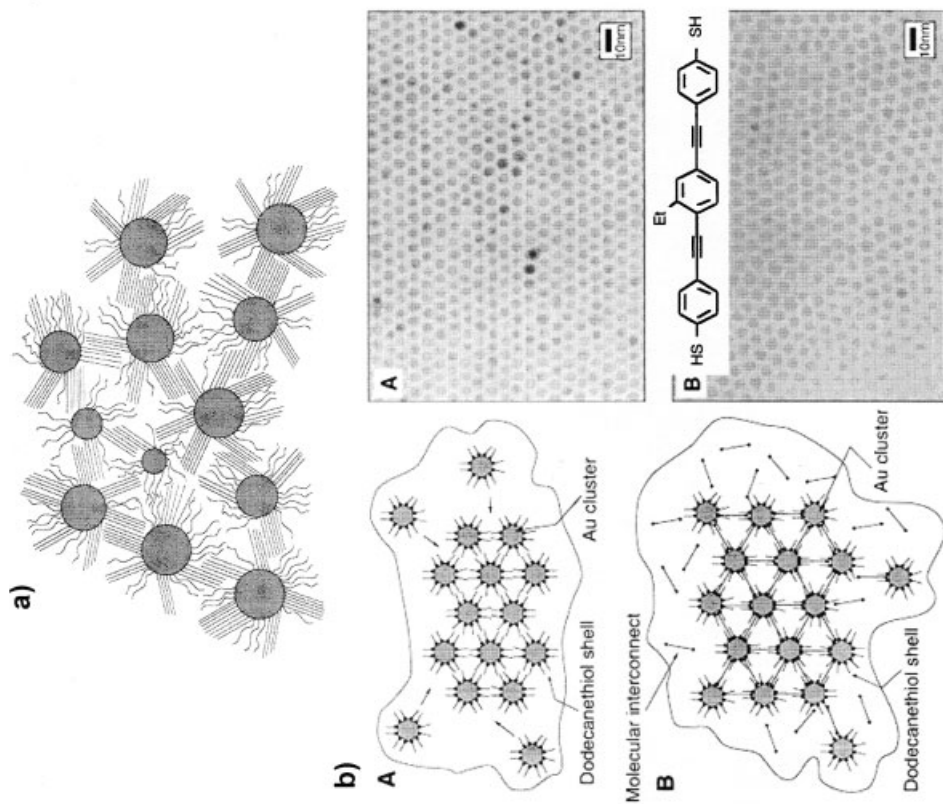
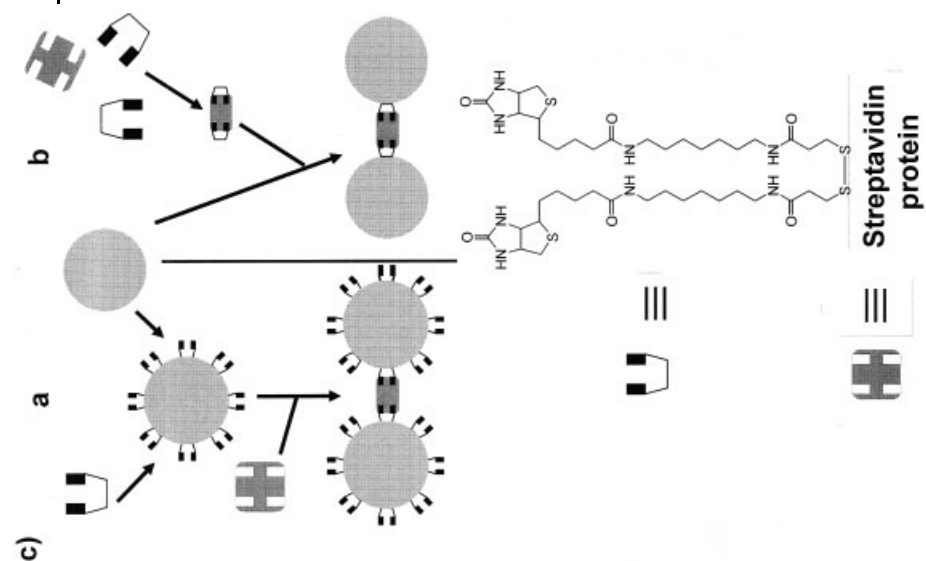
Considerable research effort was focused on systems of colloidal gold of which a broad variety of synthetic procedures were reported [140b,f]. While native colloidal gold solutions are only stable for a restricted time, Brust *et al.* [141] were able to overcome this problem by developing a simple method for the *in situ* preparation of alkyl thiol-stabilized gold nanoparticles. This synthetic route yields air-stable and easy to handle passivated nanoparticles of moderate polydispersity, and is now commonly employed for the preparation of inorganic-organic core-shell composites. Such composites are used as catalytic systems with principally two different functions of the protective 3D-SAM layer. Either the metal nanoparticle core can be used as the catalytically active center and the thiol layer is only used to stabilize the system [142], or the 3D-SAM is used as a linker system to chemically attach further catalytic functions [143].

While the method by Brust *et al.* is well-suited for the passivation of the gold colloids with simple *n*-alkanethiols, excessive purification of the decorated particles is required in the case of  $\omega$ -substituted thiols, forming polar surfaces. In this case, a second layer of the ammonium surfactant covers the nanoparticles and the purification process is long, and rarely successful. A solution to this problem was a one-phase synthesis in methanol as reported by the same group. Yee *et al.* [144] reported a simple one-phase preparation of thiol-functionalized gold, palladium, and iridium nanoparticles, using surfactant-free conditions in THF as the solvent and lithium triethylborohydride as the reducing agent. An alternative route to introduce chemical functionalities into a 3D-SAM is a post-synthesis exchange reaction, successfully employed by several research groups [145].

The main difference between a 2D-SAM on a flat surface and a 3D-SAM on a nanoparticle is their high 'surface curvature'. The entire size of the substrate is within the similar dimension as the thickness of the SAM. This does not allow the formation of a uniform crystalline SAM but can rather be pictured as a SAM

**Fig. 9.16** a) Schematic outline of the consecutive built-up of SAM/nanoparticle composites by means of charge interactions. Three different bis-benzamidines were used to serve as a linking layer, varying their alkyl chain length:  $n = 5$  pentamidine (PAM),  $n = 8$  octa-

midine (OAM) and  $n = 12$  dodecamidine (DODAM). b) Real time change in layer thickness during the adsorption of MUA-modified gold nanoparticles on bis-benzamidine-MHA modified gold surfaces as measured by *in situ* ellipsometry (modified from ref. [134]).





on a substrate with a considerable number of surface defect sites. This is also expressed by the significantly higher total amount of bonded alkanethiols on a given specific surface area on gold nanoparticles. For early in-depth investigation on 3D-SAM of alkanethiols on gold nanoparticles as well as their assembly/crystallization and order/disorder ratio as a function of the particle size and chain length of the alkanethiol shell please refer to Refs. [145–149].

### 9.3

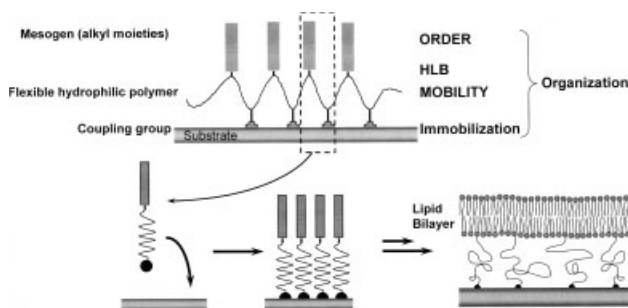
#### Polymers on Surfaces

In the second part of this Chapter the thickness of the organic layer under discussion is slightly increased and a closer look at recent developments of more complex surface-bonded systems involving polymers is outlined. Despite the introduction of flexible polymer chains, the surface coating should still be defined and uncontrolled heterogeneities minimized. Here, especially, polymer brush-type layers where self-assembled monolayers (SAMs) are used as two-dimensional template systems for the preparation of well-defined surface coatings will be subject of a more detailed discussion.

For many applications such as catalysis and possible functional devices, SAMs are simply too thin, the organized structure not flexible enough or the sterical situation within the layer too confined in order to incorporate a desired function or respond to changes in the environment in a dynamic and reversible way. One approach to increase the layer thickness of well-ordered self-assembled structures of up to 100 nm is the formation of SAM and LB multilayers by means of consecutive preparation steps (Fig. 9.1 (3)) [5, 108]. This strategy was successfully applied by several research groups, but requires the constant intervention of the experimenter to put one type of monomolecular layer on top of the other. The dynamic behavior of the layer is limited by the crystal-like organization of the system and the extreme confinement of all surface-bonded molecules. Hence, surface

**Fig. 9.17** Examples of self-assembly of nanoparticles by a) hydrophobic interactions via a shell of unfunctionalized *n*-alkanes. Depicted is a Schematic 2D Representation of the RS/Au nanoparticle packing structure in the solid state. Domains or bundles of ordered alkylthiolate chains on Au particles interdigitate into the chain domains of adjacent particles in order to compensate the free volume of the outer region of the alkyl shell (Reprinted with permission from: [146] A. Badia, L. Cuccia, L. Demers, *et al.*, *J. Am. Chem. Soc.* **1997**, 119, 2682–2692. © Copyright 1997 American Chemical Society). b) Direct comparison of hydrophobic interactions and chemical bridg-

ing. TEM micrographs of monolayer films of 3.7 nm gold nanoparticles supported on MoS<sub>2</sub>. (A) Unlinked array encapsulated by dodecanethiol. (B) Cluster network linked by a 2.0 nm-long aryl dithiol (reprinted with permission from: [138 d] R. P. Andres, J. D. Bielefeld, J. I. Henderson *et al.*, *Science* **1996**, 273, 1690–1693. © Copyright 2000 American Association for the Advancement of Science). c) Example for the self-assembly of nanoparticles using specific interactions: Two routes for aggregation of gold nanoparticles using streptavidin and a disulfide-biotin analogue (modified from ref. [139]).



**Fig. 9.18** The *polymer spacer concept* for the construction of a biomimetic cell membrane on solids. Mesogenic units, coupling groups and the flexible polymer can be combined either in form of a statistical terpolymer (above). Variation of the ratio of the three monomers allows an easy tuning of the system. In an alternative system, an end-functionalized linear hydrophilic polymer chain bearing a coupling group at the proximal and the mesogen at the distal end was employed. After grafting the polymers onto a substrate, a polymer-tethered lipid bilayer can be pre-

pared by e.g. vesicle fusion (modified from ref. [51, 150]). A polymer-tethered fluid lipid membrane can function as the optimal host matrix for membrane associated proteins. Such constructs would enable the detailed study of cell membrane associated processes such as cell-cell recognition, transport phenomena and biocatalysis. However, despite many promising approaches and candidates, a robust functional biomimetic membrane system for technological applications has not yet been developed.

defects such as interfacial roughness or chemical heterogeneity become augmented with each additional layer deposited. This can be overcome by introducing some flexibility into the system.

In 1991, Ringsdorf and coworkers [150] introduced the *polymer spacer concept* into the field of ultrathin organic layers that combines the intrinsic organization of small amphiphilic moieties and the flexibility and dynamic behavior of polymers (Fig. 9.1 (4)). Successive publications [151, 152] demonstrated the potential of this approach to overcome substrate defects, provide an 'inner compartment' with water and ion storage capabilities for water, ions (buffer) or other analytes, enable the fluidity of the layer (diffusivity of the lipids within the bilayer) and improve the elasticity of the lipid bilayer membrane. This resulted in a second-generation system to mimic a cell membrane surface as outlined by Sackmann [153]. Based on this idea, Jordan *et al.* [51, 154–156] synthesized a system based on amphiphilic end-functionalized poly(2-ethyl-2-oxazoline)s and demonstrated the impact of the delicate ratio between a flexible polymer part and the organizing lipid end group in the surface-bound lipopolymers upon the formation of a defined layer morphology, the total film thickness as well as on the stimuli responses of the amphiphilic layer.

While in neither system the total film thickness exceeded several nanometers, swelling and contact angle measurements displayed dynamic behavior of the amphiphilic surface, and reversibility of the ordering-disordering process.

To prepare thicker polymer films, one can easily spin-coat or adsorb polymers onto a planar substrate from concentrated solutions using, for example, coulomb

interactions. Layered structures can be obtained by consecutive procedures or by deposition of segregating block-copolymers. These techniques result in layered structures suitable for a variety of applications. One of the few examples demonstrating the consecutive deposition of polymers by means of a self-assembling technique was developed by Decher *et al.* [157]. He used strong coulomb-interactions to create multilayers of oppositely charged polyelectrolytes (Fig. 9.1 (7)).

However, polymer layers deposited by the mentioned techniques are in most cases subject to irreversible rearrangements because no specific, or only relatively weak, interlayer interactions are present. For stabilization, high molar mass polymers with high melting or transition temperatures are used or consecutive cross-linking reactions are applied. Within the layer, the polymers adopt random coil morphology and chemical functionalities are isotropically distributed and oriented with respect to the surface. Anisotropic orientation or enrichment of polymer bond functional groups can only be expected within the thin interfacial regions. Upon relaxation, an introduced layered structure typically dissolves [158].

By studying the properties of polymer layers on solid surfaces it soon became obvious that not only is the chemical composition of the immobilized polymer crucial for the performance of the material, but so is its morphology. This has been recognized in various fields of applications e.g. stabilization of small particles suspensions by attached polymer brush-type layers [159, 160], control of adhesion [161] or friction [162] and tailored stationary phases for chromatography [163–165].

The use of polymeric coatings in catalysis is mainly restricted to the physical and sometimes chemical immobilization of molecular catalysts into the bulk polymer [166, 167]. The catalytic efficiency is often impaired by the local reorganization of polymer attached catalytic sites or the swelling/shrinking of the entire polymer matrix. This results in problems of restricted mass transport and consequently low efficiency of the polymer-supported catalysts. An alternative could be a defined polymer coating on a solid substrate with equally accessible catalytic sites attached to the polymer (side chain) and uniform behavior of the polymer layer upon changes in the environment, such as *polymer brushes*.

The unique behavior of polymer brushes at an interface results from the fact that they consist of end-grafted, strictly linear chains [168] of the same length [169]. The grafting density has to be sufficiently high with respect to the free radius of gyration ( $R_g$ ) of the macromolecules. In order to avoid crowding, the chains are forced to stretch away from the interface, resulting in a brush height ( $h$ ) significantly larger than the typical chain dimension ( $R_g$ ) of a free chain.

In consequence, a significantly larger uniform structure is obtained for a given molecular weight. This is important for the 'reaction time' for a responding system such as a polymer brush. Entanglement and high molecular weight, broaden the relaxation time window of the response to reach a new thermodynamic equilibrium upon a change in the environment. In brush systems, entanglement is already minimized by the confinement and consequent alignment of the brushes. High molecular weight polymers are principally not necessary to obtain layer thicknesses at the nm– $\mu$ m scale for a stretched brush system (Fig. 9.1 (6)).

The layer thickness or brush height  $h$  in a good solvent scales linear with the degree of polymerization  $N$ , as well as with the grafting density  $\sigma$  as  $h \propto N \sigma^{1/3}$ . This can be written as [170]:

$$h = (12/\pi)^{1/3} N \sigma^{1/3} (\omega/\nu)^{1/3} \quad (3)$$

Because of its confinement and uniform polymer constitution, the *preorganized* polymer brush reacts *collectively* to environmental stimuli such as changes of the pH or ion strength [171–173], temperature [174], solvent quality or mechanical forces [175, 176], irradiation [177] or redox reactions [178].

Polymer brushes were found to minimize adsorption of proteins by the ‘soft’ or ‘steric’ repulsion of the flexible yet immobilized macromolecules [179], although a generally valid explanation of the protein resistant properties of some hydrophilic brushes is not available. A similar explanation can be formulated for the improvement of the colloidal stability of particle suspensions, when polymer ‘brush-type’ layers are bound to small particles. This and other intriguing features of polymer brushes prompted a remarkable experimental and theoretical research activity in order to understand and exploit the unique properties of polymer brushes.

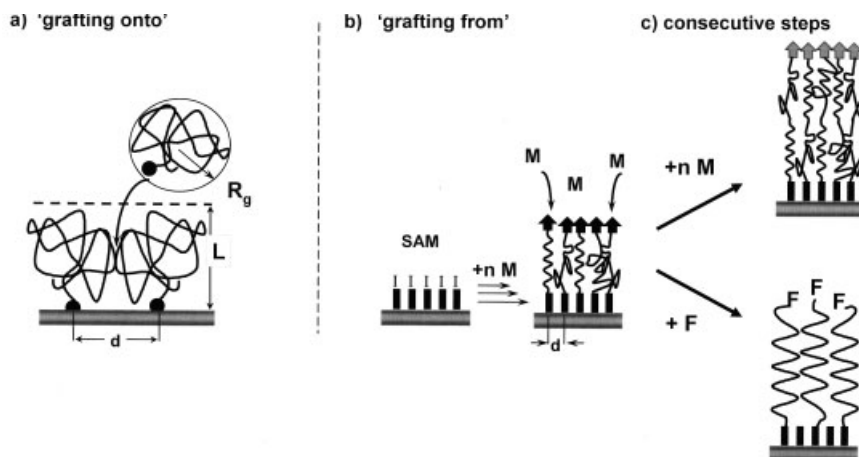
A successful theoretical description of polymer brushes has now been established, explaining the morphology and most of the brush behavior, based on scaling laws as developed by Alexander [180] and de Gennes [181]. More sophisticated theoretical models (self-consistent field methods [182], statistical mechanical models [183], numerical simulations [184] and recently developed approaches [185]) refined the view of brush-type systems and broadened the application of the theoretical models to more complex systems, although basically confirming the original predictions [186]. A comprehensive overview of theoretical models and experimental evidence of polymer brushes was recently compiled by Zhao and Brittain [187] and a more detailed survey by Netz and Adelman [188].

The mentioned properties make polymer brushes ideal systems for the preparation of preorganized ‘intelligent’ materials to serve as functional devices on significantly larger length scales [189, 190].

### 9.3.1

#### Polymer Brushes by Surface-initiated Polymerizations

Traditionally, polymer brushes have been prepared by: (a) selective physisorption of block-copolymers from bulk or solution onto a solid surface, where a shorter ‘anchor’ block adsorbs strongly onto the surface, leaving the remaining ‘buoy’ block tethered to the interface [191] or by (b) chemical grafting or chemisorption of polymer chains onto a reactive surface via a terminal coupling group [192]. However, both techniques have their limitation in terms of the maximum grafting density that can be obtained. It is easy to picture that chains that are already adsorbed, screen grafting sites still available in their vicinity, because a tethered polymer chain tries to maintain its random coil conformation (Fig. 9.19a). As the grafting density increases, the chains have to increasingly stretch to allow further



**Fig. 9.19** Preparation of polymer brushes on solid surfaces by a) chemical grafting of end-functionalized linear polymers or selective adsorption of asymmetric block copolymers and b) by surface-initiated polymerization (SIP) using initiator functions on the solid surface. The depicted SAM bearing  $\omega$ -functionalities

as initiators or initiator precursors are especially suitable for the design and control of surface-bonded initiator sites. c) Preparation of block copolymer and end-functionalized brushes via surface-initiated controlled or living polymerization techniques (modified from ref. [194]).

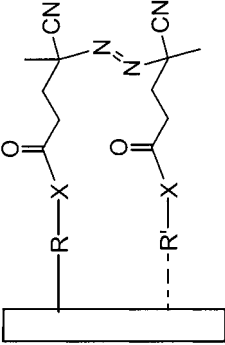
grafting, which results in a decrease of the rate of grafting kinetics [193]. At some point, a limiting situation is reached that is dominated by the free energies of stretching, chain–chain interactions, and solvation. Hence, the grafting density of a brush, formed by the traditional ‘transplanting’ methods, is self-limiting [194]. Indeed, although brushes have been theoretically successfully modeled using scaling arguments, effective synthetic routes for defined polymer brushes on solid surfaces, where the average distance between grafted polymers  $d$  is significantly smaller than  $R_g$ , have only recently been developed. The limitation by the impairing adsorption process of large polymers was overcome by the ‘grafting from’ method.

In this method, a reactive group on the surface initiates the polymerization, and the propagating polymer chain grows from the surface (Fig. 9.19b). In principle, it can be employed with all polymerization types, and a number of papers have reported high amounts of immobilized polymer using surface-initiated polymerization with various initiator/monomer systems. If controlled or living polymerization techniques are used, block copolymer or end-functionalized polymer brush systems can be prepared in consecutive reaction steps (Fig. 9.19c).

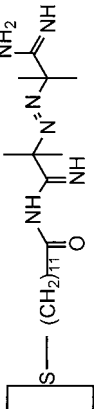
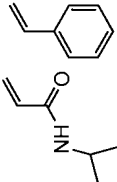
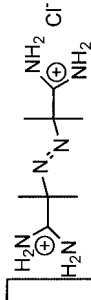
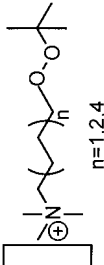
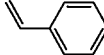
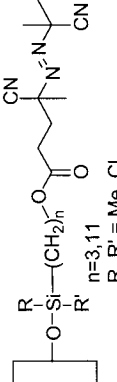
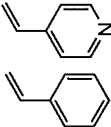
To realize surface-bonded initiating sites or their precursors, a variety of methods are applicable. Either organic (polymer) surfaces are irradiated or plasma treated to yield suitable functional groups [187, 195] or inorganic supports are covered with an interlayer of functional polymers bearing the desired groups. However, to gain control over the quantity of surface reaction sites and define the surface chemistry, interlayers of low molar mass  $\alpha,\omega$ -functionalized surface active compounds are suit-

**Tab. 9.2** Specific surface modifications and SAM systems of particles or planar substrates for the surface-initiated free radical polymerization of vinyl monomers.

Substrate	Intermediate Layer//Initiator	Monomer(s)	Reference
Carbon black		Various vinyl monomers	196–201
SiO <sub>2</sub> , TiO <sub>2</sub>	<p> <math>X = -S-Ar, -SO_2-Ar, -SO_3-Ar, -NH-Ar,</math>  <math>-C(CN)_2R, -C(CN)(COOR)R</math> </p>		202–207

$\begin{array}{c} \text{Me} \\   \\ \text{---O---Si---R---CH}_2\text{---XH //Ce(IV)} \\   \\ \text{Me} \end{array}$	$\begin{array}{c} \text{NH} \\   \\ \text{CH=CH} \\   \\ \text{O} \\   \\ \text{NH}_2 \\   \\ \text{CH=CH} \\   \\ \text{O} \\   \\ \text{HO} \\   \\ \text{COOH} \end{array}$	208-211
$\text{XH=OH, NH}_2, \text{SHr}$	$\text{R=---(CH}_2\text{)}_2\text{---N(CH}_3\text{)}_2$ $\text{---(CH}_2\text{)}_2\text{---N(C}_2\text{H}_5\text{)}_2$ $\text{---(CH}_2\text{)}_2\text{---N(CH}_3\text{)}_3^{\oplus}$ $\text{---C(CH}_3\text{)}_2\text{CH}_2\text{---SO}_3^{\ominus}$	
$\text{SiO}_2$		
$\text{SiO}_2, \text{Au}$	$\begin{array}{c} \text{NH} \\   \\ \text{---O---Si---} \\   \\ \text{---O---Si---(CH}_2\text{)}_3\text{NH} \\   \\ \text{---O---Si---(CH}_2\text{)}_3\text{O} \\   \\ \text{---O---Si---(CH}_2\text{)}_3\text{O---CH}_2\text{---CH(OH)---CH}_2\text{---O} \\   \\ \text{---S---(CH}_2\text{)}_{10}\text{S} \end{array}$	212-218

Tab. 9.2 (cont.)

Substrate	Intermediate Layer//Initiator	Monomer(s)	Reference
Au			219, 220
Mica	 		221–225
SiO <sub>2</sub>			218, 226–237



Au, SiO <sub>2</sub>			218, 238
Au			239
Au, SiO <sub>2</sub>			240
Au			241

able. For the latter, the advantages of SAM systems of  $\omega$ -functionalized silanes on oxide surfaces or thiols on metals already outlined, are especially intriguing (see again Fig. 9.6). Hence, in the following, the focus is trained on these systems.

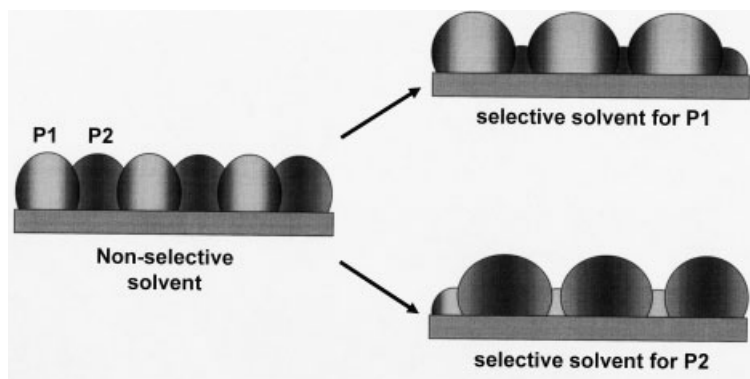
### 9.3.2

#### Surface-initiated Polymerization Using Free Radical Polymerization

To initiate free radical polymerization on a surface, the common initiators as used in solution polymerization are employed. This includes peroxides, symmetric and asymmetric azo-compounds, as well as redox systems. The initiator/monomer systems immobilized on different substrate types along with the monomers used have been compiled in Tab. 9.2. By the early 1970s, Hamann and Laible *et al.* [202–207] had reported on the preparation of polymer layers on silica and titanium dioxide particles prepared by SIP. Extensive work is reported, on a variety of azo-initiators based on 1,4-substituted aryl compounds directly bond to the oxide surface. The azo function was varied in the terminal substitution and the SIP behavior studied for most of the common vinyl monomers. Tsubokawa and Sone *et al.* [196–201] grafted polymers onto carbon black particles by SIP using azo-initiators, peroxides and redox systems with were bond via the surface phenol groups to carbon black. Since at that time elaborate characterization techniques had not yet been developed, the main criterion was the pure amount of polymer bound to the colloidal particles, taking full advantage of the high surface area of the supports and therefore the high total amount of initiator. However, the principle was demonstrated and the main initiator types of free radical SIP screened. Based on the work of these two groups, several other researchers developed SIP using more sophisticated initiator systems such as symmetric azo compounds (supposedly) bound on both sides to the substrate surface [212–218] via a thiol group on gold surfaces, a silanization reaction onto silica or glass or employing another coupling reaction on prefunctionalized surfaces using, for example  $\alpha,\omega$ -amino silanes. The decomposition of a surface-bound azo initiator results in one free and one immobilized radical. Since the initiator preparation is performed in most cases directly on the surface and the question of the number of bonds formed by one or both of the groups can only be estimated, this initiator is in principle suitable for SIP, although no defined SAM system of initiators can be formed. Especially, when thiol terminal groups are used for attachment onto gold [215], desorbed thiols can impair the SIP by acting as a chain transfer agent. Therefore, Dryer *et al.* recently addressed this point and presented a detailed study of a corresponding system using contact angle measurements, ellipsometry, ER-FTIR spectroscopy and XPS. They found that even with a relatively long  $n$ -alkyl spacer between the azo function and the thiol, the initiator forms an unorganized surface layer with the initiator bonded only by one surface-active group. The remaining thiol group is most likely oxidized by air [215a]. The poorly-defined surface morphology of the initiator is explained by the lack of a suitable mesogen as discussed in the previous part of this chapter on SAMs. The problem of poorly-defined surface chemistry during immobilization or *in situ* generation of the initiator was tackled by R  he *et*

*al.* using a preformed AIBN analog equipped with a monofunctional silane group [e.g. 226, 227] or thiol [238]. Additionally, the initiator featured a cleavable group to detach the resulting polymer brushes and analyze the amount, molecular weights and polydispersities of the polymer formed by SIP. They presented detailed studies of, for example, the effect of the polymerization temperature and surface concentration of the initiators ranging from a monolayer to submonolayer coverage upon the standard polymer analytical values. High grafting densities ( $\sigma \sim 3$  nm), high molecular weights and thick polymer brush layers have been reported. Besides the polymerization of styrene as the reference monomer to investigate SIP, functional monomers bearing a mesogen for the preparation of liquid crystalline polymer brushes [216], methacrylates bearing a dye label [238] or perfluoroalkyl chains for the preparation of low surface free energy polymer brushes [217] were polymerized. Despite the fact that free radical polymerization suffers from termination and transfer reactions, which results in a typical polydispersity index ( $PDI = M_w/M_n$ ) of 1.5 to 2, a linear relationship between the polymerization time and film thickness was found. In general, surface-initiated free radical polymerization proved to be an effective method of immobilizing polymer brushes with high molecular weights on a variety of surfaces. The polymer brush layer becomes dense so that, for example, the original support, such as colloidal silica particles, can no longer be dissolved in concentrated HF [213b, 226]. Free radical SIP seems to have much in common with bulk polymerization. This was observed by Schouten and coworkers, who reported on a pronounced Tommsdorff effect in the surface confined free radical polymerization [212].

Müller *et al.* [209–211] reported extremely thick polymer (brush) layers of poly(acrylamide) formed by SIP with redox initiators of primary alcohols and Ce(IV) which can be easily visualized by light microscopy [211]. With this initiator system, as originally developed by Mino and Kaizermann [249, 250] for the SIP of vinyl monomers from cellulose and also applied by Tsubokawa *et al.* [200, 201] for carbon black, Müller and coworkers prepared a row of polymer brush type electrolyte layers on porous silica as high capacitance ion-exchange stationary phases (there called ‘tentacle-type’) for the separation of biopolymers. Polyelectrolyte brushes can also be formed by polymer analog quaternization of poly(4-vinylpyridine) brushes as reported by Biesalski *et al.* [230, 231]. Polyelectrolyte brushes are of special interest because their morphology and physical behavior are dominated by the strong electrostatic interactions along the grafted chain and within the polymer layer [242]. As an alternative to covalent attachment of the initiator molecules, ionic groups can be used to prepare permanently grafted brushes by SIP. In fact, in the 1950s Dekking *et al.* [221, 222] used 2,2'-azobisisobutyramidine as the very first initiator systems for the free radical SIP. This class of surface initiator is relatively simple to prepare from commercially available compounds and was later revisited by other groups to form responsive polymer brushes of poly(*N*-isopropylacrylamide) (PNIPAM) on planar substrates to control bacteria attachment and detachment [220] or to form patterned polymer brushes by  $\mu$ CP of SAMs and enhancement of the patterns by SIP [219]. Suter and coworkers found that using this initiator on mica, initiation from the surface plays a minor role in the formation of the surface-



**Fig. 9.20** Grafted heterogeneous polymer brushes in different environments and principle of switching : (a) Structure in a nonselective solvent, (b) in a selective solvent for polymer P1 (e.g. PS), and (c) in a selective solvent for polymer P2 (e.g. P4VP) (modified from ref. [214]).

bound polymer but instead, a ‘grafting onto’ mechanism dominates, in which active chain ends react with the decomposition product of the initiator [223]. The same group [224, 225] alternatively used quaternary amino groups to attach peroxide initiators for the SIP of styrene on high surface area mica.

The development of surface analytical techniques enabled detailed investigations of polymer brush dynamic behavior or morphology. Today, SIP is frequently carried out on flat surfaces and studied in detail regarding these aspects. Especially, the dynamic swelling behavior of brush systems as a collectively and fast-responding functional system was studied by e.g. SPM [228], ellipsometry [194, 233, 243] or scattering methods [244, 245]. Although the preparative possibilities of free radical polymerization is limited to homopolymers or statistical copolymers, heterogeneous polymer brushes could be created. Minko and Stamm [214] successively polymerized styrene and 2-vinylpyridine on surfaces functionalized with azo initiators. They demonstrated a controlled change in the layer morphology by selective swelling (Fig. 9.20).

Laterally-defined heterogeneous polymer surfaces can be created by using a homogeneous layer of an azo initiator. UV irradiation through a mask in the presence of monomer leads to the locally confined photopolymerization [234]. A second polymerization using the remaining initiators results in patterned surfaces composed of two types of polymer brushes [238]. However, the lateral resolution of obtainable patterns is limited by the irradiation used and type of mask (in this case polymer brush patterns of 260  $\mu\text{m}$  spaced by  $\sim 40 \mu\text{m}$  were formed).

Chilkoti *et al.* took advantage of the  $\mu\text{CP}$  method to prepare patterned SAM of mercaptoundecanoic acid (MUA) for the binding of 2,2'-azobisisobutyramidine. Thermal SIP resulted in the topographical enhancement of the originally printed SAM structure with feature size of about 40  $\mu\text{m}$  [219]. Also, the selective binding of thiols onto gold can be used for spatio-selective SIP. Dryer *et al.* [215] used gold

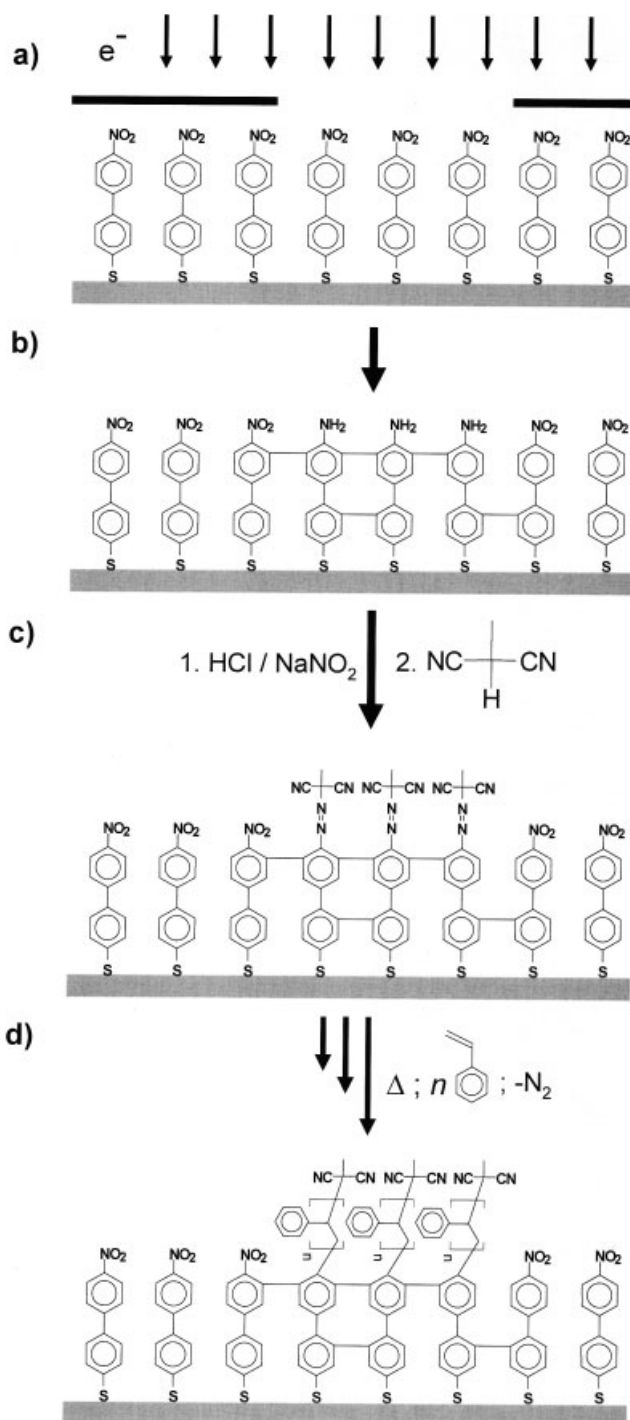
patches on silicon wafers, bonded a SAM onto the gold and used the functionalized SAM/Au patches ( $\sim 90 \times 90 \mu\text{m}^2$ ) for photopolymerization of styrene.

In recent examples, the morphology of the initiator layer was mainly that of a surface modification and not that of an organized SAM. As an alternative, one can also use a cross-linked or otherwise immobilized macromolecular interlayer containing azo or peroxide initiators [246–248], or redox systems ( $-\text{OH}/\text{Ce(IV)}$ ) [249–251]. In most of the reported work, the choice of the linker between the surface coupling group and the actual initiator is mainly determined by the chemistry of the synthesis of the initiator rather than to ensure the formation of a well-ordered SAM. For alkyl derivatives it appears that the bulky azo function inhibits the formation of a crystalline-analog SAM on gold when the entire initiator is immobilized. Surface analog reactions on SAMs may circumvent this problem but the surface chemistry has to be tailored to the steric situation at the interface (Fig. 9.6). Additionally, the problems of detached thiols as potential chain transfer agents are discussed in the corresponding reports since SAM of thiols are limited in their thermal stability or during UV irradiation.

Recently, Schmelmer *et al.* combined the chemical lithography of well-defined SAMs of 4,4'-substituted mercaptobiphenyls (see Fig. 9.15) and enhancement of surface patterns by means of SIP to create patterned polymer brushes on the micrometer and nanometer scale [241]. The selectivity, flexibility, high throughput and superior resolution of chemical lithography make it an ideal technological platform for the preparation of SAM patterns amplified by SIP. The preparation of initiator sites and a consecutive polymerization was first carried out without structuring: a SAM of 4,4'-nitromercaptobiphenyl (NMB) on Au(111) was converted to cross-linked 4,4'-aminomercaptobiphenyl (AMB) SAM by irradiation with e-beams. The terminal amino groups were then diazotized and reacted with methyl malodinitril to give a surface-bound monolayer of the 4-substituted mercaptobiphenyl azomethylmalodinitrile (cMBA) (see Fig. 9.21).

Phenylazoalkyl malodinitriles and their derivatives are known as second generation initiators for the radical polymerization of a broad variety of vinyl compounds to prepare graft copolymers in solution [252] as well as for SIP [203–207, 238]. In contrast to commonly used symmetrical azo initiators, thermal or photo-initiated decomposition yields one (bound) phenyl radical of high reactivity and one (free) malodinitrile radical which is not capable of initiating radical polymerization because of its resonance stabilization. In other words, by decomposition of the surface-bound asymmetric phenylazoalkyl initiator, the polymerization is only initiated at the surface and not by a cleaved free radical in solution, as with dialkylazoinitiators. Furthermore, previous results indicate that the radical polymerization initiated by phenylazomethyl malodinitrile follows a controlled polymerization mechanism, since in 'grafting from' reactions the degree of polymerization of the side chains can be varied with the reaction time and the typical polydispersity index is significantly lower ( $M_w/M_n \sim 1.4$ ) than in free radical polymerization. It is suspected that the methyl malonodinitrile radical acts as a reversible termination agent [253].

The monolayer of cMBA was then exposed to a solution of styrene in toluene at  $80^\circ\text{C}$ .



Inspection of the substrates with ER-FTIR spectroscopy, SPM and ellipsometry revealed that the surfaces were homogeneously covered by a polystyrene (PS) brush layer with a typical polymer layer thickness of 6.3 nm after a polymerization time of 6 h. The surface modification proved to be surprisingly stable at elevated temperatures and good solvent environments (soxhlet extraction) because of the cross-linked SAM support and the known stabilization effect of the polymer brush itself. Inspection of the SPM scans of the polymer brush in comparison with the native polycrystalline gold substrate showed the rendering of the single gold crystals, decreasing the step height of individual crystals from ~2.5 nm to approximately 1 nm and a small decrease of the root mean square roughness value of 0.7 nm in contrast to the original surface roughness of the gold substrate of 0.9 nm.

The preparation of structured polystyrene brushes was carried out following the same procedures, only the irradiation was performed through a stencil mask with circular openings of 800 nm radius that was placed on the NBT covered substrate. Fig. 9.22 shows an SEM micrograph.

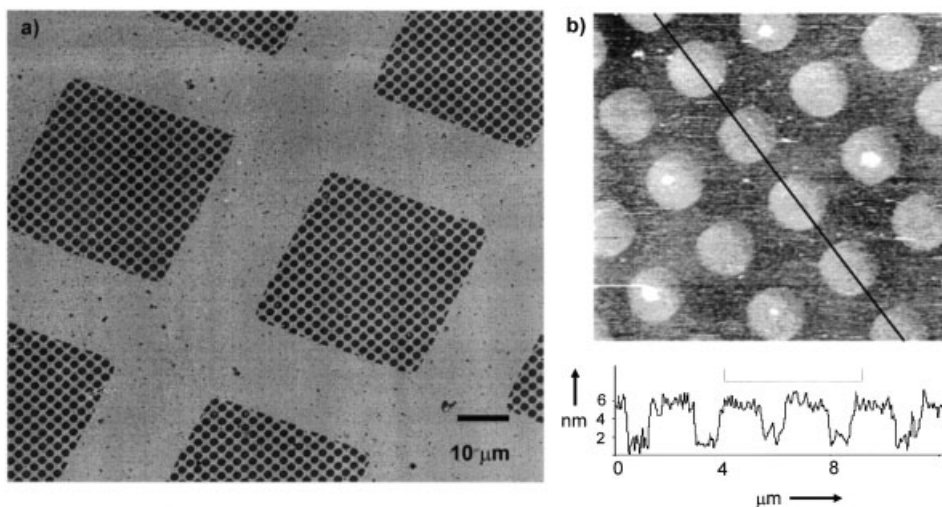
The dark dots represent areas where the NMB SAM was converted to AMB by irradiation, reacted further to cMBA and the SIP of styrene took place with good selectivity and uniformity. SPM scans revealed typical heights of the PS dots of 6 nm, a width of 1.6  $\mu\text{m}$  spaced with a periodicity of 2.5  $\mu\text{m}$  which is a one-to-one translation of the feature size of the mask. Investigation of different areas by SPM showed almost no variation of the structures.

Using a stencil mask with slits varied between 300 and 70 nm nanometer size structured polymer brushes were created following the same procedure, resulting in a one-to-one translation of the mask patterns.

The structures obtained created by the combination of chemical lithography and SIP are significantly smaller than features reported with comparable techniques. The advantage of this approach is not only the free choice of surface structures which can be created, the material contrast which can be realized by the combination of chemical lithography and amplification with SIP, but also the potential to bridge the gap in structural feature sizes ranging from the microscopic to the nanoscopic scale. Since the feature sizes reported are still limited to the features of the mask used, direct writing with a focused e-beam should result in patterned polymer brushes of features matching the size of the immobilized macromolecule.

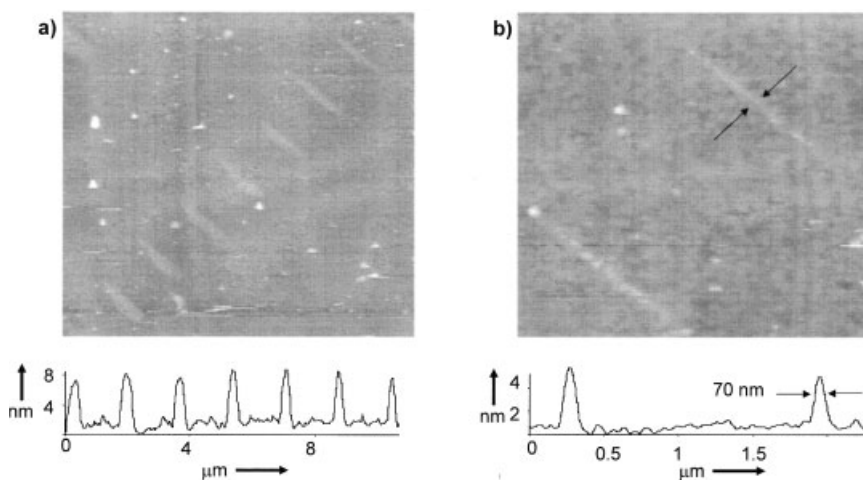
**Fig. 9.21** Reaction and preparation scheme starting from SAMs of NBT on Au(111) (a). By exposure to electron beams, intralayer cross-linking and conversion of the terminal nitro group to the amino group occurs, resulting in cABT (b). Diazotation and coupling of malonodinitrile gives a SAM bearing an asymmetric azo-initiator: cMBA (c). Finally, by

exposure to a vinyl monomer (styrene) and heating to 80 °C, the radical polymerization results in a polymer brush layer at the irradiated areas (d) (Reprinted with permission from: [241] U. Schmelmer, R. Jordan, W. Geyer, *et al.*, *Angew. Chem.* **2003**, 115, 577–581. © Copyright 2003 Wiley-VCH).



**Fig. 9.22** a) SEM micrograph of polystyrene brushes generated via SIP on a substrate that was irradiated through a stencil mask with a coarse grid with 60 μm periodicity. Each square contains an array of circular holes of 1.6 μm dots (2.5 μm periodicity). b) SPM

image of a small region of a similar substrate along with a height profile along the line indicated. (Reprinted with permission from: [241] U. Schmelmer, R. Jordan, W. Geyer, *et al.*, *Angew. Chem.* **2003**, 115, 577–581. © Copyright 2003 Wiley-VCH).



**Fig. 9.23** SPM micrographs of PS brushes generated by SIP on a chemical nanolithography substrate prepared by a stencil mask with a slit pattern. The height profiles below the images show an average profile along the

a) ~200 nm, b) ~70 nm wide lines (Reprinted with permission from: [241] U. Schmelmer, R. Jordan, W. Geyer, *et al.*, *Angew. Chem.* **2003**, 115, 577–581. © Copyright 2003 Wiley-VCH).



## 9.3.3

**Surface-initiated Polymerization Using Living Ionic Polymerization**

In comparison to the numerous accounts that are reported for free radical SIP, reports on living cationic or anionic SIP are scarce. This is mainly because the nature of the polymerization is sensitive, and the amount of initiator is tiny, and hence, the resulting total numbers of propagating polymer chains within the reactor is also small. Even amounts of impurities forming a sub-monolayer concentration on the reaction flask would strongly interfere with the living polymerization. One solution to this problem is to increase the specific surface area of the substrate by using small or porous particles and thus increasing the total number of surface-bond initiators in the reaction. Another possibility is to initiate ionic polymerization on the surface *and* in the solution to use the free propagating species as scavengers for undesired termination. In any case, the living ionic polymerization and especially anionic SIP is experimentally rather difficult to perform, especially on flat substrates with just a couple of square centimeters surface area to cover. Despite these experimental difficulties, it is worthwhile to look into living ionic SIP. The synthetic possibilities of living SIP reactions are unique, such as the formation of homopolymers with low polydispersities, synthesis of defined block copolymers and the introduction of functional end groups results in polymer brushes of uniform length, (multi)layered polymer brushes which may not be obtainable by the 'grafting to' approach, as well as polymer brushes with defined terminal end groups (Fig. 9.19). Additionally, the uniform growth of the polymer brush during polymerization and the absence of cross-linking, chain transfer and combination guarantee the formation of a well-defined brush of strictly linear chains of uniform length. In free radical polymerization the propagating species are confined within a thin surface layer which enhances the probability of side reactions such as combination and cross-linking by chain transfer. Furthermore, the decomposition of the initiator to the reactive radical species occurs throughout the propagation reaction of the polymerization. At advanced reaction time, this will lead to problems in mass transfer of the monomer through the increasingly denser polymer brush layer. Schouten [254] already pointed out that in the case of living ionic SIP where the initiation is much faster than the propagation reaction ( $k_i \gg k_p$ ) no grafting sites (propagating chain ends) are screened.

On the other hand, the observed polydispersities of polymer brushes prepared by SIP are still within the range of polymerization in solution. This may also be because the impact of transfer and other side reactions only partially shows up in the final surface-bonded brush since the fraction of created polymers which is not bonded on the surface, is simply washed away. In general, for most of the polymerization reactions employed, cross-linking, competitive side and termination reactions are augmented in surface-initiated polymerizations because of the extremely small total number of reactive chain ends, as well as their high concentration, confined in a thin layer. Recalling the characteristics of a brush, as a layer of linear chains of uniform length, controlled/living polymerization reactions are most suitable for their formation.

### 9.3.3.1 Surface-initiated Polymerization Using Living Anionic Polymerization

Recalling the demands on the polymer architecture of a polymer brush and the projected properties in terms of swelling, wetting and friction, as described in the theoretical work, the brush has to consist of linear polymer chains of the same length at high grafting densities. The closest approximation to this can be obtained by the living anionic SIP (LASIP). The experimental difficulties outlined mean that only relatively few examples of LASIP are documented in the literature.

For example, Ohkita *et al.* [255] reported that OLi surface groups created by the treatment of carbon black with *n*-BuLi are reactive enough to start LASIP of MMA and acrylonitrile (AN) but not styrene or  $\alpha$ -methylstyrene. These monomers were only polymerizable in the presence of crown ethers [256, 257].

Braun *et al.* [258] used a combination of *tert*-butyllithium (*t*-BuLi) and tetramethylethylenediamine to create initiator sites at the surface of carbon black for the LASIP of styrene. Schomaker *et al.* [259] first immobilized a methyl methacrylate derivative on colloidal silica and after activation by a Grignard reagent polymerized MMA.

Based on this approach Schouten *et al.* [254] attached a silane-functionalized styrene derivative (4-trichlorosilylstyrene) on colloidal silica as well as on flat glass substrates and silicon wafers and added a five-fold excess BuLi to create the active surface sites for LASIP in toluene as the solvent. With THF as the reaction medium, the BuLi was found to react not only with the vinyl groups of the styrene derivative but also with the siloxane groups of the substrate. It was found that even under optimized reaction conditions, LASIP from silica and especially from flat surfaces could not be performed in a reproducible manner. Free silanol groups at the surface as well as the ever-present impurities adsorbed on silica, impaired the anionic polymerization. However, living anionic polymerization behavior was found and the polymer load increased linearly with the polymerization time. Polystyrene homopolymer brushes as well as block copolymers of poly(styrene-*block*-MMA) and poly(styrene-*block*-isoprene) could be prepared.

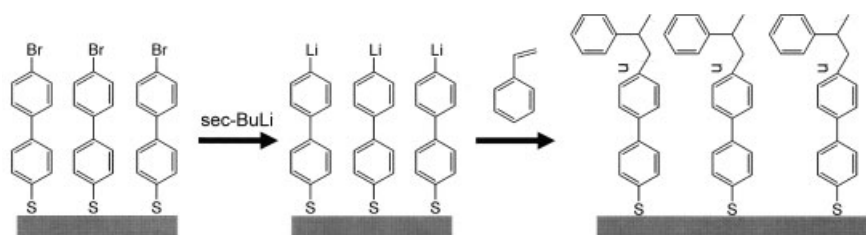
Because of the difficulty in investigating polymer layers on small particles, the characterization of the obtained materials was mainly restricted to accounts of the total amount of grafted polymer, and to estimations of the grafting density based on the remaining initiation sites. Hence, no detailed information on layer and polymer morphology or brush characteristics could be provided.

Till now, only three reports on the preparation of polymer brushes by means of surface-initiated anionic polymerization on planar substrates with accounts on the morphology and special properties can be found.

Jordan *et al.* [194] presented the only report of LASIP on planar substrates using a well-defined SAM as the initiator system.

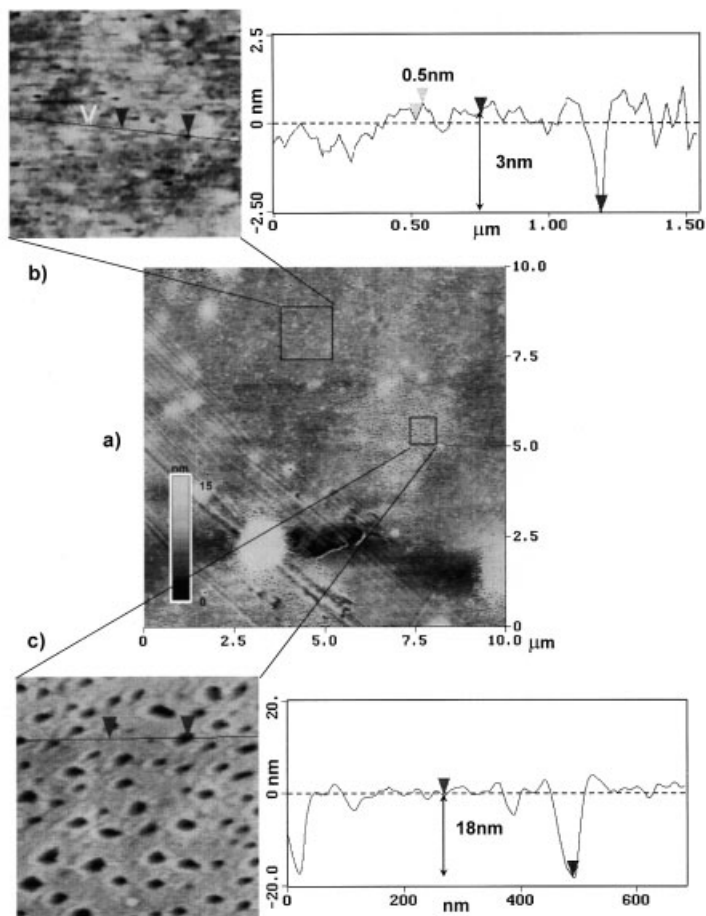
In an all-glass reactor, a SAM of 4',4-bromo-mercaptobiphenyls on Au(111) surfaces was converted to biphenyllithium moieties by treatment with *sec*-BuLi to initiate anionic polymerization of styrene on gold substrates (Fig. 9.24).

It is noteworthy that the choice of the SAM system of rigid mercaptobiphenyls thiols avoided the effect of surface reconstruction discussed previously. Analog SAMs made of longer alkanethiols (Fig. 9.7 and 9.10) may most probably not be suitable when the polymerization medium (in this case benzene/cyclohexane) is nonpolar.



**Fig. 9.24** Reaction scheme for the surface-initiated living anionic polymerization using the

rigid self-assembled monolayer of 4'-lithio-4-mercaptobiphenyl [194].



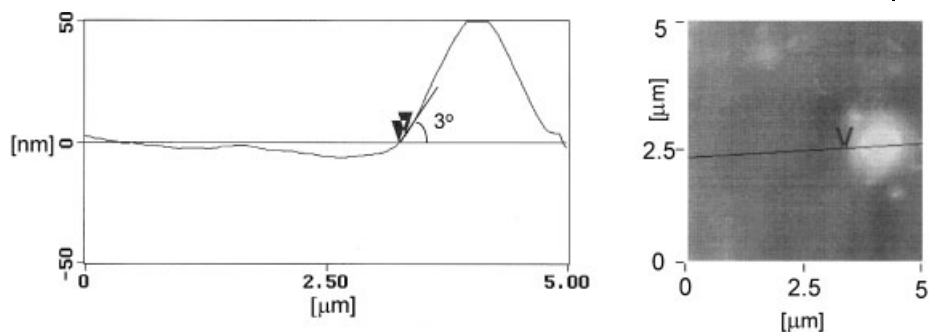
**Fig. 9.25** Surface topography of grafted polystyrene brushes layer after soxhlet extraction as probed by SPM. a) Typical scan (10 × 10) μm² with detailed scans as marked in the overview along with the dept profile analysis along the indicated lines (Reprinted with permission from: [194] R. Jordan, A. Ullman, J.F. Kang, *et al.*, *J. Am. Chem. Soc.* **1999**, 121, 1016–1022. © Copyright 1999 American Chemical Society.

This would first reduce the number of initiator sites and secondly lead to an unfavorable  $k_i/k_p$  ratio. The thickness of the resulting polystyrene brush in the dry (collapsed) state, as estimated by ellipsometry and atomic force microscopy (Fig. 9.25), was  $18 \pm 0.2$  nm. These techniques also reveal a smooth homogeneous polymer surface throughout the substrate on the macroscopic, as well as on the microscopic scale, with a roughness of 0.3–0.5 nm (rms). However, treatment of the substrate with BuLi and the complications of transferring planar substrates in and out of an all-glass reactor also gave rise to microscopic and macroscopic defects. The extremely dense polymer brush around such defect sites were partly desorbed or originally of lower grafting density because the lithiated SAM shows incomplete formation.

A polymerization degree of  $N=382$ , and grafting density of approx. 7–8 chains per  $R_g^2$ , or 3.2–3.6 nm<sup>2</sup> per chain was calculated using mean-field theory [170, 260], based on results from swelling experiments. In numerous experiments it was observed that LASIP was only possible when simultaneously, living anionic polymerization was performed in solution by the presence of small amounts of unreacted BuLi. The molecular weight of polymer created by LASIP was about  $34 \times 10^3$  g mol<sup>-1</sup>, the simultaneous polymerization in solution yielded a molecular weight of  $1.6 \times 10^6$  g mol<sup>-1</sup>. This is in agreement with observations of other groups that the SIP of controlled polymerization reactions proceeds significantly slower than in solution, because they are confined.

Polarized ER-FTIR spectra of the PS brush layer indicated strongly stretched and preferentially oriented polystyrene chains. Upon closer inspection of the  $\nu\text{CH}_x$  region (3000–2800 cm<sup>-1</sup>) of the spectra of a deposited bulk PS film and of the PS brush, the relative intensities are significantly different for both spectra. For example, while the ratio  $\nu\text{CH}_2(\text{as})/\nu\text{CH}_2(\text{s})$  is approx. 4.5 in the ‘bulk’ spectrum,  $\geq 10$  was found in the spectrum of the extracted polymer brush. Differences in ratios of CH-aromatic stretching modes are also noticeable. This indicates an apparent difference in the average chain orientation between bulk and tethered polystyrene chains. Such an orientation can only be explained if the chains are considerably stretched by the high grafting density.

One of the unusual properties of dense polymer brushes is their wetting behavior towards identical polymers [261]. In contrast to a simple liquid, which always spreads on a free surface of identical surface tension, a homopolymer may de-wet a substrate of identical chemical composition. If the interfacial macromolecules are confined in some way, i.e. tethered at one end so that they form a dense brush, an entropic barrier is established to interpenetration. Indeed, the wetting behavior of the polystyrene brush showed this effect. A 20 nm-thick layer of polystyrene was spin-coated directly onto the brush surface. After annealing of the sample above the glass transition temperature, SPM and scanning near-field optical microscopy confirms that the spin-coated polystyrene layer completely de-wets the polystyrene brush surface. The observed average contact angle of 3° is somewhat smaller than predicted by Leibler [262] in the absence of substrate deformation. In contrast to a hard surface, a brush surface can deform at the contact line in response to the vertical component of the droplet surface tension. The entropic penalty of chain stretching is balanced by minimizing the contact angle (Fig. 9.26).



**Fig. 9.26** AFM scan of a single droplet of polystyrene on top of the polystyrene brush along with its dept profile and contact angle. (Reprinted with permission from: [194])

R. Jordan, A. Ulman, J. F. Kang, *et al.*, *J. Am. Chem. Soc.* **1999**, 121, 1016–1022. © Copyright 1999 American Chemical Society).

Similarly, Ingall *et al.* [263] lithiated monolayers of short 3-bromopropylsilane on planar silica substrates to perform LASIP with AN. They obtained up to 245 nm thick PAN films within eight days of polymerization time.

Recently, Quirk and Mathers [264] performed LASIP of isoprene on silicon wafers. A chlorodimethylsilane-functionalized diphenylethene (DPE) was coupled onto the surface and lithiated with *n*-BuLi to form the initiating species. The living poly(isoprene) (PI) was end-functionalized with ethylene oxide. A brush thickness of 5 nm after two days of polymerization (9.5 nm after four days) was obtained in contrast to a polymer layer thickness of 1.9 nm by the ‘grafting onto’ method using a telechelic silane functionalized PI.

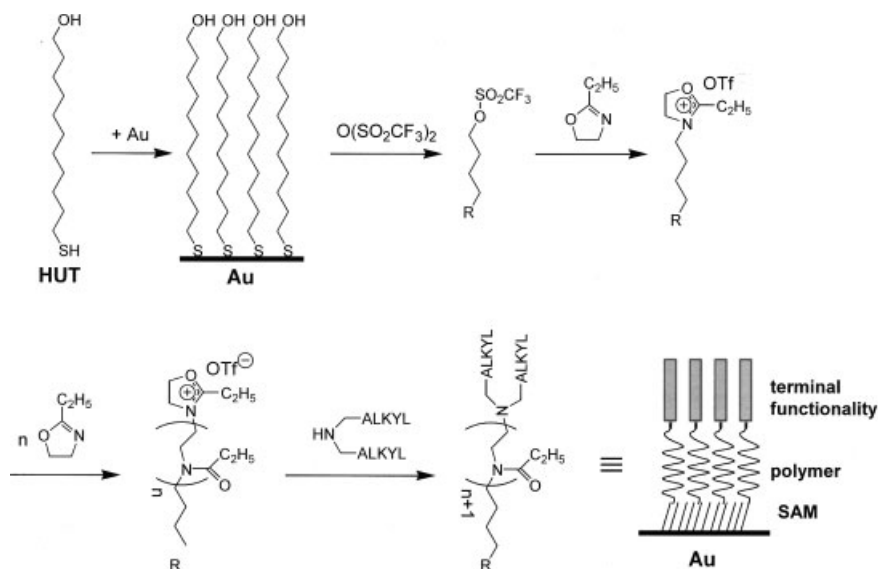
Advincula *et al.* used the same initiator type (DPE activated with *n*-BuLi) to perform LASIP from colloidal silica [265] or clay [266, 267]. The spacer between the DPE unit and the surface active group (quaternized amine for clay and chlorodimethylsilane for silica) was a long *n*-alkyl chain. In all cases, a relatively broad polydispersity for the prepared polystyrene brush ( $PDI=1.2-2$ ) was observed.

### 9.3.3.2 Surface-initiated Polymerization Using Living Carbocationic Polymerization (LCSIP)

The first report on living carbocationic surface-initiated polymerization (LCSIP) using a defined surface modification is by Vidal and Kennedy [268–270]. They prepared poly(isobutene) (PIB) brushes from silica surfaces using a silane functionalized benzylchloride activated by a Lewis acid.

In a recent review, Spange *et al.* [271] compiled LCSIP systems on inorganic substrates as well as ‘grafting onto’ methods involving carbocations in the grafting reaction and gave a detailed account on the extensive work of his group in the field of LCSIP employed directly on the silica surface.

Jordan *et al.* [272] performed LCSIP using SAMs of 11-hydroxyl undecane thiol (HUT) on planar Au(111) substrates as well as on gold nanoparticles functiona-



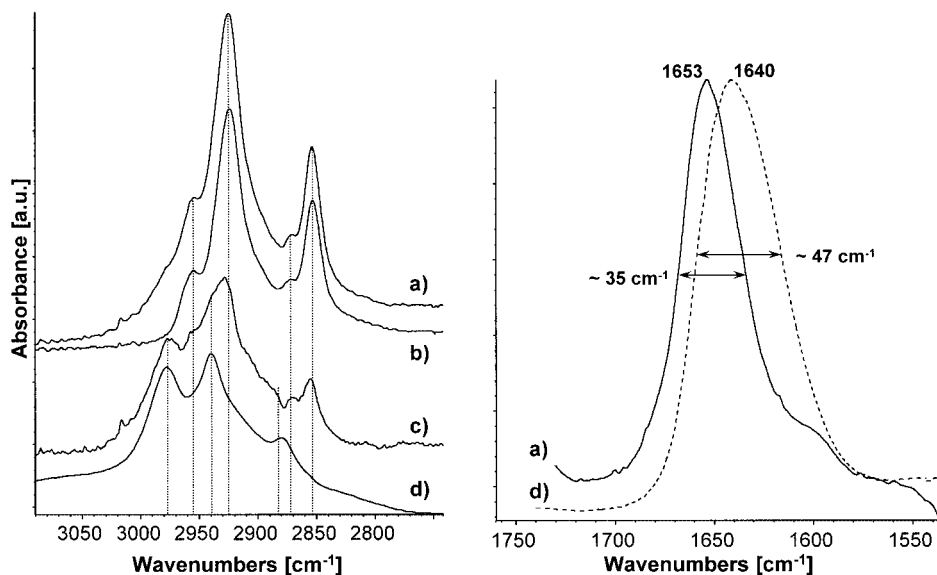
**Fig. 9.27** Reaction scheme for the preparation of amphiphilic poly(2-ethyl-2-oxazoline) brushes by means of LCSIP [272].

lized with mixed 3D-SAMs of [273]. The primary hydroxyl groups were converted by a gas phase reaction using trifluoromethanesulfonic anhydride to trifluoromethylsulfonates (triflates) as a good leaving group to initiate cationic living polymerization of 2-alkyl- and 2-phenyl-2-oxazolines. One crucial aspect of LCSIP is the choice of the surface-bond initiator for the start of the living polymerization. Since surface-confined reactions are relatively slow, LASIP or LCSIP should be initiated fast compared with the propagation reaction to ensure homogeneous growth of the polymer brush from the surface. This enables a stoichiometric polymerization on the surface and consequently results in low polydispersities. Triflates as fast initiators were introduced by Kobayashi *et al.* [274] and were found to be ideal candidates for the defined start of the living cationic polymerization of 2-oxazolines involving large initiators [51, 154–156]. The living ends of the polymer brushes were terminated with piperidine or further functionalized with *N,N*-dioctadecylamine to yield amphiphilic polymer brushes of a defined hydrophilic lipophilic balance. The reaction is outlined in Fig. 9.27.

The brush layer thickness (dry collapsed state) obtained after seven days of polymerization time and successive soxhlet extraction was found to be approx. 10 nm and very uniform ( $\pm 0.3$  nm). The uniform thickness values are provided by the homogeneous initiation, polymerization and termination reaction. Meanwhile poly(2-oxazoline) homopolymers brushes with layer thicknesses of 20 to 30 nm can be obtained [275].

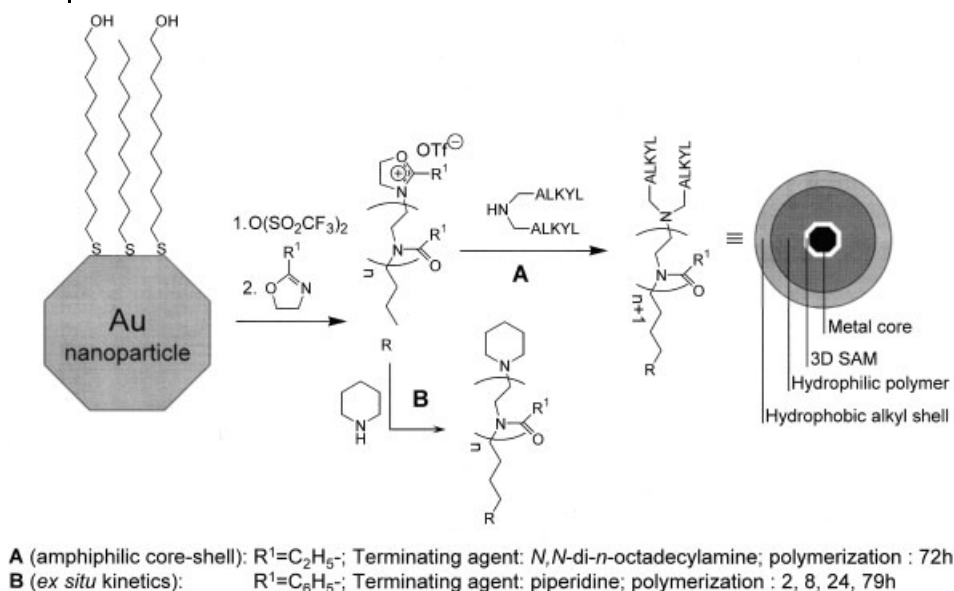
The amphiphilic brush displayed dynamic wetting behavior towards selective solvents such as water. If the substrate was immersed in water and then air-dried, an initial contact angle (sessile drop) of  $80\text{--}75^\circ$  was found, because of selective swelling

of the intermediate hydrophilic polymer brush layer and segregation of the hydrophobic moieties towards the gas-phase [51, 156, 243]. This value decreased rapidly to a stable value of  $60\text{--}62^\circ$  because of the reorganization of the amphiphilic lipopolymer layer in the presence of water. Advancing and receding contact angles showed a pronounced hysteresis of approx.  $30^\circ$ . This has been observed earlier with similar surfaces prepared by the grafting of silane functionalized lipopolymers onto silica substrates and appears to be characteristic for polymer supported alkyl monolayers [276]. The introduction of a flexible polymer interlayer enables a pronounced surface reconstruction process (compare to Section 9.2.5). One drawback of the SIP is the analysis of the polymer brush formed. Here the end-functionalization was confirmed by the wetting behavior as well as by ER-FTIR spectroscopy. To estimate the efficiency of the termination reaction, the  $\text{CH}_x$ -stretching area of both spectra was analyzed (Fig. 9.28). Subtraction of the HUT monolayer spectrum from the grafted PPEI spectrum (Fig. 9.28a) reveals an overall higher integral adsorption for the complete  $\text{CH}_x$ -stretching area (Fig. 9.28c). The characteristic bands for the  $\text{CH}_3/\text{CH}_2$ -stretching modes of the propionyl side group, appearing at  $2978$ ,  $2940$  and  $2880\text{ cm}^{-1}$ , could be unambiguously identified by comparison with the PPEI bulk spectrum (Fig. 9.28d). Furthermore, stronger adsorption at  $2926$  and



**Fig. 9.28** Analysis of the  $\text{CH}$ -stretching region ( $3000\text{--}2800\text{ cm}^{-1}$ ) and the amide I band around  $1650\text{ cm}^{-1}$ . (a) ER-FTIR spectrum of poly(2-ethyl-2-oxazoline) (PEOx) as grown on the triflate functionalized HUT SAM. (b) ER-FTIR spectrum of HUT SAM. (c) Subtraction result of (a)–(b). (d) Bulk spectrum of PEOx. In the spectrum to the left, a significant shift

of the amide I band to higher wavenumbers and decrease of the half width in the ER-FTIR spectrum of the grafted PEOx (a) can be observed. This can be explained by a different conformational freedom and/or intra- and intermolecular interactions between polymer chains in the grafted polymer when compared with the bulk phase (modified from ref. [272]).



**Fig. 9.29** Reaction scheme of the LCSIP of 2-oxazolines on gold nanoparticles: For the preparation of the amphiphilic nanocomposite 2-ethyl-2-oxazoline and *N,N*-di-*n*-octadecylamine were used as monomer and terminat-

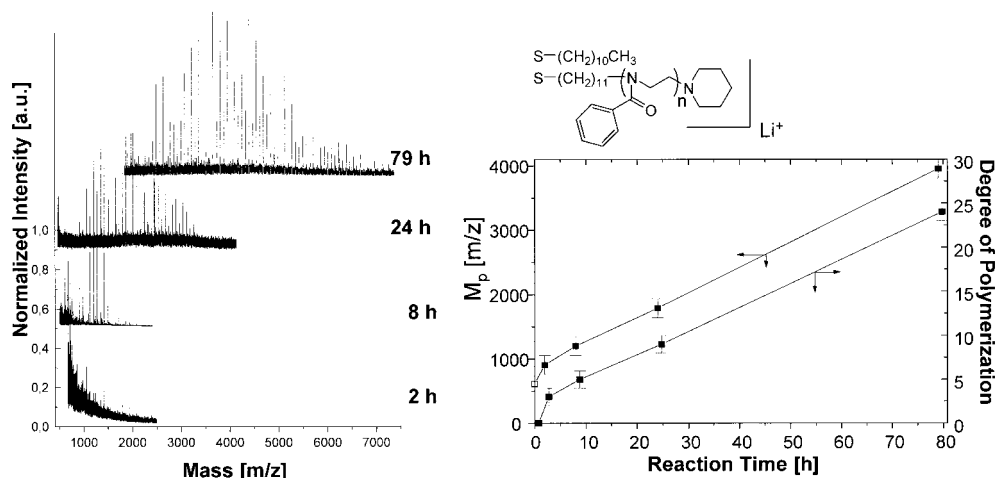
ing agent, respectively (pathway A). The kinetic studies were performed with 2-phenyl-2-oxazoline and piperidine. A schematic representation of the core-shell morphology of the amphiphilic metal-polymer composite [273].

$2854\text{ cm}^{-1}$  indicate the presence of additional long *n*-alkyl chains. This suggests a successful termination reaction of the polymerization by the *N,N*-dioctadecylamine.

However, quantitative analysis of the brush composition or extraction of standard polymer analytical values is difficult if not impossible because an extremely small total amount of polymer is immobilized on flat substrates. Therefore, Jordan *et al.* [273] performed analog LCSIP experiments on gold nanoparticles using a mixed 3D-SAM consisting of HUT and *n*-decanethiol. The triflatization of the primary OH groups of HUT and subsequent analog polymerization reaction yields core-shell amphiphilic polymer-metal nanocomposites (Fig. 9.29) whose amphiphilic nature was studied by means of LB-experiments. *Ex situ* kinetic studies of the polymerization of 2-phenyl-2-oxazoline using FTIR spectroscopy and MALDI/TOF mass spectrometry, resulted in a linear relationship between the reaction time and degree of polymerization of the grafted polymer (Fig. 9.30). This, as well as the successful end-functionalization by termination with secondary amines, confirmed the initial view of a well-defined living polymerization mechanism of 2-oxazolines using LCSIP.

In Fig. 9.30 a broadening of the molecular weight distribution at increasing time of polymerization is observable which is typical for the polymerization of 2-oxazolines. Plotting the  $m/z$  value of the most intensive mass signal versus the reaction time, a strictly linear relationship is obtained (Fig. 9.30). These results are consistent with recent experimental and theoretical studies of surface-initiated





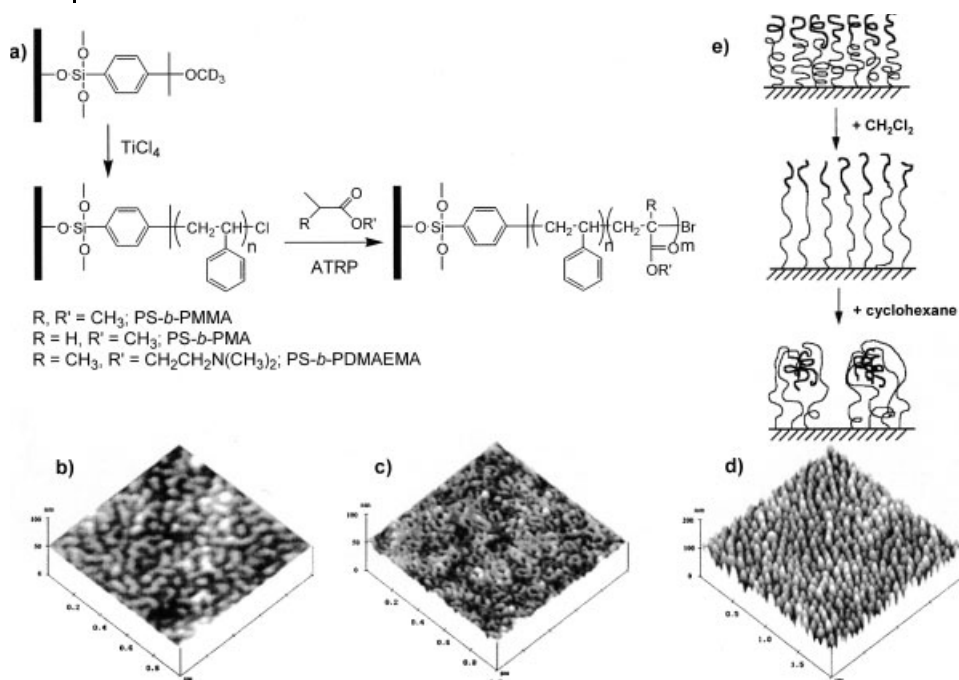
**Fig. 9.30** a) Normalized MALDI TOF mass spectrum of all fractions (taken after 2 h to 72 h of polymerization time) of poly(2-phenyl-2-oxazoline) freed by dissolving the gold core with NaCN solution and collection of the polymer. The calculated mass of the monomer unit (147.17) is in good agreement with the spacing of the mass signals ( $\Delta M = 146.93$ ) of the most prominent peaks. Based on ear-

lier findings by Tempelton *et al.* [277], the species of the isolated polymer is assumed to have an asymmetric dialkyl disulfide structure. Spectra are shifted along the y-axis for clarity. b) Plot of the most intensive mass signal ( $M_p$ ) vs. reaction time. The corresponding degree of polymerization was calculated based on the identified species as depicted (modified from ref. [273]).

atom transfer radical polymerization (ATRP) by Matyjaszewski and coworkers [278]. The initiation reaction by the alkyltriflate seems to be much faster than the propagation reaction, which is indicated by the significantly steeper slope between  $t=0$  and 2 h. This means that the induction period of the polymerization is not noticeably hindered by the surface confinement of the initiator.

In a similar approach R  he *et al.* [279] reported the preparation of poly(2-oxazoline) brushes by the ‘grafting onto’ as well as ‘grafting from’ method. For LCSIP of 2-ethyl-2-oxazolines silane functionalized undecane tosylate was first prepared and then immobilized on the substrate surface. SIP resulted in PEOx layers with thickness close to 30 nm. PEOx brushes were prepared by chemisorption of PEOx disulfides onto gold substrates. Preliminary static and dynamic swelling experiments are reported for these brushes. However, later observations [243] contradicted these findings.

Zhao and Brittain [280–282] reported the LCSIP of styrene on planar silicon wafers using surface modifications of 2-(4-(11-triethoxysilylundecyl)phenyl)-2-methoxypropane or 2-(4-trichlorosilylphenyl)-2-methoxy- $d_3$ -propane respectively. Growth of PS brushes from these SAMs has been successfully achieved; factors that influence PS thickness included solvent polarity, additives and  $TiCl_4$  concentration. Sequential polymerization by monomer addition to the same silicate substrate bearing the living polymer chains resulted in thicker PS films. FTIR-ATR studies using a deuterated initiator indicated that the initiator efficiency is low, and the



**Fig. 9.31** a) Synthesis of PS-*b*-polyacrylate brushes by LCSIP and consecutive ATRIP [282]. AFM images of the tethered PS-*b*-PMMA brushes with 23 nm thick PS layer and 14 nm thick PMMA layer b) after treatment with  $\text{CH}_2\text{Cl}_2$ , c) with cyclohexane and d) after solvent exchange from  $\text{CH}_2\text{Cl}_2$  to cyclohexane. e) Cartoon proposing a model for the regular nanopattern morphology ('pinned micelles')

after solvent exchange. (Reprinted with permission from: [282] B. Zhao, W.J. Brittain, *Macromolecules* **2000**, 33, 8813–8820. [283] B. Zhao, W.J. Brittain, W. Zhou, *et al.*, *J. Am. Chem. Soc.* **2000**, 122, 2407–2408. [284] B. Zhao, W.J. Brittain, W. Zhou, *et al.*, *Macromolecules* **2000**, 33, 8821–8827. All © Copyright 2000 American Chemical Society).

second carbocationic polymerization on the same sample involved initiation from both PS chain ends and unconsumed surface-immobilized initiators. SPM investigations revealed a uniform and smooth PS brush surface with a roughness value of 0.3 nm (rms) for a 30 nm thick PS layer. Additionally they succeeded in sequential LASIP and surface-initiated atom transfer radical polymerization (ATRIP) of MMA, MA or (*N,N*-dimethylamino)ethyl methacrylate (DMAEMA) using the terminal halogen of the polystyrene chains [280].

Surface reconstruction of the PS-PMMA brush in selective solvents gave rise to pattern formation which was investigated by SPM, wetting experiments and XPS. The obtained morphologies depended on the thickness of the brush and its composition [283, 284] (Fig. 9.31).

## 9.3.4

**Surface-initiated Polymerization Using Controlled Radical Polymerization**

While in most of the reports on SIP free radical polymerization is utilized, the restricted synthetic possibilities and lack of control of the polymerization in terms of the achievable variation of the polymer brush architecture limited its use. The alternatives for the preparation of well-defined brush systems were living ionic polymerizations. Recently, controlled radical polymerization techniques has been developed and almost immediately applied in SIP to prepare structurally well-defined brush systems. This includes living radical polymerization using nitroxide species such as 2,2,6,6-tetramethyl-4-piperidin-1-oxyl (TEMPO) [285], reversible addition fragmentation chain transfer (RAFT) polymerization mainly utilizing dithiocarbamates as iniferters (iniferter describes a molecule that functions as an initiator, chain transfer agent and terminator during polymerization) [286], as well as atom transfer radical polymerization (ATRP) where the free radical is formed by a reversible reduction-oxidation process of added metal complexes [287]. All techniques rely on the principle to drastically reduce the number of free radicals by the formation of a dormant species in equilibrium to an active free radical. By this the characteristic side reactions of free radicals are effectively suppressed.

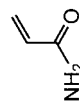
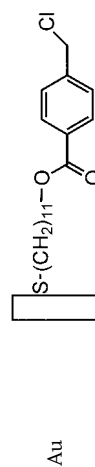
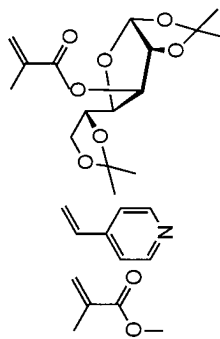
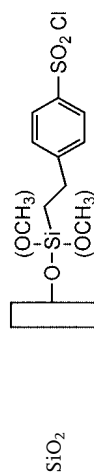
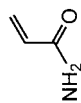
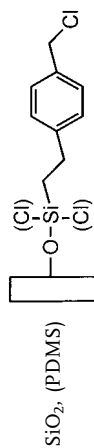
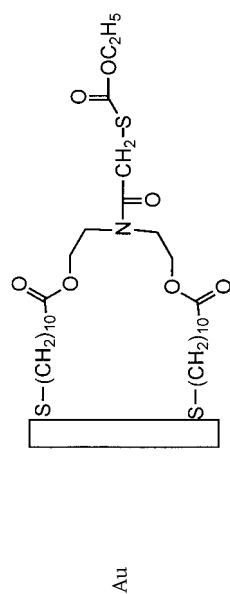
The initiator/monomer system applied in controlled radical (CR) SIP are compiled in Tab. 9.3.

Sogah *et al.* [288] immobilized a TEMPO-functionalized ionic surfactant on the surface of mica-type layered silicate and successfully polymerized styrene to give an organic-inorganic nanocomposite. Although the layered silicate delaminated when PS was incorporated within the layers, the polydispersities of the PS formed was relatively high. Hawker *et al.* [289] employed a TEMPO functionalized SAM on silica and employed besides the common styrene, the polymerization of acrylates, acryl amides and acrylonitrile. SIP with a linear increase of the brush film thickness and low polydispersities could only be obtained, when free alkoxyamine was added. A comparison of the polymer fraction as created in solution and via SIP gave almost identical molecular weights and low polydispersities of 1.14. The potential of CRSIP was demonstrated by preparing block as well as random copolymer brushes of styrene and 2-hydroxyethyl methacrylate. Laterally patterned polymer brush surfaces of poly(acrylic acid) (PAA) and poly(*t*-butylacrylate) with a resolution of approx. 25  $\mu\text{m}$  were also created, using a photoresist [290].

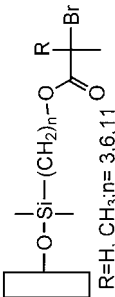
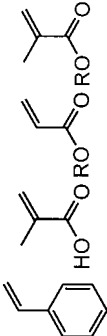
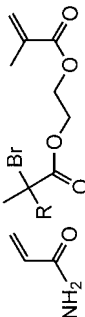
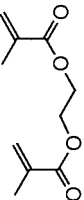
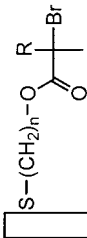
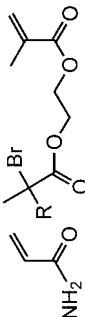
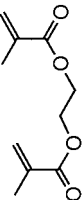
In a series of papers, Matsuda *et al.* [291–295] employed RAFT-SIP with immobilized benzyl *N,N*-diethyldithiocarbamate to form polymer brushes from styrene, methacrylamides, acrylamides and acrylates, NIPAM and *N*-vinyl-2-pyrrolidone on various surfaces. The SIP is initiated by UV irradiation of the surface-bonded dithiocarbamates. Thermoresponsive polymer brushes were prepared by the polymerization of NIPAM and investigated by XPS, wetting experiments and mainly SPM [294]. Patterned polymer brush layers were also prepared. When chloromethyl styrene was used as a comonomer, RAFT-SIP resulted in branching. By control of the branching, spatio-resolved hyperbranching of a controllable stem/branch design was realized (Fig. 9.32) [293, 295].

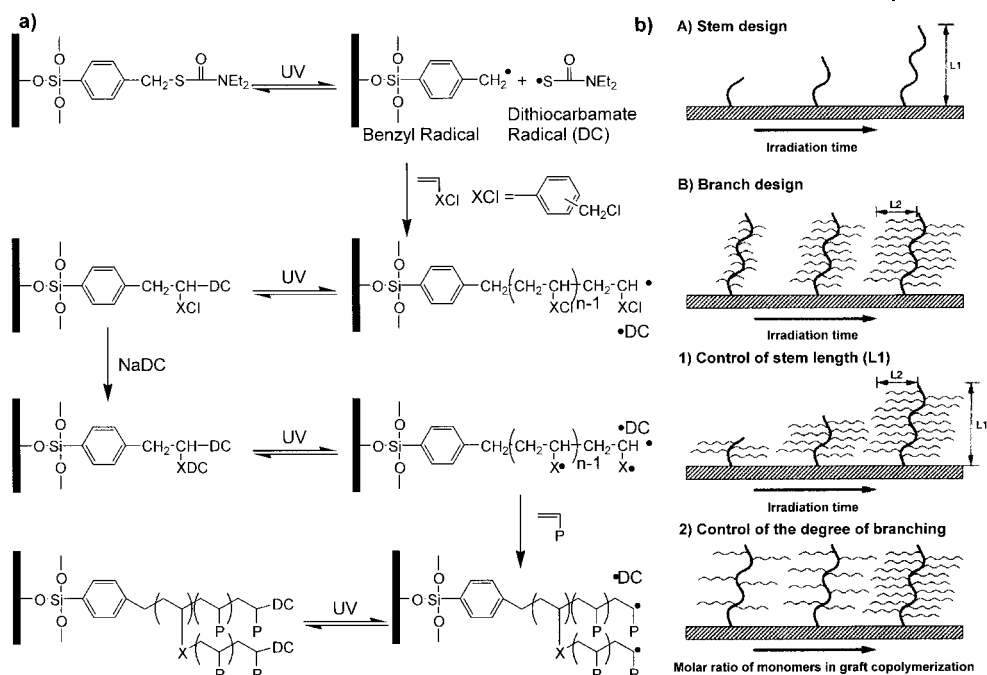
**Tab. 9.3** Specific surface modifications and SAM systems of particles or planar substrates for the surface-initiated controlled radical polymerization (CRSIP) of vinyl monomers.

Substrate	Intermediate Layer//Initiator	Monomer(s)	Reference
Silicate			288
SiO <sub>2</sub>		 	289, 290
PS, SiO <sub>2</sub> ,		     	291–296



Tab. 9.3 (cont.)

Substrate	Intermediate Layer//Initiator	Monomer(s)	Reference
SiO <sub>2</sub>	 R=H, CH <sub>3</sub> ; n= 3, 6, 11	  	278, 310–318
Au	 R=H, CH <sub>3</sub> ; n=10, 11	 	319–325



**Fig. 9.32** a) Reaction scheme for the preparation of the design of stem and branches in RAFT-SIP using dithiocarbamates [293]. b) Schematic representation of the various stem/

branch designs (Reprinted with permission from: [293] H.J. Lee, Y. Nakayama, T. Matsuda, *Macromolecules* **1999**, 32, 6989–6995. © Copyright 1999 American Chemical Society).

Hadziioannou *et al.* [296] employed an analog surface-bond initiator for RAFT-SIP on silica substrates to prepare homogeneous block copolymers of styrene and methyl methacrylate. A patterned substrate was prepared by selective deposition of the initiator.

Niwa *et al.* [297] prepared a mixed SAM from dithiols on gold which partly bears a dithiocarbamate group. The RAFT-SIP of methacrylic acid was monitored by in situ quartz crystal microbalance. The polymerization rate depended strongly on the composition of the SAM.

The mechanism and kinetics of RAFT-SIP were studied by Fukuda *et al.* [326]. Besides the expected linear increase of the molecular weight of the surface grafted polymer with the monomer conversion, they observed the appearance of a prominent low molar mass fraction which was attributed to a combination reaction of the propagating active chains.

Using a SAM of an asymmetric azo compounds Baum and Brittain [327] homo- and block copolymerized styrene, MMA and *N,N'*-dimethylacrylamide under RAFT conditions in the presence of 2-phenylprop-2-yl dithiobenzoate as the chain transfer agent.

Within the short period of time since its discovery, ATRP has developed remarkably fast to become the most employed controlled radical polymerization technique

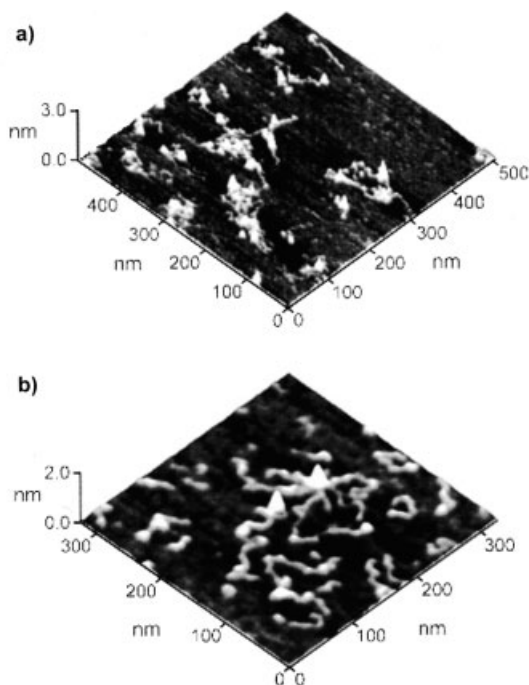
for SIP. In the first account, Wirth *et al.* [298–300] used a monolayer of silane functionalized benzyl chloride and  $\text{Cu}(\text{bpy})_2\text{Cl}$  to form polymer brushes of acrylamide as stationary phases in HPLC and in capillary electrophoresis. The polydispersity index of the grafted brush was typically between 1.15 and 1.3. Genzer *et al.* [301] immobilized this initiator onto oxidized PDMS substrates while under stress. Analogous to the preparation of MAMs, polymer brushes were produced by surface modification of the PDMS elastomer under stress and final relaxation (see Fig. 9.8). Giopireddy and Husson used an analog initiator function for ATRSIP of acrylamide featuring an undecane as a longer, effective mesogen to ensure SAM formation of the thiol on gold [309]. A similar surface initiator function was recently used by Zheng and Stöver [328] to prepare polystyrene homopolymer and poly(styrene-*b*-4-methylstyrene) on polymer resins. Fukuda *et al.* [302–308] employed a monolayer of 2-(4-chlorosulfonylphenyl)ethyl trimethoxysilane on planar and substrates and silica particles as an effective initiator group to start ATRP at the surface. Extremely high grafting densities between  $0.07\text{--}0.7$  chains  $\text{nm}^{-2}$  were obtained, similar to results obtained by LASIP. The group investigated the brush systems in terms of the impact of grafting density [305] and chain length [304] upon the surface interaction forces. Besides MMA and 4-vinylpyridine, MMA derivatives bearing sugar moieties could be polymerized in a controlled manner [303].

Brittain *et al.* [329] used a SAM on planar silica substrates, which were again functionalized with an asymmetric azo group to start the polymerization as a free radical polymerization. However, similar to the addition of dithiocarbamates, they added copper chloride and a suitable ligand to the polymerization reaction to control the free radical concentration during propagation (reverse ATRP). Secondary and tertiary  $\alpha$ -bromoesters bearing various alkyl chains as mesogens for the formation of defined SAMs and equipped with mono- or trifunctional silanes [311–314, 316–318] or thiol [319–325] groups for chemisorption onto silica or gold surfaces became especially popular. Again, in the presence of copper complexes with various ligands, this type of surface initiator is well suited to effectively initiate ATRSIP. Especially for the SIP from SAM initiator systems of limited stability, the conditions of ATRP employing  $\alpha$ -bromoesters are comparatively mild in terms of temperature [309, 320] and tolerance towards moisture. Baker *et al.* [323] and Huck *et al.* [325] performed ATRSIP with 2-hydroxyethyl methacrylate (HEMA) or MMA as well as glycidyl methacrylate in the presence of water or even in water as the solvent. Recently, a preliminary study from Rühle *et al.* [317] investigated the role of the added copper compounds for the surface-confined ATRP.

Beside planar surfaces, Patten *et al.* [310–312] and Hallensleben *et al.* [313, 314, 322] prepared well-defined nanocomposites by ATRSIP of from silica and gold nanoparticles. After spin-coating a solution of the polymer decorated particles onto mica, Hallensleben was able to image the single particles with the individual grafted polymer chains (Fig. 9.33).

Although controlled or living SIP techniques are mainly used to prepare strictly linear polymer brush layers, defined structural variations of the polymer layer give rise to new properties of the coating. Especially ATRP is useful to prepare such novel coatings. Using inimers (monomers bearing initiator functions) or bifunctional





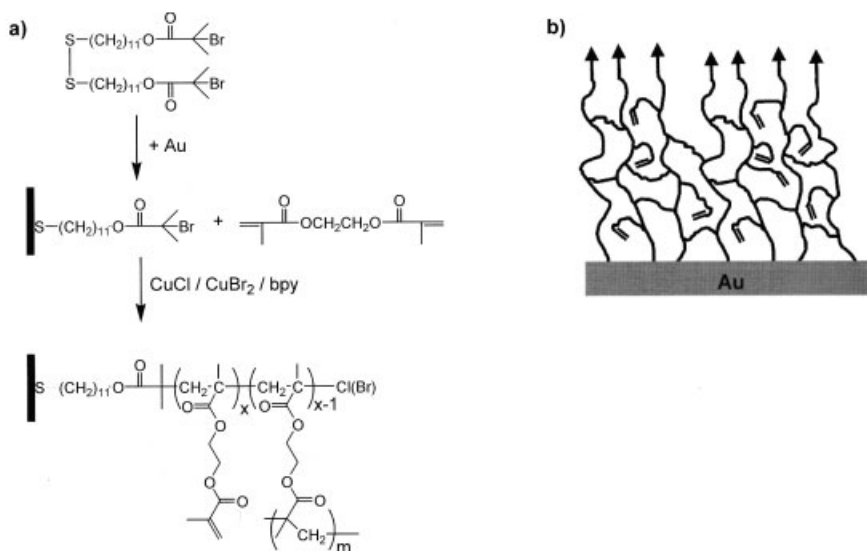
**Fig. 9.33** SPM micrograph of gold nanoparticles decorated with grafted chains of poly(*n*-butylacrylate) spin-coated onto mica. a) Deposition from chloroform and b) from THF solution. The gold cores are depicted by the white protrusions in the SPM images; the polymer chains are shown in gray. The micrographs clearly demonstrate that the polymer chains are bound to the gold cores, which

confirms the success of the ATRSIP. Figure 9.33 b) also shows that different numbers of chains of various lengths are attached to the gold particles (Reprinted with permission from: [322] S. Nuß, H. Böttcher, H. Wurm, M. L. Hallensleben, *Angew. Chem.* **2001**, 113, 4137–4139; *Angew. Chem. Int. Ed.* **2001**, 40, 4016–4018. © Copyright 2001 Wiley-VCH).

monomers, cross-linked or hyperbranched surface coatings can be prepared in a defined fashion. Figures 9.34 and 9.35 depicting two recent examples from Müller *et al.* [315] and Bruening *et al.* [321] using functional monomers for the preparation of branched or cross-linked polymer coating by means of ATRSIP on gold substrates.

ATRSIP is probably the most suitable SIP technique to prepare defined di- or triblock copolymers by successive monomer addition. This has been demonstrated in a very early paper by Matyjaszewski *et al.* [278]. Analog to the already mentioned work from Brittain *et al.*, forming diblocks by cross-over LCSIP and ATRSIP, di- [316, 330] and ABA- [318] and ABC [324] triblock copolymers could be prepared by ATRSIP alone. Again the dynamic responds (segregation, surface reconstruction) upon treatments with selective solvents in terms of surface topography and wetting behavior was investigated using various techniques including SPM.

ATRSIP was also used to amplify surface patterns, created by the  $\mu$ CP of SAMs. Shah *et al.* [319] stamped *n*-hexadecane thiol (HDT) onto planar gold substrates



**Fig. 9.34** a) Synthetic outline for the preparation of cross-linked, ultrathin poly(ethylene glycol dimethacrylate) films on gold surfaces.

**b)** Schematic illustration of a cross-linked film growing from a gold substrate (modified from ref. [321]).

and filled the remaining bare surface with a SAM bearing a tertiary  $\alpha$ -bromoester function. Locally confined ATRSIP of five different monomers resulted in patterned polymer brushes as depicted in Fig. 9.36. The additional polymer brush layer enhanced the etch resistance of the covered areas. The amplified structures were investigated by XPS, wetting experiments and SPM.

### 9.3.5

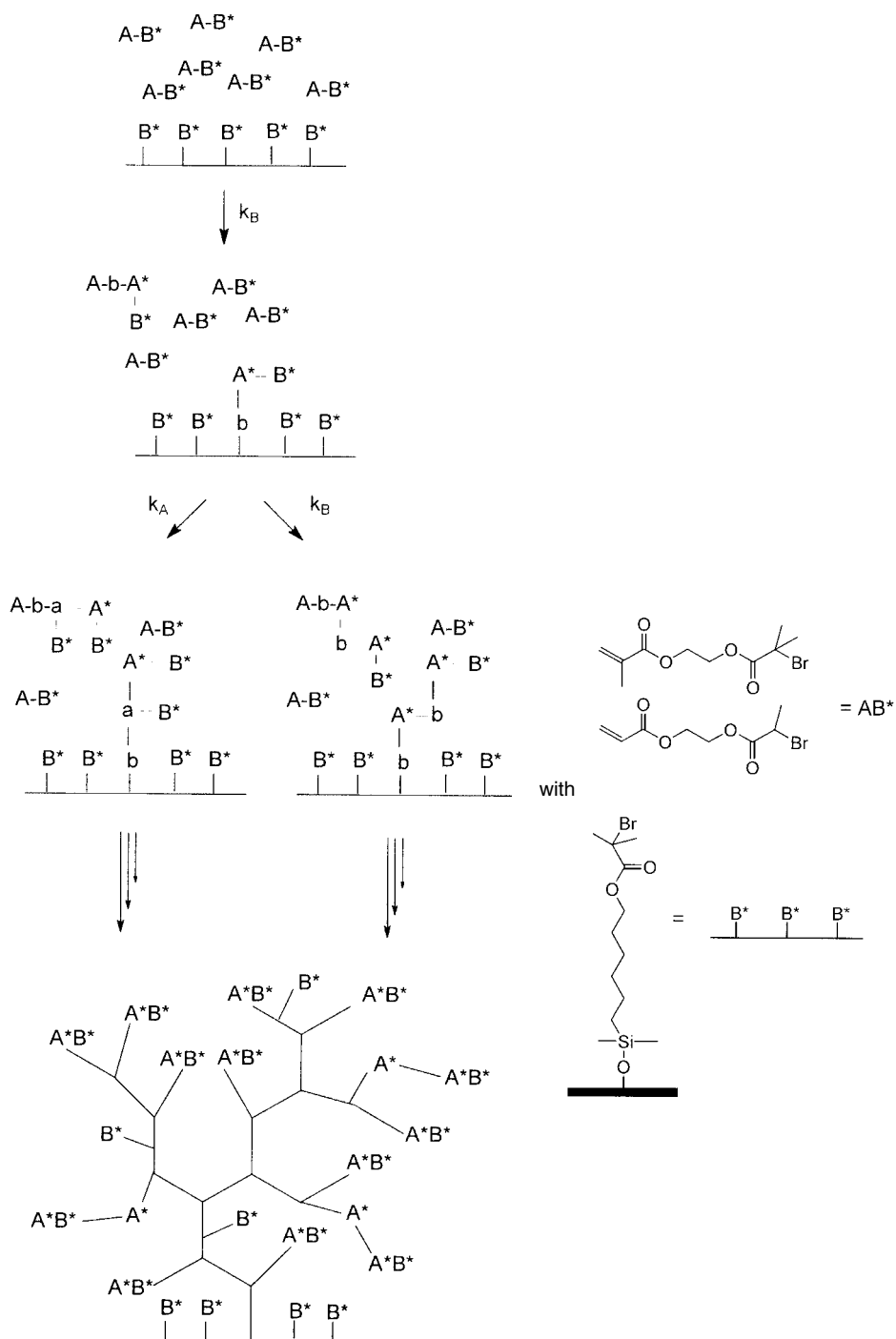
#### Surface-initiated Polymerization by Miscellaneous Techniques

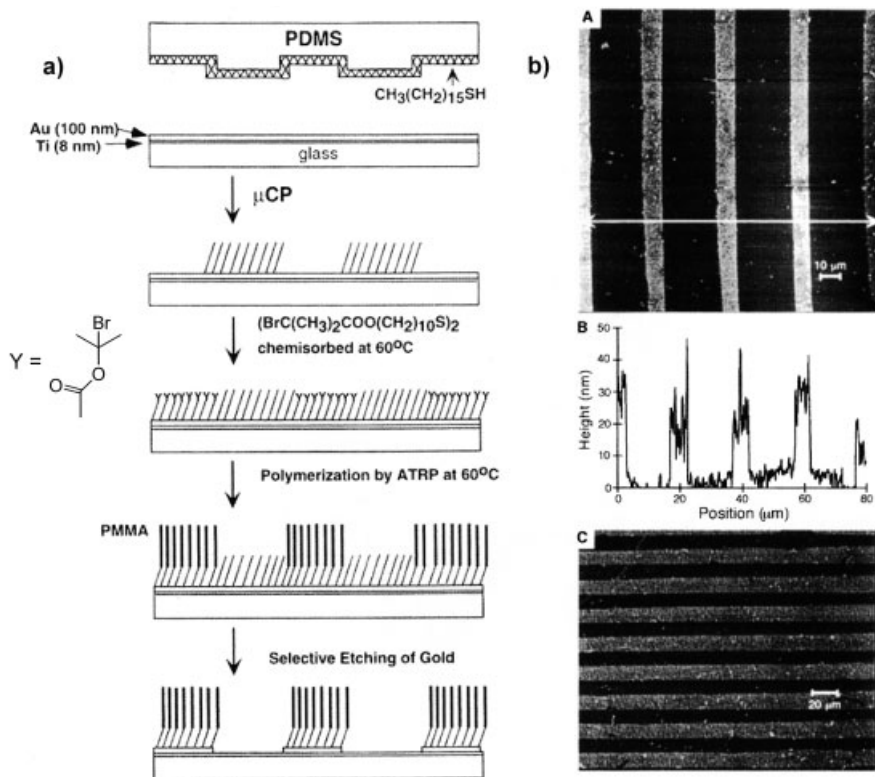
Besides the polymerization techniques discussed above, other polymerization methods have been used for the preparation of surface grafts. Recently, ring-opening metathesis polymerization (ROMP) became popular. This polymerization type will be discussed by Buchmeiser in Chapter 8. Recently, interesting accounts have appeared on solventless polymerization techniques applying (living) ROMP on surfaces to prepare structured brush surfaces of conjugated polymers [331, 332].

Tsubokawa *et al.* [196, 333] and Hamann *et al.* [207, 334, 335] pioneered the SIP of *N*-carboxyanhydrides (NCA) on carbon black and colloidal silica and Schouten *et al.*

**Fig. 9.35** Schematic illustration of the 'self-condensing vinyl polymerization' ATRSIP on planar silica substrates resulting in hyper-branched surface-bonded polymer layers.

(Reprinted with permission from: [315] H. Mori, A. Böker, G. Krausch, *et al.*, *Macromolecules* **2001**, 34, 6871–6882. © Copyright 2001 American Chemical Society).





**Fig. 9.36** a) Procedure of the preparation steps starting with the  $\mu$ CP of an inert SAM, self-assembly of a monolayer of initiator sites, ATRSIP and selective wet etching. b) (A) AFM image of a patterned brush of PMMA formed by this procedure. The bright areas correspond to PMMA brushes, while the dark regions correspond to the patterned areas of SAMs formed from HDT. (B) Cross-sectional profile of the patterned PMMA brush shown in (A). The location of the cross-sectional pro-

file is marked in (A) by the double-headed arrow. (C) Optical image of a patterned brush of PMMA after immersion into aqueous  $\text{KI}/\text{I}_2$  for 60 s. The dark areas of the image are gold protected by the PMMA brush, and the light regions correspond to the supporting glass substrate. (Reprinted with permission from: [319] R.R. Shah, D. Merrezeys, M. Husemann, *et al.*, *Macromolecules* **2000**, 33, 597–605. © Copyright 2000 American Chemical Society).

[336–338] successfully performed SIP of NCA on planar glass surfaces. The polymerization of NCA is initiated by surface-bonded primary amino groups and results in polypeptides (polyglutamates, polyasparates). The intriguing aspect of the surface-bonded polypeptides is the expected biocompatibility of such surfaces and potential control in biomineralization. Additionally, the predefined ( $\alpha$ )-helical conformation stabilized by hydrogen bonding makes the polymers rather rigid. A terminal attachment of the polymer results in rigid polymer ‘brushes’ with a high total dipole moment oriented along the axis of the  $\alpha$ -helix of the polypeptide chain. The impact of the molecular orientation of the rigid polypeptides upon the total dipole moment of

the entire polymer layer as a function of the grafting density and hence, the average orientation of the helices with respect to the surface has been investigated by Frank *et al.* [339, 340], using different deposition techniques including SIP.

Braun *et al.* [341] investigated the molecular dynamics of the rigid polypeptide brush by means of dielectric spectroscopy and prepared patterned brushes by SIP from  $\mu$ CP SAM initiators [342].

Whitesell and coworkers reported the preparation of highly organized helical peptide layers of thickness up to 200 nm [343, 344]. The major drawback of this system is a relatively high surface roughness and considerably broad molecular weight distribution. Solutions to this problem, like enzymatic digestion of the exposed helices were demonstrated [345], but it appears that the high rigidity of the brush and the polymerization mechanism itself offer no readily available options for improvement. Indeed, results regarding the grafting densities or layer thickness as reported by Whitesell *et al.* could not be reproduced by other researchers.

Surface-initiated ring-opening polymerization of  $\epsilon$ -caprolactone on  $\mu$ CP SAM initiators equipped with an oligo-ethylenoxide function is reported by Hawker *et al.* [346]. Choi and Langer used a similar SAM initiator system to polymerize L-lactide [347].

Group transfer polymerization was employed by Hertler and coworkers [348] as well as Huber *et al.* [349].

With the development of enzymatic polymerization in solution, also first accounts for SIP appeared. Loos *et al.* [350] reported on enzymatic surface polymerization of glucose-1-phosphate with potato phosphorylase as the catalyst resulting in oligo- or poly-( $\alpha$ ,1 $\rightarrow$ 4)-D-glucopyranose. As 'initiator' sites, immobilized maltoheptaose was used. Enzymatic grafting of hexyloxyphenol onto chitosan is reported by Payne and coworkers [351].

Finally, hyperbranched polymer layers by surface-initiated step polymerization was intensively studied mainly by Bergbreiter *et al.* and Crooks *et al.* Patterned surfaces were prepared on the micrometer scale and a variety of functional groups introduced interesting optical, electrochemical, biological, and mechanical properties into the films. For a recent review on surface-initiated step polymerization resulting in branched polymer layers see [352].

## 9.4

### Summary and Outlook

The preparation and properties of well-defined surface coatings, self-assembled monolayers and polymer brushes have been discussed. The approach in coating technology developed from a mere addition of surface functionalities, to the programmed assembly of molecules to form organic layers with controlled morphology on the molecular level and with designed functionality. Such layers are now used as a technology platform in all areas of surface science including catalysis. One serious drawback of SAMs, the stability, could be improved by the introduction of new SAM/substrate systems as well as the introduction of suitable mesogens. This makes the use of SAMs for the study of technologically relevant catalytic systems realistic.

The same applies to polymer brushes. The use of SAMs as initiator systems for surface-initiated polymerization results in defined polymer brushes of known composition and morphology. The different polymerization techniques, from free radical to living ionic polymerizations and especially the recently developed controlled radical polymerization allows reproducible synthesis of strictly linear, hyperbranched, dendritic or cross-linked polymer layer structures on solids. The added flexibility and functionality results in robust grafted supports with higher capacity and improved accessibility of surface functions. The collective and fast response of such layers could be used for the design of polymer-bonded catalytic systems with controllable activity.

Besides homogeneous and uniform SAMs or polymer brushes, systems of tailored heterogeneity such as mixed monolayers of two or more compounds, gradients, block copolymer brushes etc. are now under investigation. Especially, the development of patterned surfaces offers the exciting possibility to perform multiple parallel experiments on a single substrate or cascade reactions.

Presently, specific immobilization of various enzymes is studied under the aspect of the orientation and the local surface environments. The deeper understanding of biocatalytic systems together with suitable surface coating techniques may lead to biologically inspired and more complex catalytic systems grafted on solid supports.

## 9.5

### References

- 1 A. ULMAN, *Chem. Rev.* **1996**, 96, 1533–1554.
- 2 General reviews on SAMs see: a) C. D. BAIN, G. M. WHITESIDES, *Angew. Chem.* **1989**, 101, 522–528; *Angew. Chem. Int. Ed.* **1989**, 28, 506–512. b) G. M. WHITESIDES, P. E. LAIBINIS, *Langmuir* **1990**, 6, 87–96. c) J. D. SWALEN, *Annu. Rev. Mater. Sci.* **1991**, 21, 373–408. d) L. H. DUBOIS, R. G. NUZZO, *Annu. Rev. Phys. Chem.* **1992**, 43, 437–463.
- 3 Recent reviews on SAMs: a) J. XU, H.-L. LI, *J. Colloid Interface Sci.* **1995**, 176, 138–149. b) A. ULMAN, *MRS Bull.* **1995**, 30, 46–49. c) A. R. BISHOP, R. G. NUZZO, *Curr. Opin. Colloid Interface Sci.* **1996**, 1, 127–136. d) E. DELAMARCHE, B. MICHEL, H. A. BIEBUYCK, *et al.*, *Adv. Mater.* **1996**, 8, 719–729.
- 4 F. SCHREIBER, *Prog. Surf. Sci.* **2000**, 65, 151–256.
- 5 A. ULMAN, *Introduction to Thin Organic Films: From Langmuir-Blodgett to Self-Assembly*, Academic Press, Boston, **1991**.
- 6 Y. XIA, G. M. WHITESIDES, *Angew. Chem.* **1998**, 110, 568–594; *Angew. Chem. Int. Ed.* **1998**, 37, 550–575.
- 7 a) P. FENTER, A. EBERHARDT, P. EISENBERGER, *Science* **1994**, 266, 1216–1218. b) E. DELAMARCHE, B. MICHEL, H. KANG, *et al.*, *Langmuir* **1994**, 10, 4103–4108. c) S. V. ATRE, B. LIEBERG, D. L. ALLARA, *Langmuir* **1995**, 11, 3882–3893. d) P. WAGNER, M. HEGNER, H.-J. GÜNTHERODT, *et al.*, *Langmuir* **1995**, 11, 3867–3875.
- 8 E. SABATINI, J. COHEN-BOULAKIA, M. BRUENING, *et al.*, *Langmuir* **1993**, 9, 2974–2981.
- 9 J. M. TOUR, L. JONES II, D. L. PEARSON, *J. Am. Chem. Soc.* **1995**, 117, 9529–9534.
- 10 J. F. KANG, A. ULMAN, S. LIAO, *et al.*, *Langmuir* **2001**, 17, 95–106.
- 11 A. ULMAN, J. F. KANG, Y. SHNIDMAN, *et al.*, *Reviews in Molecular Biotechnology* **2000**, 74, 175–188.
- 12 A. ULMAN, *Acc. Chem. Res.* **2001**, 34, 855–863.

- 13 a) H. A. BIEBUYCK, G. M. WHITESIDES, *Langmuir* **1994**, *10*, 1825–1831. b) H. SCHÖNHERR, H. RINGSDORF, *Langmuir* **1996**, *12*, 3891–3897.
- 14 E. B. THROUGHTON, C. D. BAIN, G. M. WHITESIDES, *et al.*, *Langmuir* **1988**, *4*, 365–385.
- 15 J. E. CHADWICK, D. C. MYLES, R. L. GARRELL, *J. Am. Chem. Soc.* **1993**, *115*, 10364–10365.
- 16 K. UVDAL, I. PERSSON, B. LIEDBERG, *Langmuir* **1995**, *11*, 1252–1256.
- 17 a) P. FENTER, P. EISENBERGER, J. LI, *et al.*, *Langmuir* **1991**, *7*, 2013–2016. b) A. DHIRANI, M. A. HINES, A. J. FISHER, *et al.*, *Langmuir* **1995**, *11*, 2609–2614.
- 18 a) H. KELLER, P. SIMAK, W. SCHREPP, *et al.*, *Thin Solid Films* **1994**, *244*, 799–805. b) M. ITOH, K. NISHIHARA, K. ARAMAKI, *J. Electrochem. Soc.* **1995**, *142*, 3696–3703. c) J. B. SCHLENOFF, M. LI, H. LY, *J. Am. Chem. Soc.* **1995**, *117*, 12528–12536.
- 19 T. R. LEE, P. E. LAIBINIS, J. P. FOLKERS, *et al.*, *Pure Appl. Chem.* **1991**, *63*, 821–828.
- 20 J. J. HICKMAN, P. E. LAIBINIS, D. I. AUERBACH, *et al.*, *Langmuir* **1992**, *8*, 357–359.
- 21 B. BASSETTI, V. BENZA, P. JONA, *J. Phys. (France)* **1990**, 259–275.
- 22 See for example: a) C. W. SHEEN, J.-X. SHI, J. MAARTENSSON, *et al.*, *J. Am. Chem. Soc.* **1992**, *114*, 1514–1515. b) C. D. BAIN, *Adv. Mater.* **1992**, *4*, 591–594. c) J. F. DORSTEN, J. E. MASLAR, P. W. BOHN, *Appl. Phys. Lett.* **1995**, *66*, 1755–1757. d) K. ADELKOEFER, M. TANAKA, *Langmuir* **2001**, *17*, 4267–4273. e) C. KIRCHNER, M. GEORGE, B. STEIN, *et al.*, *Adv. Funct. Mater.* **2002**, *12*, 266–276.
- 23 G. ASHHKENASY, D. CAHEN, R. COHEN, *et al.*, *Acc. Chem. Res.* **2002**, *35*, 121–128.
- 24 Y. GU, Z. LIN, R. A. BUTERA, *et al.*, *Langmuir* **1995**, *11*, 1849–1851.
- 25 a) M. J. WIRTH, R. W. P. FAIRBANK, H. O. FATUNMBI, *Science* **1997**, *275*, 44–47. b) J. B. BRZOSKA, I. B. AZOUZ, F. RONDELEZ, *Langmuir* **1994**, *10*, 4367–4373. c) D. L. ALLARA, A. N. PARIKH, F. RONDELEZ, *Langmuir* **1995**, *11*, 2357–2360.
- 26 M. R. LINFORD, C. E. D. CHIDSEY, *J. Am. Chem. Soc.* **1993**, *115*, 12631–12632.
- 27 a) ref. 26. b) M. R. LINFORD, P. FENTER, P. M. EISENBERGER, *et al.*, *J. Am. Chem. Soc.* **1995**, *117*, 3145–3155. c) J. TERRY, M. R. LINFORD, C. WIGREN, *et al.*, *Appl. Phys. Lett.* **1997**, *71*, 1056–1058.
- 28 A. BANSAL, X. LI, I. LAUERMANN, *et al.*, *J. Am. Chem. Soc.* **1996**, *118*, 7225–7226.
- 29 a) D. L. ALLARA, R. G. NUZZO, *Langmuir* **1985**, *1*, 52–66. b) P. E. LAIBINIS, J. J. HICKINAN, M. S. WRIGHTON, *et al.*, *Science* **1989**, *245*, 845–847. c) Y.-T. TAO, M.-T. LEE, S.-C. CHANG, *J. Am. Chem. Soc.* **1993**, *115*, 9547–9555.
- 30 J. P. FOLKERS, C. B. GORMAN, P. E. LAIBINIS, *et al.*, *Langmuir* **1995**, *11*, 813–824.
- 31 a) G. CAO, H.-G. HONG, T. E. MALLOUK, *Acc. Chem. Res.* **1992**, *25*, 420–427. b) M. E. THOMPSON, *Chem. Mater.* **1994**, *6*, 1168–1175. c) H. E. KATZ, *Chem. Mater.* **1994**, *6*, 2227–2232. d) H. LEE, L. J. KEPLEY, H.-G. HONG, *et al.*, *J. Am. Chem. Soc.* **1988**, *110*, 618–620. e) M. L. SCHILLING, H. E. KATZ, S. M. STEIN, *et al.*, *Langmuir* **1993**, *9*, 2156–2160. f) H. E. KATZ, M. L. SCHILLING, S. B. UNGASHSE, *et al.* in: *Supramolecular Architecture*; (T. BEIN, ed.); ACS Symposium Series 499; American Chemical Society: Washington, DC, **1992**, 24. g) H. E. KATZ, M. L. SCHILLING, C. E. D. CHIDSEY, *et al.*, *Chem. Mater.* **1991**, *3*, 699–703. h) S. B. UNGASHSE, W. L. WILSON, H. E. KATZ, *et al.*, *J. Am. Chem. Soc.* **1992**, *114*, 8717–8719. i) H. E. KATZ, G. SCHELLER, T. M. PUTVINSKI, *et al.*, *Science* **1991**, *254*, 1485–1487.
- 32 T. J. GARDNER, C. D. FRISBIE, M. S. WRIGHTON, *J. Am. Chem. Soc.* **1995**, *117*, 6927–6933.
- 33 D. K. SCHWARZ, *Annu. Rev. Phys. Chem.* **2001**, *52*, 107–137.
- 34 H. SELLERS, A. ULMAN, Y. SHNIDMAN, *et al.*, *J. Am. Chem. Soc.* **1993**, *115*, 9389–9401.
- 35 C. A. WIDRIG, C. A. ALVES, M. D. PORTER, *J. Am. Chem. Soc.* **1991**, *113*, 2805–2810.
- 36 L. STRONG, G. M. WHITESIDES, *Langmuir* **1988**, *4*, 546–558.
- 37 C. E. D. CHIDSEY, D. N. LOIACONO, *Langmuir* **1990**, *6*, 682–691.
- 38 R. G. NUZZO, E. M. KORENIC, L. H. DUBOIS, *J. Chem. Phys.* **1990**, *93*, 767–773.
- 39 N. CAMILLONE III, C. E. D. CHIDSEY, G.-Y. LIU, *et al.*, *J. Chem. Phys.* **1993**, *98*, 3503–3511.
- 40 P. FENTER, P. EISENBERGER, *Phys. Rev. Lett.* **1993**, *70*, 2447–2450.

- 41 P. FENTER, A. EBERHARDT, P. EISENBERGER, *Science*, **1994**, 266, 1216–1218.
- 42 M.S. YEGANEH, S.M. DOUGAL, R.S. POLLIZZOTTI, *et al.*, *Phys. Rev. Lett.* **1995**, 74, 1811–1814.
- 43 R. HEINZ, J.P. RABE, *Langmuir* **1995**, 11, 506–511.
- 44 H. RIELEY, G.K. KENDALL, R.G. JONES, *et al.*, *Langmuir* **1999**, 15, 8856–8866.
- 45 K.K. UNGER, C. DU FRESNE VON HOHENESCHE, R. DITZ, *Gas and Liquid Chromatography in: Handbook of Porous Solids* (F. SCHÜTH, K. SING, J. WEITKAMP; eds.) Wiley-VCH, Weinheim **2002**, 2623–2699.
- 46 J. SAGIV, *J. Am. Chem. Soc.* **1980**, 102, 92–98.
- 47 E.F. VANSANT, P. VAN DER VOORT, K.C. VRANCKEN, *Characterization and Chemical Modification of the Silica Surface*, in: *Studies in Surface Science and Catalysis*, 93, Elsevier, Amsterdam, **1995**.
- 48 K.K. UNGER, *Porous Silica*, Elsevier, Amsterdam, **1979**.
- 49 J. KÖHLER, J.J. KIRKLAND, *J. Chromatogr.* **1987**, 385, 125–150.
- 50 W. KERN, D.A. PUOTINEN, *RCA Review* **1970**, 31, 187–189.
- 51 R. JORDAN, K. GRAF, H. RIEGLER, K.K. UNGER, *Chem. Commun.* **1996**, 1025–1026.
- 52 L.C. SANDER, S.A. WISE, *J. Chromatogr.* **1984**, 316, 163–181.
- 53 I. HALLER, *J. Am. Chem. Soc.* **1978**, 100, 8050–8055.
- 54 K.D. LORK, K.K. UNGER, J.N. KINKEL, *J. Chromatogr.* **1986**, 352, 199–221.
- 55 K. ALBERT, E. BAYER, *J. Chromatogr.* **1991**, 544, 345–370.
- 56 J.N. KINKEL, K.K. UNGER, *J. Chromatogr.* **1984**, 316, 193–200.
- 57 M.J. WIRTH, H.O. FATUNMBI, in: *Chemically Modified Surfaces* (J.J. PESEK, I.E. LEIGH; eds.), Royal Society of Chemistry, Cambridge, UK, **1994**, 203–209.
- 58 J.D. LE GRANDE, J.L. MARKHAM, C.R. KURKJIAN, *Langmuir* **1993**, 9, 1746–1753.
- 59 P. SILBERZAHN, L. LÉGER, D. AUSSERRÉ, *et al.*, *Langmuir* **1991**, 7, 1647–1651.
- 60 M.J. STEVENS, *Langmuir* **1999**, 15, 2773–2778.
- 61 D.L. ALLARA, in *Polymer Surfaces and Interfaces*, 2, (W.J. FEAST, H.S. MUNRO, R.W. RICHARDS, eds.) Wiley, Chichester, **1993**, 27–46.
- 62 A. ULMAN, S.D. EVANS, Y. SHNIDMAN, *et al.*, *J. Am. Chem. Soc.* **1991**, 113, 1499–1506.
- 63 A. JARZEBINSKA, R. ROWINSKI, I. ZAWISZA, *et al.*, *Anal. Chim. Acta* **1999**, 396, 1–12.
- 64 a) C.E.D. CHIDSEY, *Science* **1991**, 251, 919–922. b) H.O. FINKLEA, D.D. HAN-SHEW, *J. Am. Chem. Soc.* **1992**, 114, 3173–3181. c) G.K. ROWE, S.E. CREAGER, *Langmuir* **1991**, 7, 2307–2312.
- 65 a) M. MRKSICH, J.R. GRUNWELL, G.M. WHITESIDES, *J. Am. Chem. Soc.* **1995**, 117, 12009–12010. b) K. MOTESHAREI, D.C. MYLES, *J. Am. Chem. Soc.* **1994**, 116, 7413–7414. c) J. SPINKE, M. LILEY, H.-J. GUDER, *et al.*, *Langmuir* **1993**, 9, 1821–1825.
- 66 a) M. MRKSICH, G.M. WHITESIDES, *Annu. Rev. Biophys. Biomol. Struct.* **1996**, 25, 55–78. b) M.N. YOUSAF, M. MRKSICH, *J. Am. Chem. Soc.* **1999**, 121, 4286–4287.
- 67 a) C.D. TIDWELL, S.I. ERTEL, B.D. RATNER, *et al.*, *Langmuir* **1997**, 13, 3404–3413. b) C.S. CHEN, M. MRKSICH, S. HUANG, *et al.*, D.E. Ingber, *Biotech. Progr.* **1998**, 14, 356–363. c) B.T. HOUSEMAN, M. MRKSICH, *J. Org. Chem.* **1998**, 63, 7552–7555.
- 68 J. ZACCARO, J.F. KANG, A. ULMAN, *et al.*, *Langmuir* **2000**, 16, 3791–3796.
- 69 S. KIM, G.Y. CHOI, A. ULMAN, *et al.*, *Langmuir* **1997**, 13, 6650–6856.
- 70 A.R. BISHOP, R.G. NUZZO, *Curr. Opin. Colloid Interface Sci.* **1996**, 1, 127–136.
- 71 L. BERTILSSON, B. LIEBERG, *Langmuir* **1993**, 9, 141–149.
- 72 A. ULMAN, S.D. EVANS, Y. SHNIDMAN, *et al.*, *Adv. Colloid Interface Sci.* **1992**, 39, 175–224.
- 73 a) B. LIEBERG, P. TENGVALL, *Langmuir* **1995**, 11, 3821–3827. b) B. LIEBERG, M. WIRDE, Y.-T. TAO, *et al.*, *Langmuir* **1997**, 13, 5329–5334.
- 74 H. ZIMMERMANN, A. LINDGREN, W.L. SCHUHMANN, *et al.*, *Chem. Eur. J.* **2000**, 6, 592–599.
- 75 J. MADOZ-GRPIDE, J.M. ABAD, J. FERNÁNDEZ-RECIO, *et al.*, *J. Am. Chem. Soc.* **2000**, 122, 9808–9817.



- 76 F. W. SCHELLER, U. WOLLENBERGER, C. LEI, *et al.*, *Rev. Mol. Biotechnology* **2002**, *82*, 411–424.
- 77 I. O. BENITEZ, B. BUJOLI, L. J. CAMUS, *et al.*, *J. Am. Chem. Soc.* **2002**, *124*, 4363–4370.
- 78 K. TÖLLNER, R. POPOVITZ-BIRO, M. LAHAV, *et al.*, *Science* **1997**, *278*, 2100.
- 79 C. D. BAIN, E. B. TROUGHTON, Y.-T. TAO, *et al.*, *J. Am. Chem. Soc.* **1989**, *111*, 321–335.
- 80 P. E. LAIBINIS, G. M. WHITESIDES *J. Am. Chem. Soc.* **1992**, *114*, 1990–1995.
- 81 T. H. ONG, R. N. WARD, P. B. DAVIES, *et al.*, *J. Am. Chem. Soc.* **1992**, *114*, 6243–6245.
- 82 S. D. EVANS, R. SHARMA, A. ULMAN, *Langmuir* **1991**, *7*, 156–161.
- 83 a) N. KACKER, S. K. KUMAR, D. L. ALLARA, *Langmuir* **1997**, *13*, 6366–6369. b) J. HAUTMAN, M. L. KLEIN, *Phys. Rev. Lett.* **1991**, *67*, 1763–1766. c) J. HAUTMAN, J. P. BAREMAN, W. MAR, *et al.*, *J. Chem. Soc. Faraday Trans.* **1991**, *87*, 2031–2037.
- 84 J. I. SIEPMANN, I. R. McDONALD, *Phys. Rev. Lett.* **1993**, *70*, 453–456.
- 85 a) J. GENZER, K. EFIMENKO, *Science* **2000**, *290*, 2130–2133. b) J. Genzer, E. Sivaniah, E. J. KRAMER, *et al.*, *Langmuir* **2000**, *16*, 1993–1997. c) J. GENZER, E. SIVANIAH, E. J. KRAMER, *et al.*, *Macromolecules* **2000**, *33*, 1882–1887.
- 86 a) Y.-T. KIM, R. L. MCCARLEY, A. J. BARD, *J. Phys. Chem.* **1992**, *96*, 7416–7421. b) Y. S. OBENG, M. E. LAING, A. C. FRIEDLI, *et al.*, *J. Am. Chem. Soc.* **1992**, *114*, 9943–9953.
- 87 E. SABATANI, J. COHEN-BOULAKIA, M. BRUENING, *et al.*, *Langmuir* **1993**, *9*, 2974–2981.
- 88 a) A.-A. DHIRANI, R. W. ZEHNER, R. P. HSUNG, *et al.*, *J. Am. Chem. Soc.* **1996**, *118*, 3319–3320. b) R. W. ZEHNER, L. R. SITA, *Langmuir* **1997**, *13*, 2973–2979. c) R. W. ZEHNER, B. F. PEARSON, R. P. HSUNG, L. R. SITA, *Langmuir* **1999**, *15*, 1121–1127.
- 89 S. B. SACHS, S. P. DUDEK, C. E. D. CHIDSEY, *J. Am. Chem. Soc.* **1997**, *119*, 10563–10564.
- 90 S. C. CHANG, I. CHAO, Y. T. TAO, *J. Am. Chem. Soc.* **1994**, *116*, 6792–6805.
- 91 Y. T. TAO, C. C. WU, J. Y. EU, *et al.*, *Langmuir* **1997**, *13*, 4018–4023.
- 92 R. P. SCARINGE, IN: *Electron Crystallography of Organic Molecules* (J. R. FRYER, D. L. DORSET, eds.), Kluwer, Dordrecht, **1990**.
- 93 C. Y. YOUNG, R. PINDAK, N. A. CLARK, *et al.*, *Phys. Rev. Lett.* **1978**, *40*, 773–776.
- 94 A. ULMAN, R. SCARINGE, *Langmuir* **1992**, *8*, 894–897.
- 95 T. Y. B. LEUNG, P. V. SCHWARTZ, G. SCOLES, *et al.*, *Surf. Sci.* **2000**, *458*, 34–52.
- 96 J. F. KANG, S. LIAO, R. JORDAN, *et al.*, *J. Am. Chem. Soc.* **1998**, *120*, 9662–9667.
- 97 J. F. KANG, R. JORDAN, A. ULMAN, *Langmuir* **1998**, *14*, 3983–3985.
- 98 J. F. KANG, A. ULMAN, S. LIAO, *et al.*, *Langmuir* **1999**, *15*, 2095–2098.
- 99 J. F. KANG, A. ULMAN, R. JORDAN, *et al.*, *Langmuir* **1999**, *15*, 5555–5559.
- 100 S. FREY, V. STADLER, K. HEISTER, *et al.*, *Langmuir* **2001**, *17*, 2408–2415.
- 101 M. ZARNIKOV, M. GRUNZE, *J. Phys.: Condens. Mater.* **2001**, *13*, 11333–11365 and references therein.
- 102 a) G. J. KLUTH, M. M. SUNG, R. MABOUDIAN, *Langmuir* **1997**, *13*, 3775–3780. b) G. J. KLUTH, M. SANDER, M. M. SUNG, *et al.*, *J. Vac. Sci. Technol. A* **1998**, *16*, 932–936.
- 103 M. CALISTRI-YEH, E. J. KRAMER, R. SHARMA, *et al.*, *Langmuir* **1996**, *12*, 2747–2755.
- 104 a) S. BAXTER, A. B. D. CASSIE, *Text- Ind.* **1945**, *36*, T35. b) A. B. D. CASSIE, S. BAXTER, *Trans. Faraday Soc.* **1944**, *40*, 546–552.
- 105 J. N. ISRAELACHVILI, M. L. GEE, *Langmuir* **1989**, *5*, 288–289.
- 106 S. WU, *Polymer Interfaces and Adhesion*, Marcel Dekker, New York **1982**.
- 107 M. P. SOMASHEKARAPPA, S. SAMPARATH *Chem. Commun.* **2002**, 1262–1263.
- 108 A. ULMAN (ed.) *Self-assembled Monolayers of Thiols, Thin Films*, Vol. 24, Academic Press, San Diego, **1998**, 1pp.
- 109 H. A. BIEBUYCK, G. M. WHITESIDES, *Langmuir* **1994**, *10*, 4581–4587.
- 110 N. B. LARSEN, H. BIEBUYCK, E. DELAMARCHE, *et al.*, *J. Am. Chem. Soc.* **1997**, *119*, 3017–3026.
- 111 H. SCHMID, B. MICHEL, *Macromolecules* **2000**, *33*, 3042–3049.
- 112 R. D. PINER, J. ZHU, F. XU, *et al.*, *Science* **1999**, *283*, 661–663.

- 113 S. HONG, J. ZHU, C.A. MIRKIN, *Science* **1999**, 286, 523–525.
- 114 S. HONG, J. ZHU, C.A. MIRKIN, *Langmuir* **1999**, 15, 7897–7900.
- 115 G.Y. LIU, S. XU, Y. QIAN, *Acc. Chem. Res.* **2000**, 33, 457–466.
- 116 a) J.W. ZHAO, K. UOSAKI, *Langmuir* **2001**, 17, 7784–7788. b) J.W. ZHAO, K. UOSAKI, *Nano Lett.* **2002**, 2, 137–140.
- 117 C.A. MIRKIN, S. HONG, L. DEMERS, *CHEMPHYSICHEM* **2001**, 2, 37–39.
- 118 M.J. LERCEL, H.G. CRAIGHEAD, A.N. PARIKH, *et al.*, *Appl. Phys. Lett.* **1996**, 68, 1504–1506.
- 119 A. GÖLZHÄUSER, W. GEYER, V. STADLER, *et al.*, *J. Vac. Sci. Technol. B* **2000**, 18, 3414–3418.
- 120 A. GÖLZHÄUSER, W. ECK, W. GEYER, *et al.*, *Adv. Mater.* **2001**, 13, 806–809.
- 121 W. GEYER, V. STADLER, W. ECK, *et al.*, *J. Vac. Sci. Technol. B* **2001**, 19, 2732–2735.
- 122 W. ECK, V. STADLER, W. GEYER, *et al.*, *Adv. Mater.* **2000**, 12, 805–808.
- 123 G. WITTSTOCK, W. SCHUHMANN *Anal. Chem.* **1997**, 69, 5059–5066.
- 124 C. BLACKLEDGE, D.A. ENGBERTSON, J.D. McDONALD *Langmuir* **2000**, 16, 8317–8323.
- 125 V. CHECHIK, R.M. CROOKS, C.J.M. STIRLING, *Adv. Mater.* **2000**, 12, 1161–1171.
- 126 see e.g. a) K.L. PRIME, G.M. WHITESIDES, *Science* **1991**, 252, 1164–1167. b) L. HÄUSSLING, W. KNOLL, H. RINGSDORF, *et al.*, *Makromol. Chem. Macromol. Symp.* **1991**, 46, 145–155. c) R. SINGHVI, A. KUMAR, G.P. LOPEZ, *et al.*, *Science* **1994**, 264, 696–698. d) M.J. WIRTH, R.W.P. FAIRBANK, H.O. FATUNMBI, *Science* **1997**, 275, 44–47. e) J. LAHIRI, L. ISAACS, B. GRZYBOWSKI, J.D. CARBECK, *et al.*, *Langmuir* **1999**, 15, 7186–7198. f) N. HIGASHI, M. TAKAHASHI, M. NIWA, *Langmuir* **1999**, 15, 111–115. g) R.M. NYQUIST, A.S. EBERHARDT, L.A. SILKS III, *et al.*, *Langmuir* **2000**, 16, 1793–1800. h) L. HÄUSSLING, B. MICHEL, H. RINGSDORF, *et al.*, *Angew. Chem.* **1990**, 103, 568–571; *Angew. Chem. Int. Ed.* **1991**, 30, 569–572. i) C. ROBERTS, C.S. CHEN, M. MRKSICH, *et al.*, *J. Am. Chem. Soc.* **1998**, 120, 6548–6555. j) D.D. SCHLERETH, R.P.H. KOOYMAN, *J. Electroanal. Chem.* **1998**, 444, 231–240. k) J. LAHIRI, L. ISAACS, J. TIEN, *et al.*, *Anal. Chem.* **1999**, 71, 777–790. l) B.T. HOUSEMAN, M. MRKSICH, *Angew. Chem.* **1999**, 111, 876–880; *Angew. Chem. Int. Ed.* **1999**, 38, 782–785.
- 127 a) T. IHARA, M. NAKAYAMA, M. MURATA, *et al.*, *Chem. Commun.* **1997**, 1609–1610. b) A. BARDEA, F. PATOLSKY, A. DAGAN, *et al.*, *Chem. Commun.* **1999**, 21–22. c) A.B. STEEL, T.M. HERNE, M.J. TARLOV, *Anal. Chem.* **1998**, 70, 4670–4677. c) C. BERGGREN, G. JOHANSSON, *Anal. Chem.* **1997**, 69, 3651–3657. d) R. BLONDER, E. KATZ, Y. COHEN, *et al.*, *Anal. Chem.* **1996**, 68, 3151–3157. e) R. BLONDER, S. LEVI, G. TAO, *et al.*, *J. Am. Chem. Soc.* **1997**, 119, 10467–10478.
- 128 W.T. MÜLLER, D.L. KLEIN, T. LEE, *et al.*, *Science* **1995**, 268, 272–273.
- 129 M. SASTRY, M. RAO, K.N. GANESH, *Acc. Chem. Res.* **2002**, 35, 847–855.
- 130 V.L. COVLIN, A.N. GOLDSTEIN, A.P. ALIVISATOS, *J. Am. Chem. Soc.* **1992**, 114, 5221–5230.
- 131 P. GHOSH, M.L. AMIRPOUR, W.M. LACKOWSKI, *et al.*, *Angew. Chem.* **1999**, 111, 1697–1700; *Angew. Chem. Int. Ed.* **1999**, 38, 1592–1595.
- 132 M. MRKSICH, *Cell. Mol. Life Sci.* **1998**, 54, 653–662.
- 133 S. FINK, F.C.J. VAN VEGGEL, D.N. REINHOUTD, *Adv. Mater.* **2000**, 12, 1315–1328.
- 134 F. AUER, M. SCOTTI, A. ULMAN, *et al.*, *Langmuir* **2000**, 16, 7554–7557.
- 135 a) B. SELLERGREN, A. SWIETLOW, T. ARNEBRANT, *et al.*, *Anal. Chem.* **1996**, 68, 402–407. b) F. AUER, D.W. SCHUBERT, M. STAMM, *et al.*, B. SELLERGREN, *Chem. Eur. J.*, **1999**, 5, 1150–1159.
- 136 S.J. GREEN, J.J. STOKES, M.J. HOSTETLER, *et al.*, *J. Phys. Chem.* **1997**, 101, 2663–2668.
- 137 For an overview see: a) J.H. FENDLER (ed.) *Nanoparticles and Nanostructured Films*, Wiley-VCH, Weinheim, **1998**. b) Special Issue on 'Nanostructured Materials: Chem. Mater.' **1996**, 8.
- 138 a) J. SCHMITT, G. DECHER, W.J. DRESICK, *et al.*, *Adv. Mater.* **1997**, 9, 61–65. b) J. SCHMITT, P. MÄCHTLE, D. ECK, *et al.*, *Langmuir* **1999**, 15, 3256–3266 and references therein. c) C.J. LOWETH, W.P. CALDWELL, X. PENG, *et al.*, *Angew. Chem.* **1999**, 111, 1925–1929; *Angew. Chem. Int.*

- Ed. 1999, 38, 1808–1812. d) R. P. Andres, J. D. Bielefeld, J. I. Henderson, *et al.*, *Science* 1996, 273, 1690–1693.
- 139 S. CONNOLLY, D. FITZMAURICE, *Adv. Mater.* 1999, 11, 1202–1205.
- 140 For reviews on the different aspects refer to e.g.: a) J. BELLONI, *Curr. Opin. Colloid Interface Sci.* 1996, 2, 184. b) L. BRUST, *Curr. Opin. Colloid Interface Sci.* 1996, 2, 197. c) E. MATIJEVIĆ, *Curr. Opin. Colloid Interface Sci.* 1996, 1, 176–183. d) H. HABERLAND (ed.), *Clusters of atoms and molecules*; Springer-Verlag, New York, 1994. e) G. SCHMID (ed.), *Clusters and Colloids. From Theory to Applications*, VCH, New York, 1994. f) G. SCHMIDT, *Chem. Rev.* 1992, 92, 1709–1707. g) L. N. LEWIS, *Chem. Rev.* 1993, 93, 2693–2730. h) U. KREIBIG, M. VOLLMER (eds.), *Optical Properties of Metal Clusters*; Springer-Verlag, New York, 1995.
- 141 a) M. BRUST, M. WALKER, D. BETHELL, *et al.*, *J. Chem. Soc. Chem. Commun.* 1994, 801–802. b) M. BRUST, J. FINK, D. BETHELL, *et al.*, *J. Chem. Soc. Chem. Commun.* 1995, 1655–1656. c) M. BRUST, D. BETHELL, D. J. SCHIFFRIN, *et al.*, *J. Adv. Mater.* 1995, 7, 795–797. d) D. BETHELL, M. BRUST, D. J. SCHIFFRIN, *et al.*, *J. Electroanal. Chem.* 1996, 409, 137–143.
- 142 see e.g.: M. Y. BEREZIN, K.-T. WAN, R. M. FRIEDMAN, *et al.*, *J. Mol. Cat. A: Chem.* 2000, 158, 567–576.
- 143 H. LI, Y.-Y. LUK, M. MRKSICH, *Langmuir* 1999, 15, 4957–4959.
- 144 a) C. K. YEE, R. JORDAN, A. ULMAN, *et al.*, *Langmuir* 1999, 15, 3486–3491. b) C. K. YEE, M. SCOTTI, A. ULMAN, *et al.*, *J. Sokolov, Langmuir*, 1999; 15, 4314–4316.
- 145 a) M. J. HOSTELTER, S. J. GREEN, J. J. STOKES, *et al.*, *J. Am. Chem. Soc.* 1996, 118, 4212–4213. b) ref. 135 (d). c) R. S. INGRAM, M. J. HOSTETLER, R. W. MURRAY, *J. Am. Chem. Soc.* 1997, 119, 9175–9178.
- 146 A. BADIA, L. CUCCIA, L. DEMERS, *et al.*, *J. Am. Chem. Soc.* 1997, 119, 2682–2692.
- 147 L. MOTTE, M. P. PILENI, *J. Phys. Chem. B* 1998, 102, 4104–4109.
- 148 A. BADIA, W. GAO, S. SINGH, *et al.*, *Langmuir* 1996, 12, 1262–1269.
- 149 W. D. LUEDTKE, U. LANDMAN, *J. Phys. Chem.* 1996, 100, 13323–13329.
- 150 L. HÄUSSLING, W. KNOLL, H. RINGSDORF, *et al.*, *Makromol. Chem., Macromol. Symp.* 1991, 46, 145–155.
- 151 a) J. SPINKE, J. YANG, H. WOLF, *et al.*, *Biophys. J.* 1992, 63, 1667–1671. b) C. ERDELEN, L. HÄUSSLING, R. NAUMANN, *et al.*, *Langmuir* 1994, 10, 1246–1250. c) N. BUNJES, E. K. SCHMIDT, A. JONCZYK, *et al.*, *Langmuir* 1997, 13, 6188–6194.
- 152 W. KNOLL, C. W. FRANK, C. HEIBEL, *et al.*, *Reviews in Molecular Biotechnology* 2000, 74, 137–158.
- 153 E. SACKMANN, *Science* 1996, 271, 43–48.
- 154 R. JORDAN, K. MARTIN, H. J. RÄDER, *et al.*, *Macromolecules* 2001, 34, 8858–8865.
- 155 R. JORDAN, K. GRAF, H. RIEGLER, in preparation.
- 156 a) A. FÖRTIG, R. JORDAN, O. PURRUCKER, *et al.*, *Polym. Preprints* 2003, in press. b) O. PURUCKER, M. TANAKA, A. FÖRTIG, *et al.*, submitted..
- 157 a) G. DECHER, *Science* 1997, 277, 1232–1237 and references therein. b) G. DECHER, J. D. HONG, *Ber. Bunsenges. Phys. Chem.* 1991, 95, 1430–1434.
- 158 I. C. SANCHEZ (ed.), *Physics of polymer surfaces and interfaces*, Butterworth-Heinemann, Boston, 1992.
- 159 a) M. VAN DER WAARDEN, *J. Colloid Sci.* 1950, 5, 317–325. b) M. VAN DER WAARDEN, *J. Colloid Sci.* 1951, 6, 443–443. c) E. L. MACKOR, *J. Colloid Sci.* 1951, 6, 492–495. d) E. L. MACKOR, J. H. VAN DER WAALS, *J. Colloid Sci.* 1952; 7, 535–550. e) E. J. CLAYFIELD, E. C. LUMB, *J. Colloid Interface Sci.* 1966, 22, 269. f) E. J. CLAYFIELD, E. C. LUMB, *J. Colloid Interface Sci.* 1966, 22, 285.
- 160 R. ISRAELS, F. A. M. LEERMAKERS, G. J. FLEER, *Macromolecules* 1995, 28, 1626–1642.
- 161 M. AMIJI, K. J. PARK, *Biomater Sci Polym Ed* 1993, 4, 217–221.
- 162 J.-F. JOANNY, *Langmuir* 1992, 8, 989–995.
- 163 M. HANSON, K. K. UNGER, *Trends Anal. Chem* 1992, 11, 368–373.
- 164 G. SCHOMBURG, *Trends Anal. Chem* 1991, 10, 163–169.
- 165 J. H. VAN ZANTEN, *Macromolecules* 1994, 27, 6797–6807.
- 166 L. CANALI, D. C. SHERRINGTON, *Chem. Soc. Rev.* 1999, 28, 85–102.

- 167 D. ASTRUC, F. CHARDAC *Chem. Rev.* **2001**, *101*, 2991–3004.
- 168 a) E. B. ZHULINA, T. A. VILGIS, *Macromolecules* **1995**, *28*, 1008–1015. b) M. A. CARIGNANO, I. SZLEIFER, *Macromolecules* **1994**, *27*, 702–710.
- 169 a) C. F. LAUB, J. T. KOBERSTEIN, *Macromolecules* **1994**, *27*, 5016–5023. b) N. DAN, M. TIRRELL, *Macromolecules* **1993**, *26*, 6467–6473. c) E. KUMACHEVA, J. KLEIN, P. PINCUS, L. J. FETTERS, *Macromolecules* **1993**, *26*, 6477–6482.
- 170 S. T. MILNER, *Science* **1991**, *251*, 905–914.
- 171 P. PINCUS, *Macromolecules* **1991**, *24*, 2912–2919.
- 172 R. ISRAELS, F. A. M. LEERMAKERS, G. J. FLEER, *et al.*, *Macromolecules* **1994**, *27*, 3249–3261.
- 173 Y. ITO, Y. OCHIAI, Y. S. PARK, Y. IMANISHI, *J. Am. Chem. Soc.* **1997**, *119*, 1619–1623.
- 174 Y. G. TAKEI, T. AOKI, K. SANUI, *et al.*, *Macromolecules* **1994**, *27*, 6163–6166.
- 175 a) J. KLEIN, Y. KAMIYAMA, H. YOSHIZAWA *et al.*, *Macromolecules* **1993**, *26*, 5552–5560. b) D. R. M. WILLIAMS, *Macromolecules* **1993**, *26*, 5806–5098.
- 176 a) G. S. GREEST, M. MURAT, *Macromolecules* **1993**, *26*, 3108–3117. b) Y. LIU, J. QUINN, M. H. RAFAILOVICH, *et al.*, *Macromolecules* **1995**, *28*, 6347–6348 and references therein.
- 177 Y. ITO, Y. S. PARK, Y. IMANISHI, *J. Am. Chem. Soc.* **1997**, *119*, 2739–2739.
- 178 Y. ITO, S. W. NISHI, Y. S. PARK, *et al.*, *Macromolecules* **1997**, *30*, 5856–5859.
- 179 a) S. I. JOEN, J. D. ANDRADE, *J. Colloid Interface Sci.* **1991**, *142*, 159–166. b) S. I. JEON, J. H. LEE, J. D. ANDRADE, *et al.*, *J. Colloid Interface Sci.* **1991**, *142*, 149–158.
- 180 a) S. ALEXANDER, *J. Phys. (Paris)* **1977**, *38*, 983–987. b) P.-G. DE GENNES IN *Solid state physics*, (SEITZ, TURNBULL; eds.), Academic Press, New York, **1978**.
- 181 a) P.-G. DE GENNES, *J. Phys. (Paris)* **1976**, *37*, 1445–1452. b) P. G. DE GENNES, *Macromolecules* **1980**, *13*, 1069–1075 and references therein.
- 182 S. T. MILNER, T. A. WITTEN, M. E. CATES, *Macromolecules* **1988**, *21*, 2610–2619.
- 183 a) M. A. CARIGNANO, I. SZLEIFER, *J. Chem. Phys.* **1993**, *98*, 5006–5018. b) M. A. CARIGNANO, I. SZLEIFER, *J. Chem. Phys.* **1994**, *100*, 3210–3223.
- 184 a) P.-Y. LAI, K. J. BINDER, *J. Chem. Phys.* **1991**, *95*, 9288–9299. b) P.-Y. LAI, K. J. BINDER, *J. Chem. Phys.* **1992**, *97*, 586–592 and references therein.
- 185 see e.g.: R. R. NETZ, M. SCHICK, *Macromolecules* **1998**, *31*, 5105–5122.
- 186 see e.g.: A. HALPERIN, M. TIRELL, T. P. LODGE, *Adv. Polym. Sci.* **1992**, *100*, 31–71 and references therein.
- 187 B. ZHAO, W. J. BRITAIN, *Prog. Polym. Sci.* **2000**, *25*, 677–710.
- 188 R. R. NETZ, D. ADELMANN IN: *Oxide Surfaces* (J. WINGRAVE, ed.), Marcel Dekker, New York **2001**.
- 189 R. ISRAELS, D. GERSAPPE, M. FASOLKA, *et al.*, *Macromolecules* **1994**, *27*, 6679–6682.
- 190 E. M. SEVICK, D. R. M. WILLIAMS, *Macromolecules* **1994**, *27*, 5285–5290.
- 191 a) N. DAN, M. TIRRELL, *Macromolecules* **1993**, *26*, 4310–4315. b) G. F. BELDER, G. TEN BRINKE, G. HADZIIOANNOU, *Langmuir* **1997**, *13*, 4102–4105 and references therein.
- 192 a) W. ZHAO, G. KRAUSCH, M. H. RAFAILOVICH, J. SOKOLOV, *Macromolecules* **1994**, *27*, 2933–2935.
- 193 a) J. R. DORGAN, M. STAMM, C. TOPRAKCIOLU, *et al.*, *Macromolecules* **1993**, *26*, 5321–5330. b) J. C. DIJT, M. A. C. STUART, G. J. FLEER, *Macromolecules* **1994**, *27*, 3207–3218. c) J. C. DIJT, M. A. C. STUART, G. J. FLEER, *Macromolecules* **1994**, *27*, 3219–3229.
- 194 R. JORDAN, A. ULMAN, J. F. KANG, *et al.*, *J. Am. Chem. Soc.* **1999**, *121*, 1016–1022.
- 195 J. JAGUR-GRODZINSKI, *Prog. Polym. Sci.* **1992**, *17*, 361–415.
- 196 N. TSUBOKAWA, *Prog. Polym. Sci.* **1992**, *17*, 417–470 and references therein.
- 197 N. TSUBOKAWA, K. FUKIKI, Y. SONE, *Polym. J.* **1988**, *20*, 213–220.
- 198 K. FUJIKI, N. TSUBOKAWA, Y. SONE, *Polym. J.* **1990**, *22*, 661–670.
- 199 K. FUJIKI, N. TSUBOKAWA, Y. SONE, *J. Macromol. Sci., Chem.* **1991**, *A28*, 715–731.
- 200 N. TSUBOKAWA, K. FUKIKI, Y. SONE, *J. Polym. Sci., Polym. Chem. Ed.* **1986**, *24*, 191–194.

- 201 N. TSUBOKAWA, K. FUKJIKI, Y. SONE, *J. Macromol. Sci., Chem.* **1988**, A25, 1159–1171.
- 202 K. NOLLEN, V. KADEN, K. HAMANN, *Angew. Makromol. Chem.* **1969**, 6, 1–23.
- 203 N. FERY, R. HOENE, K. HAMANN, *Angew. Chem.* **1972**, 84, 359–360.
- 204 N. FERY, R. LAIBLE, K. HAMANN, *Angew. Makromol. Chem.* **1973**, 34, 81–109.
- 205 E. DIETZ, N. FERY, K. HAMANN, *Angew. Makromol. Chem.* **1974**, 35, 115–129.
- 206 R. LAIBLE, K. HAMANN, *Angew. Makromol. Chem.* **1975**, 48, 97–133.
- 207 R. LAIBLE, K. HAMANN, *Adv. Coll. Interface Sci.* **1980**, 13, 65–99.
- 208 N. TSUBOKAWA, K. MARUYAMA, Y. SONE, *et al.*, *Polym. J.* **1989**, 21, 475–481.
- 209 R. JANZEN, K. K. UNGER, W. MÜLLER, *et al.*, *J. Chromatogr.* **1990**, 522, 77–93.
- 210 W. MÜLLER, *J. Chromatogr.* **1990**, 510, 133–140.
- 211 W. MÜLLER, *Bioseparation* **1990**, 1, 265–282.
- 212 a) G. BOVEN, M. L. C. M. OOSTERLING, G. CHALLA, *et al.*, *Polymer*, **1990**, 31, 2377–2382. b) G. BOVEN, R. FOLKSMA, G. CHALLA, *et al.*, *Polym. Commun.* **1991**, 32, 50–53.
- 213 a) E. CARLIER, A. GUYOT, A. REVILLON, *et al.*, *React. Polym.* **1991**, 16, 41–49. b) E. CARLIER, A. GUYOT, A. REVILLON, *React. Polym.* **1991**, 16, 115–124.
- 214 A. SIDORENKO, S. MINKO, K. SCHENKMEUSER, *et al.*, *Langmuir* **1999**, 15, 8349–8355.
- 215 a) R. SCHMIDT, T. ZHAO, J.-B. GREEN, *et al.*, *Langmuir* **2002**, 18, 1281–1287. b) R. PAUL, R. SCHMIDT, J. FENG, *et al.*, *J. Polym. Sci. A: Polym. Chem.* **2002**, 40, 3284–3291.
- 216 B. PENG, D. JOHANNSMANN, J. RÜHE, *Macromolecules* **1999**, 32, 6759–6766.
- 217 D. H. JUNG, I. J. PARK, Y. K. CHOI, *et al.*, *Langmuir* **2002**, 18, 6133–6139.
- 218 J. RÜHE in: *Supramolecular Polymers* (A. CIFERRI, Ed.), Marcel Dekker, New York, **2000**, 565–613.
- 219 J. HYUN, A. CHILKOTI, *Macromolecules* **2001**, 34, 5644–5652.
- 220 L. K. ISTA, S. MENDEZ, V. H. PÉREZ-LUNA, *et al.*, *Langmuir* **2001**, 17, 2552–2555.
- 221 H. G. G. DEKKING, *Appl. Polym. Sci.* **1965**, 9, 1641–1651.
- 222 H. G. G. DEKKING, *Appl. Polym. Sci.* **1967**, 11, 23–36.
- 223 L. P. MEIER, R. A. SHELDEN, W. R. CASERI, *et al.*, *Macromolecules* **1994**, 27, 1637–1642.
- 224 U. VELTEN, S. TOSSATI, R. A. SCHELDEN, *et al.*, *Langmuir* **1999**, 15, 6940–6945.
- 225 U. VELTEN, R. A. SCHELDEN, W. R. CASERI, *et al.*, *Macromolecules* **1999**, 32, 3590–3597.
- 226 O. PRUCKER, J. RÜHE, *Macromolecules* **1998**, 31, 592–601.
- 227 O. PRUCKER, J. RÜHE, *Macromolecules* **1998**, 31, 602–613.
- 228 A. ROTERS, M. SCHIMMEL, J. RÜHE, *et al.*, *Langmuir* **1998**, 14, 3999–4004.
- 229 O. PRUCKER, J. RÜHE, *Langmuir* **1998**, 14, 6893–6898.
- 230 M. BIESALSKI, J. RÜHE, *Macromolecules* **1999**, 32, 2309–2316.
- 231 M. BIESALSKI, J. RÜHE, *Langmuir* **2000**, 16, 1943–1950.
- 232 A. LASCHITSCH, C. BOUCHARD, J. HABICHT, *et al.*, *Macromolecules* **1999**, 32, 1244–1251.
- 233 J. HABICHT, M. SCHMIDT, J. RÜHE, *et al.*, *Langmuir* **1999**, 15, 2460–2465.
- 234 O. PRUCKER, M. SCHIMMEL, G. TOVAR, *et al.*, *Adv. Mater.* **1998**, 10, 1073–1077.
- 235 G. TOVAR, S. PAUL, W. KNOLL, *et al.*, *J. Supramol. Sci.* **1995**, 2, 89–98.
- 236 O. PRUCKER, J. RÜHE, *MRS Symp. Proc.* **1993**, 304, 163.
- 237 J. RÜHE, *MACROMOL. SYMP.* **1997**, 126, 215.
- 238 O. PRUCKER, J. HABICHT, I.-J. PAK, *et al.*, *Mater. Sci. Eng. C* **1999**, 8-9, 291–297.
- 239 J. ZHANG, C. Q. CUI, T. B. LIM, *et al.*, *Macromol. Chem. Phys.* **2000**, 201, 1653–1661.
- 240 W. HUANG, G. SKANTH, G. L. BAKER, *et al.*, *Langmuir* **2001**, 17, 1731–1736.
- 241 a) U. SCHMELMER, R. JORDAN, W. GEYER, *et al.*, *Angew. Chem.* **2003**, 115, 577–581; *Angew. Chem. Int. Ed.* **2003**, 42, 559–563. b) R. JORDAN, J. F. KANG, A. ULMAN, *et al.*, *Polym. Preprints* **2003**, 44(1), 414–415. c) R. JORDAN, U. SCHMELMER, A. PAUL, *et al.*, *Polym. Preprints* **2003**, 44(1), 416–417. d) U. SCHMELMER, R. JORDAN, A. PAUL, *et al.*, *Polym. Preprints* **2003**, 44(1), 562–563.
- 242 a) E. B. ZHULINA, O. V. BORISOV, T. M. BIRSHTEN, *J. Phys II* **1992**, 2, 63–74.

- b) O. V. BORISOV, E. B. ZHULINA, T. M. BIRSHTEIN, *Macromolecules* **1994**, *27*, 4795–4803. c) E. B. ZHULINA, T. M. BIRSHTEIN, O. V. BORISOV, *Macromolecules* **1995**, *28*, 1491–1499. d) V. A. PRYAMITSYN, F. A. M. LEERMAKERS, E. B. ZHULINA, *Macromolecules* **1997**, *30*, 584–589. e) R. ISRAELS, F. A. M. LEERMAKERS, G. J. FLEER, *et al.*, *Macromolecules* **1994**, *27*, 3249–3261. f) 165.
- 243 F. REHFELDT, M. TANAKA, L. PAGNONI, *et al.*, *Langmuir* **2002**, *18*, 4908–4914.
- 244 T. COSGROVE, K. RYAN, *Langmuir* **1990**, *6*, 136–1342.
- 245 T. COSGROVE, T. G. HEATH, K. RYAN, *et al.*, *Macromolecules* **1987**, *20*, 2879–2882.
- 246 T. KIDCHOB, S. KIMURA, Y. IMANISHI, *J. Control. Rel.* **1998**, *50*, 205–214.
- 247 X. GUO, A. WEISS, M. BALLAUF, *Macromolecules* **1999**, *32*, 6043–6046.
- 248 a) S. MINKO, G. GAFIYCHUK, A. SIDORENKO, *et al.*, *Macromolecules* **1999**, *32*, 4525–4531. b) S. MINKO, A. SIDORENKO, M. STAMM, *et al.*, *Macromolecules* **1999**, *32*, 4532–4538. c) A. SIDORENKO, S. MINKO, G. GAFIYCHUK, *et al.*, *Macromolecules* **1999**, *32*, 4539–4543. d) S. MINKO, I. A. LUZINOV, I. Y. EVCHUK, *et al.*, *Polymer* **1996**, *37*, 177–181. e) I. A. LUZINOV, I. Y. EVCHUK, S. S. MINKO, *et al.*, *J. Appl. Polym. Sci.* **1998**, *67*, 299–305. f) I. A. LUZINOV, A. VORONOV, S. S. MINKO, *et al.*, *J. Appl. Polym. Sci.* **1996**, *61*, 1101–1109. g) I. A. LUZINOV, S. S. MINKO, V. SENKOVSKY, *et al.*, *Macromolecules* **1998**, *31*, 3945–3952.
- 249 G. MINO, S. KAIZERMANN, *J. Polym. Sci.* **1958**, *31*, 242–243.
- 250 G. MINO, S. KAIZERMANN, E. RASMUSSEN, *J. Polym. Sci.* **1959**, *38*, 393–401.
- 251 T. MATSUDA, N. SAITO, T. SUGAWARA, *Macromolecules* **1996**, *29*, 7446–7451.
- 252 O. NUYKEN, R. WEIDNER, *Adv. Polym. Sci.* **1986**, *73/74*, 147–199 and references therein.
- 253 P. C. WIELAND, O. NUYKEN, M. SCHMIDT, *et al.*, *Macromol. Rapid Commun.* **2001**, *22*, 1255–1260.
- 254 M. L. C. M. OOSTERLING, A. SEIN, A. J. SCHOUTEN, *Polymer* **1992**, *33*, 4394–4400.
- 255 K. OHKITA, N. NAKAYAMA, T. OHTAKI, *Coatings Technol.* **1983**, *55*, 35–39.
- 256 N. TSUBOKAWA, *J. Macromol. Sci.- Chem.* **1987**, *A24*, 763–775.
- 257 N. TSUBOKAWA, T. YOSHIHARA, Y. SONE, *J. Polym. Sci. A-Polym. Chem.* **1992**, *30*, 561–567.
- 258 D. BRAUN, A. KAMPFRATH, *Angew. Makromol. Chem.* **1984**, *120*, 1–41.
- 259 E. SCHOMAKER, A. J. ZWARTVEEN, G. CHALLA, *et al.*, *Polym. Commun.* **1988**, *29*, 158–160.
- 260 a) S. T. MILNER, *Europhys. Lett.* **1988**, *7*, 695–699. b) S. T. MILNER, T. A. WITTEN, M. E. CATES, *Macromolecules* **1988**, *21*, 2610–2619.
- 261 Y. LIU, M. H. RAFAILOVICH, J. SOKOLOV, *et al.*, *Phys. Rev. Lett.* **1994**, *73*, 440–443.
- 262 A. R. LEIBLER, *Proc. of the OUMS- Conference on Ordering in Macromolecular Systems*, Osaka, June **1983**.
- 263 M. D. INGALL, C. H. HONEYMAN, J. V. MERCURE, *et al.*, *J. Am. Chem. Soc.* **1999**, *121*, 3607–3613.
- 264 R. P. QUIRK, R. T. MATHERS, *Polym. Bull.* **2001**, *45*, 471–477.
- 265 Q. ZHOU, S. WANG, X. FAN, J. MAYS, *et al.*, *Langmuir* **2002**, *18*, 3324–3331.
- 266 Q. ZHOU, X. FAN, C. XIA, *et al.*, *Chem. Mat.* **2001**, *13*, 2465–2467.
- 267 X. FAN, Q. ZHOU, C. XIA, *et al.*, *Langmuir* **2002**, *18*, 4511–4518.
- 268 A. VIDAL, J. B. DONNET, J. P. KENNEDY, *J. Polym. Sci., Polym. Lett. Ed.* **1977**, *15*, 585–588.
- 269 A. VIDAL, A. GUYOT, J. P. KENNEDY, *Polym. Bull.* **1980**, *2*, 315–20.
- 270 A. VIDAL, A. GUYOT, J. P. KENNEDY, *Polym. Bull.* **1982**, *6*, 401–407.
- 271 S. SPANGE, *Prog. Polym. Sci.* **2000**, *25*, 718–849.
- 272 R. JORDAN, A. ULMAN, *J. Am. Chem. Soc.* **1998**, *120*, 243–247.
- 273 R. JORDAN, N. WEST, A. ULMAN, *et al.*, *Macromolecules* **2001**, *34*, 1606–1611.
- 274 S. KOBAYASHI, S. IJIMA, T. IGARASHI, *et al.*, *Macromolecules* **1987**, *20*, 1729–1739.
- 275 R. JORDAN, unpublished results.
- 276 C. ERDELEN, L. HÄUSSLING, R. NAUMANN, *et al.*, *Langmuir* **1994**, *10*, 1246–1250.
- 277 A. C. TEMPELTON, M. J. HOSTETLER, C. T. KRAFT, *et al.*, *J. Am. Chem. Soc.* **1998**, *120*, 1906–1911.

- 278 K. MATYJASZEWSKI, P. MILLER, N. SHUKLA, *et al.*, *Macromolecules* **1999**, 32, 8716–8724.
- 279 T. LEHMANN, J. RÜHE, *Macromol. Symp.* **1999**, 142, 1–12.
- 280 B. ZHAO, W.J. BRITAIN, *J. Am. Chem. Soc.* **1999**, 121, 3557–3558.
- 281 B. ZHAO, W.J. BRITAIN, *Macromolecules* **2000**, 33, 342–348.
- 282 B. ZHAO, W.J. BRITAIN, *Macromolecules* **2000**, 33, 8813–8820.
- 283 B. ZHAO, W.J. BRITAIN, W. ZHOU, S.Z.D. CHENG, *J. Am. Chem. Soc.* **2000**, 122, 2407–2408.
- 284 B. ZHAO, W.J. BRITAIN, W. ZHOU, *et al.*, *Macromolecules* **2000**, 33, 8821–8827.
- 285 C.J. HAWKER, *Acc. Chem. Res.* **1997**, 30, 373–382.
- 286 a) T. OTSU, M. YOSHIDA, *Makromol. Chem. Rapid Commun.* **1982**, 3, 127–132.  
b) T. OTSU, M. YOSHIDA, T. TAZAKI, *Makromol. Chem. Rapid Commun.* **1982**, 3, 133–140.
- 287 K. MATYJASZEWSKI, In *Controlled/Living Radical Polymerization*; MATYJASZEWSKI, K., Ed.; ACS Symposium Series 768; American Chemical Society: Washington, DC, **2000**.
- 288 M.W. WEIMER, H. CHEN, E.P. GIANNELIS, *et al.* *J. Am. Chem. Soc.* **1999**, 121, 1615–1616.
- 289 M. HUSSEMAN, E.E. MALMSTROM, M. MCNAMARA, *et al.*, *Macromolecules* **1999**, 32, 1424–1431.
- 290 M. HUSEMANN, M. MORRISON, D. BENOTT, *et al.*, C.J. HAWKER, *J. Am. Chem. Soc.* **2000**, 122, 1844–1845.
- 291 Y. NAKAYAMA, T. MATSUDA, *Macromolecules* **1996**, 29, 8622–8630.
- 292 Y. NAKAYAMA, T. MATSUDA, *Macromolecules* **1999**, 32, 5405–5410.
- 293 H.J. LEE, Y. NAKAYAMA, T. MATSUDA, *Macromolecules* **1999**, 32, 6989–6995.
- 294 S. KIDOAKI, S. OHYA, Y. NAKAYAMA, *et al.*, *Langmuir* **2001**, 17, 2402–2407.
- 295 Y. NAKAYAMA, M. SUDO, K. UCHIDA, *et al.*, *Langmuir* **2002**, 18, 2601–2606.
- 296 B. DE BOER, H.K. SIMON, M.P.L. WERTS, *et al.*, *Macromolecules* **2000**, 33, 349–356.
- 297 M. NIWA, M. DATE, N. HIGASHI, *Macromolecules* **1996**, 29, 3681–3685.
- 298 X. HUANG, M.J. WIRTH, *Anal. Chem.* **1997**, 69, 4577–4580.
- 299 X. HUANG, L.J. DONESKI, M.J. WIRTH, *Anal. Chem.* **1998**, 70, 4023–4029.
- 300 X. HUANG, M.J. WIRTH, *Macromolecules* **1999**, 32, 1694–1696.
- 301 T. WU, K. EFIMENKO, J. GENZER, *Macromolecules* **2001**, 34, 684–686.
- 302 M. EJAZ, S. YAMAMOTO, K. OHNO, *et al.*, *Macromolecules* **1998**, 31, 5934–5936.
- 303 M. EJAZ, K. OHNO, Y. TSUJII, *et al.*, *Macromolecules* **2000**, 33, 2870–2874.
- 304 S. YAMAMOTO, M. EJAZ, Y. TSUJII, *et al.*, *Macromolecules* **2000**, 33, 5602–5607.
- 305 S. YAMAMOTO, M. EJAZ, Y. TSUJII, *et al.*, *Macromolecules* **2000**, 33, 5608–5612.
- 306 S. YAMAMOTO, Y. TSUJII, T. FUKUDA, *Macromolecules* **2000**, 33, 5995–5998.
- 307 M. EJAZ, S. YAMAMOTO, Y. TSUJII, *et al.*, *Macromolecules* **2002**, 35, 1412–1418.
- 308 S. YAMAMOTO, Y. TSUJII, T. FUKUDA, *Macromolecules* **2002**, 35, 6077–6079.
- 309 D. GOPIREDDY, S.M. HUSSON, *Macromolecules* **2002**, 35, 4218–4221.
- 310 T. VON WERNE, T.E. PATTEN, *J. Am. Chem. Soc.* **1999**, 121, 7409–7410.
- 311 T. VON WERNE, T.E. PATTEN, *J. Am. Chem. Soc.* **2001**, 123, 7497–7505.
- 312 C. PERRUCHOT, M.A. KHAN, A. KAMITSU, *et al.*, *Langmuir* **2001**, 17, 4479–4481.
- 313 H. BÖTTCHER, M.L. HALLENSLEBEN, S. NUSS, *et al.*, *Polym. Bull.* **2000**, 44, 223–229.
- 314 H. BÖTTCHER, M.L. HALLENSLEBEN, R. JANKE, *et al.*, ATRP 'Living/Controlled Radical Grafting of Solid Particles to Create New Properties' in: *Tailored Polymers and Applications*, (Y. YAGCI, M.K. MISHRA, O. NUYKEN, K. ITO, G. WNEK eds.), VSP Publishers, New York **2000**.
- 315 H. MORI, A. BÖKER, G. KRAUSCH, *et al.*, *Macromolecules* **2001**, 34, 6871–6882.
- 316 X. KONG, T. KAWAI, J. ABE, *et al.*, *Macromolecules* **2001**, 34, 1837–1844.
- 317 J.D. JEYAPRAKASH, S. SAMUEL, R. DHAMODHARAN, *et al.*, *Macromol. Rapid Commun.* **2002**, 23, 277–281.
- 318 S.G. BOYES, W.J. BRITAIN, X. WENG, *et al.*, *Macromolecules* **2002**, 35, 4960–4967.
- 319 R.R. SHAH, D. MERRECEYES, M. HUSEMANN, *et al.*, *Macromolecules* **2000**, 33, 597–605.
- 320 J.-B. KIM, M.L. BRUENING, G.L. BAKER, *J. Am. Chem. Soc.* **2000**, 122, 7616–7617.

- 321 W. HUANG, G. L. BAKER, M. L. BRUENING, *Angew. Chem.* **2001**, *113*, 1558–1560; *Angew. Chem. Int. Ed.* **2001**, *40*, 1510–1512.
- 322 S. NUSS, H. BÖTTCHER, H. WURM, *et al.*, *Angew. Chem.* **2001**, *113*, 4137–4139; *Angew. Chem. Int. Ed.* **2001**, *40*, 4016–4018.
- 323 W. HUANG, J.-B. KIM, M. L. BRUENING, *et al.*, *Macromolecules* **2002**, *35*, 1175–1179.
- 324 J.-B. KIM, W. HUANG, M. L. BRUENING, *et al.*, *Macromolecules* **2002**, *35*, 4799–4805.
- 325 D. M. JONES, A. A. BROWN, W. T. S. HUCK, *Langmuir* **2002**, *18*, 1265–1269.
- 326 Y. TSUJII, M. EJAZ, K. SATO, *et al.*, *Macromolecules* **2001**, *34*, 8872–8878.
- 327 M. BAUM, W. J. BRITAIN, *Macromolecules* **2002**, *35*, 610–615.
- 328 G. ZHENG, H. D. H. STÖVER, *Macromolecules* **2002**, *35*, 6828–6834.
- 329 R. A. SEDJO, B. K. MIROUS, W. J. BRITAIN, *Macromolecules* **2000**, *33*, 1492–1493.
- 330 S. ANGOT, N. AYRES, S. A. F. BON, *et al.*, *Macromolecules* **2001**, *34*, 768–774.
- 331 K. M. VAETH, R. J. JACKMANN, A. J. BLACK, *et al.*, *Langmuir* **2000**, *16*, 8495–8500.
- 332 D. FU, L.-T. WENG, B. DU, *et al.*, *Adv. Mater.* **2002**, *14*, 339–343.
- 333 N. TSUBOKAWA, K. KOBAYASHI, Y. SONE, *Polym. J.* **1987**, *19*, 1147–1155.
- 334 R. KROKER, K. HAMANN, *Angew. Makromol. Chem.* **1970**, *13*, 1–22.
- 335 E. DIETZ, N. FERY, K. HAMANN, *Angew. Makromol. Chem.* **1974**, *115*–129.
- 336 M. L. C. M. OOSTERLING, E. WILLEMS, A. J. SCHOUTEN, *Polymer* **1995**, *36*, 4463–4470.
- 337 S. H. WIERINGA, A. J. SCHOUTEN, *Macromolecules* **1996**, *29*, 3032–3034.
- 338 A. HEISE, H. MENZEL, H. YIM, *et al.*, *Langmuir* **1997**, *13*, 723–728.
- 339 Y. C. CHANG, C. W. FRANK, *Macromol. Symp.* **1997**, *118*, 641–646.
- 340 Y.-C. CHANG, C. W. FRANK, G. G. FORSTMANN *et al.*, *J. Chem. Phys.* **1999**, *111*, 6136–6143.
- 341 L. HARTMANN, T. KRATZMÜLLER, H.-G. BRAUN, *et al.*, *Macromol. Rapid Commun.* **2000**, 795–868.
- 342 T. KRATZMÜLLER, D. APPELHANS, H.-G. BRAUN, *Adv. Mater.* **1999**, *11*, 555–557.
- 343 J. K. WHITESELL, H. K. CHANG, *Science* **1993**, *261*, 73–76.
- 344 J. K. WHITESELL, H. K. CHANG, *Mol. Cryst. Liq. Cryst.* **1994**, *240*, 251–258.
- 345 J. K. WHITESELL, H. K. CHANG, C. S. WHITESELL, *Angew. Chem.* **1994**, *106*, 921–924; *Angew. Chem. Int. Ed.* **1994**, *33*, 871–874.
- 346 M. HUSEMANN, D. MECERREYES, C. J. HAWKER, *et al.*, *Angew. Chem.* **1999**, *111*, 685–687; *Angew. Chem. Int. Ed.* **1999**, *38*, 647–649.
- 347 I. S. CHOI, R. LANGER, *Macromolecules* **2001**, *34*, 5361–5363.
- 348 W. R. HERTLER, D. Y. SOGAH, F. H. BOETTCHER, *Macromolecules* **1990**, *23*, 1264–1268.
- 349 D. L. HUBER, K. E. GONSALVES, G. CARLSON, *et al.* in: *Interfacial aspects of multi-component polymer materials* (D. J. Lohse, T. P. Russell, L. H. Sperling, eds.), Plenum Press, New York **1997**, 107–134.
- 350 K. LOOS, V. VON BRAUNMÜHL, R. STADLER, *et al.*, *Macromol. Rapid Commun.* **1997**, *18*, 927–938.
- 351 T. CHEN, G. KUMAR, M. T. HARRIS, *et al.*, *Biotechnology and Bioengineering* **2000**, *70*, 565–573.
- 352 R. M. CROOKS, *CHEMPHYSICHEM* **2001**, *2*, 644–654.



## 10

### Biocatalyzed reactions on polymeric supports:

#### Enzyme-labile linker groups

REINHARD REENTS, DURAISWAMY JEYARAJ and HERBERT WALDMANN

#### 10.1

##### Introduction

Combinatorial chemistry and parallel synthesis of compound libraries on polymeric supports are efficient methods for the generation of new substances with a pre-determined profile of properties [1–3]. The anchoring of one reactant to a polymeric support has the advantage that an excess of reagent may be used, while purification is kept manageable. This is particularly important if the reaction is to be carried out with several reactants in the same reaction vessel. Solid-phase synthesis involves the use of linkers between the compounds to be varied combinatorially and the solid supports which are stable during the reactions. These linkers have to be cleavable as desired, usually at the end of the synthetic sequence, with high selectivity and in high yield, without affecting the structure(s) of the product(s) that are released from the polymeric supports.

Linkers have previously usually been cleaved by classical chemical methods, for instance using strong acids. Such conditions often restrict the application of the linkers, i.e. acid-sensitive linkers are not suitable for acid-labile compounds, such as carbohydrates. Specific linkers have therefore been developed for acid-labile compounds, such as silyl ether linkages, thio ether linkages, [4] and ester linkages [5]. Although such linkers may be cleaved in the presence of acid-labile groups, they have the disadvantage that they are themselves quite labile to common chemical reagents that one might want to employ on the solid phase. For example, esters and silyl ethers are unstable to bases, and thio ethers are unstable in the presence of oxidants, such as *m*-chloroperbenzoic acid, and to electrophilic reagents, such as alkylating agents.

In principle, linker groups are polymer-enlarged versions of blocking functions used in regular solution-phase chemistry. Therefore, enzymatic transformations that may be employed for the removal of protecting groups in solution, in principle may also open up alternative opportunities for releasing compounds from polymeric supports. The linkers developed so far can be divided into exo- and endo-linkers (Fig. 10.1) cleavable by exo- respectively endo-enzymes, as proposed by Flitsch *et al.* [6].

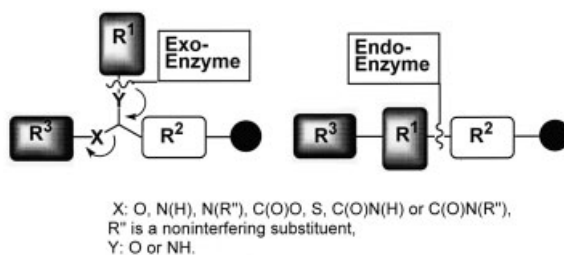


Fig. 10.1 Graphical representation of exo- and endo-linkers.

Exo-linkers are composed of three units: i) a group providing the site for enzyme catalyzed hydrolysis ( $R^1$ ); ii) a site for attachment of the target molecule ( $R^3$ ) and iii) a site for attachment to a further optional spacer ( $R^2$ ).

Endo-linkers are linkers in which the target molecule ( $R^3$ ), the group that provides a site for enzyme catalyzed hydrolysis ( $R^1$ ) and a further optional spacer ( $R^2$ ) are attached to the polymeric support in a linear arrangement. By means of enzyme-mediated dissection, the target molecule, in many cases tagged with the functional group recognized by the enzyme, is released. Examples of endo-cleavable linkers have been reported (Tab. 10.1). The endo-peptidase chymotrypsin cleaves endo-linkers towards the middle of a peptide-chain or “internally”. Not only does this limit the methodology to a very small number of enzymes, but it may also restrict the structure of molecules that can be generated. Typically but not necessarily (see Schemes 10.1 and 10.2) this method generates compounds containing C-terminal aromatic amino acids, which are necessary for recognition by chymotrypsin.

By contrast, exo-linkers do not restrict the structure of the reactant and can be cleaved by more readily-available exo-enzymes, which act at the end of a chain or “externally” (Tab. 10.2). Furthermore exo-cleavable linkers yield untagged products upon cleavage from the solid support.

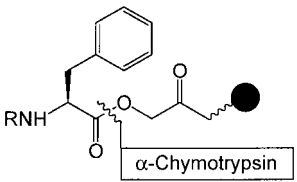
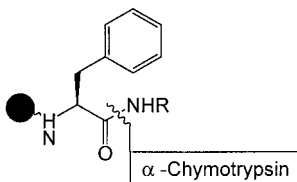
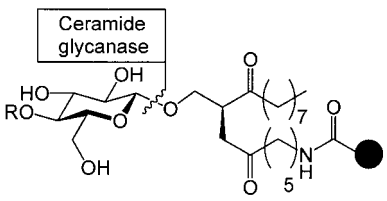
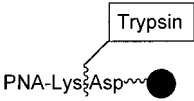
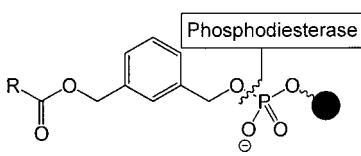
## 10.2

### Endo-linkers

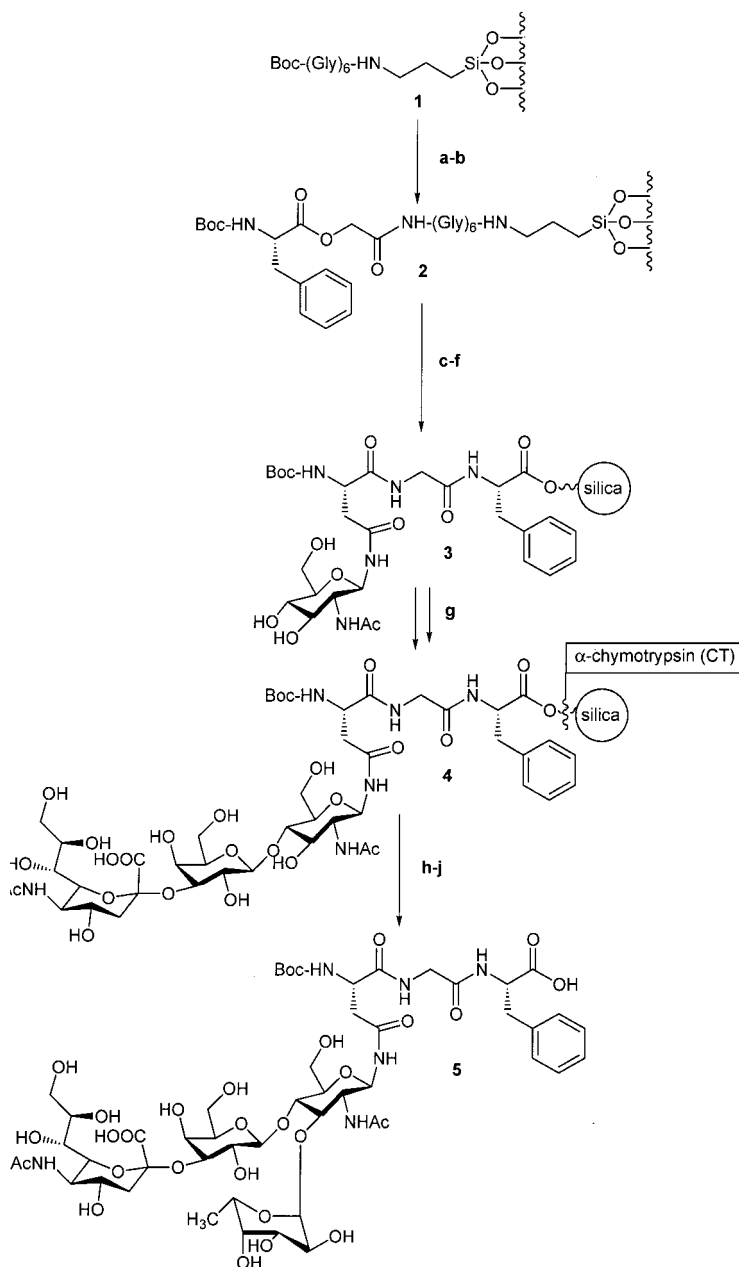
For a better overview, examples of endo-linkers and the enzymes used for the cleavage of the product from the solid phase which have been described in the literature so far are given in Tab. 10.1.

Wong *et al.* [7] introduced a silica-based solid support with a specific enzymatically cleavable linker for the synthesis of glycopeptides and oligosaccharides. They found that styrene- and sugar-based polymers tend to swell, which leads to a low coupling yield. Their choice of solid support is aminopropyl silica based on the facts that (a) it is compatible with both aqueous and organic solvents, (b) it has a large surface area accessible to biomolecules, and (c) it has sufficient density of functional groups.

Tab. 10.1 Examples of endo-linkers and respective cleavage enzymes.

Linker/Enzyme	Examples	Ref.
	Glycopeptide synthesis	7
	Oligosaccharide synthesis	8–9
	Oligosaccharide synthesis	10–11
	Peptide nucleic acid (PNA) synthesis	12
	Peptide synthesis	13

A hexaglycine spacer was attached to the solid support to give a substitution of  $0.2 \text{ mmol g}^{-1}$  of dry silica and the excess amino groups were then capped using acetic anhydride. In the next step a selectively cleavable,  $\alpha$ -chymotrypsin sensitive, phenylalanine ester (**2**) was implemented for the release of the products from the solid support under mild conditions. Subsequently it was transformed to (**3**) followed by reactions with glycosyl transferases to yield (**4**). Finally, the desired glycopeptide was cleaved from the solid support in high yield by treatment of (**4**) with  $\alpha$ -chymotrypsin (Scheme 10.1).



**Scheme 10.1** Glycopeptide synthesis and  $\alpha$ -chymotrypsin catalyzed release from the solid support. a) 25% TFA (CH<sub>2</sub>Cl<sub>2</sub>); b) O-(N-Boc-Phe)glycolic acid (7 eq), BOP, HOBT, DIEA; c) 25% TFA (CH<sub>2</sub>Cl<sub>2</sub>); d) Boc-Gly-OH (7 eq), BOP, HOBT, DIEA; e) 25% TFA (CH<sub>2</sub>Cl<sub>2</sub>); f) Boc-Asn(GlcNAc)-OH (3 eq), BOP, DIEA; g) galactosyl transferase, sialyl transferase; h) CT, H<sub>2</sub>O, pH 7.0; i) ultrafiltration; j)  $\alpha$ -1,3-fucosyltransferase, GDP-Fuc (2.5 eq), 0.1 M HEPES (pH 7.0), 95%.

Nishimura *et al.* [8–9] described a novel method for the enzymatic synthesis of oligosaccharide derivatives employing an  $\alpha$ -chymotrypsin sensitive linker. The synthesis of the water soluble *N*-acetyl-D-glucosamine (GlcNAc)-polymer (**10**), sensitive to  $\alpha$ -chymotrypsin, is shown in Scheme 10.2. Oxazoline derivative (**6**) was coupled to 6-(*N*-benzyloxycarbonyl-L-phenylalanyl)-amino-hexanol-1 (**7**) followed by *N*-deprotection of the phenylalanine and subsequent condensation with 6-acrylamidocaproic acid (**8**). De-*O*-acetylation gave the polymerizable GlcNAc derivative (**9**). Finally, copolymerization of acrylamide and monomer (**9**) in the presence of ammoniumper-sulfate (APS) and *N,N,N',N'*-tetramethyl ethylene diamine (TMEDA) gave the polymer (**10**) in high yield. The polymer (**10**) was then subjected to galactosylation and subsequent sialylation with the corresponding glycosyl transferases to yield (**11**). The final product (**12**) was cleaved from the water-soluble support by treatment with  $\alpha$ -chymotrypsin at 40 °C for 24 h in 72 % overall yield from (**10**).

Nishimura and Yamada [10–11] introduced a water-soluble polymeric support having a linker recognized by ceramide glycanase for a synthesis of ganglioside GM3 (**17**). Synthesis of the polymerizable lactose derivative (**14**) with a ceramide glycanase sensitive linker is shown in Scheme 10.3. The lactosyl ceramide (Lac-Cer) mimetic glycopolymer (**15**) is obtained from the monomeric precursor (**14**) by co-polymerization with acrylamide.

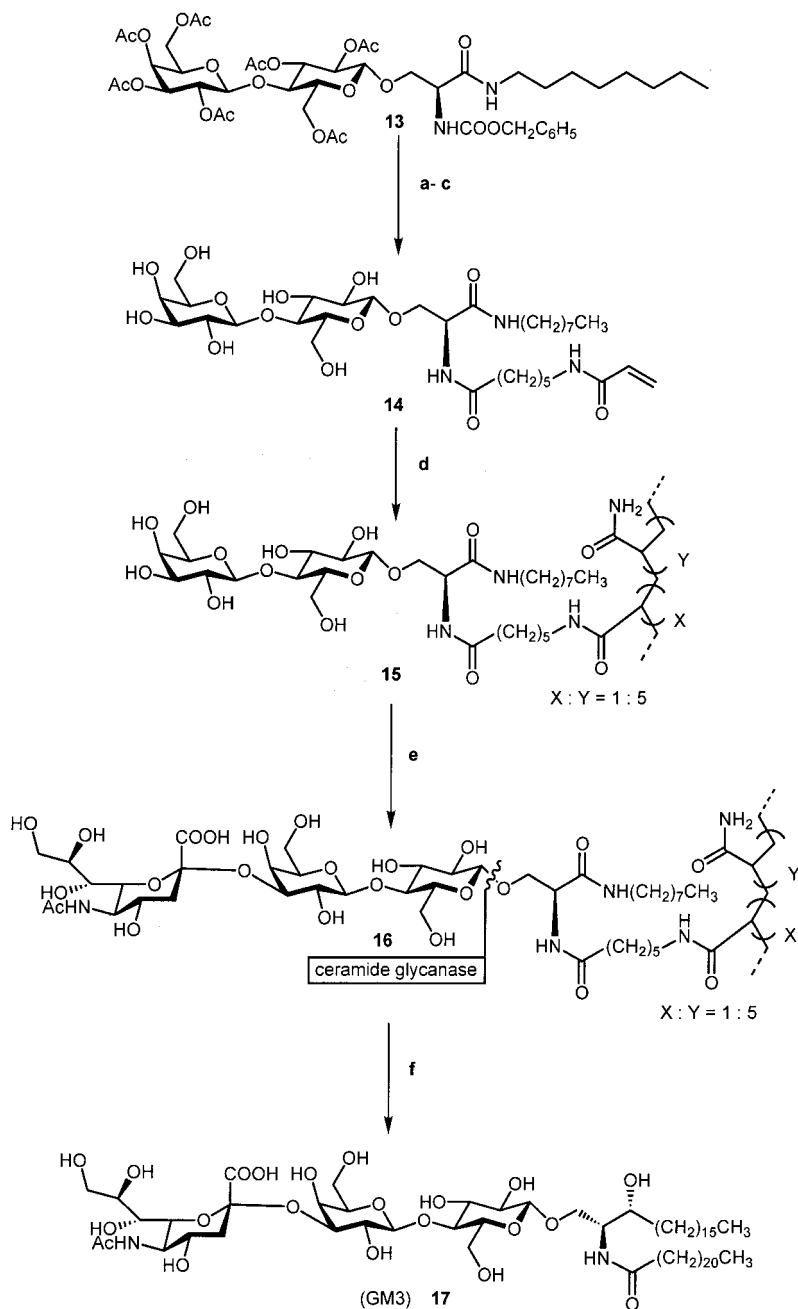
This solid support (**15**) was converted to the intermediate product (**16**) by sialylation using  $\beta$ Gal1 $\rightarrow$ 3/4GlcNAc  $\alpha$ -2,3-sialyltransferase. Finally, the polymeric support was cleaved by transglycosylation with leech ceramide glycanase in the presence of excess ceramide as acceptor to give the desired product (**17**) in high yield (Scheme 10.3). An advantage of the water-soluble polymer is that the transformation can be monitored by NMR spectroscopy during the enzymatic glycosylation steps.

Arrays of up to 1000 peptide nucleic acid (PNA) oligomers of different sequence were synthesized by Jensen *et al.* on polymer membranes (Fig. 10.2) [12]. The PNA chain was linked to the peptide spacer glutamic acid-( $\gamma$ -tert-butyl ester)-(L-aminohexanoic acid)-(L-aminohexanoic acid) (Glu [OtBu]-L-Ahx-L-Ahx) via an enzymatically cleavable Glu-Lys handle. The Glu [OtBu]-L-Ahx-L-Ahx spacer was coupled to the amino-functionalized membrane by standard Fmoc-Chemistry. Then the membranes were mounted in an ASP 222 Automated SPOT Robot and a grid of the desired format was dispensed at each position. The free amino groups outside the spotted areas were capped and further chain elongation was performed with Fmoc-protected PNA monomers to synthesize the desired PNA oligomers (**18**). After completion of the synthesis, the PNA oligomers were cleaved from the solid support by incubation with bovine trypsin solution in ammonium bicarbonate at 37 °C for 3 h.

One of the very first papers reporting about endo-linkers was published by Elmore *et al.* (Scheme 10.4) [13]. They described a new linker containing a phosphodiester group (**19**) for solid-phase peptide synthesis using a Pepsyn K (polyacrylamide) resin. After completion of coupling and deprotection cycles, the phosphodiester (**20**) was cleaved with a phosphodiesterase. In this way  $\beta$ -casomorphin, Leu-enkephalin and a collagenase substrate (**21**) were synthesized in high yields.



**Scheme 10.2** Oligosaccharide synthesis and  $\alpha$ -chymotrypsin catalyzed release from the solid support. a) Z-Phe-NH-(CH<sub>2</sub>)<sub>6</sub>-OH (**7**), CSA, (CHCl<sub>2</sub>)<sub>2</sub>, 70 °C; b) H<sub>2</sub>, Pd/C, MeOH, 50 °C; c) CH<sub>2</sub>=CHCONH(CH<sub>2</sub>)<sub>5</sub>COOH (**8**), EtOH-C<sub>6</sub>H<sub>6</sub>; d) MeONa (cat.), MeOH/THF, CH<sub>2</sub>=CHCONH(CH<sub>2</sub>)<sub>5</sub>COOH, APS, DMSO-H<sub>2</sub>O, 50 °C; e) Galactosyl transferase, Sialyl transferase; g) CT, Tris-HCl buffer, pH 7.8, 48 °C, 72% from (**10**).



**Scheme 10.3** Ceramide glycanase mediated release by transglycosylation. a) Pd/C, MeOH; b) (8), EEDQ, EtOH-C<sub>6</sub>H<sub>6</sub> c) MeONa d) CH<sub>2</sub>=CHCONH<sub>2</sub>, TMEDA, APS, DMSO-H<sub>2</sub>O, 50 °C, CMP-NeuAc, α-2,3-sialyltransferase, BSA, MnCl<sub>2</sub>, CIAP, 50 nM sodium cacodylate buffer, pH 7.49, ceramide, Triton CF-54, sodium citrate buffer, pH 6.0, 37 °C, 61%.



**Fig. 10.2** Trypsin mediated cleavage of a peptide bond in PNA oligomer synthesis



### Synthesis via symmetrical anhydrides of N-Fmoc amino acids

pH = 5.7, 7d (83%)

21

**Scheme 10.4** Synthesis of a collagenase substrate on a phosphodiesterase-scissile Linker.

In the context of enzymatic cleavage of linkers on polymeric supports particular attention was paid to the general question of whether enzymatic transformations on resins are viable and high yielding. An in-depth treatment of this problem is beyond the scope of this review. However, a few examples for the application of biocatalyzed transformations on solid supports will serve to illustrate that such transformations can indeed be employed advantageously for various purposes. Meldal *et al.* described the proteolytic cleavage of the alanine-tyrosine bond in a resin-bound decapeptide by treatment with the 27 kDa protease subtilisin BNP' to demonstrate the accessibility of the interior of the newly designed SPOCC-resin [14] to enzymes [15]. Furthermore, enzymatic hydrolysis of model isopeptides N<sup>ε</sup>-oligo(L-methionyl)-L-lysine from Bio-beads [16] by pepsin, chymotrypsin, cathepsin-C (dipeptidyl peptidase IV) and intestinal aminopeptidase-N was investigated

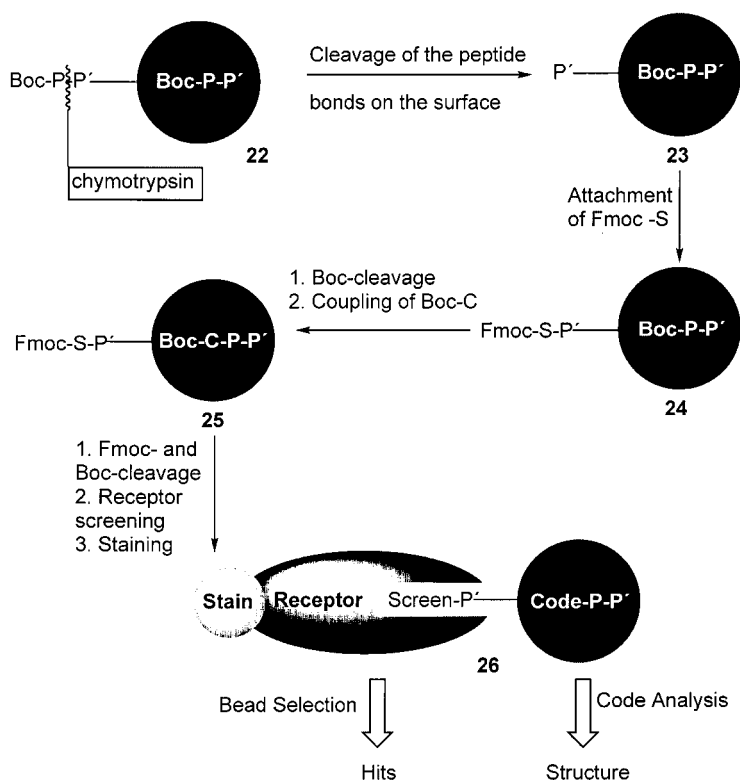


using high performance liquid chromatography to identify and quantify the hydrolysis products [17].

Larsen *et al.* reported the enzymatic cleavage of a desB30 insulin B-chain from a presequence (Lys(Boc))<sub>6</sub>. This spacer shifts the conformation of the growing peptide chain from a  $\beta$ -structure to a random coil conformation and reduces peptide-chain aggregation, which otherwise causes serious synthetic problems. Novasyn KA [18] was employed as a solid support, but unfortunately, no information about the enzyme used was reported [19].

Barany *et al.* exploited the different enzyme accessibilities of surface and interior areas of a given bead and the resulting differentiated beads were used to synthesize a peptide library on the surface and code for it in the interior of the bead [20].

This clever strategy is illustrated in Scheme 10.5. Selective cleavage of short N<sup>α</sup>-protected peptide substrates with chymotrypsin from the surface area of TentaGel-



**Scheme 10.5** Peptide encoded combinatorial peptide libraries via enzyme-mediated spatial segregation. P-P'. Substrate with a scissile bond between P and P', S. Terminal Residue of the screening structure, C. Terminal Residue of the coding structure.

AM-beads (**22**) leaves the majority of the peptide attachment sites in the interior uncleaved to afford (**23**) ("shaving" methodology). The first residue is attached using orthogonal Fmoc-chemistry to provide (**24**). Coding is achieved by using standard BOC-chemistry in the interior of the bead to yield (**25**). Repetition of this process furnishes a surface bound peptide, which is encoded internally (**26**).

This generation of two structures on the same bead allowed the investigation of the synthesized peptide library ( $1 \times 10^5$  members) with different receptors (anti- $\beta$ -endorphin antibody, streptavidin and thrombin). After the staining procedure had been carried out, the beads that showed a colour were selected for sequencing and the coding peptides present within the bead were used to deduce the binding structures. This screening led to the discovery of a new thrombin ligand, which binds with an affinity one order of magnitude higher than the natural motif.

In principle solid-phase synthesis suffers from a major disadvantage compared with solution-phase syntheses: During the syntheses no purification of the resin bound substrate is possible leading sometimes to complex product mixtures. Fernandez-Mayoralas *et al.* [21] developed a novel approach to overcome this problem using the high substrate specificity of enzymes in their synthesis of galactose-glucose-disaccharides (**31**) on a support [22]. After galactosylation of glucose immobilized to the soluble MPEG-support (**28**) using  $\beta$ -galactosidase, the unreacted monosaccharide glucose was removed by the combined use of  $\alpha$ - and  $\beta$ -glucosidases to obtain only MPEG-bounded disaccharides (**29**), Scheme 10.6). Finally the obtained disaccharides (**31**) were released from the support by ethanolysis.

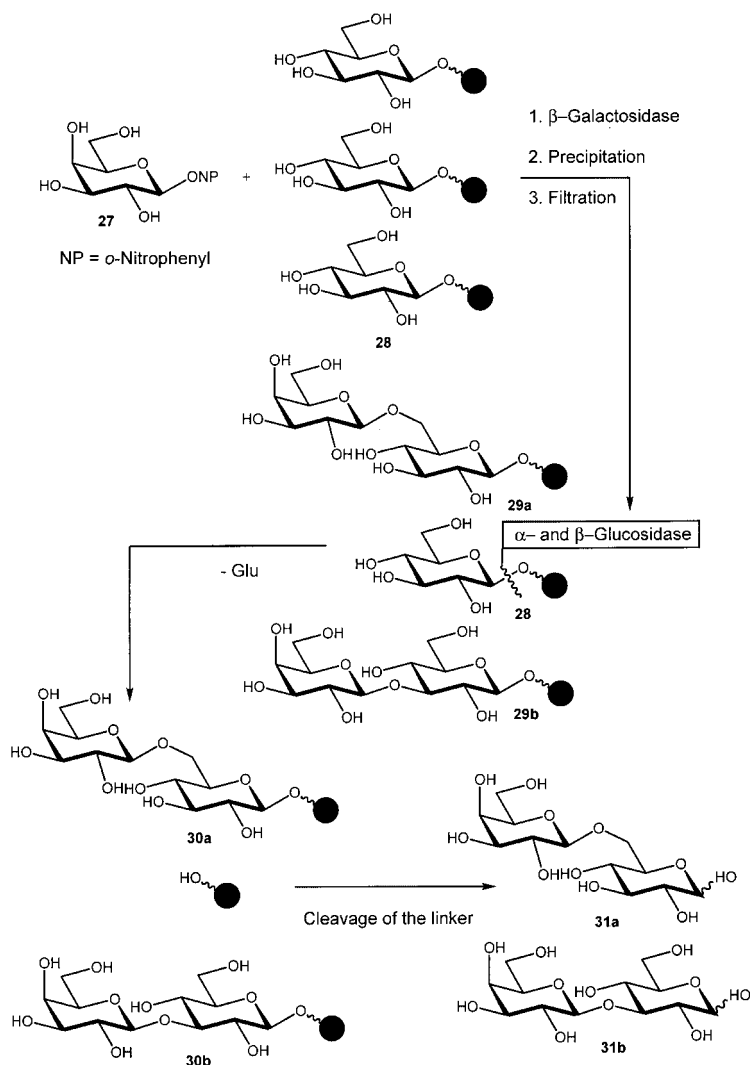
Reetz *et al.* described the solid-phase enzymatic synthesis of oligonucleotides on Kieselguhr-PDMA-resins via T4 RNA ligase. Concomitantly, they found that RNase A selectively cleaves the last bound nucleotide at the ribose sugar leaving a 3',5'-diphosphorylated oligomer on the resin, but application in synthesis has not yet been undertaken [22].

Enzyme hydrolysis of immobilized substrates was not only used for the development of linkers in solid-phase chemistry but also used as a key step to evaluate enzyme-selectivity in several assays.

Lowe *et al.* investigated the substrate selectivity of the proteases papain and chymotrypsin using PEGA-bound combinatorial peptide libraries (**32**) (Fig. 10.3) [24]. The qualitative extent of enzymatic cleavage of the resin-bound peptide in case of an accepted substrate strand was rapidly visualized by a significant reduction in the fluorescence of the beads visualized with a fluorescence microscope. Furthermore it was proven that substrate selectivity of the enzyme remain the same on the solid phase and in solution.

Meldal *et al.* developed a novel protease assay based on the long-range resonance energy transfer (FRET) [25] fluorescence quenched (FQ) pair 3-nitrotyrosine/2-aminobenzoic acid. This served to characterize enzyme specificity by direct visual inspection of the resin beads (**33**).

The libraries of enzyme substrates were obtained by split-pool synthesis to yield "one-bead-one-compound" libraries. The substrate assay was performed with a range of proteolytic enzymes such as subtilisin Carlsberg [26], cruzipain [27], protein disulfide isomerase [28–29], matrix metalloprotease MMP-9 [30], papain [31],



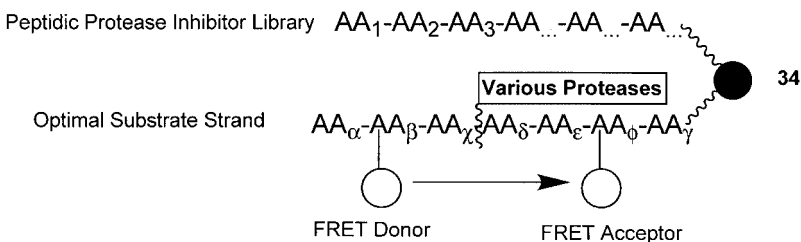
**Scheme 10.6** General strategy for the liquid-phase synthesis of disaccharides using glycosidases.

outer membrane protease T (ompT) [32], cathepsin [33] and a cysteine protease from *Leishmania mexicana* [34–35]. It was robust and gave a complete picture of the hydrolytic specificity and activity of the enzymes.

Furthermore, Meldal *et al.* developed the idea to combine the substrate cleavage on the solid phase with an inhibitor library assay in which a substrate is synthesized and coupled to a library of putative inhibitors (**34**) (Fig. 10.4). The incubation of such an inhibitor library with enzymes led to cleavage and hence fluorescence in beads containing weak inhibitors. Beads containing strong inhibitors re-



**Fig. 10.3** Protease substrate assays.

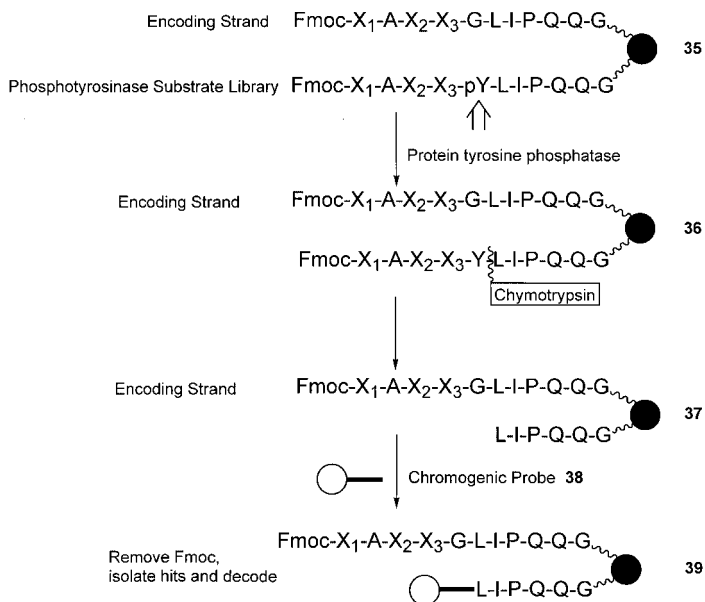


**Fig. 10.4** One bead two peptide assays.

remained dark, and after collection of such beads the inhibitor structure could be identified. This “one-bead-two-compounds” assay was developed using the optimal substrate according to the above described substrate assay and was validated with subtilisin Carlsberg [36], cruzipain [37] and matrix metalloprotease MMP-12 [38].

The library is deprotected and used in aqueous buffer for identification of inhibitors by thorough hydrolysis with  $10^{-6}$  to  $10^{-7}$  concentration of the enzyme. Assuming a volume of 3 mL for  $10^6$  beads and the use of a protease of molecular weight about 30 kDa, this corresponds to  $10^{-11}$  grams of enzyme per inhibitory assay. Thus the assay is not only efficient in terms of time required and manipulation but also reduces the amount of enzyme used, which is essential if only minute amounts of enzyme can be produced. Rossé *et al.* showed while applying this assay with human napsin A, that enzymes can even be used as crude cell extracts without further purification [39].

Balasubramanian *et al.* developed an assay to investigate tyrosine phosphatase selectivity (Scheme 10.7). Firstly a Kieselguhr-immobilized phosphopeptide library



**Scheme 10.7** Protein tyrosine phosphatase inhibitor assay.

(35) with an undecapeptide corresponding to the autophosphorylation site of epidermal growth factor receptor (EGFR<sub>988-998</sub>) as a prototype sequence was synthesized, in which the phosphotyrosine (pY) position was exchanged to 30% glycine to generate an encoding strand (Scheme 10.7) [40]. The *N*-terminus was left capped with a Fmoc protecting group. The library was subjected to on-bead dephosphorylation with a protein tyrosine phosphatase (PTP) (leukocyte antigen receptor (LAR) phosphatase) resulting in the transformation of substrates to tyrosyl peptides. The library was then subjected to proteolytic cleavage with  $\alpha$ -chymotrypsin, which is selective for those sequences that have undergone PTP-mediated dephosphorylation in the previous step. The encoding strand (37), which lacks tyrosine, remains intact throughout. The free amino termini that result from dephosphorylated sequences were coupled to carboxyfluorescein (38), an amine-reactive fluorophore to locate the positive beads. Removal of the terminal Fmoc group from the encoding strands of positive beads permits facile sequence identification by standard peptide sequencing.

The combinatorial screening experiment generated six distinct substrate sequences for LAR PTP, each of which contained at least two acidic residues in three variable positions. These results indicate that acidic residues on the *N*-terminal site of pY are important for binding and catalysis.

## 10.3

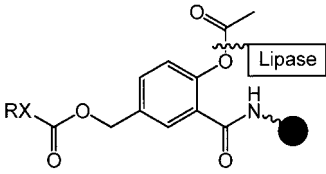
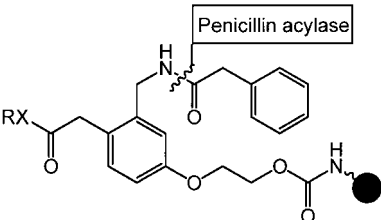
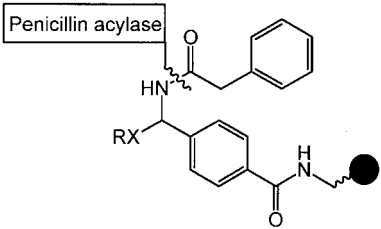
## Exo-linkers

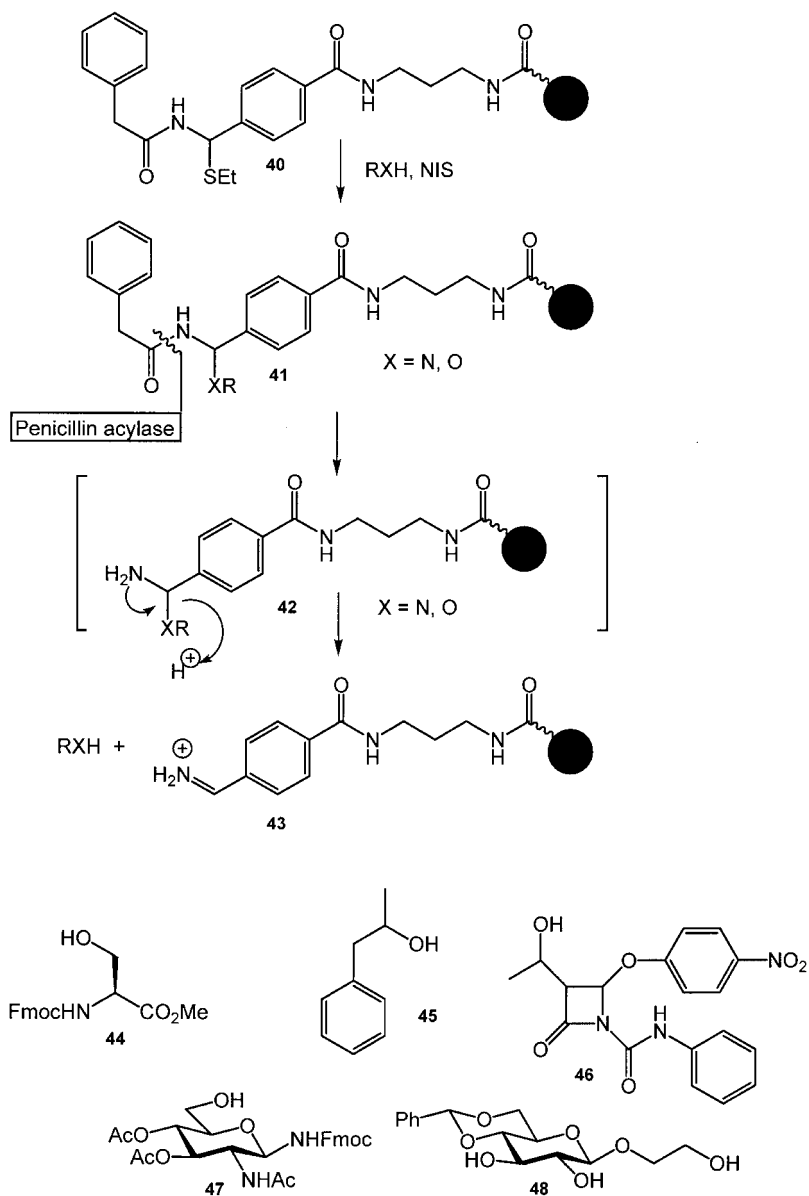
An exo-linker according to Fig. 10.1 must contain an enzyme labile group  $R^1$ , which is recognized and attacked by the biocatalyst. Possible combinations could be: phenylacetamide/penicillin amidase, ester/esterase, monosaccharide/glycosidase, phosphate/phosphatase, sulfate/sulfatase and peptides/peptidases [41]. The following systems have been worked out (Tab. 10.2).

In independent and simultaneous investigations Flitsch *et al.* [41–42] and Waldmann *et al.* [43–44] developed selectively cleavable exo-linkers, which can be cleaved with penicillin G acylase, a commercially available and widely used enzyme [45].

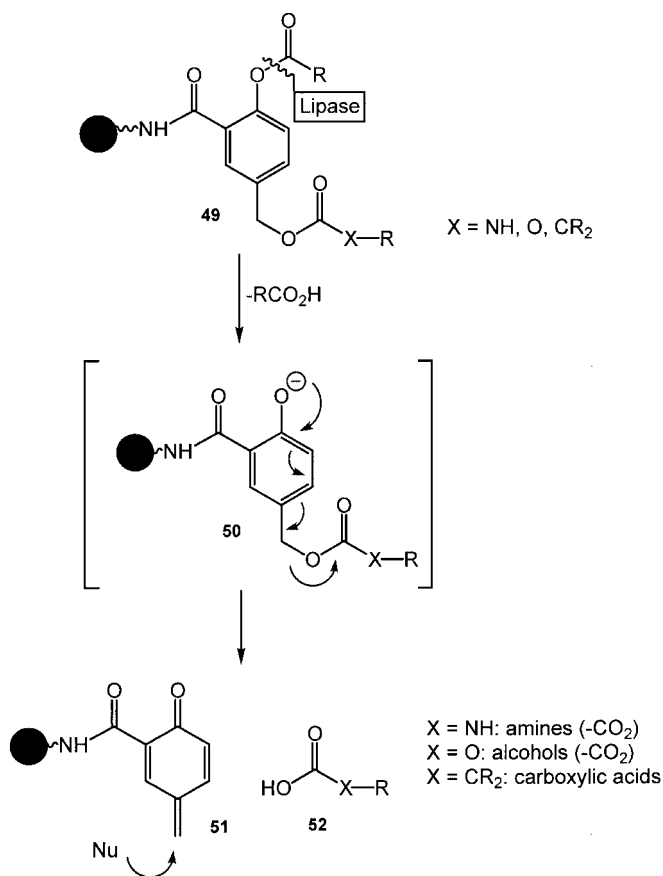
Penicillin acylase catalyzes the hydrolysis of phenylacetamides and has been used in peptide synthesis for the cleavage of protecting groups [46–47]. In linker (40) developed by Flitsch *et al.* [41–42] (Scheme 10.8) the group  $-XR$  represents the alcohol or amine group of the target molecule. Hydrolysis of the phenylaceta-

Tab. 10.2 Examples of exo-linkers and respective cleavage enzymes.

Linker/Enzyme	Examples	Ref.
	Pictet–Spengler reaction, nucleoside immobilization	48–49
	Palladium cat. C–C-couplings, Mitsunobu- and Diels–Alder reactions, 1,3-dipolar cyclo-additions	43–44
	Immobilization of alcohols (e.g. Fmoc protected serine methyl ester, glycosides) and amines (e.g. phenylalamine)	41–42



**Scheme 10.8** Loading and cleavage of a penicillin acylase scissile linker.



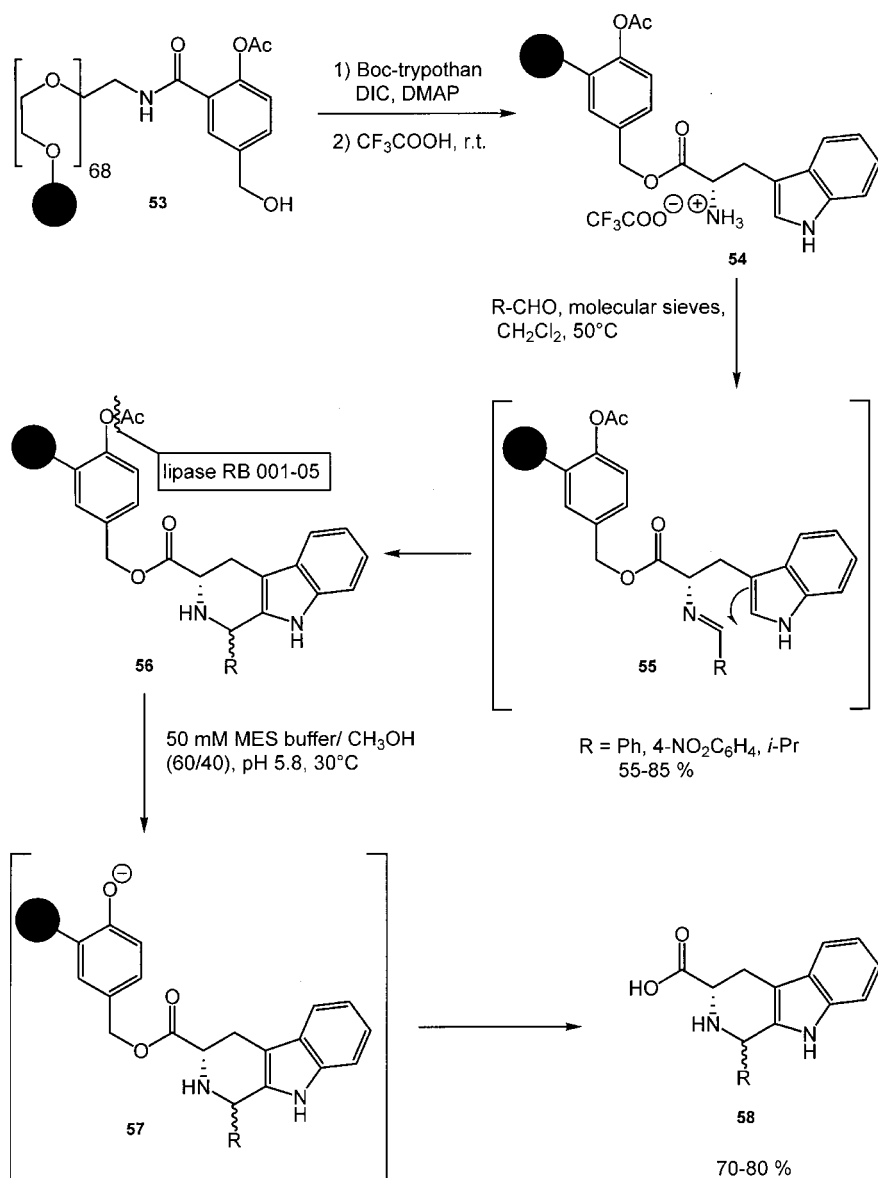
**Scheme 10.9** Principle for the development of the enzyme-labile 4-acyloxybenzyloxy linker group.

imide moiety generates hemiaminal (**42**) which readily fragments in aqueous medium and thereby releases the desired products, RXH.

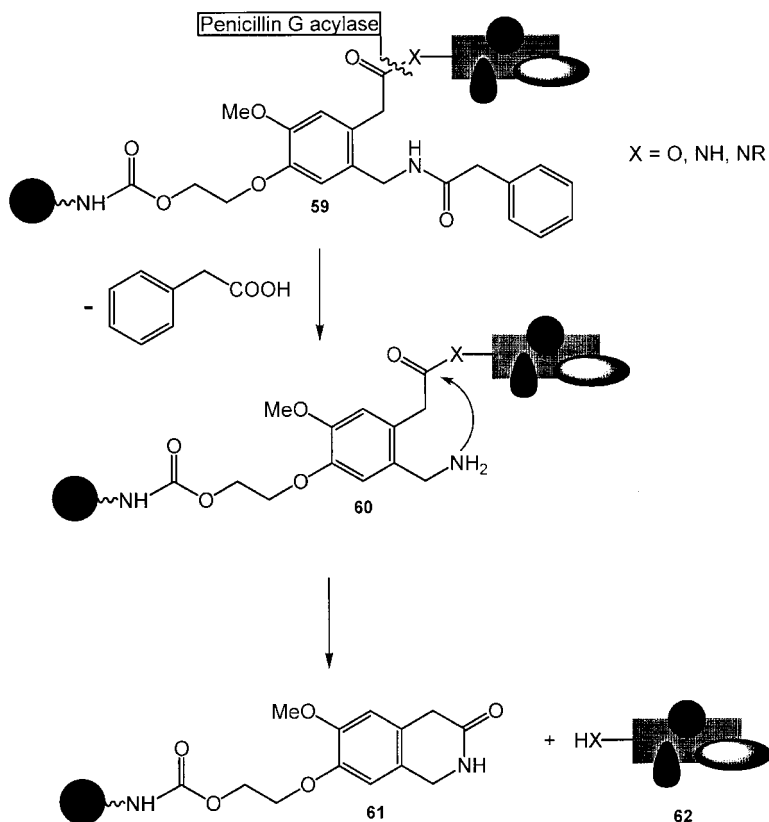
The thioethyl group present in the anchor group of (**40**) was activated by treatment with *N*-iodosuccinimide (NIS) followed by displacement with a variety of alcohols (**44–46**). To prove the possible application of this linker in solid phase carbohydrate synthesis, protected glycosides (**47**) and (**48**) were coupled to linker (**40**) and released enzymatically. Flitsch *et al.* also described the immobilization and enzymatic cleavage on a variety of amines [41]. Nevertheless, the application of this enzyme-labile linker group in multi-step syntheses on the solid phase and subsequent enzyme-initiated release from the polymeric support has not been described yet.

Waldmann *et al.* designed the exo-linker (**49**) [48–49]. The anchor group comprises a 4-acyloxy-3-carboxybenzyloxy group, which is recognized and attacked by





**Scheme 10.10** Solid phase synthesis of tetrahydro-β-carbolins and subsequent detachment by enzyme initiated fragmentation of the anchor group.



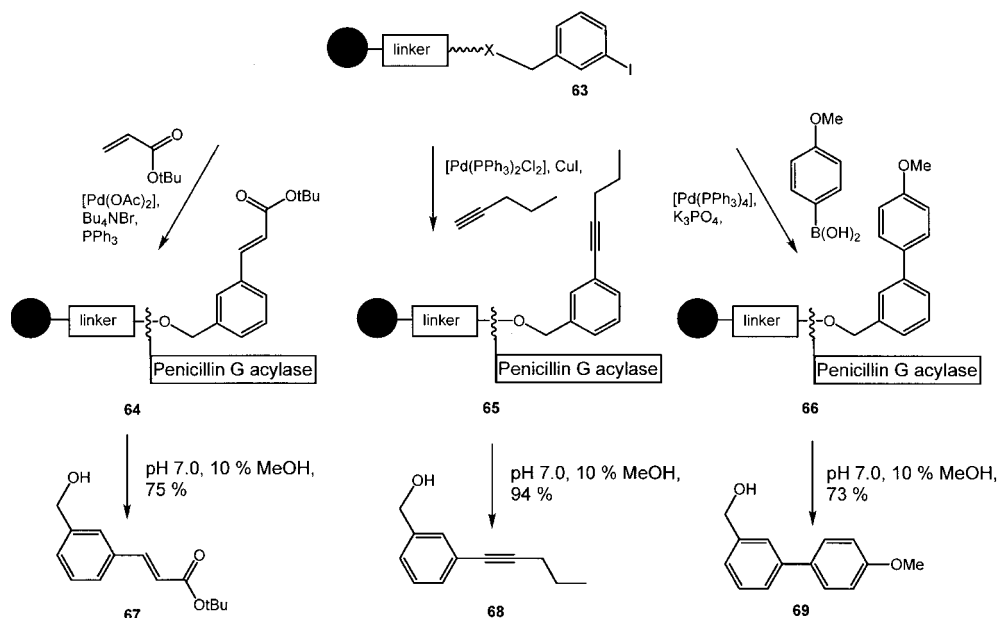
**Scheme 10.11** Principle of the enzyme-labile safety catch linker.

the biocatalyst, so that a spontaneously fragmenting intermediate is generated, thereby releasing the desired compound (Scheme 10.9) [50–52].

The linker (**49**) is attached as an amide to the solid phase. Cleavage of the acyl group by a lipase generated a phenolate (**50**), which fragments to give a quinone methide (**51**) and releases the product (**52**). The quinone methide remains on the solid phase and is trapped by water or an additional nucleophile.

Following this cleavage in principle, amines (bound as urethanes), alcohols (bound as carbonates), and carboxylic acids (bound as esters) can be detached from the polymeric carrier. The substrate specificity of the enzyme guarantees that only the intended ester is cleaved.

TentaGelS-NH<sub>2</sub> was chosen as the polymeric support, i.e. a polystyrene resin equipped with terminally NH<sub>2</sub>-functionalized oligoethylene glycol units. It has a polar surface and swells in aqueous solutions allowing the biocatalyst access to the polymer matrix [53].



**Scheme 10.12** Pd<sup>0</sup>-catalyzed reactions on enzyme labile linker-conjugates.

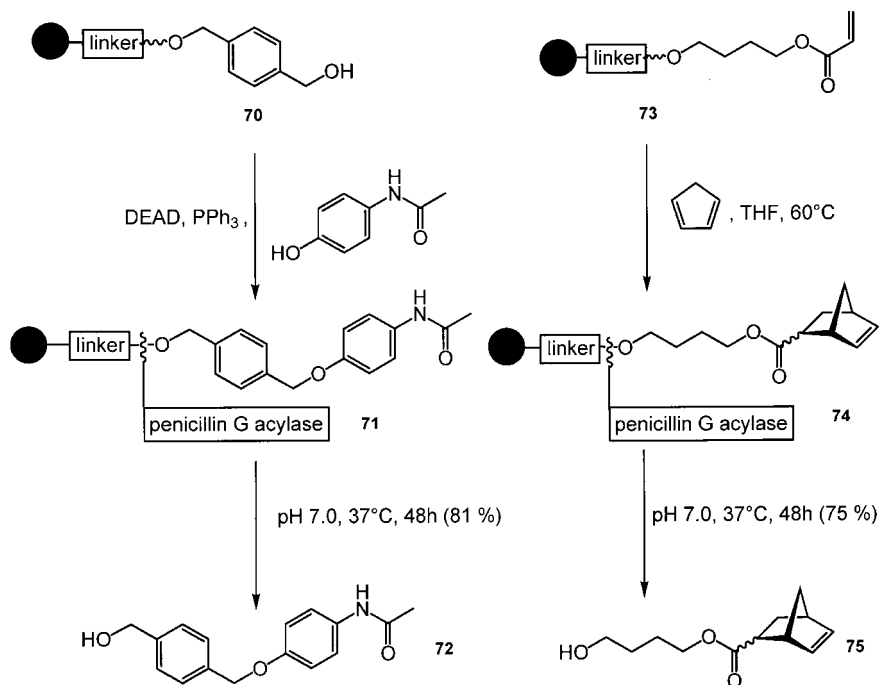
The applicability of the enzyme-labile anchor group was demonstrated by the synthesis of tetrahydro- $\beta$ -carbolins (**58**) employing the Pictet-Spengler reaction (Scheme 10.10).

The benzylic alcohol group of the linker (**53**) was first esterified with Boc-L-tryptophan, and after its *N*-terminal deprotection the support-bound tryptophan (**54**) was reacted with aliphatic and aromatic aldehydes to give imines (**55**), which cyclized immediately in reasonable to high yields to the tetrahydro- $\beta$ -carbolins (**56**). Lipase RB 001-05 selectively attacked the acetate incorporated into the linker and generated the corresponding phenolate (**57**), which then fragmented spontaneously. Following these multi-step transformations the desired tetrahydro- $\beta$ -carbolins (**58**) were obtained in 70–80% yield.

Waldmann *et al.* developed a second exo-linker following a new approach [43–44] which makes use of a safety-catch linker. It is based on the enzymatic cleavage of a functional group embodied in the linker. In this way an intermediate is generated, which subsequently cyclizes intramolecularly according to the principle of assisted removal [54–58] and thereby releases the desired target compounds (Scheme 10.11).

The linker group is immobilized as a urethane to the amino-functionalized carrier (**59**). It facilitates the attachment of a variety of molecules such as alkyl halides, alcohols or amines bound as carboxylic acid esters and amides.

According to the safety-catch principle, the separation of the desired products proceeds in a two-step process. First, penicillin G acylase hydrolyses the phenyl-



**Scheme 10.13** Mitsunobu and Diels–Alder reaction on enzyme labile linker-conjugates.

acetamide with complete chemo- and regioselectivity and under exceptionally mild conditions (pH 7.0, room temperature or 37°C) [59–61]. Then the activated intermediate generated, i.e. benzylamine (**60**), cyclizes to polymer-bound lactam (**61**) and releases the desired target molecule (**62**).

POE 6000 was used as polymeric support, a soluble polyethylene glycol derivative functionalized at both termini with an amino group and with an average molecular mass of 6000 Da [62–63]. After completion of the homogeneous reactions it can be precipitated, filtered off, and washed with diethyl ether, thereby facilitating the separation of surplus reagents and the side products. Furthermore it allows for NMR spectroscopic monitoring of the reactions [64].

Most importantly, it is soluble in aqueous solutions, thereby allowing efficient access of the enzyme to the polymer-fixed linker group.

The suitability of the polymer-linker conjugate was examined for a variety of transformations, in particular Pd<sup>0</sup>-catalyzed reactions. For instance, the polymer-bound aryl iodide (**63**) was transformed quantitatively in a Heck reaction to a cinnamic acid ester (**64**) and to biphenyl (**66**) in a Suzuki reaction. It gave an alkyne (**65**) in a Sonogashira reaction (Scheme 10.12).

The desired benzyl alcohols (**67–69**) were released by incubation of the corresponding polymer conjugates (**64–66**) with penicillin G acylase at pH 7 and 37°C

in high yields and isolated with a purity of >95% by simple extraction with diethyl ether.

Furthermore, the applicability in a Mitsunobu esterification reaction and a Diels–Alder reaction was proven (Scheme 10.13). The polymer-bound benzyl alcohol (**70**) was reacted with 4-acetamidophenol in the presence of the Mitsunobu reagent to give phenyl ether (**71**) in quantitative yield. It was released from the polymeric support in high yield.

For the Diels–Alder reaction, polymer-bound acrylic acid ester (**73**) was treated with cyclopentadiene. The cycloaddition product (**74**) was formed with an *endo/exo* ratio of 2.5:1 and with quantitative conversion. The subsequent enzymatic release delivered the corresponding alcohols (**72**, **75**) in high yield and purity.

## 10.4

### References

- 1 F. BALKENHOHL, C. VON DEM BUSSCHE HÜNNFELD, A. LANSKY, *et al.*, *Angew. Chem. Int. Ed. Engl.* **1996**, 35, 2289–2337.
- 2 J.S. FRUCHTEL, G. JUNG, *Angew. Chem. Int. Ed. Engl.* **1996**, 35, 17–42.
- 3 L.A. THOMPSON, J.A. ELLMAN, *Chem. Rev.* **1996**, 96, 555–600.
- 4 L. YAN, C.M. TAYLOR, R. GOODNOW, *et al.*, *J. Am. Chem. Soc.* **1994**, 116, 6953–6954.
- 5 R.L. HALHOMB, H.M. HUANG, C.H. WONG, *J. Am. Chem. Soc.* **1994**, 116, 11315–11322.
- 6 This nomenclature was introduced by S.L. FLITSCH *et al.* See references [41–42] and N.J. TURNER, *Curr. Org. Chem.* **1997**, 1, 21–36.
- 7 M. SCHUSTER, P. WANG, J.C. PAULSON, *et al.*, *J. Am. Chem. Soc.* **1994**, 116, 1135–1136.
- 8 K. YAMADA, S.I. NISHIMURA, *Tetrahedron Lett.* **1995**, 36, 9493–9496.
- 9 K. YAMADA, E. FUJITA, S.I. NISHIMURA, *Carbohydr. Res.* **1997**, 305, 443–461.
- 10 S. NISHIMURA, K. YAMADA, *J. Am. Chem. Soc.* **1997**, 119, 10555–10556.
- 11 The versatility of polymer-assisted enzymatic synthesis of non-natural and biologically significant glycolipid derivatives was also demonstrated by constructing pseudo-ganglioside GM3, see: K. YAMADA, S. MATSUMOTO, S.I. NISHIMURA, *Chem. Commun.* **1999**, 507–508.
- 12 J. WEILER, H. GAUSEPOHL, N. HAUSER, *et al.*, *Nucleic Acids Res.* **1997**, 25, 2792–2799.
- 13 D.T. ELMORE, D.J.S. GUTHRIE, A.D. WALLACE, *et al.*, *J. Chem. Soc. Chem. Commun.* **1992**, 1033–1034.
- 14 SPOCC resin is based on the cross-linking of long-chain Poly(ethylene glycol) (PEG) terminally substituted with oxetane by cationic ring-opening polymerization.
- 15 J. RADEMANN, M. GROTLI, M. MELDAL, *et al.*, *J. Am. Chem. Soc.* **1999**, 121, 5459–5466.
- 16 Bio-beads consists of (1% cross-linked polystyrene with 1.25 mmol chloromethyl substitution per gram of dry resin respectively benzhydrylamine polymer (1% cross-linked polystyrene with 0.24 mmol NH<sub>2</sub> per gram of dry resin, Bio-Rad Laboratories (Richmond, CA, USA).
- 17 H. GAERTNER, A. PUIGSERVER, *Eur. J. Biochem.* **1984**, 145, 257–263.
- 18 Novasyn KA consists of kieselguhr supported dimethylacrylamide functionalized with sarcosine methylester.
- 19 B.D. LARSEN, A. HOLM, *J. Pept. Res.* **1998**, 52, 470–476.
- 20 J. VAGNER, G. BARANY, K.S. LAM *et al.*, *Proc. Natl. Acad. Sci. U. S. A.* **1996**, 93, 8194–8199.
- 21 G. CORRALES, A. FERNANDEZ-MAYORALAS, E. GARCIA-JUNCEDA, *et al.*, *Biocatalysis and Biotransformation* **2000**, 18, 271–281.
- 22 MPEG consists of a polyethylene glycol 5000 monomethyl ester, see: J.J. KREPINSKY, Advances in polymer-supported solution synthesis of oligosaccharides, In *Modern Methods in Carbohydrate Synthesis*

- (eds. S.A. KHAN and R.A. O'NEILL). Harwood Academic publishers, The Netherlands, **1996**, 194–224.
- 23 C. SCHMITZ, M.T. REETZ, *Organic Letters* **1999**, 1, 1729–1731.
  - 24 S. LEON, R. QUARELL, G. LOWE, *Bioorg. Med. Chem. Lett.* **1998**, 8, 2997–3002.
  - 25 T. FÖRSTER, *Ann. Phys. N. Y.* **1998**, 6, 55–75.
  - 26 M. MELDAL, I. SVENDSEN, K. BREDDAM, *et al.*, *Proc. Natl. Acad. Sci. USA*, **1994**, 91, 3314–3318.
  - 27 E. DEL NERY, M.A. JULIANO, M. MELDAL, *et al.*, *Biochem. J.*, **1997**, 323, 427–433.
  - 28 J.C. SPETZLER, V. WESTPHAL, J.R. WINTHER, *et al.*, *J. Pep. Sci.*, **1998**, 4, 128–137.
  - 29 V. WESTPHAL, J.C. SPETZLER, M. MELDAL, *et al.*, *J. Biol. Chem.*, **1998**, 273, 39, 24992–24999.
  - 30 M. RENIL, M. FERRERAI, J.M. DELAISSÉ, *et al.*, *J. Pep. Sci.*, **1998**, 4, 195–210.
  - 31 P.M. ST. HILAIRE, M. WILLERT, M.A. JULIANO, *et al.*, *J. Comb. Chem.* **1999**, 1, 509–523.
  - 32 N. DEKKER, R.C. COX, R.A. KRAMER, *et al.*, *Biochemistry*, **2001**, 40, 1694–1701.
  - 33 J.J. PETERSON, C.F. MEARES, *Bioconjugate Chem.* **1998**, 9, 618–626.
  - 34 P.M. ST. HILAIRE, L.C. ALVES, S.S. SANDERSON *et al.*, *Chembiochem.* **2000**, 1, 155–122.
  - 35 L.C. ALVES, P.M. ST. HILAIRE, M. MELDAL *et al.*, *Molecular and Biochem. Parasitology* **2001**, 114, 81–88.
  - 36 M. MELDAL, I. SVENDSEN, *Chem. Soc. Perkin Trans. I*, **1995**, 1591–1596
  - 37 M. MELDAL, I. SVENDSEN, L. JULIANO, *et al.*, *J. Pep. Sci.* **1998**, 4, 83–91.
  - 38 J. BUCHARDT, C.B. SCHIODT, C. KROG-JENSEN, *et al.*, *J. Comb. Chem.* **2000**, 2, 624–638.
  - 39 G. ROSSÉ, E. KUENG, M.G.P. PAGE *et al.*, *J. Comb. Chem.* **2000**, 2, 461–466.
  - 40 Y.W. CHEUNG, C. ABELL, S. BALASUBRAMANIAN, *J. Am. Chem. Soc.* **1997**, 119, 9568–9539.
  - 41 FLITSCH, S.L., LAHJA, S., TURNER, N.J. Solid phase preparation and enzymic and non-enzymic bond cleavage of sugars and glycopeptides, PCT Int. Appl. **1997**, patent EP 9605535, CAN 127:81736.
  - 42 G. BÖHM, J. DOWDEN, D.C. RICE, *et al.*, *Tetrahedron Lett.* **1998**, 39, 3819–3822.
  - 43 U. GRETHER, H. WALDMANN, *Chem. Eur. J.* **2001**, 7, 959–971.
  - 44 U. GRETHER, H. WALDMANN, *Angew. Chem. Int. Ed.* **2000**, 39, 1629–1632.
  - 45 H. WALDMANN, A. REIDEL, *Angew. Chem. Int. Ed. Engl.* **1997**, 36, 647–649.
  - 46 H. WALDMANN, D. SEBASTIAN, *Chem. Rev.* **1994**, 94, 911–937.
  - 47 D. KADEREIT, H. WALDMANN, *Chem. Rev.* **2001**, 101, 3367–3396.
  - 48 B. SAUERBREI, V. JUNGSMANN, H. WALDMANN, *Angew. Chem. Int. Ed.* **1998**, 37, 1143–1146.
  - 49 H. WALDMANN, B. SAUERBREI, U. GRETHER, Enzyme cleavable linker for solid phase synthesis, (BASF A.G., Germany), Ger. Offen. **1998**, CAN 128: 114573.
  - 50 H. WALDMANN, M. SCHELHAAS, E. NÄGELE, *et al.*, *Angew. Chem. Intl. Ed. Engl.* **1997**, 36, 2238–2241.
  - 51 H. WALDMANN, E. NÄGELE, *Angew. Chem. Intl. Ed. Engl.* **1995**, 34, 2259–2262.
  - 52 T. POHL, H. WALDMANN, *J. Am. Chem. Soc.* **1997**, 119, 6702–6710.
  - 53 W. RAPP, in *Combinatorial Peptide and Non-Peptide Libraries* (ed.: G. JUNG), VCH, Weinheim **1996**, 425.
  - 54 T.W. GREENE, P.G.M. WUTS, *Protective Groups in Organic Synthesis*, Wiley and Sons, New York **1999**.
  - 55 B.F. CAIN, *J. Org. Chem.* **1976**, 41, 2029–2031.
  - 56 I.D. ENTWISTLE, *Tetrahedron Lett.* **1994**, 35, 4103–4106.
  - 57 F. CUBAIN, *Rev. Roum. Chim.* **1973**, 18, 449–461.
  - 58 G. JUST, G. ROSEBERY, *Synth. Commun.* **1973**, 3, 447–451.
  - 59 H. WALDMANN, *Liebigs Ann. Chem.* **1988**, 1175–1180.
  - 60 M.A. DINEVA, B. GALUNSKY, V. KASCHE, *et al.*, *Bioorg. Med. Chem. Lett.* **1993**, 3, 2781–2784.
  - 61 H. WALDMANN, A. HEUSER, A. REIDEL, *Synlett* **1994**, 65–67.
  - 62 D.J. GRAVERT, K.D. JANDA, *Chem. Rev.* **1997**, 97, 489–509.
  - 63 E. BAYER, M. MUTTER, *Nature* **1972**, 237, 512–513.
  - 64 J.M. DUST, Z.H. FANG, J.M. HARRIS, *Macromolecules* **1990**, 23, 3742–3746.

## 11

**Polymer-supported Olefin Metathesis Catalysts for Organic and Combinatorial Synthesis**

JASON S. KINGSBURY and AMIR H. HOVEYDA

## 11.1

**Introduction**

It is close to forty years since Merrifield's groundbreaking achievements in solid-phase polypeptide synthesis [1]. Today polymers continue to simplify a myriad of reaction procedures and product isolations in the context of a variety of new applications. Solid supports are used routinely in high-throughput synthesis of diverse libraries of organic molecules [2]. Combined with recently developed screening methods [3], solid-phase chemical synthesis allows for significant acceleration of the discovery of new biological probes and therapeutic candidates. However, such strategies may be rendered more efficient. For example, the synthesis of compounds on a polymer bead requires at least two non-complexity-generating steps (attachment to and cleavage from the resin) and the deliberate introduction of functionality (typically free hydroxyl groups) in the target compounds needed for immobilization. Challenges with 'on-resin' spectroscopic and analytical methods [4] may be viewed as another disadvantage inherent to this strategy.

A complementary approach is the synthesis of parallel libraries in solution [5], where purification is avoided through the use of polymer-supported reagents or, more preferably, catalysts. This has led to significant interest in the development of efficient solid-supported catalysts that promote a number of key transformations [6]. Transition metal-catalyzed olefin metathesis [7], in its various forms (ring-closing metathesis/RCM, ring-opening metathesis/ROM, and cross metathesis/CM), is one such general and synthetically critical transformation. Recent work in diversity-oriented synthesis has established catalytic metathesis as a method that readily and efficiently effects complex skeletal rearrangements under mild conditions [8]. Another unique feature of metathesis reactions is that either there are no byproducts formed or such side products are volatile and can be easily removed (e.g. ethylene). Key challenges associated with the immobilization of olefin metathesis catalysts include:

1. Preservation of the high activities and convenient reaction rates observed for homogeneous catalysts;
2. Development of practical procedures for catalyst recycling and the maintenance of efficient catalytic activity upon reuse;
3. Direct access to pure products that are free of toxic metal contaminants; and

4. Availability of efficient *chiral* catalysts that can be used for the asymmetric synthesis of compound libraries [9].

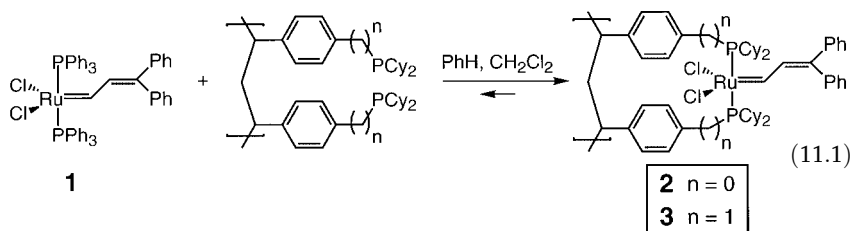
With the growing importance of modern combinatorial chemistry, additional benefits accrue for catalyst systems that readily adapt to 96 well or higher density synthesis formats.

This review offers a comprehensive summary of recent work toward the aforementioned goals. Various contributions will be discussed with the same chronology that appeared in the literature, thus allowing the reader to analyze how continuing work has addressed deficiencies uncovered in the earlier methods. Metathesis-active dendrimers are included in this survey since their large size and rigidity in principle allows for recycling by precipitation, microfiltration [10], or size-exclusion chromatographic techniques.

## 11.2

### The First Polymer-supported Ru Catalyst for Olefin Metathesis

In 1995, Grubbs and coworkers disclosed the results of their efforts to heterogenize a well-defined, single-component metal carbene [11]. Lightly cross-linked polystyrene (PS)–divinylbenzene (DVB) was employed as the support, and a convenient bisphosphine exchange reaction transferred the  $\text{Cl}_2\text{Ru}=\text{CH}-\text{CH}=\text{CPh}_2$  moiety of (**1**) [12] to dicyclohexylphosphine-functionalized resins to afford the supported vinylcarbene catalysts (**2**) and (**3**) (Eq. 11.1).  $^{31}\text{P}$  NMR spectroscopy was used to monitor the progress of this ligand substitution. As expected [13], the more electron-rich catalyst (**3**) exhibited higher activity; the metathesis of *cis*-2-pentene in  $\text{C}_6\text{D}_6$  proceeded with a turnover number (TON) of  $2\text{ h}^{-1}$ , about 7.5 times slower than that of its homogeneous counterpart (**1**). The decrease in reaction rate was attributed to three features of the system: (1) Incomplete phosphine substitution during the loading step might lead to mixed phosphine species on the resin; these complexes are known to be poor acyclic olefin metathesis catalysts [13]. (2) The heterogeneous reaction is limited by the diffusion of the reacting olefin into the cavities of the cross-linked PS-DVB support. (3) Since productive metathesis requires temporary loss of a phosphine ligand [13], rate-limiting *reassociation* of the dicyclohexylphosphine moiety during catalysis is entropically favored since it is tethered to the support.





As compensation for extended reaction times, catalyst (**3**) experienced an extended lifetime and was cycled through three complete metatheses of *cis*-2-pentene with only a minor loss in activity (20% after each cycle). Since Ru carbenes can decompose in a bimolecular coupling reaction in solution [14], these findings suggest that spacing metal complexes on a polystyrene support may enhance catalyst stability. Additionally, it was discovered that in ring-opening metathesis polymerization (ROMP) reactions the polydispersity index (PDI) of the products was much higher when supported catalysts (**2**) and (**3**) were utilized. This initial disclosure demonstrated proof-of-principle and set a standard against which later immobilization strategies could be measured.

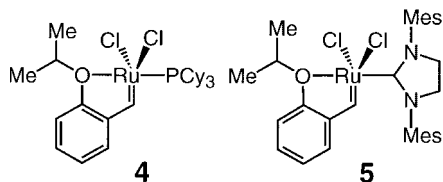
### 11.3

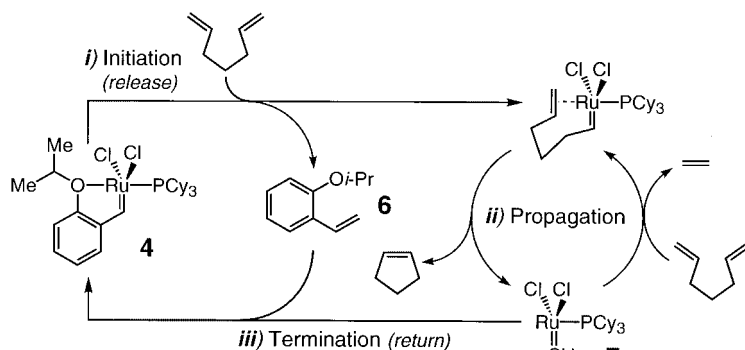
#### Homogeneous Catalysis through Heterogeneous Ru Carbenes

##### 11.3.1

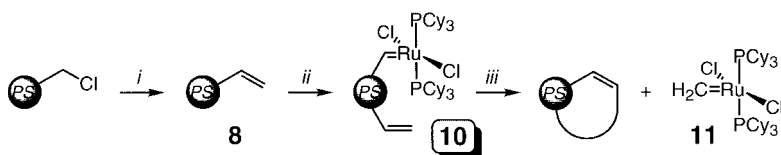
##### Recyclable Monomers Act through a 'Release/Return' Mechanism

Extensive research on monomeric Ru complexes has proven instrumental in guiding the development of improved catalyst systems. In 1999, we reported the synthesis and metathesis activity of Ru chelate complex (**4**) [15] and in 2000 the related chemistry of its more active variant (**5**) [16], bearing a 1,3-dimesityl-4,5-dihydroimidazol-2-ylidene ligand (4,5-dihydroIMes) [17]. These catalysts are exceptionally robust and recyclable: they are recovered in high (typically >90%) yield after a reaction by air-driven silica gel chromatography and can be reused in additional transformations. A plausible catalytic cycle has been put forward to account for the high activity and subsequent recovery of these complexes (shown for (**4**) in Scheme 11.1). Since catalyst initiation must involve both Ru-oxygen dissociation [13] and carbene exchange with a substrate alkene, the defining feature of this 'release/return' mechanism is the presence of liberated 2-isopropoxystyrene (**6**) during catalysis. The implication is clear: covalent attachment of a Ru catalyst to an insoluble polymer through the carbene substituent may circumvent rate limitations by rendering the propagating Ru carbenes homogeneous during catalysis. However, this strategy can only combine the benefits of homogeneous (high turnover) and heterogeneous (easy recovery) catalysis *if there is effective return of the solution-phase metal carbene (see 7, Scheme 11.1) to the polymer surface to allow for recycling*. That is, in the implementation of the above protocol, catalyst stability (vs reaction rate) becomes critical.





Scheme 11.1



Reagents: (i)  $\text{Me}_3\text{S}^+\text{I}^-$ ,  $n\text{-BuLi}$ , THF; (ii) 10 mol %  $(\text{PCy}_3)_2\text{Cl}_2\text{Ru}=\text{CHPh}$  (**9**),  $\text{CH}_2\text{Cl}_2$ , 1–2 h; (iii)  $\text{CH}_2\text{Cl}_2$ , 5 h.

Scheme 11.2

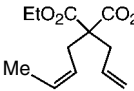
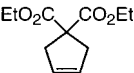
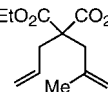
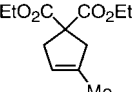
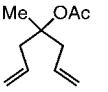
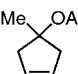
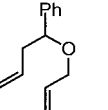
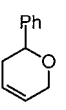
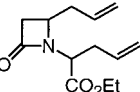
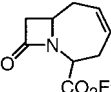
### 11.3.2

#### The First Carbene-tethered Polymeric Catalyst

Barrett and coworkers were the first to develop a polymer-bound Ru catalyst based on a release/return scenario [18]. Vinyl polystyrene [19] (**8**), prepared as shown, Scheme 11.2) was treated with Grubbs' benzylidene catalyst  $(\text{PCy}_3)_2\text{Cl}_2\text{Ru}=\text{CHPh}$  (**9**) [20] (10 mol% based on calculated vinyl resin sites,  $\text{CH}_2\text{Cl}_2$ , 1–2 h) to give orange-brown beads (**10**) and a nearly colorless filtrate solution. Phosphorous microanalysis confirmed that the loading of the available metal onto the support was quantitative. The preparation time for the catalyst resin proved important: reaction mixtures that were left longer than 2 h led to darker solutions and more highly colored washings. As shown in Scheme 11.2, this increased decomposition can result from RCM between the bound metal carbene and free vinyl groups on the resin surface ("biting back"), which releases the bisphosphine Ru methylene complex (**11**) [21] into solution [22]. Once dried, the beads (**10**) were found to be indefinitely stable to air and moisture without loss of activity.

When employed for the RCM of select diene substrates, the yields obtained with supported catalyst (**10**) matched those acquired with the homogeneous catalyst (**9**) in all but one case (entry 2, Tab. 11.1). This report places emphasis on the operational simplicity of these metathesis reactions. After suspension of the catalyst resin in a solution of substrate, the mixture was agitated for forty minutes

Tab. 11.1 Ring-closing metathesis of acyclic dienes by Ru complex (**10**).<sup>a)</sup>

Entry	Substrate	Product	Time	Conv (%) <sup>b)</sup>
1			40 min	95 (>98)
2			22 h	60 (90)
3			40 min	85 (90)
4			40 min	>98 (>98)
5			40 min	40 (45)

a) Conditions: 25 mg **10**/0.1 mmol substrate, 22 °C, CH<sub>2</sub>Cl<sub>2</sub>.

b) Determined by <sup>1</sup>H NMR analysis of the unpurified reaction mixture; figures in parantheses represent the % conversion with homogeneous catalyst **9**.

and filtered. Concentration of the filtrates and washes led to isolation of the desired products. Visual inspection of these unpurified compounds proved revealing. Whereas dark brown products were produced with (**9**), the supported system delivered materials that were essentially colorless. ICP/MS ruthenium residue analysis was used to validate these qualitative observations. As shown in Tab. 11.2 for the RCM of diethyl diallylmalonate, the use of homogeneous catalyst (**9**) gave neat cyclo-olefin contaminated at a level of 5100 ppm; Ru residues could be further reduced to 330 ppm after silica gel chromatography. In contrast, catalytic ring closure by the supported variant (**10**) resulted in just 500 ppm contamination – which was further reduced to 55 ppm by chromatography. These data compare favorably with a recent aqueous extraction procedure using the hydrophilic tris(hydroxymethyl)phosphine as a scavenger (Ru contaminant level of 200 ppm in the best case) [23].

Attempted recycling and reuse of the heterogeneous catalyst (**10**) led to dramatic losses of activity. Following quantitative RCM of diethyl diallylmalonate and simple filtration, the recovered resin was notably less active (<40% conversion) in a second run and the reaction mixture was dark in color. Such complications were attributed to the instability [14, 21] of Ru methylene (**11**) (Scheme 11.2) that propagates during the RCM of terminal diene substrates. In an effort to offset this solution-phase decomposition, the use of alkene additives was investigated. The

**Tab. 11.2** Ru contaminant level for the RCM of diethyl diallylmalonate with catalysts (**9**) and (**10**).<sup>a)</sup>

Entry	Catalyst (quantity)	Operation	Ru residue/ppm <sup>b)</sup>
1	<b>9</b> (3 mol%)	Evaporation	5100
2	<b>9</b> (3 mol%)	Evaporation and chromatography	330
3	<b>10</b> (50 mg)	Filtration and evaporation	500
4	<b>10</b> (50 mg)	Filtration, evaporation, and chromatography	55

a) Conditions: Indicated catalyst loading, 22 °C, CH<sub>2</sub>Cl<sub>2</sub>, 40 min.

b) Determined by ICP-MS.

volatile 1-hexene proved to be superior, allowing for quantitative conversion in the second round of RCM and modest activity (50% conversion) in the third. Nevertheless, this solution is not general. Ring-opening (ROM) and cross metathesis (CM) processes preclude the use of such additives since they can compete as donor olefins. The added cost and waste inherent to this approach is unattractive as well. Although the issue is not explicitly addressed, it is logical to assume that little, if any, of the released metal is recaptured by the polymer support before the onset of carbene decomposition. A more electronically or entropically suitable olefin metathesis with the support-bound alkene might be needed to restore the resting state of the catalyst.

In the context of the aforementioned shortcomings, the approach of Yao may have a distinct advantage [24]. Yao recognized that a *bidentate* carbene ligand could entropically assist the recapture of solution-phase carbenes by the solid support at the completion of a reaction. At that time, we had reported on the chemistry of monophosphine recyclable Ru complex (**4**); this system was selected by Yao to serve as a unimolecular model for his new immobilization strategy [15a]. Its bidentate styrene unit offered a convenient handle for covalent attachment to a solid support. Moreover, we had demonstrated in 1999 that the styrene ether Ru complex (**4**) catalyzes olefin metathesis with a greater propagation rate than (**9**) (due to the absence of unligated tricyclohexylphosphine in solution, see (**7**) in Scheme 11.1) [13]. In principle, the latter feature could further discourage loss of the homogeneous carbene to decomposition.

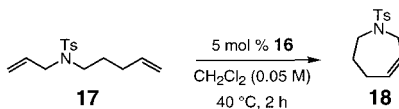
### 11.3.3

#### A Poly(ethylene glycol)-based Catalyst with Solvent-dependent Solubility

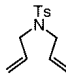
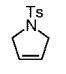
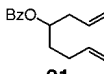
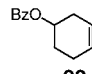
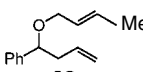
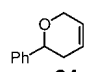
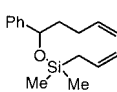
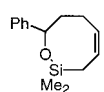
Starting from the commercially available aldehyde (**12**), styrene (**13**) was prepared by a straightforward synthetic sequence (Scheme 11.3). Subsequent esterification of the phenol with succinate-derivatized poly(ethylene glycol) monomethyl ether (MeO-PEG) appended the styrene unit to approximately 50% of the free acid groups in (**14**). The loading in (**15**) was estimated by 500 MHz <sup>1</sup>H NMR spectroscopy to be about 0.1 mmol g<sup>-1</sup>. In a final step, the polymer-bound catalyst was ob-



Tab. 11.3 Recycling of Ru complex (**16**) in the ring-closing metathesis of diene (**17**).

								
Cycle	1	2	3	4	5	6	7	8
Conv (%) <sup>a)</sup>	98	97.5	96.5	95	95	93	93	92

a) Determined by 500 MHz <sup>1</sup>H NMR analysis of the unpurified reaction mixture.Tab. 11.4 Ring-closing metathesis of acyclic dienes by Ru complex (**16**).

Cycle	Substrate (conc)	Product	Conditions	Conv (%) <sup>a)</sup>
				
1	(0.05 M)		5 mol% <b>16</b> , 40 °C, 2 h	96
2	(0.05 M)		5 mol% <b>16</b> , 40 °C, 2 h	94
3	(0.05 M)		5 mol% <b>16</b> , 40 °C, 2 h	92
4	(0.1 M)		2.5 mol% <b>16</b> , 40 °C, 3.5 h	97
5	(0.1 M)		2.5 mol% <b>16</b> , 22 °C, 12 h	>98
				
6	(0.1 M)		2.5 mol% <b>16</b> , 40 °C, 2 h	90
				
1	(0.1 M)		2.5 mol% <b>16</b> , 40 °C, 2 h	96
				
2	(0.1 M)		2.5 mol% <b>16</b> , 40 °C, 3 h	>98

a) Determined by 500 MHz <sup>1</sup>H NMR analysis of the unpurified mixture.

The results in Tab. 11.3 and 11.4 demonstrate that the PEG-bound Ru complex (**16**) maintains its efficacy through iterative cycles of RCM. Nonetheless, a steady, detectable loss of activity is evident. Slow but competing decomposition of the active species, in this case a *monophosphine carbene* ((**7**), Scheme 11.1), is likely responsible for this trend. Since decomposition of propagating carbene intermedi-

ates can occur even when a homogeneous catalyst (such as (5) or (9)) is used, gradual degradation of catalyst activity may complicate any immobilization strategy. However, it is possible that Yao's PEG-based system releases small but competent amounts of a highly active monophosphine carbene into solution that never returns to the support. It would be helpful to quantitate the amount of Ru loss in a given round of metathesis and to confirm that polymer-bound catalysts based on the release/return mechanism (Scheme 11.1) are truly recyclable, retrieving electron-deficient metal carbenes from solution.

## 11.4

### Dendrimers as Recyclable Metathesis Catalysts

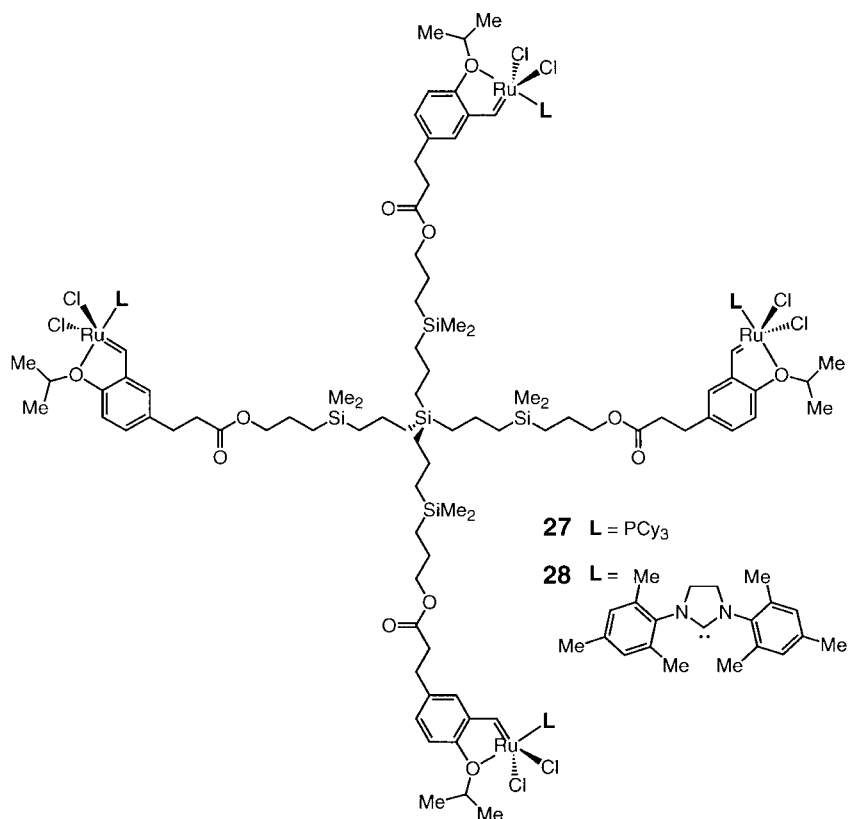
It was with these subtle issues in mind that in 1999 we began our studies in this area. Following the development of (4) and (5) as stable and recyclable metathesis catalysts, we turned our attention to the preparation of more easily recoverable complexes. Ru-based dendrimers were targeted initially because of their ease of characterization and the high level of certainty with which metal-containing sites can be introduced at their periphery. With a catalyst based on these small branching polymers, it would be possible to gauge rigorously the efficiency with which the active metal carbene leaves the ligation site and returns to the macromolecule.

#### 11.4.1

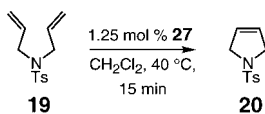
##### Synthesis and Metathesis Activity of Ru-based Carbosilane Dendrimers

Convergent syntheses (11 steps, 5 steps for longest linear sequence) of compounds (27) and (28) were optimized. Key features of the route include a Pd-catalyzed Stille coupling for installation of the requisite vinyl group and synthesis of the dendrimer core by a Pt-catalyzed hydrosilation/alkylation [25] /hydroboration [26] sequence. The final step in the synthesis of (27) involved metallation of the precursor tetraolefin by treatment with Grubbs' catalyst (9) in the presence of CuCl. The more active Ru dendrimer (28) was also obtained by ligand exchange with the vacant dendritic structure, this time with (4,5-dihydroIMes)PCy<sub>3</sub>Cl<sub>2</sub>Ru=CHPh (29) [17] as the stoichiometric metal source. The catalysts were purified to air-stable dark brown and green solids (respectively) by silica gel chromatography. The high solubility of these synthetic dendrimers in common organic solvents permitted full analysis by NMR spectroscopy and high-resolution mass spectrometry. As anticipated, this ease of characterization was only a prelude to our studies of the mechanism for the corresponding metathesis reaction.

As shown in Tab. 11.5, multi-component catalyst (27) matches the activity of its corresponding monomer (4), promoting efficient RCM of (19) in just 15 minutes at 40 °C. The reaction mixture was passed through a short column in methylene chloride to isolate the desired product. Subsequent washing of the silica with diethyl ether led to quantitative recovery of the dendritic catalyst. 400 MHz <sup>1</sup>H NMR analysis revealed that 13% of the styrene ligands on the dendrimer were va-



Tab. 11.5 Utility of dendritic (**27**) in catalyzing multiple rounds of ring-closing metathesis.



Cycle	Product yield <sup>a)</sup> (%)	Ru content <sup>b)</sup> (%)
1	99	87
2	91	76
3	96	72
4	89	64
5	92	48
6	87	41

a) Isolated yields after silica gel chromatography.

b) Determined by 400 MHz <sup>1</sup>H NMR analysis of the purified dendrimer.

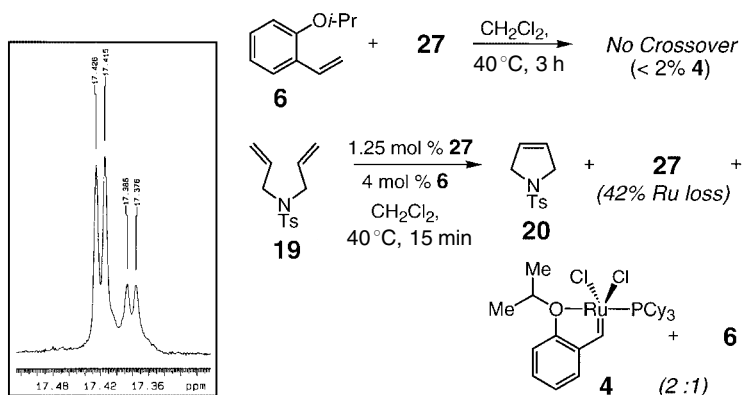


cant, presumably because of decomposition during the reaction. However, repeated use of recycled (**27**), in spite of this steady Ru loss per reaction, resulted in facile ring closure to (**20**) and isolation of the desired product in >86% yield (Tab. 11.5). It is noteworthy that the dendritic complex remains active even after 50% of its sites have been depleted of Ru (see cycle 6). As in the Yao work [24], this high level of reactivity invokes the intermediacy of a coordinatively unsaturated, monophosphine carbene ((**7**), Scheme 11.1) during catalysis. It further hints that isopropyl styrene ethers do not kinetically reassociate to the metal center as well as tricyclohexylphosphine during propagation. Since substantial turnover can accompany even minor amounts of Ru release, a recurring question again arises: How can one confirm that there is effective return of the propagating carbene to the polymer support, and that catalysts based on the bidentate styrene ether are truly recyclable?

#### 11.4.2

##### Evidence for Ru Release and Return During Olefin Metathesis

Our efforts to confront this issue were facilitated by a minor chemical shift difference for the carbene proton signals of (**4**) and (**27**) (see box, Scheme 11.4), allowing us to determine the amount of Ru bound to dendritic versus monomeric styrene ligands by integration of the appropriate downfield signals in the  $^1\text{H}$  NMR spectrum of a mixture. In a control reaction, we established that prolonged treatment of (**27**) with 2-isopropoxystyrene (**6**) results in no metal crossover (Scheme 11.4) [27]. However, repetition of the experiment *in the presence of a metathesis substrate* (**19**) gave rise to rapid RCM ( $\rightarrow$  **20**) and statistically-driven scrambling of the transition metal between monomeric and dendritic ligation sites in fifteen minutes (Scheme 11.4). These results imply that the Ru center, after reacting with a substrate alkene and leaving the dendrimer, can be trapped again by a styrene ether. These findings further suggest that a significant portion of the available metal initiates the moment a metathesis reaction begins, providing direct evi-

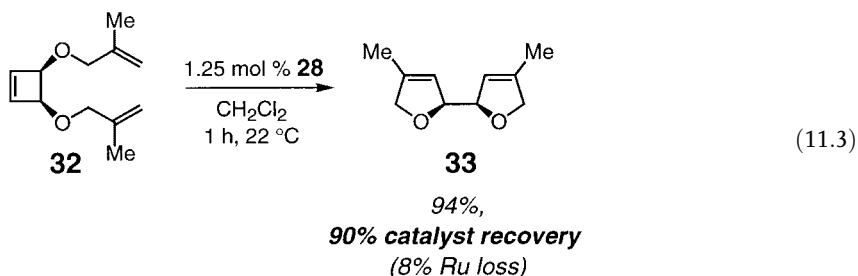
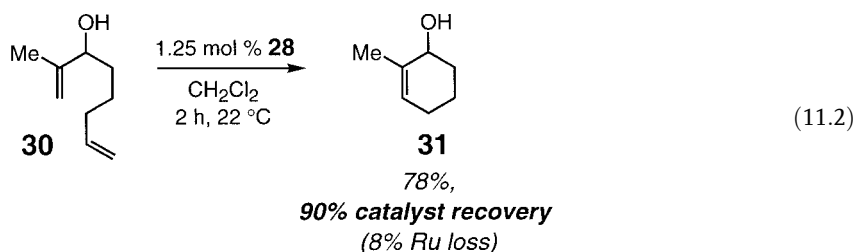


Scheme 11.4

dence for the 'release/return' mode of action defined by the structures of catalysts (4), (5), (16), (27) and (28).

Aside from their utility as mechanistic probes, dendrimers (27) and (28) are efficient metathesis catalysts that offer practical advantages over the corresponding monomers. Owing to their increased polarity, simple filtration of reaction mixtures through a short pad of silica gel is sufficient for separation of these dendrimers from reaction products. The examples shown in equations 11.2 and 11.3 are representative. Catalytic RCM of (30) in the presence of 1.25 mol% (28) (5 mol% Ru) was complete in 2 h at ambient temperature (Eq. 11.2). The desired carbocycle (31) was obtained in 78% yield after the reaction mixture was passed through silica gel in methylene chloride. A subsequent wash of the column with diethyl ether as eluant retrieved the dendrimer in pure form (90% yield, 8% Ru loss). A ring-opening/ring-closing transformation was efficient as well (Eq. 11.3). An analogous isolation procedure afforded the desired bicycle (33) and the recovered catalyst in 94% and 90% (8% Ru loss) isolated yields, respectively. These reactions underscore the importance of the more electron-releasing N-heterocyclic carbene ligand in catalyst (28), since little or no conversion was obtained when the less active phosphine-based systems such as (4) or (27) were used.

Attempts to avoid chromatography and recycle the dendrimers by precipitation

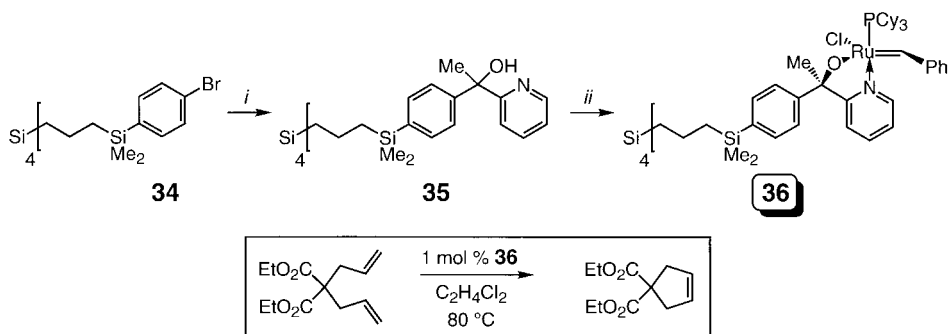


in the presence of a variety of solvents proved largely unsuccessful. Crystalline solids could be obtained in pure form, but yields were low. An alternative size-exclusion recovery strategy with microporous membranes as filters was not explored [10]. These developments motivated the experiments described below which involved the use of an alternative heterogeneous support for Ru-based complexes that preserve the bidentate styrene ether ligation.

## 11.4.3

**Dendrimer Microfiltration: A New but Underdeveloped Strategy for Catalyst Recovery**

Notwithstanding substantial current interest in small branching polymers that contain transition metal binding sites at their termini, we are aware of only one other report involving a metathesis-active dendrimer [28]. van Koten and co-workers have used poly(bromoarenes) (such as **(34)**, Scheme 11.5) as versatile starting materials for the synthesis of a variety of functionalized dendrimers in the presence of suitable electrophiles. As an example, 2-pyridylcarbinol-containing Ru carbene (**(36)**) was prepared and studied under homogeneous conditions in the RCM of diethyl diallylmalonate (see box, Scheme 11.5). Installation of the catalytic active sites proved straightforward and efficient. Lithiation of **(34)** followed by reaction with 2-acetylpyridine generated the 2-hydroxyalkylpyridyl-functionalized precursor (**(35)**). Deprotonation of **(35)** with four equivalents of *n*-BuLi and subsequent transmetalation with  $(\text{PCy}_3)_2\text{Cl}_2\text{Ru}=\text{CHPh}$  (**(9)**) afforded **(36)** as a dark green solid. When a dichloroethane solution of diethyl diallylmalonate was treated with 1 mol% (based on Ru) of catalyst **(36)** and heated to 80 °C, quantitative ring closure to diethyl-3-cyclopentene dicarboxylate was achieved (as monitored by GC), a result that compares well to that of the unimolecular catalyst. In a preliminary recycling attempt, catalyst and substrate solutions were separated by a membrane (SelRO-nanofiltration membrane MPS-60; stated molecular weight cutoff, 400). In this case, however, the reaction stopped at 20% conversion. Black precipitation in the compartment containing the dendrimer was taken as a sign of extensive catalyst decomposition. van Koten and coworkers suspect deactivation of the metathesis catalyst by the membrane surface. It should be noted that leaching of the metal through the membrane did not occur since the substrate/product solution remained clear and colorless. Such findings may prove advantageous to future developments if new filtration membranes can be developed that are compatible with the applied reaction conditions.



Reagents: (i) *n*-BuLi, THF; then 2-acetylpyridine; (ii) *n*-BuLi; then  $(\text{PCy}_3)_2\text{Cl}_2\text{Ru}=\text{CHPh}$  (**(9)**).

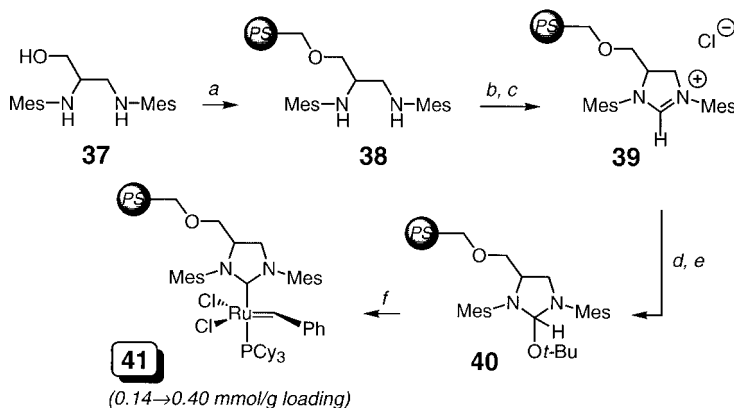
Scheme 11.5

## 11.5

## A Recent Approach to Permanent Immobilization of a Ru-based Catalyst

By virtue of their precise structure and high solubility, dendritic Ru carbenes (**27**), (**28**), and (**36**) are readily characterized molecules that preserve the high activity characteristic of their corresponding monomers. This homogeneity, however, presents challenges to practical catalyst recovery. Perhaps the ideal polymeric metathesis catalyst is one that is heterogeneous, and by judicious choice of both linker and support the inherent rate limitations can be overcome. In a recent contribution, Blechert and coworkers recognized the importance of a *single* covalent link to a ligand that *would not dissociate* during olefin metathesis [29]. Their work describes the attachment of Grubbs' catalyst (4,5-dihydroIMes)PCy<sub>3</sub>Cl<sub>2</sub>Ru=CHPh (**29**) to a solid support by its *N*-heterocyclic carbene ligand [30, 31].

The synthesis of a suitably immobilized ligand precursor was carried out as shown in Scheme 11.6. Compound (**37**) was prepared from 2,3-dibromo-1-propanol and 2,4,6-trimethylaniline following a literature procedure. A base-mediated etherification reaction with Merrifield polystyrene (1% divinyl benzene (DVB)) afforded the diamine (**38**) in quantitative yield. This material was then cyclized under acidic conditions, and anion exchange yielded the support-bound 3,4-dimethyl-4,5-dihydroimidazolium chloride (**39**). Presumably, subsequent treatment with TMSOTf was responsible for capping free amine groups on the resin that had failed to undergo cyclization. Supported chloride salt (**39**) was then converted into the 2-*tert*-butoxy-4,5-dihydroimidazoline (**40**) upon exposure to KO<sup>t</sup>-Bu in THF. In analogy to the synthesis of the soluble complex (**29**) [17], deprotection of the carbene at elevated temperature by  $\alpha$ -elimination in the presence of (PCy<sub>3</sub>)<sub>2</sub>Cl<sub>2</sub>Ru=CHPh (**9**) gave the desired support-bound complex (**41**) as a pink



Reagents: (a) 1.0 equiv KO<sup>t</sup>-Bu, DMF, 22 °C, 20 min; then 0.5 equiv Merrifield-PS (1% DVB), TBAI, DMF, 60 °C, 12 h; (b) HC(OMe)<sub>3</sub>, HCO<sub>2</sub>H, toluene, 100 °C, 100 mbar, 15 h; (c) 0.1 M HCl in THF, 22 °C, 5 min; (d) TMSOTf, 2,6-lutidine, CH<sub>2</sub>Cl<sub>2</sub>, 22 °C, 30 min; (e) KO<sup>t</sup>-Bu, THF, 22 °C, 1 h; (f) 1.5 equiv (PCy<sub>3</sub>)<sub>2</sub>Cl<sub>2</sub>Ru=CHPh (**9**), toluene, 80 °C.

Scheme 11.6

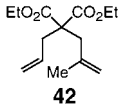
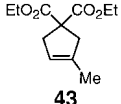
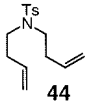
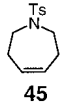
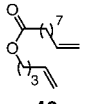
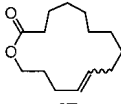
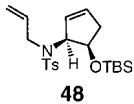
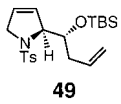
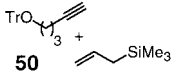
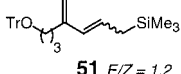
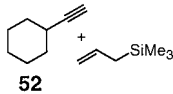
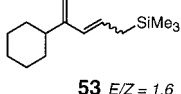
resin. The Ru loading (0.14 to 0.40 mmol g<sup>-1</sup>, determined by elemental analysis and mass increase) showed a linear dependence on the loading level of the starting Merrifield resin (0.50 to 0.90 mmol g<sup>-1</sup>). It is worthy of note that the four-step synthesis from (37) is performed entirely on the solid support.

As a model metathesis reaction, diethyl diallylmalonate was cyclized in the presence of 5 mol% (41) within forty minutes in methylene chloride at 40 °C; the product was isolated as a colorless oil after filtration and removal of volatiles. An analogous reaction with the soluble catalyst (29) was complete in less than five minutes, suggesting that metathesis reactions catalyzed by (41) are diffusion-controlled. Nonetheless, a reaction time of forty minutes is reasonable, and the validation for this chemistry lies in the simplified purification procedure and minimization of waste streams.

Notably, additional experiments involving more challenging metatheses established that the expected products were routinely obtained free of contaminants. These results have been summarized in Tab. 11.6. The more hindered diene (42) cyclized cleanly to give (43) as a colorless oil, and macrolactone (47) was obtained in 80% yield from acyclic ester (46) (entries 1 and 3). Following rearrangement of the enantiomerically pure diene (48) in the presence of ethylene, concentration of the unpurified filtrate led to spontaneous crystallization of (49) as a colorless solid (entry 4). Catalyst (41) was competent in promoting other types of metathesis processes. Yne-ene cross metathesis of acetylene (50) with allyltrimethylsilane gave 1,3-disubstituted butadiene (51) (entry 5). This material was isolated as a mixture of olefin isomers by filtration and removal of the excess volatile allylsilane under vacuum. A similar transformation involving the sterically hindered cyclohexylacetylene ((52), entry 6) was selected to highlight the enhanced activity imparted by the resin-bound *N*-heterocyclic carbene. Whereas no reaction occurs in the presence of catalyst (9), exposure of the reactants to 5 mol% (41) affords diene (53) in high yield as a colorless oil after removal of excess starting material under vacuum. It deserves mention that the qualitative assessments of product purity have been substantiated further by NMR spectroscopy.

In a final measure of catalyst utility, iterative use of (41) for the RCM of (44) was explored (entry 2, Tab. 11.6). In the best case, complex (41), with a loading of 0.14 mmol g<sup>-1</sup>, gave complete cyclization of (44) in four runs. The reaction times for complete cyclization increased from 1.5 h in the first run, to 4 h in the second, 12 h in the third, and 2 days in the fourth run. These numbers point to a gradual decline in catalyst integrity at the polymer surface. Clearly, the use of *N*-heterocyclic carbene ligation in supported Ru-based catalysts permits olefin metatheses that are impossible with catalyst systems based on tricyclohexylphosphine (see entry 6, Tab. 11.6). However, this switch to a more basic neutral ligand donor is not a general solution to extending catalyst lifetime. A follow-up study by Barrett and coworkers lends further support to this assertion (see below).

Tab. 11.6 Catalytic olefin metathesis with Ru complex (41).<sup>a)</sup>

Entry	Substrate	Product	Yield (%)
1	 42	 43	> 98
2	 44	 45	90
3	 46	 47 E/Z = 1.4	80
4 <sup>b)</sup>	 48	 49	> 98
5	 50	 51 E/Z = 1.2	> 98
6	 52	 53 E/Z = 1.6	80

a) Conditions: 5 mol% 41, 40 °C, CH<sub>2</sub>Cl<sub>2</sub>, 12–18 h.

b) Reaction performed under ethylene atmosphere.

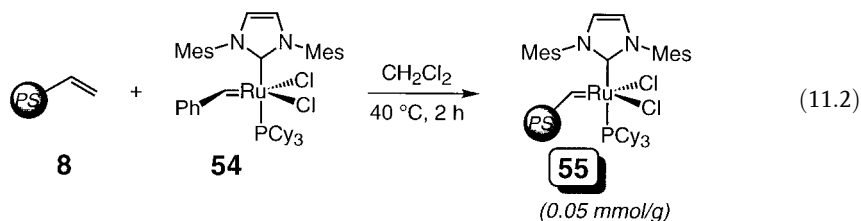
## 11.6

A PS-supported Ru Catalyst with Unsaturated *N*-Heterocyclic Carbene Ligation

Unlike the aforementioned use of the *saturated* *N*-heterocyclic carbene 4,5-dihydroIMes (see (28) and (41)), Barrett and colleagues based their second generation polystyrene-supported catalyst [32] on the corresponding *unsaturated* carbene 1,3-bis(2,4,6-trimethylphenyl)imidazol-2-ylidene (IMes) [33]. This selection was based on the reported stability of the unimolecular complex (IMes)PCy<sub>3</sub>Cl<sub>2</sub>Ru=CHPh ((54), Eq. 11.2) relative to the parent carbene (9). With (54), no decomposition was detected by NMR spectroscopy after 14 days in toluene at 60 °C. In contrast, Grubbs' complex (9) showed significant decomposition after standing for one hour in methylene chloride at 22 °C. Conclusions based on these simple experiments must be tempered, however, since propagating, electron-deficient inter-

mediates are not produced in the absence of an alkene. The above results might simply indicate the relative facility with which initiation (dissociative loss of the labile tricyclohexylphosphine) occurs in the two systems. The most appropriate measure of catalyst stability ultimately involves olefin metathesis and catalyst reuse.

In analogy to the synthesis of (**10**) (Scheme 11.2), the new boomerang catalyst was prepared by carbene exchange in (**54**) with vinylated polystyrene resin (**8**) ( $\rightarrow$  (**55**), Eq. 11.4). The catalyst loading on the polymer was established on the basis of phosphorous and nitrogen microanalyses and Ru ICP data ( $0.05 \text{ mmol g}^{-1}$ ). Direct comparison of the new supported catalyst (**55**) to the original (**10**) was carried out under optimized conditions. Reactions were performed in a Schlenk flask with rigorous exclusion of air and moisture. Between consecutive runs, the reaction mixture was removed from the resin by vacuum filtration, leaving the catalyst beads behind on the glass frit.



As shown in Tab. 11.7 for the RCM of diethyl diallylmalonate, the original catalyst (**10**) suffered complete loss of metathesis activity after only two runs (entry 1). On the other hand, the second generation catalyst (**55**) retained modest activity in the third consecutive run (entry 2). As in the prior study [18], the addition of a terminal olefin additive was required to extend the catalyst lifetime past four runs (entry 3). Use of triphenylphosphine as a second additive just ten minutes before filtration led to further improvements in activity during catalyst reuse. However, as mentioned previously, the use of additives is somewhat wasteful and exclusive, since

Tab. 11.7 RCM of diethyl diallylmalonate with catalysts (**10**) and (**55**).<sup>a)</sup>

Entry	Catalyst	Additive	Conversion (%) <sup>b)</sup>				
			1	2	3	4	5
1 <sup>c)</sup>	<b>10</b>	None	100	40	0	–	–
2	<b>55</b>	None	91	61	40	13	1
3	<b>55</b>	1-octene	100	100	96	86	60
4	<b>55</b>	1-octene and PPh <sub>3</sub>	100	100	100	88	43

a) Conditions: 2.5 mol% catalyst, 50 °C, Toluene, 2 h.

b) Determined by <sup>1</sup>H NMR analysis.

c) Performed with 5 mol% catalyst, 40 °C, CH<sub>2</sub>Cl<sub>2</sub>, 40 min.

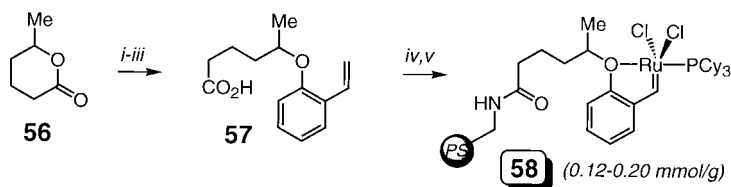
they cannot be applied to other types of metathesis (ROM and CM). Furthermore, resorting to the nonvolatile triphenylphosphine is counterproductive, requiring purification of reaction products. As for (10), these researchers suspect solution-phase decomposition of the Ru methylene species accounts for the early deactivation observed for (55) [21]. Although recovery of this system is trivial, improvements in catalyst longevity are a prerequisite to its repetitive use in combinatorial applications.

## 11.7

### A New Recyclable Catalyst Based on the Bidentate Styrene Ether

Special attributes of Yao's PEG-supported complex (16) [24] include its reliance on a soluble yet readily recoverable polymer support and its tolerance of air and reagent-grade solvents. Shortly after this study, Dowden and Savovic [34] disclosed a complementary strategy based on a subtle change in the site of polymer attachment. With our monomeric complex (4) again serving as a model [15a], these workers chose to manipulate the isopropyl portion of the styrene ether as a covalent linker unit. Thus, basic hydrolysis of racemic  $\delta$ -hexanolactone (56) with sodium methoxide, subsequent Mitsunobu reaction with 2-vinylphenol, and saponification provided (57) (Scheme 11.7). Treatment of the pendant acid group in (57) with aminomethyl polystyrene under standard conditions provided the supported bidentate ligand. Stoichiometric metallation of the resin with Grubbs' complex (9) afforded (58) with a loading of  $0.12 \text{ mmol g}^{-1}$  (as determined by phosphorous analysis). It was discovered that treatment of the free resin with five successive portions of 10 mol% (9) increased the loading to  $0.20 \text{ mmol g}^{-1}$ . Simple filtration delivered (58) as dark brown beads that were dried and stored in air indefinitely with no loss of activity.

Recycling of (58) was studied by exposure of the same batch of resin to equal, successive portions of benzyl *N,N*-diallylcarbamate (59) in the absence of a stabilizing alkene. Importantly, general laboratory-grade methylene chloride was used without degassing in an air atmosphere. Substrate solutions were added to the resin in a plastic solid phase organic synthesis tube fitted with a glass frit. The tube was then sealed and subjected to  $360^\circ$  rotation at  $22^\circ\text{C}$ . Filtration and washing

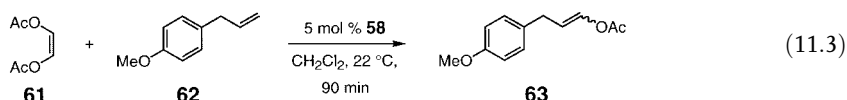


Reagents: (i) NaOMe, MeOH,  $0 \rightarrow 22^\circ\text{C}$ , 6 h, 95%; (ii) 2-vinylphenol, DIAD, PPh<sub>3</sub>, THF,  $0 \rightarrow 22^\circ\text{C}$ , 14 h, 64%; (iii) 1 M NaOH, dioxane,  $22^\circ\text{C}$ , 12 h, 88%; (iv) polystyrene-NH<sub>2</sub>, DIC, HOBT, CH<sub>2</sub>Cl<sub>2</sub>/DMF,  $22^\circ\text{C}$ , 12 h; (v) (PCy<sub>3</sub>)<sub>2</sub>Cl<sub>2</sub>Ru=CHPh (9), DCE,  $22^\circ\text{C}$ , 12 h.

Scheme 11.7



with methylene chloride directly afforded the product and recovered catalyst. As shown in Tab. 11.8, (**58**) (5 mol%) provided good yields over five runs (entry 1). A decreased catalyst loading of 1.5 mol% was sufficient for catalysis, but recycling was less efficient (entry 2). Although reaction rates were slower than those reported with homogeneous catalyst (**9**) [35], the easy manipulation of (**58**) and its tolerance of air and moisture are noteworthy. Supported catalyst (**58**) promotes cross metathesis reactions as well. As shown in Eq. 11.3, treatment of a methylene chloride solution of (*Z*)-1,4-diacetoxybut-2-ene (**61**) and 4-allylanisole (**62**) with (**58**) at 40 °C for 9 h gave the cross-coupled product (**63**) (33%) along with the anisole homodimer (18%). A subsequent RCM of (**59**) (Tab. 11.8) with the recycled resin furnished the cyclized product (85%) in 90 min, confirming the retention of catalytic activity.



Catalysis of olefin metathesis in polar, protic media is an important goal that to date has been addressed by the employment of water soluble phosphine ligands [36]. In a final demonstration of the versatility of their synthesis, Dowden and Savovic studied the effect of an alternative solid support on the solubility and activity of complex (**58**). Amine-functionalized Tentagel (0.3 mmol g<sup>-1</sup>) was employed to prepare Tentagel-(**58**); the supported catalyst showed modest RCM activity (**59** → **60**) in nondegassed methanol (31% conversion after 6 h). Although different batches of resin provided variable results, this preliminary finding does suggest that the supporting polymer can be modified depending on the desired application.

Tab. 11.8 RCM of benzyl *N,N*-diallylcarbamate with catalyst (**58**).

Entry	Conversion (%) <sup>a)</sup>						
	1	2	3	4	5	6	7
1 <sup>b)</sup>	91	81	68	67	63	46	40
2 <sup>c)</sup>	81	69	68	33	21	11	0

a) Determined by <sup>1</sup>H NMR analysis.

b) 5 mol% **58**.

c) 1.5 mol% **58**.

## 11.8

## Alternative Solid Supports Expand the Scope of Existing Catalyst Systems

## 11.8.1

## A Comparative Study of Three Poly-DVB-supported Ru Carbenes

Since different organic polymers possess unique swelling properties in a variety of solvents, perhaps known catalyst immobilization strategies could be rendered more synthetically useful simply by changing the identity of the solid support. A recent contribution by Nolan and Jafarpour describes improvements to the Barrett polystyrene-based catalysts (**10**) and (**55**) through the use of the macroporous polymer poly-divinylbenzene (poly-DVB) [37]. Homogeneous catalysts ( $(\text{PCy}_3)_2\text{Cl}_2\text{Ru}=\text{CHPh}$  (**9**), (4,5-dihydroIMes) $\text{PCy}_3\text{Cl}_2\text{Ru}=\text{CHPh}$  (**29**), and (IMes) $\text{PCy}_3\text{Cl}_2\text{Ru}=\text{CHPh}$  (**54**) were all anchored to the support, allowing for comparative analysis of the resulting polymeric Ru complexes.

The poly-DVB used in this study was synthesized from commercially available divinylbenzene by AIBN-mediated radical polymerization with toluene as a porogen (v:v 1:1). The bulk polymer was dried in vacuo and ground into a fine powder. After suspension of the polymer in toluene solutions of each of the catalyst precursors (**9**), (**29**), and (**54**), reaction mixtures were heated to 50 °C for one hour. The resulting slurries were filtered and washed with toluene to afford the corresponding poly-DVB-supported carbenes as light pink solids (**9** → **64**, **29** → **65**, and **54** → **66**). Metal loading was determined through elemental analysis to be 4 wt% for (**64**), 10 wt% for (**65**), and 3 wt% for (**66**). The authors attribute the more efficient carbene exchange (higher loading) observed for (**65**) to the increased CM activity which is typical of homogeneous catalysts bearing the saturated 4,5-dihydroIMes ligand [38].

As shown in Tab. 11.9, all three heterogeneous catalysts showed RCM activity comparable to their monomeric counterpart for the benchmark substrate diethyl diallylmalonate. Each catalyst could be recycled up to four times without significant loss of activity. Atomic absorption spectroscopy confirmed that there was little leaching of the metal into product streams. Results of these analyses showed that for catalyst (**64**), approximately 5% (of the initial 4 wt % loading) of active Ru was lost to decomposition in the solution phase after four cycles. For the more active systems (**65**) and (**66**), only 2% of the total Ru content was detectable in the cyclized product after four rounds. To further test the performance of these catalysts, the tetrasubstituted substrate diethyl bis(2-methylallyl)malonate was investigated as a RCM substrate. As anticipated, the phosphine-based precursor (**9**) and its supported variant (**64**) showed no activity in this reaction (Tab. 11.10, entries 1 and 2). However, (**66**) showed modest activity for this challenging metathesis and could be recycled four times. Although the sustained activity of (**66**) is disappointing relative to its parent (**54**), these results constitute the first example of tetrasubstituted olefin synthesis by a polymeric Ru-based catalyst, and the superiority of (**66**) over (**65**) is intriguing. The advantages of the poly-DVB complexes over the aforementioned polystyrene-supported catalysts (**10**) and (**55**) include the ease of

**Tab. 11.9** RCM of diethyl diallylmalonate with poly-DVB-supported Ru catalysts (**64**), (**65**) and (**66**).<sup>a)</sup>

Entry	Catalyst	Cycle	Yield (%) <sup>b)</sup>
1	<b>9</b>	–	85
2	<b>64</b>	1	97
3	<b>64</b>	4	81
4	<b>29</b>	–	>98
5	<b>65</b>	1	>98
6	<b>65</b>	4	>98
7	<b>54</b>	–	92
8	<b>66</b>	1	97
9	<b>66</b>	4	81

a) Conditions: 5 mol% catalyst, 22 °C, CH<sub>2</sub>Cl<sub>2</sub>, 30 min.

b) Determined by NMR or GC analysis, average of two runs.

**Tab. 11.10** RCM of diethyl bis(2-methylallyl)malonate with poly-DVB-supported Ru catalysts (**64**), (**65**) and (**66**).<sup>a)</sup>

Entry	Catalyst	Cycle	Yield (%) <sup>b)</sup>
1	<b>9</b>	–	0
2	<b>64</b>	1	2
3	<b>65</b>	1	17
4	<b>54</b>	–	75
5	<b>66</b>	1	33
6	<b>66</b>	4	22

a) Conditions: 5 mol% catalyst, 80 °C, toluene, 3 h except for entry 4 (1 h).

b) Determined by NMR or GC analysis, average of two runs.

polymer synthesis and the increased number of resin vinyl groups exposed for metal retrieval – which might in part account for the increased recycling efficiency of these systems in the absence of additives.

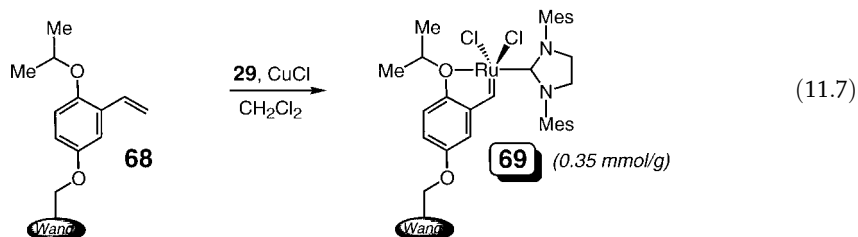
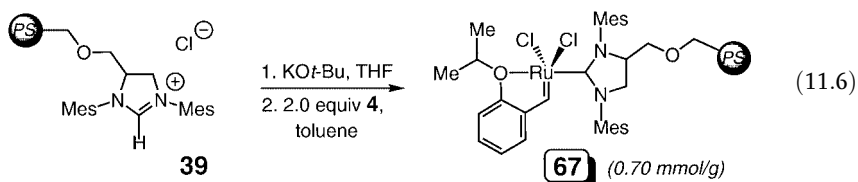
### 11.8.2

#### A Wang-supported Styrene Ether Catalyst for Stereoselective Cross Metathesis

Blechert *et al.* have also sought to expand upon prior work through simple changes to existing catalyst systems. After noticing that catalyst (**5**) is an efficient and recyclable catalyst for stereoselective CM in which one of the reaction partners is an electron-poor alkene (such as methyl vinyl ketone, methyl acrylate, and even acrylonitrile) [39], the immobilization of (**5**) through the 4,5-dihydroIMes and chelating styrene ligands was reported [40].

Following conversion of imidazolinium chloride (**39**) to the corresponding *tert*-butoxy addition product (**40**) (as for Scheme 11.6), ligand exchange at elevated

temperature in the presence of two equivalents of (4) afforded (67) as a green resin (Eq. 11.6). In addition, 2-isopropoxy-5-hydroxystyrene (prepared as shown in Scheme 11.3) was coupled to Wang resin (loading 0.72 mmol g<sup>-1</sup>) under Mitsunobu etherification conditions to provide ligand (68) in quantitative yield according to mass balance. The requisite ligand exchange with (29) was aided by the phosphine scavenger CuCl to furnish (69) as a deep green resin (Eq. 11.7). The Ru loading for each of these new catalysts (0.70 mmol g<sup>-1</sup> and 0.35 mmol g<sup>-1</sup>, respectively) was determined by Ru elemental analysis and mass balance.



Even though the RCM of diallyltosylamine ((19), see Tab. 11.4) with both catalysts was quantitative after four successive rounds under standard conditions (0.1 M methylene chloride, 40 °C, reaction times not given), studies in CM revealed remarkable differences in catalyst efficiencies. As shown in Tab. 11.11, (69) displayed enhanced activity in the reaction of terminal olefin (70) with a variety of electron-deficient partners. These cross couplings were stereoselective (>20:1) for the *trans* isomer of the product with the exception of acrylonitrile and acrolein, which gave *E/Z* ratios of 1:3 and 1:1, respectively. For the reaction with methyl vinyl ketone (entry 2), catalyst recycling was carried out. Although longer reaction times were unavoidable upon its reuse (4 h, 4 h, 12 h, 20 h, and 43 h), catalyst (69) gave quantitative conversion after each of five consecutive runs. This is a noteworthy result given that CM, being an intermolecular process, places extra demands on the longevity, efficiency, and steric tolerance of a given catalyst. Although (67) and (69) are bound to distinct polymer supports, making a direct comparison difficult, the superior activity of (69) is likely a function of its ability to release the active species into solution. Since the propagating carbene from (67) remains heterogeneous, diffusion of reacting alkenes into the cavities of the support is rate-limiting, especially in the more challenging case of CM.

In the context of Blechert's study, it is interesting that only in the CM (vs RCM) work was the deficiency associated with catalyst (67) pronounced. Aside from the

**Tab. 11.11** Cross metathesis with electron-deficient olefins catalyzed by (67) and (69).

$\text{EWG}-\text{CH}=\text{CH}_2 + \text{CH}_2=\text{CH}-\text{CO}_2\text{Ph} \xrightarrow[\text{12 h}]{\text{5 mol \% 67 or 69, CH}_2\text{Cl}_2, 40^\circ\text{C}} \text{EWG}-\text{CH}=\text{CH}-\text{CH}_2-\text{CH}_2-\text{CO}_2\text{Ph}$ <p style="text-align: center; margin-left: 150px;"><b>70</b></p>			
Entry	EWG	Conversion (%) <sup>a)</sup> with 67	Conversion (%) <sup>b)</sup> with 69
1	CN	15	98
2	COCH <sub>3</sub>	68	97
3	CO <sub>2</sub> CH <sub>3</sub>	96	97
4	CON(CH <sub>3</sub> ) <sub>2</sub>	42	40
5	CONH <i>i</i> Pr	–	96
6	CHO	–	86

a) Determined by <sup>1</sup>H NMR spectroscopy.

study of more demanding metathesis processes, what other variables can lead to innovation in this area of research? One may easily get the impression that the goals set forth in the introduction have been satisfied. A variety of supported, recyclable Ru-based catalysts are readily available that simplify reaction procedure and deliver products of high purity and low toxicity. However, nowhere is this time and cost savings more critical than in combinatorial synthesis. Ironically, in spite of this seemingly obvious connection, none of the work discussed thus far has applied the catalysts in a high-throughput setting. In fact, use of all of the above catalysts in a library synthesis could be considered disadvantageous for several reasons, including:

1. The need for multiple weighing measurements to deliver appropriate catalyst loadings to individual reaction mixtures;
2. The filtration step required to isolate the catalyst for reuse; and
3. The variable swelling of the polymer supports in different solvents which can lead to unpredictable changes in reaction volume and even cause well over-flow.

## 11.9

### Easily Recyclable Ru Catalysts for Combinatorial Synthesis

In an effort to confront these deficiencies, we have developed a procedure for the surface derivatization of small glass (sol-gel) [41] pellets and applied it to the synthesis of supported Ru catalysts [42]. As shown in Scheme 11.8, the linker *and* the active metal carbene were installed *in a single step*. Treatment of (71) with allylchlorodimethylsilane and a full equivalent of (4,5-dihydroIMES)PCy<sub>3</sub>Cl<sub>2</sub>Ru=CHPh (29) led to rapid ROCM and metallation of the styrenyl ether (→ 72). Preweighed monolithic (smallest dimension ≥ 1 mm) sol-gels were then added to the solution, and substi-

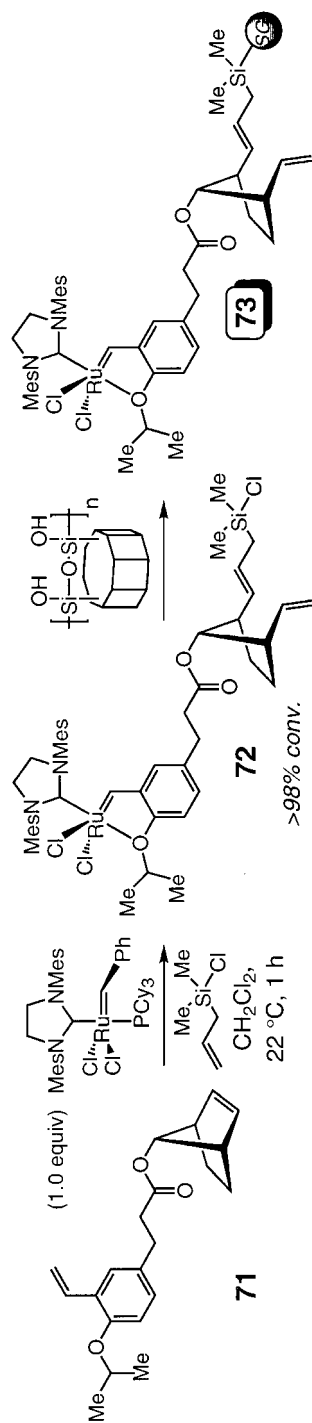
tution of the labile Si–Cl bond in (72) with free hydroxyl groups on the glass surface anchored the catalyst to the support. The resulting dark green glass pellets (73) were washed with methylene chloride and dried in vacuo. In addition, sol-gel systems (74) and (75) were prepared by this procedure starting from the corresponding norbornene precursors and possess a physical appearance similar to (73) (see Fig. 11.1).

For this study, a commercially available (Geltech) glass monolith (6 mm in diameter and 3 mm thick) was selected with an average pore size of 200 Å. The virtues of the resulting recyclable catalysts (73–75) stem directly from our choice of solid support:

1. These highly porous glasses retain a rigid and exposed interfacial surface area (typically 300–1000 m<sup>2</sup> g<sup>−1</sup>), whereas conventional organic polymer beads swell and shrink in different solvents, often with unpredictable effects on catalysis;
2. Functionalization of a monolithic (largest dimension ≥ 1 mm) gel affords a bulk catalyst sample. This obviates the need for filtration to recover the catalyst; tweezers can be used instead;
3. Gelation occurs after a sol is cast into a mold. The glass pieces can therefore be tailored to a uniform size and shape.

Sol-gel-supported Ru complexes (73–75) proved to be remarkably efficient and recyclable catalysts. With purified solvent under nitrogen atmosphere, catalyst (73) was used in the synthesis of trisubstituted olefin (77) for a total of twenty cycles (Tab. 11.12). Despite extended reaction times, all transformations proceeded to completion (>98% isolated yield). With reagent-grade solvent under air, the catalyst was employed efficiently three times (>98% conversion), yet the reaction did not proceed to completion during the fourth cycle under these conditions. The practicality of these glass-bound Ru complexes in high-throughput synthesis was demonstrated by synthesis of two olefin metathesis libraries (Scheme 11.9). The first was a set of twenty-five RCM reactions for a range of dienes with varying levels of alkene substitution. After 6 h at 22 °C under air using reagent-grade methylene chloride, reaction mixtures were *simply removed with a Pasteur pipette with rinsing and concentrated*. Reaction wells were then charged with substrates for the second, more challenging, library of ROM/RCM products (24 h, methylene chloride, 22 °C). This study established the following: (1) The supported catalysts (73–75) approach the monomeric catalyst (5) in reactivity since all reactions, including those involving trisubstituted olefins and recycled pellets (library 2), proceeded efficiently. (2) The use of glass samples of identical size allows combinatorial synthesis to be carried out *without even weighing the catalyst*. Since uniform metal loading occurs in the procedure shown in Scheme 11.8, an appropriate number of pellets of a given size can be added to a well, depending on the amount of substrate. (3) For reactions that proceeded to completion and delivered a single product, representative elemental (C, H) and ICP/MS analyses showed that the products, without any purification or work-up, were of high (often analytical) purity and the level of Ru contamination was typically below 1%.

Since the isopropyl styrene ether remains bound to the glass surface during catalysis, it is unavailable to serve as a stabilizing Lewis base for electron-deficient



### Scheme 11.8

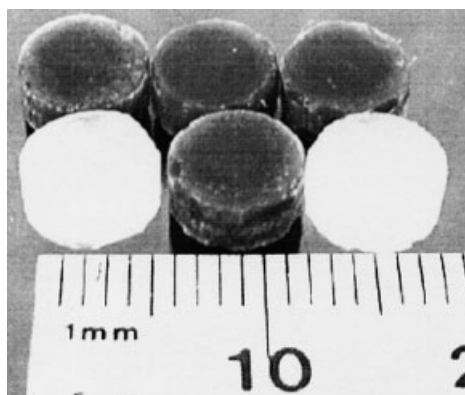
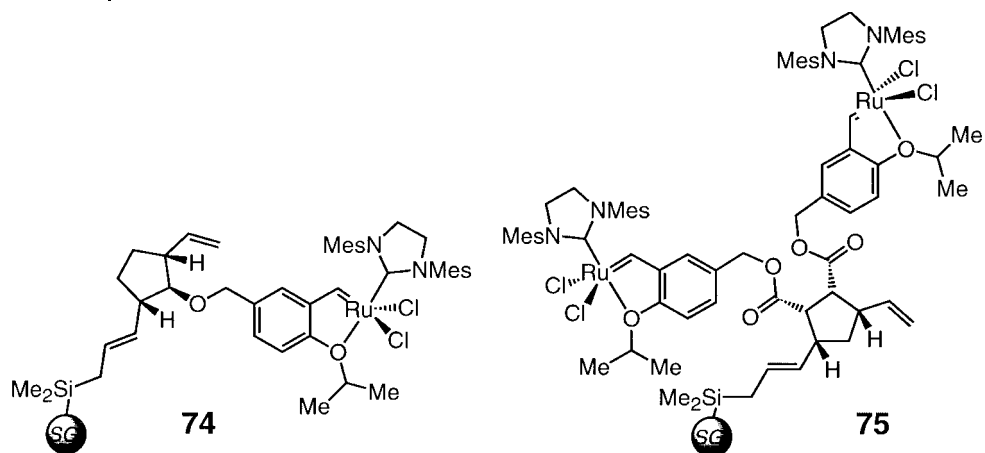
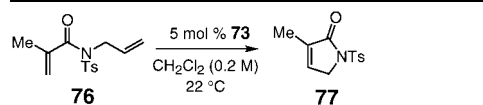


Fig. 11.1 Unfunctionalized (white) and Ru-containing (green) sol-gel monoliths.

and highly active metal complexes in solution, leading to some Ru carbene decomposition. It is therefore plausible that small amounts of Ru are released into solution, where the extremely high propagation rate for the free metal carbene gives rise to substantial levels of conversion. The glass-bound catalysts may not be recycled as efficiently when metathesis is performed in the presence of air and moisture, because this unstabilized and highly reactive unbound Ru carbene is sensitive. Studies are underway to establish to what extent, as observed with the monomeric and dendritic variants (see Scheme 11.4), the released Ru returns to the bidentate ligand at the glass surface.



Tab. 11.12 RCM studies with catalyst (**73**).

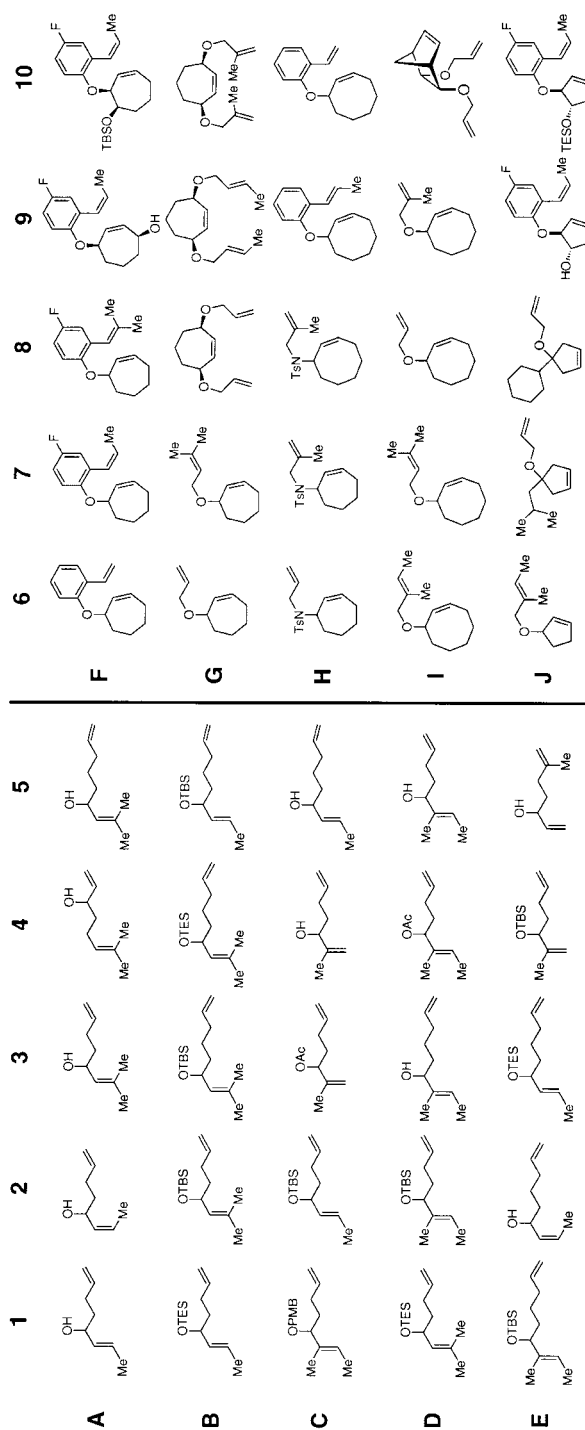
Cycle (time)	Conv (%); Yield (%)
Cycle 1 (3 h)	>98; >98
Cycle 2 (3 h)	>98; >98
Cycle 3 (3 h)	>98; >98
Cycle 4 (3 h)	>98; >98
Cycle 5 (5 h)	>98; >98
Cycle 6 (6 h)	>98; >98
Cycle 7 (6 h)	>98; >98
Cycle 8 (7 h)	>98; >98
Cycle 9 (8 h)	>98; >98
Cycle 10 (8 h)	>98; >98
Cycle 11 (9 h)	>98; >98
Cycle 12 (10 h)	>98; >98
Cycle 13 (12 h)	>98; >98
Cycle 14 (14 h)	>98; >98
Cycle 15 (14 h)	>98; >98
Cycle 16 (16 h)	>98; >98
Cycle 17 (18 h)	>98; >98
Cycle 18 (20 h)	>98; >98
Cycle 19 (22 h)	>98; >98
Cycle 20 (24 h)	>98; >98

## 11.10

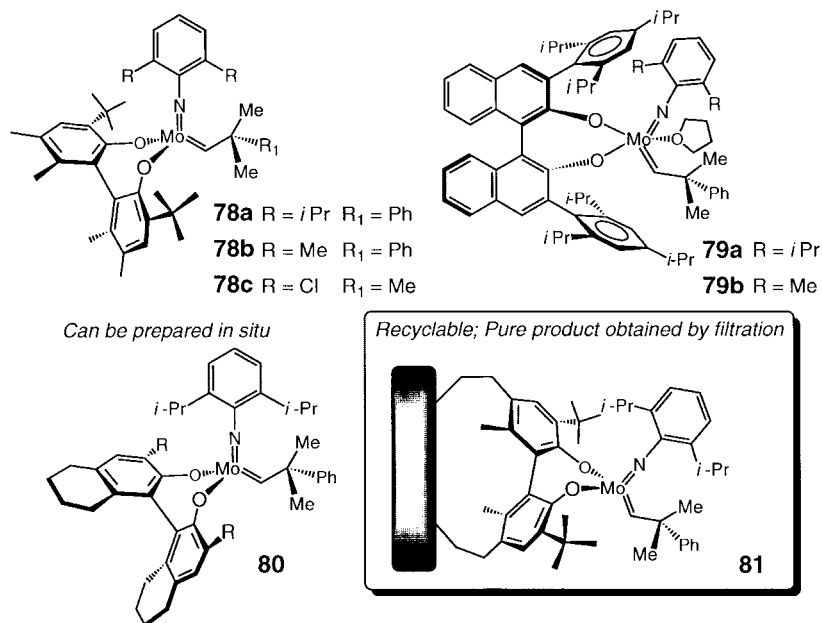
### The First Supported Chiral Metathesis Catalyst

Ongoing work in our laboratories also concerns the design and study of chiral Mo-based catalysts for asymmetric olefin metathesis [9a]. A diverse collection of chiral Mo alkylidenes (including (**78**–**80**), Scheme 11.10) is now available which provides unrivaled synthetic access to a broad range of optically enriched or pure compounds. In addition to expanding the scope and generality of these catalytic processes, rendering the use of these sensitive metal complexes more practical and convenient is an important objective. Although Ru carbenes enjoy high popularity because of their ease of handling, Mo-based catalysts are indispensable because of their superior activity and tolerance of a unique set of functional groups.

As part of this initiative, complex (**80**) (Scheme 11.10) has been advanced as a user-friendly catalyst for enantioselective metathesis [43]. Even when prepared *in situ* from commercially available solutions of the requisite metal complex and chiral ligand, (**80**) gives rise to high levels of efficiency and enantioselectivity. More recently, the first chiral solid-supported Mo alkylidene ((**81**), Scheme 11.10)



Scheme 11.9

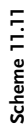


Scheme 11.10

was prepared through the use of a rigid, nonlabile linker that imposes little or no steric influence at the metal center [44].


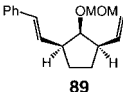
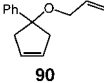
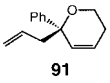
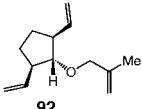
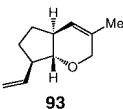
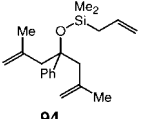
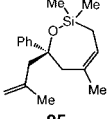
The route to the new polymer-bound catalyst (**81**) is shown in Scheme 11.11. Bromination of optically pure biphenol (**82**) in acetic acid furnished bis(cyclohexadienone) (**83**) as a yellow solid. Rearrangement in the solid state over five days occurred smoothly to give the desired dibromide (**84**) as a white powder in 86% yield for the two steps. Exposure of (**84**) to excess *p*-vinylbenzyl magnesium chloride and subsequent protection of the phenol groups with ethyl chloromethyl ether provided (**85**) in 80% yield. A peroxide-induced radical co-polymerization of (**85**) in the presence of styrene followed by deprotection under acidic conditions afforded the heterogeneous chiral ligand (**86**) as a white powder (76% overall yield). After deprotonation with excess  $\text{KN}(\text{TMS})_2$  in THF for 24 h and thorough washing, the polymer was treated with Mo bis(triflate) (**87**) for 7 h in THF to give supported complex (**81**) as a dark brown powder in 73% yield.

Preliminary experiments with the heterogeneous catalyst were encouraging. As anticipated, (**81**) is typically less efficient than the parent homogeneous catalyst (**78a**) (Scheme 11.10). The decreased activity can result from diffusion-controlled transport of substrate and product molecules through the cavities of the support. Nonetheless, the polymer-bound catalyst routinely provides comparably high levels of asymmetric induction as the corresponding homogeneous variant. As illustrated in Tab. 11.13, asymmetric ring-opening/cross metathesis (AROM/CM) of MOM-protected 7-*syn*-norbornenol (**88**) with styrene as the donor olefin was effi-



### Scheme 11.11

**Tab. 11.13** Catalytic asymmetric olefin metathesis reactions promoted by supported chiral catalyst (**81**).<sup>a)</sup>

Entry	Substrate	Product	Time (h)	Isolated Catalyst	Supported Catalyst
				Conv (%) <sup>b)</sup> ; yield (%) <sup>c)</sup> ; ee (%) <sup>d)</sup>	Conv (%) <sup>b)</sup> ; yield (%) <sup>c)</sup> ; ee (%) <sup>d)</sup>
1 <sup>e</sup>			0.5	>98; 88; >98	>98; 89; 95
2			24	>98; 88; 19	57; 45; 33
3			2	93; 84; >98	57; 41; 93
4			2	>98; 97; 93	95; 92; 81

a) Conditions: 5 mol% **81** (based on Mo), C<sub>6</sub>H<sub>6</sub> (0.1 M), 22 °C.

b) Determined by analysis of 400 MHz <sup>1</sup>H NMR spectra of unpurified mixtures.

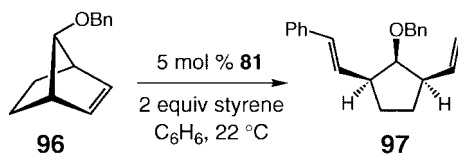
c) Isolated yields after silica gel chromatography.

d) Determined by chiral HPLC (chiralcel AD for entry 1 and chiralcel OJ for entry 4) and chiral GLC (betadex column for entries 2–3).

e) Reaction performed in the presence of 2 equiv styrene.

cient and enantioselective (entry 1). Although the ring opening/ring closing of substrate (**90**) was less efficient with (**81**) than with (**78a**) (57% vs >98% conversion, entry 2), the heterogeneous catalyst gave a noticeably higher selectivity (33% vs 19% ee). Asymmetric ring closure of compound (**92**) using (**81**) was highly enantioselective (93% ee) but again less efficient than with the monomeric catalyst (**78a**) (entry 3). Finally, desymmetrization of siloxane (**94**) in the presence of (**81**) proceeded with a lower but respectable level of asymmetric induction (81% ee, entry 4). Although initial attempts to effect asymmetric metathesis with (**81**) in the absence of solvent were unsuccessful, it was discovered that elevated substrate concentrations could be used to accelerate reactions. For example, 82% conversion to bicycle (**93**) was achieved in just 80 minutes when a 0.5 M solution of (**92**) was exposed to 5 mol% (**81**) (2% homodimeric byproducts formed).

The polymer-supported chiral catalyst is recyclable. The catalytic AROM/CM example shown in Scheme 11.12 is representative. Excellent enantioselection and ef-



Scheme 11.12

**Cycle 1:**>98% conv, 30 min; 97% *ee*

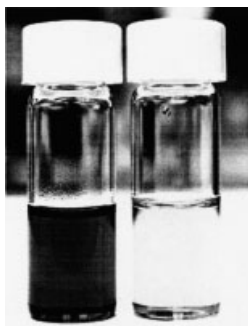
products contains 3% of total Mo initially used

**Cycle 2:**98% conv, 30 min; 98% *ee*

products contains 10% of total Mo initially used

**Cycle 3:**55% conv, 16 h; 89% *ee*

products contains 16% of total Mo initially used



**Fig. 11.2** Difference in the appearance of solutions of asymmetric olefin metathesis product (**97**) obtained from reaction of (**78a**) (left) and supported catalyst (**81**) (right).

iciency are observed in the first cycle, which leaches only 3% of the total Mo loading into the reaction product. After filtration under inert atmosphere, the polymer suffers no loss of activity in a second run, providing the desired product (**97**) in 98% *ee* within thirty minutes (10% contamination based on 5% Mo loading). The minor but steady depletion of Mo finally takes its toll in the third cycle and activity is notably diminished, yet modest conversion and high enantioselectivity are still observed. It deserves mention that in all of the above transformations catalyzed by (**81**), unpurified product solutions obtained by filtration are homogeneous and light yellow in color. In contrast, reaction products derived from homogeneous catalyst (**78a**) are dark brown in color and occasionally heterogeneous (see Fig. 11.2).

## 11.11

## Conclusions and Future Outlook

Catalytic olefin metathesis has emerged as one of the most important transformations in organic chemistry; it is a process that has already been used in the preparation of a large number of biologically important molecules. Such considerations, together with the significance of combinatorial synthesis and the pressing need for environmentally friendly and increasingly efficient processes, clearly point to the significance of practical, recyclable and effective supported metathesis catalysts. As summarized above, a number of key advances have been made in this area during the past few years. However, it would be naïve to assume that significant additional research is not required. We are still a long way away from having in hand supported catalysts that are truly practical and selectively afford products that can be used without further purification. Within this context, facile access to optically enriched materials that contain significantly lower levels of toxic metal impurities, as described in the last section of this article, is one area that should prove of considerable interest in combinatorial synthesis and medicinal chemistry. With the recent advent of both mono- [9b] and bidentate [9c] chiral ligands for Ru-catalyzed asymmetric metathesis, it is reasonable to expect increased interest in their immobilization through the use of a number of the strategies discussed in this review. The availability of enantioselective and recyclable Ru catalysts will likely have a tremendous impact on modern synthesis, complementing Mo-based systems in the high-throughput synthesis of optically enriched small molecule libraries from achiral or racemic precursors. Continued efforts to improve achiral catalysts (both monomeric and polymeric) promise to be equally rewarding when combined with other catalytic asymmetric methods. The design and development of new high-performance supports will further streamline application of these systems to combinatorial chemistry. Regardless of the future course of events, there is little doubt, given the versatility and power of modern metathesis, that supported Ru- and Mo-based catalysts have a great future.

## 11.12

## References

- 1 "Solid Phase Peptide Synthesis. I. The Synthesis of a Tetrapeptide," R. B. MERRIFIELD, *J. Am. Chem. Soc.* **1963**, 85, 2149–2154.
- 2 For a review, see: (a) "Synthesis and Applications of Small Molecule Libraries," L. A. THOMPSON, J. A. ELLMAN, *Chem. Rev.* **1996**, 96, 555–560; for a new one-bead, one-stock solution technology platform, see: (b) "An Alkylsilyl-Tethered, High-Capacity Solid Support Amenable to Diversity-Oriented Synthesis for One-Bead, One-Stock Solution Chemical Genetics," J. A. TALLARICO, K. D. DEPEW, *et al.*, *J. Comb. Chem.* **2001**, 3, 312–318.
- 3 For example: (a) "Small-Molecule Microarrays: Covalent Attachment and Screening of Alcohol-Containing Small Molecules on Glass Slides," P. J. HERGENROTHER, K. M. DEPEW, S. L. SCHREIBER, *J. Am. Chem. Soc.* **2000**, 122, 7849–7850; (b) "Printing Small Molecules as Microarrays and Detecting Protein-Ligand Interactions en Masse," G. MACBEATH,

- A. N. KOEHLER, S. L. SCHREIBER, *J. Am. Chem. Soc.* **1999**, *121*, 7967–7968.
- 4 “Monitoring the Progress and the Yield of Solid-Phase Organic Reactions Directly on Resin Supports,” B. YAN, *Acc. Chem. Res.* **1998**, *31*, 621–630.
  - 5 For the use of *soluble* polymers in synthesis, see: “Liquid-Phase Chemistry: Recent Advances in Soluble Polymer-Supported Catalysts, Reagents, and Synthesis,” P. WENTWORTH, JR., K. D. JANDA, *Chem. Commun.* **1999**, 1917–1924 and references cited therein.
  - 6 A recent review is available: “Polymer-Supported Catalysis in Synthetic Organic Chemistry,” B. CLAPHAM, T. S. REGER, K. D. JANDA, *Tetrahedron* **2001**, *57*, 4637–4662.
  - 7 “Recent Advances in Olefin Metathesis and Its Application in Organic Synthesis,” R. H. GRUBBS, S. CHANG, *Tetrahedron* **1998**, *54*, 4413–4450; (b) “Olefin Metathesis and Beyond,” A. FURSTNER, *Angew. Chem.* **2000**, *112*, 3140–3172; *Angew. Chem. Int. Ed.* **2000**, *39*, 3012–3043.
  - 8 For example: (a) “A Strategy for Macrocyclic Ring Closure and Functionalization Aimed toward Split-Pool Syntheses,” D. LEE, J. K. SELLO, S. L. SCHREIBER, *J. Am. Chem. Soc.* **1999**, *121*, 10648–10649; (b) “Pairwise Use of Complexity-Generating Reactions in Diversity-Oriented Organic Synthesis,” D. LEE, J. K. SELLO, S. L. SCHREIBER, *Org. Lett.* **2000**, *2*, 709–712; (c) “A Boronic Ester Annulation Strategy for Diversity-Oriented Organic Synthesis,” G. C. MICALIZIO, S. L. SCHREIBER, *Angew. Chem.* **2002**, *114*, 160–162; *Angew. Chem. Int. Ed.* **2002**, *41*, 152–154.
  - 9 For a review of asymmetric Mo-catalyzed metathesis, see: “Catalytic Asymmetric Olefin Metathesis,” A. H. HOVEYDA, R. R. SCHROCK, *Chem. Eur. J.* **2001**, *7*, 945–950; for reports on chiral Ru-based complexes, see: (b) “Enantioselective Ruthenium-Catalyzed Ring-Closing Metathesis,” T. J. SEIDERS, D. W. WARD, R. H. GRUBBS, *Org. Lett.* **2001**, *3*, 3225–3228; (c) “A Recyclable Chiral Ru Catalyst for Enantioselective Olefin Metathesis. Efficient Catalytic Asymmetric Ring-Opening/Cross Metathesis In Air,” J. J. VAN VELDHIJZEN, S. B. GARBER, J. S. KINGSBURY, *et al.*, *J. Am. Chem. Soc.* **2002**, *124*, 4954–4955.
  - 10 For filtration processes, see: “*Membrane Handbook*,” W. S. W. HO AND K. K. SARKAR, eds., Chapman and Hall: New York, **1992**.
  - 11 “The Syntheses and Activities of Polystyrene-Supported Olefin Metathesis Catalysts Based on  $\text{Cl}_2(\text{PCy}_3)_2\text{Ru}=\text{CH}-\text{CH}=\text{CPh}_2$ ,” S. T. NGUYEN, R. H. GRUBBS, *J. Organomet. Chem.* **1995**, *497*, 195–200.
  - 12 “Ring-Opening Metathesis Polymerization (ROMP) of Norbornene by a Group VIII Carbene Complex in Protic Media,” S. T. NGUYEN, L. K. JOHNSON, R. H. GRUBBS, *et al.*, *J. Am. Chem. Soc.* **1992**, *114*, 3974–3975.
  - 13 “Well-Defined Ruthenium Olefin Metathesis Catalysts: Mechanism and Activity,” E. L. DIAS, S. T. NGUYEN, R. H. GRUBBS, *J. Am. Chem. Soc.* **1997**, *119*, 3887–3897.
  - 14 “Ruthenium Carbene-Based Olefin Metathesis Initiators: Catalyst Decomposition and Longevity,” M. ULMAN, R. H. GRUBBS, *J. Org. Chem.* **1999**, *64*, 7202–7207.
  - 15 “A Recyclable Ru-Based Metathesis Catalyst,” J. S. KINGSBURY, J. P. A. HARRITY, P. J. BONITATEBUS, JR., *et al.*, *J. Am. Chem. Soc.* **1999**, *121*, 791–799; for a related monophosphine Ru complex that is metathesis-active, see: (b) “Ring-Opening Metathesis. A Ruthenium Catalyst Caught in the Act,” J. A. TALLARICO, P. J. BONITATEBUS, JR., M. L. SNAPPER, *J. Am. Chem. Soc.* **1997**, *119*, 7157–7158.
  - 16 “Efficient and Recyclable Monomeric and Dendritic Ru-Based Metathesis Catalysts,” S. B. GARBER, J. S. KINGSBURY, B. L. GRAY, *et al.*, *J. Am. Chem. Soc.* **2000**, *122*, 8168–8179.
  - 17 “Synthesis and Activity of a New Generation of Ruthenium-Based Olefin Metathesis Catalysts Coordinated with 1,3-Dimesityl-4,5-dihydroimidazol-2-ylidene Ligands,” M. SCHOLL, S. DING, C. W. LEE, *et al.*, *Org. Lett.* **1999**, *1*, 953–956.
  - 18 “A Recyclable ‘Boomerang’ Polymer-Supported Catalyst for Olefin Metathesis,” M. AHMED, A. G. M. BARRETT, D. C. BRADDOCK, *et al.*, *Tetrahedron Lett.* **1999**, *40*, 8657–8662.



- 19 "Efficient Procedure for the Preparation of (Vinyl)polystyrene Resin," C. SYLVAIN, A. WAGNER, C. MIOSKOWSKI, *Tetrahedron Lett.* **1998**, 39, 9679–9680.
- 20 "A Series of Well-Defined Metathesis Catalysts–Synthesis of  $[\text{RuCl}_2(\text{=CHR})(\text{PR}_3)_2]$  and Its Reactions," P. SCHWAB, M. B. FRANCE, J. W. ZILLER, *et al.*, *Angew. Chem.* **1995**, 107, 2125–2127; *Angew. Chem. Int. Ed.* **1995**, 34, 2039–2041; (b) "Synthesis and Applications of  $\text{RuCl}_2(\text{=CHR})(\text{PR}_3)_2$ : The Influence of the Alkylidene Moiety on Metathesis Activity," P. SCHWAB, R. H. GRUBBS, J. W. ZILLER, *J. Am. Chem. Soc.* **1996**, 118, 100–110.
- 21 Recent mechanistic work has shown that  $16\text{ e}^-$  Ru methylene complexes (such as bisphosphine 11) are slow to re-enter the catalytic cycle. Their reluctance to initiate can result in competitive decomposition; see: "Mechanism and Activity of Ruthenium Olefin Metathesis Catalysts," M. S. SANFORD, J. A. LOVE, R. H. GRUBBS, *J. Am. Chem. Soc.* **2001**, 123, 6543–6554.
- 22 "ROMP-Spheres: A Novel High-Loading Polymer Support Using Cross Metathesis between Vinyl Polystyrene and Norbornene Derivatives," A. G. M. BARRETT, S. M. CRAMP, R. S. ROBERTS, *Org. Lett.* **1999**, 1, 1083–1086.
- 23 "Purification Technique for the Removal of Ruthenium from Olefin Metathesis Reaction Products," H. D. MAYNARD, R. H. GRUBBS, *Tetrahedron Lett.* **1999**, 40, 4137–4140; for other approaches where Ru impurities are removed using  $\text{Pb}(\text{OAc})_4$  and a phosphine oxide (respectively), see: (b) "A Convenient Method for Removing All Highly-Colored Byproducts Generated during Olefin Metathesis Reactions," L. A. PAQUETTE, J. D. SCHLOSS, I. EFREMOV, *et al.*, *Org. Lett.* **2000**, 2, 1259–1261; (c) "A Convenient Method for the Efficient Removal of Ruthenium Byproducts Generated during Olefin Metathesis Reactions," Y. M. AHN, K. YANG, G. I. GEORG, *Org. Lett.* **2001**, 3, 1411–1413.
- 24 "A Soluble Polymer-Bound Ruthenium Carbene Complex: A Robust and Reusable Catalyst for Ring-Closing Olefin Metathesis," Q. YAO, *Angew. Chem.* **2000**, 112, 4060–4062; *Angew. Chem. Int. Ed.* **2000**, 39, 3896–3898.
- 25 For carbosilane dendrimers using an iterative alkenylation/hydrosilation sequence, see: (a) "Silane Dendrimers," A. W. VAN DER MADE, P. W. N. M. VAN LEEUWEN, *J. Chem. Soc., Chem. Commun.* **1992**, 1400–1401; (b) "Dendrimeric Silanes," A. W. VAN DER MADE, P. W. N. M. VAN LEEUWEN, J. C. DE WILDE, *et al.*, *Adv. Mater.* **1993**, 5, 466–468.
- 26 For carbosilane dendrimers using a repetitive alkenylation/hydroboration/oxidation sequence, see: "Dendritic Carbosilanes Containing Hydroxy Groups on the Periphery," C. KIM, S. SON, B. KIM, *J. Organometallic Chem.* **1999**, 588, 1–8.
- 27 In general, electronically mismatched systems undergo cross metathesis more effectively, see: "New Approaches to Olefin Cross-Metathesis," H. E. BLACKWELL, D. J. O'LEARY, A. K. CHATTERJEE, *et al.*, *J. Am. Chem. Soc.* **2000**, 122, 58–71 and references cited therein.
- 28 "Synthesis of Periphery-Functionalized Dendritic Molecules Using Polyolithiated Dendrimers as Starting Material," P. WIJCKENS, J. T. B. H. JASTRZEBSKI, P. A. VAN DER SCHAAF, *et al.*, *Org. Lett.* **2000**, 2, 1621–1624.
- 29 Recall from the Grubbs study (Eq. 11.1) the troublesome use of the *labile* phosphine ligands as the site of *bidentate* polymer attachment.
- 30 "Synthesis and Application of a Permanently Immobilized Olefin Metathesis Catalyst," S. C. SCHURER, S. GESSLER, N. BUSCHMANN, *et al.*, *Angew. Chem.* **2000**, 112, 4062–4065; *Angew. Chem. Int. Ed.* **2000**, 39, 3898–3901.
- 31 Space limitations unfortunately preclude a full discussion of two more recent approaches to permanently immobilized Ru catalysts, see: (a) "Monolithic Materials: New High-Performance Supports for Permanently Immobilized Metathesis Catalysts," M. MAYR, B. MAYR, M. R. BUCHMEISER, *Angew. Chem.* **2001**, 113, 3957–3960; *Angew. Chem. Int. Ed.* **2001**, 40, 3839–3842; (b) "A Novel Polymer-Supported Arene–Ruthenium Complex for Ring-Closing Olefin Metathesis," R. AKIYAMA, S. KOBAYASHI, *Angew. Chem.* **2002**, 114, 2714–2716; *Angew. Chem. Int. Ed.* **2002**, 41, 2602–2604.

- 32 "Second Generation Recyclable 'Boomerang' Polymer Supported Catalysts for Olefin Metathesis: Application of Arduengo Carbene Complexes," M. AHMED, T. ARNAULD, A. G. M. BARRETT, *et al.*, *Synlett* **2000**, 1007–1009.
- 33 "A Novel Class of Ruthenium Catalysts for Olefin Metathesis," T. WESKAMP, W. C. SCHATTELMANN, M. SPIEGLER, *et al.*, *Angew. Chem.* **1998**, *110*, 2631–2633; *Angew. Chem. Int. Ed.* **1998**, *37*, 2490–2493; (b) "Highly Active Ruthenium Catalysts for Olefin Metathesis: The Synergy of N-Heterocyclic Carbenes and Coordinatively Labile Ligands," T. WESKAMP, F. J. KOHL, W. HIERINGER, *et al.*, *Angew. Chem.* **1999**, *111*, 2573–2576; *Angew. Chem. Int. Ed.* **1999**, *38*, 2416–2419; (c) "Increased Ring-Closing Metathesis Activity of Ruthenium-Based Olefin Metathesis Catalysts Coordinated with Imidazolin-2-ylidene Ligands," M. SCHOLL, T. M. TRNKA, J. P. MORGAN, *et al.*, *Tetrahedron Lett.* **1999**, *40*, 2247–2250; (d) "Olefin Metathesis-Active Ruthenium Complexes Bearing a Nucleophilic Carbene Ligand," J. HUANG, E. D. STEVENS, S. P. NOLAN, *et al.*, *J. Am. Chem. Soc.* **1999**, *121*, 2647–2678.
- 34 "Olefin Metathesis in Non-degassed Solvent Using a Recyclable, Polymer Supported Alkylideneruthenium," J. DOWDEN, J. SAVOVIC, *Chem. Comm.* **2001**, 37–38.
- 35 Unfortunately, the authors do not discuss the more appropriate comparison with homogeneous catalyst 4.
- 36 "Water-Soluble Ruthenium Alkylidenes: Synthesis, Characterization, and Application to Olefin Metathesis in Protic Solvents," D. M. LYNN, B. MOHR, R. H. GRUBBS, *et al.*, *J. Am. Chem. Soc.* **2000**, *122*, 6601–6609.
- 37 "Simply Assembled and Recyclable Polymer-Supported Olefin Metathesis Catalysts," L. JAFARPOUR, S. P. NOLAN, *Org. Lett.* **2000**, *2*, 4075–4078.
- 38 "Synthesis of Trisubstituted Alkenes via Olefin Cross-Metathesis," A. K. CHATTERJEE, R. H. GRUBBS, *Org. Lett.* **1999**, *1*, 1751–1753; (b) "Synthesis of Functionalized Olefins by Cross and Ring-Closing Metatheses," A. K. CHATTERJEE, J. P. MORGAN, M. SCHOLL, *et al.*, *J. Am. Chem. Soc.* **2000**, *122*, 3783–3784; (c) "Cross Metathesis Reaction: Generation of Highly Functionalized Olefins from Unsaturated Alcohols," J. COSSY, S. BOUZBOUZ, A. H. HOVEYDA, *J. Organomet. Chem.* **2001**, *624*, 327–332.
- 39 "Synthesis and Metathesis Reactions of a Phosphine-Free Dihydroimidazole Carbene Ruthenium Complex," S. GESSLER, S. RANDL, S. BLECHERT, *Tetrahedron Lett.* **2000**, *39*, 9973–9976; (b) "Highly Selective Cross Metathesis with Acrylonitrile Using a Phosphine-Free Ru Complex," S. RANDL, S. GESSLER, H. WAKAMATSU, *et al.*, *Synlett* **2001**, 430–432.
- 40 "Highly Efficient and Recyclable Polymer-Bound Catalyst for Olefin Metathesis Reactions," S. RANDL, N. BUSCHMANN, S. J. CONNOR, *et al.*, *Synlett* **2001**, 1547–1550.
- 41 "Sol-Gel Science: The Physics and Chemistry of Sol-Gel Processing," C. J. BRINKLER and G. W. SCHERER, Academic Press: San Diego, CA, 1990.
- 42 "Immobilization of Olefin Metathesis Catalysts on Monolithic Sol-Gel. Practical, Efficient, and Easily Recyclable Catalysts for Organic and Combinatorial Synthesis," J. S. KINGSBURY, S. B. GARBER, J. M. GIFTOS, *et al.*, *Angew. Chem.* **2001**, *113*, 4381–4386; *Angew. Chem. Int. Ed.* **2001**, *40*, 4251–4256.
- 43 "A Readily Available and User-Friendly Chiral Catalyst for Efficient Enantioselective Olefin Metathesis," S. L. AELTIS, D. R. CEFALO, P. J. BONITATEBUS, JR., *et al.*, *Angew. Chem.* **2001**, *113*, 1500–1504; *Angew. Chem. Int. Ed.* **2001**, *40*, 1452–1456.
- 44 "The First Polymer-Supported and Recyclable Chiral Catalyst for Enantioselective Olefin Metathesis," K. C. HULTZSCH, J. A. JERNELIUS, A. H. HOVEYDA, *et al.*, *Angew. Chem.* **2002**, *114*, 609–613; *Angew. Chem. Int. Ed.* **2002**, *41*, 589–593.

## 12

# Monitoring and Optimizing Organic Reactions Carried Out on Solid Support

BING YAN

### 12.1

#### Introduction

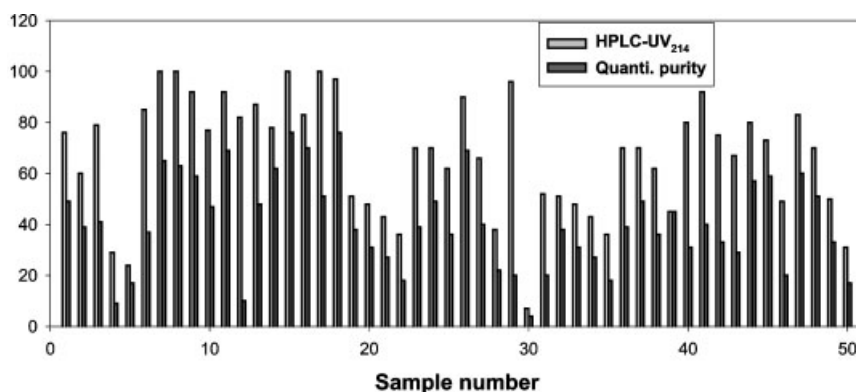
A recent survey [1] has shown that solid-phase organic synthesis (SPOS) [2] continues to hold a dominant position over the years in combinatorial synthesis [3] as more and more chemical reactions are developed on polymer support. However, the time-consuming task in solid-phase combinatorial synthesis is the optimization of reaction conditions. Compound library synthesis tends to give lower yields and higher amount of impurities in the final products unless careful optimization is carried out. Low quality libraries will lead to ambiguity and uncertainty in the biological assays. Thus, prior reaction optimization of each synthetic step including resin loading, intermediate synthetic steps, and the cleavage of desired compounds on a chosen solid support becomes imperative.

#### 12.1.1

##### Quality of Combinatorial Libraries

A decade ago, combinatorial libraries were large and compounds from those libraries were characterized less rigorously. They were rarely purified nor analyzed for their yield and purity. Recently, LC/MS/UV214 or LC/MS/ELSD has been used to characterize combinatorial libraries. These methods provide information regarding the identity and relative purity of compounds at a high throughput.

However, the relative purity does not represent the true purity of a sample. The problem with reporting relative purity is indicated in Fig. 12.1. In this experiment, we measured the absolute quantity of each compound using an authentic reference compound as calibration reference. The quantitative purity (absolute purity) was determined by calculation from the compound quantity and the total sample weight. This quantitative purity is lower than the relative purity in all cases. The total impurities in the sample include those “visible” to a UV detector such as side products, starting materials and excess reagents, and those “invisible” such as TFA, inorganic salts, plastic, resin extracts, and some remaining high boiling point solvent. The only way to improve the absolute purity is to purify all compounds including those already having a relative purity higher than 90%.



**Fig. 12.1** Comparison of the relative purity to quantitative purity for 50 compounds based on 12 different scaffolds.

### 12.1.2

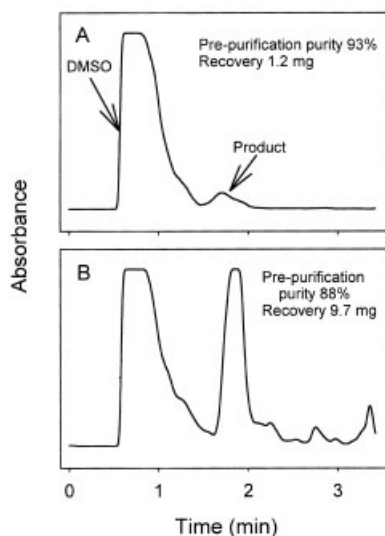
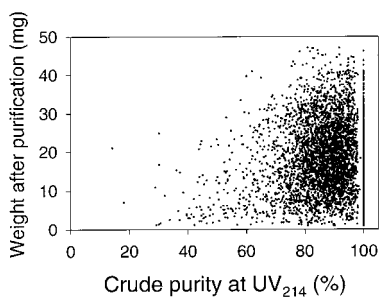
#### Purification and the Chemical Yield of Synthesis

Compound libraries are often purified by reverse phase HPLC. Loss of compound mass associated with HPLC cannot be avoided. Besides the HPLC issue, both purity and chemical yield of the synthetic product are determining factors for obtaining a reasonable quantity of pure compound (>90%). A combinatorial library containing 3170 compounds was synthesized on solid phase with an average relative purity of 80%. After purification, various amounts of compounds were obtained (Fig. 12.2). The average recovery is only 18 mg compared with the expected 45 mg. The preparative purification chromatograms (Fig. 12.3) showed that when the product peak was small, the recovery was generally low indicating the importance of the chemical yield.

Relative purity measurement and the relative purity-based reaction optimization have long been used in combinatorial synthesis. In order to make high-throughput purification a success, the yield-based optimization is essential. Chemiluminescent nitrogen detection (CLND) [4] with HPLC determines the quantitative yield after each reaction step during the library feasibility and rehearsal stages. The yield of each synthetic step provides guidance for the final library synthesis.

Solution-phase synthesis [5] often needs purification or clean-up procedures after each reaction step to remove excess reagent. These methods include scavenging, extractions and associated plate transfers. All these procedures cause the loss of the desired compound. Although the purity can be improved after treatment, the chemical yield is seriously compromised. In contrast, SPOS has a unique advantage in purifying bound compound without losing compound mass. However, if the reaction is not complete at each step, the side products will form on resin and they cannot be removed while bound to the resin. The final yield and purity will both suffer as a result. A 90% yield for a four-step synthesis will produce the final product in a disappointing 65% yield.

**Fig. 12.2** The relationship between the compound crude purity and the weight after purification for 3170 compounds.



**Fig. 12.3** Preparative HPLC chromatograms for two compounds in a library purification as in Figure 12.2.

Ideally, SPOS can be driven to completion by using the optimal reaction conditions and the excess reagent. In reality, some proprietary and expensive reagents cannot be used in large excess. For kinetics or thermodynamic reasons, not all reactions can easily go to completion. Therefore, extra efforts should be made to push a reaction closer to completion.

### 12.1.3

#### Methods for Monitoring the Reaction Completion

To determine if a solid-phase reaction is complete, on-resin analytical methods are preferable [6]. First, the quantitative or qualitative information obtained from on-resin analysis is more relevant to solid-phase reactions. Secondly, this kind of analysis is fast, direct, and without any alteration to the sample. On the other hand, analysis after cleavage would depend on the cleavage efficiency (to be discussed later) and the stability of analyte to cleavage conditions such as TFA. The

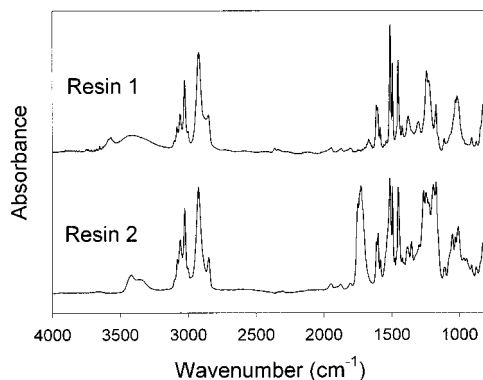
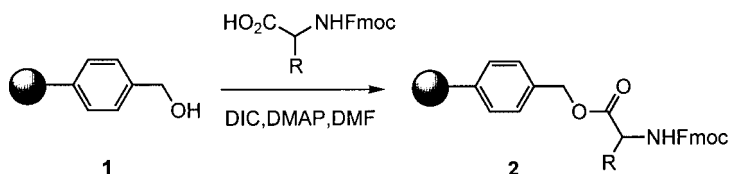


Fig. 12.4 Single bead FTIR spectra for resin-bound compounds (1) and (2).



Scheme 12.1

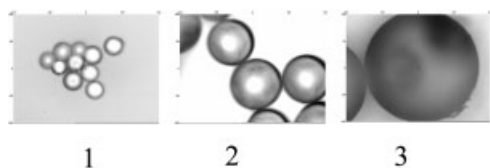
cleaved products are normally analyzed by HPLC or LC/MS/UV. The relative purity obtained has low prediction value for the solid-phase reaction monitored. An exception is the use of a quantitative detector such as CLND [4] after the complete cleavage. This quantitative analysis can measure the yield of the reaction.

A comparison of the amounts of resin-bound starting material and the product by cleave-and-analyze method might give a clue on the reaction completion. However, uncertainty will arise because (1) the resin-bound starting material and the product are not cleaved at the same rate and efficiency; (2) the decomposition may occur during the process; and (3) their UV extinction coefficients are different.

A comparison of results from reaction monitoring by two on-bead and one off-bead methods for a reaction depicted in Scheme 12.1 is described in the following. Single bead FTIR [7] showed that the starting material with a hydroxyl functional group was completely converted to product and the product carbonyl group was formed in both reactions (Fig. 12.4). Quantitative measurement of the product on resin was carried out by analyzing the Fmoc groups using UV<sub>278</sub> after cleavage with 20% piperidine for 2 h. The analysis showed that the conversion for both reactions was nearly 100%. Resin-bound compound was also cleaved with 50% TFA for 2 h and analyzed by LC/UV<sub>214</sub>/MS. This analysis after cleavage gave a relative purity of ~60% (Tab. 12.1). Product decomposition and TFA-induced leaching from resin might be responsible for extra impurities in the cleaved sample. This example showed that on-resin analysis resulted in more relevant and clear-cut conclusion. The cleave-and-analyze approach did not provide correct information on these polymer-supported reactions.

**Tab. 12.1** Comparison of on-bead and off-bead analysis.

<i>Fmoc amino acid</i>	<i>Single bead FTIR</i>	<i>Fmoc cleavage UV<sub>278</sub></i>	<i>Compound cleavage LC/UV<sub>214</sub>/MS</i>
Gly	100%	98%	62%
Ala	100%	101%	63%

**Fig. 12.5** Photographs of resin beads used in diffusion study. Pictures were taken at the same scale. The bead diameters are: 1) 35–75  $\mu\text{m}$ ; 2) 160–200  $\mu\text{m}$ ; 3) 500–560  $\mu\text{m}$ .

## 12.2

### Non-chemical Factors Affecting the Completion of Solid-phase Reactions

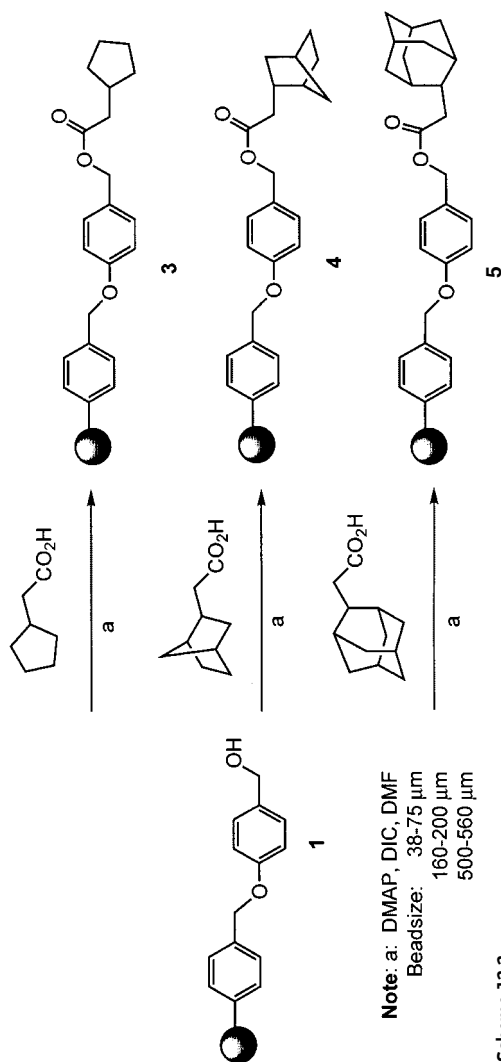
Many factors will prevent the reaction from completion and lower the yield of solid-phase synthesis. Besides chemical issues, factors like solvent [8], reagent diffusion [9], mixing method [10], site interaction [11], and others may all influence the synthesis. In this section, discussion will focus on the reagent diffusion issue in solid-phase synthesis.

Reaction kinetics on resin determine the time required for solid-phase synthesis and the likelihood of the reaction completion that determines the final purity and yield of the synthesis. Such information is important for solid-phase combinatorial synthesis using the parallel format. It is also crucial for combinatorial synthesis using the split-and-pool method. Recently, the miniaturized screening format has allowed the use of much less compound for each assay. Split synthesis using beads with a diameter of 500  $\mu\text{m}$  provided enough compound for  $\sim 7000$  assays. This established that the split synthesis is a more economical method for synthesizing combinatorial libraries for biological screening. However, the reaction rate on such macro beads might be different from that on regular beads with a diameter of 50–100  $\mu\text{m}$ . This hypothesis is attested in the following sections by studying reaction kinetics on resin beads with various diameters (Fig. 12.5) [12].

#### 12.2.1

##### Esterification Reaction Using Resin Beads of Various Sizes

In this experiment, cyclopentylacetic acid, 2-norbornaneacetic acid, and 1-admantaneacetic acid reacted, respectively, with the alcohol resins (1) (Scheme 12.2) of three sizes. These resins have different diameter ranges, namely, 35–75, 160–200, and 500–560  $\mu\text{m}$ . The relative conversion of the starting material to the product was determined by single bead FTIR method. Fig. 12.6 shows IR spectra taken at



Scheme 12.2

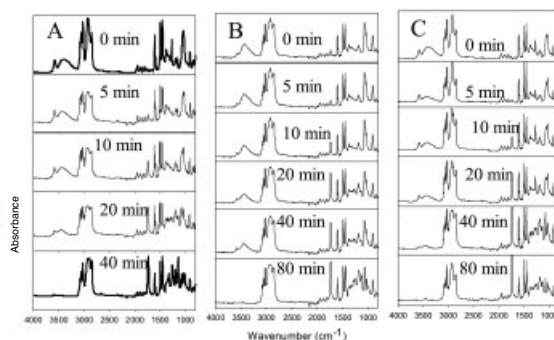


**Tab. 12.2** Rate constants ( $\times 1000$  L/s) for reactions carried out on resin beads with different sizes

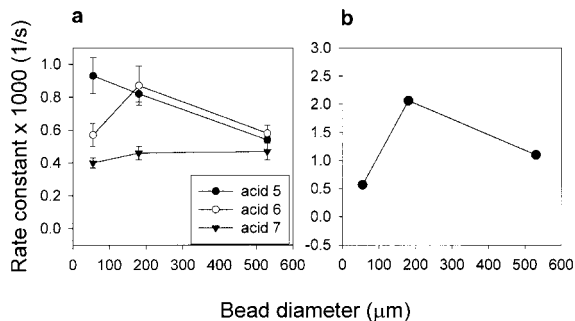
	<i>Acid 5</i>		<i>Acid 6</i>		<i>Acid 7</i>		<i>Bromination</i>
	<i>s.m.</i>	<i>prod</i>	<i>s.m.</i>	<i>prod</i>	<i>s.m.</i>	<i>prod</i>	<i>s.m.</i>
Bead 1	0.99	0.26	0.60	0.53	0.41	0.28	2.26
Bead 2	0.84	0.73	0.93	0.81	0.44	0.48	1.18
Bead 3	0.55	0.53	0.55	0.60	0.49	0.35	0.83

Note: s.m. = starting material. Prod. = product.

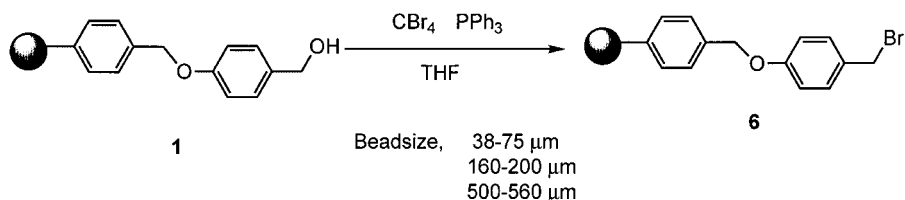
**Fig. 12.6** Single bead FTIR spectra of resins at various times during the reaction between (1) and (5). Panel A is for reaction carried out on resins with a diameter of 35–75  $\mu\text{m}$ , B is for resins with a diameter of 160–200  $\mu\text{m}$ , and C for resins with a diameter of 500–560  $\mu\text{m}$ .



**Fig. 12.7** a) The relationship between the average bead diameter and the reaction rate constant when acids 5–7 were used in the reaction (Scheme 12.2). b) The relationship between the average bead diameter and the reaction rate constant for the reaction shown in Scheme 12.3.



various times during the reaction. In reactions with all three kinds of resins, the IR bands at  $\sim 3500$   $\text{cm}^{-1}$  that represents the starting alcohol on resin decreased its intensity with time. At the same time, the IR band at  $1734$   $\text{cm}^{-1}$  increased its intensity with time. The reaction process was monitored by integrating IR peak area for the starting material and the product on resins. Curve-fit analysis provided rate constants (Tab. 12.2) for all reactions monitored based on a pseudo-first-order reaction model. The relationship between reaction rate and the bead size for three acids in esterification reaction is shown in Fig. 12.7a. Data showed that the reaction rate did not depend on the size of resin bead.



Scheme 12.3

## 12.2.2

**Bromination Reaction on Resin Beads of Various Sizes**

The bromination reaction (Scheme 12.3) was also carried out on resins (**1**) of three different sizes (Fig. 12.5). Single bead FTIR study and the kinetics analysis were carried out as in the esterification reaction studies. Rate constants are listed in Tab. 12.2. The relationship between the rate constants and the bead size is shown in Fig. 12.7b.

Triphosphine reacted with carbon tetrabromide to form an organic salt [13]. This reactive species then reacted with alcohol to form the corresponding bromide. Kinetics results showed that there is no significant difference in reaction rate when resin beads of different sizes were used. This demonstrated that the diffusion of the organic salt into bead was not rate limiting compared with the reaction rate.

## 12.3

**Monitoring the Reaction Completion**

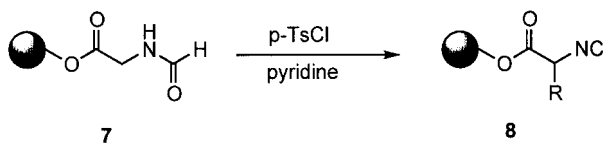
The goal of reaction monitoring is to optimize reaction conditions such as solvent, reagent ratio, temperature, concentration, mixing method, catalyst and others to push a reaction to completion. These reaction steps include the loading of scaffold, the building block additions, and the final cleavage from the polymer.

## 12.3.1

**Reaction Completion Monitored by Single Bead FTIR**

In a dehydration reaction (Scheme 12.4), the IR band of the formamide carbonyl group at  $1684\text{ cm}^{-1}$  in (**7**) decreased and eventually converted to the isonitrile band at  $2150\text{ cm}^{-1}$  in (**8**) (Fig. 12.8). In a separate example (Scheme 12.5), the conversion of the IR band from the carbonate carbonyl group in (**9**) to the IR band of the carbamide carbonyl group in (**10**) can be monitored to assure the reaction completion (Fig. 12.9). Based on FTIR analysis, the reaction time course can be analyzed by integrating peak areas of the IR bands from the starting resin and the product. From the point of view of kinetics, the side reaction product formation can be excluded if the pseudo first order rates of the starting material consumption and the product formation are identical.

Scheme 12.4



## 12.3.2

**Reaction Completion Monitored by Combination of Methods**

To check the completion of the reaction in Scheme 12.6, the single bead FTIR measurement (Fig. 12.10) alone was not conclusive because there was no IR band from the starting resin (**11**) to monitor. Resin elemental analysis (Cl) of (**11**) could conclusively show if the reaction was complete. The accuracy and the reproducibility of the resin elemental analysis methods have been evaluated before [14].

Two acylation reactions as depicted in Schemes 12.7 and 12.8 had the same issue when monitored by single bead FTIR (Figs 12.11 and 12.12). The starting resins (**13**) and (**15**) did not have convenient signal to monitor by FTIR. A chloranil test [15] specific for the secondary amines was used to confirm the complete consumption of (**13**), therefore the reaction completion. An iron-chloride-pyridine test [16] was used to confirm the complete consumption of (**15**). In both color tests, a blue color would suggest the presence of the starting material. In both cases we observed the disappearance of the blue color that indicated the reaction completion.

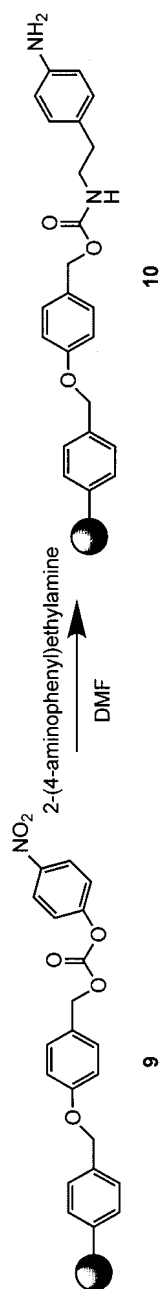
The combination of detecting methods in solid-phase reaction monitoring can add more certainty to decision making. Because there are few available color testing methods for reaction monitoring, we have developed several novel color testing methods. Dansylhydrazine [17] and Purpald [18] were both used to detecting trace amount of aldehyde groups on resins. 9-Anthrolynitrile [19] was used to effectively detecting the trace amount of hydroxyl groups on resin and PDAM [19] was used to detecting carboxyl groups on resin.

## 12.3.3

**Pitfalls to Avoid in Reaction Monitoring**

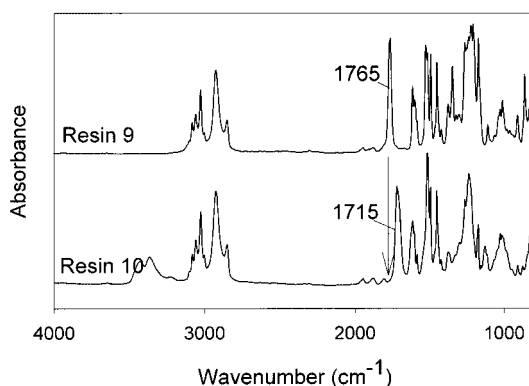
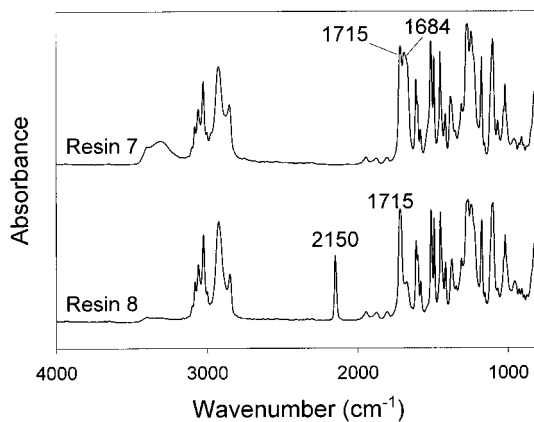
To check the completion of the reaction depicted in Scheme 12.9, single bead FTIR seemed quite conclusive because the IR band from the starting material (alcohol) has converted to the product carbonate band (Fig. 12.13). The hydroxyl stretch disappeared completely in the FTIR data. However, the possible presence of a trace amount of hydroxyl groups might not be evident in the IR spectrum. The fluorescent dye 9-anthrolynitrile reacted with resin-bound alcohol and it was very sensitive in detecting trace amount of hydroxyl groups [19]. It was used to detect the residual resin-bound alcohol and to confirm the reaction completion.

The reductive amination reaction (Scheme 12.10) has two steps: the formation of imine and the reduction of imine. The single bead FTIR results (Fig. 12.14) show the combined result of both steps. The aldehyde IR bands at 1682 and 2769  $\text{cm}^{-1}$  disappeared in the final product. However, this did not suggest that the

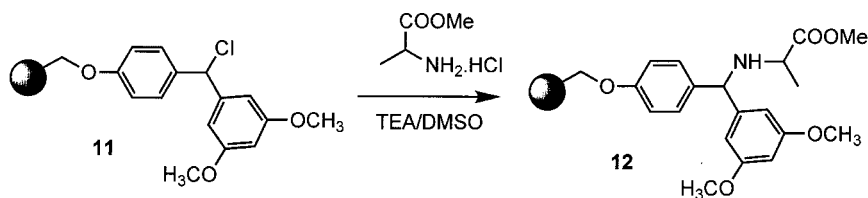


Scheme 12.5

**Fig. 12.8** Single bead FTIR spectra for resin-bound compounds (7) and (8).



**Fig. 12.9** Single bead FTIR spectra for resin-bound compounds (9) and (10).



**Scheme 12.6**

product is pure (13). If the imine formation was not complete, the remaining aldehyde would be reduced to the alcohol and the IR bands at 1682 and 2769  $\text{cm}^{-1}$  would have also disappeared. Since 9-anthroynitrile specifically reacted with alcohol and did not react with secondary amines [19], it was used to detect any trace amount of hydroxyl groups in the resin. The reductive amination could be considered complete only when the negative 9-anthroynitrile test was obtained in addition to FTIR result.

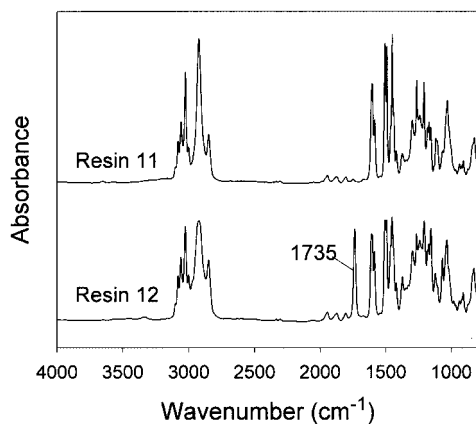
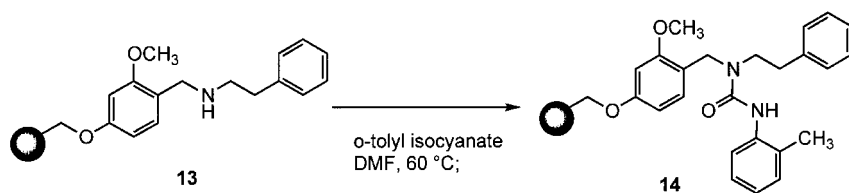
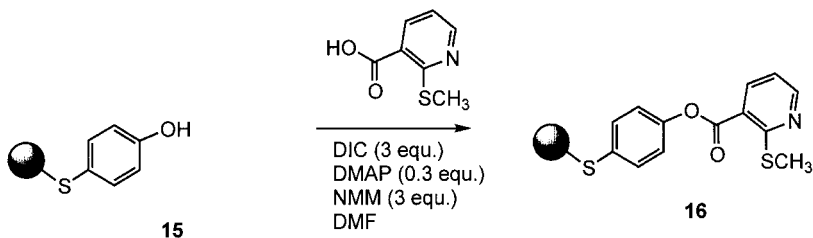


Fig. 12.10 Single bead FTIR spectra for resin-bound compounds (11) and (12).



Scheme 12.7



Scheme 12.8

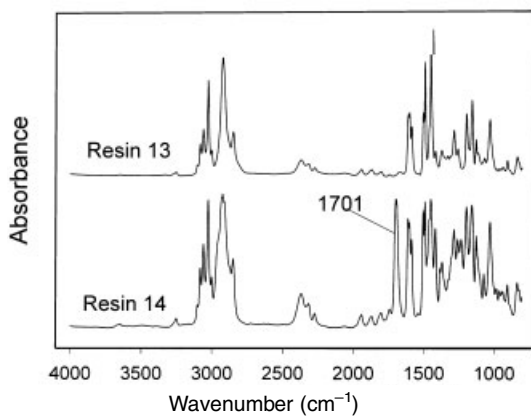
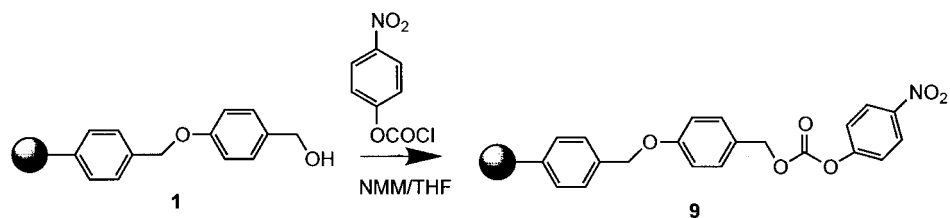
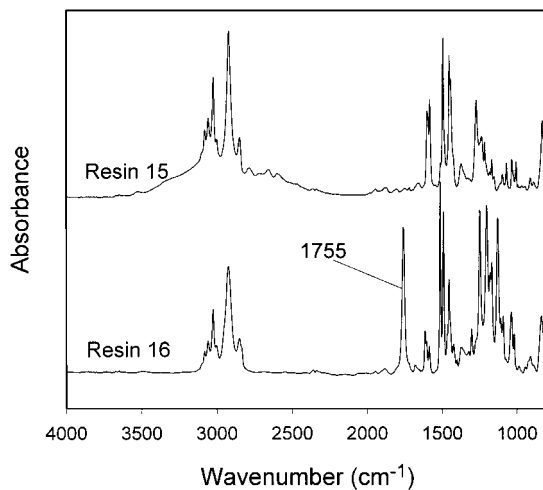
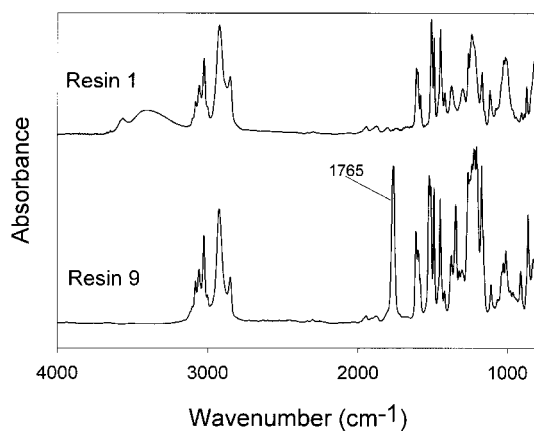


Fig. 12.11 Single bead FTIR spectra for resin-bound compounds (13) and (14).

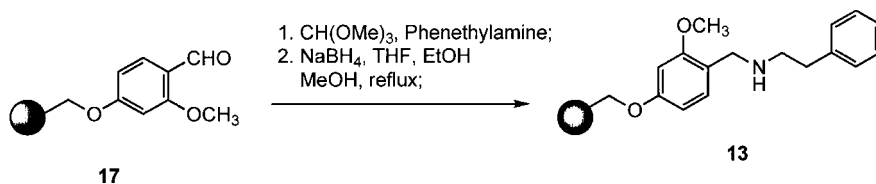
**Fig. 12.12** Single bead FTIR spectra for resin-bound compounds (**15**) and (**16**).



**Scheme 12.9**



**Fig. 12.13** Single bead FTIR spectra for resin-bound compounds (**1**) and (**9**).



Scheme 12.10

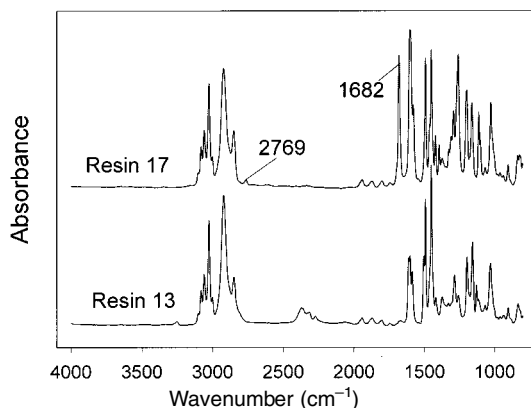


Fig. 12.14 Single bead FTIR spectra for resin-bound compounds (17) and (13).

## 12.4

### Monitoring the Cleavage Completion

The successful assembly of organic compounds on a solid support represents only part of the challenge in SPOS. After completion of synthetic sequence, the compounds must be cleaved from linkers attached to polymer by a chemical or photochemical reaction, for example, treatment of a polymer-bound compound with acids, bases, nucleophiles, redox reagents, and even photons. Acid-labile linker and amine-cleavable Marshall linker are two major classes of linkers used in combinatorial synthesis.

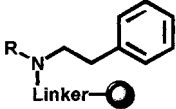

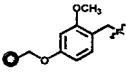
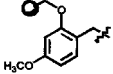
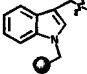
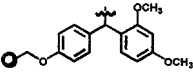
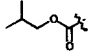
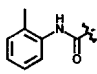
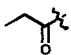
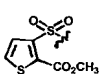
#### 12.4.1

##### Cleavage from Acid-labile Linker [20]

Many acid-labile linkers are used to assemble combinatorial libraries. Compounds are cleaved in the final step by TFA/DCM solution with various concentrations for a certain period of time. Mild cleavage conditions may lead to incomplete cleavage of the desired compound from a solid support. On the other hand harsh conditions may cause compound degradation and side reactions. Harsh conditions will also cause the partial breakdown of resin and the leaching of unidentified impurities into the final products. Harsh cleavage conditions demand the stability of all compounds under such conditions. This may limit the scope of combinatorial synthesis



Tab. 12.3<sup>a)</sup> Resins studied in TFA cleavage reactions.

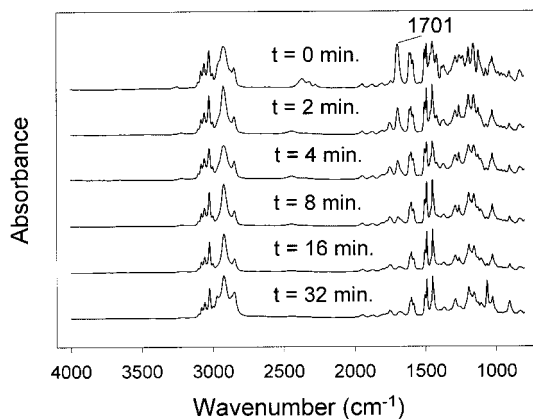
				
				
R	I	II	III	IV
				
	18, 70	19, 71	20, 67	21, 68
	22, 72	23, 72	24, 77	25, 75
	26, 71	27, 71	28, 75	29, 60
	30, 75	31, 80	32, 83	33, 57

a) The numbers in bold represent the organic molecule bound to a polymer through a representative linker (I–IV). The numbers in italics represent the crude yield of compound after cleavage with 5% TFA at room temperature for 6 h. These cleavages were done before kinetic analysis of these resins. Crude products were characterized using NMR and MS. High-resolution <sup>1</sup>H NMR (400 MHz) showed that all cleaved crude products were baseline pure.

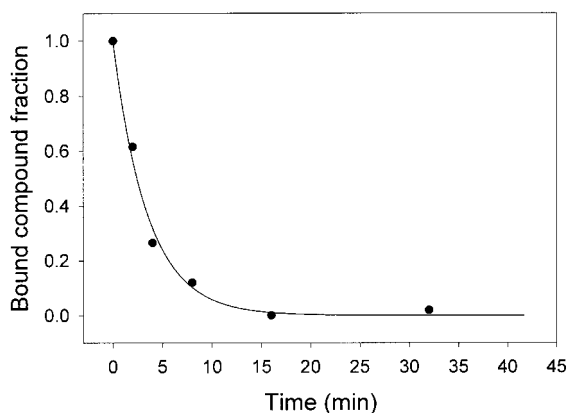
and the exploration of molecular diversity. Therefore, the selection of the optimal cleavage conditions is critical. A set of carbamates, ureas, secondary amides, and sulfonamides (Tab. 12.3) were synthesized and their cleavage from four different acid-labile linkers including benzyl, benzhydryl and indole linkers were investigated.

#### 12.4.1.1 TFA Cleavage of Resin-Bound Products

Resins were briefly swollen by suspending them in DCM for 15 min. After the solvent was drained, 1% TFA (or other concentration of TFA) in DCM was added to the resin and the mixture was mixed on a rotator. In nearly all cases, the cleavage was visualized by observing the color change on resin. Depending on the compound on resin, the color ranged from light pink to deep purple or dark brown when the cleavage occurred.



**Fig. 12.15** Single bead IR spectra of resins (**19**) at various times during the TFA cleavage reaction (5% TFA).



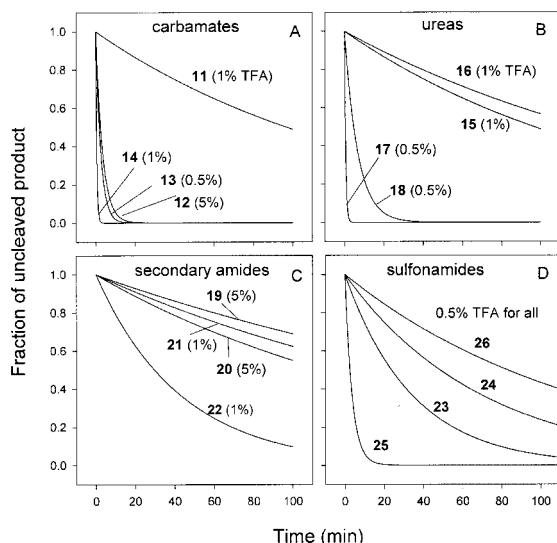
**Fig. 12.16** Time courses of TFA cleavage reactions for resin (**19**) obtained by integrations of the carbonyl bands. Lines represent the best fit obtained by PeakFit (Jandel Scientific, San Rafael, CA) analysis on a PC computer.

Resins (**19**) (~30 mg each) reacted with 5% TFA in DCM. Droplet of suspension was taken at various time intervals for single bead FTIR (Fig. 12.15) and kinetics analysis (Fig. 12.16). The data was also fitted to a first order reaction rate equation and rate constants were determined to be  $4.8 \times 10^{-3}$  (5% TFA). Cleavage of carbamides (**18**), (**20**), (**21**), ureas (**22–25**), amides (**26–29**), and sulfonamides (**30–33**) were studied in the same way.

#### 12.4.1.2 Comparison of TFA Cleavage Reactions

To compare the cleavage kinetics of various resin-bound compounds, the time course curves representing the best fit were plotted in Fig. 12.17.

For resin-bound carbamates (**18–21**), indole linker was the most acid-labile linker for this class of compounds. Rink linker ranked second. Resin (**20**) was cleaved with 0.5% TFA in 20 min. Resin (**21**) was cleaved with 1% TFA in 2 min. Resins (**18**) and (**19**) required higher concentration of TFA. Resin (**18**) was cleaved with 1% TFA in 5 h. Alternatively, resin (**19**) was cleaved with 1% TFA in 12 h and with 5% TFA in only 16 min (not shown).



**Fig. 12.17** Kinetic comparison of TFA cleavage reactions of all 16 resin-bound compounds (**18–33**). The kinetics of cleavage reaction was analyzed as in Figures 12.15 and 12.16. The curves represent the best fit and are displayed for each reaction. The first order reaction rate constants ( $s^{-1}$ ) determined for these reactions are: resins (**18**) (1%),  $1.2 \times 10^{-4}$ ; (**19**) (5%),  $4.8 \times 10^{-3}$ ; (**20**) (0.5%),  $6.5 \times 10^{-3}$ ; (**21**) (1%),

$3.4 \times 10^{-2}$ ; (**22**) (1%),  $1.2 \times 10^{-4}$ ; (**23**) (1%),  $9.5 \times 10^{-5}$ ; (**24**) (0.5%),  $3.0 \times 10^{-2}$ ; (**25**) (0.5%),  $2.5 \times 10^{-3}$ ; (**26**) (5%),  $6.2 \times 10^{-5}$ ; (**27**) (5%),  $1.0 \times 10^{-4}$ ; (**28**) (1%),  $7.9 \times 10^{-5}$ ; (**29**) (1%),  $3.9 \times 10^{-4}$ ; (**30**) (0.5%),  $4.9 \times 10^{-4}$ ; (**31**) (0.5%),  $2.4 \times 10^{-4}$ ; (**32**) (0.5%),  $4.7 \times 10^{-3}$ ; (**33**) (0.5%),  $1.4 \times 10^{-4}$ . Panels are organized as (A) carbamates; (B) ureas; (C) secondary amides; (D) sulfonamides.

For resin-bound ureas (**22–25**), Indole and Rink linkers, generally ranked 1 and 2 in cleavage kinetics, were still the most acid-labile linker for this class of compounds. Resins (**24**) and (**25**) were cleaved with 0.5% TFA in 2 and 23 min, respectively. Resins (**22**) and (**23**) were cleaved with 1% TFA in more than 10 h. The order of cleavage rates is similar to carbamate compounds.

The resin-bound secondary amides (**19–22**) are the most difficult to cleave among the compounds studied. Resin (**29**) was cleaved with 1% TFA in 2 h. Resin (**28**) was cleaved with 1% TFA in 8 h. Resins (**26**) and (**27**) required 5% TFA and 8–15 h. This was the only occasion that linker III was not the most labile bond. Rink linker, the second best in all other series, became the most labile bond.

Resin-bound sulfonamides (**30–33**) were easily cleaved by 1% TFA in 3 min or by 0.5% TFA in 2–7 h. Indole linker was still the most labile linker in this class of compounds.

Comparison of the cleavage kinetics of these 16 compounds in various TFA concentrations, a general trend was observed. Despite some small variations, the general trend is that linker III and IV, ranked 1 and 2, are more labile compared with linkers I and II.

Cleavage conditions we identified were generally milder (e.g. from 5% to 0.5% TFA) than those commonly used and reported in the literatures (e.g. from 10% to

50% TFA). Among various linkers studied in this work, the indole linker [21] was found to be the most suitable linker in terms of cleavage kinetics and actual cost. Rink linker was the second best in term of kinetics. The rate of cleavage of various functional groups linked to the above-mentioned resins was as follows: sulfonamide > carbamate ~ urea > amide. Results from this study demonstrated that optimization of cleavage conditions often led to more suitable conditions and safer release of precious compounds synthesized on a solid support.

#### 12.4.2

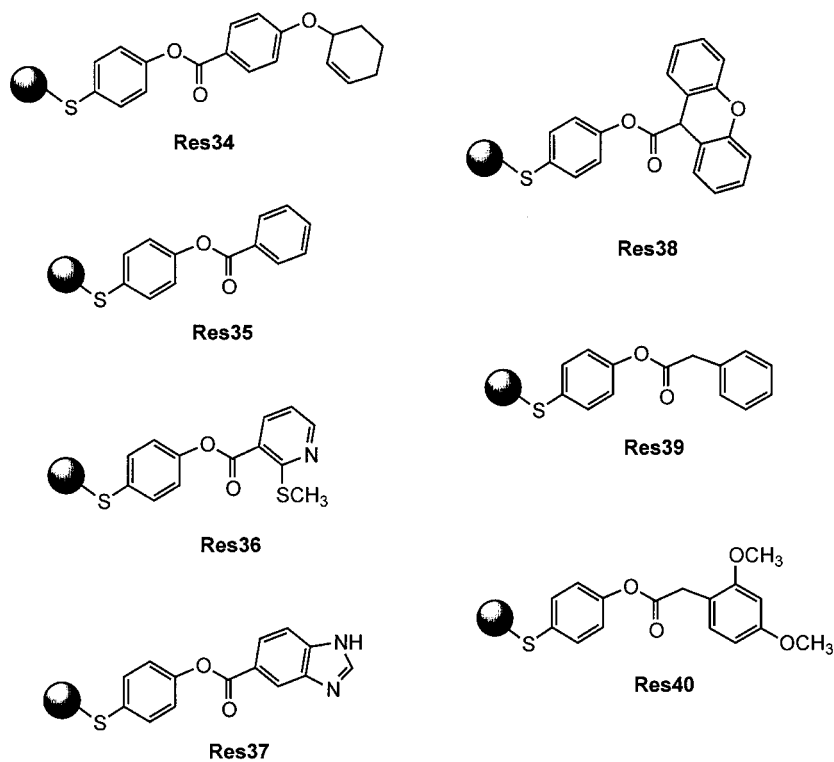
##### Cleavage from Marshall Linker [22]

The Marshall linker [23] has been widely used to synthesize compounds that can be cleaved by primary and secondary amines to afford the corresponding amides. Marshall linker was used in the synthesis of three or more diversity-site libraries because it allowed the addition of one more diversity element at the cleavage step. While the original reported linker [23] involved the oxidation of the linker before cleavage, the efficient release of the resin-bound compounds using nucleophiles from the unoxidized linker has been reported [16, 24]. Similarly to the acid-labile linkers, the kinetics of the cleavage reaction and time required for this reaction directly affect the synthesis efficiency, purity and yield of the final products. A cleavage study was carried out on seven resin-bound thiophenol esters (34–40) on Marshall linker with 3 amines (41–43) (Scheme 12.11 and Tab. 12.4).

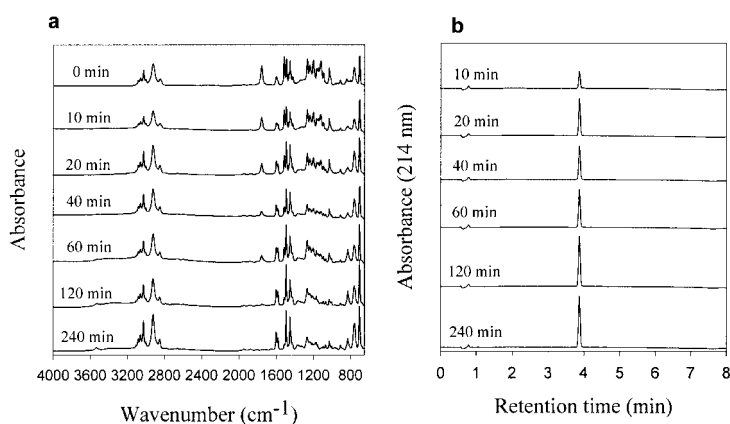
##### 12.4.2.1 Cleavage of Resin-Bound Thiophenol Esters with *n*-Butylamine

The reactivity of seven resin-bound thiophenol esters toward *n*-butylamine (41) varied depending on their structures. The reaction of aromatic thiophenol esters (resins 34–36) took about 24 h to complete as indicated by the complete disappearance of carbonyl band in single bead FTIR spectra. On the other hand, the same reaction with alkyl thiophenol esters (resins 38–40) went to completion in less than 8 hours. The reaction with benzimidazolecarboxylic thiophenol ester (resin 37) was the fastest, finished in 3 h.

Single bead FTIR spectra of resin (40) at various times during the *n*-butylamine cleavage reaction are shown in Fig. 12.18a. The HPLC/UV<sub>214</sub> chromatograms of the cleaved product in solution at various times are shown in Fig. 12.18b. The peak area of the carbonyl band at 1750 cm<sup>-1</sup> and the peak area of the product in UV chromatogram at various times were integrated and plotted against time. Both time courses were analyzed and were found to fit well to a pseudo-first-order rate equation. The rate constant, 5.41 × 10<sup>-4</sup>, was obtained from single bead FTIR analysis by directly on-bead monitoring the disappearance of starting material. The calculated rate constant, 5.39 × 10<sup>-4</sup>, was obtained from HPLC analysis by monitoring the formation of product in solution. Even though this reaction could be monitored by both methods, single bead FTIR method had the advantage of speed and convenience over HPLC/UV or LC/UV/MS for the study of reaction kinetics. Peak area



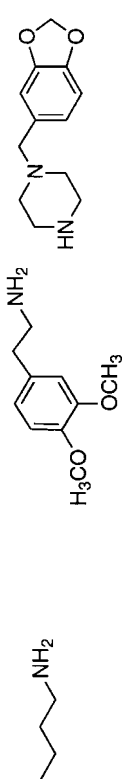
Scheme 12.11

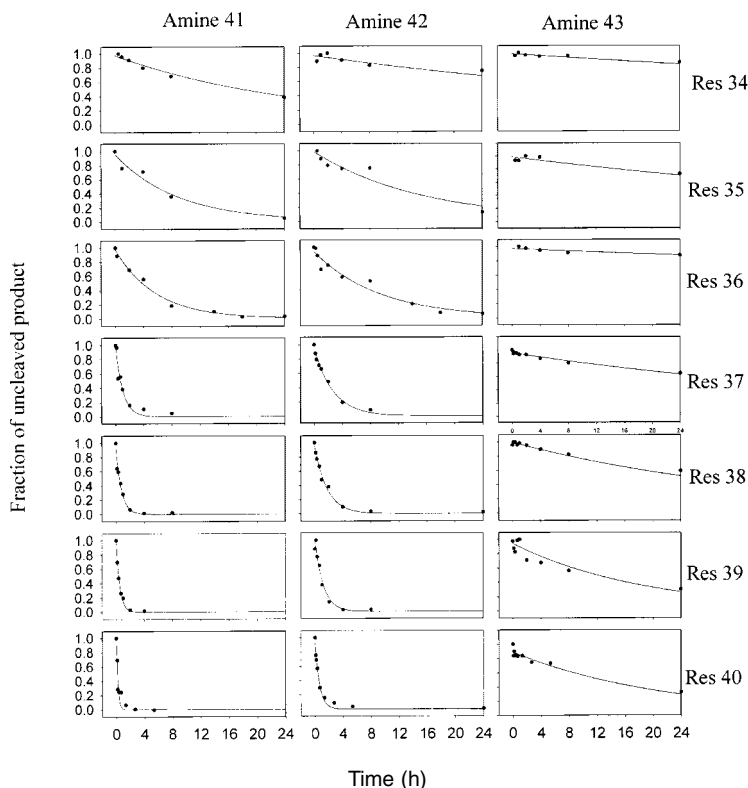


**Fig. 12.18** Single bead FTIR spectra (A) and HPLC/UV chromatograms (B) of resin (**40**) at various times during the *n*-butylamine cleavage reaction.

Tab. 12.4 Summary of IR characteristics and rate constants in Marshall resin cleavage studies.

Resin	O=C str. ( $\text{cm}^{-1}$ )	Rate constant ( $\times 10^6$ )
Aryl esters	res34	1740
	res35	1744
	res35 20 °C	1744
	res35 40 °C	1744
	res35 60 °C	1744
	res35 Ox	1744
	res36	1735
	res37	1757
	res38	1757
	res39	1760
Benzimidazole ester	res 40	1757
Alkyl esters		
Benzimidazole ester		





**Fig. 12.19** The cleavage time courses of all 21 cleavage reactions during a 24 h period and their pseudo-first-order best fit (lines).

integration and kinetic analysis procedures were applied to all resins. The rate constants are listed in Tab. 12.4. The cleavage time courses of all resin-bound phenol esters from single bead FTIR analysis and the best fit are shown in Fig. 12.19.

When *n*-butylamine was used for cleavage, the rate of the alkyl thiophenol esters were approximately 13 times faster than that of the aromatic thiophenol esters. The rate of benzimidazolecarboxylic thiophenol esters was 45 times faster than that of aromatic thiophenol esters and 3 times faster than that of the alkyl thiophenol esters.

#### 12.4.2.2 Cleavage with 3,4-Dimethoxyphenethylamine

The reactivity of seven resin-bound thiophenol esters toward 3,4-dimethoxyphenethylamine (**42**) was consistent with the trend seen in *n*-butylamine cleavage reactions i.e. benzimidazole > alkyl > aromatic. However, the rate constant for the same thiophenol esters with 3,4-dimethoxyphenethylamine was decreased by two to three fold compared with that with *n*-butylamine. The rate constant of ben-

imidazolecarboxylic thiophenol ester was 25 times higher than that of aromatic thiophenol esters and 3 times higher than that of the alkyl thiophenol esters.

#### 12.4.2.3 Cleavage with 1-Piperonylpiperazine

The reactivity of seven resin-bound thiophenol esters toward 1-piperonylpiperazine (**43**) was much lower than that seen with *n*-butylamine, but still had the same trend. The reaction of aromatic thiophenol esters (resins **(34–36)**) did not go to completion after 48 h as indicated by the substantial amount of carbonyl band in FTIR spectra (only 20–50% completion). The same reaction for alkyl thiophenol esters (resins **(38–40)**) went to 70–90% completion during the same time period. The reaction of benzimidazolecarboxylic thiophenol ester (resin **(37)**) went to 90% completion in 48 h.

#### 12.4.2.4 Effect of Temperature on Cleavage Reaction

The rate of a chemical reaction depends on temperature. A rule of thumb for many organic reactions in solution is that a 10 °C change in temperature causes a two- to three-fold change in rate of reaction [25]. To study the temperature dependence of solid-phase reactions, the cleavage reaction of resin **(35)** with *n*-butylamine at 20, 40 and 60 °C were carried out. The cleavage time courses and pseudo-first-order rate fits at these three temperatures are shown in Fig. 12.20. The rate constants from single bead FTIR analysis are listed in Tab. 12.4. Compared with the reaction at 20 °C, the solid-phase cleavage reaction of resin 3b was two times faster at 40 °C and four times faster at 60 °C.

#### 12.4.2.5 Cleavage Rate after Linker Oxidation

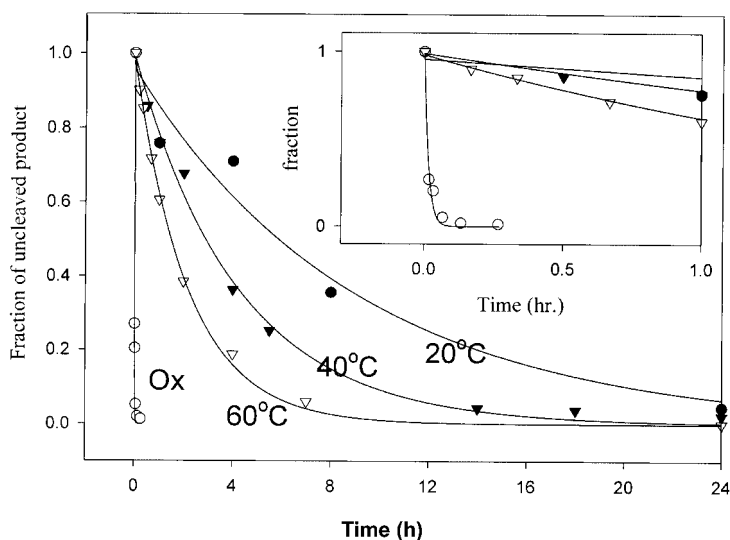
According to Marshall [23] and Beech [26], the oxidation of the thiophenol linker would increase the reaction rate. To study this effect, the linker in resin **(35)** was oxidized to sulfone/sulfoxide using mCPBA. Cleavage reaction of resin **(35)** -OX with *n*-butylamine went to completion in less than 4 min (Fig. 12.20), compared with 24 h needed for this resin under the same conditions without oxidation. The rate constant was determined to be 0.0179, which was a 580-fold increase compared with the unoxidized form. This result indicated that a linker oxidation was preferred for high yield when the products will not be affected by oxidation conditions.

## 12.5

### Concluding Remarks

Solid-phase synthesis has unique advantages in accommodating purification at each individual reaction step without losing compound mass. However, to ensure reaction completion is a challenging task. Our capability to monitor reactions on





**Fig. 12.20** The cleavage time courses of resin (35) at 20 °C (filled circle), 40 °C (filled triangle), 60 °C (triangle) and resin (35)-OX (circle) during a 24 h period and their pseudo-first-order best fit (lines).

polymer support without interrupting reaction has been greatly strengthened in recent years. Single bead FTIR, combustion elemental analysis, and on-bead color test are a few methods discussed in this chapter. The strategic purity improvement by applying high-throughput purification highly depends on the chemical yield of every member in a combinatorial library. To obtain a high chemical yield, three processes should be monitored and optimized:

1. The scaffold loading to the polymer support;
2. The intermediate reaction steps;
3. The cleavage of the final product from polymer support.

To achieve these goals, various reaction-monitoring methods have become an essential part of combinatorial synthesis process.

## 12.6

### Acknowledgements

I am indebted to Liling Fang, Jason Cournoyer, Michael Demee, Pascal Fantauzzi, Lina Liu, and Qing Tang for their valuable contributions to the development and application of reaction monitoring techniques discussed in this chapter.

## 12.7

## References

- 1 R. E. DOLLE, Comprehensive survey of combinatorial library synthesis: 1999. *J. Comb. Chem.* **2000**, 2, 383–433.
- 2 a) C. C. LEZNOFF, *Chem. Soc. Rev.* **1974**, 3, 65. b) I. W. JAMES, *Mol. Diversity* **1996**, 2, 175. c) P. H. H. HERMKENS, H. C. J. OTTENHEIJM, D. REES, *Tetrahedron*, **1996**, 52, 4527. d) R. BROWN, *Contemp. Org. Syn.* **1997**, 4, 216.
- 3 A. W. CZARNIK, S. H. DEWITT, *A Practical Guide to Combinatorial Chemistry*, American Chemical Society, Washington, D. C., **1997**.
- 4 a) W. L. FITCH, A. K. SZARDENINGS, E. M. FUJINARI, *Tetrahedron Lett.* **1997**, 38, 1689. b) E. M. FUJINARI, J. D. MANES, R. BIZANEK, *J. Chromatogr. A* **1996**, 743, 85. c) E. M. FUJINARI, J. D. MANES, *J. Chromatogr. A*, **1994**, 676, 113.
- 5 C. M. BALDINO, *J. Comb. Chem.* **2000**, 2, 89–103.
- 6 B. YAN, *Acct. Chem. Res.* **1998**, 31, 621–630.
- 7 a) B. YAN, in *Analytical methods in combinatorial chemistry*. Ch. 3, Technomic Publishing Co. Lancaster, PA, **2000**. b) B. YAN, G. KUMARAVEL, H. ANJARIA, *et al.*, *J. Org. Chem.* **1995**, 60, 5736–5738. c) B. YAN, G. KUMARAVEL, *Tetrahedron*, **1996**, 52, 843–848.
- 8 a) E. M. CILLI, E. OLIVEIRA, *J. Org. Chem.* **1996**, 61, 8992. b) G. B. FIELDS, C. G. FIELDS, *J. Am. Chem. Soc.* **1991**, 113, 4202.
- 9 a) G. CAINELLI, M. CONTENTO, F. MANOSCALCHI, *et al.*, *J. Chem. Soc. Chem. Commun.* **1982**, 725. b) M. E. WILSON, K. PAECH, W.-J. ZHOU, *et al.*, *J. Org. Chem.* **1998**, 63, 5094. c) T. GROTH, M. GROTH, M. MELDAL, *J. Comb. Chem.* **2001**, 3, 461.
- 10 W. LI, B. YAN, *Tetrahedron Lett.* **1997**, 38, 6485–6488.
- 11 a) J. I. CROWLEY, T. B. HARVEY, III., H. PAPOPORT, *J. Macromol. Sci.-Chem. A* **1973**, 1117. b) J. I. CROWLEY, H. RAPOPORT, *J. Am. Chem. Soc.* **1970**, 92, 6363. c) G. E. MARTIN, M. B. SHAMBHU, S. R. SHAKSHIR, *et al.*, *J. Org. Chem.* **1978**, 43, 4571. d) S. MAZUR, P. JAYALEKSHMY, *J. Am. Chem. Soc.* **1979**, 101, 677. e) S. MAZUR, P. JAYALEKSHMY, *J. Am. Chem. Soc.* **1976**, 98, 6710. f) B. YAN, Q. SUN, *J. Org. Chem.* **1998**, 63, 55–58.
- 12 B. YAN, Q. TANG, *Ind. Eng. Chem. Res.* **2003**, in press.
- 13 F. RAMIREZ, N. B. DESAI, N. MCKELVIE, *J. Am. Chem. Soc.* **1962**, 84, 1745.
- 14 B. YAN, C. F. JEWELL, JR., S. W. MYERS, *Tetrahedron*, **1998**, 54, 11755.
- 15 T. CHRISTENSEN, *Acta Chemica Scandinavica B*, **1979**, 33, 763.
- 16 C. R. JOHNSON, B. ZHANG, P. FANTAUZZI, *et al.*, *Tetrahedron* **1998**, 54, 4097.
- 17 B. YAN, W. LI, *J. Org. Chem.* **1997**, 62, 9354.
- 18 J. J. COURNOYER, T. KSHIRSAGAR, P. P. FANTAUZZI, *et al.*, *J. Combi. Chem.* **2002**, 4, 120–124.
- 19 B. YAN, L. LIU, C. A. ASTOR, *et al.*, *Anal. Chem.* **1999**, 71, 4564–4571.
- 20 B. YAN, N. NGUYEN, L. LIU, *et al.*, *J. Comb. Chem.* **2000**, 2, 66–74.
- 21 K. G. ESTEP, C. E. NEIPP, L. M. S. STRAMIELLO, *et al.*, *J. Org. Chem.* **1998**, 63, 5300.
- 22 L. FANG, M. DEMEE, T. SIERRA, *et al.*, *J. Combi. Chem.* **2002**, 4, 362–368.
- 23 D. L. MARSHALL, I. E. LIENER, *J. Org. Chem.* **1970**, 35, 867–868.
- 24 a) J. G. BREITENBUCHER, C. R. JOHNSON, M. HAIGHT *et al.*, *Tetrahedron Lett.* **1998**, 39, 1295–1298. c) P. P. FANTAUZZI, K. M. YAGER, *Tetrahedron Lett.* **1998**, 39, 1291–1294. d) J. G. BREITENBUCHER, H. C. HUI, *Tetrahedron Lett.* **1998**, 39, 8207–8210.
- 25 A. STREITWIESER, JR., C. HEATHCOCK, *Introduction to Organic Chemistry*, 3rd Edn Macmillan Publishing Company, page 54, **1985**.
- 26 C. BEECH, J. COOPE, G. FAIRLEY, *et al.*, *J. Org. Chem.* **2001**, 66, 2240–2245.

## 13

# Polymeric Membranes for Integrated Reaction and Separation

J. T. F. KEURENTJES

### 13.1

#### Introduction

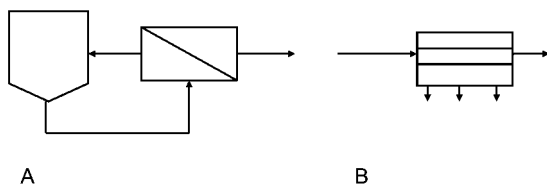
Membranes have found application for a wide variety of separations in chemical, biochemical, environmental and petrochemical processes. The first large-scale applications of membrane technology were in brackish water desalination using reverse osmosis and hemodialysis. Depending on the type of feed stream, rejection characteristics and the driving force applied, the range of membrane processes can be classified as given in Tab. 13.1. These range from filtration processes (microfiltration, ultrafiltration, nanofiltration and reverse osmosis), gas and vapor permeation, pervaporation to electromembrane processes like electrodialysis, membrane electrolysis and bipolar membrane processes. Additionally, microporous membranes have been used as a support in membrane contactors, also known as “pertraction”, for solvent extraction and gas absorption.

For the integration of reaction and separation, both polymeric and inorganic membranes have been used. In this chapter, the focus will be entirely on the application of polymeric membranes. For integrated reaction–separation systems, membranes have been used as an add-on to a reactor, i.e. a reaction followed by a membrane separation, as well as in an integrated mode, the latter also known as membrane reactors (Fig. 13.1). Because a wide variety of combinations is possible, this has led to a broad range of processes [1, 2]. Integrated systems provide several advantages over a sequential reaction–separation system. These include increased reaction rates, reduced by-product formation, a lower energy requirement and the possibility of heat integration. In general, this leads to processes that can be operated with a high degree of flexibility.

In the following, a number of integrated reaction–separation systems will be discussed, with emphasis on the application of polymeric membranes. As a result, the systems discussed will be limited to relatively low temperatures, typically below 120 °C. In Section 13.2, applications of membranes in chemical synthesis will be described. Subsequently, in Section 13.3 various examples of membrane bioreactors will be discussed.

**Tab. 13.1** Types and characteristics of widely practiced membrane processes.

<b>Process</b>	<b>Driving force</b>	<b>Applications (examples)</b>
Reverse osmosis (RO)	pressure difference	desalination of sea/brackish water concentration of whey and fruit juice waste water treatment
Nanofiltration (NF)	pressure difference	removal of small organics mono/divalention separation
Ultrafiltration (UF)	pressure difference	protein recovery purification of polymer solutions
Microfiltration (MF)	pressure difference	filtration of cell suspensions blood plasma recovery
Gas Separation (GS)	pressure difference	oxygen enriched air purification of natural gas
Pervaporation (PV)	partial vapor pressure difference	separation of isomers dehydration of organic liquids
Electrodialysis (ED)	electrical potential	demineralization removal of metals from waste water
Dialysis	concentration difference	purification of polymer solutions hemodialysis

**Fig. 13.1** Two basic types of integrated reactor–separator systems. In A the membrane is used as an add-on to the reactor, whereas in B the membrane is fully integrated.

## 13.2

### Membrane Systems for Improved Chemical Synthesis

#### 13.2.1

##### Efficient Catalyst Recycle

For the production of chemicals, food additives and pharmaceutical products, homogeneous catalysis offers some attractive features such as a high selectivity and activity, e.g. in asymmetric synthesis. However, since most homogeneous catalysts are relatively expensive, their current industrial application is limited [3]. On the other hand, heterogeneous catalysts can easily be separated from the products and can be recycled efficiently. Membrane separations with emphasis on nanofiltration and ultrafiltration will allow for a similar recyclability of homogeneous catalysts, which is important both from an environmental as well as a commercial

**Tab. 13.2** Summary of homogeneous catalyst recycling using membrane technology [3].

Reaction type	MW	Solvent <sup>a)</sup>	Membrane <sup>b)</sup>	Retention	Ref.
ZnEt <sub>2</sub> addition	9600	<i>n</i> -hexane	PAH-20	0.998	6
Reduction ketones	13800	THF	MP F-50	>0.98	7, 8
<i>Ibid.</i>		THF	MPF-50	>0.985	9, 10
Asymm. hydrogenation	>7460	water	YC05	0.991	11
Dihydroxylation	>20000	acetone/H <sub>2</sub> O	unknown	n.d.	12
Hydroformylation	>3×10 <sup>5</sup>	MeOH	PES	0.998	13
Kharash addition	1570	CH <sub>2</sub> Cl <sub>2</sub>	MPF-50	0.974	14
<i>Ibid.</i>	4940	CH <sub>2</sub> Cl <sub>2</sub>	MPF-50	0.998	14
Hydrovinylation	2800	CH <sub>2</sub> Cl <sub>2</sub>	MPF-60	>0.85	15, 16
Allylic alkylation	8252	THF	MPF-60	0.981	17
Allylic amination	>5000	CH <sub>2</sub> Cl <sub>2</sub>	MPF-60	>0.985	18
Olefin metathesis	3230	C <sub>2</sub> H <sub>4</sub> Cl <sub>2</sub>	MPF-60	n.d.	19
Allylic substitution	10200	CH <sub>2</sub> Cl <sub>2</sub>	PAH-5	0.992	20, 21
<i>Ibid.</i>	10200	CH <sub>2</sub> Cl <sub>2</sub>	MPF-50	0.999	20, 21
Asymm. hydrogenation	7550	MeOH	Centricon-3	n.d.	22
Kharash addition	2060	CH <sub>2</sub> Cl <sub>2</sub>	MPF-60	n.d.	23
Allylic amination	>40000	CH <sub>2</sub> Cl <sub>2</sub>	MPF-60	>0.994	24
Asymm. hydrogenation	929	MeOH	MPF-60	0.97	4
<i>Ibid.</i>	723	MeOH	MPF-60	0.98	4

a) Solvent in which the retention is determined. This solvent is not necessarily the solvent used for catalysis.

b) PAH-20 and PAH-5 (MWCO unknown) Hoechst Nadir; MPF-50 (MWCO=700) and MPF-60 (MWCO=400), Koch Membrane Systems; YC05 (MWCO=500), Millipore; Centricon-3 (MWCO=3000), Millipore; PES (MWCO=50000) Sartorius.

point of view. Most common homogeneous catalysts have molecular weights in the range of 100–1000. Although direct separation from the reaction mixture is sometimes possible [4], the general approach followed in this field is enlargement of the catalysts to allow for a relatively easy separation. Both polymers and dendritic structures have shown to be effective for this. The examples found in the literature are summarized in Tab. 13.2.

Kragl *et al.* [5, 6] have used a copolymer of 2-hydroxyethyl methacrylate and octadecyl methacrylate (MW=96000) coupled to a low molecular weight ligand (*α,α*-diphenyl-L-prolinol) for the enantioselective addition of diethylzinc to benzaldehyde. This polymer-enlarged catalyst system could be retained for >99.8% using a Hoechst Nadir aromatic polyamide UF membrane. Polymer-enlarged oxazaborolidines have been used for enantioselective reductions of various ketones using a solvent-stable SelRo nanofiltration membrane from Koch. The same oxazaborolidine catalyst has also been bound to polysiloxanes and polystyrenes.

The incorporation or complexation of transition metal fragments by dendrimers has led to a broad spectrum of metallodendrimers. Dendrimers are well-defined branched structures (Fig. 13.2). The dimensions of a dendrimer can easily be adjusted by changing its generation, which can be very practical for their application

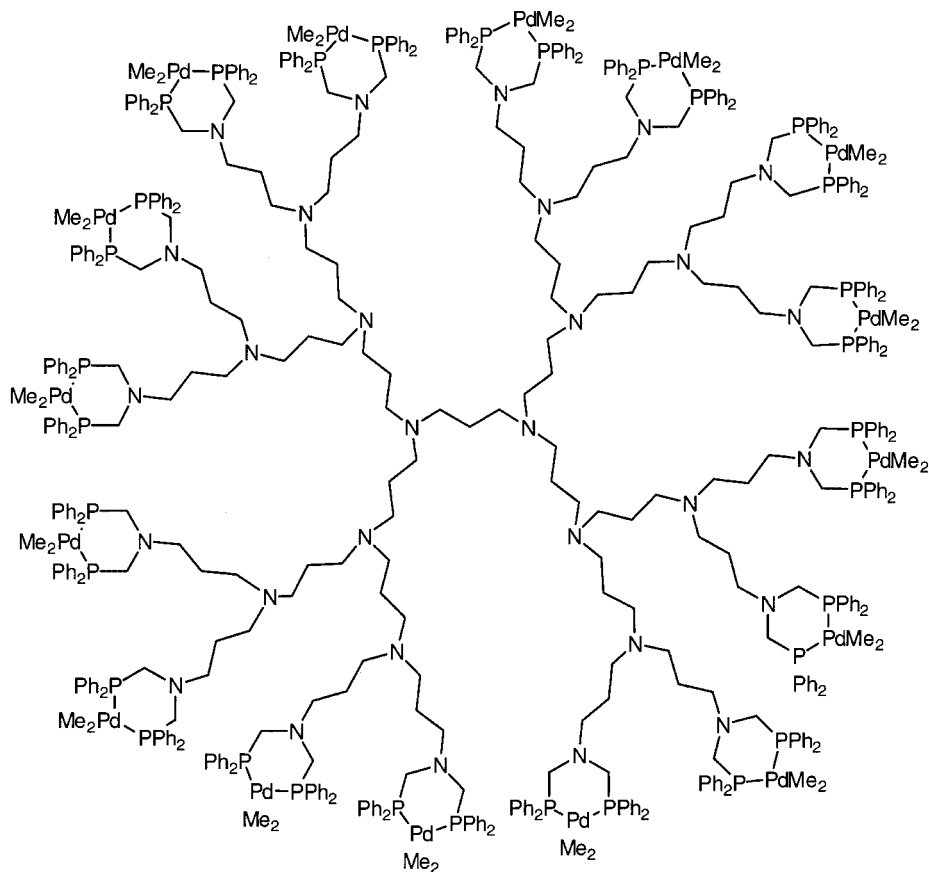


Fig. 13.2 Phosphine-functionalized metallodendrimer [3].

in a membrane separation. Various dendrimers have been applied as a catalyst support, including carbosilane dendrimers [25–27], 1,4-diaminobutane phosphino dendrimers [20, 21] and poly(propylene imine) dendrimers [29, 30].

Seen the list of demonstrated applications, numerous possibilities exist for the integration of homogeneous catalysis and a membrane separation. A complicating factor, however, is the relatively limited availability of solvent-resistant membranes. This will require a substantial development effort to obtain more solvent-stable membranes, including both polymeric and inorganic ones.

### 13.2.2

#### Pervaporation Membranes for Shifting Chemical Equilibrium

Pervaporation has become one of the standard membrane technologies with a large number of realized industrial applications. Pervaporation is used for the dehydration of organic compounds, the separation of organic compounds from aqueous solu-

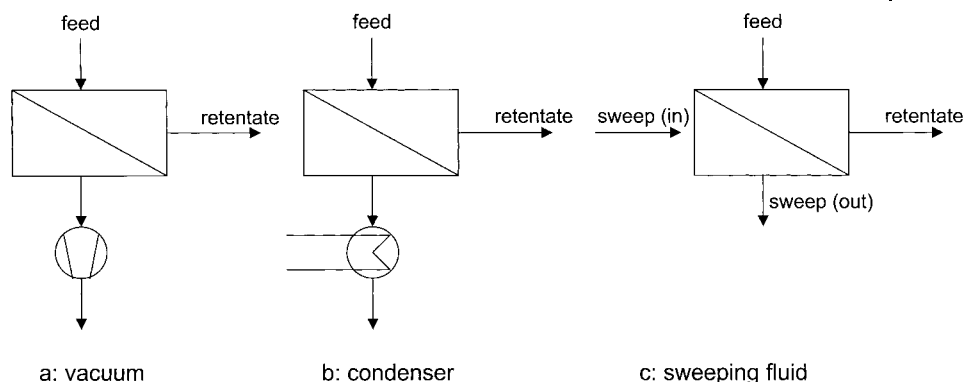


Fig. 13.3 Reduction of permeate-side partial vapor pressure [31].

tions, and the separation of organic mixtures. In pervaporation a liquid feed mixture is in contact with one side of the membrane. The separation is determined by the physical-chemical affinity between permeating species and the membrane, i.e. sorption and solubility. The driving force for transport across the membranes is created by a gradient in partial vapor pressure of the components between the feed and the permeate side, which is maintained by a reduction of the permeate-side vapor pressure, either by applying a vacuum or by using a sweep gas (Fig. 13.3).

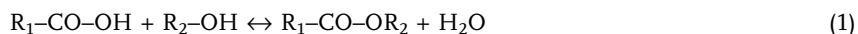
The membranes used for pervaporation are similar to reverse osmosis membranes, i.e. both are composite membranes consisting of a very thin dense permselective film on top of a nonselective porous support. In pervaporation, however, the membrane is highly swollen at the feed side and relatively “dry” at the permeate side. Two different types of pervaporation membranes based on polymeric materials were developed at about the same time in the early 1980s [31]:

1. Hydrophilic membranes with a preferential permeation of water are mainly used for the dehydration of organic solvents with an emphasis on azeotropic mixtures. Membranes for the removal of small alcohol molecules like methanol and ethanol are also of a hydrophilic nature.
2. Organophilic membranes with a preferential permeation of nonpolar compounds are used for the removal of volatile organic components from aqueous and gas streams.

The selective dense layer of hydrophilic membranes is made from different polymers with a high affinity for water. These polymers contain ions, oxygen functions like hydroxyl, ester, ether or carboxylic moieties, or nitrogen as imino or imido groups. Preferred hydrophilic polymers are polyvinylalcohol (PVA) [32], polyimides, cellulose acetate (CA) or natural polymers like chitosan [33] or alginates. Organophilic membranes usually consist of crosslinked silicones, mostly polydimethyl siloxane (PDMS) or polymethyl octyl siloxane (POMS).

In many chemical reactions like esterification, acetalisation, ketalisation or etherification, water is produced as an unwanted by-product. As esterifications are

equilibrium reactions, high yields can be obtained by adding an excess of one reactant or by constant removal of the produced water from the reaction mixture in order to shift the reaction to the product side [34, 35]:



Pervaporation forms an interesting alternative to separate water from the reaction mixture instead of distillation, especially in systems with azeotropes or low boiling reactants. Some examples of pervaporation-assisted esterifications are given in Tab. 13.3. Additionally, pervaporation can also be used for the production of polycondensation esters [36, 37].

Regarding the various options for process layouts, three basic designs can be distinguished (Fig. 13.4) [46]. In the first layout, the system consists of a reactor, a distillation column and a PV unit containing hydrophilic PVA membranes. In the reactor ethanol and an acid react to form the ester and water. The vapor phase containing ethanol and water is separated in the distillation/PV section up to 98% of ethanol. The recovered ethanol is then recycled to the reactor. In the second layout, the liquid reaction mixture is circulated over the membrane. This layout results in a high conversion rate at low energy consumption. Additionally, the ethanol-water azeotrope represents no limitation in this setup. Depending on the membrane selectivity, however, an additional treatment of the permeate may be required. As the reacting mixture is in direct contact with membrane, this requires the membrane to be stable in this environment. Inorganic membranes may be better suited for this way of operation, because of their increased stability compared with polymeric ones, especially when the formation of polyesters is in-

Tab. 13.3 Overview of pervaporation-assisted esterifications [2].

Reaction	Membrane material	Temp. (°C)	Ref.
methanol + acetic acid $\leftrightarrow$ methyl acetate + H <sub>2</sub> O	Nafion	25	38
ethanol + acetic acid $\leftrightarrow$ ethyl acetate + H <sub>2</sub> O	PVA	90	39
ethanol + acetic acid $\leftrightarrow$ ethyl acetate + H <sub>2</sub> O	Nafion 117	90	39
ethanol + acetic acid $\leftrightarrow$ ethyl acetate + H <sub>2</sub> O	Nafion 324	90	39
ethanol + acetic acid $\leftrightarrow$ ethyl acetate + H <sub>2</sub> O	PVA	80	40, 41
ethanol + acetic acid $\leftrightarrow$ ethyl acetate + H <sub>2</sub> O	PEI	75	42
ethanol + oleic acid $\leftrightarrow$ oleic acid ethyl ester + H <sub>2</sub> O	PEI	60	42
1-propanol + propionic acid $\leftrightarrow$ propionic acid propyl ester + H <sub>2</sub> O	PVA	50	43
1-propanol + propionic acid $\leftrightarrow$ propionic acid propyl ester + H <sub>2</sub> O	PVA	50	44
1-propanol + propionic acid $\leftrightarrow$ propionic acid propyl ester + H <sub>2</sub> O	PSSH-PVA	50	44
2-propanol + propionic acid $\leftrightarrow$ propionic acid propyl ester + H <sub>2</sub> O	PVA	55	43
2-propanol + propionic acid $\leftrightarrow$ propionic acid propyl ester + H <sub>2</sub> O	PVA	65	43
2-propanol + propionic acid $\leftrightarrow$ propionic acid propyl ester + H <sub>2</sub> O	PEI	85	42
1-butanol + acetic acid $\leftrightarrow$ butyl acetate + H <sub>2</sub> O	PVAc	155	45
1-butanol + acetic acid $\leftrightarrow$ butyl acetate + H <sub>2</sub> O	Nafion	25	38



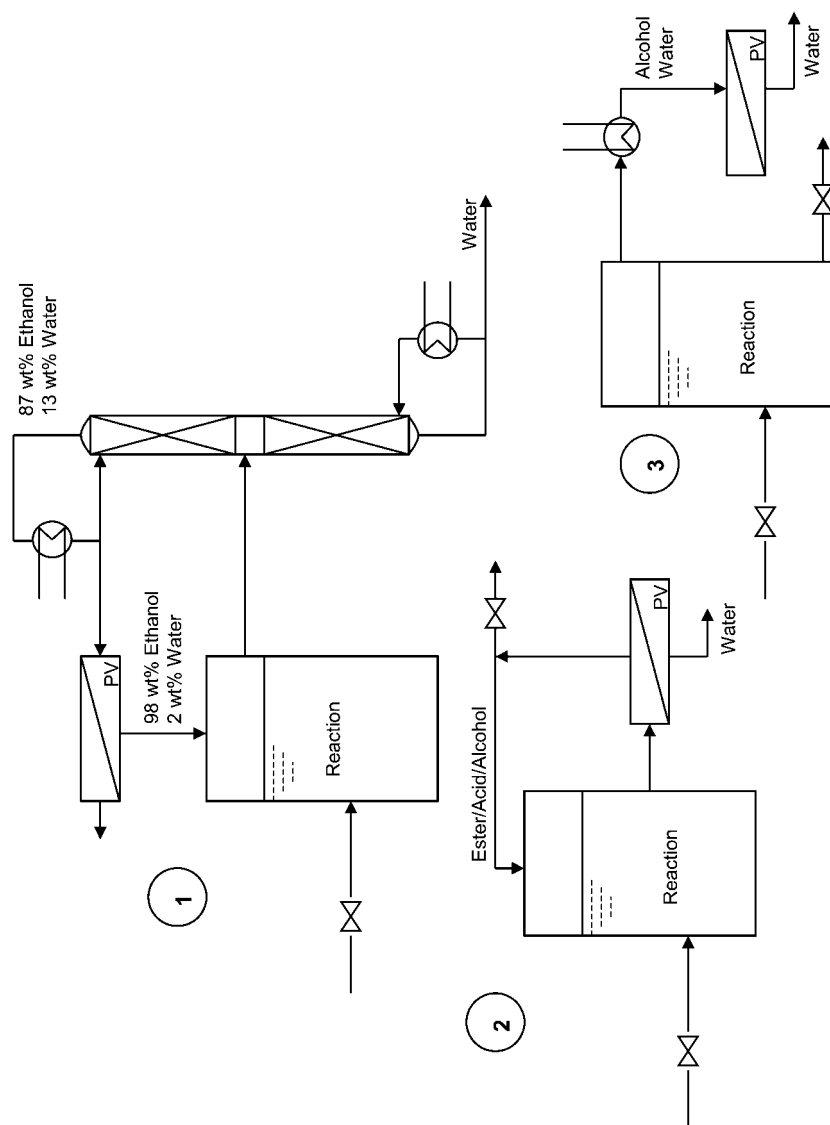


Fig. 13.4 Alternative process layouts for batch esterification by a pervaporation-reactor hybrid process [34].

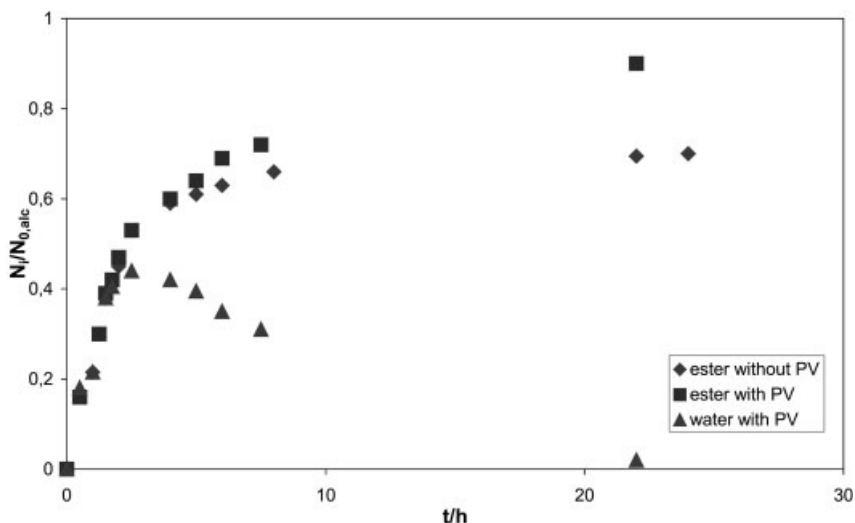
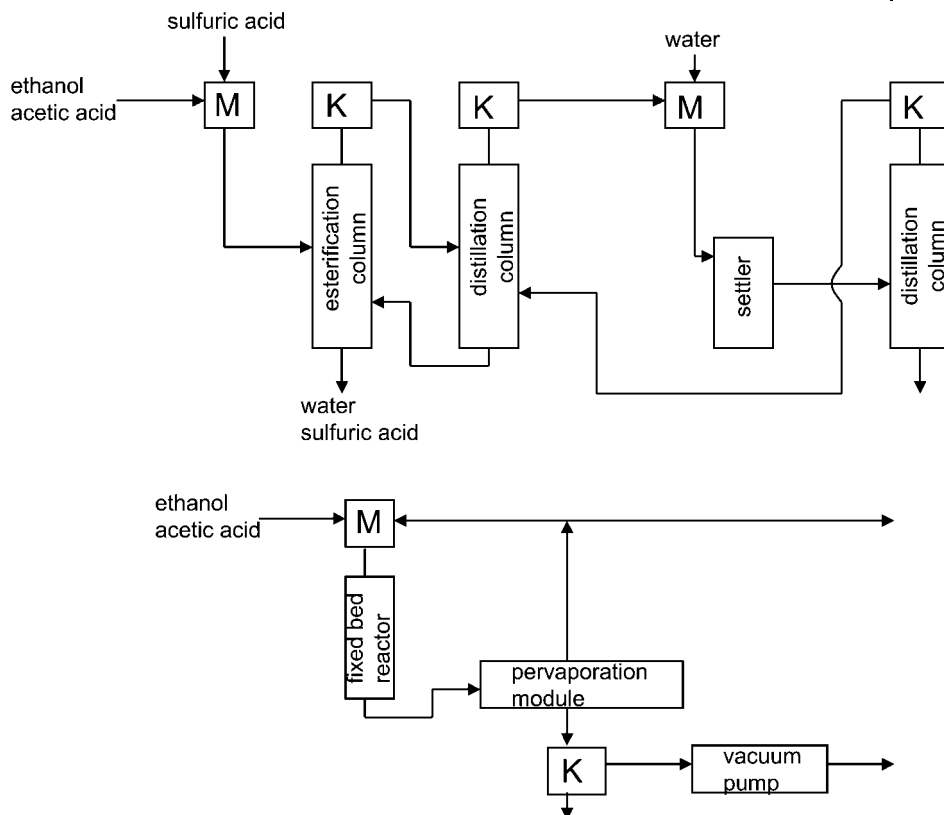


Fig. 13.5 Concentration profiles in the pervaporation-assisted esterification of 1-propanol and propionic acid.

volved. In the third layout, water is removed from the vapor in equilibrium with the reaction mixture. As the membrane is not exposed to the acid and ester, the membrane will show an extended lifetime. From an economic comparison, it follows that the second layout is the most effective with respect to energy costs, as only 7% of the energy requirement of the conventional process is required.

A process performance study has been conducted by David *et al.* [47] taking the coupling of pervaporation with the esterification reactions of 1-propanol and 2-propanol with propionic acid as a model system. Toluene sulfonic acid was applied as the homogeneous acid catalyst. A PVA-based composite membrane from GFT was used. Fig. 13.5 shows the comparison between the esterification reaction with and without pervaporation. Without pervaporation, the conversion factor reaches a limit, which corresponds to the equilibrium of the esterification reaction. Coupling of the esterification to pervaporation allows the reaction to reach almost complete conversion.

Based on experimental results and a model describing the kinetics of the system, it has been found that the temperature has the strongest influence on the performance of the system as it affects both the kinetics of esterification and of pervaporation. The rate of reaction increases with temperature according to Arrhenius law, whereas an increased temperature accelerates the pervaporation process also. Consequently, the water content decreases much faster at a higher temperature. The second important parameter is the initial molar ratio of the reactants involved. It has to be noted, however, that a deviation in the initial molar ratio from the stoichiometric value requires a rather expensive separation step to recover the unreacted component afterwards. The third factor is the ratio of membrane area to reaction volume, at least in the case of a batch reactor. For continuous opera-



**Fig. 13.6** Process scheme of the conventional reaction-distillation process (top) compared with the membrane-assisted esterification (bottom) for the production of ethyl acetate [48].

tion, the flow rate should be considered as the determining factor for the contact time of the mixture with the membrane and subsequently the permeation flux.

The catalytic esterification of ethanol and acetic acid to ethyl acetate and water has been taken as a representative example to emphasize the potential advantages of the application of membrane technology compared with conventional distillation [48], see Fig. 13.6. From the McCabe-Thiele diagram for the separation of ethanol-water mixtures it follows that pervaporation can reach high water selectivities at the azeotropic point in contrast to the distillation process. Considering the economic evaluation of membrane-assisted esterifications compared with the conventional distillation technique, a decrease of 75% in energy input and 50% lower investment and operation costs can be calculated. The characteristics of the membrane and the module design mainly determine the investment costs of membrane processes, whereas the operational costs are influenced by the lifetime of the membranes.

The esterification of tartaric acid with ethanol using pervaporation has also been studied [35]. The equilibrium composition could be shifted significantly to-

wards the final product diethyltartrate by integration of pervaporation with hydrophilic PVA-based composite membranes in the process. Based on the kinetic parameters, an optimum membrane surface area could be calculated which results in a minimal reaction time for the esterification reaction. In the case that the membrane surface area to volume ratio is too low, the water removal is rather slow, whereas at high surface area to volume ratios significant amounts of ethanol are removed as well (Fig. 13.7).

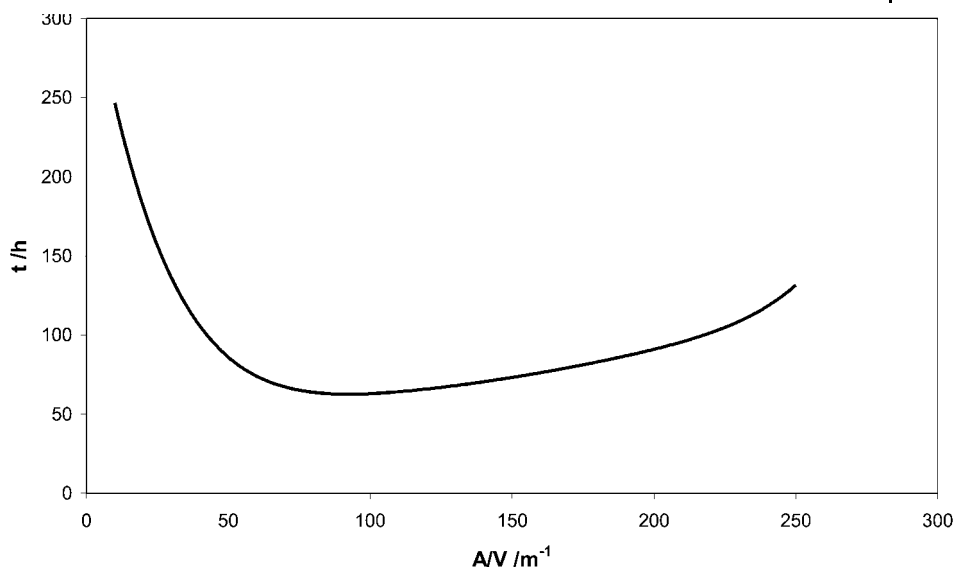
### 13.3

#### Membrane Bioreactors

In the development of cell or enzyme-based processes, many process configurations exist, including batch, fed batch and continuous operation. In general, the conversion and the separation processes (downstream processing) are regarded as separate units, and most industrial processes are based on this approach. In the last decades, however, more attention is paid to the integration of conversion and separation, leading to the development of membrane bioreactors [49, 50], and some of these concepts have reached an industrial scale. The membranes used for this type of reactors are almost exclusively polymeric, as temperatures seldomly exceed 100 °C for obvious reasons.

Generally, a distinction can be made between membrane bioreactors based on cells performing a desired conversion and processes based on enzymes. In cell-based processes, bacteria, plant and mammalian cells are used for the production of (fine) chemicals, pharmaceuticals and food additives or for the treatment of waste streams. Enzyme-based membrane bioreactors are typically used for the degradation of natural polymeric materials like starch, cellulose or proteins or for the resolution of optically active components in the pharmaceutical, agrochemical, food and chemical industry [50, 51]. In general, only ultrafiltration (UF) or microfiltration (MF)-based processes have been reported and little is known on the application of reverse osmosis (RO) or nanofiltration (NF) in membrane bioreactors. Additionally, membrane contactor systems have been developed, based on microporous polyolefin or teflon membranes [52–55].

Two types of membrane bioreactors can be distinguished: bioreactors with an external membrane system and bioreactors in which the membrane unit is integrated (this is similar to the options depicted in Fig. 13.1). In the bioreactor with the external unit, liquid is pumped from the reactor to the membrane unit where either the product or an inhibiting component can be removed. The retentate is returned to the reactor. A bleed is applied which can serve as a drain to remove biologically inactive material or biomass when it is the main product of the process. The advantage of this bioreactor is that the membrane process can be optimised separately. In the bioreactor with an integrated membrane unit the focus has been on the application of tubular and hollow fiber geometries, for which lumen-side as well as shell-side feeding can be applied. In both cases the biologically active material is present at the shell side. With lumen-side-feeding, feed



**Fig. 13.7** Required reaction time for 95% conversion in the pervaporation-assisted esterification of tartaric acid with ethanol at different membrane area per reactor volume [35].

components diffuse through the membrane into the biologically active region where products are formed. The products diffuse from the shell side back into the lumen side and are removed from the reactor. Similar to this, a shell-side-fed process can be used in which the biologically active material is fixed in the lumen and diffusion is the major transport mechanism for substrate into and product from the lumen. In the case of shell-side-feeding, the feed is forced through the biologically active region and through the membrane. Product is removed via the lumen region.

#### 13.3.1

##### Lactic Acid Production

Lactic acid is one of the major organic acids produced by fermentation. Annually about 35 000 tonnes are produced this way [56]. The work on NF-based membrane fermentors for the production of organic acids has been started with the observation that lactic acid retention of RO membranes shows a strong pH-dependence [57–59]. For selective removal of lactic acid a low pH is necessary, however, this reduces the lactic acid productivity to about  $1 \text{ g l}^{-1}\text{h}^{-1}$ . Compared with UF- and MF-based membrane fermentors this productivity is at least a factor of 10 lower [60] but product purity is much improved. Despite the higher product purity, the lactic acid concentration in the permeate ( $10 \text{ g l}^{-1}$ ) is at least a factor of 4 lower than in the case of UF- and MF-based membrane fermentors. This lower concentration requires additional energy input for product concentration, which

makes the process economically not viable. To obtain a better understanding of the organic acid separation process, lactic acid removal from model solutions and fermentation broths using RO and NF has been studied [61, 62], showing that the separation process can be fully described by considering dissociated and undissociated lactic acid as individually permeating species. These insights have been used for the development of a NF-membrane reactor. Despite improvements in membrane process performance with respect to energy consumption, the productivity and the lactic acid concentrations of the NF-membrane fermentor are similar to the RO-membrane reactor [63].

An improvement of the productivity of the NF-based process to  $7.1 \text{ g l}^{-1}\text{h}^{-1}$  is obtained by running the process semi-continuously [64]. Final lactic acid concentrations in the permeate can reach values between 10 and  $60 \text{ g l}^{-1}$ . The higher values are at the lower limit of concentrations found in UF- and MF-based processes [60]. Based on these data, a three-step repetitive process has been proposed [64]. The first step is the cell multiplication step during which pH can be controlled, the second step is an acid production step, followed by NF. In this approach a constant pH is assumed during each separate process step. However, other strategies in the acidification stage, which make use of natural acidification by the lactic acid bacteria are also possible.

### 13.3.2

#### Bioreactors for Environmental Applications

Biotreatment of large air streams in membrane contactors has been evaluated widely (Tab. 13.4 [65]). The removal of organic compounds (e.g. propylene, dichloromethane, etc.) and inorganic substances ( $\text{SO}_2$ ,  $\text{NO}_x$  etc.) has proven to be highly efficient in membrane contactors. The gas stream to be treated is led on one of the membranes, whereas an appropriate aqueous solution containing one single or a mixture of bacteria is circulated on the other side. This allows for an easy adjustment of conditions (pH and nutrients). The bacteria used can either grow as a film onto the membrane surface or can be homogeneously dispersed in the liquid. This approach has led to large-scale operations, e.g. for the treatment of traffic tunnel vent streams.

Rautenbach and Mellis [75] describe a process in which a UF-membrane fermentor and a subsequent NF-treatment of the UF-permeate are integrated. The retentate of the NF-step is recycled to the feed of the UF-membrane reactor (Fig. 13.8). This process has been commercialised by Wehrle-Werk AG as the Biomembrat<sup>®</sup>-plus system [76] and is well suited for the treatment of effluents with recalcitrant components. The process also allows for an additional treatment process, like adsorption or chemical oxidation of the NF-retentate, before returning the NF-retentate to the feed of the UF-membrane fermentor. Usually, the efficiency of these treatment processes is increased as the NF-retentate contains higher concentrations of these components. Pilot tests with landfill leachates [75] and wastewater from cotton textile and tannery industry have been reported [77]. An overview of chemical oxygen demand (COD) reduction and COD concentrations in the permeate are shown in

Tab. 13.5. This reduction rate is based on water inlet concentration and NF-permeate outlet concentration. It has to be kept in mind, however, that part of the COD will also be removed from the system by excess sludge, so that the reduction rate numbers are not indicative for the COD conversion rate. COD reduction in the treatment of industrial wastewater is 95%, while in the treatment of landfill leachates lower elimination rates have been found. However, in the treatment of landfill leachates, the application of NF as the second treatment step increased the COD reduction rate by 9 to 17% compared with the process without NF.

Tab. 13.4 Membrane bioreactors for biological waste gas treatment [65].

<i>Compound to be removed from air</i>	<i>Conc. [ppm]</i>	<i>Type of membrane</i>	<i>Nutrient supply in liquid</i>	<i>Bio-film</i>	<i>Inoculant</i>	<i>Ref.</i>
Xylenes	30–140	Silicone; tubes	Minerals	Yes	Sludge	66
<i>n</i> -Butanol	40–180	Silicone; tubes	Minerals	Yes	Sludge	66
Dichloromethane	60–220	Silicone; tubes	Minerals	No	Sludge	66
Toluene	20	HM <sup>a)</sup> ; sheet	Minerals	NA <sup>b)</sup>	<i>Pseudomonas</i> GJ40	67
Dichloromethane	47	HM; sheet	Minerals	NA	Strain DM21	67
Toluene	56	HM; sheet	Minerals	Yes	<i>Pseudomonas</i> GJ40	68
Dichloromethane	69	HM; sheet	Minerals	Yes <sup>c)</sup>	Strain DM21	68
<i>n</i> -hexane	32	Silicone; tubes <sup>d)</sup>	Minerals	?	?	69
Toluene	32	Silicone; tubes	Minerals	?	?	69
NO	5	H; sheet	Alcohols, minerals	Yes	<i>Methylobacter</i>	70
Mixture	'low'	HM; sheet	Minerals	Yes	Various strains	71
Dichloroethane	150	Silicone; spiral wound	Minerals <sup>e)</sup>	Yes	<i>Xanthobacter</i> GJ10	72
Propene	250–300	HM; sheet	Minerals	Yes	<i>Xanthobacter</i> Py2	73
Trichloroethene	20	Polysulfone; fibers	Acetate, minerals <sup>f)</sup>	Yes	Sludge	74
Propene	330–2700	HM; fibers	Minerals	Yes	<i>Xanthobacter</i> Py2	68

a) H, hydrophobic material; M, microporous material.

b) Experiments lasted less than 1 day.

c) Severe sloughing observed after 4 days.

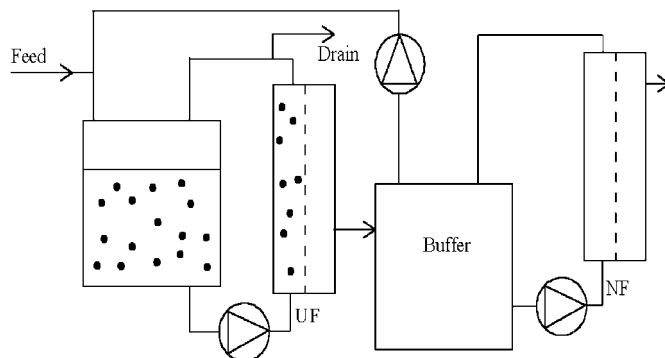
d) Reactor in a combination of a membrane bioreactor and a bubble-column and was designed for simultaneous degradation of both hydrophilic and hydrophobic contaminants from the gas phase.

e) Gas phase did not contain oxygen.

f) Liquid phase was kept anaerobic.

**Tab. 13.5** Percentage COD elimination and NF-effluent concentrations for various applications of the Biomembrat®-plus process

Application	COD elimination [%]	COD concentration NF-effluent [mg/l]	Reference
Landfill leachate	56–86	<200	75
Cotton textile industry waste	95	15	77
Tannery waste water	95	119	77

**Fig. 13.8** Flow diagram of the Biomembrat®-plus process [75].

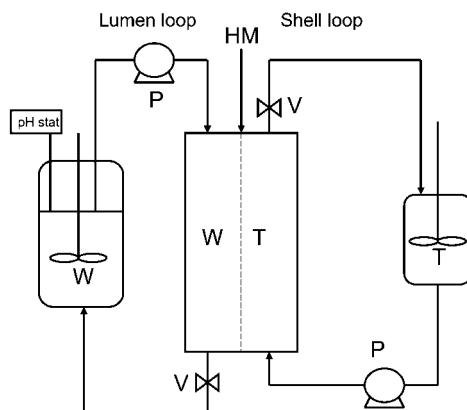
## 13.3.3

**Enzyme Reactors**

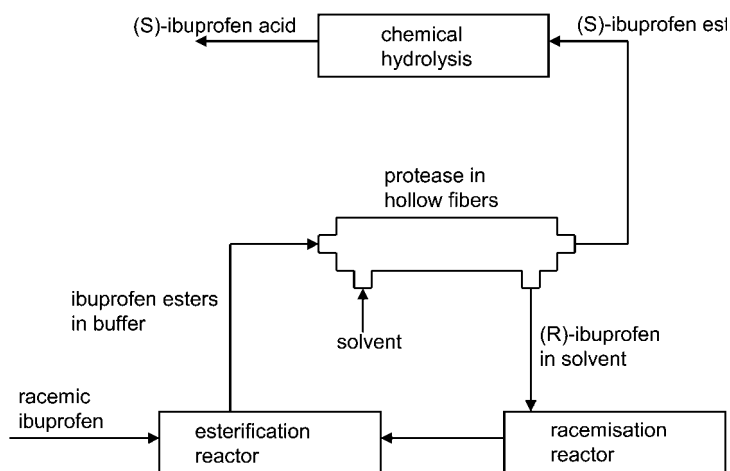
The main application of membrane reactors for liquid–liquid systems is based on intimate phase contacting, without the formation of an emulsion, thus avoiding troublesome phase splitting afterwards. Microporous membranes have proven to be particularly useful for this type of applications, since the two immiscible liquids can be kept on two sides of the membrane with their interface immobilized at the membrane surface [78–80]. The general advantages of these systems are: no dispersion is formed, thus avoiding coalescence; no density difference required between the two phases; large and known interfacial area (typically  $10\,000\text{ m}^2\text{ m}^{-3}$ ); no loading and flooding, thus allowing for widely different phase flow ratios.

An example of an industrial membrane bioreactor is the hollow-fiber membrane system for the production of (–)-MPGM (3-(4-methoxyphenyl)glycidic acid methyl ester), which is an important intermediate for the production of diltiazem hydrochloride [81, 82]. For the enantiospecific hydrolysis of MPGM a hollow-fiber ultrafiltration membrane with immobilized lipase from *Serratia marcescens* is used. (+)-MPGM is selectively converted into (2*S*,3*R*)-(+)-3-(4-methoxyphenyl)glycidic acid and methanol. The reactant is dissolved in toluene, whereas the hydrophilic product is removed via the aqueous phase at the permeate side of the membrane, see Fig. 13.9. Enantiomerically pure (–)-MPGM is obtained from the to-





**Fig. 13.9** Flow diagram of the membrane reactor for the production of (-)-MPGM. W=water, T=toluene, HM=hydrophilic membrane [81, 82].



**Fig. 13.10** Flow diagram of the Sepracor bioreactor process for the production of (S)-ibuprofen [83].

luene phase by a crystallization step. In cooperation with Sepracor Inc., a pilot-plant membrane reactor has been developed, which produces annually about 40 kg (-)-MPGM per m<sup>2</sup> of membrane surface.

In a comparable system, (*R,S*)-ibuprofen can be separated by a membrane reactor [83], see Fig. 13.10. The technique comprises a stereo-specific hydrolysis by an enzyme. Subsequently, the enantiomeric ester is extracted into the organic phase on the other side of the membrane. In the system developed by Sepracor Inc., (*R*)-ibuprofen is selectively hydrolyzed by proteases in a hollow-fiber unit and the (*S*)-ibuprofen ester can be isolated at 100% yield. This configuration also applies for enantioseparation of other acids such as naproxen and 2-chloropropionic acid.

When lipases are used for enzymatic conversions, the enzyme is mainly active at a phase boundary, which can effectively be provided by a membrane. Additionally, for conversions requiring two phases (e.g. fat splitting [84–86] and esterifications [87]), the membrane also keeps the two liquid phases (an oil and an aqueous phase, respectively) separated. This is schematically depicted in Fig. 13.11. The equilibrium reactions involved are

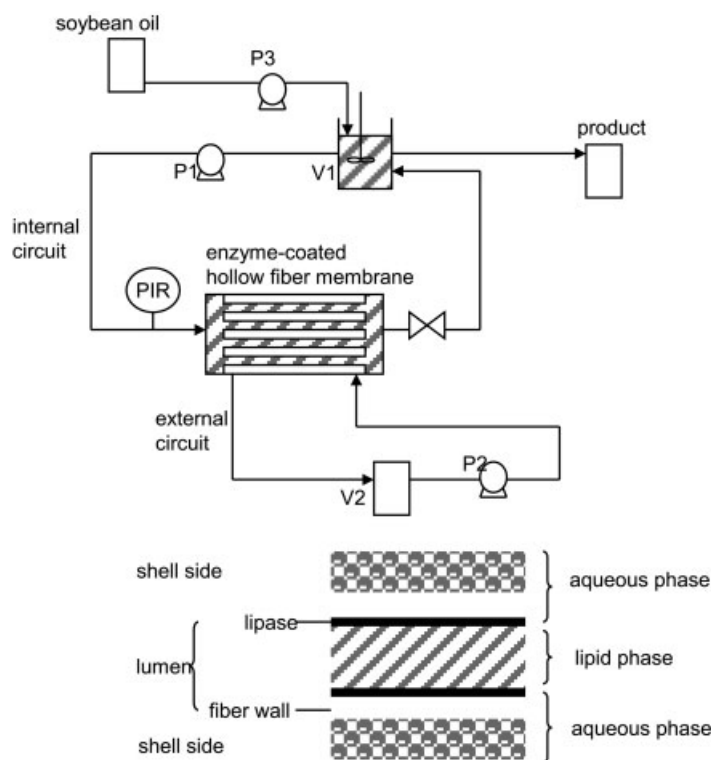
Triglycerides + water  $\leftrightarrow$  diglyceride + fatty acid

Diglyceride + water  $\leftrightarrow$  monoglyceride + fatty acid

Monoglyceride + water  $\leftrightarrow$  glycerol + fatty acid

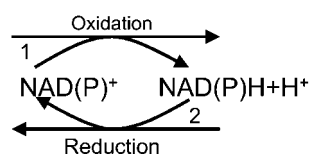
The use of both hydrophilic [85, 87] and hydrophobic [84, 86] membranes has proven to be efficient in binding the enzyme. The main advantage of this system over emulsion systems lies in the ease of the downstream processing, as no enzyme-stabilized emulsion has to be broken.

A major challenge in chemical and food industry is to perform oxidative and reductive conversions by biological means. In the application of enzymes for oxidative or reductive conversions a coenzyme like NAD(P)H or FADH<sub>2</sub> is needed. For two



**Fig. 13.11** Schematic representation of the hollow fiber membrane bioreactor for the enzymatic hydrolysis of triglycerides. A hydrophilic membrane has been used, coated with lipase on the lipid side [85].

**Fig. 13.12** General reaction scheme of NAD(P) (H)-linked enzymatic oxidation/reduction reactions.



**Tab. 13.6** Overview of retentions of various membranes for  $\text{NAD}^+$ ,  $\text{NADP}^+$ ,  $\text{NADH}$  and  $\text{NADPH}$  in different solutions.

Membrane	Component	Retention [%]	Reference
<i>Toray</i>			
Polyamide	$\text{NADP}^+$	98	90
	$\text{NAD}^+$	86	90
<i>S-Psf</i>	<i>Protein-free solutions</i>		89
	$\text{NAD}^+$ in TRA buffer	85–92	
	$\text{NAD}^+$ in phosphate buffer	39–58	
	$\text{NADH}$	83–98	
	$\text{NADPH}$	>99.5	
	<i>protein solutions</i>		
	$\text{NAD}^+$ in TRA buffer	92–96	
	$\text{NADH}$	>98	
	<i>buffer solutions (100 mM, pH 7.5)</i>		91
	$\text{NADP}^+$ in	64	
	tris(hydroxymethyl)aminomethane-HCl		
	$\text{NADP}^+$ in potassium phosphate	60	
	$\text{NADP}^+$ in glycylglycine	92	
<i>Nitto</i>			92
SPA-I	$\text{NADH}$	35	
NTR 7410	$\text{NADH}$	73	
NTR 7410x	$\text{NADH}$	92	
NTR 7430	$\text{NADH}$	99	
<i>Amicon</i>			
Y05	$\text{NADH}$	89	
<i>Desalination</i>			
DS5	$\text{NADH}$	98	
G5	$\text{NADH}$	85	
<i>Osmonics</i>			
SEPA-MX07	$\text{NADH}$	95	
<i>Nitto</i>			93
NTR 4710	$\text{NADP}^+$	61–87	
<i>Rhone Poulenc</i>			
SPS 3026	$\text{NADP}^+$	5–90	

decades studies have been made on oxidative and reductive conversions using coenzymes in enzyme reactors. As the coenzyme is the major cost determinative factor, two issues are of major importance, i.e. the regeneration of the coenzyme and retaining the coenzyme in the enzyme reactor [87]. For this regeneration two coenzyme-dependent reactions can be coupled as shown in Fig. 13.12. Reaction step 1 is the oxidation of a substrate to reduce NAD(P) to NAD(P)H. In reaction step 2, H is transferred from NAD(P)H to reduce the substrate. When NF is used to retain the coenzyme NAD(P)H the difference in retention of a membrane for NAD(P)<sup>+</sup> and NAD(P)H has to be considered. From Tab. 13.6 it can be seen that NF-membranes show a lower retention for NAD(P)<sup>+</sup> than for NAD(P)H. This poses the constraint that the conversion rates of the enzymatic system should be tuned to favor the presence of NAD(P)H to avoid coenzyme losses. Typical NF-behavior is observed when the ionic strength of the solution is increased [94], which causes the retention of NAD(P)<sup>+</sup> to decrease. In the case glucose is converted into gluconic acid a reduction in retention is also observed with an increase in gluconic acid concentration [88]. The presence of a protein or an enzyme that causes membrane fouling has an opposite effect and increases the retention of NAD<sup>+</sup> and NADH. Besides the permeation of NAD(P)H, the stability of the enzyme is also an issue. The most important factor determining the feasibility of this type of processes is the coenzyme turnover number that can be achieved, which is related to the loss of coenzyme either by permeation or by inactivation. A turnover number in excess of 500,000 is necessary to make the costs of the total membrane process not limited by the coenzyme [92]. So far, values up to 106 000 have been reported [89, 90, 94, 95].

#### 13.4

##### Concluding Remarks

For the application of membrane reactors it can be concluded that these are accepted as proven technology for many biotechnological applications. The membranes used in this area can operate under relatively mild conditions (low temperature and aqueous systems). However, there is a tremendous potential for membrane reactors in the chemical industry, which often requires application in nonaqueous systems. Long term stability of the membrane materials in these systems will require an ongoing development from the side of materials scientists. As reaction selectivity is of major importance in the production of fine chemicals and pharmaceutical products, it seems plausible to expect that membrane reactors will find their way in the production of chemicals through applications in these areas.

## 13.5

## References

- 1 K. K. SIRKAR, P. V. SHANBHAG, A. S. KOVVALI, *Ind. Eng. Chem. Res.* **1999**, 38, 3715.
- 2 M. F. KEMMERE, J. T. F. KEURENTJES, Industrial Membrane Reactors, in *Membrane Technology in the Chemical Industry* (eds.: S. P. NUNES, K. V. PEINEMANN), Wiley-VCH, Weinheim, **2001**.
- 3 H. P. DIJKSTRA, G. P. M. VAN KLINK, G. VAN KOTEN, *Acc. Chem. Res.*, in press.
- 4 K. DE SMET, S. AERTS, E. CEULEMANS, *et al.*, *Chem. Commun.* **2001**, 597.
- 5 U. KRAGL, C. DREISBACH, C. WANDREY, *Appl. Homogen. Catal. Organomet. Comp.* **1996**, 2, 832.
- 6 U. KRAGL, C. DREISBACH, *Angew. Chem.* **1996**, 108, 684; *Angew. Chem. Int. Ed.* **1996**, 35, 642.
- 7 G. GIFFELS, J. BELICZEY, M. FELDER, *et al.*, *Tetrahedron Asymm.* **1998**, 9, 691.
- 8 S. RISSOM, J. BELICZEY, G. GIFFELS, *et al.*, *Tetrahedron Asymm.* **1999**, 10, 923.
- 9 J. WÖLTINGER, A. S. BOMMARIUS, K. DRAUZ, *et al.*, *Org. Proc. Res. & Dev.* **2001**, 5, 241.
- 10 J. WÖLTINGER, K. DRAUZ, A. S. BOMMARIUS, *Appl. Catal. A.* **2001**, 221, 171.
- 11 T. DWARS, J. HABERLAND, I. GRASSET, *et al.*, *J. Mol. Cat. A: Chem.* **2001**, 168, 81.
- 12 J. WÖLTINGER, H. HENNIGES, H.-P. KRIMMER, *et al.*, *Tetrahedron Asymm.* **2001**, 2095.
- 13 E. SCHWAB, S. MECKING, *Organometallics* **2001**, 20, 5504.
- 14 A. W. KLEIJ, R. A. GOSSAGE, R. J. M. KLEIN GEBBINK, *et al.*, *J. Am. Chem. Soc.* **2000**, 122, 12112.
- 15 N. J. HOVESTAD, E. B. EGGELING, H. J. HEIDBUECHEL, *et al.*, *Angew. Chem.* **1999**, 111, 1763; *Angew. Chem. Int. Ed.* **1999**, 38, 1655.
- 16 E. B. EGGELING, N. J. HOVESTAD, J. T. B. H. JASTRZEBSKI, *et al.*, *J. Org. Chem.* **2000**, 65, 8857.
- 17 D. DE GROOT, E. B. EGGELING, J. C. DE WILDE, *et al.*, *Chem. Commun.* **1999**, 1623.
- 18 D. DE GROOT, REEK, P. C. J. KAMER, P. W. N. M. VAN LEEUWEN, *Eur. J. Org. Chem.* **2002**, 1085.
- 19 P. WIJKENS, J. T. B. H. JASTRZEBSKI, P. A. VAN DER SCHAAF, *et al.*, *Org. Lett.* **2000**, 2, 1621.
- 20 M. T. REETZ, G. LOHMER, R. SCHWICKARDI, *Angew. Chem.* **1997**, 109, 1559; *Angew. Chem. Int. Ed.* **1997**, 36, 1526.
- 21 N. BRINKMAN, D. GIEBEL, G. LOHMER, *et al.*, *J. Cat.* **1999**, 183, 163.
- 22 C. KÖLLNER, B. PUGIN, A. TOGNI, *J. Am. Chem. Soc.* **1998**, 120, 10274.
- 23 M. ALBRECHT, N. J. HOVESTAD, J. BOERSMA, *et al.*, *Chem. Eur. J.* **2001**, 7, 1289.
- 24 D. DE GROOT, B. F. M. DE WAAL, J. N. H. REEK, *et al.*, *J. Am. Chem. Soc.* **2001**, 123, 8453.
- 25 R. KREITER, A. W. KLEIJ, R. J. M. KLEIN GEBBINK, *et al.*, *Topics in Current Chemistry; Dendrimers IV*; (ed.: F. VÖGTLE), Springer, Berlin, **2001**.
- 26 A. W. KLEIJ, R. J. M. KLEIN GEBBINK, G. VAN KOTEN, *Dendrimers and other Dendritic Polymers*, (eds.: J. FRECHET, D. TOMALIA), Wiley, New York, **2002**.
- 27 G. E. OOSTEROM, J. N. H. REEK, P. C. J. KAMER, *et al.*, *Angew. Chem.* **2001**, 113, 1878, *Angew. Chem. Int. Ed.* **2001**, 40, 1828.
- 28 J. W. J. KNAPEN, A. W. VAN DER MADE, J. C. DE WILDE, *et al.*, *Nature* **1994**, 372, 659.
- 29 R. SCHERENBERG, B. COUSSENS, P. VAN VLIET, *et al.*, *Macromolecules* **1998**, 31, 456.
- 30 J. H. M. HEIJNEN, E. L. V. GOETHEER, L. J. P. VAN DEN BROEKE, J. T. F. KEURENTJES, to be published.
- 31 H. E. A. BRÜSCHKE, State-of-the-Art of Pervaporation Processes in the Chemical Industry, in *Membrane Technology in the Chemical Industry* (eds.: S. P. NUNES, K. V. PEINEMANN), Wiley-VCH, Weinheim, **2001**.
- 32 H. E. A. BRÜSCHKE, EP 096339, **1982**.
- 33 Y. P. AGEEV, S. L. KOTOVA, A. B. ZESIN, *et al.*, *Proc. 7th Internat. Conf. Pervaporation Proc.*, (ed.: R. BAKISH) Englewood, N.J., **1995**.
- 34 F. LIPNIZKI, R. W. FIELD, P. TEN., *J. Membr. Sci.* **1999**, 153, 183.
- 35 J. T. F. KEURENTJES, G. H. R. JANSSEN, J. J. GORISSEN, *Chem. Eng. Sci.* **1994**, 49, 4681.

- 36 W.J.W. BAKKER, I.A.A.C.M. BOS, W.L.P. RUTTEN, *et al*, *Int. Conf. Inorganic Membranes*, Nagano, Japan, **1998**, 448.
- 37 G.J.S. VAN DER GULIK, R.E.G. JANSSEN, J.G. WIJERS, *et al*, *Chem Eng. Sci.* **2001**, 56, 371.
- 38 L. BAGNELL, K. CAVELL, A.M. HODGES, *et al*, *J. Membrane Sci.* **1993**, 85, 291.
- 39 G.K. PEARCE, EU Pat. 0210055 A1, BP Chemicals, Ltd., **1987**.
- 40 R.M. WALDBURGER, PhD thesis, Swiss Federal Institute of Technology, Zurich, **1993**.
- 41 R.M. WALDBURGER, F. WIDMER, W. HEINZELMANN, *Chem. Ing. Tech.* **1994**, 66, 850.
- 42 H. KITA, S. SASAKI, K. TANAKA, *et al*, *Chem. Lett.* **1988**, 10, 2025.
- 43 R. GREF, M.O. DAVID, Q.T. NGUYEN, *et al*, *4th Int. Conf. Pervaporation Processes in the Chemical Industry*, Ft Lauderdale, **1989**, 344.
- 44 M.O. DAVID, PhD thesis, Institut National Polytechnique de Lorraine, Nancy, **1991**.
- 45 J.F. JENNINGS, R.C. BENNING, US PAT. 2956070, AMERICAN OIL COMP., **1960**.
- 46 A. DAMS, J. KRUG, *Proc. 5th Internat. Conf. Pervaporation Proc.*, (Ed.: R. BAKISH), Englewood, N.J., **1991**.
- 47 M.O. DAVID, R. GREF, T.Q. NGUYEN, J. NEEL, *Trans IChemE* **1991**, 69 A, 341.
- 48 R.M. WALDBURGER, F. WIDMER, *Chem. Eng. Technol.* **1996**, 19, 117.
- 49 M. CHERYAN, M.A. MEHAIA, Membrane bioreactors, in: *Membrane Separations in Biotechnology*, (ed.: W.C. MCGREGOR), Marcel Dekker, New York, **1986**.
- 50 G. BELFORT, *Biotechnol. Bioeng.* **1989**, 33, 1047.
- 51 A.S. BOMMARIUS, K. DRAUZ, U GROEGER, *et al.*, Membrane bioreactors for the production of enantiomerically pure  $\alpha$ -amino acids, in: *Chirality in industry*, (eds.: A.N. COLLINS, G.N. SHELDRAKE, J. CROSBY), Wiley, New York, **1992**.
- 52 G.T. FRANK, K.K. SIRKAR, *Biotechnol. Bioeng. Symp. Ser.* **1985**, 15, 621.
- 53 W. KANG, R. SHUKLA, K.K. SIRKAR, *Biotechnol. Bioeng.* **1990**, 34, 826.
- 54 G.T. FRANK, K.K. SIRKAR, *Biotechnol. Bioeng. Symp. Ser.* **1986**, 17, 303.
- 55 R. SHUKLA, W.K. KANG, K.K. SIRKAR, *Biotechnol. Bioeng.* **1989**, 34, 1158.
- 56 J.S. KÁSCÁK, J. KOMÍNEK, M. ROEHR, Lactic acid, in: *Biotechnology: a multi-volume comprehensive treatise*, (eds.: H.-J. REHM, G. REED, A. PÜHLER, P. STADLER), vol. 6, Wiley-VCH, Weinheim, **1996**.
- 57 B.R. SMITH, R.D. MACBEAN, G.C. COX, *Austr. J. Dairy Technol.* **1977**, 32, 23.
- 58 J.H. HANEMAAIJER, J.M.K. TIMMER, T.J.M. JEURNINK, *Voedingsmiddelentechnologie* **1988**, 21(9), 17.
- 59 L.R. SCHLICHER, M. CHERYAN, *J. Chem. Technol. Biotechnol.* **1990**, 49, 129.
- 60 J.M.K. TIMMER, J. KROMKAMP, *FEMS Microb. Rev.* **1994**, 14, 29.
- 61 J.M.K. TIMMER, H.C. VAN DER HORST, T. ROBERTSEN, *J. Membrane Sci.* **1993**, 85, 205.
- 62 J.M.K. TIMMER, J. KROMKAMP, T. ROBERTSEN, *J. Membrane Sci.* **1994**, 92, 185.
- 63 J.M.K. TIMMER, T. ROBERTSEN, J. KROMKAMP, L.E.S. BRINK, NIZO report NOV-1695, **1992**.
- 64 R. JEANTET, J.L. MAUBOIS, P. BOYAVAL, *Enzym.. Microb. Techn.* **1996**, 19, 614.
- 65 M.W. REIJ, J.T.F. KEURENTJES, S. HARTMANS, *J. Biotechnol.* **1998**, 59, 155.
- 66 U. BÄUERLE, K. FISCHER, D. BARDTKE, *STAUB Reinhaltung der Luft* **1986**, 46, 233.
- 67 S. HARTMANS, E.J.T.M. LEENEN, G.T.H. VOSKUILEN, In *Biotechniques for air pollution abatement and odour control policies*, (eds.: A.J. DRAGT, J. HAM), Elsevier, Amsterdam **1992**.
- 68 M.W. REIJ, G.T.H. VOSKUILEN, S. HARTMANS, in *Biofilms-Science and Technology*, (eds.: L.F. MELO, T.R. BOTT, M. FLETCHER, B. CAPDEVILLE), Kluwer, Dordrecht **1992**.
- 69 M. REISER, K. FISCHER, K.H. ENGESSER, *VDI Berichte* **1994**, 1104, 103.
- 70 M. HINZ, F. SATTler, T. GEHRKE, *et al*, *VDI Berichte* **1994**, 1104, 113.
- 71 R.A. BINOT, P. PAUL, S. KEUNING, *et al*, *ESA Technol. Prog. Quart.* **1994**, 4, 14.
- 72 L.M. FREITAS DOS SANTOS, U. HÖMMERICH, A.G. LIVINGSTON, *Biotechnol. Prog.* **1995**, 11, 194.
- 73 M.W. REIJ, C.D. DE GOOIJER, J.A.M. DE BONT, *et al*, *Biotechnol. Bioeng.* **1995**, 45, 107.
- 74 M.G. PARVATIYAR, R. GOVIND, D.F. BISHOP, *Biotechnol. Bioeng.* **1996**, 50, 57.

- 75 R. RAUTENBACH, R. MELLIS, *Desalination* **1994**, 95, 171.
- 76 Wehrle-Werk AG information leaflet "Biomembrat@-plus", [www.wehrle-werk.de](http://www.wehrle-werk.de), **2001**.
- 77 K. KRAUTH, *Wat. Sci. Tech.* **1996**, 34, 389.
- 78 R. PRASAD, K. K. SIRKAR, *AIChE J.* **1987**, 33, 1057.
- 79 R. PRASAD, K. K. SIRKAR, *AIChE J.* **1988**, 34, 177.
- 80 M. C. YANG, E. L. CUSSLER, *AIChE J.* **1986**, 32, 1910.
- 81 H. MATSUMAE, M. FURUI, T. SHIBATANI, *J. Ferment. Bioeng.* **1993**, 41, 979.
- 82 H. MATSUMAE, M. FURUI, T. SHIBATANI, *et al*, *J. Ferment. Bioeng.* **1993**, 75, 93.
- 83 S. L. MATSON, S. A. WALD, C. M. ZEPP, D. DODDS, PCT Int. Pat. Appl., WO 8909765, **1991**.
- 84 M. M. HOQ, T. YAMANE, S. SHIMIZU, *et al*, *J. Am. Oil Chem. Soc.* **1985**, 62, 1016.
- 85 W. PRONK, P. J. A. M. KERKHOF, C. VAN HELDEN, *et al*, *Biotechnol. Bioeng.* **1988**, 32, 512.
- 86 R. MOLINARI, M. E. SANTORO, E. DRIOLI, *Ind. Eng. Chem. Res.* **1994**, 33, 2591.
- 87 A. VAN DER PADT, M. J. EDEMA, J. J. W. SEWALT, *et al*, *J. Am. Oil Chem. Soc.* **1990**, 67, 347.
- 88 M. W. HOWALDT, K. D. KULBE, H. CHMIEL, *Ann. N.Y. Acad. Sci.* **1990**, 589, 253.
- 89 M. HOWALDT, A. GOTTLÖB, K. D. KULBE, *et al*, *Ann. N.Y. Acad. Sci.* **1988**, 542, 400.
- 90 K. SEELBACH, U. KRAGL, *Enzym. Microb. Technol.* **1997**, 20, 389.
- 91 V. KITPREECHAVANICH, N. NISHIO, M. HAYASHI, *et al*, *Biotechnol. Lett.* **1985**, 7, 657.
- 92 B. NIDETZKY, K. SCHMIDT, W. NEUHAUSER, *et al*, Application of charged ultrafiltration membranes in continuous, enzyme-catalysed processes with coenzyme regeneration, in *Separations for Biotechnology 3* (ed.: D. L. PYLE) Royal Society of Chemistry, **1994**, 351.
- 93 M. IKEMI, N. KOIZUMI, Y. ISHIMATSU, *Biotechnol. Bioeng.* **1990**, 36, 149.
- 94 S. LIN, O. MIYAWAKI, K. NAKAMURA, J. BIOSCI. *Bioeng.* **1999**, 87, 361.
- 95 B. NIDETZKY, D. HALTRICH, K. SCHMIDT, *et al*, *Biocatal. Biotransf.* **1996**, 14, 47.

## Index

### **a**

- acetone 8
- acids 145
- activated esters 88
- acyclic diene polymerization (ADMET) 346
- addition reactions 219, 221f.
- adhesion 371, 379
- adsorption 371, 380
- AgroGel 42f., 206
- AIBN 300
- alcohols 143, 145f., 150, 152, 155, 160, 162
- aldol condensation 335
- alkanes 149, 158f.
- alkane thiols 375, 397
- alkenes 147, 149, 159ff., 164
- alkyl arenes 150
- alkyl halides 150
- alkyl silanes 284
- 1-alkyne polymerization 346
- allylation reactions 219
- allylic alkylation 335, 529
- allylic amination 529
- allylic substitution 529
- alumina 55
- Alzheimer's disease 95
- Amberlite 72, 107, 118
- Amberlyst 88, 102, 107, 123f.
- amides 140, 143, 145, 147, 150, 154, 163, 165
- amines 143, 150f., 154, 162f., 169
- $\gamma$ -aminobutyric acid (GABA) neurotransmitter 113
- aminohydroxylation 216, 218
- aminomethylpolystyrene 106f., 325, 328
- $\alpha,\omega$ -amino silanes 406
- amphiphiles 280
- amphiphilic star polymers 295
- aromatic hydrazines 150
- Arrhenius law 534
- asymmetric dihydroxylation (AD) 249, 251
- asymmetric hydrogenation 282, 299, 529
- asymmetric reduction of ketones 230
- asymmetric synthesis 159, 161, 234, 468, 528
- atom transfer radical polymerization (ATRP) 291, 421, 423
- atomic absorption spectroscopy 486
- atomic-force microscopy (AFM) 411, 416
- ATRP 291f., 350, 353, 421, 423
- attenuated total reflection (ATR) FT-IR 39
- azepanones 184
- azides 150, 163
- aziridines 179
- 2,2'-azobisisobutyramidine 407
- azo compounds 150, 406
- 2,2'-azoisobutyronitrile (AIBN) 187

### **b**

- Baylis-Hillman adducts 257
- beads 11
- benzazepines 185
- benzimidazoles 185
- benzisoaxazoles 185
- benzo[b]furans 186
- 1,4-benzodiazepin-2-ones 156
- benzodiazepinediones 172f.
- benzodiazepines 144, 185
- benzofurans 155f.
- benzothiazepines 185
- benzothiazines 185
- benzotriazoles 150, 185
- benzoxazolines 186
- benzoxazinones 85, 87
- benzoxazoles 185
- BET 3
  - equation 20
  - theory 20
- biaryls 150



- Biginelli reactions 173
- bimolecular reaction 469
- biomaterial interfaces 379
- Biomembrat®-plus 538, 540
- biomineralization 432
- 2,2'-bipyridine 292
- Bischler-Napieralski reactions 185
- BJH theory 21
- Boba resin 140
- Boltorn hyperbranched polymer 317
- brush layer thickness 418
- bulk density 25
- Burgess reagent 266 f.
- (2S,4S)-*N*-*tert*-butoxycarbonyl-4-diphenylphosphino-2-diphenylphosphinomethylpyrrolidine (BPPM) 282
- c**
- calcination 208
- calorimetric measurements 18
- capillary condensation 22
- capillary electrochromatography 358
- capillary electrophoresis 15, 428
- $\epsilon$ -caprolactone 433
- carbamates 165
- carbon black 406
- carbon-carbon bond-formation 253 ff.
- carbosilane 335
- carbosilane dendrimers 313 f.
- carboxylic acids 145, 147, 151, 154
- carpanone 122
- ( $\pm$ )-carpanone 121
- $\beta$ -casomorphin 449
- casting techniques 371
- catalysis 211, 283, 305, 307, 311, 345, 371
- catch and release 62
- cathepsin D inhibitor 100
- cation exchange resin 220
- C-C bond formation 165
- cell adhesion 393
- cell growth 379
- cellulose 55, 246
- C-H activation 207
- chain-transfer agents (CTAs) 365
- chemical (nano)lithography 391
- chemical lithography 393, 409, 411
- chemiluminescent nitrogen detection (CLND) 504
- chemisorption 374, 400, 421
- Chimasorb 944, 212
- chinchona ligands 350
- chroman-4-ones 187
- chromatography 15, 271, 472
- chromium 214
- 4-chromones 187
- chymotrypsin 446
- $\alpha$ -chymotrypsin 447 ff.
- cinnolines 150, 185
- Claisen rearrangement 121
- clays 55
- coatings 371
- color tests 34
- combinatorial chemistry 53, 71, 137, 201, 345, 445, 489, 499
- combinatorial libraries 503 f.
- combinatorial synthesis 503
- compound libraries 504
- controlled radical polymerization 423, 427
- [Co(salen)] complex 338
- cotton textile industry 540
- coumarines 187
- coupling reactions 227
- cross metathesis (CM) 31, 160, 467, 472, 487, 489, 495
- cross-coupling reactions 277
- cross-linking 1, 6, 320
- cross-polarization (CP) 41
- crystallization 244, 379
- curve-fit analysis 509
- cyclative cleavage 155 f.
- cyclic peptides 156
- cycloaddition reactions 162, 170, 223
- cyclodehydrations 266 f.
- cycloelimination 156
- cyclofragmentation 156
- cyclopropanation 224
- cylindrical pore model 25, 30
- d**
- Davankov 8
- deglycobleomycin A<sub>5</sub> 175
- dehydrations 510
- dendrimers 10, 206, 295, 306, 335, 468, 475, 478, 529
- dendritic catalysts 331 f.
- dendritic effect
  - negative 332, 334
  - positive 332
- dendritic polymers 305
- dephosphorylation 457
- desorption 18
- Dess-Martin periodinane 74, 83, 263
- destructive on-bead analysis 34
- DHQ 218
- dialysis 297, 307 ff., 528
- diazonium salts 163

2,3-dichloro-5,6-dicyanobenzoquinone (DDQ) 75  
 2,6-dichloropyridine *N*-oxide (Cl<sub>2</sub>pyNO) 213  
 dicyclopentadiene (DCPD) 359  
 Diels-Alder reaction 64, 121, 170, 185, 208, 210, 223, 254, 458, 464 f.  
 diethyl diallylmalonate (DEDAM) 351, 353, 365 f., 483, 486 f.  
 diffuse reflectance FT-IR (DRIFT) spectroscopy 40  
 diffusion 380  
 2,5-dihydrofuranones 179 f.  
 2,5-dihydrofurans 179  
 dihydropyrans 181  
 dihydropyridines 181  
 dihydropyridones 181  
 dihydropyrimidinediones 181  
 dihydropyrimidines 173, 181  
 dihydroquinidine (DHQD) 217, 249  
 dihydroxylation 165, 216 ff., 529  
 diketomorpholines 184  
 diketopiperazines 155 f., 172, 181  
 4-dimethylaminopyridine (DMAP) 85, 365  
 1,4-dimethyl-1,4,7-triazacyclononane (dmtacn) 213  
*N,N*-dioctadecylamine 420  
 1,3-dipolar cycloadditions 161, 171, 223  
 dipoles 386  
 dip-pen nanolithography (DPN) 391  
 divinylbenzene (DVB) 7  
 DMAP 127  
 DNA 393  
 dormant species 291  
 DRIFT *see* diffuse reflectance FT-IR spectroscopy  
 Dubinin-Astakhov analysis 22  
 Dubinin-Radushkevich method 22  
 dynamic swelling experiments 421

## e

e-beam nanolithography 391  
 electrocatalysis 388  
 electro dialysis 527 f.  
 electron transfer 379  
 elemental analysis 511  
 elemental microanalysis 34  
 ellipsometry 384, 406, 408  
 enantiomeric excess 341  
 enantioselectivity 249, 282, 315  
 end-functionalization 419  
 endo-borneol 262  
 endo-enzymes 445

endo-linkers 446  
 enzymatic glycosylations 322  
 enzymatic polymerization 433  
 enzymatic synthesis 321  
 enzymatic transformations 445  
 enzyme reactors 540  
 (±)-epibatidine 118, 120  
 (±)-epimaritidine 118 f.  
 epothilone A 125, 132, 165, 175  
 epoxidations 207 f., 213, 215 f., 253, 355 f.  
 ER-FTIR spectroscopy 384, 386, 388, 406, 411  
 ester 150  
 esterase 458  
 esters 140 f., 143, 146, 150, 154, 160  
 1-ethyl-3-(3-dimethylaminopropyl)carbodiimide (EDC) 100  
 ethylene glycol dimethacrylate (EGDMA) 225  
 evaporation 472  
 EXAFS 46  
 exo-enzymes 445  
 exo-linkers 446, 458, 460, 463  
 extrusion 25

## f

farnesyl transferase 89  
 Felkins' iridium catalyst 121  
 fermentation 537  
 filtration 308, 336, 472 f.  
 first generation Grubbs catalyst 355  
 Fischer indol synthesis 313  
 Fischer reactions 185  
 fluid penetration 18  
 focused ion beam lithography 389  
 free radical allylation 357  
 free radical polymerization 406, 408, 413, 428  
 friction 371  
 Friedel-Crafts sulfonylation 222  
 FT-IR 46  
 – analysis 35  
 – microscopy 36  
 – spectroscopy 382  
 furans 179

## g

β-galactosidase 454  
 galactosylation 454  
 galanthamine 176, 178  
 gas adsorption 18  
 gas permeation 527  
 gas separation 528  
 gel filtration (GF) 29

gel permeation chromatography (GPC) *see*  
 also SEC 29, 244  
 gel-phase  $^{13}\text{C}$  NMR spectroscopy 42f.  
 gel-phase high resolution magic angle spin-  
 ning 32  
 gel-phase (HR-MAS) NMR 43  
 gelation 207  
 glass 207  
 glass beads 55  
 $\alpha$ -glucosidases 454  
 $\beta$ -glucosidases 454  
 glycopeptides 446f.  
 glycosidase 458  
 glycosides 144  
 glycosylations 268  
 gold 397, 406, 430  
 gold nanoparticles 418, 420, 429  
 GP IIb-IIIa antagonists 325  
 grafting densities 378, 433  
 grafting from 296, 347, 401, 409  
 grafting-to 408, 421  
 graphite 55  
 Grieco reactions 172  
 Grignard reagents 92  
 group-transfer polymerization 281  
 Grubbs' initiator *see also* Grubbs-cata-  
 lyst 346, 359, 364  
 Grubbs' catalyst *see also* Grubbs-initia-  
 tor 470, 475, 480, 484  
 Grubbs' complex 482  
 Grubbs-type ruthenium alkylidene 255  
 guanidines 150

## h

halides 150, 272  
 Hammett equation 388  
 Hantzsch reactions 173  
 head group 373  
 Heck reactions 166, 185, 207, 228, 254f.,  
 284, 287, 290, 297, 327, 332, 347f., 351,  
 355ff., 366f., 464  
 heterocycle formation 98  
 heterocycles 156  
 N-heterocyclic carbenes (NHC) 346, 478,  
 480ff.  
 hetero-Diels-Alder reaction 107  
 heterogeneous catalysis 277, 338, 345, 358,  
 364  
 1,4,4a,5,8,8a-hexahydro-1,4,5,8-*exo-endo*-dime-  
 thanonaphthalene (DCPD) 359  
 Hg intrusion porosimetry 24  
 high performance liquid chromatography  
 (HPLC) 376

high resolution patterning 393  
 high throughput 31  
 high throughput screening (HTS) 53, 137,  
 345, 349  
 high throughput synthesis 54, 202, 225,  
 234, 490, 499  
 HIV-1 reverse transcriptase inhibitors 167  
 homogeneous catalysis 277, 331f., 345, 469  
 Horner-Wadsworth-Emmons reactions 127,  
 169  
 Horvath-Kawazoe equation 22  
 HR-MAS NMR 43, 46  
 Hund-Mori reaction 92  
 HYCRAM 141f.  
 HYCRON 141f.  
 hydantoins 156, 180  
 hydrazides 154  
 hydrazines 150  
 hydrobenzo[b]furans 186  
 hydroboration 475  
 hydrodynamic volume 307f.  
 hydroformylation 65, 68, 231f., 288, 297,  
 333, 335f., 339, 529  
 hydrogen transfer reactions 230  
 hydrogenation 65, 248f., 297, 334f.  
 hydrosilylation 475  
 hydrothermal activation 377  
 hydrovinylation 334, 529  
 2-hydroxyethyl methacrylate (HEMA) 428  
 11-hydroxyundecane-1-thiol (HUT) 381  
 hyperbranched polyester support 317  
 hyperbranched polyglycerol 316  
 hyperbranched polymers 206, 295, 306,  
 334  
 hyperbranching 423  
 hysteresis loops 19

## i

(*R,S*)-ibuprofen 541  
 imidazoles 180  
 imidazoquinoxalinones 156  
 immobilization 207, 292  
 immobilized catalysts 201  
 immunoassays 395  
 indazoles 185  
 indolactam 176f.  
 indoles 143, 185  
 inductively coupled plasma-optical emission  
 spectroscopy (ICP-OES) 351  
 infrared spectroscopy 35  
 iniferters 423  
 initiation 418  
 inorganic supports 207

interleukin-1 $\beta$  converting enzyme inhibitors 103  
 inter-microglobule void volume 360  
 intrusion volume 17  
 inverse size exclusion chromatography (ISEC) 29  
 iodoarenes 150  
 iodobenzene 290, 297  
 iodophenol 255  
 ion-exchange resins 73, 203  
 ion-exchanges 407  
 ionic polymerizations 434  
 ionochocarpine 176  
 iridium nanoparticles 397  
 isochromans 187  
 2-isopropoxystyrene 477  
 isoquinolines 185  
 isoxazoles 180, 185  
 isoxazolidines 180  
 isoxazolines 180  
 IUPAC 138

## j

Janda Jel-polymer 221

## k

ketones 147  
 ketopiperazines 181  
 Kharasch reaction 335  
 Kharash addition 529  
 Knoevenagel 335  
 Knoevenagel condensation 207, 334

## l

$\beta$ -lactams 178, 180  
 lactic acid 537  
 $\beta$ -lactones 179  
 landfill leachate 540  
 Langmuir-Blodgett (LB) films 372  
 Langmuir-Blodgett technique 378  
 lanthanides 220  
 Letsinger 55  
 Leu-enkephalin 449  
 Lewis acid 219  
 libraries from libraries principle 98  
 light microscopy 407  
 light scattering 30  
 linker 138f.  
 – acetal 141  
 – acid-labile 516  
 – allylic 149  
 – amide 143  
 – BAL 140

– boronate 144, 146  
 – carbamate 143  
 – ester 143, 445  
 – fragmentation/cycloreversion cleavage 152  
 – HAL 139f.  
 – HMPA 324  
 – HMPB 322  
 – indole 518ff.  
 – ketal 141  
 – Marshall 520  
 – multifunctional 152  
 – Pbs 145  
 – photo-cleavable 151  
 – photo-labile 151  
 – Ramage 145  
 – Rink 518ff.  
 – SAC 145  
 – safety catch 152f.  
 – SAL 144f.  
 – selenium 148  
 – SEM 144, 146  
 – silico Wang 144  
 – silyl 144, 159  
 – silyl ether 445  
 – stannane-based 146f.  
 – strategies 152f.  
 – sulfone 146, 159  
 – thio ether 445  
 – THP 141  
 – traceless 138, 152, 157  
 – triazene 159  
 – triazene-based 149f.  
 – Wang 140, 327  
 lipases 542  
 lipopolymers 419  
 liquid phase-separation 308  
 liquid-liquid extraction 271, 316  
 liquid-phase synthesis 241, 243f.  
 lithium triethylborohydride 397  
 living anionic polymerization 414f.  
 living carbocationic polymerization 417  
 living polymerization 420  
 – anionic 281  
 – cationic 281  
 – radical 281  
 living radical polymerization 423  
 loading capacities 310  
 low-energy atom diffraction (LEAD) 383

## m

macrocyclic lactones 156  
 macrocyclization reactions 59

- macroligands 288, 292
  - macroporous 5
  - magic angle spinning (MAS)  $^{13}\text{C}$  NMR 9, 41
  - Magtrieve<sup>TM</sup> 118
  - MALDI/TOF mass spectrometry 420
  - manganese 214f.
  - Mannich reactions 173
  - mass spectrometry (MS) 33
    - electrospray ionization (ESI) 33
    - ESI Fourier transform ion cyclotron resonance (ESI-FT-ICR) 33
    - matrix assisted laser desorption ionization (MALDI) 33
  - McCabe-Thiele diagram 535
  - MCM-41 207, 212, 215
  - MCPBA 215
  - mechanically assembled monolayers (MAMs) 382
  - membrane bioreactors 536, 540
  - membrane electrolysis 527
  - membrane filtration 297, 307
  - membrane osmometry 30
  - membrane separation 335
  - membrane separation techniques 332
  - membrane technology 529
  - membranes 310, 527, 532, 544
  - mercaptopbiphenyls 383, 391, 409
  - Merrifield 9, 53, 55
  - Merrifield resin 140, 209, 215, 221, 227, 262, 310, 328, 339
  - mesogenic unit 372f.
    - mesopores 20
  - mesoporous 5
  - metal ion analysis 32
  - metal oxides 207
  - metal dendrimers 529
  - metalloporphyrins 380
  - metathesis 345, 366, 478, 484, 493
    - ring closing (RCM) 170, 188
    - ring opening (ROM) 170
  - metathesis reactions 156, 160, 169, 185
  - methacrylates 407
  - methanol 8
  - methylarenes 152, 158
  - methyl methacrylate (MMA) 293
  - N*-methylmorpholine-*N*-oxide 249 ff.
  - Methylobacter 539
  - 2-methyl-2-oxazoline 296
  - methylrhenumtrioxide (MTO) 213
  - micellar aggregates 281, 283
  - micellar catalysis 277 ff., 287f.
  - micelles 278, 280, 298
  - micellization 283
  - Michael addition 110, 169, 271, 334f.
  - Michael reactions 168
  - microbeads 40
  - microencapsulation 205, 227
  - microfiltration (MF) 468, 479, 527f., 536
  - microgels 265
    - micropores 20
  - microporosity 364
  - microporous 5
  - Mitsunobu reaction 256f., 259, 311, 323, 326f., 329, 458, 464f., 484, 488
  - molecular dynamics 23
  - molecular recognition 379
  - molecular weight cut-off (MWCO) 309
  - monolayers 378, 388, 419
  - monolithic 366
  - monolithic supports 358f., 363, 367
  - monoliths *see also* monolithic supports 366
  - Monte Carlo method 23
  - Monte Carlo simulations 381
  - Mukayama-type aldol reaction 220
  - multi-functional libraries 84
  - multilayer adsorption 18
  - multi-step transformations 69
- n**
- NAD(P)H 542, 544
  - Nafion 219
  - nanocomposites 420, 423, 428
  - nanocrystalline arrays 395
  - nanoelectronics 283
  - nanofiltration (NF) 295, 335, 527f., 536
  - nanografting 391
  - nanolithography 412
  - nanoparticles 283, 286, 297, 305, 395
  - nanosecond fluorescence sensing
    - devices 11
  - nanoshaving 391
  - naproxen 541
  - narrow molecular weight 30
  - natural products 156
  - NCPS 215
  - near-edge X-ray absorption fine structure spectroscopy (NEXAFS) 382, 384
  - Negishi couplings 168
  - Nenitzescu reactions 185
  - network effect 23
  - NHC 346
  - nicotine 122, 125
  - nitrones 91, 223
  - NMO 215
  - non-cross-linked polystyrene (NCPS) 247

- nondestructive on-bead analysis 35
- norbornadiene (NBDE) 359
- norbornene 95
- nornicotine 122 ff.
- N<sub>2</sub> sorption 3, 9, 18
- nuclear magnetic resonance (NMR) spectroscopy 41
- nucleation 284
- nucleic acids 154
- nylon 66 261
- o**
- n*-octadecylsilane 391
- n*-octadecyltrichlorosilane 376
- 1-octene 288
- off-bead analysis 32
- off-bead methods 506
- olefin metathesis 229, 255, 467 f., 477, 483, 485, 490, 493, 497, 529
- oligonucleotides 137, 144
- oligosaccharides 137, 144, 446 f., 449 f.
- on-bead methods 506
- Oppolzers' sultam 129
- optics 283
- optoelectronics 395
- organic synthesis 241, 305, 307, 311 f., 345
- organotin reagents 272
- oscillamide Y 175
- oscillatory baffled reactor 2
- osmotic shock 327
- oxadiazoles 180
- 7-oxanorbornene 95
- oxazoles 180
- oxazolidines 180
- oxazolidinones 180
- oxidation 164, 212, 261, 336
- (±)-oxomaritadine 119
- p**
- palladium 397
- PAMAM dendrimers 326, 330, 334
- parallel synthesis 445
- Paullones 176, 178
- Pauson-Khand reaction 233
- Pd black 284
- penicillin amidase 458
- penicillin G acylase 463 f.
- pentaerythritol 321
- peptidases 458
- peptide nucleic acid (PNA) oligomers 449
- peptides 137, 139, 144, 154, 170, 245, 393, 447
- peracetyl-macrophylloside D 176
- percolation theory 23
- perhydrodiazepinediones 184
- peroxides 406
- perruthenate 89
- pervaporation 528, 530, 534
- Pfizzner-Moffat oxidation 73
- phase separation 4
- phase transitions 374
- phase-transfer catalysts 251 f.
- phase-transfer reactions 252
- phenols 150
- Philanthotoxin 176
- Philanthotoxin-433 178
- phosphatase 458
- phosphodiesterase 449
- phosphonates 164
- photoacoustic (PA) FT-IR 40
- photopolymerization 408
- phthalazine 217 f.
- physisorption 374, 400
- physisorption isotherms 19
- Pictet-Spengler reaction 463
- pincer ligands 337, 334 f.
- piperazines 181
- piperidindiones 181
- piperidines 181
- piperidinones 181
- piperidino-thiomorpholines 101
- 1-piperonylpiperazine 524
- PIPO 212
- (±)-plicamine 124, 126
- PNIPAM 228
- PNIPAM-resins 227
- poly(2-oxazoline)s 292
- poly(4-vinylpyridine) 99, 114, 407
- poly(dimethylsiloxane)-*block*-poly(ethylene oxide) (PDMS-*b*-PEO) 285
- poly(ethylene glycol) (PEG) 205
- poly(*n*-alkylacrylamide)s 280
- poly(vinyl naphthalene) 264
- poly(vinylpyridiniumchlorochromate) (PVPCC) 67
- poly(acrylamide) 246
- poly(acrylic acid) 246
- poly(amidoamine) (PAMAM) dendrimer 12
- poly(dimethyl siloxane) (PDMS) 531
- polydispersity index (PDI) 407, 428
- polyelectrolyte brushes 407
- poly(ethylene glycol) (PEG) 245 ff., 265
- poly(ethylene imine) 246
- poly(ethyleneimine)-*block*-poly(ethyleneoxide) (PEI-*b*-PEO) 285

- poly(glycerol) 206, 298, 328
  - polymer brushes 371 f., 400 f., 407 f., 413, 433 f.
  - polymer coatings 372
  - polymer layers 371 f.
  - polymer morphology 6
  - polymer spacer concept 398
  - polymer support
    - methacrylate-based 28
  - polymer supports 1
  - polymerization 418
  - polymer-supported metal complex
    - catalysts 32
  - polymer-supported monolayers (PSMs) 371 f.
  - polymer-supported synthesis 205
  - poly(methyl octyl siloxane) (POMS) 531
  - poly(methylene oxide) 246
  - poly(peptide)s 432
  - poly(propylene oxide) 246
  - poly(saccharide)s 364
  - poly(soaps) 298, 300
  - poly(styrene) 245 ff., 260, 263, 265, 328, 483, 486
  - poly(styrene) microbeads 305
  - poly(styrene)-*block*-poly(4-vinylpyridine) (PS-*b*-P4VP) 283
  - poly(styrene)-*block*-poly(ethylene oxide) (PS-*b*-PEO) 285
  - poly(styrene)-*block*-poly(*m*-vinyltriphenylphosphine) (PS-*b*-PPH) 285
  - poly(vinyl alcohol) (PVA) 246, 531
  - pore area 25
  - pore size 5, 25
  - pore volume 25
  - pore volume  $V_p$  361
  - pores
    - macropores 20
  - porogen 4, 7, 205
  - porosity 17, 25
  - porphyrin 213
  - precipitation 244, 249, 308, 334 f., 336, 468, 473, 478
  - precipitation-crystallization 244
  - preparative SEC 307
  - propagation 421
  - protein tyrosine phosphatase (PTP) 457
  - proteins 393
  - PS-BEMP 106
  - PS-DVB 3, 17, 29, 209
  - pseudomonas 539
  - pycnometry 18
  - pyrazoles 180
  - pyrazolines 180
  - pyrazolones 180
  - pyridazines 181
  - pyridines 181
  - pyridinones 181
  - pyrimidines 181
  - pyrimidinones 181
  - pyrroles 179
  - 2,4-pyrrolidinediones 179
  - 2,5-pyrrolidinediones 179
  - pyrrolidines 179
  - pyrrolidinones 179
  - 2,5-pyrrolinediones 179
  - pyrrolinones 179
- q**
- quantitative purity 503
  - quinazolines 185
  - quinolines 185
  - quinoxalines 185
- r**
- radiation scattering 18
  - radical cyclizations 357
  - Raman spectroscopy 35, 40
  - rare earth catalysts 219
  - redox systems 406
  - reduction reactions 164
  - reductions 264
  - reductive amination 76, 511
  - Reformatsky reaction 129
  - Reissert-reaction 221
  - relative purity 503
  - release/return mechanism 469
  - resins
    - anion-exchange 205
    - collapsible macroporous 8
    - Davankov hypercross-linked 8
    - gel-type 3
    - JandaJel 270 f.
    - macroporous 3, 205
    - Merrifield 250
    - Rasta silane 310 f.
    - solvent expanded gel-type 7
    - TentaGel 250, 310, 322 ff., 462, 485
    - Wang 75, 250, 326, 330, 487
  - retrocycloaddition cleavage 156
  - reverse osmosis (RO) 527 f., 536
  - reversed-phase (RP) stationary phases 376
  - reversible addition fragmentation chain transfer (RAFT) polymerization 423
  - rhodium 288
  - Richter reactions 185

- ring-closing metathesis (RCM) 350, 353, 364, 467, 474, 476, 485, 487, 490, 493
  - ring-opening metathesis (ROM) 467, 472, 495
  - ring-opening metathesis polymerization (ROMP) 281, 346, 349, 358 f., 430
  - ring-opening metathesis precipitation polymerization 346, 366 f.
  - ring-opening polymerization 433
  - ROMPGEL 95, 97, 354
  - ROMP-spheres 353
  - ruthenium 213, 293
- S**
- saccharides 144
  - safety catch linker 462
  - salen 208, 214 ff.
  - salmeterol (Serevent®) 114
  - (R)-Salmeterol 117
  - sarcodictyin 176 f.
  - SASRIN 140
  - SASRIN resin 139
  - scanning electron micrographs (SEM) 30
  - scanning near-field optical microscopy 416
  - scanning tunneling microscopy (STM) 391
  - scavengers 14, 53, 61, 89
  - scavenger reagents
    - electrophilic 77
    - nucleophilic 77
  - scavenging techniques 76
  - scCO<sub>2</sub> 8
  - Schiff bases 97
  - Schrock initiator 346, 359
  - Schrock molybdenum alkylidene 255
  - Schwesingers' phosphazene base 104
  - second generation Grubbs catalyst 352, 366
  - secondary amides 141
  - secondary cross-linked 9
  - selenium 165
  - self-assembled monolayers (SAMs) 371 ff., 393, 397, 433
  - self-assembled multilayers 393
  - self-assembly 373, 386
  - self-supporting films 11
  - sensor technology 371
  - seseline 176
  - Sharpless epoxidations 214
  - Shell Higher Olefin Process (SHOP) 278
  - shrinking 399
  - sialic acid 268
  - silanes 376
  - silanization 377
  - Sildenafil (Viagra™) 114, 116
  - silica 55
  - single bead Fourier transform infrared (FT-IR) spectroscopy 32, 36, 509, 515 f.
  - single layer adsorption 18
  - single pulse excitation (SPE) 9
  - site isolation 204
  - size exclusion chromatography (SEC) 18, 29, 307, 468
  - skeletal density 25
  - small angle X-ray scattering 31
  - sol-gel synthesis 207
  - solid phase extraction 358
  - solid phase organic synthesis (SPOS) 31, 503
  - solid-phase reactions 507
  - solid phase synthesis 1, 3, 14, 139, 174, 305, 445, 454, 461
  - solid state <sup>13</sup>C NMR 41
  - solution phase NMR spectroscopy 32
  - solution phase synthesis 504
  - solvent imbibition 16
  - Sonogashira reactions 168, 185, 347 f., 464
  - spatial analysis 44
  - specific surface area 377
  - spin-coating 416, 428
  - split synthesis 507
  - SPOS 42, 504
  - standards 30
  - static swelling experiments 421
  - stationary phases 399, 428
  - Staudinger reaction 258, 319
  - Staudinger reduction 256
  - stencil mask 411
  - stereinduction 315
  - stereoselectivity 242
  - Stille reaction 146, 160, 167, 334 f.
  - Strain DM21 539
  - StratoSphere Plugs™ 13
  - Strecker-type synthesis 222
  - styrene 7, 255, 290, 297
  - sulfatase 458
  - sulfonamides 164
  - sulfones 146
  - sulfonic acids 146
  - sulfoxides 146
  - sulfoximines 150
  - sulfur 165
  - Sunbrite PTE-2000 320
  - supports *see also* polymer supports
    - discs 12
    - morphological characterization 15
    - plugs 12 f.
    - PolyHIPE-based 13



- self-supporting rods 12
  - supported monolithic structures 15
  - thin film based 11
  - surface coatings 433
  - surface confined heterostructures 393
  - surface engineering 378
  - surface-*gauche* defects 381
  - surface-initiated atom transfer radical polymerization (ATRSIP) 422
  - surface-initiated controlled radical polymerization (CRSIP) 424
  - surface-initiated polymerization (SIP) 400ff., 413, 430
  - suspension polymerization 2, 205
  - Suzuki reactions 146, 159, 166, 227f., 314, 316, 327, 329, 347f., 464
  - swelling 7, 16, 204, 340, 399
  - swelling/shrinking 399
  - Swern oxidation 262
  - synthesis 31
- t**
- TADDOL 208f., 220, 223
  - tail group 373
  - tannery waste water 540
  - Taxol 176f.
  - TEMPO 212
  - tentacle-type 407
  - TentaGel® 9, 42f., 206
  - termination reaction 418
  - tetrahydroazepines 184
  - tetrahydroazepinones 184
  - tetrahydropyrans 181
  - tetrahydropyridines 181
  - 2,2,6,6-tetramethyl-4-piperidin-1-oxyl (TEMPO) 423
  - tetra-substituted pyrroles 107
  - thermomorphic separation 335
  - thermoporometry 31
  - thermoreponsive polymer brushes 423
  - thiadiazoles 180
  - thiazoles 180
  - thiazolidines 180
  - thiazolidinones 180
  - thin layer chromatography (TLC) 32, 201
  - thin layers 371
  - thioacetals 270
  - thioesters 165
  - thioethers 146
  - thioketals 270
  - thiomorpholinones 184
  - thiophenes 179
  - thioureas 150
  - THP 142
  - titration 245
  - Tommsdorff effect 407
  - total porosity 360
  - transglycosylation 451
  - transition metal catalysts 226, 281
  - transmission electron microscopy (TEM) 31, 45
  - triazepanediones 184
  - triazoles 180
  - trifluoroacetic acid (TFA) 85, 139
  - triglycerides 542
  - tri-*o*-tolylphosphine 227
  - tripeptides 323
  - triphenylphosphine 56, 65, 122, 129, 227, 256, 259f., 288f., 293, 296, 329, 483
  - triphenylphosphine palladium 205
  - tris(norborn-2-en-5-ylmethylenoxy)methylsilane (NBE-CH<sub>2</sub>O)<sub>3</sub>SiCH<sub>3</sub>) 359
  - trisubstituted ureas 86
  - Trypostatin B 175
  - Tsuge reactions 185
  - turn-over frequency (TOF) 365
  - turn-over number (TON) 347
- u**
- Ugi reactions 172
  - ultrafiltration 307, 310, 335, 336, 527f., 536
  - ureas 88
  - UV irradiation 408
  - UV-active protecting group 35
- v**
- Vancomycin 148f., 176f.
  - vapor permeation 527
  - Verrucine A 175
  - Verrucine B 175
  - vinyl polystyrene 470
  - vinylbenzyl chloride 7
  - 2-vinylpyridine 408
  - volume fraction of the inter-microglobule void volume 361
  - volume fraction of the pores 361
- w**
- Wadsworth-Horner-Emmons reaction 67
  - Wang alcohol 38
  - Wang-supported alanine 38
  - wetting 371
  - wetting experiments 430
  - Wilkinsons' catalyst 67
  - Wittig olefination 156

Wittig reactions 56, 90, 160, 169, 185, 256,  
260f.

Wittig-Horner reaction 156

## **x**

Xanthobacter GJ10 539

Xanthobacter Py2 539

Xanthyletine 176

Xenon NMR 18

X-ray photoelectron spectroscopy (XPS) 384,  
406

## **y**

Yne-ene metathesis 481

## **z**

(*S*)-zearalenone 169

zeolites 55, 207

Ziegler-Natta polymerization 207